ICSM ICQMT 2024

9th ICSM 2024 — 2nd ICQMT 2024

9th INTERNATIONAL CONFERENCE on SUPERCONDUCTIVITY and MAGNETISM

&

2nd INTERNATIONAL CONFERENCE on QUANTUM MATERIALS and TECHNOLOGIES

27th April - 04th May 2024

Liberty Hotels Lykia / Ölüdeniz-Fethiye/TÜRKİYE

Abstract Book

The bridge between west and east in scientific and technological excellence of quality

www.icsm2020.org
www.icsm2023.org
www.icsmforever.org

organizers@icsmforever.org • www.icsmforever.org

Table of Contents

ORAL PRESENTATIONS	1
Public Outreach and Plenary Session	2
On the Large Scale Applications of Superconductors	3
A. Gencer	3
Vision of Ankara University as a Leading Research Institution	4
Mustafa Fener	4
Implications of Climate Change and Zero Emission Targets on Emerging Technologies	5
G.J. Levermore	5
Advances in Quantum Computing, Sensing and Metrology	6
Ziad Melhem	6
Superconducting Diode Effect	7
T. Ono	7
Plenary Session	8
SuperBrain Manifesto	9
Ivan Božović	9
Topological Quantum Matter : New Frontiers	10
M. Zahid Hasan	10
Effects of Topology in Superconductor Nanoarchitectures	11
V.M. Fomin	11
Magnon Enhanced Quantum Technologies	12
M.E. Flatté	12
Advanced REBCO-based conductors for large-scale HTS applications: Exploring limits of performance in coated conductors	13
Amit Goyal	13
Remarkable Effects of Electricity and Magnetism in Human Body	14
Tarık Yazar	14
Non-Trivial Topological and Strongly Correlated Electron States in Model-Type Low-Dimensional Magnet - Superconductor Hybrid Systems	15
Roland Wiesendanger	15
From spintronic devices to quantum spin torques	16
Pietro Gambardella	16
Superconductivity near 80 K in a bilayer nickelate under high pressure	17

Meng Wang	17
Ferrimagnetic Garnet Films and Nanocomposites for Spintronic, Photonic and Magnetoelectric Devices	18
Caroline A. Ross	18
Transport Phenomena in Bose–Einstein Magnon Condensates	19
B. Hillebrands	19
High-pressure challenges of metallic hydrogen and room-Tc superconductors	20
Ho-kwang (David) Mao	20
Quantum dynamics and transport of spins in magnets	21
Eiji Saitoh	21
Neuromorphic Computing Architecture Using Superconducting Nanowire Single Photon Detectors and Phase Change Memory Materials	22
Orkun Hasekioglu, Atilla Hasekioglu, Adil Öztürk	22
Half-Plenary Session	23
Lifshitz transition in LSCO: the exception that confirms the rule	24
Neven Barišić	24
Spin-orbit torques with two dimensional materials	25
Sergio Valenzuela	25
Coherent Quantum Control of Molecular Spin Qubits	26
K. Kundu, M.V.H. Subramanya, J. Marbey, J. Hrubý, E. Coronado, A. Gaita-Ariño, Y. Duan, J. White, W. Evans, D. Ngo, J.R. Long, P.W. Smith, S. Minasian, J. Chen, S. Hoffman, X. Zhang, H.-P. Cheng, Stephen Hill	26
Artificial Superconducting Platforms for Quantum Technologies	27
A. Braggio	27
Spintronics with Ferrimagnetic and Antiferromagnetic Insulators	28
Andrew D. Kent	28
Advances in Application of Process Informatics for Iron-Based Superconductors	29
A. Yamamoto, S. Tokuta, A. Ishii, Y. Shimada, S. Hata, K. Iida, A. Yamanaka	29
Dynamics of topological spin textures	30
M. Garst	30
Surface Superconductivity and topology in the Weyl semi metal PtBi2	31
Prof. Dr. Bernd Büchner	31
Mutual synchronization of spin Hall nano-oscillators for Ising machines and neuromorphic computing.	32
J. Åkerman	32

Orbital current generation and long distant diffusive propagation	33
YoshiChika Otani, Weiguang Gao, Junyeon Kim	33
HTS Cuprates: Advances in Fundamentals and Experimental Studies I	34
Small Pockets and the Origin of the Low Superfluid Density in the Underdoped Cuprates	35
N. Harrison, M. K. Chan	35
Charge order near the antiferromagnetic quantum critical point in a trilayer high Tc cuprate.	36
V. Oliviero, I. Gilmutdinov, D. Vignolles, S. Benhabib, N. Bruyant, A. Forget, D. Colson, W.A. Atkinson , C. Proust	36
Resilience of the AFM Mott insulating state of La2CuO4 against photodoping	37
J. Demsar	37
HTS Cuprates: Advances in Fundamentals and Experimental Studies II	38
Visualizing the Cuprate Pair Density Wave States and Periodic Lattice Displacements	39
Kazuhiro Fujita	39
Vortex Mass Determination in YBaCuO Using THz Circularly Polarized Light	40
M. Šindler, R. Tesař, C. Kadlec, J. Koláček, P. Lipavský, Wen-Yen Tzeng, Chih-Wei Luo-, Jiunn-Yuan Lin	40
Multi-band superconductivity, polarons and the steep band/flat band scenario	41
Annette Bussmann-Holder	41
Topological Quantum Matter I	42
Non-Hermitian Topological Phases of Quantum Matter	43
W.B. Rui, Z.D. Wang	43
Interplay of Topology and Geometry in Fractional Quantum Hall Liquids	44
Kun Yang	44
Quantum transport and fractional hall effect in Moiré correlated/anticorrelated interface channels	45
Farzaneh Shayeganfar, Ali Ramazani	45
Temperature-Dependent XRD and NEXAFS on Ta2Ni(Se,S)5 and Ta2(Ni,Co) Se5	46
Nour Maraytta, Peter Nagel, Fatemeh Ghorbani, Santanu Pakhira, Amir Ghiami, Matthieu Le Tacon, Stefan Schuppler, Amir-Abbas Haghighirad, Michael Merz	46
Topological Quantum Matter II	47
Effect of Nanopatterning on films in the vicinity of superconductor-insulator transition	48

A. Yu. Mironov, D.A. Nasimov, V.M. Vinokur 48

Electride Properties Inducing a Flat Band in the Sc Phase of Magnesium under High Pressure. 49

Sabri Elatresh 49

New Physics of Old Graphite 50

A. Mishchenko 50

Study if the order parameter of a superconductor modified by adatoms and molecules 51

Nicolás Lorente 51

Quantum Spin and Magnetism in Chiral Materials: CISS Effect, Solitons and Skyrmions I 52

Thermally Induced Dynamics of Magnetic Skyrmions and Their Device Functions 53

Masahito Mochizuki, Xichao Zhang, Jun Matsuki 53

Spin-wave propagation through a tunable-width nanoconstriction 54

E. Fourneau, C. Delforge, N. Lejeune, A.V. Silhanek 54

Chiral-induced Unidirectional Spin-to-charge Conversion 55

A. Moharana, Y. Kapon, F. Kammerbauer, D. Anthofer, S. Yochelis, Y. Paltiel, A. Wittmann 55

Quantum Spin and Magnetism in Chiral Materials: CISS Effect, Solitons and Skyrmions II 56

Truly chiral phonon and phonon angular momentum 57

Jun-ichiro Kishine, Takuya Satoh, Yoshihiko Togawa, Hiroaki Kusunose 57

Spin Relaxation, Diffusion and Edelstein Effect in Chiral Metal Surface 58

Yuta. Suzuki, Yusuke Kato 58

Inducing a Tunable Skyrmion-Antiskyrmion System through Ion Beam Modification of FeGe Films 59

M.B. Venuti, Xiyue S. Zhang, Eric J Lang, Sadhvikas J. Addamane, Hanjong Paik-, Portia Allen, Peter Sharma, David Muller, Khalid Hattar, Tzu-Ming Lu , Serena Eley 59

Enhancement of Intrinsic Spin Hall Effect in Chiral Topological Semimetals 60

Wei Jiang 60

Superconducting, Magnetic, Topological Arsenides and Tellurides 61

Anomalous metallic oxygen band in the potential superconductor KCa2Fe4As4O2 62

N.S. Pavlov, K.S. Pervakov, I.A. Nekrasov 62

Phase separation in single crystals of AFM semimetal EuSn2As2 63

Alena Yu. Degtyarenko, Alexander L. Vasiliev, Nikita Pavlov, Alexey V. Ovcharov, Vladimir I. Bondarenko, Andrey V. Sadakov, Kirill S. Pervakov, Vladimir M. Pudalov 63

Superconducting Gap Structure of Slightly Overdoped NaFe0.955Co0.045As Pnictides: Joint SnS-Andreev Spectroscopy and Specific Heat Study 64

S.A. Kuzmichev, A.V. Muratov, S.Yu. Gavrilkin, I.V. Morozov, A.I. Shilov, Ye.O. Rakhmanov, T.E. Kuzmicheva 64

Iron Based Superconductors (IBS): Fundamental and Applied Research under Ambient and Applied Pressures I 65

New superconductors - ternary bismuthides BaTM1.8Bi2 (TM = Au, Ag): synthesis, crystal structure and properties 66

A.I. Shilov, A.V. Sadakov, A.S. Usoltsev, A.Yu. Degtyarenko, E.O. Rakhmanov, I.V. Morozov, K.A. Lyssenko, A.N. Kuznetsov, A.V. Shevelkov 66

Research on the Anisotropy of Upper Critical Field in Iron-Based and Nickel-Based Superconductors 67

Zhixiang Shi, Yongqiang Pan, Wei Wei 67

Temperature Dependence of the Superconducting Order Parameter in Stoichiometric Alkali MetalBased Pnictide EuCsFe4As4 68

T.E. Kuzmicheva, S.A. Kuzmichev, A.Yu. Degtyarenko, K.S. Pervakov, V.A. Vlasenko 68

Sharp Peaks in Critical Current Density at Distinct Quantum Critical Points in FeSe(Te,S) Single Crystals 69

Wei Wei, Qiang Hou, Yue Sun, Zhixiang Shi 69

Superconducting Motors and Applications in Electrical Engineering I 70

Research and Development of Optimal Structure of Liquid Hydrogen Cooled High Temperature Superconducting Induction/Synchronous Motor using Self-organizing Design Method 71

T. Nakamura 71

Electromagnetic modeling of high temperature superconductors near ferromagnetic materials by using the volume integral method 72

Hocine Menana 72

Development Status of Liquid Hydrogen Cooled High-temperature Superconducting Power Generation Demonstrator 73

M. Ohya, S. Tonooka, Y. Terao, Y. Shirai, H. Kobayashi, K. Okai 73

Superconducting Motors and Applications in Electrical Engineering II 74

AC loss and stability in the REBCO stator of superconducting motors for hydrogen-electric airplanes 75

E. Pardo, A. Hussain, A. Dadhich, J. Kováč, L. Kopera 75

Numerical Study of Multi-Pole Generator with and without HTS Windings for Multi-MW Direct Drive Wind Turbines 76

Shuangrong You, Markus Mueller 76

Quantitative Analysis of AC Losses in HTS Coils Below 40K for Advanced Electric Aircraft Propulsion Systems	77
Ercan Ertekin, Calvin C. T. Chow, Alexandr Shchukin, Zhishu Qiu, Min Zhang	77
Molecular Spin Qubits toward Quantum Computer I	78
Molecular Spin Qubits Based on Molecular Magnets with S=1/2	79
Masahiro Yamashita	79
How to build quantum circuits based on electric currents and molecules	80
Nicolás Lorente	80
Fundamental Studies of F-Element Organometallics Leading to the Design of New Quantum Systems	81
P W. Smith, J. Hruby, W. Evans, S. Hill, S. G. Minasian	81
Molecular Spin Qubits toward Quantum Computer II	82
Spin and Orbital Ordering Effects in 2D-Superlattice Perovskite Films	83
Bin Hu	83
Molecular Spin Qubit in Spin Crossover Systems	84
S. Hayami	84
Magnetic Molecules Based on Transition Metal Ions as Spin Quantum Bits	85
T. Mallah, I. Tlemsani, S. Gambarella, A.-L. Barra, A. Ardavan, J. Liu.	85
Device Physics of Josephson Junctions and Their Fundamental Technologies I	86
Coherent tunneling of flux quanta in a long Josephson Junction	87
Alexey Ustinov	87
Dual-Rail Direct-Coupled Adiabatic Quantum Flux Parametron Logic for High-Density Circuit Integration	88
N. Yoshikawa, W. Komiya, Y. Hasegawa, C. Ayala	88
Gate-Controlled Resistive State of a NbTi Superconducting Wire.	89
K. Harrabi, A. Mekki, M.V. Miloševic	89
Device Physics of Josephson Junctions and Their Fundamental Technologies II	90
Higher-dimensional topology and fractional states of matter in superconducting systems	91
Wolfgang Belzig	91
Effects of Strong Capacitive Coupling Between Meta-Atoms in rf SQUID Metamaterials	92
Jingnan Cai, Steven M. Anlage	92
A Real-Time Testing Technique for High-Speed Streaming RSFQ Circuits	93

M. Eren Çelik, Timur V. Filippov, Dmitri E. Kirichenko, Mustapha Habib, Anubhav Sahu, Deepnarayan Gupta 93

Kagome Superconductivity I 94

Superconductivity and Charge Order in Kagome-Lattice Systems 95

Zurab Guguchia 95

Chiral phonons and phonon drumhead surface state in kagome CoSn-like compounds 96

A. Ptok 96

Tunable topological Dirac surface states and van Hove singularities in kagome metal GdV6Sn6 97

Ming Shi 97

Kagome Superconductivity II 98

Rotation Symmetry Breaking of Charge-density-wave State and Magnetic Topological State in Kagome Lattices 99

Zhicheng Jiang, Soohyun Cho, Dawei Shen 99

Robust charge order above room temperature in kagome superconductor LaRu3Si2 100

I. Plokhikh, Z. Guguchia 100

Unconventional superconductivity in the kagome superconductor AV3Sb5 101

Ben-Chuan Lin 101

Two-dimensional metal-organic kagome systems as candidates for the study of spin liquids or the quantum anomalous Hall effect 102

Adam Hassan Denawi, Roland Hayn, Mathieu Abel, Holger Vach 102

Effects of Topology in Superconductor Nanoarchitectures I 103

Eliashberg theory and topology of superconducting thin films 104

G.A. Ummarino, A. Zaccone 104

The unconventional normal state of twisted bilayer graphene 105

María José Calderón 105

Study of vortex dynamics in superconducting nanoarrays 106

A. Arroyo-Fructuoso, G. Hlawacek, R. Córdoba 106

Effects of Topology in Superconductor Nanoarchitectures II 107

Microscale Metasurfaces for On-chip Magnetic Flux Concentration 108

E. Fourneau, N. Lejeune, J.A. Arregi, M. Stano, A. Barrera, N. Bort-Soldevila , J. Cunill-Subiranas, Th. Pirottin, O. Morris, O. Leonard, B. Vanderheyden, N. Mestres, Ll. Balcells, N. Del-Valle, A. Sanchez, C. Navau, V. Uhlíř, S. Bending, A. Palau, A.V. Silhanek 108

Nonreciprocal spin waves in 3D screw-like ferromagnetic tubes prepared by atomic layer deposition 109

M. Xu, A. J.M. Deenen, H. Guo, D. Grundler 109

Integration of Magnons into Superconducting Quantum Circuits 110

D. García-Pons, J. Pérez-Bailón, F. Luis, D. Zueco, María José Martínez-Pérez 110

Effects of Topology in Superconductor Nanoarchitectures III 111

Supercurrent-enabled Andreev Reflection in a Chiral Quantum Hall Edge State 112

Andreas Bock Michelsen, Patrik Recher, Bernd Braunecker, Thomas L. Schmidt 112

Curved superconducting vortices in three-dimensional nanoarchitectures 113

Elina Zhakina, Luke Turnbull, Weijie Xu, Markus König, Paul Simon, Wilder Carrillo-Cabrera, Amalio Fernandez-Pacheco, Dieter Suess, Claas Abert, Vladimir M. Fomin, Claire Donnelly 113

The Challenges of Braiding with Majorana Zero Modes 114

E. Mascot, T. Hodge, D. Crawford, C. Peeters, J. Bedow, D. K. Morr, S. Rachel 114

Effects of Topology in Superconductor Nanoarchitectures IV 115

Topology-Driven Vortex Commensurability in YBCO Thin Films: Pinning Force of an Individual Vortex and Reentrant Zero Resistance 116

W. Lang, B. Aichner, M. Karrer, K. Wurster, C. Schmid, R. Hutt, C. Magén, L. Backmeister, 116

Heterostructures and hybrid systems based on high-temperature superconductors for energy-efficient Information and Communication Technologies 117

A. Palau, T. Günkel, J. Alcalà, A. Barrera, A. Fernández-Rodríguez, Marinkovic, E. Fourneau, A.V. Silhanek, J. Suñé, L.L. Balcells, N. Mestres 117

Advancements in Solving the 2D Fermi Hubbard Model at Finite Temperature: Insights from Tensor Network Methods 118

Aritra Sinha, Alexander Wietek, Marek M. Rams, Jacek Dziarmaga 118

Near-Field Microwave Microscope for Exploring Trapped Vortices in Superconductors 119

Chung-Yang Wang, Steven M. Anlage 119

Advances in Current-Induced Magnetization Control I 120

Probabilistic Computing with Magnetic p-bits: Optimization, Machine Learning and Quantum Simulation 121

Kerem Y. Çamsarı 121

Design and applications of MTJs in unconventional computing and multiphysics solutions 122

A. Grimaldi, E. Raimondo, F. Garescì, A. Giordano, M. Carpentieri, G. Finocchio 122

Electrical Switching of Magnetic Tunnel Junctions for future Electronics 123

Kewen Shi, Weisheng Zhao	123
Advances in Current-Induced Magnetization Control II	124
Theory of orbital generation, diffusion, and detection	125
Aurélien Manchon	125
Generation of orbital currents and torques for efficient manipulation of chiral spin textures for spintronics devices	126
S. Krishnia, G. Beneke, K. Raab, T. B. Winkler, M. A. Brems, P. Gerhards, K. Knobloch, N. Sebe, N. Reyren, A. Fert, H. Jaffrès, Vincent Cros, Johan Mentink, M. Kläui	126
Efficient spin-orbit torque generation in complex oxides	127
Tianxiang Nan	127
Advances in Current-Induced Magnetization Control III	128
Ultrathin metallic antiferromagnets spin current manipulation and thermal stability	129
Ozhan Ozatay	129
All-electrical angular momentum transport experiments in antiferromagnetic insulators and isolated ferromagnetic metals	130
M. Althammer	130
Coherent antiferromagnetic spintronics: new opportunities for controlling spin and electronic states of antiferromagnets	131
Jiahao Han, Shunsuke Fukami	131
Advances in Current-Induced Magnetization Control IV	132
Efficient spintronics with fully compensated ferrimagnets	133
Wanjun Jiang	133
Magnetoresistive detection of perpendicular switching in a magnetic insulator	134
Can Onur Avci	134
Spin Orbit Coupling Contribution to Anisotropic Magnetic Interaction	135
Xiangang Wan	135
Advances In Thin Films, Multi-Layers and Patterned Nanostructures I	136
Neutron Diffraction Studies of Helical Magnetic Order in Quasi-two-dimensional Layered Chiral PbMnTeO6 with Triangular Lattice	137
A.I. Kurbakov	137
Magnetic micro-, nano-structures for Sensing Magnetic Fields	138
A. Barrera, E. Fourneau, N. Bort-Soldevila, J. Cunill-Subiranas, V. Uhlir, S. Bending, C. Navau, A. Silhanek, Ll. Balcells, N. Mestres, A. Palau	138
On Spectral Weight and Plasmons in the Strange Metal Phase of Bi-2212 Bilayer System	139

Partha Goswami 139

Low Hysteresis, High Sensitivity, Fast Response and Recovery Time of Humidity Sensor 140

Muneeb ur Rahman 140

Advances In Thin Films, Multi-Layers and Patterned Nanostructures II 141

Wurtzite MnSe – Epitaxy and Optical Properties of an Altermagnetic Candidate 142

Michał J. Grzybowski, Carmine Autieri, Jaroslaw Domagala, Cezary Krasucki, Anna Kaleta, Sławomir Kret, Katarzyna Gas, Maciej Sawicki, Rafał Bożek, Jan Suffczyński, Wojciech Pacuski 142

Continuous Magnetic Transitions in Disordered LaSrCo1/2Fe1/2O4 Ruddlesden -Popper Oxide 143

D.I. Fazlizhanova, R.G. Batulin, I.V. Yatsyk, T.I. Chupakhina, Yu.A. Deeva, S.V. Levchenko 143

Quantum Transport in Branched Conducting Polymers 144

H. Matyakubov, D. Matrasulov, J. Yusupov 144

The effect of Si content on the physical properties of nanostructured (Ni75Fe25) 100-xSix alloy elaborated by mechanical alloying 145

A. Kaibi, A. Guittoum, M. Hemmous, D. Martínez-Blanco, P. Gorria, J.A. Blanco, M. Kechouane 145

Superconducting Thin Films and Interface Superconductivity I 146

Performance of Nb Thin Films with Laser Induced Surface Corrugation 147

A. Badía-Majós, N. Lejeune, E. Martínez, L. Porta-Velilla, J. Frechilla, E. Fourneau, L.A. Angurel, G.F. de la Fuente, S. Marinkovic, A.V. Silhanek 147

Tailored Magnetic Flux Channeling in Laser Patterned Nb Thin Films 148

N. Lejeune, E.Martínez , Luis Porta-Velilla, Javier Frechilla, Emile Fourneau, Luis A. Angurel, Germán F. de la Fuente, Antonio Badía-Majós, Alejandro V. Silhanek 148

Assessing the Meissner State of a Square Superconducting Thin Film by Numerical Simulations Utilizing the Fluxoid Quantization 149

Alexander Bodenseher, David Hofmann, Michael Eisterer 149

Possible Eliashberg-type superconductivity enhancement effects in a two-band superconductor MgB2 driven by narrow-band THz pulses 150

J. Demsar 150

Superconducting Thin Films and Interface Superconductivity II 151

BHO Nanocomposite GdBCO Superconducting Thin Films: Substrate Temperature, Deposition Rate and Oxygen Annealing as Means for Pushing the Critical Current Densities 152

R. Popov, J. Hänisch, B. Holzapfel 152

Modulating Superconducting Properties by FIB and Current-Induced Modifications in Nb Thin Films 153

M. Motta 153
Magnetic structure and dopant effect in quasi-one-dimensional Fe-base superconductor BaFe2Se3 154
W. Zheng, V. Balédent, P. Foury, P. Miao 154
In-plane magnetoconductivity studies in granular aluminium thin film at high reduced temperatures and magnetic fields 155
R. Pervin, U.C. Thuwal 155
Novel Quantum Magnetism in Low Dimensions I 156
The saga of BaCo2(AsO4)2 157
Pavel A. Maksimov 157
Quantum phases in ferro-antiferromagnets 158
A.L. Chernyshev 158
Possible quantum spin liquid and cluster Mott insulator phases in the Mo3O8 magnets 159
S. Streltsov 159
Novel Quantum Magnetism in Low Dimensions II 160
Condensation of bosonic pairs in quantum magnets 161
Frédéric Mila 161
Magnetizations Plateaus: Field-Induced Fragmentation of a Spin Lattice into Clusters 162
M.-H. Whangbo, H.-J. Koo, R.K. Kremer, A.N. Vasiliev 162
Magnetic frustration in octahedral networks: from antiperovskites to fcc antiferromagnets 163
M. E. Zhitomirsky, A. Gubina, T. Ziman 163
Novel Quantum Magnetism in Low Dimensions III 164
Covalent Two Dimensional Magnets and Heterostructures 165
C. Huai, M. Bian, R. Sabirianov, H. Zeng 165
Interplay Between Unusual Magnetic Anisotropy and Electronic Properties of the Near-Room-Temperature van der Waals Ferromagnet Fe4GeTe2 166
V. Kataev 166
Magnetic resonances involving integer magnons in a magnetism modulated two-dimensional electron gas 167
Lin Zhang, Yi Wang, Shu-Yu Zheng, Li Lu, Chi Zhang. 167
Novel Quantum Magnetism in Low Dimensions IV 168
Engineering of topological magnons and magnon-polarons in CrI3 ferromagnets 169
Alireza Qaiumzadeh 169

4d and 5d metals based magnets 170
O. Volkova 170
Microscopic scale of quantum phase transitions: from Heisenberg and Ising spin chains to cold gases and moiré superlattices 171
A. Rogachev 171
Strain-Driven Bidirectional Spin Orientation Control in Epitaxial High Entropy Oxide Films 172
Zhibo Zhao, Horst Hahn, Robert Kruk, Abhishek Sarkar 172
Device Physics of Josephson Junctions and Their Fundamental Technologies III 173
Circuit QED with Two PT-symmetric Non-Hermitian Qubits 174
Mikhail V. Fistul, Grigory A. Starkov, Ilya M. Eremin 174
The Josephson Balanced Comparator as a Sensor to Monitor On-chip Clock Sources for RSFQ/ERSFQ Circuits 175
Timur V. Filippov, Dmitri E. Kirichenko, Anubhav Sahu, M. Eren Çelik, Deepnarayan Gupta 175
Zero-field superconducting diode effect in a trigonal superconductor PbTaSe2 176
Y. Itahashi, Y. Iwasa 176
Device Physics of Josephson Junctions and Their Fundamental Technologies IV 177
Quantum precise bias supply and single flux quantum readout of superconducting nanowire single photon detectors 178
T. Ortlepp, S. Engert, C. Moeller and A. Reinhardt 178
YBCO resistors, nano-constriction Josephson junctions fabricated with a focused He-Ion beam 179
E. Goldobin, C. Schmid, M. Meichsner, D. Hanisch, M. Pröpper, C. Magen, M. Schilling, R. Kleiner, D. Koelle 179
Investigation of the Sputtering Conditions of Niobium and Magnetite Thin Films for Realizing Ferromagnetic Josephson Junctions 180
T. Alp, Y. Ozturk, E. Aygit, A. Rahimpour, O. Ozatay Y. Simsek 180
Device Physics of Josephson Junctions and Their Fundamental Technologies V 181
Magnetic fluctuations as a potential source of losses in superconducting quantum devices 182
Y. Krasnikova, A.A. Murthy, F. Crisa, M. Bal, Z. Sung, J. Lee, A. Cano, D.M.T. van Zanten, A. Romanenko, A. Grassellino, A. Suter, T. Prokscha, Z. Salman 182
Improving Characteristics of the Flux-Driven Josephson Traveling-Wave Parametric Amplifiers by Using Bi-SQUIDs Cells 183
A.N. Nikolaeva, V.K. Kornev, N.V. Kolotinskiy 183
Catastrophic magnetic flux avalanches in NbTiN superconducting resonators 184

L. Nulens, N. Lejeune, J. Caeyers, S. Marinkovi, I. Cools, H. Dausy, S. Basov, B. Raes, M.J. Van Bael, A. Geresdi, A.V. Silhanek, J. Van de Vondel 184

Hybrid Schroedinger-Ginzburg-Landau relaxation algorithm in description of uncoventional Josephson junction systems 185

K. Pomorski, L. Gomez, B. Stojewski, M. Kowalik, Ł. Stępień, P. Pęczkowski 185

Device Physics of Josephson Junctions and Their Fundamental Technologies VI 186

Cooper quartets designing in interacting superconducting systems 187

L. Chirolli, A. Braggio, F. Giazotto 187

Low Power Single Flux Quantum Qubit Control Circuits without High-Frequency Input 188

Jie Ren, Bicong Weng, Wei Peng 188

Identifying Dominant Magnetic Couplings in Large Superconducting Circuits 189

K. Jackman, C.J. Fourie 189

Molecular Spin Qubits toward Quantum Computer III 190

Electron Spin Resonance Measurement of a Single Molecule Magnet Terbium Phthalocyanine (TbPc2) Adsorbed on Surface Towards Quantum Computing 191

Tadahiro Komeda, Ryo Kawaguchi, Katsushi Hashimoto, Toshiyuki Kakudate, Keiichi Katoh, Masahiro Yamashita 191

Two-qubit [Dy2] molecules deposited into micro-SQUID susceptometers: in-situ characterization of their magnetic integrity 192

Ana Repollés, María Carmen Pallarés, David Aguilà, Olivier Roubeau, Verónica Velasco, Diego Gella, Leoní A. Barrios, María José Martínez-Pérez, Javier Sesé, Dietmar Drung, Thomas Schurig, Boris Le Guennic, Anabel Lostao, Guillem Aromí, Fernando Luis 192

EPR spectroscopy and spin coherence in rare-earth dimers with single-electron metal-metal bonds 193

A.A. Popov 193

Molecular Spin Qubits toward Quantum Computer IV 194

Probing Quantum Coherence in Single-Atom and Molecular Qubits Using the ESR-STM Technique 195

Christoph Wolf 195

Probing spin coupling within single molecular magnets 196

Ying-Shuang Fu 196

STM Study on Superconductors and Architecting Molecular Magnets on Surfaces 197

T. K. Yamada 197

Molecular Spin Qubits toward Quantum Computer V 198

Controlling Environmental Sensitivity in 59Co Nuclear Spin Qubits 199

O. Ungor, T. Ozvat, S. Sanchez, A. Rappé, N. Schaffner J. Zadrozny 199
Quantum Sensing of Magnetic Fields with Molecular Spins 200
M. Affronte, C. Bonizzoni, A. Ghirri 200
Integration of Molecular Quantum Bits 201
L. Tesi, F. Stemmler, D. Schäfter, M. Kern, N. Crivillers, S. Ludwigs, J. van Slageren 201
Molecular Spin Qubits toward Quantum Computer VI 202
Probing Diverse Behavior in Atomically Engineered Molecular Devices on Surfaces 203
Deung-Jang Choi 203
Charge Transfer in Adducts of Lanthanide 3,5-dinitrobenzoates with Aminobenzene Derivatives 204
P.S. Koroteev, A.B. Ilyukhin, N.N. Breslavskaya, E.N. Timokhina, E.A. Ugolkova, V.V. Minin, N.N. Efimov 204
Increasing Quantum Coherence in Molecular Spin Qubits by Fullerene Encapsulation in MOFs 205
D. Žilić, M. Kveder, L. Vujević, K. Užarević, B. Karadeniz, N. Cindro, A. Krajnc, G. Mali, M. Mazaj, A.A. Popov, S.M. Avdoshenko 205
Superconductivity and Magnetism in Heavy Fermion Systems I 206
Local Magnetism in UTe2 above the Critical Pressure 207
Riku Yamamoto 207
Multi-phase Superconductivity in the Locally Non-Centrosymmetric CeRh2As2 208
K. Semeniuk*, M. Pfeiffer,, J. Landaeta,, R. Borth, M. Nicklas, C. Geibel, M. Brando, S. Khim, E. Hassinger, 208
Low-Field Bardeen-Cooper-Schrieffer state in CeRh2As2 from Local Magnetization 209
J. Juraszek, G. Chajewski, M. Konczykowski, D. Kaczorowski, D.F. Agterberg, T. Cichorek 209
Superconductivity and Magnetism in Heavy Fermion Systems II 210
The Fermi surface of UTe2 211
A.G. Eaton 211
Probing the unusual superconductivity of UTe2 with high pressure 212
D. Braithwaite 212
The Microwave Electrodynamics of UTe2 213
Arthur Carlton-Jones, Yun-Suk Eo, Ian Hayes, Shanta Saha, Nicholas P. Butch, Johnpierre Paglione, Steven M. Anlage 213
Superconductivity-induced improper orders in nonsymmorphic systems 214
Andras Szabo, Aline Ramires 214

Superconductivity and Magnetism in Heavy Fermion Systems III	215
Correlation-Driven Topological Semimetals	216
Diego A. Zocco	216
Coexistence of Superconductivity and Ferromagnetism in High-entropy Carbides	217
Huchen Shu, Wei Zhong, Fang Hong, Binbin Yue	217
Novel Phases in Strongly Correlated Electron Systems	218
Fate of density waves in the presence of a higher-order van Hove singularity	219
D.V. Efremov, A. Zervou, J. Betouras	219
Resolving Length Scale Dependent Transient Disorder Through an Ultrafast Transition	220
Emil Bozin	220
Electronic Band Structure, Peculiarities in the Charge Density Distribution, Magnetic and Magnetoelectric Properties of La2CuO4	221
V.G. Orlov, G.S. Sergeev	221
Quantum phenomena in Si:Sb near the metal-insulator transition	222
S.L. Prischepa, A.L. Danilyuk, A.G. Trafimenko, A.A. Nazarenka	222
Advanced REBCO-Based Coated Conductors for Large-Scale HTS Applications I	223
Requirements of REBCO Coated Conductors for use in compact fusion magnets	224
Ashleigh Francis, J.L. Cheng, Brandon Sorbom	224
Progress in reducing the cost of 2G HTS tape manufactured in large volume	225
A. Molodyk, S. Lee. V. Petrykin. S. Samoilenkov	225
Recent Effort and Discussion at Shanghai Superconductor Technology for HTS Fusion Application	226
Y. Yamada, J-M Zhu , B. Song	226
Advanced REBCO-Based Coated Conductors for Large-Scale HTS Applications II	227
Homogeneous and Productive BMO-Doped REBCO Coated Conductor Developed by Hot-Wall PLD on IBAD Templated Substrate	228
Y. Iijima, M. Ohsugi, K. Kakimoto, S. Muto, S. Fujita, W. Hirata, N. Nakamura, M. Daibo	228
Development and scale up of high-performance REBCO tapes and round wires	229
Venkat Selvamanickam	229
Coated Conductor Production at SuNAM via PLD and Reactive Co-evaporation for Large Scale Applications	230
Hunju Lee	230
Advanced REBCO-Based Coated Conductors for Large-Scale HTS Applications III	231
AMSC's 2G HTS Wire manufacturing	232

D. McGahn 232
ARPA-E Investment in Manufacturing of High Temperature Superconducting Tapes 233
Laurent Pilon 233
Noncontact High Throughput Measurements of Current-Voltage Characteristics of REBCO High Temperature Superconducting Tapes Over Wide Range of Electric Fields and Current Densities 234
Takanobu Kiss, , Z. Wu, K. Higashikawa 234
Theory of Superconductivity I 235
Polarons with a quadratic interaction: analytic and numerical methods 236
S. N. Klimin, M. Houtput, J. Tempere 236
Impact of an Extended d-Wave Gap on Superconductivity: Analysis of the Critical Current Density and Upper Critical Field in Cuprate Systems 237
O.K. Ganiev, B. Yavidov, Z. Rakhmonov 237
Investigation of the Phase Change During Solid Phase Synthesis of Bi1.7Pb0.3Sr2Can-1CunOy Bismuth-Based Cuprates 238
D.R. Djurayev, A.A. Turayev, O.G. Turayev 238
Topological Quantum Matter : New Frontiers 239
M. Zahid Hasan 239
Topological and Unconventional Superconductivity in Low-Dimensional Magnet-Superconductor Hybrid Systems 240
Emergent topology in a magnet-superconductor hybrid system driven by a 2D antiferromagnetic spin texture 241
R. Lo Conte, M. Bazarnik, E. Mascot, K. Palotás, L. Rózsa, L. Szunyogh, A. Kubetzka, D.K. Morr, K. von Bergmann, R. Wiesendanger 241
Controlling Majorana modes in magnetic adatom chains 242
Oladunjoye A. Awoga, Ioannis Ioannidis, Archana Mishra, Martin Leijnse, Mircea Trif, Thore Posske 242
Influence of the Spin Configuration on the Band Structure of Yu-Shiba-Rusinov States 243
L. Rózsa 243
Topological and Unconventional Superconductivity in Low-Dimensional Magnet-Superconductor Hybrid Systems II 244
Topological Superconductivity, Majorana Zero Modes and Quantum Algorithms in Magnet-Superconductor Hybrid Systems 245
Dirk K. Morr 245
Topological superconductivity in Fibonacci quasicrystals 246
A. Kobiałka, O.A. Awoga, T. Domański, P. Holmvall, A.M. Black-Schaffer 246

Understanding of role of disorder in epitaxial superconductor-semiconductor qubits	247
Javad Shabani	247
Unconventional Superconductivity, and Tunable Quantum States	248
Multiple-Q pair density wave in proximity to a nested Fermi surface	249
Yi Zhou	249
Weyl Fermion Excitations in the CuTlSe2 Semimetal	250
T. Shiroka, D. Tay, Q. X. Dong, Z. Okvátovity, G.F. Chen, C. N. Wang	250
Itinerant diamagnetic spin-triplet superconductivity in Fe-based high entropy alloy NbTaTiZrFe	251
Jin Hee Kim, Rahmatul Hidayati, Jong-Soo Rhyee	251
Effects of Topology in Superconductor Nanoarchitectures V	252
Anomalous symmetry properties and gap structures in the Kagome superconductor CsV3Sb5	253
K. Fukushima, K. Obata, S. Yamane, Y. Hu, Y. Li, Y. Yao, Z. Wang, Y. Maeno, S. Yonezawa	253
Non-Invasive Readout of Superconducting Nanostructures	254
L. Nulens, D.A.D. Chaves, O.J.Y. Harb, J.E. Scheerder, N. Lejeune, K. Brahim, B. Raes, A.V. Silhanek, M.J. Van Bael, J. Van de Vondel	254
Quantum detector tomography for two-dimensional superconducting nano-detectors	255
A.D. Semenov, M. Sidorova, S. Cherednichenko, H.-W. Hübers	255
Advances in Current-Induced Magnetization Control V	256
Exploring magnon-magnon coupling, spin Hall magnetoresistance, and laser-driven spin textures in 2D van der Waals magnets	257
C.W.F. Freeman, M. Dabrowski, P.S. Keatley, Z. Xue, A.K. Budniak, G. Eda, O. Kazakova, R.J. Hicken, H. Kurebayashi, M. Cubukcu	257
Optimizing Bi2Te3 Thin Film Growth for Spintronic Applications	258
Aykut Can Önel, Ebrahim Zahrabi, Roya Kavkhani, Ahmad El Zatari, Arooba Maryyam, Rawana Yagan, Kerem Anar, Ferhat Katmış, Mehmet Cengiz Onbaşlı	258
Stabilization and External Fields Control of Skyrmions in Synthetic Antiferromagnetic Multilayers	259
Rawana Yagan, Arash Mousavi Cheghabouri, Mehmet C. Onbasli	259
Advances in Current-Induced Magnetization Control VI	260
Scalable Low Power Skyrmion Logic Gates and Circuits	261
A. Mousavi Cheghabouri, R. Yagan, Mehmet C. Onbasli	261
Surface Acoustic Wave Manipulation of Magnetic Domain Walls and Skyrmions	262

J. Shuai, R.G. Hunt, L. Lopez-Diaz, J.E. Cunningham, T.A. Moore 262
Artificial intelligence for magnetic materials design 263
T. Schrefl, Clemens Wager, A. Kovacs, J. Fischbacher, D. Böhm, S. Stanciu , Q. Ali, H. Moustafa, F. Lasthofer, H. Oezelt, M. Gusenbauer 263
Quantum Spin and Magnetism in Chiral Materials: CISS Effect, Solitons and Skyrmions III 264
Stabilizing skyrmion crystal in centrosymmetric magnets 265
Shizeng Lin 265
Resonant elastic small-angle soft x-ray scattering unveils anisotropic interactions in chiral magnets 266
V. Ukleev 266
On the stability boundaries of the skyrmion phase in non-centrosymmetric ferromagnets with the Dzyaloshinskii-Moriya interaction 267
S.V. Grigoriev, V.E. Timofeev, D.N. Aristov 267
Quantum Spin and Magnetism in Chiral Materials: CISS Effect, Solitons and Skyrmions IV 268
Systematic Study of Chiral Magnetism in Rare Earth Intermetallic Compounds Based on YbNi3Al9 269
S. Ohara, S. Nakamura, K. Kurauchi, M. Tsukagoshi, T. Matsumura 269
Experimental Demonstration of Molecular Chirality-Dependent Pseudo-Jahn-Teller States 270
M. Eginligil 270
Generalized Heisenberg Ferromagnet Equation with Scalar Potential 271
Zh. Beisekeyeva, K. Beisekeyev 271
Quantum cavities based on magnonic textures 272
D. García-Pons, C.A. González, J. Pérez-Bailón, F. Luis, D. Zueco, María José Martínez-Pérez 272
Large Scale Applications of Superconductors and Their Fundamental Technologies I 273
Hadrontherapy: exploring new challenges against cancer 274
S. Rossi 274
Compact Particle Therapy with Superconducting Technologies 275
A. Godeke, A. Harmant, M. Schillo 275
Recent trends in Protontherapy 276
E. Forton, V. Nuttens 276
Large Scale Applications of Superconductors and Their Fundamental Technologies II 277
Development of a novel high temperature superconducting cable with high current density and low AC losses 278

Charlie Sanabria, Alexey Radovinsky, Christopher Craighill, Kiran Uppalapati, Alex Warner, Julio Colque, Elle Allen, Sam Heller, David Chavarria, Kristen Metcalfe, Amanda Hubbard, Amy Watterson, Sarah Chamberlain, Rui Diaz-Pacheco, Benjamin Weinreb, Elizabeth Brownell, Justin Nealey, Annie Hughes, Eric Laamanen, Keshav Vasudeva, Colin McCormack, Erica Salazar Owen Duke, Matt Hicks, Jeremy Adams, Dylan Kolb-Bond, Timothy Liu, Kara Malhotra, Ashleigh Francis, JL Cheng, Maise Shepard, Aliya Greenberg, Vinny Fry, Nick Kostifakis, Carl Avola, Paul Ljubicic, Lex Palmer, Ronak Padukone, Sergey Kuznetsov, Kai Donez, Theodore Golfinopoulos, Phillip Michael, Rui Vieira, Nicolai Martovetsky, Rodney Badcock, Mike Davies, Arvid Hunze, Bart Ludbrook, Ramesh Gupta, Piyush Joshi, Shresht Joshi, Anis Ben Yahia, Hugues Bajas, Markus Jenni, Christoph Mueller, Manuel Holenstein, Kamil Sedlak Dash Weeks, Ross Rentz, Jake Benzing, Sera Evcimen, Brandon Sorbom, Daniel Brunner	278
HTS Wires, Cables, and Coils with High Je and Very Low AC Losses	279
A. Otto, L. Saraco, A. Bouthillette, B. Bouchard, A. Croteau, A. Dimino, J. Voccio	279
Significant Improvement of Electromechanical Robustness of REBCO Coated Conductors by Face-to-Face Double Stacked Architecture	280
Takanobu Kiss, Z. Wu, S. Sera, Y. Oda, R. Nagayama, K. Ibusuki, K. Imamura, M. Nakamura, K. Higashikawa	280
Large Scale Applications of Superconductors and Their Fundamental Technologies III	281
Stability and quench of HTS magnets at low temperatures the point of view	282
Vitaly S. Vysotsky	282
High Field HTS Cryogen-free Superconducting Magnets - Developments and Long Term Operation -	283
S. Awaji, A. Badel, A. Zampa, K. Takahashi, T. Okada, Y. Tsuchiya	283
The world's longest HTS DC cable line in the power system of St. Petersburg, testing results and installation	284
Andrey Kashcheev, Victor Sytnikov, Mikhail Dubinin	284
Large Scale Applications of Superconductors and Their Fundamental Technologies IV	285
Superconducting and Cryogenic Technologies for Zero-Emission Large Electric Transport Platforms at Florida State University	286
Sastry V. Pamidi	286
Neutron Radiation Challenges for HTS Fusion Magnets	287
R. Unterrainer, A. Bodenseher, M. Eisterer	287
Simulation of Magnetic Flux Trapping in Seeded YBCO for EDS Maglev Systems	288
U. Kemal Ozturk, Murat Abdioglu Ali Suat Yıldız	288
Novel Functional Magnetic Materials- Basic Approach and Applications I	289

Giant Magnetostrain and Magnetoelectric Effects in Particulate Ni-Mn-Ga/Polymer Composites	290
Volodymyr Chernenko-, Victor L'vov, Senentxu Lanceros-Mendez, Hideki Hosoda	290
Magnetically Bistable Microwires for Miniaturized Contactless Sensors.	291
R. Varga	291
Thermoelectric Properties of X2(Cs,Rb)(Bi,Sb) (X = Li, K, Na, Rb) Heusler Alloys	292
V. Buchelnikov, V. Sokolovskiy, D. Baigutlin	292
Novel Functional Magnetic Materials- Basic Approach and Applications II	293
Magnetic, optical and photothermic properties of composite ferromagnetic core-plasmonic shell nanostructures for bio-medical applications	294
L.V. Panina, V.K. Belyaev, A. Anikin, A. Gurevich, V.V. Rodionova	294
Magnetic steel health monitoring in the nano-scale	295
Angeliki Mpaliou, Tatiana Damatopoulou, Evangelos Hristoforou	295
X-ray magnetic circular dichroism in study functional magnetic materials	296
A. Rogalev, F. Wilhelm	296
Novel Functional Magnetic Materials- Basic Approach and Applications III	297
Multifunctional properties, energy storage efficiency and magnetoelectric coupling: A case study of novel (1-x)BaTiO3-xBiFe0.95Mn0.05O3 nanocomposites	298
Shahid Husain, Mehroosh Fatema	298
Development of graded magnetic anisotropy in amorphous microwires	299
A. Zhukov, P Corte-Leon , M. Ipatov, J.M. Blanco, V. Zhukova	299
Infrared study of carriers dynamics in Diluted Magnetic Semiconductor (Ba$_{1-x}$K$_{x}$)(Zn$_{1-y}$Mn$_{y}$)$_{2}$As$_{2}$	300
Z.Y. Liao, X.G. Qiu	300
Effect of atomic arrangement in the A2 crystal structure on the magnetostriction constant of Fe90.625Z9.375 (Z = Ga, Ge) alloys	301
M. Matyunina, M. Zagrebin, V. Sokolovskiy, V. Buchelnikov	301
Novel Functional Magnetic Materials- Basic Approach and Applications IV	302
Exploring the magneto-volume anomalies and the magnetic properties of R2Fe17 intermetallic alloys using large scale facilities	303
Pedro Gorria, Pablo Alvarez-Alonso, José L. Sánchez Llamazares, Jesús A. Blanco	303
Semiconductor nanoparticles for analytical chemistry	304
O.A. Goryacheva	304
Circular magnetization in Co-based amorphous wires	305

M.A. Nemirovich, N.A. Yudanov, E.I. Nefedova, Vlada V. Miroshkina, L.V. Panina	305
Theory of Superconductivity II	306
Decoding the major 122, 11,111-type iron-based superconductors: successful simulation of phase diagrams and transition temperatures	307
Chi Ho Wong, Rolf Lortz	307
Quantifying proximity-induced superconductivity from first principle	308
Zheng Liu	308
2π Domain Walls for Tunable Majorana Devices	309
D. Hauck, S. Rex, M. Garst	309
Ginzburg-Landau approximation for the Hubbard model in the external magnetic field	310
S.N. Burmistrov, L.B. Dubovskii	310
Theory of Magnetism I	311
Flat Band in Pyrochlore Oxides: A Possible Playground of Magnetism and Superconductivity	312
I. Hase	312
Interface-Driven Modulation on 2D Magnetic Heterostructures	313
R. Caglayan, A. Mogulkoc, Y. Mogulkoc	313
The effect of structural disorder on magnetic properties of Fe-Z (Z = Ga, Ge, Al) alloys: Insights from ab initio and Monte Carlo	314
M.V. Matyunina, Yu.S. Tarasova, M.A. Zagrebin, V.V. Sokolovskiy, V.D. Buchelnikov	314
New Phenomena and Applications in Molecular Magnets	315
Switchable molecular magnets: from film deposition to composite material	316
M. Fitta, A. Pacanowska, M. Jasiurkowska – Delaporte, G. Wota, B. Nowicka	316
Circuit QED with molecular spin qudits	317
Fernando Luis	317
Transforming brittle stimuli-responsive crystalline structures into temperature and pressure-sensing composites	318
A. Pacanowska, G. Wota, M. Jasiurkowska – Delaporte, B. Nowicka, M. Fitta	318
Rotational Symmetry Breaking of Nuclear Motion in the Jahn-Teller X3 Molecule Due to Casimir-Polder Interaction	319
A.D. Lyakhov, A.S. Ovchinnikov, I.G. Bostrem, J. Kishine	319
HTS Cuprates: Advances in Fundamentals and Experimental Studies III	320

T-linear electrical resistivity of high-Tc cuprates due to scattering of fermions by the Q-balls	321
S.I. Mukhin	321
New quantum criticality for the strange metal and Planckian behaviour in high temperature superconductors	322
C. Di Castro	322
Spin and charge correlation functions in hole-doped cuprates in the cluster perturbation theory	323
S.G.Ovchinnikov, V.I.Kuzmin, S.V.Nikolaev, M.M. Korshunov	323
HTS Cuprates: Advances in Fundamentals and Experimental Studies IV	324
Cuprate universal electronic spin response and the pseudogap from NMR	325
D. Bandur, J. Nachtigal, A. Lee, S. Tsankov, J. Haase	325
Cuprates, Pnictides, and Sulfosalts: Lessons in Functional Materials	326
D.K. Sunko	326
On the Tc of (La, Sr)2CuO4 - based Superconducting Superlattices	327
S.M. Otajonov, D.E. Uskenbaev, T. Saparbaev, B.Ya. Yavidov	327
HTS Cuprates: Advances in Fundamentals and Experimental Studies V	328
Revealing Collective Electronic Ordering in Space and Time	329
W. Hu	329
Elementary excitations of cuprate probed with high-resolution RIXS	330
Di-Jing Huang	330
Electromigration-driven weak resistance switching in high-temperature superconducting devices	331
Stefan Marinković, Daniel Stoffels, Simon Collienne, Emile Fourneau, Alejandro Fernández-Rodríguez, Narcís Mestres, Anna Palau, Alejandro V. Silhanek	331
Angular dependences of magnetization and critical current of second-generation HTSC tapes	332
D.S. Chikurov, A.E. Rudominskiy, M.P. Volkov	332
HTS Cuprates: Advances in Fundamentals and Experimental Studies VI	333
Universal low-temperature fluctuation of unconventional superconductors revealed: ‘Smoking gun’ leaves proper bosonic superfluidity the last theory standing	334
Anthony Hegg, Ruoshi Jiang, Jie Wang, Jinning Hou, Yucel Yildirim, Wei Ku	334
Thermodynamics and kinetics aspects of YBCO nucleation at perovskite substrates	335
M. De Angelis, M. Tomellini, V. Pinto, A. Augieri, A. Masi, A. Rufoloni, F. Rizzo, A. Angrisani Armenio, G. Campi, L. Barba, G. Celentano	335

Emergence of a Marginal FL* fractionalized Fermi liquid in underdoped Cuprates	336
P.A. Marchetti	336
Field-Induced Reversible Tuning of Oxygen Doping in High-Temperature Superconductors	337
A. Fernández-Rodriguez, J. Alcalà, T. Günkel, A. Barrera, S. Marinković, A.V. Silhanek, J. Gazquez, N. Mestres, A. Palau	337
Superconductors Under Extreme Conditions of Pressure and Strain I	338
Degenerated superconductivity and fluctuation induced phases in multiband systems: Sr2RuO4 and Ba1-xKxFe2As2	339
Hans-Henning Klauss	339
High-pressure effects on the layered scandium borocarbide superconductor	340
G. Lamura, T. Shiroka, R. Khasanov, H. Ninomiya, K. Kawashima, H. Ogino	340
Strain Tuning of Quantum Materials: Superconductivity and Magnetism	341
Elena Gati	341
Superconductors Under Extreme Conditions of Pressure and Strain II	342
µSR measurements of Sr2RuO4 under uniaxial strain	343
Vadim Grinenko	343
Do magnetism and superconductivity compete in La_2Ni_O_{7-\delta}? A muon-spin rotation/relaxation under pressure study	344
Rustem Khasanov, Dariusz Gawryluk, Zurab Guguchia	344
Structure and Superconductivity of Se at Megabar Pressure of Hydrogen	345
Zhongyan Wu, Jaeyong Kim	345
Superconductors Under Extreme Conditions of Pressure and Strain III	346
Effects of Uniaxial Strain on the Electronic Structure of 2H-NbSe2	347
T. Valla, A.K. Kundu, I.I. Klimovskikh, H. Berger	347
Extended saddle van Hove singularities in the H3S superconductor explained	348
R. Akashi	348
Superconductivity in metal sulfides under high pressure	349
Fang HONG	349
Superconductors Under Extreme Conditions of Pressure and Strain IV	350
Is quantum criticality always avoided? The case of a tricritical point	351
R.R. Ullah, J.S. Harvey, Y. Wu, H.B. Cao, J.R. Badger, P. Klavins, V. Taufour	351
Magnetic and Superconducting Properties of Iron Polyhydrides Synthesized at High Pressures	352

I. Lyubutin, A. Gavriliuk, V. Struzhkin, D. Trunov, S. Aksenov, A. Mironovich, M. Lyubutina, I. Troyan	352
Two distinct charge density wave orders and emergent superconductivity in pressurized CuTe	353
Zhaorong Yang	353
Room Temperature Superconductor May Exist for A Long Time	354
D. Zhao	354
Iron Based Superconductors (IBS): Fundamental and Applied Research under Ambient and Applied Pressures II	355
Anomalies in the DC magnetization and AC susceptibility of EuRbAs4Fe4 due to the interplay between vortex matter and Eu spins	356
A.M. Ionescu, I. Ivan, C.F. Miclea, A. Galluzzi, M. Polichetti, A. Crisan	356
Disorder in FeSe1-xSx (0 ≤ x ≤ 1) superconducting crystals	357
Cedomir Petrovic	357
Enhancement of transition temperature and critical current density of iron-based superconductors by high-pressure growth	358
Shiv J. Singh	358
Iron Based Superconductors (IBS): Fundamental and Applied Research under Ambient and Applied Pressures III	359
Single crystal growth of iron-based superconductors with complex layered structures	360
Hiraku Ogino, Yudai Yatsu, Shigeyuki Ishida, Naomichi Sakai, Rayko Simura	360
Electronic Origin of Superconductivity in Iron Chalcogenide	361
Shankar Kunwar	361
Temporal evolution of topological domain-wall defects in ferromagnetic superconductors	362
S. Köstler, A. Vagov, T.T. Saraiva, A. Yu. Aladyshkin, D.Y. Roditchev, A.A. Shanenko, V.S. Stolyarov	362
Multicomponent superconductivity and four-fermion phase in the Ba1-xKxFe2As2 system	363
Vadim Grinenko	363
Quantum Information Technology and Applications I	364
Hybrid Quantum Systems for Quantum and Nano Devices	365
Hee Chul Park	365
Detecting the symmetry breaking of the quantum vacuum in a QED system	366
Tiefu Li	366

Utilization of the Zeeman faraday effect in atomic vapor cells for laser intensity stabilization	367
Mohammad Karami, Zahra Gholami Ahangaran, Zahra Heydarinasab, Maryam Hatefi, Farrokh Sarreshtedari	367
Advancements in Quantum Technologies: Integration into Quantum Metrology and Sensing	368
A. Gokce Ozbay, L. Nur Akay, E. Sınır	368
Quantum Information Technology and Applications II	369
Superconducting Cavity Optomechanical Systems Toward Quantum Sensing	370
Junho Suh	370
Magnonic qubit based on Bose condensate	371
Yu. M. Bunkov	371
Spectral properties of branched nanoscale lattices	372
M. Akramov, C. Trunk, J. Yusupov, D. Matrasulov	372
Revitalizing the Integration of Material Characterization Techniques into Quantum Sensing, Metrology, and Quantum-Enhanced Imaging	373
L. Nur Akay, O. Bozat, E. Sınır, B. Aydogan, A. Gokce Ozbay	373
Superconductors Under Extreme Conditions of Pressure and Strain V	374
Superconductivity, and Structural and Metal-Insulator Phase Transitions: High Pressure Studies	375
Sergey L. Bud'ko	375
Ir-Sb Binary System: Unveiling Nodeless Unconventional Superconductivity Proximate to Honeycomb-Vacancy Ordering	376
V. Sazgari, Tianping Ying, J.N. Graham, C. Mielke III, D. Das, S.S. Islam, M. Bartkowiak, R. Khasanov, H. Luetkens, H. Hosono, Z. Guguchia	376
Vortex phase transitions in HTSC hydrides	377
Andrey V. Sadakov, Vladimir A. Vlasenko, Dmitrii V. Semenok, Di Zhou, Ivan A. Troyan, Vladimir M. Pudalov	377
On a Room Temperature Superconductor YCuO2+x (0<x<0.5)	378
Danijel Djurek	378
Nonuniform Magnetic Textures I	379
Angular Dependent Spin-Wave Imaging in a Rectangular Ni80Fi20 Microstrip	380
S. Pile, S. Wintz, K. Lenz, R. Narkowicz, A. Ney, J. Lindner, J. Förster, S. Mayr, M. Weigand	380
Magnon dynamics studies by time-resolved resonant X-ray scattering	381
Guido Meier, Lars Bocklage, Jakob Gollwitzer, Cornelius Strohm, Christian F. Adolff, Kai Schlage, Ilya Sergeev, Olaf Leupold, Hans-Christian Wille, Ralf Röhlsberger	381

Controlling the dynamics of magnetic domain walls and skyrmions by magnetic exchange coupling and pinning effects	382
Saül Vélez	382
Magneto-elastic Engineering of Antiferromagnetic Domain Structure	383
A. Wittmann , O. Gomonay , K. Litzius , A. Churikova , N.O. Birge , F. Büttner , S. Wintz , M. Mawass , M. Weigand , F. Kronast , L. Scipioni , A. Shepard , T. Newhouse-Illige , J.A. Greer , J. Sinova , G. Schütz , G.S.D. Beach	383
Frontiers in Magnetization Dynamics and Magnonics I	384
A Time-Multiplexed Spinwave Ising Machine	385
A. Litvinenko, R. Khymyn, V. Gonzalez, R. Ovcharov, A.A. Awad, V. Tyberkevych, A. Slavin, J. Åkerman	385
Nonreciprocal Magneto-Acoustic Waves in Piezoelectric/Ferromagnetic Hybrids	386
Matthias Küß	386
Exploiting Magnetic Tunnel Junctions for Unconventional Computing	387
D.R. Rodrigues, M. Carpentieri, G. Finocchio	387
Frontiers in Magnetization Dynamics and Magnonics II	388
Sustained Spin and acoustic waves excitations driven by fs-laser comb.	389
A.A. Awad, A.K. Chaurasiya, S. Muralidhar, A. Aleman, R. Khymyn, D. Hanstorp, J. Åkerman	389
Strong Nonreciprocity of Surface Acoustic Waves in Hybrid Magneto-Elastic Structures	390
A.N. Slavin	390
Imaging of Spin Textures and Spin Waves in 2D Magnets	391
F. Schulz, K. Litzius, L. Powalla, M.T. Birch, R.A. Gallardo, S. Satheesh, M. Weigand, T. Scholz, B.V. Lotsch, G. Schütz, M. Burghard, S. Wintz	391
Spin-Orbit Torque Driven Antiferromagnetic Oscillator	392
P.K. Rout, J. Godinho, F. Vilsmeier, R. Salikhov, Z. Soban, R.M. Otxoa, C. Back, O. Hellwig, J. Wunderlich	392
MgB2 – Materials and Applications I	393
Kinetics Mechanism on the Efficiency of C Substituting B in the MgB2 Tape Fabrication	394
Chen Guo, Dongliang Wang, Yanwei Ma, Zizhao Gan	394
Textured (00l) MgB2 Small Discs (20 mm in diameter and about 2 mm thickness) with High Levitation Forces and Trapped Magnetic Fields	395
P. Badica, M. Grigoroscuta, A. Kuncser, C. Locovei, G. Aldica, A.M. Ionescu , S.B. Guner, B. Savaskan, U.K. Ozturk, T.S. Suzuki, O. Vasylkiv	395
MgB2 - Magnetic Avalanche of Flux Lattice and Dynamics with Harmonic Susceptibilities	396

TBD	396
MgB2 – Materials and Applications II	397
Synthesis, characterization and application of new 2D material of hydrogen boride sheets derived from MgB2	398
Takahiro Kondo	398
The effect of vacuum annealing on the superconducting properties of MgB2 film deposited by magnetron sputtering on Hastelloy C276TM tape	399
I. Rudnev, I. Yanilkin, A. Gumarov, R. Batulin	399
Production of MgB2 Wire and Joint by External Magnesium Diffusion Method	400
Doğan Avcı, Hakan Yetis, Fırat Karaboğa, Daniel Gajda, Michal Babij, Lan Maria Tran, Andrzej Zaleski, İbrahim Belenli	400
Improving the magnetic levitation force performance of MgB2 bulk superconductors by conventional sintering process	401
Burcu Savaşkan, Sait Barış Güner, Kemal Öztürk, Petre Badica	401
Preliminary study on the phase formation of joints of MgB2/Fe wires by induction processes	402
Mustafa Akdoğan, Bayram Albayrak	402
Graphene and 2D Materials (2DM) – Experimental Session	403
Formation of high-quality 2D Mo2C Crystals and Their Graphene Heterostructures	404
Omer Refet Caylan,*, Elif Okay, Eren Atlı, Zişan Güler, Omer Tarik Ogurtani, Goknur Cambaz Buke	404
Synthesis and Characterization of Vertically Aligned Carbon Nanotubes (VACNTs) on SiC for Field Emission	405
Erhan Gurpinar, Tyson Back, Jon Ludwick, Marc Cahay, Goknur Cambaz Buke	405
Hunts for a Superconductive Phase in Nanographite Films	406
S.G. Lebedev	406
Searching for the working principle of flow-induced voltage in graphene	407
Qian Yang	407
Graphene and 2D Materials – Theory Session	408
The hole-doping induced ferromagnetism in quartic systems	409
M. Polat, H. Sevinçli	409
Optically induced chaotic ionization of relativistic atoms created by Coulomb impurities in graphene	410
J. Matrasulov, J. Yuspov, I. Ibragimov	410
Electronic transition in Coulomb impurities in graphene driven by ultrashort in optical pulses	411

S. Rakhmanov R. Egger, D. Matrasulov 411
Trapped Photons: transverse plasmons in layered semiconducting heterostructures 412
N. Golenić, S. de Gironcoli, V. Despoja 412
Superconducting Spintronics: Novel Quantum Circuits I 413
Optimization of superconducting pickup loops and transformers for SQUID-based quantum sensors 414
P. Febvre, C. Fourie, U. Yılmaz, A. Bozbey 414
Superconducting Neuron and Synapse for Artificial Neural Network 415
Anatolie Sidorenko 415
Density of states in the presence of spin-dependent scattering in SF bilayers. 416
A.V. Guravova, T. Karabassov, A.A. Golubov, A.S. Vasenko 416
Superconducting Spintronics: Novel Quantum Circuits II 417
Numerical analysis of SQUID effective area influenced by flux focusing and kinetic inductance 418
C.J. Fourie 418
Controlled Superconductivity in Van der Waals Superconductor/Ferromagnet Heterostructures 419
A.S. Ianovskaia, G.A. Bobkov, K.A. Bokai,, I.V. Bobkova 419
Return current of Josephson junction: influence of frustration effects 420
I.N.Askerzade 420
Design and Comparative Analysis of Wideband Superconducting Terahertz Antennas 421
A. Canberk Songur, H. Alper Gunes, Emre Kucukyilmaz, N. Orhun Tekci, A. Bozbey, M. Ünlü 421
Spin diffusion and emerging fields in altermagnets 422
A. Manchon 422
Nanocomposites: Properties and Applications I 423
Nanomagnetic Materials: Properties and Applications 424
R. Awad, A.M. Abdallah, A. Aridi, K. Habanjar 424
Ultra-Short Spin Waves Excitation in Spin Hall Nano-Oscillators 425
M. Haidar 425
Revealing the Impact of (Gd, Cr) Dual Doping Yttrium Iron Garnets Derived by Citrate Auto-Combustion Method 426
A.M. Abdallah, K. Habanjar, B. Nsouli, R. Awad 426
Investigating the Physical Properties of Gd-doped Yttrium Orthoferrites 427

S. Isber, A. M. Abdallah, K. Habanjar, R. Awad 427

(1-x) YCeIG/x MgSmO nanocomposites: Characterization and Properties 428

Khulud Habanjar, Majed Sharrouf, R. Awad 428

Nanocomposites: Properties and Applications II 429

The Influence of Defects on the Structural and Magnetic Properties of Mn/Cu Co -doped ZnO Nanoparticles 430

M.M. Seker Perez, C. Boyraz, L. Arda 430

Structural, Dielectric and Conduction Properties of Bi2Ca1.80Sm0.10Ce0.10CoO6 Nano-particles 431

Yasir Abbas, M. Anis-ur-Rehman 431

Role of Superconductivity Roadmap For Net Zero Carbon Emission Targets by 2050: Superconductivity Global Alliance (ScGA) I 432

The Superconducting Global Alliance (ScGA) for Net Zero Carbon Emission Targets by 2050 433

Ziad Melhem 433

Zero Emission Electric Aircraft through Superconducting DC Distribution Network 434

Xiaoze Pei 434

The role of Superconductivity in Transport in a Sustainable Future 435

Marco Breschi, Loïc Quéval, Arno Godeke, Ziad Melhem 435

Role of Superconductivity Roadmap For Net Zero Carbon Emission Targets by 2050: Superconductivity Global Alliance (ScGA) II 436

Superconducting Maglev as a Zero-Emission, High-Speed Ground Transportation System 437

H. Ohsaki 437

Superconducting Cable with Energy Storage Function as a Key to Next-generation Power System toward Net-zero Carbon Society 438

Kohei Higashikawa, Hitoshi Kitaguchi, Naoki Hirano, Kazuhiko Hayashi, S.M. Muyeen, Takanobu Kiss 438

Magnetic Materials Processing and Physical Properties 439

Magnetic interactions and associated effects in rare-earth iron garnets processed by different routes. 440

Cristina Bartha, Claudiu Locovei, Mihai Grigoroscuta, Andrei Alexandru-Dinu, Aurel Leca, Nicu Iacob,Cezar Comanescu, Andrei Kuncser, Petre Badica, Victor Kuncser 440

Magnetic properties and electronic structure of FeRhAs1-xZx (Z=Al, Ga, In) alloys: ab initio study 441

O. Pavlukhina, V. Buchelnikov, V. Sokolovskiy, M. Zagrebin 441

Measurements of stray magnetic fields of Co-rich amorphous microwires using a scanning GMI magnetometer 442

S.A. Gudoshnikov, G.E. Danilov, Yu.B. Grebenshchikov, A.V. Popova, V.I. Odintsov 442

A Magnetic Moment Calculation Method Based on Magnetic Gradient Tensor 443

Shiyao Wang, Sansheng Wang, Fan Liu, Junyang Fang 443

Bulk Superconductors I 444

Microstructure of Dybco bulk cylinders and rings prepared by the SDMG process 445

P. Diko, K. Zmorayova, V. Kucharova, T. Motoky, J. Shimoyama 445

Influence of V-doping on the superconductivity of non-centrosymmetric NbReSi: Interplay of superconductivity and induced charge density wave 446

S. Chakrabortty, N. Mohapatra 446

Effects of Laser-Induced Microstructuring on the Superconducting Properties of YBCO Bulk Superconductors 447

S.B. Guner, L.A. Angurel, G.F. de la Fuente, A. Gencer F. Al-Mokdad, S. Celik, M. Miryala 447

Superconductivity with high upper critical field in Ta-Hf alloys 448

P.K. Meena, S. Jangid, R.K. Kushwaha, R.P. Singh 448

Superconducting Spintronics: Novel Quantum Circuits III 449

Hybrid superconductor-ferromagnet structures with spin-polarized electron diffusion and injection 450

V.V. Ryazanov, T.E. Golikova, I.S. Lakunov, I.A. Nazhestkin, S.V. Egorov, I.E. Batov 450

Andreev bound states at nonmagnetic impurities in superconductor/antiferromagnet heterostructures 451

A.M. Bobkov, G.A. Bobkov, I.V. Bobkova, A.A. Golubov 451

Collective excitations in thin-film topological superconductor/ferromagnetic insulator heterostructures 452

T. Karabassov, I.V. Bobkova, A.M. Bobkov, A.A. Golubov, A.S. Vasenko 452

Superconducting Spintronics: Novel Quantum Circuits IV 453

Magnetic interactions in coupled systems of S/F/S Josephson junctions 454

I.V. Bobkova, G.A. Bobkov, A.M. Bobkov 454

Neel triplet correlations in Superconductor/Antiferromagnet heterostructures with spin-orbit coupling 455

G.A. Bobkov, I.V. Bobkova, A.A. Golubov 455

Supercurrents in a halfmetallic manganite 456

Yao Jungxiang, Remko Fermin, Kaveh Lahabi, and Jan Aarts 456

Superconducting Spintronics: Novel Quantum Circuits V 457

Side-channel Leakage in Superconducting Output Drivers 458

Yerzhan Mustafa, Selçuk Köse	458
High-Density Superconducting Logic and Memory Technologies	459
Oleg Mukhanov, F. Lupo, S. Adler, M. Arzeo, Ivan Nevirkovets	459
Ferromagnetic Josephson Junctions: Fundamental Science and Applications	460
Noman O. Birge	460
Superconducting Spintronics: Novel Quantum Circuits VI	461
Supercurrent Reversal in Zeeman-Split Josephson Junctions	462
A.A. Golubov, S.-I. Suzuki, Y. Asano	462
Superconductivity in Atomically Thin Films: Diodes and 2D Critical State Model	463
Filippo Gaggioli, Gianni Blatter, Kostya S. Novoselov, Vadim B. Geshkenbein	463
Controllable topological superconducting diode	464
T. Karabassov, I.V. Bobkova, A.A. Golubov, A.S. Vasenko	464
Large Scale Facilities in Magnetism, Superconductivity and Energy Related Materials I	465
Uncommon magnetism in rare-earth intermetallic compounds: neutron spectroscopy data and modern theoretical models	466
Pavel S. Savchenkov, Pavel A. Alekseev,	466
Examining the Structure-property Relationships of Sustainable Functional Ceramics Using Powder Diffraction	467
A. Manjon Sanz, C. Berger, C. Culbertson, A. Neill, M. Dolgos	467
Magnetism and lattice collapse transition in ACo2P2	468
J. Sugiyama, I. Umegaki, K. Moriyam, K. Yoshinaga, K. Ohishi, F. Elson, U. Miniotaite, R. Palm, M. Månsson, O.K. Forslund, Y. Sassa, S. Sugiyama, G.D. Morris, B. Hitti, C. Michioka, H. Ueda, K. Yoshimura	468
Large Scale Facilities in Magnetism, Superconductivity and Energy Related Materials II	469
X-Ray Magnetic Spectroscopy: Emerging Opportunities at the 4th Generation Synchrotrons	470
A. Rogalev	470
Study on Na-ion Battery Materials by Means of Small- and Wide-Angle Neutron Scattering and Muon Spin Relaxation	471
K. Ohishi, D. Igarashi, R. Tatara, Y. Kawamura, S. Takata, K. Hiroi, J. Suzuki, I. Umegaki, J. Nakamura, A. Koda, S. Komaba, J. Sugiyama	471
Large Scale Neutron Facilities in Magnetism: Neutron Diffraction Prospective	472
A. Goukassov	472
Large Scale Facilities in Magnetism, Superconductivity and Energy Related Materials III	473

The design and current status of the high-resolution neutron diffractometer at China Spallation Neutron Source 474
Ping Miao 474
In-Situ Synchrotron X-ray Diffraction Study of Silicon-based Anodes produced by Diatom Algae 475
Pedro Alonso Sánchez, Weicheng Hua, Javier Campo, Federico H. Cova, María Valeria Blanco 475
Doping Evolution of High-Energy Spin Excitations in Pr1.4-xLa0.6CexCuO4 476
M. Fujita, K. Shigiya, T. Sasaki, K. Sato, K. Tsutsumi, S. Asano 476
Large Scale Facilities in Magnetism, Superconductivity and Energy Related Materials IV 477
High-Resolution Neutron Powder Diffraction for Materials Science 478
T. Kamiyama, P. Miao 478
Pressure-Induced Second-Order Mott Transition in Quadruple Perovskites 479
A. De Giovanni Rodrigues, A. Perucchi, L. Tomarchio, M. Verseils, P. Parisiades, B. Baptiste, K. Béneut, E. Gilioli, S. Lupi, A. Gauzzi 479
XtremeD: A New Single Crystal and Powder Diffractometer Designed for Measurements at Extreme Conditions of Pressure and Magnetic Fields 480
J. Campo, S. Savvin, J.A. Rodríguez-Velamazán 480
Magnetic shape memory alloys and magnetocalorics I 481
Development of glass-coated microwires from Heusler alloys 482
V. Zhukova, M. Salaheldeen, M. Ipatov, A.Wederni, A. Zhukov 482
Magnetic Shape Memory Alloys and neutron diffraction 483
Jose M. Porro 483
Superelasticity and Elastocaloric Effect in Ni-Fe-Ga Single Crystals 484
J. Torrens-Serra, F. Masdeu, J. Pons, Y. Chumlyakov, E. Cesari 484
Magnetic shape memory alloys and magnetocalorics II 485
Unveiling Electronic Structure of Heusler-type Mn and Co Based Metamagnetic Shape Memory Alloys 486
Akio Kimura 486
Magnetic shape memory properties of Ni-Mn-Ga-based melt spun ribbons 487
M.J. Szczerba, M. Kowalska, P. Czaja, Ł. Rogal 487
Metamagnetic Shape Memory Effect with Small Dissipation Energy in Heusler-type Pd2MnGa Alloy 488
Xiao Xu, Tatsuya Ito, Atsushi Miyake, Yuto Kinoshita, Makoto Nagasako, Kohki Takahashi, Masashi Tokunaga, Ryosuke Kainuma 488
Magnetic shape memory alloys and magnetocalorics III 489

Nanotwinning in off-stoichiometric Ni-Mn-based Heusler alloys from first-principles	490
M.E. Gruner, O.N. Miroshkina, V.V. Sokolovkiy, V.D. Buchelnikov, S. Fähler	490
Shell-ferromagnetism in Heuslers	491
M. Acet	491
Additive manufacturing of Mn-based magnetic shape memory alloys for solid-state refrigeration	492
Daniel Salazar	492
Magnetic shape memory alloys and magnetocalorics IV	493
Ni45Co5Mn37In15 and Ni45Co5Mn35Sn15 alloys Metamagnetic Shape Memory Alloys Production by Mechanical Grinding.	494
J. López-García, , D.L. R. Khanna, V. Recarte, V. Sánchez-Alarcos, J.I. Pérez-Landazabal, P. LaRoca, P. Álvarez-Alonso, , J.A. Rodríguez-Velamazán	494
Dynamics of the magnetocaloric effect in Heusler alloys: results of direct measurements dTad in cyclic magnetic fields up to 8 T	495
Adler Gamzatov, A.T. Kadirbardeev, A.M. Aliev	495
Structural and Magnetic Disorder in Ni(-Co)-Mn-(In,Sn,Ti) Heusler Alloys: Impact on Electronic, Magnetic and Vibrational Properties	496
O. N. Miroshkina, B. Eggert, J. Lill, K. Ollefs, B. Beckmann, D. Koch, F. Scheibel, W. Donner, O. Gutfleisch, H. Wende, M.E. Gruner	496
The structural, electronic and transport properties of Ni-Mn-Sn Heusler alloy	497
V.V. Sokolovskiy, A.G. Gamzatov, V.D. Buchelnikov	497
Nonuniform Magnetic Textures II	498
Observations of bubble resonances in a magnetic insulator via time-resolved scanning transmission X-ray microscopy	499
P. Che, D. Gouéré, S. Wintz, A. El Kanj, A. Mucchietto, D. Grundler, G. Schütz, R. Lebrun, V. Cros, A. Anane	499
Eigenmodes of magnetic skyrmion lattices	500
Louise Desplat, Bertrand Dupé	500
Controlling Spin-Orbit Torque Driven Dynamics for Skyrmion Generation	501
L.-M. Kern, K. Litzius, V. Deinhart, M. Schneider, C. Klose, K.Gerlinger, R. Battistelli, D. Engel, C.M. Günther, K. Höflich, F. Büttner, S. Eisebitt, B. Pfau	501
Nonuniform Magnetic Textures III	502
Magnetic hopfions	503
Nikolai S. Kiselev	503
Three-Dimensional Topological Spin Textures in Curvilinear Helimagnets	504

Luke Turnbull, Max Birch, Jeffrey Neethirajan, Marisel Di Pietro Martínez, Rikako Yamamoto Marina Raboni Ferreira, Simone Finizio, Rachid Belkhou, Claas Abert, Dieter Süss, Geetha Balakrishnan, Sebastian Wintz, Claire Donnelly	504
Magnetooptic response of nanostructures with 3D geometries.	505
J. Jurczyk, N. Leo, M.A. Cascales Sandoval, A. Fernández-Pacheco	505
Nonuniform Magnetic Textures IV	506
Evaluating Skyrmion Spin Textures by Quantitative MFM	507
H.J. Hug, R. Peremedathil-Pradeep, E. Darwin, A.-O. Mandru, T. Dutta	507
Hybrid Antiskyrmions Revealed by 3d LTEM Tomography	508
J. Masell	508
Skyrmions in synthetic antiferromagnets and their fast current induced dynamics without skyrmion Hall effect	509
O. Boulle	509
Nonuniform Magnetic Textures V	510
Uncovering the nature of faint background domain patterns in amorphous ferrimagnetic multilayers	511
Tamer Karaman*, Daniel Metternich, Kai Litzius, Aladin Ullrich, Timo Schmidt, Riccardo Battistelli, Manas Patra, Manuel Valvidares, Daniel Pérez Salinas, Jordi Llobet, Christopher Klose, Michael Schneider, Bastian Pfau, Andrada-Oana Mandru, Reshma Peremadathil Pradeep, Konrad Samwer, Manfred Albrecht, Hans Josef Hug, Felix Büttner	511
X-ray microscopy imaging of stripe, skyrmion and skyrmionium states in van der Waals magnets	512
Max Birch, Lukas Powalla, Kai Litzius, Fehmi Yasin, Frank Schulz, Vanessa Nehruji, Ondrej Hovorka, Daniel Mayoh, Geetha Balakrishnan, Markus Weigand, Xiuzhen Yu, Sebastian Wintz, Gisela Schütz, Marko Burghard	512
Soft x-ray imaging of magnetic textures in permanent magnets at high fields	513
T. Nakamura, Y. Kotani, D. Billington	513
Vortex Matter, Dynamics and Pinning I	514
Vortex Pinning and Dynamics in the Ferromagnetic Iron-based Superconductor EuFe2(As1-xPx)2	515
J.A. Wilcox, S.J. Bending, I. Veshchunov, T. Ren, T. Tamegai, S. Friedemann, M.V. Milošević	515
AC Vortex Dynamics in Superconducting Devices and Applications to Novel Qubits	516
A. Glatz, A. Al Luhaibi, J.B. Ketterson	516
Non-monotonous Jc(H,T) and Relaxation Phenomena in BaFe2(As1-xPx)2	517
A. Galluzzi, A. Crisan, A. M. Ionescu, I. Ivan, A. Leo, G. Grimaldi, M. Polichetti	517

AC magnetic field analysis of the rhombic-to-square transition in the Bragg vortex glass phase in a BaFe2(As1-xPx)2 crystal.	518
M. Polichetti, A. Galluzzi, A. Ionescu, I. Ivan, G. Grimaldi, A. Leo, A. Crisan	518
Vortex Matter, Dynamics and Pinning II	519
Vortex dynamics and ion-irradiation-induced pinning in low-temperature and high-temperature superconductors: a microwave analysis	520
G. Ghigo, M. Fracasso, R. Gerbaldo, L. Gozzelino, F. Laviano, D. Torsello	520
Surface impedance measurements in superconductors in the mixed state: anisotropy, flux-flow, pinning and creep. Perspectives for rf applications in high magnetic fields.	521
E. Silva, A. Alimenti, P. Vidal García, K. Torokhtii, N. Pompeo	521
Vortex Matter Can Become Unstable: the Flux Flow Instability Tool	522
G. Grimaldi, A. Leo, M.R. Khan, N. Martucciello, A. Nigro	522
Vortex Matter, Dynamics and Pinning III	523
Using Machine Learning to Characterize Nonequilibrium Phases in Superconducting Vortex Matter	524
Charles Reichhardt	524
2D vortex lattice: a promising platform to explore the fragile-to-strong glass transition	525
I. Maccari, L. Benfatto, C. Castellani, J. Lorenzana, C. De Michele, S.Dutta, P. Raychaudhuri, B. Pokharel, J. Terzic, D. Popovic	525
Plastic vortex creep and dimensional crossovers in the highly anisotropic superconductor HgBa2CuO4+x	526
Haley M. Cole, Michael B. Venuti, Brian Gorman, Eric D. Bauer, Mun K. Chan, Serena Eley	526
Vortex Matter, Dynamics and Pinning IV	527
Vortex Penetration Into the Putative Chiral Superconductor 4HbTaS2 by Local Magnetization Measurements	528
J. Juraszek, Y.M. Thiebes, Ł. Luszyński, M. Konczykowski, R. Niewa, T. Cichorek	528
Intertype Superconductivity Evoked by the Interplay of Disorder and Multiple Bands	529
P.M. Marychev, A.A. Shanenko, A.V. Vagov	529
Microscopic analysis of the crossover between type I and II superconductivity	530
V.D. Neverov, A.V. Krasavin, A.E. Lukyanov, M.D. Croitoru, A. Vagov	530
Helicity-controlled switching of superconducting states by radiation pulse: Theoretical Analysis and Stability Assessment	531
M.D. Croitoru, B. Lounis, A.I. Buzdin	531
High Temperature Superconductors for fusion applications I	532

Recent Status of R and D and Production of 2G HTS Wires for Fusion Application at Faraday Factory Japan	533
S. Lee, V. Petrykin, I. Matvian, M. Nakamura, K. Vereschagin, M. Gaifullin, R.Valikov, H. Nanjyo, A. Borisov, V. Vyatkin, I. Veschunov, M. Okube, J. Renel, L. Pak, A. Li, S. Hasuo, V. Cheremin, M. Oka, S. Samoilenkov, A. Molodyk	533
Study of neutron radiation effects in YBCO for fusion reactors	534
D. Torsello, D. Gambino, D. Fischer, F. Ledda, S. Sparacio, Z. Hartwig, A. Trotta, F. Laviano	534
The path towards an HTS stellarator fusion power plant in Europe	535
N. Riva on behalf of the Proxima Fusion Team	535
High Temperature Superconductors for fusion applications II	536
Investigation of the Quench Behavior at Fusion Relevant Conditions of the Aluminum Slotted-Core HTS REBCO Cable	537
G. Celentano, A. Augieri, V. Corato, S. Chiarelli, G. De Marzi, R. Freda, M. Marchetti, A. Masi, L. Muzzi, V. Pinto, G. Romanelli, A. Rufoloni, A. Vannozzi, A. della Corte, A. Formichetti, A. Bragagni, M. Seri, R. Bonifetto, A. Zappatore, G. Colombo, H. Bajas, K. Sedlak	537
Performance degradation in REBCO tapes after irradiations between 20 K and 300 K	538
D.X. Fischer, A.R. Devitre, K.B. Woller, Z.L. Fischer, Z.S. Hartwig	538
Correlating the Deterioration of the Superconducting Properties of CCs by Neutron Irradiation with Small Defects.	539
Raphael Unterrainer*, Davide Gambino, Florian Semper, Alexander Bodenseher, Daniele Torsello, Francesco Laviano, Michael Eisterer	539
High Temperature Superconductors for fusion applications III	540
Current status of R and D of SCSC cable	541
N. Amemiya, Y. Sogabe, Y. Tejima, H. Hara, H. Sakamoto	541
Change in Structural and Superconducting Parameters of 2G HTS Tapes under the Influence of Irradiation	542
P. Pęczkowski	542
The influence of ion irradiation on the superconducting properties of 2G HTS wire	543
P. Degtyarenko, V. Skuratov, A. Vasiliev, V. Amelichev, S. Gavrilkin, A. Ovcharov, V. Semina, M. Novikov, A. Petrzhik, A. Tsvetkov, A. Malyavina	543
Role of Superconductivity Roadmap For Net Zero Carbon Emission Targets by 2050: Superconductivity Global Alliance (ScGA) III	544
Superconductivity Global Alliance –Analysis and Roadmaps of Transitioning superconducting technologies to the marketplace in Industry, Energy, Power, and Transport Sectors	545
Sastry Pamidi, Michael Parizh, Peter Cheetham, Mohammad Yazdani-Asrami, Loic Queval,	545

Novel Methodology for Smart Manufacturing and Inspection of Industrial Scale REBCO Coated Conductor Wires	546
Takanobu Kiss, Z. Wu, K. Higashikawa, T. Terazaki, S. Sera, Y. Tanaka, R. Valikov, M. Nakamura, A. Li, V. Petrykin, S. Lee	546
Superconducting Wind Energy – Air-cored HTS C-GEN	547
Hongye Zhang	547
Quantum Transport and Novel Broken Symmetry Ground States I	548
Higher-spin pairing and exotic superconductivity in Luttinger semimetals	549
Igor Herbut	549
Dynamical Conductivity of a Two-Dimensional Weakly Doped Holstein System	550
Z. Rukelj, D. Radić, J. Krsnik, O.S. Barišić, A.S. Mishchenko, I. Kupčić	550
Charge Stripes and Magnetotransport in the Graphene-based Materials	551
D. Radić, P. Grozić, B. Keran, A.M. Kadigrobov	551
Quantum Transport and Novel Broken Symmetry Ground States II	552
Tomasch Oscillations as Above-Gap Signature of Topological Superconductivity	553
Antonio Štrkalj, Xi-Rong Chen, Wei Chen, D.Y. Xing, Oded Zilberberg	553
Unconventional electrodynamics across the charge-density-wave transition in TiSe2	554
Dino Novko	554
Emergent electronic properties in a plastically deformed quantum material	555
D. Pelc	555
Quantum Transport and Novel Broken Symmetry Ground States III	556
The Egzotic Electromagnetic Modes in Layered van der Waals Heterostructures	557
Vito Despoja	557
Designing superconductivity in nanodevices	558
Nina Markovic	558
Experimental investigation of the electromagnetically induced transparency for different D2-line transitions of 87Rubidium	559
Zahra Heydarinasab, Mohammad Karami, Farrokh Sarreshtedari	559
Quantum Transport and Novel Broken Symmetry Ground States IV	560
Quantum Transport Equations in 2D and 3D Dirac Systems: Self-Consistent RPA Approach	561
I. Kupčić	561
Manon-driven quantum dot based spin Seebeck heat engine and refrigerator	562
P. Trocha	562
Entanglement of Many-Body Mixed States	563

F.-H. Wang, X.Y. Xu 563
Diagnosing Quantum Phases Using Long-Range Quantum Resource Behaviors 564
L.-L. Su, J. Ren, W.-L. Ma, Z.D. Wang, Y.-K. Bai 564
Superconductivity in Bi-layer Nickelates I 565
Theory for high temperature superconductivity in La3Ni2O7 566
Fu-Chun Zhang 566
Orbital-Dependent Electron Correlation in Double-Layer Nickelate La3Ni2O7 567
Xingjiang Zhou 567
Resonant x-ray scattering on superconducting nickelates 568
J. Pelliciari 568
Superconductivity in Bi-layer Nickelates II 569
Magnetic fluctuations, superconducting instability, and spin resonance in La3Ni2O7 under high pressure 570
F. Lechermann, S. Bötzel, J. Gandolf, Ilya M. Eremin 570
Theoretical analysis on the possibility of unconventional superconductivity in La3Ni2O7 and La4Ni3O10 under high pressure 571
Kazuhiko Kuroki 571
Superconducting transition behavior of La3Ni2Oy (y~ 7) polycrystalline samples with different oxygen content under high pressure 572
Ke Wang, Qiang Hou, Sheng Li, ZhiXiang Shi 572
Superconductivity in Bi-layer Nickelates III 573
Effects of oxygen reduction on the superconductivity and Ni-3d orbitals of the infinite layer nickelate 574
Ariando 574
Superconducting phase transitions in granular aluminium thin film 575
R. Pervin, U.C. Thuwal 575
Efficient Cooper Pair Splitting Without Coulomb Blockade 576
E.S. Tikhonov, V.S. Khrapai 576
Superconductivity in Lower Dimensions I 577
Impact of disorder in the charge-density-wave state of Pd-intercalated ErTe3 revealed by the electrodynamic response 578
L. Degiorgi 578
Voltage Fluctuations in a System of Capacitively Coupled Superconducting Nanowires 579
A. Latyshev, A.G. Semenov, A.D. Zaikin 579
Superconductivity Induced by Extremely Small Amount of Li in SnSe2 580

Daniel Duong, Jie Xing, Eklavya Thareja, Silu Huang, Scott Crittenden, Williams A. Shelton, Rongying Jin	580
The Transport of Non-Equilibrium Quasiparticles in a Superconductor	581
Konstantin Yu. Arutyunov, Anatoly S. Gurskiy, Dmitry L. Shapovalov	581
Superconductivity in Lower Dimensions II	582
Josephson dynamics at high transmissions: Perturbation theory	583
A.V. Galaktionov, A.D. Zaikin	583
Mechanism of quantum phase transitions in one- and two-dimensional superconductors: microscopic scale and nature of critical fluctuations	584
A. Rogachev, S. Feldman, K. Davenport	584
Quasiparticle response in semiconductor-superconductor NSN structures	585
Vadim Khrapai	585
Superconductivity in Lower Dimensions III	586
Observation of the current steps in Josephson junctions under microwave radiation	587
V.N. Antonov, R.S. Shaikhaidarov, O.V. Astafiev	587
Drag effect in capacitively coupled Josephson junctions and thin superconducting nanowires.	588
Alex Latyshev, Andrew G. Semenov, Andrei D. Zaikin	588
Nonlinear microwave response of clean superconducting films	589
A.A. Radkevich, A.G. Semenov	589
Nonuniform Magnetic Textures VI	590
Zero-field spin wave turns- correct template	591
Jan Klíma, Ondřej Wojewoda, Václav Roučka, Tomáš Molnár, Jakub Holobrádek, Michal Urbánek	591
Realization of magnetic circuits exploiting exchange and chiral lateral couplings	592
Aleš Hrabec	592
Topotronics with Magnetic Topological Materials	593
O.A. Tretiakov	593
Nonuniform Magnetic Textures VII	594
Dipolar-Stabilized Skyrmions and Antiskyrmions in Magnetic Multilayers	595
M. Albrecht	595
Reversible Topological Transformation of Skymions and Trivial Bubbles	596
T. Schmidt, S. Koraltan, M. Albrecht	596
Tunable Magnetic Equilibrium Configurations in Dipolar Helices	597
Ot Garcés, Òscar Iglesias	597

Synthesis, structural and magnetic properties of CuxMn1-xFe2O4 nanoparticles	598
P.P. Majozi, J.Z Msomi, S.J.C Masuku	598
Spintronics Materials-Devices and Applications	599
Enabling Offset-free Sensing using Spin-Orbit Torques	600
Sabri Koraltan	600
Spin pumping from insulating antiferromagnets with strong Dzyaloshinskii-Moriya interaction	601
A. Safin	601
Bismuth Ferrite Nanostructures; Magnetic-Dependent Cycloidal Ordering and Photocatalytic Activity	602
N. Thabet Mliki, I. Mallek Zouari, W. Ben Taazayet, J-M. Grenèche, L. Bessais, B. Dkhil	602
Theory of Magnetism II	603
Growing crystalline artificial magnet ice in a kagome lattice	604
Jun-Yi Ge,*, Jia-Jie Zhang, Li-Ming Tu, Vladimir N. Gladilin	604
Theoretical description of spin-driven ferroelectricity in systems with symmetric and antisymmetric exchange interactions	605
Mariya Iv. Trukhanova, Pavel Andreev	605
HTS Cuprates: Advances in Fundamentals and Experimental Studies VII	606
Recent development of Bi-2223 high temperature superconducting tapes in NIN	607
S. Zhang, L. Jin, X. Liu, X. Ma, B. Shao, G. Liu, J. Feng, C. Li, J. Li, P. Zhang	607
Fabrication of BSCCO HTS Wires by Cryogenic Drawing and Rolling under Liquid Nitrogen Temperature	608
X. Liu, S. Zhang, J. Li, J. Liu, J. Feng, C. Li, P. Zhang	608
Mass of Charge Carrier in the La2-xSrxCuO4 from Bipolaronic Model	609
B.Ya. Yavidov, S.M. Otajonov, D.E. Uskenbaev, T. Saparbaev, A.N. Kurmantayev	609
Superconducting Spintronics: Novel Quantum Circuits VII	610
Mutual Synchronization of Bi-2212 THz emitters	611
O. Kizilaslan, R. Wieland, E. Dorsch, N.V. Kinev, A.B. Ermakov, D.Koelle, H.B. Wang, P.H. Wu, V.P. Koshelets, R. Kleiner	611
Interplay between magnetism and superconductivity in a hybrid magnon-photon bilayer system in the ultrastrong coupling regime	612
A. Ghirri, C. Bonizzoni, M. Maksutoglu, A. Mercurio, O. Di Stefano, S. Savasta, M. Affronte	612
Unconventional Superconductor's Impact on Spin Dependent Transport Properties of Multi-Terminal Quantum Dot Hybrid	613

Vrishali Sonar, Piotr Trocha	613
Magnetic Materials Processing and Physical Properties II	614
Unlocking Multifunctional Potential: Mn-Ru Co-Doping Boosts Catalytic and Magnetic properties in La0.62Bi0.05Ba0.33Mn1-xRuxO3 (x = 0.0 and 0.1) Compounds	615
A. Osman Ayaş, S. Kılıç Çetin, G. Akça, D. Kaya, A. Ekicibil	615
Excellent Electromagnetic Wave Absorption of Fe3O4:MoS2 Hybrid Composites	616
M. Akyol, C. Aka, O. Akgöl, M. Karaaslan	616
Sintering Temperature Effect on Structural, Magnetic and Magnetocaloric Properties of Some Perovskite Manganite Materials	617
A. Osman Ayaş, A. Kandemir, M. Akyol, A. Ekicibil	617
Characterization of Gd3+Doped Magnesium Ferrite Synthesized by Sol- gel Method.	618
Haroon Mazhar, M. Anis-ur-Rehman	618
Magnetic Materials Processing and Physical Properties III	619
Development of persistent joints for superconducting Bi-2212 coils	620
Tayebeh Mousavi, Petr Zagura, Ingon Kim, Frederick Follows, Ziad Melhem, Steven Ball, Andrew Twin, Susannah Speller, Chris Grovenor	620
Numerical Modelling of High-Velocity EDS Hyperloop Systems with different PMG-Aluminium Rail Configurations	621
Murat Abdioglu, Hakki Mollahasanoglu, Ufuk Kemal Ozturk, Elvan Coskun, Ali Gencer	621
HRTEM studies and superconducting properties of the KCa2Fe4As4F2 single crystals	622
Alena Yu. Degtyarenko, Andrey V. Sadakov, Alexey S. Usoltsev, Juniy Ge	622
Ferrites and Rare Earth Magnetic Materials	623
Emerging RRAM Materials: An Overview of Recent Advances in Ferrites	624
M. Anis-ur-Rehman	624
Climate change, clean energy technologies and resource recovery-A pathway for sustainable development	625
Rizwan Raza	625
Large magnetoresistance of amorphous carbon film	626
Awais Siddique Saleemi, Ali Abdullah, M. Anis Ur Rehman	626
Continuous tuning of compensated ferrimagnetism in Gd 3 – x Ho x Fe 5 O 12 thin films	627
Hao Bai,*, Wenlong Si,*, Heng-An Zhou,*, Ledong Wang, Teng Xu, Yiqing Dong, Jing Zhu,†, Wanjun Jiang	627
Quantum Transport and Novel Broken Symmetry Ground States V	628

Electrical Breakdown of Excitonic Insulators	629
Yuelin Shao, Xi Dai	629
Dirac plasmon emission in photo-excited heavily doped graphene KC8	630
Josip Jakovac	630
Study of Electric and Atomic Properties at the Grain Boundary in Perovskite Materials	631
M.R. Samatov, D. Liu, A.S. Vasenko	631
Unconventional Electronic Instabilities in Kagome Metals: Insights from ARPES	632
Yong Hu	632
Bulk Superconductors II	633
In situ self-assembled double-seeds with exact-(110)/(110) alignment for growing high-performance YBCO bulks	634
Xin Yao	634
Production of Large-Size Bi-2212 Plates using Laser-Furnace Technologies	635
C. Özçelik, H. Amaveda, M. Mora, E. Martínez, G.F. de la Fuente, L.A. Angurel, B. Özçelik	635
Influence of low Oxygen Pressure on Tl-Based HTS Phase Formation	636
I.R. Metskhvarishvili, D.L. Surmanidze, T.E. Lobzhanidze, G.N. Dgebuadze, V.M. Gabunia, B.G. Bendeliani, M.R. Metskhvarishvili	636
W-Nb-Mo-V-Ta-Cr-Al Refractory High-Entropy Alloys for Potential Superconducting Materials	637
Burçak Boztemur, M. Lütfi Öveçoğlu, Duygu Ağaoğulları	637
Bulk Superconductors III	638
Bulk trapped-field superconducting magnets arranged in a linear Halbach array: important points to achieve the full potential of the magnetized superconductors	639
M. Houbart, N. Rotheudt, J.F. Fagnard, J. Dular, A.R. Dennis, D.K Namburi, J.H. Durrell,	639
Bulk MgB 2 for Applications at Liquid Hydrogen Temperatures	640
Tetiana Prikhna, , , Michael Eisterer, Canan Aksoy, Viktor Moshchil, Bernd Büchner, Tersa Puig, Dirk Lindackers, Paul Sass, Anton Shaternik, Volodymyr Sverdun, Semyon Ponomarov, Ali Gencer	640
Superconducting Properties of a Seed Infiltration Growth (BSIG) Processed REBCO Single Crystals	641
E. Coskun, F.Al-mokdad, C. Aksoy, E. Aksu, Y. Oznal, B. Cakır, K. Sonmez, Sukru Celik, A. Gencer	641
POSTER PRESENTATIONS	642
Microstructure Evolution and Magnetic Properties of Nanocrystalline Ni75Fe25 Thin Films Deposited onto Glass, Al2O3 Kapton Substrates	643
A. Kaibi, A. Guittoum, R.M. Öksüzoğlu, C.Yavru, S. Özgün, M. Boudissa	643

Investigation of the physico-chemical and superconducting properties of superconducting foams produced by the top-seed infiltration-growth (TSIG) method	644
Paweł Pęczkowski, Piotr Zachariasz, Ryszard Zalecki, Jarosław Piętosa, Jan Marek Michalik, Cezariusz Jastrzębski, Michał Ziętala, Marcin Zając, Łukasz Gondek	644
Laser-induced ultrafast insulator-metal transition in BaBiO3	645
A.E. Lukyanov, V.D. Neverov, Ya.V. Zhumagulov, A.P. Menushenkov, A.V. Krasavin, Alexei Vagov	645
Investigation of The Mechanical Behavior of Partially Substituted TB/Y AND Zn/CU Y-358 Superconductors	646
Ö. Öztürk, G. Güdücü, S. Kurnaz, T. Seydioğlu, S. Safran	646
Solar technology for the production of Bi/Pb superconducting ceramics and its properties	647
D.D. Gulamova, E.B. Eshonkulov, T.I. Gulamov, V.R. Li, G.I. Mamniashvili, G.J. Donadze, V.A. Peikrishvili	647
An investigation comparing the different phases of YBCO superconductors doped with Tb produced by the Sol-Gel Route	648
Serap Safran, Gülnur Güdücü, Özgür Öztürk, Sedat Kurnaz, Elif Aşikuzun Tokeşer, Gürcan Yildirim	648
Unconventional Superconductivity in PbMo6Se8?	649
Souvik Banerjee, A. Sundaresan	649
Synthesis, Crystal and Electronic Structure of the ATM2Bi2 Series (TM = d-Metal, A = Alkali or Alkali-Earth Metal)	650
E.O. Rakhmanov, A.I. Shilov, A.V. Sadakov, A.S. Usoltsev, A. Yu. Degtyarenko, K.A. Lyssenko, A.N. Kuznetsov, I.V. Morozov, A.V. Shevelkov	650
Irradiation Influence on Structural and Magnetic Properties of YBCO-123 Superconductor: An Investigation	651
F. Al-Mokdad, E. Aksu, S.B. Guner, E. Coskun, Y. Oznal. K. Sonmez, A. Gencer	651
The compression system of the NICA cryogenic complex	652
N.N. Agapov, A.E. Emelyanov, A.V. Konstantinov, Iu.A. Mitrofanova, D.S. Shvidkiy	652
Derivation of effective tight-binding model for coupled Josephson junction and semiconductor quantum dot systems	653
K. Pomorski, P. Pęczkowski, M. Kowalik	653
Inductively coupled superconducting rings and semiconductor rings treated by Bogomolny formalism and Schroedinger-Ginzburg-Landau relaxation method	654
Ł. Stępień, K. Pomorski, M. Kowalik, P. Pęczkowski	654
On the Path to Superconductor Broadband Receivers	655
V.K. Kornev, N.V. Kolotinskiy	655

Superconducting Perceptron Network using Hybrid QFP-RSFQ Neurons	656
M. Ameen Jardine, Coenrad J. Fourie	656
Design of a Superconducting RF Switch for Cryogenic 4-12 GHz Band Applications	657
A.O. Sakın, A.C. Sonğur, B. Akçay, M. Demircioğlu, H.A. Güneş, D. Doğan, A. Bozbey, M. Ünlü	657
Influence of Defect Structure on Superconducting Properties in Alkali Metal-Based Iron Pnictides and Selenides	658
A. Yu. Degtyarenko, I.V. Morozov, E. O. Rakhmanov, A.V. Sadakov, A.I. Shilov, S. Yu. Gavrilkin, A. Yu. Tsvetkov, S. A. Kuzmichev,, T.E. Kuzmicheva	658
The Large Thermal-Voltage Of Yttrium Iron Oxide (Y3Fe5O12)/Tungsten (W) Hybrid Structure On Spin Seebeck Effect Measurement	659
P. Wongjom, C. Wongsakulkhamkhot	659
Enhanced the Ionic Conductivity at High Temperature in RE Doped Magnesium Ferrite for Applications of Fuel Cell.	660
Haroon Mazhar, Haris Farooq Kiani, M. Anis-ur-Rehman	660
Exploring Structure-Electrical Correlations in (Mn-Zn) Nanomaterials for Memory Application	661
Rehana Rasool, M. Anis-ur-Rehman	661
Barium Hexaferrite Doped with Cobalt: A Study on Electrical Behavior for Memory Applications	662
Rabia Tariq, M. Anis-ur-Rehman	662
Temperature dependent Electrical and Dielectric properties of MgFe1.8Ce0.2O4 Ferrite.	663
Haroon Mazhar, M. Anis-ur-Rehman	663
Doping in Pyrochlore Lanthanum Zirconates to Tune Transport properties for RAMS Application	664
Arouba Abbas, M. Anis-ur-Rehman	664
Tuning Electrical Characteristics of Cobalt Ferrite through Magnesium Doping for Improved R-RAM Performance	665
Irsa Kanwal Abbasi, M. Anis-ur-Rehman	665
Enhanced Energy Storage Properties of Nd-doped Calcium Bismuth Cobaltite's Nanoparticles via Wet Chemical Method	666
Haris Farooq Kiani, Haroon Mazhar, M. Anis ur Rehman	666
The Magnetic and Electrophysical Properties of (FeIn2S4)0,97(CuIn2S4)0,03	667
S.S. Ragımov , Sh. S. Abdullaeva	667
Additive Manufacturing of R-Fe-B Type Permanent Magnets	668
V. Maltseva, A. Urzhumtsev, S. Andreev, A. Volegov	668

Magnetometric Approach to Establishing the Basic Mechanism of Magnetization Reversal Processes in Nd-Fe-B Type Permanent Magnets	669
A. Urzhumtsev, V. Maltseva, A. Volegov	669
Magnetic and magnetocaloric properties of rare earth substituted Zn-Ni nanosized ferrites	670
S.J.C. Masuku, J.Z. Msomi, A.M. Strydom, A. Xhakaza	670
Observations of the novel low field microwave absorption in ZnxCo1-xFe2-xAlxO4 ferrites	671
S.J.C. Masuku, P.P. Majozi, J.Z. Msomi, S. Mahule	671
Modulated Magnetic Structure in Weak Ferromagnet FeBO3:Mg and Iron-Garnets Tb0,26Y2,74Fe5O12, Ho0,6Y2,4Fe5O12	672
D.R.Djurayev, L.N.Niyazov, Sh.Sh.Fayziyev	672
Correlation of Structural and Electrical Characterization of La (Mn-Zn) Ferrites for Green Energy Applications	673
Sumaira Komal, M. Anis-ur-Rehman	673
Physical properties of Zn0.5Co0.5Fe2O4 ferrites doped with bismuth and tin	674
Sajida Rmeid, Khulud Habanjar, Amani Aridi, R. Awad	674
Nonlinear shift of exceptional points in coupled spin torque nanooscillators	675
O. Temnaya	675
Enhancing Ionic Conductivity: A Comprehensive Study of Phase Pure and Doped Lanthanum Zirconates for Solid Oxide Fuel Cells	676
Arouba Abbas, M. Anis-ur-Rehman	676
Structural and Electrical Properties of (Mn–Zn) Cobalt doped Spinel Ferrites for High Energy Applications	677
Rehana Rasool, M. Anis-ur-Rehman	677
Evaluating the Electrical Conductivity of Cobalt-Incorporated Barium Hexaferrite for Fuel Cell Applications.	678
Rabia Tariq, M. Anis-ur-Rehman	678
Electrical Analysis of NiCo2O4 and its composite with CNTs as electrode material for Energy Storage Devices	679
Hira Sultan, M. Anis-ur-Rehman	679
Nd Doping impact on the Dielectric Properties of (Ca-Bi) Cobaltite's Nanoparticle synthesized by WOWs Sol-gel Process for Solid Oxide Fuel Cell Application.	680
Haris Farooq Kiani, Haroon Mazhar, Rabia Shahid, M. Anis ur Rehman	680
Magnon-polaritons at the junction of two antiferromagnetic superlattices with graphene at the contact interfaces	681
R.T. Askerbeyli, Hiba Elharkati	681
Electronic Properties of Monolayer Fe3GeTe2 under Hubbard Correction	682

G.Y. Senguler, Y. Mogulkoc, A. Mogulkoc	682
Spin transfer torque and anisotropic conductance in spin orbit coupled graphene	683
Razieh Beiranvand	683
Influence of magnetic ions implantation on the critical current of HTSC composites	684
I. Rudnev, D. Abin, S. Pokrovskii, R. Batulin	684
Flux jumps, cluster distribution model and vortex phase diagram of oxygenated Al-YBCO single crystal	685
Ashna Babu, Deepshikha Jaiswal Nagar	685
Effect of different immersion times in seawater on the mechanical properties of Bi1.6Pb0.4Sr2Ca2Cu3.2O10+δ composite	686
Ahmad Najem, M. Anas, K. Habanjar, R. Awad	686
The Effect of Sr Substitution on the crystal symmetry and Superconductivity of the High Temperature Superconductor La 2-x Sr x CuO4	687
Bassam M. Mustafa	687
The Electrical Properties of the several HTS Tape Joints for the Superconducting Fault Current Limiter	688
D.M. Durão, S. Costa, C. Aksoy, I. Catarino, J.M. Pina, A. Pronto	688
Investigations of Some Properties of High-Temperature Iron-Based Superconductor 〖Ba〗_(1-x) 〖Rb〗_x 〖Fe〗_2 〖As〗_(2) Using Effective Two-Band Model	689
Derejaw Gardew, Gebregziabher Kahsay, Tamiru Negussie	689
Electronic structure of InCo2As2 and KInCo4As4: LDA+DMFT	690
N.S. Pavlov, I.R. Shein, K.S. Pervakov, I.A. Nekrasov	690
Tunneling Spectroscopy of Ba(Fe,Ni)2As2 Pnictides in the Normal State	691
I.A. Nikitchenkov, , A.D. Ilina, K.S. Pervakov, V.A. Vlasenko, S.A. Kuzmichev, T.E. Kuzmicheva	691
Doping Evolution of the Superconducting Gap Structure of the 122 Family Pnictides and Chalcogenides	692
T.E. Kuzmicheva, S.A. Kuzmichev, I.V. Morozov, A.I. Shilov, Ye.O. Rakhmanov, K.S. Pervakov, V.A. Vlasenko	692
Analysis of the Effect of Aliovalent Substitutions in Ca/K-1144 Iron Based Superconductors.	693
A. Duchenko, F. Varsano, A. Augieri, L. Barba, G. Campi, G. Celentano, L. Gigli, J.R. Plaisier, N. Pompeo, A. Rufoloni, Z.-H. Sung, A. Masi	693
High-pressure synthesis and Mn doping effect CaKFe4As4Superconductor	694
Manasa Manasa, Mohammad Azam, Tatiana Zajarniuk, Svitlana Stelmakh, Tomasz Cetner, Andrzej Morawski, Andrzej Wisniewski, Shiv J. Singh	694
High-pressure synthesis optimization and its effect on the superconducting properties of Sm-based oxypnictide	695

Mohammad Azam, Manasa Manasa, Tatiana Zajarniuk, Ryszard Diduszko, Tomasz Cetner, Andrzej Morawski, Andrzej Wiśniewski, Shiv J. Singh	695
Comparison of Operating Characteristics of DC Circuit Breaker According to The Response of Superconducting Elements in MMC-HVDC	696
Dae-Seong Jang, Hyo-Sang Choi	696
Fault Current Interruption in MTDC Systems Using Superconducting LC Resonant DC Circuit Breaker: Resonant Frequency	697
Jihye Kim, Hyosang Choi	697
Analysis on Current Limiting Characteristics of Three-Phase Transformer Type SFCL using Double Quench Due to Single-Line Ground Fault	698
Shin-Won Lee, Tae-Hee Han, Seok-Cheol Ko, Sung-Hun Lim	698
DC Current Limiting Characteristics of Flux-Lock Type SFCL using Twice Quench	699
Sung-Hun Lim, Seok-Cheol Ko, Tae-Hee Han	699
Peak Fault Current Limiting Characteristics of Trigger Type SFCL using Twice Quench	700
Sung-Hun Lim, Seok-Cheol Ko, Tae-Hee Han	700
50-80 kA conductors for large HTS fusion magnets	701
V. Vysotskiy, E. Zapretilina, V. Zubko, A. Krasilnikov, A. Mednikov, V. Ovsyannikov, I. Rodin, D. Stepanov, V. Sytnikov, S. Fetisov	701
High-speed superconducting magnetic bearings for ring spinning: experimental and numerical analysis	702
M. Baloochi, T. Espenhahn, M. Hossain, A. Abdkader, Chokri Cherif, K. Nielsch, R. Hühne	702
Persistent current switch of a whole-body 1.5T superconducting MRI magnet	703
A. Nandawadekar, M. Singh, S. Kar	703
Compression eliminates charge traps by stabilizing perovskite grain boundary structure: ab initio analysis with machine learning force field	704
A.S. Vasenko, D. Liu, M.R. Samatov, O.V. Prezhdo	704
Hall Effect in SmxMn1–xS solid solutions	705
A.M. Kharkov, R.V. Runov, A.V. Gelgorn	705
Giant X-ray circular dichroism in a time-reversal invariant antiferromagnet	706
Jun Okamoto, Ru-Pan Wang, Yen-Yi Chu, Hung-Wei Shiu, Amol Singh, Hsiao-Yu Huang, Chung-Yu Mou, Sucitto The, Horng-Tay Jeng, Kai Du, Xianghan Xu, Sang-Wook Cheong, Chao-Hung Du, Chien-Te Chen, Atsushi Fujimori,, Di-Jing Huang	706
Enhancing Magnetic Sensing Capabilities Beyond Conventional Techniques	707
M. Soğan, M. Dilara Pütkül, A. Gokce Ozbay, A. Ozbay , H. Tatlıpınar	707
Ultrahigh Curie temperature in Co2Fe1+xGe1-x Heusler alloys via powder metallurgy	708

Yifeng Zhang, Chang Xue,Zhenjie Feng, Jincang Zhang	708
Ultrahigh Curie temperature in Co2Fe1+xGe1-x Heusler alloys via powder metallurgy	709
Yifeng Zhang, Chang Xue,Zhenjie Feng, Jincang Zhang	709
Stability of the magnetocaloric effect in La-Fe-Si alloys under long-term exposure to the cyclic magnetic fields	710
N.Z. Abdulkadirova, A.G. Gamzatov, A.M. Aliev, J. Wang, Fengxia Hu	710
Critical Role of the Magnetocrystalline Anisotropy on the Frequency-dependent Hyperthermia Performance of Magnetite Nanoparticles	711
D. Failde, V. Ocampo, D. Serantes, Ò. Iglesias	711
Effect of milling time on the Mossbauer spectra of Ni50.52Mn9.03Fe11.93Ga28.52 and Ni52.27Mn11.66Fe13.25Ga22.83 alloys	712
H.S. Yilmaz, S. Delice, H. Güngüneş	712
Preparation of Polymer-coated Magnetic Nanoparticles as Targeted Drug Delivery Systems	713
O. Gok, S.N. Ozkan E. Ozkul, M.N. Atilmis, P.S. Unlu	713
Evaluation of Superconducting Phase Transitions in MgB2/Fe Wires Produced Through Different Methods	714
Naki Kaya	714
Examining the Effect of Carbon Nanotube on the Dielectric Properties of MgB2 Superconductor	715
P. Oruç, A. Seçkin, N. Kaya, S. Cavdar, H. Koralay	715
Microhardness Analysis of MgB2 Produced with Carbon-Encapsulated Boron	716
P. Oruç, A. Seçkin, S. Cavdar, H. Koralay	716
Crystal Size Analysis of MgB2 Superconductor Produced Utilizing Carbon-Accumulated Boron	717
A. Seckin, P. Oruç, S. Cavdar, H. Koralay	717
Superexchange-Coupling Driven Magnetostriction in van der Waals Molecular Solids	718
Dong-Yang Li, Yuan-Qi Zhai, Yan-Zhen Zheng	718
Preparation and Characterization of Different Magnetic Nanoferrites for the Treatment of Contaminated Water	719
Mariam Rabaa, Amani Aridi, Ramadan Awad	719
Effect of milling time on the Particle Size and Magnetic Properties of Fe-25%Ni-5%Si-15%Co and Fe-28%Ni-5%Si-15%Co alloys	720
H. Kuyubaşi, S. Delice, H. Güngüneş	720
Characterisation of a Magnetic Iron Oxide Biocomposite for Wastewater Remediation Via an External Magnetic Field	721
B. Nasirli, İ. Tosun Satir, Ç. Dönmez Güngüneş	721

Synthesis and electron spin resonance study of Zn 0.7 Ni 0.3 (RE) 0.1 Fe 1.9 O 4 (Re = Gd, Sm, Dy)	722
S.J.C. Masuku, J.Z. Msomi, S. Mahule	722
Magnetic and ESR study of CuxNi1-xFe2O4 nanosized compounds	723
P.P. Majozi, J.Z. Msomi, S. Mahule	723
Temperature dependent structural and magnetic properties of permalloy (Ni80Fe20) nanotubes	724
S. Parajuli, K. Javed, M. Irfan, X. M. Zhang, C. Cheng, X.F. Han	724
Exceptionally Slow, Long Range, and Non-Gaussian Fluctuations Anticipate the Critical Singularity Far Away from the Charge Density Wave Transition.	725
Sk Kalimuddin, Sudipta Chatterjee Arnab Bera, Hasan Afzal, Satyabrata Bera, Deep Singha Roy, Soham Das, Tuhin Debnath, Bhavtosh Bansal Mintu Mondal	725
Molecular Magnetism Based on Rare-Earth Dimer Encapsulated in Fullerene Cages	726
Matheus Barbosa, Wei Yang, Fupin Liu, Alexey Popov	726
Tuning strategy for Curie-temperature enhancement in the van der Waals magnet Mn1+x Sb2-xTe4	727
M. Sahooa,b, M.C. Rahnb, E. Kochetkovaa,d, A. Tcakaeve, V.B. Zabolotnyye, E. Weschkeh, V. Hinkove,c, A. Alfonsova, V. Kataeva, B. Büchnera,c,b, A.U.B. Woltera,c, J.I. Faciof, L.T. Corredora, A. Isaevaa,d	727
Magnetic properties of the double perovskite Ba2CoNbO6	728
D.V. Popov, R.G. Batulin, M.A. Cherosov, I.V. Yatsyk, T.I. Chupakhina, Yu.A. Deeva, R.M. Eremina	728
Magnetic phase diagram of Kitaev Quantum Spin Liquid candidate Na3Co2SbO6	729
K.K. Bestha, M. Sahoo, R.C. Morrow, A. Malyuk, B. Buechner, L.T.C. Bohorquez, A.U.B. Wolter	729
Magnetic ordering in (Ni,Mn,Cu)3BO5	730
R.M. Eremina, R.G. Batulin, V.A. Shustov, E.M. Moshkina, I.I. Fazlizhanov	730
Tunable carrier-mediated ferromagnetism in a Van der Waals semiconductor up to room temperature	731
Xiao Chang, Tingyu Qu, Barbaros Oezyilmaz	731
Mathematical model and neural networks for the dynamic hysteresis losses calculation	732
A. Nouicer	732
Motion of a Charged Particle in a Mutually Perpendicular Uniform Magnetic and Electric Fields	733
M.R. Rajabov, B.G. Pashayev	733
Fully superconducting electrical machines in various applications	734

N. Ivanov, V. Kaderov, N. Malevich	734
Study of a new superconducting inductor for an axial field synchronous machine	735
Hakim Douar, Larbi Hadjout, Ailam El Hadj	735
Signatures of spin-triplet-pairing state in two-dimensional niobium diselenide	736
T. Qu, X. Chang, B. Oezyilmaz	736
Dynamics and Influence of Helium and Vacuum on Gap Relaxation Time in Superconducting Bridges	737
A. Mekki, K. Harrabi, M. Milosevic	737
Advances in the Thermoelectric Measurements of 2D Superconductor Utilizing Contact Printed Circuit Boards	738
S. Shokri, C.N. Saggau, T. Confalone, M. Martini, Y. Lee, F. Caglieris, H. Reith, D. Berger, G.D. Gu, V.M. Vinokur, K. Nielsch, N. Poccia	738
Quasi-two-dimensional anisotropic superconductivity in Li intercalated 2H-TaS2	739
T. Agarwal, C. Patra, A. Kataria, Rajeswari R. Chowdhury, R. P. Singh	739
Anatomy of band structure of newest apparent near-ambient superconductor LuH3-xNx	740
N.S. Pavlov, I.R. Shein, K.S. Pervakov, V.M. Pudalov, I.A. Nekrasov	740
Exceptionally Slow, Long Range, and Non-Gaussian Fluctuations Anticipate the Critical Singularity Far Away from the Charge Density Wave Transition	741
Sk Kalimuddin, Sudipta Chatterjee, Arnab Bera, Hasan Afzal, Satyabrata Bera, Deep Singha Roy, Soham Das, Tuhin Debnath, Bhavtosh Bansal, Mintu Mondal	741
Optical conductivity of Dynes Superconductors: experiment and theory	742
M. Šindler, C. Kadlec, and F. Herman	742
Problems on Representing Mechanism of The Phenomenon of High Temperature Superconductivity	743
Djuraev Davron Rahmonovich, Ahadov Abdullo Amrullojon ogli	743
Correlation Carrier Concentration with Critical Temperature of Superconductors	744
D.R. Djuraev, J.S. Abdulloyev, A.A. Turayev	744
Boosting the Solution of Bogoliubov – de Gennes Equations by the Neural Network	745
A.V. Krasavin, V.D. Neverov, A.E. Lukyanov, M.D. Croitoru, A. Vagov	745
Quantum Hall and Light Responses in a 2D Topological Semimetal	746
Sariah Al Saati, Karyn Le Hur	746
Vortex dynamics and dissipation effects in non-simply connected thin films	747
V. Pashkovskaia, A. Vagov, A. Shanenko, A. Vasenko, T.T. Saraiva	747
The Effect of Pinning Arrays with Moiré Structure on the Critical Current Density in Superconducting Media	748

Z. Owjifard, M. Hosseini, A. Tavana	748
Current-induced Vortex Dynamics in Superconducting Diabolo and Screw Geometries	749
A.J.M. Deenen, D. Grundler	749
Dynamic Changes in the Critical State and the Structure of Magnetic Flux Fronts in an NbTi Superconductor	750
V.V. Chabanenko, I. Abaloszewa, V.F. Rusakov, O.I. Kuchuk, O.M. Chumak , A. Abaloszew, A. Nabiałek, R. Puz´niak	750
Transport properties of MgB2/Fe small mono-core wires fabricated by magnetic induction	751
M. Akdoğan, A. Rajab Ahmed, B. Albayrak	751
Optoelectronic Properties of Organic Thin Film Al/N-Si/ZnCo2O4/TPA-DA-IPA/Al Heterojunction	752
Şükrü Çavdar, Pınar Oruc, Haluk Koralay, Serkan Eymur, Nihat Tuğluoğlu	752
Structural and magnetic properties of (Co/Eu) doped ZnO Nanoparticles	753
Y. Kandil, A. Guler, C. Boyraz, L. Arda	753
The Impact of Defects on Structural and Magnetic Properties in Y/B Co-doped ZnO Nanoparticles	754
S. Veziroğlu K. Özdoğan, L. Arda	754
The Influence of Defects on the Structural, Magnetic, and Photocatalytic Properties of Mg/Fe co-doped ZnO Nanoparticles	755
K. Senturk, L. Arda	755

ORAL PRESENTATIONS

27.04.2024 SATURDAY - 03.05.2024 FRIDAY

Public Outreach and Plenary Session

27.04.2024 SATURDAY

Abstract ID: 1625

ON THE LARGE SCALE APPLICATIONS OF SUPERCONDUCTORS IN THE ENERGY SECTOR IN RENEWABLES, NUCLEAR ENERGY, WASTE TREATMENT AND PUBLIC TRANSPORT

A. Gencer[1,2]

[1] *Ankara University, Science Faculty, Phys. Dept., 06100-Tandogan- Ankara, TURKIYE*
[2] *Ankara University, Center of Excellence for SUperconductivity Research, (CESUR), 06830 - Golbasi-Ankara, TURKIYE*
E-mail: aligencer06@gmail.com

Sustainable Development is to meet the needs of societal development goals while simultaneously sustaining the ability of natural systems to provide the natural resources and ecosystem services on which the economy and society depend on. Since the discovery of superconductivity in 1911, there have been many milestone achievements in the large scale applications of superconductors. In this presentation, a brief summary of Turkey's efforts and the leading countries in superconductor technologies based on energy applications in view of decarbonized economy with zero-carbon emission targets will be provided along with historical progress of the low temperature physics, Quantum Science & Technology and cryogenics engineering with enabling technologies. With respect to the 12. Development plan of Turkiye for the years of 2024-2028 (on page 106, clause 510.3), moduler fusion technologies are to be developed. Technology has become more advanced with many sophisticated functionalities over the recent times after long period of industrial revolutions. The impact of superconductivity in the global world with technological development will be discussed mentioning the potential highlights of compact fusion reactors with the use of high temperature superconductors as the potentially disruptive Technologies in view of energy, environmental and superconducting materials. We shall explore to find the answer for the advances and potential challenges for the advances compact fusion reactor technologies together with potential technologies to be used nuclear waste treatment in the conventional fission nuclear reactors. In addition, use of superconductor technology in public transport will be discussed.

Abstract ID: 1754

Vision of Ankara University as a Leading Research Institution

Mustafa Fener[1]

[1] *Ankara University -vice Rector*

E-mail: TBD

TBD

Abstract ID: 1651

IMPLICATIONS OF CLIMATE CHANGE AND ZERO EMISSION TARGETS ON EMERGING TECHNOLOGIES

G.J. Levermore

The University of Manchester, Dept of Mechanical, Aerospace and Civil Engineering, Manchester, M13 9PL, UNITED KINGDOM
E-mail: geoff.levermore@manchester.ac.uk

Climate change, along with the rising urban heat island, is discussed leading to the fact that the UNFCCC (IPCC) 1.5C Paris target will be missed and that hopefully the temperature rise through the century, compared to pre-industrial times, will be restricted to 2C. Some scenarios are considered and the technology to support them are discussed, especially relating to improved solar PV and larger wind turbines with the importance of superconductivity to enable bigger wind turbines to be produced. Emerging technology is suggested as the solution to combating climate change rather than lifestyle change, apart from dietary alterations. The paper concludes with the ethical principles needed for equity in the world so that a robust solution to climate change can be made.

Abstract ID: 1493

ADVANCES IN QUANTUM COMPUTING, SENSING AND METROLOGY

Ziad Melhem

Oxford Quantum Solutions Ltd, Oxford, OX2 9SB, UK
E-mail: ziad.melhem@oxqsol.com

Quantum applications like quantum information processing (QIP) or quantum computing, quantum sensors, and quantum metrology research rely on the ability to build and manipulate nano-devices based on quantum principles, with an ultimate control at the level of single quantum at various operating conditions including low temperature. Quantum states can be used to perform computations, make measurements (metrology), and sense objects with a precision that far exceeds what is possible classically. The primary idea is to exploit quantum effects such as taking advantage of quantum mechanical effects, such as superposition and quantum interference. to beat the shot-noise limit in metrology and the limitation in sensing. Nanotechnology applications will be dependent on modular platforms and environments that allow probing and manipulation of matter at the nanoscale and are simple to use and manage. These environments will be used to assemble, align, and analyse functional, nano-, and microstructures leading to new innovative solutions.

This plenary talk will review recent advances in quantum computing, sensing, and metrology applications. This will include an introduction to the respective technologies and environments, primary requirements, challenges in developing quantum solutions, and current progress by industrial players in developing commercial quantum solutions.

Abstract ID: 1103

SUPERCONDUCTING DIODE EFFECT

T. Ono[1,2]

[1] *Institute for Chemical Research, Kyoto University, JAPAN*
[2] *Center for Spintronics Research Network, Kyoto University, JAPAN*
E-mail: ono@scl.kyoto-u.ac.jp

The diode effect is fundamental to electronic devices and is widely used in rectifiers and AC-DC converters. However, conventional diodes have an energy loss due to finite resistance. We found the superconducting diode effect (SDE) in Nb/V/Ta superlattices with a polar structure, which is the ultimate diode effect exhibiting a superconducting state in one direction and a normal state in the other [1-3]. SDE can be considered as the nonreciprocity of the critical current for the metal-superconductor transition. We also found the reverse effect, i.e., the nonreciprocal critical magnetic field under the application of the supercurrent [4]. We also found that the polarity of the superconducting diode shows a sign reversal as a magnetic field is increased [5], which can be considered as the crossover and phase transitions of the finite-momentum pairing states predicted theoretically [6]. SDE in Nb/V/Ta superlattices needs an application of an external magnetic field to break the time reversal symmetry, which is a disadvantage in applications. We recently succeeded in demonstrating SDE in a zero-field by introducing ferromagnetic layers in superlattices [7, 8]. The polarity of the SDE is controlled by the magnetization direction of the ferromagnetic layer, leading to development of novel non-volatile memories and logic circuits with ultralow power consumption.

This work was partly supported by JSPS KAKENHI Grant Numbers (18H04225, 18H01178, 18H05227, 20H05665, 20H05159, 21K18145), MEXT Initiative to Establish Next-generation Novel Integrated Circuits Centers (X-NICS) Grant Number JPJ011438, the Cooperative Research Project Program of the Research Institute of Electrical Communication, Tohoku University, and the Collaborative Research Program of the Institute for Chemical Research, Kyoto University.

References

[1] F. Ando *et al.*, J. Magn. Soc. Japan **43**, 17 (2019).
[2] F. Ando *et al.*, Nature **584**, 373 (2020).
[3] F. Ando *et al.*, Jpn. J. Appl. Phys. **60**, 060902 (2021).
[4] Y. Miyasaka *et al.*, Appl. Phys. Express **14**, 073003 (2021).
[5] R. Kawarazaki *et al.*, Appl. Phys. Express **15** 113001 (2022).
[6] A. Daido *et al.*, Phys. Rev. Lett. **128**, 037001 (2022).
[7] H. Narita *et al.*, Nat. Nanotechnol. **17**, 823 (2022).
[8] H. Narita *et al.*, Adv. Mater., 10.1002/adma.202304083.

Plenary Session

28.04.2024 SUNDAY

Abstract ID: 1474

SUPERBRAIN MANIFESTO

Ivan Božović[1,2]

[1]*Brookhaven National Laboratory, Upton, NY 11973, USA*
[2]*Yale University, New Haven, CT 06520, USA*
E-mail: bozovic@bnl.gov

So far, superconducting electronics have found only niche applications. The future support for research in this field hinges on envisioning products with potentially big markets.

An opportunity may have presented itself with the most dramatic event of our times: the rise of Artificial Intelligence, anticipated to penetrate all aspects of our lives. For now, AI is implemented using digital semiconductor electronics. But brains are not digital, and to emulate one neuron, one needs many transistors. Moreover, one neuron is typically connected to 10,000 or more other neurons, and such interconnectivity cannot be achieved in 2D topology.

Here, superconducting electronics offer elegant alternatives. A Josephson junction has a nonlinear *I-V* characteristic and can act like an artificial synapse. A superconducting nanowire can detect a single photon; it can receive inputs from many others by exchanging photons – i.e., at the speed of light and without energy dissipation. However, current superconducting computing is based on low-T_c superconductors, requiring complex, bulky, expensive, and power-hungry cryogenic equipment. High-T_c superconductors (HTS) could offer great improvement.

In this talk, I will review recent progress in fabricating HTS tunnel junctions, nanowires, and single-photon detectors. These devices operate at much higher temperatures, making cryogenics simpler, smaller, and cheaper. They can also reach much higher frequencies, up to the THz regime, several hundred times faster than the semiconductors, at a tiny fraction of energy cost.

We now have the building blocks for producing a table-top, HTS-based neuromorphic computer as a superb hardware platform for implementing AI on a vast scale. But reaching that goal requires substantial, focused, and sustained funding. That, in turn, would shape the future of our field and our students.

Abstract ID: 1661

TOPOLOGICAL QUANTUM MATTER: THE KAGOME FRONTIERS

M. Zahid Hasan

Department of Physics, Princeton University, Princeton, NJ 08544, USA
E-mail: mzhasan@princeton.edu

Topology plays a key role in describing quantum matter which has been greatly explored in recent decades [for an introduction, see, M.Z. Hasan & C.L. Kane Rev. Mod. Phys. 82, 3045 (2010) [1]]. In talk, I present how tuning a topological insulator featuring a Dirac fermion can be used as a platform to realize emergent Weyl fermion and "fractional" Fermi surfaces [1, 2]; and can lead to correlated magnetic, Chern, or many-body states [1-3]. The Kagome lattice which features Dirac fermions, flat bands, and van Hove singularities can serve as another platform to explore topology, superconductivity and many-body density-wave phenomena [3-7]. These novel "topological quantum matter" harbor properties that may lead to the development of next-generation quantum devices.

References

[1] M.Z. Hasan, C.L. Kane, *Topological insulators*, Rev. Mod. Phys. **82**, 3045 (2010).
[2] I. Belopolski, *et.al.*, *Discovery of topological Weyl fermion lines and drumhead surface states in a room temperature magnet*, Science **365**, 1278-1281 (2019).
[3] T. Neupert, M. Denner, J.-X. Yin, R. Thomale, M. Z. Hasan; *Charge order and superconductivity in kagome materials*, Nature Phys. **18**, 137–143 (2022).
[4] J-X. Yin, Y.-X. Jiang, X. Teng *et al.*, *Discovery of charge order and corresponding edge state in a Kagome magnet*, Phys. Rev. Lett. **129**, 166401 (2022).
[5] X. Teng, L. Chen, F. Ye *et al.*, *Discovery of charge density wave in a correlated Kagome lattice antiferromagnet*, Nature **609**, 490-495 (2022).
[6] C. Mielke, D. Das, J.-X. Yin *et al.*, *Time-reversal symmetry-breaking charge order in a kagome superconductor*, Nature **602**, 245 (2022).
[7] J. Yin, B. Lian, M.Z. Hasan, *Topological Kagome magnets and superconductors*, Nature **612**, 647-657 (2022).

Abstract ID: 1356

EFFECTS OF TOPOLOGY IN SUPERCONDUCTOR NANOARCHITECTURES

V.M. Fomin[1,2]

[1] *Institute for Emerging Electronic Technologies, Leibniz Institute for Solid State and Materials Research (IFW) Dresden, D-01069 Dresden, GERMANY*
[2] *Laboratory of Physics and Engineering of Nanomaterials, Department of Theoretical Physics, Moldova State University, MD-2009 Chişinău, REPUBLIC OF MOLDOVA*
E-mail: v.fomin@ifw-dresden.de

Nanostructures extended into the third dimension have become a hallmark of the modern research in condensed-matter physics due to the emergence of a variety of phenomena driven by geometry and topology. Recent advances of high-tech fabrication techniques, e.g., strain-driven self-rolling and focused-ion/electron-beam direct writing, have allowed for creation of geometrically complex and topologically nontrivial 3D architectures at the nanoscale, ranging from open nanotubes and Möbius stripes to nanohelices and petals, which determine novel electronic, magnetic, optical and transport properties [1 to 3]. The non-planar geometry of a nanoarchitecture leads to a submicron-scale inhomogeneity of the normal component of the magnetic field, which decisively affects the edge barriers for vortex (de)nucleation [4] and defines the nontrivial topology of screening currents [5]. A topological transition between the vortex and phase-slip regimes under a strong transport current or in a high enough magnetic field in open superconductor Nb nanotubes is manifested through a hysteresis effect [6]. Just before the transition from the upper branch to the lower one, the way of nucleation and annihilation of vortices in the region with suppressed superconductivity experiences readjustment [7] (see Fig. 1). Dynamic topological transitions and coexistence between different regimes of superconducting dynamics in open superconductor nanotubes occur under an ac-modulated transport current [8]. The effects of topology in superconductor nanoarchitectures open unprecedented potentialities for on-demand design, functionalization, and integration of nanodevices [1, 2].

This work was supported by the COST Action CA21144 "Superconducting Nanodevices and Quantum Materials for Coherent Manipulation".

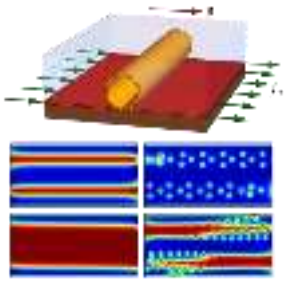

Fig. 1: *Control of the dynamics of vortices in open superconductor Nb nanotubes through the inhomogeneous normal component of the applied magnetic field* ***B****. Vortices are aligned in the areas near its maximal/minimal values. A topological transition between the vortex and phase-slip regimes leads to the novel hysteresis effect. (After [7])*

References

[1] V.M. Fomin, *Self-rolled Micro- and Nanoarchitectures: Topological and Geometrical Effects* (De Gruyter, Berlin–Boston, 2021) 148 pp.
[2] V.M. Fomin, O.V. Dobrovolskiy, Appl. Phys. Lett. **120**, 090501 (2022).
[3] J. Wang, S. Valligatla, Y. Yin, L. Schwarz, M. Medina-Sánchez, S. Baunack, C.H. Lee, R.Thomale, S. Li, V.M. Fomin, L. Ma, O.G. Schmidt, Nature Photonics **17**, 120-125 (2023).
[4] V.M. Fomin, R.O. Rezaev, O.G. Schmidt, Nano Lett. **12**, 1282-1287 (2012).
[5] R.O. Rezaev, E.I. Smirnova, O.G. Schmidt, V.M. Fomin, Communication Physics **3**, 144 (2020).
[6] I. Bogush, V.M. Fomin, Phys. Rev. B **105**, 094511 (2022).
[7] I. Bogush, V.M. Fomin, Phys. Status Solidi RRL **17**, 2300064 (2023).
[8] V.M. Fomin, R.O. Rezaev, O.V. Dobrovolskiy, Sci. Reports **12**, 10069 (2022).

Abstract ID: 1557

MAGNON ENHANCED QUANTUM TECHNOLOGIES

M.E. Flatté[1,2]

[1] *Department of Physics and Astronomy, University of Iowa, Iowa City, IA 52242, USA*
[2] *Department of Applied Physics, Eindhoven University of Technology, Eindhoven, THE NETHERLANDS*
E-mail: receipts@filingdoc.net

Quantum technologies require high-fidelity quantum information processing, such as quantum gates, and conversion of quantum information from one physical form to another. Quantum gates between fermionic qubits, such as spins, often rely on bosonic mediators such as photons or phonons. Each type of mediator has strengths and weaknesses, for example photons can be exceptionally low loss but their wavelengths at convenient (GHz) frequencies are huge, making quantum processors enormous. Over the past several years we have explored the advantages of magnons as mediators in quantum technologies. We predicted strong coupling between magnons and microwave photons [1], recently achieved in a lithographically compatible framework [2]. We further have proposed using magnons to enable micron-scale entangling gates between spin qubits [3] and as novel ``flying qubits" in a magnetic quantum bus [4]. Recently the coupling strengths relevant to such proposals have been verified [5]. I will also sketch a next step, to use exchange coupling between spin-photon interfaces and magnetic materials, and the potential of such an approach for microwave to optical quantum transduction.

Work supported by DOE BES.

References

[1] Ö.O. Soykal, M.E. Flatté, Phys. Rev. Lett. **104**, 077202 (2010).
[2] Q. Xu, H.F.H. Cheung, D.S. Cormode, T.O. Puel, S. Pal, H. Yusuf, M. Chilcote, M.E. Flatté, E. Johnston-Halperin, G.D. Fuchs, Advanced Science Early View 2310032 (2024). **https://doi.org/10.1002/advs.202310032**
[3] M. Fukami, D.R. Candido, D.D. Awschalom, M.E. Flatté, Phys. Rev. X Quantum **2**, 040314 (2021).
[4] D.R. Candido, G.D. Fuchs, E. Johnston-Halperin, M.E. Flatté, Mater. Quantum Technol. **1**, 011001 (2021).
[5] M. Fukami, J.C. Marcks, D.R. Candido, L.R. Weiss, B. Soloway, S.E. Sullivan, N. Delegan, F.J. Heremans, M.E. Flatté, D.D. Awschalom, PNAS **121**, e2313754120 (2024).

Abstract ID: 1646

ADVANCED REBCO-BASED CONDUCTORS FOR LARGE-SCALE HTS APPLICATIONS: EXPLORING LIMITS OF PERFORMANCE IN COATED CONDUCTORS

Amit Goyal[1,2,3]

[1] *Laboratory for Heteroepitaxial Growth of Functional Materials & Devices, NYS Center on Plastics Recycling Research & Innovation, New York, USA*
[2] *The RENEW (Research and Education in eNergy, Environment & Water) Institute, New York, USA*
[3] *Department of Chemical & Biological Engineering, State University of New York (SUNY) at Buffalo, New York, USA*
E-mail: agoyal@buffalo.edu

Current status related to commercialization of three platform technologies will be discussed: (1) Rolling-Assisted-Biaxially-Textured Substrates; (2) LMOe-enabled IBAD MgO Substrates technology, for fabrication of kilometer-long HTS wires and (3) Phase Separation and Strain-driven Self-Assembly technology for creating controlled nanostructures in kilometer-long wires. A majority of companies world-wide, fabricating long-lengths of HTS wires, use one or more of these technologies for fabricating the high-performance, single-crystal-like HTS wires. However, the price/performance metric of coated conductors is not yet favorable for most large-scale applications. The key to making the price/performance metric more favorable is to significantly enhance the critical current density, J_c (H,T) of coated conductors.

Engineered nanoscale defects within $REBa_2Cu_3O_{7-\delta}$ (REBCO) based coated conductors are of great interest for enhancing the performance via vortex-pinning, especially in high-applied magnetic fields. We have previously reported excellent J_c's and flux-pinning in YBCO films with self-assembled BZO columnar defects in the entire operating temperature regime from 4.2 K-77 K via correlated pinning from extended defects at mid to higher operating temperatures as well as collective pinning from oxygen point defects arising due to the local strain near YBCO/BZO interfaces at lower operating temperatures. We will report on our recent work to probe the limits of critical current density possible via defect engineering. We have obtained record values of critical current density, J_c, and pinning force, F_p, in REBCO coated conductors with selfassembled BZO nanocolumns fabricated using pulsed laser ablation. A J_c of ~175-180 MA/cm^2 at self-field and ~80-85 MA/cm^2 at 7 T was measured at 4.2 K. At 20K, J_c of ~135-140 MA/cm^2 at self-field and ~60 MA/cm^2 at 7 T was observed. A very high pinning force, F_p, of ~6 TN/m^3 and ~4 TN/m^3 were observed at 4.2 K and 20 T respectively. These are the highest values of J_c and F_p reported to date. These results establish that significant performance enhancements are possible and hence the associated reduction in costs that could potentially be realized in optimized, commercial HTS wires. In addition, we have experimentally reconfirmed the effect of local micro-strain resulting in oxygen point defects due to the large lattice-misfit between REBCO and BZO as well as the effect of Ca-doping in REBCO coated conductors to mitigate the microstrain. These results can help guide industry towards realizing significantly higher performance in commercial coated conductors or HTS wires.

Abstract ID: 1657

REMARKABLE EFFECTS OF ELECTRICITY AND MAGNETISM IN HUMAN BODY

Tarık Yazar

Ankara University, Medical Faculty, Ibn-i Sina Hospital, Ankara, TURKIYE
E-mail: yazartarik@gmail.com

As a physicist and a medical doctor, I will deliver this public lecture to make an awareness of what is actuality happening in our bodies as human beings. In my undergraduate years, I was fascinated to learn the physics of Piezo Electric Effect, and after graduation to be a physics engineer, I have also done medical school to be a specialist in the orthopedics. In my talk, I will mention the importance of Piezo electric effect, share a few real cases and the heal process in some of my patients over the last 30 years. But after having look at the wide topics of presentations in the conference program, I also noticed that there have been many other applications of superconductors (e.g. SQUID) and many other quantum applications with the use big data, and artificial intelligence (AI) together with neuromorphic computing.

Abstract ID: 1271

NON-TRIVIAL TOPOLOGICAL AND STRONGLY CORRELATED ELECTRON STATES IN MODEL-TYPE LOW-DIMENSIONAL MAGNET - SUPERCONDUCTOR HYBRID SYSTEMS

Roland Wiesendanger

Dept. of Physics, University of Hamburg, Jungiusstr. 11, 20355 Hamburg, GERMANY
E-mail: wiesendanger@physnet.uni-hamburg.de

Artificially designed and tailored materials provide a most valuable platform for revealing exciting physical phenomena in solid state systems without influences of disorder and impurity effects. The scanning tunneling microscope (STM) is one of the most powerful tools to create artificial nanostructures with each individual atom being of well-defined chemical nature and in a predetermined spatial position [1]. In this talk, I will focus on low-dimensional (1D and 2D) magnet - superconductor hybrid (MSH) systems which are fabricated from the bottom-up, atom-by-atom, by using an atomically sharp STM tip. Such low-dimensional MSH systems provide ideal platforms for realizing textbook-like physics, including the emergence of topological superconductivity [2] and associated Majorana quasiparticles [3,4], the emergence of 2D Kondo lattice physics, the quantum-mechanical projection of electronic states in nano-scale electronic cavities, as well as proximity-induced superconductivity in individual quantum levels of artificially created nano-scale quantum dots [5]. Most importantly, the emerging exotic electronic states can be revealed with unprecedented spatial-, energy-, and spin-resolution making use of spin-polarized scanning tunneling microscopy and spectroscopy [6] with superconducting and highly spin-polarized probe tips being atomically sharp and well defined [7]. As an outlook, we will discuss exciting opportunities for a bottom-up design of unconventional superconducting states based on atomically well-defined MSH systems.

References

[1] R. Wiesendanger, *Scanning Probe Microscopy and Spectroscopy: Methods and Applications*, Cambridge University Press, Cambridge (1994).
[2] L. Schneider *et al.*, Nature Physics **17**, 943 (2021).
[3] D. Crawford *et al.*, npj Quantum Materials **7**, 117 (2022).
[4] L. Schneider *et al.*, Nature Nanotechnol. **17**, 384 (2022).
[5] L. Schneider *et al.*, Nature **621**, 60 (2023).
[6] R. Wiesendanger, Rev. Mod. Phys. **81**, 1495 (2009).
[7] L. Schneider *et al.*, Science Advances **7**, eabd7302 (2021).

Abstract ID: 1650

FROM SPINTRONIC DEVICES TO QUANTUM SPIN TORQUES

Pietro Gambardella

Department of Materials, ETH Zurich, Hönggerbergring 64, 8093 Zurich, SWITZERLAND
E-mail: pietro.gambardella@mat.ethz.ch

Nonequilibrium spin and orbital currents mediate the transfer of angular momentum between neighbouring materials. Decoupling these currents from the flow of electronic charges opens avenues for the electrical control of the magnetization in both metals and insulators, encompassing ferromagnets and antiferromagnets, on short temporal and spatial scales. I will present recent results that unravel the generation, transport, and absorption of angular momenta in magnetic and nonmagnetic heterostructures, surpassing the limitations of conventional spin currents. I will also discuss the application of spin torques to perform quantum operations on individual spins. Model systems for these experiments consist of free radicals coupled to magnetic electrodes, where spin rotations and decoherence are controlled by the applied voltage and current.

Abstract ID: 1102

SUPERCONDUCTIVITY NEAR 80 K IN A BILAYER NICKELATE UNDER HIGH PRESSURE

Meng Wang

School of Physics, Sun Yat-Sen University, Guangzhou, 510275 CHINA
E-mail: wangmeng5@mail.sysu.edu.cn

High-transition-temperature (high-T_c) superconductivity in cuprates has been discovered for more than three decades, but the underlying mechanism remains a mystery. Cuprates are the only unconventional superconducting family that hosts bulk superconductivity with T_cs above the liquid nitrogen boiling temperature at 77 Kelvin. We found superconductivity in single crystals of $La_3Ni_2O_7$ grown by the high-pressure floating zone method with a maximum T_c of 80 K at pressures between 14.0-43.5 gigapascals [1,2]. Our collaborators have independently confirmed the high Tc superconductivity on our samples [3,4]. The superconducting phase under high pressure exhibits an orthorhombic structure of *Fmmm* space group with the $3d_{x2-y2}$ and $3d_{z2}$ orbitals of Ni cations strongly mixing with oxygen *2p* orbitals. Density functional theory calculations suggest the superconductivity emerges coincidently with the metallization of the σ-bonding bands under the Fermi level, consisting of the $3d_{z2}$ orbitals with the apical oxygens connecting Ni-O bilayers. The recent ARPES and infrared measurements are consistent with our theoretical expectations [5,6]. Thus, the discoveries not only reveal important clues for the high-T_c superconductivity in this Ruddlesden-Popper double-layered perovskite nickelates but also provide a new family of compounds to investigate the high-T_c superconductivity mechanism.

Reference

[1] Z. Liu, H.L. Sun, M.W. Huo, *et al.,* Sci. China-Phys. Mech. Astron. 66, 217411(2023).
[2] H.L. Sun, M.W. Huo, X.W. Hu *et al.,* Nature 621, 493-498(2023).
[3] Y.N. Zhang, M. Wang, H.Q. Yuan *et al.,* arXiv:2307.14819(2023).
[4] J. Hou, M. Wang, J.G. Cheng *et al.,* arXiv:2307.09865(2023).
[5] Z. Liu, Y.M. Dai, M. Wang, H.H. Wen *et al.,* arXiv:2307.02950(2023).
[6] J. Yang, L. Zhao, M. Wang, X.J. Zhou *et al.,* arXiv:2309.01148(2023).

Abstract ID: 1126

FERRIMAGNETIC GARNET FILMS AND NANOCOMPOSITES FOR SPINTRONIC, PHOTONIC AND MAGNETOELECTRIC DEVICES

Caroline A. Ross

Department of Materials Science and Engineering, MIT
77 Massachusetts Ave, Room 13-4005, Cambridge MA 02139, USA
E-mail: caross@mit.edu

Iron garnets (IGs) are exciting materials for spintronics, with TmIG and TbIG/Pt bilayers exhibiting interfacial DMI and field-free spin orbit torque switching, [1] and BiYIG exhibiting relativistic domain wall velocities of 4.3 km/s [2] and spin wave-driven domain wall motion [3], as well as excellent magnetooptical properties in the IR for photonic devices [4]. Garnets have an enormous range of compositions and properties, accessible by controlling the site occupancy, stoichiometry and ordering of species on the three cation sites. For example, excess rare earth raises the compensation temperature and lowers the Curie temperature [5], cation ordering in mixed garnets such as EuTmIG leads to a strong growth-induced anisotropy, and bilayer and multilayered garnets grow coherently with layers as thin as half a unit cell, exhibiting properties different from those of the end-members. Garnet/perovskite nanocomposite structures can be grown on a patterned substrate, enabling ferroelectric and ferrimagnetic behavior. We will show how engineering these remarkable materials enables a range of devices including high performance integrated photonic isolators and high speed domain wall devices.

References

[1] Caretta *et al.*, Nature Commun., **11**, 1090 (2020).
[2] Caretta *et al.*, Science **18**, 1438 (2020).
[3] Fan *et al.*, Nat. Nanotechnol. **18**, 1000 (2023).
[4] Bi *et al.*, Nat. Photonics **5**, 758 (2011).
[5] Rosenberg *et al.*, Small **2023**, 2300824 (2023).

Abstract ID: 1507

TRANSPORT PHENOMENA IN BOSE–EINSTEIN MAGNON CONDENSATES

B. Hillebrands

Fachbereich Physik and Landesforschungszentrum OPTIMAS,
Rheinland-Pfälzische Technische Universität (RPTU) Kaiserslautern-Landau,
67663, Kaiserslautern, GERMANY
E-mail: hilleb@rptu.de

The field of magnonics is seen as a path to better information processing technology [1]. The basic idea is to use magnons, the quanta of spin waves, as information carriers. Magnonic Bose-Einstein condensates, with their unique properties, are of particular interest and could serve as a crucial entity. They can be generated at room temperature, enable wave-based computational applications such as quantum classical qubit computation [2], and are spatially localized due to their zero group velocity. I will discuss the transport properties of magnon BECs via the excitation of magnon supercurrents [3-5] and address the application potential.

Funded by the Deutsche Forschungsgemeinschaft (DFG, German Research Foundation)–TRR 173/2–268565370 Spin +X (Project B04).

References

[1] P. Pirro, V.I. Vasyuchka, A.A. Serga, B. Hillebrands, Nat. Rev. Mater. **6**, 1114 (2021).
[2] M. Mohseni, V.I. Vasyuchka, V.S. L'vov, A.A. Serga, B. Hillebrands, Commun. Phys. **5**, 196 (2022).
[3] D.A. Bozhko, A.A. Serga, P. Clausen, V.I. Vasyuchka, F. Heussner, G.A. Melkov, A. Pomyalov, V.S. L'vov, B. Hillebrands, Nat. Phys. **12**, 1057 (2016).
[4] D.A. Bozhko, A.J.E. Kreil, H.Yu. Musiienko-Shmarova, A.A. Serga, A. Pomyalov, V.S. L'vov, B. Hillebrands, Nat. Commun. **10**, 2460 (2019).
[5] M.R. Schweizer, A.J.E. Kreil, G. von Freymann, B. Hillebrands, A.A. Serga, J. Appl. Phys. **132**, 183908 (2022).

Abstract ID: 1433

HIGH-PRESSURE CHALLENGES OF METALLIC HYDROGEN AND ROOM-Tc SUPERCONDUCTORS

Ho-kwang (David) Mao[1,2]

[1]*Shanghai Advanced Research in Physical Sciences, Pudong, Shanghai, 201203,CHINA*
[2]*Center for High Pressure Science and Technology Advanced Research, Haidian, Beijing, 100094, CHINA*
E-mail: maohk@hpstar.ac.cn

Elemental hydrogen under extreme pressure is of great interest to the physics community, due to its predicted pressure-induced metallization, room-temperature superconductivity and a novel quantum state combining superconductivity and superfluidity at near zero temperature. To reach such state is a formidable task that requires reaching and holding hydrogen sample at 500 GPa and characterizing its physical material properties in-situ at high pressures. The exciting goal has become an incentive for the relentless drive of high-pressure science and technology during the past 50 years. Finally the metallization of hydrogen [1] and multiple phase transitions under static compression have been reported in the recent years. The key challenges on the rich physics are now focused on the bonding structure and electron dynamics of the dense hydrogen that rely on further advancement in Xray diffraction [2], Xray spectroscopy [3], and nuclear magnetic resonance [4] up to the maximum pressure.

A by-product of the metallic hydrogen quest is its very high Debye temperature and phonon frequency leading to very high superconducting temperature (T_c). Near room-temperature T_c of 250 K was achieved in LaH_{10} which acts like an impurity doped metallic hydrogen at less extreme pressure of 170 GPa [5]. In addition to the continuous efforts to perfect the transport and magnetic measurements of superconductivity at extreme pressure [6], the experimental challenges in understanding the fundamental physics of hydrogen-dominant superconductors remain on the bonding structure and electron dynamics of the dense hydrogen surrounding the "impurity" cations.

Room-temperature superconductor is a dream material only if it could be used at ambient pressure conditions. Such prerequisite is contradictory with our fundamental understanding of hydrogen-dominant high-T_c superhydrides that require enormous pressure for dissociating the H_2 diatomic bonds to form the calculated hydrogen atomic cages. Current research community efforts are thus devoted to casting a wide combinatorial net of two-, three-, or four-component superhydrides, using chemical pressures to maximize the T_c while minimize the required external pressure. Another perspective is to seal the pressure and high-T_c superhydrides in superhard capsule [8, 9] to preserve the pressure and the corresponding superior properties for ambient applications. The final goal of room-T_c superconductor may be met halfway by combined progresses from both directions.

References

[1] P. Loubeyre, F. Occelli, P. Dumas, Nature, **577**, 631 (2020).
[2] C. Ji *et al.*, Nature, **573**, 558 (2019).
[3] B. Li *et al.*, Phys. Rev. Lett., **126**, 036402 (2021).
[4] T. Meier, D. Laniel, F. Trybel, Matter and Radiation at Extremes, **8**, 018401 (2023).
[5] A.P. Drozdov *et al.*, Nature, **569**, 528 (2019).
[6] V.V. Struzhkin, H.K. Mao, National Science Review, nwae005 (2024).
[7] F. Peng *et al.*, Phys. Rev. Lett., **119**, 107001 (2017).
[8] H.K. Mao, W.L. Mao, Matter and Radiation at Extremes, **7**, 068102 (2022).
[9] Z. Zeng *et al.*, Nature, **608**, 513 (2022).

Abstract ID: 1130

QUANTUM DYNAMICS AND TRANSPORT OF SPINS IN MAGNETS

Eiji Saitoh[1,2,3]

[1]*Department of Applied Physics, University of Tokyo, JAPAN*
[2]*ACenter for Emergent Matter Science (CEMS), RIKEN, JAPAN*
[3]*AIMR, Tohoku University, JAPAN*
E-mail: saitohlab-sec-group@g.ecc.u-tokyo.ac.jp

Spin dynamics and transport in condensed matter are key elements that contribute to various spintronics functions. Recent developments in spin measurement and spectroscopy techniques have enabled us to approach quantum spin transport and explore novel operating principles of spintronics devices. In this talk, I will introduce recent topics in quantum spin, nonlinear transport, and dynamics, as well as their applications in material property development. The topics covered will be as follows: (1) Quantum spin liquids exhibiting spin pumping and spin Seebeck effects [1,2], (2) Nuclear spin pumping and nuclear spin Seebeck effects [3,4], (3) State tomography for parametric transitions, (4) Magnon thermal squeezing, and (5) Persistent coherence beyond magnetization damping [5].

References

[1] D. Hirobe , M. Sato , T. Kawamata , Y. Shiomi , K. Uchida , R. Iguchi , Y. Koike , S. Maekawa, E. Saitoh, Nature Physics **13**, 30–34 (2017).
[2] Y. Chen , M. Sato , Y. Tang , Y. Shiomi , K. Oyanagi , T. Masuda , Y. Nambu , M. Fujita , E. Saitoh, Nature Communications **12**, 5199 (2021).
[3] Y. Shiomi , J. Lustikova , S. Watanabe , D. Hirobe , S. Takahashi , E. Saitoh, Nature Physics **15**, 22–26 (2019).
[4] T. Kikkawa , D. Reitz , H. Ito , T. Makiuchi , T. Sugimoto , K. Tsunekawa , S. Daimon , K. Oyanagi , R. Ramos , S. Takahashi , Y. Shiomi , Y. Tserkovnyak , E. Saitoh, Nature Communications **12**, 4356 (2021).
[5] T. Makiuchi *et al.*, Nature materials (accepted).

Abstract ID: 270

NEUROMORPHIC COMPUTING ARCHITECTURE USING SUPERCONDUCTING NANOWIRE SINGLE PHOTON DETECTORS AND PHASE CHANGE MEMORY MATERIALS

Orkun Hasekioglu, Atilla Hasekioglu, Adil Öztürk

TÜBİTAK Informatics and Information Security Research Center, 41400 Gebze / Kocaeli, TURKIYE
E-mail: orkun.hasekioglu@gmail.com

Computing with light using integrated optics has seen huge progress over the last 3-4 years in multiple fields such as neuromorphic computing, quantum computing and on-chip data storage. This has created a vast ecosystem that relies on high-speed reconfigurations of nanophotonic circuits (such as their use as synapses or routing applications) and ultrafast yet high-resolution, low-power photodetection. Currently, it is impossible to combine all these functionalities into an integrated platform that fits onto a single chip. In RESPITE, by utilizing superconducting Joule switches as neurons, multi-level phase change memory elements as synaptic weights, and superconducting single-photon detector arrays as retina we will demonstrate a novel platform which combines vision and cognition on a single chip. This new platform will allow in-sensor neuromorphic computing with unprecedented performance levels. The platform will have attoJoule switching power consumption, sub-nanosecond latency, and compactness.

Half-Plenary Session

28.04.2024 SUNDAY

Abstract ID: 1497

LIFSHITZ TRANSITION IN LSCO: THE EXCEPTION THAT CONFIRMS THE RULE

Neven Barišić[1,2]

[1] *Institute of Solid State Physics, TU Wien, Wiedner Hauptstraße 8, 1040 Wien AUSTRIA*
[2] *Department of Physics, University of Zagreb, Bijenička c. 32, 10000 Zagreb, CROATIA*
Email: nbarisic@phy.hr

In cuprates, experimentally established universalities of transport coefficients as well as optical conductivity have led to two simple relations that fully capture their phenomenology.First is the charge conservation relation:

$$1 + p = n_{\mathrm{loc}} + n_{\mathrm{eff}}$$

where, p is the doping while n_{eff} is the carrier density and n_{loc} is the density of localized charge within a CuO_2 plaquette. Importantly, p, n_{eff} and n_{loc} are experimentally determined directly. Second is the expression for the superfluid density:

$$\varrho_S = n_{\mathrm{eff}} \cdot (O_S\, n_{\mathrm{loc}}).$$

where O_S, is the compound-dependent constant fine-tuned by the local crystal structure. It arises from the *p–d–p* fluctuation by the Cu-localized holes visiting the neighboring planar–oxygen atoms and can be determined from NMR.

Here, we demonstrate that the measured evolution of the resistivity and Hall coefficients in cuprates can be obtained directly from the measured Fermi-surfaces solely by truncating the textbook FL integrals to the observed (doping- and temperature-dependent) Fermi arcs. Particularly instructive is the case of LSCO, which undergoes a non-universal, material-specific Lifshitz transition within the relevant doping range. Despite this complication, the calculated evolution of transport coefficients perfectly aligns with those measured.

Abstract ID: 1516

SPIN-ORBIT TORQUES WITH TWO DIMENSIONAL MATERIALS

Sergio Valenzuela

Catalan Institute of Nanotechnology, Campus UAB, ICN2 Building, Bellaterra, SPAIN
E-mail: SOV@icn2.cat

Van der Waals (vdW) heterostructures, including those comprising topological insulators (TIs) of the Bi_2Te_3 family of materials, have disruptive potential for magnetic random-access memory applications [1]. The boundary states of a TI can generate a non-equilibrium spin density to control the magnetization of a ferromagnet (FM) by means of the spin-orbit torques (SOTs). Recent reports have demonstrated large SOT efficiencies with TIs, however, to identify the microscopic mechanisms at play, as well as to maximize the SOT, a deep understanding and control of the properties of the TI/FM interface is needed. In this talk, I will first introduce the potential advantages of vdW heterostructures and of TIs for non-volatile spintronics memories. I will then describe the relevance of their boundary states and of preserving the quality of the TI/FM interface. I will show that the introduction of a (non-magnetic) metallic [2] or graphene [3] interlayer between the TI and the FM, when FM is a transition metal, can notably suppress Te diffusion into the FM and change the nature of the SOT and its efficiency [2]. Finally, I will argue that the discovery of vdW FMs, which can be grown as high-quality thin films [4,5], can further improve the TI/FM interface, as the weak vdW interaction between the TI and the vdW FM can limit chemical reactions, intermixing and electronic hybridization. Our recent results using Fe_3GeTe_2 demonstrate large SOTs and magnetization switching with currents densities about 10^{10} A/m^2 [6].

References

[1] H. Yang *et al.*, Nature **606**, 663(2022).
[2] F. Bonell *et al.*, Nano Lett. **20**, 5893 (2020).
[3] R. Galceran *et al.*, Adv. Mater. Interfaces **9**, 2201997 (2022).
[4] M. Ribeiro *et al.*, npj 2D Mater. Appl. **6**, 10 (2022).
[5] J.M.J. Lopes *et al.*, 2D Mater. **8**, 041001 (2021).
[6] T. Guillet *et al.*, Nano Lett. **24**, 822 (2024).

Abstract ID: 1358

COHERENT QUANTUM CONTROL OF MOLECULAR SPIN QUBITS

K. Kundu[1], M.V.H. Subramanya[1,2], J. Marbey[1,2], J. Hrubý[1], E. Coronado[3], A. Gaita-Ariño[3], Y. Duan[3], J. White[4], W. Evans[4], D. Ngo[5], J.R. Long[5,6], P.W. Smith[6], S. Minasian[6], J. Chen[7], S. Hoffman[7], X. Zhang[7], H.-P. Cheng[7], Stephen Hill[1,2]

[1]National High Magnetic Field Laboratory, Tallahassee, FL 32310, USA
[2]Department of Physics, Florida State University, Tallahassee, FL 32306, USA
[3]ICMOL, Universitat de Valencia, 46980 Paterna, Valencia, Spain
[4]Department of Chemistry, University of California Irvine, CA 92697, USA
[5]College of Chemistry, University of California Berkeley, CA 94720, USA
[6]Lawrence Berkeley National Laboratory, Berkeley, CA 94720, USA
[2]Department of Physics, University of Florida, Gainesville, FL 32611, USA
E-mail: shill@magnet.fsu.edu

This presentation will describe various approaches aimed at controlling the quantum dynamics of electronic spins associated with nanoscale molecular magnets, both via chemical approaches [1-4] and through high-power, broadband pulsed ESR method developments employing an arbitrary waveform generator [5]. The first approach involves the spin-orbital moments ($J = L + S$) of lanthanide ions, whereby synthetic tuning of their molecular coordination environment gives rise to so-called clock transitions (CTs) – avoided Zeeman level crossings at which the spin dynamics become desensitized to fluctuations (noise) in the local magnetic field [1]. In this way, CTs provide optimal operating points at which the electron spin dynamics decouples from the surrounding nuclear bath, leading to enhanced coherence [3]. The CT frequency can be controlled via crystal-field engineering in the case of integer spin-orbital moments [1,4], and the on-site hyperfine interaction in the half-integer case [2]. The presentation will include comprehensive results of pulsed ESR measurements [1-3] and quantum dynamics simulations [3] in order to demonstrate electron-nuclear decoupling in several different molecular spin qubit systems. The second approach involves the use of frequency chirped pulses (spanning a 1 GHz bandwidth [5]) to achieve coherent population transfer among the $2S + 1 = 8$ states associated with a spin $S = {}^7/_2$ Gd^{III} molecular qudit, a key step towards implementing simple quantum gates using such molecules [1]. Chirped pulses may also be used to achieve non-thermal spin populations among pairs of Gd^{III} Zeeman levels allowing, e.g., exceptional polarization of the $m_S = -½$ to ½ transition, which can be driven four times faster than the usual $S = ½$ qubit for a comparable drive. This and weak spin-lattice relaxation highlight the potential use of Gd^{III} spins for molecular quantum technologies.

References

[1] A. Gaita-Ariño, F. Luis, S. Hill, E. Coronado, Nat. Chem. **11**, 301 – 309 (2019).
[2] K. Kundu, S. Hill *et al.*, Nat. Chem. **14**, 392 – 397 (2021).
[3] K. Kundu, S. Hill et al., Comms. Phys. **6**, 38 (2023).
[4] R. Stewart, S. Hill et al., J. Am. Chem. Soc. (under revision, 2024).
[5] M. V. H. Subramanya, J. Marbey, K. Kundu, J. McKay, S. Hill, Appl. Magn. Reson. **54**, 165 – 181 (2023).

Abstract ID: 1489

ARTIFICIAL SUPERCONDUCTING PLATFORMS FOR QUANTUM TECHNOLOGIES

A. Braggio[1,2]

[1]*Istituto di Nanoscienze CNR-NANO, P.zza San Silvestro 12 Pisa, ITALY*
[2]*NEST, Scuola Normale Superiore, P.zza San Silvestro 12 Pisa, ITALY*
E-mail: alessandro.braggio@nano.cnr.it

The demand of fast low-consumption electronics combined with the quantum technologies requests, such as quantum computers, requires to solve complex heat management issue in multicomponent systems. In particular the recent bipolar thermoelectric effects as induced by spontaneous particle-hole symmetry-breaking [1] in gap-asymmetric superconducting tunnel junctions under a strong temperature gradient [2] could be helpful to provide on-chip power by heat harvesting. It also promises new possible applications [3-5]. Furthermore, the superconductors are optimal platforms also to realize novel quantum material exploiting the proximization capabilities of the superconductors over the electronic degrees of freedom [6,7] and novel thermoelectrical and coherent effects in topological systems [8,9].

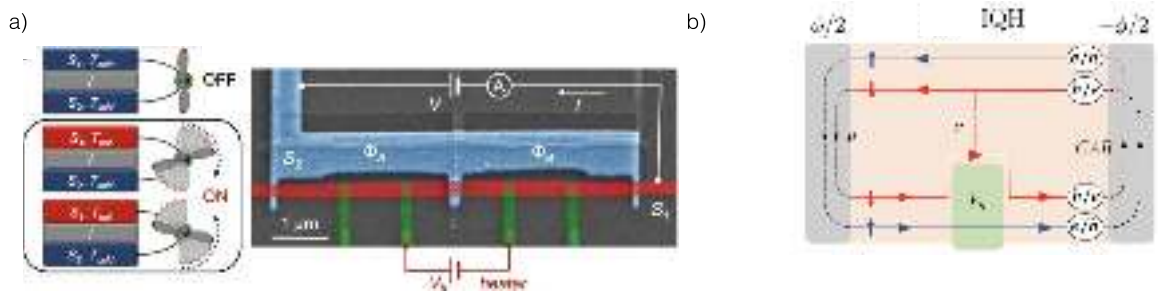

Fig. 1: *a) Bipolar thermoelectric Josephson junction[1,2] b) Topological Josephson junction (JJ) simulating a time-reversal symmetric JJ from a time reversal broken phase such as Integer Quantum Hall (IQH) [6].*

References

[1] G. Marchegiani, A. Braggio, F. Giazotto Phys. Rev. Lett. **124**, 106801 (2020).
[2] G. Germanese, F. Paolucci, G. Marchegiani, A. Braggio, F. Giazotto, Nature Nanotech. **17**, 1084 (2022).
[3] S. Battisti, G. De Simoni, L. Chirolli, A. Braggio, F. Giazotto, Phys. Rev. Research **6**, L012022 (2024).
[4] L. Bernazzani, G. Marchegiani, F. Giazotto, S. Roddaro, A. Braggio, Phys. Rev. Applied **19**, 044017 (2023).
[5] G. Germanese, F. Paolucci, G. Marchegiani, A. Braggio, F. Giazotto Patent, Filling number: 102021000032042, 21/12/2021(2021); G. Germanese, F. Paolucci, A. Braggio, F. Giazotto Patent, Filling number: 102023000001854, date:06/02/2023(2023).
[6] G. Blasi, G. Haack, V. Giovannetti, F. Taddei, A. Braggio, Phys. Rev. Research **5**, 033142 (2023).
[7] L. Chirolli, A. Braggio, F. Giazotto, arXiv:2401.04202
[8] G. Blasi, F. Taddei, L. Arrachea, M. Carrega, A. Braggio, Phys. Rev. Lett. **124**, 227701 (2020); G. Blasi, F. Taddei, L. Arrachea, M. Carrega, A. Braggio, Phys. Rev. B **102**, 241302(R) (2020).
[9] G. Blasi, F. Taddei, V. Giovannetti, A. Braggio, Phys. Rev. B **99**, 064514 (2019).

Abstract ID: 1570

SPINTRONICS WITH FERRIMAGNETIC AND ANTIFERROMAGNETIC INSULATORS

Andrew D. Kent

New York University, Department of Physics, New York, NY 10003 USA
E-mail: adk1@nyu.edu

The discovery that electric currents can excite spin waves and reverse the magnetization of a magnetic material by transporting spin angular momentum has had a significant impact on magnetism research and technology [1,2]. While the initial focus of the field was on ferromagnetic materials and magnetic tunnel junctions, new research opportunities are with materials and nanostructures with different types of magnetic order, electronic structure and geometries. In this talk, I will provide an overview of my group's experiments investigating current-induced excitation and reorientation of the Néel vector in antiferromagnetic materials, including experiments in my group on hematite (α-Fe_2O_3) thin films [3-5]. I will also discuss means of quantifying spin-torques in antiferromagnetic thin films using harmonic Hall effect, which make it possible to determine the form and magnitude of the spin-torques that act on the Néel vector [4,5]. Further, I will discuss a new type of spin Hall nanooscillator based on hybrid magnetic nanostructures, specifically ferromagnetic metal/ferrimagnetic insulator heterostructures, permalloy/epitaxial lithium aluminium ferrite [6]. These heterostructures are particularly interesting due to the very low damping of the ferrimagnetic insulators, which enables the excitation of spin-waves at lower currents and oscillators with both higher output power and quality factors. This new type of spin Hall nanooscillator has potential applications in neuromorphic computing, by enabling electrically isolated oscillators to communicate through spin waves in an extended insulating ferrimagnetic film.

References

[1] A. Brataas, A.D. Kent, H. Ohno, *Current-induced torques in magnetic materials*, Nature Materials **11**, 372 (2012).
[2] A.D. Kent, D.C. Worledge, *A new spin on magnetic memories*, Nature Nanotechnology **10**, 187 (2015).
[3] E. Cogulu, N.N. Statuto, Y. Cheng, F. Yang, R.V. Chopdekar, H. Ohldag, A.D. Kent, *Direct imaging of electrical switching of antiferromagnetic Néel order in a-Fe_2O_3 epitaxial films*, Physical Review B **103**, L100405 (2021).
[4] E. Cogulu, H. Zhang, N.N. Statuto, Y. Cheng, F. Yang, R. Cheng, A.D. Kent, *Quantifying spin-orbit torques in antiferromagnet/heavy metal heterostructures*, Physical Review Letters **128**, 247204 (2022).
[5] Y. Cheng, E. Cogulu, R.D. Resnick, J.J. Michel, N.N. Statuto, A.D. Kent, F. Yang, *Third harmonic characterization of antiferromagnetic heterostructures*, Nature Communications **13**, 3659 (2022).
[6] H. Ren, X.Y. Zheng, S, Channa, G. Wu, D.A. O'Mahoney, Y. Suzuki, A.D. Kent, *Hybrid spin Hall nano-oscillators based on ferromagnetic metal/ferrimagnetic insulator heterostructures*, Nature Communications **14**, 1406 (2023).

Abstract ID: 1587

ADVANCES IN APPLICATION OF PROCESS INFORMATICS FOR IRON-BASED SUPERCONDUCTORS

A. Yamamoto[1,5], S. Tokuta[1,5], A. Ishii[2,5], Y. Shimada[3,5], S. Hata[3,5], K. Iida[4,5], A. Yamanaka[1,5]

[1] Tokyo University of Agriculture and Technology, Tokyo 184-8588, JAPAN
[2] NIMS, Tsukuba 305-0047, JAPAN
[3] Kyushu University, Fukuoka 816-8580, JAPAN
[4] Nihon University, Narashino 275-8575, JAPAN
[5] JST-CREST, Kawaguchi 332-0012, JAPAN
E-mail: akiyasu@cc.tuat.ac.jp

Iron-based superconductors (IBSs) are a promising candidate for strong magnet applications owing to their high upper critical field with small electromagnetic anisotropy [1] and large critical angle [2]. In particular, 122-phase IBSs have attracted attention and high critical current density [3-5] exceeding 10^7 A/cm^2 and prototypes of tesla-class magnets were reported [6,7]. In this talk, we report the recent progress on the advanced materials science integrated with data science, such as fully convolutional neural network for micro-phase analysis [8], a tailored software BOXVIA for data-driven process design [9,10] and multiscale nano/micro-structural analysis with integrated modeling [11,14], for the processing of spark plasma sintered polycrystalline K-doped Ba122-phase superconductors which were synthesized from mechanochemically prepared precursor by high energy milling [15-17].

Acknowledgement

This work was supported by JST CREST (JPMJCR18J4).

References

[1] H. Hosono *et al.*, Materials Today **21**, 278 (2018).
[2] T. Katase *et al.*, Nat. Commun. **2**, 409 (2011).
[3] K. Iida, D. Qin, C. Tarantini, T. Hatano, C. Wang, Z. Guo, H. Gao, H. Saito, S. Hata, M. Naito, A. Yamamoto, NPG Asia Materials **13**, 68 1-9 (2021).
[4] D. Qin, K. Iida, T. Hatano, H. Saito, Y. Ma, C. Wang, S. Hata, M. Naito, A. Yamamoto, Phys. Rev. Mat. **5**, 014801 (2021).
[5] D. Qin, K. Iida, Z. Guo, C. Wang, H. Saito, S. Hata, M. Naito, A. Yamamoto, Super. Sci. Technol. Letters **35**, 09LT01 (2022).
[6] J.D. Weiss *et al.*, Supercond. Sci. Technol. Fast Track Commun. **28**, 112001 (2015).
[7] H.W. Ding *et al.*, Supercond. Sci. Technol. Letters **36**, 11LT01 (2023).
[8] Y. Hirabayashi, H. Iga, H. Ogawa, S. Tokuta, Y. Shimada, A. Yamamoto, npj Comput. Mater. **10**, (2024).
[9] A. Ishii, R. Kamijyo, A. Yamanaka, A. Yamamoto, SoftwareX **18**, 101019 (2022).
[10] A. Ishii, S. Kikuchi, A. Yamanaka, A. Yamamoto, J. Alloys Compd. **966**, 171613 (2023).
[11] Y. Shimada, S. Tokuta, A. Yamanaka, A. Yamamoto, T.J. Konno, J. Alloys Compd. **923**, 166358 (2022).
[12] Z. Guo, K. Muraoka, H. Gao, Y. Shimada, T. Harada, S. Tokuta, Y. Hasegawa, A. Yamamoto, S. Hata, Acta Materialia **266**, 119648 1-9 (2024).
[13] A. Ishii, A. Yamanaka, E. Miyoshi, Y. Okada, A. Yamamoto, MSMSE **29**, 065012 (2021).
[14] A. Ishii, A. Yamamoto, A. Yamanaka, STAM Method **3**, 2239133 (2023).
[15] S. Tokuta, A. Yamamoto, APL Materials **7**, 111107 1-6 (2019).
[16] S. Tokuta, Y. Shimada, A. Yamamoto, Super. Sci. Technol. **33**, 094010 (2020).
[17] S. Tokuta, Y. Hasegawa, Y. Shimada, A. Yamamoto, iScience **25**, 103992 (2022).

Abstract ID: 1506

DYNAMICS OF TOPOLOGICAL SPIN TEXTURES

M. Garst

Institute of Theoretical State Physics & Institute of Quantum Materials and Technology, Karlsruhe Institute of Technology, 76131 Karlsruhe, GERMANY
E-mail: markus.garst@kit.edu

Topological strings are effectively one-dimensional objects that can be found in diverse systems such as domain walls in magnetic films, vortex filaments in fluids or, potentially, cosmic strings in the universe. Usually, these stringlike objects can elastically bend and twist, and this elasticity also determines their dynamical behavior at low energies. A particular example are magnetic skyrmions that are smooth topological textures of the magnetization that are localized within a two-dimensional plane. They arise in magnetic systems that lack inversion symmetry where they are stabilized by the Dzyaloshinskii-Moriya interaction. In bulk materials, magnetic skyrmions extend in the third direction forming an effective string.

These strings can be dynamically excited resulting in various vibrational modes. We provide an overview of the dynamics of skyrmion strings [1], that can be found in chiral magnets like MnSi or FeGe, and we compare theoretical predictions with magnetic resonance spectroscopy [2], spin-wave spectroscopy [3], inelastic neutron scattering [4] and Brillouin light scattering [5]. At low energies the dynamics is determined by an effective elasticity theory. We show that a single string supports non-linear solitary waves [6] similar to vortex filaments in fluids. Moreover, these strings can be destabilized by spin currents flowing along the string direction thus providing a mechanism to topologically unwind these topological textures [7].

References

[1] M. Garst, J. Waizner, D. Grundler, J. Phys. D: Appl. Phys. **50**, 293002 (2017).
[2] T. Schwarze *et al.,* Nat. Mater. **14**, 478 (2015).
[3] S. Seki *et* al., Nat. Commun. **11**, 256 (2020).
[4] T. Weber *et al.*, Science **375**, 1025 (2022).
[5] P. Che, R. Ciola, M. Garst, D. Grundler *et al,* in preparation.
[6] V.P. Kravchuk *et al.*, Phys. Rev. B **102**, 220408(R) (2020).
[7] S. Okumura, V.P. Kravchuk, M. Garst, Phys. Rev. Lett. **131**, 066702 (2023).

Abstract ID: 1535

SURFACE SUPERCONDUCTIVITY AND TOPOLOGY IN THE WEYL SEMI METAL $PtBi_2$

Prof. Dr. Bernd Büchner

IFW Dresden, Helmholtzstraße 20, Dresden, GERMANY
E-mail: b.buechner@ifw-dresden.de

By means of angle-resolved photoemission spectroscopy (ARPES) and ab initio calculations, we identify topological Fermi arcs on two opposing surfaces of the non-centrosymmetric Weyl material trigonal $PtBi_2$. We show these states become superconducting at temperatures around 10 K. Remarkably, the corresponding coherence peaks appear as the strongest and sharpest excitations ever detected by photoemission from solids. Superconductivity is also found in our STM measurements showing in addition spatial inhomogeneity of the superconducting gap. In some samples superconducting gaps as large as 20 meV are revealed by STM resembling the phenomenology found in high-T_c superconductors. However bulk probes such as magnetization, transport and thermodynamics do not show superconductivity. This is consistent with the absence of gaps in bulk electronic states measured by ARPES. Our findings indicate that superconductivity in $PtBi_2$ can occur exclusively at the surface, rendering it a possible platform to host Majorana modes in intrinsically topological superconductor–normal metal–superconductor junctions.

Abstract ID: 1499

MUTUAL SYNCHRONIZATION OF SPIN HALL NANO-OSCILLATORS FOR ISING MACHINES AND NEUROMORPHIC COMPUTING

J. Åkerman[1,2,3]

[1]*Department of Physics, University of Gothenburg, Gothenburg 412 96, SWEDEN*
[2]*Center for Science and Innovation in Spintronics, Tohoku University, 2-1-1 Katahira, Aoba-ku, Sendai 980-8577 JAPAN*
[3]*Research Institute of Electrical Communication, Tohoku University, 2-1-1 Katahira, Aoba-ku, Sendai 980-8577 JAPAN*
E-mail: johan.akerman@physics.gu.se

Mutually synchronized spin hall nano-oscillators (SHNOs) [1,2] have emerged as one of the most promising types of spintronic devices for neuromorphic computing as individual SHNOs in large arrays can be voltage [3] and memristor [4] controlled. Very recently, the first experimental steps towards SHNO-based Ising Machines were also taken [5], and their potential was evaluated theoretically [6]. In my talk, I will describe the general idea behind Ising Machines and some of the existing implementations such as D-Waves Quantum Annealer and the Optical Coherent Ising Machine from NTT Research. I will then discuss how we have tried to build similar Ising Machines using SHNO arrays. I will describe the key elements required for such an SHNO-based Ising Machine, including much larger mutually synchronized SHNO arrays of up to 15,000 oscillators and individual electrical, memristive, and optical [7] control of SHNOs. Time permitting, I will also discuss our work on spin wave and surface acoustic wave based Ising Machines [8,9].

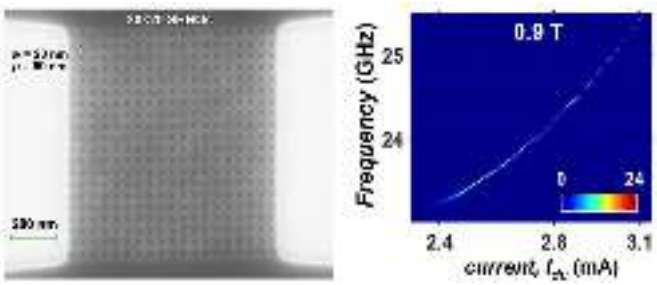

Fig. 1: *Left) Scanning electron micro-graph of a 20 × 20 nano-constriction SHNO array with width w = 20 nm and a center-to-center separation of p = 50 nm. Right) Power spectral density (PSD) of the magnetization auto-oscillation of an array of 15,000 mutually synchronized SHNOs.*

References

[1] A.A. Awad *et al.*, Nature Physics **13**, 292 (2017).
[2] M. Zahedinejad *et al.*, Nature Nanotechnology **15**, 47 (2020).
[3] H. Fulara *et al.*, Nature Communications **11**, 4006 (2020).
[4] M. Zahedinejad *et al.*, Nature Materials **21**, 81 (2022).
[5] A. Houshang *et al.*, Physical Review Applied **17**, 014003 (2022).
[6] B.C. McGoldrick *et al.*, Physical Review Applied **17**, 014006 (2022).
[7] S. Muralidhar *et al.*, Applied Physics Letters **120**, 262401 (2022).
[8] A. Litvinenko *et al.*, Communications Physics **6**, 227 (2023).
[9] A. Litvinenko *et al.*, arXiv:2311.06830 (2023).

Abstract ID: 1353

ORBITAL CURRENT GENERATION AND LONG DISTANT DIFFUSIVE PROPAGATION

YoshiChika Otani[1,2], Weiguang Gao[1], Junyeon Kim[2]

[1] *Center for Emergent Matter Science, RIKEN, Wako, Saitama, JAPAN*
[2] *Institute for Solid State Physics, The University of Tokyo, Kashiwa, Chiba, Tokyo, JAPAN*
E-mail: yotani@riken.jp & yotani@issp.u-tokyo.ac.jp

The emerging field of spintronics is currently focused on exploring the potential of electron orbital angular momentum (OAM) as a functionality analogous to electron spin. Recently, it has been discovered that nonequilibrium OAM accumulation can be generated through both the interfacial orbital Edelstein effect (OEE) [1,2] and the bulk orbital Hall effect (OHE) [3]. Notably, these conversions between charge and orbital states do not necessitate spin-orbit interaction.

In our study, we present compelling evidence of both direct and inverse OEE in lateral transport structures. These structures include interfaces of orbital accumulation generator/detector Al2O3/Cu and detector/injector ferromagnetic nanowires. Through systematic exploration of separation distance and Cu thickness dependencies, our findings demonstrate that the conversion adheres to the Onsager reciprocity relation. Furthermore, we observe an orbital diffusion length exceeding 110 nm, indicating the existence of a lateral orbital transport channel at the Al2O3/Cu interface.

Our experimental results not only contribute to a foundational understanding of OAM manipulation but also establish a basis for the future precise control of OAM in spintronics applications.

References

[1] J. Kim, *et al.*, Phys. Rev. B **103(2)**, L020407 (2021).
[2] J. Kim, *et al.*, Phys. Rev. Matter. **7(11)**, L111401 (2023).

HTS Cuprates: Advances in Fundamentals and Experimental Studies I

28.04.2024 SUNDAY

Abstract ID: 1330

SMALL POCKETS AND THE ORIGIN OF THE LOW SUPERFLUID DENSITY IN THE UNDERDOPED CUPRATES

N. Harrison[1], M. K. Chan[1,2]

[1]*Los Alamos National Labs, Los Alamos, New Mexico 87545, USA*
[2]*National Science Foundation, 2415 Eisenhower Avenue Alexandria, Virginia 22314, USA*
E-mail:nharrison@lanl.gov

The underdoped high temperature superconducting cuprates have been shown to exhibit anomalously small carrier and superfluid densities in the pseudogap regime, together with an approximate scaling of the superconducting transition temperature with the density of doped holes [1,2]. One possibility that has been suggested is that the Fermi surface upon which pairing occurs consists of small Fermi surface pockets. Angle-resolved photoemission spectroscopy has only seen Fermi surface arcs instead of pockets [3], whereas quantum oscillation studies have revealed small pockets only at very low temperatures inside what is thought to be a charge-density wave state [4]. Here, we report using angle-resolved magnetoresistance oscillation measurements at very high temperatures above T_c, revealing direct evidence for small Fermi surface pockets in this regime. Such an observation tightly constrains possible models for the pseudogap and enables us to understand the origin of the small superfluid density.

References

[1] Y.J. Uemura *et al.*, Phys. Rev. Lett. **62**, 2317 (1989).
[2] S. Badoux *et al.*, Nature **531**, 210 (2016).
[3] M.R. Norman *et al.*, Nature **392**, 157 (1998).
[4] S.E. Sebastian, N. Harrison, G.G. Lonzarich, Rep. Prog. Phys. **75**, 102501 (2012).

CANCELLED

Abstract ID: 1444

CHARGE ORDER NEAR THE ANTIFERROMAGNETIC QUANTUM CRITICAL POINT IN A TRILAYER HIGH T_c CUPRATE

V. Oliviero[1], I. Gilmutdinov[1], D. Vignolles[1], S. Benhabib[1], N. Bruyant[1], A. Forget[2], D. Colson[2], W.A. Atkinson [3], C. Proust[1]

[1]LNCMI-EMFL, CNRS UPR3228, Univ. Grenoble Alpes, Univ. Toulouse, INSA-T, Grenoble and Toulouse, FRANCE
[2]Service de Physique de l'Etat Condensé, CEA Saclay (CNRS-URA 2464), Gif sur Yvette 91191, FRANCE
[3]Department of Physics and Astronomy, Trent University, Peterborough, K9L 0G2, Ontario, CANADA
E-mail: vincent.oliviero@lncmi.cnrs.fr

One of the surprising features of cuprate superconductors is the extent to which the interplay between antiferromagnetic order (AFM), charge density waves (CDW), and superconductivity is ubiquitous across different families [1]. High magnetic field transport measurements provide a powerful technique to study the underlying Fermi surface. The discovery by Quantum Oscillations (QO) of a small electron pocket in the CDW state of underdoped $YBa_2Cu_3O_{6+x}$ [2] and single-layer $HgBa_2CuO_{4+\delta}$ [3] was recently followed by the observation of small hole pockets deep in the AFM doped Mott phase of 5- and 6-layer cuprates [4,5]. Multilayer cuprates are a valuable avenue for exploring the interplay between these orders: in the underdoped trilayer $HgBa_2Ca_2Cu_3O_{8+\delta}$ (Hg1223) [5], both signatures of CDW and AFM orders are present at p = 0.08 - 0.09.

In this talk, I will present a new high magnetic field study of Hg1223 at higher doping (p = 0.10 - 0.11) where, for the first time in a cuprate superconductor, we are able to infer a Fermi surface reconstruction from an AFM state (hole pockets) to a biaxial charge density wave state (electron pocket). This phase transition is tracked at low temperature in the QO spectrum and in the Hall effect, and our interpretation is based on numerical simulations that account for the three-layered structure of Hg1223.

References

[1] B. Keimer, S. Kivelson, M. Norman, S. Uchida, J. Zaanen, *From quantum matter to high-temperature superconductivity in copper oxides*, Nature **518**, 179 (2015).

[2] N. Doiron-Leyraud, C. Proust, D. LeBoeuf, *et al.*, *Quantum oscillations and the fermi surface in an underdoped high-T_c superconductor*, Nature **447**, 565 (2007).

[3] N. Barisic, S. Badoux, M.K. Chan, *et al.*, *Universal quantum oscillations in the underdoped cuprate superconductors*, Nature Phys. **9**, 761 (2013).

[4] S. Kunisada, S. Isono, Y. Kohama *et al.*, *Observation of small fermi pockets protected by clean CuO_2 sheets of a high-T_c superconductor*, Science **369**, 833 (2020).

[5] K. Kurokawa, S. Isono, Y. Kohama *et al.*, *Unveiling phase diagram of the lightly doped high-T_c cuprate superconductors with disorder removed*, Nature communications, **14(1)**, 4064 (2023).

[6] V. Oliviero, S. Benhabib, I. Gilmutdinov, *et al.*, *Magnetotransport signatures of antiferromagnetism coexisting with charge order in the trilayer cuprate $HgBa_2Ca_2Cu_3O_{8+\delta}$*, Nature Comm. **13**, 1568 (2022).

Abstract ID: 1593

RESILIENCE OF THE MOTT INSULATING STATE OF La_2CuO_4 AGAINST PHOTODOPING

J. Demsar

Institute of Physics, Johannes Gutenberg University Mainz, 55128 Mainz, GERMANY
E-mail: demsar@uni-mainz.de

We study transient photo-doping phenomena in La_2CuO_4, an archetypal antiferromagnetic Mott insulating parent compound of the cuprate high-T_c superconductor. We capture the dynamics of the transient state by tracking the time-evolution of THz photoconductivity and the complex dielectric function $\varepsilon(\omega,t)$ from 0.5 – 2.6 eV in optically-thin films upon optical excitation across the charge transfer (CT) gap, coving a large range of excitation densities from 0.001 to ~0.12 absorbed photons [electron-hole (e-h) pairs] per Cu. Analysis of $\Delta\varepsilon(\omega,t)$ demonstrates in a pronounced photoinduced reduction of the CT gap concomitant with the appearance of mid-infrared absorption and a weak free carrier response, all simultaneously relaxing on a (sub)picosecond scale. Up to the highest excitation densities, where at comparable chemical-doping levels a metallic state is realized, the free carrier contribution remains negligible, underscoring the robustness of the underlying electronic correlations. Recovery is density-independent up to 0.01 e-h pairs per Cu. The low free-carrier spectral weight and the overall fast recombination suggest that relaxation proceeds via pair-wise recombination of nearly bound e-h pairs through multi-magnon emission. At densities beyond 0.01 e-h pairs per Cu the relaxation rate starts to increase, which we attribute to melting of the antiferromagnetic background and many-body recombination.

HTS Cuprates: Advances in Fundamentals and Experimental Studies II

28.04.2024 SUNDAY

Abstract ID: 1480

VISUALIZING THE CUPRATE PAIR DENSITY WAVE STATES AND PERIODIC LATTICE DISPLACEMENTS

Kazuhiro Fujita

Condesed Matter Physics and Materials Science Department, Brookhaven National Laboratory, Upton, NY 11973, USA

E-mail: kfujita@bnl.gov

In this talk, we will review recent developments of the Spectroscopic Imaging Scanning Tunneling Microscopy (SI-STM) studies for the cuprate superconductors. Firstly, recent studies of the resonant X-ray scattering on the cuprate superconductors have revealed a strong renormalization of the phonon dispersion, indicating that the cuprate Charge Density Wave (CDW) state couples to the lattice degree of freedom [1]. We introduce a novel Scanning Tunneling Microscopy (STM) based technique to directly visualize a local lattice distortion of the $Bi_2Sr_2CaCu_2O_{8+\delta}$. This technique revealed a spatial modulation of the lattice distortion that is coupled to the unidirectional d-symmetry CDW in the pseudogap states [2].

Secondly, another recent discovery is the pair density wave states in the cuprate pseudogap states. The defining characteristic of Cooper pairs with finite center-of-mass momentum is a spatially modulating superconducting energy gap $\Delta(\boldsymbol{r})$, which is predicted to exist in the cuprates as the pair density wave (PDW) state. Although Cooper-pair tunneling has detected indirect evidence of a cuprate PDW, the definitive signature in single-electron tunneling of a periodic $\Delta(\boldsymbol{r})$ modulation has never been observed. Here, using a new approach, we discover strong $\Delta(\boldsymbol{r})$ modulations in $Bi_2Sr_2CaCu_2O_{8+\delta}$ that have eight-unit-cell periodicity or wavevectors $\boldsymbol{Q}\sim 2p/a_0(1/8,0)$; $2p/a_0(0,1/8)$ [3].

Finally, we will discuss how such a PDW impact on the local-density-of-states $N(\boldsymbol{r},E)$. In addition, we will talk about a relationship of the $N(\boldsymbol{r},E)$ modulation to the lattice structure and discuss how they are linked to the phonon anomalies detected in the recent X-ray measurements [4].

This work was done in collaboration with Zengyi Du, Hui Li Sanghyun Joo, Elizabeth P. Donoway, Jinho Lee, J. C. Séamus Davis, Genda Gu, Peter D. Johnson, Abhay N. Pasupathy, John M. Tranquada. *These works were supported by the US Department of Energy, Office of Basic Energy Sciences, contract No. DEAC02-98CH10886.*

References

[1] W.S. Lee *et al.*, Natutre. Phys. **17**, 53 (2021).
[2] Z. Du *et al.*, Phys. Rev. X **13**, 021025 (2023).
[3] Z. Du and H. Li *et al.*, Nature **580**, 65-70 (2020).
[4] Z. Du *et al.*, J. of Phys. Soc. of Jpn. **90**, 111003 (2021).

Abstract ID: 1229

VORTEX MASS DETERMINATION IN YBaCuO USING THz CIRCULARLY POLARIZED LIGHT

M. Šindler[1], R. Tesař[1], C. Kadlec[1], J. Koláček[1], P. Lipavský[2], Wen-Yen Tzeng[3], Chih-Wei Luo[4–6], Jiunn-Yuan Lin[6]

[1]*Institute of Physics, Czech Academy of Sciences, 18200 Prague 8, CZECH REPUBLIC*
[2]*Faculty of Mathematics and Physics, Charles University, 121 16, Prague 2, CZECH REPUBLIC*
[3]*Department of Electronic Engineering, National Formosa University, Yunlin 632, TAIWAN*
[4]*Department of Electrophysics, National Yang Ming Chiao Tung University, Hsinchu 30010, TAIWAN*
[5]*National Synchrotron Radiation Research Center, Hsinchu, 30076, TAIWAN*
[6]*Institute of Physics, National Yang Ming Chiao Tung University, Hsinchu 30010, TAIWAN*
E-mail: sindler@fzu.cz

The determination of the mass of Abrikosov vortices in superconductors is a long standing issue. Whereas the theoretical approximations span over 8 orders of magnitude, only two experimental evaluations had been previously performed, one using an electro-acoustic method [1], the second one magneto-optical imaging [2]. Here we demonstrate a method of its detection in $YBa_2Cu_3O_{7-d}$ films.

Our method is inspired by the standard determination of cyclotron mass of charge carriers in semiconductors in magnetic field through measuring the cyclotron resonance. In the case of vortices, we probe their interaction with circularly polarized far-infrared light under external magnetic field of up to ±10 T. It differs for the clockwise and anti-clockwise polarized light cases, resulting in the so-called circular dichroism, which manifests itself as a difference in the transmittance of the light through the superconducting sample. We propose a model to relate the ratio of transmittances of opposite helicity or alternatively of opposite magnetic field to the mass of the vortices [4].

We have investigated thin $YBa_2Cu_3O_{7-d}$ films of various doping – underdoped, optimally doped and overdoped ($Y_{0.7}Ca_{0.3}Ba_2Cu_3O_{7-\delta}$) case. All samples used in this study were prepared by pulsed laser deposition. The sample parameters have been determined by usual techniques (DC resistivity and standard time-domain THz spectroscopy [5]) or taken from the literature. With such inputs, we show that the theory of the vortex mass developed by Kopnin and coworkers [6] matches our experimental data without any additional fitting parameter. Kopnin's theory assumes vortex mass as a complex tensor, which reflects a delay between a change of the vortex velocity and a change of the total momentum of quasiparticles in its core. In the DC limit, all values become purely real.

References

[1] V.D. Fil *et al.*, Low Temp. Phys. **33**, 1019 (2007).
[2] D. Golubchik *et al.*, Phys. Rev. B **85**, 060504 (2012).
[3] R. Tesař *et al.*, Sci. Rep. **11**, 21708 (2021).
[4] R. Tesař *et al.*, https://doi.org/10.48550/arXiv.2312.00652
[5] M. Šindler *et al.*, https://doi.org/10.48550/arXiv.2309.17408
[6] L.N. Kopnin, V.M. Vinokur, Phys. Rev. Lett. **81**, 3952 (1998).

Abstract ID: 1403

MULTI-BAND SUPERCONDUCTIVITY, POLARONS AND THE STEEP BAND/FLAT BAND SCENARIO

Annette Bussmann-Holder

Max-Planck-Institute for Solid State Research, Heisenbergstr. 1, D-70569 Stuttgart, GERMANY
E-mail: a.bussmann-holder@fkf.mpg.de

The basic features of multi-band superconductivity and its implications are derived. In particular, it is shown that enhancements of the superconducting transition temperature take place due to interband interactions, which substantially enhance the effective electron-electron coupling. In addition, the isotope effects differ markedly from the typical BCS scheme as soon as polaronic coupling effects are present. Special cases of the model are polaronic coupling in one band as realized e.g. in cuprates, coexistence of a flat band and a steep band like in MgB_2, crossovers between extreme cases. The advantages of the multiband approach as compared to the single band BCS model are elucidated and its rather frequent realization in actual systems is discussed.

Topological Quantum Matter I

28.04.2024 SUNDAY

Abstract ID: 1420

NON-HERMITIAN TOPOLOGICAL PHASES OF QUANTUM MATTER

W.B. Rui[1,2], Z.D. Wang[1,2]

[1]*Department of Physics and HK Institute of Quantum Science & Technology, The University of Hong Kong, Hong Kong, CHINA*
[2]*Quantum Science Center of Guangdong-Hong Kong-Macau Great Bay Area, Shenzhen, CHINA*
E-mail: zwang@hku.hk

Symmetry plays a key role in exploring many topological phases. In this talk, non-Hermitian spatial symmetries, a class of symmetries that have no counterparts in Hermitian systems, and particularly how normal and exceptional topological semimetals can be stabilized by these symmetries, will be elaborated. Different from internal ones, spatial symmetries act nonlocally in momentum space and enforce global constraints on both band degeneracies and topological quantities at different locations. Notably, the nonlocal Hermitian conjugate pair of exceptional or normal band degeneracies may be enforced by non-Hermitian spatial symmetries. Remarkably, it is found that these pairs lead to the symmetry-enforced violation of the Fermion doubling theorem in the long-time limit. On the other hand, for time-reversal and sublattice symmetries, there are six ramified symmetry classes leading to novel topological classifications with various non-Hermitian skin effects. As artificial crystals are the main experimental platforms for non-Hermitian physics, there exists the symmetry barrier for realizing topological physics in the six ramified symmetry classes. Here we present a general mechanism to cross the symmetry barrier. Using the general mechanism, we systematically construct spinless models for all non-Hermitian spinful topological phases in one and two dimensions, which are experimentally realizable. Our work suggests that gauge structures may significantly enrich non-Hermitian physics at the fundamental level.

The work was supported by the NSFC/RGC JRS grant (RGC Grant No. N_HKU774/21), the CRF (Grant No. C6009-20G) and GRF (Grant Nos. 17310622 &17303023) of Hong Kong.

References

[1] W.B. Rui, Z. Zheng, C.J. Wang, Z.D. Wang, Phys. Rev. Lett. **128**, 226401 (2022).
[2] W.B. Rui, Y.X. Zhao, Z.D. Wang, Phys. Rev. Lett. **131**, 176402 (2023).

Abstract ID: 225

INTERPLAY OF TOPOLOGY AND GEOMETRY IN FRACTIONAL QUANTUM HALL LIQUIDS

Kun Yang

Florida State University, USA
E-mail: kunyang@magnet.fsu.edu

Fractional Quantum Hall Liquids (FQHL) are the ultimate strongly correlated electron systems, and the birth place of topological phase of matter. Early theoretical work has emphasized the universal or topological aspects of quantum Hall physics. More recently it has become increasingly clear that there is very interesting bulk dynamics in FQHL, associated with an internal geometrical degree of freedom, or metric. The appropriate quantum theory of this internal dynamics is thus expected to take the form of a "quantum gravity", whose elementary excitations are spin-2 gravitons. After briefly reviewing the topological aspect of FQHL, I will discuss in this talk how to probe the presence of this internal geometrical degree of freedom experimentally in the static limit, and detect the graviton excitation in spectroscopic measurements, in particular how to reveal its chirality. Comparison will be made with recent experimental and numerical work, and discussions on future experimental probe of the graviton chirality as well as its significance will be presented.

Abstract ID: 1436

QUANTUM TRANSPORT AND FRACTIONAL HALL EFFECT IN MOIRÉ CORRELATED/ANTICORRELATED CHANNELS

Farzaneh Shayeganfar[1,2], Ali Ramazani[3]

[1]*Department of Aerospace Engineering, University of Michigan, Ann Arbor, Michigan 10485 USA*
[2]*Department of Physics and Energy Engineering, Amirkabir University of Technology, Tehran, IRAN*
[3]*Department of Mechanical Engineering, Massachusetts Institute of Technology, Cambridge, MA 02139, USA*
E-mail: fshayega@umich.edu

Twisted bilayer graphene (tBLG) including interlayer interaction and rotational disorder shows anomalous electronic transport as a function of twist-angles (tAs). Quantum criticality of metal-insulator transitions of twisted nanostructures has been recently discovered and characterized by their transport measurement [1]. In this work, we address a new perspective of hybridization of fermions in twisted graphene nanoribbons (tGN) by representing a physical map of electronic properties and electronic transport of circular (with anticorrelated surfaces) and rectangular (with correlated surfaces) twisted tGN channels for two regimes of small and large tAs. Analysis of band structure reveals a phase transition of metal to semiconductor occurs in rectangular (correlated) case, sweeping small tAs to large ones. Local flat bands at the AA stacking of small and magic angles of circular (anticorrelated) twisted nanoribbons are formed by effective hybridization of local fermion momenta as f-orbitals and itinerant conduction electrons as c-orbitals, while electrons of extended topological conduction bands are responsible for transport and delocalization. This implies a different transport mechanism; where he energy resolved transmission of circular (anticorrelated) channels reveals pseudo-band and pseudo-gap depending on tAs. Moreover, rectangular channels with correlated surfaces indicate more electronic transmission than anticorrelated counterparts with wider pseudo-bands. Furthermore, the hybridization of f- and c- orbitals create the fractional Hall conductivity of circular (anticorrelated) tGNs. This study probes exotic quantum states in twisted van der Waals (vdW) homostructure with correlated/anticorrelated interfaces, engineering the quantum transport of twisted nanoribbons as building blocks for future quantum circuits and Hall sensors.

CANCELLED

Abstract ID: 1027

TEMPERATURE-DEPENDENT XRD AND NEXAFS ON $Ta_2Ni(Se,S)_5$ AND $Ta_2(Ni,Co)Se_5$

Nour Maraytta[1], Peter Nagel[1,2], Fatemeh Ghorbani[1], Santanu Pakhira[1], Amir Ghiami[1,2], Matthieu Le Tacon[1], Stefan Schuppler[1,2], Amir-Abbas Haghighirad[1], Michael Merz[1,2]

[1]*Institute for Quantum Materials and Technologies, Karlsruhe Institute of Technology, Kaiserstr. 12, 76131 Karlsruhe, GERMANY*
[2]*Karlsruhe Nano Micro Facility (KNMFi), Karlsruhe Institute of Technology, Kaiserstr. 12, 76131 Karlsruhe, GERMANY*
E-mail: nour.maraytta@kit.edu

The excitonic insulator (EI) is a a coherent electronic phase which was predicted to be realized in narrow gap semiconductors and semimetals with small band overlap driven by poorly screened coulomb interaction between conduction band electrons and valence band holes [1, 2]. Ta_2NiSe_5 is one of the few promising candidates for an EI. The compound undergoes a second order structural phase transition from an orthorhombic (*Cmcm*) to a monoclinic (*C2/c*) phase at $T_C \sim 328$ K [3]. A semimetal-to-insulator (SI) transition is observed at T_C which is associated with an EI transition due to electronic correlations [4, 5]. The EI scenario in Ta_2NiSe_5 is supported by optical measurements [4], X-ray photoemission spectroscopy (XPS), angle resolved photoemission spectroscopy (ARPES) [6], and by band structure calculations [7].

With S substitution for Se in Ta_2NiSe_5, the transition temperature decreases and the magnitude of the band gap increases towards the BEC side of the phase diagram. On the other hand, for $Ta_2(Ni,Co)Se_5$, both the transition temperature and the magnitude of the semi-metallic band gap are reduced, suggesting that Co substitution drives the system towards the BCS side of the phase diagram [4, 8].

Here, we will present a combined study of (i) temperature-dependent SXRD and (ii) NEXAFS on Ta_2NiSe_5, Ta_2NiS_5, and $Ta_2Ni_{0.9}Co_{0.1}Se_5$. Our SXRD data show a clear 2nd order structural phase transition in Ta_2NiSe_5 and $Ta_2Ni_{0.9}Co_{0.1}Se_5$, while no structural change was found in Ta_2NiS_5 down to 80 K. The transition is accompanied with a shortening in the bond lengths which increases the hybridization between the relevant Ta, Ni, and Se orbitals. This agrees well with our NEXAFS data: a stronger hybridization is seen for Ta_2NiSe_5 and $Ta_2Ni_{0.9}Co_{0.1}Se_5$ together with a significant T-dependent change of the spectral weight and, thus, a T-dependent charge transfer between these orbitals is observed. In contrast, the in- and out-of-plane spectra of Ta_2NiS_5 are predominatly isotropic and thus, no T-dependent charge transfer between the corresponding orbitals is observed. The results from our SXRD and NEXAFS studies are fully consistent with and show strong indications for an excitonic insulator scenario in Ta_2NiSe_5 and $Ta_2Ni_{0.9}Co_{0.1}Se_5$ whereas this can be ruled out for Ta_2NiS_5.

References

[1] N.F. Mott, Phil. Mag. **6**, 287 (1961).
[2] D. Jerome, T.M. Rice, W. Kohn, Phys. Rev. **158**, 462 (1967).
[3] S.A. Sunshine, J.A. Ibers, Inorg. Chem. **24**, 3611 (1985).
[4] Y.F. Lu, Nat. Commun. **8**, 14408 (2017)
[5] K. Katsumi, Phys. Rev. Lett. **130**, 106904 (2023).
[6] M.D. Watson, Phys. Rev. Research **2**, 013236 (2020)
[7] T. Kaneko, Phys. Rev. B **87**, 035121 (2013).
[8] T. Mitsuoka, J. Phys. Soc. Jpn **89**, 124703 (2020).

Topological Quantum Matter II

28.04.2024 SUNDAY

Abstract ID: 1560

EFFECT OF NANOPATTERNING ON FILMS IN THE VICINITY OF SUPERCONDUCTOR-INSULATOR TRANSITION

A. Yu. Mironov[1,2], D.A. Nasimov[1], V.M. Vinokur[2]

[1] *A.V. Rzhanov Institute of Semiconductor Physics, 630090 Novosibirsk, RUSSIA*
[2] *Terra Quantum AG, 9400 Rorschach, SWITZERLAND*
E-mail: mironov@isp.nsc.ru

We present the results of the study of low-temperature linear and non-linear transport properties of disordered nanopatterning NbTiN film. Nanopatterning enables the transformation of a thin superconducting NbTiN film into a system of superconducting and insulating islands or wires. The simplest objects of this kind are perforated films and arrays of superconducting islands in an insulating matrix. Nanoperforation drives the critically disordered superconducting film into an insulating state, which transits into a superinsulating one upon decreasing temperature. However, it is impossible to convert a superconducting film far from the superconductor-insulator transition into an insulating film using nanoperforation. The creation of superconducting islands in an insulating matrix allows both to convert any superconducting film into a superinsulating system and to create a superconducting one based on the initially insulating system. Note that the transport properties of such systems periodically depend on the magnetic field. Superinsulating wires, in turn, make it possible to dramatically enhance the capacitive and inductive characteristics of the system, which is important for the creation of various quantum cryogenic devices, such as qubits or SQUIDS

Fig. 1: *(a) Sample structure and SEM images of the disordered nanoperforated NbTiN film, (b) Temperature dependence of resistance of initial and perforated films (c) Color plot of the differential conductance as function of the magnetic field and the dc bias*

Abstract ID: 206

ELECTRIDE PROPERTIES INDUCING A FLAT BAND IN THE SC PHASE OF MAGNESIUM UNDER HIGH PRESSURE

Sabri Elatresh

King Fahd University of Petroleum and Minerals (KFUPM), Dhahran, SAUDI ARABIA
E-mail: sabri.elatresh@kfupm.edu.sa

The magnesium phase diagram has garnered significant attention due to its structural properties, electride formation, and melting behavior. Recent observations reveal multiple crystal structure transitions in magnesium, including non-close-packed phases at extreme pressures [1]. In this study, we employ a structure prediction method based on the liquid state, coupled with first-principles calculations, to reassess the solid-phase stability of the Sc phase in magnesium. Furthermore, we delve into the analysis of electride formation and its role in the creation of a flattened band structure.

Acknowledgment

This work is supported by King Fahd University of Petroleum and Minerals (KFUPM), Saudi Arabia, Deanship of Scientific Research. S. E extends gratitude to all the authors of reference [1] for insightful discussions.

References

[1] M.G. Gorman, S.F. Elatresh, A.E. Lazicki, M. Cormier, D. McGonegle, R. Briggs, A.L. Coleman, S. Rothman, L. Peacock, J. Bernier, Y. Ping, F. Coppari, D. Braun, G.W. Collins, J.H. Eggert, J.S. Wark, S. Bonev, M.I. McMahon, *Crystal structures of magnesium electrides at terapascal pressures*, Nature Physics ISSN 1745-2481 (2022).

Abstract ID: 226

NEW PHYSICS OF OLD GRAPHITE

A. Mishchenko

Department of Physics and Astronomy, The University of Manchester, Oxford Road, Manchester, UK
E-mail: artem.mishchenko@gmail.com

Our team has re-examined an old natural mineral – graphite – and revealed plenty of new unconventional physics harbouring there. In this talk, I will delve into these surprising findings in graphite, hoping to inspire further exploration and potential applications in this material.

First, by applying the van der Waals technology to graphite crystals, we made devices with exceptional electronic quality, which led to the discovery of a new type of quantum Hall effect (QHE). This novel QHE, which we refer to as 2.5 dimensional, or 2.5D QHE persists even in films of graphite hundreds of graphene layers thick and shows striking dependence on layer number parity [1]. While in thinner graphite films, a number of exotic phenomena like fractional 2.5D QHE, magnetic ordering, and spontaneous valley polarisation, were observed, opening new avenues towards future quantum technologies.

Second, in addition to van der Waals technology we utilized crystallographic alignment – a technique behind burgeoning field of twistronics – to control the topology of electronic states at the graphite surface via m moiré superlattices. To our surprise, changes in the surface states of graphite drastically changed the bulk states as well – in high magnetic fields, fractal states of Hofstadter's butterfly penetrate deep into the bulk of graphite – leading to the discovery of 2.5D fractal QHE [2]. Our work paves the way to novel control of 3D materials using the approach of twistronics, borrowed from 2D research field.

Last but not least, I will discuss how the control of interlayer stacking between graphene layers provides a pathway to program quantum properties of graphite films. For instance, tuning the stacking order allowed us to fabricate films of rhombohedral graphite and study their transport properties for the first time ever, which resulted in discovery of strong electronic correlations typically unattainable in such simple systems as graphite [3, 4]. Control of the stacking order provides an alternative approach to program quantum properties of layered crystals, and without the need for moiré superlattices of twistronics.

References

[1] J. Yin, S. Slizovskiy, Y. Cao, *et al.*, *Dimensional reduction, quantum Hall effect and layer parity in graphite films*, Nat. Phys. **15**, 437 (2019).

[2] C. Mullan, S. Slizovskiy, J. Yin, *et al.*, *Mixing of moiré-surface and bulk states in graphite*, Nature **620**, 756 (2023).

[3] Y. Yang, Y.-C. Zou, C.R. Woods, *et al.*, *Stacking order in graphite films controlled by van der waals technology*, Nano Letters **19**, 8526 (2019).

[4] Y. Shi, S. Xu, Y. Yang, *et al.*, *Electronic phase separation in multilayer rhombohedral graphite*, Nature **584**, 210 (2020).

Abstract ID: 1423

STUDY OF THE ORDER PARAMETER OF A SUPERCONDUCTOR MODIFIED BY ADATOMS AND MOLECULES

Nicolás Lorente

Centro de Física de Materiales (CSIC-EHU), Donostia International Physics Center, Donostia – San Sebastián, ESPAGNE

E-mail: Nicolas.lorente@ehu.eus

We have studied the in-gap states induced by magnetic impurities on an s-wave superconductor. This is a fascinating subject that creates new electronic structures and new properties on a superconductor. In the present work, we have focused on the quantum phase transitions that appear when the interaction between the magnetic impurity and the superconductor is so strong that leads to a change of the wave function of the ground state of the full system. This can be studied by following the evolution of the order parameter (or gap) as a function of the interaction and the number of impurities on the susbtrate. Our findings reveal that the order parameter not only reflects the fundamental characteristics of the superconductor but also provides insights into the topology of the resultant band structure induced within it.

Quantum Spin and Magnetism in Chiral Materials: CISS Effect, Solitons and Skyrmions I

28.04.2024 SUNDAY

Abstract ID: 1096

THERMALLY INDUCED DYNAMICS OF MAGNETIC SKYRMIONS AND THEIR DEVICE FUNCTIONS

Masahito Mochizuki, Xichao Zhang, Jun Matsuki

Waseda University, Dept. of Applied Physics, Okubo, Shinjuku-ku, Tokyo, 169-8555, JAPAN
E-mail: masa_mochizuki@waseda.jp

Thermally induced dynamics of magnetic topology in magnets has turned out to host rich phenomena and device functions, which are subjects of intensive studies in the research of spintronics recently. In this presentation, we discuss following two phenomena related with thermal motion of skyrmions, which were revealed in our recent theoretical studies.

Heat-electricity conversion with skyrmions in the presence of thermal gradient [1,2]. A confined skyrmion crystal exhibits rotational motion when a radial temperature gradient is present due to an inverse effect of the topological magnon Hall effect [2]. We discuss that this thermally induced rotational motion of skyrmions can be exploited for the DC-voltage generation. A moving skyrmion texture generates a spinmotive force perpendicular to its moving direction. Consequently, the rotational motion of skyrmions confined in a circular disk generates DC electric voltage in the radial direction. The proposed phenomenon can be exploited as spintronic thermoelectric devices to realize the heat-electricity conversion.

Active-matter-like behaviors of skyrmions due to the chiral Brownian motion [3]. Skyrmions as chiral objects show chiral nature in interactions with nanostructures, which can lead to intriguing phenomena. We discuss that the Brownian dynamics of skyrmions interacting with a chiral flower-like obstacle in a ferromagnet exhibits topology-dependent outcomes, which can be regarded as a spontaneous mesoscopic order-from-disorder phenomenon driven by thermal fluctuations. This phenomenon can be utilized to control the skyrmion position and distribution without any external driving force and can be exploited as a new way to design topology-sorting devices.

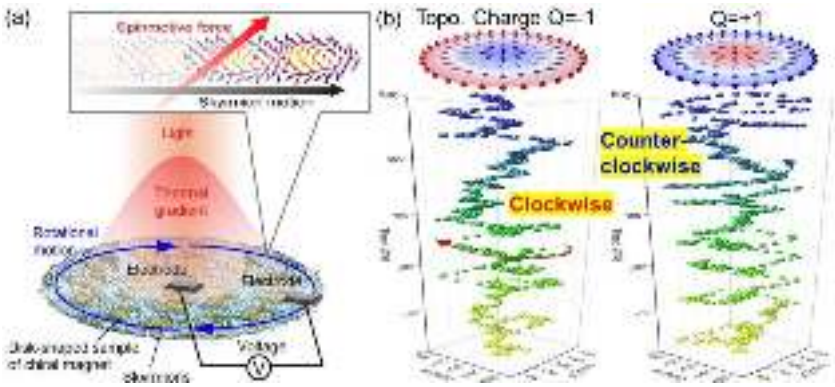

Fig. 1: *(a) Schematics of the thermoelectric effect of magnetic skyrmions (b) Chiral Brownian motion of skyrmions as a source of active-matter-like behaviors.*

References

[1] J. Matsuki, M. Mochizuki, Phys. Rev. B **107**, L100408 (2023).
[2] M. Mochizuki *et al.*, Nature Materials **13**, 241 (2014).
[3] X. Zhang, M. Mochizuki et al., Nano Letters **23**, 11793 (2023).

Abstract ID: 1194

SPIN-WAVE PROPAGATION THROUGH A TUNABLE-WIDTH NANOCONSTRICTION

E. Fourneau, C. Delforge, N. Lejeune, A.V. Silhanek

Université de Liège, EPNM, QMAT, CESAM, Liège, BELGIUM
E-mail: emile.fourneau@uliege.be

Spin waves are collective oscillations of electron spins propagating in any magnetically ordered material and transporting spin currents. The manipulation of spin waves holds intriguing similarities to light optics, offering the potential to emulate the functionality of bulky optical devices at the microscopic scale while remaining compatible with conventional microelectronics. The creation of such devices involves thin film nanostructuring through doping or precise structural modifications [1]. Therefore, exploring topographically complex waveguides has been identified as an essential step towards advanced manipulation possibilities, such as graded refractive index spin-wave structures for steering or focusing.

In this work, we investigate the propagation of spin waves through in-situ lithographed nanoconstrictions. By performing spin wave spectroscopy experiments coupled with AFM lithography, we manage to characterize the efficiency of spin wave transmission while locally shrinking the waveguide. Supported by micromagnetic simulations, we demonstrate that within a certain width range of a central constriction, decreasing the size of the constriction actually increases the signal transmission (i.e., the minimum transmission is not obtained for zero-width junctions). We speculate that this unexpected minimum arises from the interference between the wave transmitted by dipolar magnetic coupling through the gap of the constriction and the wave diffracted by the constriction. Notably, the interference pattern can be altered by adjusting the constriction geometry and is influenced by the wavelength of the incident wave, providing a broad spectrum of tuning parameters for potential applications.

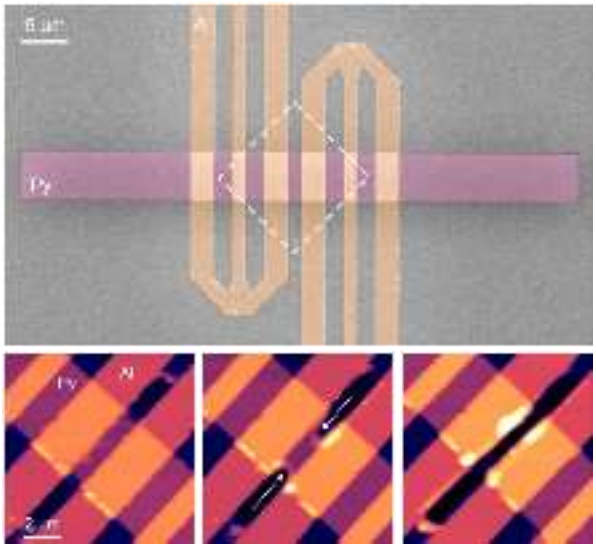

Fig. 1: *False-colored SEM image of the propagation spin-wave spectroscopy setup showing Al antennas and a 5-µm-wide Py waveguide (top panel). The three bottom panels present AFM topography of the junction at different stages of the in-situ etching of the constriction.*

References

[1] M. Kiechle, *et al.*, Small **19**, 220793 (2023).

Abstract ID: 1161

CHIRAL-INDUCED UNIDIRECTIONAL SPIN-TO-CHARGE CONVERSION

A. Moharana[1], Y. Kapon[2], F. Kammerbauer[1], D. Anthofer[1], S. Yochelis[2], Y. Paltiel[2], A. Wittmann[1]

[1] *Johannes Gutenberg University, Mainz, GERMANY*
[2] *Hebrew University Jerusalem, ISRAEL*
E-mail: a.wittmann@uni-mainz.de

The observation of spin-dependent transmission of electrons through chiral molecules has led to the discovery of chiral-induced spin selectivity. The remarkably high efficiency of the spin polarizing effect in chiral molecules has recently gained significant interest due to the high potential for novel sustainable hybrid chiral molecule magnetic applications. However, the fundamental mechanisms underlying the chiral-induced phenomena at the hybrid molecule-metal interface remain to be understood fully.

In our work, we explore the impact of chirality on spin angular momentum in hybrid metal/chiral molecule thin film heterostructures. For this, we inject a pure spin current from a ferromagnetic insulator at ferromagnetic resonance and investigate the effective interfacial spin-orbit coupling at the hybrid chiral interface. Notably, we observe a chiral-induced unidirectionality in the spin-to-charge conversion. Furthermore, angle-dependent measurements reveal that the spin selectivity is maximum when the spin angular momentum is aligned with the chiral axis.

Our findings validate the central role of spin angular momentum for the chiral-induced spin selectivity effect, paving the path toward three-dimensional functionalization of hybrid molecule-metal devices via chirality.

References

[1] R. Naaman *et al.*, Nat. Rev. Chem. **3**, 250 (2019).

Quantum Spin and Magnetism in Chiral Materials: CISS Effect, Solitons and Skyrmions II

28.04.2024 SUNDAY

Abstract ID: 1370

TRULY CHIRAL PHONON AND PHONON ANGULAR MOMENTUM

Jun-ichiro Kishine, Takuya Satoh, Yoshihiko Togawa, Hiroaki Kusunose

The Open Univ. Japan, Chiba, JAPAN
E-mail: kishine@ouj.ac.jp

Recently, there has been increased interest in studying how the chirality of materials interacts with the angular momentum carried by phonons in crystal structures. This research aims to uncover new material functionalities by utilizing the inherent diversity of quantum numbers in matter and transmitting them through phonons.

The main question driving this investigation is: How do vibrations in crystals (phonons) reveal the chirality of the material? While the profound impact of chirality on properties like magnetism and conductivity in molecules and crystals is well-known, the study of how chirality affects phonons has gained attention only in recent years.

In this presentation we seek to clarify the connection between crystal chirality and phonon angular momentum, providing a simpler understanding of chirality in materials. We will explore this link through a theoretical framework and recent Raman scattering experiments conducted on chiral crystals. Our goal is to define chiral phonons clearly and demonstrate the relationship between the pseudo-angular momentum of chiral phonons and the spin of photons in Raman scattering. This attempt will contribute to the broader discussion on the role of chirality in material properties and open new routes for advancements in the design and application of chiral materials.

References

[1] K. Ishito, H. Mao, Y. Kousaka, Y. Togawa, S. Iwasaki, T. Zhang, S. Murakami, J.-I. Kishine, T. Satoh, Nature Physics **19**, 35 (2023).
[2] A. Kato, J.-I. Kishine, J. Phys. Soc. Jpn. **92**, 075002 (2023).
[3] Y. Togawa, A.S. Ovchinnikov, J.-I. Kishine, J. Phys. Soc. Japan **92**, 081006 (2023).
[4] Y. Togawa, A.S. Ovchinnikov, J. Kishine, J. Phys. Soc. Japan **92**, 081006 (2023).
[5] J.-I. Kishine, H. Kusunose, H.M. Yamamoto, Israel J. Chem. **62** (11-12), e202200049 (2022).
[6] K. Ishito, H. Mao, K. Kobayashi, Y. Kousaka, Y. Togawa, H. Kusunose, J. Kishine, T. Satoh, Chirality **35**, 338 (2023).

Abstract ID: 1524

SPIN RELAXATION, DIFFUSION AND EDELSTEIN EFFECT IN CHIRAL METAL SURFACE

Yuta. Suzuki[1], Yusuke Kato[1,2]

[1] *The University of Tokyo, Dept. of Physics, 113-0083, Tokyo, JAPAN*
[2] *The University of Tokyo, Dept. of Basic Science, 153-8902, Tokyo, JAPAN*
E-mail: yusuke@phys.c.u-tokyo.ac.jp

Motivated by recent reports on chirality-induced-spin-selectivity (CISS) in metals [1-4] and a superconductor [5], we study electron spin transport at spin-splitting surface of chiral-crystalline-structured metals and Edelstein effect at the interface, by fully solving the linearized Boltzmann transport equation [6]. We first define spin relaxation time and spin diffusion length for two-dimensional systems with anisotropic spin–orbit coupling through the spectrum of the integral kernel in the collision integral. We then explicitly take account of the interface between the chiral metal and a nonmagnetic metal with finite thickness. For this composite system, we derive analytical expressions for efficiency of the charge current–spin current interconversion as well as other coefficients found in the Edelstein effect. We also develop the Onsager's reciprocity in the Edelstein effect in accord with experiments so that it relates local input and output, which are respectively defined in the regions separated by the interface. We finally provide a transfer matrix corresponding to the Edelstein effect through the interface, with which we can easily represent the Onsager's reciprocity as well as the charge–spin conversion efficiencies we have obtained. We confirm the validity of the Boltzmann transport equation in the present system starting from the Keldysh formalism. Our scheme is particularly useful to study the spin transport at the interface and in the bulk system with an anisotropic spin-orbit-coupling. It also applies to the Rashba model and other spin-splitting systems.

References

[1] A. Inui, R. Aoki, Y. Nishiue, K. Shiota, Y. Kousaka, H. Shishido, D. Hirobe, M. Suda, J.-i. Ohe, J.-i. Kishine, H.M. Yamamoto, Y. Togawa, Phys. Rev. Lett. **124**, 166602 (2020).
[2] Y. Nabei, D. Hirobe, Y. Shimamoto, K. Shiota, A. Inui, Y. Kousaka, Y. Togawa, H.M. Yamamoto, Appl. Phys. Lett.**117**, 052408 (2021).
[3] K. Shiota, A. Inui, Y. Hosaka, R. Amano, Y. Ōnuki, M. Hedo, T. Nakama, D. Hirobe, J.-i. Ohe, J.-i. Kishine, H.M. Yamamoto, H. Shishido, Y. Togawa, Phys. Rev. Lett. **127**, 126602 (2021).
[4] H. Shishido, R. Sakai, Y. Hosaka, Y. Togawa, Appl. Phys. Lett. **119**, 182403 (2021).
[5] R. Nakajima, D. Hirobe, G. Kawaguchi, Y. Nabei, T. Sato, T. Narushima, H. Okamoto, H.M. Yamamoto, Nature **613**, 479 (2023).
[6] Y. Suzuki, Y. Kato, Phys. Rev. B **107**, 115305 (2023).

Abstract ID: 1016

INDUCING A TUNABLE SKYRMION-ANTISKYRMION SYSTEM THROUGH ION BEAM MODIFICATION OF FeGe FILMS

M.B. Venuti[1], Xiyue S. Zhang[2], Eric J Lang[3], Sadhvikas J. Addamane[4], Hanjong Paik[6–8], Portia Allen[1], Peter Sharma[5], David Muller[2,6], Khalid Hattar[4,9], Tzu-Ming Lu[4], Serena Eley[1,10]

[1]*Department of Physics, Colorado School of Mines, Golden, CO USA*
[2]*Department of Applied Physics, Cornell University, Ithaca, NY USA*
[3]*Department of Nuclear Engineering, University of New Mexico, Albuquerque, NM USA*
[4]*Center for Integrated Nanotechnologies, Sandia National Laboratories, Albuquerque, NM USA*
[5]*Sandia National Laboratories, Albuquerque, NM USA*
[6]*Platform for the Accelerated Realization, Analysis, and Discovery of Interface Materials, Cornell University, Ithaca, NY USA*
[7]*School of Electrical & Computer Engineering, University of Oklahoma, Norman, OK USA*
[8]*Center for Quantum Research and Technology, University of Oklahoma, Norman, OK USA*
[9]*Department of Nuclear Engineering, University of Tennessee, Knoxville, TN USA*
[10]*Department of Electrical & Computer Engineering, University of Washington, Seattle, WA USA*
E-mail: serename@uw.edu

Skyrmions are nanoscale whirlpools of magnetic moments that arise in certain magnetic materials and are potentially useful as information carriers in next-generation low-energy spintronic devices. To exploit skyrmions in spintronics, we must be able to controllably manipulate them, which necessitates understanding how to create, annihilate, and move them. It also requires understanding how the skyrmion lattice is affected by disorder, dictating how skyrmions will either maneuver around or be pinned by energy barriers within the material's disorder landscape. Here, we report on a systematic study of the effects of disorder on the skyrmion phase in FeGe films. Specifically, we irradiate epitaxial B20-phase FeGe films with 2.8 MeV Au^{4+} ions at varying fluences, inducing varying sizes and densities of amorphous regions within the crystalline matrix. Using low-temperature electrical transport and magnetization measurements, we observe a strong topological Hall effect with a double-peak feature that may serve as a signature of skyrmions and antiskyrmions. These results may contribute to the development of information storage devices that use skyrmions and anitskyrmions as storage bits.

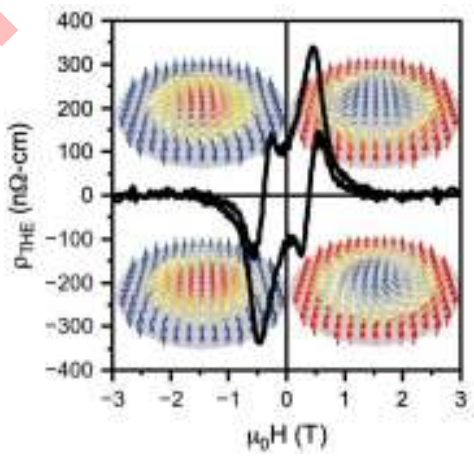

Fig. 1: *Topological Hall resistivity at 100 K of ion-irradiated FeGe film. Each quadrant is labelled with the corresponding topological spin texture type and polarization associated with the peak in that region.*

CANCELLED

Abstract ID: 214

ENHANCEMENT OF INTRINSIC SPIN HALL EFFECT IN CHIRAL TOPOLOGICAL SEMIMETALS

Wei Jiang

School of Physics, Beijing Institute of Technology, Beijing, CHINA
E-mail: tj.jwei@gmail.com

The spin Hall effect (SHE), which transduces charge current into spin current, is one of the essential cornerstones of spintronics. Here we propose a new intrinsic SHE (ISHE) enhancement mechanism in topological semimetals with high Chern numbers, and present a series of promising material candidates with large intrinsic spin Hall conductivities (ISHC) and spin Hall angles (SHA) for potential spintronic applications. By way of model Hamiltonian calculations and statistical analysis of 260 non-magnetic semimetals with chiral crystal structure, we unravel a positive correlation between the maximum Chern number and the ISHE, i.e., the ISHC and, under specific conditions, the SHA. Such positive correlations in topological gapless systems represent a novel mechanism to enhance ISHE, distinct from the conventional spin-orbit induced anticrossing mechanism in gapped systems. Additionally, our first-principles calculations of 38 chiral topological semimetals from space group 198, which can support zero-dimensional nodes with the highest Chern number (C = 4), reveal multiple realistic materials with large ISHC and even larger SHAs than Pt. Our discovery not only enriches the fundamental understanding of SHE but also provides an ideal material system conducive to efficient charge-to-spin conversion applications.

Superconducting, Magnetic, Topological Arsenides and Tellurides

28.04.2024 SUNDAY

Abstract ID: 1191

ANOMALOUS METALLIC OXYGEN BAND IN THE POTENTIAL SUPERCONDUCTOR $KCa_2Fe_4As_4O_2$

N.S. Pavlov[1,2], K.S. Pervakov[2], I.A. Nekrasov[1,2]

[1]*Institute of Electrophysics UB RAS, 620016, Yekaterinburg, RUSSIA*
[2]*Lebedev Physical Institute RAS, 119991, Moscow, RUSSIA*
E-mail: pavlovns@gmail.com

After the discovery of superconductivity in self-doped iron-based 1144 ($KCaFe_4As_4$ [1,2]) and 12442 ($KCa_2Fe_4As_4F_2$ [3]) systems in 2016 many other compound was synthesized and investigated. Most of the studies of 12442 systems with oxygen contain 3+ and 1+ cations. And we decide to investigate a hole self-doped iron-based potential superconductor $KCa_2Fe_4As_4O_2$ with 2+ (Ca) and 1+ (K) cations. The electronic structure, magnetism and Fermi surface of $KCa_2Fe_4As_4O_2$ were studied by a first-principes DFT/GGA approach [4]. The self-doping value is obtained from DFT is 0.75 hole on Fe-3d states for $KCa_2Fe_4As_4O_2$. Surprisingly, for the $KCa_2Fe_4As_4O_2$ it was found that except the Fe-3d bands the O-2p bands also cross the Fermi level (Fig. 1). In general, the O-2p states are usually fully occupied in transition metal oxides. Here it is not the case due to the fact that CaO layer gives some of the electrons to the FeAs layer, thus leaving O-2p states partially occupied. The O-2p states form additional Fermi surface sheet with propeller-like shape around Γ-point and modify the Fe-3d Fermi surface sheets due to the hybridization. To prove the presence of an anomalous metallic O-2p band in $KCa_2Fe_4As_4O_2$, a comparative study with 12442 systems ($KCa_2Fe_4As_4F_2$, $RbGd_2Fe_4As_4O_2$, $CsSm_2Fe_4As_4O_2$) was performed. Finally, the main differences between the appearance of the metallic O-2p band in the case of $KCa_2Fe_4As_4O_2$ and in the case of $LaBaCuO_4$ and $YBa_2Cu_3O_7$ cuprate superconductors were studied in detail. Thus $KCa_2Fe_4As_4O_2$ is a potential superconductor with unusual properties.

This work was supported in part by Russian Science Foundation, grant No. 23-12-00307.

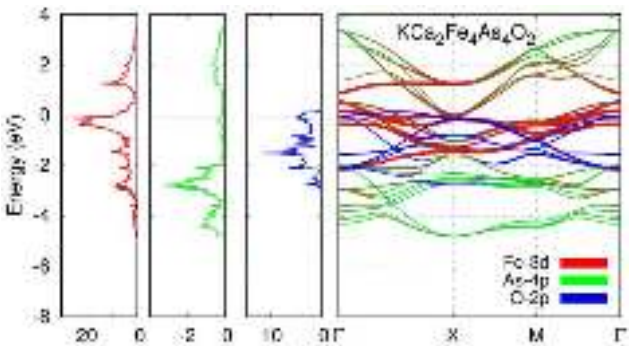

Fig. 1: DFT/GGA *density of states (left) of $KCa_2Fe_4As_4O_2$ and band structure (right) with contribution of Fe-3d, As-4p and O-2p states.*

References

[1] A. Iyo, K. Kawashima, T. Kinjo, T. Nishio, *et al.*, J. Am. Chem. Soc. **138**, 3410 (2016).
[2] D. Mou, T. Kong, W.R. Meier, F. Lochner, *et al.* Phys. Rev. Let. **117**, 277001 (2016).
[3] Z.C. Wang, C.Y. He, S.Q. Wu, Z.T. Tang, *et al.* J. Am. Chem. Soc. **138**, 7856 (2016).
[4] N.S. Pavlov, K.S. Pervakov, I.A. Nekrasov, Comput. Mater. Sci. **218**, 111916 (2023).

Abstract ID: 1198

PHASE SEPARATION IN SINGLE CRYSTALS OF AFM SEMIMETAL $EuSn_2As_2$

Alena Yu. Degtyarenko[1], Alexander L. Vasiliev[2], Nikita Pavlov[3], Alexey V. Ovcharov[4], Vladimir I. Bondarenko[2], Andrey V. Sadakov[1], Kirill S. Pervakov[1], Vladimir M. Pudalov[1]

[1] *V.L. Ginzburg Centre for High-Temperature Superconductivity and Quantum Materials P.N. Lebedev Physical Institute of the RAS, 53, Leninsky ave., 119991 Moscow, RUSSIA*
[2] *Shubnikov Institute of Crystallography of Federal Scientific Research Centre "Crystallography and Photonics" of the RAS, 59 Leninsky ave., Moscow 119333, RUSSIA*
[3] *Institute for Electrophysics of the RAS, 106 Amundsen St., Ekaterinburg, 620016, RUSSIA*
[4] *National Research Centre "Kurchatov Institute", 1 Kurchatov Sq, Moscow 123182, RUSSIA*
E-mail: degtyarenkoayu@lebedev.ru

Currently, layered van-der Waals materials with non-trivial band structure and magnetic ordering of the host lattice are in the focus of research interest. The object of our studies, the layered semimetal $EuSn_2As_2$, below 24 K experiences an AFM ordering of the Eu sublattice in the ab-plane [1-3]. This compound manifests a number of remarkable features in magnetic properties, DC-transport and electron spin resonance. Particularly, in DC-magnetization, a weak nonlinearity is observed in low fields (< 0.03T) applied in the easy ab-plane, the AC susceptibility in ab-plane often shows an upturn towards lowest temperatures in the same low field interval [3, 4-6] and in the electron spin resonance measurements the ESR spectrum contains an additional line [7] that is irrelevant to the AFM resonance. In this work, we experimentally found these puzzling features to originate from the presence of rare planar nanodefects embedded into the bulk AFM single crystal. By HRTEM we determined that the planar defects extend by about 5μm in the ab-plane and consist of three layers of Eu atoms with Sn- and a reduced number of As-atoms between them. By a combination of EDX, HRTEM, and EELS we identified the local phase as $EuSnAs_2$. Due to a reduced distance between the Eu layers in the planar nanodefect, the Eu atoms experience a weak FM-type ordering below ~25 K. Our high resolution magnetization measurements in weak fields indeed revealed a ferromagnetic type hysteresis, whereas the DFT calculations of the defect confirmed the weak in-plane ferromagnetic moment. The presence of the FM nanodefects in the bulk AFM crystal is responsible for the above features in transport and magnetic properties. On the other hand, such natural metamaterial is an interesting object for studies and even might find practical applications.

This research was supported by RFBR (#21-52-12043).

References

[1] M.M. Otrokov, *et al.*, Nature **576**, 416 (2019).
[2] P. Wang, *et al.*, Innov. **2**,100098 (2021).
[3] S. Pakhira, *et al.*, Phys. Rev. B **104**, 174427 (2021).
[4] Hang Li *et al.*, Phys. Rev. X **9**, 041039, (2019).
[5] H.-C. Chen *et al.*, Chin. Phys. Lett. **37**, 4, 047201 (2020).
[6] H. Li, *et al.*, Phys. Rev. B **104**, 054435 (2021).
[7] I.A. Golovchansky, *et al.*, J. Supercond. Nov. Magn. **562**,169713 (2022).

Abstract ID: 1668

SUPERCONDUCTING GAP STRUCTURE OF SLIGHTLY OVERDOPED $NaFe_{0.955}Co_{0.045}As$ PNICTIDES: JOINT SNS-ANDREEV SPECTROSCOPY AND SPECIFIC HEAT STUDY

S.A. Kuzmichev[1,2], A.V. Muratov[1], S.Yu. Gavrilkin[2], I.V. Morozov[3], A.I. Shilov[2], Ye.O. Rakhmanov[2,3], T.E. Kuzmicheva[2]

[1]Lebedev Physical Institute, Russian Academy of Sciences, 119991, Moscow, RUSSIA
[2]Lomonosov Moscow State University, Faculty of Physics, 119991, Moscow, RUSSIA
[3]Lomonosov Moscow State University, Department of Chemistry, 119991, Moscow, RUSSIA
E-mail: kuzmichevate@lebedev.ru

Single crystals of alkali metal based $NaFe_{0.955}Co_{0.045}As$ superconducting (SC) pnictides (the 111 family) with slightly overdoped composition and $T_c \approx 20$ K are grown using "self-flux" technique [1]. Here, we present a comprehensive study of the SC order parameter of $NaFe_{0.955}Co_{0.045}As$ using incoherent multiple Andreev reflection effect (IMARE) spectroscopy of planar "break-junctions" [1] (direct local probe), and specific heat (SH) measurements (bulk probe). Lattice SH was modelled within the Debye-Einstein framework. We show a multiple-gap superconductivity and determine the magnitudes and characteristic ratios of the SC order parameters: possibly anisotropic in the k-space large SC gap Δ_L with nodeless extended s-wave symmetry and $2\Delta_L(0)/k_BT_c \approx 4$–6 (the range corresponds to the anisotropy degree), and isotropic small SC gap Δ_S with $2\Delta_S(0)/k_BT_c \approx 1.5$–2.0 [2]. Both characteristic ratios are close to those determined by IMARE spectroscopy of underdoped $NaFe_{0.979}Co_{0.021}As$ compounds [3,4]. Temperature dependences of the SC gaps $\Delta_{L,S}(T)$ directly determined using IMARE spectroscopy are also presented.

The work is supported by RSF project no. 22-72-10082.

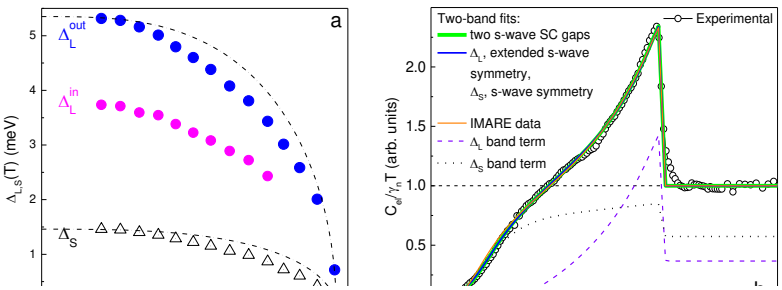

Fig. 1: *(a) Temperature dependence of the SC order parameters. (b) Electronic SH with two-band fits.*

References

[1] S.A. Kuzmichev, T.E. Kuzmicheva, Low Temp. Phys. **42**, 1008 (2016).
[2] S.A. Kuzmichev, *et al.*, Eur. Phys. J. Plus (2024) [in press].
[3] S.A. Kuzmichev, *et al.*, JETP Lett. **117**, 612 (2023).
[4] L.A. Morgun, *et al.*, Materials **16**, 6421 (2023).

Iron Based Superconductors (IBS): Fundamental and Applied Research under Ambient and Applied Pressures I

28.04.2024 SUNDAY

Abstract ID: 1528

NEW SUPERCONDUCTORS - TERNARY BISMUTHIDES Ba*TM*$_{1.8}$Bi$_2$ (*TM* = Au, Ag): SYNTHESIS, CRYSTAL STRUCTURE AND PROPERTIES

A.I. Shilov[1,2], A.V. Sadakov[2], A.S. Usoltsev[2], A.Yu. Degtyarenko[2], E.O. Rakhmanov[1], I.V. Morozov[1], K.A. Lyssenko[1,3], A.N. Kuznetsov[1,4], A.V. Shevelkov[1]

[1] *Department of Chemistry, Lomonosov Moscow State University, Moscow, 119991, RUSSIA*
[2] *V.L. Ginzburg Centre for High-Temperature Superconductivity and Quantum Materials P.N. Lebedev Physical Institute of the Russian Academy of Sciences (LPI RAS), 53, Leninsky Ave., 119991 Moscow, RUSSIA*
[3] *Faculty of Chemistry, National University Higher School of Economics, Moscow, 109028, RUSSIA*
[4] *Kurnakov Institute of General and Inorganic Chemistry of RAS, Moscow, 119991, RUSSIA*
E-mail: miv448@mail.ru

Recently discovered bismuthides with the $BaAu_2Sb_2$ structure type demonstrate interesting properties and electronic structures. We report successful crystal growth, crystal structure, band structure calculations, DOS and physical properties for $BaAg_{1.8}Bi_2$ and $BaAu_{1.8}Bi_2$. Grown crystals were characterized by a combination of single crystal X-ray diffraction and EDX spectroscopy. Both compounds crystallized in a new variation of $BaAu_2Sb_2$ structure type and demonstrated superconducting properties.

The superconducting transition temperature of $BaAg_{1.8}Bi_2$ is 5.5K, and $BaAu_{1.8}Bi_2$ is about 5K. The specific susceptibility of the compound with silver is an order of magnitude higher than that of the compound with gold. The critical field for both compounds is about 2 T.

The report will present the results of studying the magnetic and transport properties of the resulting compounds, as well as data from Andreev spectroscopy. The results of band structure calculations and DOS shed light on the differences between these bismuthides and the famous superconducting arsenides.

This work is supported by RSCF grant 22-43-02020.

Abstract ID: 1442

RESEARCH ON THE ANISOTROPY OF UPPER CRITICAL FIELD IN IRON-BASED AND NICKEL-BASED SUPERCONDUCTORS

Zhixiang Shi, Yongqiang Pan, Wei Wei

Key Laboratory of Quantum Materials and Devices of Ministry of Education, School of Physics, Southeast University, Nanjing 211189, CHINA
E-mail: zxshi@seu.edu.cn

Since cuprate superconductors' discovery, unconventional pairing remains a key issue in condensed matter physics. Many proposed superconducting pairing scenarios put forth by scientists have been challenging to reconcile, necessitating additional experimental clues and validation.

In our work, the value of H_{c2} of $Fe_{1+y}Te_{0.6}Se_{0.4}$ single crystals with controlled amounts of excess Fe was obtained by resistivity measurements over a wide range of temperatures down to ~1.5 K, and magnetic fields up to ~60 T. The crossover of the H_{c2}^{c}-T and H_{c2}^{ab}-T curves was found to be independent of the excess Fe content. The angle dependence of H_{c2} was also checked. The H_{c2} (θ) symmetry at higher temperature near T_c could be fitted by anisotropic G-L model, and novel fourfold symmetry of H_{c2} at lower temperature was found. Based on our spin-orientation-locking pairing model, the crossover behavior originates from the anisotropic spin-paramagnetic effect, and the novel four-fold symmetry of H_{c2} could be understood by the theoretical analysis.

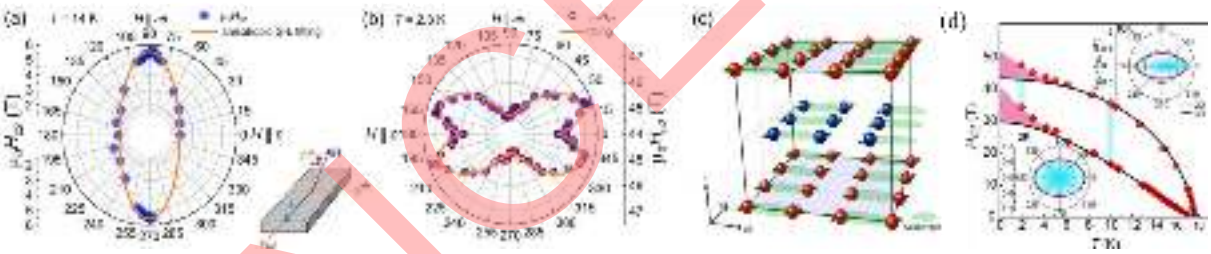

Fig. 1: *Polar angle dependence of H_{c2} at (a) 14 K and (b) 2.3 K for $Fe_{1+y}Te_{0.6}Se_{0.4}$. (c) Schematic diagram of the spin-orientation-locking phenomenon of Cooper pairs. (d) H_{c2} represents the upper critical field for H//c and H⊥c determined by taking a criterion of 50% R_n; Inset: Polar angle dependence of H_{c2} at 2 K and 10 K.*

Using the same approach, in the recently emerging superconductivity of infinite-layer nickelates with the isostructural and isoelectronic characteristics of cuprates, a very large H_{c2}, ~40 T for $H//c$ and ~52 T for $H\perp c$, was confirmed. Angle dependence of H_{c2} confirms the crossover of superconductivity from 2D to 3D as the temperature decreases.We discussed that the interstitial orbital effect causes the weakening of anisotropy. The observed abnormal upturning of H_{c2} at low temperatures is found to be a universal behavior independent of film quality and rare-earth elements. Therefore, it should not be the FFLO state due to the fact that it is in the dirty limit and insensitive to disorder. If FFLO states are absent in nickel-based superconductors under clean conditions, we question whether the upper critical field will exhibit a crossover similar to that observed in $Fe_{1+y}Te_{0.6}Se_{0.4}$ at lower temperatures or in nickel-based superconductors with higher T_c. That is, whether the nickel base has a strong anisotropic spin magnetic effect similar to the iron base.

The relevant content has been published in Physical Review B (2023, 107(22): L220503) and Journal of Alloys and Compounds (2024, 976: 173262.).

CANCELLED

Abstract ID: 1208

TEMPERATURE DEPENDENCE OF THE SUPERCONDUCTING ORDER PARAMETER IN STOICHIOMETRIC ALKALI METAL BASED PNICTIDE $EuCsFe_4As_4$

T.E. Kuzmicheva[1], S.A. Kuzmichev[1,2], A.Yu. Degtyarenko[1], K.S. Pervakov[1], V.A. Vlasenko[1]

[1]Lebedev Physical Institute, Russian Academy of Sciences, 119991, Moscow, RUSSIA
[2]Lomonosov Moscow State University, Faculty of Physics, 119991, Moscow, RUSSIA
E-mail: kuzmichevate@lebedev.ru

Superconducting (SC) pnictides $EuCsFe_4As_4$ of the novel 1144 structural family show a long magnetic order in the Eu planes below T_c, thus attracting both theoreticians and experimenters. With it, due to its rapid degradation in presence of even trace amounts of H_2O and O_2, SC properties of $EuCsFe_4As_4$ remain still understudied.

Here, using incoherent multiple Andreev reflection effect (IMARE) spectroscopy of planar "break-junctions" [1], we determine the structure of the SC order parameter in $EuCsFe_4As_4$ single crystals [2–4]. We show a multiple-gap superconductivity with possibly anisotropic SC condensate with the large SC gap (a nodeless extended s-wave symmetry), and a "weak" SC condensate with the small SC gap. The magnitudes, characteristic ratios, and temperature dependences of the SC gaps are directly determined. A weak crossband coupling in the k-space was estimated. We present large data statistics in order to show the reproducibility of the IMARE results, and compare the obtained SC gap structure with that of other alkali metal based SC pnictides.

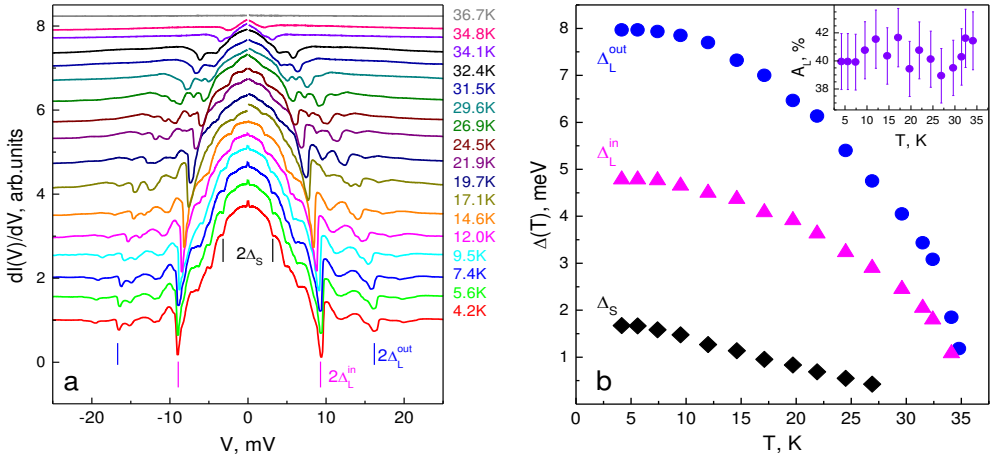

Fig. 1: *(a) dI(V)/dV spectrum of SnS break-junction in $EuCsFe_4As_4$ single crystal. (b) Temperature dependence of the SC order parameters and possible k-space anisotropy of Δ_L (inset).*

References

[1] S.A. Kuzmichev, T.E. Kuzmicheva, Low Temp. Phys. **42**, 1008 (2016).
[2] S.A. Kuzmichev, *et al.*, JETP Lett. **116**, 723 (2023).
[3] T.E. Kuzmicheva, *et al.*, J. Supercond. Novel Magn (2024). DOI:/10.1007/s10948-023-06681-7
[4] A.Yu. Degtyarenko, *et al.*, JETP Lett (2024). DOI:10.1134/S002136402360338X

Abstract ID: 1441

SHARP PEAKS IN CRITICAL CURRENT DENSITY AT DISTINCT QUANTUM CRITICAL POINTS IN FeSe(Te,S) SINGLE CRYSTALS

Wei Wei, Qiang Hou, Yue Sun, Zhixiang Shi

Key Laboratory of Quantum Materials and Devices of Ministry of Education, School of Physics, Southeast University, Nanjing 211189, CHINA
E-mail: 230218228@seu.edu.cn

The role of quantum critical points (QCPs) in both superconducting and normal states has attracted widespread attention. The study of it can provide valuable clues for the emergence of non-Fermi liquid behavior and the mechanisms underlying unconventional superconductivity. Nevertheless, the existence of superconductivity itself hinders the investigating of the QCPs beneath superconducting domes. Here, the persistent critical current density (J_c), free from the influence of vortex pinning changes, was utilized as a probe for the QCPs in Te- and S-doped FeSe single crystals. Within superconducting states, sharp peaks in J_c have been observed just at the QCPs, which supports for the existence of hidden QCPs beneath the superconducting dome. At the same time, an enhancement of J_c near $FeSe_{0.1}Te_{0.9}$ was also observed, an enhancement was observed in this work, the origin of which (from AFM QCP or other reasons) has been discussed. These results not only confirme the exsitence of QCPs in FeSe(Te,S), but also suggest that J_c could be an effective method to probe QCP, which can be applied to various materials.

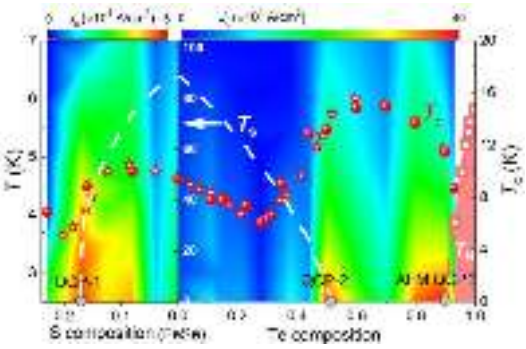

Fig. 1: *A contour map of Jc under the self-field (H =0 T) is constructed for FeSe(Te,S) using our experimental data, which is superimposed on the T-x phase diagram. The $J_c(T)$ at zero magnetic field of $FeSe_{0.96}S_{0.04}$ is derived from the study of Mahmoud Abdel-Hafiez et al..[1] Dashed white lines, solid circles, and pink areas correspond to T_s, T_c, and T_N, respectively. The open stars represent the $T_c(x)$ values from Ref. [2].*

References

[1] M. Abdel-Hafiez, Y.Y. Zhang, Z.Y. Cao, *et al.*, Phys. Rev. B **91**, 165109 (2015).
[2] K. Mukasa, K. Ishida, S. Imajo, *et al.*, Phys. Rev. X **13**, 011032 (2023).

Superconducting Motors and Applications in Electrical Engineering I

28.04.2024 SUNDAY

Abstract ID: 1276

RESEARCH AND DEVELOPMENT OF OPTIMAL STRUCTURE OF LIQUID HYDROGEN COOLED HIGH TEMPERATURE SUPERCONDUCTING INDUCTION/SYNCHRONOUS MOTOR USING SELF-ORGANIZING DESIGN METHOD

T. Nakamura

Kyoto University, Dept. of Electrical Engineering, 6158510, Kyoto, JAPAN
E-mail: nakamura.taketsune.2a@kyoto-u.ac.jp

Our group is conducting research and development on High Temperature Superconducting Induction/Synchronous Motor (HTS-ISM) [1] for liquid hydrogen circulation pumps, liquid hydrogen-cooled transport equipment (buses, aircraft, etc.). The HTS-ISM is an induction motor whose squirrel-cage winding is made of the HTS, and it has several features such as high efficiency [2], high output density [3], rotating stability against acceleration and deceleration drive [4], and room temperature operation with reduced output [2]. In order to put the HTS-ISM into practical use in near future, it is necessary to achieve high efficiency for variable speed operation and high-power density at startup and overload conditions. The rotating characteristic of the HTS-ISM, however, is sensitively affected by its magnetic structure. Therefore, it is necessary to establish a precise design method for the machine structure.

In this study, we propose a self-organizing design method that allows the stator slot and rotor bar structures to be uniquely determined without relying on empirical rules [5]. This design starts from a line current approximation model that ignores the conductor cross-sectional areas of the stator and the rotor, and systematically expands the areas, based on certain synthesis conditions until the desired current density is reached. A systematic design that does not depend on the experience of the designer is possible with the design method. Fig. 1 shows a design example of several kW class HTS-ISM. The detailed procedure of the self-organizing design method will be presented. Also, a design result of a 100 kW class HTS-ISM for liquid hydrogen circulation pump is also to be reported and discussed.

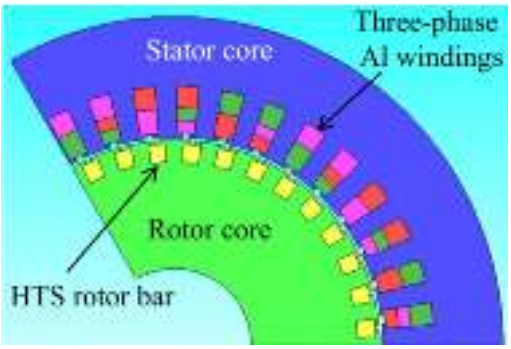

Fig. 1: *Example of self-organizing design result of HTS-ISM.*

Acknowledgements

I would like to thank R. Minonishi for his assistance of some of the analysis. This work was supported by JSPS KAKENHI under Grants no. 22H01471.

References

[1] G. Morita, T. Nakamura, I. Muta, Supercond. Sci. Technol. **19(6)**, 473-478 (2006).
[2] T. Nakamura, M. Yoshikawa, T. Terazawa, K. Matsuki, Y. Gao, T. Kiss, IEEE Trans. Appl. Supercond. **33(5)**, 5200205 (2023).
[3] T. Nakamura, K. Ikeda, T. Karashima, S. Guo, M. Yoshikawa, Y. Itoh, T. Terazawa, Y. Ohashi, Proc. of 2018 International Symposium on Power Electronics, Electrical Drives, Automation and Motion (SPEEDAM 2018), 1179-1184 (2018).
[4] K. Muranaka, T. Nakamura, S. Okajima, T. Ogasa, N. Amemiya, Y. Itoh, IEEE Trans. Appl. Supercond. **26(4)**, 5201205 (2016).
[5] T. Nakamura, Y. Kido, in preparation

Abstract ID: 1129

ELECTROMAGNETIC MODELING OF HIGH TEMPERATURE SUPERCONDUCTORS NEAR FERROMAGNETIC MATERIALS BY USING THE VOLUME INTEGRAL METHOD

Hocine Menana

Group of Research in Electrical Engineering of Nancy (GREEN), University of Lorraine, F-54000 Nancy, FRANCE
E-mail: hocine.menana@univ-lorraine.fr

Electromagnetic modeling is essential for the design and characterization of superconducting power systems. The strong dependency of the critical current density to the magnetic field, particularly in high temperature superconductors (HTS), implies the use of local quantities. Numerical methods are thus often needed.

On the other hand, superconducting systems often appear as multi-conductor assemblies separated by significant air regions, partly due to cryogenic parts, and presenting multiscale dimensions. The use of volume integral methods requiring only the discretization of the active parts is then favored [1-2]. However, the presence of ferromagnetic materials in some applications of HTS, such as electrical machines, complicates modeling by integral methods.

In this work, an original approach is developed for the volume integral modeling (VIM) of the electromagnetic field in HTS materials near ferromagnetic materials with linear and nonlinear magnetic permeability (Fig.1). A comparison with the finite element method (FEM) highlights the advantages of the proposed approach in terms of rapidity and precision.

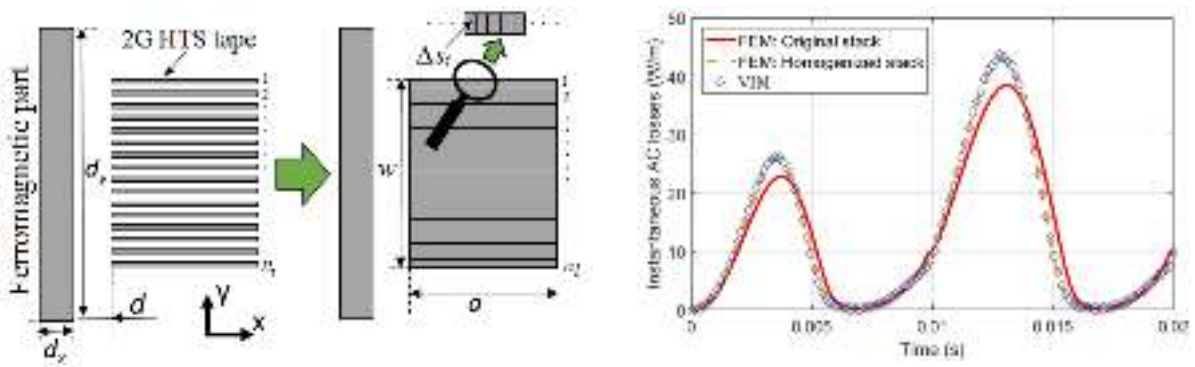

(a) (b)

Fig. 1: *(a) The modelled system, (b) Time evolution of the ac losses in the HTS tapes.*

References

[1] F. Sirois, F. Grilli, Supercond. Sci. Technol., **vol. 28, no. 4**, Art. no. 043002 (2015).
[2] Y. Statra, H. Menana, B. Douine, IEEE Transactions on App. Supercond., **vol. 31, no. 1**, 202, Art. no. 5900306.

Abstract ID: 1374

DEVELOPMENT STATUS OF LIQUID HYDROGEN COOLED HIGH-TEMPERATURE SUPERCONDUCTING POWER GENERATION DEMONSTRATOR

M. Ohya[1], S. Tonooka[2], Y. Terao[3], Y. Shirai[4], H. Kobayashi[5], K. Okai[6]

[1]*Kwansei Gakuin University, School of Engineering, 669-1330, Sanda, Hyogo, JAPAN*
[2]*Mitsubishi Electric Corporation, 661-0001, Amagasaki, Hyogo, JAPAN*
[3]*University of Tokyo, 277-0882, Kashiwa, Chiba, JAPAN*
[4]*Kyoto University, 606-8317, Kyoto, Kyoto, JAPAN*
[5]*Japan Aerospace Exploration Agency, 252-5210, Sagamihara, Kanagawa, JAPAN*
[6]*Japan Aerospace Exploration Agency, 182-0012, Chofu, Tokyo, JAPAN*
E-mail: Masayoshi-Ohya@kwansei.ac.jp

A hydrogen society is being promoted in Japan, and hydrogen power generation using imported liquid hydrogen is being considered [1]. The economic challenge is the cost of liquefaction [2], and effective utilization of the cold heat of liquid hydrogen is essential. We are developing a liquid hydrogen-cooled high-temperature superconducting (HTS) generator [3]. As shown in Fig. 1, liquid hydrogen is used to cool the superconducting field coil, and the evaporated gas is sent to a hydrogen gas turbine. The system can be built without a refrigerator and has almost zero cooling cost. The New Energy and Industrial Technology Development Organization (NEDO) Leading Research Program (FY2022-2024) was launched and we have designed a 10 kW /1800 rpm HTS power generation demonstrator. A cross-sectional view of the demonstrator is shown in Fig. 2. Only the field coils are superconducting and are cooled using liquid hydrogen. Four 300-turn racetrack-type double pancake coils were arranged to form a four-pole rotor. The demonstrator is currently being assembled, and the results of rotation and cooling tests before shipping will be reported at the conference.

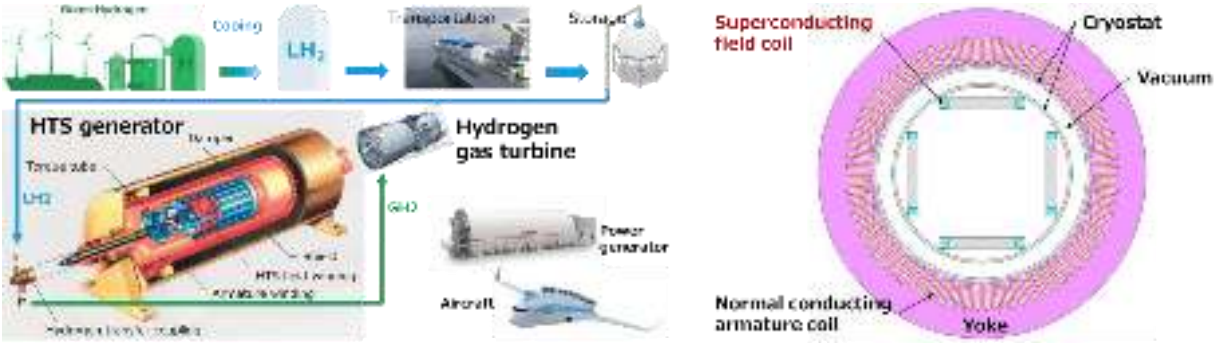

Fig. 1: *Hydrogen power generation system with liquid hydrogen-cooled HTS generator and cross-sectional view of 10 kW-class demonstrator.*

This presentation is based on results obtained from a project, JPNP14004, subsidized by the New Energy and Industrial Technology Development Organization (NEDO).

References

[1] Y. Kanehana, 2nd Hydrogen Energy Ministerial Meeting (2019).
[2] DOE Hydrogen and Fuel Cells Program Record, No. 19001 (2019).
[3] M. Ohya *et al.*, IEEE Trans. Appl. Supercond., 10.1109/TASC.2024.3354697 (2024).

Superconducting Motors and Applications in Electrical Engineering II

28.04.2024 SUNDAY

Abstract ID: 1604

AC LOSS AND STABILITY IN THE REBCO STATOR OF SUPERCONDUCTING MOTORS FOR HYDROGEN-ELECTRIC AIRPLANES

E. Pardo, A. Hussain, A. Dadhich, J. Kováč, L. Kopera

Institute of Electrical Engineering, Slovak Academy of Sciences, Bratislava, SLOVAKIA
E-mail: enric.pardo@savba.sk

Superconducting motors and generators are very promising for air-borne applications, thanks to their high power-over-weight ratio. They are specially interesting for hydrogen-electric aircrafts, since hydrogen can act as both fuel and coolant. In these motors, stators made of REBCO high-temperature superconductors (HTS) containing multi-tape conductors cause high AC loss, which needs to be reduced. In this work, we present both modelling results of motors with REBCO stators and measurements of single coils down to 25 K. For AC loss modelling, we analyze a 1 MW propulsion motor with distributed REBCO winding in the stator. Modelling is made by a novel in-house method based on the Minimum Electro-Magnetic Entropy Production (MEMEP) that takes the full interaction between the iron yoke and the superconducting windings into account. Computations show that due to the distributed winding geometry of the stator, using parallel-tape conductors with tapes isolated along their length reduces the AC loss to the theoretical limit of ideally transposed cables. Thanks to this and other strategies, REBCO stators are able to experience very low AC loss without striations or using complex transposed wires. We also model the electrothermal properties of the stator coils under either alternating or DC voltage, which represent usual operation and fault conditions, respectively. Faults could be caused by malfunctioning of the power source, for instance. We model this configuration by coupling our electromagnetic MEMEP model with our thermal model, which is based on finite differences. We found that although the coils can withstand several hundreds of volts in AC current amplitude, the same voltage in DC can irreversibly damage the stator winding. Finally, we also present AC loss measurements on single coils down to 25 K and at frequencies from 18 to 500 Hz. These measurements are based on electric means. This provides high accuracy, which enables us to identify the nature of several AC loss contributions.

Abstract ID: 1633

NUMERICAL STUDY OF MULTI-POLE GENERATOR WITH AND WITHOUT HTS WINDINGS FOR MULTI-MW DIRECT DRIVE WIND TURBINES

Shuangrong You, Markus Mueller

The University of Edinburgh, School of Engineering, EH9 3FG, Edinburgh, U.K.
E-mail: syou2@ed.ac.uk

Numerical modeling is an effective approach for investigating electromagnetic performance and AC loss behaviors of high-temperature superconductor (HTS) generators, which demonstrate promising potential for achieving competitive energy costs in offshore wind turbine applications. In this work, we have numerically investigated a modular wind turbine generator, featuring 176 rotor poles. Each 4-pole group severing as a modular unit, facilitating convenient installation and removal. Four design types are considered for this generator. Design-1 follows a conventional structure and serves as a reference design, utilizing permanent magnets for the rotor and copper windings for the stator. Design-2 and design-3 incorporate partial HTS structures. Design-2 replaces the stator copper coils with HTS coils, while Design-3 substitutes the rotor permanent magnets with HTS windings. Design-4 features a fully HTS design, with both the rotor and stator consisting of HTS windings. 3D static FEM models were constructed to investigate the magnetic field distribution across the four design types, while 2D dynamic FEM models, incorporating periodic conditions and moving mesh, were employed to analyze force and AC loss behaviors. Simulation results indicate that both partial HTS structure and fully HTS design offer higher power density compared to the conventional non-superconducting design. However, careful consideration of AC loss in superconducting windings is essential, as it can increase cryogenic load and overall weight of the generator.

Abstract ID: 1603

QUANTITATIVE ANALYSIS OF AC LOSSES IN HTS COILS BELOW 40K FOR ADVANCED ELECTRIC AIRCRAFT PROPULSION SYSTEMS

Ercan Ertekin[1], Calvin C. T. Chow[1,2], Alexandr Shchukin[1], Zhishu Qiu[1], Min Zhang[1]

[1] *Applied Superconductivity Laboratory, University of Strathclyde, G1 1RD, Glasgow, UNITED KINGDOM*
[2] *Department of Electrical and Electronic Engineering, The University of Hong Kong, Pokfulam, Hong Kong SAR, CHINA*
E-mail: ercan.ertekin@strath.ac.uk

Electric or hybrid aviation technologies are increasingly recognized as pivotal for achieving net-zero emissions in the aerospace sector. Superconducting machines, characterized by their high power-to-weight ratio, are poised to fulfill the advancing propulsion requirements of this domain. The design of future cryogenic systems and the attenuation of alternating current (AC) losses in high-temperature superconducting (HTS) machines necessitate experimental data on AC losses across a spectrum of operational temperatures. Consequently, gaseous helium's employment as a cryogen emerges as a versatile solution, catering to the operational demands of HTS power applications.

Building upon our antecedent research, which delineated the fabrication of multi-filamentary HTS coils and corroborated a significant diminution in AC losses, the present study endeavors to quantify additional AC loss reductions across diverse HTS windings within a rotational machine environment, specifically under the cryogenic threshold of 40K. This investigation introduces a novel fully HTS machine, integrated with a cryogenic helium circulation system for cooling, designed to facilitate an environment conducive to measuring the AC losses in HTS stator windings at sub-40K temperatures. Subsequent to the experimental phase, Finite Element Modelling (FEM) will be employed to corroborate the findings, thereby providing a computational framework to augment future system designs. It is anticipated that the cooling strategy, leveraging a cryogenic gas circulation system, will enhance the performance and power density of fully HTS machines, culminating in an optimized machine efficiency.

References

[1] T. Lan *et al.*, *Multifilament HTS cables to reduce AC loss: Proof-of-concept experiments and simulation*, IEEE Transactions on Applied Superconductivity, **vol. 33, no. 6**, pp. 1-12, Art no. 5901512 (2023).

Molecular Spin Qubits toward Quantum Computer I

28.04.2024 SUNDAY

Abstract ID: 1373

MOLECULAR SPIN QUBITS BASED ON MOLECULAR MAGNETS WITH S = ½

Masahiro Yamashita

Department of Chemistry, Graduate School of Science, Tohoku University, 6-3, Aramaki-Aza-Aoba, Aoba-Ku, Sendai 980-8578, JAPAN

E-mail: masahiro.yamashita.c5@tohoku.ac.jp

Nobel Prizes in Physics were given to Professors A. Aspect, J. F. Clauser, and A. Zeilinger due to the experimental evidence of "Quantum Entanglement" in 2022. "Quantum Entanglement" is strongly related to qubits and quantum computers. Computer performance has developed remarkably over the last few decades. A bit of a conventional computer is composed of a combination of 0 and 1, whereas that of a quantum computer is composed of a superposition of 0 and 1, that is, $\psi = a|0> + b|1>$. Hence, it is called a quantum bit (qubits). Therefore, the quantum computer is drastically superior from the viewpoints of performance, speed, capacity, etc. Qubit candidates for quantum computers are created by using superconducting loops, nitrogen vacancies in diamond, trapped atoms, photons, and quantum dots. These candidates have merits and demerits, such as their coherence time, operating temperature, etc. Therefore, I will focus on molecular spin qubits based on molecular magnets with S=1/2..

As for molecular spin qubits for quantum computer, we must increase T_1 (spin-lattice relaxation time) and T_2 (spin-spin relaxation time). Therefore, we will focus on the following three strategies:**(1) Crystal Engineering Method;** To compare 0D [VO(TPP)] and 3D [VO(TCPP-Zn_2-bpy)] (3D-MOF) to investigate the influence of the spin-lattice relaxation (T_1) in 0D and 3D lattices. Due to the rigid lattice of 3D-MOF, the Rabi nutation was observed even at room temperature (Fig.1). **(2) g-Tensor Engineering Method;** To compare [VO(TPP) and [CrN(TPP)] to investigate the contribution of the anisotropy of their g-values for the spin relaxation. Due to the large anisotropy of g-values, [CrN(TPP)] shows the short life time. **(3) Orbital Engineering Method;** To compare [Ni(cyclam)X_2]ClO_4 and TBA[Ni(mnt)$_2$] to investigate the relationship between the different occupied orbitals and spin relaxation. [Ni(cyclam)$(NO_3)_2$]ClO_4 has the longer life time due to the rigid molecular structure.

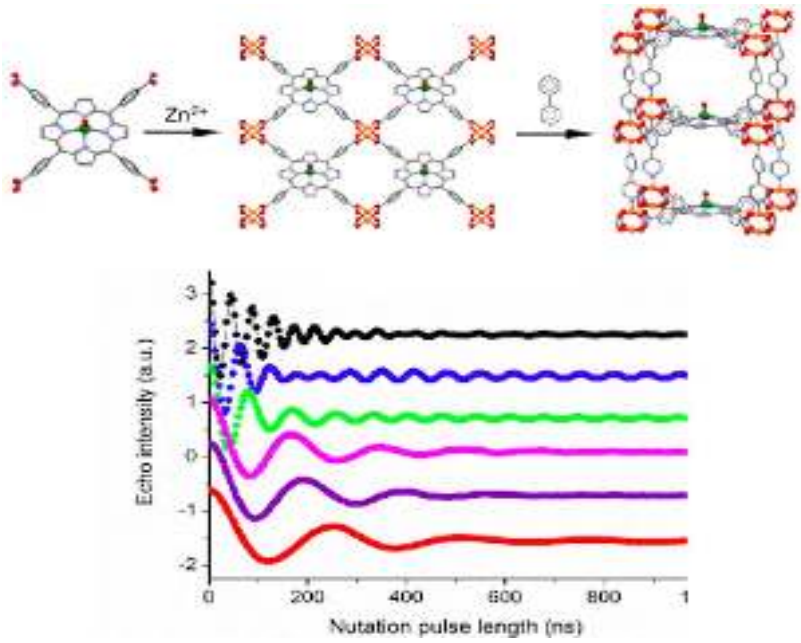

Fig.1: *3D MOF from 0D VO(TCPP) and Rabi Nutation at room temperature.*

Abstract ID: 1424

HOW TO BUILD QUANTUM CIRCUITS BASED ON ELECTRIC CURRENTS AND MOLECULES

Nicolás Lorente

Centro de Física de Materiales (CSIC-EHU), Donostia International Physics Center, Donostia – San Sebastián, ESPAGNE
E-mail: Nicolas.lorente@ehu.eus

A scanning tunnelling microscope (STM) can drive the spin evolution of a single atom, molecule or nanostructure on a solid surface [1]. The localized tunneling electron current on a single atom, modulated at microwave frequencies, reveals excitations attributed to spin resonance (ESR). We have developed a theory based on quantum master equations with non-equilibrium Green's functions and software to simulate ESR-STM instances under realistic conditions of temperature, external fields, and conductance [2-5]. In addition to a survey of the experiments and theory of continuous-wave and pulsed ESR, I will suggest the realization of the usual quantum circuit, Fig. 1, that converts a product state to a Bell state. The sequence begins with a Hadamard gate acting on the first spin. Subsequent evolution demonstrates the realization of the Hadamard gate, coupled with current-induced decoherence for extended evolution times. To assess our gate, we evaluate its fidelity against the desired Bell state, allowing us to discuss the simulated gate's performance using tunneling currents and solid-state-hosted atomic spins.

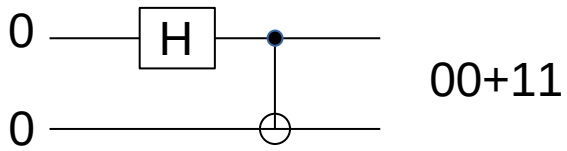

Fig. 1: *Quantum circuit simulated with the interaction of two Ti atoms on an MgO substrate, driven by a scanning tunneling microscope.*

References

[1] K. Yang *et al.*, Science **366**, 509 (2019).
[2] J. Reina-Gálvez *et al.*, PRB **100**, 035411 (2019).
[3] J Reina-Gálvez, Lorente, Delgado, Arrachea Phys. Rev. B **104**, 245415 (2021).
[4] J Reina-Gálvez, Wolf, Lorente Phys. Rev. B **107**, 235404 (2023).
[5] https://github.com/qphensurf/

Abstract ID: 1055

FUNDAMENTAL STUDIES OF F-ELEMENT ORGANOMETALLICS LEADING TO THE DESIGN OF NEW QUANTUM SYSTEMS

P W. Smith[1], J. Hruby[2], W. Evans[3], S. Hill[2,4], S. G. Minasian[1]

[1]*Lawrence Berkeley National Laboratory, Berkeley, CA 94720, USA*
[2]*National High Magnetic Field Laboratory, Tallahassee, FL 32310, USA*
[3]*University of California, Irvine, CA 92697, USA*
[4]*Florida State University, Tallahassee, FL, 32310, USA*
E-mail: sgminasian@lbl.gov

The ability to create and control coherence in a quantum object, or "qubit", is key to the development of new concepts in quantum information science (QIS), including sensing, communication, and computing. Fundamentally, interrogating and manipulating quantum phenomena are at direct odds with sustaining coherence, as interactions between a qubit and its environment lead to decoherence and thus a loss of information. As such, long coherence times can often come at the expense of control over initialization and read-out, scalability, and entanglement. Coherence times in electron-spin molecular qubits are improved at avoided energy-level crossings where the dependence of the transition frequency on the magnetic field vanishes. As such, the transverse relaxation time (T_2) is less sensitive to magnetic noise, engendering resistance to decoherence from near-neighbor magnetic sites and other nuclear spins in the molecule. Organometallic systems are particularly desirable because ligand field interactions in metallocenes can be adjusted by changing ring size and ring substituents to control both metal–C_{ring} distances and the electron withdrawing or donating character of the ligand itself. This presentation describes a general strategy for identifying molecules with high-frequency clock transitions based on systems wherein a d-electron is coupled to a crystal-field singlet state of an f-configuration, resulting in a minimally anisotropic ground state with strong hyperfine coupling. Using this approach, a 9.834 GHz clock transition was identified in a molecular Pr complex, [K(crypt)][Cp'$_3$Pr^{II}], leading to T_2 enhancements up to threefold relative to other transitions in the spectrum (Fig. 1). This result indicates the promise of the design principles outlined here for further development of f-element systems for quantum information applications.

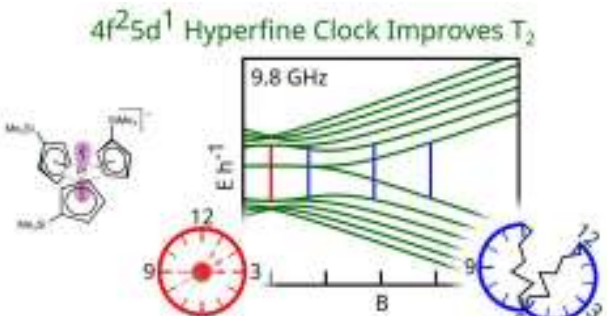

Fig. 1: *Representation of the improvement in coherence times at a clock transition.*

References

[1] M.Shiddiq, D. Komijani, Y. Duan, A. Gaita-Ariño, E. Coronado, S. Hill, *Enhancing coherence in molecular spin qubits via atomic clock transitions*, Nature, **531**, 348–351 (2016).

[2] J.M. Zadrozny, A.T. Gallagher, T.D. Harris, D.E. Freedman, *A porous array of clock qubits*, J. Am. Chem. Soc., **139**, 7089–7094 (2017).

[3] K. Kundu, J.R. White, S.A. Moehring, J.M. Yu, J.W. Ziller, F. Furche, W.J. Evans, S.A Hill, *9.2-GHz clock transition in a Lu(II) molecular spin qubit arising from a 3,467-MHz hyperfine interaction*, Nat. Chem., 14, 392–397 (2022).

Molecular Spin Qubits toward Quantum Computer II

28.04.2024 SUNDAY

Abstract ID: 1610

SPIN AND ORBITAL ORDERING EFFECTS IN 2D-SUPERLATTICE PEROVSKITE FILMS

Bin Hu

Department of Materials Science and Engineering, University of Tennessee, Knoxville, Tennessee 37996, USA
E-mail: bhu@utk.edu

2D-superlattice perovskite films can be conveniently prepared by using refined spin-coating method. Interestingly, the spin-cast 2D-superlattice perovskite films simultaneously carry spin and orbital momentum. Consequently, using spin and orbital momentum has become a critical approach to control the multifunctional properties. However, exploring spin and orbital ordering effects still demands much effort to understand their coupling relations in different length and time scales. To respond to this demand, we have been using magnetic field effects, circularly polarized luminescence, and circularly polarized pump-probe transient absorption technique to experimentally investigate spin and orbital spin and orbital ordering effects in 2D-superlattice perovskite films. We find that the orbital orders in 2D-superlattice perovskite films can be optically operated by using circularly polarized laser excitation, shown as circularly polarized luminescence with right and left-handedness selected by right-handed and left-handed circularly polarized laser excitations, respectively. More interestingly, we find that, when 2D-superlattice perovskite film is prepared on the ferromagnetic cobalt (Co) substrate, a circularly polarized laser excitation can surprisingly induce a magnetization within the entire 2D-superlattice perovskite film, leading to an optically induced magnetization indicated by polarized neutron reflectometry measurements. This optically induced magnetization provides direct evidence that the orbital order in 2D-superlattice perovskite film can establish a long-range interaction with the spin order in Co substrate. Furthermore, we find that switching the spin order between positive and negative magnetic field directions can switch the orbital orders between right and left handedness, shown by spin-switchable circularly polarized luminescence in 2D-superlattice perovskite films prepared on Co substrate. This observation presents the fundamental possibilities that spin order and orbital order can mutually switch and select towards realizing optically-active quantum materials. This presentation will discuss the fundamental details on mutually switchable spin and orbital ordering effects in 2D-superlattice perovskite films.

Abstract ID: 1618

MOLECULAR SPIN QUBIT IN SPIN CROSSOVER SYSTEMS

S. Hayami

Kumamoto University, Dept. of Chemistry, 8608555, Kumamoto, JAPAN
E-mail: hayami@kumamoto-u.ac.jp

Spin qubits are promising systems that can perform at room temperature. NV center in diamond is very stable and shows long time spin-spin relaxation, T_2, and promising as a spin-cubit. However, controlling the array of NV centers is difficult and remains a challenge. Recently, attempts have been made to create spin-cubits from molecules (molecular spin qubit), among these, spin qubits created from metal complexes are one of the most promising materials because of their controllability of ligands and metal ions.

Here we focus on spin crossover (SCO) cobalt(II) compounds. SCO cobalt(II) compounds show spin transition between $S = 1/2$ and $S = 3/2$. We can control the spin states by a various of ligands. Furthermore, we can control not only the spin states but also molecular distortion by molecular design. We would like to discuss about possibility of molecular spin qubit in SCO systems.

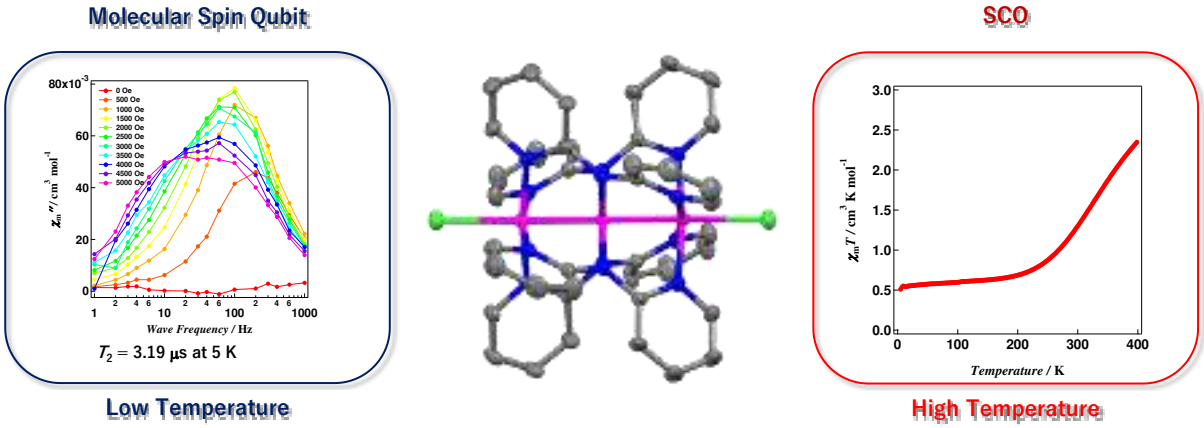

Abstract ID: 1565

MAGNETIC MOLECULES BASED ON TRANSITION METAL IONS AS SPIN QUANTUM BITS

T. Mallah[1], I. Tlemsani[1], S. Gambarella[2], A.-L. Barra[3], A. Ardavan[4], J. Liu.[4]

[1] *Université Paris-Saclay, Institut de Chimie Moléculaire et des Matériaux d'Orsay, 91400 Orsay, FRANCE*
[2] *Université Grenoble Alpes, CEA ,CNRS, INAC, SyMMES, 38042 Grenoble, FRANCE*
[3] *Laboratoire National des Champs Magnétiques Intenses, CNRS, 38042 Grenoble, FRANCE*
[4] *Departmentof Physics, Clarendon Laboratory, University of Oxford, Oxford OX1 3PU, UNITED KINGDOM*
E-mail: talal.mallah@universite-paris-saclay.fr

The ground spin state of transition metal complexes is, in most cases, well separated from the excited states. The nature of the ligands (electronic effects) and the geometry of the complex, may lift the degeneracy of the spin state sublevels (for S > ½) and leads to a low-lying two-level system (in the absence of external magnetic field for non-Kramers levels and in the presence of a magnetic field for Kramers doublets) that may behave as a spin quantum bits. This is the case of the two mononuclear complexes Ni(II) and Mn(II) whose structure is depicted in Figure 1. For Ni(II) calculations and Electron Paramagnetic Resonance (EPR) spectroscopy show that that the $M_S = \pm 1$ sub-levels are lower in energy that $M_S = 0$ ($D = -10.5$ cm^{-1}) and its degeneracy is lifted thanks to a slight rhombicity ($E = 0.15$ cm^{-1}). The gap (2E) between the two low-lying levels that defines the qubit frequency is very close the X-band microwave energy (0.3 cm^{-1}), so that a clock transition is expected at zero applied magnetic field [1].

In this presentation, we show that, thanks to the clock transition at zero field, the coherence of the superposed state is well protected from the magnetic fluctuations of the spin bath. We will also briefly discuss the effect of an electric field on the modulation of the electronic parameters characterizing the quantum bit in the case of half-integer spin mononuclear complexes (Mn(II), S = 5/2, Figure 1-right), with a view to electrically addressing quantum bits.

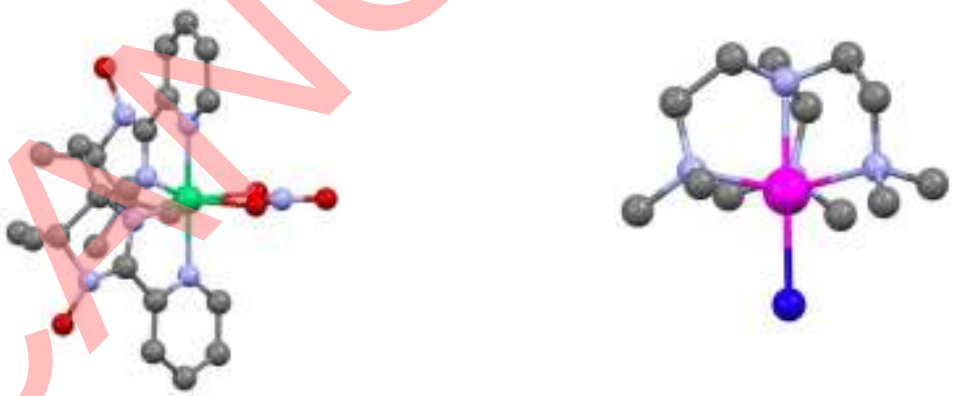

Fig. 1: *view of the structure of the mononuclear Ni(II) (left) and Mn(II) (right) complexes.*

References

[1] M. Rubin-Osanz *et al.*, Chem. Sci. **12**, 5123 (2021).

CANCELLED

Device Physics of Josephson Junctions and Their Fundamental Technologies I

28.04.2024 SUNDAY

Abstract ID: 1396

COHERENT TUNNELING OF FLUX QUANTA IN A LONG JOSEPHSON JUNCTION

Alexey Ustinov

Institute of Physics, Karlsruhe Institute of Technology, 76131 Karlsruhe, GERMANY
E-mail: alexey.ustinov@kit.edu

Quantized vortices of supercurrent in a superconductor are accompanied by magnetic flux penetrating the material and play a key role in determining the properties of superconducting materials and devices. The dynamics of such magnetic fluxons is essentially classical, while some earlier studies have hypothesised a collective quantum dynamics. However, the proposition that a magnetic fluxon as a macroscopic entity can exist in a coherent superposition of two or more spatially distinct states has received no experimental evidence till now. We experimentally study the quantum dynamics of magnetic fluxons in long Josephson junctions made of a high kinetic inductance material, in which the effective mass of the fluxon is reduced by orders of magnitude [1]. By probing the fluxon states with a weak microwave signal, we observe a direct evidence for a quantum coherent superposition of spatially distinct magnetic flux configurations. The spectrum of the system has a two-level character, with a coherence time of Rabi oscillations between the states on the order of few microseconds [2]. The observed phenomenon of the quantum superposition between spatially distinct magnetic flux states adds a novel perspective to the well established quantum coherence in lumped circuits such as superconducting qubits.

References

[1] M. Wildermuth, L. Powalla, J.N. Voss, J. Schön, A. Schneider, M.V. Fistul, H. Rotzinger, A.V. Ustinov, Appl. Phys. Lett., **120**, 112601 (2022).

[2] M. Wildermuth, J.N. Voss, M. Kristen, A. Schneider, M.V. Fistul, H. Rotzinger, A.V. Ustinov, *to be published* (2024).

CANCELLED

Abstract ID: 1395

DUAL-RAIL DIRECT-COUPLED ADIABATIC QUANTUM FLUX PARAMETRON LOGIC FOR HIGH-DENSITY CIRCUIT INTEGRATION

N. Yoshikawa[1,2], W. Komiya[2], Y. Hasegawa[2], C. Ayala[1]

[1]*Institute of Advanced Sciences, Yokohama National University, JAPAN*
[2]*Department of Electrical and Computer Engineering, Yokohama National University, JAPAN*
E-mail: nyoshi@ynu.ac.jp

Adiabatic quantum-flux-parametron (AQFP) logic is an extremely energy-efficient superconducting logic that relies on adiabatic gate switching. Its minimal switching energy, more than five orders of magnitude lower than state-of-the-art CMOS logic, makes it a promising technology for future high-performance computing. Presently, a superconductor transformer connects the output signal from the AQFP gate to the next gate. This configuration works well for creating a NOT gate due to easy current signal polarity negation through the negatively coupled transformer. However, the magnetic coupling of the superconductor transformer does not scale with shrinking feature sizes in submicron processes, posing challenges for the high-density integration of AQFP circuits in the future. To address this issue, we have proposed dual-rail direct-coupled adiabatic quantum flux parametron logic (D^2QFP). This approach is based on the dual-rail logic style but efficiently constructs AND/OR logic without increasing the number of junctions compared to conventional AQFP logic, thanks to the use of offset gates. Moreover, D^2QFP exhibits superior robustness, driving capability, and lower power consumption compared to conventional AQFP logic. In this presentation, we will introduce simulation results regarding the basic performance of D^2QFP logic. Additionally, we have implemented basic gates and circuits of D^2QFP logic, such as an AND/OR gate and a half-adder (see Figure1), and verified their proper operation at 4.2K. We will also discuss the prospects for future scaling of D^2QFP logic in this presentation.

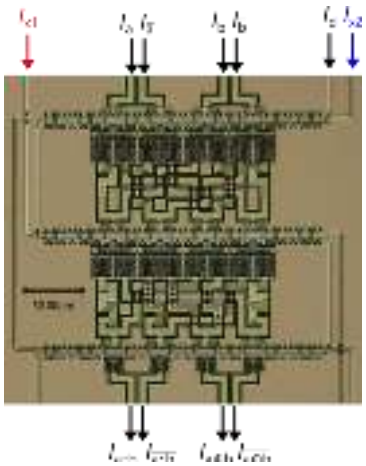

Fig. 1: *Microphotograph of a D^2QFP Half Adder.*

Abstract ID: 1572

GATE-CONTROLLED RESISTIVE STATE OF A NbTi SUPERCONDUCTING WIRE

K. Harrabi[1,2], A. Mekki1[1,3], M.V. Miloševic[4]

[1] Physics Department, King Fahd University of Petroleum and Minerals, 31261 Dhahran, SAUDI ARABIA
[2] Interdisciplinary Research Center (RC) for Intelligent Secure Systems, KFUPM, Dhahran 31261, SAUDI ARABIA
[3] Center for Advanced Material, King Fahd University of Petroleum and Minerals, Dhahran 31261, SAUDI ARABIA
[4] Department of Physics & NANOlab Center of Excellence, University of Antwerp, BELGIUM
E-mail: harrabi@kfupm.edu.sa

A current-driven superconductor loses dissipationless properties upon surpassing the depairing threshold, and enters a non-equilibrium state encompassing resistive phase-slip and hot-spot phenomena. In that regime, the superconductors exhibit most sensitivity to additional external excitations, be it magnetic, electronic, thermal, which forms the broad base for their use as advanced quantum sensors.

In this study, we employed a gate electrode to apply a perpendicular voltage (an electric field) to a NbTi filament driven by electric current, to demonstrate the control of the critical state of the filament by the gate voltage. Our investigation revealed that gate voltage not only affects the threshold current of the resistive state, but it also prompted a transformative change in subsequent dissipation behavior, transitioning from hotspot formation to the appearance of phase slip lines. We have also systematically mapped out the delay times for the onset of dissipation, critically important to the responsiveness of diverse electronic applications, such as single-photon detection. More generally, our research illuminates the complex interplay between gate voltage, critical current reduction, and dissipation, diversifying the applicability of superconducting nanostructures in cryogenic electronic applications of the 21st century.

Device Physics of Josephson Junctions and Their Fundamental Technologies II

28.04.2024 SUNDAY

Abstract ID: 1486

HIGHER-DIMENSIONAL TOPOLOGY AND FRACTIONAL STATES OF MATTER IN SUPERCONDUCTING SYSTEMS

Wolfgang Belzig

Department of Physics, Universität Konstanz, 78457 Konstanz, GERMANY
E-mail: wolfgang.belzig@uni-konstanz.de

Topology ultimately unveils the roots of the perfect quantization observed in complex systems. The 2D quantum Hall effect is the celebrated archetype. Remarkably, topology can manifest itself even in higher-dimensional spaces defined by control parameters playing the role of synthetic dimensions. However, so far, a very limited number of implementations of higher-dimensional topological systems have been proposed, a notable example being the so-called 4D quantum Hall effect. In this talk I will show that mesoscopic superconducting systems can implement higher-dimensional topology and represent a formidable platform to study a quantum system with a purely nontrivial second Chern number [1]. I further demonstrate that the absorption intensity in microwave spectroscopy [2] is quantized and the integer is directly related to the second Chern number. Finally, I discuss that these systems also possess a non-Abelian Berry phase or exotic topologies like tensor monopoles. Another class of nontrivial topology relates to fractional states of matter occurring in quantum Hall systems due Coulomb interactions. I will present a realisation of a fractional state of a superconducting nanostructure that manifests itself in an analogy to the fractional conductance, that can be measured experimentally in a specially engineered circuit of Josephson junctions [3].

References

[1] H. Weisbrich, R.L. Klees, G. Rastelli, W. Belzig, *Second chern number and non-abelian berry phase in superconducting systems*, PRX Quantum **2**, 010310 (2021).

[2] R.L. Klees, G. Rastelli, J.C. Cuevas, W. *Belzig Microwave spectroscopy reveals the quantum geometric tensor of topological Josephson matter*, Phys. Rev. Lett. **124**, 197002 (2020).

[3] H. Weisbrich, R.L. Klees, O. Zilberberg, W. Belzig, *Fractional transconductance via non-adiabatic topological cooper pair pumping*, arxiv: 2212.11757 (2022).

Abstract ID: 1115

EFFECTS OF STRONG CAPACITIVE COUPLING BETWEEN META-ATOMS IN RF SQUID METAMATERIALS

Jingnan Cai, Steven M. Anlage

[1]*Quantum Materials Center, Physics Department, University of Maryland, College Park, MD 20742-4111, USA*
E-mail: anlage@umd.edu

The self-resonant radio frequency Superconducting Quantum Interference Device (rf SQUID) has been established as a unique building block for microwave frequency metamaterials [1-4]. We consider two-dimensional arrays of rf SQUIDs constructed in a way to create strong *capacitive*, as well as inductive, coupling between the meta-atoms. New collective properties of the materials arise from these strong interactions, allowing for new applications, such as travelling-wave parametric amplification [5]. The nonlinearity and nonlocal coupling of rf SQUID metamaterials endow them with interesting dynamical properties, such as chaos and chimera states, both of which have been studied extensively by theorists in the context of rf SQUID metamaterials [6,7]. Laser scanning microscopy [8] with single SQUID resolution is employed to study collective states of the nonlinear metamaterial with strong inductive coupling. We set up and solve the equations of motion for the gauge-invariant phase on the Josephson junctions in each SQUID, and include the ability of SQUID loops to share high-frequency displacement currents (but not dc currents) through capacitive overlap of their loop wiring. The capacitive coupling gives rise to qualitatively new self-resonant response of rf SQUID metamaterials (Fig. 1), and is demonstrated through analytical theory, numerical modeling, and experiment in the 10-30 GHz range on strongly coupled rf SQUID metamaterials.

Fig. 1: *(Left) A fabricated 12x12x2 rf SQUID metamaterial array made from Nb/AlO$_x$/Nb thin film technology. (Right) Schematic of four corner-coupled rf SQUIDs with capacitive coupling and the 9 resulting linearized eigenmodes of the system, organized into three classes.*

This work is supported by the National Science Foundation through Grant # NSF DMR-2004386, and the U.S. Department of Energy through grant # DESC0017931.

References

[1] C. Du, H. Chen, S. Li, Phys. Rev. B **74**, 113105 (2006).
[2] N. Lazarides, G. P. Tsironis, Appl. Phys. Lett. **90**, 163501 (2007).
[3] M. Trepanier, *et al.*, Phys. Rev. X **3**, 041029 (2013).
[4] D. Zhang, *et al.*, Phys. Rev. X **5**, 041045 (2015).
[5] M.A. Castellanos-Beltran, K.W. Lehnert, Appl. Phys. Lett. **91**, 083509 (2007).
[6] K. Fesser, A.R. Bishop, Appl. Phys. Lett. **43**, 123 (1983).
[7] J. Hizanidis, N. Lazarides, G.P. Tsironis, Chaos **28**, 063117 (2018).
[8] Alexander P. Zhuravel, *et al.*, Appl. Phys. Lett. **114**, 082601 (2019).

Abstract ID: 1495

A REAL-TIME TESTING TECHNIQUE FOR HIGH-SPEED STREAMING RSFQ CIRCUITS

M. Eren Çelik[1], Timur V. Filippov[1], Dmitri E. Kirichenko[1], Mustapha Habib[1], Anubhav Sahu[1], Deepnarayan Gupta[2]

[1]HYPRES Inc., NY, USA
[2]Formely with HYPRES Inc., NY, USA
E-mail: mecelik@hypres.com

Various superconducting digital circuits have been demonstrated at very high clock rates, particularly for streaming applications. However, transferring data between room-temperature electronics and the superconducting chip can create a bottleneck for high-speed testing and error debugging. To address this problem, we use a testing technique that enables controlled access to real-time streaming data [1]. We accomplish this by placing the circuit in a custom test bench environment and providing it with a clock signal at the full rate. The clock signal is then applied to multiple input signals as required using a splitter tree. A controlled fixed pattern is applied to the circuit using an array of DC-controlled switches, thus generating a constant output of either logical zeros or ones. Finally, the output of the circuit is split into its true and complementary forms by employing a set of DFF and NOT cells per output line. This way it becomes possible to observe high, low, and average output voltage levels and any bit error would manifest itself as a toggling of the voltage level from high to low or vice versa. By observing the output voltage levels at full speed, it would be possible to estimate the bit error rate of the circuit.

To demonstrate the effectiveness of this testing structure, we used a family of parallel counters designed as digital benchmark circuits [2]. We selected these circuits because of their repeating internal structure, their ability to support high-speed throughput, and the predictability of their functionality. Various test results, including pass-fail tests, pattern dependency tests, symmetry tests, and operating margins for various frequencies, are reported as well.

References

[1] S.B. Kaplan, A.F. Kirichenko, O.A. Mukhanov, S. Sarwana, *A prescaler circuit for a superconductive time-to-digital converter*, IEEE Transactions on Applied Superconductivity, **vol. 11, no. 1**, pp. 513-516, (2001); doi: 10.1109/77.919395.

[2] M. Eren Çelik *et al.*, *Fast RSFQ and ERSFQ parallel counters*, IEEE Transactions on Applied Superconductivity, **vol. 30, no. 7**, pp. 1-4, (2020); Art no. 1302404, doi: 10.1109/TASC.2020.3010692.

Kagome Superconductivity I

28.04.2024 SUNDAY

Abstract ID: 1101

SUPERCONDUCTIVITY AND CHARGE ORDER IN KAGOME-LATTICE SYSTEMS

Zurab Guguchia

Laboratory for Muon Spin Spectroscopy, Paul Scherrer Institute, Villigen PSI, SWITZERLAND
E-mail: zurab.guguchia@psi.ch

Kagome lattices are intriguing and rich platforms for studying the intertwining of topology, correlation, and magnetism [1-5]. The unique geometry gives rise to frustration, correlated quantum orders, and topology, owing to its special features: the electronic structure shows a flat band, inflection points leading to van Hove singularities, and Dirac cones. These materials have been subject to tremendous experimental and theoretical studies not only due to their exciting physical properties but also as systems that may solve critical technological problems.

In this talk, I will review recent experimental progress on superconductivity and magnetic fingerprints of charge order in several kagome-lattice systems from the local-magnetic probe point of view by utilizing muon-spin rotation under extreme conditions, i.e., hydrostatic pressure, uniaxial strain, ultra low temperature and high magnetic field. The systems include: **(1)** The series of compounds AV_3Sb_5 (A = K, Rb, Cs) with V kagome lattice which form the first kagome-based family that exhibits a cascade of symmetry-broken electronic orders, including charge order and superconductivity. In these systems, we discovered a time-reversal symmetry-breaking charge ordered state and tunable unconventional superconductivity [6-8]. **(2)** Bilayer kagome material ScV_6Sn_6, in which we observed hidden magnetism in charge ordered state [9]. **(3)** The system $LaRu_3Si_2$ with Ru kagome layers, in which we discovered above room temperature charge order [10]. In $LaRu_3Si_2$, we also found [11] that the electron-phonon coupling alone can only explain a small fraction of T_c from calculations, which suggests other factors enhancing T_c such as the correlation effect from the kagome band structure.

References

[1] I. Syozi, Prog. Theor. Phys. **6**, 306 (1951).
[2] E. Liu *et al.*, Nature Physics **14**, 1125 (2018).
[3] J.-X. Yin *et al.*, Nature **583**, 533 (2020).
[4] L. Ye *et al.*, Nature **555**, 638 (2018).
[5] Z. Guguchia *et al.*, Nature Communications **11**, 559 (2020).
[6] C. Mielke III *et al.*, and Z. Guguchia, Nature **602**, 245 (2022).
[7] Z. Guguchia *et al.*, Nature Communications **14**, 153 (2023).
[8] Z. Guguchia, R. Khasanov, H. Luetkens. NPJ Quantum Materials **8**, 41 (2023).
[9] Z. Guguchia *et al.*, Nature Communications **14**, 7796 (2023).
[10] I. Plokhikh *et al.*, and Z. Guguchia, arXiv:2309.09255 (2023).
[11] C. Mielke III *et al.*, and Z. Guguchia, Phys. Rev. Materials **5**, 034803 (2021).

Abstract ID: 227

CHIRAL PHONONS AND PHONON DRUMHEAD SURFACE STATE IN KAGOME CoSn-LIKE COMPOUNDS

A. Ptok

Institute of Nuclear Physics Polish Academy of Sciences, PL-31342 Kraków, POLAND
E-mail: aptok@mmj.pl

Typically, a single phonon mode realizes vibration related to linear motion. However, in the presence of n-folded (n>2) rotational symmetry, the phonon wavefunction possesses additional (geometric) phase, which allows for the realization of chiral phonons by single, non-degenerate phonon branches, i.e. circular motion of the atoms around the equilibrium positions. Previous theoretical studies demonstrated that chiral phonons can be found in ideal two-dimensional hexagonal lattices [1,2]. Here, we present our results of ab initio studies of chiral phonons in several compounds, such as CoSn-like systems (with P6/mmm symmetry, and containing both kagome and honeycomb sublattices) [3], magnetic topological insulators TBi2Te4 (T=Mn,Fe) [4], binary compounds ABi (A=K,Rb,Cs) containing chiral Bi chains [5], and orthorhombic ternary YAlSi compound [6]. Furthermore, we discuss the case of RhPb implementing the distorted kagome lattice [7]. For these compounds, realization of the phonon drumhead-like surface state is possible.

References

[1] L. Zhang, Q. Niu, Phys. Rev. Lett. **115**, 115502 (2015).
[2] H. Chen, W. Wu, S.A. Yang, X. Li, L. Zhang, Phys. Rev. B **100**, 094303 (2019).
[3] A. Ptok, A. Kobiałka, M. Sternik, J. Łazewski, P.T. Jochym, A.M. Oleś, S. Stankov, P. Piekarz, Phys. Rev. B **104**, 054305 (2021).
[4] A. Kobiałka, M. Sternik, A. Ptok, Phys. Rev. B **105**, 214304 (2022).
[5] J. Skórka, K.J. Kapcia, P.J. Jochym, A. Ptok, Matter. Today Commun. **35**, 105888 (2023).
[6] S. Basak, A. Ptok, Crystals **12**, 436 (2022).
[7] A. Ptok, W.R. Meier, A. Kobiałka, S. Basak, M. Sternik, J. Łażewski, P.T. Jochym, M.A. McGuire, B.C. Sales, H. Miao, P. Piekarz, A.M. Oleś, Phys. Rev. Research **5**, 043231 (2023).

Abstract ID: 1033

TUNABLE TOPOLOGICAL DIRAC SURFACE STATES AND VAN HOVE SINGULARITIES IN KAGOME METAL GdV_6Sn_6

Ming Shi

Center for correlated matter and school of Physics, Zhejiang University, 310058 Hangzhou, CHINA
E-mail: shi20001231@outlook.com

Transition-metal-based kagome materials at van Hove filling are a rich frontier for the investigation of novel topological electronic states and correlated phenomena. To date, in the idealized two-dimensional kagome lattice, topologically nontrivial Dirac surface states (TDSSs) have not been unambiguously observed, and the manipulation of TDSSs and van Hove singularities (VHSs) remains largely unexplored. Here, we reveal TDSSs originating from a $\mathbb{Z}_2$ bulk topology and identify multiple VHSs near the Fermi level (E_F) in the magnetic kagome material GdV_6Sn_6. Remarkably, using *in-situ* surface potassium deposition, we successfully realize manipulation of the TDSSs and VHSs. The Dirac point of the TDSSs can be tuned from above to below E_F, which reverses the chirality of the spin texture at the Fermi surface. These results not only establish GdV_6Sn_6 as a fascinating platform for studying the nontrivial topology, magnetism and correlation effects native to kagome lattices, but also open up a new avenue for the potential application of spintronic devices based on kagome materials.

CANCELLED

Kagome Superconductivity II

28.04.2024 SUNDAY

Abstract ID: 1062

ROTATION SYMMETRY BREAKING OF CHARGE-DENSITY-WAVE STATE AND MAGNETIC TOPOLOGICAL STATE IN KAGOME LATTICES

Zhicheng Jiang[1,2], Soohyun Cho[1], Dawei Shen[1,2]

[1]*National Synchrotron Radiation Laboratory, University of Science and Technology of China, 42 South Hezuohua Road, Hefei, Anhui 230029, CHINA*
[2]*School of Nuclear Science and Technology, University of Science and Technology of China, Hefei, 230026, CHINA*
E-mail:

Recently, the vanadium based Kagome superconductors AV_3Sb_5 (A = K, Rb, Cs) have drawn great attention because of the various intriguing phenomena discovered in this class of materials, including the charge density wave (CDW), unusual electronic structures with nontrivial band topology, giant anomalous Hall effect, and superconductivity [1]. Remarkably, the recent discovery of C_2 symmetric nematic phase intertwined with the superconductivity in AV_3Sb_5 could be related to the unusual superconducting state at lower temperature, and the superconducting mechanism is reminiscent of the nematic superconducting state in copper or iron-based superconductors.

Although the electronic nematicity has been studied in literatures using real-space microscopy and transport measurements, the direct evidence on the CDW driven rotational symmetry breaking (RSB) of the electronic structure in the reciprocal space is still missing. The underlying mechanism of the electronic nematicity and its relationship to the CDW transition remain elusive. Here, utilizing the micron-scale spatially resolved angle-resolved photoemission spectroscopy, we have directly observed the electronic nematicity in the reciprocal space of kagome superconductors KV_3Sb_5, which is a significant progress beyond the latest reports on RSB of local electronic structure in AV_3Sb_5 [2]. Besides, we experimentally demonstrated the hint of rotation symmetry breaking in $RbTi_3Bi_5$, which is isostructural to AV_3Sb_5 but in the absence of the concomitant intertwined CDW [3]. Moreover, we identified that the combined symmetry $S=\theta\tau_{1/2}$ plays a crucial role in the antiferromagnetic ground state of $EuTi_3Bi_4$, which ensures the stability of topological surface states in the case of time-reversal symmetry breaking [4]. Our findings thus provide critical pieces of the jigsaw which go towards solving puzzles in kagome lattices.

References

[1] S. Cho *et al.*, PRL **127**, 155302 (2021).
[2] Z. Jiang *et al.*, Nano Lett. **23**, 5625 (2023).
[3] Z. Jiang *et al.*, Nat. Commun. **14**, 4892 (2023).
[4] Z. Jiang *et al.*, e-print arXiv: 2309.01579 (2023).

CANCELLED

Abstract ID: 1170

ROBUST CHARGE ORDER ABOVE ROOM TEMPERATURE IN KAGOME SUPERCONDUCTOR $LaRu_3Si_2$

I. Plokhikh, Z. Guguchia

Paul Scherrer Institut, CH-5232 Villigen PSI, SWITZERLAND
E-mail: igor.plokhikh@psi.ch

The traditional Japanese woven bamboo pattern known as kagome, noted for its geometric beauty, is remarkably prevalent in the crystal structures of various solid materials. This unique topology leads to fascinating physical phenomena in the realms of frustrated magnetism and superconductivity. Due to its susceptibility to theoretical modeling, kagome materials present a compelling platform for discovering, tuning, and comprehending the unconventional phases of quantum matter.

The focus of the present work is $LaRu_3Si_2$, with one of the highest critical temperatures (T_c = 7 K) among kagome superconductors. The structural motif of this material represents Ru-based kagome layers placed between $LaSi_2$ hexagonal nets. Previous theoretical studies hint at the possibility of charge order instabilities in this material due to the d_{z^2} flat bands close to the Fermi level [1]. Our current single-crystal X-ray diffraction investigation of the pristine and Fe-doped $LaRu_3Si_2$ reveals a cascade of structural phase transitions as a function of temperature [2]. Above 600 K, the material crystallizes in an undistorted P6/mmm structure (HT-hex), which doubles along the *c*-direction upon cooling (LT-hex, Fig. 1). Below ~400 K, additional charge order (CO-I) reflections with q_1 = ($^1/_4$ 0 0) evolve, followed by the second charge order transition into CO-II with q_2 = ($^1/_6$ 0 0) below 180 K.

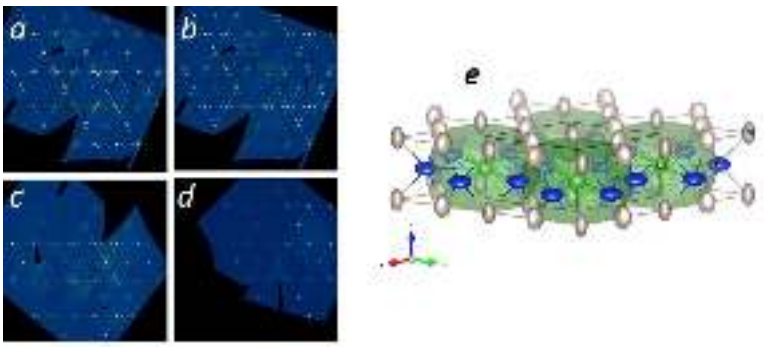

Fig. 1. *Overview of reconstructed reciprocal space along c-axis for CO-II at 80K (a), CO-I below 400K (b, c), LT-hex at 500K (d) phases and an undistorted crystal structure of $LaRu_3Si_2$ (HT-hex, e).*

In the talk, apart from detailing the transition in reciprocal space, we will explore the corresponding structural transformations observed in real space and discuss their potential implications on superconductivity.

References

[1] C. Mielke III, *et al.*, Z. Guguchia, *Nodeless Kagome superconductivity in $LaRu_3Si_2$*, Phys. Rev. Mat. **5**, 034803 (2021).

[2] I. Plokhikh, C. Mielke III, *et al.*, D.J. Gawryluk, Z. Guguchia, *Charge order above room-temperature in a prototypical kagome superconductor $La(Ru_{1-x}Fe_x)_3Si_2$*, arXiv:2309.09255

Abstract ID: 1416

UNCONVENTIONAL SUPERCONDUCTIVITY IN THE KAGOME SUPERCONDUCTOR AV_3Sb_5

Ben-Chuan Lin

International Quantum Academy, Southern University of Science and Technology, CHINA
E-mail: linbc@sustech.edu.cn

The recently discovered kagome superconductors offer a promising platform for investigating intertwined orders and novel states, including topology, superconductivity, charge density waves, and more. The interplay among these orders can spontaneously break rotational symmetry, giving rise to exotic phenomena such as nematicity or even nematic superconductivity. Here we present our findings on the two-fold symmetric superconductivity in thin-flake AV_3Sb_5 in response to a direction-dependent in-plane magnetic fields, in contrast to the inherent six-fold structural symmetry of the crystal lattice. The two-fold symmetry was evidenced through a combination of magnetoresistance transport experiments, critical magnetic field measurements, and observations of anisotropic superconducting gaps. Notice that though the normal states have two-fold symmetry due to the charge density wave driven nematicity, it doesn't guarantee the two-fold symmetry observed in the superconducting states, particularly within the inversion-symmetric kagome superconductors. We propose that the unconventional spin-orbit-parity-coupled superconductivity is responsible for the anisotropic superconducting gap. Besides this, I will also present an update on our findings at this forthcoming meeting in April.

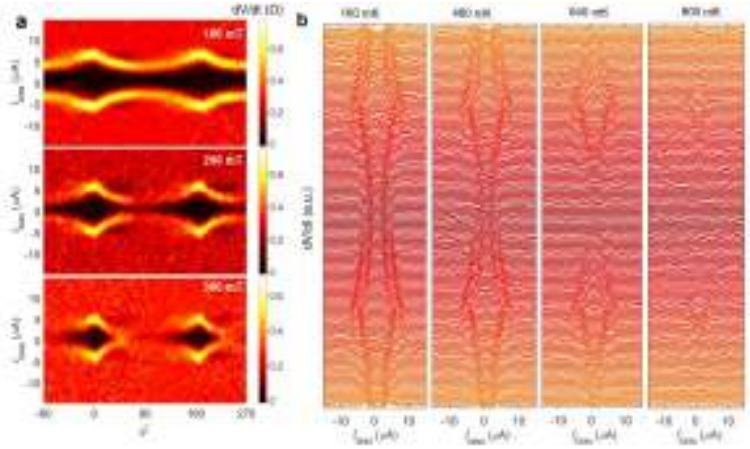

Fig. 1: *Two-fold symmetric superconductivity observed in the kagome superconductor.*

References

[1] S. Wang, B.-C. Lin, et al., *Two-fold symmetric superconductivity in the Kagome superconductor RbV_3Sb_5*, Commun. Phys. **7**, 15 (2024).
[2] *Unconventional superconductivity in the kagome superconductor AV_3Sb_5* (Unpublished).

Abstract ID: 1162

TWO-DIMENSIONAL METAL-ORGANIC KAGOME SYSTEMS AS CANDIDATES FOR THE STUDY OF SPIN LIQUIDS OR THE QUANTUM ANOMALOUS HALL EFFECT

Adam Hassan Denawi[1], Roland Hayn[2], Mathieu Abel[2], Holger Vach[1]

[1]CNRS, LPICM, École Polytechnique, IP Paris, Palaiseau 91128, FRANCE
[2]Aix Marseille Université, CNRS, IM2NP UMR 7334, 13397 Marseille, FRANCE
E-mail: hassan.denawi@polytechnique.edu

The Kagome Heisenberg antiferromagnet has emerged as a pivotal model for investigating highly frustrated magnetism, drawing attention for its unique electronic and transport characteristics on kagome lattices. These properties, reminiscent of the Dirac point in graphene with symmetry-protected band-crossing points, have sparked interest in the exploration of topological quantum materials. Recent findings highlighting ferromagnetic kagome metals further underscore the significance of kagome systems as potential platforms for such materials.

We theoretically examined metal-organic free-standing monolayers of $TM_3C_6O_6$, where 3d transition metals (TM) establish coordination bonds with C_6O_6 ligands. The resulting Kagome lattice, renowned for its unconventional topological and magnetic features, served as a focal point. Kagome lattice materials are acknowledged as topological quantum materials, exhibiting a Dirac point (in the nonmagnetic case for two spin directions) or a Weyl point (in a ferromagnetic material with only one spin direction) at a high symmetry point in the Brillouin zone.

The pronounced frustration in the kagome lattice holds significance in magnetism, offering avenues for exploring spin liquids. Our investigation encompassed all possible 3d transition metals (TM) from Sc to Cu in $TM_3C_6O_6$ [1,2], revealing diverse realizations of unconventional systems. Particularly noteworthy were instances of Heisenberg kagome antiferromagnets with varying values of local spin, presenting opportunities for exploring the spin liquid state. Additionally, we observed the presence of the kagome lattice with ferromagnetic interactions, facilitating the spin ice state. These findings contribute to the evolving understanding of topological quantum materials in kagome systems.

References

[1] A.H. Denawi, X. Bouju, M. Abel, J. Richter, R. Hayn, Physical Review Materials **7**, 74201 (2023).
[2] N. Shaiek, H. Denawi, M. Koudia, R. Hayn, S. Schäfer, I. Berbezier, C. Lamine, O. Siri, A. Akremi, M. Abel, Advanced Materials Interfaces **9**, 2201099 (2022).

CANCELLED

Effects of Topology in Superconductor Nanoarchitectures I

29.04.2024 MONDAY

Abstract ID: 1041

ELIASHBERG THEORY AND TOPOLOGY OF SUPERCONDUCTING THIN FILMS

G.A. Ummarino[1,2], A. Zaccone[3]

[1]*Department of Applied Science and Technology, Politecnico di Torino, Corso Duca degli Abruzzi 24, 10129 Torino, ITALY*
[2]*Department of Semiconductor Quantum Electronics, National Research Nuclear University MEPhI, Moscow Engineering Physics Institute, Kashira Hwy 31, 115409 Moskva, RUSSIA*
[3]*Department of Physics "A. Pontremoli," University of Milan, via Celoria 16, 20133 Milan, ITALY*
E-mail: giovanni.ummarino@polito.it

We present a generalization, in the Eliashberg framework, of a BCS theory of superconductivity in good metals which are confined along one of the three spatial directions, such as thin films. By solving in a numerical way these new Eliashberg type equations we find the dependence of the superconducting critical temperature T_c as a function of the confinement size L, in quantitative agreement with experimental data with no adjustable parameters. Upon increasing the confinement, a crossover from a spherical Fermi surface, which contains two growing hollow spheres corresponding to states forbidden by confinement, to a strongly deformed Fermi surface, is predicted. This crossover represents a new topological transition, driven by confinement, between two Fermi surfaces belonging to two different homotopy classes. This topological transition provides a mechanistic explanation of the commonly observed non-monotonic dependence of T_c upon film thickness with a maximum which, according to our theory, coincides with the topological transition.

References

[1] R. Travaglino, A. Zaccone, J. Appl. Phys. **133**, 033901 (2023).
[2] M. Baggioli, C. Setty, A. Zaccone Phys. Rev. B **101**, 214502 (2020).

Abstract ID: 1122

THE UNCONVENTIONAL NORMAL STATE OF TWISTED BILAYER GRAPHENE

María José Calderón

Instituto de Ciencia de Materiales de Madrid, ICMM-CSIC, SPAIN
E-mail: calderon@icmm.csic.es

Twisted bilayer Graphene (TBG) shows a great variety of correlated states. Among the experimental observations, the cascades in the spectroscopic properties [1] and in the compressibility [2] happen in larger ranges of energy, twist angle and temperature than other effects, pointing to a hierarchy of phenomena. In this talk I will show that the spectral weight reorganization associated to the formation of local moments and heavy quasiparticles can explain the cascade signatures without invoking symmetry breaking orders [3]. Our results are based on Dynamical Mean Field Theory plus Hartree calculations. We reproduce the cascade flow of spectral weight, the oscillations of the remote band energies, the asymmetric jumps of the inverse compressibility, and the presence of resistive states. We predict a strong momentum differentiation in the incoherent spectral weight associated to the fragile topology of TBG. I will also show how strong correlations impact other measurements that can be performed in order to characterize the unconventional normal state of these moiré systems.

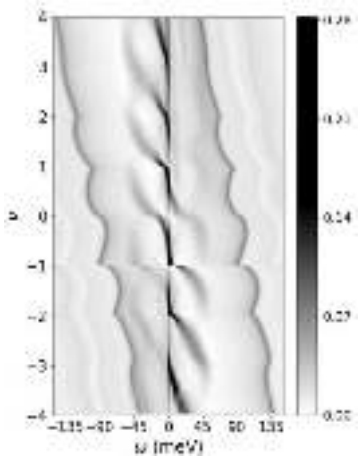

Fig. 1: *Contour plot of the density of states obtained from the Dynamical Mean Field Theory plus Hartree calculations versus doping n and energy w. Cascades of incoherent spectral weight resemble scanning tunneling microscopy experiments [1]. The cascades at positive and negative energies are shifted in doping. Figure from Ref. [3].*

References

[1] D. Wong *et al.*, Nature **582**, 198 (2020); Y. Choi *et al.*, Nature **589**, 536 (2021).
[2] U. Zondiner *et al.*, Nature **582**, 203 (2020).
[3] A. Datta, A. Camjayi, M.J. Calderón, E. Bascones, Nature Communications **14**, 5036 (2023).

Abstract ID: 1169

STUDY OF VORTEX DYNAMICS IN SUPERCONDUCTING NANOARRAYS

A. Arroyo-Fructuoso[1], G. Hlawacek[2], R. Córdoba[1]

[1]*Universitat de València (UV), Institute of Molecular Science (ICMol), Catedràtic José Beltrán Martínez, 46980, Paterna, SPAIN*
[2]*Helmholtz-Zentrum Dresden-Rossendorf (HZDR), Bautzner Landstraße, 01328, Dresden, GERMANY*
E-mail: alba.arroyo@uv.es

The fabrication of superconducting (SC) nanoarrays has acquired interest in the investigation of collective phenomena [1] for their use in computer technology. The production of these devices is a complex multi-step process with a high processing time. The use of a direct-write technique makes possible the growth of nanostructures in the three dimensions on targeted location in a single step with a very high lateral resolution (sub-10 nm) [2,3]. Here, we used a direct-write technique to grow SC nanoarrays. The acquired STEM images reveal the successful growth of two types of nanoarrays: 1) gentle thickness modulation (GM) between SC nanoobjects and 2) steep thickness modulation between SC nanoobjects (SM). The SC properties in both types of nanoarrays were studied by magnetotransport measurements. Minimums of resistance at high values of magnetic field were observed in GM and SM. In the case of GM samples, the reduced thickness between ellipses creates pinning sites for vortex motion resulting in the so- called matching effect a certain values of applied magnetic field (Fig. 1)[4]. In the case of SM samples, where SC nanoobjects are separated by a normal region, the specific geometry of the nanoarray prevents the formation of an Abrikosov lattice. This impossibility leads vortices to arrange in various lattice configurations, resulting in magnetic frustration [5].

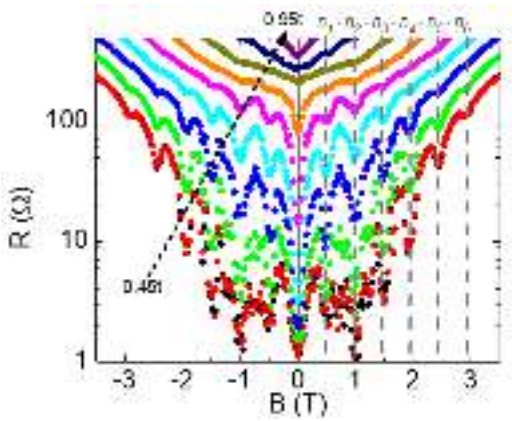

Fig. 1: *Resistance vs. applied magnetic field measurement of a typical GM nanoarray.*

These results indicate that employing a direct-write technique enables the controlled growth of nanostructures with diverse characteristics, facilitating the study of exciting physical phenomena in the area of fluxonics.

Acknowledgments

This work is supported by the Grant RYC2020-029075-I funded by MCIN/AEI/ 10.13039/501100011033 and by "ESF Investing in your future", the Generalitat Valenciana (SEJIGENT/2021/012T) and the European Cooperation in Science and Technology COST Action CA16218 (FIT4NANo) and CA21144 (SuperQuMap).

References

[1] Y. Imry, L. Gunther, Phys. Rev., 10, 11 (1974).
[2] P. Orús, *et al.*, Nanotechnology, 32, 8 (2021).
[3] R. Córdoba, *et al*, Nano Lett., 19, 12 (2019).
[4] L. Backmeister, *et al.*, Nanomaterials, 12, 19 (2022).
[5] G. Ithier, *et al.*, Phys. Rev. B, 72, 13 (2005).

Effects of Topology in Superconductor Nanoarchitectures II

29.04.2024 MONDAY

Abstract ID: 1142

MICROSCALE METASURFACES FOR ON-CHIP MAGNETIC FLUX CONCENTRATION

E. Fourneau[1], N. Lejeune[1], J.A. Arregi[2], M. Stano[2], A. Barrera[3], N. Bort-Soldevila[4], J. Cunill-Subiranas[4], Th. Pirottin[5], O. Morris[6], O. Leonard[6], B. Vanderheyden[5], N. Mestres[3], Ll. Balcells[3], N. Del-Valle[4], A. Sanchez[4], C. Navau[4], V. Uhlíř[2,7], S. Bending[6], A. Palau[3], A.V. Silhanek[1]

[1]*Université de Liège, EPNM, QMAT, CESAM, Liège, BELGIUM*
[2]*CEITEC BUT, Brno University of Technology, Brno, CZECHIA*
[3]*Institut de Ciència de Materials de Barcelona, ICMAB-CSIC, Bellaterra, SPAIN*
[4]*Departament de Física, Universitat Autònoma de Barcelona, Bellaterra, SPAIN*
[5]*Department of Electrical Engineering and Computer Science, Université de Liège, BELGIUM*
[6]*University of Bath, Centre for Nanoscience and Nanotechnology, Bath, UNITED KINGDOM*
[7]*Brno University of Technology, Institute of Physical Engineering, Brno, CZECHIA*
E-mail: asilhanek@uliege.be

Magnetic metamaterials inspired by optics transformation and combining ferromagnetic and superconducting layers have demonstrated promising perspectives to improve the efficiency of macroscopic magnetic flux concentrators [1]. Following this proof-of-concept, we investigate the effects of downscaling these devices (Fig. 1), resulting in thin film metasurfaces suitable for on-chip integration [2]. We scrutinize the influence of the non-linear magnetic response of the ferromagnetic components, their magnetic irreversibility, the formation of magnetic domains, as well as the effects of geometry and size of the devices. We demonstrate that well-designed magnetic metasurfaces with microscale lateral dimensions can have a large concentration gain but also the unique property of isotropic amplification, i.e., constant field concentration without a preferential direction of the external magnetic field. Our results prove that the implementation of metasurfaces at the microscale opens up new technological possibilities for enhancing the performance of magnetic field detectors and remotely charging small electric devices, thus paving the way towards new approaches in information and communication technologies.

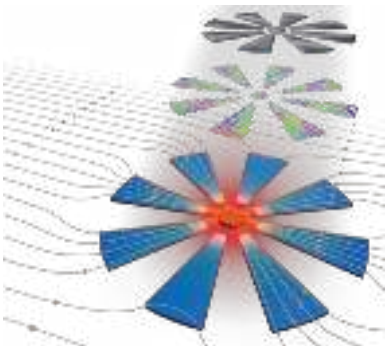

Fig. 1: *Magnetic response of a 8-petal magnetic metasurface obtained using finite-element simulation, micromagnetic simulation and magneto-optical Kerr effect microscopy.*

References

[1] J. Prat-Camps, C. Navau, A. Sanchez, Appl. Phys. Lett **105**, 234101 (2014).
[2] E. Fourneau *et al.*, Adv. Mater. Technol. **2**, 2200042 (2023).

Abstract ID: 1149

NONRECIPROCAL SPIN WAVES IN 3D SCREW-LIKE FERROMAGNETIC TUBES PREPARED BY ATOMIC LAYER DEPOSITION

M. Xu[1], A. J.M. Deenen[1], H. Guo[1], D. Grundler[1,2]

[1]*Laboratory of Nanoscale Magnetic Materials and Magnonics (LMGN), Institute of Materials (IMX), School of Engineering, Ecole Polytechnique Fédérale de Lausanne (EPFL), 1015 Lausanne, SWITZERLAND*
[2]*Institute of Electrical and Micro Engineering, EPFL, 1015 Lausanne, SWITZERLAND*
E-mail: dirk.grundler@epfl.ch

Chiral magnets offer helical arrangement of magnetic moments leading to nonreciprocal transport. Relevant natural chiral magnets have provided helical and conical spin structures with low spin-wave damping below room temperature [1,2]. Using two-photon lithography and atomic layer deposition of 30-nm-thick Ni, we have synthesized hollow ferromagnetic tubes with a spirally corrugated surface. The tubes had an outer diameter of about 1 micrometre. Using micro-focused Brillouin light scattering spectroscopy scanning over the surface of tubes, we observed asymmetric Stokes and anti-Stokes signals attributed to magnon nonreciprocity at room temperature. The asymmetries depended on their structurally defined handedness and the magnetic field orientation. The experimental findings were supported by micromagnetic simulations. Importantly, we noted a field-programmable magnetic chirality at zero field in the remanent state. Our findings highlight the potential of our additive manufacturing methodology [3] for creating curvature-controlled magnonic waveguides which could serve as building blocks for nonreciprocal GHz signal steering in 3D device architectures.

The work is supported by SNSF via grant 197360.

References

[1] T. Schwarze *et al.*, Nat. Mater. **14**, 478 (2015).
[2] P. Che *et al.*, Phys. Rev. Res. **3**, 033104 (2021).
[3] H. Guo *et al.*, Adv. Mater. **35**, 2303292 (2023).

Abstract ID: 1150

INTEGRATION OF MAGNONS INTO SUPERCONDUCTING QUANTUM CIRCUITS

D. García-Pons, J. Pérez-Bailón, F. Luis, D. Zueco, María José Martínez-Pérez

Instituto de Nanociencia y Materiales de Aragón CSIC-Universidad de Zaragoza, Calle Pedro Cerbuna 12, 50009 Zaragoza, ESPAÑA
E-mail: pemar@unizar.es

Circuit Quantum Electrodynamics (QED) is enormously powerful, allowing, e.g., the manipulation and interrogation of superconducting or magnetic qubits and quantum sensing of individual spins. All these interesting applications are built upon the condition of strong coupling between the qubit and a quantized field of excitations. Besides photons, the solid state offers a wide variety of bosonic excitations that can be emitted or absorbed such as, e.g., magnons, the quantum version of spin waves.

Magnonic cavities are expected to play an important role since they shall allow building coherent qubit-qubit interactions between distant spin qubits, a challenge difficult to overcome with conventional electromagnetic cavities. One fundamental step towards achieving this goal is the integration of magnonic cavities into superconducting circuits, commonly employed for qubit manipulation and readout. In this context, we present our progress in integrating patterned magnetic nanostructures hosting both homogeneous and topologically protected textures into superconducting devices. Additionally, we perform broadband ferromagnetic resonance measurements and cavity experiments that demonstrate that the light-matter coupling strength can be estimated using either open superconducting transmission lines or resonant cavities, yielding very good agreement. Finally, we describe a simple theoretical framework based on electromagnetic and micromagnetic simulations that successfully accounts for the experimental results. This approach can be used to design hybrid quantum systems exploiting magnetostatic mode excited in ferromagnets of arbitrary size and shape and to tune their operation conditions.

Effects of Topology in Superconductor Nanoarchitectures III

29.04.2024 MONDAY

Abstract ID: 1211

SUPERCURRENT-ENABLED ANDREEV REFLECTION IN A CHIRAL QUANTUM HALL EDGE STATE

Andreas Bock Michelsen[1,2], Patrik Recher[3,4], Bernd Braunecker[1], Thomas L. Schmidt[2]

[1]*SUPA, School of Physics and Astronomy, University of St. Andrews, North Haugh, St. Andrews KY16 9SS, UNITED KINGDOM*
[2]*Department of Physics and Materials Science, University of Luxembourg, 1511 Luxembourg, LUXEMBOURG*
[3]*Institut für Mathematische Physik, Technische Universität Braunschweig, 38106 Braunschweig, GERMANY*
[4]*Laboratory for Emerging Nanometrology, 38106 Braunschweig, GERMANY*
E-mail: thomas.schmidt@uni.lu

A chiral quantum Hall (QH) edge state placed in proximity to an s-wave superconductor experiences induced superconducting correlations. Recent experiments have observed the effect of proximity coupling in QH edge states through signatures of the mediating process of Andreev reflection. We present the microscopic theory behind this effect by modeling the system with a many-body Hamiltonian, consisting of an s-wave superconductor, subject to spin-orbit coupling and a magnetic field, which is coupled by electron tunneling to an integer or fractional QH edge state. By integrating out the superconductor we obtain an effective pairing Hamiltonian in the QH edge state. We clarify the qualitative appearance of nonlocal superconducting correlations in a chiral edge state and analytically predict the suppression of electron-hole conversion at low energies (Pauli blocking) and negative resistance as experimental signatures of Andreev reflection in this setup. In particular, we show how two surface phenomena of the superconductor, namely, Rashba spin-orbit coupling and a supercurrent due to the Meissner effect, are essential for the Andreev reflection.

References

[1] A.B. Michelsen, P. Recher, B. Braunecker, T.L. Schmidt, Phys. Rev. Research **5**, 013066 (2023).

Abstract ID: 1222

CURVED SUPERCONDUCTING VORTICES IN THREE-DIMENSIONAL NANOARCHITECTURE

Elina Zhakina[1], Luke Turnbull[1], Weijie Xu[1], Markus König[1], Paul Simon[1], Wilder Carrillo-Cabrera[1], Amalio Fernandez-Pacheco[2], Dieter Suess[3,4], Claas Abert[3,4], Vladimir M. Fomin[5,6], Claire Donnelly[1,8]

[1]*Max Planck Institute for Chemical Physics of Solids, Nöthnitzer Str. 40, 01187 Dresden GERMANY*
[2]*Institute of Applied Physics, TU Wien, Wiedner Hauptstr. 8-10/134,1040 Vienna, AUSTRIA*
[3]*Physics of Functional Materials, Faculty of Physics, University of Vienna, Kolingasse 14-16, A-1090, Vienna, AUSTRIA*
[4]*Research Platform MMM Mathematics-Magnetism Materials, University of Vienna, Vienna, 1090, AUSTRIA*
[6]*Institute for Emerging Electronic Technologies, Leibniz IFW Dresden, Helmholtzstraße 20, D-01069 Dresden, GERMANY*
[7]*Moldova State University, strada A. Mateevici 60, MD-2009 Chişinău, REPUBLIC OF MOLDOVA*
[8]*International Institute for Sustainability with Knotted Chiral Meta Matter (WPI-SKCM2), Hiroshima University, Hiroshima 739-8526, JAPAN*
E-mail: elina.zhakina@cpfs.mpg.de

Three-dimensional nanostructuring offers new possibilities to control the emergent properties of quantum materials via geometric effects. In nanomagnetism, for example, the introduction of curvature can lead to exotic dynamic effects, as well as curvature-induced chirality and anisotropy. In superconductivity, the introduction of three-dimensional geometries offers a route to controlling the emergent properties of the system, such as spatial variations in the supercurrents and vortex dynamics leading to phase slips [1, 2], with new opportunities for devices. However, while the investigation of 3D magnetic nanostructures is now well established, three-dimensional superconducting systems remain in their infancy due to outstanding challenges in their fabrication and characterization [2].

In this work, we present the local control over the emergent properties in superconductors by patterning three-dimensional nano geometries with focused electron-beam-induced-deposition [3]. Specifically, we grow a prototype direct-write three-dimensional superconducting nanostructure with a critical temperature of about 5 K. With a local nanowire diameter in the order of 180 nm, our structure lies in between two fundamental superconducting length scales: the coherence length and the London penetration depth, such that our confinement effects manifest in the interaction of the structure with the applied magnetic field. With local and non-local transport measurements, we experimentally confirm the presence and propagation of superconducting vortices through our 3D superconducting nanostructure. We gain insight into the 3D nature of the vortices by performing finite element three-dimensional time-dependent Ginsburg-Landau simulations, revealing the superconducting vortices to be curvilinear and exhibit non-trivial field-dependent pinning effects. Beyond the propagation of the vortices, the geometric confinement leads to a local anisotropy in the upper-critical magnetic field, allowing for the local design of the superconducting state. With these fabrication capabilities and local control of the superconducting properties, the evaluation of arbitrary 3D geometries becomes possible, leading to opportunities for the design and realization of 3D superconducting nanoarchitectures.

References

[1] V. Fomin *et al.*, Appl. Phys. Lett. **120**, 090501 (2022).
[2] R. Córdoba, Rosa, *et al.*, Nano letters **19.12**, 8597-8604 (2019).
[3] L. Skoric *et al.*, Nano Letters **20 (1)**, 184-191 (2020).

Abstract ID: 1660

THE CHALLENGES OF BRAIDING WITH MAJORANA ZERO MODES

E. Mascot[1], T. Hodge[1], D. Crawford[1], C. Peeters[1], J. Bedow[2], D. K. Morr[2], S. Rachel[1]

[1] *University of Melbourne, School of Physics, 3010, Parkville, AUSTRALIA*
[2] *University of Illinois at Chicago, Dept. of Physics, 60607, Chicago, USA*
E-mail: eric.mascot@unimelb.edu.au

Majorana zero modes have been celebrated as a promising avenue for achieving topologically protected quantum computing. Recent experiments show strong evidence for the presence of Majorana zero modes. However, doubts persist regarding their practical viability. To address this, numerical simulations become essential for assessing their real-world potential. A novel method [1] has simplified such simulations and drastically reduced the computational cost. We have conducted a comprehensive investigation on the impact of factors such as disorder, low-lying sub-gap states, and dissipation to elucidate the limitations of a topological quantum computer. In this talk, I will present the current progress of these simulations.

References

[1] E. Mascot, T. Hodge, D. Crawford, J. Bedow, D.K. Morr, S. Rachel. *Many-body Majorana braiding without an exponential Hilbert space*, Phys. Rev. Lett. **131**, 176601 (2023).

Effects of Topology in Superconductor Nanoarchitectures IV

29.04.2024 MONDAY

Abstract ID: 1303

TOPOLOGY-DRIVEN VORTEX COMMENSURABILITY IN YBCO THIN FILMS: PINNING FORCE OF AN INDIVIDUAL VORTEX AND REENTRANT ZERO RESISTANCE

W. Lang[1], B. Aichner[1], M. Karrer[2], K. Wurster[2], C. Schmid[2], R. Hutt[2], C. Magén[3], L. Backmeister[1], P.A. Korner[1], J.M. De Teresa[3], R. Kleiner[2], E. Goldobin[2], D. Koelle[2]

[1]*University of Vienna, Faculty of Physics, 1090 Vienna, AUSTRIA*
[2]*Universität Tübingen, Physikalisches Institut, Center for Quantum Science (CQ) and LISA+, 72076, Tübingen, GERMANY*
[3]*Universidad de Zaragoza, Instituto de Nanociencia y Materiales de Aragón (INMA), 50009 Zaragoza, SPAIN*
E-mail: wolfgang.lang@univie.ac.at

The study of how topology influences the distribution of Abrikosov vortices in a superconductor hinges on the precise creation of a vortex-pinning potential landscape. It is essential to magnetically couple these vortices, ensuring their separation does not exceed the London penetration depth at the target operating temperature. This temperature must be substantially below the superconductor's critical temperature T_c to mitigate the effects of thermodynamic fluctuations. Achieving the necessary nanoscale precision is particularly challenging in copper-oxide superconductors due to their intricate atomic structure and sensitivity to environmental factors. Traditional lithographic methods face significant limitations in this context, but these can be circumvented by employing the focused beam of a helium ion microscope (He-FIB). The 30 keV He^+ ion beam is utilized to create hexagonal arrays of defect columns, spaced 25 nm or 30 nm apart, in thin films of $YBa_2Cu_3O_{7-\delta}$. Within these nanocolumns, T_c is completely suppressed due to pair-breaking caused by numerous point defects. These defects are primarily generated by the interaction of helium ions with oxygen atoms in the thin film.

The unique topology of our pinning landscapes results in several notable phenomena. At high magnetic fields, reaching several tesla, we observe vortex commensurability effects. These effects include the formation of an ordered Bose glass of vortices stemming from the interplay between vortex pinning at regular and irregular sites [1,2]. Moreover, we observe reentrant zero resistance at an applied magnetic field of 3.8 T, accompanied by a pronounced peak in both the critical current and the pinning force density of the vortex ensemble. The observation of commensurability effects, when the vortex density aligns with the precisely known density of defect columns, enables us to determine the pinning force exerted on a single vortex by an artificial defect. We will also discuss how this pinning force varies with temperature.

Acknowledgments

The research was funded by a joint project of the Austrian Science Fund (FWF), grant I4865-N, and the German Research Foundation (DFG), grant KO 1303/16-1. It is based upon work from COST Actions CA21144 (SuperQuMap), CA19140 (FIT4NANO), and CA19108 (Hi-SCALE) supported by COST (European Cooperation in Science and Technology).

References

[1] L. Backmeister *et al.*, Nanomaterials, **12**, 3491 (2022).
[2] B. Aichner *et al.*, Condens. Matter **8**, 32 (2023).

Abstract ID: 1300

HETEROSTRUCTURES AND HYBRID SYSTEMS BASED ON HIGH-TEMPERATURE SUPERCONDUCTORS FOR ENERGY-EFFICIENT INFORMATION AND COMMUNICATION TECHNOLOGIES

A. Palau[1], T. Günkel[1], J. Alcalà[1], A. Barrera[1], A. Fernández-Rodríguez[1], Marinkovic[2], E. Fourneau[2], A.V. Silhanek[2], J. Suñé[3], L.L. Balcells[1], N. Mestres[1]

[1]*Institut de Ciència de Materials de Barcelona, ICMAB-CSIC, Bellaterra, 08193, SPAIN*
[2]*Experimental Physics of Nanostructured Materials, Q-MAT, CESAM, Université de Liège, B-4000 Liège, BELGIUM*
[3]*Departament d'Enginyeria Electrònica, Universitat Autònoma de Barcelona, 08193, SPAIN*
E-mail: palau@icmab.es

Today advances to store and analyze massive information offer huge opportunities and unprecedented benefits in business, healthcare, security, society, and industrial applications. Design and fabrication of novel materials and heterostructures with improved tailored properties are needed to achieve high performance in a sustainable way. Multifunctional materials based on complex oxides offer unique opportunities to tune their magnetic or electric properties with multiple external inputs, thus providing the basis for realizing energy-efficient electronic devices. Among numerous outstanding properties of strongly correlated multifunctional oxides, superconducting cuprates are of special interest due to their inherent energy efficiency.

This work is focused on the study of nanostructures, multilayers, and hybrid systems based on high-temperature superconducting cuprates with innovative functionalities which can contribute to the development of sustainable Information and Communication Technologies. $YBa_2Cu_3O_{7-x}$ (YBCO) structures have been combined with ferromagnetic (Permalloy, CoFeB, Co, $La_{1-x}Sr_xMnO_3$), insulating oxides (CeO_2, Al_2O_3), and metallic (Ag, Au) materials to explore novel interactions and useful physical phenomena. The performance of the explored devices has been modified through material engineering – oxygen doping, crystallographic defects, epitaxy, strain, interfacial or geometric effects [1].

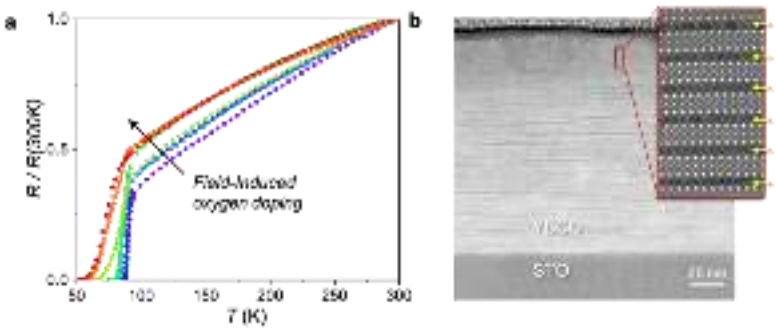

Fig. 1: *(a) Tunning of the superconducting critical temperature though field induced oxygen doping. (b) TEM image of a YBCO film with field-induced interstitial defects (stacking-faults).*

References

[1] Alcalà *et al.*, Scientific Reports (In press), Marinkovíc *et al.*, ACS Nano, **14**, 11765 (2020), Palau *et al.*, ACS Appl. Mater. Interfaces **10**, 30531(2018), Rouco *et al.*, Nano Letters **19**, 4174 (2019), Palau *et al.*, Advanced Science **3**, 1600207 (2016), Stangl *et al.*, Sientific Reports, **11**, 8176 (2021).

Abstract ID: 1632

ADVANCEMENTS IN SOLVING THE 2D FERMI HUBBARD MODEL AT FINITE TEMPERATURE: INSIGHTS FROM TENSOR NETWORK METHODS

Aritra Sinha, Alexander Wietek, Marek M. Rams, Jacek Dziarmaga

Max Planck Institute for the Physics of Complex Systems, Dresden, GERMANY
E-mail: asinha@pks.mpg.de

The **Fermi Hubbard Model (FHM)** stands as a cornerstone in the study of interacting electrons on a lattice, encapsulating the fundamental aspects of condensed matter physics. Despite its apparent simplicity, accurately solving the model in two dimensions for the ground state and at finite temperatures has posed a significant challenge. Recent advancements in tensor network methods, particularly through **matrix product states (MPS)** on **cylindrical geometry** and **infinite projected entangled pair states (iPEPS)** on a genuinely **2D infinite** plane [1], have ushered in a new era of understanding the model's ground states. Yet, the exploration of finite temperature regimes, especially for larger lattices, remains an arduous frontier. In our research, we employ the **Neighborhood Tensor Update (NTU)** algorithm in conjunction with iPEPS to facilitate the imaginary time evolution (involved in the calculation of thermal states), successfully accessing temperatures as low as 0.17 times the hopping rate [2]. This approach has focussed on **slightly doped** lattices within strong coupling regimes, revealing **disruptions in the background antiferromagnetic order** that hint at complex underlying physics. To probe even deeper into the low-temperature regime, we introduce a novel algorithm that integrates **Minimally Entangled Typical Thermal States (METTS)** with finite PEPS, a method distinguished for its efficiency in simulating finite temperature quantum systems at significantly reduced computational costs [3]. Parallelly we also employ MPS on cylinder geometries using METTS to understand the phase diagram of the Hubbard model from disordered states at high temperatures to ordered states down to very low temperatures offering a 'handshake' with the ground state [4]. Our findings highlight the intricate regimes at finite temperatures, identifying **incipient phase-separated** regimes characterized by **coexistence** of **charge-clustered antiferromagnetic** regions and **hole-rich** zones. This phase separation manifests as a peak in the charge structure factor at the lowest momentum mode distinguishing it from the peak at a fixed momentum at very low temperatures when the stripe-phase physics sets in. Further we discuss the possible role of charge clustering for the physics of FHM at intermediate temperatures.

References

[1] Bo-Xiao Zheng *et al.*, *Stripe order in the underdoped region of the two-dimensional Hubbard model*, Science **358**, 6367 (2017).

[2] A. Sinha, M.M. Rams, P. Czarnik, J. Dziarmaga, *Finite temperature tensor network study of the Hubbard model on an infinite square lattice*, Phys. Rev. B **106**, 195105 (2022).

[3] A. Sinha, M.M. Rams, J. Dziarmaga, *Efficient representation of minimally entangled typical thermal states in two dimensions via projected entangled pair states*, Phys. Rev. B **109**, 045136 (2024).

[4] A. Sinha, A. Wietek, (in preparation).

Abstract ID: 1116

NEAR-FIELD MICROWAVE MICROSCOPE FOR EXPLORING TRAPPED VORTICES IN SUPERCONDUCTORS

Chung-Yang Wang, Steven M. Anlage

Quantum Materials Center, Physics Department, University of Maryland, College Park, MD 20742-4111, USA
E-mail: anlage@umd.edu

Understanding and removing trapped vortices is essential for optimizing the performance of flux-quantum-based digital superconducting devices. In this study, we employ a near-field magnetic microwave microscope with sub-micron spatial resolution [1-4] to shake trapped vortices with a local and intense RF magnetic field and analyze the response. The sample used in this study is a Nb film containing intentionally-created non-superconducting holes designed to act as pinning sites for DC vortices. To create these trapped vortices, a DC magnetic field is applied as the Nb film cools down across its critical temperature. The microwave microscope applies an intense microwave magnetic field at frequency *f* to a sub-micron area of the sample. We then monitor the local response of the superconductor due to screening currents flowing at frequencies *2f* and *3f* to learn about the nonlinear response of the material [1-4]. Time-dependent Ginzburg-Landau (TDGL) simulations in COMSOL [3, 4] (see Fig. 1) predict that the wiggling of trapped vortices, induced by a locally-applied RF magnetic field, typically results in a strong second harmonic (*2f*) response. The experimental results validate the predictions, demonstrating a strong second harmonic response. The dependence of this response on the strength of the DC magnetic field and the temperature are investigated to understand the distribution and pinning strength of the vortices.

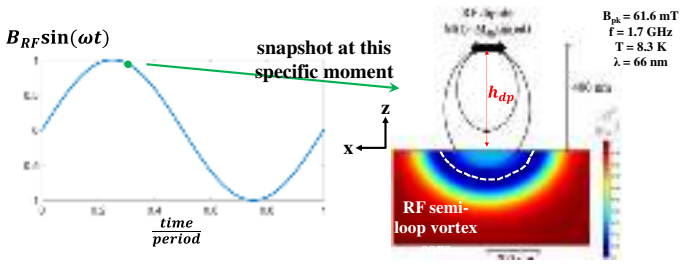

Fig. 1: *TDGL simulation of a bulk Nb surface being stimulated by an rf magnetic dipole at f = 1.7 GHz, showing the superconducting order parameter around an rf vortex semi-loop [3,4].*

This work is funded by US Department of Energy / High Energy Physics through grant # DE-SC0017931.

References

[1] Tamin Tai, *et al.*, *Nanoscale nonlinear radio frequency properties of bulk Nb: Origins of extrinsic nonlinear effects*, Phys. Rev. B **92**, 134513 (2015).
[2] Bakhrom Oripov, *et al.*, *High frequency nonlinear response of superconducting cavity-grade Nb surfaces*, Phys. Rev. Applied **11**, 064030 (2019).
[3] Bakhrom Oripov, Steven M. Anlage, *Time-dependent Ginzburg-Landau treatment of rf magnetic vortices in superconductors: Vortex-semiloops in a spatially nonuniform magnetic field*, Phys. Rev. E **101**, 033306 (2020).
[4] Chung-Yang Wang, *et al.*, *Microscopic examination of srf-quality Nb films through local nonlinear microwave response*, arXiv:2305.07746.

Advances in Current-Induced Magnetization Control I

29.04.2024 MONDAY

Abstract ID: 1336

PROBABILISTIC COMPUTING WITH MAGNETIC P-BITS: OPTIMIZATION, MACHINE LEARNING AND QUANTUM SIMULATION

Kerem Y. Çamsarı

[1]*Department of Electrical and Computer Engineering, University of California, Santa Barbara, Santa Barbara, 93106 USA*
E-mail: camsari@ucsb.edu

The slowing down of Moore's era has coincided with escalating computational demands from Machine Learning and Artificial Intelligence. An emerging trend in computing involves building physics-inspired computers that leverage the intrinsic properties of physical systems for specific domains of applications. Probabilistic computing with p-bits, or probabilistic bits, has emerged as a promising candidate in this area, offering an energy-efficient approach to probabilistic algorithms and applications [1-4].

Several implementations of p-bits, ranging from standard CMOS technology to nanodevices, have been demonstrated. Among these, the most promising p-bits appear to be based on stochastic magnetic tunnel junctions (sMTJ) [2]. sMTJs harness the natural randomness observed in low-barrier nanomagnets to create energy-efficient and fast fluctuations, up to GHz frequencies [4]. In this talk, we will discuss how magnetic p-bits can be combined with conventional CMOS to create hybrid probabilistic-classical computers for various applications. We will provide recent examples of how p-bits are naturally applicable to combinatorial optimization, such as solving the Boolean satisfiability problem [3], energy-based generative machine learning models like deep Boltzmann machines, and quantum simulation for investigating many-body quantum systems.

Through experimentally informed projections for scaled p-computers using sMTJs, we will demonstrate how physics-inspired probabilistic computing can lead to GPU-like success stories for a sustainable future in computing.

References

[1] S. Chowdhury, A. Grimaldi, N.A. Aadit, S. Niazi, M. Mohseni, S. Kanai, H. Ohno, S. Fukami, L. Theogarajan, G. Finocchio, S. Datta, K.Y. Camsari, *A full-stack view of probabilistic computing with p-bits: devices, architectures and algorithms*, IEEE Journal on Exploratory Solid-State Computational Devices and Circuits, (2023)

[2] W.A. Borders, A.Z. Pervaiz, S. Fukami, K.Y. Camsari, H. Ohno, S. Datta, *Integer factorization using stochastic magnetic tunnel junctions*, Nature, **573**, 390-393 (2019)

[3] N.A. Aadit, A. Grimaldi, M. Carpentieri, L. Theogarajan, J.M. Martinis, G. Finocchio, K.Y. Camsari, *Massively parallel probabilistic computing with sparse ising machines*, Nature Electronics (2022)

[4] N.S. Singh, S. Niazi, S. Chowdhury, K. Selcuk, H. Kaneko, K. Kobayashi, S. Kanai, H. Ohno, S. Fukami K.Y. Camsari, *Hardware demonstration of feedforward stochastic neural networks with Fast MTJ-based p-bits*, IEDM (2023)

Abstract ID: 1172

DESIGN AND APPLICATIONS OF MTJs IN UNCONVENTIONAL COMPUTING AND MULTIPHYSICS SOLUTIONS

A. Grimaldi[1], E. Raimondo[1], F. Garescì[2], A. Giordano[2], M. Carpentieri[3], G. Finocchio[1]

[1]*University of Messina, MIFT Dept., 98166, Messina, ITALY*
[2]*University of Messina, Dept. Of Engineering, 98158, Messina, ITALY*
[3]*Politecnico di Bari, Dept. of Electrical and Information Engineering, 70126, Bari, ITALY*
E-mail: andrea.grimaldi@unime.it

The progress of magnetic tunnel junctions (MTJs) is driving the development of applications in a wide range of fields. Recently, we have proposed how to develop a new class of spintronic accelerometers [1] that are compact and can drive the acceleration detection only by reading a change in a voltage across an MTJ working as diode. In addition, considering the growing scientific interest in Ising machines (IMs) [2], we have considered [3] how MTJs can be used for the design of two emerging IM paradigms: probabilistic Ising machines (PIMs) [4] and oscillatory Ising machines (OIMs) [5].

OIMs are implemented by generating in-plane self-oscillations using a dc STT current combined with ac STT current at double the oscillation frequency.

PIMs can be implemented using out-of-plane MTJs with unperturbed stable energy minima along the z-axis. An SOT current pulse can be used to temporarily bring the magnetization in-plane, and an STT current can be used to tune which states it relaxes to after the pulse.

Acknowledgements

This work was supported under the project number 101070287 — SWAN-on-chip — HORIZON-CL4-2021-DIGITAL-EMERGING-01, the projects PRIN 2020LWPKH7 – The Italian factory of micromagnetic modeling and spintronics and PRIN_20225YF2S4 – Magneto-Mechanical Accelerometers, Gyroscopes and Computing based on nanoscale magnetic tunnel junctions (MMAGYC), funded by the Italian Ministry of University and Research.

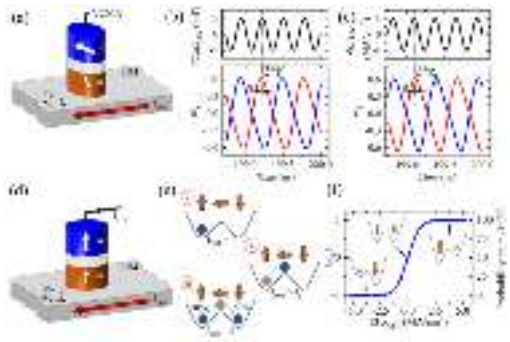

Fig. 1: *(a) MTJ schematic of the OIM. (b)-(c) Binarized phase (red and blue) of the oscillation. In the top panels, the external signal: an ac VCMA effect in (a) and an ac STT current in (b). (d) MTJ schematic of the PIM. (e) The stable magnetization (i) is brought to a metastable state (ii) before relaxing back to either of the two stable states (iii). (f) Relaxation state probability tuned using an STT current.*

References

[1] A. Meo *et al.*, Phys. Rev. Appl. **20**, 034003 (2023).
[2] N. Mohseni *et al.*, Nat. Rev. Phys. **4**, 363-379 (2022).
[3] A. Grimaldi *et al.*, Phys. Rev. Appl. **20** (2023).
[4] T. Wang, J. Roychowdhury, in Lecture Notes in Computer Science, 232-256 (2019).
[5] S. Chowdhury *et al.*, JXCDC **9**, 1-11 (2023).

Abstract ID: 1601

ELECTRICAL SWITCHING OF MAGNETIC TUNNEL JUNCTIONS FOR FUTURE ELECTRONICS

Kewen Shi, Weisheng Zhao

Fert Beijing Institute, MIIT Key Laboratory of spintronics, School of Integrated Circuit Science and Engineering, Beihang University, Beijing 100191, CHINA
E-mail: shikewen@buaa.edu.cn

Current induced magnetization switching of magnetic tunnel junction (MTJ) is crucial for low-power and high-speed magnetic random-access memory (MRAM). In this report, we will focus on the key achievements and advanced technologies in the typical electrical switching strategies from the spin transfer torque (STT) MRAM to the spin-orbit torque (SOT) MRAM. During the SOT writing process, an extra in-plane magnetic field is always required to break the balance for deterministic reversal. Herein, we propose the interplay effect of STT and SOT to effectively achieve low-power and field-free switching in perpendicular MTJs. Afterwards, to purchase the higher density and faster speed, antiferromagnetic has become one of novel information storage candidates to replace the conventional ferromagnetic due to its zero-stray field, high-precession frequency and high stability. However, achieving efficient electrical detection and manipulation remains a persistent challenge. Therefore, we report the recent discoveries of the SOT-induced switching in antiferromagnetic random-access memory (ARAM), presenting a potential solution for high-energy-efficient and high-density storages. The distinctive features of various electrical switching strategies make MRAM promising candidates for replacing traditional memories, with the prospect of widespread applications in future electronics.

References

[1] A. Du, *et al.*, *Electrical manipulation and detection of antiferromagnetism in magnetic tunnel junctions*, Nature Electronics **6**, 425–433 (2023).

[2] Z. Guo, *et al.*, *Spintronics for energy-efficient computing: An overview and outlook*, Proceedings of the IEEE **109**, 1398–1417 (2021).

[3] M. Wang, *et al.*, *Field-free switching of a perpendicular magnetic tunnel junction through the interplay of spin–orbit and spin-transfer torques*, Nature Electronics **1**, 582–588 (2018).

[4] D. Xiong, et al. *Antiferromagnetic spintronics: An overview and outlook*, Fundamental Research **2**, 522–534 (2022).

[5] D.Q. Zhu, *et al.*, *First demonstration of three terminal MRAM devices with immunity to magnetic fields and 10 ns field free switching by electrical manipulation of exchange bias*, IEEE International Electron Devices Meeting (IEDM) 17.5.1-17.5.4, (2021).

[6] S. Peng, *et al.*, *Exchange bias switching in an antiferromagnet/ferromagnet bilayer driven by spin–orbit torque*, Nature Electronics **3**, 757–764 (2020).

Advances in Current-Induced Magnetization Control II

29.04.2024 MONDAY

Abstract ID: 1252

THEORY OF ORBITAL GENERATION, DIFFUSION, AND DETECTION

Aurélien Manchon

Aix-Marseille Univ, CNRS, CINaM, Marseille, FRANCE
E-mail: aurelien.manchon@univ-amu.fr

Recent progress in the physics of spin-charge interconversion mediated by spin-orbit coupling has shed new light on the orbital angular momentum degree of freedom. Indeed, while the orbital ordering driven by the crystal-field potential governs the interplay between crystal structure and electronic properties of strongly correlated materials such as Mott insulators, the possibility of transporting the orbital information in these materials has remained an open question so far. In the context of metallic spintronics though, it has been progressively realized that the orbital angular momentum can be generated out of equilibrium, transported, and detected, rather similarly to the spin angular momentum.

The interconversion between charge and orbital currents, via orbital Hall and orbital Rashba effects for instance, might be much more efficient than its spin counterpart because it arises from the orbital texture imposed by the crystal-field potential rather than from spin-orbit coupling. Therefore, corresponding phenomena such as orbital torque and orbital magnetoresistance have been proposed and experimentally reported. Recent phenomenological models of orbital diffusion have been recently proposed but lack quantitative predictability by overlooking microscopic details. Understanding the way orbital currents and densities propagate in metals and accumulate at interfaces requires determining transport coefficients such as orbital conductivity or diffusivity, as well as the ability to interconvert spin currents into orbital currents via spin-orbit coupling.

In this presentation, I intend to provide a discussion of the theoretical aspects of orbital generation, transport, and detection. After introducing general ideas about orbital ordering and orbital angular momentum, I will first discuss the orbital-charge interconversion mechanisms, orbital Hall, and orbital Edelstein effects. I will insist on the distinction between intra-atomic and inter-atomic orbital contributions in these two effects [1]. Then, I will present a quantum theory of orbital diffusion and uncover several mechanisms governing orbital torque and magnetoresistance phenomena, including orbital diffusivity, spin-orbit polarization, orbital swapping, and orbital mixing conductance [2,3]. These new concepts are crucial to the understanding of experimental results and can be computed from first principles. Finally, I will discuss the possibility of detecting orbital densities optically using the orbital Kerr effect. I will particularly emphasize the central role played by the second-order Hall effect, which is a companion phenomenon to the orbital Edelstein effect.

References

[1] Pezo *et al.*, *Orbital Hall effect in crystals: inter-atomic versus intra-atomic contributions*, Phys. Rev. B **106**, 104414 (2021); *Orbital Hall physics in two-dimensional Dirac materials*, Phys. Rev. B **108**, 075427 (2023).

[2] A. Manchon, A. Pezo, K.-W. Kim, K.-J. Lee, *Orbital diffusion, polarization and swapping in centrosymmetric metals*, arXiv:2310.04763

[3] Ning et al., *unpublished*

[4] D.G. Ovalle, A. Pezo, A. Manchon, *Orbital Kerr effect and terahertz detection via the nonlinear Hall effect*, arXiv:2311.11889

Abstract ID: 1187

GENERATION OF ORBITAL CURRENTS AND TORQUES FOR EFFICIENT MANIPULATION OF CHIRAL SPIN TEXTURES FOR SPINTRONICS DEVICES

S. Krishnia[1], G. Beneke[1], K. Raab[1], T. B. Winkler[1], M. A. Brems[1], P. Gerhards[2], K. Knobloch[2], N. Sebe[3], N. Reyren[3], A. Fert[3], H. Jaffrès[3], Vincent Cros[3], Johan Mentink[4], M. Kläui[1]

[1]*Institut für Physik, Johannes Gutenberg-Universität Mainz, 55128, Mainz, GERMANY*
[2]*Infineon Technologies Dresden, 01099 Dresden, GERMAN*
[3]*Laboratoire Albert Fert, CNRS, Thales, Université Paris-Saclay, 91767, Palaiseau, FRANCE*
[4]*Radboud University, Institute for Molecules and Materials, 6525 AJ Nijmegen, THE NETHERLANDS*
E-mail: skrishni@uni-mainz.de

In the last decade, spin-orbit torque (SOT) has been widely investigated for both fundamental physics and for its technological interest, such as the development of SOT random access memories [1] and more recently, for skyrmion-based neuromorphic applications [2]. Conventionally, the large SOTs have long been achieved by two main charge-to-spin conversion mechanisms, i.e. the spin Hall effect and/or the Rashba effect, intrinsically linked to a strong spin-orbit coupling. However, recent theories have predicated that an electric current can also induce a transverse flow of orbital angular momentum (OAM) in metals and/or at interfaces via orbital Hall effect and orbital Rashba Edelstein effect (OREE), even in the absence of spin-orbit coupling. This OAM can diffuse in adjacent metal and/or ferromagnet, exerting a torque on the magnetic layer leading to a significant improvement in efficiencies [3].

In this talk, I will discuss recent experimental findings regarding the generation of orbital currents via OREE and its action on the magnetization. Specifically, I will highlight the efficient enhancement of torques on magnetic insulators [4] and 3*d* magnetic metals due to the orbital current generated at the Cu/CuOx interface [5]. Additionally, I will discuss emergence of giant torques from metallic Co/Al light element interface and its nature, thanks the helical orbital texture at the interface [6]. In the second part of the talk, I will explore the utilization of spin-orbit and orbital torques for the manipulation of chiral spin textures in the context of energy-efficient memory devices and unconventional computing with a particular focus on real-time gesture recognition [7].

References

[1] M. Miron *et al.*, Nature **476**, 189 (2011).
[2] K. Everschor-Sitte *et al.*, J. Appl. Phys. **124**, 240901 (2018).
[3] D. Go *et al.*, Europhys. Lett. **135,** 37001 (2021).
[4] S. Ding *et al.* Phys. Rev. Lett. **125**, 177201 (2023).
[5] S. Krishnia *et al.* arXiv:2309.15987 (2023).
[6] S. Krishnia *et al.* Nano Lett. **23**, 6785 (2023).
[7] G. Beneke *et. al.*, (submitted)

Abstract ID: 1246

EFFICIENT SPIN-ORBIT TORQUE GENERATION IN COMPLEX OXIDES

Tianxiang Nan

School of Integrated Circuits, Tsinghua University, Beijing 100084, CHINA
E-mail: nantianxiang@mail.tsinghua.edu.cn

Spin-orbit torque devices operate based on the spin-to-charge interconversion, where charge-current flowing through materials and interfaces with the strong spin-orbit interaction generates spin-current via the spin-Hall effect. Heavy metals have been extensively studied as efficient spin-source materials due to their strong SOC of conduction electrons. To further improve the performance of spin-orbit torque devices, new materials systems and spin-to-charge conversion mechanisms have recently been explored. In this talk, I will review the recent advances of complex oxides with strong spin-to-charge conversion. Due to the strong interplay between the spin, charge, lattice and orbital degrees of freedom, these complex oxides can provide tuning knobs to control the electronic structure and the engineering of spin-to-charge conversion by crystalline symmetry. I will also show our recent demonstration of high spin-torque efficiency in delafossite thin films with ultra-low resistivity.

CANCELLED

Advances in Current-Induced Magnetization Control III

29.04.2024 MONDAY

Abstract ID: 1347

ULTRATHIN METALLIC ANTIFERROMAGNETS SPIN CURRENT MANIPULATION & THERMAL STABILITY

Ozhan Ozatay

Bogazici University, Department of Physics, Istanbul, TURKEY
E-mail: ozhan.ozatay@boun.edu.tr

Antiferromagnetic spintronics is currently regarded as a promising technology as a potential replacement for the ferromagnetic counterpart due to many benefits including superior scalability, lack of neighboring bit cross talk in memory devices, high radiation endurance and THz frequency dynamics. A technological realization of such devices necessitates a solid understanding of the behaviour of antiferromagnetic thin films in the ultrathin limit including thermal stability and susceptibility to torque applied by spin currents for easy manipulation of the Neel vector. However, this is quite challenging since conventional characterization techniques for ferromagnets such as reversal with a magnetic field application in practical limits and magnetic imaging in a university lab environment do not work. One needs to resort to more advanced techniques such as X-ray Magnetic Circular Dichroism or neutron diffraction for proper probing of the spin sublattices in a central lab environment.

Here we discuss our characterization of ultrathin antiferromagnetic metallic films including IrMn, PtMn, NiMn, PdMn and FeMn using two different techniques: one in which we rely on a pure spin current generated at the interface with Pt to momentarily reorient the spin sublattices following a field cooling procedure with three different orientations [1] where we study the effect of increasing the number of repetitions in heavy metal/ antiferromagnet bilayers for enhancement of spin torque from multiple interfaces and two in which we do temperature dependent ferromagnetic resonance of NiFe/ AFM bilayers [2] and correlate with exchange bias obtained from hysteresis measurements to uncover the blocking temperature-

Neel temperature relationship. We will discuss the strategy for engineering antiferromagnetic ultrathin films for device applications based on the experimental results.

We acknowledge support from TUBITAK under project numbers 118F116 and 118F431 and Bogazici University Research Fund BAP under project number 17161.

References

[1] J.H. Park, *et. al.*, Sci. Rep. **6**, 31996 (2016).
[2] L. Frangou, *et. al.*, Phys. Rev. Lett. **116**, 077203 (2016).

Abstract ID: 1295

ALL-ELECTRICAL ANGULAR MOMENTUM TRANSPORT EXPERIMENTS IN ANTIFERROMAGNETIC INSULATORS AND ISOLATED FERROMAGNETIC METALS

M. Althammer[1,2]

[1] *Walther-Meißner-Institut, Bavarian Academy of Sciences and Humanities, Garching, GERMANY*
[2] *TUM School of Natural Sciences, Physics Department, Technical University of Munich, Garching, GERMANY*
E-mail: Matthias.althammer@wmi.badw.de

Pure spin currents, i.e., the flow of angular momentum without an accompanying charge current, represent a new paradigm in spintronics. Most importantly, pure spin currents can be transported by fermions, i.e., electrons, in electrical conductors, and bosons, i.e., by magnons, the quantized spin excitations in magnetically ordered systems. This talk will present our recent progress in probing angular momentum transport via all-electrical measurements in antiferromagnetic insulators [1-4] and isolated metallic ferromagnet strips [5].

In the first part, I will show that the quantized spin excitations of an ordered antiferromagnet with opposite chirality represent pairs of spin-up and -down magnons. A magnonic pseudospin can characterize this two-level nature. Over the last years, we studied the associated dynamics of antiferromagnetic pseudospin and observed the magnon Hanle effect in hematite thin films [1-4]. Its realization via electrically injected and detected spin transport in an antiferromagnetic insulator demonstrates its high potential for devices and as a convenient probe for magnon eigenmodes and the underlying spin interactions in the antiferromagnet [2,3]. Here, we observe a nonreciprocity in the Hanle signal measured in hematite using two spatially separated platinum electrodes as spin injector/ detector [4]. Interchanging their roles was found to alter the detected magnon spin signal. We explain these observations in terms of a spin transport direction-dependent pseudofield. The latter leads to a nonreciprocity, controllable via the applied magnetic field. The observed nonreciprocal response in the readily available hematite films opens exciting opportunities for realizing exotic physics predicted so far only for antiferromagnets with unique crystal structures.

The second part will present our recent progress toward separating electronic and magnonic contributions to angular momentum transport in metallic ferromagnets [5]. To this end, we electrically excite and detect spin transport between two parallel and electrically insulated ferromagnetic metal strips on top of a diamagnetic substrate. Charge-to-spin current conversion within the ferromagnetic strip generates electronic spin angular momentum transferred to magnons via electron-magnon coupling. We observe a finite angular momentum flow to the second ferromagnetic strip across a diamagnetic substrate over micron distances, which is electrically detected in the second strip by the inverse charge-to-spin current conversion process. We discuss phononic and dipolar interactions as the likely cause of angular momentum transfer between the two strips.

References

[1] T. Wimmer *et al.*, Phys. Rev. Lett. **125**, 247204 (2020).
[2] A. Kamra *et al.*, Phys. Rev. B **102**, 174445 (2020).
[3] J. Gückelhorn *et al.*, Phys. Rev. B **105**, 094440 (2022).
[4] J. Gückelhorn *et al.*, Phys. Rev. Lett. **130**, 247204 (2023).
[5] R. Schlitz *et al.*, arXiv:2311.05290 (2023)

Abstract ID: 1132

COHERENT ANTIFERROMAGNETIC SPINTRONICS: NEW OPPORTUNITIES FOR CONTROLLING SPIN AND ELECTRONIC STATES OF ANTIFERROMAGNETS

Jiahao Han[1,2], Shunsuke Fukami[1,2,3,4,5]

[1]*RIEC, Tohoku University, JAPAN*
[2]*AIMR, Tohoku University, JAPAN*
[3]*CSIS, Tohoku University, JAPAN*
[4]*CIES, Tohoku University, JAPAN*
[5]*Inamori Research Institute of Science, JAPAN*
E-mail: jiahao.han.c8@tohoku.ac.jp

Antiferromagnets are considered as promising materials to build high-performance spintronic devices, forming a paradigm so-called the antiferromagnetic (AFM) spintronics. In this field, a lot of efforts had been spent on the switching and readout of static AFM order. Meanwhile, spin coherence, the key to explore the wave features of spin polarization and to integrate spintronics with quantum technologies, had been barely touched. Recently, unique effects of spin transport and manipulation based on coherent AFM dynamics have emerged, ushering a new frontier called coherent AFM spintronics. In this talk, we first analyze the fundamental effects of this developing field and illustrate how they lead to potential applications in ultrafast memory, terahertz signal generation, and novel computing [1].

In particular, we discuss our recent progresses in the topics of AFM magnon transport [2] and non-collinear AFM dynamics under spin-orbit torque (SOT) [3,4]. In the former, using an easy-plane AFM insulator α-Fe_2O_3, we found efficient magnon transport over micrometer scale, which arises from the interference of two linearly polarized propagating magnons forming a circularly polarized effective magnon [2]. This birefringence-like transport offers opportunities for vector-based computing and non-volatile control of spin transmission. In the latter, we study the SOT-driven dynamics, which interacts with the topological electonics states, of a non-collinear antiferromagnet Mn_3Sn. We observed a persistent rotation of the chiral-spin structure under SOT [3]. We also found a handedness anomaly in the SOT-driven dynamics of Mn_3Sn: when spin current is injected, the collective magnetic order parameter (octupole moment) rotates oppositely to the individual moments, leading to a switching polarity distinct from ferromagnets [4]. These studies endow non-collinear antiferromagnets with unique properties and functionalities that are unachievable in ferromagnets and collinear antiferromagnets, providing additional pathways for electrical control of magnetic order.

A portion of this work was supported by JSPS Kakenhi 19H05622 and 22F32037.

References

[1] J. Han, *et al.*, Nat. Mater. **22**, 684 (2023).
[2] J. Han, *et al.*, Nat. Nanotechnol. **15**, 563 (2020).
[3] Y. Takeuchi, *et al.*, Nat. Mater. **20**, 1364 (2021).
[4] J.-Y. Yoon, *et al.*, Nat. Mater. **22**, 1106 (2023).

Advances in Current-Induced Magnetization Control IV

29.04.2024 MONDAY

Abstract ID: 1342

EFFICIENT SPINTRONICS WITH FULLY COMPENSATED FERRIMAGNETS

Wanjun Jiang

Department of Physics and State Key Laboratory of Low-Dimensional Quantum Physics, Tsinghua University, 100084, CHINA
E-mail: jiang_lab@tsinghua.edu.cn

Compensated ferrimagnets with perpendicular-magnetic anisotropy, fast spin dynamics controlled by spin-orbit torques, and the ability to display topological spin textures are highly desirable for efficient spintronic applications. This presentation demonstrates that rare-earth transition-metal (RE-TM) compounds possess those attributes [1]. For example, we reveal the microscopic origin of the perpendicular anisotropy and interfacial Dzyaloshinskii-Moriya interaction in the FeTb based system [1-2]. Further, the stabilization of topological spin textures containing FeTb will be discussed [3,4]. Lastly, I will show our recent results on the magnetization switching of ultrathick FeTb and FeGd layers by using the current induced spin torques, the ionic liquid gating, and the mechanical strain methods.

References

[1] H.-A. Zhou *et al.*, *Efficient spintronics with fully compensated ferrimagnets*, Journal of the Physical Society of Japan **90 (8)**, 081006 (2021).
[2] T. Xu *et al.*, *Evolution of compensated magnetism and spin-torque switching in ferrimagnetic* $Fe_{1-x}Tb_x$, Phys. Rev. Appl. **19**, 034088 (2023).
[3] T. Xu *et al.*, *et al.*, *Imaging the spin chirality of ferrimagnetic Néel skyrmions stabilized on topological antiferromagnetic* Mn_3Sn, Physical Review Materials **5**, 084406 (2021).
[4] T. Xu *et al.*, *Systematic control of ferrimagnetic skyrmions via composition modulation in Pt/Fe1−xTbx/Ta multilayers*, ACS Nano **17**, 7920 (2023)."

CANCELLED

Abstract ID: 1617

MAGNETORESISTIVE DETECTION OF PERPENDICULAR SWITCHING IN A MAGNETIC INSULATOR

Can Onur Avci

Institut de Ciència de Materials de Barcelona, Campus de la UAB, Bellaterra, 08193, SPAIN
E-mail: cavci@icmab.es

Spintronics offers promising routes for efficient memory, logic, and computing technologies. The central challenge in spintronics is electrically manipulating and detecting magnetic states in devices. The electrical control of magnetization via spin-orbit torques is effective in both conducting and insulating magnetic layers [1,2]. However, the electrical readout of magnetization in the latter is inherently difficult, limiting its use in practical applications. Here, we demonstrate magnetoresistive detection of perpendicular magnetization reversal in an electrically insulating ferrimagnet, terbium iron garnet (TbIG) [3]. To do so, we use TbIG|Cu|TbCo, where TbCo is a conducting ferrimagnet and serves as the reference layer, and Cu is a nonmagnetic spacer. Current injection through Cu|TbCo allows us to detect the magnetization reversal of TbIG with a simple resistance readout during an external magnetic field sweep. By examining the effect of measurement temperature, TbCo composition, and Cu thickness on the sign and amplitude of the magnetoresistance, we conclude that the spin-dependent electron scattering at the TbIG|Cu interface is the underlying cause [4]. Technologically-feasible magnetoresistive detection of perpendicular switching in a ferrimagnetic garnet is a breakthrough, as it opens broad avenues for novel insulating spintronic devices and concepts.

References

[1] A. Manchon *et al.*, Rev Mod. Phys. **91**, 035004 (2019).
[2] C.O. Avci, J. Phys. Soc. Japan **90**, 081007 (2021).
[3] S. Damerio, C.O. Avci, J. Appl. Phys. **133**, 073902 (2023).
[4] S. Damerio et al., arXiv:2311.07350 (2023).

Abstract ID: 1390

SPIN ORBIT COUPLING CONTRIBUTION TO ANISOTROPIC MAGNETIC INTERACTION

Xiangang Wan

Deparment of Physics, Nanjing University, Nanjing 210093, CHINA
E-mail: xgwan@nju.edu.cn

Anisotropic magnetic exchange interactions lead to a surprisingly rich variety of the magnetic properties. Considering the spin orbit coupling (SOC) as perturbation, we extract the general expression of a bilinear spin Hamiltonian, including isotropic exchange interaction, antisymmetric Dzyaloshinskii-Moriya (DM) interaction and symmetric Γ term. Though it is commonly believed that the magnitude of the DM and Γ interaction correspond to the first and second order of SOC strength respectively, we clarify that the term proportional to λ^2 also has contribution to DM interaction. Based on combining magnetic force theorem and linear-response approach, we have presented the method of calculating anisotropic magnetic interactions, which now has been implemented in the open source software WienJ. Furthermore, we introduce another method which could calculate the first and second order SOC contribution to the DM interaction separately, and overcome some shortcomings of previous methods. Our methods are successfully applied to several typical weak ferromagnets for 3d, 4d and 5d transition metal oxides. We also predict the conditions where the DM interactions proportional to λ are symmetrically forbidden while the DM interactions proportional to λ^2 are nonzero, and believe that it is widespread in certain magnetic materials.

References

[1] Di Wang, Xiangyan Bo, Feng Tang, Xiangang Wan, Phys. Rev. B **108**, 085140 (2023).

Advances In Thin Films, Multi-Layers and Patterned Nanostructures I

29.04.2024 MONDAY

Abstract ID: 1019

NEUTRON DIFFRACTION STUDIES OF HELICAL MAGNETIC ORDER IN QUASI-TWO-DIMENSIONAL LAYERED CHIRAL $PbMnTeO_6$ WITH TRIANGULAR LATTICE

A.I. Kurbakov

Petersburg Nuclear Physics Institute, NRC Kurchatov Institute, 188300, Gatchina, RUSSIA
E-mail: kurbakov_ai@pnpi.nrcki.ru

Careful analysis of neutron diffraction data of the $PbMnTeO_6$ powder collected on a high-resolution diffractometer HRPT (PSI, Switzerland) unambiguously determined octahedral (trigonal antiprismatic) coordination for all cations within chiral space group *P312* [1] in contrast to previously announced space group *P-62m* with trigonal prismatic coordination for all three atom species [2]. This result was obtained through the use of neutron diffraction, since both structural models have identical arrangement of cations and only differ in positions of oxygen, which was difficult to see by X-ray diffraction. The combination of a quasi-two-dimensional layered structure and triangular arrangement of Mn^{4+} magnetic ions leads to a complex magnetic system with a significant role of short-range correlations far above $T_N \sim 20$ K. All of the above makes $PbMnTeO_6$ a promising material with possible unique multiferroic properties. We traced the occurrence of long-range magnetic ordering in $PbMnTeO_6$ using a low-temperature neutron powder diffraction experiment on DMC diffractometer (PSI, Switzerland), which has a high angular resolution at low scattering angles, where magnetic scattering is mainly concentrated. Neutron diffraction data demonstrate an absence of any structural phase transition in $PbMnTeO_6$ between RT and 1.6 K and the appearance of additional reflections related to an antiferromagnetic long-range ordering below T_N. The presence of residual diffuse neutron scattering in the first magnetic peaks region is clearly visible above 15 K. Similar behavior is usually observed for low-dimensional systems where short-range spin correlations increase with transition temperature approaching. Processing of low-temperature neutron diffraction data shows that to describe a rather complex spin ordering in $PbMnTeO_6$, it is necessary to use two incommensurate modulations with respect to the triangular crystal system of magnetic ions Mn^{4+}, which are determined by the propagation vectors $\boldsymbol{k}_1$ and $\boldsymbol{k}_2$. The observed result strongly indicates the complicated frustrated origin of spin ordering in $PbMnTeO_6$. The observed ground state presents a non-collinear 120-degree spin structure, that is helically modulated along the *c*-direction. The best agreement to the experimental data was obtained for the propagation vector $\boldsymbol{k}_1 = (1/3\ 1/3\ 0.4077(2))$, which corresponds to the commensurate magnetic unit cell in the *ab* plane and a spiral ordering along the layers stacking direction with a characteristic period of spiral equal to ~13.2 Å. Besides, we also observed the second incommensurate modulation for magnetic structure with the propagation vector $\boldsymbol{k}_2 = (1/3\pm\delta_1\ 1/3\pm\delta_1\ 0.15375\pm\delta_2)$. An additional nontrivial magnetic contribution to the magnetic neutron scattering reflects the complex nature of the noncentrosymmetric chiral crystal structure. Using theoretical approaches of high temperature expansion (HTE), density matrix renormalization group (DMRG) and linear spin wave theory (SWT), we suggested the $S = 3/2$ triangular-lattice Heisenberg model as an effective spin model to explain the measured magnetic properties in $PbMnTeO_6$. The dominant nearest-neighbor interaction was estimated as $J_1 = 12 \pm 2$K by fits of magnetic susceptibility, magnetization curve, and magnetic part of specific heat between experimental and numerical results. Furthermore, the spiral ordering along the layers stacking direction and incommensurate modulation of propagation vector in the *ab* plane are explained by the introduction of frustrated inter-layer couplings and a small anisotropic distortion of triangular lattice, respectively.

References

[1] M.D. Kuchugura, Dalton Trans. **48**, 17070 (2019).
[2] S.W. Kim, Inorg. Chem. **55** , 1333 (2016).

Abstract ID: 1287

MAGNETIC MICRO-, NANO-STRUCTURES FOR SENSING MAGNETIC FIELDS

A. Barrera[1], E. Fourneau[2], N. Bort-Soldevila[3], J. Cunill-Subiranas[3], V. Uhlir[5], S. Bending[4], C. Navau[3], A. Silhanek[2], Ll. Balcells[1], N. Mestres[1], A. Palau[1]

[1]*Insitut de Ciencia de Materials de Barcelona, CSIC, Bellaterra 08193, SPAIN*
[2]*Université de Liège, B-4000 Sart Tilman, BELGIUM*
[3]*Universitat Autónoma de Barcelona, Bellaterra 08193, SPAIN*
[4]*University of Bath, Bath, BA2 7AY, UNITED KINGDOM*
[5]*Institute of Physical Engineering, Brno University of Technology, 616 69 Brno, CSECHIA*
E-mail: abarrera@icmab.es

Magnetoresistive devices based on the anisotropic magnetoresistance effect (AMR) and the associated planar Hall effect (PHE) have been widely studied for different sensor applications due to its interesting properties, such as high sensitivity, thermal stability, and easy fabrication.

Here, we evaluate both the longitudinal and the transverse magnetoresistance performance of magnetic bars with tuned shape magnetic anisotropy at different temperatures, magnetic field values and orientations (Figure 1). Micromagnetic simulations are used to evaluate the electrical response of the devices and correlate them with the magnetic domain distribution within the bars [1]. We show that the device performance and range of magnetic field operation may be controlled by tuning the shape anisotropy through the strip length, width and thickness. We will also evaluate the effect of implementing magnetic metasurfaces for tunning the strip magnetoresistance response [2].

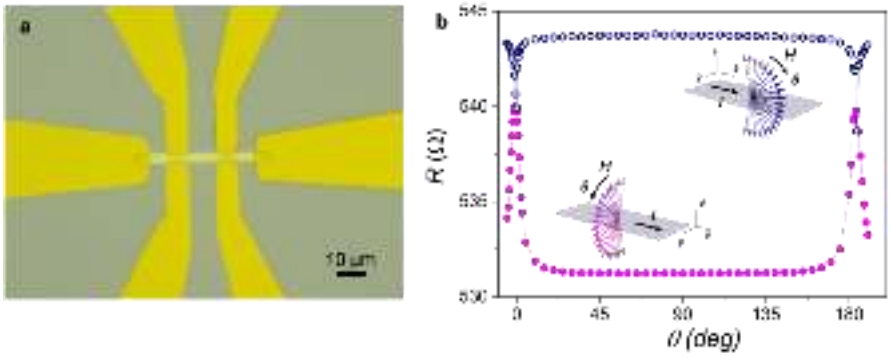

Fig. 1: *a) Optical image of a permalloy magnetic strip with longitudinal and transversal voltage contacts. b) anisotropic magnetoresistance of a permalloy strip measured by rotating the applied magnetic field in a plane parallel and perpendicular to the current.*

References

[1] A. Barrera *et al.*, *Tunable perpendicular magnetoresistive sensor driven by shape and substrate induced magnetic anisotropy,* Adv. Sensor Res. , **2**,2200042 (2022).

[2] E. Fourneau *et al.* , *Microscale metasurfaces for on-chip magnetic flux concentration*, Adv. Mater. Technol. , **8**, 2300177 (2023).

Abstract ID: 1040

ON SPECTRAL WEIGHT AND PLASMONS IN THE STRANGE METAL PHASE OF Bi-2212 BILAYER SYSTEM

Partha Goswami

D.B.College, University of Delhi, Kalkaji, New Delhi-110019, INDIA
E-mail: physicsgoswami@gmail.com

We consider a bismuth-based cuprate Bi-2212 bilayer system, which is a fully gapped chiral $d_{x^2-y^2} + id_{xy}$superconductor (SC) [1] with T_c close 90 K. The pseudo-gap (PG) phase of this system was assumed to be chiral d-density wave (CDDW) ordered earlier [1]. We find non-trivial spin texture in **k**-space in PG phase, which is an outcome of the broken inversion symmetry for the bilayer system. In particular, features of the strange metal(SM) phase constitute almost a Gordian knot [2-4]. For example, no dispersing and long-lived plasmon were observed here [3], though the system is a good conductor by most standards, and the variation in resistance is linear (similar to misaligned sheets of graphene) rather than the standard quadratic. Beyond the linearity, there is an additional anomaly unique to SM phase, viz. a Fermi liquid (FL)like Hall angle. In this communication we start with CDDW ordered scenario, and show that dispersing plasmons ($\omega \sim q^{1/2}$) do exist for this system in SM phase. Upon making use of the quantum fluctuation dissipation theorem, we also find that a strange crossover between PG and SM takes place characterized by sign reversal of the spectral weight change.

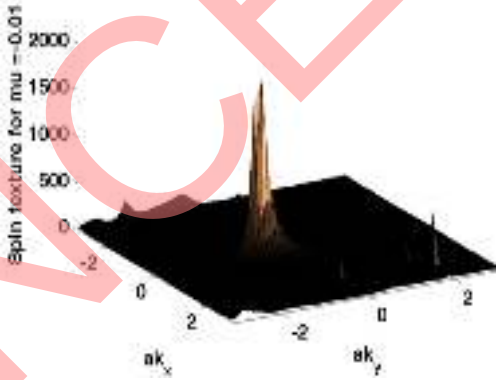

Fig. 1: *Three - dimensional plot of the spin texture in the pseudo-gap phase as a function of the wave number components.*

References

[1] Zhang, S. Tewari, V.M. Yakovenko, S. Das Sarma, Phys. Rev. B **78**, 174508 (2008); S. Tewari, C. Zhang, V.M. Yakovenko, S. Das Sarma, Phys. Rev. Lett. **100**, 217004 (2008).
[2] S.T. Van den Eede, T.J.N. van Stralen, C.F.J. Flipse, H.T.C. Stoof, arXiv:2311. 03142 [cond-mat.str-el] (2023).
[3] T.J.N. Van Stralen, *Probing charge density oscillations in the cuprate superconductor Bi-2212 using Electron Energy Loss Spectroscopy*, MSc Thesis, Eindhoven University of Technology (2023).
[4] A. Nikolaenko, S. Sachdev A.A. Patel, Physical Review Research **5**, 043143 (2023).

CANCELLED

Abstract ID: 1032

LOW HYSTERESIS, HIGH SENSITIVITY, FAST RESPONSE AND RECOVERY TIME OF HUMIDITY SENSOR

Muneeb ur Rahman

Department of Physics, Islamia College Peshawar, Peshawar 25120, KP, PAKISTAN
E-mail: muneeb@icp.edu.pk

Compound 2-((2-chloro-4-methylphenylimino)methyl)-5diethylamino)phenol was used for the first time in the fabrication of humidity sensor. The solution of the compound was deposited on interdigitated Ag-Pd electrodes using drop casting technique. The scanning electron micrographs (SEM images) revealed that the surface morphology consisted of flat surface along with pores and pore-channels of various shapes and sizes. Porosity and conduits facilitated and accommodated more H_2O molecules and played key role in the sensing mechanism. When applied frequency was increased from 25 Hz to 2 MHz, the capacitance of the device was decreased from 48.8 pF to 3.92 pF. However, when humidity was changed from 39.4 %RH to 90 %RH the capacitance of the device was enhanced from 8.68×10^{-10} Farad to 4.1×10^{-9} Farad. The regression or goodness of fit (R^2) values were 0.96 and 0.94 which are very close to unity and represented the best fit of both the curves to improve linearity. The sensor showed rapid response time (3.5sec) and recovery time (9.4sec), which are much quicker than our previous published results. The present sensor showed high sensitivity of 47299%, which is higher than conventional humidity sensor. The hysteresis of the sensor was low (3.63%).Thus, the rapid response/recovery time, high sensitivity, and low hysteresis of the sensor appear to be very promising candidate for efficient capacitive humidity sensor.

CANCELLED

Advances In Thin Films, Multi-Layers and Patterned Nanostructures II

29.04.2024 MONDAY

Abstract ID: 1447

WURTZITE MnSe – EPITAXY AND OPTICAL PROPERTIES OF AN ALTERMAGNETIC CANDIDATE

Michał J. Grzybowski[1], Carmine Autieri[2], Jaroslaw Domagala[3], Cezary Krasucki[1,3], Anna Kaleta[3], Sławomir Kret[3], Katarzyna Gas[3,4], Maciej Sawicki[3], Rafał Bożek[1], Jan Suffczyński[1], Wojciech Pacuski[1]

[1]*Faculty of Physics, University of Warsaw, POLAND*
[2]*International Research Centre Magtop, Institute of Physics, Polish Academy of Sciences, Warsaw, Poland*
[3]*Institute of Physics, Polish Academy of Sciences, Warsaw, POLAND*
[4]*Center for Science and Innovation in Spintronics, Tohoku University, Sendai, JAPAN*
E-mail: Michal.Grzybowski@fuw.edu.pl

A coexistence of a magnetically compensated collinear order and spin-splitting of the bands is a peculiar phenomenon [1,2] that attracts a lot of attention. It is present in the class of materials, which have been recently called altermagnets [2]. Such behaviour arises from the specific symmetry operations that connect the spin sublattices. We present a novel candidate of this class, semiconductive wurtzite MnSe [3]. We demonstrate experimentally through structural characterization techniques that it is possible to obtain thin films of both the intriguing wurtzite phase of MnSe and more common rock-salt MnSe using molecular beam epitaxy on GaAs substrates. The choice of buffer layers during the growth plays a crucial role in determining the resulting phase of MnSe and consequently extends the array of materials available for the physics of altermagnetism. We present basic optical properties of structures containing wurtzite MnSe. We show that despite strong photoluminescence of MnSe close to 1.6 eV, this material can be a good barrier for CdSe quantum wells (QW) emitting at higher energies, close to 1.8 eV.

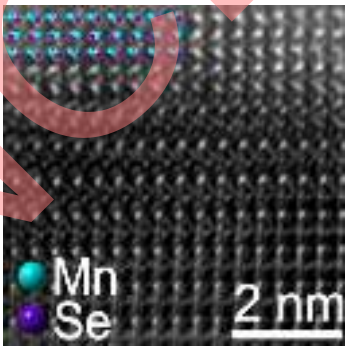

Fig. 1: *The scanning transmission electron microscopy reveals the intriguing wurtzite phase of MnSe obtained by the molecular beam epitaxy.*

References

[1] L.-D. Yuan *et al.*, Phys. Rev. B. **102**, 014422 (2020).
[2] L. Šmejkal *et al.*, Phys. Rev. X **12**, 040501 (2022).
[3] M.J. Grzybowski *et al.*, Nanoscale, In Press (2024), DOI:10.1039/d3nr04798a.; arXiv:2309.06422 (2023).

CANCELLED

Abstract ID: 1057

CONTINUOUS MAGNETIC TRANSITIONS IN DISORDERED $LaSrCo_{1/2}Fe_{1/2}O_4$ RUDDLESDEN-POPPER OXIDE

D.I. Fazlizhanova[1], R.G. Batulin[2], I.V. Yatsyk[3], T.I. Chupakhina[4], Yu.A. Deeva[4], S.V. Levchenko[1]

[1]Skolkovo Institute of Science and Technology, Moscow 121205, RUSSIA
[2]Kazan (Volga Region) Federal University, 420008 Kazan, RUSSIA
[3]Zavoisky Physical-Technical Institute, Federal Research Center "Kazan Scientific Center of RAS", 420029 Kazan, RUSSIA
[4]Institute of Solid State Chemistry of the Russian Academy of Sciences (UB), Ekaterinburg, 620990, RUSSIA
E-mail: dina.fazlik@gmail.com

The continuous magnetic transitions were observed in $LaSrCo_{1/2}Fe_{1/2}O_4$ Ruddlesden-Popper oxide by combining magnetization, specific heat, and electron paramagnetic resonance measurements.

Susceptibility measurements in 100 Oe field in zero-filed cooling (ZFC) mode and field cooling mode (FC) are presented in Fig 1. To exclude the external nature of the negative magnetization we conducted additional measurements under the negative trapped fields (NPF) reducing the field in the superconducting magnet from a high positive value to zero and the positive trapped field (PTF) after reducing the magnetic field from the high negative value. The results indicate high sensitivity (several Oe) to magnetic field cooled.

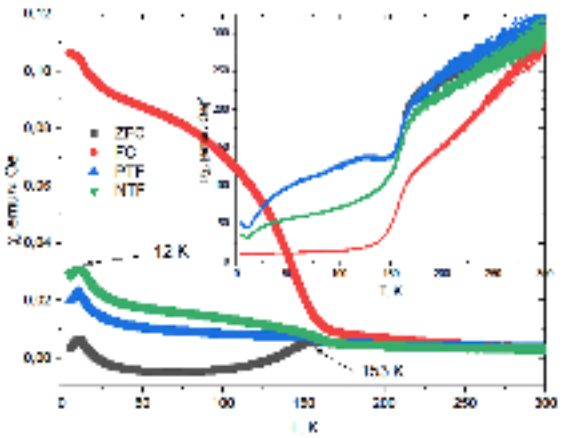

Fig. 1: *Magnetic susceptibility at 100 Oe applied fields. The insets show the inverse susceptibility and Curie-Weiss fit.*

A continuous ferromagnetic transition is observed at 160 K. At the same temperature the first faint hysteresis loop is observed. The saturation magnetization decreased with increasing temperature, whereas. the coercive field and remnant magnetization reached their highest values at T=100 K. The reason for this behavior and the absence of Curie-Weiss law in the measured temperature range in small magnetic fields is Co spin state transitions.

According to the density functional theory calculations, the most favorable magnetic configuration (including Co spin states) varies with the distribution of doping. We established that Fe-Fe interaction is antiferromagnetic whereas Co-Co and Co-Fe are ferromagnetic.

Abstract ID: 1270

QUANTUM TRANSPORT IN BRANCHED CONDUCTING POLYMERS

H. Matyakubov[1], D. Matrasulov[2], J. Yusupov[3]

[1]Urganch State Pedagogical Institute, 220100, Gurlan Str., Urgench, UZBEKISTAN
[2]Turin Polytechnic University in Tashkent, 17 Niyazov Str., 100095, Tashkent, UZBEKISTAN
[3]Kimyo International University in Tashkent, 156 Usman Nasyr Str., 100121 Tashkent, UZBEKISTAN
E-mail: hikmat.shuhratovich@gmail.com

Conducting polymers are the functional materials, which found broad spectrum of practical applications in organic electronics and related areas. An important problem required from the viewpoint of device optimization in the context of conducing polymers is tuning of their electronic properties. In many organic electronic devices, especially in organic photovoltaics, conducting polymers appear in the form of low-dimensional branched structures[1-7]. Therefore, developing physically realistic models for charge transport in such branched conducting polymers is a key problem for improving of functional properties of organic semiconductors and organic electronic devices. In this work we propose model for charge transport in branched conducting polymers in quantum regime, by considering such charge carriers as excitons and polarons. Within such approach, low-dimensional conducting polymer structures are modelled in terms of quantum graphs. These latter are branched quantum wires connected to each other at the nodes (vertices). Physically acceptable constraints for ballistic and diffusive regimes for charge transport are revealed. Ballistic regime is considered as to be caused by the absence of backscattering at the nodes. Charge current and current-voltage characteristics are computed for different branching architectures.

References

[1] R.J. Kline, M.D. McGehee, J. Macromol. Sci. C **46**, 27 (2006).
[2] W.R. Salaneck, R.H. Friend, J.L. BreHdas, Phys. Rep. **319**, 231 (1999).
[3] A.J. Heeger, Rev. Mod. Phys. **73**, 681 (2001).
[4] A.J. Heeger, S. Kivelson, J.R. Schrieffer, W.-P. Su, Rev. Mod. Phys. **60**, 781 (1988).
[5] T. Soganci, O. Gumusay, H.C. Soyleyici, M. Ak, Polymer **134**, 187 (2018).
[6] D. Babajanov, H. Matyokubov, D. Matrasulov, J. Chem.Phys. **149**, 164908 (2018).
[7] J.R. Yusupov, Kh.Sh. Matyokubov, K.K. Sabirov, D.U. Matrasulov, Chem. Phys., **537**, 110861 (2020).

Abstract ID: 1406

THE EFFECT OF SI CONTENT ON THE PHYSICAL PROPERTIES OF NANOSTRUCTURED $(Ni_{75}Fe_{25})_{100-x}Si_x$ ALLOY ELABORATED BY MECHANICAL ALLOYING

A. Kaibi[1,2], A. Guittoum[3], M. Hemmous[3], D. Martínez-Blanco[4], P. Gorria[5], J.A. Blanco[6], M. Kechouane[1]

[1]*University Larbi Tébessi - Route de Constantine, 12002, Tébessa - ALGERIA*
[2]*University Larbi Tébessi - Route de Constantine, 12002, Tébessa - Algeria Physics of Materials Laboratory (PML), Faculty of physics, Algiers, USTHB, BP 32 El Alia, ALGERIA*
[3]*Nuclear Research Centre of Algiers, 02 Bd Frantz Fanon, BP 399, Alger-Gare, Algiers, ALGERIA*
[4]*SCTs, University of Oviedo, EPM, 33600 Mieres, SPAIN*
[5]*Department of Physics, EPI, University of Oviedo, 33203 Gijón, SPAIN*
[6]*Department of Physics, University of Oviedo, Calvo Sotelo St., 33007 Oviedo, SPAIN*
E-mail: kaibi_amel@yahoo.fr

The present work deals with the effect of Si content on the physical properties of nanostructured $(Ni_{75}Fe_{25})_{100-x}$ Si_x (x=0, 3.5, 6.5, 9, 12 and 15 at %) powders elaborated by mechanical alloying for a milling time of 96 h [1]. The microstructure, hyperfine and magnetic properties of the powders were investigated, as a function of Si content, by means of X-ray diffraction (XRD), Scanning Electron Microscopy (SEM), Mössbauer Spectroscopy and Vibrating Sample magnetometry (VSM). From XRD spectra, the formation of FCC disordered Ni(Fe, Si) solid solution was evidenced after 96 h. As Si content increases, the lattice parameter and the grains size decreases (from ~28 to 15 nm); while the microstrain level decreases from 0.98% to 0.65%. From SEM micrographs, we showed that powders particles become round in shape and decreases in size with increasing Si content. For all Si content, the adjustment of Mössbauer spectra confirmed the formation of disordered ferromagnetic NiFeSi phase. From hysteresis curves, we have extracted the values of saturation magnetization and coercive field for all powders. The evolution of M_s and H_c as a function of Si content will be discussed.

References

[1] A. Kaibi, A. Guittoum, N. Fenineche, N. Souami, M. Kechouane, Sens. Lett. **Vol. 11**, pp. 1–7 (2013).

CANCELLED

Superconducting Thin Films and Interface Superconductivity I

29.04.2024 MONDAY

Abstract ID: 1477

PERFORMANCE OF Nb THIN FILMS WITH LASER INDUCED SURFACE CORRUGATION

A. Badía-Majós[1], N. Lejeune[2], E. Martínez[1], L. Porta-Velilla[1], J. Frechilla[1], E. Fourneau[2], L.A. Angurel[1], G.F. de la Fuente[1], S. Marinkovic[2], A.V. Silhanek[2]

[1]*Instituto de Nanociencia y Materiales de Aragón (INMA), CSIC-Universidad de Zaragoza, Zaragoza, 50009, SPAIN*
[2]*Experimental Physics of Nanostructured Materials, Q-MAT, CESAM, Université de Liège, Liège, 4000, BELGIUM*
E-mail: anabadia@unizar.es

Surface groove motifs with lateral modulation about 250 nm have been fabricated on 200 nm thick Nb films by pulsed laser irradiation [1]. Control over the groove depth and their geometrical layout is achieved by means of the laser beam and scanning parameters. The patterned samples display distinctive microstructural and physical properties as it has been investigated by means of Scanning and Transmission Electron Microscopy (SEM & TEM), Atomic Force Microscopy (AFM), Magneto Optical Imaging (MOI), SQUID magnetometry, and electrical resistivity measurements. The basic observations are: (i) superconducting and normal state currents flow anisotropically as dictated by the microstructure. Higher critical current densities and lower resistivity display along the grooves direction and are modulated by the depth of the channels, (ii) in the superconducting state, magnetic flux penetration is enhanced along the channels (safe for the flux avalanche regime at the lower temperatures), (iii) together with an increase of the critical current density J_c along the grooves (as compared to the pristine sample values), a reduction of the critical temperature T_c is observed for the laser treated samples. DT_c is noticeably dependent on the processing atmosphere, (iv) a prominent anomaly in the sample's magnetoresistance accompanies the anisotropic behavior of the laser treated samples. Enabled by the flexibility of the laser scanning operation, we may fabricate 'a la carte' structures that allow to control the flux penetration, exit or trapping in the superconductor. Validated by MOI, simulations based on the critical state model have proven to be an excellent tool for designing flux structures with micrometer-level precision.

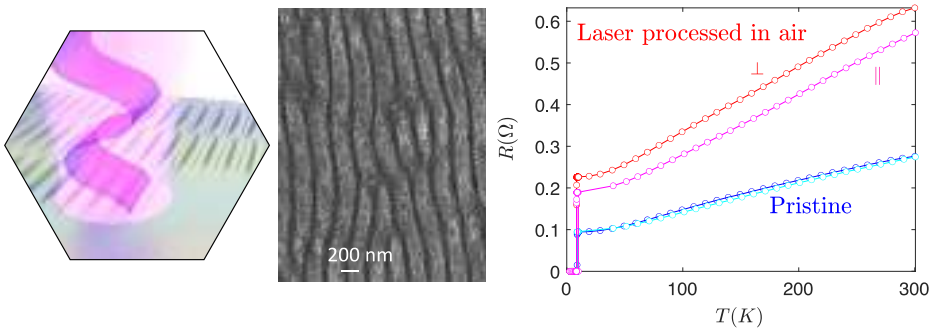

Fig. 1: *Left: Sketch of the pulsed laser technique scanning over the sample surface. Middle: SEM image showing the formation of periodic surface structures in Nb. Right: Resistivity of the films either parallel or perpendicular to the channels.*

References

[1] A. Badía-Majós *et al.*, *Laser nanostructured metasurfaces in Nb superconducting thin films*, Appl. Surf. Sci. **649**, 159164 (2024).

Abstract ID: 1049

TAILORED MAGNETIC FLUX CHANNELING IN LASER PATTERNED Nb THIN FILMS

N. Lejeune[1], E.Martínez[2] , Luis Porta-Velilla[2], Javier Frechilla[2], Emile Fourneau[1], Luis A. Angurel[2], Germán F. de la Fuente[2], Antonio Badía-Majós[2], Alejandro V. Silhanek[1]

[1] *Experimental Physics of Nanostructured Materials, Q-MAT, CESAM, Université de Liège, Liège, 4000, BELGIUM*
[2] *Instituto de Nanociencia y Materiales de Aragón (INMA), CSIC-Universidad de Zaragoza, Zaragoza, 50009, SPAIN*
E-mail: nlejeune@uliege.be

Femtosecond ultraviolet laser patterning has been employed on 200nm Nb thin films to generate highly anisotropic groove domains, resulting in a threefold increase in critical current density parallel to the ripples compared to both transverse current and unpatterned Nb [1]. This technique, in conjunction with strategically designed patterns, can alter the conventional out-of-plane magnetic flux penetration in square superconducting samples. By combining regions of untreated Nb with regions where vertical/horizontal ripples are introduced, the method modifies the flux penetration pathways, deviating from the typical middle-of-the-sides entry point where demagnetization factors are maximized. Verification of the domain creation was successfully achieved through Scanning Electron Microscopy (SEM) and Atomic Force Microscopy (AFM) inspections, while Magneto Optical (MO) imaging of the samples at temperatures down to 3.7 K confirmed the modified flux penetration.

Near the critical temperature (T_c), where thermomagnetic avalanches are absent, experimental evidence demonstrates that flux penetration aligns with the landscape predicted by critical state model simulations. This alignment is further validated by employing the Biot-Savart law to invert MO images, allowing for the derivation of current density maps in the sample. The agreement between predictions and experimental results is found to be excellent.

Additionally, a U-shaped pattern, comprising closed rectangular ripple domains in Landau patterns, was designed to facilitate flux channeling. This design guides the flux through a narrow channel, preventing its penetration into the remainder of the sample as confirmed by MO imaging. Flux penetration along the two sides of the U-shape converges in the middle before allowing flux entry into the rest of the device. Notably, by applying a decreasing oscillatory perpendicular field on the sample, a reproducible short-wavelength spatial alternation of packets of fluxons (approximately 100 μm in size) can be trapped along the canal. This method of inducing anisotropic penetration behavior proves to be fast and highly scalable for large samples.

References

[1] A. Badía-Majós, *et al.*, *Laser nanostructured metasurfaces in Nb superconducting thin films*, Preprint (2023). URL https://ssrn.com/abstract=4591497.

Abstract ID: 1190

ASSESSING THE MEISSNER STATE OF A SQUARE SUPERCONDUCTING THIN FILM BY NUMERICAL SIMULATIONS UTILIZING THE FLUXOID QUANTIZATION

Alexander Bodenseher, David Hofmann, Michael Eisterer

Atominstitut TU Wien, Stadionallee 2, 1020 Vienna, AUSTRIA
E-mail: alexander.bodenseher@tuwien.ac.at

Empirical observations have shown that the product of normal state conductivity and critical temperature is proportional to the superfluid density, which in turn is inversely proportional to the squared penetration depth $\rho_s \propto 1/\lambda^2$[1]. This relation – known as Homes' scaling – seems to hold for many conventional and unconventional superconductors. However, its validity and theoretical explanation are still under debate. Furthermore, the superfluid density correlates to the depairing current density $J_d \propto \frac{\rho_s}{\xi}$ and the core energy of a flux vortex and consequently the available energy gain for efficient flux pinning enabling high critical current densities. Measurements of the critical temperature and normal state conductivity are quite straightforward; however, measurements of the penetration depth are not as trivial, but are highly desirable and may help to elucidate fundamental mechanisms of superconductivity.

Different approaches have been reported in literature to measure the penetration depth, ranging from muon spin resonance, mutual inductance measurements, microwave resonance spectroscopy, to magnetization measurements i.e. measuring the magnetic moment of the sample and comparing it to a perfect diamagnetic response with χ=-1. The mathematics is straightforward for an infinite geometry; however, complications arise for finite sample geometries due to demagnetization effects.

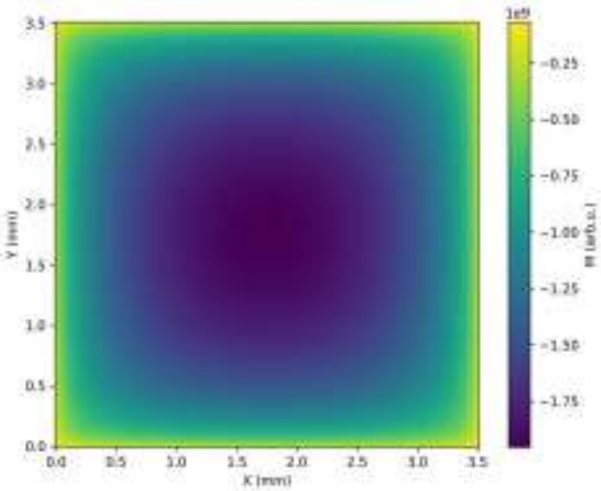

Fig. 1: *Simulation of the local magnetization for the ideal Meissner state for a square film with a side length of 3.5mm and a thickness of 1μm.*

We present a novel approach for numerically calculating the response of superconducting square thin films in the Meissner phase in a homogenous magnetic field utilizing the fluxoid quantization and taking advantage of symmetries while spanning the grid over our sample. Advantages, limitations, numeric details, the influence of the film thickness and overall geometry will be discussed and put into context of ac SQUID magnetometry experiments.

References

[1] C.C. Homes, S.V. Dordevic, M. Strongin, D.A. Bonn, R. Liang, W.N. Hardy, S. Komiya, Y. Ando, G. Yu, N. Kaneko, X. Zhao, M. Greven, D.N. Basov, T. Timusk; Nature **430**, 539 (2004); DOI: 10.1038/nature02673

Abstract ID: 1594

ELIASHBERG-TYPE SUPERCONDUCTIVITY ENHANCEMENT EFFECTS IN A TWO-BAND SUPERCONDUCTOR MgB_2 DRIVEN BY NARROW-BAND THz PULSES

J. Demsar

Institute of Physics, Johannes Gutenberg University Mainz, 55128 Mainz, GERMANY
E-mail: demsar@uni-mainz.de

We study THz-driven condensate dynamics in epitaxial thin films of MgB_2, a prototype two-band superconductor (SC) with weak interband coupling. The temperature and excitation density dependent dynamics follow the behavior predicted by the phenomenological bottleneck model for the single-gap SC, implying adiabatic coupling between the two condensates on the ps timescale. The amplitude of the THz-driven suppression of condensate density reveals an unexpected decrease in pair-breaking efficiency with increasing temperature - unlike in the case of optical excitation. The reduced pair-breaking efficiency of narrow-band THz pulses, displaying minimum near ≈ 0.7 T_c, is attributed to THz-driven, long-lived, non-thermal quasiparticle distribution, resulting in Eliashberg-type enhancement of superconductivity, competing with pair-breaking.

References

[1] S. Sobolev, *et al.*, Phys. Rev. Lett. **131**, 186903 (2023).

Superconducting Thin Films and Interface Superconductivity II

29.04.2024 MONDAY

Abstract ID: 1223

$BaHfO_3$ NANOCOMPOSITE $GdBa_2Cu_3O_{7-\delta}$ SUPERCONDUCTING THIN FILMS: SUBSTRATE TEMPERATURE, DEPOSITION RATE AND OXYGEN ANNEALING AS MEANS FOR PUSHING THE CRITICAL CURRENT DENSITIES

R. Popov, J. Hänisch, B. Holzapfel

Karlsruhe Institute of Technology, Institute for Technical Physics, 76344, Eggenstein-Leopoldshafen, GERMANY
E-mail: ruslan.popov@kit.edu

Rapid development in Coated Conductors (CC) production over the last decades brings closer the day, when technologies based on high temperature superconductors (HTS) will be a part of the day-to-day life. However, together with the issue of increasing the production speed and reducing the production costs, various challenges remain in the field of the materials science. One of those is acquiring superconducting layer with the highest critical current density (J_c), since this provides the best performance and more compact design.

RE$Ba_2Cu_3O_{7-\delta}$ (*RE*=Rare Earth, *RE*BCO) based superconductors especially $YBa_2Cu_3O_{7-\delta}$ (YBCO), have shown potential for improving characteristics in such applications as motors, generators, fault current limiters and magnets. The most common approach that has been used to enhance J_c of *RE*BCO-based thin films is the introduction of artificial pinning centers (APC) such as $BaHfO_3$ (BHO), $BaZrO_3$ $BaSnO_3$ and a variety of others. In *RE*BCO thin films grown by pulsed laser deposition (PLD) strain effects lead to BHO self-assembling into nanocolumns, which are threading through the films and may pin the flux lines along entire length, thus, drastically increasing in-field J_c. Additionally, it has been shown that by controlling the substrate temperature (T_{sub}) and the deposition rate (v_{dep}) one may have the possibility to tailor the shape and size of BHO nanocolumns.

In this work we focus on PLD-grown $GdBa_2Cu_3O_{7-\delta}$ (GdBCO) superconducting thin films containing BHO nanocomposites. In order to uncover the capabilities of this compsite, the first step is dedicated to optimization of T_{sub} and v_{dep} (here controlled by the laser frequency). The second step is dedicated to oxygen annealing, another important part of the superconducting thin film preparation. Oxygen annealing, which is required to create the superconducting phase of *RE*BCO-based thin films, has not often been addressed as a tool for increasing J_c. Therefore, GdBCO thin films containing BHO nanocomposites are prepared at various oxygen annealing conditions, mainly annealing temperature and annealing time. Their structural and transport properties are discussed in correlation with the annealing conditions.

CANCELLED

Abstract ID: 1234

MODULATING SUPERCONDUCTING PROPERTIES BY FIB AND CURRENT-INDUCED MODIFICATIONS IN Nb THIN FILMS

M. Motta

Departamento de Física, Universidade Federal de São Carlos, 13565-905 São Carlos, SP, BRAZIL
E-mail: m.motta@df.ufscar.br

Several promising technologies, such as superconducting qubits and photon counters, are based on nanoengineered thin films. Ubiquitous in most superconducting materials and a common result of nanofabrication processes, weak links are known for their limiting effects on the transport of electric currents. Recently, focused ion beam (FIB) and electromigration have become prominent techniques allowing the tuning of the properties of Nb-based superconducting weak links [1,2]. Firstly, we studied the effects of a single FIB-milled weak link in Nb films [3]. By performing quantitative magneto-optical imaging experiments and thermomagnetic model simulations, we correlate the existence of local maxima in the magnetization loops of FIB-patterned Nb films to a magnetic field-induced weak-to-strong-link transformation increasing their critical current. This phenomenon arises from the nanoscale interaction between quantized magnetic flux lines and FIB-induced modifications of the device microstructure. Secondly, we investigate the targeted and localized material modifications produced by electropulsing on Al capped Nb microbridges with multiterminal configuration [4]. The affected regions on the Nb/Al bilayer terminals are revealed by an in-lens secondary electrons detector in a scanning electron microscope and by Kelvin-probe force microscopy, both suggesting a decrease of the work function in the modified areas. In contrast to that, the affected areas are neither apparent through an Everhart-Thornley secondary electrons detector nor through atomic force microscopy, which indicates little morphological changes on the microstructure. We demonstrate that the extension of the electroannealed regions is strongly influenced by the terminal geometry, resulting in weak links which affect the superconducting transition. These findings can be exploited in developing new superconducting electronic devices, to attenuate or amplify the supercurrent through a circuit element, and as a strategy to enhance the critical currents in weak-link-bearing devices.

The author thanks CAPES, CNPq, and FAPESP for financial support.

References

[1] M.I. Valerio-Quadros *et al.*, Materials, **14**, 7274 (2021).
[2] J. Lombardo *et al.*, Nanoscale **10**, 1987 (2018).
[3] D. Chaves *et al.*, Phys. Rev. B **108**, 1149, 022602 (2023).
[4] S. Marinkovic *et al.*, Phys. Rev. App. **19**, 054009 (2023).

Abstract ID: 1543

MAGNETIC STRUCTURE AND DOPANT EFFECT IN QUASI-ONE-DIMENSIONAL Fe-BASE SUPERCONDUCTOR $BaFe_2Se_3$

W. Zheng[1], V. Balédent[2], P. Foury[2], P. Miao[1]

[1] *Spallation Neutron Source Science Center, Dongguan, 523803, P. R. CHINA*
[2] *Université Paris-Saclay, CNRS, Laboratoire de Physique des Solides, 91405, Orsay, FRANCE*
E-mail: zhengwengen@163.com

The recent discovery of superconductivity under pressure in the quasi-one-dimensional Fe-based material $BaFe_2Se_3$ [1] has sparked interest in understanding its unique properties. The low dimensionality of the Fe spin-ladders simplifies the development of theoretical models and offers insights into the mechanism of superconductivity. Previous research has identified a block-like magnetic structure in $BaFe_2Se_3$ [2]. In this study, we conducted a single crystal neutron diffraction experiment to investigate the magnetic structure of $BaFe_2Se_3$ at ambient pressure. The C_am magnetic space group with a tilt of moment in the (a, c) and (b, c) planes was identified. Besides, thanks to the powder neutron diffraction under pressure, we successfully investigated the frontier between magnetic and superconducting phases in $BaFe_2Se_3$. As shown in Figure 1, a transition from a block-like magnetic structure to a stripe-like order was observed around 3 GPa. we examined the impact of Ni/Te substitution of Fe on the magnetic structure of $BaFe_2Se_3$, providing valuable insights into the material's behavior.

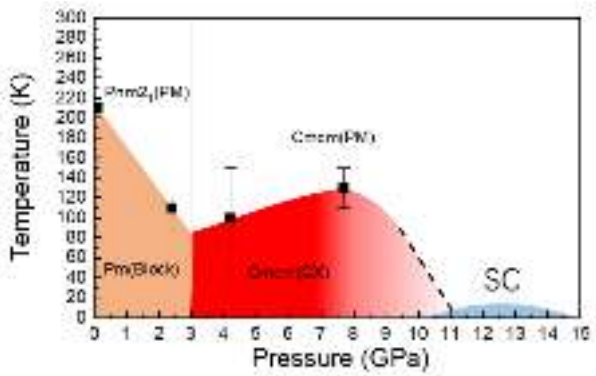

Fig. 1: *Phase diagram of $BaFe_2Se_3$ obtained from powder neutron diffraction under pressure.*

References

[1] J. Ying, *et al.*, Phys. Rev. B **95**, 241109(R) (2017).
[2] J.M. Caron, *et al.*, Phys. Rev. B **84**, 180409 (2011).

Abstract ID: 260

IN-PLANE MAGNETOCONDUCTIVITY STUDIES IN GRANULAR ALUMINIUM THIN FILM AT HIGH REDUCED TEMPERATURES AND MAGNETIC FIELDS

R. Pervin[1,2], U.C. Thuwal[1]

[1]*Indian Institute of Techlogy Kanpur, Dept. of Physics, 208016, Kanpur, INDIA*
[2]*Beijing Institute of University, Dept. of Physics, 102401, Beijing, CHINA*
E-mail: rukshanapervin92@gmail.com

We demonstrate an interplay among superconducting fluctuations, weak-localization and electron-electron interaction by low-temperature magnetotransport measurements for 40 nm thick granular aluminum film. The logarithmic temperature dependence of the resistance, signature of the 2D electron-electron interaction, has been reported when the external fields exceed the upper critical field, indicating that the sample is in two-dimensional limit in its normal state. The temperature dependence of inverse phase scattering time $(\tau_\phi)^{-1}$ is investigated which shows anomalous outcomes from the MR analysis.

References

[1] T.I. Baturina, S.V. Postolova, A.Y. Mironov, A. Glatz, M.R. Baklanov, V.M. Vinokur, EPL **97**, 17012 (2012).
[2] S. Yadav, V. Kaushik, M.P. Saravanan, S. Sahoo, Phys. Rev. B **107**, 014511 (2023).

CANCELLED

Novel Quantum Magnetism in Low Dimensions I

29.04.2024 MONDAY

Abstract ID: 1620

THE SAGA OF $BaCo_2(AsO_4)_2$

Pavel A. Maksimov[1,2]

[1] *Bogolyubov Laboratory of Theoretical Physics, Joint Institute for Nuclear Research, Dubna, Moscow region, 141980 RUSSIA*
[2] *M.N. Miheev Institute of Metal Physics of Ural Branch of Russian Academy of Sciences, S. Kovalevskaya St. 18, 620990 Ekaterinburg, RUSSIA*
E-mail: pmaksimo@uci.edu

A honeycomb compound $BaCo_2(AsO_4)_2$ has been studied since 1970s, where using inelastic neutron scattering it was shown to exhibit a spiral state. It was argued to be stabilized by the interplay of ferromagnetic nearest neighbour and antiferromagnetic third-neighbor interactions [1]. Recently, $BaCo_2(AsO_4)_2$ was also put in spotlight due to recent interest in cobalt-based honeycomb materials [2]. They were proposed to host Kitaev exchange model [3], an exactly solvable model that has Majorana excitations with topological properties [4]. Recent INS also showed that $BaCo_2(AsO_4)_2$ has unique double-zigzag ground state [5] and a plateau in the magnetization process [1,2].

We have performed an extensive search through a eight-parameter phase space of the Kitaev-Heisenberg model and showed that third-neighbor anisotropic Kitaev-type interaction is the one necessary for stabilization of double-zigzag, which we also confirmed by DMRG calculations [6]. We have also calculated field phase diagram for the minimal model that stabilizes double-zigzag ground state and establish a parameter regime where experiemntally observed sequence of magnetic phase transitions is realized. Moreover, we have calculated magnetic spectrum in the polarized phase for magnetic field in two directions, which allowed us to extract parameters of the exchange model for $BaCo_2(AsO_4)_2$.

I would like to acknowldge support from Russian Science Foundation grant 23-12-00159.

References

[1] L.-P. Regnault, P. Burlet, J. Rossat-Mignod, Physica B+C **86–88**, 660 (1977).
[2] R. Zhong, T. Gao, N.P. Ong, R.J. Cava, Sci. Adv. **6**, eaay6953 (2020).
[3] H. Liu, J.Chaloupka, G. Khaliullin, Phys. Rev. Lett. **125**, 047201 (2020).
[4] A. Kitaev, Annals of Physics 321, 2 (2006).
[5] L.-P. Regnault, C. Boullier, J.E. Lorenzo, Heliyon **4**, e00507 (2018).
[6] P.A. Maksimov, A.V. Ushakov, Z.V. Pchelkina, Y. Li, S.M. Winter, S.V. Streltsov, Phys. Rev. B **106**, 165131 (2022).

Abstract ID: 1010

QUANTUM PHASES IN FERRO-ANTIFERROMAGNETS

A.L. Chernyshev

Department of Physics and Astronomy, University of California, Irvine, 92697, USA
E-mail: sasha@uci.edu

Quantum spin nematics and unconventional magnetically ordered phases are among the exotic states that can be stabilized in quantum magnets with competing interactions. I will report on our recent results concerning paradigmatic S=1/2 J_1–J_2 square-lattice [1] and J_1–J_3 honeycomb-lattice [2] ferro-antiferromagnetic models, with the former focusing on the search for the quantum spin nematics and the latter on the emergence of the classically unstable quantum phases, potentially relevant to a large group of Kitaev materials. The minimally-augmented spin-wave theory is advertised as an effective tool to explore quantum phases beyond their classically stable ranges. Our works provides vital guidance to the intense experimental searches of the quantum spin nematics and other unconventional quantum phases, arming them with realistic expectations.

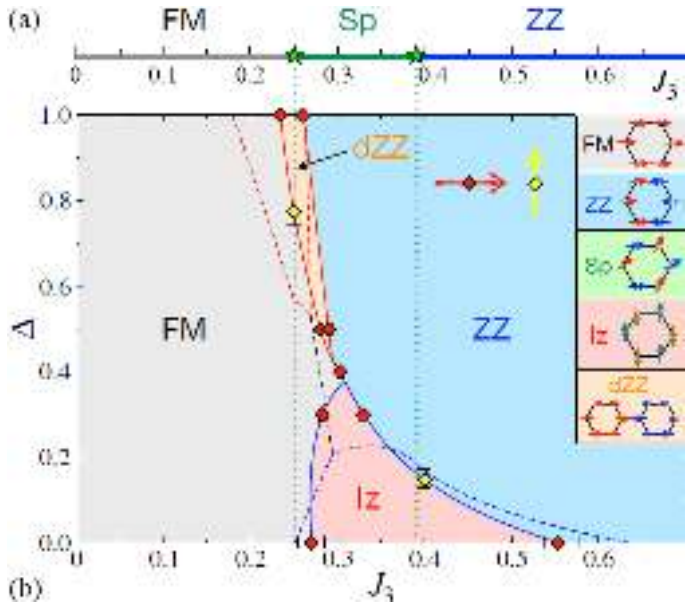

Fig. 1: *From [2]. The classical (a) and quantum (b) phase diagrams of the J_1–J_3 honeycomb-lattice ferro-antiferromagnetic model.*

References

[1] S. Jiang, J. Romhanyi, S.R. White, M.E. Zhitomirsky, A.L. Chernyshev, Phys. Rev. Lett. **130**, 116701 (2023).
[2] S. Jiang, S.R. White, A.L. Chernyshev, arXiv:2304.06062 (2023).

Abstract ID: 1643

POSSIBLE QUANTUM SPIN LIQUID AND CLUSTER MOTT INSULATOR PHASES IN THE Mo_3O_8 MAGNETS

S. Streltsov

RUSSIA
E-mail: streltsov@imp.uran.ru

We unveil the microscopic origin of largely debated magnetism in the Mo_3O_8 quantum systems. Upon considering an extended Hubbard model at 1/6 filling on the anisotropic Kagomé lattice formed by the Mo atoms, we argue that its ground state is determined by the competition between kinetic energy and intersite Coulomb interactions, which is controlled by the trimerisation of the Kagomé lattice into the Mo_3O_{13} clusters, and the sign of hopping parameters, specifying the electron localisation at such clusters. Based on first-principles calculations, we show that the strong interaction limit reveals a plaquette charge order with unpaired spins at the resonating hexagons that can be realised in $LiZn_2Mo_3O_8$, and whose origin is solely related to the opposite signs of intracluster and intercluster hoppings, in contrast to all previous scenarios. On the other hand, both $Li_2InMo_3O_8$ and $Li_2ScMo_3O_8$ are demonstrated to fall into the weak interaction limit where the electrons are well localized at the Mo_3O_{13} clusters. While the former is found to exhibit a long-range antiferromagnetic order, the latter is more likely to reveal short-range order with quantum spin liquid-like excitations [1].

We have also studied the electronic structure of Mo trimers in $LiZn_2Mo_3O_8$ by means of the hard x-ray photoemission spectroscopy. The Mo $3d_{5/2}$ core level peak is accompanied by a shoulder on the lower energy side, indicating that the shoulder and main peaks are derived from Mo^{3+} and Mo^{4+} species in the trimers being a direct experimental evidence of the Mo^{3+}/Mo^{4+} charge fluctuations due to formation of molecular orbitals or intersite Coulomb interaction [2,3]. Importance of the spin-orbit coupling on magnetic properties (and in particular on anisotropy of the exchange interaction) of Mo_3O_8 quantum systems will be also discussed.

We will also discuss possibility of a spin-liquid state realization in various Kitaev materials.

The work is supported by the grant RSF 23-12-00159.

References

[1] S.A. Nikolaev, I.V. Solovyev, S.V. Streltsov, NPJ Quantum Materials **6**, 25 (2021).
[2] R. Nakamura, D. Takegami, M. Ferreira-Carvalho, A. Melendez-Sans, M. Okawa, M. Yoshimura, K.-D. Tsuei, A.V. Ushakov, S. Nikolaev, H. Xu, Y. Sui, N.L. Saini, L.H. Tjeng, S.V. Streltsov, T. Mizokawa unpublished.
[3] A.I. Poteryaev, S.V. Streltsov, unpublished.

Novel Quantum Magnetism in Low Dimensions II

29.04.2024 MONDAY

Abstract ID: 1071

CONDENSATION OF BOSONIC PAIRS IN QUANTUM MAGNETS

Frédéric Mila

Institute of Physics, Ecole Polytechnique Fédérale de Lausanne, 1015 Lausanne, SWITZERLAND
E-mail: frederic.mila@epfl.ch

Closing the gap with a magnetic field in gapped antiferromagnets can be interpreted as a Bose-Einstein condensation of triplets, and the resulting phase is gapless with low-lying triplet excitations that can be observed with inelastic neutron scattering. In this talk I will discuss an alternative scenario where the gap closing is due to the condensation of spin-2 bound states, a possibility put forward two decades ago in the context of the Shastry-Sutherland model and of its almost exact realization, the compound $SrCu_2(BO_3)_2$ [1]. The resulting phase is a spin nematic phase which, in bosonic language, corresponds to a pair condensation without single particle condensation, and it has been shown to be stabilized in a field range above condensation in models with correlated hopping [2]. The detection of such a phase is quite challenging however because standard spectroscopies do not couple to spin-2 excitations. Motivated by recent inelastic neutron scattering in $SrCu_2(BO_3)_2$ up to 26 T, I will argue that very clear although indirect evidence can be detected as a characteristic kink in the lowest triplet branch at the magnetic field where the spin-2 bound state condenses, leading to the first experimental confirmation of the possibility to realize a spin nematics by applying a magnetic field to a gapped antiferromagnet [3].

References

[1] For an early review, see S. Miyahara and K. Ueda, J. Phys.: Condens. Matter **15**, R327–R366 (2003).
[2] R. Bendjama, B. Kumar, F. Mila, Phys. Rev. Letters **95**, 110406 (2005).
[3] E. Fogh, M. Nayak, O. Prokhnenko, M. Bartkowiak, K. Munakata, J.-R. Soh, A.A. Turrini, M.E. Zayed, E. Pomjakushina , H. Kageyama, H. Nojiri, K. Kakurai, B. Normand, F. Mila, H.M. Rønnow, Nature Comm., in press.

Abstract ID: 1097

MAGNETIZATIONS PLATEAUS: FIELD-INDUCED FRAGMENTATION OF A SPIN LATTICE INTO CLUSTERS

M.-H. Whangbo[1,2], H.-J. Koo[2], R.K. Kremer[3], A.N. Vasiliev[4,5]

[1]*Department of Chemistry, North Carolina State University, Raleigh, NC 27695-8204, USA*
[2]*Department of Chemistry and Research Institute for Basic Sciences, Kyung Hee University, Seoul 02447, REPUBLIC OF KOREA*
[3]*Max Planck Institute for Solid State Research, Heisenbergstrasse 1, Stuttgart D-70569, GERMANY*
[4]*Lomonosov Moscow State University, Low Temperature Physics and Superconductivity Dept., 119991, Moscow, RUSSIA*
[5]*National University of Science and Technology, Functional Quantum Materials Lab., 119049, Moscow, RUSSIA*
E-mail: anvas2000@yahoo.com

We aim to answer several questions concerning the phenomenon of magnetization plateau, namely, why only certain magnets exhibit magnetization plateaus, why there occur several different types of magnetization plateaus, and what controls the widths of magnetization plateaus. The key to answering these questions is to analyze the magnetic structures of those magnets exhibiting magnetic plateaus based on their spin lattices, which in turn requires the analysis of both the structural chemistry associated with the magnetic ions and the spin exchange interactions between these magnetic ions. Our study reveals that the spin lattice of a magnet can be divided into ferrimagnetic fragments. By considering how these fragments respond to a magnetic field, one can understand why magnetization plateaus are formed and why different types of magnetization plateaus emerge depending on how these fragments are interconnected together. By analyzing the interactions between such ferrimagnetic fragments, we show that there are two types of mechanisms leading to magnetization plateaus, namely, the intra-cluster and the inter-cluster mechanisms. The intra-cluster mechanism, which occurs when the ferrimagnetic fragments are ferromagnetically coupled, produces typically a wide plateau width. The inter-cluster mechanism, which takes place when the interactions between the ferrimagnetic fragments can be ferromagnetic or antiferromagnetic, typically generates a narrow plateau. Then, we classify magnets exhibiting magnetization plateaus into several different categories and discuss their magnetic plateau phenomena; magnets whose spin lattices are fragmented into diamagnetic fragments under field, those whose spin lattices are partitioned into ferrimagnetic fragments under field, and those with complex magnetic structures. Finally, we summarize our conclusions. Our study suggests strongly that the spin lattice of a magnet exhibiting a magnetic plateau is broken into ferrimagnetic fragments by the magnetic field because of Zeeman energy, thereby altering the energy spectrum from that predicted for the spin lattice in the absence of the field. We illustrate the above-mentioned concept by experimental results obtained on various inorganic compounds including $Cs_2Cu_3(SeO_3)_4{\cdot}2(H_2O)$ [1], $Na_2Cu_5(Si_2O_7)_2$ [2] and $Pb_2Cu_{10}O_4(SeO_3)_4Cl_7$ [3].

References

[1] A.V. Moskin, E.S. Kozlyakova, L.V. Shvanskaya, D.A. Chareev, H.-J. Koo, M.-H. Whangbo, A.N. Vasiliev, Dalton Trans. **52**, 118 (2023).
[2] A.M. dos Santos, P. Brandao, A. Fitch, M.S. Reis, J. Sol. St. Chem. **180**, 16 (2007).
[3] A.N. Vasiliev, P.S. Berdonosov, E.S. Kozlyakova, O.V. Maximova, A.F. Murtazoev, V.A. Dolgikh, K.A. Lyssenko, Z.V. Pchelkina, D.I. Gorbunov, S.-H. Chung, H.-J. Koo, M.-H. Whangbo, Dalton Trans. **51**, 15017 (2022).

Abstract ID: 1213

MAGNETIC FRUSTRATION IN OCTAHEDRAL NETWORKS: FROM ANTIPEROVSKITES TO fcc ANTIFERROMAGNETS

M. E. Zhitomirsky[1,2], A. Gubina[1], T. Ziman[2]

[1]*Pheliqs, Institute of Interdisciplinary Research, CEA, 38054 Grenoble, FRANCE*
[2]*Institute Laue-Langevin, 38042 Grenoble, FRANCE*
E-mail: mike.zhitomirsky@gmail.com

Geometrically frustrated magnets typically consist of of either triangular or tetrahedral blocks of magnetic ions. A novel frustrated motif is provided by octahedral blocks. Magnetic ions form a corner-sharing network of octahedra in antiperovskites and Mn_3X intermetallics, whereas edge-shared octahedra emerge for the J_1–J_2 spin model on a face-centered cubic lattice for a special ratio of two exchanges $J_2/J_1 = 0.5$. We illustrate an emergent complex behavior of octahedral antiferromagnets by studying the magnetization process of the classical J_1–J_2 fcc antiferromagnet. We find up to eight different phases in magnetic field including two fractional magnetization plateaus.

Novel Quantum Magnetism in Low Dimensions III

29.04.2024 MONDAY

Abstract ID: 1302

COVALENT 2D MAGNETS AND HETEROSTRUCTURES

C. Huai[1], M. Bian[1], R. Sabirianov[2], H. Zeng[1]

[1]*Department of Physics, University at Buffalo, The State University of New York, Buffalo, NY, USA*
[2]*Department of Physics, University of Nebraska-Omaha, Omaha, NE, USA*
E-mail: haozeng@buffalo.edu

The recent realization of atomically thin vdW magnets by exfoliation and characterization of 2D magnets down to the monolayer limit has rekindled interest in 2D magnetism [1-3]. However, most of the existing research has focused on a limited number of exfoliated vdW systems, many of which possess relatively low magnetic ordering temperatures and are often chemically unstable. In this talk, I will explore a class of lesser explored materials dubbed covalent 2D magnets [4,5]. These 2D magnets emerge from the self-intercalation of native 3d transition metal atoms in between layers of transition metal dichalcogenides, forming ultrathin, covalently bonded layered magnets denoted by the chemical formula $M_{1+\delta}X_2$. The degree of self-intercalation provides a unique mechanism to control exchange coupling, magnetic order, and spin texture, presenting a distinct avenue for the manipulation of 2D magnetism. I will first talk about the synthesis of these materials, focusing on Cr_2Te_3 and Fe_3Se_4, as well as 2D magnet/2D semiconductor heterostructures. Subsequently, I will delve into their magnetic properties and unconventional anomalous Hall effect (AHE), which we attribute to the intrinsic band structure associated with the intercalated cations with canted spin moment. We suggest that AHE can be used to probe hidden magnetic order and self-intercalation provides an additional tuning knob for the Berry curvature and AHE.

We acknowledge support from the US National Science Foundation (Grant No. DMR-2242796, ECCS-2042085, MRI-1229208, and MRI-1726303).

References

[1] B. Huang, *et al.*, Nature **546**, 270-273 (2017).
[2] C. Gong, *et al.*, Nature **546**, 265-269 (2017).
[3] K.F. Mak, *et al.*, Nature Reviews Physics **1**, 646-661 (2019).
[4] M. Bian, *et al.*, Materials Research Letters **9**, 205-212 (2021).
[5] M. Bian, *et al.*, Adv Mater **34**, 2200117 (2022).

Abstract ID: 204

INTERPLAY BETWEEN UNUSUAL MAGNETIC ANISOTROPY AND ELECTRONIC PROPERTIES OF THE NEAR-ROOM-TEMPERATURE VAN DER WAALS FERROMAGNET Fe_4GeTe_2

V. Kataev

Leibniz Institute for Solid State and Materials Research IFW Dresden, 01069 Dresden, GERMANY
E-mail: v.kataev@ifw-dresden.de

Layered van der Waals (vdW) magnetic compounds attract currently large attention as they may display an intrinsically low-dimensional magnetic behavior and as such offer an extensive materials base for exploring fundamental quantum magnetic properties of strongly correlated two-dimensional (2D) electron systems [1-4]. Furthermore, they appear as very promising functional materials which in the mono- or few-layer form can be used as a magnetic part of spintronic devices [5]. For that, particular beneficial would be a combination of metallic conductivity and a high ferromagnetic ordering temperature T_C. The latter property requires the presence of significant magnetic anisotropy to stabilize magnetic order in the 2D limit. The family of Fe-rich vdW intermetallic compounds Fe_nGeTe_2 (n = 3, 4, 5) appears as a promising candidate in this respect. In particular, Fe_4GeTe_2 attracts special attention because of its high, nearly room-temperature value of $T_C \approx 270$ K, high transport spin polarization and a large anomalous Hall effect [6-8].

In this talk, we will report a detailed sub-THz, multi-frequency electron spin resonance (ESR) study of Fe_4GeTe_2 that provided detailed quantitative insights into the nature of the unusual magnetic anisotropy (MA) of this compound. In particular, the analysis of the ESR data enabled us to disentangle the nature of a peculiar spin reorientation transition taking place in Fe_4GeTe_2 at $T_{SR} \sim 110$ K. We will discuss striking correlations between the changes in the temperature dependence of MA and characteristic features of transport properties occurring at similar temperatures [7] that suggest an inherent coupling between magnetic and electronic degrees of freedom in Fe_4GeTe_2.

This work has been done in collaboration with J. J. Abraham, B. Büchner, and A. Alfonsov (Leibniz IFW Dresden, Germany), R. Pal, P. Mandal, and A. Pal (S. N. Bose National Centre for Basic Sciences, Calcutta, 700106, India), and S. Mondal (Saha Institute of Nuclear Physics, Calcutta 700064, India).

References

[1] C. Gong *et al.*, Nature **546**, 265 (2017)
[2] B. Huang *et al.*, Nature **546**, 270 (2017).
[3] M.M. Otrokov *et al.*, Nature **576**, 416 (2019).
[4] S. Yang *et al.*, Adv. Sci. **8**, 2002488 (2021).
[5] Y. Khan *et al.*, Nano Today **34**, 100902 (2020).
[6] D. Rana *et al.,* Phys. Rev. B **107**, 224422 (2023).
[7] R. Pal *et al.*, arXiv 2303.07440 (2023).
[8] S. Bera *et al.*, Phys. Rev. B **108**, 115122 (2023).

Abstract ID: 234

MAGNETIC RESONANCES INVOLVING INTEGER MAGNONS IN A MAGNETISM MODULATED TWO-DIMENSIONAL ELECTRON GAS

Lin Zhang[1,2], Yi Wang[1,3], Shu-Yu Zheng[4], Li Lu[4], Chi Zhang.[1,3,5]

[1] *Institute of Semiconductors, Chinese Academy of Science, State Key Laboratory of Superlattices and Microstructures (SKLSM), P.O. Box 912, 100083, Beijing, CHINA*
[2] *North China Electric Power University, Department of Mathematics and Physics, 102206, Beijing, CHINA*
[3] *College of Material Science and Opto-Electronic Technology, 100190, Beijing, CHINA*
[4] *Institute of Physics, Chinese Academy of Sciences, Beijing National Laboratory for Condensed Matter Physics, 100190, Beijing, CHINA*
[5] *CAS Center for Excellence in Topological Quantum Computation, 100190, Beijing, CHINA*
E-mail: zhangchi@semi.ac.cn

We conduct an experimental study of high-mobility two-dimensional electron gas (2DEG) in GaAs/AlGaAs quantum wells modulated by strong magnetism at an in-plane magnetic field (B). The modulated magnetic fields are performed via the single stripe and gratings which are made of the heavy rare earth metal Terbium thin films on the sample surface. We observe that the robust ferromagnetic resonances (FMRs) persist to a temperature of 50-70 K in both the stripe and grating samples, for the ferromagnetism (FM) phase of the magnetic metal exists at above 100 K. The high-order (with integer number $j \equiv \hbar\omega/g\mu_B B = 1, 2, ...$) magnetic resonances that involve integer magnons can also be observed in the single stripe structure via the microwave photovoltaic detection and magnetoresistance under microwave irradiation. In addition, the resonance features around $j = 1/2$ are robust in the single stripe modulated sample, which suggests the spinons with spin-1/2 collective excitations in a 1D Heisenberg model [1].

References

[1] F. Meier, D. Loss, Phys. Rev. Lett. **90**, 167204 (2003).

CANCELLED

Novel Quantum Magnetism in Low Dimensions IV

29.04.2024 MONDAY

Abstract ID: 1608

ENGINEERING OF TOPOLOGICAL MAGNONS AND MAGNON-POLARONS IN CrI_3 FERROMAGNETS

Alireza Qaiumzadeh

QuSpin, NTNU, Trodnehim, NORWAY
E-mail: a.qaiumzadeh@gmail.com

The ferromagnetic layered van der Waals CrI_3 is the first 2D magnet discovered in 2017 and open a new door to spintronics [1]. This material shows a topological magnon band gap at its K symmetry points. The microscopic origin of the gap is unclear. Both Kitaev and Dzyaloshinskii-Moriya interactions may create such a gap, see Fig. 1. In this presentation, I talk about our recent theoretical proposal to uncover the microscopic origin of the topological magnon gap. I show that how topological properties of magnon bands and magnon-polaron bands can be tuned by an external magnetic field. Our work opens a new pathway toward engineering of topological properties of novel 2D magnets [2,3].

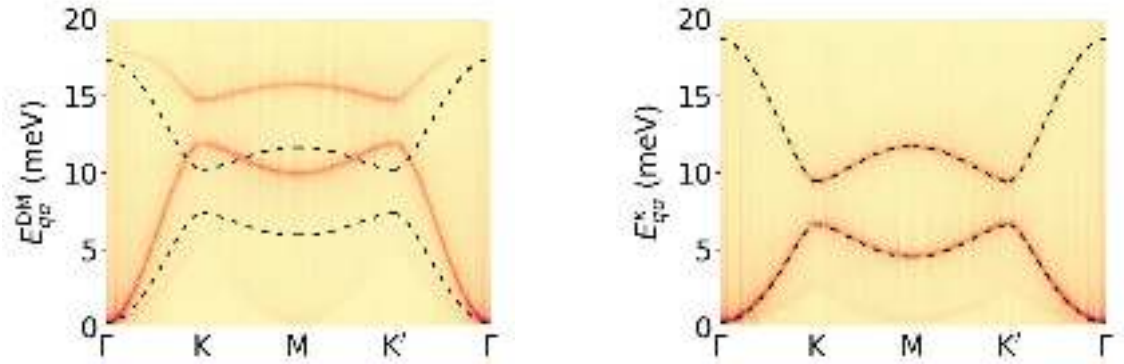

Fig. 1: *Magnon dispersion of single layer CrI_3 in the out-of-plane magnetization configuration in the absence of magnetic field for DM model (left) and Kitaev model (right) as obtained from atomistic spin simulations (color map) and linear spin wave theory (black dashed lines).*

References

[1] B. Huang *et al.*, Nature **546**, 270 (2017)
[2] J. Kløgetvedt, A. Qaiumzadeh, Phys. Rev. B **108**, 224424 (2023).
[3] V. Brehm, P. Sobieszczyk, J. Kløgetvedt, R.F.L. Evans, E.J.G. Santos, A. Qaiumzadeh, arXiv:2312.09903.

Abstract ID: 1144

4d AND 5d METALS BASED MAGNETS

O. Volkova

[1]*Functional Quantum Materials Laboratory, National University of Science and Technology "MISiS", Moscow 119049, RUSSIA*
[2]*Lomonosov Moscow State University, Moscow 119991 RUSSIA*
E-mail: os.volkova@yahoo.com

The recent discovery of an almost purely two-dimensional ferromagnetic state in van der Waals compounds makes these materials promising for the development of new spintronic devices [1]. The key for the strengthening of long-range magnetic order is in magnetocrystalline anisotropy which shifts interest from 3d metal compounds, i.e. CrI_3, $Cr_2Ge_2Te_6$ [2], to systems with 4d-5d metals. Their d-orbitals overlap better with the ligands which enlargers their splitting and enhances magnetocrystalline anisotropy [3]. However, these compounds are usually non-magnetic. Rare cases of magnetic response using connections with $MoOBr_3$ and WBr_5 as an example will be introduced in present talk.

References

[1] Y.H. Lee, Science **382**, eadl0823 (2023).
[2] K.F. Mak, J.Shan, D.C. Ralph, Nature Reviews Physics **1**, 646-661 (2019).
[3] J.B. Goodenough, Magnetism and the Chemical Bond, (New York: Interscience Publ., 1963), p.377.

Abstract ID: 1081

MICROSCOPIC SCALE OF QUANTUM PHASE TRANSITIONS: FROM HEISENBERG AND ISING SPIN CHAINS TO COLD GASES AND MOIRÉ SUPERLATTICES

A. Rogachev

University of Utah, Dept. of Physics and Astronomy, 84112, Salt Lake City, Utah, USA
E-mail: rogachev@physics.utah.edu

We have developed a phenomenological model of quantum phase transitions (QPTs) which shows that despite scale-invariance of systems near critical point of a QPT, the experimental data still contain information related to the microscopic processes and scales governing a transition. The model is based on observation that near QPTs, various physical quantities follow the generic exponential dependence predicted by the scaling theory of localization (the figure shows some examples); this dependence includes as a parameter a microscopic seeding scale of the renormalization group, L_0. We also found that for interacting systems, the temperature cuts the renormalization group flow at the dephasing length set by a distance travelled by a system-specific semi-classical elementary excitation over the Planckian time, $\tau = \hbar/k_B T$. We adopted the model for magnetic systems by setting the dephasing length to $L_\varphi = c\hbar/k_B T$ for Ising and $L_\varphi = \hbar/\sqrt{k_B T m}$ for Heisenberg chains. We found that, in both cases, the experimental L_0 matches the physically expected minimal scale, the distance between spins. We further show that the model agrees with the microscopic theory for the Heisenberg spin chain and also how it can be used to explain the Mott QPT for bosons in 2d optical lattice and for fermions in dichalcogenide moiré bilayer (panel c in the figure). Refs. [1-3] demonstrate that the model is truly generic and works for many other systems.

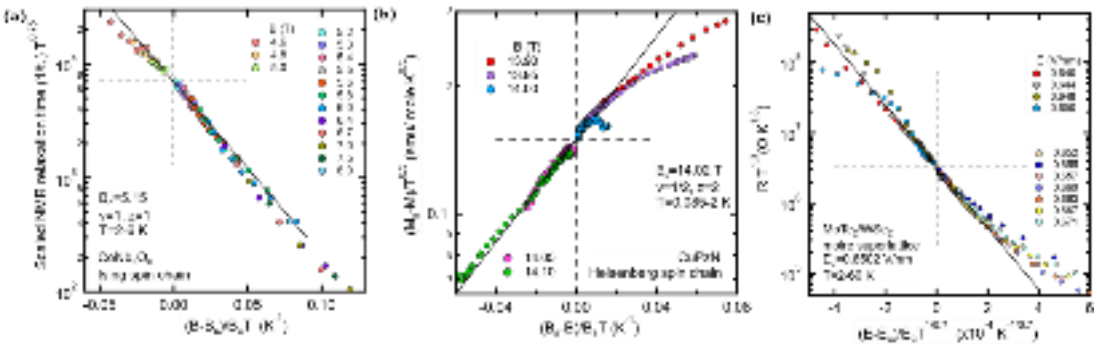

Fig. 1: *(a) Scaled NMR relaxation rate $1/t_1$ plotted versus scaled magnetic field for Ising spin chain material $CoNb_2O_6$ (b) Scaled magnetization versus scaled magnetic field for Heisenberg spin chain material CuPzN (c) Scaled resistance per square versus scaled electrical field for $MoTe_2/WSe_2$ moiré superlattice*

References

[1] A. Rogachev, *Microscopic scale of quantum phase transition: from doped semiconductors to spin chains, cold gases and moiré superlattices*, e-print arXiv:2309.00749 (2023).

[2] A. Rogachev, K. Davenport, *Microscopic scale of pair-breaking quantum phase transitions in superconducting films, nanowires and $La_{1.92}Sr_{0.08}CuO_4$*, e-print arXiv:2309.00747 (2023).

[3] A. Rogachev, *Quantum phase transitions in quantum Hall and other topological systems: role of the Planckian time*, e-print arXiv:2309.00747 (2023).

Abstract ID: 1426

STRAIN-DRIVEN BIDIRECTIONAL SPIN ORIENTATION CONTROL IN EPITAXIAL HIGH ENTROPY OXIDE FILMS

Zhibo Zhao, Horst Hahn, Robert Kruk, Abhishek Sarkar

Institute of Nanotechnology, Karlsruhe Institute of Technology, Eggenstein-Leopoldshafen, 76344 Karlsruhe, GERMANY
E-mail: zhao.zhibo@kit.edu

High entropy oxides (HEOs), based on the incorporation of multiple-principal cations into the crystal lattice, offer the possibility to explore previously inaccessible oxide compositions and unconventional properties. Here it is demonstrated that despite the chemical complexity of HEOs external stimuli, such as epitaxial strain, can selectively stabilize certain magneto-electronic states. Epitaxial $(Co_{0.2}Cr_{0.2}Fe_{0.2}Mn_{0.2}Ni_{0.2})_3O_4$-HEO thin films are grown in three different strain states: tensile, compressive, and relaxed. A unique coexistence of rocksalt and spinel-HEO phases, which are fully coherent with no detectable chemical segregation, is revealed by transmission electron microscopy. This dual-phase coexistence appears as a universal phenomenon in $(Co_{0.2}Cr_{0.2}Fe_{0.2}Mn_{0.2}Ni_{0.2})_3O_4$ epitaxial films. Prominent changes in the magnetic anisotropy and domain structure highlight the strain-induced bidirectional control of magnetic properties in HEOs. When the films are relaxed, their magnetization behavior is isotropic, similar to that of bulk materials. However, under tensile strain, the hardness of the out-of-plane (OOP) axis increases significantly. On the other hand, compressive straining results in an easy OOP magnetization and a maze-like magnetic domain structure, indicating the perpendicular magnetic anisotropy. Generally, this study emphasizes the adaptability of the high entropy design strategy, which, when combined with coherent strain engineering, opens additional prospects for fine-tuning properties in oxides.

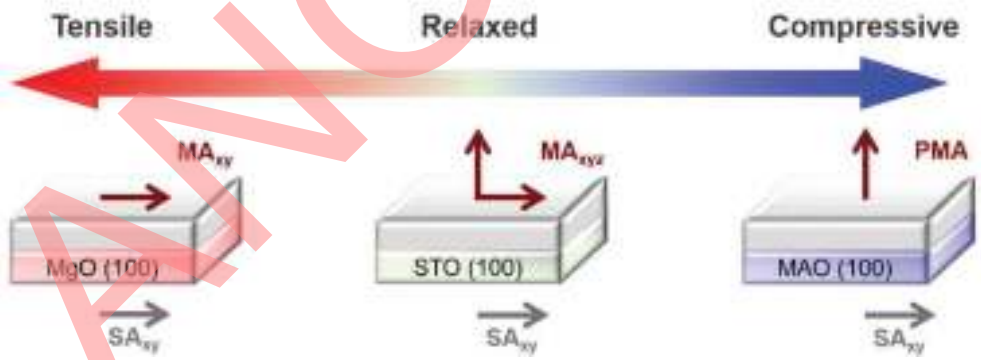

Fig. 1: *Schematic of strain-driven bidirectional spin reorientation in epitaxial HEO thin films, indicating the hardness of the out-of-plane (OOP) upon tensile straining (MgO) and easiness of the OOP upon compressive strain (MAO). The relaxed film on STO behaves similar to the bulk, that is, isotropic, however, the shape anisotropy (SA) makes the in-plane (xy) axis slightly easier compared to the OOP.*

CANCELLED

Device Physics of Josephson Junctions and Their Fundamental Technologies III

29.04.2024 MONDAY

Abstract ID: 1099

CIRCUIT QED WITH TWO *PT*-SYMMETRIC NON-HERMITIAN QUBITS

Mikhail V. Fistul[1], Grigory A. Starkov[2], Ilya M. Eremin[1]

[1]*Institut für Theoretische Physik III, Ruhr-Universität Bochum, Bochum GERMANY*
[2]*Institute for Theoretical Physics and Astrophysics, University of Würzburg, Würzburg, GERMANY*
E-mail: Mikhail.Fistoul@ruhr-uni-bochum.de

Combining non-hermiticity and interactions yields novel effects in non-equilibrium quantum many-body systems. Motivated by recent experiments on single non-Hermitian superconducting [1] or spin-qubits [2] we present here a detailed analysis of an exemplary *PT* -symmetric circuit QED composed of two biased non-Hermitian qubits embedded in a lossless resonator [3]. We consider a resonant quantum circuit as $|\omega_r - \Omega| \ll \omega_r$, where Ω and ω_r are qubits and resonator frequencies, respectively, providing well-defined groups of quasi-degenerate resonant states. Non-Hermiticity is introduced via a staggered gain/loss parameter, *g*, of individual qubits.

We develop the generalized Schrieffer-Wolff transformation and derive the effective Hamiltonian suitable for various quasi-degenerate non-Hermitian systems. Using the direct numerical diagonalization we obtain the dependence of low-lying eigenspectrum on the interaction strength between a single qubit and the resonator, *g*, and the gain (loss) parameter *g* (see, Fig. 1a), and compare that with the eigenvalues obtained analytically using the effective Hamiltonian of resonant states. We identify the *PT* -symmetry broken and unbroken phases, the Exceptional points (*EP*s) of second and third order, and provide a complete phase diagram *g-g* of low-lying resonant states (see Fig. 1b). We relate the formation of *EP*s to the additional *P*-pseudo-Hermitian symmetry of the system [4]. We also show that in *PT* -symmetric circuit QED non-Hermiticity mixes the "dark" and the "bright" states.

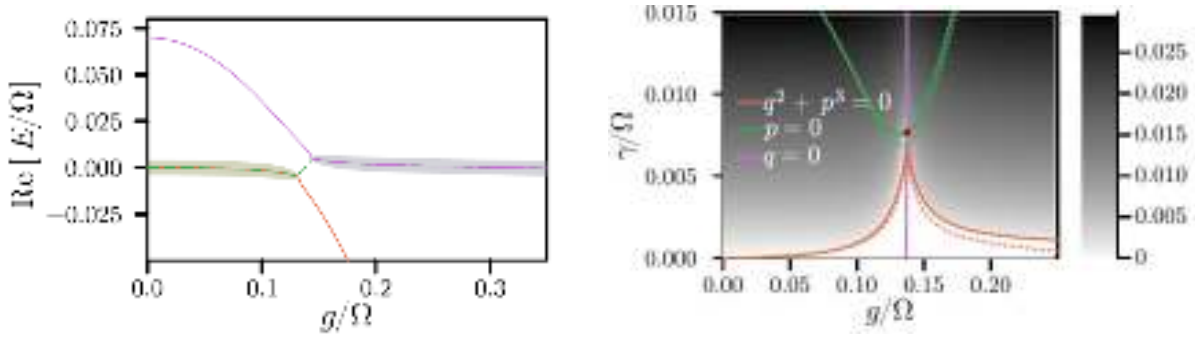

(a) **(b)**

Fig.1: *a) Typical eigenvalues of PT-symmetric QED system. The value of g/W=0.004. b) The phase diagram of low-lying resonant states. The red lines separate PT-symmetry preserved and broken phases.*

References

[1] W. Chen, M. Abbasi, Y.N. Joglekar, K.W. Murch, Phys. Rev. Lett. **127**, 140504 (2021).
[2] Y. Wu, *et al.*, Science 364, 878 (2019).
[3] G.A. Starkov, M.V. Fistul, I.M. Eremin, Phys. Rev. B **108**, 235417 (2023).
[4] G.A. Starkov, M.V. Fistul, I.M. Eremin, Phys. Rev. A **108**, 022206 (2023).

Abstract ID: 1105

THE JOSEPHSON BALANCED COMPARATOR AS A SENSOR TO MONITOR ON-CHIP CLOCK SOURCES FOR RSFQ/ERSFQ CIRCUITS

Timur V. Filippov[1], Dmitri E. Kirichenko[1], Anubhav Sahu[1], M. Eren Çelik[1], Deepnarayan Gupta[2]

[1]Hypres, 10523, Elmsford, USA
[2]Formerly with Hypres, 10523, Elmsford, USA
E-mail: tfilippov@hypres.com

The Josephson balanced comparator (BC) is a key component for all RSFQ/ERSFQ logic cells. Its frequency-dependent properties (gray zone and threshold current value) define the maximum clock frequency and bit error rate (BER) of RSFQ/ERSFQ circuits. The balanced comparator can also be used for various monitoring purposes. In this paper, we focus on on-chip clock sources and analyze several of them by means of BCs. We show experimentally how local overheating, associated with sub-optimally designed analog clock sources, can compromise the HF performance of a balanced comparator as well as an RFSQ/ERSFQ circuit on the same chip. We also investigate a clock source based on an external HF generator followed by an on-chip DC/SFQ converter and a frequency doubler. We use the balanced comparator's performance to optimize the on-chip part of the clock source at high frequencies. In addition, we confirm the advantage of overshunting the comparator driver to achieve higher clock frequency and lower BER. All test circuits were designed for the SFQ5ee fabrication node at MIT-LL, but conclusions can be applied to all other fabrication processes.

Abstract ID: 1133

ZERO-FIELD SUPERCONDUCTING DIODE EFFECT IN A TRIGONAL SUPERCONUDUCTOR $PbTaSe_2$

Y. Itahashi[1], Y. Iwasa[1,2]

[1]*Department of Applied Physics & Quantum Phase Electronics Center, University of Tokyo, Tokyo 113-8656, JAPAN*
[2]*RIKEN Center for Emergent Matter Science, Wako 351-0198, JAPAN*
E-mail: iwasay@riken.jp

Nonlinear transport is one of the peculiar properties in noncentrosymmetric superconductors. Transition metal dichalcogenide based superconductors offer a unique platform of the study of nonlinear transport because of their layered structure of the trigonal unit layers where the in-plane inversion symmetry is broken. $PbTaSe_2$ is known as a noncentrosymmetric bulk superconductor, where the trigonal monolayer is stacked in the same orientation so that the bulk keeps the trigonal symmetry. This is in sharp contrast to the well known 2H structure, recovering the centrosymmetry in bulk, because the trigonal layers form an altenate stacking.

We investigated the second order nonlinear transport, nonlinear anomalous Hall effect (NAHE), and the higher order nonlinear effect, the superconducting diode effect (SDE) in $PbTaSe_2$. Despite its nonpolar structure without Berry curvature dipole, we observed a NAHE both in the normal state and around the superconducting transition temperature. The NAHE signal in the superconducting state is two orders of magnitude larger than that in the normal state, in a similar manner to the nonreciprocal superconducting transport [1].

SDE is attracting a significant interest in the noncentrosymmetric superconductors. In contrast to the heavily investigated SDE under magnetic field *B*, the zero field counterpart or *B* even SDE is very limited [2]. In particular, for investigation of intrinsic mechanisms of SDE, symmetry dependent transport measurements are highly crucial. We have measured SDE on unstrained $PbTaSe_2$, and found there is no zero-field SDE, despite that it is symmetry allowed. In sharp contrast, we found that the zero-field SDE effect was induced in the strained $PbTaSe_2$ [3]. Based on these results, we discuss SDE under time reversal symmetry, which has been believed to be crucial for the occurrence of SDE.

References

[1] Y.M. Itahashi *et al.*, Nat. Comm. **13**, 1659 (2022).
[2] H. Wu *et al.*, Nature **604,** 653 (2022).
[3] F. Liu *et al.*, submitted.

Device Physics of Josephson Junctions and Their Fundamental Technologies IV

29.04.2024 MONDAY

Abstract ID: 1272

QUANTUM PRECISE BIAS SUPPLY AND SINGLE FLUX QUANTUM READOUT OF SUPERCONDUCTING NANOWIRE SINGLE PHOTON DETECTORS

T. Ortlepp[1,2], S. Engert[2], C. Moeller[1] and A. Reinhardt[1]

[1]*CiS Forschungsinstitut fuer Mikrosensorik GmbH, Erfurt, GERMANY*
[2]*Institut Dr. Foerster GmbH &Co. KG, Reutlingen, GERMANY*
E-mail: tortlepp@cismst.de

We propose a new biasing concept for superconducting nanowire single photon detectors (SNSPD) [1]. It features the frequency-voltage relation of a Josephson junction to generate a bias supply with quantum precision. The inductance of the detector is about 100 nH. Since the detector inductance is much larger than other parasitic inductances, we can neglect the parasitic inductance of the connection. In the first experiments, we intentionally slow down the time constant by using a very small bias resistor. We obtain an intrinsic time constant of about 100µs. Corresponding to this time constant, the generated current pulses for the Josephson junction through the SNSPD cause in time-average a constant bias current. For example, a Josephson junction with switching frequency of 9.7MHz and a resistor of 1mOhm generates a bias current of 20µA in the SNSPD. Further, the time constant of the SNSPD creates a temporary storage of a detection event to enable the synchronous readout of detector arrays. The quantum bias concept is characterized by a very low resistor and a frequency controlled noise-free quantum voltage source. The SNSPD as well as the Josephson junction are based on superconducting thin film technology and can be fabricated in general on the same substrate. This enables compact packaging and reduces the potential impact of disturbances. Further, the low resistor causes only limited Johnson-Nyquist-noise and thus in the case of a SNSPD array the dissipated heat from the resistors is reduced by some orders of magnitude, which leads to a reduction of required cooling power. We demonstrate experimental results on the bias supply of an SNSPD by using a bias regulated Josephson junction in the configuration of a balanced comparator [2-4].

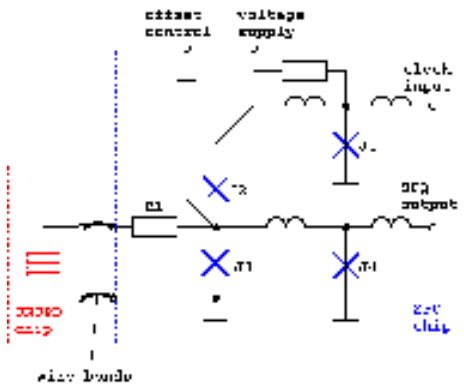

Fig. 1: *Circuit schematic for the SNSPD connected to the single flux quantum circuit.*

References

[1] A. Semenov, *et. al.*, Journal of Modern Optics, **vol. 56, no. 2-3**, pp. 345-351 (2009).
[2] T. Ortlepp, *et. al.*, Physica C, **vol. 500**, pp. 20-24 (2014).
[3] T.V. Filippov. *et. al.*, IEEE Trans. on Magnetics, **vol. 27, no. 2**, pp. 2452-2455 (1991).
[4] T.V. Filippov, *et. al.*, Proc. of the IEEE Int. Superc. Electronics Conf., pp. 1-3 (2019).

Abstract ID: 1315

YBCO RESISTORS, NANO-CONSTRICTION JOSEPHSON JUNCTIONS FABRICATED WITH A FOCUSED He-ION BEAM

E. Goldobin[1], C. Schmid[1], M. Meichsner[1], D. Hanisch[2], M. Pröpper[2], C. Magen[3], M. Schilling[2], R. Kleiner[1], D. Koelle[1]

[1]*Universität Tübingen, Physikalisches Institut, Center for Quantum Science (CQ) and LISA+, 72076, Tübingen, GERMANY*
[2]*Institut für Elektrische Messtechnik und Grundlagen der Elektrotechnik, Technische Universität Braunschweig, 38106, Braunschweig, GERMANY*
[3]*Instituto de Nanociencia y Materiales de Aragón (INMA), CSIC-Universidad de Zaragoza, 50009, SPAIN*
E-mail: gold@uni-tuebingen.de

Several groups demonstrated that irradiation with a focused He ion beam (He-FIB) of different dose values can be used to "write" Josephson barriers i.e. Josephson junctions (JJs), highly resistive lines and amorphous areas (e.g. SQUID holes) in thin epitaxial $YBa_2Cu_3O_7$ (YBCO) film bridges [1-3].

In this contribution we, first, demonstrate that irradiating sections (ca. 30 × 2000 nm^2) of YBCO thin (~30 nm) film bridges grown on LSAT substrate by a carefully selected He-FIB dose ~ 40 ions/nm^2 one can fully suppress the critical temperature T_c of YBCO without destroying its crystal structure. Thus, in the same fabrication step it is possible to create not only JJs, but also dose-dependent normal resistances that can be used e.g. as shunt resistors in different applications.

Second, to create competitive superconducting electronic devices such as digital logic, signal processing and memory cells, their size nowadays is expected to be below 100 nm. Barrier JJs mentioned above will be useless as their Josephson energy will be comparable to the thermal energy k_BT at T=4.2K. The solution is to use e.g. constriction JJs (cJJs). Previous efforts to fabricate nano-constrictions in YBCO using He-FIB were limited by minimum feature sizes down to ~100 nm. TEM analysis showed that high dose lines used to "draw" the constrictions using He-FIB actually amorphize irradiated regions, creating stress in the crystal and destroying its superconducting properties on the scale ~100 nm from the high-dose line.

Here we overcome this limitation and demonstrate constriction JJs (cJJs) that are fabricated by using the same technique as for resistors – a constriction is defined by fully suppressing T_c of YBCO outside the cJJs without destroying the crystal structure. Even for cJJs with constriction width w down to 6 nm, we observe RSJ-like I–V characteristics with small excess currents and characteristic voltages V_c above 2.6 mV at 4.2K, making such JJs interesting for applications. Our results demonstrate a serious step towards miniaturization of high-T_c Josephson devices.

References

[1] B. Müller *et al.*, Phys. Rev. Applied **11**, 044082 (2019).
[2] S.A. Cybart *et al.*, Nat. Nanotechno. **10**, 598 (2015).
[3] E.Y. Cho *et al.*, Appl. Phys. Lett. **113**, 022604 (2018).

Abstract ID: 1519

INVESTIGATION OF THE SPUTTERING CONDITIONS OF NIOBIUM AND MAGNETITE THIN FILMS FOR REALIZING FERROMAGNETIC JOSEPHSON JUNCTIONS

T. Alp[1,2], Y. Ozturk[1,2], E. Aygit[1,2], A. Rahimpour[1,2], O. Ozatay,[3] Y. Simsek[1,2]

[1] *Sabancı University Nanotechnology Research and Application Center, Istanbul, TURKEY*
[2]*Faculty of Engineering and Natural Sciences, Sabancı University, Tuzla İstanbul, TURKEY*
[2] *Department of Physics, Boğazici University, Istanbul, TURKEY*
E-mail: ysimsek@sabanciuniv.edu

Ferromagnetic Josephson junctions have attracted a great deal of interest for superconducting electronics and cryogenic memory devices since their sandwiched heterostructures exhibit the coexistence of superconductivity and magnetism, which comprises rich physics concepts such as Fulde-Ferrell-Larkin-Ovchinnikov pairing, Andreev bound states, anomalous current-phase behavior due to phase shifting, spin triplet supercurrent valving due to ferromagnetic tunneling domains and mutual proximity effects. These versatile junctions offer new approaches in developing new cryogenic quantum devices such as phase qubits, spin valve-based memory circuits and phase shifters for programmable logic circuits. In this work, an optimized sputtering system have been systematically studied to achieve high superconducting characteristics in niobium layers and ferromagnetic-insulator characteristics in iron oxide layers for ultimately realizing new-type π-junctions. For this purpose, a series of niobium and iron oxide thin films on MgO and Al_2O_3 substrates have been grown under various magnetron sputtering conditions from niobium and magnetite targets respectively. Their structural electrical and magnetic characteristics have been analyzed by X-ray diffraction, Raman spectroscopy, vibrating sample magnetometry, magnetic force microscopy, and electrical transport measurements. The best growth condition was employed to deposit each layer of coplanar Nb/Fe3O4/Nb junction arrays. The prerequisite signatures of π-junctions were investigated in their Fraunhofer patterns, and temperature dependence of I_c and I_cR_N products. The effects of the growth and fabrication conditions on these properties are discussed in order to realize ideal ferromagnetic-insulator based Josephson junction layers for applications of cryogenic memory and phase qubits.

Acknowledgement

This work was supported by Scientific and Technical Council of Turkey (TUBITAK) with a project number of 118C339.

Device Physics of Josephson Junctions and Their Fundamental Technologies V

29.04.2024 MONDAY

Abstract ID: 223

MAGNETIC FLUCTUATIONS AS A POTENTIAL SOURCE OF LOSSES IN SUPERCONDUCTING QUANTUM DEVICES

Y. Krasnikova[1], A.A. Murthy[1], F. Crisa[1], M. Bal[1], Z. Sung[1], J. Lee[1], A. Cano[1], D.M.T. van Zanten[1], A. Romanenko[1], A. Grassellino[1], A. Suter[2], T. Prokscha[2], Z. Salman[2]

[1]*Superconducting Quantum Materials and Systems Center (SQMS), Fermi National Accelerator Laboratory, Batavia, IL 60510, USA*
[2]*Laboratory for Muon Spin Spectroscopy, Paul Scherrer Institute, CH-5232 Villigen PSI, SWITZERLAND*
E-mail: yuliak@fnal.gov

Muon spectroscopy is a powerful tool to detect even weak magnetism presence [1]. Low-energy range (up to 30 keV) gives a unique opportunity to study thin films and disordered systems. It was proven that pentoxide of niobium hosts the main losses for Nb SRF cavities and considered as a potential host of TLS (two-level systems) fluctuators [2]. We have used a low-energy highly polarized muon beam and have detected magnetic fluctuations in niobium pentoxide in a wide temperature range with the rate of about 100 MHz below 35 K and down to 2.7 K. These fluctuations are most likely caused by oxygen deficiency in niobium pentoxide. Magnetic fluctuations are directly associated with magnetic flux noise and might lead to dephasing and decoherence in quantum devices. The connection of these fluctuators with the TLS model remains unclear due to the lack of experimental data to establish a transition to a low-temperature (mK) regime. However, we have microscopically checked the purity of the grown Nb_2O_5 film and could claim that no other impurities were detected, therefore it evidently shows that the presence of pentoxide on top of a surface by itself could be critical for superconducting devices' performance. To our best knowledge, it is the first study of magnetic dynamics solely in niobium pentoxide.

References

[1] Blundell, J. Stephen *et al.*, *Muon Spectroscopy: An Introduction* (2021).
[2] A. Romanenko *et al.*, Phys. Rev. Applied **13**, 034032 (2020).

Abstract ID: 1038

IMPROVING CHARACTERISTICS OF THE FLUX-DRIVEN JOSEPHSON TRAVELING-WAVE PARAMETRIC AMPLIFIERS BY USING Bi-SQUIDs CELLS

A.N. Nikolaeva, V.K. Kornev, N.V. Kolotinskiy

Lomonosov Moscow State University, 119991, Moscow, RUSSIA
E-mail: nkolotinsky@gmail.com

Parametric amplifiers are known as ultimate-low-noise amplifiers; however, such conventional cavity-based amplifiers are burdened with a gain-bandwidth trade-off. To overcome the drawback, travelling-wave parametric amplifiers (TWPA) were suggested. TWPAs are based on using waveguide lines with nonlinear reactive parameters (of capacitive or inductive types) such as a kinetic-inductance microwave line [1] or artificial lines composed of lumped cells with nonlinear capacitors or inductances. As far as the superconducting kinetic inductance of Josephson junctions $L_j=L_{j0}/Cos\ \varphi$ is strongly nonlinear (here $L_{j0}=\Phi_0/2\pi I_c$, $\Phi_0 =h/2e$, I_c are the Josephson-junction critical current and the Josephson-junction phase) the artificial lines composed of superconducting cells containing Josephson junctions are generally used in the designs of Josephson Travelling Wave Parametric Amplifiers (JTWPA) [2-5]. The amplifiers can work at low and very low temperatures and provide the extremely high sensitivity approaching quantum limit level. Therefore, JTWPAs are currently considered as promising readout devices for their use in the field of precision quantum measurements (including single-photon detectors), quantum communications and quantum computing (see [6, 7] and review [5]).

In this presentation, we discuss characteristics of the artificial waveguide lines composed of lumped element cells in connection with designing the Josephson travelling wave parametric amplifiers and consider the attainable increase in dynamic range of the two-line flux-driven amplifier [8] with substitution dc SQUID cells for bi-SQUID cells [9]. As the performed numerical simulation evidences, dynamic range of the amplifier can be increased by a factor of 2 to 3 due to the current redirection mechanism inside the cells.

This research was funded by Russian Science Foundation (RSCF), grant number 19-72-10016-P.

References

[1] M.R. Vissers, R.P. Erickson, *et al.*, *Low-noise kinetic inductance traveling-wave amplifier using three wave mixing*, Appl. Phys. Lett., **108**, p. 012601 (2016).

[2] O. Yaakobi, L. Friedland, C. Macklin, I. Siddiqi, *Parametric amplification in Josephson junction embedded transmission lines*, Phys. Rev. B, **87**, 144301 (2013).

[3] M.T. Bell, A. Samolov, *Traveling-wave parametric amplifier based on a chain of coupled asymmetric SQUIDs*, Phys. Rev. Appl., **4, no. 2**, Art no. 024014 (2015).

[4] A.B. Zorin, *Josephson traveling-wave parametric amplifier with three-wave mixing*, Phys. Rev. Appl., **6**, Art. no.034006 (2016).

[5] M. Esposito, A. Ranadive, L. Planat, N. Roch, *Perspective on traveling wave microwave parametric amplifiers*, Appl. Phys. Lett., **119**, 120501 (2021).

[6] Ch. Macklin, *et al.*, *A near–quantum-limited Josephson traveling-wave parametric amplifier*, Science, **350, no. 6258**, pp. 307-310 (2015).

[7] M. Haider, *et al.*, *A Josephson traveling wave parametric amplifier for quantum coherent signal processing*, 2019 IEEE MTT-S Int. Microwave Symp. (IMS), IEEE (2019).

[8] A.B. Zorin, *Flux-driven Josephson traveling-wave parametric amplifier*, Phys. Rev. Appl., **12, no. 4**, Art no. 044051 (2019).

[9] A.N. Nikolaeva, V.K. Kornev, N.V. Kolotinskiy, *Bi-squid versus dc squid in flux-driven traveling-wave parametric amplifier*, Applied Sciences, **13(14)**, 8236 (2023).

Abstract ID: 1240

CATASTROPHIC MAGNETIC FLUX AVALANCHES IN NbTiN SUPERCONDUCTING RESONATORS

L. Nulens[1], N. Lejeune[2], J. Caeyers[1], S. Marinković[2] , I. Cools[3], H. Dausy[1], S. Basov[1], B. Raes[1], M.J. Van Bael[1], A. Geresdi[3], A.V. Silhanek[2], J. Van de Vondel[1]

[1] *Quantum Solid-State Physics, Department of Physics and Astronomy, KU Leuven, Celestijnenlaan 200D, Leuven, B-3001, 9 BELGIUM*
[2] *Experimental Physics of Nanostructured Materials, Q-MAT, CESAM, Université de Liège, Allée du 6 Août 19, Sart Tilman, 12 B-4000, BELGIUM*
[3] *Quantum Device Physics Laboratory, Department of Microtechnology and Nanoscience, Chalmers University of Technology, Goteborg, Kemivägen 9, SE-412 58, SWEDEN*
E-mail: lukas.nulens@kuleuven.be

Superconducting coplanar waveguide (CPW) resonators have become an essential component of quantum circuits due to their ability to read different qubit systems. These CPW resonators combine a conventional fabrication method with superior quality factors needed to perform circuit quantum electrodynamics [1]. To obtain this high performance, the CPW resonators must be screened from external damping sources among which magnetic flux quanta play a particularly detrimental role. Although efficient magnetic screening can be achieved, this is not always a viable option since some qubit implementation schemes require inevitable exposure to a magnetic field [2].

In this work, we investigate the impact of the magnetic field penetration on the resonance frequency of NbTiN superconducting resonators by a combination of magneto-optical imaging and high-frequency measurements. At temperatures below approximately half of the superconducting critical temperature, the development of magnetic flux avalanches manifests itself as jumps in the resonance frequency of the coplanar resonators. A clear change in the rate of decreasing resonance frequency with magnetic field is observed when a magnetic perforation event regime sets the transition between a Meissner-like phase in the ground plane and flux injection into the central feedline. These regimes are directly visualized by magneto-optical imaging and the impact of avalanches in the ground plane and the resonator is discerned (as shown in Figure 1). At high working temperatures, a smooth flux penetration is shown to prevail. We propose some hints and strategies to mitigate the influence of avalanches on the response of the resonators and to improve the magnetic resilience of coplanar resonators. Our findings demonstrate that superconducting resonators represent a valuable tool to investigate the magnetic flux dynamics in superconducting materials. Moreover, the current blooming of niobium-based superconducting radio-frequency devices makes this report timely by unveiling the severe implications of magnetic flux dynamics.

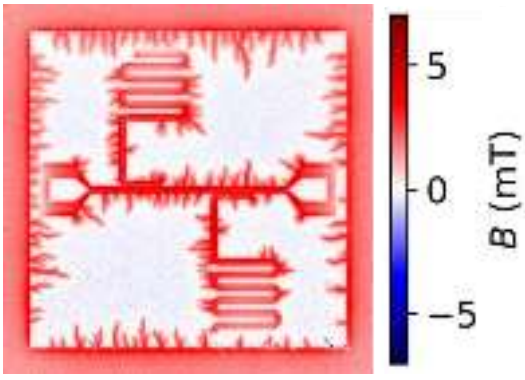

Fig. 1: *magneto-optical image taken at 5 K with a magnetic field of 1.3 mT.*

References

[1] A. Megrant, *et al.*, Appl. Phys. Letters **100**, 113510 (2012).
[2] Y. Kubo, *et al.*, Phys. Rev. Letters **105**, 140502 (2010).

Abstract ID: 236

HYBRID SCHROEDINGER-GINZBURG-LANDAU RELAXATION ALGORITHM IN DESCRIPTION OF UNCOVENTIONAL JOSEPHSON JUNCTION SYSTEMS

K. Pomorski[1,2], L. Gomez[3], B. Stojewski[1,2], M. Kowalik[4], Ł. Stępień[5], P. Pęczkowski[6]

[1]Łódź University of Technology, Institute of Physics, Wólczańska 271/221, 90-451 Łódź, POLAND
[2]Quantum Hardware Systems, Babickiego 10/195, 94-056 Łódź, POLAND
[3]NanoJunctions Company, 1401 Russell St, Covington, KY 41011, USA
[4]Rzeszów University of Technology, Faculty of Mathematics and Applied Physics, Powstańców Warszawy 8, 35-959 Rzeszów, POLAND
[5]The Pedagogical University in Cracow, Podchorążych 2, 30-084 Cracow, POLAND
[6]Cardinal Wyszyński University, Faculty of Mathematics and Natural Sciences, School of Exact Sciences, Institute of Physical Sciences, K.Wóycickiego 1/3, 01-938 Warsaw, POLAND
E-mail: kdvpomorski@gmail.com

New Josephson junction systems [1-3] are proposed and go into direction of integration between semiconductor and superconducting electronics. Replacement of microwave waveguides inducing the state of Josephson junctions with chain of coupled semiconductor quantum dots gives chance for more compact scalable superconducting qubits. At the same time topologically protected states are emerging, what gives the perspective of scalable and repetitive quantum circuits. All considerations are done in framework of Wannier qubits [5] interacting perturbatively with Josephson junction basing on Schroedinger model of quantum dots and Bogoliubov-de Gennes model of superconducting nanostructures. Furthermore, the Schroedinger-Ginzburg-Landau algorithm [4] is able to describe properties of unconventional Josephson junction made by placement of non-superconducting or ferromagnetic strip on the top of superconductor [6-7, 3].

References

[1] K. Pomorski, P. Pęczkowski, R. Staszewski, Cryogenics **109**, 103117 (2020).
[2] K. Pomorski, P. Giounanlis, E. Blokhina, D. Leipold, P. Pęczkowski, R. Bogdan Staszewski, Proc. SPIE **11054**, 11054M (2019).
[3] K. Pomorski, P. Prokopow, Phys. Stat. Soli. B **249(9)**, 1805-1813 (2012).
[4] B. Stojewski, Relax*ation algorithm in description of superconducting structures*, Defended Master of Science Thesis (2022).
[5] K. Pomorski, Math. Comp. Simul. **209**, 362-407 (2023).
[6] A. Maeda, H. Kitano, L. Gomez, T. Kubo, K. Ota, T. Ohashi, J.Phys.: Conf. Ser. **43**, 1151 (2006).
[7] A. Maeda, L. Gomez, Patent US8200304B2 (2009).

Device Physics of Josephson Junctions and Their Fundamental Technologies VI

29.04.2024 MONDAY

Abstract ID: 1413

COOPER QUARTETS DESIGN IN INTERACTING SUPERCONDUCTING SYSTEMS

L. Chirolli[1], A. Braggio[2], F. Giazotto[2]

[1]*Quantum Research Center, Technology Innovation Institute, Abu Dhabi, UAE*
[2]*NEST, Istituto Nanoscienze CNR, and Scuola Normale Superiore, I-56127 Pisa, IT*
E-mail: luca.chirolli@tii.ae

Quantum design of Cooper quartets in a double quantum dot system coupled to ordinary superconducting leads is presented as a novel platform for the study of an elusive many-body state of matter, that is at the basis of the phenomenon of charge-4e superconductivity. A fundamentally novel, maximally correlated ground state, in the form of a superposition of vacuum $|0\rangle$ and four-electron state $|4e\rangle$, emerges as a narrow resonance and it is promoted by an attractive interdot interaction. A novel phenomenology in the dissipationless transport regime is elucidated, that yields typical flux quantization in units of h/4e and manifests in non-local multi-terminal coherence and in two-Cooper pair transport properties mediated by the quartet ground state. The results open the way to the exploration of correlation effects and non-local coherence in hybrid superconducting devices, parity-protected quantum computing schemes and more generally, the work poses the basis for the design and simulation of novel correlated states of matter starting from ordinary ingredients available in a quantum solid state lab.

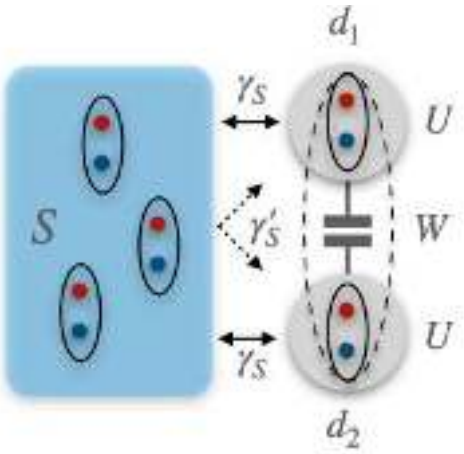

Fig. 1: *Platform for design and simulation of a Cooper quartet.*

Abstract ID: 252

LOW POWER SINGLE FLUX QUANTUM QUBIT CONTROL CIRCUITS WITHOUT HIGH-FREQUENCY INPUT

Jie Ren, Bicong Weng, Wei Peng

Shanghai Institute of Microsystem and Information Technology (SIMIT), Chinese Academy of Sciences (CAS), 865 Changning Road, Shanghai 200050, PEOPLE'S REPUBLIC OF CHINA
E-mail: jieren@mail.sim.ac.cn

Superconducting single flux quantum (SFQ) integrated circuits are expected to be applied to the manipulation of qubits in universal quantum computers because of their low operating temperature, low energy consumption, low noise, and high scalability. We propose a structure of scalable SFQ qubit control circuit (SQCC) that only requires low-frequency input. The circuit realizes the output of SFQ pulse train with adjustable frequency and controllable number of pulses. It can be used for the control of single-qubit Clifford operations. All input signals in this method are low-frequency, which enables the control of large-scale qubits to be free from the limitations of hardware consumption by high-frequency inputs from room temperature. The use of LV-RSFQ and ERSFQ design makes the circuit achieve very low power consumption, providing the basis for scaling circuits that control more qubits. The proposed circuits were fabricated under the SIMIT-Nb03 process and the function of the circuit was verified by testing. To further improve the fidelity of the qubit control, we then present optimized designs for different pattern requirements of qubit control, building upon the SQCC without high-frequency input. The circuit capable of generating arbitrary patterns currently achieves a maximum adjustable number of 400, with a corresponding frequency output of 20 GHz. It has been successfully fabricated using the SIMIT Nb03 process and has passed functionality measurement tests. The optimized circuit opens up possibilities for improved qubit control and advancements in quantum computing applications.

Abstract ID: 1463

IDENTIFYING DOMINANT MAGNETIC COUPLINGS IN LARGE SUPERCONDUCTING CIRCUITS

K. Jackman[1,2], C.J. Fourie[1,2]

[1]*Department of Electrical and Electronic Engineering, Stellenbosch University, Stellenbosch, 7600, SOUTH AFRICA*
[2]*SUN Magnetics, Stellenbosch, 7600, SOUTH AFRICA*
E-mail: kjackman@sun.ac.za

Addressing the critical challenge of modeling inductively coupled circuits in superconducting integrated circuit design, we introduce a novel method for identifying dominant magnetic couplings in large, inductively coupled superconducting circuits. This method marks a significant advance in simplifying the complex and often imprecise task of determining potential inductor couplings in an equivalent circuit. We present a technique for extracting coupling coefficients from the admittance parameters of a multi-port network and propose a strategy for minimizing these coefficients. This reduction is essential for decreasing circuit complexity while ensuring accuracy remains within a specified threshold. Additionally, our approach facilitates the extraction of all potential magnetic couplings between inductors. This approach substantially improves the design and optimization processes of superconducting integrated circuits, striking an optimal balance between circuit simplicity and modeling accuracy.

Molecular Spin Qubits toward Quantum Computer III

29.04.2024 MONDAY

Abstract ID: 1419

ELECTRON SPIN RESONANCE MEASUREMENT OF A SINGLE MOLECULE MAGNET TERBIUM PHTHALOCYANINE ($TbPc_2$) ADSORBED ON SURFACE TOWARDS QUANTUM COMPUTING

Tadahiro Komeda[1], Ryo Kawaguchi[1], Katsushi Hashimoto[2], Toshiyuki Kakudate[3], Keiichi Katoh[4], Masahiro Yamashita[5,6]

[1]*Institute of Multidisciplinary Research for Advanced Materials (IMRAM, Tagen), Tohoku University, JAPAN*
[2]*Department of Physics, Tohoku University, JAPAN*
[3]*Department of Industrial Systems Engineering, Hachinohe College, JAPAN*
[4]*Department of Chemistry, Josai University, JAPAN*
[5]*Department of Chemistry, Tohoku University, JAPAN*
[6]*School of Materials Science and Engineering, Nankai University JAPAN*
E-mail: tadahiro_komeda@hotmail.com

The application of magnetic molecules to the materials of the devices for the quantum information process attracts attention. It is critical to make the sharp spin state of the molecule coupled efficiently with the electric current and substrate. The double-decker phthalocyanine complex of bis(phthalocyaninato)terbium(III) ($TbPc_2$) molecule showed intriguing single-molecule magnet (SMM) behaviour, which was demonstrated to be served after transferred on the substrates of Au(111) and Ag(111).

A scanning tunneling microscope and spectroscopy (STM/STS) are employed to examine the structural configuration and the spin state. The experiment was done in UHV conditions at the temperature of 400 mK. RF signal and outer magnetic field are introduced to the tunneling junction between the spin-polarized tip and the Au(111) substrate. NaCl film of several monolayers is inserted as a thin interface layer.

The schematic illustration is in Fig. 1, with STM images of the $TbPc_2$ molecule. As shown in Fig. 1(d), a sharp resonance feature is observed to enhance the tunnelling current. As shown in Fig. 2, the resonance condition shows a Zeeman condition with g~2.0 representing the Pc ligand's delocalized unpaired π orbital spin.

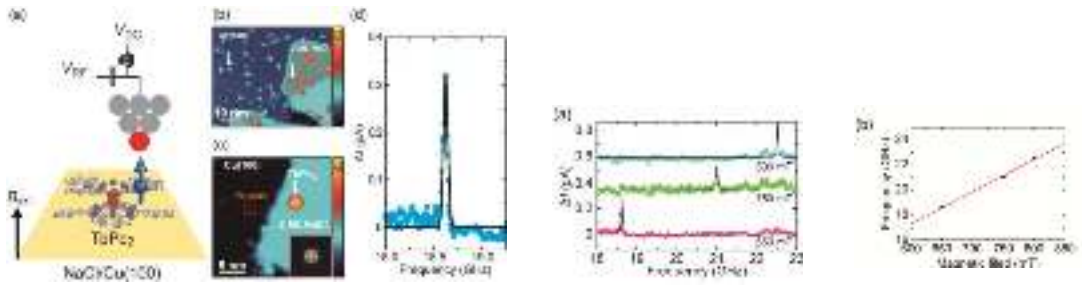

Fig. 1: *(left) (a) Schematics of ESR-STM. (b) Single-molecule magnet $TbPc_2$ film and (c) isolated $TbPc_2$ on NaCl film.*
Fig. 2: *(right) (a) Enhanced tunneling current at the resonant condition of RF signal and the magnetic field. The RF frequency at the resonant condition shifts with the magnetic field, which is summarized in (b).*

References

[1] R. Kawaguchi, K. Hashimoto, T. Kakudate, K. Katoh, M. Yamashita, T. Komeda, Nano Lett., **23**, 213-219 (2023).

Abstract ID: 1496

TWO-QUBIT [Dy_2] MOLECULES DEPOSITED INTO MICRO-SQUID SUSCEPTOMETERS: IN-SITU CHARACTERIZATION OF THEIR MAGNETIC INTEGRITY

Ana Repollés[1], María Carmen Pallarés[1,2], David Aguilà[3,4], Olivier Roubeau[1], Verónica Velasco[3,4], Diego Gella[1], Leoní A. Barrios[3,4], María José Martínez-Pérez[1], Javier Sesé[1], Dietmar Drung[5], Thomas Schurig[5], Boris Le Guennic[6], Anabel Lostao[1,2,7], Guillem Aromí[3,4], Fernando Luis[1]

[1]*Instituto de Nanociencia y Materiales de Aragón (INMA), CSIC-Universidad de Zaragoza, 50009, Zaragoza, SPAIN*
[2]*Laboratorio de Microscopias Avanzadas (LMA), Universidad de Zaragoza, 50018 Zaragoza, SPAIN*
[3]*Departament de Química Inorgànica i Orgànica, Universitat de Barcelona, Diagonal 645, 08028 Barcelona, SPAIN*
[4]*Institut of Nanoscience and Nanotechnology of the University of Barcelona (IN2UB), Barcelona, SPAIN*
[5]*Physikalisch-Technische Bundesanstalt (PTB), Abbestraße 2-12, D-10587 Berlin, GERMANY*
[6]*Univ Rennes, CNRS, ISCR (Institut des Sciences Chimiques de Rennes) - UMR 6226, F-35000 Rennes, FRANCE*
[7]*Fundación ARAID, 50018 Zaragoza, SPAIN*
E-mail: fluis@unizar.es

The integration of magnetic molecules into superconducting circuits is key for developing hybrid quantum computing architectures. Here, we study [Dy_2] molecular dimers deposited onto micro-SQUID susceptometers. The results of magnetic and heat capacity experiments, backed by theoretical calculations, show that each [Dy_2] dimer can act as a two-qubit quantum processor. Arrays of [Dy_2] molecules have been optimally integrated inside the 20 μm wide loops of micro-SQUID sensors by means of Dip-Pen Nanolithography. The equilibrium magnetic susceptibility and the spin tunneling dynamics measured in situ evidence that these molecules preserve the spin ground states, magnetic interactions and magnetic asymmetry that characterize them in bulk. These results show that it is possible to interface multi-qubit molecular complexes with superconducting circuits without disturbing their relevant properties and hints at the potential of soft nanolithography to achieve this goal in practice.

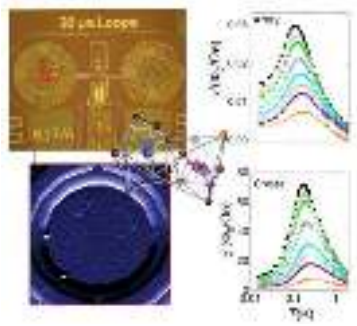

Fig. 1: *Image of a micro-SQUID ac susceptometer (top left) and of a [Dy_2] nanoarray deposited on one of its pick-up coils (bottom left). Linear ac susceptibility measured on an array (top right) compared to that measured on a bulk crystal (bottom right).*

Abstract ID: 1290

EPR SPECTROSCOPY AND SPIN COHERENCE IN RARE-EARTH DIMERS WITH SINGLE-ELECTRON METAL-METAL BONDS

A.A. Popov

[1]*Leibniz IFW Dresden, 01069, Dresden, GERMANY*
E-mail: a.popov@ifw-dresden.de

Encapsulation of magnetic species within robust molecular containers is a natural route towards stable and processable molecule magnets. Fullerenes provide an ideal platform for this goal since they are able to stabilize simple yet unconventional metallic species in their interior space and thereby. A spectacular example of this sort is the realization of the metal-metal bonding within the fullerene cage, which for a long time deemed not possible in conventional lanthanide chemistry. Particularly interesting are single-electron metal-metal bonds in dimetallofullerenes as the way to create very strong magnetic interactions between lanthanide magnetic moments [1-3], or as the way to realize very strong hyperfine coupling due to the large s-orbital contribution to the M−M bonding orbital [4]. In this contribution we will overview CW and pulsed EPR studies of endohedral rare-earth dimers inside fullerene cages, with the main focus on spin distribution and relaxation times.

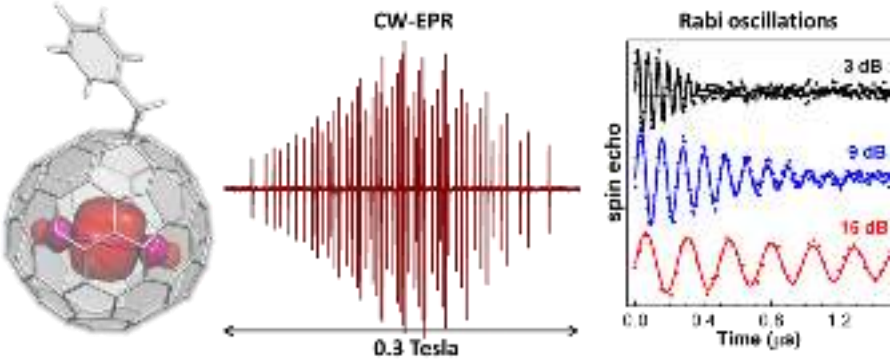

Fig. 1: *Spin-density distribution in $Sc_2@C_{80}(CH_2Ph)$ with single-electron Sc–Sc bond, X-band EPR spectrum in solution, and Rabi oscillation in frozen solution.*

References

[1] F. Liu, D.S. Krylov, L. Spree, S.M. Avdoshenko, N.A. Samoylova, M. Rosenkranz, A. Kostanyan, T. Greber, A.U.B. Wolter, B. Büchner, A.A. Popov. Nat. Commun. **8**, 16098 (2017).

[2] F. Liu, G. Velkos, D.S. Krylov, L. Spree, M. Zalibera, R. Ray, N.A. Samoylova, C.-H. Chen, M. Rosenkranz, S. Schiemenz, F. Ziegs, K. Nenkov, A. Kostanyan, T. Greber, A.U.B. Wolter, M. Richter, B. Büchner, S.M. Avdoshenko, A.A. Popov. Nat. Commun. **10**, 571 (2019).

[3] F. Liu, L. Spree, D.S. Krylov, G. Velkos, S.M. Avdoshenko, A.A. Popov. Acc. Chem. Res. **52** (10), 2981-2993 (2019).

[4] R.B. Zaripov, Y.E. Kandrashkin, K.M. Salikhov, B. Büchner, F. Liu, M. Rosenkranz, A.A. Popov, V. Kataev. Nanoscale **12**, 20513–20521 (2020).

Molecular Spin Qubits toward Quantum Computer IV

29.04.2024 MONDAY

Abstract ID: 1400

PROBING QUANTUM COHERENCE IN SINGLE-ATOM AND MOLECULAR QUBITS USING THE ESR-STM TECHNIQUE

Christoph Wolf

Center for Quantum Nanoscience, Institute for Basic Science (IBS), Seoul 03760, KOREA
EWHA Womans University, Seoul 03760, KOREA
E-mail: wolf.christoph@qns.science

The combination of electron spin resonance (ESR) and the scanning tunneling microscope yields a technique with unprecedented combination of spatial (~Å) and energy (~μeV) resolution. [1] In recent years, this has enabled the study of quantum-coherent phenomena of individual atoms and molecules on surfaces. Only very recent, we were able to show that this platform enables the bottom-up construction of nano-structures with quantum-coherent functionality – which, in principle, could be used to simulate complex quantum systems in hardware. [2]

In this talk, I want to give an overview over the recent discoveries of quantum-coherent phenomena in atoms, molecules and artificial nanostructures based on the ESR-STM technique and non-equilibrium transport simulation.[3] I want to explore the limits and opportunities of these systems with an outlook on their application as novel platform for the study of many-body quantum physics.

References

[1] Baumann *et al.*, Science **350**, 417-420 (2015).
[2] Wang *et al.*, Science **382**, 87-92 (2023).
[3] Reina *et al.*, Phys. Rev. B **107**, 235404 (2023).

Abstract ID: 1067

PROBING SPIN COUPLING WITHIN SINGLE MOLECULAR MAGNETS

Ying-Shuang Fu

Huazhong University of Science and Technology, School of Physics, 430074, Wuhan, CHINA
E-mail: yfu@hust.edu.cn

Understanding the spin coupling within single molecular magnets is essential for designing emergent quantum states. Using scanning tunneling microscopy and spectroscopy (STM/STS), we investigate a molecular magnet Tb_2Pc_3 interacting with a superconducting Pb(111) substrate, which hosts Yu-Shiba-Rusinov (YSR) states. Upon adsorption of the molecule on Pb, the degeneracy of its lowest unoccupied molecular orbitals (LUMO) is lifted, and the lower LUMO forms a radical spin via charge transfer. This leads to Kondo screening and YSR states. The YSR states display two pairs, where the inner pair energy exhibits prominent variation with the Kondo strength, but the outer pair shifts only slightly. Our theory unveils the YSR states originate from two weakly coupled LUMO ligand spins, paving the way for understanding complex many-body excitations [1]. We also achieved manipulation of the chirality of Tb_2Pc_3. The otherwise achiral Tb_2Pc_3 becomes chiral after being embedded into self-assembled monolayer films of $TbPc_2$ on Pb(111) substrate. The chirality of spin distribution in Tb_2Pc_3 is manifested via the spatial mapping of its Kondo resonance state from its ligand orbital. Our first-principles calculations demonstrate that the spin and molecular chirality are associated with a small rotation followed by a structural distortion of its top Pc, in agreement with the experimental observation. By constructing tailored molecular clusters with STM tip, single Tb_2Pc_3 molecule can be manipulated among achiral, and differently handed chiral configuration of spin distributions reversibly [2]. This provides a way for designing chiral spin enantiomers for fundamental studies and developing functional spintronic devices.

References

[1] H. Xia *et al.*, Nat. Commun. Nat. Commun. **13**, 6388 (2022).
[2] X. Liao *et al.*, JACS, under review.

Abstract ID: 1070

STM STUDY ON SUPERCONDUCTORS AND ARCHITECTING MOLECULAR MAGNETS ON SURFACES

T. K. Yamada[1,2]

[1]*Chiba University, Dept. of Materials Science, 2638522, Chiba, JAPAN*
[2]*Chiba University, Molecular Chirality Research Centre, 2638522, Chiba, JAPAN*
E-mail: toyoyamada@faculty.chiba-u.jp

Various individual organic compounds encompassing magnetic entities, called single molecular magnets (SMMs), have been intensively studied as promising candidates for advancing Quantum bits (Q-bits). Despite the substantial diversity inherent in these SMMs, facilitating a wide variety of Q-bit arrays requires a longer spin lifetime. The electronic decoupling from the conduction electrons could be a crucial breakthrough for realizing a longer lifetime reaching the scale of seconds. 2D materials, exemplified by graphene, transition metal dichalcogenides, or insulating films, have been investigated as potential mediums for this decoupling layer. Alternatively, the superconductor materials could be another candidate to protect the YSR state using the superconducting gap.

In our study, we present empirical findings obtained through scanning tunneling microscopy/spectroscopy (STM/STS) results performed on three distinct systems: (1) Caroli-de Gennes-Matricon (CdGM) states observed in multiple-flux-quanta vortices on the Pb surface [1], (2) the YSR state induced by the TCNQ molecule adsorbed on the Nb tip [2], and (3) zero-bias anomaly (ZBA) manifested in CuPc situated on the MgO/Fe(001)-p(1x1)O [3].

We further demonstrate the development of a 2D Q-bit array employing magnetic atoms and molecules on a surface, a pivotal step in the realization of Q-bit device fabrication. While the top-down drop-casting technique for SMMs struggles with controlling structural alignment, advanced bottom-up approaches utilizing on-surface growth through the assembly of precursor molecules and magnetic atoms offer a novel platform, leading to a 2D magnetic array [4,5].

References

[1] T. Gozlinski, Q. Li, R. Heid, R. Nemoto, R. Willa, T.K. Yamada, J. Schmalian, W. Wulfhekel, Sci. Adv. **9**, eadh9163 (2023).
[2] C.G. Ayani, F. Calleja, I.M. Ibarburu, P.C. Aguilar, N.K.M. Nazriq, T.K. Yamada, M. Garnica, A.L. Vazquez de Parga, R. Miranda, Nanoscale **14**, 15111 (2022).
[3] N.K.M. Nazriq, P. Krueger, T.K. Yamada, Applied Surface Science **618**, 156628 (2023).
[4] T.K. Yamada, R. Nemoto, F. Nishino, T. Hosokai, C.H. Wang, M. Horie, Y. Hasegawa, S. Kera, P. Krüger, Journal of Materials Chemistry C, (2024)
DOI: 10.1039/D3TC03339B.
[5] T. K. Yamada, S. Kera, *et al.*, under review.

Molecular Spin Qubits toward Quantum Computer V

29.04.2024 MONDAY

Abstract ID: 1006

CONTROLLING ENVIRONMENTAL SENSITIVITY IN ^{59}Co NUCLEAR SPIN QUBITS

O. Ungor,[1,2] T. Ozvat,[1] S. Sanchez,[1] A. Rappé,[1] N. Schaffner,[2] J. Zadrozny[1,2]

[1] The Ohio State University, Dept. of Chemistry, Columbus, OH 43220 USA
[2] Colorado State University, Dept. of Chemistry, Fort Collins, CO 80523 USA
E-mail: zadrozny.13@osu.edu

Magnetic nuclei are chemically sensitive qubit objects with the potential to translate concepts of spin control and design from the field of quantum information to novel bioimaging technologies. In this presentation, I will discuss mechanisms of amplifying the environmental sensitivity of magnetic nuclei. Magnetic nuclei have small magnetic moments, and therefore suppressed sensitivity relative to the other prominent molecular qubit system in magnetic resonance – unpaired electrons. In this work we present ways of synthetic tuning the environmental sensitivity of ^{59}Co magnetic nuclei to amplify it.[1-5] In the process, we found new species bearing magnetic nuclei that demonstrate the environmental sensitivity of unpaired electrons.

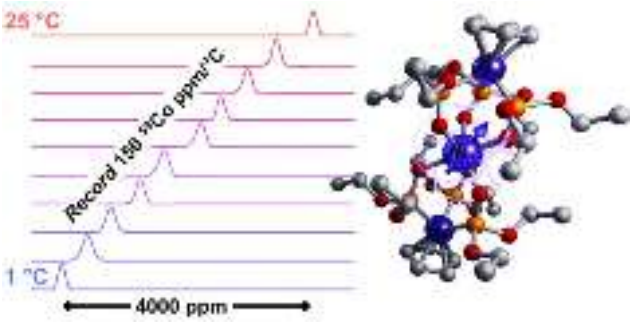

Fig. 1: *Overview of results to be presented.*

References

[1] T.M. Ozvat, M.E. Peña, J.M. Zadrozny, Chem. Sci. **10**, 6727 (2019).
[2] T.M. Ozvat, G.E. Sterbinsky, A.J. Campanella, A.K. Rappé, J.M. Zadrozny, Dalton Trans. **49**, 16380 (2020).
[3] T.M. Ozvat, S.H. Johnson, A.K. Rappé, J.M. Zadrozny, Magnetochemistry, **6**, 58 (2020).
[4] T.M. Ozvat, A.K. Rappé, J.M. Zadrozny, Inorg. Chem. **61**, 778 (2022).
[5] Ö. Üngör, T.M. Ozvat, Z. Ni, J.M. Zadrozny, J. Am. Chem. Soc. **144**, 9132 (2022).

Abstract ID: 1606

QUANTUM SENSING OF MAGNETIC FIELDS WITH MOLECULAR SPINS

M. Affronte[1,2], C. Bonizzoni[1,2], A. Ghirri[2]

[1] *Dipartimento di Scienze Fisiche, Informatiche e Matematiche, Università di Modena e Reggio Emilia, via G. Campi 213/A, Modena 41125, ITALY*
[2] *Istituto Nanoscienze—CNR, Centro S3, via G. Campi 213/A, Modena 41125, ITALY*
E-mail: marco.affronte@unimore.it

To prove that molecular spins hold potential for quantum technologies, we have recently shown that it is possible to embed molecular spin ensembles into planar superconducting microwave (MW) resonators [1] and to coherently manipulate them though resonators by using suitable sequences of MW pulses [2], eventually down to sub-nanoliter sample volumes [3]. Molecular spins can work also as temporary memories for information [2], in which the readout of output signal/s can be further assisted by machine learning methods to improve either amplitude or phase inference [4]. Due to their long coherence time, the relatively easy possibility of manipulation and readout and their intrinsic quantum nature and properties (such as entanglement), molecular spins has been proposed also for quantum sensing schemes [5]. However, experimental demonstrations of sensing schemes involving such spins have not been reported yet. Here we test molecular spins for quantum sensing of magnetic fields [6]. To this end, we first consider a diluted VO(TPP) molecular spin ensemble embedded into a planar MW superconducting resonator, as in Fig. 1.a. The sensing protocol consists in a MW pulse sequence which is used to coherently drive the spins and to obtain a Hahn's echo, while the radiofrequency (RF) signal to be detected is sent during the free spin precession time through an additional RF coil. We show that it is possible to detect changes in both echo amplitude and phase and to relate them to the presence and the parameters (amplitude, phase) of the RF field, as in Fig. 1.b [6].We extend our sensing protocol to the case in which Dynamical Decoupling sequences, such as Carr-Purcell-Meiboom-Gill [2] and Period Dynamical Decoupling are used, and we apply them to drive an ensemble of diluted BDPA organic radical [6,3]. The effect of the RF field on the echo is found to increase with the number of π pulses used in the MW sequence. The resulting magnetic field sensitivity can reach values as high as $nT/\sqrt{Hz}$ with a relatively low number (4-5) of π pulses applied, which is comparable with the typical values reported for Nitrogen Vacancy centers magnetometry performed through Optically Detected Magnetic Resonance spectroscopy [6]. These results show, for the first time, quantum sensing protocols can be successfully implemented with molecular spins.

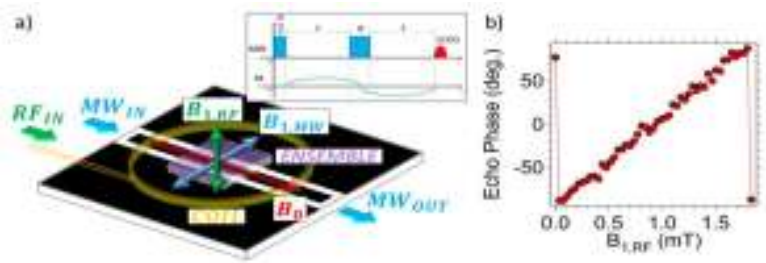

References

[1] C. Bonizzoni *et al.*, Advances in Physics: X, **3** 1435305, (2018).
[2] C. Bonizzoni *et al.*, npj Quantum Inf., **6**, 68 (2020).
[3] C. Bonizzoni *et al.*, Appl. Magn. Reson., **54**, 143 (2023).
[4] C. Bonizzoni *et al.*, Phys. Rev. Applied, **18**, 064074 (2022).
[5] F. Troiani *et al.*, J. Magn. Mag. Mat., **491**, 165534 (2019).
[6] C. Bonizzoni *et al.*, submitted, Preprint on arXiv:2311.13504 (2023).

Abstract ID: 1514

INTEGRATION OF MOLECULAR QUANTUM BITS

L. Tesi[1], F. Stemmler[1], D. Schäfter[1], M. Kern[1], N. Crivillers[2], S. Ludwigs[3], J. van Slageren[1]

[1]University of Stuttgart, Institute of Physical Chemistry, Stuttgart 70569, GERMANY
[2]Institut de Ciència de Materials de Barcelona (ICMAB-CSIC), 08193 Bellaterra, SPAIN
[3]University of Stuttgart, Institute of Polymer Chemistry, Stuttgart 70569, GERMANY
E-mail: slageren@ipc.uni-stuttgart.de

Quantum technologies are set to change the world we live in in many more ways than one. Immense advances have been made, but potential show-stoppers, especially concerning scalability, loom on the horizon. Therefore, the search for an alternative quantum technological platform is on. Molecular quantum bits are the basis for such an alternative platform, because they are highly scalable, tunable and positionable. Coherence times have been shown by ourselves and others to be competitive with other quantum technological platforms [1-3]. Current challenges in the field are individual readout and device integration.

Here we present our two recent advances in this area. First, we have immobilized molecular qubits in self-assembled monolayers on surfaces. We have conclusively proven monolayer formation. We have demonstrated quantum coherence in the immobilized qubits, which is an essential step towards device integration [4]. Secondly, we have developed hybrid materials of molecular qubits with semiconducting polymers. We have shown by organic field-effect transistor measurements that the electrical properties of the polymers are unimpeded by the incorporation of the quantum bits. Furthermore, the embedded molecular qubits were shown to still possess long coherence times, even in the presence of mobile charge carriers [5]. These are important steps on the way to electrical readout of (individual) molecular quantum bis in spintronic devices.

References

[1] K. Bader, D. Dengler, S. Lenz, B. Endeward, S.D. Jiang, P. Neugebauer, J. van Slageren, Nat. Commun. **5**, 5304 (2014).
[2] D. Schäfter, J. Wischnat, L. Tesi, J.A. De Sousa, E. Little, J. McGuire, M. Mas-Torrent, C. Rovira, J. Veciana, F. Tuna, N. Crivillers, J. van Slageren, Adv. Mater. **35**, 2302114 (2023).
[3] J.M. Zadrozny, J. Niklas, O.G. Poluektov, D.E. Freedman, ACS Cent. Sci. **1**, 488 (2015).
[4] L. Tesi, F. Stemmler, M. Winkler, S.S.Y. Liu, S. Das, X. Sun, M. Zharnikov, S. Ludwigs, J. van Slageren, Adv. Mater. **35**, 2208998 (2023).
[5] M. Kern, L. Tesi, D. Neusser, N. Rußegger, M. Winkler, A. Allgaier, Y.M. Gross, S. Bechler, H.S. Funk, L.-T. Chang, J. Schulze, S. Ludwigs, J. van Slageren, Adv. Funct. Mater. **31**, 2006882 (2021).

Molecular Spin Qubits toward Quantum Computer VI

29.04.2024 MONDAY

Abstract ID: 1591

PROBING DIVERSE BEHAVIOR IN ATOMICALLY ENGINEERED MOLECULAR DEVICES ON SURFACES

Deung-Jang Choi[1,2,3]

[1] *Centro de Fisica de Materiales, CFM/MPC (CSIC-UPV/EHU), Paseo Manuel de Lardizabal 5, 20018 Donostia-San Sebastian, SPAIN*
[2] *Donostia International Physics Center (DIPC), Paseo Manuel de Lardizabal 4, 20018 Donostia-San Sebastian, SPAIN*
[3] *Ikerbasque, Basque Foundation for Science, 48013 Bilbao, SPAIN*
E-mail: djchoi@dipc.org

We investigate the contrasting behavior of molecular devices with superconducting junctions [1], utilizing nickelocene molecules and single Fe atoms in conjunction with Pb electrodes at low temperatures. We combine the complex ordering ability of molecules with their local magnetic properties to tailor spin structures on surfaces. Using nickelocene molecules and a superconducting tip, we detect small shifts in spin-flip excitation thresholds, revealing distinct environments of molecules within an ordered layer. This approach unveils insights into the adsorption configuration of a complex molecular structure, suggesting a strong noncollinear magnetic-moment arrangement within nickelocene layers [2]. Expanding our exploration, one device exhibits low-bias features due to the superposition of multiple Andreev reflections (MAR) and Fe-induced in-gap states, while the other showcases interference between MAR and in-gap states, demonstrating the remarkable diversity achievable with identical components [3]. Our study highlights the potential for creating atomically engineered devices with diverse behaviors and intricate spin structures by merging molecular ordering and magnetic properties on surfaces.

References

[1] D.-J. Choi, N. Lorente, J. Wiebe, K. von Bergmann, A.F. Otte, A.J. Heinrich, *Colloquium: Atomic spin chains on surfaces*, Review of Modern Physics **91**, 041001 (2019).

[2] C. Mier, B. Verlhac, L. Garnier, R. Robles, L. Limot, N. Lorente, D.-J. Choi, *Superconducting scanning tunneling microscope tip to reveal sub-millielectronvolt magnetic energy variations on surfaces*, J. Phys. Chem. Letters **12**, 2983 (2021).

[3] *Two molecular devices for superconducting spintronics*, Submitted.

Abstract ID: 1349

CHARGE TRANSFER IN ADDUCTS OF LANTHANIDE 3,5-DINITROBENZOATES WITH AMINOBENZENE DERIVATIVES

P.S. Koroteev[1], A.B. Ilyukhin[1], N.N. Breslavskaya[1], E.N. Timokhina[2], E.A. Ugolkova[1], V.V. Minin[1], N.N. Efimov[1]

[1]*Kurnakov Institute of General and Inorganic Chemistry of RAS, 119991, Moscow, RUSSIA*
[2]*Emanuel Institute of Biochemical Physics of RAS, 119991, Moscow, RUSSIA*
E-mail: nnefimov@narod.ru

Recently we obtained and studied charge transfer (CT) complexes containing binuclear Ln 3,5-dinitrobenzoates and *N,N*-dimethylaniline ($[Ln_2(DNBZ)_6(DMSO)_4]\cdot x$DMA; DMA = Me_2NPh; DNBZ = 3,5-$(NO_2)_2C_6H_3CO_2^-$) [1] or *N,N,N′,N′*-tetramethylphenylenediamine ($[Ln_2(DNBZ)_6(DMSO)_4]\cdot x$TMPD$\cdot y$MeCN; TMPD = 1,4-$(Me_2N)_2C_6H_4$) [2] which represent an original type of hybrid compounds. Supramolecular structures of those complexes are formed due to stacking interactions between donor aromatic amine molecules and acceptor DNBZ fragments. With use of diaminodurene (DAD), and 1,2-phenylenediamine (PDA), two new original series of CT adducts, $[Ln_2(DNBZ)_6(DMSO)_4]\cdot$4DAD (Ln = Sm, Gd-Er, Y; DAD = 1,4-$(H_2N)_2C_6Me_4$) and $[Ln_2(DNBZ)_6(DMSO)_2]_2\cdot$PDA$\cdot$4MeCN (Ln = Gd-Er), were obtained.

CT in the complexes was characterized by UV-vis and reflectance spectra. The CW EPR and dc magnetic measurements allowed us to unequivocally confirm paramagnetism of Y compounds with DAD and TMPD due to CT. The ESEEM technique helps to understand and attribute the presence of nonzero electron density on organic fragments involved in CT – DAD/TMPD and DNBZ.

All experimental data were sutisfactorily reproduced by DFT calculations (see Fig.).

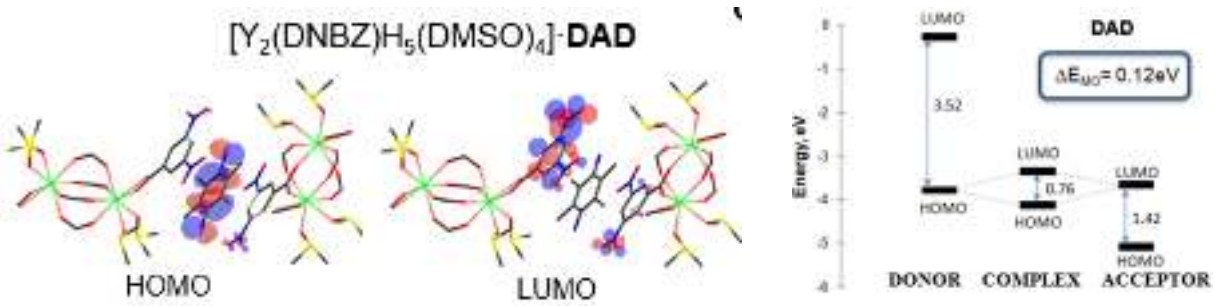

Fig. 1: *Scheme of molecular orbitals for $[Ln_2(DNBZ)H_5(DMSO)_4]\cdot$DAD (left), and energy diagrams (right) for DAD (donor), $[Ln_2(DNBZ)H_5(DMSO)_4]_2\cdot$DAD (complex) and $[Ln_2(DNBZ)H_5(DMSO)_4]$ (acceptor).*

The work was supported by the Russian Science Foundation (project 22-73-10189).

References

[1] P.S. Koroteev, A.B. Ilyukhin, N.N. Efimov *et al.*, Polyhedron, **89**, 238 (2015).
[2] P.S. Koroteev, A.B. Ilyukhin, N.N. Efimov *et al.*, Inorg. Chim. Acta, **442**, 86 (2016).

Abstract ID: 1212

INCREASING QUANTUM COHERENCE IN MOLECULAR SPIN QUBITS BY FULLERENE ENCAPSULATION IN MOFs

D. Žilić[1], M. Kveder[1], L. Vujević[1], K. Užarević[1], B. Karadeniz[1], N. Cindro[2], A. Krajnc[3], G. Mali[3], M. Mazaj[3], A.A. Popov[4], S.M. Avdoshenko[4]

[1]Ruđer Bošković Institute, 10000, Zagreb, CROATIA
[2]University of Zagreb, 10000, Zagreb, CROATIA
[3]National Institute of Chemistry, 1001, Ljubljana, SLOVENIA
[4]Leibniz IFW Dresden, 01069, Dresden, GERMANY
E-mail: dzilic@irb.hr

Increasing quantum coherence time is one of the fundamental steps for the development of quantum technologies [1,2]. We have investigated molecular spin qubits realized as dilute copper(II)– or vanadyl(II)–porphyrins in two diamagnetic zirconium metal-organic framework (MOF) matrices: MOF-525 and PCN-223. Pulse electron spin resonance (ESR) experiments showed that incorporating fullerene into MOFs increases the electron spin–lattice and phase–memory relaxation times, T_1 and T_m, respectively. Besides the reduction of the amount of nuclear spin-bearing solvent guests in MOFs, the observed prolonged relaxation times can be explained by the modulation of the phonon density of states upon fullerene encapsulation [3].

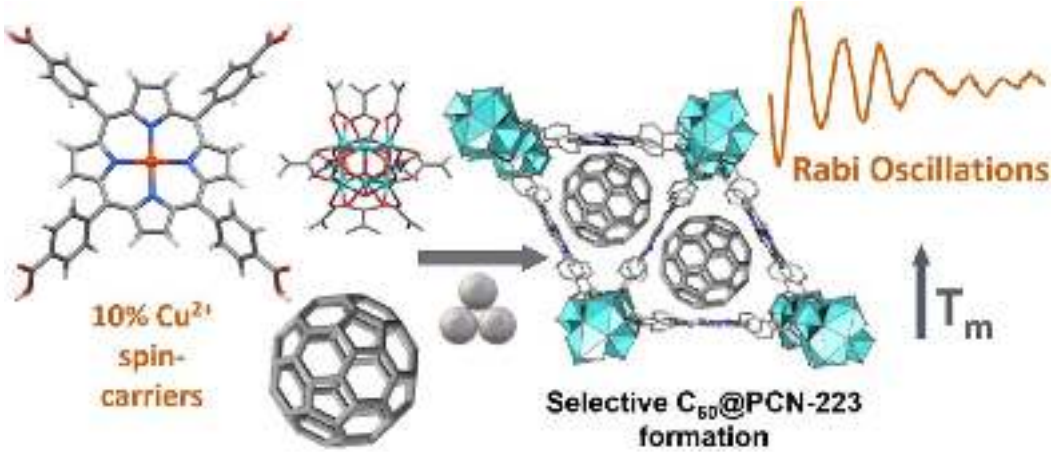

Fig. 1: *Fullerene encapsulation in MOF led to increasing relaxation times in molecular spin qubits.*

References

[1] A. Gaita-Ariño, F. Luis, S. Hill, E. Coronado, Nat. Chem. **11** 301 (2019).
[2] C.-J. Yu, M.D. Krzyaniak, M.S. Fatallah, M.R. Wasielewski, D.E. Freedman, Chem. Sci. **10** 1702 (2019).
[3] L. Vujević, B. Karadeniz, N. Cindro, A. Krajnc, G. Mali, M. Mazaj, S.M. Avdoshenko, A.A. Popov, D. Žilić, K. Užarević, M. Kveder. Chem. Sci. **14** 9389 (2023).

Superconductivity and Magnetism in Heavy Fermion Systems I

29.04.2024 MONDAY

Abstract ID: 1106

LOCAL MAGNETISM IN UTe_2 ABOVE THE CRITICAL PRESSURE

Riku Yamamoto

Los Alamos National Laboratory MPA-Q, 87544, Los Alamos, New Mexico, U.S.A.
E-mail: riku.yamamoto@lanl.gov

The interplay between superconductivity and magnetism is one of the central issues in condensed matter physics. Certain uranium compounds, such as UGe_2 under pressure, URhGe, and UCoGe, exhibit coexistence of ferromagnetism and odd-parity superconductivity. In contrast, above the critical pressure P_C = 1.4 GPa, odd-parity superconductor UTe_2 exhibits two distinct magnetic states that do not coexist microscopically with superconductivity [1-3]. The lower magnetic transition temperature (T_{C1}) has been well studied by macroscopic measurements and argued to be an antiferromagnetically ordered state [2,3]. Indeed, very recent inelastic neutron scattering has revealed a long-range incommensurate antiferromagnetic order [4]. By contrast, the magnetic state with higher transition temperature (T_{C2}) has remained rather controversial with respect to its nature as well as its relationship to the transition at T_{C1}.

In this talk, we will utilize ^{125}Te nuclear magnetic resonance (NMR) to shed light on the microscopic local magnetism in UTe_2 above P_C. In particular, we will discuss static and dynamic magnetism from site-dependent measurements of ^{125}Te NMR. By comparing the NMR results with recent neutron scattering data [5], we will show the importance of short-range magnetic interactions for the magnetism in UTe_2 [5].

This has been collaboration with M. O. Ajeesh, S. M. Thomas, J. D. Thompson, E. D. Bauer, F. Ronning, S. E. Brown, P. F. S. Rosa, and M. Hirata.

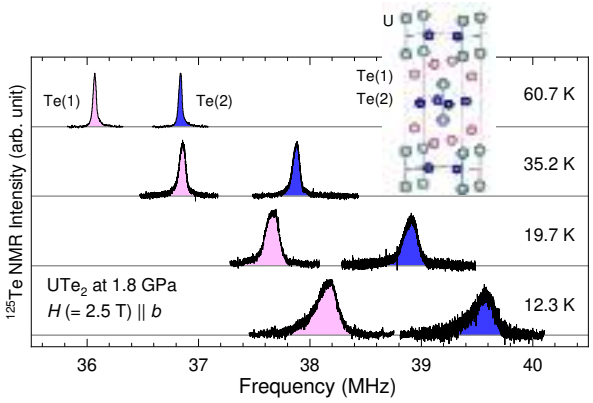

Fig. 1: *Temperature dependence of ^{125}Te NMR spectra of UTe_2 at 1.8 GPa.*

References

[1] S. Ran *et al.*, Science **365**, 684 (2019).
[2] D. Braithwaite *et al.*, Commun Phys **2**, 147 (2019).
[3] S.M. Thomas *et al.*, Sci. Adv. **6**, eabc 8709 (2020).
[4] W. Knafo *et al.*, arXiv:2311.05455 [cond-mat.str-el]
[5] R. Yamamoto *et al.*, to be submitted.

Abstract ID: 1171

MULTI-PHASE SUPERCONDUCTIVITY IN THE LOCALLY NON-CENTROSYMMETRIC $CeRh_2As_2$

K. Semeniuk[1*], M. Pfeiffer[2,1], J. Landaeta[2,1], R. Borth[1], M. Nicklas[1], C. Geibel[1], M. Brando[1], S. Khim[1], E. Hassinger[2,1]

[1]Max Planck Institute for Chemical Physics of Solids, 01187 Dresden, GERMANY
[2]Dresden University of Technology, Institute for Solid State and Materials Physics, 01062 Dresden, GERMANY
E-mail: konstantin.semeniuk@cpfs.mpg.de

The Kondo-lattice compound $CeRh_2As_2$ is an extremely rare unconventional superconductor. It displays a field-induced transition between two superconducting states, proposed to have the order parameters of the even and odd parity [1,2]. This unique transition is likely enabled by the exceptionally strong electronic correlations and the crystalline structure of the material — the globally centrosymmetric lattice contains two Ce sites located in locally non-centrosymmetric environments. In the absence of magnetic field, the superconductivity is preceded by another ordered state "Phase I" [3,4]. The microscopic nature of Phase I is currently unknown, with magnetic and quadrupolar orders proposed as candidates.

The nature of Phase I and its interplay with the superconductivity are important questions for validating the parity-switching interpretation. Here, we summarise results of the latest measurements of thermodynamic, magnetic, and charge transport properties of $CeRh_2As_2$, including studies under hydrostatic pressure. We find that the material is located close to a quantum critical point of Phase I, which is responsible for the remarkably strong correlations and drives the superconductivity. At the same time, the superconducting phase switching exists independently of Phase I, reinforcing the even-/odd-parity scenario.

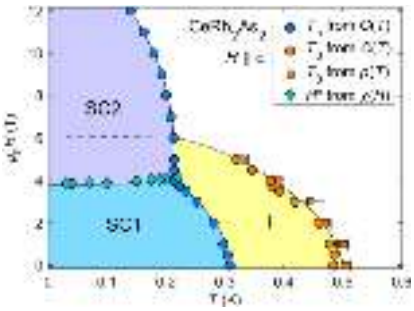

Fig. 1: *Phase diagram of $CeRh_2As_2$ against temperature (T) and c-axis magnetic field (H), according to measurements of heat capacity (C), resistivity (ϱ), and magnetic susceptibility (χ). The transition at $\mu_0H^*\approx4$ T separates the two superconducting phases SC1 and SC2. T_c and T_0 are the critical temperatures of the superconductivity and Phase I, respectively.*

References

[1] S. Khim, J. Landaeta *et al.*, Science, **373**, 1012–1016 (2021).
[2] J. Landaeta *et al.*, Phys. Rev .X, **12**, 031001 (2022).
[3] D. Hafner *et al.*, Phys. Rev. X, **12**, 011023 (2022).
[4] K. Semeniuk *et al.*, Phys. Rev. B, **107**, L220504 (2023).

Abstract ID: 1614

LOW-FIELD BARDEEN-COOPER-SCHRIEFFER STATE IN $CeRh_2As_2$ FROM LOCAL MAGNETIZATION

J. Juraszek[1], G. Chajewski[1], M. Konczykowski[2], D. Kaczorowski[1], D.F. Agterberg[3], T. Cichorek[1]

[1] *Institute of Low Temperature and Structure Research, Polish Academy of Sciences, 50-422 Wroclaw, POLAND*
[2] *LSI, École Polytechnique, CNRS, Institut Polytechnique de Paris, 91120 Palaiseau, FRANCE*
[3] *Department of Physics, University of Wisconsin–Milwaukee, Milwaukee, WI 53201, USA*
E-mail: t.cichorek@intibs.pl

The arguably most promising avenue for creating Majorana bound states relies on spin-triplet odd-parity superconductivity, yet this long-sought state of matter has remained elusive. The recently discovered superconductor $CeRh_2As_2$ with a critical temperature $T_c \approx 0.34$ K is thought to be the first and currently the only known material demonstrating a field-induced transition between spin-singlet even-parity and spin-triplet odd-parity superconducting states when subjected to a magnetic field of ≈ 3 T aligned parallel to the *c*-axis of its tetragonal crystal structure [1]. Under ambient pressure and in zero field, this heavy-fermion compound also undergoes a phase transition of an unknown origin at $T_0 \approx 0.5$ K and exhibits signs of -antiferromagnetism below 0.25 K [2]. Here, we examine a low-field even-parity state of $CeRh_2As_2$ using micro-Hall-probe magnetometry for local magnetization measurements down to $0.02T_c$. We observe a relatively small anisotropy of the lower critical field, the temperature dependencies of which for both crystallographic directions display a single-band isotropic *s*-wave behavior predicted by the Bardeen-Cooper-Schrieffer theory. Furthermore, we observe a small but distinct increase in *a*-axis magnetization starting around T_0, although attempts to detect a magnetic signal along the *c*-axis have been unsuccessful. Our findings impose important constraints on the superconducting and normal-state order parameters of $CeRh_2As_2$.

This work was supported by the Polish National Science Centre NCN (Project OPUS23 No. 2022/45/B/ST3/04117).

References

[1] S. Khim *et al.*, *Field-induced transition within the superconducting state of $CeRh_2As_2$*, Science **373**, 1012 (2021).
[2] M. Kibune *et al.*, *Observation of antiferromagnetic order as odd-parity multipoles inside the superconducting phase in $CeRh_2As_2$*, Phys. Rev. Lett. **128**, 057002 (2022).

Superconductivity and Magnetism in Heavy Fermion Systems II

29.04.2024 MONDAY

Abstract ID: 1186

THE FERMI SURFACE OF UTe_2

A.G. Eaton

Cavendish Laboratory, Department of Physics, University of Cambridge, UK
E-mail: age28@cam.ac.uk

The formulation of accurate microscopic models to explain unconventional superconductivity in a given material is strongly contingent on having an accurate understanding of that material's Fermi surface. This talk will review our recent high magnetic field quantum oscillation studies [1,2] of the spin-triplet superconductor candidate UTe_2. Our measurements reveal a remarkably simple Fermi surface, unlike the case of numerous other heavy fermion systems, which increases the likelihood of accurate microscopic models to soon be attained.

References

[1] A.G. Eaton *et al.*, Nature Communications **15**, 223 (2024).
[2] T.I. Weinberger *et al.*, arXiv:2307.00568 (2023).

Abstract ID: 1216

PROBING THE UNUSUAL SUPERCONDUCTIVITY OF UTe_2 WITH HIGH PRESSURE

D. Braithwaite

Univ. Grenoble Alpes, Grenoble INP, CEA, IRIG-PHELIQS, F-38000 Grenoble FRANCE
E-mail: daniel.braithwaite@cea.fr

The unconventional superconductivity in the strongly correlated system UTe_2 displays a plethora of fascinating properties [1,2]. Its behaviour in magnetic field is striking, as the upper critical field, H_{C2}, reaches values over 60T, of the same order of magnitude as the high-T_c superconductors, whereas the superconducting critical temperature of UTe_2 is only 2 K. Moreover, the extremely anisotropic and unusual shape of H_{C2} reveals unique features: re-entrant superconductivity in high field [3], a reinforcement of the superconducting pairing strength with field [4], and a field induced change of the superconducting order parameter, and possibly even of the underlying mechanism for superconductivity [5]. However, the microscopic mechanisms leading to these phenomena are not yet known.

As in many strongly correlated electron systems, high pressure is an extremely effective parameter in UTe_2 to tune the microscopic interactions, significantly modifying the macroscopic properties. This brings insight into understanding the striking phenomena described above as well as leading to new discoveries in this material.

I will introduce the experimental techniques used in the CEA Grenoble for studies under pressure. Then I will present our results on UTe_2 under high pressure using various experimental techniques showing that pressure significantly enhances superconductivity, and even more interestingly, induces a transition between two superconducting order parameters [6]. Then I will give a brief overview of the present understanding of UTe_2 under pressure, including our more recent measurements under pressure and pulsed magnetic fields up to 60 T [7]. These new elements improve our understanding of the interplay between magnetism and superconductivity in this remarkable system.

References

[1] S. Ran *et al.*, Science **365**, 684 (2019).
[2] D. Aoki *et al.*, Journal of the Physical Society of Japan **88**, 043702 (2019).
[3] S. Ran *et al.*, Nat Phys **15**, 1250 (2019).
[4] G. Knebel *et al.*, Journal of the Physical Society of Japan **88**, 063707 (2019).
[5] A. Rosuel *et al.*, 2022), p. arXiv:2205.04524.
[6] D. Braithwaite *et al.*, Communications Physics **2**, 147 (2019).
[7] M. Vališka *et al.*, Physical Review B **104**, 214507 (2021).

Abstract ID: 1117

THE MICROWAVE ELECTRODYNAMICS OF UTe_2

Arthur Carlton-Jones, Yun-Suk Eo, Ian Hayes, Shanta Saha, Nicholas P. Butch, Johnpierre Paglione, Steven M. Anlage

[1]*Quantum Materials Center, Physics Department, University of Maryland, College Park, MD 20742-4111, USA*
E-mail: anlage@umd.edu

The complex surface impedance of a superconductor provides many insights into its properties, such as the pairing mechanism, super- and normal-fluid responses, Fermi surface, and possibly it's topological properties. We explore the surface impedance of UTe_2 single crystals as a function of temperature using resonant cavity measurements for a variety of microwave-frequency modes. The UTe_2 crystals studied are from both older, [1] and newer generations, [2] with the latter showing higher transition temperatures. We determine a composite surface impedance for each mode using resonance data combined with the independently measured normal state dc resistivity tensor (see Fig. 1). We are able to determine the combination of crystallographic directions excited in each mode using the anisotropy of the resistivity. Studying several modes yields the surface impedance corresponding to each axis. We find a power-law temperature dependence for the magnetic penetration depth at low temperatures in both the a- and c-directions, which may arise from point nodes on the Fermi surface. We find the zero-temperature penetration depth to be largest for the c-direction, which is consistent with current understanding of the Fermi surface shape. The surface resistance demonstrates a relatively large residual loss at zero temperature, and the c-direction is the most lossy. We compare to theoretical expectations of the electrodynamic properties of topological superconductors.

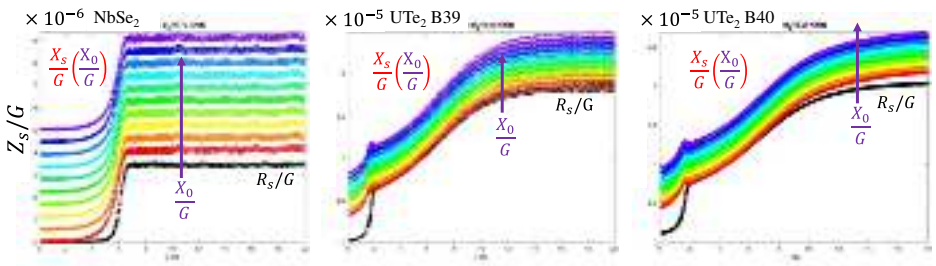

Fig. 1: *Plots of microwave $R_s(T)/G$ (black) and $X_s(T)/G$ (colors), where G is the geometrical factor of the sample/resonator, for $NbSe_2$ and two UTe_2 samples. The value of X_0/G is varied systematically in each plot. The UTe_2 samples show strong normal-state surface impedance temperature dependence.*

This work is supported by NSF DMR-2004386.

References

[1] S. Bae, H. Kim, S. Ran, Y.S. Eo, I-Lin Liu, W. Fuhrman, J. Paglione, N.P. Butch, S.M. Anlage, *Anomalous normal fluid response in a chiral superconductor*, Nature Communications **12**:2644 (2021).

[2] Yun Suk Eo, Shouzheng Liu, Shanta R. Saha, Hyunsoo Kim, Sheng Ran, Jarryd A. Horn, Halyna Hodovanets, John Collini, Tristin Metz, Wesley T. Fuhrman, Andriy H. Nevidomskyy, Jonathan D. Denlinger, Nicholas P. Butch, Michael S. Fuhrer, L. Andrew Wray, Johnpierre Paglione, *c-axis transport in UTe_2: Evidence of three-dimensional conductivity component*, Phys Rev B **106 (6)**, L060505 (2022).

Abstract ID: 1391

SUPERCONDUCTIVITY-INDUCED IMPROPER ORDERS IN NONSYMMORPHIC SYSTEMS

Andras Szabo[1], Aline Ramires[2]

[1]*Institute for Theoretical Physics, ETH Zurich, 8093 Zurich, SWITZERLAND*
[2]*Paul Scherrer Institute, 5232 Villigen PSI, SWITZERLAND*
E-mail: aszabo@phys.ethz.ch

Improper phases are characterized by a secondary order parameter setting in as a direct consequence of a primary order. For example, in the context of multiferroics, improper ferroelectrics develop electric polarization controlled by a primary magnetic or distortive order parameter. In this work, I highlight an overlooked mechanism that couples superconductivity to orders in the charge or spin sectors, such that the latter emerge as improper orders, and highlight the crucial role of nonsymmorphic symmetries therein. In particular, a bilinear in the superconducting order parameter can couple linearly to orders that are odd under inversion symmetry in centrosymmetric systems. To elucidate these observations, I use the notion of an extended symmetry group, which I analyze in real space. These findings may explain some of the unusual observations with respect to the interplay of superconductivity and magnetism in the recently discovered multiphase heavy-fermion superconductor, $CeRh_2As_2$.

References

[1] A. Szabo, A. Ramires, e-print arXiv:2309.05664 (2023).

Superconductivity and Magnetism in Heavy Fermion Systems III

29.04.2024 MONDAY

Abstract ID: 1545

CORRELATION-DRIVEN TOPOLOGICAL SEMIMETALS

Diego A. Zocco

Institute of Solid State Physics, Vienna University of Technology, 1040 Vienna, AUSTRIA
E-mail: zocco@ifp.tuwien.ac.at

The Weyl-Kondo semimetal (WKSM) state has recently been established experimentally and theoretically [1-3], and evidenced in the heavy fermion compound $Ce_3Bi_4Pd_3$ [1,3]. In this state, transport and thermodynamic signatures of topology are strongly amplified, due to the flat dispersion inherent to heavy fermion materials and the pinning of Weyl nodes to the Fermi energy. Heavy fermion compounds are well known for their sensitivity to external control parameters such as magnetic field and pressure, providing exceptional playgrounds for testing the tunability and control of–a priori robust–topological phases. In this talk, I will present two such cases. In $Ce_3Bi_4Pd_3$ we found that the application of relatively modest magnetic fields suppresses the topological signatures; we attribute this effect to the annihilation of Weyl nodes at a topological quantum phase transition [4]. $CeRu_4Sn_6$ has been suggested to be another topological semimetal [5,6]. Interestingly, inelastic neutron scattering experiments revealed that the material is quantum critical without tuning [7]. Our pressure- and magnetic field-tuning investigations reveal a dome-shaped WKSM phase, suggesting that this phase is stabilized by the quantum critical fluctuations [8].

The work in Vienna was supported by the Austrian Science Fund (FWF projects I4047, SFB F86 "Q-M&S", and I5868-N/FOR 5249 "QUAST"), the European Microkelvin Platform (H2020 project 824109 "EMP"), and the European Research Council (ERC Advanced Grant 101055088 "CorMeTop").

References

[1] S. Dzsaber *et al.*, Phys. Rev. Lett. **118**, 246601 (2017).
[2] H.-H. Lai *et al.*, Proc. Natl. Acad. Sci. U.S.A. **115**, 93 (2018).
[3] S. Dzsaber *et al.*, Proc. Natl. Acad. Sci. U.S.A. **118**, e2013386118 (2021).
[4] S. Dzsaber *et al.*, Nat. Commun. **13**, 5729 (2022).
[5] M. Sundermann *et al.*, Sci Rep **5**, 17937 (2016).
[6] Y. Xu *et al.*, Phys. Rev. X **7**, 011027 (2017).
[7] W.T. Fuhrman *et al.*, Sci. Adv. **7**, eabf9134 (2021).
[8] D.M. Kirschbaum *et al.*, in preparation

Abstract ID: 1244

COEXISTENCE OF SUPERCONDUCTIVITY AND FERROMAGNETISM IN HIGH-ENTROPY CARBIDES

Huchen Shu[1], Wei Zhong[1], Fang Hong[2,3,4], Binbin Yue[1]

[1] *Center for High Pressure Science & Technology Advanced Research, 10 East Xibeiwang Road, Haidian, 100193, Beijing, CHINA*
[2] *Beijing National Laboratory for Condensed Matter Physics, Institute of Physics, Chinese Academy of Sciences, 100190, Beijing, CHINA*
[3] *School of Physical Sciences, University of Chinese Academy of Sciences, 100190, Beijing, CHINA*
[4] *Songshan Lake Materials Laboratory, Dongguan, 523808, Guangdong, CHINA*
E-mail: yuebb@hpstar.ac.cn

Generally, superconductivity (SC) is expected to be absent in magnetic systems. However, this assumption was disturbed by unconventional superconductors, such as cuprates, iron-based superconductors, and the recently-discovered nickelate, since their superconductivity is proposed to be related to the electron-electron interaction mediated by the spin fluctuation. The study of the correlation between SC and magnetism (mostly antiferromagnetism) has been an important topic in understanding the SC mechanism. However, the coexistence of superconductivity and ferromagnetism (FM) is still rare in both conventional and unconventional superconductors. In this work, we report the coexistence of these two quantum orderings in high-entropy carbide ceramics $(Mo_{0.2}Nb_{0.2}Ta_{0.2}V_{0.2}W_{0.2})C_{0.9}$ (Mo-HEC), $(Ta_{0.25}Ti_{0.25}Nb_{0.25}Zr_{0.25})C$ (Ta-HEC), and they are expected to be conventional superconductors. A clear magnetic hysteresis loop was observed in these high-entropy carbides, indicating a ferromagnetic (FM) ground state, with such an FM ordering even existing at room temperature. A sharp superconducting transition is observed in Mo-HEC with a T_c of 3.4 K and an upper critical field of ~3.35 T. Meanwhile, superconductivity is suppressed to some extent, and the zero-resistance state disappears in Ta-HEC, in which stronger ferromagnetism is presented. The upper critical field of Ta-HEC is only ~1.5 T, though they show a higher transition temperature near 5.7 K. The ferromagnetism stems from the carbon vacancies that often occur during the high-temperature synthesis. The observation of superconductivity in high-entropy carbide ceramics provides an alternative exotic platform to study the correlation between superconductivity and magnetism, significantly benefitting the design of multifunctional electronic devices.

Novel Phases in Strongly Correlated Electron Systems

29.04.2024 MONDAY

Abstract ID: 1352

FATE OF DENSITY WAVES IN THE PRESENCE OF A HIGHER-ORDER VAN HOVE SINGULARITY

D.V. Efremov[1], A. Zervou[2], J. Betouras[3]

[1]IFW Dresden, Hemholzstr 20, 01069 Dresden, GERMANY
[2]Department of Physics and Centre for the Science of Materials, Loughborough University, Loughborough LE11 3TU, UK
E-mail: d.efremov@ifw-dresden.de

Many phases arise in close proximity to each other through the interplay of spin and charge degrees of freedom. The best-known example is superconductivity, which occurs in close proximity to magnetic or charge-density wave phases in high-temperature superconductors and dichalcogenides. In this talk, we address the competition of spin and charge degrees of freedom leading to spin-density wave phases, charge-density wave phases, and topological phases. We come to the possibility of increasing the critical temperature by increasing the density of states. A well-known example is van Hove singularities, where the Fermi surface undergoes a topological transition. Higher order singularities, where several disconnected pockets of the Fermi surface touch simultaneously, can naturally occur at high symmetry points in the Brillouin. Such multicritical singularities can lead to stronger divergences in the density of states than canonical van Hove singularities. As a concrete example of the high order topological transitions at the Fermi surface, we show how they can be used in the analysis of experimental data on $Sr_3Ru_2O_7$ [1,2]. Understanding the mechanisms involved opens new root in the development of materials for complex quantum phases.

References

[1] D.V. Efremov, A. Shtyk, A.W. Rost, C. Chamon, A.P. Mackenzie, J.J. Betouras, Phys. Rev. Lett. **123**, 207202 (2019).
[2] A. Zervou, D.V. Efremov, J.J. Betouras, Phys. Rev. Research **5**, L042006 (2023).

Abstract ID: 256

RESOLVING LENGTH SCALE DEPENDENT TRANSIENT DISORDER THROUGH AN ULTRAFAST TRANSITION

Emil Bozin

Condensed Matter Physics and Materials Science Division,
Brookhaven National Laboratory, Upton, New York 11973, UNITED STATES OF AMERICA
E-mail: emil.bozin@gmail.com

The development of materials with specialized and highly efficient properties increasingly relies on complex local structures that stray from the ideal of a perfect crystal. Advancements in electronics technology drive a need for materials that switch between distinct states: either electrical (e.g., memristors, ferroelectrics), magnetic (e.g., ferromagnets, antiferromagnets) or structural (e.g., charge density wave states). A key example is the metal-insulator transition. It is well established that local structure plays a central role in many equilibrium phase transitions driven by the competition of energy and entropy. Some non-equilibrium phase transitions can be triggered on demand using ultrafast laser pulses. Local structure has also been implicated in these transitions, but this is less understood due to a lack of appropriate means to quantify length scale dependent local disorder in these ultra-fast transient states.

The pair distribution function method has propelled structural studies beyond idealized crystal models, enabling atomic structure studies of quantum materials over varying length scales. It has indeed been instrumental in revealing concealed from detection nanoscale behaviors that have been increasingly frequently critical for comprehensive understanding of establishment of quantum phases. Applying this method with ultrafast time resolution has the potential to similarly disrupt the study of structural dynamics and phase transitions. Here, we demonstrate such a measurement of $CuIr_2S_4$, an archetypal spin singlet dimer system, optically pumped from its low temperature Ir-dimerized phase. Dimers are optically removed without spatial correlation, generating a structure whose level of disorder depends strongly on length scale. The re-development of structural ordering over tens of picoseconds is directly tracked over both space and time as a transient state is approached. This measurement demonstrates both the crucial role of local structure and disorder in non-equilibrium processes and the feasibility of accessing this information in quantum materials with state-of-the-art XFEL facilities [1].

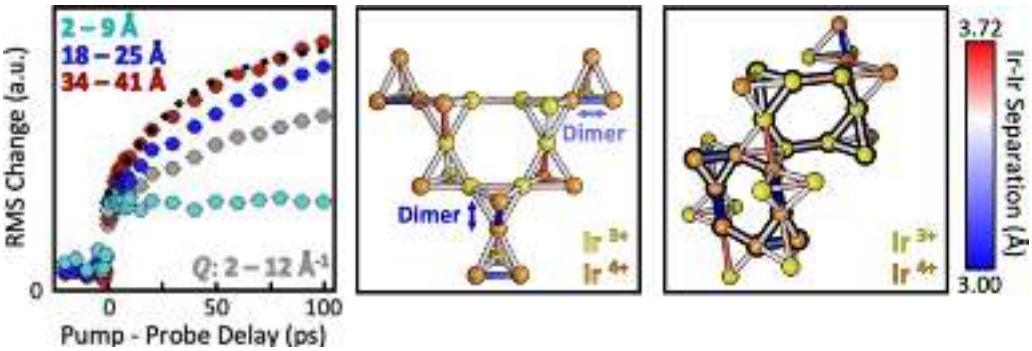

Fig. 1: *Length-scale dependent transient response in a non-equilibrium state of $CuIr_2S_4$ dimer system.*

References

[1] J. Griffiths, A. Suzana, L. Wu, S. Marks, V. Esposito, S. Boutet, P. Evans, J.F. Mitchell, M. Dean, D. Keen, I. Robinson, S. Billinge, E. Bozin, e-print arXiv: 2310.03857 2024).

Abstract ID: 1082

ELECTRONIC BAND STRUCTURE, PECULIARITIES IN THE CHARGE DENSITY DISTRIBUTION, MAGNETIC AND MAGNETOELECTRIC PROPERTIES OF La_2CuO_4

V.G. Orlov, G.S. Sergeev

National Research Centre "Kurchatov Institute", 123182, Moscow, RUSSIA
E-mail: valeryorlov3@gmail.com

Calculations of the electronic band structure of the orthorhombic phase of La_2CuO_4, which is a parent compound for a number of high T_c superconducting (HTSC) families, were performed within the framework of the Density Functional Theory using WIEN2k computer program [1]. The exchange potential of Becke and Johnson modified by Tran and Blaha [2] and the electron-electron correlations in the local density approximation were used as the exchange-correlation functional. Spin-polarized calculations revealed the semiconducting antiferromagnetic ground state of the orthorhombic La_2CuO_4 with the band gap E_g=2 eV and the magnetic moment of copper atoms M_{Cu}=0.725 μ_B [3] without requiring additional parameters such as Hubbard's U describing strong correlations of Cu d-electrons. Calculated features of the electronic band structure, as well as optical properties of the orthorhombic La_2CuO_4 [3] were in agreement with the experimental data. The calculated charge density distribution in the orthorhombic La_2CuO_4 was analyzed with the aim to find saddle critical points of the bond type (Bond Critical Points (BCPs)). Parameters of the BCPs allow the classification of the types of chemical bonding in crystals [4]. Based on performed analysis a conclusion on the absence of covalent bonding in La_2CuO_4 was made [3]. In agreement with our previous studies of the charge density distribution peculiarities in HTSC [5], a hypothesis was proposed about the presence in the orthorhombic La_2CuO_4 of a specific mechanism of the chemical bonding characterized by charge density fluctuations. It should also be noted that we revealed [5] the correlation between the value of the Laplacian of the charge density ϱ_b in the BCP with the largest value of ϱ_b and the critical temperature T_c of the HTSC. On the base of this correlation we were able [6] to predict T_c of about 150-160 K for the supposed by Korean scientists superconductor $Pb_9Cu(PO_4)_6O$, which is lower than the room temperature, but is also of great interest.

There are two magnetic classes – $D_{2h}(D_2)$ and $D_{2h}(C_{2v})$ that imply the existence of the linear magnetoelectric effect (LMEE) in the orthorhombic La_2CuO_4, the symmetry of which is described by the space group *Cmce* (D_{2h}^{18}). The relationship between the appearance of superconductivity in a crystal and such properties as fluctuation character of chemical bonding and LMEE is discussed in this work.

References

[1] P. Blaha, K. Schwarz, G.K.H. Madsen, D. Kvasnicka, J. Luitz, R. Laskowski, F. Tran, L.D. Marks, *WIEN2k, An Augmented Plane Wave + Local Orbitals Program for Calculating Crystal Properties* (Karlheinz Schwarz, Vienna University of Technology, Austria, 2021). ISBN 3-9501031-1-2.
[2] F. Tran, P. Blaha, Phys. Rev. Lett. **102**, 226401 (2009).
[3] V.G. Orlov, G.S. Sergeev, Journal of Experimental and Theoretical Physics, **137**, 95 (2023).
[4] R.F.W. Bader, *Atoms in Molecules: A Quantum Theory. International Series of Monographs on Chemistry 22* (Oxford Science Publications, Oxford 1990).
[5] V.G. Orlov, G.S. Sergeev, Physica B **536**, 839 (2018).
[6] V.G. Orlov, G.S. Sergeev, AIP Advances **13**, 115006 (2023).

Abstract ID: 229

QUANTUM PHENOMENA IN Si:Sb NEAR THE METAL-INSULATOR TRANSITION

S.L. Prischepa[1,2], A.L. Danilyuk[1], A.G. Trafimenko[1], A.A. Nazarenka[1]

[1]*Belarusian State University of Informatics and Radioelectronics, 220013, Minsk, BELARUS*
[2]*National Research Nuclear University MEPhI, 115409, Moscow, RUSSIA*
E-mail: prischepa@bsuir.by

We report the quantum phenomenon in antimony-doped silicon (Si:Sb) with a concentration of 10^{18} cm^{-3} (dielectric side of the metal/insulator transition). A study of the Hall effect in the temperature range T = 2-300 K in a magnetic field up to H = 80 K showed that at T > 100 K, a normal Hall effect is observed. At 28 K < T < 90 K, it is modified and an activation mechanism with an energy of 1.7 meV is added to the band mechanism. In the region of 5 K < T < 25 K, the Hall voltage is influenced by both band and activation mechanisms, as well as hopping conductivity. This causes the appearance of significant fluctuations in the dependence of the Hall voltage on the magnetic field $V_H(H)$. In this case, the linear dependence of $V_H(H)$ is still manifested. Below 5 K, the growth of $V_H(H)$ vanishes, i.e., the band mechanism ceases to contribute. The Hall voltage $V_H(H)$ fluctuates relative to zero $V_H(H) = 0$, its value is determined by the influence of the magnetic field on hopping and simple activation electron transfer. The latter manifests itself at T < 4 K [1]. At 3 K, the quantum Hall effect (QHE) begins to manifest itself, as evidenced by the sublinear dependence of $V_H(H)$ and signs of the appearance of a plateau on it. At T = 2 K, a pronounced plateau appears on $V_H(H)$, which indicates a significant manifestation of QHE. This dependence is also characterized by a change in the Hall voltage sign in the region of H = 50-60 kOe. Such a set of effects indicates the presence, firstly, of an electronic system with non-trivial properties, and secondly, of a change in the mechanisms of influence of the magnetic field on such an electronic system. As shown in our works [1-3] the electronic system in Si:Sb is unstable and highly correlated, characterized by activation transport in the 2-4 K region and hopping in the 5-20 K region.

The transport properties of the Si:Sb system have been studied in the temperature range 2-4 K and the regularities of the behavior of the electron correlated system of the upper Hubbard band (UHB), which occurs when nonequilibrium injected electrons are localized on impurity atoms of antimony (D^- states) [1,2]. It is shown that in the region of relatively low currents (~0.005 A/cm^2), an electron correlated system characterized by the relation between the Coulomb energy repulsion U and band width W, U/W ~ 4, is similar to a Mott insulator. It destroys with an increase in current density (an increase in the concentration of conduction electrons) and turns into a system of band electrons (loses the properties of a correlated system). Electronic transport is characterized by a crossover of the temperature coefficient of resistance, the presence of Coulomb repulsion, delocalization of the D^- states of the UHB with an increase in the concentration of electrons in the conduction band. All these phenomena point to nontrivial mechanisms of quantum transport of charge carriers, which we explain by spin-dependent processes of electron localization on neutral antimony impurities (formation of UHB) and transport along it, transitions between UHB states and the conduction band, polarization and relaxation of the spins of unpaired electrons of neutral antimony atoms (including on the spins of ^{121}Sb nuclei (spin 5/2), ^{123}Sb (spin 7/2) and the evolution of singlet D^- states in a magnetic field.

References

[1] A.L. Danilyuk *et al.*, Appl. Phys. Lett. **109**, 222104 (2016).
[2] A.L. Danilyuk *et al.*, J. Phys.: Condens. Matter. **32**, 225702 (2020).
[3] A.L. Danilyuk *et al.*, Adv. Condens. Matter Phys. **2017,** 5038462 (2017).

CANCELLED

Advanced REBCO-Based Coated Conductors for Large-Scale HTS Applications I

29.04.2024 MONDAY

Abstract ID: 1584

REQUIREMENTS OF REBCO COATED CONDUCTORS FOR USE IN COMPACT FUSION MAGNETS

Ashleigh Francis, J.L. Cheng, Brandon Sorbom

Commonwealth Fusion Systems, 01434, Devens, MA, USA
E-mail: afrancis@cfs.energy

Commonwealth Fusion Systems (CFS) is building the world's first compact net energy fusion device using magnetic confinement, the SPARC tokamak, made possible by utilizing the recent advances in the commercial production of 2G REBCO coated conductors. The SPARC tokamak comprises three high field magnet systems: the poloidal field coils, the central solenoid, and 18 non-insulated toroidal field magnets designed to operate in the 20K, 20T range, requiring 10,000 kms of 4mm wide tape. The design, safe operation, and quench protection of high field fusion magnets requires the detailed characterization of the field (B), angle (Θ), and temperature (T) dependence of the critical current (Ic) of these tapes at the operational range for each magnet system. Additionally the REBCO conductors must be able to withstand the large stresses and strains required for operation and quench in the challenging conditions SPARC will see, adding additional specifications for the conductors to meet and retain their performance. The impact of the manufacturing processes the conductors are subjected to must also be well understood and designed for. This talk will summarize the present and future requirements needed for REBCO coated conductors to make use of them in high field fusion magnets and present on the methods for characterizing the conductor performance along with the results of large magnet tests at CFS.

Abstract ID: 1566

PROGRESS IN REDUCING THE COST OF 2G HTS TAPE MANUFACTURED IN LARGE VOLUME

A. Molodyk, S. Lee. V. Petrykin. S. Samoilenkov

Faraday Factory Japan, 192-0032, Tokyo, JAPAN
E-mail: a.molodyk@faradaygroup.com

In the recent years, Faraday Factory Japan (FFJ) has become the world leading manufacturer of 2G HTS tape. In this talk we analyse the factors that contribute to FFJ success.

The HTS layer formulation based on YBCO with Y_2O_3 nanoparticles demonstrates excellent superconducting performance at low temperature in high magnetic field, making FFJ HTS tape a competitive product for building high-field magnets, in particular, for compact fusion. In addition to that, the YBCO-Y_2O_3 formulation has proven itself very robust and amenable to fast manufacturing scale-up, allowing to maintain the high performance and yield when annual production volume was increased more than 20 times in just 4 years.

Over more than a decade on the 2G HTS tape market, the selling price of FFJ HTS tape halved with each ten-fold increase of production and sales (Fig. 1). This has been possible thanks to the approach we take to scale-up. When increasing the production volume, we improve all three elements that determine the capacity of a manufacturing line: (1) throughput (tape line speed), (2) process up-time, and (3) manufacturing yield. This has been an ongoing effort at FFJ that secures the continuous reduction of production cost with scale-up, as opposed to the alternative approach of merely multiplying identical production units that has a limited potential to cost reduction.

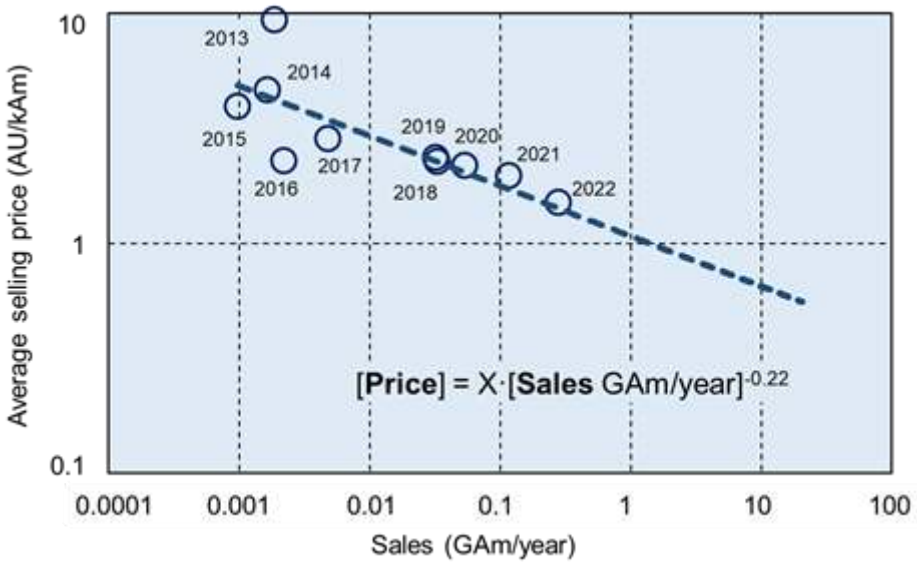

Fig. 1: *Actual selling price learning curve of Faraday Factory Japan. Prices are shown in arbitrary units. Price goes down approximately 2 times when sales grow 10 times.*

Abstract ID: 1428

RECENT EFFORT AND DISCUSSION AT SHANGHAI SUPERCONDUCTOR TECHNOLOGY FOR HTS FUSION APPLICATION

Y. Yamada[1,2], J-M Zhu [1], B. Song[1]

[1] *Shanghai Superconductor Technology Co., Ltd, Shanghai, CHINA*
[2] *Chubu University, Thin Film R&D Center, Kasugai, JAPAN*
E-mail: yutakayamada@isc.chubu.ac.jp

Recent progress of the mass production of HTS-CC (Coated Conductor) and the application for compact fusion attract much interest in HTS community. In this presentation, I first summarize the recent effort at Shanghai Superconductor Technology for the low-cost and mass production especially as well as I_c and J_c properties. In the latter half of this talk, I will especially introduce R&D discussion aiming for compact fusion applications: such as, high I_c, mechanical property problems and cost or price issues applicable for the competitive level as an alternative electric power source of the compact fusion base on the data of low temperature fusion data of JT60SA or ITER.

Fig. 1: *Annual Production Plan of Shanghai Superconductor Technology for 12mm wide REBCO Tape*

Advanced REBCO-Based Coated Conductors for Large-Scale HTS Applications II

29.04.2024 MONDAY

Abstract ID: 1569

HOMOGENEOUS AND PRODUCTIVE BMO-DOPED REBCO COATED CONDUCTOR DEVELOPED BY HOT-WALL PLD ON IBAD TEMPLATED SUBSTRATE

Y. Iijima, M. Ohsugi, K. Kakimoto, S. Muto, S. Fujita, W. Hirata, N. Nakamura, M. Daibo

Fujikura Ltd., 1440, Mutsuzaki, Sakura-shi, Chiba, 285-8550, JAPAN
E-mail: yasuhiro.iijima@jp.fujikura.com

REBCO coated conductors have successfully been developing as the unique practical wires available especially for emerging applications used in extremely high field and strong hoop stress as high-end NMR systems or "compact" nuclear fusion reactors, etc., which could not be reached by LTS wires as Nb_3Sn. The combined process of ion-beam-assisted deposition (IBAD) and pulsed-laser-deposition (PLD) can form wires that have excellent and uniform in-field J_c properties with robust mechanical strain strength, in long piece length with business scale productivity, though it is the oldest approach to manufacture coated conductors [1].

PLD is a non-equilibrium vapor process characterized to be much supersaturated high-rate growth, come from fine, rapid and activated evaporation by ultraviolet pulse laser [2]. It allows to control high density dislocations and small-size secondary phase particles, dispersed inside uniformly textured REBCO films growing at extremely high rates [3]. Thus, PLD could form REBCO wires with both homogenous high in-field J_c and high production throughput, which could derive affordable manufacturing cost despite the operation of high-powered UV laser.

These PLD advantages should be facilitated if the most severe parameter of substrate temperature were enough controlled during long length contentious depositions. We had designed and developed "Hot-Wall Type" reel-to-reel PLD apparatuses, which realized quite robust and reproducible temperature uniformity by furnace like heating system [4]. As a result, we succeeded in commercialization of long length and uniform REBCO wires including scattered short length $BaHfO_3$ nano-rods, which have less angular dependent, but higher J_c compared to non-doped samples, which also had a random pinning like scaling behaviour observed in wide temperature range [5]. Almost no dependence on growth rate was observed of I_c /I_{c0} properties for high in-field I_c at 20 K 20 T, as far as using industrial UV laser currently available. We are now investing toward cost reduction and increase of production capacity, with non-spoiled uniformity for long piece length, up to 1.4 km long currently obtained for 4 mm wide tape. Transport tests of 16-layered pancake coils have conducted to assess the longitudinal uniformity of in-field J_c for $BaHfO_3$ doped REBCO wires [6].

A part of this work is based on results from a project subsidized by the New Energy and Industrial Technology Development Organization (NEDO), and results performed at the High Field Laboratory for Superconducting Materials, IMR, Tohoku University.

References

[1] Y. Iijima, K. Matsumoto, Supercond. Sci. Tech. **13**, 68-81 (2000).
[2] J.G. Ulbrandt, *et al.*, Phys. Rev. B **101**, 241406 (2020).
[3] J.L. MacManus-Driscoll, S.C. Wimbush, Nature Reviews Materials **6**, 587–604 (2021).
[4] Y. Iijima, *et al.*, IEEE Trans. Appl. Supercond., **25**, 6604104 (2015).
[5] S. Fujita, *et al.*, IEEE Trans. Appl. Supercond., **29**, 8001505 (2019).
[6] S. Muto, *et al.*, IEEE Trans. Appl. Supercond, in press.

Abstract ID: 1515

DEVELOPMENT AND SCALE UP OF HIGH-PERFORMANCE REBCO TAPES AND ROUND WIRES

Venkat Selvamanickam[1,2]

[1]*Department of Mechanical Engineering, Advanced Manufacturing Institute, Texas Center for Superconductivity, University of Houston, Houston, Texas, USA*
[2]*AMPeers LLC, Houston, Texas, USA*
E-mail: selva@uh.edu

Since the first pilot-scale manufacturing of REBCO tapes in 2006 [1] and demonstration of first in-grid demonstration of REBCO device in 2007 [2], significant progress has transpired for implementation of REBCO conductors in many applications. Challenges still remain for widespread use of REBCO conductors: cost, availability, robustness, and application-specific formats. We have been developing advanced REBCO conductors to address these challenges, with very high critical currents especially in high magnetic fields, deposition process for high efficiency use of precursors, double-sided tapes, high-strength tapes, and round REBCO wires with excellent flexibility. Fabrication processes for these advanced REBCO tapes and round wires have been scaled up to 50 meters. Prototype devices are being fabricated with these longer conductors. The recent advances in the development of scale of our high-performance REBCO tapes and round wires will be presented.

This work was supported by awards from the U.S. Department of Energy and the U.S. Navy.

References

[1] V. Selvamanickam *et al.*, IEEE Trans. Appl. Supercond. **17,** 3231 (2007).
[2] V. Selvamanickam *et al.*, IEEE Trans. Appl. Supercond. **19,** 3225 (2009).

Abstract ID: 1599

COATED CONDUCTOR PRODUCTION AT SuNAM VIA PLD AND REACTIVE CO-EVAPORATION FOR LARGE SCALE APPLICATIONS

Hunju Lee

SuNAM Co., Ltd., 52 Seungryanggil, Wongok, Anseong, Gyeonggi, SOUTH KOREA
E-mail: hlee@i-sunam.com

SuNAM has been providing Coated Conductors (CC) for various applications, including grid uses, through the Reactive Co-evaporation-Deposition and Reaction (RCE-DR) method. This includes the first commercial cable commissioned in Korea and several Fault Current Limiters (FCL). To meet the demands of grid applications, we installed a new RCE system with higher power and improved stability.

However, fusion and other high field devices require more CCs than grid applications. We have had limited success in producing CCs for these applications using the RCE system, which is only effective in the mid-field range up to 5-6 Tesla. Therefore, we set up a PLD system to incorporate pinning. The characteristics of the CCs obtained from the PLD system are presented. Microstructures, transport properties, and electromechanical characteristics of CCs from both PLD and RCE-DR systems are compared in this study. The deposition of a thick layer of GdBCO(YBCO) via RCE upon a thin YBCO(GdBCO) layer by PLD resulted in the rearrangement of Re2O3 particles. The implications of this behavior on the possible control of pinning and throughput enhancement will also be discussed.

Part of this work was supported by the National Research Foundation of Korea (NRF) grant funded by the Korea government (MSIT) (No. 2022M3I9A1076681).

Advanced REBCO-Based Coated Conductors for Large-Scale HTS Applications III

29.04.2024 MONDAY

Abstract ID: 1538

AMSC's 2G HTS WIRE MANUFACTURING

D. McGahn

AMSC, USA
E-mail: noel.martin@amsc.com

AMSC has been manufacturing its Amperium® 2G HTS wire in long lengths and large scale for well over a decade. AMSC's factory has the capacity to support known commercial applications at the wire performance levels required by the end users. AMSC's end of the line lamination process is configurable, resulting in stable, robust wire properties that are tailored to the end product requirements. AMSC's Amperium® wire has proven itself in the most demanding commercial applications including the Electric Utility Grid, and US Navy Warships. The status of AMSC's wire manufacturing facility and its focus for the future will be discussed.

CANCELLED

Abstract ID: 1613

ARPA-E INVESTMENT IN DOMESTIC MANUFACTURING OF HIGH TEMPERATURE SUPERCONDUCTING TAPES

Laurent Pilon

Advanced Research Project Agency – Energy, 950 L'Enfant Plaza, Washington, DC, USA
E-mail: laurent.pilon@hq.doe.gov

This talk will discuss the recent investment of the Advanced Research Project Agency – Energy (ARPA-E) to support the development of advanced manufacturing methods to produce high-temperature superconducting (HTS) tapes in the United States. While there are many areas of improvement and investigation associated with HTS tapes that may be inextricably related, the primary focus of ARPA-E's investment is on novel fabrication methods of HTS tapes that can concurrently (i) increase the continuous tape length, (ii) reduce the electrical variation along the tape or wire, and (iii) increase the overall production rate while (iv) significantly reducing the production costs, and (v) maintaining a high level of tape performance characterized by its critical current per unit width and its engineering current density. Enabling widely available long, high quality, and low-cost high-temperature superconducting (HTS) tapes could facilitate the development of energy technologies with major implications for the United States' transition to a net-zero energy future. Energy technologies of particular interest where HTS tapes could be used include power transmissions, electric aviation, energy storage, and power generation (e.g., fusion, wind).

Abstract ID: 1576

NONCONTACT HIGH THROUGHPUT MEASUREMENTS OF CURRENT-VOLTAGE CHARACTERISTICS OF REBCO HIGH TEMPERATURE SUPERCONDUCTING TAPES OVER WIDE RANGE OF ELECTRIC FIELDS AND CURRENT DENSITIES

Takanobu Kiss[1, 2], Z. Wu[2], K. Higashikawa[1,2]

[1] *Res. Inst. of Superconductor Science and Systems, Kyushu Univ., Fukuoka 819-0395, JAPAN*
[2] *Dept. of Electrical Engineering, Kyushu Univ., Fukuoka 819-0395, JAPAN*
E-mail: kiss@sc.kyushu-u.ac.jp

Current-voltage (*I-V*) characteristic of high-temperature superconducting (HTS) tape is one of the most fundamental and critical characteristics required for HTS based device applications and understanding the material-performances. Temperature and magnetic field dependent *I-V* characteristics are generally measured by the transport four-terminal method using a short sample. However, it has limitations in the requirements such as 1) measurements which require high current bias, 2) measurement at ultra-low electric field region which becomes relevant in the persistent current mode operation of the superconducting magnet, 3) analysis spatial variation in a long wire under the practical environment including at low temperature and magnetic field. The authors have been developing evaluation methods for current transport characteristics to meet these demands using magnetic measurement, which is positioned as a complementary method with the four-terminal method. In the conventional magnetizing method, critical current density (J_c) is derived on the basis of the critical state model assuming the uniformity of the sample and a constant J_c, therefore, the inhomogeneity in the sample and the dynamics of the magnetic moment are not sufficiently considered. In this talk, the principle of the measurement method developed by the authors will be described, and recent results and future prospects will be discussed. The main contents are as follows. For REBCO coated conductor tapes, we derived *I-V* characteristics by dynamical magnetic measurement using a magnetic microscope. The results showed good agreement with that of four-terminal measurements [1]. *I-V* characteristics in the ultra-low electric field ranges such as 10^{-11} V/m, which is difficult to reach by the four-terminal method, was also successfully measured [1]. In addition, a reel-type high-speed magnetic microscopy of long tapes has been developed for continuous measurements of the longitudinal profile of the local J_c in practical operation conditions including 4.2 K and under external magnetic fields. Furthermore, based on the enormous magnetic microscopic images, a new technique introducing image analysis based on machine-learning [2] has been developed. We have succeeded in detecting local J_c lowering domains in the long tapes automatically. This allows us to acquire detailed information on the spatial distribution and statistical information of the obstacles in long length HTS tapes. By fusing such macro-scale information with vortex dynamics in HTS tapes, we developed a mathematical model to describe the current transportation properties of the long HTS tapes accurately.

Acknowledgements

This work was supported by JSPS KAKENHI Grant Number JP19H05617.

References

[1] Z. Wu, K. Higashikawa, T. Kiss, IEEE TAS, **Vol. 33, No. 5**, 6601705 (2023).
[2] N. Somjaijaroen, T. Kiss, *et al.*, IEEE TAS, **Vol. 32, No. 6**, 6601504 (2022).

Theory of Superconductivity I

29.04.2024 MONDAY

Abstract ID: 1455

POLARONS WITH A QUADRATIC INTERACTION: ANALYTIC AND NUMERICAL METHODS

S. N. Klimin, M. Houtput, J. Tempere

Theorie van Kwantumsystemen en Complexe Systemen (TQC), Universiteit Antwerpen, B-2610 Antwerpen, BELGIUM
E-mail: sergei.klimin@uantwerpen.be

The nonlinear electron-phonon interaction has recently gained attention from both experimentalists and theorists [1–4], as it is considered a necessary and important component in explaining various phenomena such as optical response, superconductivity, and temperature dependence of mobility.

This presentation is devoted to our recent theoretical investigations of the effects of nonlinear electron-phonon coupling. We pay particular attention to comparing numerical treatment with analytical methods. Our focus is on revisiting the Gross-Tulub approximation [5,6] in polaron theory extended for non-parabolic finite-width conduction bands, which has proven to be an effective tool for the analytic calculation of polaron parameters. It is in line with the results of the diagrammatic Monte Carlo technique [7] in a wide range of the coupling strength of the nonlinear interaction.

References

[1] P.M. Dee, J. Coulter, K.G. Kleiner, S. Johnston, Commun. Phys. **3**, 145 (2020).
[2] D.E. Kiselov, M.V. Feigel'man, Phys. Rev. B **104**, L220506 (2021).
[3] D. van der Marel, F. Barantani, C.W. Rischau, Phys. Rev. Research **1**, 013003 (2019).
[4] A. Kumar, V.I. Yudson, D.L. Maslov, Phys. Rev. Lett. **126**, 076601 (2021).
[5] E.P. Gross, Phys. Rev., **100**, 1571 (1955).
[6] A.V. Tulub, J. Exp. Theoret. Phys. **14**, 1828 (1961).
[7] S. Ragni, T. Hahn, Z. Zhang, N. Prokof'ev, A. Kuklov, S. Klimin, M. Houtput, B. Svistunov, J. Tempere, N. Nagaosa, C. Franchini, A.S. Mishchenko, Phys. Rev. B **107**, L121109 (2023).

Abstract ID: 1435

IMPACT OF AN EXTENDED *d*-WAVE GAP ON SUPERCONDUCTIVITY: ANALYSIS OF THE CRITICAL CURRENT DENSITY AND UPPER CRITICAL FIELD IN CUPRATE SYSTEMS

O.K. Ganiev[1,2,3,4], B. Yavidov[5], Z. Rakhmonov[6]

[1]*New Uzbekistan University, 100007, Tashkent, UZBEKISTAN*
[2]*Central Asian University, 111221, Tashkent, UZBEKISTAN*
[3]*Institute of Nuclear Physics, 100214, Tashkent, UZBEKISTAN*
[4]*National University of Uzbekistan, 100174, Tashkent, UZBEKISTAN*
[5]*Nukus State Pedagogical Institute Named After Ajiniyaz, 230105, Nukus, UZBEKISTAN*
[6]*Engineering Physics Institute, Samarkand State University, 140104, Samarkand, UZBEKISTAN*
E-mail: orif.ganiev@gmail.com

In a *d*-wave superconductor, the superconducting gap (which describes the energy required to break a pair of superconducting electrons) exhibits a particular symmetry known as *d*-wave symmetry. Hole-doped cuprate superconductors, such as some high-temperature superconductors, have been shown to exhibit a *d*-wave superconducting gap described by the equation $\Delta=\Delta_0\mathrm{Cos}(2\theta)$. ARPES experiments have provided critical evidence for this gap structure [1-3]. In certain cuprate superconductors, particularly those based on bismuth (Bi-based cuprates), ARPES studies have revealed deviations from the idealized $d_{x^2-y^2}$ - wave symmetry. These deviations can be attributed to various factors, including the specific electronic structure of these materials and the presence of additional complexities [4]. In electron-doped cuprate superconductors, the superconducting gap structure is also intricate, often involving additional terms or modulations of the gap magnitude on the Fermi surface [5]. Earlier studies [6-9] have put forward compelling evidence that indicates a noteworthy distinction in the angular dependence of the gap function within electron-doped cuprates compared to the standard functional form $\Delta_0\mathrm{Cos}(2\theta)$.

In this study, we examine the influence of *d*-wave symmetry, including its higher angular harmonics (i.e., extended *d*-wave gap symmetry), on the key characteristics of cuprates. These characteristics include the critical temperature (T_c), the magnitude and structure of the superconducting gap, the superfluid density (ρ_s), the coherence length, the penetration depth, the critical current density (J_c), and the upper critical field (H_{c2}). By employing the Chandrasekhar and Einzel approach, we carefully calculate the superfluid density, taking into account the variations in the superconducting gap with respect to temperature and angle. This, in turn, allows for an accurate fitting of the temperature-dependent experimental data for ρ_s, J_c, and H_{c2} in cuprate superconductors.

References

[1] Z.-X. Shen *et al.*, Phys. Rev. Lett. **70**, 1553 (1993).
[2] H. Ding *et al.*, Phys. Rev. B **54**, R9678 (1996).
[3] C.C. Tsuei, J.R. Kirtley, Rev. Mod. Phys. **72**, 969 (2000).
[4] J. Mesot *et al.*, Phys. Rev. Lett. **83**, 840 (1999).
[5] T. Kondo *et al.*, Phys. Rev. Lett. **98**, 267004 (2007).
[6] G. Blumberg *et al.*, Phys. Rev. Lett. **88**, 107002 (2002).
[7] H. Matsui *et al.*, Phys. Rev. Lett. **95**, 017003 (2005).
[8] L. Shan *et al.*, Phys. Rev. B **72**, 144506 (2005).
[9] I. Eremin, E. Tsoncheva, A.V. Chubukov, Phys. Rev. B **77**, 024508 (2008).

CANCELLED

Abstract ID: 1459

INVESTIGATION OF THE PHASE CHANGE DURING SOLID PHASE SYNTHESIS OF $Bi_{1.7}Pb_{0.3}Sr_2Ca_{n-1}Cu_nO_y$ BISMUTH-BASED CUPRATES

D.R. Djurayev[1,4], A.A. Turayev[2,4], O.G. Turayev[3,4]

[1]Doctor of Physical and Mathematical Sciences, professor
[2]Doctor of Philosophy in Physical and Mathematical Sciences, (PhD)
[3]Doctoral student of Bukhara State University, UZBEKISTAN
[4]Bukhara State University, Bukhara, UZBEKISTAN
E-mail: drabbobur@gmail.com

There are different preparation technologies of any kind of cuprates. This article talks about the technology of obtaining bismuth-based cuprates and the aspects that need to be paid attention to in this process. The advantages and disadvantages of obtaining BSCCO cuprate by solid state reaction method are presented. At the same time, it was mentioned why cuprates of this type of superconducting phase appear in several phases instead of one, and these reasons are explained in a simple way. The steps for obtaining BSCCO cuprate by the solid state reaction method are listed in sequence. The constituents of the BSCCO composite material, the role of each element in the mixture was studied under an optical microscope. The formation of the overall structure near the melting temperature was analyzed by microscopic images.

CANCELLED

Abstract ID: 1661

TOPOLOGICAL QUANTUM MATTER: THE KAGOME FRONTIERS

M. Zahid Hasan

Department of Physics, Princeton University, Princeton, NJ 08544, USA
E-mail: mzhasan@princeton.edu

Topology plays a key role in describing quantum matter which has been greatly explored in recent decades [for an introduction, see, M.Z. Hasan & C.L. Kane Rev. Mod. Phys. 82, 3045 (2010) [1]]. In talk, I present how tuning a topological insulator featuring a Dirac fermion can be used as a platform to realize emergent Weyl fermion and "fractional" Fermi surfaces [1, 2]; and can lead to correlated magnetic, Chern, or many-body states [1-3]. The Kagome lattice which features Dirac fermions, flat bands, and van Hove singularities can serve as another platform to explore topology, superconductivity and many-body density-wave phenomena [3-7]. These novel "topological quantum matter" harbor properties that may lead to the development of next-generation quantum devices.

References

[1] M.Z. Hasan, C.L. Kane, *Topological insulators*, Rev. Mod. Phys. **82**, 3045 (2010).
[2] I. Belopolski, *et.al.*, *Discovery of topological Weyl fermion lines and drumhead surface states in a room temperature magnet*, Science **365**, 1278-1281 (2019).
[3] T. Neupert, M. Denner, J.-X. Yin, R. Thomale, M. Z. Hasan; *Charge order and superconductivity in kagome materials*, Nature Phys. **18**, 137–143 (2022).
[4] J-X. Yin, Y.-X. Jiang, X. Teng *et al.*, *Discovery of charge order and corresponding edge state in a Kagome magnet*, Phys. Rev. Lett. **129**, 166401 (2022).
[5] X. Teng, L. Chen, F. Ye *et al.*, *Discovery of charge density wave in a correlated Kagome lattice antiferromagnet*, Nature **609**, 490-495 (2022).
[6] C. Mielke, D. Das, J.-X. Yin *et al.*, *Time-reversal symmetry-breaking charge order in a kagome superconductor*, Nature **602**, 245 (2022).
[7] J. Yin, B. Lian, M.Z. Hasan, *Topological Kagome magnets and superconductors*, Nature **612**, 647-657 (2022).

Topological and Unconventional Superconductivity in Low-Dimensional Magnet-Superconductor Hybrid Systems

30.04.2024 TUESDAY

Abstract ID: 1043

EMERGENT TOPOLOGY IN A MAGNET-SUPERCONDUCTOR HYBRID SYSTEM DRIVEN BY A 2D ANTIFERROMAGNETIC SPIN TEXTURE

R. Lo Conte[1,2], M. Bazarnik[2,3], E. Mascot[2,4], K. Palotás[5], L. Rózsa[6], L. Szunyogh[5], A. Kubetzka[2], D.K. Morr[7], K. von Bergmann[2], R. Wiesendanger[2]

[1]Zernike Institute for Advanced Materials, University of Groningen, 9747 AG Groningen, THE NETHERLANDS
[2]Department of Physics, University of Hamburg, D-20355 Hamburg, GERMANY
[3]Institute of Physics, Poznan University of Technology, Piotrowo 3, 60-965 Poznan, POLAND [4]School of Physics, University of Melbourne, Parkville, VIC 3010, AUSTRALIA
[5]Department of Theoretical Physics, Institute of Physics, Budapest University of Technology and Economics, Műegyetem rkp. 3., H-1111 Budapest, HUNGARY
[6]Wigner Research Center for Physics, Konkoly-Thege Miklós út 29-33, 1121 Budapest, HUNGARY
[7]Department of Physics, University of Illinois at Chicago, Chicago, IL 60607 USA
E-mail: r.lo.conte@rug.nl

In the recent years, pioneering studies have been carried out on magnet/superconductor hybrid systems [1-4], motivated by their potential to host emergent quantum phases such as topological superconductivity [5]. So far, the attention has been mainly focused on hybrid systems with a ferromagnetic order [1,3,4,6], which are understood as gapped topological superconductors with a finite Chern number [7, 8] defining the amount of end states and propagating edge modes.

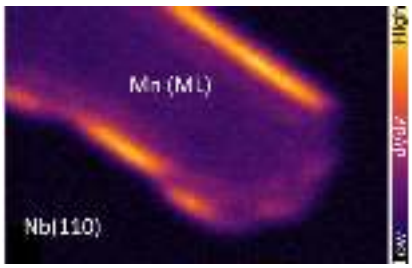

Fig. 1: *In-gap edge modes observed in a antiferromagnetic Mn(ML) island on a Nb(110) substrate via scanning tunneling spectroscopy.*

In my talk, I will discuss the discovery of a topological nodal-point superconducting phase in a hybrid system consisting of antiferromagnetic manganese (Mn) monolayer (ML) islands on top of the *s*-wave superconductor niobium (Nb) [9,10]. The novel topological superconducting phase was discovered via a low-temperature spin-polarized scanning tunneling microscopy and spectroscopy investigation. Low-energy edge modes are observed at the boundaries of the magnetic islands, separating the topological phase from the trivial one (Fig. 1). In accordance to tight-binding calculations, the relative spectral weight of the edge modes depends on the edge's atomic configuration, which is a fingerprint of the discovered two-dimensional (2D) topological superconducting state. These results establish the combination of antiferromagnetism and superconductivity as a novel route to design 2D topological quantum phases.

References

[1] S. Nadj Perge *et al.*, Science **346**, 602 (2014).
[2] H. Kim *et al.*, Science Advances **4**, eaar5251 (2018).
[3] A. Palacio-Morales *et al.*, Science Advances **5**, eaav6600 (2019).
[4] L. Schneider *et al.*, Nature Physics **17**, 943 (2021).
[5] J. Li *et al.*, Nature Communications **7**: 12297 (2016).
[6] S. Kezilebieke *et al.*, Nature **588**, 424 (2020).
[7] A.P. Schnyder, *et al.*, Physical Review B **78**, 195125 (2008).
[8] C. Chiu, *et al.*, Review of Modern Physics **88**, 035005 (2016).
[9] R. Lo Conte *et al.*, Physical Review B **105**, L100406 (2022).
[10] M. Bazarnik, R. Lo Conte *et al.*, Nature Communications **14**, 614 (2023).

Abstract ID: 1047

CONTROLLING MAJORANA MODES IN MAGNETIC ADATOM CHAINS

Oladunjoye A. Awoga, Ioannis Ioannidis, Archana Mishra, Martin Leijnse, Mircea Trif, Thore Posske

E-mail: ioannis.ioannidis@uni-hamburg.de

We propose controlling the hybridization between Majorana zero modes at the ends of magnetic adatom chains on superconductors by an additional magnetic adatom deposited close by. By tuning the additional adatom's magnetization, position, and coupling to the superconductor, we can couple and decouple the Majorana modes as well as control the ground state parity. The scheme is independent of microscopic details in ferromagnetic and helical magnetic chains on superconductors with and without spin-orbit coupling, which we show by studying their full microscopic models and their common low-energy description. Our results show that scanning tunneling microscopy and electron spin resonance techniques are promising tools for controlling the Majorana hybridization in magnetic adatoms-superconductor setups, providing a basis for Majorana parity measurements, fusion, and braiding techniques.

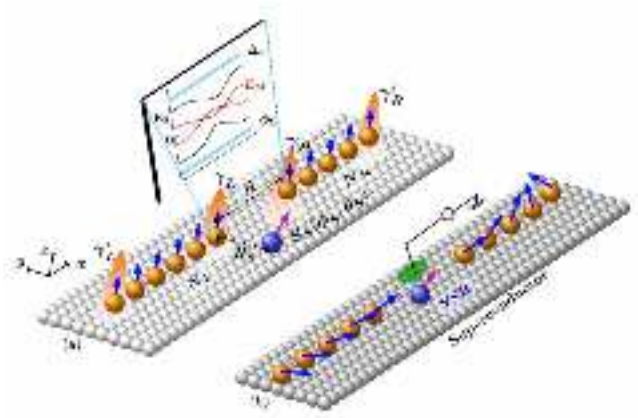

Fig. 1: *Proposed setups. Manipulation of the inter-chain Majorana coupling by placing an additional magnetic adatom between the chains and controlling its' position, orientation and bare energy.*

Reference

[1] O. Awoga, I. Ioannidis *et al.*, e-print arXiv:2308.07961 (2023).
[2] L. Schneider, P. Beck *et al.*, Nat. Nanotechnol. **17**, 384–389 (2022).

Abstract ID: 1167

INFLUENCE OF THE SPIN CONFIGURATION ON THE BAND STRUCTURE OF YU-SHIBA-RUSINOV STATES

L. Rózsa[1,2]

[1]*HUN-REN Wigner Research Centre for Physics, Department of Theoretical Solid State Physics, H-1525 Budapest, HUNGARY*
[2]*Budapest University of Technology and Economics, Department of Theoretical Physics, H-1111 Budapest, HUNGARY*
E-mail: rozsa.levente@wigner.hun-ren.hu

Magnetic impurities in conventional superconductors locally break Cooper pairs, leading to the emergence of Yu-Shiba-Rusinov (YSR) bound states. Chains of YSR impurities have been theoretically predicted to give rise to Majorana bound states, which hold promises for realizing topological quantum computers. A fundamental understanding of the formation of YSR states in small atomic clusters is essential for revealing the topological properties of the YSR band structure. The accurate theoretical modelling of YSR states represents a considerable challenge, since it requires a simultaneous description of the electronic structure, the magnetic ordering of the impurities and superconductivity on significantly different energy scales.

Here, first-principles simulations are combined with tight-binding model calculations to determine the influence of the electronic and magnetic structure on the band structure of YSR states. In ferromagnetic chains the spin-orbit coupling opens a minigap in the bands around the Fermi energy where end states are formed, but the small size of this gap in typical material platforms is found to lead to a long-range extension and interactions between these precursors of Majorana bound states [1]. Introducing nonmagnetic heavy-metal capping layers proximity coupled to the superconductor is expected to enhance the spin-orbit coupling, yet it may fail to considerably increase the size of the minigap in ferromagnetic chains [2]. The minigap is larger in antiferromagnetic chains where the spin-orbit coupling is not necessary for its formation, but the well-localized end states in this minigap typically have a topologically trivial origin [3]. The theoretical concepts are illustrated by experimental realizations in specific materials.

References

[1] L. Schneider, P. Beck, J. Neuhaus-Steinmetz, L. Rózsa, T. Posske, J. Wiebe, R. Wiesendanger, Nat. Nanotechnol. **17**, 384 (2022).
[2] P. Beck, B. Nyári, L. Schneider, L. Rózsa, A. Lászlóffy, K. Palotás, L. Szunyogh, B. Ujfalussy, J. Wiebe, R. Wiesendanger, Commun. Phys. **6**, 83 (2023).
[3] L. Schneider, P. Beck, L. Rózsa, T. Posske, J. Wiebe, R. Wiesendanger, Nat. Commun. **14**, 2742 (2023).

Topological and Unconventional Superconductivity in Low-Dimensional Magnet-Superconductor Hybrid Systems II

30.04.2024 TUESDAY

Abstract ID: 1484

TOPOLOGICAL SUPERCONDUCTIVITY, MAJORANA ZERO MODES AND QUANTUM ALGORITHMS IN MAGNET-SUPERCONDUCTOR HYBRID SYSTEMS

Dirk K. Morr

University of Illinois at Chicago, USA
E-mail: dkmorr@uic.edu

Magnet-Superconductor Hybrid (MSH) systems have proven to be versatile platforms for the engineering of topological superconductivity and the ensuing Majorana zero modes, an important step towards the realization of topological quantum computing. In particular, the experimental ability to create MSH system with widely varying magnetic structures -- from ferromagnetic and skyrmion-like to antiferromagnetic – has provided an unprecedented opportunity to manipulate and explore topological phases.

In this talk, I will review some recent progress in the theoretical prediction and experimental realization of novel topological superconducting phases – ranging from strong and higher order topological superconductors to topological nodal-point superconductivity -- in MSH systems. Moreover, I will demonstrate how the real-time manipulation of the magnetic structure in MSH systems provides a new path to braiding MZMs, revealing their non-Abelian statistics, and to the creation of topological quantum gates and quantum algorithms.

Abstract ID: 1332

TOPOLOGICAL SUPERCONDUCTIVITY IN FIBONACCI QUASICRYSTALS

A. Kobialka[1], O.A. Awoga[12], T. Domański[3], P. Holmvall[1], A.M. Black-Schaffer[1]

[1]Department of Physics and Astronomy, Uppsala University, Box 516, S-751 20 Uppsala, SWEDEN
[2]Solid State Physics and NanoLund, Lund University, Box118, 22100 Lund, SWEDEN
[3]Institute of Physics, M. Curie-Sklodowska University, 20-031 Lublin, POLAND
E-mail: aksel.kobialka@physics.uu.se

Majorana bound states offer a route to fault-tolerant quantum computing and, therefore, could be highly useful for quantum technologies. However, their practical implementation has proven to be challenging. Consequently, finding systems where such states are easier to realize becomes desirable. One system which, perhaps counterintuitively, can enhance correlated states of matter is a quasicrystal (QC) [1,2]. QCs lack translational invariance, but still exhibit a long-range order in the form of discrete scale invariance. This peculiar combination leads to interesting properties such as critical behavior, the opening of topological gaps, and topological invariants that are otherwise only possible in higher-dimensional systems. Stemming from previous inquiry [3], we set out to study how these properties influence the realization of Majorana bound states, in particular in a Fibonacci QC nanowire. We find that the Majorana bound states overcome the aperiodic structure, and that the pre-existing gaps of the quasicrystal trigger additional, non-trivial, topological phase transitions. Furthermore, these states are robust against disorder and incommensurability. On the other hand, the latter removes trivial edge modes, offering the ability to switch the trivial states on or off. These results promote quasicrystals as a nominal platform for further studies of Majorana bound states and point out issues in potential experimental realization

References

[1] D. Levine, P.J. Steinhardt, Phys. Rev. Lett. **53**, 2477 (1984).
[2] A. Jagannathan, Rev. Mod. Phys. **93**, 045001 (2021)
[3] A. Kobiałka, N. Sedlmayr, M.M. Maśka, T. Domański, Phys. Rev. B **101**, 085402 (2020).

Abstract ID: 203

UNDERSTANDING OF ROLE OF DISORDER IN EPITAXIAL SUPERCONDUCTOR-SEMICONDUCTOR QUBITS

Javad Shabani

Physics Department, New York University, Center for Quantum Information Physics 726 Broadway, New York, NY USA
E-mail: jshabani@nyu.edu

Progress in the emergent field of topological superconductivity relies on synthesis of new material combining superconductivity, low density, and spin-orbit coupling (SOC). Theory indicates that the interface between a one-dimensional semiconductor with strong SOC and a superconductor hosts Majorana-modes with nontrivial topological properties [1]. We discuss the recent developments in epitaxial growth of Al on InAs nanowires was shown to yield a high-quality superconductor-semiconductor system with uniformly transparent interfaces. We have developed a two-dimensional (2D) surface InAs quantum wells with epitaxial superconducting Aluminum [2], yielding a planar system with exceptional structural and transport characteristics [3]. We present new qubits based on semiconductor weak links dubbed Gatemons. These qubits show great promise on this platform for realization of topological qubits where we unprecedented control over proximity effect in semiconductors using a gate voltage [4]. We discuss the role of disorder and how they could enable potential circuit applications for low power circuits, gate-based topological qubits as well as superconducting qubits for computation [5].

References

[1] J. Alicea, Rep. Prog. Phys. **75**, 076501 (2012).
[2] J. Shabani *et al.*, Phys. Rev. B **93**, 155402 (2016).
[3] W. Mayer, J. Yuan, K. Wickramasinghe, T. Nguyen, M. Dartiailh, J. Shabani, Superconducting proximity effect in epitaxial Al-InAs heterostructures, Appl. Phys. Lett. **114**, 103104 (2019).
[4] M.C. Dartiailh, W. Mayer, J. Yuan, K.S. Wickramasinghe, A. Matos-Abiague, I. Žutić, J. Shabani, *Phase signature of topological transition in Josephson Junctions*, Phys. Rev. Lett. **126**, 036802 (2021).
[5] C. Richardson, V. Lordi, S. Misra, J. Shabani, *Materials science for quantum information science and technology*, MRS Bulletin, **45(6)**, 485-497 (2020).

Unconventional Superconductivity, and Tunable Quantum States

30.04.2024 TUESDAY

Abstract ID: 1009

MULTIPLE-Q PAIR DENSITY WAVE IN PROXIMITY TO A NESTED FERMI SURFACE

Yi Zhou

Institute of Physics, Chinese Academy of Sciences, Beijing 100190, CHINA
E-mail: yizhou@iphy.ac.cn

We show that spontaneous time-reversal-symmetry (TRS) breaking can naturally arise from the interplay between pair density wave (PDW) ordering at multiple momenta and nesting of Fermi surfaces (FS). Concretely, we consider the PDW superconductivity on a hexagonal lattice with nested FS at 3/4 electron filling, which is related to a recently discovered superconductor CsV3Sb5. Because of nesting of the FS, each momentum on the FS has at least two counterparts on the FS to form finite momentum Cooper pairs, resulting in a TRS and inversion broken PDW state with stable Bogoliubov Fermi pockets. Possible implications to the Kagome superconductor CsV3Sb5 and future experiments will be discussed.

References

[1] Jin-Tao Jin, Kun Jiang, Hong Yao, Yi Zhou, Phys. Rev. Lett. **129**, 167001 (2022).

CANCELLED

Abstract ID: 1066

WEYL FERMION EXCITATIONS IN THE $CuTlSe_2$ SEMIMETAL

T. Shiroka[1,2], D. Tay[1], Q. X. Dong[3], Z. Okvátovity[4], G.F. Chen[3], C. N. Wang[5]

[1]*Laboratorium für Festkörperphysik, ETH Zürich, CH-8093 Zurich, SWITZERLAND*
[2]*Laboratory for Muon Spin Spectroscopy, PSI, CH-5232 Villigen PSI, SWITZERLAND*
[3]*Beijing National Laboratory for Condensed Matter Physics, CAS, Beijing 100190, CHINA*
[4]*Dept. of Theoretical Physics, Budapest University of Technology, 1521 Budapest, HUNGARY*
[5]*Department of Physics, University of Fribourg, CH-1700, Fribourg, SWITZERLAND*
E-mail: tshiroka@phys.ethz.ch

The unusual band topology of Weyl semimetals allows them to host Weyl fermions as quasi-particles, in turn providing access to their exotic physics in a condensed-matter system [1,2]. However, realizing and experimentally identifying ideal Weyl semimetals is a challenging task. Here, we report on $CuTlSe_2$, a Weyl semimetal candidate compound, whose properties were studied by both bulk-probe techniques (SQUID magnetometry and Hall-effect measurements) and local-probe methods (μSR and NMR) [3]. The small and temperature-independent muon-spin relaxation rate up to 140 K suggests that $CuTlSe_2$ shows no intrinsic magnetism of electronic origin and that it preserves time-reversal symmetry. On the other hand, the temperature-dependent local magnetic susceptibility, as obtained from copper-NMR measurements, is clearly distinct from that of conventional semimetals. In pristine $CuTlSe_2$, the Cu Knight shift increases as the temperature is lowered towards 100 K. At the same time, between 20 K and 100 K, $1/(T_1T)$ follows a characteristic T^2 scaling (see figure). A generic microscopic model, which considers the linear- and quadratic electronic-band contributions, successfully corroborates our experimental findings, including here the Tl- and Se-NMR data. We interpret the T^2 dependence as the hallmark of low-energy Weyl fermion excitations. In general, the $CuTlSe_2$ case demonstrates that a combination of different techniques can provide valuable insight into the properties of complex correlated electron materials.

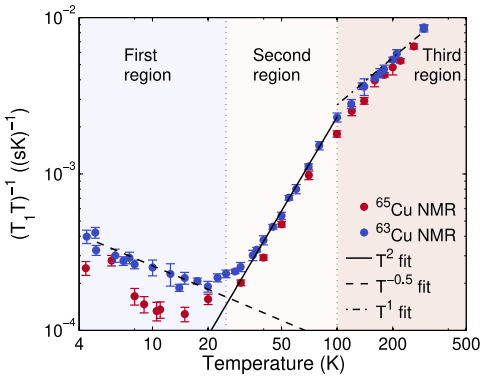

Fig. 1: *Spin-lattice relaxation rate vs temperature in $CuTlSe_2$. Of the three regions, the first two highlight a Weyl-semimetal behavior.*

References

[1] B. Yan, C. Felser, Annu. Rev. Condens. Matter Phys. **8**, 337 (2017).
[2] T. Wehling, A. Black-Schaffer, A. Balatsky, Adv. Phys. **63**, 1–76 (2014).
[3] C.N. Wang *et al.*, submitted to Nat. Commun. (2023).

Abstract ID: 1100

ITINERANT DIAMAGNETIC SPIN-TRIPLET SUPERCONDUCTIVITY IN Fe-BASED HIGH ENTROPY ALLOY NbTaTiZrFe

Jin Hee Kim, Rahmatul Hidayati, Jong-Soo Rhyee

Department of Applied Physics and Institute of Natural Sciences, Integrated Education Institute for Frontier Science and Technology (BK21 Four), Kyung Hee University, Yongin 17104, KOREA
E-mail: jsrhyee@khu.ac.kr

The spin-triplet pairing in superconductivity is of great interest to find exotic topological and quantum states of matter such as Majorana fermions, spin fluctuation-mediated superconductivity, etc. There has been much effort to find unconventional ferromagnetic superconductors, but the materials candidates are rare and limited such as Uranium-based superconductors. Here we found evidence of diamagnetically aligned spin-triplet superconductivity in Fe-based high entropy alloy NbTaTiZrFe compound. The significant diamagnetic signal below 42 K with a superconducting transition temperature Tc = 7 K in zero-field-cooled magnetic susceptibility changes to ferromagnetic transition in field-cooled conditions. The diamagnetic spin-triplet pairing is supported by various experimental and theoretical evidences such as significant diamagnetic signal at low fields with strong ferromagnetic coercive force Hcoer = 1800 Oe, ferromagnetic spin flip signal only for the diamagnetic state, and metallic ferromagnetism confirmed by the scanning magnetic force microscopy and spin-resolved density of states. The spin-triplet diamagnetic/ferromagnetic superconductivity is controllable by offset field conditions (direct- and oscillation-off) to remove a residual magnetic field at room temperature. The diamagnetically aligned spin-triplet superconductivity is an unprecedented finding and can be a good platform to investigate the Majorana fermion and its potential applicability to quantum computation.

CANCELLED

Effects of Topology in Superconductor Nanoarchitectures V

30.04.2024 TUESDAY

Abstract ID: 1263

ANOMALOUS SYMMETRY PROPERTIES AND GAP STRUCTURES IN THE KAGOME SUPERCONDUCTOR CsV_3Sb_5

K. Fukushima[1], K. Obata1, S. Yamane[1,2], Y. Hu[1], Y. Li[3], Y. Yao[3], Z. Wang[3], Y. Maeno[1,4], S. Yonezawa[1,2]

[1]Dept. of Phys. Grad. School of Sci., Kyoto Univ., Kyoto, Kyoto 606-8502, JAPAN
[2]Dept. of Electronic Sci. and Eng., Grad. School of Eng., Kyoto, Kyoto 606-8510, JAPAN
[3]Beijing Institute of Technology, Beijing 100081, P. R. CHINA
[4]Toyota Riken - Kyoto University Research Center, Kyoto 606-8501, JAPAN
E-mail: yonezawa.shingo.3m@kyoto-u.ac.jp

Recently, AV_3Sb_5 (A = K, Rb, Cs) with vanadium Kagome net has been attracting tremendous attention [1]. This family exhibits charge-density-wave (CDW) order around 80-100 K, and further exhibits superconductivity below around 3 K for A = Cs and 1 K for A = K and Rb. Various experiments indicate that both orderings are accompanied by non-trivial symmetry breakings such as rotational and time-reversal symmetry breakings.

In this work, in order to reveal unconventional nature of superconductivity in CsV_3Sb_5, we investigate in-plane anisotropies of its superconductivity by means of field-angle-resolved calorimetry [2]. We discovered that this compound exhibits unique in-plane superconducting anisotropy consisting of both nematic and six-fold features [2]. In particular, we observed that the six-fold anisotropy observed in the in-plane H_{c2} robustly persists very close to zero-field T_c. This observation is in contrast with the "emergent rotational symmetry" in hexagonal superconductors, namely the near absence of six-fold superconducting anisotropy, based on the standard Ginzburg-Landau theory [3-5]. Our observation of the violation of this symmetry property is well interpreted as a multi-component order parameter coupled with a crystalline-symmetry lowering, as discussed in the contexts of hexagonal and trigonal superconductors such as UPt_3 [3,4] and doped Bi_2Se_3 [5].

We also found that low-temperature low-field specific-heat anisotropy, detecting low-energy quasiparticle excitation, exhibits clear oscillation, indicating a node-like structure in the superconducting gap [6].

In this presentation, we explain these experimental results and their implications on the unconventional nature of superconductivity in CsV_3Sb_5.

References

[1] For recent reviews, see T. Neupert *et al.*, Nature Phys. **18**, 137 (2022); K. Jiang *et al.*, Natl. Sci. Rev. **10**, nwac199 (2023).
[2] K. Fukushima, SY *et al.*, arXiv:2303.11072.
[3] J.A. Sauls, Phys. Rev. B **53**, 8543 (1996).
[4] P.L. Krotkov, V.P. Mineev, Phys. Rev. B **65**, 224506 (2002).
[5] J.W.F. Venderbos *et al.*, Phys. Rev. B **94**, 094522 (2016).
[6] K. Fukushima, SY *et al.*, in preparation.

Abstract ID: 1202

NON-INVASIVE READOUT OF SUPERCONDUCTING NANOSTRUCTURES

L. Nulens[1], D.A.D. Chaves[2], O.J.Y. Harb[1], J.E. Scheerder[3], N. Lejeune[4], K. Brahim[3], B. Raes[3], A.V. Silhanek[4], M.J. Van Bael[1], J. Van de Vondel[1]

[1]*Quantum Solid-State Physics, Department of Physics and Astronomy, KU Leuven, Celestijnenlaan 200D, B-3001 Leuven, BELGIUM*
[2]*Departamento de Física, Universidade Federal de São Carlos, 13565-905, SP, BRAZIL*
[3]*Imec, Kapeldreef 75, 3001 Leuven, BELGIUM*
[4]*Experimental Physics of Nanostructured Materials, Q-MAT, CESAM, Université de Liège Allée du 6 Août 19, Sart Tilman, B-4000, BELGIUM*
E-mail: jorisvandevondel1981@gmail.com

Understanding the dynamics of phase slips, topological fluctuations of the superconducting order parameter, in superconducting loops is very important for the development of future nanodevices. These loops show tremendous potential as building blocks for superconducting qubits [1], could be used for memory devices with topological protection [2], and determine the observed critical current profile in Superconducting Quantum Interference Devices (SQUIDs). Understanding these phase slips necessitates the capability to probe the number of flux quanta and determine the kinetic inductance associated with the Cooper pair density in such structures. Here we utilize a niobium resonator as a non-invasive probe capable of exploring the superconducting properties of an aluminum loop positioned close to the resonator. By locally applying a magnetic field, adjusting the temperature, and modifying the loop dimensions using focused ion beam milling, we induce changes in the kinetic inductance of the loop, which are directly manifested in the resonance frequency. This approach highlights the promise of our proof-of-principle spectroscopy device as a tool for exploring the local Cooper pair density within inductively coupled superconducting nanostructures. Moreover, it provides an effective platform for manipulating and detecting phase slips, offering insights into the dynamics of these quantum phenomena.

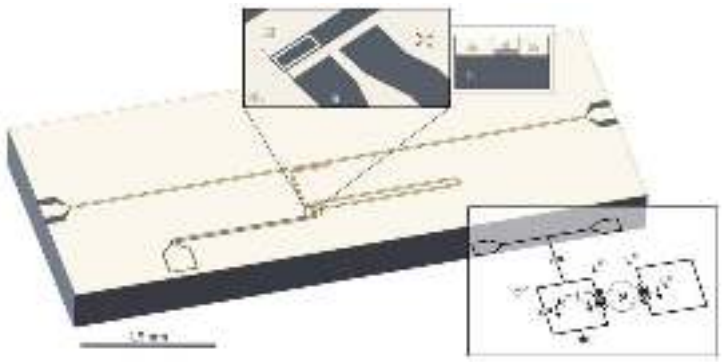

Fig. 1: *schematic representation of the device, comprised of a λ/4 resonator capacitively coupled to the central feedline. The circuit diagram representation of the resonator-loop system is provided in the bottom inset.*

References

[1] J.E. Mooij, C.J.P.M. Harmans. New Journal of Physics **7,** 219 (2005).
[2] N. Ligato *et al.*, Nat Commun **12**, 5200 (2021).

Abstract ID: 1286

QUANTUM DETECTOR TOMOGRAPHY FOR TWO-DIMENSIONAL SUPERCONDUCTING NANO-DETECTORS

A.D. Semenov[1], M. Sidorova[2], S. Cherednichenko[3], H.-W. Hübers[1,4]

[1]*DLR Institute of optical systems, 12489 Berlin, GERMANY*
[2]*Nanyang Technological University, 639798 SINGAPORE*
[3]*A Chalmers University of Technology, Department of Microtechnology and Nanoscience, SE-41296, Gothenburg, SWEDEN*
[4]*Humboldt-University, Department of Physics, 12489 Berlin, GERMANY*
E-mail: alexei.semenov@dlr.de

Quantum tomography is a well-established characterization tool [1]. The major goal of this technique is to reconstruct the quantum state of an incident light by measuring statistical distribution of the clicks produced by the detector in response to arriving photons. If the statistics of light is known, the method can be applied to detectors. Thus, quantum *detector* tomography (QDT) adds a new dimension to the application area of detectors non-resolving the photon number. So far QDT was successfully applied to characterize superconducting nanodetectors with a small active area [2] comparable to the size of the local nonequilibrium state which is produced by the absorbed photon. Another restriction of the established QDT technique is the width of the spectral detection threshold broadened by fluctuations inherent to the detection mechanism [3].

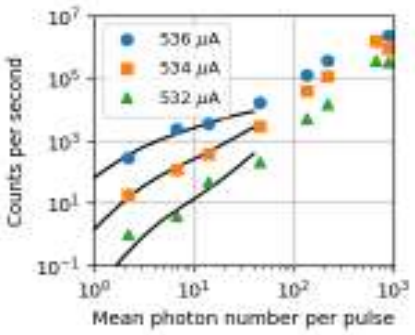

Fig. 1: *Count rate of the MgB_2 strip (symbols) as function of the mean number of photons per pulse at three bias currents specified in the legend. Solid lines show model fits.*

Here we propose a mathematical approach allowing for QDT characterization of multiphoton two-dimensional detectors which exhibit position dependent detection efficiency and relatively broad detection threshold. The proposed modification of QDT incorporates the solution of the partition problem for photon distribution over active detector area. Applicability of our approach was demonstrated with superconducting nanostrips from magnesium diboride (MgB_2). The plot shows the count rate of a straight nanostrip with a length of 100 micrometers, a width of 150 nm, and a thickness of 8 nm at several bias currents as function of the mean number of photons per pulse impinging the strip area. The strip was exposed to pulsed light with the wavelengths 800 nm at a repetition rate of $8 \cdot 10^7$ sec^{-1}. At the smallest current, the count rate follows the power law with the exponent 2 which decreases to almost 1 at the largest current. The best fit, however, was obtained for thresholds in the form of the error function centered at three, four and five photon energies (from top to bottom) with the variance equal to the squared photon energy. Centering the threshold to the energy of just one photon results in the saturated count rate as function of the mean photon number.

References

[1] J.S. Lundeen, A. Feito, H. Coldenstrodt-Ronge, K.L. Pregnell, C. Silberhorn, T.C. Ralph, J. Eisert, M.B. Plenio, I.A. Walmsley, Nat. Phys. **5**, 27–30 (2008).

[2] J.J. Renema, G. Frucci, Z. Zhou, F. Mattioli, A. Gaggero, R. Leoni, M.J.A. de Dood, A. Fiore, M.P. van Exter, Optics Express **20**, **No. 3**, pp. 2806-2813 (2012).

[3] A.D. Semenov, M. Sidorova, M.A. Skvortsov, A. Kuzmin, K. Ilin, M. Siegel, Phys. Rev. B **102**, 184508 (2020).

Advances in Current-Induced Magnetization Control V

30.04.2024 TUESDAY

Abstract ID: 1177

EXPLORING MAGNON-MAGNON COUPLING, SPIN HALL MAGNETORESISTANCE, AND LASER-DRIVEN SPIN TEXTURES IN 2D VAN DER WAALS MAGNETS

C.W.F. Freeman[1,2], M. Dabrowski[3], P.S. Keatley[3], Z. Xue[1], A.K. Budniak[4], G. Eda[4], O. Kazakova[2], R.J. Hicken[3], H. Kurebayashi[1], M. Cubukcu[1,2]

[1]*London Centre for Nanotechnology, University College London, WC1H 0AH, London, UK*
[2]*National Physical Laboratory, TW11 0LW, Teddington, UK*
[3]*Department of Physics and Astronomy, University of Exeter, EX4 4QL, Exeter, UK*
[4]*Department of Physics, National University of Singapore, 117551, SINGAPORE*
E-mail: m.cubukcu@ucl.ac.uk

The antiferromagnetic magnons and the manipulation of magnetization through spin current and laser excitation in 2D van der Waals (vdW) materials, holds significant promise for applications in quantum information and spintronics [1]. We have demonstrated ultra-strong magnon-magnon coupling in the gigahertz (GHz) band in a two-dimensional (2D) van der Waals (vdW) antiferromagnet, $CrPS_4$, achieving a maximum normalized coupling strength of 0.5 (see Fig. 1). Our investigation revealed that the coupling strength can be tuned by temperature and by magneto-crystalline anisotropy. Additionally, we presented spin Hall magnetoresistance in a 2D vdW antiferromagnetic-based device, Pt/$CrPS_4$/h-BN, illustrating the potential to exfoliate 2D antiferromagnets into thin layers and manipulate their magnetization through spin currents [2]. Finally, we showed that laser excitation can generate different type of spin textures at room temperature and zero field in a 2D vdW ferromagnet, Fe_3GaTe_2 [3]. These findings provide an ideal platform for development of magnonic quantum and spintronics devices based on 2D magnets.

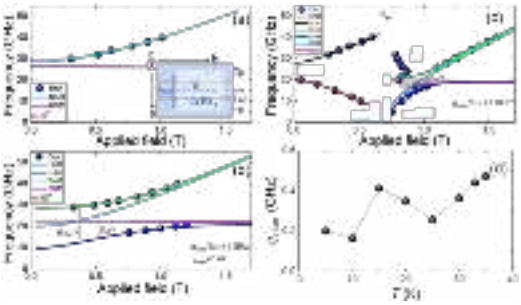

Fig. 1: *The frequency-dependent ferromagnetic resonance (FMR) results were obtained at 15 K, with the magnetic field applied along the b-axis (a), θ=45° (b), along the c-axis (c) (dots) and the fitting (lines). (d) The normalized magnon-magnon coupling rate (η_{inter}) is depicted as a function of temperature at θ=45° Inset: Schematic representation of the arrangement between the coplanar waveguide, $CrPS_4$ crystal, and external magnetic field.*

References

[1] C. Tang, *et al.*, Phys. Rep. **1032**, 1-36. (2023).
[2] C.W.F. Freeman, M. Cubukcu, *et al.*, *Tunable ultra-strong magnon-magnon coupling and spin Hall magnetoresistance in a 2D van der Waals antiferromagnet*, unpublished.
[3] C.W.F. Freeman, M. Cubukcu, *et al.*, *Room-temperature laser-driven spin textures in a 2D van der Waals magnet*, unpublished.

Abstract ID: 1268

OPTIMIZING Bi_2Te_3 THIN FILM GROWTH FOR SPINTRONIC APPLICATIONS

Aykut Can Önel[1], Ebrahim Zahrabi[1], Roya Kavkhani[1], Ahmad El Zatari[1], Arooba Maryyam[1], Rawana Yagan[1], Kerem Anar[1], Ferhat Katmış[2], Mehmet Cengiz Onbaşlı[1]

[1] Koç University, Dept. of Engineering, 34450, İstanbul TURKEY
[2]Massachusetts Institute of Technology, 02139, Massachusetts USA
E-mail: ayonel@ku.edu.tr

Advancements in spintronics, crucial for low-power, high-efficiency electronics, face challenges such as integrating spintronic components with silicon CMOS technology and achieving room-temperature operation. Two-dimensional (2D) materials are key to overcoming these hurdles due to their unique properties suitable for spintronic applications [1,2]. Our research focuses on optimizing Bi_2Te_3 thin films using Molecular Beam Epitaxy (MBE) on Al_2O_3 (0001) and Si (111) substrates. We investigated the effects of substrate temperature, varying from 25°C to 180°C after initial attempts at 230°C resulted in no film formation. Lower temperatures led to homogeneous films but with multiple crystalline phases. Characterization involved X-ray Diffraction (XRD), X-ray Reflectivity (XRR), and profilometer measurements for film quality and thickness. X-ray Photoelectron Spectroscopy (XPS) revealed multiple peaks in Bi 4f and Te 3d spectra, indicating the presence of both Bi_2Te_3 and metallic Bi and Te, suggesting stoichiometric complexities. Atomic Force Microscopy (AFM) confirmed the expected triangular surface morphology. This study underscores the importance of substrate temperature in Bi_2Te_3 film growth and highlights the nuanced challenges in achieving optimal film quality. Our findings contribute significantly to the development of Bi_2Te_3 for spintronic applications, marking a step forward in the field of advanced electronic materials.

References

[1] W. Han, Y. Otani,, S. Maekawa, npj Quantum Materials **3**, 27 (2018).
[2] X. Lin, W. Yang, K.L. Wang, W. Zhao, Nature Electronics **2**, 274 (2019).

Abstract ID: 1247

STABILIZATION AND EXTERNAL FIELDS CONTROL OF SKYRMIONS IN SYNTHETIC ANTIFERROMAGNETIC MULTILAYERS

Rawana Yagan[1], Arash Mousavi Cheghabouri[1], Mehmet C. Onbasli[1,2]

[1] *Koç University, Dept. of Electrical and Electronics Engineering, 34450, Istanbul, TURKEY*
[2] *Koç University, Dept. of Physics, 34450, Istanbul, TURKEY*
E-mail: ryagan@ku.edu.tr

Skyrmions in synthetic antiferromagnetically coupled (SAF) multilayers have demonstrated considerable potential for future device applications in memory and logic operations owing to the nanoscale dimensions, offering high-density, quick response, and low-power throughput. They offer a more comprehensive range of stability conditions and dynamic performance than conventional ferromagnetic (FM) skyrmions, namely their immunity against topological Hall effect and stray fields. Uncertainty exists regarding the requirements for stabilizing SAF skyrmions and how the material properties, external drive conditions, and spatial defects affect this stability. By extending the ferromagnetic skyrmion theory [1] to antiferromagnetically coupled FM/NM/FM multilayers (here: Co/CoFeB/Ir/CoFeB/Co) [2], we present the theory of stabilizing SAF skyrmions. According to the output of our micromagnetic model, equilibrium skyrmions with radii between 1 and 50 nm can be produced by varying material parameters, including saturation magnetization (M_s), Dzyaloshinskii-Moriya interaction (DMI) constant, uniaxial anisotropy (K_u), and interlayer exchange. Based on the balance between these parameters and the intralayer exchange, Zeeman, and shape anisotropy energies, skyrmions on both ferromagnetic layers are stabilized. Next, we study the impact of adiabatic drive, out-of-plane external magnetic field, and perpendicular external current density drive on skyrmion velocity and SAF skyrmion decoupling thresholds. SAF skyrmions can move at speeds up to 196 m/s when the external magnetic field increases (up to 120 mT). We trace the decoupling current under an external magnetic field where the skyrmion requires a lower current to decouple under higher field power. According to the phase diagram of skyrmion velocity under various magnetic fields and current bias, skyrmions can be driven at current densities between 10^8 and $3x10^{11}$ A/m^2 without experiencing topological Hall effect or decoupling and with velocities about 3-10 times greater than the typical ferromagnetic skyrmion. Finally, we examine the spatial effects of the skyrmion nanotrack, including edge line effects and in-plane anisotropy variation modeled with Voronoi tessellation. SAF skyrmion shows stable drive under an acceptable window of these parameters where limited performance exists in extreme conditions inhibiting the skyrmion's forward motion along the track. These findings could provide valuable insights into the functions of SAF skyrmions and their utilization in memory and logic devices.

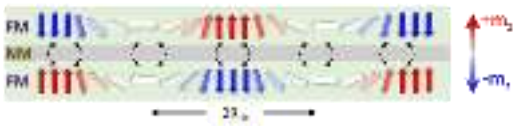

Fig. 1: *Skyrmion pair created at the interfaces* of the *SAF multilayers coupled through normal metal (NM) layer via RKKY interaction [2].*

References

[1] F. Büttner, I. Lemesh, G. Beach, Sci. Rep. **8**, **4464**, 1-12 (2018)
[2] R. Yagan, A.M. Cheghabouri, M.C. Onbasli, Nanoscale Advances, **5(17)**, 4470–4479 (2023).

Advances in Current-Induced Magnetization Control VI

30.04.2024 TUESDAY

Abstract ID: 1249

SCALABLE LOW POWER SKYRMION LOGIC GATES AND CIRCUITS

A. Mousavi Cheghabouri[1], R. Yagan[1], Mehmet C. Onbasli[1,2]

[1]*Department of Electrical and Electronics Engineering, Koç University, Sarıyer, 34450 Istanbul, TURKEY*
[2]*Department of Physics, Koç University, Sarıyer, 34450 Istanbul, TURKEY*
E-mail: monbasli@ku.edu.tr

Skyrmions are nanoscale chiral magnetic spin structures that could be used for dense information storage as well as processing with ultra-low power, nonvolatility and wide bandwidth [1]. These spin structures could not be used for any scalable logic system previously, because most logic gates that use skyrmions are not cascadable and drive currents are not compatible. In this study, we use micromagnetic modelling to establish a clear control of skyrmion motion in magnetic nanowires under magnetic field and current bias conditions. Next, we develop a universal Boolean gate logic system that can implement arbitrary combinational logic circuits. The cascadable and field-free logic components demonstrated are NOR, AND, OR, NAND, XNOR gates and a voltage-controlled periodic skyrmion clock generator [2,3]. Using these gates and blocks, we demonstrate the operation of a FULL ADDER skyrmion digital logic circuit.

We provide a timing, current drive, and energy consumption analysis for the Co/Pt materials. The magnetic energy consumption for the components ranges between 2.30 to 9.60 $\times$ 10^{-18} J. The energy consumption due to Joule heating in these devices ranges between 1.30 to 6.72$\times$ 10^{-13} J. We discuss the routes for eliminating Joule heating by substituting Co/Pt with semiconductor/magnetic insulator interfaces that have large spin-orbit coupling.

We designed and we present a toolkit that lays the foundation for bridging the gap between theoretical exploration and practical implementation of skyrmion-based computing. The skyrmion block components might help reduce energy consumption per logic operation after eliminating Joule heating. Our insights and designs might help skyrmions be used in the state-of-the-art electronic design automation.

References

[1] A. Fert, V. Cros, J. Sampaio, *Skyrmions on the track*, Nat. Nanotechnol. **8**, 152 (2013).
[2] A. Cheghabouri, F. Katmis, M.C. Onbasli, *Cascadable direct current driven skyrmion logic inverter gate*, Phys. Rev. B **105**, 054411 (2022).
[3] A.M. Cheghabouri, M.C. Onbasli, *Direct current-tunable MHz to multi-GHz skyrmion generation and control*, Sci. Rep. **9**, 9496 (2019).

Abstract ID: 1292

SURFACE ACOUSTIC WAVE MANIPULATION OF MAGNETIC DOMAIN WALLS AND SKYRMIONS

J. Shuai[1], R.G. Hunt[1], L. Lopez-Diaz[2], J.E. Cunningham[3], T.A. Moore[1]

[1]*School of Physics and Astronomy, University of Leeds, Leeds, LS2 9JT, U.K.*
[2]*Department of Applied Physics, Universidad de Salamanca, Salamanca, 37008, SPAIN*
[3]*School of Electronic and Electrical Engineering, University of Leeds, Leeds, LS2 9JT, U.K.*
E-mail: t.a.moore@leeds.ac.uk

Surface acoustic waves (SAWs) are potentially interesting for energy-efficient control of magnetic domain wall (DW) and skyrmion motion via magneto-elastic coupling[1]. One issue is that SAW-induced heating may also contribute to DW motion. Here, the heating of a SAW device was measured locally using an on-chip Pt film as a thermometer (Fig 1(a,b)). Interdigitated transducers of center frequency 48 MHz were patterned either side of a strip of Ta(5.0)/Pt(2.5)/Co(0.9)/Ta(5.0) thin film (thicknesses in nm, Fig. 1(c)). Measurements of DW velocity by Kerr microscopy (Fig. 1(d)) show that with a 10 K temperature increase and no SAWs applied, the velocity increases from 33±3 μm/s to 104±8 μm/s at an external field of 65 Oe. The temperature rises by 10 K and DW motion is enhanced (418±8 μm/s) in the presence of standing SAWs, but not travelling SAWs[2]. We have performed micromagnetic simulations to examine the effect of SAWs on DW and skyrmion velocities in this material[3,4]. In Fig. 1(e) we combine a longitudinal travelling SAW and a transverse standing SAW to precisely transport skyrmions by exploiting a balance of SAW-induced forces.

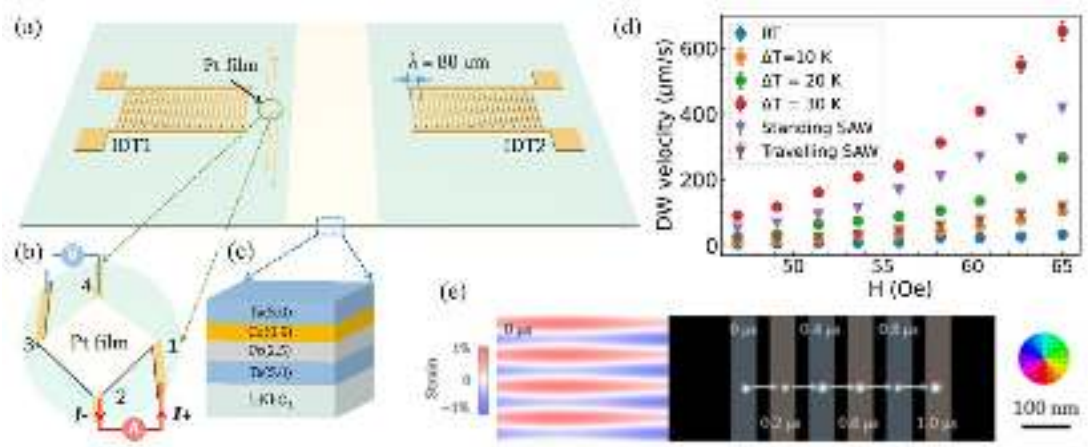

Fig. 1: *Schematic of the SAW device (a) and the on-chip Pt thermometer (b). (c) Structure of the Ta/Pt/Co/Ta film. (d) DW velocity at different temperatures or in the presence of SAWs, plotted against the applied magnetic field. (e) Snapshot of skyrmion motion in the presence of longitudinal travelling SAW and transverse standing SAW.*

References

[1] J. Puebla, Y. Hwang, S. Maekawa, Y. Otani, Appl. Phys. Lett. **120**, 220502 (2022).
[2] J. Shuai, R.G. Hunt, T.A. Moore, J.E. Cunningham, Phys. Rev. Appl. **20**, 014002 (2023).
[3] J. Shuai, L. Lopez-Diaz, J.E. Cunningham, T.A. Moore, Phys. Rev. B **108**, 104420 (2023).
[4] J. Shuai, T.A. Moore, L. Lopez-Diaz, J.E. Cunningham, arXiv:2305.16006 (2023).

Abstract ID: 1558

ARTIFICIAL INTELLIGENCE FOR MAGNETIC MATERIALS DESIGN

T. Schrefl[1,2], Clemens Wager[1], A. Kovacs[2], J. Fischbacher, D. Böhm, S. Stanciu, Q. Ali[1], H. Moustafa[2], F. Lasthofer[2], H. Oezelt[2], M. Gusenbauer[2]

[1] *Doppler Laboratory for magnet design through physics informed machine learning, University of Continuing Education Krems, Wiener Neustadt, AUSTRIA*
[2] *Department for Integrated Sensor Systems, University of Continuing Education Krems, Wiener Neustadt, AUSTRIA*
E-mail: thomas.schrefl@donau-uni.ac.at

Artificial intelligence (AI) has played a significant role in materials design for decades [1]. Unlike other fields, materials science lacks the vast amounts of data typically required for advanced AI applications. As a result, AI in materials research often relies on classical algorithms such as partial least squares regression and genetic optimization. We demonstrate that combining these approaches can be highly effective in optimizing permanent magnet materials, taking into account both performance and the criticality of raw materials [2]. A series of regression models serve as a surrogate for rapid evaluation of material properties during the optimization process. This enables inverse design, where the optimizer suggests the ideal chemical composition and structure of magnetic materials based on desired properties. Datasets for machine learning can be generated through high-throughput micromagnetic simulations of synthetic microstructures, derived from experimental images [2]. This breakthrough allows for the exploration of novel magnet structures with specified properties using generative AI. We provide a proof of concept of materials design through the integration of measurements, imaging, micromagnetic simulations, and generative AI.

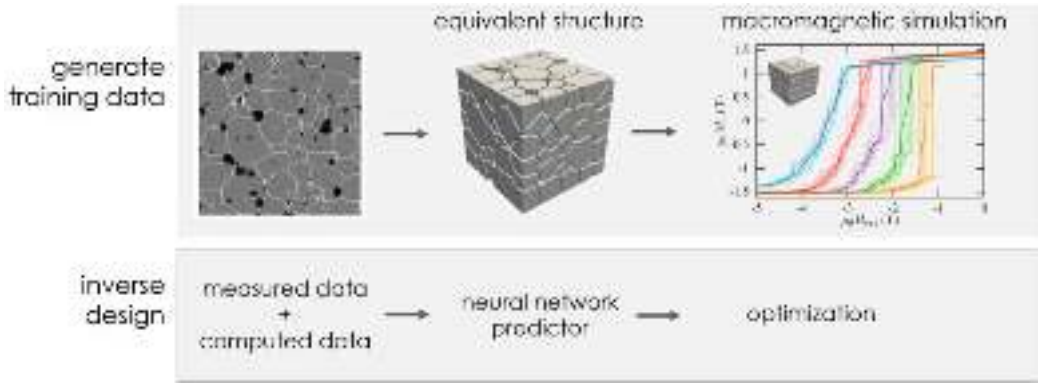

Fig. 1: *Image-based prediction, optimization, and generation of magnetic materials by combining experimental measurements, imaging, micromagnetic simulations, and generative artificial intelligence.*

The financial support by the Austrian Federal Ministry of Labour and Economy, the National Foundation for Research, Technology and Development and the Christian Doppler Research Association is gratefully acknowledged.

References

[1] K. Rajan, Materials Today **8**, 38 (2005).
[2] A. Kovacs, J. Fischbacher *et al.*, Front. Mater. **9**, 1094055 (2023).

Quantum Spin and Magnetism in Chiral Materials: CISS Effect, Solitons and Skyrmions III

30.04.2024 TUESDAY

Abstract ID: 1013

STABILIZING SKYRMION CRYSTAL IN CENTROSYMMETRIC MAGNETS

Shizeng Lin

Theoretical division and CINT, Los Alamos National Laboratory, USA
E-mail: szl@lanl.gov

Magnetic skyrmions are topological excitations that have many promising device applications. However, most materials that host skyrmions require breaking the inversion symmetry. In this talk, I will present a mechanism to stabilize topological nontrivial texture in centrosymmetric magnets through the interplay among frustration, spin anisotropy, and lattice geometry. I will discuss the skyrmion lattice stabilized by RKKY interaction in the Kondo lattice. I will then discuss a transformation between various topological spin textures, such as skyrmions, merons, and vortices on a square lattice with compass-like interaction. In the last part of the talk, I will present a novel skyrmion stabilizing mechanism through local Dzyaloshinskii-Moriya interaction in centrosymmetric magnets. I will also discuss the effect of the topological spin texture on conduction electrons.

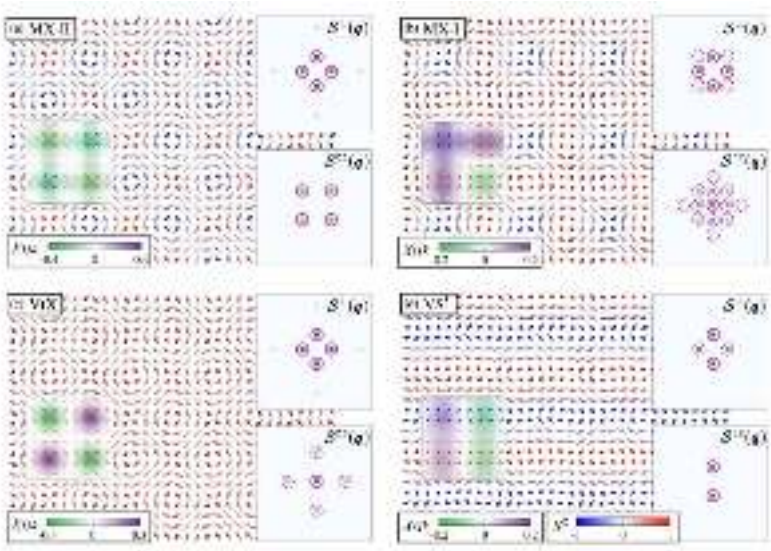

Fig. 1: *Meron and vortex crystals in centrosymmetric magnets.*

References

[1] Z. Wang, Y. Su, S.-Z. Lin, C.D. Batista, Phys. Rev. Lett. **124**, 207201 (2020).
[2] Z. Wang, Y. Su, S.-Z. Lin, C.D. Batista, Phys. Rev. B **103**, 104408 (2021).
[3] S.-Z. Lin, arXiv:2112.12850.

Abstract ID: 1015

RESONANT ELASTIC SMALL-ANGLE SOFT X-RAY SCATTERING UNVEILS ANISOTROPIC INTERACTIONS IN CHIRAL MAGNETS

V. Ukleev

Helmholtz-Zentrum Berlin für Materialien und Energie, 14109 Berlin, GERMANY
E-mail: v.ukleev@gmail.com

Resonant elastic small-angle soft x-ray scattering (REXS) serves as a unique and powerful tool, offering unprecedented reciprocal-space resolution, to delve into long-periodic spin textures in noncentrosymmetric magnets. The distinctive sample environment further facilitates the exploration of uncharted spin texture transformations and extraction of small parameters inaccessible through other methods. In this consolidated study, we present recent REXS investigations on the chiral magnetoelectric Cu_2OSeO_3 and the chiral room-temperature skyrmion host $Co_8Zn_8Mn_4$.

In the case of Cu_2OSeO_3, our REXS studies in vector magnetic fields expose the significant role of anisotropic exchange interaction (AEI) at low temperatures (< 35 K). The AEI strongly influences the conical spiral pitch variation in Cu_2OSeO_3, impacting the orientation of exotic low-temperature states, including a tilted conical spiral and a disordered skyrmion phase [1]. These findings underscore the importance of previously neglected cubic and exchange anisotropies in defining the magnetic phase diagrams of noncentrosymmetric magnets [2].

Additionally, we delve into the chiral helimagnet $Co_8Zn_8Mn_4$, β-Mn-type alloy, revealing its peculiar temperature-dependent behavior in the spiral pitch and structural transition of the metastable skyrmion texture [3-5]. REXS in vectorial magnetic fields provides insights into the temperature-dependent anisotropic properties, showcasing a competition between exchange and cubic magnetocrystalline anisotropies. Our theoretical model, incorporating anisotropy contributions from AEI and uniaxial strain, allows for the quantitative extraction of the AEI parameter.

These comprehensive studies using REXS not only unveil the rich and exotic magnetic phase diagrams of noncentrosymmetric magnets but also extend their tunability, thereby providing a significant platform for further fundamental explorations and potential applications in energy-saving technologies.

References

[1] A. Chacon, *et al.*, Nat. Phys. **14**, 936 (2018).
[2] P.R. Baral, *et al.*, Phys. Rev. Res. **5**, L032019 (2023).
[3] K. Karube, *et al.*, Nat. Materials **15**, 1237 (2016).
[4] D. Morikawa, *et al.*, Nano letters **17**, 1637 (2017).
[5] V. Ukleev, *et al.*, Phys. Rev. B **99**, 144408 (2019).

Abstract ID: 1384

ON THE STABILITY BOUNDARIES OF THE SKYRMION PHASE IN NON-CENTROSYMMETRIC FERROMAGNETS WITH THE DZYALOSHINSKII-MORIYA INTERACTION

S.V. Grigoriev[1,2], V.E. Timofeev[1,2], D.N. Aristov[1,2]

[1]*Petersburg Institute of Nuclear Physics, NRC "Kurchatov Institute", Gatchina, 188300, RUSSIA*
[2]*St. Petersburg State University, St. Petersburg, 198504, RUSSIA*
E-mail: grigor@lns.pnpi.spb.ru

The cubic noncentrosymmetric structure of the B20 compounds causes the formation of a spin spiral with a wave vector $k_S = D/J$ balanced by the competition of antisymmetric Dzyaloshinskii-Moriya (DM) interaction and the ferromagnetic exchange interaction (Back-Jensen model) [1,2]. The application of a magnetic field H transforms the helix into a conical structure, which collapses into a field-induced ferromagnet at point H_{C2}. This field is defined by the interaction hierarchy through $g\mu_B H_{C2} = Ak_S^2$. Small-angle neutron scattering experiments demonstrate the appearance of a Skyrmion Lattice (SkL) instead of a conical structure [3]. The SkL is formed under the influence of an applied magnetic field within a narrow range of fields [H_{A1}, H_{A2}] and only near T_C. It manifests itself as a hexagonal structure of magnetic vortices, with the vortex axis parallel to the magnetic field and three identical wave vectors placed in a plane perpendicular to the field. The SkL wave vector k is practically equal to that of the helix k_S showing that the SkL is built on the same hierarchy of interactions [3,4].

We discuss the results of small-angle neutron scattering experiments on a single crystal of manganese monosilicide MnSi, which demonstrate the very fact of existence and determine the limits of the stability of SkL. To understand the physical picture of the appearance of a new phase, a simplified model is proposed that describes the stability boundaries of the SkL, in which the energies of interaction with the magnetic field of the conical structure and the SkL are compared. It is shown that the SkL is closest in energy to a conical spiral at field $H_A = \alpha H_{C2}$, with the coefficient α being equal to the ratio of the z-projection of an average moment $\mu_{Sk,z}$ inside the SkL unit cell to the total moment μ at a given temperature $\alpha = \mu_{Sk,z}/\mu = 0.4$. The field H_A is characterized by equality of the projections to the field axis z of average moments of SkL $\mu_{Sk,z}$- and the conical structure $\mu_{c,z}$-, thus giving better physical ground picture of the SkL appearance in all ferromagnets with the DM interaction.

When taking dipole forces (demagnetization factor) into account, the lower and higher boundaries of the SkL stability on the field scale (H_{A1}, H_{A2}) are found. It appears that the SkL becomes energetically more favourable than a conical structure within a certain range around H_A near Tc. Within the simplified model the criticality is taken into account throughout magnetization value that, being small, stabilizes the SkL and stabilizes the conical structure becoming larger upon temperature decrease. A careful theoretical analysis in the stereographic projection approach [5] and further numerical calculations supports main conclusions of the simplified model. It also shows necessity of taking additionally into account different positive additives coming from the critical fluctuations to the energies of SkL and the conical phase.

In conclusion, we show that the position of the SkL on the field scale (close to $H_A = \alpha H_{C2}$) in the (H-T) phase diagram of the in non-centrosymmetric ferromagnets with the Dzyaloshinskii-Moriya interaction is determined, firstly, by the balance of the two main interactions via the value of H_{C2} and, secondly, by the the z-projection of an average moment $\mu_{Sk,z}$ inside the SkL unit cell via the its ratio to the total moment $\alpha = \mu_{Sk,z}/\mu = 0.4$. The position of the SkL close to Tc is determined by the dipole forces (demagnetization factors) those are different for the SkL and conical structure. The SkL is energetically favourable at small magnetization but loses the competition to the conical structure at large magnetization, i.e. at the intermediate and low temperatures.

References

[1] P. Bak, M.H. Jensen, J. Phys. **C13**, L881 (1980).
[2] O. Nakanishi, A. Yanase, A. Hasegawa, M. Kataoka, Solid State Commun. **35**, 995 (1980).
[3] S. Muhlbauer, B. Binz, F. Jonietz, C. Pfleiderer, A. Rosch, A. Neubauer, R. Georgii, and P. Boni, Science **323**, 915 (2009).
[4] S.V. Grigoriev, N.M. Potapova, E.V. Moskvin, V.A. Dyadkin, Ch.Dewhurst, S.V. Maleyev, JETP Letters **100**, 238-243 (2014).
[5] V.E. Timofeev, A.O. Sorokin, D.N. Aristov, JETP Letters **109**, 207–212 (2019).

Quantum Spin and Magnetism in Chiral Materials: CISS Effect, Solitons and Skyrmions IV

30.04.2024 TUESDAY

Abstract ID: 1401

SYSTEMATIC STUDY OF CHIRAL MAGNETISM IN RARE EARTH INTERMETALLIC COMPOUNDS BASED ON $YbNi_3Al_9$

S. Ohara[1], S. Nakamura[1], K. Kurauchi[2], M. Tsukagoshi[2], T. Matsumura[2]

[1]*Department of Physical Science and Engineering, Graduate School of Engineering, Nagoya Institute of Technology, 466-8555, Nagoya, JAPAN*
[2]*Department of Quantum Matter, ADSE, Hiroshima University, Higashihiroshima, Hiroshima 739-8530, JAPAN*
E-mail: ohara@nitech.ac.jp

In recent years, there has been a growing interest in chiral magnetism in rare earth intermetallic compounds. This interest was sparked by the discovery of chiral helical magnetic order in $YbNi_3Al_9$ and EuPtSi [1-4]. Unique spin structures, such as chiral soliton lattice and skyrmion lattice, were observed in each of these compounds under magnetic fields.

In rare earth intermetallic compounds, the magnetic interactions between rare earth magnetic ions are mediated by conduction electrons. This aspect distinguishes them from the previously studied chiral magnetism in insulator or itinerant magnet. In rare earth intermetallic compounds, it is believed that the asymmetric magnetic interaction, known as the DM interaction (DMI), is also mediated by conduction electrons [5]. So far, the mechanism of DMI in rare earth intermetallic compounds remains unclear.

To understand the DMI in rare earth intermetallic compounds, it is essential to develop various chiral magnetic materials for comparison. In this context, $YbNi_3Al_9$ proves to be a suitable candidate for research. $YbNi_3Al_9$ crystallizes in the $ErNi_3Al_9$-type structure, exhibiting a chiral nature with the space group $R32$ (#155) and the crystal point group D_3 [6]. The crystal structure is layered, with rare-earth ions forming a two-dimensional honeycomb network. Materials with the same crystal structure can be obtained for rare earth elements of Y and from Gd to Lu. In compounds where Al is replaced with Ga, synthesis is possible for Y, Nd, Sm, and from Gd to Lu. The partial substitution of Ni allows for the exploration of carrier-doping effects through Co or Cu substitution, as well as the investigation of the influence of Pd or Pt substitution.

We have determined the magnetic structures of $YbNi_3Al_9$, $ErNi_3Ga_9$, $DyNi_3Ga_9$ and $GdNi_3Ga_9$ using neutron diffraction and resonant X-ray scattering measurements [2, 7-9]. In each case, a chiral helix, Ising magnetic order unaffected by DMI, chiral helical order competing with ferroquadrupolar ordering, and long-period antiferromagnetic chiral helical order are observed. The details of these magnetic structures and the control of DMI through elemental effects will be presented.

References

[1] S. Ohara *et al.*, JPS Conf. Proc., **3**, 017016 (2014).
[2] T. Matsumura *et al.*, J. Phys. Soc. Jpn., **86**, 124702 (2017).
[3] M. Kakihana *et al.*, J. Phys. Soc. Jpn., **87**, 023701 (2018).
[4] K. Kaneko *et al.*, J. Phys. Soc. Jpn., **88**, 013702 (2019).
[5] J. Kishine, A.S. Ovchinnikov, *Theory of Monoaxial Chiral Helimagnet*, Solid State Physics, **66** Elsevier, pp.1–130 (2015).
[6] R.E. Gladyshevskii *et al.*, Acta Cryst. **B49**, 468 (1993).
[7] H. Ninomiya *et al.*, Physica B, **536**, 392-396 (2017).
[8] M. Tsukagoshi *et al.*, Phys. Rev. B., **105**, 014428 (2022).
[9] S. Nakamura *et al.*, Phys. Rev. B., **108**, 104422 (2023).

Abstract ID: 258

EXPERIMENTAL DEMONSTRATION OF MOLECULAR CHIRALITY-DEPENDENT PSEUDO-JAHN-TELLER STATES

M. Eginligil

Nanjing Tech University (NanjingTech), Key Laboratory of Flexible Electronics (KLoFE) & Institute of Advanced Materials (IAM), School of Flexible Electronics (Future Technologies), 210009, Nanjing, CHINA
E-mail: iameginligil@njtech.edu.cn

The Jahn-Teller (JT) effect, symmetry breaking of nonlinear nuclear configurations through vibronic coupling with degenerate electronic states (DES) in molecules [1], has led to great breakthrough in molecular science and engineering. One immediate consequence of the JT effect, the pseudo-JT (PJT) effect [2], a direct indicator of the molecular instability, can be the reason of sub-meV split excited DES that can be used to discriminate enantiomers [3], such as chiral camphor. Although Raman circular intensity differential has been employed to identify the nondegenerate vibrational states in chiral camphor [4], there has been no evidence of peculiarly-split pseudo-JT (PS-PJT) states. In this work, linearly polarized Raman measurements were performed to demonstrate these doubly degenerate PJT states and their molecular chirality dependence for D (right chiral) and L (left chiral) camphor ($C_{10}H_{16}O$). The splitting of the PJT-based excited-DES was found to be 1.8 x 0.2 cm^{-1} in resonance Raman scattering (at ~ 649 cm^{-1}) by two chiral centers on carbon ring of camphor. This observation can be attributed to the symmetry reduction from D_{6h} to D_{3h} (and C_{2v}) and chiral C_3 [5] becoming intact, by placing camphor on a SiO_2/Si substrate. The enantiomeric PS-PJT states exhibited clear differences between camphor enantiomers by the noncoincidence effect, the depolarization ratio, and the molecular orientation. The occupancy ratio of the states was four times larger in one enantiomer compared to the other, manifesting molecular chirality-dependent polarization rotation [6]. In addition to revelation of the PS-PJT states, this proof-of-concept study may open new doors in studies of chiral molecules and related applications.

References

[1] H.A. Jahn, E. Teller, Proc. of the Royal Society A, **161**, 220–235 (1937).
[2] I.B. Bersuker, Chem. Rev. **113**, 1351–1390 (2013).
[3] Y.-N. Chiu, J. Phys. Chem. **88**, 5820–5826 (1984).
[4] L.D. Barron, J. Chem. Soc., Perkin Trans. **2**, 1074–1079 (1977).
[5] J. Kishine, H. Kusunose, H.M. Yamamoto, Isr. J. Chem. e202200049 (2022).
[6] S.-K. Zhao, B. Baltabayeva, M.-R. Zhang, J.-M. Wang, Y.-F. Hao, M. Eginligil, W. Huang, doi.org/10.21203/rs.3.rs-3770494/v1 (2024).

Abstract ID: 1666

GENERALIZED HEISENBERG FERROMAGNET EQUATION WITH SCALAR POTENTIAL

Zh. Beisekeyeva[1], K. Beisekeyev[2]

[1] *L.N. Gumilyov Eurasian National University, Dept. of General and Theoretical Physics, 010000, Astana, KAZAKHSTAN*
[2] *Astana IT University, Dept. Intelligence Systems and Cybersecurity 010000, Astana, KAZAKHSTAN*
E-mail: sagidullayeva.zh@gmail.com

Currently, the theory of solitons is rapidly developing. A soliton is a structurally stable solitary wave propagating in a nonlinear medium. Due to their special properties, solitons behave like particles (particle-like wave): when interacting with each other or with some other disturbances, they are not destroyed, but continue to move, keeping their structure unchanged. This property can be used to transmit data over long distances without interference. This opens up enormous possibilities for the use of solitons. Solitons and soliton-like waves can be observed in various fields of physics. The mathematical description of solitons has also been developed. Over the past decades, the theory of nonlinear evolutionary equations has advanced so much that nonlocal models have emerged: spatial, temporal, and spatiotemporal.

The study of spin systems is one of the fundamental problems of modern physics. However, questions related to the description of integrable spin systems with potential remain open, and this direction has become one of the active areas of research in the field of physics and mathematics in recent years. Within the framework of soliton theory, the definition of interactions of spins and spin chains quite succinctly includes the theory of integrable systems. An important subclass of nonlinear evolution equations - integrable spin systems that describe the dynamics of propagation of wave packets in magnets - includes the generalized Heisenberg ferromagnet equation. This research examines generalized Heisenberg ferromagnet equation with scalar potential and its equivalents. A fundamental understanding of spin systems, as well as systems with potentials, and their study will help expand our understanding of magnetic materials and spin dynamics. This will make it possible to study various aspects such as the structure of spin waves, magnetic domains and interactions between spins, which is important for the development of new materials and technologies based on magnetism.

Acknowledgments

This research has been funded by the Science Committee of the Ministry of Science and Higher Education of the Republic of Kazakhstan (Grant No. AP14972423)

References

[1] T. Dauxois, M. Peyrard, Physics of Solitons (Cambridge: Cambridge University Press, 2006).
[2] R. Myrzakulov, S. Vijayalakshmi, G. Nugmanova, M. Lakshmanan, Phys. Lett. A **233** (1999).
[3] P. Lax, Commun. on Pure and App. Math. **21**, (1968).
[4] Zh. Sagidullayeva, G. Nugmanova, R. Myrzakulov, N. Serikbayev, Symmetry **14(7)** 1374 (2022).
[5] Zh. Sagidullayeva, Journal of Physics: Conference Series, **2667** (2023).

Abstract ID: 1151

QUANTUM CAVITIES BASED ON MAGNONIC TEXTURES

D. García-Pons, C.A. González, J. Pérez-Bailón, F. Luis, D. Zueco, María José Martínez-Pérez

Instituto de Nanociencia y Materiales de Aragón CSIC-Universidad de Zaragoza, Calle Pedro Cerbuna 12, 50009 Zaragoza, ESPAÑA
E-mail: pemar@unizar.es

Solid state quantum computing and quantum sensing technologies are based on the strong coupling between qubits and a quantized field of excitations. Besides photons, the solid state offers a wide variety of bosonic excitations that can be emitted or absorbed such as, e.g., magnons, the quantum version of spin waves.

Magnonic cavities offer the advantage of operating at reduced wavelengths compared to electromagnetic resonators of the same frequency. Here, we investigate the integration of magnonic cavities based on topological magnetic solitons as, e.g., magnetic vortices. The latter are extremely stable magnetic textures exhibiting a very rich dynamical behavior in the sub-GHz to tens of GHz range. We focus on the coupling of individual spin qubits to vortex cavities for sensing and quantum computing applications.

Large Scale Applications of Superconductors and Their Fundamental Technologies I

30.04.2024 TUESDAY

Abstract ID: 1561

HADRONTHERAPY: EXPLORING NEW CHALLENGES AGAINST CANCER

S. Rossi

The National Centre for Oncological Hadrontherapy (CNAO), ITALY
E-mail: sandro.rossi@cnao.it

At the beginning of the third millennium, one out of three European citizens experiences cancer at least once in the course of her/his life. Radiotherapy is involved in almost half of the successful treatments of these patients and includes several modalities. Hadrontherapy is one of the most advanced and personalized clinical approach and uses ion beams (like protons and carbon ions), which have useful properties (namely precision and radiobiological efficacy) for the treatment of rare tumours.

The modern era of hadrontherapy started in the nineties of last century, with the construction of hospitals equipped with accelerators and dose delivery systems fully devoted to clinical applications. Technology and human expertise have continuously made progresses over the last decades, and nowadays proton therapy systems are very sophisticated, highly reliable and commercially available. The expansion of carbon ion radiotherapy has been much more limited, as it requires large investments, high operational costs, sufficient space for larger accelerators, and a team of specialists familiar with the physical and biological peculiarities of these particles. Technological advancements (like the introduction of new superconducting magnets) aim at developing tools and strategies to improve treatment outcome, reduce dimensions and cost and favour the diffusion of hadrontherapy.

This talk will report on the rationale of hadrontherapy and will give an overview of its status in the world. It will also present the technologies associated to hadron beams production and their use, including accelerators, dose delivery systems, patient positioning and the imaging devices. An overview of the most promising R&D topics is also included.

CNAO (Italian acronym that stands for National Centre for Oncological Hadrontherapy) is a clinical facility, located in Pavia (North of Italy), which has treated more than 5000 oncological patients with particle beams. In this presentation the results, the technologies and the R&D programmes of CNAO are outlined, as examples to better describe this field. Attention is also paid to the European project HITRIplus, that gathers a wide multidisciplinary consortium conceived to favour the access of a larger number of patients to this advanced treatment modality, to pursue R&D in accelerators and its related technologies and to open the European carbon ion centres to the clinical and research communities.

Abstract ID: 1622

COMPACT PARTICLE THERAPY WITH SUPERCONDUCTING TECHNOLOGIES

A. Godeke, A. Harmant, M. Schillo

Compact PT, Hengelo, THE NETHERLANDS
E-mail: agodeke@icloud.com

High-energy ion particle beams for the treatment of cancers enables much more localized targeting of tumors than is possible with conventional X-rays. This results in large reductions of undesirable radiation dosages in healthy tissue and organs, leading to a significantly improved quality-of-life for patients after their treatment, as well as a reduced chance of secondary cancers. For critical areas such as head and neck, and for pediatric patients, particles are the only radiation option.

Despite the advantages, there are globally only about 230 particle treatment-rooms available, compared to about 20,000 X-ray facilities. One of the main reasons for this reduced market penetration of particle therapy are the huge facility-size and -cost: The typical cost for a single-room proton facility, including building, is 35 to 50 MUSD and the cost of carbon facilities is even higher, while the cost for a typical X-ray facility is below 10 MUSD.

In this presentation, novel superconducting approaches to particle therapy are described, leading to systems that can be operated using existing commercial treatment soft- and hardware, to provide a much shorter time-to-market and clinical acceptance. Extreme compactness is achieved by the introduction of challenging, but realistic, superconducting components. The resulting projected system size- and cost-levels for proton systems are competitive with X-ray solutions, while for carbon-ion systems extreme reductions in size and cost are enabled compared to existing solutions. Increased availability of particle therapy can therefore be expected, helping the millions of patients that currently do not have access to these superior treatment modalities.

Abstract ID: 1663

RECENT TRENDS IN PROTONTHERAPY

E. Forton, V. Nuttens

Ion Beam Applications, B-1348 Louvain la Neuve, BELGIUM
E-mail: vincent.nuttens@iba-group.com

It is well-known that Radiation therapy started with the use of gamma rays and Xrays to treat tumours, but that ion beams (e.g. proton or carbon beams) can be used to treat cancer tumours with unrivalled accuracy. Today, Proton Therapy is a growing cancer treatment modality thanks to its ability to reduce long and short-term side effects. And it is still evolving.

In this keynote, we will start with an overview of the benefits of protons over photons for cancer treatment. We will then introduce the typical layout of a proton therapy system. Then, we will describe and discuss a few of the current challenges in the field and how they may be tackled with system modifications and improvements, with a focus on how superconductivity may contribute, bearing in mind high-level system constraints like total cost of ownership or environmental impacts.

Large Scale Applications of Superconductors and Their Fundamental Technologies II

30.04.2024 TUESDAY

Abstract ID: 1382

DEVELOPMENT OF A NOVEL HIGH TEMPERATURE SUPERCONDUCTING CABLE WITH HIGH CURRENT DENSITY AND LOW AC LOSSES

Charlie Sanabria[1], Alexey Radovinsky[1], Christopher Craighill[1], Kiran Uppalapati[1], Alex Warner[1], Julio Colque[1], Elle Allen[1], Sam Heller[1], David Chavarria[1], Kristen Metcalfe[1], Amanda Hubbard[2], Amy Watterson[2], Sarah Chamberlain[2], Rui Diaz-Pacheco[1], Benjamin Weinreb[1], Elizabeth Brownell[1], Justin Nealey[1], Annie Hughes[1], Eric Laamanen[1], Keshav Vasudeva[1], Colin McCormack[1], Erica Salazar[1], Owen Duke[1], Matt Hicks[1], Jeremy Adams[1], Dylan Kolb-Bond[1], Timothy Liu[1], Kara Malhotra[1], Ashleigh Francis[1], JL Cheng[1], Maise Shepard[1], Aliya Greenberg[1], Vinny Fry[1], Nick Kostifakis[1], Carl Avola[1], Paul Ljubicic[1], Lex Palmer[1], Ronak Padukone[1], Sergey Kuznetsov[1], Kai Donez[1], Theodore Golfinopoulos[2], Phillip Michael[2], Rui Vieira[2], Nicolai Martovetsky[3], Rodney Badcock[4], Mike Davies[4], Arvid Hunze[4], Bart Ludbrook[4], Ramesh Gupta[5], Piyush Joshi[5], Shresht Joshi[5], Anis Ben Yahia[5], Hugues Bajas[6], Markus Jenni[6], Christoph Mueller[6], Manuel Holenstein[6], Kamil Sedlak[6], Dash Weeks[7], Ross Rentz[7], Jake Benzing[7], Sera Evcimen[8], Brandon Sorbom[1], Daniel Brunner[1]

[1]*Commonwealth Fusion Systems, Cambridge, Massachusetts, USA*
[2]*Plasma Science and Fusion Center, Massachusetts Institute of Technology, Cambridge, Massachusetts, USA*
[3]*Oak Ridge National Laboratory, Oak Ridge, Tennessee, USA*
[4]*Robinson Research Institute, Victoria University of Wellington, Wellington, NEW ZEALAND*
[5]*Brookhaven National Laboratory, Upton, New York, USA*
[6]*Ecole Polytechnique Federale de Lausanne Swiss Plasma Center, Lausanne, Vaud, SWITZERLAND*
[7]*Applied Chemicals and Materials Division, National Institute of Standards and Technology, Boulder, Colorado, USA*
[8]*Pratik Development LLC, Boston, MA, USA*
E-mail: charlie@cfs.energy

Commonwealth Fusion Systems (CFS) is entering the manufacturing stages of the SPARC tokamak, a Q>1 fusion device based on the high-field compact concept proposed by MIT and CFS. A pulsed device such as SPARC, will require low AC loss, high current density conductor in its Central Solenoid (CS) and Poloidal FIeld (PF) coils to generate the flux required to initiate, drive, and shape the plasma. To achieve this, CFS has developed a novel cable technology based on the Twisted Stacked-Tape Cable (TSTC) conductor and the VIPER conductor developed by MIT and CFS. This new conductor—optimized for AC losses—has an engineering critical current density in the range of ~100 A/mm^2 (20 K, 20 T) and is capable of sustaining up to 300 kN/m of IxB loading per tape stack. Additionally, it can survive up to 570 MPa of transverse compression at the unit cell level without current capacity degradation and over 260 MPa at the insulated winding pack level without insulation breakdown. Furthermore, quench detection capabilities using fiber optic sensors have been demonstrated at SPARC-relevant currents and temperatures. A comprehensive test has been carried out by making a four-layer, 5.7 T (peak-field) magnet tested at 50 kA and 20 K in MIT in Feb 2024. The development of this technology and its demonstration coil—as well as its contribution to fusion energy—will be the focus of this talk.

Acknowledgements

This work was funded by ARPA-E Award Number DE-AR0001259 and by Commonwealth Fusion Systems.

Abstract ID: 1571

HTS WIRES, CABLES, AND COILS WITH HIGH JE AND VERY LOW AC LOSSES

A. Otto, L. Saraco, A. Bouthillette, B. Bouchard, A. Croteau, A. Dimino, J. Voccio

Solid Material Solutions LLC, North Chelmsford, Massachusetts, 01863 USA
E-mail: alex.otto@solidmaterialsolutions.com

This paper provides an in-depth update on critical advances achieved in the development of new HTS conductor and coil designs with combinations of performance and loss at operating temperature, field, and ramp rate, that meet commercial requirements and that are unmatched by HTS tapes. Specifically, new types of low loss HTS wires, cables and coils based on the Bi2212 material have recently been developed for AC and fast ramp usage modes with operating temperatures in the 25 K to 40 K range. A series of baseline wire designs were first developed with the required low ac losses and high Jc / Je levels, along with long length manufacturing capability. Low loss cable designs and cable fabrication where then developed for these wire types, with their high Je's and custom Ic levels in the target temperature and field ranges also at commercial levels. With the availability of long cables, generic and application specific coil developments were initiated with focus on racetrack and saddle coil designs. To date 64 test coils have been produced in studies aimed at developing all critical coil design features, along with wind-and-react and react-and-wind fabrication techniques for small and large coils. Je's in the latest designs are at levels required for drop-in ac field generating components that, when sufficiently developed will enable drastic advances in the performance of diverse, large market end user product systems. These include for example stator coils for much higher power density motors and generators required for transoceanic electric plane development, as well as compact ion beam cancer treatment systems for affordable installation in same large numbers as X-Ray systems, with the benefit of far less healthy tissue damage and treatment of areas where X-Rays are too damaging, such as in the brain. With baseline technologies established, current development is focused on customized and optimized cable designs and advanced coil design and fabrication development to meet very demanding commercial specifications set for these next generation components so that they enable drastic end user system advances. Application of these and other new Bi2212 conductor designs to fusion reactor and accelerator coils are also reviewed.

Abstract ID: 1574

SIGNIFICANT IMPROVEMENT OF ELECTROMECHANICAL ROBUSTNESS OF REBCO COATED CONDUCTORS BY FACE-TO-FACE DOUBLE STACKED ARCHITECTURE

Takanobu Kiss[1,2], Z. Wu[2], S. Sera[2], Y. Oda[2], R. Nagayama[2], K. Ibusuki[2], K. Imamura[2], M. Nakamura[2,3], K. Higashikawa[1,2]

[1] *Res. Inst. of Superconductor Science and Systems, Kyushu Univ., Fukuoka 819-0395, JAPAN*
[2] *Dept. of Electrical Engineering, Kyushu Univ., Fukuoka 819-0395, JAPAN*
[3] *Faraday Factory Japan LLC, Kanagawa 252-0132, JAPAN*
E-mail: kiss@sc.kyushu-u.ac.jp

Since the current is carried in a monolithic thin superconducting layer in a REBCO coated conductor (CC), it is significantly affected by local obstacles in the current transport. In particular, a large electric field concentration occurs in the vicinity of the obstacle under low temperature environment where the *n*-value becomes large. Furthermore, the yield of coil is not high enough at present stage due to a difficulty of mechanical handling of the thin CC tape and/or the weakness of delamination strength. It is an urgent task to improve electromechanical robustness and to develop REBCO conductor with coil grade in order to realize reproducible coil I_c as same to the designed value expected from strand I_c. The authors proposed a Face-to-Face Double Stacked (FFDS) conductor which composites two REBCO wires facing superconducting layer side each other. In this talk, the current transport properties of the FFDS conductor will be described including 1) superior tolerance against local obstacles in the strands, 2) overcurrent response, and 3) mechanical bending properties. In particular, to study the bending properties in the diameter less than 10 mm, we proposed a novel test method which enables continuous bending tests including the small diameter range far below the diametral 10 mm, which is difficult by the conventional test method. By implementing this method to an actual equipment, we have succeeded in measuring current-voltage characteristics of the FFDS sample in-situ immersed in liquid nitrogen while applying bending strain continuously. It was demonstrated that the REBCO FFDS conductor can sustain 95 % of the initial I_c even at 7.25 mm in diameter. Current transport test with DC and AC bias to a small coil made by the FFDS conductor with 20 mm inner-diameter will also be presented.

Acknowledgements

This work was supported by JSPS KAKENHI Grant Number JP19H05617.

Large Scale Applications of Superconductors and Their Fundamental Technologies III

30.04.2024 TUESDAY

Abstract ID: 1112

STABILITY AND QUENCH OF HTS MAGNETS AT LOW TEMPERATURES THE POINT OF VIEW

Vitaly S. Vysotsky

All-Russian Scientific R&D Cable Institute, Moscow, 111024 RUSSIA
E-mail: vysotsky@ieee.org

Current trends in magnets for fusion devices are to use high temperature superconductors (HTS) at low temperatures, below 20 K, to achieve magnetic fields above 20 Tesla. In most cases, coated conductors or 2G HTS tapes are considered prime candidates for use in such magnets due to their superior mechanical properties and high current density. However, one of the main problems of high-field HTS magnets is protection from loss of superconductivity (stability) and transition to the normal state (quenching). Standard approaches to stability analysis may not work for thin asymmetrical HTS 2G tapes and their combinations into high current conductors. Normal origination and propagation analysis approaches that are well developed for low Tc magnets may not work at low temperatures for HTS magnets. Various physical parameters of HTS windings at low temperatures lead to a slow propagation speed of the normal zone, which is difficult to detect, especially in large magnets. Even the very definition of a normal zone can be very ambiguous for HTS windings with their high critical temperature. The strong nonlinearity of the system and natural inhomogeneities that arise during the manufacture of initial HTS conductors create points of possible localization of temperature and destruction of the device. Many experiments have demonstrated the very slow propagation of normal or resistive zones with a clear localization of the warm zone, where most of the stored energy during the discharge of HTS magnets causes overheating and overvoltage. Detecting the onset of quenching in the large magnet/coil required to activate the protection circuits is also a very difficult task.

It was shown before that HTS windings can be considering as very non-linear media with heating and cooling [1]. In such a media high temperature localization, similar to "blow up" regimes can occur. In this paper we consider the possibility to use approaches developed in [1] adapted for stability, quench and heat localization analysis of HTS magnets at low temperatures. We trust that such approaches could be useful and fruitful for predicting of stability and quench development in large HTS windings at temperatures below 20 K.

References

[1] A.L. Rakhmanov *et al.*, Cryogenics, **v.40, N1**, pp.19-27 (2000).

Abstract ID: 1600

HIGH FIELD HTS CRYOGEN-FREE SUPERCONDUCTING MAGNETS - DEVELOPMENTS AND LONG TERM OPERATION

S. Awaji, A. Badel, A. Zampa, K. Takahashi, T. Okada, Y. Tsuchiya

High Field Laboratory for Superconducting Materials, IMR, Tohoku University, 980-8577, Sendai, JAPAN
** Present address is Neel Institute / G2Elab, Grenoble, FRANCE*
E-mail: awaji@tohoku.ac.jp

Cryogen-free superconducting magnets (CSMs) and cryogen-free hybrid magnets (CHMs) have been developed at the High Field Laboratory for Superconducting Materials (HFLSM), IMR, Tohoku University since 1992 [1]. In particular, the high temperature superconducting materials have been used for the high field insert magnet since 2004. The 20 T-CSM and the 25T-CSM were developed with $Ag/Bi_2Sr_2Ca_2Cu_2O_3$ (Ag/Bi2223) insert coils, in 2013 and 2016, respectively [2, 3]. We have operated both CSMs as a user magnet for 18 years for 20T-CSM and 8 years for the 25T-CSM [4]. During the long-term operation, some failures and quenches have occurred, and we have learned lessons from the failures. For example, we confirmed the quench protection with a dump resistance works quite well for accidental quenches even in the Bi2223 magnets. Because of high cryo-stability in high temperature superconductors (HTSs), we can discharge the Bi2223 insert without any normal zone in the windings, which leads to the reduction of the temperature rise even after the quench. In addition, we have many failures with REBCO coils under the developments of the 20T-CSM and 25T-CSM. The lessons learned enable us to find the "Robust REBCO coil structure", which is a two REBCO tape wound pancake with edge-impregnation with thin FRP plates [5]. It will be used for an on-going project of 33T-CSM. The cryostat with f320mm-14 T LTS outsert magnets, power supplies, cooling and control system without REBCO insert were installed in 2024 March. The 19 T REBCO insert magnet is to be installed in 2026.

The CSMs have been developed at HFLSM under collaboration with Toshiba Energy System and Solutions Corporation, Sumitomo Heavy Industrial, Furukawa Electric and Fujikura. The Bi2223 tapes were manufactured by Sumitomo Electric.

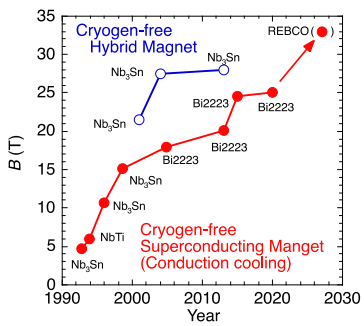

Fig. 1: *Progress of cryogen-free superconducting magnets (CSM) and hybrid magnets (CHM) at HFLSM.*

References

[1] K. Watanabe, S, Awaji J. Low Temp. Phys. **133**, 17 (2003).
[2] S. Awaji *et al.,* Adv. Cryo. Eng. **59**, 732(2014);AIP Conf. Proc. **1573**, 732 (2014).
[3] S. Awaji *et al.,* Supercond. Sci. Technol., **30** 065001 (2017).
[4] K. Takahashi *et al.,* IEEE TAS, **34**, 4601905 (2024).
[5] S. Awaji *et al.,* IEEE TAS, **31**, 4300105 (2021).

Abstract ID: 1145

THE WORLD'S LONGEST HTS DC CABLE LINE IN THE POWER SYSTEM OF ST. PETERSBURG, TESTING RESULTS AND INSTALLATION

Andrey Kashcheev, Victor Sytnikov, Mikhail Dubinin

ROSSETI R&D Center, Moscow, RUSSIA
E-mail: avkashcheev@yandex.ru

The development and implementation of electric power equipment based on the application of the superconductivity effect is a progressive direction in the development of electric power systems. High-temperature superconducting (HTS) cable lines are considered as a real alternative to the use of traditional equipment in the reconstruction of electrical networks. An example of such alternative is the HTS DC cable line project in power system of St. Petersburg.

The report is devoted to the development, manufacture and practical implementation of a high-temperature superconducting DC cable line with a length of 2,400 meters at a voltage of 20 kV with an operating current of 2500A into the power grid of St. Petersburg, the second largest megacity in Russia. A high-temperature DC cable line will connect two independent energy districts of the city at medium voltage without increasing fault currents. Cable line will increase the operational controllability of the network, as well as it will enable a controlled flow of power between energy districts.

The report provides information on the design of the cable, terminal and connection joints and the cryostat of the cable line. The results of intermediate, resource and complex electrical tests of the cable line assembly at a specialized test site are presented. The scheme of the cryogenic system and the characteristics of the cryogenic loop with a length of 5000 meters are described.

The report highlights the process of laying a high-temperature cable line in the conditions of dense urban development in St. Petersburg. The cable line, consisting of six segments, is installed in one of the central districts of the city and all technological nodes of the cable line are designed in such a way as to ensure the possibility of unhindered monitoring and repair during operation. The operation of this high-temperature cable line will is essential to gain practical experience in using extended high-temperature cable lines in the power systems of megacities, and to move on to replicating the developed solutions and mass implementation of highly efficient high-efficiency HTS DC and AC cable lines into the power systems of cities.

CANCELLED

Large Scale Applications of Superconductors and Their Fundamental Technologies IV

30.04.2024 TUESDAY

Abstract ID: 1628

SUPERCONDUCTING AND CRYOGENIC TECHNOLOGIES FOR ZERO-EMISSION LARGE ELECTRIC TRANSPORT PLATFORMS AT FLORIDA STATE UNIVERSITY

Sastry V. Pamidi

The Center for Advanced Power Systems & FAMU-FSU College of Engineering
Tallahassee, Florida 32310, UNITED STATES OF AMERICA
E-mail: pamidi@caps.fsu.edu

There is increased interest in developing large electric transport platforms, such as electric aircraft and ships, to curb greenhouse gas emissions from the transportation sector. Superconducting technologies will provide the necessary power density to achieve the electrification of large transport platforms. Liquid hydrogen-fueled platforms provide the synergy to reduce the complexity of superconducting technologies because the liquid fuel at 20 K can serve as a cryogenic heat sink. However, the research facilities required to develop the technologies are expensive and take time to establish. Hence, collaborations and joint developments are an option to quickly progress, validate initial design options, and build and test prototype propulsion, power distribution, and cryogenic systems. The Center for Advanced Power Systems (CAPS) and the FAMU-FSU College of Engineering have established testbeds for high temperature superconducting power distribution systems, cryogenic electrical insulation systems, cryogenic fluid circulation systems, advanced AC loss measurement systems at LH2 temperature relevant to developing electric aircraft and ships [1-6]. The presentation will describe the facilities and examples of collaborative development efforts. The primary purpose of the presentation is to offer and encourage collaboration opportunities to make the most use of the advanced research facilities at CAPS. However, the research facilities required to develop the technologies are expensive and take time to establish. Hence, collaborations and joint developments are an option to quickly progress, validate initial design options, and build and test prototype propulsion, power distribution, and cryogenic systems.

The work is supported by NASA and the Office of Naval Research.

References

[1] S. Telikapalli, P. Cheetham, C.H. Kim, S.V. Pamidi, *Helium gas cooled and insulated superconducting coaxial dipole cable for electric transport*, IEEE Transactions on Dielectrics and Electrical Insulation, **vol. 30, no. 5**, pp. 2165-2172 (2023); doi: 10.1109/TDEI.2023.3269008.

[2] P. Cheetham *et al.*, *SuPErShip – A multidisciplinary collaborative study on system-level benefits of superconducting power devices on electric ships*, IEEE Transactions on Applied Superconductivity, **vol. 33, no. 5**, pp. 1-4, Art no. 5401204 (2023); doi: 10.1109/TASC.2023.3256962.

[3] S. Telikapalli, J. Stright, P. Cheetham, C.H. Kim, S. Pamidi, *Failure mode effects and analysis of superconducting power distribution and related cryogenic components for all-electric ship*, IEEE Transactions on Applied Superconductivity, **vol. 33, no. 5**, pp. 1-6, Art no. 5400506 (2023); doi: 10.1109/TASC.2023.3243562.

[4] P.C. Saha *et al.*, "*CLEAN: Cryogenic Link for Electric Aircraft Propulsion*, IEEE Transactions on Applied Superconductivity, **vol. 33, no. 5**, pp. 1-6, Art no. 3800406 (2023); doi: 10.1109/TASC.2023.3241600.

[5] D.C. van Der Laan, C.H. Kim, S.V. Pamidi, J.D. Weiss, *A turnkey gaseous helium-cooled superconducting CORC®dc power cable with integrated current leads*, Superconductor Science and Technology, **35(6)**, 065002 (2022).

[6] D.C. van der Laan, J.D. Weiss, C.H. Kim, L. Graber, S. Pamidi, *Development of CORC® cables for helium gas cooled power transmission and fault current limiting applications*, Superconductor Science and Technology, **31**, 085011 (2018).

Abstract ID: 1304

NEUTRON RADIATION CHALLENGES FOR HTS FUSION MAGNETS

R. Unterrainer, A. Bodenseher, M. Eisterer

Atominstitut, TU Wien, Vienna, AUSTRIA
E-mail: michael.eisterer@tuwien.ac.at

Nuclear fusion promises to be a practically inexhaustible energy source and research on its exploitation started in the 1940s, unfortunately, only successful for nuclear weapons so far. Attempts for producing energy for the benefit of humankind set in nearly simultaneously but turned out to be much more challenging. Two different approaches to create a plasma hot and dense enough to produce more energy by fusion reactions than required for its generation were followed since the very beginning: The first being inertial confinement that mimics the mechanism in nuclear weapons. The nuclear fuel is heated and compacted extremely fast resulting in a very dense plasma with a high fusion rate limited to the timescale the plasma needs to expand during the resulting explosion. Recently, a net energy gain, where the fusion energy exceeded the energy deposited in the nuclear fuel ($Q>1$) was achieved for the first time. The second approach relies on a magnetic confinement of the charged particles and can in principle lead to a continuously burning plasma. However, a net energy gain was not realized so far. In both cases, the progress was continuous but slow, since there was no immediate need for fusion power plants. The first fusion device aiming at a useful energy gain (ITER, $Q \approx 10$) has been under construction for many years now and it will take more than another decade until experiments with a burning plasma will start. Europe plans a first demonstration reactor (DEMO) producing electricity for the second half of this century.

The situation changed with the broad public awareness of the climate change creating an immediate need for alternative energy sources. Fusion was reconsidered but the existing programs were obviously too slow to face the challenge; thus new, privately funded initiatives took the stage. The vast majority of these projects is based on the idea to increase the magnetic field for confinement, which is only possible by using high temperature superconductors. A higher magnetic field enhances the power density of the burning plasma and enables much compacter designs, which in turn promises a significant cost reduction and commercial viability of fusion power plants.

However, the increased power density leads to other challenges, among them the increased neutron (and heat flux) density. A small fraction of the neutrons will reach the superconducting magnets degrading their performance and hence limiting their lifetime.

Results of neutron irradiation experiments on high temperature superconducting tapes performed at the TRIGA reactor in Vienna will be presented. Their implication for the lifetime of conventional and compact fusion reactor concepts will be compared. Mechanism for the degradation of the conductor performance will be introduced and related to the neutron induced defect structure. Finally, possible mitigation strategies will be discussed.

This work has been carried out within the framework of the EUROfusion Consortium, funded by the European Union via the Euratom Research and Training Programme (Grant Agreement No 101052200 — EUROfusion). Views and opinions expressed are however those of the author(s) only and do not necessarily reflect those of the European Union or the European Commission. Neither the European Union nor the European Commission can be held responsible for them.

Abstract ID: 1635

SIMULATION OF MAGNETIC FLUX TRAPPING IN SEEDED YBCO FOR EDS MAGLEV SYSTEMS

U. Kemal Ozturk[1,*], Murat Abdioglu[1,2] Ali Suat Yıldız[3]

[1] *Electromagnetic Guidance and Acceleration Research Group (EMGA), Department of Physics, Faculty of Science, Karadeniz Technical University, 61080, Trabzon, TURKIYE*
[2] *Department of Mathematics and Science Education, Faculty of Education, Bayburt University, 69000, Bayburt, TURKIYE*
[3] *Department of Mechanical Engineering, Faculty of Engineering and Natural Sciences, Sivas University of Science and Technology, 58000, Sivas, TURKIYE*
E-mail: kozturk6167@gmail.com

Today, three-seeded YBCO superconductors – PMG rail configurations (PMG: Permanent Magnet Guideway) are used in maglev applications requiring high levitation and guidance, but due to the high cost of PMG rail, alternative systems are needed [1]. In this study, the simulation of magnetic flux trapping in bulk HTS (High Temperature Superconductor) is carried out by finite element method using the H-φ formulation. A three-seeded bulk YBCO (HTS) with dimensions of 64 mm x 33 mm x 14 mm was divided into three equal slices to obtain the appropriate magnetic flux distribution. The (MB_pulse)*(t/tou)*exp(1-(t/tou)) function was used in COMSOL Multiphysics 6.2 for magnetic field trapping in three-seeded YBCO sample, where MB_pulse and tou represent pick value of pulse magnetic flux density and time constant respectively. The magnetic flux trapped bulk YBCO was moved at different speeds (up to 600 km/h) on an aluminum rail of certain thickness and the magnetic levitation and magnetic drag forces were calculated using Lorent's law in "Rotating Machinery, Magnetic (rmm)" physics in COMSOL. The conventional levitation and drag force curve depending on the velocity were obtained as in PMG-Aluminium rail configuration for EDS maglev system [2]. It is also seen that levitation and drag forces can reach optimum values by changing the magnetic flux orientations and geometries of magnetic flux trapped YBCO superconductors.

Acknowledgement

This work and the attendance in to the conference were supported by the Scientific and Technological Research Council of Türkiye (TUBITAK), with project number of 122F432 and the Scientific Research Projects Coordination Unit of Karadeniz Technical University with project No. FBA-2021-9814.

References

[1] K. Ozturk, A. Badía-Majós, M. Abdioglu, D.B. Dilek, H. Gedikli, *Experimental and numerical investigation of levitation force parameters of novel multisurface Halbach HTS–PMG arrangement for superconducting Maglev system*, IEEE Transactions on Applied Superconductivity, **31(7)**, 1-12 (2021).

[2] L. Beauloye, B. Dehez, *Permanent magnet electrodynamic suspensions applied to maglev transportation systems: A review*, IEEE Transactions on Transportation Electrification, **9(1)**, 748-758 (2022).

Novel Functional Magnetic Materials- Basic Approach and Applications I

30.04.2024 TUESDAY

Abstract ID: 1088

GIANT MAGNETOSTRAIN AND MAGNETOELECTRIC EFFECTS IN PARTICULATE Ni-Mn-Ga/POLYMER COMPOSITES

Volodymyr Chernenko[1-3], Victor L'vov[4], Senentxu Lanceros-Mendez[1,2], Hideki Hosoda[5]

[1]*Basque Center for Materials, Applications and Nanostructures and University of Basque Country, Leioa 48940, SPAIN*
[2]*Ikerbasque, Basque Foundation for Science, Bilbao 48009, SPAIN*
[3]*Int. Res. Frontiers Initiative, Tokyo Institute of Technology, Yokohama 226-8503, JAPAN*
[4]*Institute of Magnetism NASU and MESU, Kyiv, 03142, UKRAINE*
[5]*Institute of Innovative Research, Tokyo Institute of Technology, Yokohama 226-8503, JAPAN*
E-mail: vladimir.chernenko@gmail.com

We will overview and analyse the latest advances in the research field of ferromagnetic shape memory alloys (FSMAs), particulalrly related to the development of multifunctional NiMnGa/polymer composites.

1. The technological details and know-how for elaboration of the magnetostrain active NiMnGa particles/polymer composites as novel actuator materials will be outlined [1,2]. A specially designed route was proposed to fabricate the single crystalline microparticles of NiMnGa FSMA which enabled a magnetic field induced strain (MFIS) of bulk NiMnGa/silicone composite equal to 4% in the field of 0.9 T. This MFIS was reversible after field removal giving rise to the new outstanding effect of composite which we called as a magnetic field induced rubber-like behavior. The mechanism of this effect has been clarified by X-ray microCT 3D imaging. Such composites can be implemented in novel actuators or haptic devices.

2. Thin film composites containing an ensemble of NiMnGa particles distributed in the P(VDF-TrFE) piezopolymer were found to exhibit an unprecedented resonance amplification of the magnetoelectric (ME) signal [3,4]. The giant values of ME coefficient equal to 18.0 and 6.05 $V \cdot cm^{-1} \cdot Oe^{-1}$ under AC magnetic drive field of 0.2 Oe and DC bias field of 485 and 1300 Oe were experimentally measured in the austenitic and martensitic states of particles, respectively. The physical mechanism of the proposed ME response amplification has been disclosed theoretically considering the influences of magnetic susceptibility and volume magnetostriction exhibiting by the Ni-Mn-Ga particles on the resonant elastic oscillation of the piezoelectric polymer matrix. Such composites can be used, e.g., for vibration energy harvesting.

References

[1] P. Sratong-On, V.A. Chernenko, J. Feuchtwanger, H. Hosoda. Sci. Rep. **9**, 1 (2019).
[2] D.K. Han, W.-T. Chiu, M. Tahara, V. Chernenko, S. Lanceros-Mendez, H. Hosoda. Sci. Rep. **13**, 7160 (2023).
[3] P. Martins, A. C. Lima, V.A. L'vov, N. Pereira, P Sratong-on, H. Hosoda, V. Chernenko, S. Lanceros-Mendez. Appl. Mater. Today **29**, 101682 (2022).
[4] V.A. L'vov, P. Martins, N. Pereira, Díez Ander Garcí, H. Hosoda, V. Chernenko, S. Lanceros-Mendez. Composites Science and Technology **241,** 110101 (2023).

Abstract ID: 1250

MAGNETICALLY BISTABLE MICROWIRES FOR MINIATURIZED CONTACTLESS SENSORS

R. Varga[1,2]

[1]RVmagnetics a.s., Nemcovej 30, 040 01 Kosice, SLOVAKIA
[2]CPM TIP UPJS, Tr. SNP 1, 040 01 Kosice, SLOVAKIA
E-mail: varga@rvmagnetics.com

Modern applications in industry, medicine or information technology require materials which, in addition to their mechanical, electrical, magnetic and other functional properties, are also characterized by the ability to provide information about their condition. Modern physics recognizes several new physical processes that can be advantageously used to produce such multifunctional materials.

Wire shape of any materials brings advantages in easy automation of large production and simplicity of further applications in automatic production of equipment [1]. One of such materials is glass-coated microwire with positive magnetostriction. These are characterized by a unique magnetization process - the movement of a single domain wall along the entire wire [1]. Understanding the movement of single domain wall at high speeds and its dependence on external parameters subsequently allows the use of microwires as contactless sensors of temperature, stress, magnetic field, etc [2].

Within this contribution we will describe all advantages and disadvantages of applications based on magnetically bistable microwire. Magnetic bistability, that allows for separation of magnetic field and temperature/stress contribution, shape of the signal, that simplifies reading and leads to the possibility to transform the measured parameter (temperature, stress, magnetic field) into time.

Different applications of contactless sensors for temperature, stress, magnetic field, electrical current, position, humidity, etc. will be presented. Simple cheap electronics will be introduced that allows for construction of unique passive contactless sensors in medicine [3], engineering [4], IT, automotive, and many other areas.

Acknowledgement

This work was partially supported by the project APVV-16-0079 of the Slovak Research and Development Agency, and project VEGA 1/0180/23 of the Scientific Grant Agency of the Ministry of Education, Science, Research and Sport of the Slovak Republic.

References

[1] J. Alam *et al.*, Journal of Magnetism and Magnetic Materials, **513**, 167074 (2020).
[2] R. Jurc *et al.*, Sensoric *Application of Glass-coated Magnetic Microwires, in Magnetic Nano- and Microwires* (2nd Edition), (Woodhead Publishing, 2020).
[3] J. Milkovicova *et al.*, Sensors & Actuators: A. Physical **366**, 115007 (2024).
[4] M. Al Ali *et al.*, Measurement **208**, 112458 (2023).

Abstract ID: 1182

THERMOELECTRIC PROPERTIES OF X_2(Cs,Rb)(Bi,Sb) (X = Li, K, Na, Rb) HEUSLER ALLOYS

V. Buchelnikov, V. Sokolovskiy, D. Baigutlin

Chelyabinsk State University, Dept. of Cond. Matter Physics, 454001, Chelyabinsk, RUSSIA
E-mail: buche@csu.ru

The main problem of application of thermoelectric (TE) materials is related to their efficiency. The figure of merit ZT of most TE materials at 300 K is small [1]. The ZT for SnSe single crystal is 2.6 at 923 K [2]. At 300 K the ZT of SnSe single crystal is equal to 0.12. So, there is a problem of searching the TE materials with large ZT at 300 K. For SnSe crystal, the ZT at 300 K can be increased up to 1.2 by application of pressure [3]. The half-Heusler alloys are also promising for TE applications [4]. However, the maximum of ZT for half-Heusler alloys is about 1.5 for high temperatures. At 300 K the ZT of half-Heusler alloys is very small. Full Heusler compounds are also promising TE materials. However, the high thermal conductivity of the lattice, leading to limited TE efficiency, still prevents their widespread use in practical applications. Recently, new full Heusler alloys with low lattice thermal conductivity have been predicted [5,6]. In this work the TE properties of new full Heusler alloys X_2(Cs,Rb)(Bi,Sb) (X = Li, K, Na, Rb) are investigated within DFT calculations and BoltzTraP2 code. It is shown that the lattice thermal conductivity at 300 K is low than 1 W/mK (Fig. 1). This results in large ZT of alloys which can achieves the value about 3 or large (Fig. 1).

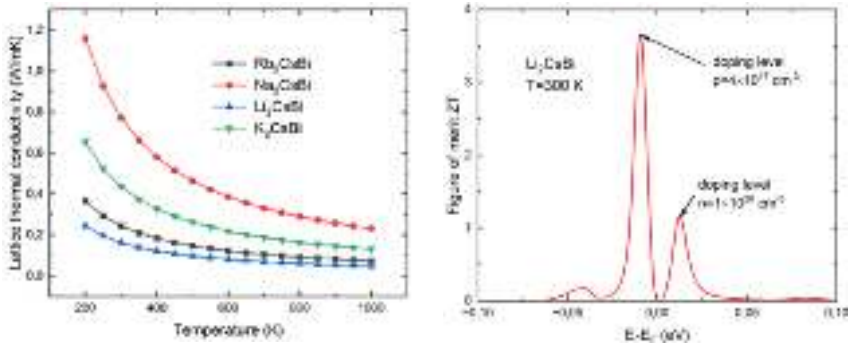

Fig. 1: *Calculated lattice thermal conductivity for X_2CsBi (X = Li, K, Na, Rb) as a function of temperature (left panel) and figure of merit as a function of chemical potential for Li_2CsBi (right panel) at constant electron relaxation time 10^{-13} s.*

This work was supported by the Russian Science Foundation (project No. 22-12-20032, https://rscf.ru/project/22-12-20032/).

References

[1] Liuyijie Huang, *et al.*, Thermal Sci. and Eng. Progress **45,** 102064 (2023).
[2] L.-D. Zhao, *et al.*, Nature **508**, 373 (2014).
[3] Jinlong Ma, *et al.*, Int. J. Heat and Mass Transfer **221**, 125063 (2024).
[4] G Rogl, PF Rogl: Crystals **13**, 1152 (2023).
[5] Jiangang He, *et al.*, Phys. Rev. Letters 117, 046602 (2016).
[6] Shuming Zeng, *et al.*, Int. J. Heat and Mass Transfer **217**, 124628 (2023).

Novel Functional Magnetic Materials- Basic Approach and Applications II

30.04.2024 TUESDAY

Abstract ID: 1398

MAGNETIC AND OPTICAL PROPERTIES OF COMPOSITE FERROMAGNETIC CORE-PLASMONIC SHELL NANOSTRUCTURES FOR BIO-MEDICAL APPLICATIONS

L.V. Panina[1,2], V.K. Belyaev[1], A. Anikin[1], A. Gurevich[2], V.V. Rodionova[1]

[1]*Immanuel Kant Baltic Federal University, Kaliningrad, RUSSIA*
[2]*National University of Science and Technology, MISiS, Moscow, RUSSIA*
E-mail: drlpanina@gmail.com

Nanomaterials open up new possibilities for improving methods of cancer treatment. To improve efficiency, several mechanisms of therapy has been considered based on multifunctional particle architectures. Combination of magnetic and plasmonic properties can be used for therapy involving magnetic hyperthermia and photothermia. In addition, magnetomechanical effect for point destruction of pathological cells can be exerted.

For such applications, mesoscale particles in the form of rods, tubes and discs are proposed. Such particles have a large surface area relative to volume, and when they are covered with gold or other plasmonic metals this results in an increased extinction cross section at plasmon resonance. Using as a core transition metal contributes to an increase in saturation magnetization and a high aspect ratio also provides higher magnetic anisotropy. All these factors lead to the increase of heat release during magnetic hyperthermia and photothermia. In addition, ferromagnetic particles in with anisotropic shape can transmit mechanical force to a cell when an alternating magnetic field is applied. In the present paper, a comparative analysis of the optical, magnetic and photothermal properties of several types of multifunctional particles is presented. The optical density could be tuned to produce an absorption peak at the NIR region by changing the particle shape and coating material. For example, covering the gold nanoparticles with thin magnetic shells shifts the absorption peak to the red region. Alternatively, magnetic particles of an anisotropic shape (discs, rods, tubes) covered with plasmonic metal also demonstrate enhanced red shift of plasmon resonance. Thus, Ni nanotubes covered with gold demonstrates a wide absorption region with a peak at 700 nm as shown in Fig 1. Such particles with ferromagnetic core and gold shell can be nontoxic and can give access to combined magnetic, magnetomechanic and photothermal therapies.

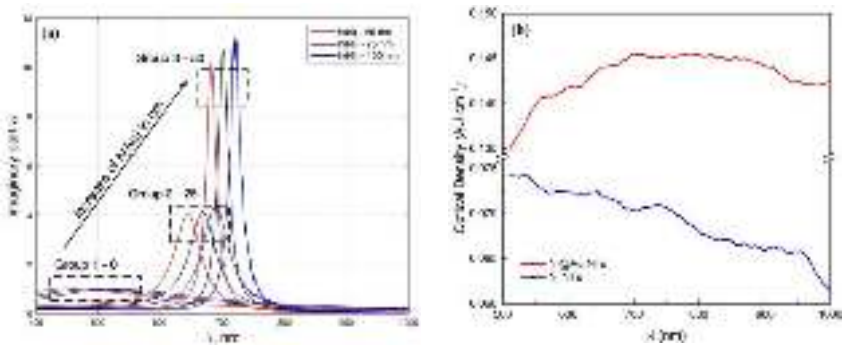

Fig. 1. *a) Calculated spectra of the imaginary part of electric polarizability of Ni NTs and Ni@Au NTs for different thickness of nickel and gold layers (inner diameter - 300 nm. b) Experimental optical density spectra of Ni NTs (blue curve) and Ni@Au NTs (red curve) with concentration of 100 μg/ml.*

Acknowledgment: the work was supported by RSF (grant No 21-72-20158).

Abstract ID: 1333

MAGNETIC STEEL HEALTH MONITORING IN THE NANO-SCALE

Angeliki Mpaliou, Tatiana Damatopoulou, Evangelos Hristoforou

Laboratory of Electronic Sensors, School of Electrical and Computer Engineering, National Technical University of Athens, Zografou Campus, Athens 15780, GREECE
E-mail: damatat5@central.ntua.gr

The aim of the current work is to demonstrate the ability of determining the number, density and distribution of dislocations and nano-precipitations in steels. Magnetization process is evidently dependent on the microstructure of the magnetic substance. The presence of dislocations and nano-precipitates affects both magnetic domain wall mobility and magnetic domain rotation. Thus, the B-H loops, the Barkhausen noise, the magnetoacoustic emission and the surface magnetic permeability of steels are modified with the level of plastic deformation, the presence of sub-grains in the grain, as well as the size and distribution of nano-precipitates in the grain. These four types of magnetic measurements are in agreement with microstructural changes observed mainly by electron back scattering diffraction (EBSD), but also with transmission electron microscopy (TEM) and XRD based stress tensor analysis. The dependence of the magnetic properties change on the microstructure is modeled with respect to the dependence of domain wall motion and domain rotation on dislocations and nano-precipitates. A typical dependence of the crystalline mis-orientation angle in a grain on the coercive field is illustrated in Figure 1, while Figure 2 shows the agreement in the increase of the Barkhausen noise with the Vicker's hardness, thus allowing for a magnetic non destructive determination of hardness in steels. As a result of the whole magnetic procedure, one may use the above mentioned magnetic techniques in order to determine the level of plastic deformation of steels, in other words the nano-cracks of steels, thus improving significantly the existing state of the art in steel non-destructive testing and offering the possibility of early stage steel health monitoring.

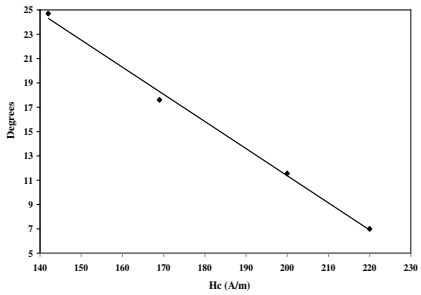

Fig. 1: *Typical dependence of the crystalline misorientation angle in a grain on the coercive field.*

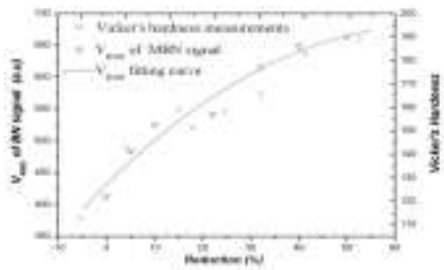

Fig. 2: *Agreement in the increase of the Barkhausen noise with the Vicker's hardness.*

Abstract ID: 1314

X-RAY MAGNETIC CIRCULAR DICHROISM IN STUDY FUNCTIONAL MAGNETIC MATERIALS

A. Rogalev, F. Wilhelm

ESRF - The European Synchrotron 38000 Grenoble, FRANCE
E-mail: rogalev@esrf.fr

Discovery of X-ray magnetic circular dichroism (XMCD) 35 years ago [1] marks a major breakthrough in magnetism research reaching objectives that previously would have been unattainable. The XMCD is obtained as a difference in the X-ray absorption spectra of a magnetized sample recorded with left and right circularly polarised photons. In a way, it may be seen as the high-energy counterpart to the magneto-optical effects in the visible discovered by Faraday and Kerr. Unlike the latters, XMCD benefits of the unique advantage to be element specific and orbital selective since it originates from transitions of a core electron of an absorbing atom into its empty states picked out via the selection rules. Furthermore, derivation of magneto-optical sum rules [2,3] has greatly strengthened the XMCD, offering a unique capability of quantitative determination of the orbital and spin contributions to the total magnetic moment carried by the absorbing atom. Availability of high fluxes of circularly polarized X-rays at the 3rd generation synchrotron radiation facilities make this technique widely available. Sophisticated end stations have facilitated its use, offering a large variety of sample environments, including high magnetic field, ultralow temperature, high pressure, etc.

Concomitant advances in X-ray instrumentation and theoretical approaches have metamorphosed XMCD from a scientific curiosity to a workhorse technique in modern magnetism research and have paved the way to further new applications of XMCD in chemistry, earth science, biology and other field of science.

Concomitant advances in X-ray instrumentation and theoretical approaches have metamorphosed XMCD from a scientific curiosity to a workhorse technique in modern magnetism research and have paved the way to further new applications of XMCD in chemistry, earth science, biology and other field of science.

Here we present only two examples that illustrate how XMCD helps to unravel magnetic properties of functional magnetic materials on an atomistic scale. The first example concerns magnetocaloric materials featuring the first order transition either purely magnetic, e.g. metamagnetic transition in MnAu2 or magneto-structural, i.e., field induced structural transformations in FeRh alloys. The second one deals with elusive metastable phases in Nd-Fe alloys that are of key importance for permanent magnet technologies.

References

[1] G. Schütz *et al.*, Phys. Rev. Lett. **58**, 737 (1987).
[2] B.T. Thole *et al.*, Phys. Rev. Lett. **68**, 1943 (1992).
[3] P. Carra *et al.*, Phys. Rev. Lett. **70**, 694 (1993).

CANCELLED

Novel Functional Magnetic Materials- Basic Approach and Applications III

30.04.2024 TUESDAY

Abstract ID: 1503

MULTIFUNCTIONAL PROPERTIES, ENERGY STORAGE EFFICIENCY AND MAGNETOELECTRIC COUPLING: A CASE STUDY OF NOVEL (1-x)$BaTiO_{3-x}BiFe_{0.95}Mn_{0.05}O_3$ NANOCOMPOSITES

Shahid Husain, Mehroosh Fatema

Department of Physics, Aligarh Muslim University, Aligarh, INDIA
E-mail: s.husaincmp@gmail.com

In high-power and pulsed electronic systems, high dielectric permittivity, and substantial energy storage efficiency serve a crucial role for potential applications. Similarly, magnetoelectric multiferroics have sparked tremendous interest due to its multifunctional applications. Magnetoelectric composites have a competitive edge over single-phase multiferroics due to greater coupling interface between the two phases. Hence, in this work, we propose the synthesis of nanocrystalline composites (1-x)$BaTiO_3$-x$BiFe_{0.95}Mn_{0.05}O_3$ ($0 \leq x \leq 0.3$) via solid state reaction route. The samples are characterized to investigate its structural, morphological, dielectric, ferroelectric, piezoelectric, magnetic and magnetoelectric properties. XRD patterns reveal successful loading of magnetic phase on the $BaTiO_3$ matrix. A dense microstructure as revealed from the FESEM micrographs, contributes to the improved dielectric and ferroelectric response of the samples. The low temperature dielectric measurements reveal distinct phase transitions with colossal rise in permittivity values of nanocomposites. The energy storage efficiency rises from 33.8% for pristine BTO to 72.5% for the 10 mol% doped nanocomposite. Piezoelectric (d_{33}) coefficients exhibit optimum values for all the samples. Strong ME coupling up to 0.42 $mVcm^{-1}Oe^{-1}$ has been attained in this system. The identified characteristics make these nanocomposites a promising candidate for energy storage and magnetoelectric devices.

Abstract ID: 1092

DEVELOPMENT OF GRADED MAGNETIC ANISOTROPY IN AMORPHOUS MICROWIRES

A. Zhukov[1,2,3,4], P Corte-Leon [1,2,3], M. Ipatov[1,2], J.M. Blanco[2,3], V. Zhukova[1,2,3]

[1]*Dept. Polymers and Advanced Materials, Univ. Basque Country, UPV/EHU San Sebastián 20018, SPAIN*
[2]*Dept. Appl. Phys., Univ. Basque Country EIG, UPV/EHU, 20018, San Sebastian, SPAIN*
[3]*EHU Quantum Center, University of the Basque Country, UPV/EHU, SPAIN*
[4]*IKERBASQUE, Basque Foundation for Science, 48011 Bilbao, SPAIN*
E-mail: arkadi.joukov@ehu.es

Soft magnetic materials are demanded for numerous applications [1,2]. Therefore, studies of magnetic wires have attracted great interest owing to outstanding magnetic properties, like the giant magnetoimpedance (GMI) or the magnetic bistability and related single domain wall (DW) propagation. These properties make them quite attractive for a number of technological applications [1,2]. An important advantage of the glass-coated magnetic microwires prepared using the Taylor-Ulitovsky technology is that the wire diameter can be significantly reduced (an order of magnitude). Another advantages of such microwires are better corrosion resistance and mechanical properties. Therefore, such microwires are suitable for emerging applications including biomedicine, non-destructive control of external stimuli (stress, temperature) in smart composites, magnetic memories and logics, magnetic and magnetoelastic sensors or electronic surveillance [2,3].

Recently we observed that, the hysteresis loops Fe-rich microwires are substantially affected by the stress-annealing conditions (temperature or stress). In Co-rich microwires even conventional annealing at different temperatures produce similar modification of the hysteresis loops [2]. Therefore, we proposed simple method to prepare glass-coated microwires with graded magnetic anisotropy by annealing at variable temperature [2]. Previously, graded magnetic anisotropy was obtained by rather sophisticated method involving modification of the chemical composition during the sample preparation [4]. Magnetic materials with a graded magnetic anisotropy presenting controllable spatial distribution of the magnetic anisotropy can show unusual magnetic properties, like controllable nucleation or pinning of domain walls [2,5].

We have studied the magnetic properties and domain wall dynamics in Fe-rich and Co-rich microwires subjected to stress-annealing. For the wires stress-annealed at variable temperatures we obtained a graded magnetic behavior with local hysteresis loops shapes and properties (coercivity, remanent magnetization) changing along the sample length. In the samples subjected to local stress-annealing we created an artificial source of DW injection allowing the manipulation of the DW dynamics. The observed stress-induced anisotropy could be related to the internal stresses relaxation after annealing and the interplay of compressive "back-stresses" arisen after stress annealing and axial internal stresses.

References

[1] K. Mohri, *et al.*, IEEE Trans. Magn., Mag, **26**, 1789-1781 (1990).
[2] A. Zhukov, *et al.*, J. Phys. D: Appl. Phys., **55**, 253003 (2022).
[3] M.H. Phan, H.X. Peng, Progr. Mater. Sci., **53**, 323-420 (2008).
[4] C.L. Zha, *et al.*, J. Appl. Phys. Lett. **97**, 182504 (2010).
[5] R. Skomski, T.A. George, D.J. Sellmyer, J. Appl. Phys. 2008, **103**, 07F531 (2008).

Abstract ID: 1107

INFRARED STUDY OF CARRIERS DYNAMICS IN DILUTED MAGNETIC SEMICONDUCTOR $(Ba_{1-x}K_x)(Zn_{1-y}Mn_y)_2As_2$

Z.Y. Liao, X.G. Qiu

Beijing National Laboratory for Condensed Matter Physics, Institute of Physics, Chinese Academy of Sciences, P.O. Box 603, Beijing 100190, CHINA
E-mail: xgqiu@iphy.ac.cn

Dilute magnetic semiconductors (DMSs) with carrier-mediated ferromagnetism has triggered much interest due to great potential for spintronics application. Understanding the ferromagnetism (FM) induced by the charge carriers will guide us for increasing the Curie temperature of DMSs. Here, with infrared spectroscopy we systematically study the optical conductivity of 122-type DMSs $(Ba_{1-x}K_x)(Zn_{1-y}Mn_y)_2As_2$. A remarkable mid-infrared broad peak centered around 0.25 eV can be observed, which derives from the As-4p valence-band states to the unoccupied Mn-3d states. As the temperature drops down to FM phase, the spectral weight of Drude component transfers to the mid-infrared Lorentz part, indicating a localization of charge carriers. It may originate from the strong p-d exchange at low temperature. When increasing K-doping, the Drude spectral weight increases and the Curie temperature enhances. These results support the p-d exchange model to describe the carrier-mediated ferromagnetism in $(Ba_{1-x}K_x)(Zn_{1-y}Mn_y)_2As_2$.

Abstract ID: 1308

EFFECT OF ATOMIC ARRANGEMENT IN THE A2 CRYSTAL STRUCTURE ON THE MAGNETOSTRICTION CONSTANT OF $Fe_{90.625}Z_{9.375}$ (Z = Ga, Ge) ALLOYS

M. Matyunina, M. Zagrebin, V. Sokolovskiy, V. Buchelnikov

Chelyabinsk State University, 454001, Chelyabinsk, RUSSIA
E-mail: matunins.fam@mail.ru

Multifunctional iron-based compounds are of interest due to their unusual mechanical, magnetic, electrical, and magnetostrictive properties [1–4]. The addition of a non-magnetic element such as Ga or Ge leads to a significant increase in the magnitude of magnetostriction [2,5]. The magnetostriction curve of Fe-Ga alloys demonstrates two peaks of magnetostriction λ_{001} at 19 at.% and 27 at.% of Ga content [2], [4,5]. The Fe-Ge systems exhibit only one peak at 10 at.% of Ge content [2,6]. According to the experimental results for $Fe_{100-x}Z_x$ (Z = Ga, Ge) alloys in the range of 0-10 at.%, A2 phase is predominant for all these alloys [7]. In this work, using density functional theory implemented in the VASP software package [8,9], we assessed the influence of the arrangement of atoms in the crystal structure of A2 alloys $Fe_{90.625}Z_{9.375}$ (Z = Ga, Ge) on the magnetostriction constant λ_{001}. The generalized gradient approximation in the PBE scheme [10] was used for treating exchange correlation effects. Geometric optimization and calculation of the magnetocrystalline anisotropic energy (E_{MCA}) were done for the A2 structure (#229 group of symmetry) with the 32 atom-supercell for $Fe_{90.625}Z_{9.375}$ composition ($Fe_{29}Z_3$ in terms of the supercell approach) in three different configurations. The spin-orbit coupling was included in calculating the $E_{MCA.}$ Expressions from [11] were used to estimate magnetostriction, and E_{MCA} was defined as the energy difference of the system with the spin orientation of Fe atoms along the [001] and [111] directions.

In the $Fe_{90.625}Ge_{9.375}$ alloy, the maximum value of $\lambda_{001}=14.34\times10^{-6}$ was found for the configuration with the "$D0_3$-type" arrangement of atoms in the A2 structure. The second largest magnetostriction value of -11.98×10^{-6} belongs to the configuration with "B2-type" ordering. In the Fe-Ga alloy, the maximum λ_{001} was found for the most energetically favorable configuration with the "$D0_3$-type" arrangement of atoms and is 37.01×10^{-6}. The experimental value in $Fe_{91.4}Ga_{8.6}$ alloy is 64×10^{-6} [2] and 45×10^{-6} in the $Fe_{91}Ge_9$ alloy [2].

Support by the Ministry of Science and Higher Education of the Russian Federation within the framework of the Russian State Assignment under contract No. 075-00187-24-00 is acknowledged.

References

[1] G. Petculescu *et al.*, J. Appl. Phys., **105**, 07A932-2 (2009).
[2] J.B. Restorff *et al.*, J. Appl. Phys., **111**, 023905-12 (2012).
[3] I.S. Golovin *et al.*, J. Alloys Compd., **688**, 310-319 (2016).
[4] T.A. Lograsso *et al.*, J. Alloys Compd., **350**, 95-101 (2003).
[5] A.E. Clark *et al.*, J. Appl. Phys., **93**, 8621-8623 (2003).
[6] D. Wu *et al.*, J. Appl. Phys., **10**, 07B307-3 (2008).
[7] O. Kubaschewski., *Iron-Binary Phase Diagrams*, (Springer-Verlag, Berlin, 1982).
[8] G. Kresse, J. Furthmuller, Phys. Rev. B., **54**, 11169 (1996)
[9] G. Kresse, D. Joubert, Phys. Rev. B, **59**, 1758 (1999)
[10] J.P. Perdew *et al.*, Phys. Rev. Lett., **77,** 3865 (1996).
[11] M. Matyunina *et al.*, JMMM, **476**, 120–123 (2019).

Novel Functional Magnetic Materials- Basic Approach and Applications IV

30.04.2024 TUESDAY

Abstract ID: 1534

EXPLORING THE MAGNETO-VOLUME ANOMALIES AND THE MAGNETIC PROPERTIES OF R_2Fe_{17} INTERMETALLIC ALLOYS USING LARGE SCALE FACILITIES

Pedro Gorria[1], Pablo Alvarez-Alonso[1], José L. Sánchez Llamazares[2], Jesús A. Blanco[1]

[1]*Department of Physics, Faculty of Sciences, University of Oviedo, 33007 Oviedo, SPAIN*
[2]*División de Materiales Avanzados, IPICYT, San Luis Potosí 78216, MEXICO*
E-mail: pgorria@uniovi.es

Although the 'INVAR effect' was discovered at the end of XIX century, still today there is an intense research activity in this topic at the crossover between Solid State and Materials Science. This effect, primarily investigated by Guillaume in a ferromagnetic fcc $Fe_{65}Ni_{35}$ binary alloy, consists of an almost constant -'invariant'- lattice parameter or unit cell volume of the material (nearly zero or low thermal expansion, LTE) in a wide temperature range just above the Curie temperature [1]. INVAR alloys are commonly exploited as functional materials for applications requiring temperature-independent geometry (i.e. precision sensors for aerospace technology or high-resolution screens). Therefore, the search for new INVAR materials and/or new processing methods to enlarge the temperature range for LTE above room temperature is a current challenging issue [2]. Moreover, ferromagnetic INVAR materials display other anomalies in their physical properties, such as the negative pressure dependence of the Curie temperature and the hyperfine field distribution, the elastic moduli or the heat capacity among others, which are commonly referred to as *magneto-volume anomalies* [1].

R_2Fe_{17} compounds (R = rare earth) exhibit a variety of magnetic behaviors (ferro-, antiferro-, or ferri-magnetic and more complex magnetic orderings such as helimagnetism or fan magnetic structures) depending on the rare earth element [3]. Likewise, all of them display large magneto-volume anomalies induced by the strong dependence of the magnetic exchange interaction on the Fe-Fe interatomic distances [4,5]. In addition, these binary intermetallics show a moderate magneto-caloric effect, MCE, with values of the magnetic entropy change, ~ 6 $Jkg^{-1}K^{-1}$ (for $\mu_o\Delta H$ = 5 T) at room temperature (for R = Nd, Pr) [6-8].

In this talk we will show our investigations on the magneto-volume anomalies and the magnetic properties of R_2Fe_{17} alloys in polycrystalline, nanostructured and rapid quenched samples using neutrons and synchrotron radiation facilities under extreme conditions (*T* and *P*).

We acknowledge the financial support from MICINN (Spain) and CONACyT (Mexico).

References

[1] E.F. Wassermann, J. Magn. Magn. Mater. **100**, 346 (1991).
[2] P. Gorria *et al.,* Phys Rev. B **69**, 214421 (2004); *ibid* **80**, 064421 (2009).
[3] K.H.J. Buschow Rep. Prog. Phys. **40**, 1179 (1977).
[4] P. Gorria *et al.,* Acta Mater. **57**, 1724 (2009).
[5] P. Alvarez-Alonso *et al.,* Phys Rev. B **86**, 184411 (2012); Acta Mater. **61**, 7931 (2013).
[6] P. Alvarez, P. Gorria *et al.,* J. Phys.: Condens. Matter **22**, 216005 (2010).
[7] C.F. Sánchez-Valdes *et al.,* Appl. Phys. Lett., **104**, 212401 (2014).
[8] J.L. Garrido- Alvarez *et al.,* J. Alloys Compd., **979**, 173575 (2024).

Abstract ID: 1483

SEMICONDUCTOR NANOPARTICLES FOR ANALYTICAL CHEMISTRY

O.A. Goryacheva

Saratov State University, Institute of Chemistry, 410012, Astrakhanskaya 83, Saratov, RUSSIA
E-mail: olga.goryacheva.93@mail.ru

Quantum dots (QDs) are semiconductor nanocrystals with unique optical properties. Typically, the core and the shell are composed of type II–VI, IV–VI, and III–V semiconductors. However, a crystal can also consist of three-component systems including precious metals. The use of QDs in analytical chemistry and bioanalysis is due to a wide absorption spectrum, unified synthesis, high fluorescence quantum yield, and the ability to vary the fluorescence color shift during synthesis. Most QDs are obtained by high-temperature organic synthesis and are ultimately colloidally stable in organic solvents. For use in test methods, particles that are stable in water, buffers and biological fluids are needed.

Several hydrophilization methods exist for QDs, which allow them to be used in analytical methods based on fluorescence detection. Different approaches allow you to optimize the test system for analytes.

Silanization is the process of coating a QD with a hydrophilic shell using the ligand exchange method. The shell thickness process can be varied at the synthesis stage due to the number of reagents and parameters of the inverse microemulsion [1]. Siloxanes with modifying groups make it possible to obtain a hydrophilic surface and different groups are capable of conjugation. Antibody conjugation is used in ELISA and LFIA [2]. Several analytes can be detected on a test strip due to different fluorescence colors. In this way, both low-molecular substances and proteins can be detected [3].

Use of thinner shells such as short-chain polymers. Such structures are used for non-radiative energy transfer. Förstor resonance energy transfer is realized through a pair of quantum dots as a donor and gold nanoparticles as an energy acceptor. Immunochemical test methods maintain low detection limits even in small sample volumes [4].

Mercapto groups on the surface of a QD allow it to be used as an independent detector. The AgInS structure can be obtained with these groups during synthesis; cadmium containing QDs require an additional hydrophilization step. Detection occurs due to the quenching of QD fluorescence when an analyte attaches to the QD surface. The presence of anthracycline antibiotics may be limited in buffers and biofluids[5].

The reported study was funded by the Russian Science Foundation: project number 21-73-10046.

References

[1] O.A. Goryacheva, *et al.*, Anal. Bioanal. Chem. 1–13 (2022).
[2] O.A. Goryacheva, *et al.*, ACS Appl. Mater. Interfaces **12**, 24575–24584 (2020).
[3] O.A. Goryacheva, *et al.*, Talanta Open **7**, 100186 (2023).
[4] O.A. Goryacheva, *et al.*, Talanta **225**, 121973 (2021).
[5] S.A. Mescheryakova, *et al.*, Biosensors **13**, 596 (2023).

CANCELLED

Abstract ID: 1619

CIRCULAR MAGNETIZATION IN Co-BASED AMORPHOUS WIRES

M.A. Nemirovich[1], N.A. Yudanov[1], E.I. Nefedova[1], Vlada V. Miroshkina[2], L.V. Panina[1,3]

[1] National University of Science and Technology, MISIS, Moscow, RUSSIA
[2] Saint Petersburg Electrotechnical University "Leti", RUSSIA
[3] Research and Educational Center "Smart Materials and Biomedical Applications", Immanuel Kant Baltic Federal University, Kaliningrad, RUSSIA
E-mail: drlpanina@gmail.com

Co-based amorphous wires are one of the best materials which exhibit large and sensitive magnetoimpedance effect. This is based on specific change in circular magnetisation caused by axial magnetic field. This justifies interest in studying the circular magnetisation reversal at elevated frequencies up to 250 kHz. In this paper, the influence of such factors as excitation frequency, annealing current, conductor length, and external magnetic field on circular magnetization in Co-rich amorphous wires with glass cover have been investigated. Analysis of various permeability parameters made it possible to decompose the magnetization process into domain wall displacements (reversible and irreversible) and magnetisation rotation.

$Co_{66.6}Fe_{4.28}B_{11.51}Si_{14.48}Ni_{1.44}Mo_{1.69}$ amorphous wires of varying length 10-50 mm with slightly negative magnetostriction were used in these experiments. An AC current is applied to the wire, which produces an easy-axis driving circular magnetic field. For relatively low frequencies when the skin effect is not very strong the inductive component V_L of the voltage across the wire is proportional to the change in the circular magnetisation. The induced circular magnetisation reversal can be measured by filtering out an inductive voltage signal across the wire using well-known balanced bridge circuit technique. Then, only the magnetic contribution to V_L is measured. Integrating the voltage signal yields the circular magnetisation loops. Inverse dependences of the voltage amplitude on the frequency of the applied current in the range of 50-250 kHz were obtained due to increase in the domain wall damping.

Experiments have confirmed that changes in the microwire structure, such as those caused by current annealing, have a significant effect on the induced voltage. A decrease in the amplitude of this voltage was observed with increasing annealing current, which indicates suppression of circumferential anisotropy. A linear dependence of the increase in the amplitude of the output voltage on the length of the microwire was obtained.

Additionally, it was found that the external magnetic field H_{ex} has a significant influence on the induced voltage: with its increase, a sharp decrease in the signal amplitude was observed. On the other hand, examining the hysteresis loops demonstrates that the application of H_{ex} activates the rotational processes, confirming two competing processes contributing to MI.

Non-linear circular magnetization results in generation of higher frequency harmonics which show stronger dependence on H_{ex}, which can be directly used in sensor construction.

References

[1] L.V. Panina, H. Katoh, K. Mohri, K. Kawashima, IEEE Trans. Magn. **29**, 2524 (1993).
[2] I. Betancourt, *I. Magnetization dynamics of amorphous ribbons and wires studied by inductance spectroscopy*, Materials, **4**, 37-54 (2011).

Theory of Superconductivity II

30.04.2024 TUESDAY

Abstract ID: 1131

DECODING THE MAJOR 122, 11,111-TYPE IRON-BASED SUPERCONDUCTORS: SUCCESSFUL SIMULATION OF PHASE DIAGRAMS AND TRANSITION TEMPERATURES

Chi Ho Wong, Rolf Lortz

Department of Physics, The Hong Kong University and Science and Technology, Hong Kong, CHINA
E-mail: chkhwong@ust.hk

This study presents a comprehensive approach to understanding the complex behavior of iron-based superconductors, which are important in the field of low-temperature physics. We amalgamate several existing theoretical models and incorporate experimental data to simulate the superconducting phase diagrams of the "122, 11, 111-type" iron-based compounds, including $Ba_{1-x}K_xFe_2As_2$, $CaFe_2As_2$, $SrFe_2As_2$, FeSe, FeSe/$SrTiO_3$, LiFeAs and NaFeAs. This model takes into account various factors such as the momentum dependence of the superconducting gap, spin-orbital coupling, antiferromagnetism, spin density wave, induced XY potential on the tetrahedral structure, and electron-phonon coupling. To improve the computational accuracy, we refine the electron-phonon scattering matrix using the ARPES data, which captures the relevant electrons involved in iron-based superconductivity. Using this innovative approach, we are able to calculate their superconducting transition temperatures as functions of pressure reasonably. In addition, this model is able to predict that $MgFe_2As_2$ remains non-superconducting regardless of the applied pressure.

References

[1] C.H. Wong, R. Lortz, Phy, Rev, Res (2023, in press).
[2] C.H. Wong, R. Lortz, Materials, **16(13)**, 4674 (2023)

Abstract ID: 1084

QUANTIFYING PROXIMITY-INDUCED SUPERCONDUCTIVITY FROM FIRST PRINCIPLE

Zheng Liu

Institute for Advanced Study, Tsinghua University, Beijing 100084, CHINA
E-mail: zheng-liu@tsinghua.edu.cn

Proximity induced superconductivity in theory and experiment has attracted much attention in recent years, and is usually modeled by the electron tunneling approximation. We discuss how this approximation can be hybridized with first-principles calculation to achieve a quantitative characterization starting from the microscopic interfacial structure. By using the graphene-Zn heterostructure as an example, we compare this approximated treatment to the full *ab inito* anisotropic Eliashberg formalism. Based on the calculation results, we discuss how superconductivity is affected by the interfacial environment.

Abstract ID: 1140

2π DOMAIN WALLS FOR TUNABLE MAJORANA DEVICES

D. Hauck[1], S. Rex[2,3], M. Garst[1]

[1]*Karlsruhe Institute of Technology, Institute for Theoretical Solid State Physics, Karlsruhe, GERMANY*
[2]*Karlsruhe Institute of Technology, Institute for Quantum Materials and Technologies, Karlsruhe, GERMANY*
[3]*Karlsruhe Institute of Technology, Institute for Theoretical Condensed Matter Physics, Karlsruhe, GERMANY*
E-mail: daniel.hauck@kit.edu

Superconductor-magnet hybrid structures provide a platform for investigating topological phases with localized Majorana states. Such states have previously been predicted for elongated Skyrmions in the magnetic layer. Here we consider 2π domain walls which are easier to realize and tweak experimentally. We show that localized Majorana states can be found in these systems and investigate possible ranges of parameters. This establishes 2π domain walls as tunable elements for the realization of Majorana devices.

Abstract ID: 1086

GINZBURG-LANDAU APPROXIMATION FOR THE HUBBARD MODEL IN THE EXTERNAL MAGNETIC FIELD

S.N. Burmistrov, L.B. Dubovskii

NRC "Kurchatov Institute", 123182 Moscow, RUSSIA
E-mail: ldubovskii@mail.ru

The Hubbard model is studied in the external magnetic field. The analysis is carried out phenomenologically within the framework of the Ginzburg-Landau theory with the order parameter describing the opposite spin electrons. The study is performed for the nearly half-filled lower Hubbard band in the metallic state. The final equations are the Pauli-like ones for the opposite spins and nonlinear as a result of interaction between electrons with the opposite spins. The equations can analytically be solved for the spatially homogeneous distributions in a number of most interesting cases. In particular, the problem on the metal-insulator transition is analyzed for the nearly half-filled Hubbard sub-bands. The critical magnetic field at which the transition from the metallic state to the insulator one takes place is found under the paramagnetic spin effect.

CANCELLED

Theory of Magnetism I

30.04.2024 TUESDAY

Abstract ID: 1160

FLAT BAND IN PYROCHLORE OXIDES: A POSSIBLE PLAYGROUND OF MAGNETISM AND SUPERCONDUCTIVITY

I. Hase

[1]*National Institute of Advanced Industrial Science and Technology, 305-8568, Tsukuba, Ibaraki, JAPAN*
E-mail: i.hase@aist.go.jp

Valence electrons in crystal usually have energy dispersion due to its itinerancy. However, in some special cases, electrons lose the energy dispersion due to the quantum interference. The resulting dispersion-less band is called as a flat band. Flat band can be seen in several lattice models, including 2D Kagome lattice and 3D pyrochlore lattice. Due to its anomalous nature, it is known that the flat band can induce many fascinating properties like quantum Hall effect, exact ferromagnetism, superconductivity, and so on [1,2].

Achieving this flat band in real materials is a challenging task. In order to achieve an electronic state similar to the above model, we focused on pyrochlore oxides with having an s-orbital in the outermost shell and performed systematic first-principles electronic state calculations. As a result, we found that many compounds, including $Sn_2Nb_2O_7$ and $Pb_2Sb_2O_7$, have nearly flat bands near the Fermi level [3,4].

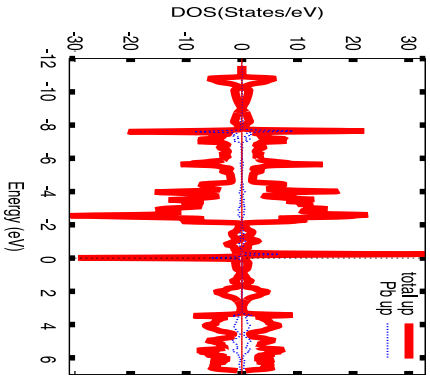

Fig. 1: *Density of States of Ferromagnetic $Pb_2Sb_2O_7$. Note that this compound does not include any magnetic atoms.*

References

[1] O. Derzhko, J. Richter, M. Maksymenko, Intl. J. Mod. Phys. B **29**, 1530007 (2015).
[2] Z. Liu, F. Liu, Y. -S. Wu. Chin. Phys. B **23**, 077308 (2014).
[3] I. Hase, T. Yanagisawa, Y. Aiura, K. Kawashima, Phys. Rev. Lett. **120**, 196401 (2018).
[4] I. Hase, Y. Higashi, H. Eisaki, K. Kawashima, Sci. Rep. **13**, 4743 (2023).

Abstract ID: 1544

INTERFACE-DRIVEN MODULATION ON 2D MAGNETIC HETEROSTRUCTURES

R. Caglayan[1], A. Mogulkoc[2], Y. Mogulkoc[3]

[1]*Ankara University, Graduate School of Natural and Applied Sciences, Dept. of Physics, 06100, Ankara, TURKEY*
[2]*Ankara University, Faculty of Sciences, Dept. of Physics, 06100, Ankara, TURKEY*
[3]*Ankara University, Faculty of Engineering, Dept. of Physics Engineering, 06100, Ankara, TURKEY*
E-mail: rcaglayan@ankara.edu.tr

Two-dimensional (2D) magnets have gained significant interest following the discovery of prominent materials such as CrI_3, $Cr_2Ge_2Te_6$, and Fe_3GeTe_2, which hold promise for state-of-the-art applications in spintronics and nanoelectronics [1]. In particular, 2D magnetic heterostructures enable precise control over magnetic properties and electronic behavior by manipulating the interfaces between the stacked layers. Such magnetic heterostructures, characterized by their high sensitivity and performance, play a pivotal role in providing the foundation for devices like magnetic tunnel junctions (MTJs) and spin valves, which enable critical applications such as magnetic random-access memory (MRAM) and hard disc drives (HDDs). The interlayer distance within heterostructures dictates magnetic coupling strength and electronic properties. Modulating this distance enables control over magnetic properties **(see Fig. 1)** and facilitates the emergence of chiral magnetic structures [2]. Due to the broken inversion symmetry together with a strong spin-orbit coupling, the significant Dzyaloshinskii-Moriya interaction (DMI) is induced at the interface of the heterostructures, which may stabilize the chiral magnetic textures. DMI driven topological chiral magnetic structures, especially skyrmions, provide high density and low energy consumption in race-track memory devices and have attracted much attention in recent years with the potential to replace conventional magnetic domain walls [3].

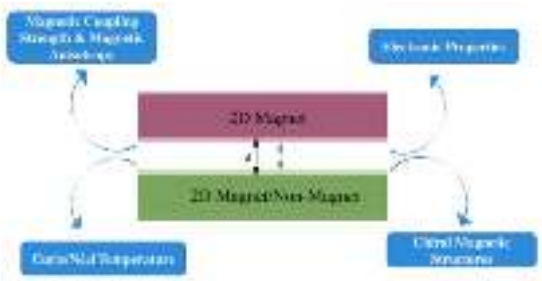

Fig. 1: *Schematic representation of interlayer-controlled modulation in 2D magnetic heterostructures.*

Acknowledgement

This work was supported by the FLAG-ERA grant MNEMOSYN, by MCIN/AEI/10.13039/501100011033 and European Union "NextGenerationEU/PRTR" under grant PCI2021-122035-2A-2a

References

[1] S. Xing, J. Zhou, X. Zhang, S. Elliott, Z. Sun, Progress in Materials Science, **132**, 101036 (2023).
[2] E. Skoropata, J. Nichols, J.M. Ok, R.V. Chopdekar, E.S. Choi, A. Rastogi, H.N. Lee, Science Advances, **6(27)**, eaaz3902 (2020).
[3] R. Tomasello, V. Puliafito, E. Martinez, A. Manchon, M. Ricci, M. Carpentieri, G. Finocchio, Journal of Physics D: Applied Physics, **50(32)**, 325302 (2017).

Abstract ID: 1294

THE EFFECT OF STRUCTURAL DISORDER ON MAGNETIC PROPERTIES OF Fe-*Z* (*Z* = Ga, Ge, Al) ALLOYS: INSIGHTS FROM *ab INITIO* AND MONTE CARLO

M.V. Matyunina, Yu.S. Tarasova, M.A. Zagrebin, V.V. Sokolovskiy, V.D. Buchelnikov

Chelyabinsk State University, 454001, Chelyabinsk, RUSSIA
E-mail: miczag@mail.ru

The magnetostrictive Fe-Ga alloys are the most popular object for investigation in the last two decades. The Fe-Ga alloys are successful magnetostrictive materials, which demonstrated two peaks of saturation magnetostriction $\lambda_{001} = 395\times10^{-6}$ and 350×10^{-6} at room temperature for compositions with $x \approx 19$ at.% and $x \approx 27$ at.%, respectively [1]. After the discovery of giant magnetostriction in Fe-Ga alloys other Fe-based alloys such as Fe-*Z* (*Z* = Ge, Al) have been investigated in more detail. Each of these alloys has magnetostriction of saturation that increases as more Fe atoms are substituted with solute atoms [2]. According to the experimental results for $Fe_{100-x}Z_x$ (Z = Ga, Ge, Al) alloys in the range of 0-10 at.% A2 phase is predominant for all these alloys [3]. Besides, the concentration dependencies of magnetostriction constant are the same for the considered alloys [4-6]. In this study, we investigate the effect of structural disorder on magnetic properties of Fe-Z (Z = Ga, Ge, Al) alloys in the A2 phase by means of the density functional theory.

The calculations were carried out by using the Vienna Ab initio simulation package (VASP) [7,8]. For the calculations, we used lattice parameters obtained by optimizing the geometry of the crystal structure taking into account the approach of 54-atom supercells. 10 configurations of A2 crystal structure (*Im-3m* no. 229 space group, prototype α-Fe) with Fe and (Ga, Ge, Al) atoms randomly distributed were considered.

As a result, magnetic properties such as magnetic moment, Curie temperatures, tetragonal magnetostriction constant λ_{001} of $Fe_{100-x}Z_x$ (Z = Ga, Ge, Al) (3.7, 5.5, 9.3 at. %) alloys have been obtained.

This work was supported by Russian Science Foundation (Project #24-22-20086).

References

[1] A.E. Clark *et al.*, J. Appl. Phys. **93**, 8621 (2003).
[2] K.H.J. Buschow, *Handbook of Magnetic Materials* (Elsevier Science B.V, Amsterdam, 2012).
[3] O. Kubaschewski, *Iron-Binary Phase Diagrams* (Springer-Verlag, Berlin, 1982).
[4] A.E. Clark *et al.*, J. Appl. Phys. **93**, 8621 (2003).
[5] J.B. Restorff *et al.*, J. Appl. Phys. **111**, 023905 (2012).
[6] E.M. Summers *et al.*, J. Mater. Sci. **42**, 9582 (2007).
[7] G. Kresse, J. Furthmuller, Phys. Rev. B. **54**, 11169 (1996).
[8] G. Kresse, D. Joubert, Phys. Rev. B. **59**, 1758 (1999).

New Phenomena and Applications in Molecular Magnets

30.04.2024 TUESDAY

Abstract ID: 1338

SWITCHABLE MOLECULAR MAGNETS: FROM FILM DEPOSITION TO COMPOSITE MATERIAL

M. Fitta[1], A. Pacanowska[1], M. Jasiurkowska – Delaporte[1], G. Wota[2], B. Nowicka[2]

[1]*Institute of Nuclear Physics, Polish Academy of Sciences, 31-342, Kraków, POLAND*
[2]*Faculty of Chemistry, Jagiellonian University, 30-387, Kraków, POLAND*
E-mail: Magdalena.Fitta@ifj.edu.pl

Molecular magnets are typically synthesized in crystal form, characterized by unfavorable mechanical properties. To explore the potential applications of these compounds, a crucial step involves their surface deposition or dispersion within an organic polymer matrix. In our research, we focused on producing thin films and nanocomposites of CN-bridged networks that exhibit switchable magnetic properties in response to variations in temperature, pressure, or humidity [1, 2]. Various physical and chemical methods were employed for film fabrication, selected based on the formation processes and stability conditions of the networks. These methods encompassed the bottom-up approach, involving in situ formation of the coordination network on the substrate surface, and the top-down approach, which included crystal size reduction through ultrasonic and mechanical homogenization, or adjustment of synthetic conditions. Our investigation delved into the impact of different deposition techniques on the film morphology and how the switchable properties of bulk samples were influenced by grain size reduction and interface interactions (Fig. 1) [3]. Additionally, we developed nanocomposites comprising coordination network particles embedded in the organic polymer matrix, presented as surface-deposited membranes or electrospun mats.

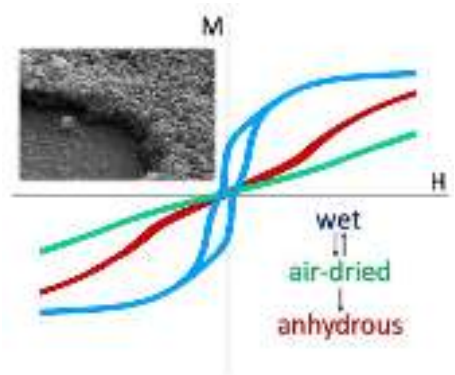

Fig. 1: *SEM images of the $[Ni(cyclam)]_3[Cr(CN)_6]_2$ film and the shape of magnetic hysteresis depending on the degree of hydration.*

References

[1] B. Nowicka *et al.*, Cryst Growth Des. **16**, 4736 (2016).
[2] M. Reczyński *et al.*, Angew. Chem. Int. Ed. **60**, 2330 (2021).
[3] A. Pacanowska *et al.*, Adv. Mater. Interfaces **10**, 2201834 (2023).

Abstract ID: 1378

CIRCUIT QED WITH MOLECULAR SPIN QUDITS

Fernando Luis

Instituto de Nanociencia y Materiales de Aragón (INMA), CSIC-Universidad de Zaragoza, 50009, Zaragoza, SPAIN
E-mail: fluis@unizar.es

Scaling up quantum processors remains very challenging, even for today's most successful platforms, on account of the need of reducing and correcting errors. Magnetic molecules can provide some competitive advantages. Molecular complexes able to encode up to 6 qubits or, in general, *d*-dimensional qudits in their electronic and nuclear spin states [1-3] can act as universal quantum processors or even correct errors [3]. Exploiting them calls for a solid-state platform to control, read-out and wire them up [3,4]. I'll discuss recent experiments aimed at achieving this goal by coupling molecular spins, mainly diluted in diamagnetic crystals, to superconducting resonators. A high cooperativity coupling to electronic and even nuclear spins has been achieved [5]. We also find that spin clock states optimize the spin-photon coupling and the isolation from magnetic noise. The results provide the basis for reading out electro-nuclear spin qudits and for implementations of quantum algorithms [4].

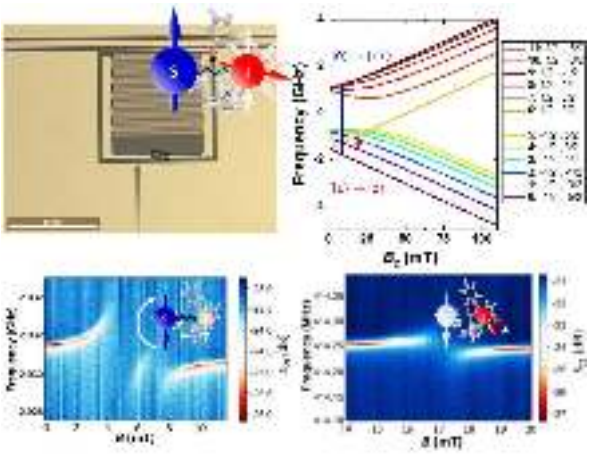

Fig. 1: *A single crystal of ^{173}Ybtrensal, which hosts an electronic spin qubit coupled to a d = 6 nuclear spin qudit, is coupled to a lumped element superconducting resonator. Microwave transmission experiments show that the spin-photon coupling reaches high cooperativity, which allows using the circuit to read out the qudit states.*

References

[1] G. Aromí, D. Aguilà, P. Gamez, F. Luis, O. Roubeau, Chem. Soc. Rev. **41**, 537 (2012).
[2] A. Gaita-Ariño, F. Luis, S. Hill, E. Coronado, Nature Chem. **11**, 301 (2019).
[3] S. Carretta, D. Zueco, A. Chiesa, Á. Gómez-León, F. Luis, Appl. Phys. Lett. **118**, 240501 (2021).
[4] A. Chiesa, S. Roca, S. Chicco, M.C. de Ory, A. Gómez-León, A. Gomez, D. Zueco, F. Luis, S. Carretta, Phys. Rev. Applied **19**, 064060 (2023).
[5] V. Rollano *et al.*, Commun. Phys. **5,** 246 (2022).

Abstract ID: 1205

TRANSFORMING BRITTLE STIMULI-RESPONSIVE CRYSTALLINE STRUCTURES INTO TEMPERATURE AND PRESSURE-SENSING COMPOSITES

A. Pacanowska[1], G. Wota[2], M. Jasiurkowska – Delaporte[1], B. Nowicka[2], M. Fitta[1]

[1]*Institute of Nuclear Physics, Polish Academy of Sciences, 31-342, Krakow, POLAND*
[2]*Jagiellonian University, Faculty of Chemistry, 30-387, Krakow, POLAND*
E-mail: aleksandra.pacanowska@ifj.edu.pl

In contemporary scientific and technological pursuits, there has been a concerted effort to explore novel multifunctional materials whose properties can be dynamically modulated by external stimuli, including light, pressure, and electric or magnetic fields. Organic-inorganic structures, synthesized through facile wet-chemistry processes, represent compelling candidates in this domain. This unique class, featuring metal-to-metal charge transfer (MMCT), showcases inherent bistability and responsiveness, making it exceptionally promising for advancing molecular switches and sensors.

To enhance the processability and stability of these materials for practical applications and integration into devices, a viable strategy involves embedding functional frameworks into polymer matrices. This approach facilitates the transformation of brittle crystals into flexible polymeric composites while preserving the functionality of the molecular systems.

In our recent investigation, attention was directed towards the multi-responsive chain-like coordination compound $\{NH_4[Ni(cyclam)][Fe(CN)_6]\cdot 5H_2O\}_n$ (where cyclam = 1,4,7,11-tetraazacyclotetradecane). This compound of poor stability demonstrates a reversible thermal MMCT phase transition with bistability in the room temperature range, characterized by a sharp and broad thermal hysteresis loop[1]. Through the application of electrospinning, sub-micro and nanoparticles of the bistable material were incorporated into fibres of poly(ε-lactone) (PCL) and poly(2-vinylpyridine-co-styrene) (P2VP-PS) (see Fig. 1). Notably, switchable properties are preserved in the composite materials, as evidenced by optical observation and magnetic measurements. Furthermore, the polymer matrix increases the stability of the compound expanding its scope of applicability as a working temperature or pressure sensor.

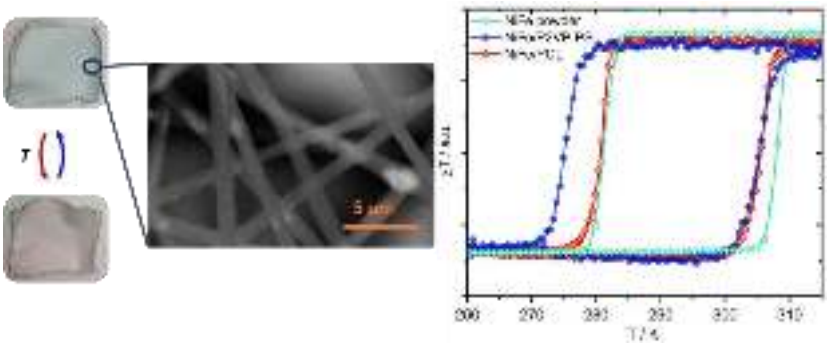

Fig. 1: *Left image: Photographs and SEM image of eletrospun fibres loaded with* $\{NH_4[Ni(cyclam)][Fe(CN)_6]\cdot 5H_2O\}_n$ *Right image: Comparison of magnetic susceptibility measurement of loaded electrospun fibres of PCL and P2VP-PS and compound as powder.*

References

[1] M. Reczyński, *et al.*, Angew. Chem. Int. Ed. **60** 2330 (2021).

Abstract ID: 1125

ROTATIONAL SYMMETRY BREAKING OF NUCLEAR MOTION IN THE JAHN-TELLER X_3 MOLECULE DUE TO CASIMIR-POLDER INTERACTION

A.D. Lyakhov[1], A.S. Ovchinnikov[1], I.G. Bostrem[1], J. Kishine[2]

[1]*Ural Federal University, Institute of Natural Science and Mathematics, 620002, Ekaterinburg, RUSSIA*
[2]*The Open University of Japan, Division of Natural and Environmental Sciences, 261-8586, Chiba, JAPAN*
E-mail: alexander.ovchinnikov@urfu.ru

The Casimir-Polder effect is the well-known phenomenon in physics that describes the attraction between a neutral atom and a surface due to quantum fluctuations [1]. Recently, it has been shown that the existence of degenerate low-lying energy atomic levels plays an important role in this effect and can lead to the Casimir torque acting on the atom [2]. A plausible way to verify this assumption is to exploit Jahn-Teller (JT) molecules. In particular, we propose to use JT X_3 molecules, belonging to the point group symmetry C_{3v}, in which the well-known linear $E \otimes e$ problem is realized [3].

When the molecule is brought close to a surface of the gyrotropic media, it experiences attraction to the surface due to the Casimir-Polder force. Special features of the rotovibrational spectrum of the JT molecule and broken time-reversal symmetry in the gyrotropic medium make it possible to realize in practice the model of rotational symmetry breaking in a Kramers twolevel system. As a result of the interaction, the molecule plane is reoriented perpendicular to the interface, and the ground-state Kramers degeneracy is lifted. The new stable state has a broken rotational (time-reversal) symmetry, which leads to the appearance of a nonzero orbital magnetic dipole moment and the accumulation of the topological Berry phase [4].

Good candidates for testing the theory could be the alkaline trimers Li_3, Na_3, and K_3. These molecules are stable and possess the ground electronic E-term in the correct triangular configuration [5]. If so, these compounds could be attributed to temporal crystals, a concept introduced by F. Wilczek [6,7], in which the ground state of the system demonstrates repeating oscillations in time, sustained, in this case, by vacuum fluctuations of the electromagnetic field.

References

[1] H.G.B. Casimir, D. Polder, Phys. Rev. **73**, 360 (1948).
[2] M.G. Silveirinha, Phys. Rev. B **100**, 165146 (2019).
[3] I.B. Bersuker, Jahn-Teller Effect (Cambridge University Press, Cambridge, 2006).
[4] A.D. Lyakhov, A.S. Ovchinnikov, I.G. Bostrem, J. Kishine, Phys. Rev. B **108**, 115429 (2023).
[5] J.L. Martins, R. Car, J. Buttet, J. Chem. Phys. **78**, 5646 (1983).
[6] A. Shapere, F. Wilczek, Phys. Rev. Lett. **109**, 160402 (2012).
[7] F. Wilczek, Phys. Rev. Lett. **109**, 160401 (2012).

HTS Cuprates: Advances in Fundamentals and Experimental Studies III

30.04.2024 TUESDAY

Abstract ID: 1005

T-LINEAR ELECTRICAL RESISTIVITY OF HIGH-T_c CUPRATES DUE TO SCATTERING OF FERMIONS BY THE Q-BALLS

S.I. Mukhin[1,2]

[1] *NUST MISIS, Dept. of Theoretical Physics and Quantum Technologies, 119049, Moscow, RUSSIA*
[2] *Leiden University, Lorentz Institute, 2300 RA Leiden, THE NETHERLANDS*

Proposed by the author Q-ball mechanism of the pseudogap state and high-T_c superconductivity in cuprates [1,2] was recently supported by comparison [3,4] with micro X-ray diffraction data in $HgBa_2CuO_{4+y}$ obtained earlier [5]. This provides a remarkable opportunity to investigate X-ray diffraction produced by the quantum thermodynamic time crystals represented by the Euclidean Q-balls considered in the aforementioned theory. It is demonstrated in the present work, that T-linear and T^2 temperature dependences of electrical resistivity in the Q-ball phase arise due to scattering of electrons on the condensed charge/spin fluctuations inside the Q-balls and collective motion of the charge density fluctuations respectively [6]. This gives a clue concerning possible mechanisms of the experimentally measured persistent T-linear behaviour of electrical resistivity in the strange metal phase of high-T_c cuprates above T^* followed by T^2 temperature dependence at lower temperatures above T_c [7]. New quantum field theoretical method of calculations of the resistivity due to scattering on the fluctuations is devised and used in the work.

References

[1] S.I. Mukhin, Condens. Matter **7**, 31 (2022).
[2] S.I. Mukhin, Ann. Phys. **447**, 169000 (2022).
[3] G. Campi, L. Barba, N.D. Zhigadlo, A.A. Ivanov, A.P. Menushenkov, A. Bianconi, Condens. Matter **8**, 15 (2023).
[4] S.I. Mukhin, Condens. Matter **8**, 16 (2023).
[5] G. Campi, A. Bianconi, N. Poccia, G. Bianconi, L. Barba, G. Arrighetti, D. Innocenti, J. Karpinski, N.D. Zhigadlo, S.M. Kazakov, et al., Nature, **525**, 359 (2015).
[6] S. I. Mukhin, e-print arXiv:2304.1087 (2023).
[7] N. Barišić, Y. Li, G. Yu, X. Zhao, M. Dressel, A. Smontara, M. Greven, PNAS **110**, 12235 (2013).

Abstract ID: 1509

NEW QUANTUM CRITICALITY FOR THE STRANGE METAL AND PLANCKIAN BEHAVIOUR IN HIGH TEMPERATURE SUPERCONDUCTORS

C. Di Castro

Accademia dei Lincei; Department of Physics, University of Roma "Sapienza", Pazza A. Moro Roma I-00185, ITALY
E-mail: carlo.dicastro@roma1.infn.it

After reviewing the main aspect of high temperature superconductors, I will stress how the recent high-resolution RIXS (resonant inelastic X-ray scattering) experiments have given a new impulse to the physics of cuprates [1]. In particular, the newly discovered short-range dynamical charge density fluctuations with short correlation length [2], precursors of the three-dimensional charge density waves, account for the long-standing problem of the strange metal behaviour of the cuprates [3]. Due to their broadness, charge density fluctuations mediate an almost isotropic scattering among the fermi quasiparticles. Above the superconducting critical temperature and around optimal doping, within a time-dependent Landau-Ginzburg approach, isotropic scattering provides the famous strange metal behaviour and the linear-in-T resistivity. This is realized for temperatures greater than the characteristic energy (proportional to the inverse correlation length squared and to the inverse dissipation parameter) [3]. However, the linearity in T of the resistivity and a divergent specific heath [4], are observed down to the lowest temperatures (the so called Planckian behavior) by experiments in the presence of high pulsed magnetic field to suppress superconductivity. To account of these results at low T, we must reduce the characteristic energy of the fluctuations finite by increasing the damping while the correlation length stays. Namely, we are suggesting a new paradigm [5] and [6] in contrast with the standard criticality models. Usually, the diverging correlation length is invoked to produce quantum criticality as the temperature goes to zero, here instead the strange criticality with linear in T resistivity and a diverging specific heat are accounted for by the increase of the damping parameter only. When the damping increases by lowering the temperature, the charge density fluctuations relax at longer and longer times giving rise to an anomalous criticality for a glass of small islands of charge density fluctuations correlated in time not in space.

References

[1] R. Arpaia, G. Ghiringhelli, *Charge order at high temperature in cuprate superconductors*, J. Phys. Soc. Jpn. **90**, 111005 (2021).

[2] R. Arpaia, S. Caprara, R. Fumagalli, G. De Vecchi, Y.Y. Peng, E. Andersson, D. Betto, G. M. De Luca, N. B. Brookes, F. Lombardi, M. Salluzzo, L. Braicovich, C. Di Castro, M. Grilli, G. Ghiringhelli, *Dynamical charge density fluctuations pervading the phase diagram of a copper-based high-T_c superconductor*, Science **365**, 906 (2019).

[3] G. Seibold, R. Arpaia, Y. Y. Peng, R. Fumagalli, L. Braicovich, C. Di Castro, M. Grilli, G. Ghiringhelli, S. Caprara, *Strange metal behaviour from charge density fluctuations in cuprates*, Commun. Phys. **4**, 7 (2021).

[4] Michon, *et al.*, *Thermodynamic signatures of quantum criticality in cuprate superconductors*, Nature **567**, 218222 (2019).

[5] S. Caprara, C. Di Castro, G. Mirarchi, G. Seibold, M. Grilli, *Dissipation-driven strange metal behavior*, Commun. Phys. **5**, 10 (2022).

[6] R. Arpaia *et al.*, *Signature of quantum criticality in cuprates by charge density fluctuations*, Nat Commun. **14**, 7198 (2023); https://doi.org/10.1038/s41467-023-42961-5

CANCELLED

Abstract ID: 1022

SPIN AND CHARGE CORRELATION FUNCTIONS IN HOLE-DOPED CUPRATES IN THE CLUSTER PERTURBATION THEORY

S.G.Ovchinnikov[1], V.I.Kuzmin[1], S.V.Nikolaev[2], M.M. Korshunov[1]

[1] *Kirensky Institute of Physics, Federal Research Center KSC SB RAS, 660036, Krasnoyarsk, RUSSIA*
[2] *Siberian Federal University, 660041, Krasnoyarsk, RUSSIA*
E-mail: sgo@iph.krasn.ru

The physics of high-Tc superconducting cuprates is obscured by the effect of strong electronic correlations. One way to overcome this problem is to seek an exact solution at least within a small cluster and expand it to the whole crystal. Such an approach is at the heart of cluster perturbation theory (CPT). Here, we developed CPT for the dynamic spin and charge susceptibilities (spin-CPT and charge-CPT), with the correlation effects explicitly taken into account by the exact diagonalization. We applied spin-CPT and charge-CPT to the p-d two-band Hubbard model for the cuprates obtained from the three-band Emery model and calculated one- and two-particle correlation functions, namely, electronic spectral function and spin and charge susceptibilities. The doping dependence of the spin susceptibility was studied within spin-CPT and CPT-RPA, that is, the CPT generalization of the random phase approximation (RPA). In the underdoped region, both our methods resulted in the signatures of the upper branch of the spin excitation dispersion with the lowest excitation energy at the (π, π) wave vector and no presence of low-energy incommensurate excitations. In the high doping region, both methods produced a low energy response at four incommensurate wave vectors in qualitative agreement with the results of the inelastic neutron scattering experiments on overdoped cuprates. Spin susceptibility map for Ω=0.2 and 3 doping levels from spin-CPT with 3x3 unit cell is shown in the Figure.

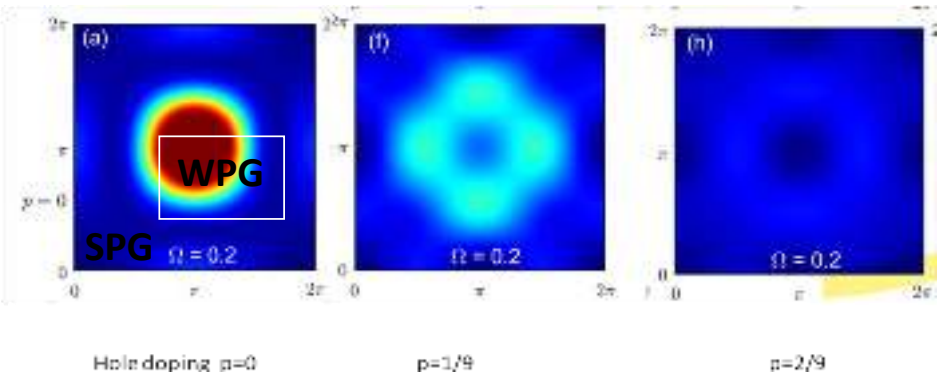

References

[1] V.I. Kuz'min, S.V. Nikolaev, M.M. Korshunov, S.G. Ovchinnikov, *One- and two-particle correlation functions in the cluster perturbation theory for cuprates*, Materials, **Vol. 16**, N Is. 13.- Ст.4640 (2023).

HTS Cuprates: Advances in Fundamentals and Experimental Studies IV

30.04.2024 TUESDAY

Abstract ID: 1649

CUPRATE UNIVERSAL ELECTRONIC SPIN RESPONSE AND THE PSEUDOGAP FROM NMR

D. Bandur, J. Nachtigal, A. Lee, S. Tsankov, J. Haase

University of Leipzig, Felix Bloch Institute for Solid State Physics, Linnestr. 5, 04103 Leipzig, GERMANY
E-mail: j.haase@physik.uni-leipzig.de

High-temperature superconductivity, in particular in the cuprates, is central to condensed matter physics, and telltale experimental laws for guiding theory are desirable. Here we report on such a universal property from the linear response of the electronic matter to a homogeneous static magnetic field. From it, two different types of carriers are identified. The universal behavior concerns the carriers from hybridized copper and oxygen orbitals that span the defining element, the CuO2 plane, of the superconducting cuprates. Their spin response is similar to that of a material independent metallic density of states which carries a temperature independent, but doping dependent pseudogap that closes beyond optimal doping. The second electronic spin component has a strong family and doping dependent density of states, and it involves only Cu (isotropic orbitals, except for La-214). The condensation of both types of carriers is interconnected and sets the critical temperature of superconductivity (T_c). The inter-planar component can condense at the same or lower temperatures compared to that of the planar component, and a certain match in density of states seems to be required for the highest T_c. The second component reminds one of the proposed involvement of another Cu axial orbital that relates to the distance or presence of the apical oxygen and the charge distribution in the CuO2 plane, which correlates with the maximum T_c, as well [1].

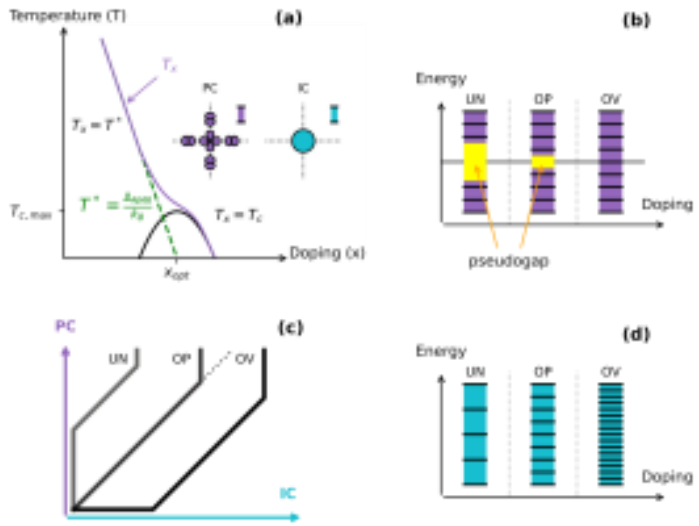

Fig. 1: *Two different types of carriers (PC, IC) are present in the cuprates. Planar carriers (PCs) are associated with the CuO2 plane; inter-planar carriers (ICs) mostly reside on Cu 4s orbitals. (a) Phase diagram with pseudogap temperature T* (from NMR). (b) PC universal density of states (DOS) with a doping dependent pseudogap. (d) IC DOS increases from under (UN) to overdoped (OV) materials. (c) Carrier condensation behavior for different doping levels.*

References

[1] D. Bandur *et al.*, arXiv:2309.11874v3

Abstract ID: 1451

CUPRATES, PNICTIDES, AND SULFOSALTS: LESSONS IN FUNCTIONAL MATERIALS

D.K. Sunko

Department of Physics, Faculty of Science, University of Zagreb, Bijenička cesta 32, HR-10000 Zagreb, CROATIA
E-mail: dks@phy.hr

Murunskite $K_2FeCu_3S_4$ is a representative sulfosalt isostructural to the pnictides, but with electronic properties more similar to the insulating parent compounds of the cuprates [1]. Here it is used as a bridge to compare the chemical and physical roles of metal and ligand orbitals in cuprates and pnictides.

In cuprates, I will argue that ionicity, covalency, and metallicity are tightly interwoven to give rise to high-temperature superconductivity (SC). Their most remarkable property is the interaction of an ionically localized hole in the Cu-O *3d-2p* bond with a Fermi liquid metallized via the Cu-O *4s-2p* bond, which is critically important for the superconducting mechanism [2]. In the pnictides, the ionic and metallic sectors are separate. The former sets the lattice spacing via the Fe *3d e2g* orbitals binding the ligands, and the second proceeds via direct *3d t2g* orbital overlaps between the iron atoms, in which superconductivity is found together with significant magnetic correlations [3]. In murunskite, the greater covalency of sulfur orbitals compensates for total disorder in the Fe atom positions, giving rise to an agglomeration of fractal magnetic clusters coexisting with perfect crystallographic order and exhibiting a surprisingly robust antiferromagnetism (AF) [4]. Because the open ligand orbitals play an important role in it, the essentially local AF of murunskite is more similar to the SC of the cuprates than to the AF of the pnictides, in which the ligands are passive.

On the basis of these examples, it is argued that the development of next-generation paradigms in functional materials must treat the physical and chemical roles of atomic orbitals on an equal footing. These meet in the dual role of the chemical potential, which simultaneously accounts for the level density of metallic carriers and for the balance of chemical reactions between constituents in the solid state. A recent insight into the physical limitations of the Hohenberg-Mermin-Wagner theorem for both magnetism and SC [5] is encouraging for the fabrication of 2D materials and heterostructures to harness such understanding.

References

[1] D. Tolj *et al.*, Applied Materials Today **24**, 101096 (2021).
[2] N. Barišić, D.K. Sunko, J Supercond. Nov. Magn. **35**, 1781–1799 (2022) and refs. therein.
[3] D.K. Sunko, J Supercond. Nov. Magn. **33**, 27–33 (2019) and refs. therein.
[4] D. Tolj *et al.*, The Surprising Magnetism of Murunskite (2024), ms. in preparation.
[5] G. Palle, D.K. Sunko, Journal of Physics A: Mathematical and Theoretical **54**, 315001 (2021).

Abstract ID: 1386

ON THE T_c OF $(La,Sr)_2CuO_4$ -BASED SUPERCONDUCTING SUPERLATTICES

S.M. Otajonov[1], D.E. Uskenbaev[2], T. Saparbaev[2], B.Ya. Yavidov[1]

[1]*Nukus state pedagogical institute named after Ajiniyaz, 230105 Nukus, UZBEKISTAN*
[2]*S. Seifullin Kazakh Agrotechnical University, 010011, Astana, KAZAKHSTAN*
E-mail: otajonovsardorbek23@gmail.com

Superconducting (SC) superlattices (SL) are promising potential structures for future electronics. The properties of SL depend on many factors. It is well known that the SC properties of SL are determined by the materials which they are made from and by the growth conditions and etc. In addition, it was found that the value of the critical temperature of SC, T_c, of $(La,Sr)_2CuO_4$ -based SC SL depends also on the number of stacking periodicity ($N_{stc.p}$) [1,2]. The latter works reported T_c of $La_{1.85}Sr_{0.15}CuO_4/Sm_2CuO_4$ (LSCO/SCO) SC SL with different $N_{stc.p}$. Namely, it was found that SC SL LSCO/SCO with $N_{stc.p}$=15/15, 30/30 and 60/60 have $T_{c,on}$ equal to 15K, 25K and 30K, respectively (for bulk LSCO $T_{c,on}$=38K). Although this and similar structures have been studied in more detail in recent decades [3,4], it cannot be said that all the properties of such structures are well understood. This concerns issues such as the influence of lattices mismatch strain, the influence of film thickness, the effect of dimensionality and etc. Another feature of these SL is that the charge carriers in LSCO are of a polaronic nature [5]. In this regard, it is useful to study the dependence of T_c of the LSCO/SCO SC SL on $N_{stc.p}$ in the light of bipolaronic superconductivity, as an alternative to the de Gennes-Werthamer (dGW) theory [6,7]. Such a study becomes even more relevant if we take into account that the dGW theory underestimates T_c at small $N_{stc.p}$ (corresponding film thickness <15 nm). For this reason, we have studied the dependence of T_c of the LSCO/SCO SC SL on $N_{stc.p}$ within the framework of extended Holstein-Hubbard model and bipolaronic scenario of high-T_c superconductivity. The basic idea and methodology of our study can be found in our recent paper [8]. In our consideration T_c of LSCO/SCO SC SL is associated with the Bose-Einstein condensation (BEC) temperature, T_{BEC}, of an ideal gas of the intersite bipolarons and correspondence between $N_{stc.p}$ and LSCO thin film thickness (d_f) in SL is established via formula $d_f = c_f\ N_{stc.p}/2$. For the estimation of T_{BEC} we used the following lattice parameters: for LSCO a_b=0.378 nm and c_b=1.323 nm, for SCO a_s=0.391 nm. The Cu-O_{apex} distance of bulk LSCO is set to be equal to 0.241115 nm which is a characteristic scale for the LSCO lattice. In addition, we set T_{BEC}=38K for the very thick LSCO film (1 mm) in SL. We calculated T_{BEC} at different film thicknesses (d_f) and found that T_{BEC} of SL with 15/15, 30/30 and 60/60 stacking periodicity equals to 17.07K, 23.81K and 29.05K, respectively. These findings clearly signal on the existence of certain correlation between $T_{c,on}$ and T_{BEC}. We hope to obtain even better agreement with experiment by performing calculations taking into account the subtle features of the crystal lattice. The detailed numerical work on the issue is in progress.

References

[1] H. Tabata *et al.*, Appl. Phys. Lett. **58**, 1444 (1991).
[2] H. Tabata *et al.*, Phys. Rev. Lett. **70**, 2633 (1993).
[3] O. Yuli *et al.*, Phys. Rev. Lett. **101**, 057005 (2008).
[4] K. Sen *et al.*, Phys. Rev. B **95**, 214506 (2017).
[5] A. Bussmann-Holder *et al.*, Eur. Phys. Lett. **101**, 47004 (2013).
[6] P.G. de Gennes, Rev. Mod. Phys. **36**, 225 (1964).
[7] N.R. Werthamer, Phys. Rev. **132**, 2440 (1963).
[8] B. Yavidov, D. Khajibaev, J. Low Temp. Phys. **213**, 291 (2023).

CANCELLED

HTS Cuprates: Advances in Fundamentals and Experimental Studies V

30.04.2024 TUESDAY

Abstract ID: 1245

REVEALING COLLECTIVE ELECTRONIC ORDERING IN SPACE AND TIME

W. Hu

National Synchrotron Light Source II, Brookhaven National Laboratory, 11973, Upton, NY, USA
E-mail: wenhu@bnl.gov

The Fluctuations are widely believed to provide the key to address significant unresolved questions in condensed-matter physics and materials science, such as the role of thermal fluctuations and material defects in magnetic materials or the role of fluctuations and nanometre-scale material inhomogeneities in high-T_c superconductivity. To image fluctuating dynamics, we developed a new analysis technique, named coherent correlation imaging (CCI) [1], to directly image fluctuating and dynamic collective electronic ordering in materials with high time and space resolution. To develop and demonstrate the CCI method, we applied CCI to study previously inaccessible magnetic fluctuations in a highly degenerate magnetic stripe domain state with nanometer-scale resolution (Fig. 1(a)). It resulted in direct visualization of domain wall dynamics for the first time. Our spatiotemporal data enable us to reconstruct the pinning energy landscape (Fig. 1(b)) and to thereby explain the dynamics observed on a microscopic level. Moreover, CCI paves the way for addressing some large fundamental questions, such as the contribution of pinning and topology in phase transitions and the role of spin and charge order fluctuations in high-temperature superconductivity.

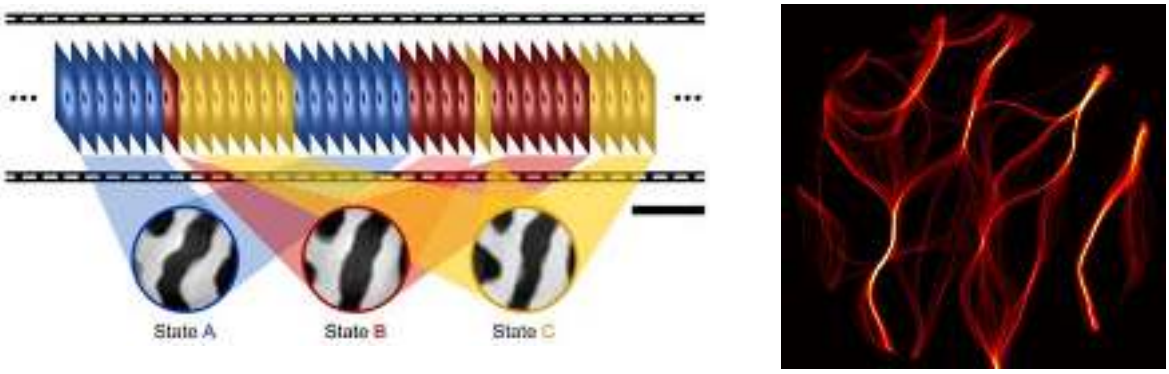

(a) **(b)**

Fig. 1: *(a) Principle of time-resolved coherent correlation imaging, (b) Superposition of magnetic domains accumulate over time, and thus define the presence of pinning sites.*

References

[1] C. Klose, F. Büttner, W. Hu, C. Mazzoli, K. Litzius, R. Battistelli, I. Lemesh, J.M. Bartell, M. Huang, C.M. Günther, M. Schneider, A. Barbour, S.B. Wilkins, G.S.D. Beach, S. Eisebitt, B. Pfau, Nature **614**, 256-261 (2023).

Abstract ID: 1291

ELEMENTARY EXCITATIONS OF CUPRATE PROBED WITH HIGH-RESOLUTION RIXS

Di-Jing Huang

National Synchrotron Radiation Research Center, Hsinchu 30076, TAIWAN
E-mail: djhuang@nsrrc.org.tw

Recent advancements in synchrotron radiation instrumentation have enabled high-resolution resonant inelastic X-ray scattering (RIXS) to become a powerful technique for probing elementary excitations with momentum resolution and providing direct information about the dynamics arising from fluctuations of spin, charge, and orbital degrees of freedom. This talk will begin with a review of the advances in high-resolution RIXS instrumnetation [1], followed by examples of RIXS studies on quantum materials such as cuprate superconductors [2, 3], and spin-orbit materials [4].

The superconductivity of cuprates has remained a mystery since its discovery decades ago. Above the superconducting transition temperature (T_c) in cuprate superconductors, various physical quantities show an enigmatic electronic excitation gap called a pseudogap. The mechanisms of the pseudogap formation and the superconductivity itself are core issues of high-T_c superconductivity. The pseudogap and strange- metal phases observed in cuprates above T_c are puzzling. One approach to resolving this puzzle is based on the scenario of quantum phase transition, which is driven by non-thermal fluctuations at absolute zero temperature, playing a crucial role in shaping the phase diagram of high-temperature cuprate superconductors. We have investigated the doping-dependent high-resolution RIXS of $La_{2-x}Sr_xCuO_4$ to unravel the quantum fluctuations of charge-density waves. Our findings provide the spectroscopic signature of quantum critical scaling in cuprates, in which the pseudogap and strange-metal phases correspond to the renormalized classical and the quantum critical scaling regimes, respectively.

In addition, electron quasiparticles play a crucial role in simplifying the description of many-body physics in solids with surprising success. However, conventional Landau's Fermi-liquid and quasiparticle theories for high-temperature superconducting cuprates have received skepticism from various angles. Whether the framework of electron fractionalization captures the essential physics of the pseudogap and superconducting phases of cuprates is still an open issue. We will also show that excitonic excitation of optimally doped $Bi_2Sr_2CaCu_2O_{8+\delta}$ with energy far above the superconducting-gap energy scale, about 1 eV or higher, is unusually enhanced by the onset of superconductivity. Our findings prove the involvement of such high-energy excitons in superconductivity. Therefore, the observed enhancement in the spectral weight of excitons imposes a crucial constraint on theories for the pseudogap and superconducting mechanisms.

References

[1] A. Singh *et al.*, J. Synchrotron Radiat. **28**, 977 (2021).
[2] H.Y. Huang *et al.*, Phys. Rev. X **11**, 04138 (2021).
[3] A. Singh, Nat. Commun. **13**, 7906 (2022).
[4] H.Y. Huang *et al.*, npj Quantum Materials **7**, 33 (2022).

Abstract ID: 1221

ELECTROMIGRATION-DRIVEN WEAK RESISTANCE SWITCHING IN HIGH-TEMPERATURE SUPERCONDUCTING DEVICES

Stefan Marinković[1], Daniel Stoffels[1], Simon Collienne[1], Emile Fourneau[1], Alejandro Fernández-Rodríguez[2], Narcís Mestres[2], Anna Palau[2], Alejandro V. Silhanek[1]

[1]*Experimental Physics of Nanostructured Materials, Q-MAT, CESAM, Université de Liège, B-4000 Sart Tilman, BELGIUM*
[2]*Institut de Ciència de Materials de Barcelona, ICMAB-CSIC, Campus UAB, 08193 Bellaterra, SPAIN*
E-mail: smarinkovic@uliege.be

Complex oxides are at the heart of modern functional material design. In particular, the perovskite ABO_3 structure is seen in compounds used in oxide solar cells, resistive memories, fuel cell catalysts, superconducting tapes, quantum bits and programmable magnets, making it one of the most studied material families. One important advantage of these systems[1,2] is that their properties may be controlled in situ to change between various electronic states, usually by means of thermal or electric conditioning. In this work, we investigate the two-terminal resistive switching properties of the perovskite-like oxide $YBa_2Cu_3O_{7-\delta}$ when the system is driven by electric current. We perform all-electrical switching to characterize and control low-amplitude resistance changes, and we implement finite element modelling[3] to explain how these effects can be properly accounted for by oxygen-vacancy counterflow induced by electric bias. The presented research sheds new light on the bulk displacement of oxygen atoms in perovskite materials with potential for sensing and memory technologies.

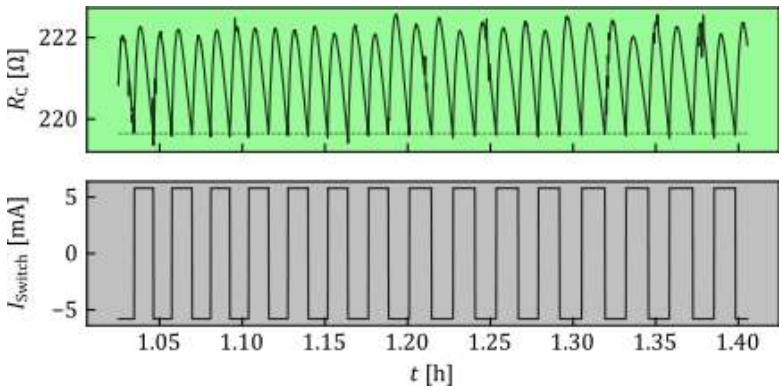

Fig. 1: R*everesible resistive switching in a micropatterned YBCO film via square wave current of 5.8 mA amplitude. The green panel correspond to a constriction resistance vs. time measurement, while the gray panel shows the applied DC current. The switching resistance criterion is set manually after a short initialization phase and is shown with the dashed horizontal line. This criterion determines the position at which the current polarity is switched. Note that the constriction has a dome shaped R(t) curve. This is explained by an oxygen-vacancy counterflow following the current direction where the deoxygenation front repeatedly passes trough the central constriction during switching.[3] Experiment performed in ambient conditions.*

References

[1] S. Marinković, A. Fernández-Rodríguez *et al.*, ACS Nano **14(9)**, 11765-11774 (2020).
[2] S. Marinković, A. Fernández-Rodríguez *et al.*, Adv. Mater. Interfaces **220953**, (2022).
[3] S. Collienne, S. Marinković *et al.*, Adv. Electron. Mater. **220953**, (2022).

Abstract ID: 1077

ANGULAR DEPENDENCES OF MAGNETIZATION AND CRITICAL CURRENT OF SECOND-GENERATION HTSC TAPES

D.S. Chikurov, A.E. Rudominskiy, M.P. Volkov

Ioffe Institute, 194021, Saint-Petersburg, RUSSIA
E-mail: d.chikurov@mail.ioffe.ru

To create magnetic systems using second-generation HTSC tapes, knowledge of the dependence of the critical current on the magnitude and direction of the magnetic field is required. The anisotropy of the critical current when the magnetic field is oriented along and across can be very significant and depend on the specific composition of the HTSC compound and the parameters of the technological cycle. In this work, the anisotropy of the critical currents of a SuperOx tape is determined using the flux capture method in a continuous HTSC ring [1] at several temperatures. The method used makes it possible to non-contact measure the dependence of the critical current on the magnitude and orientation of the magnetic field for tapes with high critical currents. Using the same foil, measurements were made of the dependence of magnetization on the magnitude of the magnetic field for a number of angles α between the plane of the tape and the direction of the magnetic field.

Figure 1 shows a family of M(H) dependences measured at a temperature of 77 K and a number of angles α from 0 to 90 degrees.

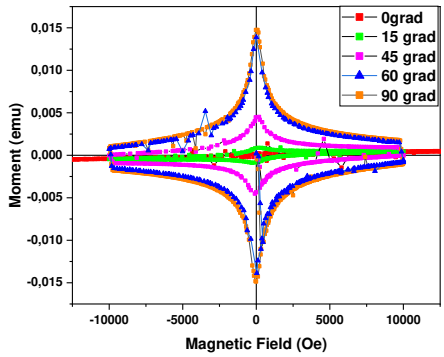

Fig. 1: *Dependences of M(H) of a piece of HTSC tape measured at different orientations of the magnetic field relative to the plane of the tape at a temperature of 77 K.*

A discussion of the anisotropy of magnetization and its correlation with the anisotropy of the critical current of the strip is carried out.

The authors express their gratitude to the SuperOx company for the samples provided. The work was supported by the Russian Science Foundation grant No. 23-29-00390.

References

[1] D.S. Chikurov, A.E. Rudominskiy, M.P. Volkov, J. Sib. Fed. Univ. Math. Phys., **16(6)**, 838–844 (2023).

HTS Cuprates: Advances in Fundamentals and Experimental Studies VI

30.04.2024 TUESDAY

Abstract ID: 1596

UNIVERSAL LOW-TEMPERATURE FLUCTUATION OF UNCONVENTIONAL SUPERCONDUCTORS REVEALED: "SMOKING GUN" LEAVES PROPER BOSONIC SUPERFLUIDITY THE LAST THEORY STANDING

Anthony Hegg[1], Ruoshi Jiang[1], Jie Wang[1], Jinning Hou[1], Yucel Yildirim[2], Wei Ku[1,3,4]

[1] *Tsung-Dao Lee Institute & School of Physics and Astronomy, Shanghai Jiao Tong University, Shanghai 200240, CHINA*
[2] *Department of Energy Systems Engineering, Bilgi University, Istanbul 34060, TURKEY*
[3] *Key Laboratory of Artificial Structures and Quantum Control (Ministry of Education), Shanghai 200240, CHINA*
[4] *Shanghai Branch, Hefei National Laboratory, Shanghai 201315, PEOPLE'S REPUBLIC OF CHINA*
E-mail: weiku@sjtu.edu.cn

Low-temperature thermal fluctuations offer an essential window in characterizing the true nature of a quantum state of matter, a quintessential example being Fermi liquid theory. In the long-standing pursuit toward a fundamental understanding of unconventional superconductivity, the most essential low-temperature thermal fluctuation of superfluidity has unfortunately been greatly overlooked. Here, we examine the leading thermal fluctuation of the superfluid density across numerous families ranging from relatively conventional to highly unconventional superconductors (MgB_2, bismuthates, doped buckyballs, heavy fermions, Chevrel clusters, intermetallics, κ-organics, transition metal dichalcogenides, ruthenates, iron-pnictides, cuprates, and kagome metals). Amazingly, in all of them an unprecedented universal T^3 depletion materializes in the low-temperature superfluid density, even in the believed-to-be-conventional MgB_2. This reveals a new quantum superfluid state of matter and requires a necessary change of paradigm in describing modern superconductors. We demonstrate that such unorthodox yet generic behavior can be described by an proper particle-conserving theory of bosonic superfluidity hosting a long-lived "true condensate".

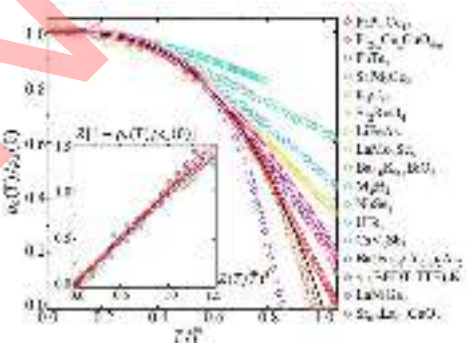

References

[1] arXiv:2402.08730

CANCELLED

Abstract ID: 1289

THERMODYNAMICS AND KINETICS ASPECTS OF YBCO NUCLEATION AT PEROVSKITE SUBSTRATES

M. De Angelis[1,2], M. Tomellini[1], V. Pinto[2], A. Augieri[2], A. Masi[2], A. Rufoloni[2], F. Rizzo[2], A. Angrisani Armenio[2], G. Campi[3], L. Barba[4], G. Celentano[2]

[1]*Tor Vergata University, Dept. of Chemical Sciences, Via della Ricerca Scientifica, 00133, Rome, ITALY*
[2]*Superconductivity Laboratory, Dept. of Fusion and Technologies for Nuclear Safety and Security, ENEA, Via E. Fermi 45, 00044, Frascati (Rome), ITALY*
[3]*Institute of Crystallography, CNR, Via Salaria Km 29.300, I-00015, Monterotondo (Rome), ITALY*
[4]*Institute of Crystallography, CNR, SS14 Km 163.5, I-34142, Basovizza (Trieste), ITALY*
E-mail: michele.deangelis.01@alumni.uniroma2.eu

The typical layered structure of superconducting cuprates, such as $YBa_2Cu_3O_{7-y}$ (YBCO), requires proper alignment of conduction planes to ensure optimal transport properties. For this reason, YBCO thin films must be grown with a specific orientation. The best superconducting properties are observed in the YBCO grown along the *c*-axis, perpendicular to the substrate. Against the background of extensive scientific literature on the growth of YBCO on crystalline substrate by chemical deposition technique [1-5], only a few works concern the study of the nucleation process, although it is crucial for the growth of the film [2-5]. A thermodynamic and kinetic model for the growth of YBCO has been proposed in references [5, 6]. This model is based on the calculation of the free energy of oxide formation using thermodynamic data, experimental and theoretical, for the formation reaction of YBCO, to obtain information on the preferential growth of the film along the *a* or *c*-axis. Among the parameters that enter the model of [6] and that rule crystal orientation during the growth, the partial pressure of water (P_{H2O}) and the temperature of crystallization (T_{cryst}) can be monitored during the film preparation. The study reported in ref. [6] highlights the role of the adhesion work between film and substrate, since it determines the nucleation barrier for oriented growth. This study is significant to identify the optimal conditions for the growth along the *c*-axis of YBCO crystals.

In this work, the process of epitaxial growth of YBCO films obtained with the fluorine based Metal Organic Decomposition technique was investigated, with the objective of studying the effect of the process parameters, namely P_{H2O} and T_{cryst} , on the degree of orientation of the film, to verify the model proposed in ref. [6]. The obtained samples have been fully characterized through the analysis of morphology, microstructure, and superconducting properties. This study allowed to deepen the qualitative understanding of the role of these parameters on the epitaxial growth mechanisms. Although the thermodynamic model is in accord with the experimental data, the kinetic model of ref. [6] has been improved to achieve a better description of the experimental output. In addition, the use of two substrates ($SrTiO_3$ and $LaAlO_3$) highlighted the importance of the role of the interface in YBCO's growth processes. In fact, a substantial difference has emerged between the two used substrates, so the variation of the investigated parameters has a different effect on the nucleation and growth of the films. This is particularly important to produce YBCO on an industrial scale.

References

[1] T. Araki, I. Hirabayashi, Supercond. Sci. Technol. **16**, R71 (2003).
[2] X. Obradors *et al.*, Supercond. Sci. Technol. **25**, 123001 (2012).
[3] Y. Ichino *et al.*, Trans. Appl. Supercond. **13**, 2735 (2003).
[4] X. Obradors *et al.*, Physica C: Superconductivity and its Applications **482**, 58 (2012).
[5] V. F. Solovyov *et al.*, Supercond. Sci. Technol. **18**, 239 (2005).
[6] V. Pinto *et al.*, Supercond. Sci. Technol. **33**, 115006 (2020).

Abstract ID: 1021

EMERGENCE OF A MARGINAL FL* FRACTIONALIZED FERMI LIQUID IN UNDERDOPED CUPRATES

P.A. Marchetti[1,2]

[1] *Dipartimento di Fisica e Astronomia, Università di Padova, Padova, ITALY*
[2] *INFN, Sezione di Padova, Padova, ITALY*
E-mail: marchetti@pd.infn.it

Using the terminology of [1] we denote by FL* a fractionalized Fermi Liquid (FL) satisfying a suitable version of Luttinger theorem related to topological order. In FL* systems besides standard holes (relevant for hole-doped cuprates discussed here) carrying charge and spin, the quasi-particle excitations are the holons carrying only charge and the spinons carrying only spin. The hole is a bound state, or in general a resonance, made of holon and spinon and the corresponding Landau quasi-particle is the true low-energy excitation, holon and spinon being well defined particle-like excitations only far away from the region of small energy close to the hole Fermi surface. Following reference [2] we define a FL* Marginal if the relaxation rate of the hole at zero temperature is proportional to the absolute value of the energy, measured from the Fermi surface.

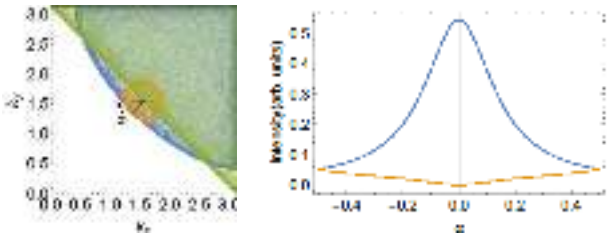

Figure (**left**) *Exterior of the Magnetic BZ (green), interior of the tight-binding FS for the hole (blue), interior of the small FS in PG derived in the FL* formalism (orange) in the first quadrant of the BZ for $t'/t = 0.25$ and doping $\delta = 0.07$; a angle along the small FS in PG.* (**right**) *Intensity of the symmetrized Spectral weight of the hole along the small FS in PG at $T = 20K$. The intensity inside the MBZ is in blue, that outside in yellow. a is measured in units of π and the origin is shifted by -1 outside of the MBZ.*

We apply our FL* formalism [3] for hole-doped cuprates, based upon a 2D t-t'-J model expressed in terms of gapped spinons and (semionic) gapless holons, to the "pseudogap phase" (PG), i.e. at small doping and low temperature but still in the non-superconducting phase. We show that in PG in this formalism the slave-particle gauge interaction binding holon and spinon into the hole resonance produces a Marginal FL* nature of the hole whose spectral weight is essentially concentrated on Fermi arcs [4], see Figure. Such Marginal nature is in agreement with experimental results [5] for a doping not too high.

References

[1] T. Senthil, S. Sachdev, M. Vojta, Phys. Rev. Lett. **90**, 216403 (2003); A.Paramekanti, A.Vishwanath, Phys. Rev . B **70**, 245118 (2004).
[2] C.M. Varma, P.B. Littlewood, S. Schmitt-Rink, E. Abrahams, A.E. Ruckenstein, Phys. Rev. Lett. **63**, 1996 (1989).
[3] P.A. Marchetti, F. Ye, Z.-B. Su and L. Yu, Phys. Rev. B **100**, 035103 (2019); P.A. Marchetti, Condens. Matter **5**, 12 (2020).
[4] P.A. Marchetti paper submitted to Condensed Matter (2023).
[5] T. Valla *et al.*, Science, **285**, 2110 (1999); J.M. Bok *et al.*, Phys. Rev. B **81**, 174516 (2010); J.M. Bok *et al.*, Sci. Adv. **2**, 1501329 (2016).

Abstract ID: 1259

FIELD-INDUCED REVERSIBLE TUNING OF OXYGEN DOPING IN HIGH-TEMPERATURE SUPERCONDUCTORS

A. Fernández-Rodriguez[1], J. Alcalà[1], T. Günkel[1], A. Barrera[1], S. Marinković[2], A.V. Silhanek[2], J. Gazquez[1], N. Mestres[1], A. Palau[1]

[1]ICMAB-CSIC, 08193, Bellaterra, SPAIN
[2] Université de Liège, EPNM, QMAT, CESAM, Liège, BELGIUM
E-mail: afernandez3@icmab.es

Modulation of carrier density in strongly correlated oxides offers the unique opportunity to induce different phases in the same material, which dramatically change their physical properties. Specially, the possibility of reversibly modifying the metal-insulator transition (MIT) in perovskite oxides, using an electric field as the external control parameter, is a very active area of research in condensed matter physics, and a promising technique to generate new solid-state devices with interesting functionalities. This work is focused on the study of the electric manipulation of the metal (superconducting) to insulator transition in high-temperature superconductor $YBa_2Cu_3O_{7-d}$ thin films by field-induced oxygen doping [1].

We demonstrate that non-volatile volume phase transitions can be locally modulated to generate superconducting transistor-like devices with free-resistance channels, or multi-terminal memristive structures for neuromorphic applications [2]. We will provide experimental evidence of selective displacement of oxygen atoms through, temperature-dependent resistance (Fig 1 (a)), Hall measurements (Fig 1 (b)), micro-Raman, Transmission Electron Microscopy and in-situ X-ray absorption spectroscopy investigations. The effect of oxygen doping on critical temperature, T_c, and critical current density, J_c, is thoroughly investigated [3]. Moreover, we will show the potential to tune the oxygen content in an extended region of a YBCO bridge by mass-selective migration of oxygen atoms induced by electromigration [4].

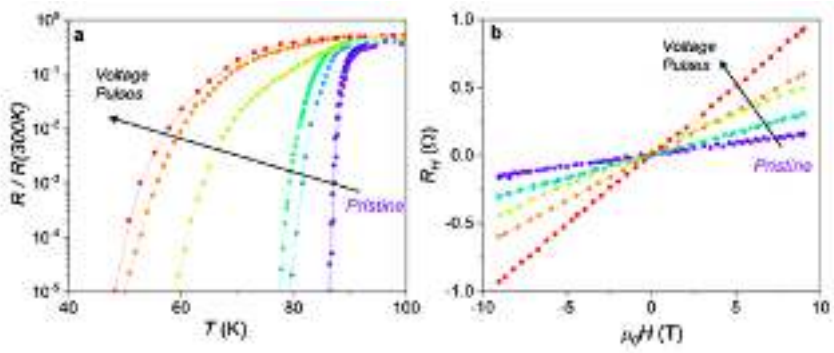

Fig. 1: *Modulation of the critical temperature (a) and the carrier density (b) in YBCO thin films by field-induced oxygen doping.*

References

[1] A. Palau *et al.* ,ACS Applied Materials & Interfaces, **10**, 30522 (2018).
[2] A. Fernandez-Rodriguez *et al.*, Materials, **13**, 281 (2020).
[3] J. Alcalà *et al.* (submitted)
[4] X.D.A. Baumans *et al.*, Appl. Phys. Lett. **114**, 012601 (2019), S. Marinkovic *et al.*, ACS Nano **14**, 11765 (2020).

Superconductors Under Extreme Conditions of Pressure and Strain I

30.04.2024 TUESDAY

Abstract ID: 1072

DEGENERATED SUPERCONDUCTIVITY AND FLUCTUATION INDUCED PHASES IN MULTIBAND SYSTEMS: Sr_2RuO_4 AND $Ba_{1-x}K_xFe_2As_2$

Hans-Henning Klauss

IFMP, Technische Universität Dresden, 01069 Dresden, GERMANY
E-mail: henning.klauss@tu-dresden.de

From the very beginning of quantum mechanics the concept of degeneracy of states has been an important topic throughout the quantum world. For example, the Landau-Zener dynamics of avoided level crossing describes quantum tunneling in single-molecule magnets as well as the deficiency in the flux of solar electron neutrinos at the earth. In solid state physics degeneracy can lead to multi-component order-parameters in symmetry broken phases such as superconductors and magnets. The topologically non-trivial skyrmion phase in the itinerant ferromagnet MnSi can be described as a triple-$\boldsymbol{q}$ antiferromagnet.

In particular in multi-band superconductors the degeneracy of superconducting order parameters with the same or different symmetry can lead to a coherent superposition. Unlike in magnets these states are experimentally difficult to detect. One indication is the appearance of time-reversal symmetry breaking (TRSB) superconductivity.

In my talk I will discuss two important systems in this context. In Sr_2RuO_4 we used uniaxial and hydrostatic pressure muon spin relaxation (μSR) experiments [1,2] to prove the two-component nature of the superconducting state using the concept of explicit symmetry breaking under uniaxial pressure. I will present uniaxial pressure studies along (100) and (110) directions in this system and discuss the implications on the superconducting state.

In $Ba_{1-x}K_xFe_2As_2$ we found TRSB superconductivity in μSR experiments at high doping x~0.8 due to the competition of single-component order parameters with different symmetry [3]. This competition appears close to a Lifshitz transition of the multi-band fermi surface. Supported by detailed thermodynamic and transport experiments we found a new TRSB phase also *above* T_C. This state can be understood as a fluctuation-induced Z_2 symmetry breaking with four fermion correlations [4].

This work was supported by DFG (GR 4667, GRK 1621, and SFB 1143).

References

[1] V. Grinenko, S. Ghosh, *et al.*, Nat. Phys. (2021).
[2] V. Grinenko, *et al.*, Nat. Comm. (2021).
[3] V. Grinenko, *et al.*, *Nat. Phys.* (2020).
[4] V. Grinenko, *et al.*, *Nat. Phys.* (2021).

Abstract ID: 1073

HIGH-PRESSURE EFFECTS ON THE LAYERED SCANDIUM BOROCARBIDE SUPERCONDUCTOR

G. Lamura[1], T. Shiroka[2,3], R. Khasanov[3], H. Ninomiya[4], K. Kawashima[5], H. Ogino[4]

[1]*CNR-SPIN, Genova, 16152, ITALY*
[2]*Laboratorium für Festkörperphysik, ETH Hönggerberg, 8093 Zürich, SWITZERLAND*
[3]*Paul Scherrer Institute, 5232 PSI Villigen, SWITZERLAND*
[4]*National Institute of Advanced Industrial Science and Technology (AIST), Tsukuba, JAPAN*
[5]*IMRA Japan Co., Ltd., Kariya, JAPAN*
E-mail: gianrico.lamura@spin.cnr.it

High-pressure research provides valuable hints on the nature of superconductivity. Typically, T_c decreases with increasing pressure, as observed in many simple- and transition-metal superconductors [1]. Layered systems, however, often show exceptions: (i) in cuprates, T_c versus p shows a domelike behavior, (ii) the $MoTe_2$ Weyl semimetal becomes supercon-ducting above 4.5 kbar [2], (iii) in MoB_2 T_c rises to 32 K at 1000 kbar [3], (iv) while, in the graphite intercalated compound CaC_6, T_c increases almost linearly with pressure [4]. The last examples highlight the intriguing case of layered compounds containing light elements, where the chemical/hydrostatic pressure can significantly affect the phonon spectra and the electron-phonon coupling strength, both crucial to achieve high T_c values. In this framework, the discovery of superconductivity in $Sc_{20}BC_{27}$ is particularly relevant [5]. This compound has a layered tetragonal structure, consisting of alternating ScC- and C- or B-layers along the crystallographic c-axis. At ambient pressure, the superconductivity has its onset at 7.7 K [5].

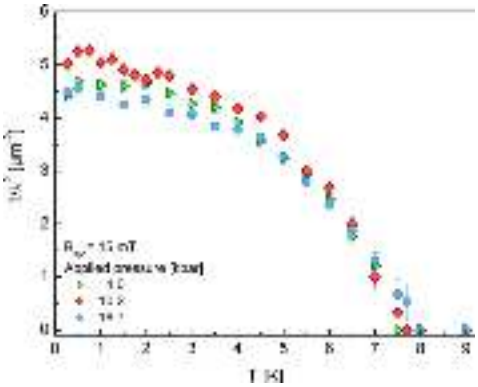

Figure 1: *Magnetic penetration depth vs. temperature, taken at B_{app} = 15 mT in an applied pressure of 4, 10.2, and 16.7 kbar.*

Here, we present systematic muon spectroscopy (μSR) study as a function of temperature and hydrostatic pressure on polycrystalline $Sc_{20}BC_{27}$. Two series of transverse-field TF-μSR experiments in applied magnetic fields B_{app} = 15, 30 mT at three different applied pressures: p ≃ 4, 10.2, and 16.7 kbar were performed down to 0.27 K. As shown in the figure, the magnetic penetration depth presents a modulation under applied pressure. Moreover, we observe a moderate increase in T_c with pressure. We discuss these findings and the evolution of the superfluid density in the framework of a two-band BCS *s-wave* model.

References

[1] J.S. Schilling, *High-pressure effects*, "*Handbook of High-Temperature Superconductivity. Theory and Experiment*" (Springer, New York, 2007).
[2] Z. Guguchia *et al.*, *Nature Comm.* **8**, 1082 (2017).
[3] C. Pei *et al.*, *Natl. Sci. Rev.* **10**, nwad034 (2023).
[4] A. Gauzzi *et al.*, *Phys. Rev. Lett.* **98**, 067002 (2007).
[5] H. Ninomiya *et al.*, *Inorg. Chem.* **58**, 15629 (2019).

Abstract ID: 1079

STRAIN TUNING OF QUANTUM MATERIALS: SUPERCONDUCTIVITY AND MAGNETISM

Elena Gati

Max-Planck-Institute for Chemical Physics of Solids, 01187 Dresden, GERMANY
E-mail: elena.gati@cpfs.mpg.de

In recent years, uniaxial stress has emerged as an extremely powerful tool to modify the delicate balance between competing ground states in correlated quantum materials. This notion is rooted in the power of uniaxial stress to deliberately control the lattice symmetry of a given quantum material. In this talk, we will provide an overview of the technical advances [1], that allow for the high-precision control of quantum materials by uniaxial stress. Using specific research examples from the fields of iron-based superconductivity [2] and quantum magnetism [3], we will illustrate how uniaxial pressure has already and will continue to be a key tool to answer fundamental questions and discover novel phenomena in the area of quantum materials.

Work is supported by the German Science Foundation through TRR 288—422213477 and the SFB 1143 (project-id 247310070).

References

[1] E. Gati, L. Xiang, S.L. Bud'ko, P.C. Canfield, Annalen der Physik, **2000248** (2020) (invited review article)
[2] A. Valadkhani, B.Z. Céspedes, S. Mandloi, M. Xu, J. Schmidt, S.L. Bud'ko, P.C. Canfield, R. Valentí, E. Gati, arXiv: 2307.10604 (2023).
[3] E. Gati, B. Schmidt, S.L. Bud'ko, A.P. Mackenzie, P.C. Canfield, npj Quant. Mat. **8**, 69 (2023).

Superconductors Under Extreme Conditions of Pressure and Strain II

30.04.2024 TUESDAY

Abstract ID: 1306

μSR MEASUREMENTS OF Sr_2RuO_4 UNDER UNIAXIAL STRAIN

Vadim Grinenko

Tsung-Dao Lee Institute, Shanghai Jiao Tong University, Pudong, Shanghai 200240, CHINA
E-mail: vadim.grinenko@sjtu.edu.cn

Muon spin rotation (μSR) and polar Kerr effect measurements provide evidence for a time-reversal symmetry breaking (TRSB) superconducting state in Sr_2RuO_4 [1,2]. In our previous μSR studies of Sr_2RuO_4, we observed that T_{TRSB} and T_c split under ⟨100⟩ uniaxial stresses, thereby supporting a hypothesis of TRSB superconductivity [3]. Together with the observation that T_{TRSB} and T_c track each other under hydrostatic stress and also under an introduction of disorder [4], these observations suggest a symmetry-protected even-parity chiral superconducting state, $d_{xz}\pm id_{yz}$. However, so far, the splitting of the transitions under uniaxial ⟨100⟩ stress has been seen only in μSR measurements. In contrast with expectations for a chiral state, a second anomaly was not resolved either in heat capacity [5] nor in elastocaloric effect [6] measurements under ⟨100⟩ uniaxial stress. These contradictory results call for a search for additional evidence that TRSB phase transition is indeed present below T_c under uniaxial stress.

I will present our preliminary μSR data under an applied magnetic field, demonstrating that the intervortex interactions is sensitive to the TRSB transition when $T_{TRSB} < T_c$. Our data can be interpreted as an indication of vortex clustering in the vicinity of T_{TRSB}. The vortex clustering is expected in two-component superconductors due to the divergent TRSB coherence lengths at T_{TRSB} [7], while penetration depth varies smoothly across the transition [8].

Also, we performed zero-field μSR measurements under uniaxial stress applied along a ⟨110⟩ lattice direction [9]. We have obtained preliminary evidence for suppression of T_{TRSB} below T_c at a rate much higher than the suppression rate of T_c. This result indicates that condensation energy associated with the TRSB state might be very small compared to that associated with the superconductivity overall. Our data provide a possible consistency between μSR and thermodynamic probes and additional evidence for the phase transition at T_{TRSB} characterised by divergent coherence length.

References

[1] J. Xia *et al.*, Phys. Rev. Lett. **97**, 167002 (2006).
[2] G.M. Luke *et al.*, Nature **394**, 558 (1998).
[3] V. Grinenko, *et al.*, Nat. Phys. **17,** 748–754 (2021).
[4] V. Grinenko, *et al.*, Nat Commun **12,** 3920 (2021).
[5] Y.-S. Li *et al.*, Proc. Nat. Acad. Sci. USA **118**, e2020492118 (2021).
[6] Y.-S. Li *et al.*, Nature **607**, 276–280 (2022).
[7] E. Babaev, M. Speight, Phys. Rev. B **72**, 180502(R) (2005).
[8] J. Garaud *et al.*, Phys. Rev. B **98**, 014520 (2018).
[9] V. Grinenko, *et al.*, Phys. Rev. B **107**, 024508 (2023).

Abstract ID: 1235

DO MAGNETISM AND SUPERCONDUCTIVITY COMPETE IN $La_2Ni_3O_{7-\delta}$? A MUON-SPIN ROTATION/RELAXATION UNDER PRESSURE STUDY

Rustem Khasanov[1], Dariusz Gawryluk[2], Zurab Guguchia[1]

[1] *Laboratory for Muon Spin Spectroscopy, Paul Scherrer Institute, CH-5232 Villigen PSI, SWITZERLAND*
[2] *Laboratory for Multiscale Materials Experiments, Paul Scherrer Institut,CH-5232 Villigen PSI, SWITZERLAND*
E-mail: rustem.khasanov@psi.ch

Our muon-spin rotation/relaxation (μSR) experiments in $La_2Ni_3O_{7-\delta}$ unveil the presence of commensurate magnetic order, aligning with the critical temperature associated with the density wave anomaly, concurrent with superconductivity. One of the pivotal finding is the observation that pressure induces an elevation in the magnetic ordering temperature, by approximately 6 K at p=2.3 Gpa, underscoring the resilience of magnetism under external pressure. Significantly, this behavior stands in stark contrast to the substantial suppression, specifically by 40 K within the same pressure range, of the transport anomaly associated with the density wave instability (see Fig. 1). The distinctive pressure-induced response in $La_2Ni_3O_{7-\delta}$ implies the simultaneous existence of two separate orders in its ground state: magnetic and most likely charge density wave orders. Remarkably, our results point to a pressure-induced decoupling between these two distinct orders. In cuprates or hole-doped nickelates like $La_{2-x}Sr_xCuO_4$, the relationship between spin and charge orders is notably intricate, with both orders being strongly intertwined and exhibiting similar responses to external parameters. However, this intricate interplay differs in $La_2Ni_3O_{7-\delta}$, where the behavior of spin and charge orders deviates from this pattern. Here, the response to external parameters reveals a distinct and less correlated behavior between spin and charge orders compared to the observed intertwining in cuprates and hole-doped nickelates. This distinction underscores the unique electronic characteristics and order interplay in $La_2Ni_3O_{7-\delta}$, adding to the complexity of the superconducting mechanism in this nickel oxide system.

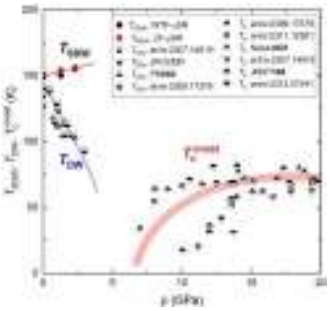

Fig.1: *The pressure-temperature phase diagram of $La_2Ni_3O_{7-\delta}$. The data are from Refs. [1-8].*

References

[1] Wang *et al.*, arXiv:2309.17378.
[2] Zhang *et al.*, arXiv:2307.14819.
[3] Hosoya *et al.*, J. Phys. Conf. Series **121**, 052013 (2008).
[4] Wu *et al.*, Phys. Rev. B **63**, 245120 (2001).
[5] Sun *et al.*, Nature **621**, 493 (2023).
[6] Zhang *et al.*, J. Mater. Sci. Technol. **185**, 147 (2024).
[7] Hou *et al.*, Chin. Phys. Lett. **40**, 117302 (2023).
[8] Puphal *et al.*, arXiv:2312.07341.

Abstract ID: 1189

STRUCTURE AND SUPERCONDUCTIVITY OF Se AT MEGABAR PRESSURE OF HYDROGEN

Zhongyan Wu, Jaeyong Kim

Department of Physics, Institute for High Pressure, Hanyang University, Seoul 04763, KOREA
E-mail: kimjy@hanyang.ac.kr

The structure and electronic transport properties of the chalcogen elements under hydrogen pressure to 180 GPa were measured. The enhanced superconductivity values for Se were obtained and on the verge of the β-Po–bcc phase transition, up to 9.4 K at 140 GPa. The superconducting transition is evidenced by a direct zero resistance drop and was further verified through its suppression under an external magnetic field with $\mu_0 H_c(0) = 0.26\,T$ at 140 GPa. An abnormally high resistance peak preceding the drop to zero resistance exhibits granular superconductivity. Our studies demonstrate that selenium does not react with hydrogen at 182 GPa at room temperature or 102 GPa with laser heating to 3000 K, suggesting that the synthesis of selenium hydride requires higher energy conditions than the ones suggested in theoretical predictions. The results of structural evolvements of Te under hydrogen will be also presented.

Superconductors Under Extreme Conditions of Pressure and Strain III

30.04.2024 TUESDAY

Abstract ID: 1445

EFFECTS OF UNIAXIAL STRAIN ON THE ELECTRONIC STRUCTURE OF 2H-$NbSe_2$

T. Valla[1], A.K. Kundu[2], I.I. Klimovskikh[1], H. Berger[3]

[1] *Donostia International Physics Center, 20018 Donostia-San Sebastian, SPAIN*
[2] *National Synchrotron Light Source II, Brookhaven National Laboratory, Upton, New York 11973, USA*
[3] *Institute of Condensed Matter Physics, Ecole Polytechnique Fédérale de Lausanne, 1015 Lausanne, SWITZERLAND*
E-mail: tonica.valla@dipc.org

Interplay of superconductivity and density wave orders has been at the forefront of research of correlated electronic phases for a long time. The balance between these two competing orders can be tuned by means of lattice deformation, i.e. pressure or strain. 2H-$NbSe_2$ is considered to be an ideal system for studying this interplay, but the origin of charge density wave in this material is still unresolved. Here, by using angle-resolved photoemission spectroscopy, we revisit the charge density wave order and study the effects of uniaxial strain on the electronic structure of 2H-$NbSe_2$. Our results indicate previously undetected signatures of charge density waves on the Fermi surface. The application of small amount of uniaxial strain induces substantial changes in the electronic structure and lowers its symmetry. This, and the altered lattice should affect both the charge density wave phase and superconductivity and should be observable in the macroscopic properties.

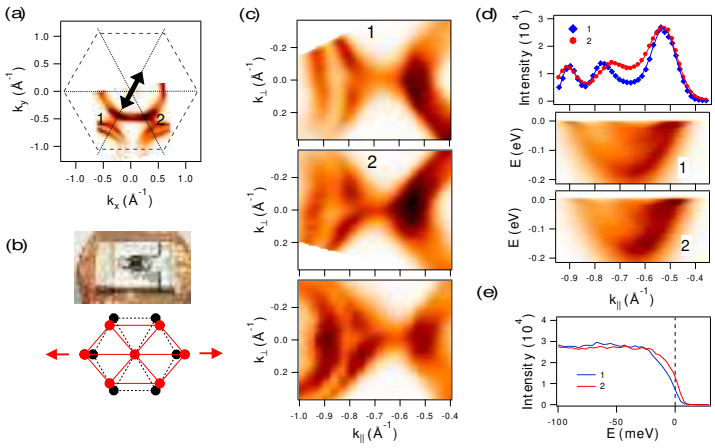

Fig. 1: *Uniaxially strained 2H-$NbSe_2$. a) Fermi surface (FS) of the sample when the tensile strain is applied along the GK line indicated by an arrow. (b) Bi-metal strain jig (top) and schematic of the change in the crystal structure under uniaxial strain. (c) close-up of the FS from (a) (strained sampel) and relaxed sample (bottom). (d) Intensity at the Fermi level (top) and dispersion of the bands along the two GK lines from (a). (e) Spectra at two van Hove singularities at lines 1 and 2, showing a small shift under strain.*

Abstract ID: 1466

EXTENDED SADDLE VAN HOVE SINGULARITIES IN THE H_3S SUPERCONDUCTOR EXPLAINED

R. Akashi

National Institutes for Quantum Science and Technology, Ookayama, Tokyo, JAPAN
E-mail: akashi.ryosuke@qst.go.jp

The sulfur superhydride H_3S is a milestone system for high pressure research [1], as it ignited a surge of studies for finding high-temperature hydride superconductors under extreme pressure. The prominent feature of this system from theoretical point of view is narrow peak in the density of states at the Fermi level, which has been found by the first-principle calculations. Considering this feature several simulations successfully reproduced the observed high T_c along with the Eliashberg theory for phonon-mediated superconductivity [2,3]. However, why such peak occurs has eluded simple explanation. Several attempts are actually made [4] to build tight-binding models that reproduce the electronic structure, though they commonly required many tight-binding parameters. Here we report a successful modeling based on an opposite view: nearly uniform electron model [5]. The linearly extended van Hove singularity as the origin of the DOS peak is consistently explained with very few model parameters, which solves the DOS-concentration mechanism underlying the high-T_c superconductivity. The current result appears to reflect the significant departure of the system from molecular orbital regime to weakly diffracted uniform gas.

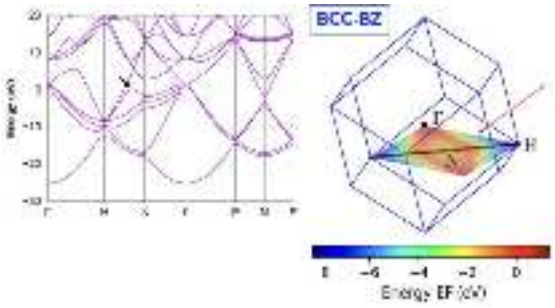

Fig. 1: *The electronic band structure in H_3S and its heatmap plot from first principles calculation, where arrows indicate extended van Hove singularities.*

References

[1] A.P. Drozdov *et al.*, Nature (London) **525**, 73 (2014).
[2] I. Errea *et al.*, Phys. Rev. Lett. **114**, 157004 (2015).
[3] R. Akashi *et al.*, Phys. Rev. Lett. **117**, 075503 (2016).
[4] R. Akashi, Phys. Rev. B **101**, 075126 (2020).
[5] R. Akashi, arXiv:2306.04238

Abstract ID: 1119

SUPERCONDUCTIVITY IN METAL SULFIDES UNDER HIGH PRESSURE

Fang HONG

Beijing National Laboratory for Condensed Matter Physics, Institute of Physics, Chinese Academy of Sciences, Beijing 100190, CHINA

E-mail: hongfang@iphy.ac.cn

Various exotic physical properties exist in metal sulfides, such as charge density wave, superconductivity and metal-insulator transition. Dependent on the ratio between metal and sulfur atoms, metal sulfides can be in forms of 1D, 2D and 3D structures, and it provides an ideal platform to study the structure-property correlation. Here, we are going to show the pressure-induced superconductivity in pristine insulating metal sulfides, from 1D-HfS_3 to 2D-SnS_2 to 3D-PbS. Though these compounds are in form of different structures, their structural phase transition trends show some similarity. There are isostructural phase transitions in 1D-HfS_3 and 2D-SnS_2, and a NaCl-CsCl (cubic-cubic) transition is presented in PbS. The critical pressure of superconducting transition is ~50 GPa for 1D-HfS_3 and 2D-SnS_2, while it is only ~20 GPa for PbS. It is noted that PbS has a high Tc of 12.3 K, which is the only one with Tc > 10 K below 100 GPa in the whole metal sulfide family, as seen in Fig.1. Similar with the superconductivity in superhydrides, the light element S dominates the superconducitivity in most metal sulfides and the metal atom plays a role of chemical pre-compression. Our systematic works on metal sulfides will inspire the exploration of new superconductors and be of great benefit on the investigation of superconductivity mechanism.

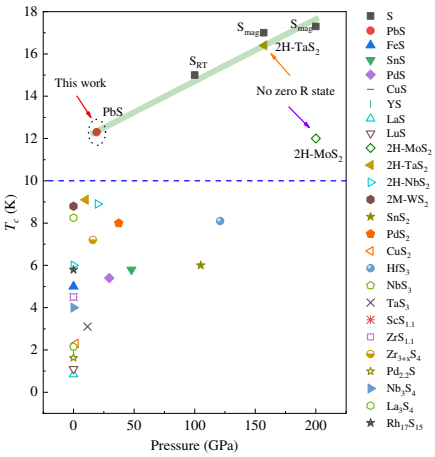

Fig. 1: *The Tc-P chart for binary metal sulfide superconductors and pure sulfur.*

References

[1] H. Zhang, W. Zhong, Y. Meng, B. Yue, X. Yu, J.-T. Wang, F. Hong, *Superconductivity above 12 K with possible multiband features in CsCl-type PbS*, Phys. Rev. B, **107**, 174502 (2023).

[2] Binbin Yue, Wei Zhong, Xiaohui Yu, Fang Hong, *Superconductivity in the van der Waals crystal SnS_2 up to 105 GPa*, Phys. Rev. B; **105**, 104514 (2022).

[3] Binbin Yue, Wei Zhong, Wen Deng, Ting Wen, Yonggang Wang, Yunyu Yin, Pengfei Shan, Jian-Tao Wang, Xiaohui Yu, Fang Hong, *Insulator-to-superconductor transition in quasi-one-dimensional HfS_3 under pressure*, J. Am. Chem. Soc.; **145**, 1301-1309 (2023).

Superconductors Under Extreme Conditions of Pressure and Strain IV

30.04.2024 TUESDAY

Abstract ID: 1343

IS QUANTUM CRITICALITY ALWAYS AVOIDED? THE CASE OF A TRICRITICAL POINT

R.R. Ullah[1], J.S. Harvey[1], Y. Wu[2], H.B. Cao[2], J.R. Badger[3], P. Klavins[1], V. Taufour[1]

[1]*Department of Physics and Astronomy, University of California Davis, USA*
[2]*Neutron Scattering Division, Oak Ridge National Laboratory, USA*
[3]*Department of Chemistry, University of California Davis, USA*
E-mail: valentin.taufour@hotmail.com

When phase transitions happen at zero temperature, physicists often observe new phases, or new phenomena. These new effects represent nature's way of avoiding quantum critical phase transitions.

I will discuss a special case where two transitions are driven to zero temperature at the same time. Near this special transition point, called a quantum tricritical point, we observe the emergence of a new magnetic phase, and that the transition is of the first order at low temperature. Using chemical substitution, we drive $LaCrSb_3$ towards a quantum tricritical point. The phase diagram showcases the avoidance of quantum criticality and our results suggest that other quantum tricritical points might be universally avoided as well [1-5].

Funding from UC Laboratory Fees Research Program (LFR-20-653926). This research used resources at the HFIR, a DOE Office of Science User Facility operated by the ORNL.

References

[1] Taufour *et al.*, Phys. Rev. Lett., **105**, 217201 (2010).
[2] Taufour *et al.*, Phys. Rev. Lett., **117**, 037207 (2016).
[3] Kaluarachchi *et al.*, Nature Communications, **8**, 546 (2017).
[4] Kaluarachchi *et al.*, Phys. Rev. B, **97**, 045139 (2018).
[5] Brubaker *et al.*, Phys. Rev. B, **101**, 214408 (2020).

Abstract ID: 1502

MAGNETIC AND SUPERCONDUCTING PROPERTIES OF IRON POLYHYDRIDES SYNTHESIZED AT HIGH PRESSURES

I. Lyubutin[1], A. Gavriliuk[1,2], V. Struzhkin[3], D. Trunov[2], S. Aksenov[2], A. Mironovich[2], M. Lyubutina[1], I. Troyan[1]

[1]*Shubnikov Institute of Crystallography, FSRC "Crystallography and Photonics", SRC «Kurchatov Institute», 119333, Moscow, RUSSIA*
[2]*Institute for Nuclear Research, Russian Academy of Sciences, 117312, Moscow, RUSSIA*
[3]*Center for High Pressure Science and Technology Advanced Research (HPSTAR), Beijing 100094, CHINA*
E-mail: lyubutinig@mail.ru

CANCELLED

First, we established that the ferromagnetic *bcc* phase α-Fe, upon transition to the *hcp* phase ε-Fe at pressures above 15 GPa, becomes nonmagnetic up to 4 K [1]. The properties of iron hydrides have not previously been experimentally studied, but theory predicts that some iron hydrides may be superconductors [2]. In this work, several iron polyhydrides FeH*x* were synthesized by laser heating of an iron–borazane (NH_3BH_3) sample in diamond anvil cells at pressures up to 200 GPa and temperatures up to 2000 K. The magnetic and electronic properties of FeH*x* compounds were studied by nuclear forward scattering spectroscopy on Fe-57 nuclei (NFS -synchrotron Mössbauer spectroscopy) at high pressures in the temperature range of 4–300 K in external magnetic fields up to 5 T [1,3]. The superconducting properties of FeH*x* compounds were studied by measuring the electrical resistance *R*(*T*) at high pressures (180–216 GPa) in the temperature range of 8–300 K [4]. In the samples synthesized at pressures of 77–157 GPa, the NFS data indicate the formation of seven FeH*x* compounds with very different electronic and magnetic properties. The Neel temperature T_N, determined for the FeH_2 phase at 82 GPa, is about 174 K [3]. Another surprising result is the discovery of one of the FeHx phases, of unknown composition, which at 128 GPa remains magnetically ordered in the temperature range 4 - 300 K, and the extrapolated value of T_N can reach ~ 2100 K ! [3]. The existence of a magnetic phase of an iron compound at such a record high pressure is unique and has not been observed to date. Our previous X-ray and NFS studies [3] show that superconductivity does not appear in iron polyhydrides saturated with hydrogen up FeH_4. Then, as a result of additional syntheses at pressures up to 216 GPa, superconducting phases of iron polyhydrides FeHx(I) and FeHx(II) were synthesized for the first time. Based on the obtained *R(T)* data, two superconducting phases of FeH_x with the maximum critical transition temperatures $T_c \approx 25.0$ and 27.7 K were identified [4]. Superconductivity in iron hydrides, revealed by measuring the resistance R(T), is confirmed by a number of additional methods. We assume that the superconducting phases obtained in our work can correspond to the FeH_5 structure (sp. gr. *I*4/*mmm*) or/and the FeH_6 structure (sp. gr. *Cmmm* or *C*2/*c*), which were predicted in [2].

This work was carried out with the financial support of the Russian Science Foundation (grants # 22-12-00163 and # 22-12-00163). X-ray diffraction and NFS studies were performed with the support of the Department of Crystal Physics of the Kurchatov Complex of Crystallography and Photonics.

References

[1] A.G. Gavriliuk, *et al.*, JETP Letters **117**, 126 (2023); DOI: 10.1134/S0021364022602986
[2] A.G. Kvashnin, *et al.*, J. Phys. Chem. C, **122**, 4731 (2018); DOI: 10.1021/acs.jpcc.8b01270
[3] A.G. Gavriliuk, *et al.*, JETP Letters, **116**, 804 (2022); DOI: 10.1134/S0021364022602433
[4] A.G. Gavriliuk, *et al.*, JETP Letters, **118**, 742 (2023); DOI: 10.1134/S0021364023603159

Abstract ID: 1446

TWO DISTINCT CHARGE DENSITY WAVE ORDERS AND EMERGENT SUPERCONDUCTIVITY IN PRESSURIZED CuTe

Zhaorong Yang

High Magnetic Field Laboratory, Chinese Academy of Sciences, Hefei 230031, CHINA
E-mail: zryang@issp.ac.cn

Understanding the interplay between superconductivity and other collective electronic phenomena has always been one of the central issues within the condensed matter and material physics communities. Here, we report a high-pressure study of quasi-one-dimensional CDW material CuTe through ultralow-temperature (400 mK) electrical transport and temperature-dependent Raman spectroscopy measurements and first-principles calculations. We provide solid evidence that the pristine CDW order (CDW1) transforms into a distinct CDW order (CDW2) at 6.5 GPa. Calculations show that the driving force of CDW1 is due to the nesting effect and that of CDW2 probably arises from the electronic correlated interaction. Strikingly, pressure-induced superconductivity is observed with a dome-like phase diagram, and its transition displays an extraordinary broadening along with the crossover from CDW1 to CDW2. These results demonstrate that pressurized CuTe provides a promising playground for understanding the intricate interplay of multiple CDWs and superconductivity.

References

[1] Shuyang Wang, Qing Wang, Chao An, Yonghui Zhou, Ying Zhou, Xuliang Chen, Ning Hao, Zhaorong Yang, Matter **6**, 1-12 (2023).

Abstract ID: 1148

ROOM TEMPERATURE SUPERCONDUCTOR MAY EXIST FOR A LONG TIME

D. Zhao

Honda Research Institute, 70 Rio Robles, San Jose, CA 95134, USA
E-mail: dong_zhao@honda-ri.com

The LK-99's roller coaster story about its superconductivity inspired the worldwide interest on exploring new room temperature superconductors. However, a report specified that room temperature superconductors may have been made many years ago because certain thorium compounds, such as ThI_2, exhibited the superconducting property at least at room temperature and under atmosphere pressure [1]. The most important feature of ThI_2, as reported, is its unique property of the coexistence of high electrical conductivity and diamagnetism at ambient condition. This distinctive property is in line with that of the superconductors and thus, the ThI_2's room temperature superconductivity can be concluded. ThI_2 was prepared in 1963 [2] and structurally analyzed in 1968 [3]. The results from these works enabled the ThI_2 a unique molecular formula of $[Th^{4+}(e^-)_2](I^-)_2$ as sketched in figure 1.

Fig. 1: *The molecular coordination of the $[Th^{4+}(e^-)_2](I^-)_2$ that the 2 electrons on Th cation is paired while the 2 iodides are bent at 138.1°, pushed by the electron pair on the Th cation.*

Fig. 2: *A schematic of the $[Th^{4+}(e^-)_2](I^-)_2$'s 2-D network where the circles represent the electron pairs with 2 electrons spinning in different directions.*

In use of the $[Th^{4+}(e^-)_2](I^-)_2$'s structural information, figure 2 is obtained through outlining 16 unit cells by means of only drawing the electron pairs on the Th cations on a specific crystallographic plane. This 2-D planar network grants the electron pairs to hop on it to form the supercurrent in a 2-D anisotropic manner. It is noticed that the style of the electron pairing in $[Th^{4+}(e^-)_2](I^-)_2$ is different from that of the Cooper pairs in the BCS theory. Consequently a new superconducting mechanism is established. Unlike the "three-particle paring" fashion in the Cooper pairs, the new pairing is a pure "two-particle" electron-electron pairing style that named as the "Zhao pair". The nature of the "Zhao pairs" is that two electrons are residing on its Th cation in a closely correlated fashion and never gets separated if the compound's superconducting state is preserved. The network showing in figure 2 received the name of the "Zhao pair network" because it allows the "Zhao pairs" to hop over it to generate the supercurrent. Therefore, the new mechanism of superconductivity is that the "Zhao pairs" are migrating on the "Zhao pair network" to present the material's superconducting property.

References

[1] D. Zhao, G.J. Zhao, WO 2017/164978 A2
[2] R.J. Clark, J.D. Corbett, Inorg. Chem. **2,** 460 (1963).
[3] L.J. Guggenberger, R.A. Jacobson, Inorg. Chem. **7,** 2257 (1968).

Iron Based Superconductors (IBS): Fundamental and Applied Research under Ambient and Applied Pressures II

30.04.2024 TUESDAY

Abstract ID: 1023

ANOMALIES IN THE DC MAGNETIZATION AND AC SUSCEPTIBILITY OF $EuRbAs_4Fe_4$ DUE TO THE INTERPLAY BETWEEN VORTEX MATTER AND EU SPINS

A.M. Ionescu[1], I. Ivan[1], C.F. Miclea[1], A. Galluzzi[2], M. Polichetti[2], A. Crisan[1]

[1]*National Institute of Materials Physics, 405A Atomistilor Str., 077125 Magurele, ROMANIA*
[2]*Department of Physics "E.R. Caianiello", University of Salerno, Via Giovanni Paolo II, 132, 84084 Fisciano, ITALY*
E-mail: acrisan652@gmail.com

Among the iron-based superconducting systems, the so-called 1144 materials, especially $CaKAs_4Fe_4$ received much interest lately due to their very high critical current density, pinning potential, vortex melting line as well as low anisotropy [1,2]. More recently it was discovered a novel 1144 material, $EuRbAs_4Fe_4$, in which superconductivity with a critical temperature of 37 K coexists with magnetic ordering of Eu spins at 15K [3]. We have performed multi-harmonic AC susceptibility studies and DC magnetization and magnetic relaxation measurements on high quality $EuRbAs_4Fe_4$ single crystals. All the results show various anomalies due to the co-existence of Abrikosov vortices and Eu spins, even at temperatures much higher than the temperature of magnetic ordering. Among other interesting features, our results are consistent with a special Meissner phase (see Fig. 1) due to the diverging penetration depth close to the critical temperature and coexisting of magnetic domains in the mixed state.

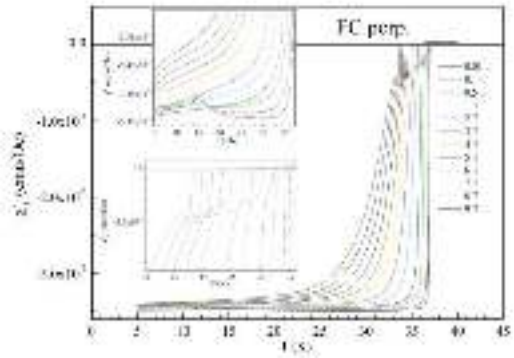

Fig. 1: *Temperature dependence of the fundamental in-phase AC susceptibility, in various applied DC fields. Insets represent zooms near the temperature of spin orientation (top) and, respectively, near the critical temperature (bottom).*

References

[1] I. Ivan, A. M. Ionescu, D. N. Crisan, A. Crisan, Int. J. Mol. Sci., **24**, 7896, (2023).
[2] A. M. Ionescu, I. Ivan, C. F. Miclea, D. N. Crisan, A. Galluzzi, M. Polichetti, A. Crisan, Cond. Matt., **8**, 93, (2023).

Abstract ID: 1383

DISORDER IN $FeSe_{1-x}S_x$ ($0 \leq x \leq 1$) SUPERCONDUCTING CRYSTALS

Cedomir Petrovic

Shanghai Advanced Research in Physical Sciences (SHARPS), CHINA
E-mail: cedomir_petrovic@yahoo.com

Connections among crystal chemistry, disorder and critical temperature T_c have been at the forefront of superconductivity, one of the most widely studied phenomena in physics, chemistry and materials science alike. In Fe-based superconductors T_c correlates with the average anion height above the Fe plane, i.e. with the geometry of the $FeAs_4$ or $FeCh_4$ (Ch = Te, Se, S) tetrahedron. By synthesizing $FeSe_{1-x}S_x$ ($0 \leq x \leq 1$) single crystal alloys with atomic defects we find that their T_c is not correlated with the anion height of other Fe superconductors. Instead, changes in $T_c(x)$ and tetragonal-to-orthorombic (nematic) transition $T_s(x)$ on cooling are correlated with Bragg plane and Fe vibrations disorder in direction orthogonal to Fe planes and thereby induced scattering rates $(1/\tau)(x)$ [1,2]. The disorder stems from deformed $Fe(Se,S)_4$ tetrahedra with different Fe-Se and Fe-S bond distances. Moreover, high-temperature metallic resistivity in the region of strong disorder exceeds Mott limit and provides an example of the strong violation of Matthiesen's rule and Mooij law which is known to be a dominant when adding moderate disorder past the Drude/Matthiassen's regime in all materials [2]. Scattering mechanism of Mott limit-exceeding resistivity is unrelated to phonons and arises for strong Se/S atom disorder in tetrahedral surrounding of Fe. Observations point to intricate connection between nanostructure details and unconventional scattering mechanism, possibly related to charge-nematic or magnetic spin fluctuations [2,3].

References

[1] Aifeng Wang *et al.*, Inorg. Chem. **61**, 11036 (2022).
[2] Aifeng Wang *et al.*, Nano Lett. **22**, 6900 (2022).
[3] Yu Liu *et al.*, Nanoscale Horizons (in press 2023).

Abstract ID: 1399

ENHANCEMENT OF TRANSITION TEMPERATURE AND CRITICAL CURRENT DENSITY OF IRON-BASED SUPERCONDUCTORS BY HIGH-PRESSURE GROWTH

Shiv J. Singh

Institute of High-Pressure Physics (IHPP), Polish Academy of Sciences, Sokolowska 29/37, Warsaw, POLAND
E-mail: shivjees@gmail.com

Iron-based superconductor (FBS) has the highest transition temperature of 36 K for $CaKFe_4As_4$ as a stoichiometric superconductor and 58 K for *RE*FeAsO (*RE* = La, Ce, Sm) as a doped system [1-2]. A large amount and high-quality bulk samples are generally needed to explore their intrinsic properties and for the fabrication of superconducting wires and tapes [1-3]. However, preparing a high-quality and large amount of bulk sample is always challenging by the conventional synthesis process at ambient pressure (CSP) [4-6]. To overcome this problem, high-pressure synthesis can be a unique way to improve the sample quality and superconducting properties of FBS [4-6]. In this presentation, we report a comprehensive study of the critical transition temperature, grain connectivity, and the critical current densities of these families by preparing the various polycrystalline F-doped (Sm/Gd)FeAsO and $CaKFe_4As_4$ samples using high gas pressure and high-temperature synthesis (HP-HTS) and CSP methods. Our HP-HTS technique can generate an inert gas pressure of up to 1.8 GPa in a cylinder chamber with a large sample space (~15 cm) and fitted with a three-zone furnace capable of reaching 1700°C [5]. All prepared samples are characterized by structural, microstructural, transport, and magnetic measurements to reach the final conclusions. High-pressure synthesis enhanced the transition temperature by 2 K for $CaKFe_4As_4$ whereas it is almost constant for the 1111 family. For both families, the sample quality, sample density, and grain connections are improved, and the critical current density is enhanced by two orders of magnitude (~10^5 A/cm^2, 5 K, 0 T) compared to that (~10^3 A/cm^2, 5 K, 0 T) of CSP. We discuss the optimization of the pressure growth conditions, the sample quality of the bulk, superconducting properties, and the granular behavior of these families with respect to CSP and the high-pressure synthesis process, which is very useful for the processing of 1111 and 1144 superconducting compounds. These findings will be of great interest to the condensed matter research community and have a significant impact on both fundamental and applied studies of all FBS superconductors especially for the fabrication of superconducting wires and tapes.

Acknowledgments

The work was funded by SONATA-BIS 11 project (Registration number: 2021/42/E/ST5/00262) funded by National Science Centre (NCN), Poland. SJS acknowledges financial support from National Science Centre (NCN), Poland through Project number 2021/42/E/ST5/00262.

References

[1] S.J. Singh *et al.*, Crystals. **12,** 20 (2022); Phys. Rev. Materials **2**, 074802 (2018).
[2] S.J. Singh, A. Morawski, Jenny Stanford Publishing: New York, NY, USA, 2021; pp. 283–314
[3] J. Shimoyama, Supercond. Sci. Technol. **27**, 044002 (2014)
[4] M. Manasa *et al.*, IEEE Trans. Appl. Supercond. **34**, 7300605 (2023).
[5] M. Azam *et al.*, Materials **16 (15)**, 5358 (2023); Crystals **13 (10)**, 1525 (2023).
[6] M. Azam *et al.*, IEEE Trans. Appl. Supercond. **34**, 7300205 (2023); **34**, 7300405 (2023).

Iron Based Superconductors (IBS): Fundamental and Applied Research under Ambient and Applied Pressures III

30.04.2024 TUESDAY

Abstract ID: 1438

SINGLE CRYSTAL GROWTH OF IRON-BASED SUPERCONDUCTORS WITH COMPLEX LAYERED STRUCTURES

Hiraku Ogino[1], Yudai Yatsu[1,2], Shigeyuki Ishida[1], Naomichi Sakai[2], Rayko Simura[3]

[1]*National Institute of Advanced Industrial Science and Technology (AIST), Tsukuba, Ibaraki 305-8568, JAPAN*
[2]*Shibaura Institute of Technology, Koto, Tokyo 135-8548, JAPAN*
[3]*Tohoku University, Sendai, Miyagi 980-8577, JAPAN*
E-mail: h-ogino@aist.go.jp

Important feature of iron-based superconductor (IBS)s is the variety of their crystal structures. IBSs are generally known for their low anisotropy, which is also highly dependent on the crystal structure. Especially, IBSs having perovskite-type block layers have thick block layers, and interesting properties such as very large anisotropy and interlayer Josephson junctions [1] are reported. However, in this system only single crystals of $Sr_2VFeAsO_3$ with ~300mm have been reported [2]. On the other hand, various compounds exist in this system, such as $Ca_{n+1}(Sc,Ti)_nFe_2As_2O_{n+3}$[3], which has a thicker block layer and a higher superconducting transition temperature(T_c) more than 40 K as shown in Fig.1 (a). In this presentation, we report on the successful fabrication and structural analysis of single crystals of $Ca_{n+1}(Sc,Ti)_nFe_2As_2O_{n+3}$.

The samples were prepared by the self-flux method using FeAs. The starting composition, flux and raw material ratio were adjusted based on the composition of $Ca_5(Sc,Ti)_4Fe_2As_2O_{11}$:FeAs = 1:4. The phase identification and structural analysis by X-ray diffraction, observation and compositional analysis by scanning electron microscope (SEM-EDS), magnetization measurement by magnetic property measurement system (MPMS), and electrical resistance measurement by four-terminal method were evaluated.

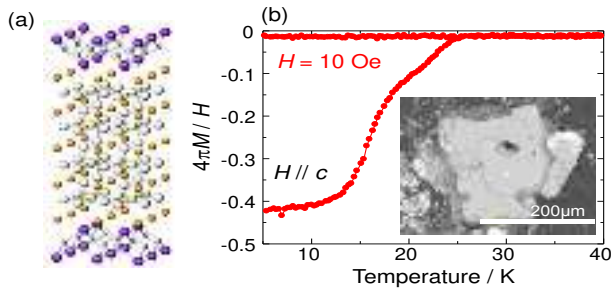

Fig. 1: *(a) Crystal structure, (b) temperature dependence of magnetization and SEM image $Ca_5(Sc,Ti)_4Fe_2As_2O_{11}$ single crystal.*

By optimizing the above conditions, we succeeded in synthesizing single crystals of $Ca_5(Sc,Ti)_4Fe_2As_2O_{11}$. Although in some cases $Ca_6(Sc,Ti)_5Fe_2As_2O_{14}$ formed at the same time, in other cases $Ca_5(Sc,Ti)_4Fe_2As_2O_{11}$ were exclusively formed. Single crystals of several hundred microns square were successfully isolated as shown in Fig. 1(b). The crystal structure of the crystal was analyzed by single crystal structure analysis. The basic structure is stacking of FeAs and four perovskite layers as previously reported, and the (Sc,Ti) sites are Ti-rich and the oxygen sites inside the oxide layer are split sites to suppress the atomic displacement parameter. Superconductivity above 30 K was observed by magnetization and resistivity measurements. Further details of physical properties will be discussed in the presentation.

References

[1] P.J.W. Moll *et al.*, Nat. Phys. **10**, 644 (2014). [2] [3]
[2] K. Katagiri, T. Sasagawa, Physica C **484**, 16 (2013).
[3] H. Ogino *et al.,* Appl. Phys. Let. **97**, 072506 (2010).

Abstract ID: 1030

ELECTRONIC ORIGIN OF SUPERCONDUCTIVITY IN IRON CHALCOGENIDE

Shankar Kunwar

King Fahd University of Petroleum and Minerals, Dept. of Physics, 31261, Dhahran, KSA
E-mail: kunwar@kfupm.edu.sa

Superconductivity is a quantum mechanical phenomenon where two fermi electrons pair up and forms a bosonic condensate. In conventional superconductors, the pairing mechanism is very well understood, where the pairing is mediated by the lattice vibrations [1]. However, despite extensive studies, the pairing mechanism in unconventional superconductors such as the high-T_c cuprates and the iron-based superconductors, is still under debate. Instead of phonon mediation, several studies suggest the electronic origin of the pairing mechanism in high-T_c superconductors [2]. To investigate the pairing mechanism in one of the iron-based superconductors we studied the tunneling spectroscopy on one of the iron-based superconductors, $FeSe_{0.5}Te_{0.5}$, using high-resolution Scanning Tunneling Microscope (STM). We found inhomogeneity in tunneling spectra and have broadened coherence peaks. The superconducting energy gap Δ is determined from coherence peaks and found it to be 4.6±0.5 meV. The deep hump feature, which manifest as the peaks at energy E higher than coherence peak in the derivative of tunneling spectra, shown in dotted lines in **Fig 1**, represents the signature of paring glue [3]. The pairing mode energy Ω is determined by subtracting the gap Δ from the energy E, resulting in a value of 7.2±1.1 meV. The value is consistent with the spin resonance mode energy measured by the neutron scattering experiments. Our study unveils the anti-correlation between the mode energy and the superconducting gap, one of the signature properties of the electron-meditated pairing mechanism, emphasizing the electronic origin of the superconducting glue in iron-based superconductors [4].

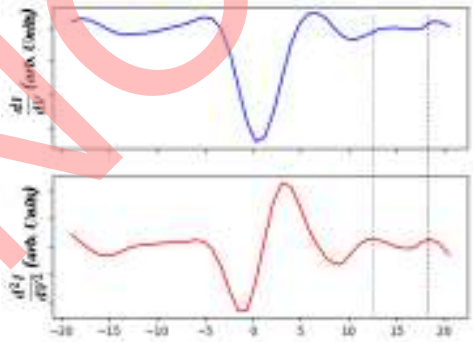

Fig. 1: *Top: Differential Conductance spectra with coherence peaks and at bottom derivative of the differential conductance with clear two peaks on the right side outside the gap energy as the signature of pairing glue.*

References

[1] J. Bardeen, L.N. Cooper, *et at.*, Physical Review, **108(5)**, 1175-1204 (1957).
[2] F.C. Niestemski, S. Kunwar, *et. al.*, Nature **450**, 1058 –1061 (2007).
[3] W.L. McMillan, J.M. Rowell, *et al.*, Phys. Rev. Lett., **14**, 108 (1965).
[4] C. Chen, C. Liu, *et al.*, Nano Lett. **20**, 2056−2061 (2020)..

CANCELLED

Abstract ID: 1193

TEMPORAL EVOLUTION OF TOPOLOGICAL DOMAIN-WALL DEFECTS IN FERROMAGNETIC SUPERCONDUCTORS

S. Köstler[1], A. Vagov[2], T.T. Saraiva[2], A. Yu. Aladyshkin[2,3,4], D.Y. Roditchev[5], A.A. Shanenko[2], V.S. Stolyarov[4,5]

[1]Bayreuth University, 95447 Bayreuth, GERMANY
[2]HSE University, 101000 Moscow, RUSSIA
[3]Institute for Physics of Microstructures RAS, Nizhny Novgorod, GSP-105, 603950 RUSSIA
[4]Moscow Institute of Physics and Technology, 141700 Dolgoprudny, RUSSIA
[5]Institut des Nano-Sciences de Paris-Sorbonne Universite, Paris 75005, FRANCE
E-mail: alexei.vagov@uni-bayreuth.de

The coexistence of seemingly contradictory phenomena, such as superconductivity and ferromagnetism in $EuFe_2(As_{1-x}P_x)_2$, gives rise to a variety of effects not observed in materials that exhibit either ferromagnetism or superconductivity alone [1]. The interplay between two competing order parameters, characterizing the magnetic and superconducting subsystems, leads to the emergence of complex magnetization patterns, contributing to a highly diverse phase diagram [1,2]. In this unique system, ferromagnetic bulk domain walls are stabilized, and can coexist with vortices and anti-vortices of the superconducting condensate [2]. In our study, we show that the formation of ferromagnetic domain walls in the Meissner state of such a material is accompanied by the temporal evolution of topological Y-shaped defects of the domain wall structure. Through experimental observation of the magnetization pattern on the surface of the bulk sample, we identified the slow motion of the defects along the domain walls. The experimental findings align with the theoretical analysis of emerging patterns, utilizing a model that combines the Ginzburg-Landau theory for the superconducting condensate and the Landau-Lifshitz-Gilbert equations for magnetization.

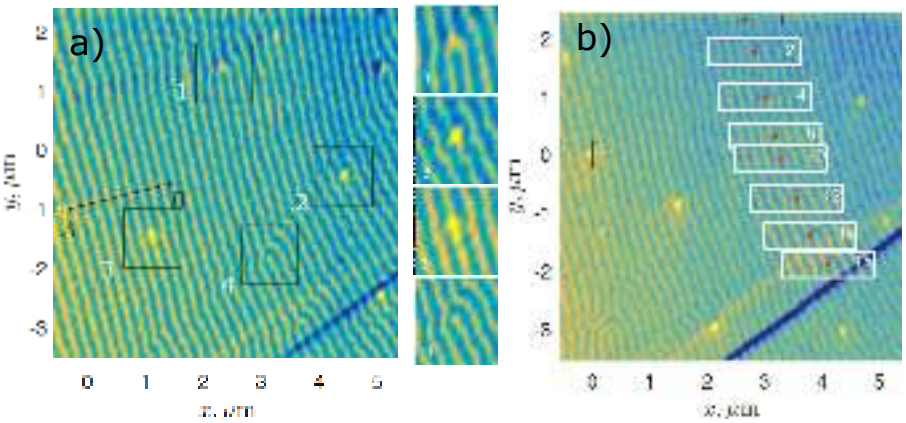

Fig. 1: *a) Domain walls in $EuFe_2(As_{1-x}P_x)_2$ at T=18K; defects in boxes 1-4 are enlarged in the corresponding panels; 2 and 3 are vortex defects, 1 and 4 are topological Y-shaped defects. b) A defect (red spot) moves downwards along the domain wall (time-frame insets are numbered as 1-15).*

References

[1] V.A. Stolyarov *et al.*, Sci. Adv. **4**, eaat1061 (2018).
[2] A. Vagov *et al.*, Comm. Physics **6**, 284 (2023).

Abstract ID: 1310

MULTICOMPONENT SUPERCONDUCTIVITY AND FOUR-FERMION PHASE IN THE $Ba_{1-x}K_xFe_2As_2$ SYSTEM

Vadim Grinenko

Tsung-Dao Lee Institute, Shanghai Jiao Tong University, Pudong, Shanghai 200240, CHINA
E-mail: vadim.grinenko@sjtu.edu.cn

In general, magnetism and superconductivity are antagonistic to each other. However, there are several families of superconductors in which superconductivity coexists with magnetism, and a few examples are known where the superconductivity itself induces spontaneous magnetism. The best-known of these compounds are Sr_2RuO_4 and some non-centrosymmetric superconductors. In this talk, I will present our finding superconducting phase with broken time-reversal symmetry (BTRS) of the centrosymmetric multiband superconductor $Ba_{1-x}K_xFe_2As_2$ ($0.7 \lesssim x \lesssim 0.85$), Fig.1 [1,2]. We observe spontaneous magnetic fields in this doping range using the muon spin relaxation (μSR) technique and spontaneous Nernst effect measurements. BTRS superconductivity implies a complex multicomponent superconducting order parameter. The evidence for multicomponent superconductivity in $Ba_{1-x}K_xFe_2As_2$ is provided by observation of fractional vortices [3].

Theoretically, materials that break multiple symmetries allow, under certain conditions, the formation of four-fermion condensates above the superconducting critical temperature (T_c). Such states can be stabilized by phase fluctuations. I will present a set of experimental observations that evidence the presence of a fermionic quadrupling condensate that breaks the Z_2 time-reversal symmetry [4,5]. This phase forms at the summit of BTRS dome in $Ba_{1-x}K_xFe_2As_2$ and is distinct in symmetry from normal and superconducting states. In this phase, a long-range order exists not between Cooper pairs but only between pairs of Cooper pairs.

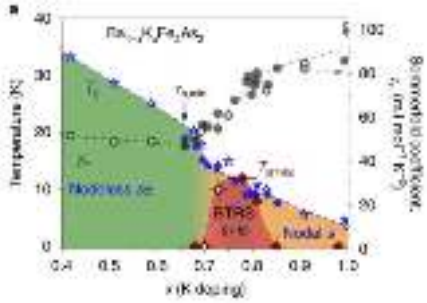

Fig. 1: *Left axis: doping dependence of the superconducting transition temperature T_c and the onset temperature T_{BTRS} of the BTRS state. Right axis: doping dependence of the Sommerfeld coefficient (γ_n). The figure is taken from Ref. [2].*

References

[1] V. Grinenko *et al.*, Phys. Rev. B **95**, 214511 (2017).
[2] V. Grinenko *et al.,* Nat. Phys. **16**, 789–794 (2020).
[3] Y. Iguchi *et al.,* Science **380**, 1244-1247(2023).
[4] V. Grinenko *et al.,* Nat. Phys. **17**, 1254 (2021).
[5] I. Shipulin *et al.,* Nat Commun **14**, 6734 (2023).

Quantum Information Technology and Applications I

30.04.2024 TUESDAY

Abstract ID: 1464

HYBRID QUANTUM SYSTEMS FOR QUANTUM AND NANO DEVICES

Hee Chul Park

Pukyong National University, Dept. of Physics, 44200, Busan, REPUBLIC OF KOREA
E-mail: hc2725@gmail.com

We have conducted a comprehensive study of hybrid quantum systems at mesoscopic scales, proposing an intriguing system that is a movable superconducting grain. We explore the potential of a nanomechanical superconducting shuttle as a promising model for investigating "flying qubits". Within this study, we examine a nanoelectromechanical system that comprises a Cooper pair box qubit executing nanomechanical vibrations between two bulk superconductors. We demonstrate that the application of a bias voltage to the superconductors can generate states characterized by entanglement between qubit states and quantum 'cat states,' representing a superposition of coherent states of the nanomechanical oscillator [1].

References

[1] D. Radic, S.-J. Choi, H.C. Park, J. Suh, L. Gorelik, R. Shekhter, *Nanomechanical cat states generated by a dc voltage-driven Cooper pair box qubit*, npj, Quantum, Info., **8**, 74 (2022).

Abstract ID: 268

DETECTING THE SYMMETRY BREAKING OF THE QUANTUM VACUUM IN A QED SYSTEM

Tiefu Li

School of Integrated Circuits, Tsinghua University, CHINA
E-mail: litf@tsinghua.edu.cn

In ultrastrong coupling regime, a qubit–resonator system has an entangled quantum vacuum with a nonzero average photon number. We experimentally observe the vacuum by the induced symmetry breaking of a dispersively coupled probe qubit. This result opens a way to experimentally explore the novel quantum-vacuum effects.

Hybrid quantum systems in the ultrastrong, and even more in the deep-strong, coupling regimes can exhibit exotic physical phenomena and promise new applications in quantum technologies. In these nonperturbative regimes, a qubit–resonator system has an entangled quantum vacuum with a nonzero average photon number in the resonator, where the photons are virtual and cannot be directly detected. The vacuum field, however, can induce the symmetry breaking of a dispersively coupled probe qubit. We experimentally observe this Higgs-like quantum-vacuum symmetry breaking induced by the field of a lumped-element superconducting resonator deep-strongly coupled with a flux qubit. The violation of the Xmon parity selection rule comes from virtual paths enabled by its interaction with an electromagnetic resonator whose parity symmetry is significantly broken by the deepstrong light–matter interaction with a flux qubit. The experimental results are in very good agreement with our theoretical analysis. The proposed setting offers a novel way to explore quantum-vacuum effects emerging in the light–matter ultra-strong and deep-strong coupling regimes and can be used as a tool to explore the coherence properties of quantum vacua in this exotic hybrid quantum system, and the occurrence of superradiant phase transitions in Dicke-like systems.

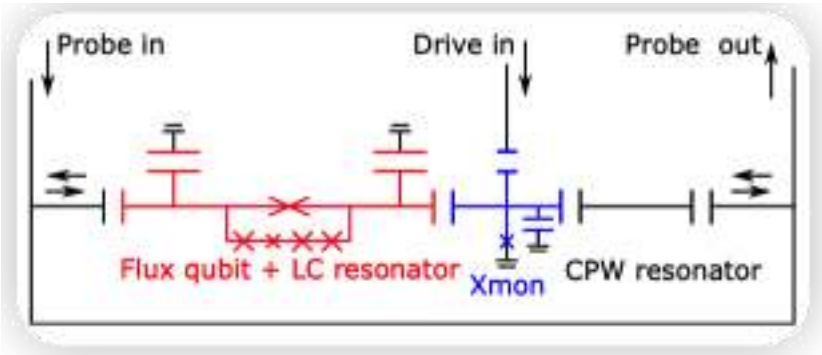

Fig. 1: *Circuit diagram of the device.*

References

[1] S.P. Wang, *Probing the symmetry breaking of a light–matter system by an ancillary qubit*, Nature Communications, **14**, 4397 (2023).

[2] S.P. Wang, Ph*oton-dressed Bloch-Siegert shift in an ultrastrongly coupled circuit quantum electrodynamical system*, Phys. Rev. Appl., **13**, 054063 (2020).

Abstract ID: 250

UTILIZATION OF THE ZEEMAN FARADAY EFFECT IN ATOMIC VAPOR CELLS FOR LASER INTENSITY STABILIZATION

Mohammad Karami, Zahra Gholami Ahangaran, Zahra Heydarinasab,
Maryam Hatefi, Farrokh Sarreshtedari

Quantum Resonance Research Laboratory, Department of Physics, College of Science, University of Tehran, 143-9955961, Tehran, IRAN
E-mail: hatefi.maryam94@gmail.com

Zeeman faraday effect is a well-known quantum effect which describes the changing of the light polarization in the presence of an external magnetic field [1]. This phenomenon is wildly used in atomic physics for different purposes, including optical isolation [2,3], atomic line filtering [4], laser frequency stabilization [5,6] and etc. In this work, we have shown that this effect could be efficiently used for laser intensity stabilization which is required for different atomic experiments. Fig.1 shows the schematics of our experimental setup. The wavelength of the laser (a homemade ECDL) is adjusted on the $6S_{1/2}$-$6P_{1/2}$ transition (D1 line) of the Cesium [7]. The principle of the proposed stabilization method is based on the operation of atomic line filters. When the output beam of the laser passes the first PBS, a linear polarization is achieved. As the second PBS is placed perpendicular to the first PBS, in the absence of magnetic field, the photodetector does not receive any signal. By applying the magnetic field, because of the Faraday rotation, the light polarization axis changes and the laser beam could pass the second PBS. This implies that the value of the applied magnetic field determines the value of the output laser intensity. We have engineered this dependency for laser intensity stabilization. For characterization of the stabilization method, the ECDL laser beam is modulated using an acousto-optical modulator (AOM) and the stability of the output power is investigated.

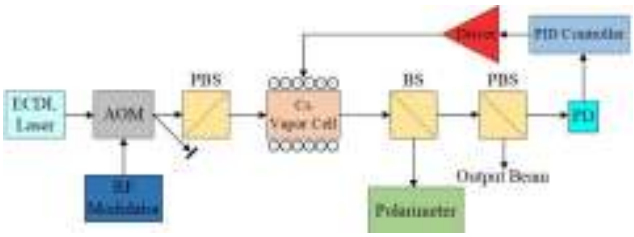

Fig.1: *The schematics of experimental setup for the laser intensity stabilization.*

References

[1] H. Chen, C.Y. She, P. Searcy, E. Korevaar, *Sodium-vapor dispersive Faraday filter*, Optics Letters **18(12)**, 1019-21 (1993).
[2] L.J. Aplet, J.W. Carson, *A Faraday effect optical isolator*, Applied Optics **3(4)**, 544-5 (1964).
[3] S. Fischer, *The Faraday optical isolator. Journal of optical communications*, **8(1)**, 18-21 (1987).
[4] M.A. Zentile, D.J. Whiting, J. Keaveney, C.S. Adams, I.G. Hughes, *Atomic Faraday filter with equivalent noise bandwidth less than 1 GHz*, Optics Letters 40(9), 2000-3 (2015).
[5] J. Keaveney, W.J. Hamlyn, C.S. Adams, I.G. Hughes, *A single-mode external cavity diode laser using an intra-cavity atomic Faraday filter with short-term linewidth< 400 kHz and long-term stability of< 1 MHz*, Review of Scientific Instruments **87(9)** (2016).
[6] A.L. Marchant, S. Händel, T.P. Wiles, S.A. Hopkins, C.S. Adams, S.L. Cornish, *Off-resonance laser frequency stabilization using the Faraday effect*, Optics Letters **36(1)**, 64-6 (2011).
[7] M. Karami, Z. Heydarinasab, F. Sarreshtedari, *Sub-Doppler dichroism as a useful tool in alkali atom hyperfine spectroscopy*, Laser Physics **vol. 33, no. 12**, pp. 125701 (2023).

Abstract ID: 257

ADVANCEMENTS IN QUANTUM TECHNOLOGIES: INTEGRATION INTO QUANTUM METROLOGY AND SENSING

A. Gokce Ozbay[1], L. Nur Akay[1,2], E. Sınır[1]

[1]TUBITAK National Metrology Institute, UME, Quantum Metrology Division, 41470, Gebze, Kocaeli, TURKIYE
[2]Yıldız Technical University, Institute of Natural Sciences, 34210, Esenler, Istanbul, TURKIYE
E-mail: gokce.ozbay@tubitak.gov.tr

Overcoming conventional paradigms, quantum information science and technology, or QIST, is in the forefront of revolutionary advances in information processing, communication, and sensing. Developments in metrology have paved the way to making better sensing platforms. Especially after the re-definition of the SI units, utilizing Quantum properties of matter has become crucial since references for units such as Ampere, Kelvin and Second had to rely on universal constants (electron charge, speed of light, Planck constant, etc.). Atomic clocks, ion-traps, superconducting Josephson Junction devices, color centers in diamond materials are few examples quantum devices that are currently employed or being explored for quantum sensing and reference standards. Metrology aims to improve measurement accuracies, increase sensitivities and provide traceability in quantum sensing. As the market for quantum computation and quantum communication grows, the need for traceable qubit measurements is foreseeable [1].

In this presentation we demonstrate how exploring new horizons in measurement standards and sensing capabilities enriches how we perceive and make use of quantum properties of materials. Research and industry applications alike stand to gain considerably from the integration of quantum metrology and quantum sensing into science and technology. We emphasize means of detecting quantum states of atoms and electrons via electrical measurements, fluorescence, photoelectric effects. Our works concentrates on integration of Quantum Anomalous Hall Effect devices into metrology as primary reference standards, exploring the use of diamond color centers in magnetometry, gravimetry and bio-sensing and memristive devices that have resistances tuned by electrical bias history. We also highlight the key role of a quantum roadmaps which guides governments, institutions and industry in future development of quantum technologies, raising awareness on quantum sensing abilities paving way to new consortiums.

References

[1] D. David Awschalom, *et al.*, *A Roadmap for Quantum Interconnects*, (ANL-22/83). Argonne National Laboratory, United States (2022).

[2] A. Laucht, *et al.*, *Roadmap on quantum nanotechnologies*, Nanotechnology **32**, 162003 (2021).

Quantum Information Technology and Applications II

30.04.2024 TUESDAY

Abstract ID: 1359

SUPERCONDUCTING CAVITY OPTOMECHANICAL SYSTEMS TOWARD QUANTUM SENSING

Junho Suh

Pohang University of Science and Technology, Dept. of Physics, 44200, Pohang, SOUTH KOREA
E-mail: junhosuh@postech.ac.kr

Mechanical oscillators have become device platforms for utilizing phonons as a resource for quantum technology. In this talk, I describe our recent results on developing superconducting cavity optomechanical devices and their quantum sensing applications. First, our cavity optomechanical devices with superconducting niobium implement optomechanical interactions at microwave frequency to demonstrate significant enhancement in the operating temperature, magnetic fields, and microwave powers [1]. The devices exhibit a microwave frequency comb emerging from nonlinear interactions between the microwave and mechanical oscillation [2]. Second, we explore new directions for mechanical quantum sensors with novel material systems. By employing semiconductor or topological insulator nanowires as mechanical oscillators, the nanowire oscillators demonstrate new functionalities such as precision microwave bolometers and quantum capacitance sensors [3,4]. Our works illustrate potential routes to harness the versatility of mechanical quantum oscillators for quantum sensing and transduction in hybrid quantum systems.

References

[1] J. Cha *et al.*, Nano Lett. **21**, 1800 (2021).
[2] J. Shin *et al.*, Nano Lett. **22**, 5459 (2022).
[3] J. Kim *et al.*, Phys. Rev. Appl. **15**, 034075 (2021).
[4] M. Kim *et al.*, Nat. Comm. **10**, 4522 (2019).

Abstract ID: 219

MAGNONIC QUBIT BASED ON BOSE CONDENSATE

Yu. M. Bunkov

Russian Quantum Center, Skolkovo, Moscow, RUSSIA
E-mail: y.bunkov@rqc.ru

Bose-Einstein condensation occurs at an appropriate density of bosonic particles, depending on their mass and temperature. We were able to experimentally observe the transition from the spin wave regime to the magnon Bose-Einstein condensed state (mBEC) with an increase in the magnon density due to microwave pumping. We used an optical setup based on the Faraday rotation effect to record the spatial distribution of the magnon density and phase.

We used the sample of 6 μm YIG film in the form of an ellipse with axes 4.5 by 1.5 mm. A strip line 0.2 mm wide excited magnons near one of the ends of the sample. The external magnetic field was directed out of plan of the film. We have investigated the propagation of magnons outside the region of excitation. At a low amplitude of resonant microwave excitation, we observed the formation of spin waves, the parameters of which are in good agreement with calculations based on the Landau-Lifshitz-Gilbert (LLG) equations for the experimental conditions.

At a critical density of excited magnons, its properties changed dramatically. Instead of a pattern of spin waves, a coherent precession was observed even far from the region of excitation. This pattern clearly corresponds to Bose condensation of magnons [1]. We performed a spatial Fourier analysis of the signal outside the excitation region as a function of the excitation energy and found a sharp transition from a wide spectrum in the spin wave mode to a narrow line in the BEC mode. The critical magnon density for the transition corresponds to a 3° deviation of the magnetization, which is in good agreement with the prediction [2].

The Bose condensation of magnons studied by us is formed from magnons with k = 0. It has the same basic properties as the magnon BEC in antiferromagnetic superfluid 3He discovered in 1984 [3-5]. In both cases, it has direct analogies with the atomic Bose condensate. We propose to use a magnon Bose condensate to read out information after quantum computations that use all the spins of a sample simultaneously.

This work was supported by the Russian Science Foundation (project no. 22-12-00322)

References

[1] P.E. Petrov, *et al.*, Optics Express **31**, 8335 (2023).
[2] Yu. M. Bunkov, V.L. Safonov, J. Magn. Magn. Mat. **452**, 30 (2018).
[3] A.S. Borovik-Romanov, *et al.*, JETP Letters,**40**, 1033 (1984).
[4] Yu. M. Bunkov, J. Low Temp. Phys., **138**, 753 (2005).
[5] Yu. M. Bunkov, G.E. Volovik, Phys. Rev. Lett. **98**, 265302 (2007).

CANCELLED

Abstract ID: 1609

SPECTRAL PROPERTIES OF BRANCHED NANOSCALE LATTICES

M. Akramov[1], C. Trunk[2], J. Yusupov[3], D. Matrasulov[4]

[1] *National University of Uzbekistan, 100174, Tashkent, UZBEKISTAN*
[2] *Institute of Mathematics, TU Ilmenau, 98693, Ilmenau, GERMANY*
[3] *Kimyo International University in Tashkent, 100121, Tashkent, UZBEKISTAN*
[4] *Turin Polytechnic University in Tashkent, 100095, Tashkent, UZBEKISTAN*
E-mail: mashrabresearcher@gmail.com

We propose an approach to quantize discrete networks (graphs with discrete edges). We introduce a new exact solution of discrete Schrödinger equation as

$$\Psi^{(a)}\left(x_n^{(a)}\right) = Ag_+^{x_n^{(a)}/a} + Bg_-^{x_n^{(a)}/a}, \tag{1}$$

where $x_n^{(a)} = na$, a is the step size, n is an integer number. Graphical representation of convergence of the solution (1) to the solution of the continuous case with decrease of the step size a is shown in Fig. 1.

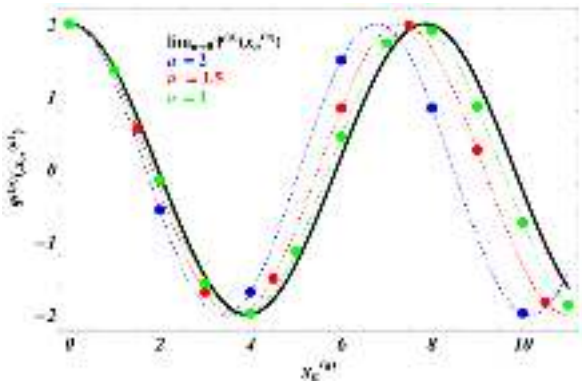

Fig. 1: *Analytic solution of discrete Schrödinger equation in Eq. (1) with different values of the step size* a *and limit of the solution at* $a \to 0$ *for parameters* $k = 0.8, A = B = 1$.

The solution (1) is used to write the solution for quantum graphs. General form of the secular equation for finding eigenvalues is derived. Application of this approach is done for the star graph. The model we proposed can be applied to broad variety of problems in quantum science and technology, where nanoscale branched lattices such as quantum wire networks, graphene nanoribbon networks, branched molecular wires, etc.

Acknowledgement

The work is supported by the World Bank Project "Modernizing Uzbekistan National Innovation System" (Ref. No. REP-05032022/235) and the Innovation Development Agency of the Republic of Uzbekistan (Ref. No. F-2021-440).

References

[1] T. Kottos, U. Smilansky, Ann.Phys., **76**, 274 (1999).
[2] G. Berkolaiko, Arxiv:1603.07356v2 (2016).

Abstract ID: 255

REVITALIZING THE INTEGRATION OF MATERIAL CHARACTERIZATION TECHNIQUES INTO QUANTUM SENSING, METROLOGY, AND QUANTUM-ENHANCED IMAGING

L. Nur Akay[1,2], O. Bozat[1], E. Sınır[1], B. Aydogan[1], A. Gokce Ozbay[1]

[1]TUBITAK National Metrology Institute, UME,Quantum Metrology Laboratory, 41470, Gebze, Kocaeli, TÜRKIYE
[2]Yıldız Technical University, Institute of Natural Sciences,Department of Physics, 34210, Esenler, Istanbul, TÜRKIYE
E-mail: lnurakay@gmail.com

Ground-breaking developments in and quantum technologies have broadened the horizons of integration of quantum science into device applications. Most Quantum Roadmaps point to Quantum Sensing and Metrology as one of the pillars of Quantum technologies; the other two being Quantum Communication and Quantum Computing [1]. Advances in metrology and quantum sensing, i.e. how we accurately measure things with much higher sensitivities, cultivates quantum technologies such as quantum computation and communication which in turn serves in better quantum sensing abilities creating a virtuous cycle.

Here we present how recent developments in material characterization techniques lead the way to more enhanced quantum devices and quantum metrology standards. Understanding and optimizing thin film materials forges engineering of Nano-constructed devices utilizing these materials. Hence a key element into constructing a thin-film based material with desired physical and electronic properties is measurement of the film with various techniques. We explore measurement platforms such as Grazing Incidence XRD, Ion-Microscopy, Photo-Luminescence, Tip-Enhanced Raman Spectroscopy and most importantly Atomic Force Microscopy methods with various mapping capabilities such as conductance, surface work functions, heat capacities and magnetic and electrostatic forces [2]. We elaborate on how these techniques can be utilized in engineering Quantum Devices. Quantum Enhanced Imaging is a key part of Quantum roadmaps, as well. One such example is how vacancies in diamond coupled with Nitrogen centers shaped the way we sense magnetic fields and combine this with microscopic imaging. Recently we have integrated metrologically traceable Conducting-Atomic Force Microscopy techniques to the infrastructure of Nano-scale metrology within the scope of a European Metrology Partnership project called ELENA. The trajectory of quantum technologies is guided by such precision measurements which in turn provides professionals and decision makers with a strategic roadmap.

References

[1] D. David Awschalom, *et al.*, *A Roadmap for Quantum Interconnects*, (ANL-22/83). Argonne National Laboratory, United States (2022).

[2] K. Bongs, S. Bennett, A. Lohmann, *Quantum sensors will start a revolution- If we deploy them right*, Nature **617**, 672-675 (2023).

Superconductors Under Extreme Conditions of Pressure and Strain V

01.05.2024 WEDNESDAY

Abstract ID: 1586

SUPERCONDUCTIVITY, AND STRUCTURAL AND METAL-INSULATOR PHASE TRANSITIONS: HIGH PRESSURE STUDIES

Sergey L. Bud'ko

Ames National Laboratory and Department of Physics and Astronomy, Iowa State University, Ames, Iowa 50011, USA
E-mail: budko@ameslab.gov

A brief overview of our recent studies of superconductivity, in particular in materials that exhibit structural (first order) phase transitions under pressure will be provided. Whereas in BCS superconductors like $PbTaSe_2$ and $BaBi_3$ superconductivity is robust and persists (with a change in T_c) through the structural phase transition [1,2], in unconventional, pure and Ni-substituted $CaKFe_4As_4$ [3,4] the structural, half-collapsed tetragonal, transition coincides with an abrupt loss of bulk superconductivity. Possible reasons, ranging from fragile magnetic fluctuations to different "structural perturbation strength", for such distinct behavior will be discussed. Additionally the results showing suppression of metal-insulator transition and stabilization of superconductivity by pressure in Re_3Ge_7 [5] will be presented and discussed.

This work is supported by the U.S. DOE, Basic Energy Sciences, Materials Science and Engineering Division under Contract No. DE-AC02-07CH11358.

References

[1] U. S. Kaluarachchi, *et al.*, Phys. Rev. B, **95**, 224508 (2017).
[2] L. Xiang, *et al.*, Phys. Rev. B **98**, 214509 (2018).
[3] U. S. Kaluarachchi, *et al.*, Phys. Rev. B **96**, 140501(R) (2017).
[4] L. Xiang, *et al.*, Phys. Rev. B **97**, 174517 (2018).
[5] S. Huyan *et al.*, arXiv:2401.09592 (2024).

Abstract ID: 1598

Ir-Sb BINARY SYSTEM: UNVEILING NODELESS UNCONVENTIONAL SUPERCONDUCTIVITY PROXIMATE TO HONEYCOMB-VACANCY ORDERING

V. Sazgari[1], Tianping Ying[2,3], J.N. Graham[1], C. Mielke III[1], D. Das[1], S.S. Islam[1], M. Bartkowiak[4], R. Khasanov[1], H. Luetkens[1], H. Hosono[2], Z. Guguchia[1]

[1] *Laboratory for Muon Spin Spectroscopy, Paul Scherrer Institute, CH-5232 Villigen PSI, SWITZERLAND*
[2] *Materials Research Center for Element Strategy, Tokyo Institute of Technology, Yokohama 226-8503, JAPAN*
[3] *Beijing National Laboratory for Condensed Matter Physics, Institute of Physics, Chinese Academy of Sciences, Beijing 100190, CHINA*
[4] *Laboratory for Neutron and Muon Instrumentation, SWITZERLAND*
E-mail: vahid.sazgari@psi.ch

Vacancies play a crucial role in solid-state physics, but their impact on materials with strong electron-electron correlations has been underexplored. A recent study on the Ir-Sb binary system, $Ir_{16}Sb_{18}$ revealed a novel extended buckled-honeycomb vacancy (BHV) order [1, 2]. Superconductivity is induced by suppressing the BHV ordering through high-pressure growth with excess Ir atoms or isovalent Rh substitution, although the nature of superconducting pairing has remained unexplored. Here, we conduct muon spin rotation experiments probing the temperature-dependence of the effective magnetic penetration depth λ_{eff} (T) in $Ir_{1-\delta}Sb$ (synthesized at 5.5 GPa with T_C = 4.2 K) and ambient pressure synthesized optimally Rh-doped $Ir_{1-x}Rh_xSb$ (x=0.3, T_C = 2.7 K). The exponential temperature dependence of the superfluid density n_S/m^* at low temperatures indicates a fully gapped superconducting state in both samples. Notably, the ratio of T_C to the superfluid density is comparable to previously measured unconventional superconductors. A significant increase in n_S/m^* in the high-pressure synthesized sample correlates with T_C, a hallmark feature of unconventional superconductivity. This correlation is intrinsic to superconductivity in the Ir-Sb binary system, with the ratio of T_C and the Fermi temperature T_F about 20 times lower than in hole-doped cuprates. We further demonstrate a similar effect induced by chemical pressure (Rh substitution) and hydrostatic pressure in $Ir_{1-x}Rh_xSb$, highlighting that the dome-shaped phase diagram is a fundamental feature of the material. These findings underscore the unconventional nature of the observed superconductivity and classify IrSb as the first unconventional superconducting parent phase with ordered vacancies. We also anticipate further theoretical investigations to elucidate the microscopic relationship between superconductivity and vacancy ordering in $Ir_{16}Sb_{18}$.

Abstract ID: 1214

VORTEX PHASE TRANSITIONS IN HTSC HYDRIDES

Andrey V. Sadakov[1], Vladimir A. Vlasenko[1], Dmitrii V. Semenok[2], Di Zhou[2], Ivan A. Troyan[3], Vladimir M. Pudalov[1,4]

[1] *V.L. Ginzburg Centre for High-Temperature Superconductivity and Quantum Materials P.N. Lebedev Physical Institute of the RAS, 53, Leninsky ave., 119991 Moscow, RUSSIA*
[2] *Center for High Pressure Science & Technology Advanced Research, Bldg. #8E, ZPark, 10 Xibeiwang East Rd, Haidian District, Beijing, 100193, CHINA*
[3] *Shubnikov Institute of Crystallography, Federal Scientific Research Center Crystallography and Photonics, Russian Academy of Sciences, 59 Leninsky Prospekt, Moscow 119333, RUSSIA*
[4] *National Research University Higher School of Economics, Moscow, 101000, RUSSIA*
E-mail: andrey.sadakov@gmail.com

Careful studies have been carried out on the behavior of the vortex structure in yttrium and thorium hydrides within the framework of the theory of vortex glass (VG), as well as the theory of thermally activated flux flow (TAFF) [1, 2]. This kind of research on hydrides is being carried out for the first time. First of all, it was interesting how high critical temperatures of isotropic cubic HTSC hydrides (YH_6 and ThH_{10} [3, 4]) (compared to layered anisotropic HTSC cuprates) would affect the dynamics and phase transitions of the vortex structure. As is known, in cuprates (and also to a lesser extent in other anisotropic HTSCs - iron-based pnictides and chalcogenides), rich vortex physics, with various pinning regimes and phase transitions, is ensured by a combination of factors - high critical temperature, small values of the coherence length, large values of penetration depth and large values of the anisotropy parameter. Under such conditions, the role of temperature fluctuations is very large, and it dictates the course of processes in the vortex system. In hydrides, the critical temperature is even higher (for ThH_{10} Tc = 153 K, for YH_6 Tc = 215 K), the penetration depth and coherence length are comparable, but the anisotropy parameter is equal to unity (isotropic cubic crystals). Therefore, studies of the vortex system and phase transitions in hydrides are of particular interest.

For yttrium hydride YH6, transport measurements were carried out in magnetic fields. The data was processed within the VG and TAFF models. It was found that the behavior of linear resistance in a magnetic field as it approaches zero resistance behaves as a power function, which, in accordance with the VG theory, indicates a phase transition from vortex liquid to vortex glass. The values of $T_g(H)$ were obtained – the so-called. melting curve, as well as the value of the critical exponent s, which indicates the dimension of the vortex system. The critical exponent is practically independent of the magnetic field and takes a value of 3.5-3.9, which corresponds to a three-dimensional vortex system. At temperature above T_g, the vortex system is in a liquid state, and within the TAFF model we have identified a region on the T-H phase diagram where the movement of the vortices is regulated by the activation mechanism. A detailed phase diagram was constructed [5]. For thorium hydrides ThH_{10}, transport measurements were carried out and current-voltage characteristics were taken in magnetic fields to determine the phase transition in the vortex system. It turned out that, unlike yttrium hydride, the critical exponent s in the ThH_{10} system is very small (1.4 – 2.0) and, in accordance with the VG theory, this indicates a quasi-two-dimensional dimension of the vortex system. The results of scaling the current-voltage characteristics showed that the best scaling is provided by the values of the critical exponents, which also correspond to the two-dimensional case [6].

References

[1] M.P.A. Fisher, Phys. Rev. Lett. **62**, 1415 (1989).
[2] G. Blatter, M.V. Feigel'man, V.B. Geshkenbein, A.I. Larkin,V.M. Vinokur, Rev. Mod. Phys. **66**, 1125 (1994); S. Pakhira, *et al.*, Phys. Rev. B **104**, 174427 (2021).
[3] I.A. Troyan, D.V. Semenok, A.G. Kvashnin, A.V. Sadakov, O.A. Sobolevskiy, V.M. Pudalov, A.G. Ivanova, V.B. Prakapenka, E. Greenberg, A.G. Gavriliuk *et al.*, Adv. Mater. **33**, 2006832 (2021).
[4] D.V. Semenok, A.G. Kvashnin, A.G. Ivanova, V. Svitlyk, V.Y. Fominski, A.V. Sadakov, O.A. Sobolevskiy, V.M. Pudalov, I.A. Troyan, A.R. Oganov, Mater. Today **33**, 36 (2020).
[5] A.V. Sadakov, V.A. Vlasenko, I.A. Troyan, O.A. Sobolevskiy, D.V. Semenok, D. Zhou,V.M. Pudalov, J. Phys. Chem. Lett. **14**, 6666 (2023).
[6] A.V. Sadakov, V.A. Vlasenko, D.V. Semenok, D. Zhou, I.A. Troyan, A.S. Usoltsev, V.M. Pudalov, *Quasi two-dimensional vortex matter in ThH_{10} superhydride*, arXiv preprint arXiv:2311.01318 (2023).

CANCELLED

Abstract ID: 1655

ON A ROOM TEMPERATURE SUPERCONDUCTOR $YCuO_{2+x}$ (0<x<0.5)

Danijel Djurek

Alessandro Volta Applied Ceramics (AVAC), 49247 Zlatar Bistrica, Augusta Šenoe 14. CROATIA
E-mail: danijel@avac.hr

Discovery of the superconductivity [1] at T_C = 93 K in the mixed phase $Y_{1.2}Ba_{0.8}CuO_{4-x}$ was followed by numerous announcements of possible transitions at higher temperatures, even close to room temperature. Two groups [3,4] found in Y-Ba-Cu-O systems the traces of delafossite $Y_2Cu_2O_5$, while Ishiguro and co-workers previously synthesized $CuYO_2$ [4]. The author reported [5] that Y-Ba-Cu-O system, treated in vacuum, undoubtedly contains one Meissner type phase more, appearing at 282 K, and that it may be identified as $YCuO_2$.

Preparation of $YCuO_2$ starts with nanopowders Y_2O_3 and CuO (Alpha Aesar) or Y_2O_3 + Cu_2O, nanopowder Cu_2O prepared in the laboratory by milling. Both powders are mixed in a ceramic mortar and mixed powders were pressed in an uniaxial die. The pressed pellets were heated for 24 hours at temperature 673-720 K. The final fraction of $YCuO_2$ (insulator) is 7 – 15 percents. The crystal unit cell is hexagonal, a = 0.352 nm, c = 1.142 nm, and other phases are non reacted Y_2O_3, CuO and pure copper. Treatment in H_2 atmosphere (2 bars) at 673 K results in Y_2O_3 and Cu. Metallic state is established by annealing in small oxygen pressures (up to 200 mbar), and annealing temperature extends up to 850 K.

Samples exhibit the resistive and diamagnetic transitions above the ice point, while the reproducibility is complete. Temporal stability in air is extended up to 3-4 months when samples convert back to insulators. Subsequent treatment in oxygen atmosphere up to 850 K re-establishes the metallic state, while heating above 1090 K decomposes the samples to metallic yttrium and copper.

References

[1] M.K. Wu *et al.*, Phys.Rev. Lett. **58**, 908 (1987).
[2] J.M. Tarascon *et al.*, Phys. Rev. B **35**, 7115 (1987).
[3] J. Aride *et al.*, Solid State Comm. **72**, 459 (1989).
[4] T. Ishiguro *et al.*, Solid State Chem. **49**, 232 (1983).
[5] D. Djurek, Condens. Matter, **9(1)**, (2024); DOI:10.3390.

CANCELLED

Nonuniform Magnetic Textures I

01.05.2024 WEDNESDAY

Abstract ID: 1326

ANGULAR DEPENDENT SPIN-WAVE IMAGING IN A RECTANGULAR $Ni_{80}Fi_{20}$ MICROSTRIP

S. Pile[1], S. Wintz[2,3], K. Lenz[4], R. Narkowicz[4], A. Ney[1], J. Lindner[4], J. Förster[2], S. Mayr[5,6], M. Weigand[3]

[1] *Johannes Kepler University Linz, 4040 Linz, AUSTRIA*
[2] *Max Planck Institute for Intelligent Systems, 70569 Stuttgart, GERMANY*
[3] *Helmholtz-Zentrum Berlin für Materialien und Energie, 12489 Berlin, GERMANY*
[4] *Helmholtz-Zentrum Dresden-Rossendorf, Institute of Ion Beam Physics and Materials Research, 01328 Dresden, GERMANY*
[5] *Paul Scherrer Institut, 5232 Villigen PSI, SWITZERLAND*
[6] *Laboratory for Mesoscopic Systems, Department of Materials, ETH Zurich, 8093 Zurich, SWITZERLAND*
E-mail: santa.pile@jku.at

Geometric confinement and external static magnetic field can have a big influence on the spin-wave behavior. Researching the latter is very important for further design of magnonic devices [1]. In the present work we focus on a fundamental understanding of the spin-wave behavior in confined rectangular microstrips under a uniform MW field excitation depending on a mutual orientation of the strip and the external static magnetic field.

The development of planar microresonators/microantennas that include a micro- loop allows for quit high sensitivity in comparison to cavity resonators due to increased filling factor [2]. That makes it possible to measure FMR of a single thin microstrip including resonance lines corresponding to spin-wave excitations [3]. TR-STXM [4] can be used for direct, time-dependent imaging of the spin-wave dynamics across the nm-thin microstrips at the GHz frequency range with elemental selectivity.

FMR mode and spin waves in a single rectangular $Ni_{80}Fi_{20}$ microstrip (1x5x0.03 μm) were analyzed by means of angular dependent FMR, TR-STXM and micromagnetic simulations [5]. Orientation of the in-plane external static magnetic field was varied with respect to the microstrip's long edge, revealing the field orientation influence on the spin waves.

Acknowledgements

We thank the Helmholtz-Zentrum Berlin for the allocation of synchrotron radiation beamtime. We also thank T. Feggeler and H. Stoll for their help during the TR-STXM measurements and A. Halilovic for valuable contributions to the lithography process. Additionally, we would like to thank M. Bechtel for technical support at the beamline. The authors would like to acknowledge financial support from the Austrian Science Fund, Project No. ESP 4 and project No. I-3050 during the early stage of the work. S.M. would like to acknowledge funding from the Swiss National Science Foundation (SNSF) under Grant No. 172517.

References

[1] A.V. Chumak *et al.*, IEEE Transactions on Magnetics **58**, 1–72 (2022).
[2] R. Narkowicz *et al.*, J. Magn. Reson **175**, 275–284 (2005).
[3] S. Pile *et al.*, Phys. Rev. B **105**, 094415 (2022).
[4] M. Weigand *et al.*, Crystals **12**, 1029 (2022).
[5] A. Vansteenkiste *et al.*, AIP ADVANCES **4**, 107133 (2014).

Abstract ID: 1108

MAGNON DYNAMICS STUDIES BY TIME-RESOLVED RESONANT X-RAY SCATTERING

Guido Meier[1], Lars Bocklage[2], Jakob Gollwitzer[2], Cornelius Strohm[2], Christian F. Adolff[2], Kai Schlage[2], Ilya Sergeev[2], Olaf Leupold[2], Hans-Christian Wille[2], Ralf Röhlsberger[2,3,4,5]

[1]*Max-Planck Institute for the Structure and Dynamics of Matter, Luruper Chaussee 149, 22761 Hamburg GERMANY*
[2]*Deutsches Elektronen-Synchrotron DESY, Notkestraße 85, 22607 Hamburg, GERMANY*
[3]*Friedrich-Schiller Universität Jena, Max-Wien-Platz 1, 07743 Jena, GERMANY*
[4]*Helmholtz-Institut Jena, Fröbelstieg 3, 07743 Jena, GERMANY*
[5]*GSI Helmholtz Zentrum für Schwerionenforschung GmbH, Planckstraße 1, 64291 Darmstadt GERMANY*
E-mail: guido.meier@mpsd.mpg.de

Coherent elastic scattering, namely, nuclear resonant scattering (NRS) unites a number of different scattering processes that can be used to investigate properties of condensed matter especially of magnetic structures. Since NRS is an X-ray technique, it opens the possibility to combine it with diffraction methods to obtain very high spatial resolution down to atomic length scales. For example, nuclear resonant X-ray diffraction in grazing incidence geometry can be used to determine the lateral magnetic configuration in a lattice of ferromagnetic nanostructures [1]. However, also spin dynamics can be probed by nuclear resonant scattering of synchrotron radiation [2]. Here a single coherent mode is induced by resonant excitation with radio frequency magnetic fields and mapped by NRS.

By exploiting the time structure of the synchrotron in a pump-probe experiment ultrafast and precise control of quantum systems at X-ray energies can be studied. These energies involve photons with oscillation periods below one attosecond. Coherent dynamic control of quantum systems at these energies is one of the major challenges in hard X-ray quantum optics. We demonstrate that the phase of a quantum system embedded in a solid can be coherently controlled via a quasi-particle with sub-attosecond accuracy. In particular, we tune the quantum phase of a collectively excited nuclear state via transient magnons with a precision of one zeptosecond. These small temporal shifts are monitored interferometrically via quantum beats between different hyperfine-split levels. This experiment demonstrates zeptosecond interferometry and shows that transient quasi-particles enable accurate control of quantum systems embedded in condensed matter environments [3, 4].

References

[1] K. Schlage, L. Dzemiantsova, L. Bocklage, H.-C. Wille, M. Pues, G. Meier, R. Röhlsberger, *Nuclear resonant surface diffraction of synchrotron radiation*, Phys. Rev. Lett. **118**, 237204 (2017).

[2] L. Bocklage, Ch. Swoboda, K. Schlage, H.-C. Wille, L. Dzemiantsova, S. Bajt, G. Meier, R. Röhlsberger, *Spin precession mapping at ferromagnetic resonance via nuclear resonant scattering of synchrotron radiation*, Phys. Rev. Lett. **114**, 147601 (2015).

[3] L. Bocklage, J. Gollwitzer, C. Strohm, C. F. Adolff, K. Schlage, I. Sergeev, O. Leupold, H.-C. Wille, G. Meier, R. Röhlsberger, *Coherent control of collective nuclear quantum states via transient magnons*, Science Adv. **7**, eabc3991 (2021).

[4] K.P. Heeg, L. Bocklage, C. Strohm, C. Ott, D. Lentrodt, J. Haber, H.-C. Wille, R. Rüffer, J. Gollwitzer, C.F. Adolff, K. Schlage, I. Sergeev, O. Leupold, G. Meier, C.H. Keitel, R. Röhlsberger, T. Pfeifer, J. Evers, *Reply to: On yoctosecond science*, Nature **608**, E18 (2022).

Abstract ID: 271

CONTROLLING THE DYNAMICS OF MAGNETIC DOMAIN WALLS AND SKYRMIONS BY MAGNETIC EXCHANGE COUPLING AND PINNING EFFECTS

Saül Vélez

Universidad Autónoma de Madrid, 28049 Madrid, SPAIN
E-mail: saul.velez@uam.es

Controlling magnetism at the nanoscale is essential for the development of new electronic technologies. Efficient electric manipulation of magnetic textures can be achieved via angular momentum transfer from a metal electrode to a magnetic texture by exploiting spin-orbit interactions. However, the static and dynamic properties of the magnetic textures are often fixed by the materials combinations and a dynamic manipulation of those properties is challenging. In this talk, we will show how we can stabilize and dynamically manipulate chiral domain walls and skyrmions via magnetic exchange coupling and pinning effects.

First, we will show that chiral domain walls and skyrmions can be stabilized in $Tm_3Fe_5O_{12}$ (TmIG) thin films and controllably driven them by proximity electric currents (Fig. 1) [1,2]. Interestingly, we will demonstrate that the mobility of the magnetic textures in TmIG can be modified by exchange coupling them to an in-plane magnetized $Y_3Fe_5O_{12}$ (YIG) layer, which distorts the spin textures leading to a directional-dependent rectification of their dynamics. This effect, which is equivalent to a magnetic ratchet, is exploited to control the flow of domain walls and skyrmions in devices. Second, we will show that exchange bias effects in Co/Cr_2O_3 interfaces can also be used to control the dynamics of domain walls in Co in a non-volatile manner, leading to a directional growth of the magnetic textures upon field reversal, asymmetric diode-like dynamic effects under the application of electric currents, and velocity modulations up to one order of magnitude in the presence of pinning[3]. Finally, we will show that pinning effects can also influence the displacement and growth of skyrmion bubbles.

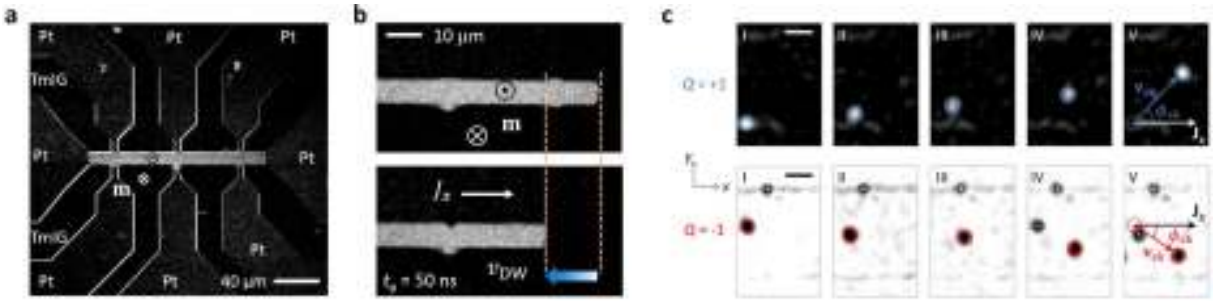

Fig. 1. **a**, *Magneto-optical Kerr effect (MOKE) image of a TmIG/Pt device showing current-induced switching of TmIG (bright region).* **b**, *Demonstration of current-driven wall motion. A current pulse $J_x \sim 10^{12}$ A m^{-2} in Pt drives the walls in TmIG at velocities v_{DW} of 300 m/s.* ***c***, *MOKE images showing the displacement of skyrmions in YIG/TmIG/Pt following a sequence of current pulses. The topological charge of the skyrmions (Q), which can be controlled by the orientation of the skyrmion core (bright/dark), results in a transverse deflection of the skyrmions.*

References

[1] S. Vélez *et al.*, Nature Comm. **10**, 4750 (2019).
[2] S. Vélez *et al.*, Nature Nanotech. **17**, 834 (2022).
[3] B.J. Jacot *et al.*, Phys. Rev. B. **106**, 134411 (2022).

Abstract ID: 1138

MAGNETO-ELASTIC ENGINEERING OF ANTIFERROMAGNETIC DOMAIN STRUCTURE

A. Wittmann [1,2], O. Gomonay [1], K. Litzius [2,3], A. Churikova [2], N.O. Birge [2,4], F. Büttner [5], S. Wintz [3], M. Mawass [5], M. Weigand [5], F. Kronast [5], L. Scipioni [6], A. Shepard [6], T. Newhouse-Illige [6], J.A. Greer [6], J. Sinova [1], G. Schütz [3], G.S.D. Beach [2]

[1] *Johannes Gutenberg University, 55128 Mainz, GERMANY*
[2] *Massachusetts Institute of Technology, Cambridge, Massachusetts 02139, USA*
[3] *Max Planck Institute for Intelligent Systems, 70569 Stuttgart, GERMANY*
[4] *Michigan State University, East Lansing, Michigan 48912, USA*
[5] *Helmholtz-Zentrum für Materialien und Energie GmbH, 14109 Berlin, GERMANY*
[6] *PVD Products, Wilmington, Massachusetts 01887, USA*
E-mail: a.wittmann@uni-mainz.de

Antiferromagnets are at the forefront of research in spintronics and demonstrate high potential for revolutionizing memory technologies. However, many of the underlying phenomena remain to be explored. This work investigates the domain structure in a thin-film canted antiferromagnet α-Fe_2O_3 in an external magnetic field.

We observe a strongly field-dependent domain structure in α-Fe_2O_3. Using x-ray magnetic linear dichroism (XMLD) and spin Hall magnetoresistance (SMR) measurements, we find that the internal long-range destressing fields driving the formation of domains do not follow the hexagonal crystal symmetry but fluctuate due to magneto-elastic interactions arising from substrate clamping as shown in Fig. 1 [1]. This leads to locally varying effective anisotropy in thin films allowing for the stabilization of long-range complex domain structures.

The insights gained from our work serve as a foundation for further studies of electrical and optical manipulation of complex magnetic textures in antiferromagnetic thin films via strain.

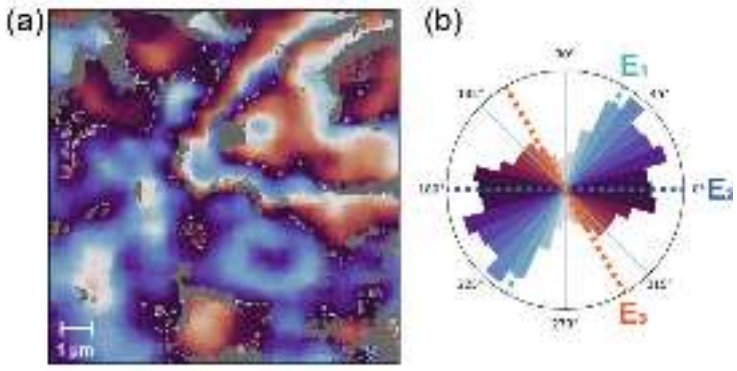

Fig. 1: *(a) Vector map of the α-Fe_2O_3 domain structure constructed from angle-dependent XMLD x-ray photoemission electron microscopy images. The orientation of the Néel vector represented by different colors is shown in the histogram in (b). The height of the bars in the circular histogram marks the frequency of occurrence of the given orientation of the Néel vectors on a linear scale (adapted from [1]).*

References

[1] A. Wittmann *et al.*, Phys. Rev. B **106**, 224419 (2022).

Frontiers in Magnetization Dynamics and Magnonics I

01.05.2024 WEDNESDAY

Abstract ID: 1078

A TIME-MULTIPLEXED SPINWAVE ISING MACHINE

A. Litvinenko[1], R. Khymyn[1], V. Gonzalez[1], R. Ovcharov[1], A.A. Awad[1], V. Tyberkevych[2], A. Slavin[2], J. Åkerman[1,3,4]

[1]University of Gothenburg, 412 96, Gothenburg, SWEDEN
[2]Department of Physics, Oakland University, 48309, Rochester, Michigan, USA
[3] Center for Science and Innovation in Spintronics, Tohoku University, 2-1-1 Katahira, Aoba-ku, Sendai 980-8577, JAPAN
[4] Research Institute of Electrical Communication, Tohoku University, 2-1-1 Katahira, Aoba-ku, Sendai 980-8577, JAPAN
E-mail: artem.litvinenko@physics.gu.se

We present a versatile platform for miniature low-power Ising machines that support and rapidly solve large-scale combinatorial problems. The spinwave Ising Machines (SWIM) is a new class of time-multiplexed Ising machines [1] that are implemented with an arbitrary-interconnected array of spinwave radio frequency (RF) pulses propagating in a ring oscillator with additional measurement and control feedback system implemented with an FPGA (Fig. 1). Spinwaves propagate 5 to 7 orders of magnitude slower than the speed of light and can be easily interconverted into RF signals which are easily manipulated with off-the-shelf energy efficient electronic RF components. Altogether, the use of spinwaves allows for dramatic miniaturization, reduction of power consumption, and significant improvement of frequency stability in time-multiplexed Ising machines.

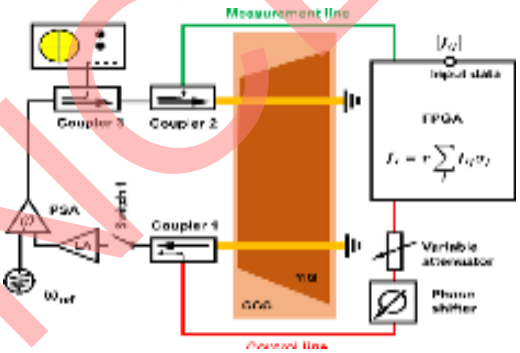

Fig. 1: *Spinwave Time-multiplexed Ising machine.*

Here, we present the design, the development, and the potential of the SWIM concept. The SWIM main loop consists of linear and parametric amplifiers, a YIG spinwave delay line where the spinwave RF pulses propagate, and an RF switch that controls the formation of RF pulses inside the ring. The feedback loop consists of the measurement and control block followed by a variable phase shifter and an attenuator.

Our work creates a pathway for miniature low-power and commercially feasible Ising machines for solving a wide range of large-scale optimization problems.

References

[1] A. Litvinenko, R. Khymyn, V.H. Gonzalez, R. Ovcharov, A.A. Awad, V. Tyberkevych, A. Slavin, J. Åkerman. Communications Physics **6 (1)**, 227 (2022).

CANCELLED

Abstract ID: 1124

NONRECIPROCAL MAGNETO-ACOUSTIC WAVES IN PIEZOELECTRIC/FERROMAGNETIC HYBRIDS

Matthias Küß

Institute of Physics, University of Augsburg, 86135 Augsburg, GERMANY
E-mail: matthias.kuess@physik.uni-augsburg.de

Surface acoustic waves (SAWs) have made their way into both technology and research over the last few decades. These "nano earthquakes" are easily excited and detected on piezoelectric crystals and have many different applications, most notably for RF signal processing in telecommunications. Surface acoustic waves are in general propagating reciprocally, which means that SAW propagation does not change under inversion of the propagation direction and limits the usage of SAWs for reciprocal devices.

Resonant magnetoelastic coupling of SAWs with spin waves (SWs) is the basis for an energy-efficient approach towards SW manipulation [1]. In addition, magnetoelastic interaction affects the properties of the SAW, which in turn can be used to devise new types of microwave devices. Since SWs are known to show a pronounced nonreciprocal behavior, SAW-SW coupling is a straightforward approach to obtain nonreciprocal transmission of SAWs.

In this talk, I will give a brief introduction in the resonant coupling between SAWs and SWs which is modeled by magnetoacoustic driving fields [2]. The symmetry of the SAW-SW coupling depends crucially on the mode of the SAW [3]. Large nonreciprocal transmission of SAWs is demonstrated in magnetic systems with a nonreciprocal dispersion relation $f(+k) \neq f(-k)$, such as in ferromagnetic/heavy metal bilayers with the interfacial Dzyaloshinskii-Moriya interaction (DMI) [4] and synthetic antiferromagnets composed of two ferromagnetic layers separated by a thin nonmagnetic spacer layer [5]. Because of the large tunability of the SW dispersion of synthetic antiferromagnets, the nonreciprocal transmission of the SAWs can be optimized to be very large (>100 dB) and to show a wide-band-like behavior.

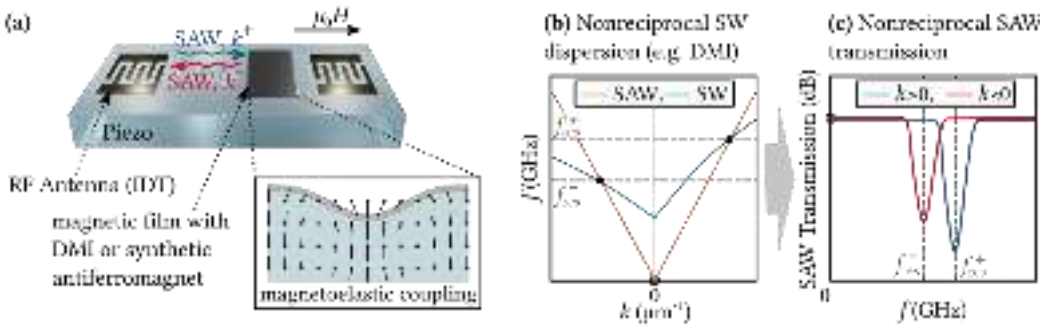

Fig. 1: *The magnetoelastic coupling between SAWs and SWs with a nonreciprocal dispersion can result in a nonreciprocal SAW transmission in piezoelectric/ferromagnetic hybrids.*

References

[1] W.-G. Yang, H. Schmidt, Appl. Phys. Rev. **8**, 021304 (2021).
[2] L. Dreher, *et al.*, Phys. Rev. B **86**, 134415 (2012).
[3] M. Küß, *et al.*, Phys. Rev. Applied **15**, 034046 (2021).
[4] M. Küß, *et al.*, Phys. Rev. Lett. **125**, 217203 (2020).
[5] M. Küß, *et al.*, ACS Appl. Electron. Mater. **5**, 5103 (2023).

Abstract ID: 1265

EXPLOITING MAGNETIC TUNNEL JUNCTIONS FOR UNCONVENTIONAL COMPUTING

D.R. Rodrigues[1], M. Carpentieri[1], G. Finocchio[2]

[1]*Department of Electrical and Information Engineering, Politecnico di Bari, Bari, 70126, ITALY*
[2]*Department of Mathematics and Computer Science, Physical and Earth Sciences, University of Messina, Messina, 98166, ITALY*
E-mail: davi.rodrigues@poliba.it & mario.carpentieri@poliba.it & giovanni.finocchio@unime.it

Unconventional Computing represents a paradigm shift in computing, drawing inspiration from brain- and physics-related mechanisms to outperform traditional computing paradigms.[1,2] Our work focuses on the use of spintronic devices, in particular magnetic tunnel junctions (MTJs), as a promising hardware realization for various Unconventional Computing paradigms. MTJs possess key properties such as non-volatility, non-linear functional response, scalability, and stochastic behavior, making them ideal candidates. We demonstrate the versatility of MTJs in the implementation of spiking neural networks (SNNs),[3] dynamical neural networks (DNNs),[4] and Ising machines (IMs).[5] SNNs, known for their biomimetic nature, use asynchronous spiking events to encode information, offering highly parallel operation, in-situ memory, and reduced power consumption. We present a hybrid MTJ design as a scalable, compact, and low-power solution that can be seamlessly integrated into hybrid CMOS hardware for SNNs, emulating both the Leaky-Integrate-and-Fire (LIF) and the complex Huxley-Hodgkin (H-H) models.[3] In addition, we propose an MTJ-based DNN that exploits the non-linear functional response and non-volatility of MTJs for classification tasks.[4] The training process is facilitated by modulating the control parameters, which is achieved through optimal control theory. Finally, we demonstrate that three-terminal MTJs seamlessly accommodate two distinct realizations of Ising Machines: coherent Ising machines (cIMs) and probabilistic Ising machines (pIMs).[5] A comparative analysis highlights the performance, strengths, and weaknesses of these IM models, emphasizing potential synergies through compatible interactions between the paradigms. This research opens new avenues for advancing unconventional computing through innovative spintronic-based hardware implementations.

References

[1] J. Grollier, *et al.*, *Neuromorphic spintronics*, Nature Electronics **3.7**, 360-370 (2020).
[2] G. Finocchio, D.R. Rodrigues, *et al.*, e-print arXiv:2301.06727 (2023)
[3] D.R. Rodrigues, *et al.*, Physical Review Applied **19.6**, 064010 (2023).
[4] D.R. Rodrigues, *et al.*, IEEE Trans. on Nano. **22**, 800-805 (2023).
[5] A. Grimaldi, D.R. Rodrigues, *et al.*, Physical Review Applied **20.2**, 024005 (2023).

Frontiers in Magnetization Dynamics and Magnonics II

01.05.2024 WEDNESDAY

Abstract ID: 1267

SUSTAINED SPIN AND ACOUSTIC WAVES EXCITATIONS DRIVEN BY fs-LASER COMB

A.A. Awad[1,2,3], A.K. Chaurasiya[1], S. Muralidhar[1], A. Aleman[1], R. Khymyn[1], D. Hanstorp[1], J. Åkerman[1,2,3]

[1]*University of Gothenburg, Kemivägen 9, 41296, Göteborg, SWEDEN*
[2]*Research Institute of Electrical Communication (RIEC), Tohoku University, Sendai 980-8577, JAPAN*
[3]*Center for Science and Innovation in Spintronics(CSIS),Tohoku University,2-1-1 Katahira, Aoba-ku, Sendai 980-8577, JAPAN*
E-mail: ahmad.awad@gu.se

Spinwaves provide an immense potential for information technology with scalable, faster and energy-efficient tunable devices; Thanks to Spinwave group velocity, low power operation and easy tunability and excitation using different means including magnetic, electrical field and spin polarized currents. Sustained SWs could be excited electrically using either microwave sources or direct current and by focused optical pulses [1] on a thin magnetic film. It has been observed that the optical excitation of the magnetic order occurs a few orders of magnitude faster than electrical excitation [2]. However, due to the decay time of the SWs, the optically induced emission of SWs is not continuous. To obtain sustainable spinwaves, repetitive pulses with a very short period between pulses should be used. Meanwhile such approach presents an attractive means of excitation for magnonics research, there are still very few works addressing such an option [3]. A recent approach uses instead a μ-focused Brillouin light scattering (BLS) technique to investigate the optically excited spin dynamics [4]. Using such approach provide a much higher sensitivity to coherent and incoherent SWs and provide additionally information on elastically excited excitations, the pioneer results showed spinwave stimulated emission tunable using the applied magnetic field magnitude and direction, and wavevector selective [5].

We have shown that high-frequency laser combs be used to generate coherent, sustained spin waves (SWs) in a range of thicknesses of Permalloy films. In plane SWs and perpendicular standing spinwaves PSSWs are excited up to the third order (18 multiples of the laser repetition rate) are observed [6]. Additionally, we demonstrated that the excitation scheme could be considered as a point-like source of continuous spin waves, as predicted by theory, caustic spinwave patterns are observed [7]. This field-controlled propagation pattern and directionality of optically driven short-wavelength spin waves provide additional degrees of freedom when designing magnonic devices. Furthermore, taking advantage of the BLS sensitivity to the elastic excitation we show that it is possible to characterize both the elastic and magnetic excitation waves generated by the ultrafast demagnetization in magnetic thin films.

References

[1] M. van Kampen *et. al.*, Phys. Rev. Lett. **88**, 22 (2002).
[2] B. Koopmans *et. al.*, Nat. Mats. **9**, 259 (2010).
[3] M. Jäckl *et. al.*, Phys. Rev. X **7**, 021009 (2017).
[4] A. Aleman *et. al.*, Optics Express **28**, 29540 (2020).
[5] S. Muralidhar *et. al.*, Phys. Rev.B **126**, 224423 (2020).
[6] A.A. Awad *et. al.*, App. Phys. Lett. **120**, 012405, (2022).
[7] S. Muralidhar *et. al.*, Phys. Rev. Lett. **126**, 037204 (2021).

Abstract ID: 1334

STRONG NONRECIPROCITY OF SURFACE ACOUSTIC WAVES IN HYBRID MAGNETO-ELASTIC STRUCTURES

A.N. Slavin

Oakland University, Dept. of Physics, 48309, Rochester, Michigan, USA
E-mail: slavin@oakland.edu

A novel method of inducing a giant nonreciprocity of surface acoustic waves (SAW) hybridized with nonreciprocal spin waves (SW) in a layered structure based on a *synthetic antiferromagnet* (two ferromagnetic layers magnetized in the opposite directions, see Fig.1a) has been proposed in [1, 2]. In a structure (Fig.1a) the SWs propagating in opposite directions have dramatically different group velocities (slopes), and in one direction ($k_x > 0$) the SW group velocity can almost exactly match the group velocity of the SAWs in all the frequency range of the SAW existence, thus causing a strong magneto-acoustic interaction leading to the strong insertion losses of hybridized SAW/SW (see Fig.1 b). In the opposite propagation direction ($k_x < 0$) the losses of SAW could be 100 times smaller (see Fig.1 c), thus creating a giant isolation of several dB for each micrometer of propagation (see Fig.1 d).

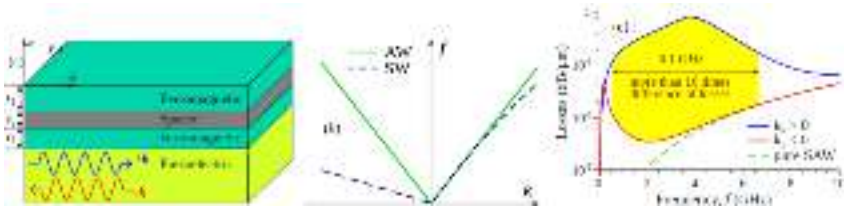

Fig. 1. *Giant nonreciprocity of hybridized SAW/SW in a layered structure comprising two antiferromagnetically ordered ferromagnetic layers supporting a nonreciprocal SW and a piezoelectric layer supporting a reciprocal SAW: (a) sketch of a layered structure; (b) dispersion laws of nonreciprocal SWs (blue) and reciprocal SAWs (green); (c) insertion losses of SAWs showing a giant isolation of contra-propagating signals.*

The proposed artificial layered structure can be used in many applications, for instance, to enable full-duplex communication over multiple frequency channels or to ensure unidirectional data flow in wave-based data processing devices. The proposed wave nonreciprocity is achieved by purely passive means and does not consume any power, which is useful for applications in IoT devices, where low power consumption is of a critical importance. The nonreciprocal isolation in the device Fig. 1 was theoretically evaluated [1] and measured [2] to be of several dB/mm of propagation distance. The isolation exceeds 10 dB in the frequency range of 6.0 GHz (from 0.6 to 6.6 GHz). This frequency band of SAW nonreciprocity is almost 100 times wider, than the nonreciprocity bands in the conventional *ferromagnetic* structures with narrow-band magnetoelastic interaction between SW and SAW [3]. It was also theoretically understood, that the effect of the wide-band SAW nonreciprocity is robust with respect to the wave propagation angle ϕ (in respect to the direction of the layers static magnetization), and that perfect alignment of the magnetization direction is not necessary for the experimental observation and utilization of the effect.

References

[1] R. Verba, V. Tiberkevich, A. Slavin, Phys. Rev. Applied **12,** 054061 (2019).
[2] D.A. Bas *et al.*, Phys. Rev. Applied **18,** 044003 (2022).
[3] R. Verba *et al.*, Appl. Phys. Lett. **103**, 082407 (2013).

Abstract ID: 1340

IMAGING OF SPIN TEXTURES AND SPIN WAVES IN 2D MAGNETS

F. Schulz[1], K. Litzius[2], L. Powalla[3], M.T. Birch[4], R.A. Gallardo[5], S. Satheesh[3], M. Weigand[6], T. Scholz[3], B.V. Lotsch[3], G. Schütz[1], M. Burghard[3], S. Wintz[1,6]

[1]Max Planck Institute for Intelligent Systems, 70569 Stuttgart, GERMANY
[2]Universität Augsburg, 86159 Augsburg, GERMANY
[3]Max Planck Institute for Solid State Research, 70569 Stuttgart, GERMANY
[4]RIKEN Center for Emergent Matter Science, 351-0198 Wako, JAPAN
[5]Universidad Técnica Federico Santa María, 2390123 Valparaíso, CHILE
[6]Helmholtz-Zentrum Berlin für Materialien und Energie, 14109 Berlin, GERMANY
E-mail: sebastian.wintz@psi.ch

The study of magnetism in reduced dimensions is not only of significant fundamental interest but also offers potential applications for materials with unique functionalities [1-3]. Here, we will address the direct imaging of spin textures and spin dynamics in two-dimensional (2D) magnets using x-ray microscopy [4,5]. Using scanning transmission x-ray microscopy (STXM), we investigated the formation and stability of skyrmions and higher order topological states in Fe_3GeTe_2 flakes [4]. Moreover, the propagation of spin waves was directly observed in Fe_5GeTe_2 flakes using time-resolved (TR)-STXM [5] (Fig.1), revealing spin-wave characteristics of 2D magnets that are distinct from their 3D counterparts.

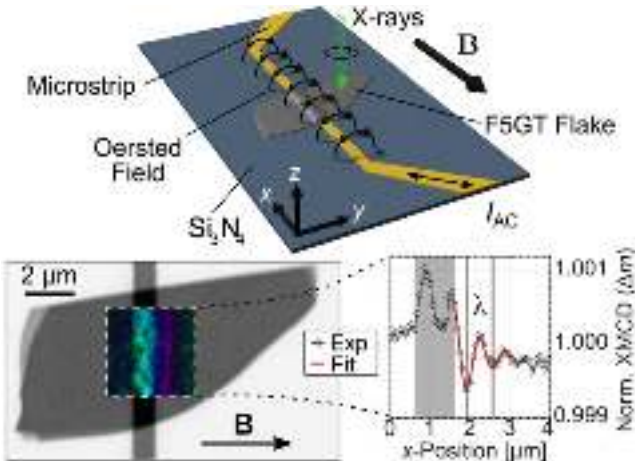

Fig. 1: *Sketch of Fe_5GeTe_2 sample (top), static and dynamic STXM imaging with smagnetic field applied along the microstrip (bottom left) and integrated spin-wave profile (bottom right), from [5].*

References

[1] C. Gong *et al.*, Nature **546**, 265 (2017).
[2] B. Ding *et al.*, Nano Lett. **20**, 868 (2020).
[3] Y.J. Bae *et al.,* Nature **609**, 282 (2022).
[4] L. Powalla *et al.*, Adv. Mater. **35**, 2208930 (2023).
[5] F. Schulz *et al.,* Nano Lett. **23**, 10126 (2023).

Abstract ID: 1611

SPIN-ORBIT TORQUE DRIVEN ANTIFERROMAGNETIC OSCILLATOR

P.K. Rout[1], J. Godinho[1], F. Vilsmeier[2], R. Salikhov[3], Z. Soban[4], R.M. Otxoa[5], C. Back[2], O. Hellwig[3,6], J. Wunderlich[1,4]

[1] *University of Regensburg, GERMANY*
[2] *Technical University of Munich, GERMANY*
[3] *Helmholtz-Zentrum Dresden-Rossendorf, GERMANY*
[4] *Institute of Physics, Czech Academy of Sciences, Prague, CZECH REPUBLIC*
[5] *Hitachi Cambridge Labyoratory, Cambridge, UNITED KINGDOM*
[6] *Chemnitz University of Technology, GERMANY*
E-mail: joerg.wunderlich@physik.uni-regensburg.de

Antiferromagnetic materials have unique properties due to their alternating exchange-coupled magnetic moment arrangements, leading to exchange-field enhanced fast and complex spin dynamics. Most intriguingly, excitation in antiferromagnets with locally broken inversion symmetry can be realized by current-induced spin-orbit torque (SOT), and complex self-oscillation modes near the critical spin-flop transition have been predicted when excited by antidamping SOT.

In this work, we realize an antiferromagnetic oscillator within a nanoconstriction patterned from a synthetic antiferromagnetic (SAF) multilayer. By exploiting the magnetic rectification effect (MRE), we first identify spin-orbit torque-driven excitations of optical and acoustic antiferromagnetic modes. Then, by adding a DC current to our radiofrequency excitation, we identify damping and anti-damping like SOT contributions by both MRE and Brillouin light scattering (BLS). Using spatially and temporally resolved magneto-optical Kerr effect (tr-MOKE) measurements, we observe pi-phase shifted current-induced oscillations of the Néel order in individual reversed antiferromagnetic domains at zero applied magnetic field. Finally we find first indications of self-oscillations near the critical spin-flop transition by MRE measurements, which appear only for DC currents above a critical current density.

CANCELLED

MgB2 – Materials and Applications I

01.05.2024 WEDNESDAY

Abstract ID: 1155

KINETICS MECHANISM ON THE EFFICIENCY OF C SUBSTITUTING B IN THE MgB_2 TAPE FABRICATION

Chen Guo[1], Dongliang Wang[1,2], Yanwei Ma[1,2], Zizhao Gan[3]

[1] *Institute of Electrical Engineering, Chinese Academy of Sciences, 100190, Beijing, PEOPLE'S REPUBLIC OF CHINA*
[2] *University of Chinese Academy of Sciences, 100190, Beijing, PEOPLE'S REPUBLIC OF CHINA*
[3] *School of Physics, Peking University, 100190, Beijing, PEOPLE'S REPUBLIC OF CHINA*
E-mail: dongliangwang@mail.iee.ac.cn

Effective carbon doping is essential for MgB_2 superconductors due to its enhancement on in-field critical current density. However, C-doped MgB_2 samples prepared with different boron powders exhibit varying levels of C substitution efficiency, which directly affect the superconducting properties. In this article, to further investigate the factors influencing C substitution efficiency, a two-stage carbon doping process was established based on the in-situ X-ray diffraction (XRD) measurement. The process begins with the initial in-situ ternary reaction of Mg, B and C, followed by the subsequent diffusion of C into the MgB_2 lattice. Through the analysis of thermodynamic equations, it can be inferred that the key factor in improving the C substitution efficiency for MgB_2 is to align the activity of the B and C precursor powders, which enables a greater participation of carbon in the initial stage of the ternary reaction. According to the systematic study on nano-C doped MgB_2 tapes, the C substitution efficiency in MgB_2 tapes prepared using nano amorphous boron powder is notably lower compared to those prepared using micron crystalline boron powder. These findings suggest that high-activity amorphous B powder necessitates a C dopant with a lower activation energy to enhance its C substitution efficiency.

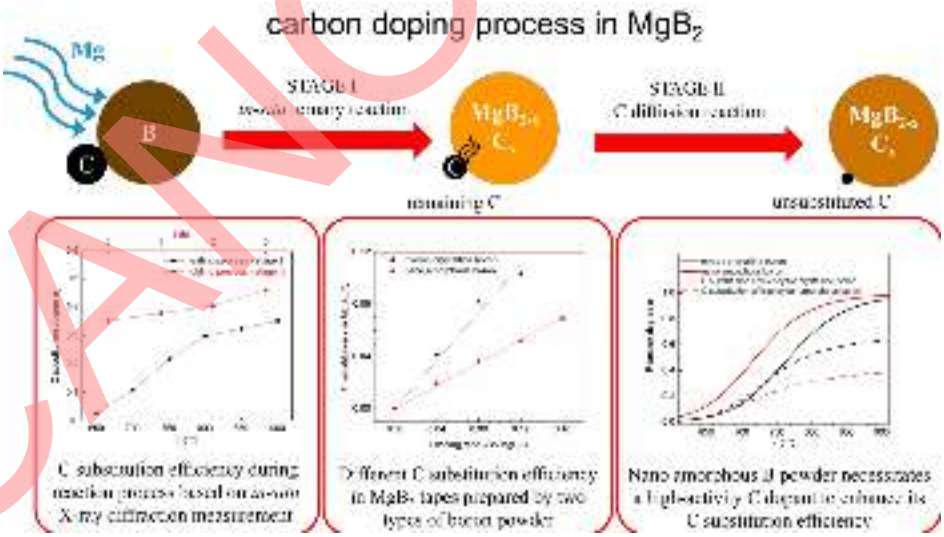

Fig. 1: *Carbon doping process in MgB_2.*

References

[1] C. Guo, D. Wang, X. Zhang, M. Han, M. Tang, C. Liu, X. Liu, F. Liu, H. Liu, Y. Ma, Z. Gan, Materials Today Physics **37**, 101217 (2023).

CANCELLED

Abstract ID: 1385

TEXTURED (00l) MgB_2 SMALL DISCS (20 mm IN DIAMETER AND ~2 mm THICKNESS) WITH HIGH LEVITATION FORCES AND TRAPPED MAGNETIC FIELDS

P. Badica[1], M. Grigoroscuta[1], A. Kuncser[1], C. Locovei[1], G. Aldica[1], A.M. Ionescu[1], S.B. Guner[2], B. Savaskan[3], U.K. Ozturk[3], T.S. Suzuki[4], O. Vasylkiv[4]

[1]National Institute of Materials Physics, 077125 Magurele, ROMANIA
[2]Recep Tayyip Erdogan University, 53100 Rize, TURKIYE
[3]Karadeniz Technical University, 61830 Trabzon, TURKIYE
[4]National Institute for Materials Science, 305-0047 Tsukuba, JAPAN
E-mail: badica2003@yahoo.com

Powder mixtures ($(MgB_2)_{0.99}A_{0.01}$) of MgB_2 and two types of additives (A) were prepared by dry mixing using a mechanical mill with plastic jars and balls. The raw powder and the as-prepared powder mixtures were subject to magnetic orientation process by slip casting under a magnetic field of 12 T [1]. To obtain a reference sample, also a raw powder without additive was processed by slip casting under zero magnetic field. Next, slip casted bodies were spark plasma sintered (SPS). The final sintered disks have a diameter of 20 mm and a thickness of 1.8-2.3 mm. X-ray diffraction measured on the top and bottom surface of the disks indicates on high degree of (00l) texture of MgB_2 with some differences between surfaces. On both surfaces of the disks, magnetic levitation forces were measured at 20 and 25 K. Trapped magnetic fields were also measured at 12 and 20 K with a Hall sensor positioned at the center of the disk surface. Zero-field cooling vertical levitation force attained high values of maximum 19.5 N at 20 K for a textured added sample comparative to about 15 N for the reference sample. The hysteresis between the curves of levitation force for approaching and departing from the surface of the sample is very small, but slightly increases at 25 K for a vertical levitation force that decreases with maximum 1N at higher temperature. Oriented added samples have shown on the surface of the disk trapped magnetic fields with a maximum value of about 4T at 20 K and 5.8 T at 12K.

Authors acknowledge E-COST-GRANT-CA19108-47678c7 and UEFISCDI, Romania through Core Program PC2-PN23080202 and PFE-35.

References

[1] M.A. Grigoroscuta, G.V. Aldica, M. Burdusel, V. Sandu, A. Kuncser, I. Pasuk, A.M. Ionescu, T.S. Suzuki, O. Vasylkiv, P. Badica, Journal of Magnesium and Alloys **10**, 2173–2184 (2022).

Abstract ID: TBD

TBD

TBD

[1] *TBD*
E-mail: TBD

TBD

MgB2 – Materials and Applications II

01.05.2024 WEDNESDAY

Abstract ID: 1430

SYNTHESIS, CHARACTERIZATION AND APPLICATION OF NEW 2D MATERIAL OF HYDROGEN BORIDE SHEETS DERIVED FROM MgB_2

Takahiro Kondo

[1] *Institute of Pure and Applied Sciences, University of Tsukuba, JAPAN*
E-mail: takahiro@ims.tsukuba.ac.jp

As new 2D materials, we have experimentally synthesized hydrogen boride (HB) sheets from MgB_2 [1]. HB sheets are composed of boron and hydrogen at a 1:1 stoichiometric ratio, which can be formed by an ion-exchange reaction between protons and magnesium cations in MgB_2 with exfoliation. In the HB sheets, boron atoms form a hexagonal 2D network, in which hydrogen atoms are bound to boron by three-center-two-electron bonds (B–H–B) and two-center-two-electron bonds (B–H) [2]. Experimental studies have clarified that HB sheets exhibit solid acid catalytic activity [3], metal ion reducibility [4], semimetal electronic properties [5], gas-sensor applicability [2], stability against water [6], CO_2 adsorption/conversion property including C-C coupling [7], and a light-responsive hydrogen release function [8, 9]. In the presentation, recent progress of HB sheets will be introduced.

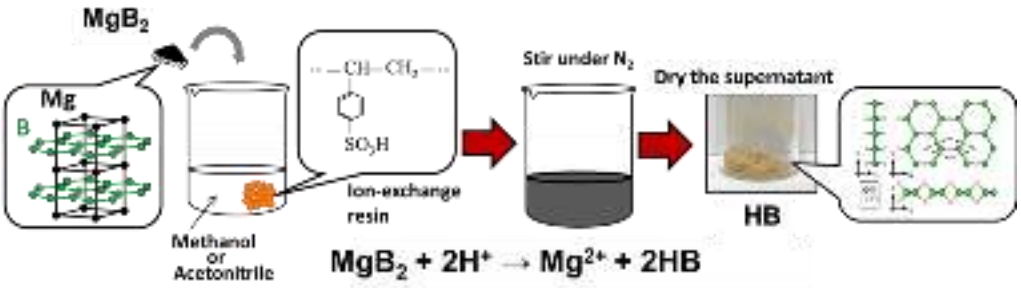

Fig. 1: *Schematic image of synthesis of hydrogen boride (HB) sheets from MgB_2.*

These works were done with Mr. H. Nishino, Prof. T. Fujita, Dr. N. T. Cuong, Dr. S. Tominaka, Prof. M. Miyauchi, Mr. N. Watanabe, Dr. S. Iimura, Dr. A. Hirata, Dr. N. Umezawa, Prof. S. Okada, Prof. E. Nishibori, Mr. A. Fujino, Mr. R. Ishibiki, Mr. T. Goto, Prof. A. Yamamoto, Dr. K. Horiba, Mr. K. Matsushita, Dr. M. Masuda, Prof. I. Hamada, Prof. Dr. A. Yamaguchi, Mr. R. Kawamura, Dr. J. M Oliva-Enrich, Dr. S. Ito, Dr. Tateishi, Prof. Niibe, Prof. J. N. Kondo, Dr. T. Fujitani, Prof. I. Matsuda, Prof. J. Nakamura, Prof. H. Hosono and other co-workers.

References

[1] H. Nishino, T. Fujita, N.T. Cuong, *et al.*, J. Am. Chem. Soc. **139**, 13761 (2017).
[2] S. Tominaka, R. Ishibiki, A. Fujino, K. Kawakami, *et al.*, Chem **6**, 406 (2020).
[3] A. Fujino, *et al.*, ACS Omega, **4**, 14100 (2019); A. Fujino, *et al.*, PCCP **23**, 7724 (2021).
[4] S.I. Ito, T. Hirabayashi, R. Ishibiki, R. Kawamura, *et al.*, Chem. Lett. **49**, 789 (2020).
[5] I. Tateishi, N.T. Cuong, C.A.S. Moura, *et al.*, Phys. Rev. Mate. **3**, 024004 (2019).
[6] K.I. Rojas, N.T. Cuong, H. Nishino, Commun. Mate. **2**, 81 (2021).
[7] T. Goto, S. Ito, S.L. Shindem *et al.*, Commun. Chem. **5**, 118 (2022).
[8] R. Kawamura, N. Cuong, T. Fujita, R. Ishibiki, *et al.*, Nat. Commun. **10**, 4880 (2019).
[9] M. Hikichi, J. Takeshita, N. Noguchi, S. Ito, *et al.*, Adv. Mater. Int. **10**, 2300414 (2023).

Abstract ID: 1046

THE EFFECT OF VACUUM ANNEALING ON THE SUPERCONDUCTING PROPERTIES OF MgB_2 FILM DEPOSITED BY MAGNETRON SPUTTERING ON HASTELLOY C276™ TAPE

I. Rudnev[1,2], I. Yanilkin[1], A. Gumarov[1], R. Batulin[1]

[1]*Kazan Federal University, 420008, Kazan, RUSSIA*
[2]*National Research Nuclear University MEPhI, 115409, Moscow, RUSSIA*
E-mail: iarudnev@mephi.ru

MgB_2 is a "conventional" superconductor with the highest critical temperature at about 39 K. Despite this high superconducting transition temperature, magnesium diboride is less used than NbTi and Nb_3Sn, which is due to the peculiarities of synthesizing this compound and other reasons. The melting temperatures of magnesium and boron are significantly different: 650 °C and 2075 °C, respectively. This difference in properties makes it difficult to obtain magnesium diboride (thin film, for instance) with desired composition and good crystallinity, because of even slight heating of MgB_2 leads to evaporation of magnesium from it, and changes stoichiometry. At the same time the influence of high temperature is necessary to obtain superconductivity in MgB_2. The solution is possible in various ways: annealing the Mg-B material (or simply boron) in magnesium vapor (a), synthesizing the material at elevated temperatures and with an excess flow of magnesium (b), cold synthesis of the material of the desired stoichiometry, protecting its surface from magnesium evaporation and annealing in a vacuum (c). Our work is devoted to finding the optimal technology for producing MgB_2 film by magnetron sputtering on Hastelloy C276™ tape. We investigated options (b) and (c) and established the effects of vacuum annealing on the superconducting properties (superconducting transition temperature and critical current) of films for both methods. In method (b), we obtained $T_c \approx 23$ K (Fig. 1), in method (c), $T_c \approx 10$ K.

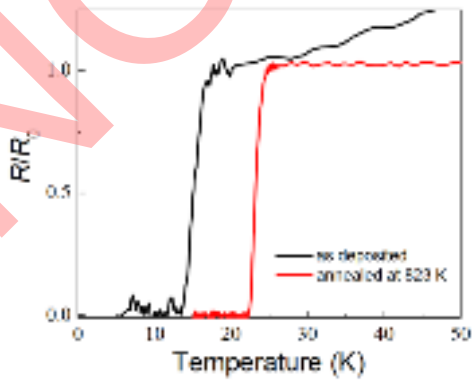

Fig. 1: *Increase in superconducting transition temperature upon vacuum annealing.*

The study was supported by the RSF grant 22-72-10088, https://rscf.ru/project/22-72-10088/

CANCELLED

Abstract ID: 1111

PRODUCTION OF MgB_2 WIRE AND JOINT BY EXTERNAL MAGNESIUM DIFFUSION METHOD

Doğan Avcı[1,2], Hakan Yetis[2], Fırat Karaboğa[3], Daniel Gajda[4], Michal Babij[4], Lan Maria Tran[4], Andrzej Zaleski[4], İbrahim Belenli[2]

[1]*Quantum Metrology Laboratory, National Metrology Institute, TUBITAK, Gebze, TÜRKIYE*
[2]*Physics deparment, Bolu Abant İzzet Baysal University, Bolu, TÜRKIYE*
[3]*Mehmet Tanrıkulu Vocat. Sch. Hlth. Serv., Bolu Abant İzzet Baysal University, Bolu, TÜRKIYE*
[4]*Institute of Low Temperature and Structure Research PAS, Wroclaw, POLAND*
E-mail: davci.0209@gmail.com

It is difficult to achieve a solid connection when joining IMD MgB_2 wires because the IMD wire has a thin MgB_2 ring layer. We implemented an innovative filling method designed to improve the connection between the IMD wire core and the joint bulk. This approach, called the "Half-EMD" (H-EMD) method, is a wire design with an outer diameter of 0.81 mm and containing longitudinally compressed semi-cylindrical columns of magnesium and boron. Electric transport measurements were performed at 4.2 K under different external magnetic fields. It is noteworthy that the undoped H-EMD wire carries 64 A DC current under 6 T at 4.2 K. On the other hand, a magnetic field as high as 24.3 mT was trapped within the single-turn coil formed by superconducting joint. The calculated value of the supercurrent circulating in the closed superconducting loop is approximately 200 A. The resistance value calculated based on the decay of the magnetic field trapped in the superconducting loop for 12 hours was found to be 3.14×10^{-15} Ω.

Abstract ID: 1526

IMPROVING THE MAGNETIC LEVITATION FORCE PERFORMANCE OF MgB_2 BULK SUPERCONDUCTORS BY CONVENTIONAL SINTERING PROCESS

Burcu Savaşkan[1], Sait Barış Güner[2], Kemal Öztürk[3], Petre Badica[4]

[1]*Department of Energy Systems Engineering, Faculty of Technology, Karadeniz Technical University, Trabzon 61830, TÜRKIYE*
[2]*Department of Physics, Faculty of Arts and Sciences, Recep Tayyip Erdogan University, Rize, TÜRKIYE*
[3]*Electromagnetic Guidance and Acceleration Research Group (EMGA), Department of Physics, Faculty of Science, Karadeniz Technical University, 61080, Trabzon, TÜRKIYE*
[4]*National Institute of Materials Physics, Atomistilor street 405A, 077125 Magurele, ROMANIA*
E-mail: bsavaskan75@gmail.com

Superconductivity in MgB_2 was discovered in 2001. The transition temperature of 39 K is relatively high, exceeding the values of low temperature (LTS) superconductors. Therefore, MgB_2 as a more suitable superconductor for applications working in liquid helium-free and low cost closed-cycle refrigerator systems. MgB_2 consists of abundant elements Mg and B in nature, without relatively expensive noble (e.g. Nb in LTS) or rare earth elements (as in HTS). It is biocompatible, biodegradable, and ecofriendly [1]. It has higher mechanical strength than high temperature superconducting (HTS) materials. Additionally, MgB_2 has the advantage of a relatively long coherence length (about one order of magnitude larger than for HTS) and low anisotropy when compared to HTS. This work investigates in-situ and ex-situ co-synthesis method to improve levitation performance of MgB_2 bulks at different sintering temperatures. Different weight percentages with the ratio of x wt.% ex situ powder were added to 1.5 g in situ powder via conventional sintering process where x=0, 10, 20, 25, and 30, respectively.

References

[1] P. Badica, D. Batalu, Green Chem. Lett. Rev. **15**, 646–657 (2022).

CANCELLED

Abstract ID: 1662

PRELIMINARY STUDY ON THE PHASE FORMATION OF JOINTS OF MgB_2/Fe WIRES BY INDUCTION PROCESSES

Mustafa Akdoğan, Bayram Albayrak

Department of Physics, Bolu Abant İzzet Baysal University, Bolu, 14300, TÜRKIYE
E-mail: mustafaakd@gmail.com

Superconducting MgB_2/Fe wires are promising for various high-performance applications. Joining two separate MgB_2/Fe wires is crucial for constructing complex superconducting systems. In this preliminary study, we investigate the phase formation at the joints of two separate MgB_2/Fe wires using induction processes. The joints undergo induction heating under varying process parameters to understand their influence on phase formation and resulting superconducting properties. Characterization techniques, including X-ray diffraction and microstructural analysis, are employed to analyze the phases formed at the joint interface. The results offer insights into the feasibility of using induction processes to produce high-quality joints between two separate MgB_2/Fe wires, which is essential for advancing superconducting applications.

Graphene and 2D Materials (2DM) – Experimental Session

01.05.2024 WEDNESDAY

Abstract ID: 1380

FORMATION OF HIGH-QUALITY 2D Mo2C CRYSTALS AND THEIR GRAPHENE HETEROSTRUCTURES

Omer Refet Caylan[1,2,*], Elif Okay[1], Eren Atlı[1], Zişan Güler[1], Omer Tarik Ogurtani[3], Goknur Cambaz Buke[1]

[1]Department of Materials Science and Nanotechnology Engineering; Micro and Nanotechnology Graduate Program, TOBB University of Economics and Technology, 06560, Ankara, TURKIYE
[2]National Nanotechnology Research Center, UNAM, Bilkent University, 06800, Ankara, TURKIYE
**Currect Affiliation: Department of Mechanical Engineering MIT, Massachusetts, USA*
[3]Department of Metallurgical and Materials Engineering, Middle East Technical University, 06531 Ankara, TURKIYE
E-mail: goknurcambaz@gmail.com

The discovery of graphene, with its extraordinary properties, has catalyzed the investigation, synthesis, and application of innovative 2D materials, establishing itself as a vibrant domain within condensed matter physics and materials science research. Beyond graphene, exploration into alternative 2D materials has gained momentum, with Mo2C emerging as a notable addition to the 2D materials family. In recent years, Mo2C has attracted considerable attention for its potential applications in quantum information science and engineering, particularly owing to its thickness-dependent superconductivity. This study delves into the controlled growth of Mo2C crystals through Chemical Vapor Deposition (CVD) on Cu substrates.

Examining critical processing parameters such as catalyst thickness, gas ratios and amounts, process temperature, duration, and the coexistence of graphene, this research sheds light on the intricacies of controlled growth. The findings underscore the pronounced impact of copper layer thickness on the resulting thickness of Mo2C crystals. Moreover, the study extends beyond optimizing Mo2C crystal growth to delve into the synthesis of tailored Mo2C crystals tailored for specific applications. The developed forward model not only enhances our understanding of Mo2C crystal growth but also serves as a foundation for further advancements and exploration of related material analogs.

This material is based on the work supported by the Air Force Officeof Scientific Research, award numbers: FA9550-19-1-7048, FA9550-22-1-0358.

Abstract ID: 1298

SYNTHESIS AND CHARACTERIZATION OF VERTICALLY ALIGNED CARBON NANOTUBES (VACNTs) ON SiC FOR FIELD EMISSION

Erhan Gurpinar[1], Tyson Back[2], Jon Ludwick[3], Marc Cahay[3], Goknur Cambaz Buke[1]

[1]Micro and Nanotechnology, Graduate School of Engineering and Science; Department of Materials Science and Nanotechnology Engineering, TOBB University of Economics and Technology, Ankara, TURKEY
[2]AFRL Materials and Manufacturing Directorate, WPAFB, OH, USA
[3]Department of Electrical and Computer Engineering, University of Cincinnati, Cincinnati, OH, USA
E-mail: erhann.gurpinar@gmail.com

The use of carbon nanotubes (CNTs) as field electron emitters has garnered attention due to their high aspect ratio, mechanical strength, and thermal stability. However, challenges such as vertical alignment, catalyst impurities, contact resistance, adherence to substrates, and controlled growth methods hinder their application in high-power field emission (FE) devices. Catalyst impurities, in many cases metallic particles, cause unreliable electron emission response, can reduce electron emission density, and can also be responsible for other undesirable side effects; either by melting and or evaporation of the catalyst. In addition, bonding of CNT to any substrate is a formidable task since carbon does not wet and bond to other materials easily. As a result of these intrinsic properties of carbon, the bond strength between CNT and substrates is weak causing two engineering challenges. First, weak interface between CNT and substrate increases electrical resistance at the interface. Second, equally importantly, a weak interface creates heat spikes at high power applications which is a significant challenge in pulsed power conditions.

To overcome these challenges, in this study we investigated the controlled formation mechanism of catalyst-free vertically aligned CNTs (VACNTs) on silicon carbide (SiC) substrates through vacuum decomposition and evaluate their field emission performance.

This study is supported by the Air Force Office of Scientific Research grant number FA9550-19-1-7048.

Abstract ID: 1410

HUNTS FOR A SUPERCONDUCTIVE PHASE IN NANOGRAPHITE FILMS

S.G. Lebedev

Department of Experimental Physics of the Institute for Nuclear Research of Russian Academy of Sciences, 60th October Anniversary prospect, 7a, Moscow, 117312, RUSSIA
E-mail: lebedev@inr.ru

Report describes some unconventional electromagnetics properties of nanographite (NG) films which reminiscent room temperature superconductivity. NG film is the composite of 20-30Å graphite clusters embedded in amorphous matrix. At such a small dimension the superconductivity can be explained by the attraction of all electrons to all kernels of atoms constituting the graphite cluster. Possibilities of room temperature weak superconductivity in nanographite films are supported by the observation of reversed Josephson Effect (which is the transformation of microwave irradiation falling on the sample into the direct current through this sample) and its temperature dependence. This dependency is fully reminiscent the behavior of known superconductors. Another effect is switching conductivity from high to very small value at some critical current (which can be used in electrical switchers), pinning of vortices on columnar topological structure of film observed in magnetic force microscope. In the article, an attempt is made to explain the appearance of coherent optical radiation upon conductivity switching in nanographite films by the movement of magnetic vortices and the thermomagnetic instability of their magnetic structure. Under the effort to find the state of global phase coherence in the nanographite films, the Josephson current at room temperature was detected, to the best of our knowledge, for the first time, when measuring the current-voltage characteristics.

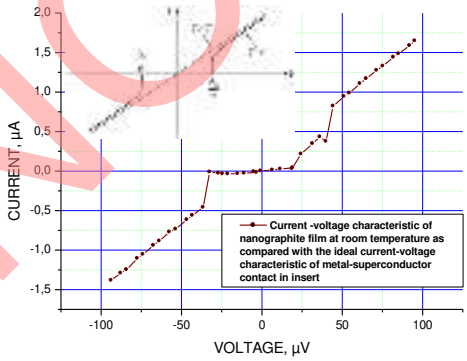

Fig. 1: *CVC of a nanographite film at low currents and room temperature.*

CANCELLED

Abstract ID: 230

SEARCHING FOR THE WORKING PRINCIPLE OF FLOW-INDUCED VOLTAGE IN GRAPHEME

Qian Yang

Department of Physics and Astronomy, The University of Manchester, Oxford Road, Manchester, UK
E-mail: qian.yang@manchester.ac.uk

The quantum interaction at the carbon-liquid interface has attracted widespread research interest in recent years. One of the most intriguing phenomena is that liquid flows through carbon nanotubes and monolayer graphene surface can induce a detectable voltage. Various studies conducted until now lead to diverse, sometimes conflicting, mechanisms behind this phenomenon, including fluctuating ratchets[1], adsorption and desorption of ions, Coulomb drag, pseudocapacitance[2], streaming potential, or phonon drag[3]. Although numerous experiments have been done to prove these concepts, no consensus has been established. Our experimental work aims at investigating the flow-induced voltage in graphene at the mesoscopic level, to gain better understanding of ion-electron interactions and how quantum frictions contribute to this phenomenon comprehensively. To this end, we choose mechanically exfoliated graphene to minimize the disorder usually induced in graphene from other processes, such as CVD graphene. By carefully tuning the liquid flow rate through graphene surface, the electrical response of the graphene was measured using low-noise DC measurements. In our preliminary results, deionized water shows the most significant signal for electricity generation, compared to that of high concentration KCl solution. This counterintuitive result indicates that the electrical double layer plays a pivotal role in flow-induced voltage, since concentrated solutions would induce a compact Stern layer and screen out electric interactions between the fluid and the graphene. Our results provide a microscopic picture of the solid-liquid interface that is ubiquitous in many important fields including catalysis, biology and electrochemistry.

References

[1] S. Ghosh, A.K. Sood, N. Kumar, *Carbon nanotube flow sensors*, Science, **299**, 1042 (2003).
[2] J. Yin, X. Li, J. Yu, Z. Zhang, J. Zhou, W. Guo, *Generating electricity by moving a droplet of ionic liquid along grapheme*, Nature Nano. **9**, 378 (2014).
[3] M. Lizée, A. Marcotte, B. Coquinot, N. Kavokine, K. Sobnath, *et al.*, *Strong electronic winds blowing under liquid flows on carbon surfaces*, Phys. Rev. X **13**, 011020 (2023).

Graphene and 2D Materials – Theory Session

01.05.2024 WEDNESDAY

Abstract ID: 213

THE HOLE-DOPING INDUCED FERROMAGNETISM IN QUARTIC SYSTEMS

M. Polat, H. Sevinçli

Izmir Institute of Technology, Department of Materials Science and Engineering, 35430 Urla, İzmir, TURKEY
E-mail: mpolat.mustafa@gmail.com

The scarcity of two-dimensional (2D) materials with intrinsic ferromagnetism is one of the major challenges in the field of spintronics and stimulates the investigation of atomically-thin ferromagnetic (FM) materials. Currently, a broad class of 2D materials, including metal halides, sulfides, oxides, and nitrides are reported to develop a half-metallic ground state upon hole doping, and these hole-doped 2D materials appear to be promising candidates for high-temperature spintronic applications [1]. In particular, some of these single-layers such as GaSe, GaS, InSe, SnN, and the group-V elements with a honeycomb crystal structure are of great interest due to the Mexican-hat-shaped quartic dispersion near the top of the valence band [2-4]. In fact, the quartic dispersion results in a sharp van Hove singularity in the density of state near the Fermi level, leading to the spontaneous formation of spin-polarized ground state upon hole doping. Using the second-nearest neighbor tight-binding approximation + U (the Hubbard model), we examine the FM ground state properties of the hole-doped quartic systems such as quasi-one-dimensional and 2D systems. The electron-electron interactions lead to a non-magnetic to FM transition in armchair nanotubes (ANT) and 2D materials within the Stoner model of band ferromagnetism. However, the same ground state has completely different features if the system is the zigzag nanoribbon (ZNR), as shown in Fig.1.

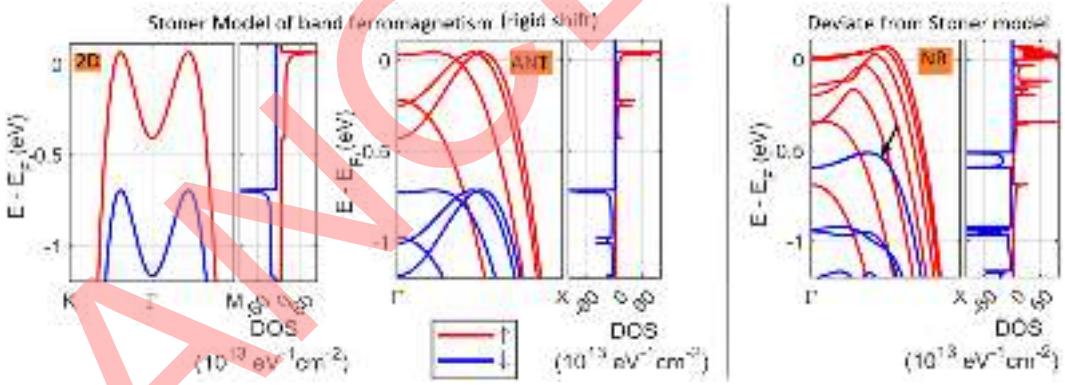

Fig. 1: *The effects of geometry on the formation mechanicsm of itenerant ferromagnetism. In all panels, $U/t_1 = 2$ and $\rho = 3.13 \times 10^{13}/cm^2$. Both 2D and ANT systems exhibit a Stone-type magnetic instability upon hole doping, whereas the ZNR geometry results in a bandwidth broadening and dispersion changes in its majortiy spin channel. These changes in the band structure is a signature of a deviation from the rigid band displacement model.*

References

[1] Ruishen Meng *et al.*, npj Comput. Mater. **8(1)**, 230 (2022).
[2] Ting Cao *et al.*, PRL **114(23)**, 236602 (2015).
[3] Konstantina Iordanidou *et al.*, ACS Appl. Nano Mater. **1(12)**, 6656–6665 (2018).
[4] Hâldun Sevinçli. Nano Lett. **17(4)**, 2589–2595 (2017).
[5] Mustafa Polat, Hâldun Sevinçli, *Doping-induced magnetism in Mexican-hat-shaped quartic dispersion systems: A mean-field Hubbard approach* (Under review/PRB) (2023).

CANCELLED

Abstract ID: 1200

OPTICALLY INDUCED CHAOTIC IONIZATION OF RELATIVISTIC ATOMS CREATED BY COULOMB IMPURITIES IN GRAPHENE

J. Matrasulov[1], J. Yuspov[2], I. Ibragimov[2]

[1]*Uzbekistan, Tashkent, National University of Uzbekistan, 4 University Str., 100174, Tashkent, UZBEKISTAN*
[2]*Kimyo International University in Tashkent, 156 Usman Nasyr Str., 100121 Tashkent, UZBEKISTAN*
E-mail: jasur1362@gmail.com

Charged impurities in graphene are powerful tool for studying of relativistic quantum mechanics and QED in low dimensions. This becomes possible due to the fact that they can "mimic" one- and two-dimensional relativistic atoms, where electron dynamics is described in terms of ultrarelativistic Dirac equation. Different aspects of (artificial) relativistic atoms created in graphene by Coulomb impurities have been studied so far, both theoretically and experimentally [1-3]. Despite this fact, some issues of the problem are remaining as less studied. These concerns for instance, the problem of charged impurities driven by external optical (microwave) field, where chaotization of atom can occur. The latter implies diffusive ionization of atom due to the chaotization of atomic electron's motion. In this work we consider one- and two-dimensional relativistic atom created in graphene by Coulomb impurity driven by external linearly polarized monochromatic (optical) field. Both classical and quantum regimes of motion are considered.

For classical regime, we explore phase space portraits and Poincare surfaces of section, as well as compute Lyapunov exponents from the viewpoint of entering of atom into the chaotic regime. For quantum regime, we study diffusive ionization of atomic electron by computing probability and cross section of ionization. Also, average kinetic energy of atomic electron is computed.

This work is supported by the grant of the Agency of Innovative Development of the Republic of Uzbekistan, World Bank Project "Modernizing Uzbekistan National Innovation System" (Ref. Nr. REP-05032022/235).

References

[1] H. Friedrich, D. Wintgen, T*he hydrogen atom in a uniform magnetic field — An example of chaos*, Physics Reports, **V. 183**, pp. 37.

[2] D. Delande, J.C. Gay., *Quantum chaos and statistical properties of energy levels: numerical study of the hydrogen atom in a magnetic field*, Physical Review Letters, **V. 56**, pp. 2006 (1986).

[3] W. Schweizer, R. Niemeier, H. Friedrich, G. Wunner, H. Ruder, *Lyapunov exponents for classical orbits of the hydrogen atom in a magnetic field*, Physical Review A, **V. 38**, pp. 1724 (1988).

Abstract ID: 1394

ELECTRONIC TRANSITION IN COULOMB IMPURITIES IN GRAPHENE DRIVEN BY ULTRASHORT IN OPTICAL PULSES

S. Rakhmanov[1] R. Egger[2], D. Matrasulov[3]

[1]*Chirchik State Pedagogical University, 104 Amur Temur Str., 111700 Chirchik, UZBEKISTAN*
[2]*Institut für Theoretische Physik, Heinrich-Heine-Universität, 40225 Düsseldorf, GERMANY*
[3]*Turin Polytechnic University in Tashkent, 17 Niyazov Str., 100095 Tashkent, UZBEKISTAN*
E-mail: saparboy92@gmail.com

We provide a theory for electronic transitions induced by ultrashort electromagnetic pulses in two-dimensional artificial relativistic atoms which are created by a charged impurity in a gapped graphene monolayer. Using a nonperturbative theoretical approach, based on modified version sudden-perturbation approximation, we compute the electronic excitation, ionization, and electron-hole pair creation probabilities and cross sections. This approach becomes exact in the limit of δ-type pulses. The essential assumption behind our theory is therefore that the pulse is very short. Analytical expressions for the electronic transition amplitude have been obtained from the time-dependent Dirac equation, where we find that the dependence on external field parameters enters solely via the effective momentum transfer. Using this theoretical approach, the probabilities for excitation, ionization, and pair creation can then be computed as a function of the momentum transfer q.

This work is supported by the Grant REP-05032022/235 ("Ultrafast phenomena and vacuum effects in relativistic artificial atoms created in graphene"), funded under the MUNIS Project, supported by the World Bank and the Government of the Republic of Uzbekistan.

References

[1] V.I. Matveev, *Sudden-perturbation approximation for the dirac equation*, Theor. Math. Phys. **142**, 48 (2005).

Abstract ID: 259

TRAPPED PHOTONS: TRANSVERSE PLASMONS IN LAYERED SEMICONDUCTING HETEROSTRUCTURES

N. Golenić[1,2], S. de Gironcoli[1], V. Despoja[2]

[1]*Scuola Internazionale Superiore di Studi Avanzati (SISSA), Via Bonomea 265, 34136 Trieste, ITALY*
[2]*Institute of Physics (IFS), Bijenička 46, 10000, Zagreb, CROATIA*
E-mail: ngolenic@sissa.it

We elucidate the properties of a transversal polarization mode known as the trapped photon (T-ph) in thin-film semiconducting heterostructures of WS2 separated by dielectric hBN layers. The T-ph shares similarities with the longitudinal 2D Dirac plasmon mode (DPP) found in (doped) conductive crystals, however, its oscillatory strength is many times greater in comparison to the DPP. Additionally, its intensity and energy can be fine-tuned by adjusting the number of semiconducting layers rather than doping, allowing for enhanced photon-electron-hole or photon-exciton binding. In our work1, we demonstrate that T-ph is a fundamental mode present in all thin-film materials which support dipole-active electronic transitions and is equivalent to the transversal plasmon mode in monolayer graphene predicted by Mikhailov et al.2 However, in conductive crystals, T-ph remains elusive due to strong screening by the intraband electron-hole continuum. We further emphasise that T-ph is quite different from the extensively studied photon-cavity modes as it does not appear due to light-confinement within a resonant cavity structure. Instead, T-ph arises from the coupling between light and either single particle electron-hole transitions or collective oscillations of bound electron-hole pairs (excitons) in the material. Due to the evanescent character of T-ph, it is rather difficult to observe experimentally, hence we simulate an s-SNOM experiment we devised specifically to experimentally confirm its presence in WS2/hBN heterostructures. In conclusion, the unique properties and tunability of the trapped photon mode present exciting possibilities for its application in optoelectronics, sensing, and quantum information processing. As such, further exploration of this mode could lead to significant advances in these fields.

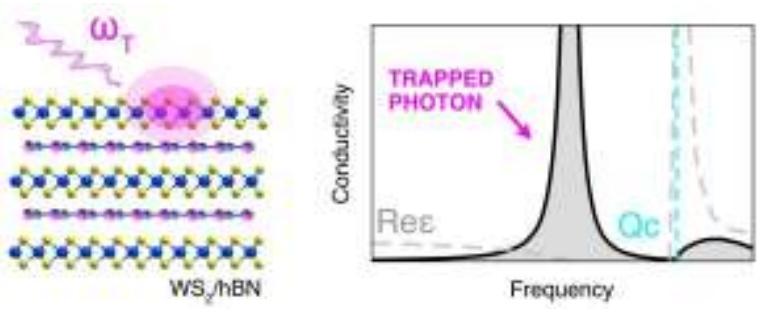

Fig. 1: *(left) The T-ph mode excited at the surface of a WS_2 /hBN van der Waals heterostructures with a SNOM driving frequency ω_T. (right) The T-ph conductivity peak below the light conus confirms the emergence of a robust transversely polarised exciton-polariton mode with plasmonic character.*

References

[1] N. Golenić, V. Despoja, *Trapped photons: transverse plasmons in layered semiconducting heterostructures*, submitted for review (2023).

[2] S.A. Mikhailov, K. Ziegler, *New electromagnetic mode in graphene*, Phys. Rev. Letters, **99(1)**, 016803 (2007).

Superconducting Spintronics: Novel Quantum Circuits I

01.05.2024 WEDNESDAY

Abstract ID: 1456

OPTIMIZATION OF SUPERCONDUCTING PICKUP LOOPS AND TRANSFORMERS FOR SQUID-BASED QUANTUM SENSORS

P. Febvre[1], C. Fourie[2], U. Yılmaz[1,3], A. Bozbey[4]

[1]CROMA, University Savoie Mont Blanc, 73376 Le Bourget du Lac, FRANCE
[2]Stellenbosch University, Stellenbosch, 7600, SOUTH AFRICA
[3]now at IQM, Munich, GERMANY
[4]TOBB ETU, 06560, Ankara, TURKEY
E-mail: Pascal.Febvre@univ-savoie.fr

SQUIDs sensors are among the most developed devices in superconducting electronics as they are used in a wide range of applications, from magnetometry applications as magnetometers or gradiometers [1], to determine the values of inductances on-chip of low-T_c [2-3] and high-T_c [4] superconducting circuits, mostly for research studies, and also as quantum sensors based on DC- or rf-SQUIDs [5]. For a long time the limited availability of 3D design tools for superconducting devices and circuits, combined with the non-linear physics of Josephson devices, has often led to simple geometries for SQUID flux pickup loops and transformers, whose properties can be deduced from analytical calculations and fine-tuned from experimental feedback.

Fig. 1: *Multi-slot washer loop used for the inductance and effective area analysis with Inductex.*

In this work we take advantage of the existence of powerful 3D inductance extraction tools like Inductex [3] to investigate a range of more complex geometries of pickup loops in order to optimize their effective area and the effective area to inductance ratio for the cases where properties are difficult to assess with an analytical approach. We started with multi-slot pickup loops [6] such as the one in Fig.1 whose properties have been determined experimentally to verify the analysis. From there we show new, and sometimes less conventional geometries, that allow to optimize the effective area and the inductance over effective area ratio for specific applications.

Finally some specific transformers will also be optimized with the same approach for quantum sensing applications.

References

[1] J. Clarke, A.I. Braginski, *The SQUID Handbook: Applications of SQUIDs and SQUID Systems*, John Wiley & Sons, 2006.

[2] J.-C. Villegier, B. Delaet, V. Larrey, P. Febvre, J.W. Tao, G. Angenieux, *Extraction of material parameters in NbN multilayer technology for RSFQ circuits*, Physica C: Superconductivity, **vol. 326–327**, pp. 133–143 (1999); doi: 10.1016/S0921-4534(99)00410-4.

[3] C.J. Fourie, O. Wetzstein, T. Ortlepp, J. Kunert, *Three-dimensional multi-terminal superconductive integrated circuit inductance extraction*, Supercond. Sci. Technol., **vol. 24, no. 12**, p. 125015 (2011); doi: 10.1088/0953-2048/24/12/125015.

[4] T. Wolf *et al.*, *YBCO Josephson junctions and striplines for RSFQ circuits made by ion irradiation*, IEEE Transactions on applied superconductivity, **vol. 23, no. 2**, pp. 1101205–1101205 (2013).

[5] V.I. Shnyrkov, A.P. Shapovalov, V.Y. Lyakhno, A.A. Kalenyuk, A. Dumik, P. Febvre, *An RF SQUID readout for a flux qubit-based microwave single photon counter*, Supercond. Sci. Technol. **36**, 035005 (2023).

[6] E. Dantsker, S. Tanaka, J. Clarke, *High-T_c superconducting quantum interference devices with slots or holes: Low 1/f noise in ambient magnetic fields*, Appl. Phys. Letters, **vol. 70, no. 15**, pp. 2037–2039 (1997).

Abstract ID: 1237

SUPERCONDUCTING NEURON AND SYNAPSE FOR ARTIFICIAL NEURAL NETWORK

Anatolie Sidorenko[1,2]

[1]*Technical University of Moldova, D.Ghitu Institute of Electronic Engineering and Nanotechnologies, Academiei 3/3 Chisinau, 2028 MOLDOVA*
[2]*Skobeltsyn Institute of Nuclear Physics, M.V. Lomonosov Moscow State University, Moscow, RUSSIA*
E-mail: sidorenko.anatoli@gmail.com

The need to radically reduce energy consumption is becoming a decisive parameter limiting the development of new supercomputers. A promising solution is the development of computers with a brain-like architecture - artificial neural networks (ANNs) with superconducting basic elements. That requires the development of two main elements of neural network - a nonlinear switch, a neuron, and linear connecting elements, a synapse [1].

The results of the design and research of artificial neurons based on superconducting spin valves and superconducting synapses based on superconductor-ferromagnetic hybrid nanostructures are presented. Study of proximity effect in the multilayer superconductor/ferromagnetic (S/F) nanostructures with ferromagnetic layers of various thicknesses and coercive fields, as well as superconducting layers of constant thickness equal to the coherence length of superconductor is presented and discussed.

In Nb/Co superlattices a change in the superconducting order parameter in thin niobium films is observed due to a switch from parallel to antiparallel magnetic ordering of adjacent ferromagnetic layers. Such superlattices can be used as suitable basic elements of superconducting spintronics for ANN engineering [2,3]. Creating an ANN using these two basic elements - artificial neurons and artificial synapses, makes it possible to build a computer with several orders of magnitude lower power consumption compared to the existing computers built on semiconductor elements.

The research was supported by RSF project No. 22-79-10018 “Controlled kinetic inductance based on superconducting hybrid structures with magnetic materials”.

References

[1] I.I. Soloviev, N.V. Klenov, S.V. Bakurskiy, M.Y. Kupriyanov, A.L. Gudkov, A.S. Sidorenko, *Beyond Moore’s technologies: operation principles of a superconductor alternative*, Beilstein J. Nanotechnol., **8**, pp. 2689–2710 (2017); https://doi.org/10.3762/bjnano.8.269.

[2] I.I. Soloviev, A.E. Schegolev, N.V. Klenov, S.V. Bakurskiy, M. Yu Kupriyanov, M.V. Tereshonok, A.V. Shadrin, V.S. Stolyarov, A.A. Golubov, *Adiabatic superconducting artificial neural network: Basic cells*, Journal of Applied Physics, **124**, 152113 (2018), https://doi.org/10.1063/1.5042147.

[3] A. Schegolev, N. Klenov, S. Bakurskiy, I. Soloviev, M. Kupriyanov, M. Tereshonok, A. Sidorenko, *Tunable superconducting neurons for networks based on radial basis functions*, Beilstein J. Nanotechnol., **13**, pp. 444–454 (2022).

Abstract ID: 1128

DENSITY OF STATES IN THE PRESENCE OF SPIN-DEPENDENT SCATTERING IN SF BILAYERS

A.V. Guravova[1], T. Karabassov[1], A.A. Golubov[2], A.S. Vasenko[1]

[1]*National Research University Higher School of Economics, 101000 Moscow, RUSSIA*
[2]*University of Twente, 7500 AE Enschede, THE NETHERLANDS*
E-mail: guravovaa@mail.ru

We present a quantitative study of the density of states (DOS) in SF bilayers (where S is a bulk superconductor and F is a ferromagnetic metal) in the diffusive limit. We solve the quasiclassical Usadel equations in the structure considering the presence of magnetic and spin–orbit scattering. For practical reasons, we propose the analytical solution for the density of states in SF bilayers in the case of a thin ferromagnet and low transparency of the SF interface. This solution is confirmed by numerical calculations using a self-consistent two-step iterative method. The behavior of DOS dependencies on the interface transparency parameter γ_B, the F-layer thickness d_f, the exchange field h, magnetic and spin–orbit scattering times is discussed [1].

A.V.G., T.K and A.S.V. acknowledges support from the Mirror Laboratories Project of HSE University.

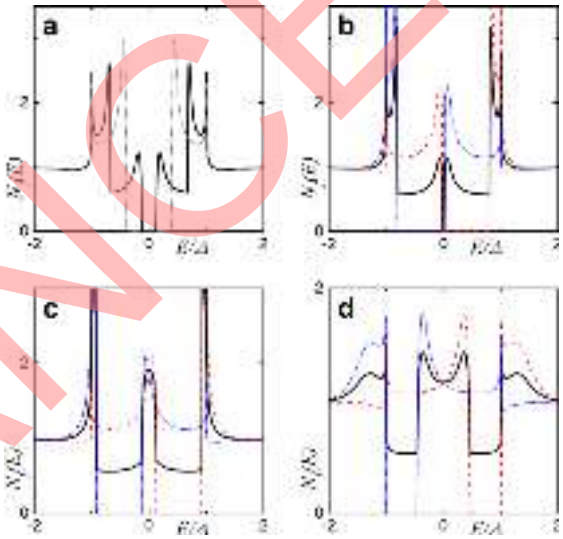

Fig. 1: *The evolution of the DOS plotted for increasing values of the exchange field h. Here, $\gamma_B = 5$, $d_f = 0.5\xi_f$. In plot (a), the gray dotted line represents the case of $h = 0$ (i.e., the NS bilayer). In plots (a)–(d), black solid lines correspond to the total DOS while red dashed lines show $N_{f\uparrow}(E)$ and blue dash-dotted lines show $N_{f\downarrow}(E)$. (a) Black solid line calculated for $h = 0.4\perp$, and all lines are calculated for (b) $h = 0.8\perp$, (c) $h = \perp$, and (d) $h = 1.6\perp$ [1].*

References

[1] T. Karabassov, V.D. Pashkovskaia, N.A. Parkhomenko, A.V. Guravova, E.A. Kazakova, B.G. Lvov, A.A. Golubov, A.S. Vasenko, Beilstein J. Nanotechnol., **13**, 1418 (2022).

CANCELLED

Superconducting Spintronics: Novel Quantum Circuits II

01.05.2024 WEDNESDAY

Abstract ID: 1454

NUMERICAL ANALYSIS OF SQUID EFFECTIVE AREA INFLUENCED BY FLUX FOCUSING AND KINETIC INDUCTANCE

C.J. Fourie

Department of Electrical and Electronic Engineering, Stellenbosch University, Stellenbosch, 7600, SOUTH AFRICA
E-mail: coenrad@sun.ac.za

Superconducting quantum interference devices (SQUIDs) are very sensitive magnetic flux to voltage sensors with application from magnetic sensors through analogue and digital superconductor electronics to quantum devices. The effective flux capture area of a SQUID affects the field-to-flux conversion efficiency and the magnetic field noise sensitivity [1, 2], but also the spatial resolution for nano-SQUIDs [3]. The effective area can be estimated from the geometric area of the SQUID and pickup loops, but this can differ significantly from measurements due to the effects of kinetic inductance – especially in high temperature SQUIDs – and flux focusing from the loop layouts or nearby feedback geometries [3]. The numerical inductance extractor, InductEx [4], with recent capabilities that allow compact simulation model extraction from arbitrary layouts, can be used to calculate the effective area of any SQUID layout. We show, in comparison with measured and published results, how the effects of flux focusing and temperature dependent kinetic inductance can be modeled when a SQUID layout is analysed. We also discuss how these results and modeling methods allow SQUID optimization for magnetic field noise sensitivity of spatial resolution.

References

[1] L.P. Lee. J. Longo, V. Vinetskiy, R. Cantor, *Low-noise $YBa_2Cu_2O_{7-d}$ direct-current superconducting quantum interference device magnetometer with direct signal injection*, Appl. Phys. Lett., **vol. 66**, pp. 1539-1541, 1995.

[2] D. Koelle, A.H. Miklich, F. Ludwig, E. Dantsker, D.T. Nemeth, J. Clake, *DC SQUID magnetometers from single layers of $YBa_2Cu_3O_{7-d}$*, Appl. Phys. Lett., **vol. 63**, pp. 2271-2273, 1003.

[3] Z. Qing, T. Yuchien, L. Jinjin, L. Hao, J. Kaili, Z. Yuan, C. Wenhui, M. Zhang, W. Xueshen, *High transfer coefficient niobium nana-SQUID integrated with a nanogap modulation flux line*, Mesas. Sci. Technol. **Vol. 32**, Art. ID. 025001, 2020.

[4] C.J. Fourie, O. Wetzstein, T. Ortlepp, J. Kunert, *Three-dimensional multi-terminal superconductive integrated circuit inductance extraction*, Supercond. Sci. Technol., **vol. 24, no. 12**, Art. ID. 125015, 2011.

Abstract ID: 1637

CONTROLLED SUPERCONDUCTIVITY IN VAN DER WAALS SUPERCONDUCTOR/FERROMAGNET HETEROSTRUCTURES

A.S. Ianovskaia[1], G.A. Bobkov[1], K.A. Bokai[2,1], I.V. Bobkova[1]

[1] *Moscow Institute of Physics and Technology, 141701, Dolgoprudny, RUSSIAN FEDERATION*
[2] *St. Petersburg State University, 7/9 Universitetskaya nab., St. Petersburg, 199034, RUSSIA*
E-mail: ianovskaia.as@phystech.edu

It is a well-known fact that in thin-film hybrid superconductor/ferromagnet (S/F) structures the exchange field induced in the superconductor suppresses superconductivity [1]. This effective field appears as a result of the proximity effect with the ferromagnet. Quasi-2D and van der Waals S/F heterostructures provide a convenient platform for realizing phenomena associated with proximity effects, because in this case the interface region extends over the entire material. Due to the low number of monoatomic layers in the heterostructure, the effects of hybridization of electronic spectra turn out to be important in the described heterostructures, due to which the superconducting state will be greatly modified. The degree of hybridization, and hence superconductivity, can be controlled using the gate voltage, which is of great scientific interest. In this talk we discuss the modification of the superconducting state in quasi-2D and van der Waals S/F heterostructures. In addition, we report how the behavior of the superconducting state depends on a change in the number of monolayers: from non-trivial behavior in the monolayer regime to behavior that almost corresponds to the conventional bulk case.

The support by the RSF via the project #24-22-00186 is acknowledged.

References

[1] G. Sarma, Journal of Physics and Chemistry of Solids, **24**, 1029 (1963).

Abstract ID: 1188

RETURN CURRENT OF JOSEPHSON JUNCTION: INFLUENCE OF FRUSTRATION EFFECTS

I.N. Askerzade[1,2]

[1] *Department of Computer Engineering and Center of Excellence of Superconductivity Research, Ankara University, TR06100, TURKEY*
[2] *Khazar University, Bashir Safar-Oghlu St, 122, Baku AZ1009, AZERBAIJAN*
E-mail: imasker@eng.ankara.edu.tr

The nonlinear behaviour in Josephson junctions (JJ) is easily accessible for experimental measurements in addition to circuit simulations and numerical analysis [1]. Josephson junctions based on high-Tc superconductors and other types of superconducting structures contain second harmonics [2-4]. There is growing interest to this multi-band superconductors in which superconductivity in different bands couples through interband coupling. Detail investigation of dynamics of switching of JJ, based in new superconductors seems also interesting for the study of order parameter structure in these compounds. The influence of multiple tunneling channels on JJ dynamics becomes also actual due to the fabrication of JJ, based on many band compounds such as iron-based or MgB_2 [2].

Thus, in this presentation it was calculated the return current of with frustration effect. JJ systems formed Single-Band/Many-Band compounds. It was shown that in all cases of the presence of additional channels leads to changing in return current in the different regimes. Frustration effects on Josephson penetration depth was analyzed [5] in long Single-Band/Many-Band superconductors.

This study partially supported by TÜBİTAK grant No 118N093.

References

[1] K.K. Likharev, *Introduction to Josephson dynamics*, New York, Gordon Beach, 1986
[2] I. Askerzade, A. Bozbey, M. Canturk, *Modern aspects of Josephson dynamics and superconductivity electronics*, (Springer, Berlin), 211 p., 2017
[3] M. Canturk, I.N. Askerzade, IEEE Applied Superconductivity, **21**, 3541 (2011).
[4] M. Canturk, I.N. Askerzade, IEEE Applied Superconductivity, 22,1400106 (2012).
[5] I.N. Askerzade, D. Matrasulov, M. Salati, JSNM, 2022, 10.1007/s10948-022-06343-0

Abstract ID: 1639

DESIGN AND COMPARATIVE ANALYSIS OF WIDEBAND SUPERCONDUCTING TERAHERTZ ANTENNAS

A. Canberk Songur, H. Alper Gunes, Emre Kucukyilmaz, N. Orhun Tekci, A. Bozbey, M. Ünlü

TOBB University of Economics and Technology, Dept. of Electrical and Electronics Engineering, 06510, Cankaya, Ankara, TURKEY
E-mail: a.songur@etu.edu.tr

This paper presents the design and numerical validation of novel terahertz wide-band on-chip antennas utilizing niobium (Nb) having a critical temperature of 9.2K as a superconducting material. Leveraging the superconducting properties of niobium enhances the antenna performance by minimizing ohmic losses. The compact nature of the antenna makes it suitable for applications with stringent size constraints. For the terahertz superconducting antenna designs and simulations, the Zimmermann Conductivity-based surface impedance values were implemented into antennas in the CST program at 4K and in the 0.8 - 2 THz band [1,2].

The antenna structures are optimized for high performance, compact integration, and exceptional directive characteristics. Three distinct antenna types are proposed, comprising bowtie and spiral antennas exhibiting effective radiation characteristics within the 0.8 - 2 THz band. Initially, a bowtie antenna, tailored to deliver broadband radiation within the 0.8 - 2 THz range, will be introduced. Following this antenna, two self-complementary superconducting antennas have been devised to match the resistance of the superconducting state, which escalates as junction size decreases at THz frequencies. The bowtie antenna, crafted for the 0.8 - 2 THz band, has been rendered self-complementary, enhancing antenna performance through the incorporation of corrugation and stub structures. Lastly, a custom-designed high-gain Archimedean spiral THz antenna has been developed. These three distinct terahertz emitters are developed on a Silicon substrate. A specially designed terahertz lens has been developed to increase antenna gain. By employing an extended hemispherical-shaped terahertz lens, peak gain exceeding 12 dBi has been attained for all three antennas. Additionally, beam steering can be achieved through the utilization of the aforementioned lens with the developed terahertz superconducting antenna array. The lens design has been specifically crafted to facilitate beam steering of a 4-element superconducting terahertz antenna array, enabling beam steering of up to 30 degrees. Beam steering application from such a terahertz superconducting antenna array can be important for future studies [3].

The proposed niobium-based on-chip antennas can open avenues for compact and efficient radio frequency components in integrated circuits, catering to the growing demand for miniaturized and high-performance wireless systems. The presented work contributes to the exploration of superconducting materials in antenna design and their integration into on-chip platforms for diverse applications.

References

[1] W. Zimmermann, E.H. Brandt, M. Bauer, E. Seider, L. Genzel, *Optical conductivity of BCS superconductors with arbitrary purity*, Physica C: Superconductivity, **183**, 1-3: 99-104 (1991).
[2] D.P.L. Aude, *Modeling superconductors using surface impedance techniques*, BSc Thesis, MIT (2010).
[3] A.C. Songur, A.O. Sakin, H.A. Gunes, B. Akcay, M. Unlu, *A terahertz lens antenna array design for beam steering in time-domain*, The 13th International Conference on Metamaterials, Photonic Crystals and Plasmonics (2023).

Abstract ID: 1253

SPIN DIFFUSION AND EMERGING FIELDS IN ALTERMAGNETS

A. Manchon

Centre Interdisciplinaire de Nanoscience de Marseille (CINaM), Aix-Marseille University, FRANCE
E-mail: aurelien.manchon@univ-amu.fr

In recent years, it has been realized that antiferromagnets host a wealth of intriguing electronic transport effects, including anomalous Hall effect, spin-orbit torque, magnetic spin Hall effect, non-relativistic current-driven Edelstein effect, etc [1]. Whereas the classification of the various families of antiferromagnets is yet to be completed, one particular category of such materials is attracting researchers' attention. This category gathers antiferromagnets whose sublattices are related by a rotation symmetry [2]. A remarkable feature is that the electronic band structure may exhibit anisotropic opposite spin-splitting along symmetry-related directions of the momentum space. The systematic search for such antiferromagnets, sometimes called "spin-split antiferromagnets" or "altermagnets", is currently ongoing and a few noticeable physical properties have been highlighted, including the emergence of a spin-polarized current along low symmetry directions of the crystal structure, its associated magnetic spin Hall effect, or spin splitter effect, the anisotropic dispersion of magnons, and the emergence of an anomalous Hall effect when spin-orbit coupling is turned on [3]. Experimentally, to the best of our knowledge, altermagnetism has been reported in RuO_2, MnTe, $MnTe_2$, and Mn_3Si_5.

Whereas important efforts have been paid to the electronic properties of potential candidates and the basic physical phenomena, the realization of spin devices based on altermagnets requires defining an appropriate set of spin transport equations, akin to the Valet-Fert theory in ferromagnetic multilayers. In the present work, based on the quantum kinetic equation, we develop the spin drift-diffusion transport equation in metallic altermagnets. To do so, we focus on a C_{4h} altermagnet that displays anisotropic spin splitting with a d-wave symmetry. The theory reveals the anisotropic diffusive transport together with unique spin dynamics on the coupled sublattices. We then apply this theory to a moving magnetic texture and compute the emergent electromagnetic field experienced by the spin-polarized electrons. In particular, we find that the topological charge and spin Hall effect induced by a two-dimensional altermagnetic texture, such as an altermagnetic skyrmion, induce completely different symmetries compared to both ferro- and antiferromagnetic skyrmions.

References

[1] Bonbien *et al.*, *Topological aspects of antiferromagnets*, J. Phys. D: Appl. Phys. **55 (10)**, 103002 (2022).
[2] Yuan *et al.*, *Giant momentum-dependent spin splitting in centrosymmetric low-Z antiferromagnets*, Phys. Rev. B **102**, 014422 (2020); Smejkal *et al.*, *Beyond Conventional Ferromagnetism and Antiferromagnetism: A Phase with Nonrelativistic Spin and Crystal Rotation Symmetry*, Phys. Rev. X **12**, 031042 (2022).
[3] e.g., Gonzalez-Hernandez *et al.*, *Efficient Electrical Spin-Splitter Based on Non-Relativistic Collinear Antiferromagnetism*, Phys. Rev. Letters **126**, 127701 (2021).

Nanocomposites: Properties and Applications I

01.05.2024 WEDNESDAY

Abstract ID: 1549

NANOMAGNETIC MATERIALS: PROPERTIES AND APPLICATIONS

R. Awad[1], A.M. Abdallah[2], A. Aridi[3], K. Habanjar[2]

[1]Physics Department, Faculty of Science, Alexandria University, Alexandria, EGYPT
[2]Physics Department, Faculty of Science, Beirut Arab University, Beirut, LEBANON
[3]Chemistry Department, Faculty of Science, Beirut Arab University, Beirut, LEBANON
E-mail: ramadan.awad@alexu.edu.eg

One of the important categories in the field of materials science is nanomagnetic materials due to the strategic interest in recent applications. Usually, Nanomagnetic materials are based on d- and f-electron systems. This work summarizes the basics of preparations characterization, and physical properties together with the corresponding applications of nanomagnetic materials. It is well known that the magnetic properties of materials are strongly dependent on the shape and the size of particles. They could be changed from paramagnetic or antiferromagnetic in the bulk state to ferromagnetic or superparamagnetic in the nanoscale region, depending on the critical particle size.

The nanomagnetic materials, including metals, oxide materials, ferrites, and composite, are fabricated by different methods such as arc method, coprecipitation, auto-combustion, and high-speed ball milling. The fabrication method could be chosen according to the required particle size and yield as well as the applications.

They are characterized and investigated by different techniques, X-ray powder diffraction, Transmission and scanning electron microscopies, Fourier transformation infrared, UV-vis spectroscopy, Photoluminescence, X-ray photoemission, and Raman spectroscopy. These techniques are used for determining the structures, morphologies, vibration bonds, oxidation states, and optical properties.

The magnetic properties of these materials are investigated using vibrating samples magnetometer, SQUID magnetometer, Mössbauer spectroscopy, and electron paramagnetic resonance. These measurements give information about the type of nanomagnetic materials and the distributions of cations inside these materials.

Finally, the applications of these materials such as spintronics, data storage, magnetic sensors, water treatment, permanent magnets, and biomedical applications are discussed.

CANCELLED

Abstract ID: 1648

ULTRA-SHORT SPIN WAVES EXCITATION IN SPIN HALL NANO-OSCILLATORS

M. Haidar

Department of Physics, American University of Beirut, P.O. Box 11-0236, Riad El-Solh, Beirut 1107-2020, LEBANON
E-mail: mh280@aub.edu.lb

While the CMOS-based technology is approaching its fundamental constraints, high-performance electronic devices are experiencing extreme challenges in terms of power consumption and miniaturization. Spin Wave (SW) excitation offers a promising alternative as it allows for substantial low power consumption resulting from the absence of the ohmic losses. In addition, SW-based technology allows for further scalability of devices, due to its shorter wavelengths (λ) which span a wide range from a macroscopic length down to nanometers. Propagating SWs can be effectively excited using spin-transfer torques mechanism, by utilizing spin-polarized current [1-3]. In spin-Hall nano-oscillators (SHNOs) devices, SWs could be excited with λ = 250 nm. In this paper, we study the excitation of propagating SWs with short wavelengths in nanowire-based spin-Hall oscillators while varying the width of the nanowire, w = 10 - 50 nm. We employ micromagnetic simulations to determine λ of propagating SWs as a function of w in 1.7 nm thin CoFeB layer [4].

Our results showed that SWs with shorter λ are excited in narrow widths at higher magnetic fields and higher currents. In addition, we find a linear relation between λ and w. We attribute the emission of short wavelength due to the quantization of SWs in the nanowire. Our results show that ultrashort SWs with wavelengths as short as 80 nm can be generated in metallic-based SHNOs, with a group velocity of 1.6 μm/ns, and an attenuation length of 0.7 μm. This is a promising result where the integration of SHNOs in magnonics may lead to further scalability of electronic devices.

References

[1] H. Fulara *et al.*, Science Advances **5**, 10.1126/sciadv.aax84 (2019).
[2] M. Succar, M. Haidar, J. Appl. Phys. **133**, 093901 (2023).
[3] M. Evelt *et al.*, Phys. Rev. Applied **10**, 041002 (2018).
[4] M. Haidar *et al.*, J. Magn. Magn. Mater. **587**, 171336 (2023).

Abstract ID: 1555

REVEALING THE IMPACT OF (Gd, Cr) DUAL DOPING YTTRIUM IRON GARNETS DERIVED BY CITRATE AUTO-COMBUSTION METHOD

A.M. Abdallah[1], K. Habanjar[1], B. Nsouli[2], R. Awad[3]

[1] *Physics Department, Faculty of Science, Beirut Arab University, Beirut, LEBANON*
[2] *Lebanese Atomic Energy Commission, NCSR, Beirut 11-8281, LEBANON*
[3] *Physics Department, Faculty of Science, Alexandria University, Alexandria, EGYPT*
E-mail: a.mabdallah@bau.edu.lb

Yttrium Iron Garnets (YIG) are a class of materials with high relative permittivity and a ferrimagnetic nature. In this work, two dopants are partially replaced simultaneously in their structure to tailor their optical and magnetic properties. The nonmagnetic Y^{3+} ions are partially replaced by the magnetic Gd^{3+} ions and Cr^{3+} ions partially substitute Fe^{3+} ions with equal concentrations. These dual-doped YIG are synthesized by the citrate auto-combustion method, having the chemical formula of $Y_{3-x}Gd_xFe_{5-x}Cr_xO_{12}$, for x = 0, 0.05, 0.1, 0.15, and 0.2. The structural, morphological, optical, and magnetic properties are studied to investigate the impact of (Gd, Cr) dual dopants on YIG. The X-ray diffraction patterns revealed the formation of the YIG phase, along with minor traces of yttrium orthoferrite and hematite as impurities. The advantage of the dual dopants was recorded by enhancing the main phase formation and reducing the secondary phases. Moreover, the scanning electron microscope depicted the formation of multiple pores within the structure, owing to the liberated gases during the synthesis. The X-ray photoelectron spectroscopy demonstrated the multivalent states of the elements and the high-resolution valence energy state was recorded to unveil the effect of the dual dopants on the electronic properties of YIG. The UV-visible spectroscopy registered notable absorbance for the samples, from which the energy gap is calculated. Moreover, the vibrating sample magnetometer enabled the measurements of the magnetic properties of the samples. The dual dopants tailored the magnetic properties of the ferrimagnetic YIG samples.

CANCELLED

Abstract ID: 1551

INVESTIGATING THE PHYSICAL PROPERTIES OF Gd-DOPED YTTRIUM ORTHOFERRITES

S. Isber[1], A. M. Abdallah[2], K. Habanjar[2], R. Awad[3]

[1] *Physics Department, American University of Beirut, Bliss Street PO Box 11-0236, Beirut, LEBANON*
[2] *Physics Department, Faculty of Science, Beirut Arab University, Beirut, LEBANON*
[3] *Physics Department, Faculty of Science, Alexandria University, Alexandria, EGYPT*
E-mail: si00@aub.edu.lb

The urge to reduce the sizes of electronic components has switched the attention to novel nanomaterials. A great challenge is faced by synthesizing multiferroic nanomaterials, having both ferromagnetic and ferroelectric properties in the nanoscale. One class of advanced multiferroic materials is yttrium orthoferrites ($YFeO_3$); to alter its physical properties, we doped the pure system of $YFeO_3$ by gadolinium (Gd), with 2.5, 5, 10, 15, and 20 at.%. This new material was synthesized by auto-combustion method, having 1 M of citric acid ($C_6H_8O_7$) as the fuel for the reaction. The synthesized samples were investigated by X-ray diffraction to confirm the crystal structure and phase purity. The Gd-dopants caused a phase transformation from hexagonal to rhombohedral $YFeO_3$ structure and reduced the hematite impurity phase. The morphology of the synthesized samples was studied by transmission electron microscope (TEM) and scanning electron microscope (SEM). The effect of the gadolinium concentration on the functional groups and the absorbance spectra was investigated by Fourier transform infrared (FTIR) and UV-visible spectroscopies. Moreover, the photoluminescence spectra detected the changes in the defect states within the system. Finally, the effect of Gd concentration at room temperature on the magnetic properties was measured using a vibrating sample magnetometer. the experimental M-H loops were fitted to the different models of the law of approach to saturation, and various magnetic parameters were extracted such as, the saturation magnetization, coercivity, retentivity, squareness ratio, and magnetic anisotropy.

Abstract ID: 1556

(1-x) YCeIG/x MgSmO NANOCOMPOSITES: CHARACTERIZATION AND PROPERTIES

Khulud Habanjar[1], Majed Sharrouf[1], R. Awad[2]

[1] *Beirut Arab University, Dept. of Physics, Beirut, LEBANON*
[2] *Alexandria University, Dept. of Physics, Alexandria, EGYPT*
E-mail: k.habanjar@bau.edu.lb

The co-precipitation technique was used to synthesize pure nanoparticles of $Mg_{0.95}Sm_{0.05}O$ (MgSmO), $Y_{2.5}Ce_{0.5}Fe_5O_{12}$ (YCeIG), followed by ball-milling to obtain their (1-x) YCeIG/x MgSmO nanocomposites, with x = 0.0, 0.1, 0.2, 0.4 and 0.8. From structural characterization, X-ray diffraction patterns show a decrease in the intensity peaks of $Y_3Fe_5O_{12}$ and CeO_2 phases with a simultaneous increase in the $YFeO_3$ phase with the formation of $MgFe_2O_4$ as secondary phases. Both transmission and scanning electron microscopies (TEM and SEM) show the alteration of YCeIG morphology and its grain size as MgSmO is added. This is due to the difference in grain size, depicted in the micrographs. The elemental composition was confirmed by X-ray photoelectron spectroscopy (XPS). The inclusion of MgSmO and $Y_{2.5}Ce_{0.5}Fe_5O_{12}$ in one matrix is confirmed by Raman spectroscopy. Vibrating sample magnetometer (VSM) analysis reveals the single-phase-like hysteresis loops, indicating the good exchange coupling between different nanoparticles. The saturation magnetization (M_s), remanent magnetization (M_r), and coercivity (H_c) were altered in the considered samples.

CANCELLED

Nanocomposites: Properties and Applications II

01.05.2024 WEDNESDAY

Abstract ID: 1539

THE INFLUENCE OF DEFECTS ON THE STRUCTURAL AND MAGNETIC PROPERTIES OF Mn/Cu CO-DOPED ZnO NANOPARTICLES

M.M. Seker Perez[1], C. Boyraz[1], L. Arda[2]

[1] *Marmara University, Department of Mechanical Engineering, 34854, Istanbul, TURKEY*
[2] *Bahcesehir University, Department of Mechatronic Engineering, 34349 Istanbul, TURKEY*
E-mail: lutfi.arda@eng.bau.edu.tr

The ongoing interest in ZnO doped with transition metals persists due to its significant properties [1]. This study aims to investigate the impact of defects formed during the synthesis of Mn/Cu-doped ZnO nanoparticles via the sol-gel method on their structural and magnetic characteristics.

Mn/Cu-doped ZnO nanoparticles were synthesized using the sol-gel technique. X-ray diffraction and Rietveld analysis confirmed the formation of the desired structure without any secondary phases. Surface morphology, shapes, size, and elemental compositions of Mn/Cu-doped ZnO nanoparticles were examined using Scanning Electron Microscopy (SEM) and electron dispersion spectroscopy (EDS). The magnetic properties of $Zn_{0.95-x}Mn_xCu_{0.01}O$ (0.0, 0.01, 0.02, 0.03, 0.04 and 0.05) nanoparticles were investigated using the Quantum Designed Physical Property Measurement System. Photoluminescence spectra of Mn/Cu-doped ZnO nanoparticles were analyzed to observe crystal features, defect types, and defect densities. This study sheds light on the influence of defects formed in Mn/Cu-doped ZnO nanoparticles with varying doping ratios, synthesized via the sol-gel method, on their structural and magnetic attributes.

References

[1] T. Dietl, Semicond. Sci. Technol., **17**, pp. 377 (2002).

CANCELLED

Abstract ID: 1014

STRUCTURAL, DIELECTRIC AND CONDUCTION PROPERTIES OF $Bi_2Ca_{1.80}Sm_{0.10}Ce_{0.10}CoO_6$ NANO-PARTICLES

Yasir Abbas, M. Anis-ur-Rehman

Applied Thermal Physics Laboratory, Department of Physics COMSATS University Islamabad, Islamabad 45550, PAKISTAN
Email: marehman@comsats.edu.pk

The perovskite cobaltite $Bi_2Ca_{1.80}Sm_{0.10}Ce_{0.10}CoO_6$ Nano-particles, was synthesized by co-precipitation method. We revealed the substance under investigation's a monoclinic structure using the analysis of X-ray diffraction data. The formation of Bi (Ca)-O and Co-O nanocomposites, as well as some impurity phase of CaCo3 nanoparticle, was confirmed by X-ray diffraction (XRD) and Fourier transform infrared spectroscopy (FTIR). The presence of $Bi_2Ca_{1.80}Sm_{0.10}Ce_{0.10}CoO_6$ was verified by morphological analysis using energy dispersive spectroscopy and scanning electron microscopy. The thermal stability of $Bi_2Ca_{1.80}Sm_{0.10}Ce_{0.10}CoO_6$ was examined using thermogravimetric analysis (TGA). Electrical and dielectric properties have been examined with respect to frequency and temperature variation. In the complex impedance study, we observed the existence of both grain and grain boundary effects. The studied sample is regarded as semiconducting because it exhibits a negative temperature coefficient. The studied properties of $Bi_2Ca_{1.80}Sm_{0.10}Ce_{0.10}CoO_6$ show that it is suited for energy devices.

CANCELLED

Role of Superconductivity Roadmap For Net Zero Carbon Emission Targets by 2050: Superconductivity Global Alliance (ScGA) I

01.05.2024 WEDNESDAY

Abstract ID: 1615

THE SUPERCONDUCTING GLOBAL ALLIANCE (SCGA) FOR NET ZERO CARBON EMISSION TARGETS BY 2050

Ziad Melhem

Oxford Quantum Solutions Ltd., Oxford, OX2 9SB, UNITED KINGDOM
E-mail: ziad.melhem@oxqsol.com

The Superconductivity Global Alliance (ScGA) is a collective initiative dedicated to advancing the understanding and application of superconductivity toward a greener, healthier, more prosperous, and sustainable future.

Superconductivity has the potential to provide means towards zero-emission targets, enabling extensive usage of wind power generation, facilitating zero-emission transportation, realising robust and resilient electricity, enabling fusion power, superconducting quantum computing, water purification, new medical diagnosis and therapy tools, and new scientific breakthroughs.

To harness the enormous potential of superconductors in addressing our societal future needs, and to realize the potential of superconductors in addressing our societal future needs as identified in the United Nations' 17 Sustainable Development Goals (SDGs, also called the Global Goals, new thinking, and innovations are needed to translate demonstrator devices into successful market applications. At the heart of this process, we propose to establish three-way partnerships between the superconductivity community, public and private investors, and industrials.

This talk will present an update on the Superconducting Global Alliance (ScGA) initiative for a cleaner and sustainable future and address providing superconducting technologies for zero emissions targets by 2050.

Abstract ID: 1517

ZERO EMISSION ELECTRIC AIRCRAFT THROUGH SUPERCONDUCTING DC DISTRIBUTION NETWORK

Xiaoze Pei

University of Bath, UK
E-mail: x.pei@bath.ac.uk

Electrification of aviation will be central to achieve ambitious environmental targets for the reduction of carbon emission, fuel burn and noise. A revolutionary concept is hydrogen-powered electric propulsion aircraft. A reliable high-power density and high efficiency superconducting DC distribution network will be a key enabling and transformative technology to achieve large-scale hydrogen-powered electric aircraft. Safety and reliability are paramount considerations in the development of electric propulsion aircraft. This presentation will focus on the system design, control, and fault protection for cryogenic and superconducting DC distribution networks.

The Institute for Advanced Automotive Propulsion Systems (IAAPS) at University of Bath is a world-leading centre of excellence supporting the transport industry in the transition to net zero. The presentation will start with a brief introduction to the state-of-the-art facilities at IAAPS.

Abstract ID: 1518

THE ROLE OF SUPERCONDUCTIVITY IN TRANSPORT IN A SUSTAINABLE FUTURE

Marco Breschi[1], Loïc Quéval[2], Arno Godeke[3], Ziad Melhem[4]

[1]University of Bologna, ITALY
2 Centrale Supélec, Université Paris Saclay, FRANCE
[3]Senior Consulting for Superconductivity, Hengelo, THE NETHERLANDS
[4]Oxford Quantum Solutions Ltd., Oxford, OX2 9SB, UNITED KINGDOM
E-mail: marco.breschi@unibo.it

Climate-driven incentives to reduce greenhouse-gas emissions yield increased focus on international transport, which accounts for 16.2% of the emissions. While electrification of the world's automobile industry is commencing, driven by government policies and industry, large-scale polluters that transport large amounts of people or cargo, are not yet sufficiently addressed. Trains, airplanes, and ships all are of sufficient scale to accommodate superconducting technologies.

Commercial aviation alone accounts for about 2.5% of global carbon emissions. The number of passengers traveling by air is increasing at a rate of more than 4% annually, leading to estimates that the overall annual consumption of jet fuel will be approximately 120 billion liters by 2040. These numbers are in stark contrast to goals for the aviation sector that foresee a 75% reduction in CO2, a 90% reduction in NOx, and 65% lower perceived noise emissions, compared with a typical new aircraft in the year 2000. This calls for disruptive technological solutions, such as hybrid-electric propulsion systems for aviation, to reduce emissions. The maritime transportation can also achieve significant improvements from superconductivity. Electric propulsion is inherently more efficient since it allows including energy storage-systems that decouple production and consumption, thus allowing to operate the motors and generators at their maximum performance. The use of superconducting materials could make it possible to achieve the high power- densities and power-to-weight ratios required for aviation and maritime transportation. This work addresses state-of-the-art and the challenges for the commercial introduction of superconducting technologies in these two applications.

Role of Superconductivity Roadmap For Net Zero Carbon Emission Targets by 2050: Superconductivity Global Alliance (ScGA) II

01.05.2024 WEDNESDAY

Abstract ID: 1554

SUPERCONDUCTING MAGLEV AS A ZERO-EMISSION, HIGH-SPEED GROUND TRANSPORTATION SYSTEM

H. Ohsaki

University of Tokyo, Graduate School of Frontier Sciences, Kashiwa 277-8561, JAPAN
E-mail: ohsaki@k.u-tokyo.ac.jp

The Superconducting maglev system is based on the technologies of the electrodynamic suspension (EDS) for levitation, and the linear synchronous motor (LSM) for propulsion [1-3]. Onboard superconducting magnets are key components in the superconducting maglev system and work as field magnets for LSM and magnetic field source for EDS. The superconducting maglev system has been developed in Japan for more than 50 years for use in super-highspeed rail applications, and its technology is already completed. Now a commercial line, Chuo Shinkansen, is under construction between Tokyo and Nagoya [2]. Chuo Shinkansen was planned as a Tokaido Shinkansen Bypass connecting three major metropolitan areas in Japan: Tokyo, Nagoya and Osaka. The maximum speed is 505 km/h in the revenue service. Between Tokyo and Osaka, the system will provide airplane-like speeds while emitting significantly less carbon dioxide than airplanes. Based on the current status of Japan's electric power system, the greenhouse gas emissions from the Chuo Shinkansen are about 1/3 of those from airplanes. If the grid side that supplies the electric power becomes carbon neutral, this super high-speed rail will become a true zero-emissions transportation system.

References

[1] K. Sawada, Proceedings of the IEEE **97**, 1881-1885 (2009).
[2] https://scmaglev.jr-central-global.com/
[3] https://northeastmaglev.com/

Abstract ID: 1531

SUPERCONDUCTING CABLE WITH ENERGY STORAGE FUNCTION AS A KEY TO NEXT-GENERATION POWER SYSTEM TOWARD NET-ZERO CARBON SOCIETY

Kohei Higashikawa[1], Hitoshi Kitaguchi[2], Naoki Hirano[3], Kazuhiko Hayashi[4], S.M. Muyeen[5], Takanobu Kiss[1]

[1] *Kyushu University, Fukuoka 819-0395, JAPAN*
[2] *National Institute for Materials Science, JAPAN*
[3] *National Institute for Fusion Science, JAPAN*
[4] *Sumitomo Electric Industries, Ltd., JAPAN (Retired)*
[5] *Qatar University, QATAR*
E-mail: kohei@super.ees.kyushu-u.ac.jp

Mass introduction of renewable energy is essential to achieve a net-zero carbon society. On the other hand, output power fluctuation from renewable energy represented by solar and wind power generation is severe, and coping with it has become a major challenge. As a solution to this problem, we have proposed a next-generation power system using superconducting cables with energy storage function [1-3]. The cable is named the SMES cable, which will contribute to the realization of an innovative power system that combines both the high-speed response characteristic of SMES and the large capacity that has been the weak point of SMES. This concept will allow a power system itself to absorb severe output power fluctuations from renewable energy, and will a decisive factor for mass introduction of renewable energy. This presentation will report on results of a five-year Japanese national program [4] and current efforts on this research.

This work was supported by a NEDO Feasibility Study Program (Uncharted Territory Challenge 2050), JSPS KAKENHI Grant Number JP20H02132, and Qatar-Japan Research Collaboration Program Grant Number M-QJRC-2023-317.

References

[1] K. Higashikawa *et al.*, *Novel power system with superconducting cable with energy storage function for large-scale introduction of renewable energies*, IEEE Transactions on Applied Superconductivity**, vol. 29, no. 5**, ArtID. 5402204 (2019).

[2] K. Higashikawa *et al.*, *Development of superconducting cable with energy storage function and evaluation of its functionality in dc microgrid with renewable energy sources*, IEEE Transactions on Applied Superconductivity, **vol. 33, no. 5**, ArtID. 5400405 (2023).

[3] K. Higashikawa *et al.*, *Energy efficiency improvement of renewable-rich DC microgrids by SMES cables*, IEEE Transactions on Applied Superconductivity, **vol. 34, no. 3**, ArtID. 5700205 (2024).

[4] NEDO Feasibility Study Program (Uncharted Territory Challenge 2050).

Magnetic Materials Processing and Physical Properties

01.05.2024 WEDNESDAY

Abstract ID: 1008

MAGNETIC INTERACTIONS AND ASSOCIATED EFFECTS IN RARE-EARTH IRON GARNETS PROCESSED BY DIFFERENT ROUTES

Cristina Bartha, Claudiu Locovei, Mihai Grigoroscuta, Andrei Alexandru-Dinu, Aurel Leca, Nicu Iacob,Cezar Comanescu, Andrei Kuncser, Petre Badica, Victor Kuncser

National Institute of Materials Physics, Atomistilor 405A, Magurele, ROMANIA

E-mail: cristina.bartha@infim.ro

This work focuses on the investigation of magnetic properties of $RE_3Fe_5O_{12}$ garnets (RE=Tb, Dy, Tb and Gd) processed by different routes (one of them being our original method that combines a modified hydrothermal method for nanoparticles synthesis, followed by their sintering by Spark Plasma Sintering). Rare earth iron garnets are materials with practical potential for spintronics (i.e. magnetic switching devices, other types of logic and electromagnetically controlled devices etc.) duo to their structural characteristics with a significant impact on their magnetic properties. The magnetism of these materials is characterized by two types of couplings, small net magnetic moment, fast domain wall moving speed, small stray field and less susceptibility to external field interferences [1-2]. It has been shown that the magnetic behavior of samples processed by our original processing method differs significantly from that of samples obtained by the classical method (solid phase reaction) due to the structural defects. X-ray diffraction accompanied by the Rietveld analysis reveals the coexistence in all samples of two garnet phases, one with ideal stoichiometry and a phase that presents cationic vacations. The materials obtained by hydrothermal synthesis has a percentage of about 7 ÷10 % garnet phase with vacations, compared to the materials processed by the classical method, which has a percentage between 22÷38 % of defected garnet phase. Local electronic and magnetic configurations in the proposed samples were investigated by temperature dependent Mössbauer Spectroscopy. The Mössbauer spectra of the analyzed samples correspond to the garnet oxide structures being similar to those reported in the literature. The ideal structure of a $RE_3Fe_5O_{12}$ garnet type is cubic and has 24 RE^{3+} ions on position **c** (dodecahedral), 16 ions of Fe^{3+} on position **a** (octahedral) and 24 ions of Fe^{3+} on position **d** (tetrahedral) [3]. For all measured samples, the relative areas highlight the formation of two garnet phases, in agreement with Rietveld analysis. Magnetic properties and related functionalities are very sensitive to the local electronic configurations influenced by cationic distribution and defects generated by the variation of the oxygen stoichiometry and therefore can be fully understood only on the basis of the Mössbauer spectroscopy data. The calculated magnetic moments are consistent with the phases ratio determined by Rietveld and Mossbauer spectroscopy respectively.

Authors acknowledge project PN-III-P2-2.1-PED-2021-2007 (contract no. 676 PED/2022) funded by the Romanian Ministry of Research, Innovation, and Digitalization through UEFSCDI.

References

[1] K. Kim *et al.*, Nat. Mater, **16**, 1187-1192 (2017).
[2] D. Kim *et al.*, Nature Materials **18**, 685–690 (2019).
[3] Tsidaeva *et al.*, Nanomaterials, **11 (4)**, 972 (2021).

CANCELLED

Abstract ID: 1050

MAGNETIC PROPERTIES AND ELECTRONIC STRUCTURE OF $FeRhAs_{1-x}Z_x$ (Z=Al, Ga, In) ALLOYS: ab INITIO STUDY

O. Pavlukhina[1], V. Buchelnikov[1], V. Sokolovskiy[1,2], M. Zagrebin[1]

[1]*Chelyabinsk State University, 454001, Chelyabinsk, RUSSIA*
[2]*National University of Science and Technology 'MISiS', 119049, Moscow, RUSSIA*
E-mail: pavluhinaoo@mail.ru

The Fe-Rh-based alloy have attracted a lot of attention due to the observation of shape memory effect [1], magnetocaloric effect [2] etc. Heusler-based half-metals have attracted significant interest for spintronics applications [3]. The properties of $FeRhAs_{1-x}Z_x$ (Z= Al, Ga, In) (x = 0, 0.25, 0.5, 0.75, 1) alloys are investigated by using the density functional theory calculations as implemented in the VASP package. The ab initio calculations have been carried out by using the 12-atom supercell approach. The half-Heusler alloys crystallize in non-centrosymmetric cubic structure (space group F-43m). They can crystallize in three possible configurations, namely *a*, *β* and γ phases. Our results suggest that $FeRhAs_{1-x}Z_x$ (Z=Al, In) (x = 0, 0.25, 0.5, 0.75, 1) and $FeRhAs_{1-x}Ga_x$ (x = 0.25, 0.5, 0.75, 1) compounds are most stable in *γ* phase, FeRhAs compound are most stable in *β* phase. Additionally, we calculate the total and partial densities of states for the $FeRhAs_{1-x}Z_x$ alloys. We estimate also the spin polarization of alloys as follows: $P = (N\uparrow(E_F) - N\downarrow(E_F))/(N\uparrow(E_F) + N\downarrow(E_F))$, where $N\uparrow(E_F)$ and $N\downarrow(E_F)$ are the electron density states at the Fermi level (E_F) for the spin up and spin down states. We find that for $FeRhAs_{0.5}Ga_{0.5}$ the spin polarization is equal to 100% (Fig. 1). It is seen, also that an addition of fourth element to the triple half-Heusler alloy shifts the Fermi level.

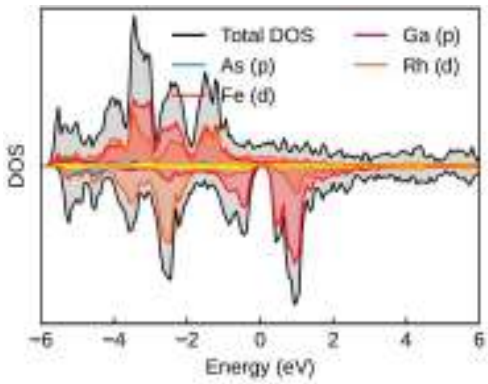

Fig. 1: *The density of electronic states for the $FeRhAs_{0.5}Ga_{0.5}$ alloys. Zero energy indicates the position of the Fermi level.*

This work was supported by RSF-Russian Science Foundation No. 22-12-20032.

References

[1] J. Winterlik, Phys Rev. B. **79**, 064508 (2009).
[2] A. Hirohata, K. Takanashi, J. Phys. D. **47**, 193001 (2014).
[3] C. Felser, L. Wollmann, APL Mater. **3**, 041518 (2015).

Abstract ID: 1054

MEASUREMENTS OF STRAY MAGNETIC FIELDS OF Co-RICH AMORPHOUS MICROWIRES USING A SCANNING GMI MAGNETOMETER

S.A. Gudoshnikov[1,2], G.E. Danilov[1], Yu.B. Grebenshchikov[1,2], A.V. Popova[1,2], V.I. Odintsov[2]

[1]National University of Science and Technology «MISiS», 119049, Moscow, RUSSIA
[2]Pushkov Institute of Terrestrial Magnetism, Ionosphere and Radio Wave Propagation RAS 108840, Troitsk, Moscow, RUSSIA
E-mail: gudosh@izmiran.ru

A scanning magnetometer based on magnetoimpedance (GMI) sensor with ~1 mm spatial resolution and 10 nT magnetic field sensitivity [1] was used for studying stray magnetic fields of 5-10 mm segments of $Co_{69}Fe_4Cr_4Si_{12}B_{11}$ amorphous ferromagnetic microwires (AFM) with metallic nuclear diameter of 18.4 μm and outer diameters 32.5 μm, produced by Ulitovsky - Taylor technique. Spatial magnetic images and vertical component profiles of stray magnetic fields of the studied AFM were obtained in longitudinal homogeneous magnetic field of Helmholtz coils with strength in the range of ± 600 A/m. As an example, Fig.1 shows a 3D magnetic image of the remnant magnetization of the 5-mm Co-rich AFM segment premagnetized in a longitudinal magnetic field. During measurements, characteristic values have been determined for the anisotropy field, the average magnetization and the closure domain width of the AFM segments for different values of the magnetizing fields.

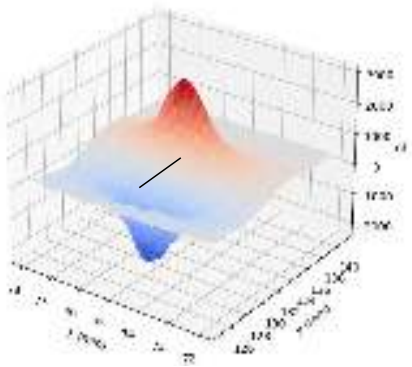

Fig.1: *3D magnetic images of the remnant magnetization of the 5-mm Co-rich AFM sample premagnetized in a longitudinal magnetic field.*

The authors gratefully acknowledge the financial support of the Strategic Academic Leadership Program "Priority 2030", project SP-1.

References

[1] G.E. Danilov, Yu. B. Grebenshchikov, Metals, **13(4)**, 800 (2023).

Abstract ID: 1134

A MAGNETIC MOMENT CALCULATION METHOD BASED ON MAGNETIC GRADIENT TENSOR EIGENVALUES

Shiyao Wang, Sansheng Wang, Fan Liu, Junyang Fang

Beihang University, School of Physics, 102206, Beijing, CHINA
E-mail: wave_wang@buaa.edu.cn

To master the magnetic characteristics of the target is the premise of magnetic anomaly detection, and the most intuitive and important physical quantity describing the magnetic characteristics of a target is the magnetic moment. The measurement of target magnetic moment is of great significance for target detection, location, and identification. This paper proposes a magnetic moment calculation method based on magnetic gradient tensor eigenvalues. In this method, the formulas for inverting the magnitude and direction of the target magnetic moment from the magnetic gradient tensor eigenvalues and eigenvectors were derived. We constructed a full tensor magnetic gradient array using three-axis magnetic sensors, and conducted simulations and experiments on different factors that affect the accuracy of magnetic moment calculation. Simulation data and actual experimental data verified the effectiveness of this method. The results show that the target magnetic moment calculated from the simulated and measured magnetic gradient tensor data agreed well with the theoretical values. Under the applicable conditions of this method, the calculation error of the magnetic moment modulus value is ≤ 0.5 Am², and the directional error is ≤ 5°. This method can achieve rapid inversion of magnetic moments under geomagnetic environment and ordinary laboratory noise environment. The scheme is simple and easy to use, with strong feasibility and reliability. In addition, the selection and analysis method of factors affecting measurement accuracy in this article is also applicable to other applications of magnetic gradient tensor.

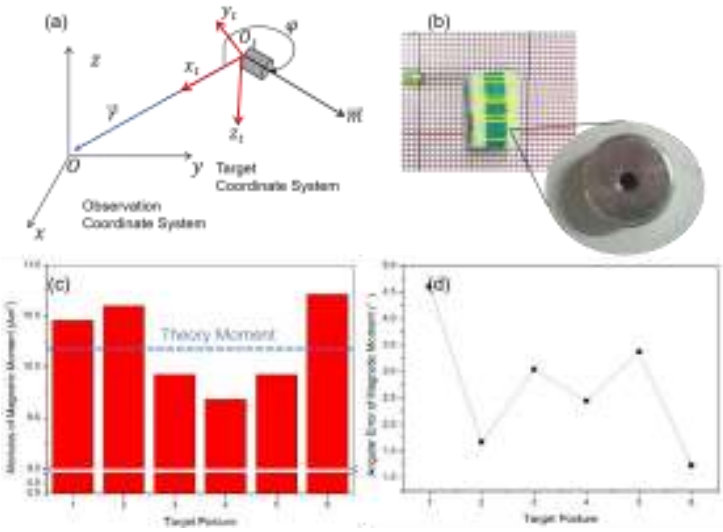

Fig. 1: *Measuring a magnetic target with this method: (a) Observation and coordinate systems; (b) The magnetic target under test; (c) Measured modulus of magnetic moment; (d) Angle error of magnetic moment.*

Bulk Superconductors I

01.05.2024 WEDNESDAY

Abstract ID: 1146

MICROSTRUCTURE OF DYBCO BULK CYLINDERS AND RINGS PREPARED BY THE SDMG PROCESS

P. Diko[1], K. Zmorayova[1], V. Kucharova[1], T. Motoky[2], J. Shimoyama[2]

[1]*Institute of Experimental Physics SAS, Watsonova 47, 040 01 Košice, SLOVAKIA*
[2]*Department of Physical Sciences, Aoyama Gakuin University, 5-10-1 Fuchinobe, Chuo-ku, Sagamihara, Kanagawa 252-5258, JAPAN*
E-mail: dikos@saske.sk

The Microstructure of bulk single-grain DyBCO superconductors with a nominal composition of 7 mol $DyBa_2Cu_3O_{y+3}$ mol Dy_2BaCuO_5 (Dy211) + 10 wt. % Ag20 + 0.5 wt. % CeO prepared by single-direction melt growth (SDMG) was studied using polarized light and electron microscopy. Microstructural parameters such as subgrain structure, porosity, size and macroscopic distribution of Dy211 particles, Eu diffusion into the sample from the EuBCO seed, as well as the position of the remaining tetragonal non-oxygenated regions in cylindrical and ring-shaped samples were characterized. It turns out that at the beginning of growth, the structure is more inhomogeneous, which is also manifested by the appearance of bands with a higher concentration of Dy211. The formation mechanism of these bands is related to the occurrence of growth steps at the c-growth front, which were formed as a result of presumed multinucleated c-growth from a large seed. Steps at the growth front cause the formation of a-subsectors with higher concentrations of Dy211 particles. The macroscopic thermal dilatational stresses induced in the samples upon cooling from the processing temperature were estimated from the measured dependence of the Gd211 concentration on the distance from the seed (Fig. 1).

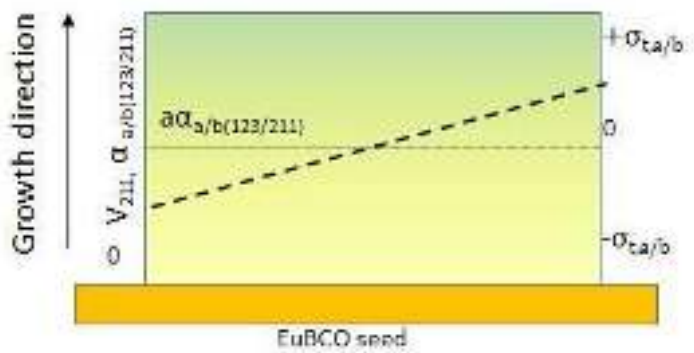

Fig. 1: *Schematic illustration of the development of residual thermal stresses in the SDMG sample. V211 is the volume fraction of 211 particles,* $a_{a/b(123/211)}$ *is the coefficient of thermal expansion of the composite 123/211 for given* V_{211}, $aa_{a/b(123/211)}$ *is the average coefficient of thermal expansion of the 123/211 sample,* $\sigma_{t,a/b}$ *is the stress in the a/b-plane.*

This work was accomplished within the framework of the projects: APVV-17-0625, APVV-21-0387, VEGA No. 2/0044/19, No. 2/0094/22 and in part by NEDO Uncharted Territory Challenge 2050 (22M1C01Y) and in part by a research grant program of Nippon Sheet Glass Foundation for Materials Science and Engineering.

Abstract ID: 1478

INFLUENCE OF V-DOPING ON THE SUPERCONDUCTIVITY OF NON-CENTROSYMMETRIC NbReSi: INTERPLAY OF SUPERCONDUCTIVITY AND INDUCED CHARGE DENSITY WAVE

S. Chakrabortty, N. Mohapatra

School of Basic Sciences, Indian Institute of Technology Bhubaneswar, Odisha, 752050 INDIA
E-mail: niharika@iitbbs.ac.in

The coexistence and competition between superconductivity and density wave order is one of the unresolved issues in the field of superconductivity as both these phenomena are related to the Fermi surface instabilities [1]. In this paper, we report a detailed investigation of the superconducting properties of the distorted Kagome system, NbReSi, and its doped variants, $Nb_{1-x}V_xReSi$, crystallizing in a non-centrosymmetric structure. The initial studies on NbReSi have shown the observation of a very high upper critical field (H_{C2}), that approaches the Pauli-Clogston limit [2,3]. The crystal symmetry was found to remain the same with a substitution limit of up to 10% with a marginal variation in the lattice parameters. The results of our resistivity and magnetic susceptibility measurements reveal a gradual suppression of T_C, the lower and upper critical fields with increasing the doping percentage. The most notable observation is the signature of the induced density wave order in the doped samples. Moreover, we have shown the multiband nature of the superconductivity being consistent with the s-wave pairing in these systems.

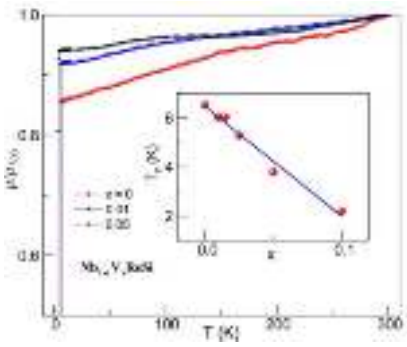

Fig. 1: *The temperature variation of normalized resistivity for $Nb_{1-x}V_xReSi$ (Inset shows the variation of T_C with doping concentration).*

References

[1] F.H. Yu *et al.*, Nat. Commun. **12**, 3645 (2021).
[2] H. Su *et al.*, Phys. Rev. Mat. **5**, 114802 (2021).
[3] K. Motla *et al.*, Phys. Rev. B **105**, 94523 (2022).

Abstract ID: 1536

EFFECTS OF LASER-INDUCED MICROSTRUCTURING ON THE SUPERCONDUCTING PROPERTIES OF YBCO BULK SUPERCONDUCTORS

S.B. Guner[1,2], L.A. Angurel[3], G.F. de la Fuente[3], A. Gencer[2] F. Al-Mokdad[2], S. Celik[2,4], M. Miryala[5]

[1] Department of Physics, Faculty of Arts and Sciences, Recep Tayyip Erdogan University, 53100 Rize, TURKEY
[2] Ankara University, Center of Excellence for Superconductivity Research, 06500, Golbasi, Ankara, TURKEY
[3] Instituto de Nanociencia y Materiales de Aragón (CSIC-Universidad de Zaragoza), María de Luna, 3, 50018, Zaragoza, SPAIN
[4] Department of Energy Systems, Faculty of Engineering and Architecture, Sinop University, 57000, Sinop, TURKEY
[5] Graduate School of Science and Engineering, Regional Environment Systems, Shibaura Institute of Technology Koto-ku, Tokyo, 135-8548, JAPAN
E-mail: sbarisguner@gmail.com

Since the discovery of high-temperature superconductors, researchers have employed various fabrication methods to produce bulk samples with controlled microstructure, with top-seeded melt growth (TSMG) emerging as one of the most effective techniques. TSMG is particularly useful in producing large-grain YBCO bulk for potential applications such as electrical motors, magnetic bearings, generators, flywheels, and energy storage devices. In magnetic levitation and trapped field systems, large-sized high-temperature superconductor (HTS) bulk materials show promise considering their superconducting properties. The geometry and size of the bulk sample play crucial roles in achieving high magnetic levitation forces and critical current densities (Jc) for levitation and trapped field applications. The trapped field initially increases with the sample radius, eventually reaching a saturation value above certain diameters. This work explores the effect that ultrashort pulse laser irradiation exerts on the properties of YBCO bulk superconductors. YBCO bulk single grains with different diameters are first fabricated using the TSMG technique. Magnetic levitation force (MLF), Trapped Field (TF), scanning electron microscope (SEM), and X-ray diffraction (XRD) analyses are performed on the top surface of YBCO samples. Laser processes are then applied to the top surface, and subsequent MLF, TF, SEM, and XRD measurements are conducted on the treated YBCO samples. Results will be presented in order to describe how the ultra-short pulse laser affects the microstructure and properties of the superconductor.

Acknowledgements

This work was supported by COST CA19108 High-Temperature Superconductivity for Accelerating the Energy Transition (Hi-SCALE) STSM Action and Spanish MCIN/AEI/10.13039/501100011033 (Project PID2020-113034RB-I00) and Gobierno de Aragón (research group T54_23R). All the magnetic levitation force measurements were performed in the MLFMS designed under TUBİTAK project no: 110T622 and whose patent application number is 2013/13638.

Abstract ID: 1085

SUPERCONDUCTIVITY WITH HIGH UPPER CRITICAL FIELD IN Ta-Hf ALLOYS

P.K. Meena, S. Jangid, R.K. Kushwaha, R.P. Singh

Department of Physics, Indian Institute of Science Education and Research Bhopal, Bhopal, 462066, INDIA
E-mail: pavan19@iiserb.ac.in

Recently, there has been considerable interest in exploring superconducting alloys for potential applications in superconducting devices [1-4]. In this study, I will present our findings on superconductivity in Ta_xHf_{1-x} alloys, utilizing magnetization, electrical resistivity, and specific heat measurements on polycrystalline samples [5].

The crystal structures of these alloys are composition-dependent. Notably, when we substituted Hf (a Type-I superconductor with a critical temperature, T_C, of 0.12 K) with Ta (also a Type-I superconductor with a T_C of 4.4 K), a remarkable enhancement in T_C was observed, along with a transition to Type-II superconductivity featuring high upper-critical fields. This transition is of particular interest from the perspective of materials science. Our specific heat measurements provided evidence of strong coupling superconductivity, aligning with conventional principles of superconductivity. These metallic alloys exhibit both metallic properties and a high upper-critical field, making them highly promising for practical superconducting devices like SQUID and qubits.

References

[1] T.G. Berlincourt *et al.*, Phys. Rev. **131**, 140 (1963).
[2] J.K. Hulm *et al.*, Phys. Rev. **123**, 1569 (1961).
[3] K.M. Wong *et al.*, Phys. Rev. B **30**, 1253 (1984).
[4] A.P. Place *et al.*, Nat. Commun. **12**, 1779 (2021).
[5] P.K. Meena *et al.*, Phys. Rev. Materials **7**, 084801 (2023).

CANCELLED

Superconducting Spintronics: Novel Quantum Circuits III

02.05.2024 THURSDAY

Abstract ID: 1511

HYBRID SUPERCONDUCTOR-FERROMAGNET STRUCTURES WITH SPIN-POLARIZED ELECTRON DIFFUSION AND INJECTION

V.V. Ryazanov[1,2], T.E. Golikova[1], I.S. Lakunov[1], I.A. Nazhestkin[2], S.V. Egorov[1], I.E. Batov[1]

[1]Institute of Solid State Physics, Russian Academy of Sciences, Chernogolovka, 142432 RUSSIA
[2]Moscow Institute of Physics and Technology, Dolgoprudny, 141700 RUSSIA
E-mail: valery.ryazanov@gmail.com

Effects of spin-polarized electron diffusion and injection on superconducting transport in superconducting ferromagnet/superconductor (SF) nanostructures were investigated. Planar Josephson multiterminal nanostructures of several geometries (Fig.1, for example) were realized and studied. Interesting peculiarities in the supercurrent behavior and in the differential resistance were observed. A modification of the supercurrent-carrying density of states [1] made it possible to detect a double transition with inversion of the superconducting phase difference. The spin-polarized electron diffusion into the Josephson barrier provided spin splitting of the mini-gap induced in the barrier and the multiple Andreev reflection peculiarities.

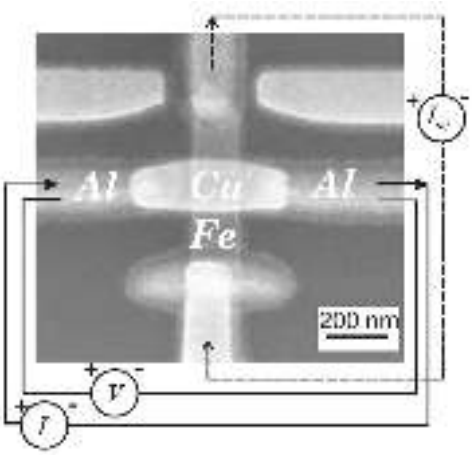

Fig. 1: *A micrograph of one of the S-N/F-S structure with spin-injection.*

References

[1] T.E. Golikova *et al.*, Supercond. Sci. Tech. **34,** 095001 (2021).

Abstract ID: 1044

ANDREEV BOUND STATES AT NONMAGNETIC IMPURITIES IN SUPERCONDUCTOR/ANTIFERROMAGNET HETEROSTRUCTURES

A.M. Bobkov[1], G.A. Bobkov[1], I.V. Bobkova[1], A.A. Golubov[2]

\[1]*Moscow Institute of Physics and Technology, 141701, Dolgoprudny, RUSSIA*
[2]*Faculty of Science and Technology and MESA+ Institute for Nanotechnology, University of Twente, 7500 AE Enschede, THE NETHERLANDS*
E-mail: bobkov.am@mipt.ru

Andreev bound states can occur at single impurities in superconductors if the impurities suppress superconductivity for a given system [1]. In particular, well-known Yu-Shiba-Rusinov states occur at magnetic impurities in conventional s-wave superconductors [2-4]. Here we demonstrate that nonmagnetic impurities in S/AF heterostructures with conventional intraband s-wave pairing also produce Andreev bound states. Analogously to the Yu-Shiba-Rusinov bound states the bound states in S/AF bilayers are spin split, but the spin of a particular bound state is determined by the sublattice to which the impurity belongs. The standard decay of the bound state LDOS is superimposed by atomic oscillations related to the staggered character of the exchange field in the host material and by another oscillating pattern produced by finite-momentum Neel triplet pairing [5] generated at the impurity. The influence of Ising spin-orbit coupling on the impurity bounds states in van der Waals S/AF heterostructures is also discussed.

The work is supported by RSF project #24-22-00186.

References

[1] A.V. Balatsky, I. Vekhter, J.-X. Zhu, Rev. Mod. Phys. **78**, 373 (2006).
[2] Y. Luh, Acta Physica Sinica **21**, 75 (1965).
[3] H. Shiba, Progress of Theoretical Physics **40**, 435 (1968).
[4] A.I. Rusinov, Sov. Phys. JETP **29**, 1101 (1969).
[5] G.A. Bobkov, V.M. Gordeeva, A.M. Bobkov, I.V.Bobkova, Phys. Rev. B **108**, 184509 (2023).

Abstract ID: 1029

COLLECTIVE EXCITATIONS IN THIN-FILM TOPOLOGICAL SUPERCONDUCTOR/FERROMAGNETIC INSULATOR HETEROSTRUCTURES

T. Karabassov[1], I.V. Bobkova[2], A.M. Bobkov[2], A.A. Golubov[3], A.S. Vasenko[1,4]

[1]HSE University, 101000 Moscow, RUSSIA
[2]Moscow Institute of Physics and Technology, Dolgoprudny, 141700 RUSSIA
[3]University of Twente, 7500 AE Enschede, THE NETHERLANDS
[4]I.E. Tamm Department of Theoretical Physics, P.N. Lebedev Physical Institute, Russian Academy of Sciences, 119991 Moscow, RUSSIA
E-mail: iminovichtair@gmail.com

The collective excitations in the superconducting systems have been intensively studied over the last decades. In conventional superconductors there are two basic collective modes: phase and amplitude (Higgs) modes [1]. Experimental investigations of the Higgs mode became particularly active due to the development of the THz spectroscopy which provided the opportunities to implement the nonlinear coupling to the amplitude mode. The idea of realizing alternative approach of the linear coupling is not novel. In particular, it has been shown theoretically that the spin-wave excitation can couple to the Higgs mode in the linear regime in systems with spin-orbit coupling [2]. However, the question of mutual impact of the spin-wave excitation and superconducting system together with the possibility of mode hybridization in such composite systems is underinvestigated. Employing the Keldysh formalism for the quasiclassical Green's functions in the diffusive limit we obtain fully self-consistent solution of the problem in the presence of the weak magnon excitation. We demonstrate that in the system under consideration the magnon has a direct impact on the pair potential. This leads to the excitation of the Higgs mode. We study the mutual influence of the collective modes in the system both in the helical ground state and in the finite momentum superconducting state. We demonstrate that these two cases are qualitatively different. While in the helical state the spectrum of the spin-wave becomes anisotropic, in the finite momentum superconducting state the sperctrum obtains chirality [3]. Moreover, we study the conditions for the hybridization of the superconducting and magnonic modes.

References

[1] R. Shimano, N. Tsuji, *Higgs mode in superconductors*, Annual Review of Condensed Matter Physics **11**, 103 (2020).

[2] Y. Lu, R. Ojajärvi, P. Virtanen, M.A. Silaev, T.T. Heikkilä, *Coupling the higgs mode and ferromagnetic resonance in spin-split superconductors with rashba spin-orbit coupling*, Phys. Rev. B **106**, 024514 (2022).

[3] T. Karabassov, I.V. Bobkova, A.M. Bobkov, A.A. Golubov, A.S. Vasenko, in preparation.

Superconducting Spintronics: Novel Quantum Circuits IV

02.05.2024 THURSDAY

Abstract ID: 1045

MAGNETIC INTERACTIONS IN COUPLED SYSTEMS OF S/F/S JOSEPHSON JUNCTIONS

I.V. Bobkova, G.A. Bobkov, A.M. Bobkov

Moscow Institute of Physics and Technology, 141701, Dolgoprudny, RUSSIA
E-mail: bobkova.iv@phystech.edu

A coupled chain of S/F/S Josephson junctions with an anomalous phase shift of the ground state is a system that realizes long-range interaction between the magnetic moments of weak links [1]. The interaction is of a magnetoelectric nature and is mediated by the condensate phase of superconductors. The system represents a paradigmatic platform for the study of collective magnetic states controlled by the superconducting phase. The talk will discuss stable magnetic configurations [2] and magnetic eigenmodes of such a system [3].

The work is supported by RSF via the project # 22-42-04408.

References

[1] G.A. Bobkov, I.V. Bobkova, A.M. Bobkov, Phys. Rev. B **105**, 024513 (2022).
[2] G.A. Bobkov, I.V. Bobkova, A.M. Bobkov, arXiv:2310.16543
[3] G.A. Bobkov, I.V. Bobkova, A.M. Bobkov, arXiv:2311.15613

Abstract ID: 1058

NEEL TRIPLET CORRELATIONS IN SUPERCONDUCTOR/ANTIFERROMAGNET HETEROSTRUCTURES WITH SPIN-ORBIT COUPLING

G.A. Bobkov[1], I.V. Bobkova[1], A.A. Golubov[2]

\[1]Moscow Institute of Physics and Technology, 141701, Dolgoprudny, RUSSIA
[2]Faculty of Science and Technology and MESA+ Institute for Nanotechnology, University of Twente, 7500 AE Enschede, THE NETHERLANDS
E-mail: bobkov.ga@phystech.edu

The influence of Rashba spin-orbit coupling (SOC) on superconducting correlations in thin-film or (quasi)2D superconductor/antiferromagnet (S/AF) structures with compensated interfaces can lead to unique effect of anisotropic enhancement of proximity-induced triplet correlations. It manifests itself in the anisotropy of the superconducting critical temperature Tc with respect to orientation of the Neel vector relative to the S/AF interface, which is opposite to the behaviour of Tc in superconductor/ferromagnet structures. This anisotropy is controlled by the chemical potential of the superconductor and, therefore, can be adjusted in (quasi)2D structures.

The work is supported by RSF project #24-22-00186

Abstract ID: 1118

SUPERCURRENTS IN A HALFMETALLIC MANGANITE

Yao Jungxiang, Remko Fermin, Kaveh Lahabi, and Jan Aarts

Huygens-Kamerlingh Onnes Laboratory, PO Box 9504, 2300 RA Leiden, THE NETHERLANDS
E-mail: aarts@physics.leidenuniv.nl

Fully spin-polarized supercurrents would be a valuable addition to the toolbox of superspintronics. A candidate halfmetallic ferromagnet for this purpose is the perovskite manganite $La_{0.7}Sr_{0.3}MnO_3$ (LSMO), which has mostly been studied in all-oxide combination with perovskite superconductors, in particular $YBa_2Cu_3O_7$. Here we demonstrate clear supercurrents in lateral Josephson junctions fabricated from a bilayer of LSMO and superconducting NbTi. The weak link is formed by a trench in the NbTi layer, made by Focused Ion Beam milling, and FIB milling also defines the junction geometry. The trench width, and therefore the junction length, was of the order 20 nm. Finding (strong) supercurrents in such junctions is surprising, since no magnetic inhomogeneity was built into the system. In bar-shaped junctions, we find a Fraunhofer-type interference pattern when applying an out-of-plane magnetic field, indicating homogeneous current flow. Disk-shaped junctions show a different pattern, indicating stronger currents along the edge of the disk. We find Josephson couplings (I_cR_N products) around 50 μV, which is large compared to all-metal junctions. We surmise that sufficient magnetic inhomogeneity exists in the LSMO layer close to the interface with NbTi to work as triplet generator. Following up on these results, we used e-beam lithography and a hard mask process to fabricate long junctions, also starting from a bilayer. Again we find supercurrents, even up to a record junction length of 1.3 μm, and with high current densities, of the order of 10^9 A/m^2 at 2 K. Combining oxide magnets with (s-wave) alloy superconductors appears a promising new route to realizing superconducting spintronics.

Superconducting Spintronics: Novel Quantum Circuits V

02.05.2024 THURSDAY

Abstract ID: 1179

SIDE-CHANNEL LEAKAGE IN SUPERCONDUCTING OUTPUT DRIVERS

Yerzhan Mustafa, Selçuk Köse

Department of Electrical and Computer Engineering, University of Rochester, Rochester, NY, 14627, UNITED STATES
E-mail: selcuk.kose@rochester.edu

Single flux quantum (SFQ) logic is a type of superconducting digital electronics that can operate at high frequencies of tens to hundreds of GHz and consume low energy per switching activity (10^{-19} J) [1]. SFQ technology can be used in high performance applications such as data centers and cloud computing. Additionally, it is a promising candidate for large-scale in-fridge control and readout circuitry of superconducting quantum computers [2]. Due to the low voltage amplitude (around 1 mV) and picosecond duration of SFQ pulse signals, the SFQ circuits cannot be directly interfaced with semiconductor (e.g., CMOS) technology. As a result, special superconducting output drivers are used to amplify and convert the SFQ pulses to DC voltage signals.

Over the recent years, there has been a growing interest in the hardware security of SFQ circuits [3]. In [4], a power side-channel leakage in standard SFQ logic gates has been studied. By measuring the variations in the power supply of SFQ chip at room temperature, a malicious adversary can decode critical information about the internal signal states. Due to the low dynamic power dissipation of SFQ logic gates (e.g., AND, OR, NOT, XOR, etc.), the largest side-channel leakage has been observed in SFQ-to-DC converter interface circuit [4]. Besides SFQ-to-DC converter, which is commonly used in testing and verification, other types of superconducting output drivers are used in, e.g., CMOS memory interface and high-speed digital data links. In this work, we analyze the side-channel leakage in various superconducting output drivers such as SFQ-to-DC converter, superconducting quantum interference device (SQUID) stack, and Suzuki stack (Josephson latching driver).

The superconducting output driver circuits are designed for MIT Lincoln Lab SFQ5ee 10 kA/cm^2 process and simulated in JoSIM. It is found that the SQUID stack has the largest side-channel leakage of ΔI_B = 220 μA (i.e., the difference in the bias current when the output voltage is low and high). However, when normalized to the total bias current ($\Delta I_B/I_B$), the Suzuki stack has the largest leakage of 8.7%. Additionally, the effect of thermal noise (at the temperature of 4.2 K) on the side-channel leakage is studied by plotting histograms of simulated bias current for each superconducting output driver circuit.

Based on the analyzed side-channel leakage data, several side-channel attacks are proposed. Particularly, we focus our discussion on attacks on system components of quantum computers such as qubit control and readout, communication with Josephson-CMOS memory, and room temperature electronics.

References

[1] G. Krylov, E.G. Friedman, *Single Flux Quantum Integrated Circuit Design* (Springer, 2022).
[2] O. Mukhanov, *et al.*, Proc. of IEEE International Electron Devices Meeting (2019), pp. 31.2.1–31.2.4.
[3] T. Jabbari, *et al.*, *Design Automation of Quantum Computers*, edited by R.O. Topaloglu (Springer, 2023), pp. 135–165.
[4] Y. Mustafa, S. Köse, IEEE Trans. Appl. Supercond. **33**, 6, 1304307 (2023).

Abstract ID: 1154

HIGH-DENSITY SUPERCONDUCTING LOGIC AND MEMORY TECHNOLOGIES

Oleg Mukhanov[1], F. Lupo[2], S. Adler[1], M. Arzeo[2], Ivan Nevirkovets[3]

[1] SEEQC, Inc., Elmsford, NY, USA
[2] SEEQC-EU, Srl, Naples, ITALY
[3] Northwestern University, Evanston, IL, USA
E-mail: omukhanov@seeqc.com

Lack of dense, high operational margin superconducting logic and memory technology has been a major limiting factor in utilizing superconducting electronics for many decades. To solve these problems, we introduced a radically new Superconductor Sustainable Ballistic Fluxon (SSBF) circuit technology. In SSBF circuits, data single flux quanta (fluxons) propagate ballistically through the low loss, bias-free, high-density superconducting gates composed of unshunted Josephson junctions. For the first time, the long-sought ballistic data processing becomes practical and scalable for the useful processor size. This is made possible by the key innovation – the digital phase source (DPS) delivering the quantized energy replenishment compensating the losses in ballistic circuits when needed and where needed.

We also introduced a new memory element which can be integrated to form a high density, high energy efficient, fully addressable memory array and compatible with SSBF digital technology. This memory element is a hybrid superconducting (S) ferromagnetic (F) device. Electric current applied along the S electrode can change the magnetization of the F layer in such a way that, for one current direction, a magnetic flux penetrates the junction perpendicular to the layers, whereas for the opposite direction, the perpendicular magnetic flux can be removed. In the former state, the modulation pattern of the Josephson critical current in the magnetic field may acquire minimum near zero field and restores its usual shape with maximum in the second state. This possibility of electric control, and a large discrimination between the Josephson critical current levels for the two states which will be preserved upon reduction of the device dimensions, is important for integration of memory arrays with high parameter margins.

Abstract ID: 1181

FERROMAGNETIC JOSEPHSON JUNCTIONS: FUNDAMENTAL SCIENCE AND APPLICATIONS

Noman O. Birge

Michigan State University, Dept. of Physics and Astronomy, East Lansing, MI 48824, USA
E-mail: birge@msu.edu

Ferromagnetic Josephson junctions have been a topic of intense interest for over 20 years, ignited both by the experimental demonstration of π-junctions [1,2] and by the theoretical prediction of spin-triplet supercurrent in junctions with suitable noncollinear magnetic inhomogeneity [3,4]. Ferromagnetic π-junctions show promise for improving the performance of superconducting digital logic and memory [5], while spin-triplet devices have sparked the imagination of the community and led to a new field often called "superconducting spintronics." Our group has contributed to both areas. For superconducting memory applications, we demonstrated that a junction containing two magnetic layers – one hard (fixed) and one soft (free) – can be switched between the 0 and π phase states by reversing the direction of the soft magnetic layer [6]. A similar switch has been achieved in spin-triplet junctions containing three magnetic layers – two fixed and one free [7]. We have recently written a review to highlight the large number of magnetic materials that have been used by groups around the world to study both fixed and controllable π-junctions [8].

We are now turning our attention to two new problems: i) creation of π-junctions with zero net magnetic moment; and ii) creation of a so-called "φ_0-junction", where the ground-state phase φ_0 across the junction can take on an arbitrary value [9,10]. φ_0-junctions have been demonstrated in several exotic systems with large spin-orbit coupling, but not yet in junctions containing only conventional ferromagnetic materials. There are several steps needed to achieve such φ_0-junctions [11]; I will discuss our progress toward that goal. If there is time, I may comment on a "holy grail" of superconducting spintronics – manipulation of the magnetic state of a junction by the supercurrent. Achieving that goal will be difficult, given the mismatch between typical Josephson energies and magnetic anisotropy energies.

References

[1] V.V. Ryazanov, *et al.*, Phys. Rev. Lett. **86**, 2427 (2001).
[2] N. Kontos, *et al.*, Phys. Rev. Lett. **89**, 137007 (2002).
[3] F.S. Bergeret, A.F. Volkov, K.B. Efetov, Phys. Rev. Lett. **86**, 4096 (2001).
[4] M. Houzet, A.I. Buzdin, Phys. Rev. B **76**, 060504(R) (2007).
[5] I. Soloviev, *et al.*, Beilstein J. Nanotechnol **8**, 2689 (2017).
[6] E.C. Gingrich, B.M. Niedzielski, *et al.*, Nature Phys. **12**, 564 (2016).
[7] J.A. Glick, *et al.*, Science Advances **4**, eaat9457 (2018).
[8] N.O. Birge, N. Satchell, arXiv:2401.04219
[9] A. Buzdin, Phys. Rev. Lett. **101**, 107005 (2008).
[10] .A. Silaev, I.V. Tokatly, F.S. Bergeret, Phys. Rev. B **95**, 184508 (2017).
[11] V. Aguilar, *et al.*, Phys. Rev. B **102**, 024518 (2020).

Superconducting Spintronics: Novel Quantum Circuits VI

02.05.2024 THURSDAY

Abstract ID: 1350

SUPERCURRENT REVERSAL IN ZEEMAN-SPLIT JOSEPHSON JUNCTIONS

A.A. Golubov[1,2], S.-I. Suzuki[1], Y. Asano[3]

[1] *Faculty of Science and Technology and + Institute MESA for Nanotechnology, University of Twente, 7500 AE Enschede, THE NETHERLANDS*
[2] *Moscow Institute of Physics and Technology, Dolgoprudny, Moscow Region 141700, RUSSIA*
[3] *Department of Applied Physics, Hokkaido University, Sapporo 060-8628, JAPAN*
E-mail: a.golubov@utwente.nl

We theoretically study the current-phase relation in a Josephson junction comprising the Zeeman-split superconductors (ZSs) and a normal metal (N). We show that at low temperatures the Josephson current in the ZS/N/ZS junctions exhibits a supercurrent reversal at a certain phase difference $\phi_c \in (0, \pi)$. By calculating the spectral Josephson current, we demonstrate that the band splitting due to the Zeeman interaction causes the level crossing in the spectra of the Andreev bound states and the sign reversal of the Josephson current, similar to the known case of an SFIFS junction (F is a ferromagnet, I is an insulator). Additionally, we propose an alternative method to observe the supercurrent reversal. We have demonstrated that ϕ_c depends on the Rashba spin-orbit interaction in the normal segment. The spin precession of a quasiparticle due to the spin-orbit interaction modifies the energy spectra of the Andreev levels and ϕ_c. In experiments, the amplitude of the spin-orbit interaction is tunable by applying the gate voltage. Therefore, by measuring the CPR by tuning the spin-orbit coupling, one would be able to observe the anomalous current reversal.

Acknowledgements

S.-I. S. acknowledges Overseas Research Fellowships by JSPS. The work is partially supported by RSF under grant number 23-72-30004

Abstract ID: 1457

SUPERCONDUCTIVITY IN ATOMICALLY THIN FILMS: DIODES AND 2D CRITICAL STATE MODEL

Filippo Gaggioli[1], Gianni Blatter[1], Kostya S. Novoselov[2], Vadim B. Geshkenbein[1]

[1]*Institut für Theoretische Physik, ETH Zurich, CH-8093 Zurich, SWITZERLAND*
[2]*Institute for Functional Intelligent Materials, National University of Singapore, 117544, SINGAPORE*
E-mail: dimagesh@itp.phys.ethz.ch

A superconducting diode carries dissipationless supercurrents in one direction, but resistive normal currents at finite voltages in the opposite direction, a phenomenon that occurs when the critical current is different in magnitude depending on the polarity. They offer perfect voltage rectification if an alternating current of magnitude between these values is applied. Despite the similar names coined, diodes and superconducting diodes have key symmetry differences due to their vastly different microscopic physics [1].

The comprehensive understanding of superconductivity is a multi-scale task that involves several levels, starting from the electronic scale determining the microscopic mechanism, going to the phenomenological scale describing vortices and the continuum-elastic scale describing vortex matter, to the macroscopic scale relevant in technological applications. The prime example for such a macro-phenomenological description is the Bean model that is hugely successful in describing the magnetic and transport properties of bulk superconducting devices. Motivated by the development of novel devices based on superconductivity in atomically thin films, such as twisted-layer graphene, here, we present a simple macro-phenomenological description of the critical state in such two-dimensional (2D) thin films. While transverse screening and demagnetization can be neglected in these systems, thereby simplifying the task in comparison with usual film- and platelet shaped samples, surface- and bulk pinning are important elements to be included. We use our 2D critical state model to describe the transport and magnetic properties of 2D thin-film devices, including the phenomenon of non-reciprocal transport in devices with asymmetric boundaries and the superconducting diode effect.

References

[1] P.J.W. Moll, V.B. Geshkenbein, Nature Physics **19**, 1379 (2023).

Abstract ID: 1020

CONTROLLABLE TOPOLOGICAL SUPERCONDUCTING DIODE

T. Karabassov[1], I.V. Bobkova[1], A.A. Golubov[2], A.S. Vasenko[1]

[1]HSE University, 101000 Moscow, RUSSIA
[2]University of Twente, 7500 AE Enschede, THE NETHERLANDS
E-mail: avasenko@hse.ru

Currently the superconducting diode effect (SDE) has become an active area of research due to its large application potential [1]. Various systems that can behave as superconducting diodes have been recently theoretically proposed and experimentally discovered. The SDE can be realized in two-dimensional superconducting systems if both inversion and time-reversal symmetries are broken. Experimentally it can be achieved in hybrid structures by proximity to a three-dimensional (3D) topological insulator (TI) [2] or in superconductors with Rashba spin-orbit coupling. On the other hand, the time-reversal symmetry can be broken by the in-plane magnetic field, or alternatively in hybrid structures by proximity to a ferromagnetic insulator with the in-plane exchange field [2]. In this work we discuss the possibility of the diode hybrid device with controllable polarity. We propose the structure that consists of two separated superconducting islands with proximity induced ferromagnetism deposited on top of the 3D TI, see **Fig. 1**. Using the quasiclassical formalism of the Usadel equations [2-4] we demonstrate that the sign of the diode efficiency can be controlled by tuning the magnetization of a single superconducting island [5]. Moreover, we show that the diode efficiency can be substantially increased in such device [5].

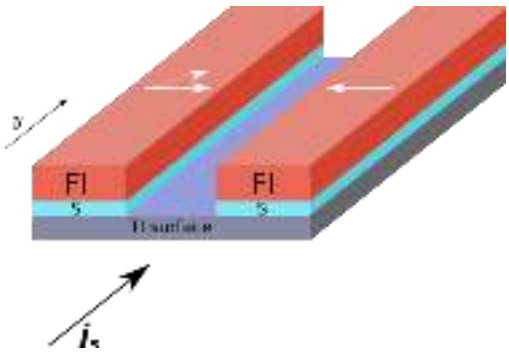

Fig. 1: *Schematic illustration of the controllable topological superconducting diode.*

T.K and A.S.V. acknowledges support from the Mirror Laboratories Project and the Basic Research Program of the HSE University.

References

[1] M. Nadeem, M.S. Fuhrer, X. Wang, Nat. Rev. Phys. **5**, 558 (2023).
[2] T. Karabassov, I.V. Bobkova, A.A. Golubov, A.S. Vasenko, Phys. Rev. B **106**, 224509 (2022).
[3] T. Karabassov, E.S. Amirov, I.V. Bobkova, A.A. Golubov, E.A. Kazakova, A.S. Vasenko, Condens. Matter **8(2)**, 36 (2023).
[4] T. Karabassov, I.V. Bobkova, V.M. Silkin, B.G. Lvov, A.A. Golubov, A.S. Vasenko, accepted in Phys. Scr., e-print arXiv: 2305.00549 (2023).
[5] T. Karabassov, I.V. Bobkova, A.A. Golubov, A.S. Vasenko, in preparation.

Large Scale Facilities in Magnetism, Superconductivity and Energy Related Materials I

02.05.2024 THURSDAY

CANCELLED

Abstract ID: 1422

UNCOMMON MAGNETISM IN RARE-EARTH INTERMETALLIC COMPOUNDS: NEUTRON SPECTROSCOPY DATA AND MODERN THEORETICAL MODELS

Pavel S. Savchenkov[1,2], Pavel A. Alekseev[2,1]

[1]*National Research Nuclear University MEPhI, 115409, Moscow, RUSSIA*
[2]*National Research Centre "Kurchatov Institute", 123098, Moscow, RUSSIA*
E-mail: savch92@gmail.com

Rare-earth intermetallic compounds are characterized by the presence of a long-range magnetic order due to the interaction of local magnetic moments periodically located within the crystal lattice. This report considers the possibility of forming an ordered state in cases where there is no opportunity to observe the local moment of the f-electronic shell in a traditional sense [1,2]. These are, first of all, systems with a singlet ground state of a rare earth ion. In such systems, under a certain ratio between the dipole matrix element connecting the singlet to the excited state and the magnitude of the interionic interaction at each lattice site, an induced magnetic moment can form and a simultaneous ordering of such moments can occur. This phenomenon, called "induced" magnetism, is discussed in this report using the example of the intermetallic compound PrNi. Some results of experimental investigations of induced magnetism in PrNi and related systems are presented. Primarily, the information extractable from neutron magnetic inelastic scattering spectra is analyzed and developed theoretical and model-based representations are discussed.

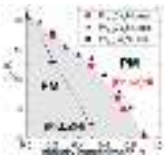

Fig. 1: *The relationship between T_C and x in $Pr_{1-x}La_xNi$ (black squares) and $Pr_{1-x}Ce_xNi$ (red circles). The blue triangles represent the T_C calculations for $Pr_{1-x}Ce_xNi$ using a microscopic state model. The calculation result for $Pr_{1-x}La_xNi$ is presented as dashed line. The grey area indicates the region of the ferromagnetic state of the (Pr,Ce)Ni system, which is significantly larger than for (Pr,La)Ni.*

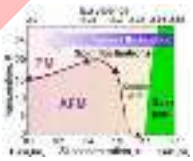

Fig. 2: *Magnetic phase diagram for $EuCu_2(Si_xGe_{1-x})_2$. The valence values shown on the upper scale. The solid brown line represents the phase boundary between the antiferromagnetic (AFM) and paramagnetic (PM) states. The triangles indicate the values obtained from neutron powder diffraction experiments. The yellow region (Kondo + HF), extending down to x = 0.4 and overlapping with the AFM region, represents the spin-fluctuation regime where a quasielastic response is observed. The green colored region represents the low temperature spingap regime.*

Special attention is devoted to explaining the influence of defects of various natures in the rare-earth sublattice (nonmagnetic impurity La - $Pr_{1-x}La_xNi$ and intermediate-valence (IV) Ce - $Pr_{1-x}Ce_xNi$) on the conditions for the emergence of long-range magnetic order (see Fig. 1). Another type of "unconventional" magnetism explored in the report is the observed coexistence of magnetic order and fast spin fluctuations in certain intermetallic compounds of Eu. This coexistence initially appears anomalous due to the intermediate valence state of the rare earth ion (see Fig. 2). This report presents the results of experiments investigating the influence of high hydrostatic pressures (up to 15 GPa) on the long-range magnetic order in $EuCu_2Si_2$ and provides evidence for the uniformity of the intermediate valence state of Eu in $EuCu_2(Si_xGe_{1-x})_2$. Based on a comprehensive analysis of the results from a combination of neutron experiments and calculations within the framework of induced magnetism theory, a realistic description of the mechanisms underlying the formation of an ordered antiferromagnetic state against a background of uniform intermediate valence is proposed for $EuCu_2(Si_xGe_{1-x})_2$.

References

[1] P.S. Savchenkov, P.A. Alekseev, Crystals, **13(8)**, 1238 (2023).
[2] P. S. Savchenkov, P.A. Alekseev, *et al.*, J. Phys.: Condens. Matter, **30(5)**, 055801 (2018).

Abstract ID: 1449

EXAMINING THE STRUCTURE-PROPERTY RELATIONSHIPS OF SUSTAINABLE FUNCTIONAL CERAMICS USING POWDER DIFFRACTION

A. Manjon Sanz[1,2], C. Berger[2], C. Culbertson[2], A. Neill[1], M. Dolgos[2,3]

[1]*Oak Ridge National Laboratory, 37830, Oak Ridge, USA*
[2]*Oregon State University, 97331, Corvallis, USA*
[3]*University of Calgary, T2N 1N4, Calgary, CANADA*
E-mail: manjonsanzam@ornl.gov

Understanding the structure of a material is critical to understand their physical properties. $PbZr_{1-x}Ti_xO_3$ (PZT) is a ceramic perovskite material that has exceptional piezoelectric properties. PZT plays an important role in industry and has many commercial applications. However, the toxicity of lead has stimulated a lot of interest in the discovery of Pb-free ferroelectric materials. Here, we use X-ray and neutron powder diffraction to investigate the structure of a few lead-free ferroelectric systems:

1) Ambient pressure stable perovskite oxides with all Bi^{3+} on the *A*-site are rare, with only four examples known. We present the full structural analysis of the orthorhombic phase of $(1 - x)Bi(Ti_{3/8}Fe_{2/8}Mg_{3/8})O_3 - xCaTiO_3$, which crystallizes in $Pna2_1$ symmetry with [001] polarization. This symmetry is rare and has only been reported twice for perovskites at ambient conditions. Analysis of maximum entropy method models using synchrotron radiation powder X-ray diffraction reveals a disordered A-site configuration, and the Maximum Entropy Method/Rietveld technique generates a structural model of this extreme disorder.

2) Bismuth-based perovskites are established as good ferroelectric materials, but it is still necessary to improve their piezoelectric properties to compete with PZT. For the system $(1-x)\ BaTiO_3 - (x)\ BiInO_3$, we study the electromechanical properties and the structure in the region $0.03 \leq x \leq 0.12$.

3) The system $(1-x)\ BaZr_{0.2}Ti_{0.8}O_3\ -x\ Ba_{0.7}Ca_{0.3}TiO_3$ is the first Pb-free piezoelectric material with a significantly high enough $d_{33} \sim 620$ pC/N at $x = 0.50$, that could replace PZT in certain applications. Here, we re-investigate its phase diagram as a function of temperature.

Abstract ID: 1485

MAGNETISM AND LATTICE COLLAPSE TRANSITION IN ACo_2P_2

J. Sugiyama[1], I. Umegaki[2], K. Moriyam[3], K. Yoshinaga[4], K. Ohishi[1], F. Elson[5], U. Miniotaite[5], R. Palm[5], M. Månsson[5], O.K. Forslund[6], Y. Sassa[5], S. Sugiyama[7], G.D. Morris[8], B. Hitti[8], C. Michioka[4], H. Ueda[4], K. Yoshimura[4]

[1]*CROSS Neutron Science and Technology Center, 319-1106, Tokai, JAPAN*
[2]*High Energy Accelerator Research Organization (KEK), 319-1106, Tokai, JAPAN*
[3]*Institute of Solid State Physics, University of Tokyo, 277-8581, Kashiwa, JAPAN*
[4]*Dept. of Chemstry, Kyoto University, 606-8502, Kyoto, JAPAN*
[5]*Dept. of Applied Physics, KTH Royal Institute of Technology, SE106-91, Stockholm, SWEDEN*
[6]*Physik-Institut, Universität Zürich, CH-8057 Zürich, SWITZERLAND*
[7]*Dept. of Applied Physics, Nagoya University, 464-8602, Nagoya, JAPAN*
[8]*Centre of Molecular and Materials Science, TRIUMF, V6T 2AS, Vancouver, CANADA*
E-mail: juns@triumf.ca

A structural phase transition from an uncollapsed tetragonal (uc*T*) phase to a collapsed tetragonal (c*T*) phase in $ThCr_2Si_2$-type ACo_2P_2 (*A*=Ca, Sr, RE) compounds is known to change the magnetic nature drastically [1]. This is caused by the following two factors:

1) the change in the valence state of P from P^{3-} in the uc*T* phase to $[P\text{-}P]^{4-}$ in the c*T* phase [2].
2) the decrease in the P-P bond length from the uc*T* phase to the c*T* phase.

The former also changes the valence state of Co and/or RE, while the latter changes the strength of the magnetic interaction along the *c*-axis. We have studied the change in magnetism of ACo_2P_2 with a microscopic magnetic tool: i.e., muon spin rotation and relaxation (m^+SR).

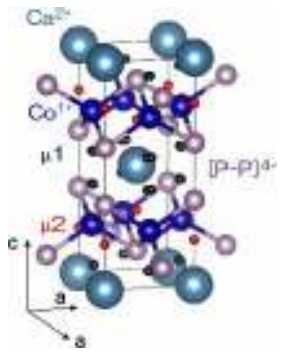

Fig. 1: *The crystal structure of $CaCo_2P_2$ in a collapsed tetragonal phase, in which two P ions form a covalent-like bond along the c-axis [1].*

In a solid solution system between nonmagnetic uc*T*-$SrCo_2P_2$ and antiferromagnetic (AF) c*T*-$CaCo_2P_2$ with T_N = 90 K [3], a magnetic but disordered phase was found to appear bwtween x = 0.5 and 0.7 in $Sr_{1-x}Ca_xCo_2P_2$, where the lattice collapsed transition occurs at around x = 0.5. Here, a "disordered" phase means the phase, for which m^+SR provides no oscillation but relaxation, and corresponds to a random spin-glass state, short-range ordered state, or highly fluctuating state. In another solid solution system between AF uc*T*-$EuCo_2O_2$ with T_N = 66.5 K and AF c*T*-$CaCo_2P_2$ [4], a disordered ferromagnetic (FM) phase was found to appear below 210 K at around x = 0.6, where the lattice collapse transition completes.

Here, we summarize our m^+SR results on ACo_2P_2 [3-6] to understand the interrelationship between the lattice collapse transition and magnateic nature.

References

[1] R. Hoffmann, C. Zheng, J. Phys. Chem. **89**, 4175 (1985).
[2] M. Reehuis *et al.*, J. Alloys Compd. **266**, 4175 (1998).
[3] J. Sugiyama *et al.*, Phys. Rev. B **91**, 144423 (2015).
[4] I. Umegaki *et al.*, submitted to Phys. Rev. B (2024).
[5] O.K. Forslund *et al.*, Phys. Scr. **96**, 125864 (2021).
[6] O.K. Forslund *et al.*, Sci. Rep. **12**, 17526 (2022).

Large Scale Facilities in Magnetism, Superconductivity and Energy Related Materials II

02.05.2024 THURSDAY

Abstract ID: 1487

X-RAY MAGNETIC SPECTROSCOPY: EMERGING OPPORTUNITIES AT THE 4TH GENERATION SYNCHROTRONS

A. Rogalev

ESRF, The European Synchrotron, 38000, Grenoble, FRANCE
E-mail: rogalev@esrf.fr

Recent achievements and discoveries based on application of X-ray spectroscopic techniques to materials with intriguing magnetic properties will be highlighted. The ESRF beamlines offer unique possibilities in the field of magnetic spectroscopy using XMCD/XMLD under multiple extreme conditions of high field, low temperatures and high pressure as well as magnetic dichroism in Resonant Inelastic X-ray Scattering and Fluorescence. The emerging new opportunities for magnetism research offered by the 4th generation high brilliance synchrotron sources, such as ESRF-EBS, will be thoroughly discussed.

CANCELLED

Abstract ID: 1488

Na-ION BATTERY MATERIALS STUDIED BY MEANS OF SMALL- AND WIDE-ANGLE NEUTRON SCATTERING AND MUON SPIN RELAXATION

K. Ohishi[1], D. Igarashi[2], R. Tatara[2], Y. Kawamura[1], S. Takata[3], K. Hiroi[3], J. Suzuki[1], I. Umegaki[4], J. Nakamura[4], A. Koda[4], S. Komaba[2], J. Sugiyama[1]

[1]*Neutron Science and Technology Center, Comprehensive Research Organization for Science and Society (CROSS), Tokai, Ibaraki 319-1106, JAPAN*
[2]*Department of Applied Chemistry, Tokyo University of Science, Shinjuku-ku, Tokyo 162-0826, JAPAN*
[3]*J-PARC Center, Japan Atomic Energy Agency (JAEA), Tokai, Ibaraki 319-1195, JAPAN*
[4]*Muon Science Laboratory, Institute of Materials Structure Science, High Energy Accelerator Research Organization (KEK), Tokai, Ibaraki 319-1106, JAPAN*
E-mail: k_ohishi@cross.or.jp

The recent surge of Li-ion batteries has triggered an increased interest to investigate Na-ion battery materials [1,2], because Na is more abundant than Li, resulting in lower material costs. Although many Na transition metal oxides are available as a cathode material for the Na-ion battery due to the size difference between Na^+ and transition-metal ions, there is, at present, no suitable anode material [1]. The most common anode materials for the Li-ion battery, i.e., graphite and soft carbon, are not compatible for the Na-ion battery, because graphite is electrochemically inactive in an intercalation and deintercalation reaction of Na^+ ions. Since non-graphitizable carbon (hard carbon) is electrochemically active as a Na insertion host, hard carbon is heavily investigated as an anode material for the Na-ion battery. However, the relationship between the structure of hard carbon and dynamics of Na insertion is still not fully clarified despite huge efforts in the past decade [2]. We have therefore attempted to study the microscopic structural nature of sodium intercalated hard carbon (NaC_x) with a small- and wide-angle neutron scattering (SANS and WANS) technique and the dynamics of Na diffusion in NaC_x with a muon spin relaxation (μ^+SR) technique. This is because SANS is very sensitive to microscopic structural environments, while μ^+SR provides an intrinsic self-diffusion coefficient of Li^+ (D^i_{Li}) in many Li-ion battery materials, such as, Li_xCoO_2 [4], Na_xCoO_2 [5], and LiC_6 [6].

The SANS and WANS experiments were performed at room temperature on TAIKAN (BL15) at the MLF, J-PARC [7]. The μ^+SR experiment was performed on S1 surface muon beamline at the MUSE MLF, J-PARC. The neutron scattering revealed the increase of interlayer distance between graphenes and decrease of the size of nanopores with increasing sodium intercalation in hard carbon. The muon spin relaxation revealed that a systematic increase in the field fluctuation rate with increasing temperature evidenced a thermally activated sodium diffusion. Assuming the two-dimensional diffusion of Na-ion in the graphene layers, the self-diffusion coefficient of Na-ion was estimated to be 2.6×10^{-11} cm^2/s at 310 K, with a thermal activation energy of 39(7) meV. At the presentation, we will discuss about the results of SANS and μ^+SR, in addition to the recent results of operando-μ^+SR on $LiCoO_2$ [9] and $NaCoO_2$.

References

[1] N. Yabuuchi *et al.*, Chem. Rev. **114**, 11636 (2014).
[2] K. Kubota *et al.*, Chem. Mater. **32**, 2961 (2020).
[3] F.W. Clarke, H.S. Washington, USGS Numbered Series **285** (1953).
[4] J. Sugiyama *et al.*, Phys. Rev. Lett. **103**, 147601 (2009).
[5] M. Månsson, J. Sugiyama, Phys. Scr. **88**, 068509 (2013).
[6] I. Umegaki *et al.*, Phys. Chem. Chem. Phys. **19**, 19058 (2017).
[7] S. Takata *et al.*, JPS Conf. Proc. **8,** 036020 (2015).
[8] K. Ohishi *et al.*, ACS Phys. Chem. Au **2**, 98 (2022).
[9] K. Ohishi *et al.,* ACS Appl. Energy Mater. **5**, 12538 (2022).

Abstract ID: 1492

LARGE SCALE NEUTRON FACILITIES IN MAGNETISM: NEUTRON DIFFRACTION PROSPECTIVE

A. Goukassov

Laboratoire Léon Brillouin, CEA-CNRS, CE-Saclay, 91191 Gif-sur-Yvette, FRANCE
E-mail: arsen.goukassov@cea.fr

A common tool for studying the magnetic structure and properties of materials is the neutron single crystal and powder diffraction (ND). On the first generation large scale neutron facilities like HFIR, ISIS and ILL it has been widely used to determine the magnetic structure of a large number of various magnetic materials, to study the effects of temperature, pressure, and magnetic field on the magnetic order. However, a major limitation of this technics was a relatively large (millimeter) sample size needed in the experiments. With the appearance of new high brilliance neutron sources like SNS, J-Park and ESS neutron diffraction opens new route to the studies of micrometric samples in extreme experimental conditions.

Polarized neutron diffraction (PND), while being one of the best tools to study the spin densities and local magnetic anisotropy in magnetic compounds also suffered from the same handicap. In spite of this, due to its high sensitivity to small magnetic moment it has been successfully used in the studies of frustrated magnetism and became a reference in mapping the local anisotropy of molecular magnets [1]. PND is based on the susceptibility approach, where measured flipping ratios are used to fit the local magnetic susceptibility tensors for each magnetic site, which allows quantifying the magnetic anisotropy at the atomic level [2]. Recently, this approach has been extended to study the magnetic anisotropy in powders [3], which opens large possibilities in the studies of highly interesting powder materials, like frustrated magnets], multiferroics, single molecule magnets or nanoscale systems.

In the talk, we illustrate the possibilities which open the new large scale neutron facilities in magnetism and review the challenges we must overcome in the neutron diffraction and in particular in the polarized neutron diffraction to make this powerful techniques easily accessible and best performing.

References

[1] D. Luneau, B. Gillon. Magnetochemistry **7**, 158 (2021).
[2] A. Gukasov, P.J. Brown, Journal of Physics: Condensed Matter **14**, 8831-39 (2002).
[3] I.A. Kibalin, A. Gukasov, Phys. Rev. Res. **1**, 033100 (2019), ibid., **2**, 033509 (2020).

CANCELLED

Large Scale Facilities in Magnetism, Superconductivity and Energy Related Materials III

02.05.2024 THURSDAY

Abstract ID: 1500

THE DESIGN AND CURRENT STATUS OF THE HIGH-RESOLUTION NEUTRON DIFFRACTOMETER AT CHINA SPALLATION NEUTRON SOURCE

Ping Miao[1,2]

[1]*Institute of High Energy Physics, Chinese Academy of Sciences, Beijing 100049, CHINA*
[2]*Spallation Neutron Source Science Center, Dongguan 523803, CHINA*
E-mail: miaoping@ihep.ac.cn

A new neutron diffractometer is under construction at China Spallation Neutron Source, which aims to reaching a world-leading resolution of $\Delta d/d \leq 0.05\%$ and bearing a moderate flexiblity of varying resoultion and brightness. Fully elliptical geometry in both vertical and horizontal directions is impletmented in neutron guides and high-frequency T0 chopper is adopted to increase the flux gain of short wavelength neutrons, which could impove the statistics at long-Q range, so that high Q-resolution pair distribution function analysis could potentially be realized. The diffratometer is designed to have large solid- angle coverage of 3He PSD detectors, spanning from 5 degree to 177 degree in the horizonal plane and from -28 degree to 28 degree in the vertical plane. Its flexibility allows versatile diffraction measurements, encompassing long-time data collection of the high- resolution powder diffraction patterns, quick measurement of small powder samples, as well as single-crystal diffraction measurement.

Abstract ID: 1453

IN-SITU SYNCHROTRON X-RAY DIFFRACTION STUDY OF SILICON-BASED ANODES PRODUCED BY DIATOM ALGAE

Pedro Alonso Sánchez[1], Weicheng Hua[2], Javier Campo[1], Federico H. Cova[3], María Valeria Blanco[1,2]

[1]Nanoscience and Materials Institute of Aragon (CSIC-University of Zaragoza) and Condensed Matter Physics Department of the University of Zaragoza, Sciences Faculty, C/Pedro Cerbuna 12, 50009, Zaragoza, SPAIN
[2]Department of Material Science and Engineering, Norwegian University of Science and Technology, NO-7491, Trondheim, NORWAY
[3]ALBA CELLS, 08290, Cerdanyola del Vallés, Barcelona, SPAIN
E-mail: p.alonso@unizar.es

Silicon (Si) has been revealed as a promising material for next generation Lithium-ion battery (LIB) anodes, displaying a high theoretical capacity of 4200 mAg^{-1}, which is about 10 times higher than the capacity of graphite anodes. However, Si undergoes substantial volume changes (up to 300%) during the (de)lithiation reactions resulting in mechanical degradation and important capacity fade, which dramatically shortens the cycle life of the anode. Different approaches have been proposed to avoid cracks formation and to improve cycling life, such as reducing particle size of silicon, limiting voltage window during the (de)lithiation, or designing silicon-graphite (Si/Gr) blended anodes that offers a balance between high capacity (from Si) and stable cycling performance (from Gr). On the other hand, complexity of silicon (de)lithiation reactions and its interplay with other materials present in the anode, makes large facility techniques ideal for the study of Si-based anodes. In this work, we present an in-operando synchrotron X-ray diffraction study for the first five (de)lithiation cycles of a Si/Gr anode. Structural changes of both, Si and Gr, were tracked during the entire experiment (see Fig. 1) with a high temporal resolution. For the first time, reversible lithiation and delithiation reactions of Si conserving its crystal structure are reported and, at the same time, typical amorphization of Si is also observed. The interplay between Gr and Si during the five cycles is also analyzed. The results provide a deeper understanding of the (de)lithiation of crystalline Si which is indispensable for the development of Si-based anodes with optimized performance.

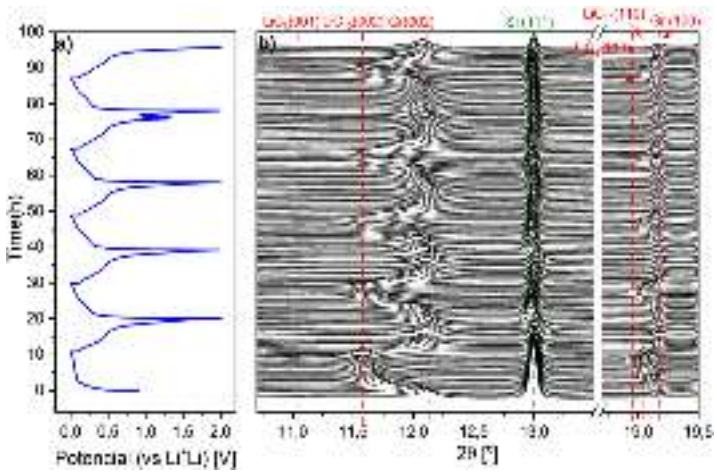

Fig. 1: *Galvanostatic cycle curves (a) with diffractograms collected from in situ XRD (b).*

Abstract ID: 1494

DOPING EVOLUTION OF HIGH-ENERGY SPIN EXCITATIONS IN $Pr_{1.4-x}La_{0.6}Ce_xCuO_4$

M. Fujita[1], K. Shigiya[2], T. Sasaki[2], K. Sato[2], K. Tsutsumi[2], S. Asano[2]

[1]*Tohoku University, Institute for Materials Research, 980-8577, Sendai, JAPAN*
[2]*Tohoku University, Department of Physics, 980-8578, Sendai, JAPAN*
E-mail: fujita@tohoku.ac.jp

We studied the effects of Ce-doping and post-growth annealing on the high-energy spin excitations in the electron-doped $Pr_{1.4-x}La_{0.6}Ce_xCuO_4$ by neutron scattering techniques. For the as-grown parent compound $Pr_{1.4-x}La_{0.6}CuO_4$, a well-defined spin-wave excitation was observed with a zone boundary energy of ~300 meV. No apparent annealing effect on the dispersion relation was observed, consistent with the results of resonant inelastic X-ray scattering measurements on Nd_2CuO_4 [1]. However, the scattering intensity in the entire energy range was drastically reduced due to annealing. With increasing x for the as-grown compounds, the spin excitation spectra become steep along the energy direction and decrease the intensity. On the other hand, the annealing effects on the spectra weaken at the larger x region, that is, the spectral shape and the intensity are insensitive to the annealing. We discuss the similarities and differences between the Ce-doping and annealing effects and their relation to the appearance of superconductivity.

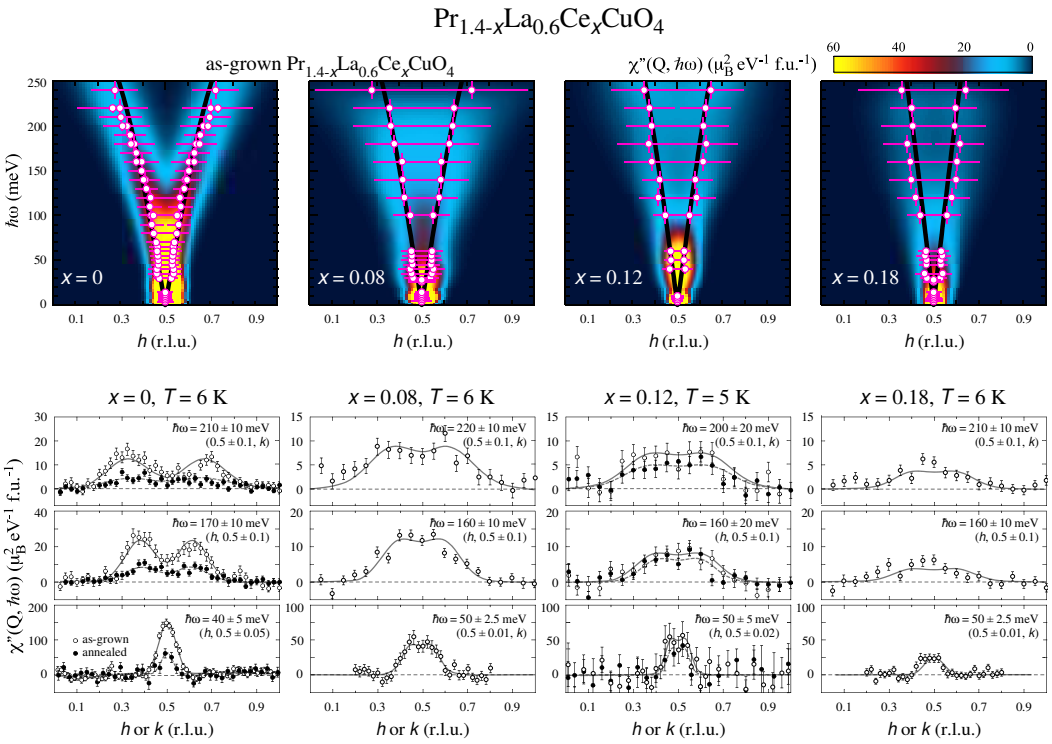

Fig. 1: *Spin excitation spectra (upper figures) in the energy-momentum space and (lower figures) at constant-energies shown for the $Pr_{1.4-x}La_{0.6}Ce_xCuO_4$ for x = 0, 0.08, 0.12 and 0.18.*

References

[1] K. Ishii, Phys. Rev. Mat. **5**, 024803 (2021).

Large Scale Facilities in Magnetism, Superconductivity and Energy Related Materials IV

02.05.2024 THURSDAY

Abstract ID: 1595

HIGH-RESOLUTION NEUTRON POWDER DIFFRACTION FOR MATERIALS SCIENCE

T. Kamiyama[1,2], P. Miao[1,2]

[1] *CSNS, IHEP, Chinese Academy of Sciences, Beijing 100049, CHINA*
[2] *Spallation Neutron Source Science Center (SNSSC), Dongguan 523803, CHINA*
E-mail: kamiyama@ihep.ac.cn

The advantage of the time-of-flight (TOF) method in diffraction experiments for materials science is to utilize a wide range of energy spectra simultaneously. Egelstaff proposed the TOF method for the structure study in the 1950s [1], and Lowde theoretically discussed the intensity gain of the TOF method over the angle-dispersive method in 1956 [2]. Buras and Leciejewicz realized the TOF powder diffraction using a Fermi chopper in 1963 [1, 3, 4]. In pulsed neutron sources using an electron linac, Rensselaer (New York), Tohoku Univ. (Sendai), and Harwell (Harwell) carried out TOF diffraction from 1967, independently. Since then, several pulsed neutron source projects have emerged such as 0.5 MW pulse reactor project (EURATOM, Italy) and a 0.5 MW Linac Booster project (Japan), but none of them were realized.

On the other hand, Carpenter pushed on pulsed spallation neutron project using proton accelerators and constructed facilities ZING-P, ZING-P'(1974,1977) and IPNS (1982). Inspired by the ZING-P, Watanabe and Ishikawa developed a user facility KENS (1980) using a booster synchrotron for the KEK proton synchrotron. IPNS and KENS became the first full-scale user facility of spallation neutron for materials science, and ISIS (1984) and LANSCE (1983) followed. When "the high-T_c superconductor fever" occurred, high-resolution powder neutron diffractometers in these facilities made the essential contribution as expected in the first step in materials science research: determining the crystal structures of newly discovered oxides one after another. The resolution of most of these diffractometers is 0.2 - 0.5 % and the complexity of most of the high-T_c oxide superconductors is suitable for the resolution. However, there remained many topics which could not be tackled by the resolution. These topics are expected to be solved by super-high-resolution diffractometers with 0.05 % resolution: HRPD at ISIS, SuperHRPD at MLF, J-PARC, and TREND at CSNS. HRPD has been the only super-high-resolution diffractometer for 20 years until SuperHRPD started in 2008. In 2024, TREND will join one of them.

The super-high-resolution diffraction is suitable for detecting tiny distortions on symmetry-breaking as well as extracting reliable structure factors from overlapping reflections in complex structures. Here I will talk about high-resolution TOF neutron diffraction and its application to physical science and energy materials.

References

[1] V.L. Aksenov, A.M. Balagurov, Physics - Uspekhi **59**, 279 (2016).
[2] R.D. Lowde, Acta Cryst. **9**, 151 (1956).
[3] B. Buras, J. Leciejewicz, W. Nitc, I. Sosnowska, J. Sosnowski, F. Shapiro, Nukleonika **9**, 523 (1964).
[4] https://www.iucr.org/news/newsletter/volume-15/number-1/crystallography-in-poland.
[5] R.M. Brugger, R.B. Bennin, T.G. Worlton, Phys. Lett. **24A**, 714 (1967).

Abstract ID: 1243

PRESSURE-INDUCED SECOND-ORDER MOTT TRANSITION IN QUADRUPLE PEROVSKITES

A. De Giovanni Rodrigues[1,2], A. Perucchi[3], L. Tomarchio[4], M. Verseils[5], P. Parisiades[2], B. Baptiste[2], K. Béneut[2], E. Gilioli[6], S. Lupi[4,7], A. Gauzzi[2]

[1]Federal University of São Carlos, São Carlos, SP, BRAZIL
[2]IMPMC, Sorbonne Université, CNRS and MNHN, 4, place Jussieu, Paris, FRANCE
[3]Elettra – Sincrotrone Trieste SCpA, 34149 Basovizza, Trieste, ITALY
[4]Department of Physics, Sapienza University, Piazzale Aldo Moro 5, Rome, ITALY
[5]Synchrotron Soleil, L'Orme des Merisiers, Saint Aubin, Gif-sur-Yvette, FRANCE
[6]Istituto Materiali per Elettronica e Magnetismo – CNR, 43100 Parma, ITALY
[7]IOM-CNR, Basovizza, Trieste, ITALY
E-mail: andrea.gauzzi@sorbonne-universite.fr

We argue that, in quadruple perovskites $AA'_3B_4O_{12}$ [1,2], a (a+a+a+) rotation of the BO_6 octahedra in the aristotype perovskite structure ABO_3 [3] leads to a high-density structure that hinders structural distortions under high pressures. We show that this unique structural feature permits the realization of a second-order insulator-to-metal transition induced by pressure at P_{cr} =17.5 GPa in the Mott system $(NaMn_3)Mn_4O_{12}$ [4]. Specifically, by means of a systematic Raman scattering and infrared reflectivity study as a function pressure, we find that both Raman and infrared modes display a continuous behavior across P_{cr}, which indicates the absence of structural changes at the insulator-metal transition and that the transition is of purely electronic origin [5]. We also observe a progressive enhancement of an asymmetry Fano term with pressure up to P_{cr} in the Raman line shape, consistent with a scenario of incipient metallic phase. We therefore envisage that a suitable spectral analysis of this line shape offers an opportunity to unveil the effective Hamiltonian of the transition.

References

[1] A. Deschanvres, B. Raveau, F. Tollemer, Bull. Chim. Soc. Fr. **11**, 4077 (1967).
[2] M. Marezio, P. Dernier, J. Chenavas, J. Joubert, Journal of Solid State Chemistry **6**, 16 (1973).
[3] A.M. Glazer, Acta Crystallographica Section B: Structural Crystallography and Crystal Chemistry **28**, 3384 (1972).
[4] D. Delmonte, F. Mezzadri, F. Orlandi, G. Calestani, Y. Amiel, E. Gilioli, Crystals **8**, 81 (2018).
[5] A. De Giovanni Rodrigues *et al.* (2023), under review.

Abstract ID: 1659

XTREMED: A NEW SINGLE CRYSTAL AND POWDER DIFFRACTOMETER DESIGNED FOR MEASUREMENTS AT EXTREME CONDITIONS OF PRESSURE AND MAGNETIC FIELDS

J. Campo[1], S. Savvin[1], J.A. Rodríguez-Velamazán[2]

[1] *Instituto de Nanociencia y Materiales de Aragón, CSIC - Universidad de Zaragoza, 50009, Zaragoza, SPAIN*
[2] *Institut Laue-Langevin, 38042, Grenoble, FRANCE*
E-mail: javier.campo@csic.es

Neutron diffraction has unique capabilities for the research under extreme conditions, mainly in two large areas: crystallography/geosciences and magnetism/solid-state physics. The growing interest for these problems is attested by the quantity and quality of publications, by the number of experiments proposed at the different neutron sources and by the new instrumentation projects under development all around the world. Therefore, the project for the construction of an "eXtreme conditions Diffractometer (XtremeD)" at Institut Laue-Langevin for both single crystals and powders, operating at high pressures (>30 GPa) and high magnetic fields (up to 15-17 Tesla), is being considered and will be presented here [1].

The scientific areas in which the projected instrument can make significant contributions and the main technical characteristics of the project are discussed in this presentation. The main idea of XtremeD is to combine a large solid-angle detector with an optional highly-focused beam on the sample, thus providing high flux while maintaining low background. The principal features of XtremeD will be the following:

- Optimisation for small samples: optional and variable focusing optics (choice of the focusing point).
- Large 2D position-sensitive detector for powders and single crystals.
- Sample environment adapted for high pressure (variety of pressure cells, up to 30 GPa for the moment, but with a goal of 50 GPa after the envisaged developments) and high magnetic fields (up to 15 Tesla in continuous mode, with the possibility of higher pulsed fields).
- Radial oscillating collimator and neutron shielding to suppress background.
- Choice of monochromators (Si, PG), take-off angles (40º-120º), and wavelengths (0.9– 4 Å).

The scientific possibilities that this instrument will provide and the main technical characteristics of the instrument performance in different conditions will be the focus of this presentation.

The Scientific Advisory Committee and the Working Team of XtremeD are acknowledged for the preparation of the scientific case and for the realization of the technical project, respectively.

References

[1] J.A. Rodríguez-Velamazán *et al.*, J. Phys. Conf. Ser. **325**, 012010 (2011).

Magnetic shape memory alloys and magnetocalorics I

02.05.2024 THURSDAY

Abstract ID: 1091

DEVELOPMENT OF GLASS-COATED MICROWIRES FROM HEUSLER ALLOYS

V. Zhukova[1,2,3], M. Salaheldeen[1,2,3,4], M. Ipatov[1,2], A.Wederni[1,2], A. Zhukov[1,2,3,5]

[1]Dept. Polym.Adv. Mater., Univ. Basque Country, UPV/EHU San Sebastián 20018, SPAIN
[2]Dept. Appl. Phys., Univ. Basque Country EIG, UPV/EHU, 20018, San Sebastian, SPAIN
[3]EHU Quantum Center, University of the Basque Country, UPV/EHU, SPAIN
[4]Physics Department, Faculty of Science, Sohag University, Sohag 82524, EGYPT
[5]IKERBASQUE, Basque Foundation for Science, 48011 Bilbao, SPAIN
E-mail: arkadi.joukov@ehu.es

The Heusler alloy have caught considerable attention owing to a number of interesting features such as large magnetic field-induced strain, the ferromagnetic shape-memory effect, magnetic field induced martensitic transition, a substantial magnetocaloric effect (MCE), Magnetoresistance effect (MR) or the half-metallic behaviour [1,2]. The conventional method for preparation of Heusler alloys is arc-melting followed by long high temperature annealing [1,2]. For increasing of the heat exchange rate the materials miniaturization involving preparation of either thin wires or thin films is beneficial [1,2]. However, there are a number of issues and difficulties with the preparation of low dimensional Heusler alloys. The modern Taylor-Ulitovsky fabrication technique enable to fabricate ultra-thin and uniform glass-covered microwires consisting of a metallic nucleus (diameter 0.1-100 μm) covered by flexible and insulating glass coating (thickness 2-30 μm) [3].

Recently we have successfully used the Taylor-Ulitovsky fabrication technique for preparation of Heusler alloy glass-coated microwires [3]. Up to now we have prepared and studied Ni_2MnGa, Ni_2MnIn, Co_2MnSi, Co_2MnSiC, Ni_2FeSi, Co_2FeSi, Co_2MnGe glass-coated microwires with metallic nucleus diameters from 3 to 80 μm [3].

The preparation Taylor-Ulitovsky technique involves the simultaneous rapid melt quenching of a composite microwire (a metallic nucleus inside a glass capillary) when it passes through a stream of coolant (water). Therefore, annealing conditions strongly affect the magnetic properties and Curie temperature, T_c, of as-prepared microwires from Heusler alloys. Here we report on the preparation and processing, magnetic and structural properties of Heusler-type glass-coated microwires. Particularly, a ferromagnetic ordering T_c, near room temperature and the hysteresis on temperature dependence of magnetization (see Fig.1) related to the first-order martensitic phase transition have been observed in properly annealed NiMnGa microwires.

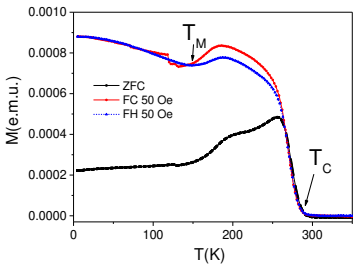

Fig. 1: *Temperature dependence of magnetic moment of properly annealed NiMnGa microwires.*

As a final conclusion, we have demonstrated that Taylor-Ulitovsky technology is a promising route of obtaining large amount of the quasi-unidimensional miniaturized Heusler alloy materials.

References

[1] D.C. Dunand, P. Müllner, Adv. Mater. **23**, 216-232 (2011).
[2] V.A. Chernenko, Scr. Mater. **40**, 523-527 (1999).
[3] A. Zhukov, M. Ipatov, J.M. Blanco, P. Corte-Leon, V. Zhukova, *Heusler-type glass-coated microwires: Fabrication, characterization, and properties*, ch.9.,in book "Magnetic Nano- and Microwires" Ed.: Manuel Vázquez, Woodhead Publishing Series in Electronic and Optical Materials, Cambridge, UK: Woodhead Publishing, pp. 255-294, 2020, ISBN: 0081028326, 9780081028322, doi: 10.1016/B978-0-08-102832-2.00009-8

Abstract ID: 1127

MAGNETIC SHAPE MEMORY ALLOYS AND NEUTRON DIFFRACTION

Jose M. Porro[1,2]

[1]*BCMaterials, UPV/EHU Science Park, Leioa 48940, SPAIN*
[2]*Ikerbasque, Basque Foundation for Science, Bilbao 48013, SPAIN*
E-mail: jm.porro@bcmaterials.net

Magnetic Shape Memory Alloys (MSMAs) are a group of active materials that undergo phase transitions (resulting in large recoverable mechanical deformations) induced by temperature, stress and/or magnetic fields. Their superfast response and high energy density make them ideal candidates to be implemented in the field of sensors and actuators. The magnetic properties of MSMAs depend on the magnetic coupling between atoms that, in turn, depends on the atomic positions within the lattice. Neutron diffraction is a powerful tool that allows to depict not only the atomic site occupancies in ma metal alloys, but also the magnetic site densities in each atomic position within the lattice. In this talk a combination of powder neutron diffraction, in polycrystalline samples, and non-polarized/polarized single crystal neutron diffraction measurements, in single crystals, will be discussed for different sets of MSMAs. Throughout the talk, we will discuss how the Rietveld refinements of the neutron diffractograms acquired for the different alloys studied allowed us to determine the atomic site occupancies of the alloys, whose changes are directly related with differences on the magnetic properties of the alloys.

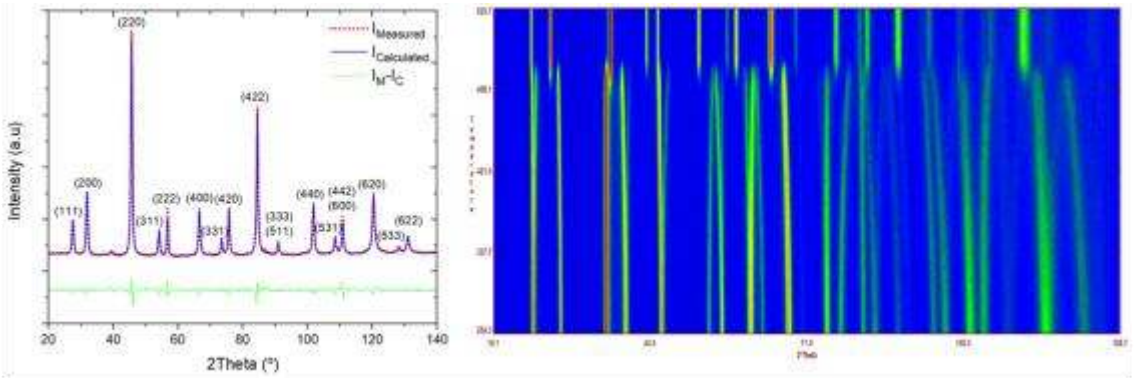

Fig. 1: *(left) Representative example of a Rietveld refinement of the austenite phase of a Magnetic Shape Memory Alloy. (right) Neutron powder thermodiffractogram of a Magnetic Shape Memory Alloy evidencing the Martensite Transformation at around 510 K.*

References

[1] P. Lázpita, J.M. Barandiarán, J. Gutiérrez, C. Mondelli, A. Sozinov, V.A. Chernenko, Phys. Rev. Letters, **119 (15)**, 155701 (2017).

[2] A. Pérez-Checa, J.M. Porro, J. Feuchtwanger, P. Lázpita, T.C. Hansen, C. Mondelli, A. Sozinov, J.M. Barandiarán, K. Ullakko, V. Chernenko, Acta Materialia, **196**, 549-555 (2020).

[3] M. Namvari, V. Chernenko, A. Saren, J.M. Porro, K. Ullakko, J. Alloys Compd. **944**, 169184 (2023).

Abstract ID: 1192

SUPERELASTICITY AND ELASTOCALORIC EFFECT IN Ni-Fe-Ga SINGLE CRYSTALS

J. Torrens-Serra[1], F. Masdeu[2], J. Pons[1], Y. Chumlyakov[3], E. Cesari[1]

[1]*University of the Balearic Islands, Dept. of Physics, E07122 Palma de Mallorca, SPAIN*
[2]*University of the Balearic Islands, Dept. of Industrial Engineering and Construction, E07122 Palma de Mallorca, SPAIN*
[3]*Tomsk State University, Lenina Street, 634050, Tomsk, RUSSIA*
E-mail: jaume.pons@uib.es

Ferromagnetic shape memory alloys (FSMAs) demonstrate prominent functionalities related to their giant magneto-strain and caloric effects, together with shape memory properties. Off-stoichiometric Heusler-type Ni_2MnGa alloys constitute the prototype FSMA family, with magnetic field induced strains as large as 12%. However, the brittle behavior of Ni–Mn-Ga alloys motivated researchers to uncover other magnetic alloys like Co-Ni-Ga, Co-Ni-Al or Ni–Fe-Ga, with enhanced ductility achieved by controlled precipitation of the ductile γ phase. In this presentation, the superelasticity and elastocaloric effects of $Ni_{51.5}Fe_{21.5}Ga_{27}$ single crystals will be reported. The mechanical behavior strongly depends on the compression axis orientation. The best superelasticity performance was achieved in the [001] orientation, showing fully recoverable strains around 4% in a wide temperature window of more than 130 K. For the [012] and [011] orientations, the superelastic window before sample fracture was reduced to only ~ 40 K and ~ 30 K, respectively. The elastocaloric effect was characterized from the temperature change measured during quasi-adiabatic unloading at a strain rate of $6{\cdot}10^{-2}$ s (100 times faster than standard conditions) using a K-type thermocouple attached to the sample surface. DT_{ad} values around −5 K were measured at a test temperature of 240 K, with a slight dependency on the axis orientation. Moreover, the adiabatic cooling decreases slightly with the increase of the test temperature, which is related to the decrease of transformation strain observed at increasing temperatures. The effect of $L2_1$ atomic ordering was also investigated in samples submitted to water quenching or slow furnace cooling treatments, to achieve low and high levels of ordering degree, respectively. The ordered samples showed a flatter transformation plateau in the *s-e* curves as well as an enhanced elastocaloric response in the [001] orientation, as shown in Fig. 1.

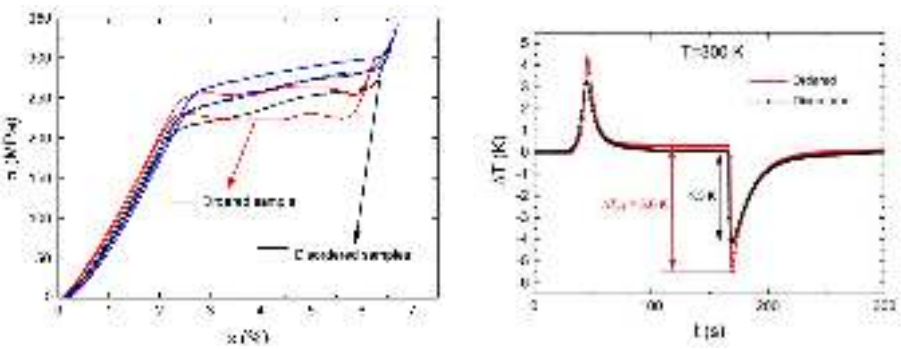

Fig. 1: *Comparative response of samples with different degrees of $L2_1$ atomic order. (a) Stress-strain superelastic cycles; (b) elastocaloric effect.*

Acknowledgements

Work performed in the frame of project PID2022-138108OB-C31 financed by MCIN/AEI/10.13039/ 501100011033/FEDER, UE.

Magnetic shape memory alloys and magnetocalorics II

02.05.2024 THURSDAY

Abstract ID: 1266

UNVEILING ELECTRONIC STRUCTURE OF HEUSLER-TYPE Mn AND Co BASED METAMAGNETIC SHAPE MEMORY ALLOYS

Akio Kimura

Graduate School of Advanced Science and Engineering, Hiroshima University, 739-8526, Higashi-hiroshima, JAPAN
E-mail: akiok@hiroshima-u.ac.jp

Heusler metamagnetic shape memory alloys (MetaMSMAs) have garnered significant attention owing to their substantial functional responses, such as the giant magnetocaloric, elastocaloric, and barocaloric effects. These remarkable physical properties are linked to a substantial change in magnetization through the first-order martensitic transformation (MT). In this study, we focus on two Heusler alloys to elucidate the origin of MT from the perspective of electronic structure and element-specific magnetic properties using soft X-ray magnetic circular dichroism (XMCD) and hard X-ray photoelectron spectroscopy (HAXPES).

We investigated the electronic structure change upon the MT of Heusler-type MetaMSMA $Mn_{1.92}Ni_{1.61}Fe_{0.10}Sn_{0.37}$ exhibiting the giant magnetocaloric properties by HAXPES and first-principles calculations. The temperature-dependent HAXPES measurements revealed that the electronic structure just below E_F was drastically changed in the same way for the prototypical Ni-based FMSMAs and MetaMSMAs. These experimentally observed features were well reproduced by the calculations of the stoichiometric Mn_2NiSn assuming the ferromagnetic ground state and the reasonable E_F shift. The comparison of the experimental and theoretical results signifies that both the Mn and Ni 3d states dominate the DOS near E_F in Mn-based MetaMSMAs, which leads to the lattice instability by the band Jahn-Teller effect.

As a second topic, we present quaternary compounds based on $Co_2Cr(Ga,Si)$ with specific compositions that exhibit a reentrant martensitic transformation, wherein the tetragonal martensite phase reverts to the cubic ferromagnetic phase upon cooling [2]. We find that the high density of states, comprised of both Co 3d and Cr 3d orbitals, induces lattice instability and stabilizes the martensite phase within a specific temperature range. Ultimately, the developed magnetic moments at low temperature stabilize the cubic ferromagnetic phase through magnetic exchange interaction by opening the half-metallic gap. The manifestation of half-metallic shape memory alloys could usher in a new era of materials design with multiple functions through the precise tuning of electronic structures.

These studies were conducted in close collaboration with V. Chernenko (Basque Country Univ.), K. Sumida (Hiroshima Univ.), and R. Kainuma (Tohoku Univ.).

References

[1] P. Lazpita, M. Sasmaz, J.M. Barandiaran, V.A. Chernenko, Acta Mater. **155**, 95 (2018).
[2] X. Xu, T. Omori, M. Nagasako, A. Okubo, R.Y. Umetsu, T. Kanomata, K. Ishida, R. Kainuma, Appl. Phys. Lett. **103**, 164104 (2013).

Abstract ID: 1238

MAGNETIC SHAPE MEMORY PROPERTIES OF Ni-Mn-Ga-BASED MELT SPUN RIBBONS

M.J. Szczerba[1], M. Kowalska[1], P. Czaja[1,2], Ł. Rogal[1]

[1]*Institute of Metallurgy and Materials Science, Polish Academy of Sciences, 30-059, Kraków, POLAND*
[2]*Department of Materials Science and Engineering, Stanford University, Stanford, CA 94305, USA*
E-mail: m.szczerba@imim.pl

The Ni-Mn-Ga-based alloys are a subject of intense studies, because of their unique magneto-mechanical coupling [1]. Such studies were primarily performed using single crystalline materials. In the case of polycrystalline materials much focus was placed on ribbons produced by the melt spinning technique studying magnetic field-induced bending as well as elastocaloric properties [2,3]. Thus, in this study we have focused on the experimental analysis of the magnetic-field-induced bending effect induced in Ni-Mn-Ga-based alloys produced by the melt spinning technique. Materials in the ribbon's form were produced by different linear velocity having a major impact on both the martensitic transformation temperature as well as the magneto-mechanical properties. Additionally, the effect of annealing, at the temperature range of 100°C – 900°C, on microstructure, martensitic transformation temperature and magnetic field-induced bending effect were examined. Initiation of the bending effect was observed at very low magnetic field of 0.06T. The maximum deformation was generated by external magnetic field of less than 0.3T. Additional, fatigue properties of the bending effect were examined taking into account the microstructural and defect evolution observed by transmission electron microscopy techniques. These obtained results are important for materials design and optimization of the magnetic-field-induced bending effect recently shown in Ni-Mn-Ga-based melt-spun ribbons.

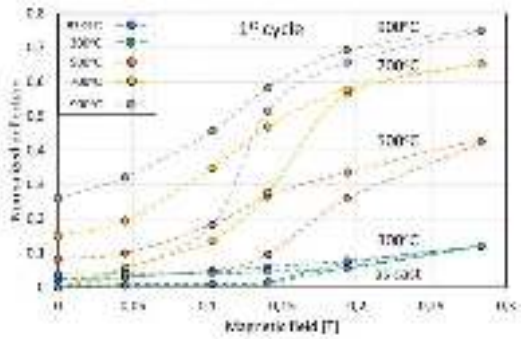

Fig. 1: *Shape change of as-cast and annealed Ni-Mn-Ga ribbons measured as normalized deflection during bending induced by external magnetic field.*

This work is funded by the National Science Centre, Poland under grant 2021/43/B/ST8/02745.

References

[1] A. Sozinov, N. Lanska, A. Soroka, W. Zou, Appl. Phys. Lett. **102**, 021902 (2013).
[2] E. Villa, F. Villa, B. Rodriguez Crespo, P. Lazpita, D. Salazar, H. Hosoda, V. Chernenko, J. Alloys Compd., **965**, 171437 (2023).
[3] M.J. Szczerba, Scripta Mater **205**, 114203 (2021).

Abstract ID: 1210

METAMAGNETIC SHAPE MEMORY EFFECT WITH SMALL DISSIPATION ENERGY IN HEUSLER-TYPE Pd_2MnGa ALLOY

Xiao Xu[1,2], Tatsuya Ito[1,3], Atsushi Miyake[4,5], Yuto Kinoshita[4], Makoto Nagasako[5], Kohki Takahashi[5], Masashi Tokunaga[4], Ryosuke Kainuma[1]

[1]Tohoku University, School of Engineering, 980-8579, Sendai, JAPAN
[2]Tohoku University, Organization for Advanced Studies, 980-8577, Sendai, JAPAN
[3]Japan Atomic Energy Agency, J-PARC Center, 319-1195, Tokai, JAPAN
[4]The University of Tokyo, The Institute for Solid State Physics, 227-8581, Kashiwa, JAPAN
[5]Tohoku University, Institute for Materials Research, 980-8577, Sendai, JAPAN
E-mail: xu@material.tohoku.ac.jp

Metamagnetic shape memory alloys (MMSMAs) show reversible martensitic transformation under the application of a magnetic field [1]. The MMSMAs are attractive functional materials due to their possible applications as magnetic actuators and sensors. However, the dissipation energy is generally large for these alloys, which limits their applications. In this talk, we introduce a new Heusler-type Pd_2MnGa MMSMA with an extremely small dissipation energy [2]. As shown in Fig. 1(a), at 120 K, all the three alloys show magnetic-field-induced reverse martensitic transformation, but the dissipation energy of the Pd_2MnGa alloy is estimated to be only roughly 1/100 of those of Ni-Co-Mn-In [3] and Ni-Co-Mn-Ga [4]. Moreover, as shown in Fig. 1(b), a large magnetic-field-induced strain of more than 2500 ppm can be obtained, indicating the possibility for the use as a high-efficiency MMSMA [2].

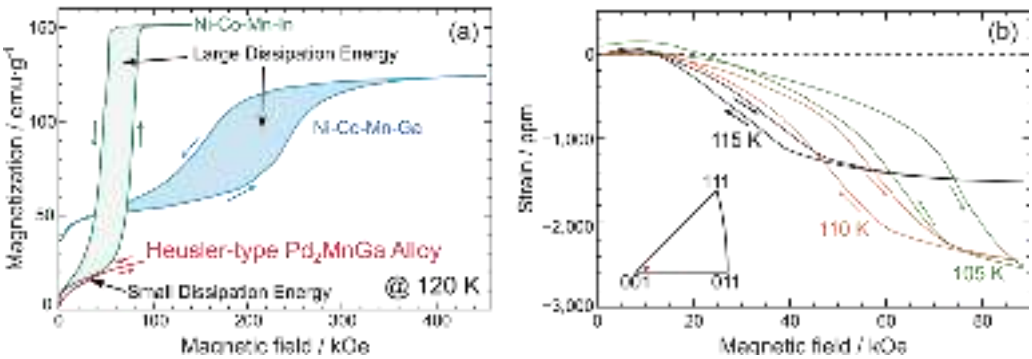

Fig. 1: (a) *Magnetization curves for the current Heusler-type Pd_2MnGa alloy [2] in comparison with Ni-Co-Mn-In [3] and Ni-Co-Mn-Ga [4] metamagnetic shape memory alloys.* (b) *The magnet-field- induced strain measured for a single-crystal Pd_2MnGa alloy [2].*

References

[1] R. Kainuma, *et al.*, Nature **439**, 957 (2006).
[2] T. Ito, *et al.*, Adv. Sci. **10**, 2207779 (2023).
[3] W. Ito, *et al.*, Appl. Phys. Lett. **92**, 021908 (2008).
[4] T. Kihara, *et al.*, Scripta Mater. **181**, 25 (2020).

Magnetic shape memory alloys and magnetocalorics III

02.05.2024 THURSDAY

Abstract ID: 1284

NANOTWINNING IN OFF-STOICHIOMETRIC Ni-Mn-BASED HEUSLER ALLOYS FROM FIRST-PRINCIPLES

M.E. Gruner[1], O.N. Miroshkina[1], V.V. Sokolovkiy[2], V.D. Buchelnikov[2], S. Fähler[3]

[1]University of Duisburg-Essen and Center for Nanointegration, CENIDE, 47048 Duisburg, GERMANY
[2]Department of Condensed Matter Physics, Chelyabinsk State University, 454001 Chelyabinsk, RUSSIA
[3]Helmholtz-Zentrum Dresden-Rossendorf, 01069 Dresden, GERMANY
E-mail: Markus.Gruner@uni-due.de

Depending on composition and chemical order, Ni-Mn-based Heusler alloys exhibit a combination of functional ferroic properties, which render them useful for magnetic shape memory applications or as magnetocaloric materials. This is linked to the presence of hierarchically twinned modulated structures in martensite, which can be interpreted as adaptive, self-organized arrangement of [110]-aligned nanotwins consisting of non-modulated tetragonal building blocks as was shown previously for the paradigmatic case of stoichiometric Ni_2MnGa [1]. A band-Jahn-Teller-type reconstruction of the Fermi surface of cubic $L2_1$ austenite which in particular softens the [110] transversal acoustic phonons. First-principles calculations in the framework of density functional theory suggest that this allows for a downhill transformation path from cubic austenite to nanotwinned martensite [2]. Frustrated antiferromagnetic coupling between neighboring Mn atoms which give rise to competing repulsive and attractive interactions in the nonmodulated $L1_0$ martensite stabilize the twin interfaces [3]. Our recent calculations address the interdependence of magnetism, chemical order and nanotwinning in Ni-Mn-based Heusler systems beyond Ni-Mn-Ga and their relevance for the functional properties with particular emphasis on off-stoichiometric compositions in magnetocaloric systems.

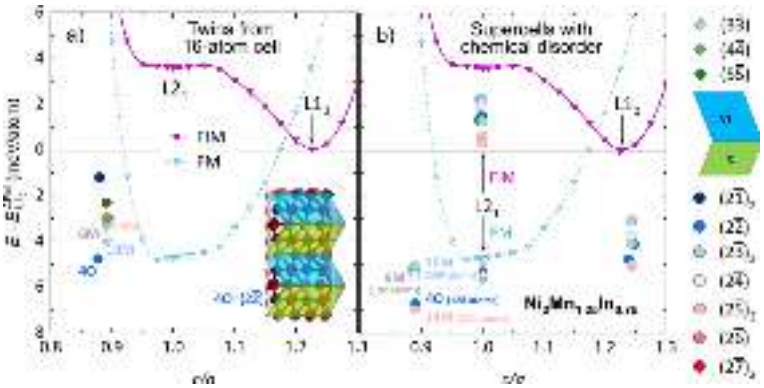

Fig. 1: *a) Energy of nano- twinned $Ni_2Mn_{1.25}In_{0.75}$ constructed from pseudo-ordered ferrimagnetic (FIM) 16 atom $Ni_8Mn_5In_3$. b) Larger supercells with partial Mn/In disorder: Nanotwinned cells vs. $L1_0$ (FIM) and $L2_1$ (FIM and FM). In both cases, FIM nanotwins compete close- ly with FM $L2_1$.*

References

[1] R. Niemann, U.K. Rößler, M.E. Gruner, O. Heczko, L. Schultz, S. Fähler, Adv. Eng. Mater. **14**, 562-581 (2012).
[2] M.E. Gruner, S. Fähler, P. Entel, Phys. Stat. Sol. (b) **251**, 2067-2079 (2014).
[3] M.E. Gruner, R. Niemann, P. Entel, R. Pentcheva, U.K. Rössler, K. Nielsch, S. Fähler, Sci. Rep. **8**, 8489 (2018).

Abstract ID: 1470

SHELL-FERROMAGNETISM IN HEUSLERS

M. Acet

Physics Faculty, Duisburg-Essen University, Lotharstr, 1, 47048 Duisburg, GERMANY
E-mail: mehmet.acet@uni-due.de

Shell-ferromagnetism is the decomposition of Ni-Mn based Heuslers with 5 at% Al, Ga, In, Sn, or Sb. When heat treated at elevated temperatures under a magnetic field, it decomposes into 2-5 nm cubic full Heusler precipitates surrounded by a tetragonal NiMn matrix. At the precipitate/matrix interface, the moments align with strong pinning in the annealing-field direction so that these spins can only be fully rotated in fields exceeding 10 T, and they can withstand temperatures up to 500 K. Depending on the direction of the applied field, the anisotropy can be set continuously to any angle between 0° and 90°, both in bulk-plate and thin-film materials. Here, we discuss the growth mechanisms and the magnetic and structural properties of shell-ferromagnets.

Abstract ID: 1367

ADDITIVE MANUFACTURING OF Mn-BASED MAGNETIC SHAPE MEMORY ALLOYS FOR SOLID-STATE REFRIGERATION

Daniel Salazar

BC Materials, Basque Center for Materials, Applications and Nanostructures, UPV/EHU Science Park, Leioa 48940, SPAIN

E-mail: daniel.salazar@bcmaterials.net

Existing social problems require the development of novel, environmentally friendly technologies and the ability to create 3D structures in a sustainable and profitable way. Advances in caloric materials, such as magneto- or elasto-caloric compounds, as integral components of the next wave of energy-efficient devices, present new opportunities to investigate potential advancements in additive manufacturing. Metamagnetic shape memory alloys emerge as promising options for magnetic refrigeration, thanks to their high entropy change during the first-order martensitic transformation. However, it is essential to note that their crystalline phase becomes unstable at elevated temperatures above 300 ºC.

In this study, we formulated original inks and pastes designed for room temperature extrusion printing techniques, enabling the creation of intricate 3D structures using high-performance NiMnSn-based magnetocaloric powders. A green matrix composed of cellulose and water as a solvent was used. The ink, comprising over 85 wt.% of powder, was carefully developed to achieve optimal viscosity, resulting in the ability to produce a maximum of 250 layers with the highest printing resolution (0.5mm wall thickness).

The proposed treatment process for the printed structures involves two main steps: (i) specialized thermal treatments to dry the printed structures, removing the polymer by calcination, followed by sintering to obtain an all-metal structure, and (ii) nickel electrodeposition to safeguard the printed structure against corrosion. Furthermore, we demonstrate that incorrectly printed workpieces can be recycled by dissolving them in water, significantly minimizing material loss and improving the cost-effectiveness and environmental friendliness of the printing process.

Magnetic shape memory alloys and magnetocalorics IV

02.05.2024 THURSDAY

Abstract ID: 1278

$Ni_{45}Co_5Mn_{37}In_{15}$ AND $Ni_{45}Co_5Mn_{35}Sn_{15}$ ALLOYS METAMAGNETIC SHAPE MEMORY ALLOYS PRODUCTION BY MECHANICAL GRINDING

J. López-García[1, 2], D.L. R. Khanna[3], V. Recarte[3], V. Sánchez-Alarcos[3], J.I. Pérez-Landazabal[3], P. LaRoca[4], P. Álvarez-Alonso[1, 2], J.A. Rodríguez-Velamazán[5]

[1] Department of Physics, Faculty of Science, University of Oviedo 33007, SPAIN
[2] Instituto Universitario de Tecnología Industrial de Asturias, Universidad de Oviedo, Gijón 33203, SPAIN
[3] Science Department, Universidad Pública de Navarra, Campus de Arrosadía, Pamplona 31006, SPAIN
[4] Centro Atómico Bariloche (CNEA), CONICET, S.C. de Bariloche 8400, ARGENTINE
[5] Institut Laue Langevin, 71 Avenue des Martyrs, Grenoble Cedex 38042, FRANCE
E-mail: lopezjavier@uniovi.es

During the last decade, metamagnetic shape memory alloys have attracted much interest due to their potential applications in fields such as sensors due to magnetoresistance or magnetic refrigeration due to the magnetocaloric effect. However, one of the main drawbacks is their poor mechanical properties, in particular the high brittleness. Composites made from polymer matrix with metamagnetic shape memory powder alloys have been recently proposed and developed to overcome the intrinsic brittleness of the bulk. Likewise, controlled powder production is needed for the additive manufacturing technique [1,2].

$Ni_{45}Co_5Mn_{37}In_{15}$ and $Ni_{45}Co_5Mn_{35}Sn_{15}$ alloys were subjected to a high-energy ball-milling and samples were obtained at different milling times. The ball milling promotes a mechanically-induced martensitic transformation as well as the appearance of amorphous-like non-transforming regions, following a double stage; for short milling times (below 30 min), a strong size reduction and martensite induction occur. On the opposite, for longer times, the increase of strains predominates and consequently a larger amount of non-transforming regions appears. The effect of the microstructural defects brought by milling (as dislocations) on both the enthalpy change at the martensitic transformation and the high field magnetization of the austenite has been quantitatively estimated and correlated to the internal strains. The mechanically- induced defects do not change the ferromagnetic coupling between Mn atoms for $Ni_{45}Co_5Mn_{35}Sn_{15}$ and for $Ni_{45}Co_5Mn_{37}In_{15}$ milled on austenite side, on contrary that occurs for $Ni_{45}Co_5Mn_{37}In_{15}$ milled in martensite.

References

[1] H. Hosoda, *et. al.*, Sci. Technol. Adv. Mater., **5**, 4, (2004).
[2] J. Feuchtwanger, *et. al.*, J. Appl. Phys., **97**, 10, 10, (2005).

Abstract ID: 1366

DYNAMICS OF THE MAGNETOCALORIC EFFECT IN HEUSLER ALLOYS: RESULTS OF DIRECT MEASUREMENTS ΔT_{ad} IN CYCLIC MAGNETIC FIELDS UP TO 8 T

Adler Gamzatov, A.T. Kadirbardeev, A.M. Aliev

Amirkhanov Institute of Physics, DFRC, RAS, 367003, Makhachkala, RUSSIA
E-mail: gamzatov_adler@mail.ru

It is known that the kinetics/dynamics of the magnetostructural martensite-austenite phase transition in Heusler alloys is associated with nucleation and growth processes, and these processes are very sensitive to external influences such as temperature, magnetic field and pressure. The process of nucleation of the austenitic phase and the movement of the phase boundary between phases determine the duration of the martensitic transition. Recently, irreversible magnetostructural phase transitions have been of great interest. The main reason for the irreversibility of the magnetocaloric effect (MCE) in Heusler alloys is hysteresis near the magnetostructural phase transition (MSPT). As a rule, the negative effect of hysteresis on the MCE is reported. The purpose of this paper is to study the influence of cyclic magnetic fields on the value and dynamics of the inverse and direct MCE in the $Ni_{47}Mn_{40}Sn_{13}Cu_1$ alloy. Direct measurements of the MCE were carried out in cyclic magnetic fields up to 8 T with frequency 0.2 Hz.

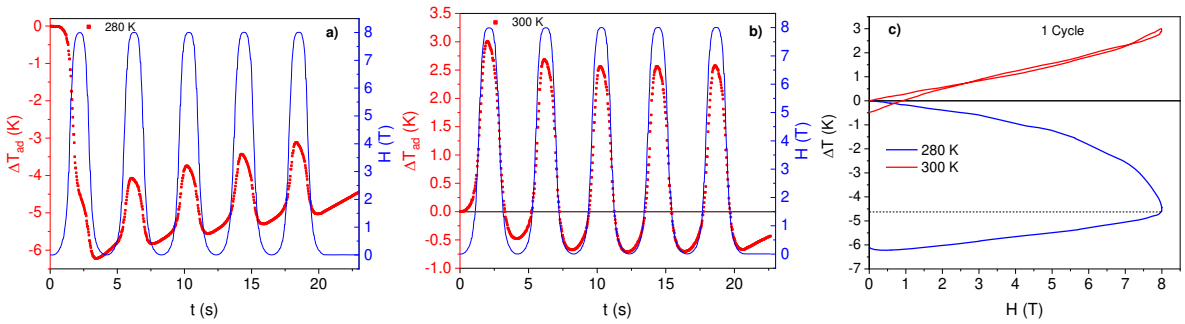

Fig. 1: *Temporal dependence ΔT_{ad} in cyclic magnetic fields 8 T a) near the MSPT at T=280 K and b) near the T_C at T=300 K c) $\Delta T_{ad}(H)$ for the first cycles of turning on/off the magnetic field 8 T at T=280 K and 300 K.*

Fig.1 (a,b) shows the time dependences of ΔT_{ad} for $Ni_{47}Mn_{40}Sn_{13}Cu_1$ in a cyclic magnetic field of 8 T (5 cycles of on/off magnetic field) at temperatures of 280 K and 300 K near the MSPT and near the T_C, respectively. As we can see, when the magnetic field is first turned on near the MSPT, an inverse MCE ($\Delta T_{ad}<0$) with a value of ΔT_{ad}=-6.2 K is observed, with the second and subsequent on/off cycles the effect becomes direct ($\Delta T_{ad}>0$). Fig.1(c) shows the dependences $\Delta T_{ad}(H)$ for the first cycles of on/off magnetic field. The field dependences of the MCE at different temperatures in the regimes of increasing and decreasing magnetic field of 8 T show that near T_C the effect is completely reversible. Near the MSPT (at temperatures of 280 K), the inverse MCE is irreversible, i.e. a magnetic field of 8 T is not enough to complete the phase transition and therefore, when the magnetic field is turned off, the temperature of the sample does not return to its initial state. Moreover, the irreversibility (T=280 K) increases when the magnetic field is turned off. This is due to the fact that when the magnetic field was turned on, part of the martensite passed into the austenitic ferromagnetic phase and when the field was turned off due to the paraprocess, partially formed ferromagnetic austenite, we observe a further decrease in the inverse effect.

The study was supported by the Russian Science Foundation grant No. 22-19-00610.

Abstract ID: 1293

STRUCTURAL AND MAGNETIC DISORDER IN Ni(-Co)-Mn-(In,Sn,Ti) HEUSLER ALLOYS: IMPACT ON ELECTRONIC, MAGNETIC AND VIBRATIONAL PROPERTIES

O. N. Miroshkina[1], B. Eggert[1], J. Lill[1], K. Ollefs[1], B. Beckmann[2], D. Koch[2], F. Scheibel[2], W. Donner[2], O. Gutfleisch[2], H. Wende[1], M.E. Gruner[1]

[1]*University of Duisburg-Essen, Theoretical Physics and Center for Nanointegration (CENIDE), 47057, Duisburg, GERMANY*
[2]*Technical University of Darmstadt, Institute of Materials Science, 64287, Darmstadt, GERMANY*
E-mail: olga.miroshkina11@gmail.com

X_2YZ Heusler alloys are promising class of the materials for the magnetic shape memory and magnetocaloric application. They demonstrate a strong coupling between lattice, electronic, and magnetic degrees of freedom. It allows for many multifunctional properties, which depend strongly on chemical and anti-site disorder. We investigate the effect of disorder on the vibrational properties and complex magnetic ordering mechanisms in magnetocaloric Ni(-Co)-Mn-(In,Sn,Ti) Heusler alloys by means of density functional theory (DFT). In our recent work [1], we showed that *p*-main-group element concentration together with positional disorder raised from Mn excess indirectly affect the magnetic exchange between the 3*d*-metal atoms in Ni-Mn-(In,Sn). This can be employed to control the magnetization of the transition-metal sublattice. For a near-stoichiometric Ni_2MnSn [2], Sn partial vibrational density of states (VDOS) are found to be sensitive to magnetic and anti-site disorder on the transition metal site, which results in a distinctive redistribution and broadening of the Sn-VDOS. We showed that the inversion of optical modes at Γ predicted previously for other Ni-Mn-based Heusler compounds and involving the displacement of Ni and the heavier Sn atoms is also a characteristic property of Ni_2MnSn. In the FM B2-ordered Ni-Co-Mn-Ti investigated in this work, mode inversion is not presented. Here, the *Z* element, Ti, is the lightest, and provides the most of its contribution to the high-frequency vibrations as expected. Similar to *p-d* Ni_2MnSn case, magnetic disorder leads to significant redistribution of the vibrational spectrum and results in hardening of the VDOS. DFT calculated XAS for FM NiCoMnTi captures the characteristic features in the L_3-peak of measured spectrum. Meantime, paramagnetic alignment modelled in the collinear disordered-local moment scheme leads to a more pronounced shoulder in the Mn L_3-peak contradicting the experiment. The absorption intensity at the L_3-edge is proportional to the 3*d* DOS function of unoccupied states above the Fermi level. Thus, combined with electronic structure calculations, Ni, Co and Mn L-edge XAS provides information on the degree of long range magnetic and structural disorder in all-*d*-metal Ni-Co-Mn-Ti. These examples illustrate how the disorder can be exploited to tune magnetic and vibrational properties of Heusler alloys and design high-performance magnetocaloric materials.

This work was funded by the German Research Foundation (Deutsche Forschungsgemeinschaft, DFG) within Collaborative Research Center/Transregio (CRC/TRR) 270, Project-ID 405553726. Large-scale DFT calculations were performed on the Lichtenberg HPC at the NHR Centers NHR4CES at TU Darmstadt (Project No. p0020039).

References

[1] F. Cugini *et al.*, Phys. Rev. B **105**, 174434 (2022).
[2] O. Miroshkina *et al.*, Phys. Rev. B **106**, 214302 (2022).

Abstract ID: 1248

THE STRUCTURAL, ELECTRONIC AND TRANSPORT PROPERTIES OF Ni-Mn-Sn HEUSLER ALLOY

V.V. Sokolovskiy[1], A.G. Gamzatov[2], V.D. Buchelnikov[1]

[1]*Chelyabinsk State University, 454001, Chelyabinsk, RUSSIA*
[2]*Amirkhanov Institute of Physics of DFRC of RAS, Makhachkala, 367003, RUSSIA*
E-mail: vsokolovsky84@mail.ru

Currently, a less attention has been dedicated to the research of the thermophysical characteristics of Heusler alloys, including a comprehensive examination of heat transmission processes near the martensitic transition, where a relatively poor thermal conductivity, similar phonon and electron component values, and a variety of anomalies were observed [1,2]. For the most cases, these findings are associated with the coexistence of phases and the competition of their contributions to thermal conductivity.

In the present work, using the *ab initio* approach we discuss the transport properties of $Ni_{46.875}Mn_{40.625}Sn_{12.5}$ compound, which is close to the experimental sample $Ni_{47}Mn_{40}Sn_{13}$. It is shown that the martensitic tetragonal phase is energetically preferable as compared to the austenitic cubic phase. Free energy approach, which includes the electronic, vibrational, and magnetic contributions, predicts the martensitic transition temperature T_m of 210 K in agreement with experiment (Fig. 1a). Both phases are ferrimagnetically ordered but with different spin configuration of Mn atoms. Analysis of changes in electronic and phonon thermal conductivities of *n*-doped $Ni_{46.875}Mn_{40.625}Sn_{12.5}$ at T_m showed their almost similar contribution to the total change in thermal conductivity, which is calculated to be 4.63 W/m K, whereas the experimental one is about 4.2 W/m K.

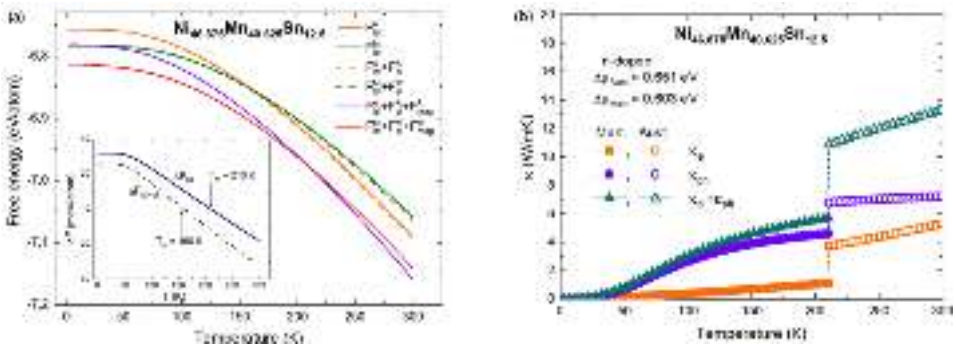

Fig. 1: *(a) Free energy of cubic austenite and tetragonal martensite of $Ni_{46.875}Mn_{40.625}Sn_{12.5}$ as a function of temperature. Three contributions to the free energy are presented: (i) $F = F_{lat}$; (ii) $F = F_{lat} + F_{el}$; (iii) $F = F_{lat} + F_{el} + F_{mag}$. The inset shows the temperature free energy difference between $L2_1$ and $L1_0$ phases. (b) Thermal conductivity decomposed into electronic ($\varkappa_e$) and phonon ($\varkappa_{ph}$) components for austenite and martensite as a function of temperature: n-doped case with $\Delta\mu\approx0.651$ eV and $\Delta\mu\approx0.603$ eV. Here $\Delta\mu$ corresponds to chemical potential at Fermi energy level of a compound*

This work was supported by the RSF-Russian Science Foundation No. 22-12-20032.

References

[1] Q. Zheng *et al.*, Adv. Eng. Mater. **21**, 1801342 (2019).
[2] A.G. Gamzatov *et al.*, Intermetallics **143**, 107491 (2022).

Nonuniform Magnetic Textures II

02.05.2024 THURSDAY

Abstract ID: 1325

OBSERVATIONS OF BUBBLE RESONANCES IN A MAGNETIC INSULATOR VIA TIME-RESOLVED SCANNING TRANSMISSION X-RAY MICROSCOPY

P. Che[1], D. Gouéré[1], S. Wintz[2,3], A. El Kanj[1], A. Mucchietto[4], D. Grundler[4,5], G. Schütz[2], R. Lebrun[1], V. Cros[1], A. Anane[1]

[1]*Laboratoire Albert Fert, CNRS/Thales, Université Paris-Saclay, 91767 Palaiseau, FRANCE*
[2]*Max Planck Institute for Intelligent Systems, 70569 Stuttgart, GERMANY*
[3]*Helmholtz-Zentrum Berlin für Materialien und Energie GmbH, 14109 Berlin, GERMANY*
[4]*Laboratory of Nanoscale Magnetic Materials and Magnonics, Institute of Materials (IMX), École Polytechnique Fédérale de Lausanne (EPFL), Lausanne, SWITZERLAND*
[5]*Institute of Electrical and Micro Engineering (IEM), ÉCOLE Polytechnique Fédérale de Lausanne (EPFL), Lausanne, Switzerland*
E-mail: ping.che@cnrs-thales.fr

Magnetic bubbles and bubble lattices are of great importance for investigations in magnonics because of their non-trivial magnon band structures [1] and skew scattering predicted between spin waves and magnetic bubbles [2]. Understanding their resonance and scattering processes with spin waves are fundamental to bubble-based devices. Magnetic bubbles, e.g. skyrmions, are found in multiple material systems, such as bulk chiral magnets and ultra-thin multilayers consisting of ferromagnetic layers and normal metal layers with strong spin-orbit coupling. However, those systems host bubbles and skyrmions either typically at cryogenic temperature or the damping parameters are significantly increased. In this work, magnetic bubbles down to 250 nm-diameter in low-damping 20 nm-thick Bi-doped YIG [3] were stabilized by controlling the anisotropy (see Fig.1(a)). We utilize the Maxymus time-resolved scanning transmission X-ray microscope (STXM) at Bessy IIto image the spin dynamic behavior of the bubbles. Below 100 MHz, multiple types of magnetic bubble resonance were observed, as shown in Fig. 1(b), depending on the shape of the bubbles. Above 100 MHz, spin waves excited from the antenna propagate through the area of resonating magnetic bubbles and interact with them. The phase image in Fig. 1(c) clearly indicates the wavefront in the region of the bubbles and bubble lattices. Isolated bubble resonances were also observed at different applied fields. Our observations offer insight into the manipulation of magnetic bubbles using spin waves and pave the way for bubble-based magnonic device designs. We acknowledge financial support from the Horizon 2020 Framework Program of the European Commission under FET-Open grant agreement no.899646 (k-NET) and from SNSF via grant 197360.

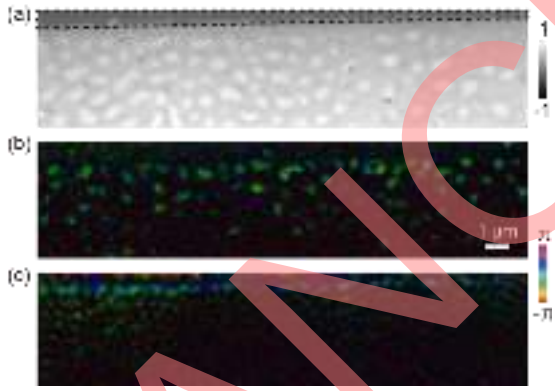

Fig. 1: *(a) Static X-ray transmission image of bubble and lattices in Bi-doped YIG film. The black dotted frame marks the edge of the antenna. White and black colors represent the X-ray transmission signal. (b and c) Phase distribution of bubble dynamics at 70 MHz and 360 MHz, respectively.*

References

[1] T. Weber, D. M. Fobes, J. Waizner, *et al.*, Science **375**, 1025–1030 (2022).
[2] C. Schütte, M. Garst. Phys. Rev. B **90**, 094423 (2014).
[3] D. Gouéré, H. Merbouche, A. El Kanj, *et al.*, Phys. Rev. Mater. **6**, 114402 (2022).

CANCELLED

Abstract ID: 1409

EIGENMODES OF MAGNETIC SKYRMION LATTICES

Louise Desplat[1,2], Bertrand Dupé[2,3]

[1]*CNRS, Spintec, Université Grenoble Alpes, 38000, Grenoble FRANCE*
[2]*Nanomat/Q-mat/CESAM, Université de Liège, B 4000, Liège, BELGIUM*
[3]*Fonds de la Recherche Scientifique (FNRS), B 1000, Bruxelles, BELGIUM*
E-mail: louise.desplat@gmail.com

We explore the interplay between topology and eigenmodes by changing the stabilization mechanism of skyrmion lattices (skX). We focus on two prototypical ultrathin films hosting an hexagonal (Pd/Fe/Ir(111) [1]) and a square (Fe/Ir(111) [2]) skyrmion lattice, which can both be described by an extended Heisenberg Hamiltonian.

We first examine whether the Dzyaloshinkskii-Moriya, or the exchange interaction when taken as the leading energy term affects the modes of the hexagonal skX of Pd/Fe/Ir(111). In both cases, we find that the lowest frequency modes correspond to internal degrees of freedom of individual skyrmions, and suggest a classification based on azimuthal and radial numbers *(l,p)*, with up to *l=6*, and *p=2*. We also show that the gyration behavior induced by an in-plane field [3] corresponds to the excitation of *l=1* deformation modes with varying radial numbers.

Second, we examine the square lattice of skyrmions of Fe/Ir(111). Its stabilization mechanism is dominated by the 4-spin interaction as obtained in Ref. [2]. After relaxation, the unit cell does not carry a topological charge, and the eigenmodes do not correspond to internal skyrmion deformations. By reducing the 4-spin interaction, an integer topological charge is recovered, but the charge carriers do not possess internal degrees of freedom, nor are they separated by energy barriers. We conclude that a 4-spin dominated Hamiltonian does not yield skyrmion lattice solutions, and that therefore*, a nontrivial topology does not imply the existence of skyrmions* [4].

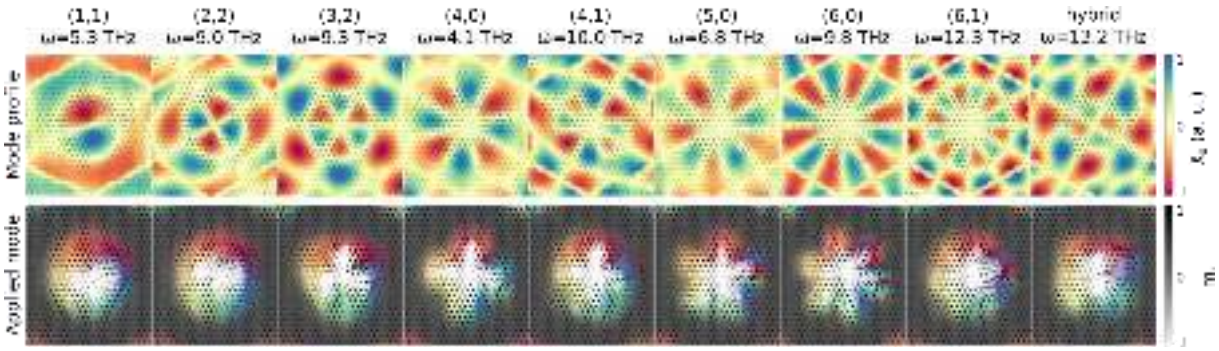

Fig. 1: *Example of modes of the skX of Pd/Fe/Ir(111), classified by azimuthal and polar numbers (l,p). Top: mode out-of-plane profile, bottom: mode applied to the skX state.*

References

[1] B. Dupé, M. Hoffmann, C. Paillard, S. Heinze, Nat. Commun. **5**, 4030 (2014).
[2] S. Heinze, *et al.*, Nat. Phys. **7**, 713 (2011).
[3] M. Mochizuki, Phys. Rev. Lett. **108**, 017601 (2012).
[4] L. Desplat, B. Dupé, Phys. Rev. B **107**, 144415 (2023).

Abstract ID: 1397

CONTROLLING SPIN-ORBIT TORQUE DRIVEN DYNAMICS FOR SKYRMION GENERATION

L.-M. Kern[1], K. Litzius[2], V. Deinhart[3,4], M. Schneider[1], C. Klose[1], K.Gerlinger[1], R. Battistelli[3], D. Engel[1], C.M. Günther[5], K. Höflich[4,3], F. Büttner[2,3], S. Eisebitt[1,6], B. Pfau[1]

[1]*Max Born Institute for Nonlinear Optics and Short Pulse Spectroscopy, Berlin, GERMANY*
[2]*Experimental Physics V, University of Augsburg, Augsburg, GERMANY*
[3] *Helmholtz-Zentrum Berlin für Materialien und Energie, Berlin, GERMANY*
[4]*Ferdinand-Braun-Institut, Leibniz-Institut für Höchstfrequenztechnik, Berlin, GERMANY*
[5]*Technische Universität Berlin, Zentraleinrichtung Elektronenmikroskopie, Berlin, GERMANY*
[6]*Technische Universität Berlin, Institut für Optik und Atomare Physik, Berlin, GERMANY*
E-mail: kern@mbi-berlin.de

Spin-orbit torques (SOT) act as a universal driver for manipulating nanoscale magnetic systems [1]. In combination with materials exhibiting high Dzyaloshinskii-Moriya interaction, SOTs are recognized for inducing well-controlled deterministic magnetization dynamics, making them reliable drivers for the creation and motion of magnetic skyrmions. However, direct imaging of the associated magnetization dynamics at the intrinsic nanometer length and nano- to picosecond timescales has proven challenging due to a lack of reproducibility. Recently, the control of magnetic textures like skyrmions on the nanometer scale has been demonstrated [2,3]. Employing focused helium ion irradiation, we can artificially engineer anisotropy defects which serve as preferred nucleation sites for skyrmions in ferromagnetic thin films with perpendicular magnetic anisotropy (PMA) [3]. In addition, these tailored defects can act as origin and return point for the SOT-driven magnetization dynamics [4].

In this study, we demonstrate a time-resolved x-ray imaging experiment to probe the response of the local magnetization during and shortly after the SOT pulse. Combined with micromagnetic modelling, we uncover coherent defect-mediated spin canting, instabilities, and topological transformations. Moreover, our images expose previously unseen skyrmion shedding. Notably, we discover that fluctuations significantly impact the observed magnetization dynamics, leading to transiently chaotic turbulences and spin-wave emission, even at moderate drive current, and resulting in deterministic final configurations [4]. Our findings highlight the potential of chaos-mediated pathways for topological switching, offering a promising trajectory to exploit complex non-linear dynamics in spintronics materials under controlled conditions.

References

[1] Q. Shao, *et al.*, *Roadmap of spin–orbit torques*, IEEE Transactions on Magnetics 57.7, 1-39 (2021).
[2] L.-M. Kern, *et al.*, *Tailoring optical excitation to control magnetic skyrmion nucleation*, Phys. Rev. B **106.5**, 054435 (2022).
[3] L.-M. Kern, *et al.*, *Deterministic generation and guided motion of magnetic skyrmions by focused He^+-ion irradiation*, Nano Letters **22.10**, 4028-4035 (2022).
[4] L.-M. Kern, *et al.*, *Time-resolved imaging reveals transiently chaotic spin-orbit-torque-driven dynamics under controlled conditions*, arXiv: 2401.12130 [cond-mat-mes-hall]

Nonuniform Magnetic Textures III

02.05.2024 THURSDAY

Abstract ID: 1075

MAGNETIC HOPFIONS

Nikolai S. Kiselev

Peter Grünberg Institute and Institute for Advanced Simulation, Forschungszentrum Jülich and JARA, 52425 Jülich, GERMANY
E-mail: n.kiselev@fz-juelich.de

Magnetic skyrmions are two-dimensional topological solitons resembling vortex-like strings in the magnetization field. Usually, skyrmion strings penetrate an entire sample from one surface to another and thus are localized only in two dimensions. In contrast, hopfions are topological solitons localized in all three dimensions and manifest as closed loops of skyrmion strings. In the simplest case, a hopfion can take the shape of a ring. While hopfions were theoretically predicted in specific magnetic systems [1], their direct observation has been elusive since, in most magnetic systems, isolated hopfions are unstable. Our recent experimental discovery revealed that in crystals of cubic chiral magnets, hopfions become stable when linked with skyrmion strings [2]. These configurations look like a skyrmion string or a bunch of skyrmion strings surrounded by a hopfion ring [Fig. 1].

In this talk, I will present the direct observation of such hopfions in B20-type FeGe plates using transmission electron microscopy. Various aspects of hopfion rings will be discussed, including a reliable protocol for hopfion ring nucleation, a quantitative comparison between theory and experiment, a homotopy group analysis of these topological states, and an examination of zero modes of hopfion rings moving along skyrmion strings.

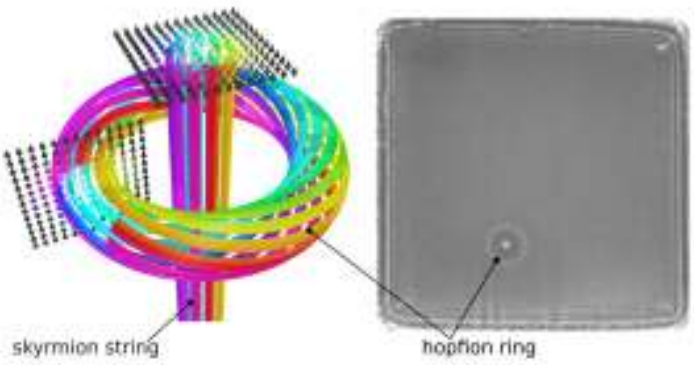

Fig. 1: *(Left) Schematic representation of the hopfion ring linked with the skyrmion string. (Right) Over-focused Lorentz TEM image capturing a hopfion ring with a single skyrmion string in a square-shaped FeGe plate of size 1 μm × 1 μm × 180 nm.*

References

[1] F.N. Rybakov *et al.*, APL Mater. **10**, 111113 (2022).
[2] F. Zheng *et al.*, Nature **623**, 718 (2023).

Abstract ID: 1207

THREE-DIMENSIONAL TOPOLOGICAL SPIN TEXTURES IN CURVILINEAR HELIMAGNETS

Luke Turnbull[1], Max Birch[2], Jeffrey Neethirajan[1], Marisel Di Pietro Martínez[1], Rikako Yamamoto[1,3], Marina Raboni Ferreira[1,4], Simone Finizio[5], Rachid Belkhou[6], Claas Abert[7], Dieter Süss[7], Geetha Balakrishnan[8], Sebastian Wintz[9], Claire Donnelly[1,3]

[1]*Max Planck Institute for Chemical Physics of Solids, 01187, Dresden, GERMANY*
[2]*RIKEN Center for Emergent Matter Science, 351-0198, Saitama, JAPAN*
[3]*International Institute for Sustainability with Knotted Chiral Meta Matter (WPI-SKCM2), Hiroshima University, 739-0046 Hiroshima, JAPAN*
[4]*Laboratório Nacional de Luz Síncrotron, 13083-100 Campinas, BRAZIL*
[5] *Swiss Light Source, Paul Scherrer Institute, 5232 Villigen PSI, SWITZERLAND*
[6]*Synchrotron SOLEIL, Saint Aubin, FR-91192, FRANCE*
[7]*Faculty of Physics, University of Vienna, 1090 Vienna, AUSTRIA*
[8]*Department of Physics, University of Warwick, Coventry, CV4 7AL, UK*
[9]*Institute Nanospectroscopy, Helmholtz-Zentrum Berlin, 12489 Berlin, GERMANY*
E-mail: Luke.Turnbull@cpfs.mpg.de

Precise control over the magnetic energy landscape is key for the stabilization and control of complex magnetization textures. Until now this has been commonly achieved by exploiting the bulk Dzyaloshinskii-Moriya interaction (DMI), an intrinsic chiral interaction that arises due to broken crystalline inversion symmetry. However, the physical properties of three-dimensional spin textures are also dependent on the geometry, topology and chirality of the host system. Indeed, the introduction of geometric symmetry breaking through curvature can provide extrinsic control over the energy landscape and formation of magnetic textures [2,3].

Here we combine intrinsic and extrinsic interactions in patterned toroidal helimagnets, resulting in a local control of the DMI. Specifically, by patterning nanoscopic tori of single crystal helimagnets using focused ion beam patterning and imaging their magnetic configuration via resonant soft x-ray imaging, we combine extrinsic curvature-induced symmetry breaking with the intrinsic DMI of the helimagnet. We observe a strong geometric influence, leading to a radial helical texture that, with finite element micromagnetic simulations, we can attribute to the presence of non-trivial three-dimensional chiral configurations. This combination of intrinsic and extrinsic DMI not only stabilizes non-trivial remanent states, but also enables the local nucleation of field-induced textures such as skyrmions and chiral bobbers [4]. Our work highlights the impact of curvature on chiral helimagnetism, offering opportunities to tailor chiral magnetic textures within curvilinear geometries [5].

References

[1] N. Nagaosa, Y. Tokura, Nat. Nanotech **8**, 899–911 (2013).
[2] A. Fernández-Pacheco, *et al.*, Nat. Commun. **8**, 15756 (2017).
[3] D.D. Sheka, Appl. Phys. Lett. 7 **118**, (23): 230502 (2021).
[4] A.O. Leonov, K. Inoue, Phys. Rev. B **98**, 054404 (2018).
[5] L.A. Turnbull, *et al.*, In preparation

Abstract ID: 1305

MAGNETOOPTIC RESPONSE OF NANOSTRUCTURES WITH 3D GEOMETRIES

J. Jurczyk, N. Leo, M.A. Cascales Sandoval, A. Fernández-Pacheco

Technical University of Vienna, Institute of Applied Physics, 1040, Vienna, AUSTRIA
E-mail: jurczyk@iap.tuwien.ac.at

In recent years, nonuniform magnetic textures have gained substantial attention from the scientific community, due to their interesting properties and potential application in spintronic devices. One of the strategies for the realisation of such textures is through the manufacturing of complex-shape 3D nanostructures [1,2]. However, the complex geometry and magnetic configurations of such systems demand for the development of characterisation methods which combine high spatial resolution with high sensitivity. Magneto-optical Kerr effect (MOKE) magnetometry is a standard magnetic characterisation technique, usually employed to investigate both nanostructures and thin film planar systems [3]. Recently, the dark-field MOKE (DF-MOKE) method has been developed in our group, to characterise magnetic properties of 3D nanostructures [4]. In DF-MOKE, the magneto-optical signals coming from different planes of a 3D nano-geometry are detected independently, exploiting the specular reflection at different angles from each plane.

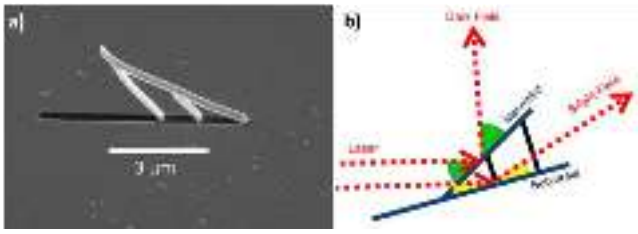

Fig. 1: *a) FEBID-3D printed ramped nanowire made of Permalloy b) schematics of dark-field MOKE detection for a nanowire grown at an angle on a substrate, with both planes leading to two distinct specular reflections (Taken from [4])*

In this contribution, the DF-MOKE characterisation of 3D magnetic nanostructures with different geometries and materials will be presented. The nanostructures under investigation were prepared using FEBID-based direct 3D nano-printing using our f3ast software [5]. Among the structures characterised, we will discuss results in ramp-shaped domain wall conduits, and in double-helix nano-geometries exhibiting complex 3D spin textures. We will discuss the sensitivity of the method and present its application to not only measure signal reflected from a single nanostructure, but also from sets of nanostructures close to each other. These results highlight the potential of DF-MOKE for advanced investigation of 3D magnetic nanostructures, including single nano-objects and arrays.

Acknowledgments

This work was supported by the European Community under the Horizon 2020 Program, Contract No. 101001290 (3DNANOMAG).

References

[1] A. Fernández-Pacheco, R. Streubel, O. Fruchart *et al.*, Nat Commun **8**, 15756, (2017)
[2] C. Donnelly, A. Hierro-Rodríguez, C. Abert, *et al.*, Nat. Nanotechnol. **17**, 136–142, (2022)
[3] D.A. Allwood *et al.*, J. Phys. D: Appl. Phys. **36**, 2175, (2003)
[4] L. Skoric, C. Donnelly, A. Hierro-Rodriguez *et al.*, ACS Nano **16**, 8860-8868, (2022)
[5] L. Skoric *et al.*, Nano Lett. **8**, 184–91 (2020).

Nonuniform Magnetic Textures IV

02.05.2024 THURSDAY

Abstract ID: 1313

EVALUATING SKYRMION SPIN TEXTURES BY QUANTITATIVE MFM

H.J. Hug[1,2], R. Peremedathil-Pradeep[1,2], E. Darwin[1], A.-O. Mandru[1], T. Dutta[1,3]

[1] *Empa, Materials Science and Technology, 8600 Dübendorf, SWITZERLAND*
[2] *University of Basel, Department of Physics, 4056 Basel, SWITZERLAND*
[3] *Department of Electronics and Electrical Engineering IIT, Guwahati, INDIA*
E-mail: hans-josef.hug@empa.ch

The development of complex magnetic multilayer structures hosting skyrmions necessitates comprehensive high-throughput studies, particularly to understand the dependence of the micromagnetic state on various system parameters. These structures include, for example, ferromagnetic multilayers with interfacial Dzyaloshinskii-Moriya interaction (DMI) aimed at generating skyrmion spin textures, rare-earth multilayers designed to tune saturation magnetization, and additional multilayers crafted to provide exchange fields. A prominent tool in this research is quantitative Magnetic Force Microscopy (qMFM) [1,2], especially when performed under vacuum conditions. This sophisticated lab-based technique enables rapid and detailed analysis of spin textures in individual systems, providing crucial insights that complement more macroscopic magnetic characterization techniques such as magnetometry and Brillouin light scattering.

qMFM has been instrumental for the development of ferro/ferri/ferromagnet multilayers supporting the coexistence of tubular skyrmions penetrating all layers, and incomplete skyrmions existing solely in the outer ferromagnetic multilayers [3]. Subsequent studies focused on adjusting the relative densities of these distinct spin textures by altering the thickness of layers in the ferromagnetic multilayer [4]. Here recent results (Fig. 1.) obtained on the reduction of the skyrmion diameter in ferrimagnetic multilayers, where the skyrmion magnetization patterns were deconvolved from the measured MFM data will be discussed.

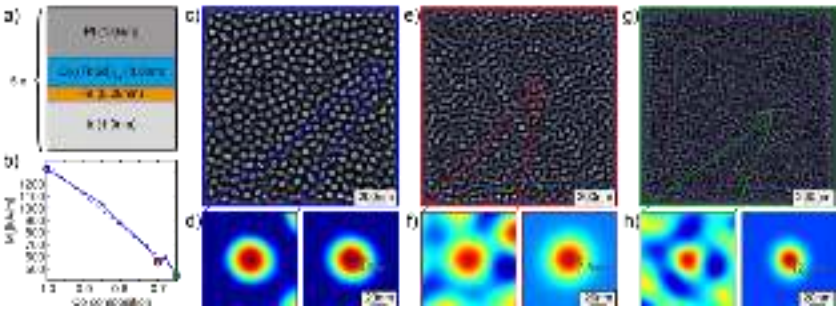

Fig. 1: *Skyrmions in ferrimagnet multilayers. a) multilayer structure. b) M_s(Co composition). c), e), and f) 2x2μm² M_s-patterns obtained by deconvolution MFM Δf-data of Co contents of 1, 0.7, 0.65, respectively. d), f), and h) left sides: zoomed skyrmion M_s-patterns from the overview images c), e), and g), respectively; right sides: gaussian fits to determine skyrmion radii.*

References

[1] Y. Feng, *et al.*, J. Magn. Magn. Mater. **551**, 169073 (2022).
[2] Y. Feng, A.-O. Mandru, O. Yıldırım, H.J. Hug, Phys. Rev. Appl.**18**, 024016 (2022).
[3] A.O. Mandru *et al.*, Nature Communications **11**, 6365 (2020).
[4] Yıldırım *et al.*, ACS Appl. Mater. Inter. **14**, 34002 (2022).

Abstract ID: 1337

HYBRID ANTISKYRMIONS REVEALED BY 3d LTEM TOMOGRAPHY

J. Masell[1,2]

[1]*Karlsruhe Institute of Technology (KIT), Institute for Theoretical Solid State Physics, 76049, Karlsruhe, GERMANY*
[2]*RIKEN Center for Emergent Matter Science, 351-0198, Wakō, JAPAN*
E-mail: jan.masell@kit.edu

Magnetic skyrmions are nowadays found in a variety of different material classes, ranging from single crystals to sputtered films. They often emerge on length scales much larger than the atomic distance where they appear as vortex-like, rotationally symmetric whirls. Their anti-vortex-like partners, consequently dubbed anti-skyrmions, naturally break this rotational symmetry which leads to a plethora of new effects. However, only a limited number of antiskyrmion-hosting materials are known and, previously, they all belonged to the D2d symmetry class, even though crystals with S4 symmetry were predicted to also host antiskyrmions. [1] Recently, we found thermodynamically stable antiskyrmions in S4-symmetric doped schreibersite compounds, where they coexist as square-shaped solitons alongside elliptical skyrmions [2,3] and manipulable, anisotropic helices [4].

In this talk, I will present our recent finding [5] that antiskyrmions in 3D systems may not be pure antiskyrmion tubes but, in addition, feature skyrmion caps where they connect to the surfaces of the material. Extensive 3d micromagnetic simulations suggest that this topological transition in the soliton string is a quite ubiquitous phenomenon in soft magnets, where antiskyrmions gain Dzyaloshinskii-Moriya exchange energy in the bulk whereas Néel skyrmions on the surfaces are optimal in terms of magnetostatic energy. Tomographic reconstructions of field-free off-axis electron holography images of antiskyrmions in thin films of Pd-doped (Fe,Ni)3P indeed show these hybrid textures and confirm that there is a zoo of new 3D textures awaiting discovery.

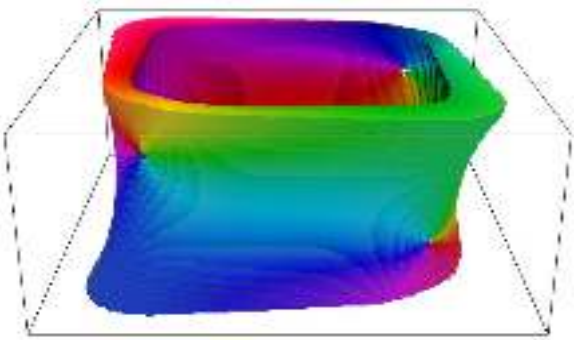

Fig. 1: *Hybrid antiskyrmion tube: antiskyrmion in the bulk with Néel-skyrmion caps on the surfaces. Result of micromagnetic simulations. Only pixels with $|m_z|<1/6$ are shown. The color indicates the in-plane direction of the magnetization.*

References

[1] A.N. Bogdanov, D.A. Yablonskii, Sov. Phys. JETP **68**, 101-103 (1989).
[2] K. Karube, L.C. Peng, J. Masell, *et al.*, Nat. Mater. **20**, 335-340 (2021).
[3] K. Karube, L.C. Peng, J. Masell, *et al.*, Adv. Mater. **34**, 2108770 (2022).
[4] F. Yasin, J. Masell, *et al.*, Nat. Commun. **14**, 7094 (2023).
[5] F. Yasin, J. Masell, *et al.*, Adv. Mater. (accepted 2024).

Abstract ID: 1372

SKYRMIONS IN SYNTHETIC ANTIFERROMAGNETS AND THEIR FAST CURRENT INDUCED DYNAMICS WITHOUT SKYRMION HALL EFFECT

O. Boulle

Spintec, Grenoble, FRANCE
E-mail: olivier.boulle@cea.fr

Skyrmions are topological spin textures which hold great promise as nanoscale bits of information in memory and logic devices [1]. The recent demonstration of room temperature skyrmions [2,3] as well as their current induced motion in industry compatible sputtered thin films have lifted important roadblocks toward the realization of skyrmion based devices. However, their development is impeded by a too low current induced velocity (about 100 m/s) [4] as well as the skyrmion Hall effect, namely a motion transverse to the current direction due to their topological charge which can lead to their annihilation in tracks. Antiferromagnetic (AF) skyrmions allow these limitations to be lifted owing to their vanishing magnetization and net zero topological charge, promising fast dynamics without skyrmion Hall effect. In this presentation, I will address the stabilization and current induced manipulation of skyrmion in compensated synthetic antiferromagnetic (SAF). I will first show that skyrmions can be stabilized at room temperature in Pt/Co/Ru based compensated SAFs and nucleated using local current injection or ultrafast laser pulses [5]. I will then show that SAF skyrmions can be moved by current at velocities over 900 m/s without skyrmion Hall effect. Micromagnetic simulations and analytical models using experimental parameters show that this enhanced skyrmion velocity can be explained by the compensation of the topological charges as well as an enhanced spin orbit torque in the synthetic antiferromagnet. I will conclude the talk with recent results on the electrical nucleation and detection of a skyrmion in magnetic tunnel junctions, which is another important milestone for skyrmion based devices [6]. Our results open important paths toward the realization of logic and memory devices based on the fast manipulation of skyrmions.

References

[1] A. Fert, V. Cros, J. Sampaio, Nat. Nanotechnol. **8**, 152 (2013).
[2] O. Boulle, Nature Nano., **11**, 449 (2016).
[3] A. Fert, N. Reyren, V. Cros, Nat Rev Mater **2**, 17031 (2017).
[4] R. Juge *et al.*, Phys. Rev. Appl. **12**, 044007 (2019).
[5] R. Juge *et al.*, Nature Communication, **13**, 4807 (2022).
[6] J. Urrestarazu Larranaga *et al.*, arXiv:2308.00445 (2023).

Nonuniform Magnetic Textures V

02.05.2024 THURSDAY

Abstract ID: 269

UNCOVERING THE NATURE OF FAINT BACKGROUND DOMAIN PATTERNS IN AMORPHOUS FERRIMAGNETIC MULTILAYERS

Tamer Karaman[1*], Daniel Metternich[1,2], Kai Litzius[1], Aladin Ullrich[3], Timo Schmidt[3], Riccardo Battistelli[1,2], Manas Patra[1,2], Manuel Valvidares[4], Daniel Pérez Salinas[4], Jordi Llobet[4], Christopher Klose[5], Michael Schneider[5], Bastian Pfau[5], Andrada-Oana Mandru[6], Reshma Peremadathil Pradeep[6], Konrad Samwer[7], Manfred Albrecht[3], Hans Josef Hug[6], Felix Büttner[1,2]

[1] *Experimental Physics V, University of Augsburg, Augsburg, GERMANY*
[2] *Helmholtz-Zentrum Berlin, Berlin, GERMANY*
[3] *Experimental Physics IV, University of Augsburg, Augsburg, GERMANY*
[4] *ALBA Synchrotron Light Source, Barcelona, SPAIN*
[5] *Max Born Institute for Nonlinear Optics and Short Pulse Spectroscopy, Berlin, GERMANY*
[6] *Empa, Swiss Federal Laboratories for Materials Science and Technology, Dubendorf, SWITZERLAND*
[7] *I. Physics Institute, University of Göttingen, Friedrich-Hund-Platz 1, Göttingen, GERMANY*
E-mail: tamer.karaman@uni-a.de

Chiral rare-earth transition metal (RE-TM) ferrimagnets stand out as promising candidates for spintronics, particularly in skyrmion-based device applications [1,2]. This category of ferrimagnets hosts a wide array of appealing material properties, including bulk DMI of Néel type [2], bulk-originating perpendicular magnetic anisotropy, and vanishing stray fields [3]. Our study of DyCo monolayers revealed intriguing domains through high-precision Magnetic Force Microscope imaging, revealing a host layer beneath the normal domain pattern that guides the as-grown configuration and is persistent even under a 7 T magnetic field. The low density and subtle contrast of these domains presented difficulties in X-ray techniques. Nevertheless, our recent advancement with a Dy/Co multilayer system exhibited enhanced density modulation, facilitating study through diverse methods, including Lorentz Transmission Electron Microscopy and X-ray synchrotron measurements. The element-specific small-angle X-ray scattering (SAXS) reveals intriguing results, showcasing distinct SAXS rings at the resonances of Dy and Co-edges, suggesting an element-specific atomic density modulation at nanometer-scale length scales. This study uncovers the mystery behind unusual faint background phenomena in amorphous ferrimagnetic RE-TM thin films, seeking the nature of these occurrences and elucidating the distinct patterns observed through various techniques. With the potential to unlock a new chapter in understanding textures in solid-state systems, we expect our experimental results to capture the attention of researchers in spintronics, as well as those studying amorphous materials in diverse contexts.

References

[1] A. Fert, *et al.*, Nat. Rev. Mater. **2**, 17031 (2017).
[2] S.K. Kim, *et al.*, Nat. Mater. **21**, 24–34 (2022).
[3] L. Caretta, *et al.*, Nat. Nanotechnol. **13**, 1154–1160 (2018).

Abstract ID: 1345

X-RAY MICROSCOPY IMAGING OF STRIPE, SKYRMION AND SKYRMIONIUM STATES IN VAN DER WAALS MAGNETS

Max Birch[1,2], Lukas Powalla[3], Kai Litzius[1], Fehmi Yasin[2], Frank Schulz[1], Vanessa Nehruji[4], Ondrej Hovorka[4], Daniel Mayoh[5], Geetha Balakrishnan[5], Markus Weigand[6], Xiuzhen Yu[2], Sebastian Wintz[1,6], Gisela Schütz[1], Marko Burghard[2]

[1]*Max Planck Institute for Intelligent Systems, 70569 Stuttgart, GERMANY*
[2]*RIKEN Center for Emergent Matter Science, Wako 351-0198, JAPAN*
[3]*Max Planck Institute for Solid State Research, 70569 Stuttgart, GERMANY*
[4]*Faculty of Engineering and Physical Sciences, University of Southampton, Southampton SO17 1BJ, UK*
[5]*Department of Physics, University of Warwick, Coventry CV4 7AL, UK*
[6]*Helmholtz-Zentrum Berlin für Materialien und Energie GmbH, Institut Nanospektroskopie, 12489 Berlin, GERMANY*
E-mail: maximilian.birch@riken.jp

Two-dimensional (2D) magnets have emerged as an exciting new platform for the design of spintronic devices [1]. While significant work has been performed on the transport properties of these systems, including some prototype heterostructure designs [2,3], detailed understanding of the basic magnetic behaviour is incomplete. In this talk, I will discuss our wide-ranging x-ray microscopy imaging results on a selection of exfoliated flakes of 2D magnets, including $Fe_{3-x}GeTe_2$, $Fe_{5-x}GeTe_2$, and $Cr_2Ge_2Te_6$ showing observations of stripe, skyrmion and higher-order composite skyrmion or skyrmion bag states. The results reveal the level of control of the magnetic spin textures which can be achieved by varying the flake thickness and structural composition of these systems, attained via manipulation of the out-of-plane anisotropy [4-6]. We explore the stability of these magnetic states by elucidating the magnetic phase diagram of all these materials following various applied field and temperature histories. Furthermore, I will detail our attempts at employing manipulation of the hosted spin textures, including current pulse-induced skyrmion nucleation and motion [7,8]. Finally, I will explain our observations of the composite skyrmions with higher-order topology, for example skyrmionium and skyrmion bag states, and the resulting implications for the concept of topological protection in real skyrmion materials [9,10].

References

[1] K.S. Burch, D. Mandrus, J.-G. Park, Nature **563**, 47 (2018).
[2] Z. Wang, *et al.*, Nano Lett. **18**, 4303 (2018).
[3] S. Albarakati, *et al.*, Sci. Adv. **5**, eaaw0409 (2019).
[4] M.T. Birch, L. Powalla, *et al.*, Nat. Commun. **13,** 3035 (2022).
[5] M.T. Birch, L. Powalla, *et al.*, 2D Materials – accepted (2024).
[6] M.T. Birch, *et al.*, In preparation (2024).
[7] L. Powalla, M.T. Birch, *et al.*, Nano Lett. **22**, 9236-9243 (2022).
[8] K. Litzius, *et al.*, In Preparation (2024).
[9] L. Powalla, M.T. Birch, *et al.*, Adv. Mater. **35,** 2208930 (2023).
[10] L. Powalla, M.T. Birch, *et al.*, Phys. Rev. B **108,** 214417 (2023).

Abstract ID: 1324

SOFT X-RAY IMAGING OF MAGNETIC TEXTURES IN PERMANENT MAGNETS AT HIGH FIELDS

T. Nakamura[1,2], Y. Kotani[2], D. Billington[3]

[1]Tohoku University, International Center for Synchrotron Radiation Innovation Smart, 980-8577, Sendai, JAPAN
[2]Photon Science Innovation Center, 980-0845, Sendai, JAPAN
[3]Cardiff University, School of Physics and Astronomy, CF24 3AA, Cardiff, UNITED KINGDOM
E-mail: tetsuya.nakamura.b5@tohoku.ac.jp

High-performance permanent Nd-Fe-B sintered magnets with high $(BH)_{max}$ are indispensable materials for energy generation and saving technologies. Crucially, the coercive force depends on the magnetic microstructure, and optimizing the microstructure can improve magnetic properties. Therefore, we focus on the magnetic domain changes associated with the demagnetization process to obtain crucial information relating the inhomogeneous microstructure of sintered magnets to their magnetic properties. However, the coercivity of the polished surface of Nd-Fe-B sintered magnets is obviously degraded, precluding techniques like magnetic Kerr microscopy because it can only measure smooth and reflective surfaces. From soft x-ray magnetic circular dichroism (XMCD) measurements of fractured surfaces, we found that the magnetism of the fractured surface is largely maintained [1]. However, there was no soft x-ray microscope that could apply magnetic fields over 1 T. Therefore, we have developed a scanning soft XMCD microscope with an 8 T superconducting magnet [2] and have succeeded in observing the magnetic domains throughout the demagnetization processes in Nd-Fe-B [3] and Sm-Co [4] magnets. Recently, we have achieved soft XMCD imaging at temperatures down to 12 K. The figure shows the temperature dependence of the magnetic domains on the surface of a $Nd_2Fe_{14}B$ grain which was exposed in the thermally demagnetized state of the fractured surface. The magnetic domains change between 150 and 100 K because of the spin reorientation transition at 135 K. Significantly, the soft XMCD imaging technique at high magnetic fields and low temperatures is not only applicable to permanent magnets, but also for magnetocaloric materials, and so on. We hope the present studies and developments will accelerate interesting and important research to determine how a microscopically inhomogeneous magnetic distribution connects to the macroscopic magnetic properties.

This work was supported by MEXT Program: Data Creation and Utilization-Type Material Research and Development Project Grant Number JPMXP1122715503.

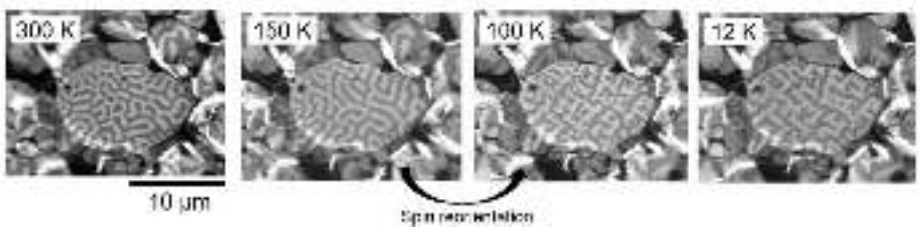

Fig. 1: *Magnetic domains recoded by XMCD at the Fe L_3-edge in a Nd-Fe-B sintered magnet.*

References

[1] T. Nakamura, Y. Kotani *et al.*, Appl. Phys. Lett. **105**, 202404 (2014).
[2] Y. Kotani, D. Billington, T. Nakamura *et al.*, J. Synchrotron Rad. **25**, 1444 (2018).
[3] D. Billington, Y. Kotani, T. Nakamura *et al.*, Phys. Rev. Mater. **2**, 104413 (2018).
[4] Y. Matsuura, T. Nakamura *et al.*, Appl. Phys. Lett. **117**, 022409 (2020).

Vortex Matter, Dynamics and Pinning I

02.05.2024 THURSDAY

Abstract ID: 1285

VORTEX PINNING AND DYNAMICS IN THE FERROMAGNETIC IRON-BASED SUPERCONDUCTOR $EuFe_2(As_{1-x}P_x)_2$

J.A. Wilcox[1], S.J. Bending[1], I. Veshchunov[2], T. Ren[2], T. Tamegai[2], S. Friedemann[3], M.V. Milošević[4]

[1]*Dept. of Physics, University of Bath, Claverton Down, Bath, BA2 7AY, UK*
[2]*Dept. of Applied Physics, University of Tokyo, Hongo, Bunkyo-ku, Tokyo 113-8656, JAPAN*
[3]*H. H. Wills Physics Laboratory, University of Bristol, Tyndall Avenue, Bristol, BS8 1TL, UK*
[4]*Dept. of Physics, University of Antwerp, Groenenborgerlaan 171, B-2020 Antwerp, BELGIUM*
E-mail: s.bending@bath.ac.uk

The iron-based $EuFe_2(As_{1-x}P_x)_2$ superconducting system exhibits a complex phase diagram characterized by various magnetically ordered phases [1]-[3]. Within the composition range of approximately $0.15 < x < 0.3$, a region of superconductivity emerges, reaching a maximum transition temperature of $T_c \simeq 25$ K at $x \simeq 0.21$. Intriguingly, this superconducting dome coexists with a ferromagnetic phase below $T_{FM} \simeq 19$ K. Conventional wisdom dictates that ferromagnetism and singlet superconductivity should be incompatible because the strong ferromagnetic exchange interaction destroys the singlet Cooper pairing. However, here the spatial separation of the superconducting FeAs layers and the magnetically ordered Eu ions within the $EuFe_2(As_{1-x}P_x)_2$ crystal structure enables the coexistence of these two competing orders. This unique situation presents an exciting opportunity to investigate the impact of the emerging magnetic order on the dynamics of vortices in the superconducting state as it is "switched on" below T_{FM}. In this presentation we will report a systematic investigation of the temperature-dependent magnetic hysteresis and magnetic relaxation of $EuFe_2(As_{1-x}P_x)_2$ single crystals, comparing samples in which $T_{FM} < T_c$ and $T_c < T_{FM}$. Our results indicate that the observed magnetic irreversibility is strongly dependent on the presence of *both* the magnetic and superconducting orders. In particular, our investigations reveal the pronounced impact of the underlying ferromagnetic microstructure on the vortex dynamics.

References

[1] Z. Ren *et al.*, Phys. Rev. Lett. **102**, 137002 (2009).
[2] S. Zapf *et al.*, Phys. Rev. Lett. **110**, 237002 (2013).
[3] V.S. Stolyarov *et al.*, Sci. Adv. **4** eaat1061 (2018).

Abstract ID: 1664

AC VORTEX DYNAMICS IN SUPERCONDUCTING DEVICES AND APPLICATIONS TO NOVEL QUBITS

A. Glatz[1], A. Al Luhaibi[2,3], J.B. Ketterson[2]

[1] *Department of Physics, Northern Illinois University, DeKalb, Illinois, USA*
[2] *Department of Physics and Astronomy, Northwestern University, Evanston, Illinois, USA*
[3] *Physics Department, King Fahd University of Petroleum and Minerals, Dhahran, SAUDI ARABIA*
E-mail: glatz@anl.gov

In this talk I will show some applications of AC driven patterned superconductors.

Using the time dependent Ginzburg-Landau formalism we have shown that above some critical current, a commensurate vortex lattice moving in a periodic pinning landscape of circular holes can generate an oscillating electric field at a certain inter pinning-site vortex hopping frequency, f_0. The latter depends, not only on the system characteristics (lattice constant, hole size, and hole pinning strength), but also on the applied current. Adding an AC component to the applied DC current allows us to lock the hopping frequency to a range of applied frequencies which is near f_0 [1]. Since the applied current density can be varied, the systems studied here constitute miniature, current-tunable, oscillators that operate at cryogenic temperatures. They can be patterned directly into a strip-line wave guides with their output transmitted to other remote devices, e.g., microwave resonators in transmon qubits.

Furthermore, we show that a heterogeneous superconducting film containing periodic defects can serve as a nonlinear inductor. Moreover, we were able to characterize the nonlinear inductivity by exploiting the similarity between the calculated E-J curves and the behavior of Josephson junctions, which diverges at the critical current density [2]. These properties suggest devices based on hole arrays have the potential to be used as circuit elements in future quantum devices.

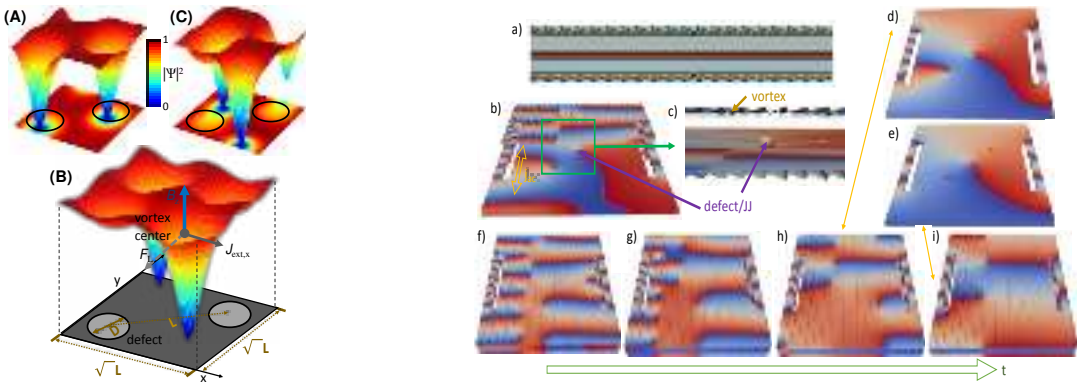

Fig. 1: *Left: Different stages of oscillation vortex dynamics in patterned superconducting films [1]. Right: Simulation of multilayer complex patterned superconducting logic devices with trapped vortices and ratchet structures.*

Finally, I will give a brief outline of our studies on AC driven superconducting logic devices with the aim of vortex mitigation strategies.

References

[1] A. Al Luhaibi, A. Glatz, J.B. Ketterson, Phys. Rev. B **106**, 224516 (2022).
[2] A. Al Luhaibi, A. Glatz, J.B. Ketterson, Phys. Rev. Applied., in production (2024).

Abstract ID: 1060

NON-MONOTONOUS $J_c(H,T)$ AND RELAXATION PHENOMENA IN $BaFe_2(As_{1-x}P_x)_2$

A. Galluzzi[1,2], A. Crisan[3], A. M. Ionescu[3], I. Ivan[3], A. Leo[2], G. Grimaldi[2], M. Polichetti[1,2]

[1]*Department of Physics "E.R. Caianiello", University of Salerno, via Giovanni Paolo II, 132, Fisciano (SALERNO), I-84084, ITALY*
[2]*CNR-SPIN Salerno, via Giovanni Paolo II, 132, Fisciano (SALERNO), I-84084, ITALY*
[3]*National Institute of Materials Physics, 405A Atomistilor Str., 077125 Magurele, ROMANIA*
E-mail: agalluzzi@unisa.it

Among the iron-based superconductors, the 122 family is for many aspects the most perspective in view of power applications of superconductivity. The interest around this compounds increase when intriguing vortex phenomena such as the Second Magnetization Peak (SMP) in field or the Peak Effect (PE) in temperature manifest because they allow to obtain strong transport current performance at high magnetic fields and temperatures. They originate from distinct non-linear modulations of the magnetic field and temperature dependencies of the critical current density $J_c(H,T)$. In this work, an overdoped $BaFe_2(As_{1-x}P_x)_2$ single crystal presenting the SMP and PE phenomena has been studied by performing DC magnetic field measurements. Starting from the superconducting hysteresis loops, the J_c values have been extracted and used for studying the pinning regime acting in the sample. In particular, by fitting the $J_c(T)$ curves, a change in the pinning regime has been individuated. Finally, the relaxation measurements m(t) have been performed at different magnetic fields and temperatures. From the analysis of the m(t) curves, the creep rate S and the pinning energy U have been studied as a function of the field and temperature showing a non-monotonous complex behavior linked to the SMP and PE phenomena. In order to better understand and visualize the regions where the vortex activity was more intense, the 2D counter plots of S(H,T) and U(H,T) have been drawn together with the vortex phase diagram of the sample.

CANCELLED

Abstract ID: 1059

AC MAGNETIC FIELD ANALYSIS OF THE RHOMBIC-TO-SQUARE TRANSITION IN THE BRAGG VORTEX GLASS PHASE IN A $BaFe_2(As_{1-x}P_x)_2$ CRYSTAL

M. Polichetti[1,2], A. Galluzzi[1,2], A. Ionescu[3], I. Ivan[3], G. Grimaldi[2], A. Leo[4], A. Crisan[3]

[1]University of Salerno, Dept. of Physics - 84084, Fisciano (SALERNO), ITALY
[2]CNR-SPIN Salerno - 84084, Fisciano (SALERNO), ITALY
[3]National Institute of Materials Physics - 077125 Magurele, ROMANIA
[4]CNR-SPIN Genova - 16152, Genova, ITALY
E-mail: mpolichetti@unisa.it

An overdoped $BaFe_2(As_{1-x}P_x)_2$ single crystal showing the presence of a rhombic-to-square transition (RST) together with the appearance of a second magnetization peak (SMP) in the field dependence of the critical current density $J_c(H_{DC})$ has been analysed in dynamic conditions by using the AC magnetic field. In particular, the AC complex magnetic susceptibility of the material has been studied as function of the temperature, at different AC frequencies and both in absence and in presence of a DC magnetic field H_{DC} with varying intensities superposed to the AC one. The first harmonics of the AC magnetic susceptibility as function of the temperature $\chi_1^*(T)$ behave much differently depending on the intensity of the applied DC field. At zero DC fields, both the real $\chi_1'(T)$ and the imaginary $\chi_1''(T)$ components of the complex AC susceptibility show a typical behavior as expected in absence of dynamic vortex structural transition, namely a step-like transition in the shielding properties that worsens with increasing temperature, totally disappearing at Tc, and peak in the power losses in correspondence of the full penetration of the applied AC field in the sample. The $\chi_1^*(T)$ measurements taken at different AC frequencies do not show any particular feature apart from what it is expected in presence of relaxation phenomena, with a very similar behavior in the various $\chi_1'(T)$, and a peak translation in the corresponding $\chi_1''(T)$, measured at different frequencies. On the contrary, at larger fields ($H_{DC}\geq 1$ T) the monotonic curve describing the decrease of the shielding properties with temperature gives way to a more complex behavior in $\chi_1'(T)$ characterized by a sudden increase of the shielding at a given field-dependent temperature $Ts(H_{DC})$, reaching a maximum at even higher temperature, and then decreasing again as T approaches T_c. This behaviour reflects also in the associated power losses, with the presence of several local maxima and minima in the same curve of $\chi_1''(T)$. Differently from the curves at zero DC field, for these curves the effect of changing frequencies in $\chi_1^*(T)$ is more evident. The values $Ts(H_{DC})$ in the $\chi_1'(T)$ curves at various DC fields were plotted in the H-T phase diagram of the sample, and a correspondence with the RST line has been evidenced, giving the possibility to detect and analyze the behavior of the RST in AC magnetic field. In particular, not only a clear dependence of the RST on the frequency appears but also, from the study of the 3rd harmonics components of the AC susceptibility $\chi_3^*(T)$, more detailed information have been obtained about the vortex dynamics governing the system before, during and after the RST.

CANCELLED

Vortex Matter, Dynamics and Pinning II

02.05.2024 THURSDAY

Abstract ID: 1175

VORTEX DYNAMICS AND ION-IRRADIATION-INDUCED PINNING IN LOW-TEMPERATURE AND HIGH-TEMPERATURE SUPERCONDUCTORS: A MICROWAVE ANALYSIS

G. Ghigo[1,2], M. Fracasso[1,2], R. Gerbaldo[1,2], L. Gozzelino[1,2], F. Laviano[1,2], D. Torsello[1,2]

[1]*Politecnico di Torino, Dept. of Applied Science and Technology, 10129, Turin, ITALY*
[2]*INFN, Sez. Torino, 10125, Turin, ITALY*
E-mail: gianluca.ghigo@polito.it

The microwave properties of superconductors have been investigated for fundamental and application-oriented purposes by means of several techniques. Among them, resonant methods generally have higher sensitivity and accuracy with respect to nonresonant ones, though they are limited to a single or to few discrete frequencies. We have focused on coplanar waveguide resonator (CPWR) techniques, useful to characterize both thin-films and small single crystals [1].

In this presentation, an overview is given of selected results obtained on films of both low-T_c (NbTi, Nb_3Sn) and high-T_c superconductors (YBCO), by means of the CPWR technique in the 8-11 GHz range and in the presence of dc magnetic fields up to 4 T. The characterization is given in terms of the London and Campbell penetration depths, the complex impedance, the vortex-motion-induced complex resistivity, and the vortex pinning properties [2,3]. The complete set of vortex-pinning parameters and the flux flow resistivity are shown and discussed in the framework of high frequency vortex dynamics models.

We also studied the effects of the introduction of controlled defects by means of ion irradiation on the vortex pinning properties and nonlinearity thresholds [2,3]. Different ion beams were used for this study, ranging from 1.5-MeV protons to 1.2-GeV Pb ions, producing qualitatively different defects as for dimensions and morphology, i.e. from point-like defects and nanosized cascades to columnar defects. Specific effects of irradiation are discussed in detail, beside the expected increase of the general pinning capability.

References

[1] G. Ghigo, D. Torsello, *Microwave Analysis of Unconventional Superconductors with Coplanar-Resonator Techniques*, Springer Cham (2022).

[2] G. Ghigo, D. Torsello, L. Gozzelino, M. Fracasso, M. Bartoli, C. Pira, D. Ford, G. Marconato, M. Fretto, I. De Carlo, N. Pompeo, E. Silva, Sci. Rep. **13**, 9315 (2023).

[3] G. Ghigo *et al.*, submitted.

Abstract ID: 1282

SURFACE IMPEDANCE MEASUREMENTS IN SUPERCONDUCTORS IN THE MIXED STATE: ANISOTROPY, FLUX-FLOW, PINNING AND CREEP PERSPECTIVES FOR RF APPLICATIONS IN HIGH MAGNETIC FIELDS

E. Silva[1,2], A. Alimenti[1,2], P. Vidal García[1,2], K. Torokhtii[1], N. Pompeo[1,2]

[1]*Dept. of Industrial, Electronic and Mechanical Engineering, University Roma Tre, 00146 Roma, ITALY*
[2]*INFN, Sezione di Roma Tre, 00146 Roma, ITALY*
E-mail: enrico.silva@uniroma3.it

Superconductors in the vortex state recently became the subject of interest for microwave and RF applications in experiments for fundamental physics, such as haloscopes for dark matter search [1], and the beam screen for the Future Circular Collider (FCC) at CERN [2]. As such, the surface impedance $Z=R+iX$ is the quantity of interest. Moreover, measurements of the same observable can shed light on more fundamental properties of the vortex state. In fact, multifrequency microwave measurements of the surface impedance Z of superconductors represent a powerful investigation tool. The dynamic properties such as flux-flow resistivity ϱ_{ff}, the pinning constant k_p, the thermal flux creep can be investigated deep in the irreversible state but still in the linear response regime. Intrinsic and pinning anisotropy can be singled out, thus isolating the effect of extended defects from the effective-mass anisotropy [3].

Thus, the high-frequency (microwave) experimental investigation can give important information on the electronic state (through the flux-flow resistivity, vortex cores are probed), the control and optimization of defects to improve pinning (through the pinning constant k_p and the flux-creep factor), as well as the anisotropy.

We employ several single or dual frequency dielectric loaded resonators, operating at frequencies between 8 GHz and 27 GHz, to measure the surface impedance $Z(H,T,\theta)$ as a function of the applied field H, the temperature T and the field orientation θ. We report measurements taken in magnetic fields up to 12 T (up to 1.2 T in the variable orientation setup), in temperature ranges from 4 K up to T_c. Special care is taken to evaluate the uncertainty and the reliability of the derived quantities.

In this presentation we review and compare the flux flow resistivity, the pinning constant, the creep factor obtained in conventional and unconventional superconductors: NbTi, Nb_3Sn, MgB_2, $FeSe_xTe_{1-x}$, YBCO, and we add new results on Tl- and Fe- based superconductors. Different flux-flow and pinning regimes are identified and discussed. Thin films, thick films and bulks are investigated. Finally, we present a perspective on the potential of different superconductors for haloscopes and for the FCC beam screen.

Acknowledgments

This work has been partially supported by MIUR-PRIN Project "HIBiSCUS" - Grant 201785KWLE, MUR-PRIN Project "IronMOON" Grant No. 2022BPJL2L, INFN CSN5 project "SAMARA" and FCC collaboration under MoU Addendum FCC-GOV-CC-0218 (KE5084/ATS). We acknowledge sample preparation and useful discussions with A. Augieri, P. Badica, V. Braccini, S. Calatroni, G. Celentano, A. Crisan, C. Gatti, G. Ghigo, M.A. Grigoroscuta, J. Gutierrez, A. Leveratto, A. Mancini, A. Masi, V. Pinto, C. Pira, S. Posen, T. Puig, M. Putti, F. Rizzo, D. Torsello.

References

[1] D. Alesini *et al.*, Phys. Rev. D **99**, 101101(R) (2019).
[2] S. Calatroni, IEEE Trans. Appl. Supercond. **26**, 3500204 (2016).
[3] N Pompeo *et al.*, Supercond. Sci. Technol. **33**, 114006 (2020); **33**, 044017 (2020).

Abstract ID: 1064

VORTEX MATTER CAN BECOME UNSTABLE: THE FLUX FLOW INSTABILITY TOOL

G. Grimaldi[1], A. Leo[1], M.R. Khan[1], N. Martucciello[1], A. Nigro[1,2]

[1]CNR-SPIN c/o University of Salerno, via Giovanni Paolo II 132 I-84084 Fisciano (SA), ITALY
[2]Physics Department "E. R. Caianiello", University of Salerno, via Giovanni Paolo II 132 I-84084 Fisciano (SA), ITALY
E-mail: gaia.grimaldi@spin.cnr.it

The influence of geometry, material anisotropy and orientation of applied magnetic field, as well as of material pinning on the phenomenon of vortex lattice instability (VLI) can become a useful tool to analyze the non-equilibrium regime of high-speed moving vortices. In superconducting materials, such instability can be observed in the current-voltage characteristics as an abrupt voltage jump to the normal state. In general, it is also well known that fast vortex dynamics is responsible of detrimental dissipation. Different insight into fundamental mechanisms such as quasi-particle energy relaxation can be retrieved from a properly tuning of the temperature, applied magnetic field as well as pinning landscape, or from the right compromise between the width and the thickness depending on the chosen material. In particular, the nanoscale effect on VLI has been studied by scaling down the sample thickness, while in HTS nanowires the goal of achieving the vortex lattice instability has been just obtained. Here, we present an overall picture of manipulating geometry and pinning to control vortex velocity in thin films of different materials, including Nb, ReBCO and Fe(Se,Te). The aim is dual: attaining higher vortex velocities pushing towards the operating limits in any superconducting device and gaining a deeper understanding of vortex and quasi-particle dynamics in extreme out-of-equilibrium conditions. Our findings show, for instance, that regardless of the superconducting material, a nanoscale effect of the thickness leads to a direct voltage switching (quenching) from the superconducting to the normal state. In addition, we demonstrate that just by changing geometrical parameters such as thickness, a different balance between quasi-particle scattering and recombination processes can be attained. We also show that a deep knowledge of the material anisotropy can boost high-speed limits of vortex dynamics, thus resulting in more robust quenching currents against external fields.

References

[1] M.R. Khan, A. Leo, A. Nigro, A. Galluzzi, M. Polichetti, V. Braccini, M. Cialone, M. Scuderi, G. Grimaldi, Materials **14**, 5289 (2021).
[2] A. Leo, A. Nigro, G. Grimaldi, Low Temp. Phys **46**, 375-378 (2020).
[3] A. Leo, A. Nigro, V. Braccini, G. Sylva, A. Provino, A. Galluzzi, M. Polichetti, C. Ferdeghini, M. Putti, G. Grimaldi, Supercond. Sci. Technol. **33**, 104005 (2020).
[4] G. Grimaldi, A. Leo, F. Avitabile, N. Martucciello, A. Galluzzi, M. Polichetti, S. Pace, A. Nigro, Nanotechnology **30** (42), 424001 (2019).
[5] G. Grimaldi, A. Leo, A. Nigro, S. Pace, V. Braccini, E. Bellingeri, C. Ferdeghini, Sci. Rep. **8** (2018) 4150.

Acknowledgments

Work partially supported by MUR-PRIN project "QUESTIONs" - grant no. P2022KWFBH and PON Research and Competitiveness 2007-2013 under grant agreement PON NAFASSY, PONa3_00007. Further, support by the European Cooperation in Science and Technology via COST Action CA19108 (HiSCALE) is acknowledged.

Vortex Matter, Dynamics and Pinning III

02.05.2024 THURSDAY

Abstract ID: 1369

USING MACHINE LEARNING TO CHARACTERIZE NONEQUILIBRIUM PHASES IN SUPERCONDUCTING VORTEX MATTER

Charles Reichhardt

Theoretical Division and Center for Nonlinear Studies, Los Alamos National Laboratory, USA
E-mail: reichhardt@lanl.gov

The dynamics of superconducting vortices moving over random disorder is a long-standing problem that has been studied experimentally as well as computationally through transport, imaging, neutron scattering, and noise. There is now strong evidence that driven vortices can exhibit distinct nonequilibrium phase transitions, such as plastic to moving smectic [1,2]; however, there are likely many other kinds of distinct flow phases that would depend on the type of landscape over which the vortices are moving, such as periodic pinning, arrays, or extended defects, or on whether the flow is elastic or plastic. Here, we employ several different types of machine learning approaches to identify different kinds of vortex dynamics in random and periodic arrays where various ML measures, such as a principal component analysis, capture the transition from disordered to moving smectic and moving crystals and also give evidence of different types of partially ordered flows. Our result opens up a new way to examine vortex dynamics and nonequilibrium phenomena in many-body systems in general.

References

[1] C. J. O. Reichhardt, A. del Campo, C. Reichhardt, *Kibble-Zurek mechanism for nonequilibrium phase transitions in driven systems with quenched disorder*, Commun. Phys. **5**, 173 (2022).

[2] S. Maegochi, K. Ienaga, S. Okuma, *Kibble-Zurek mechanism for dynamical ordering in a driven vortex system*, Phys. Rev. Lett. **129**, 227001 (2022).

CANCELLED

Abstract ID: 1468

2D VORTEX LATTICE: A PROMISING PLATFORM TO EXPLORE THE FRAGILE-TO-STRONG GLASS TRANSITION

I. Maccari[1], L. Benfatto[2], C. Castellani[2], J. Lorenzana[2], C. De Michele[2], S.Dutta[3], P. Raychaudhuri[3], B. Pokharel[4], J. Terzic[4,5], D. Popovic[4]

[1] Condensed Matter Theory Group, Paul Scherrer Institut, Villigen 5232, SWITZERLAND
[2]Department of Physics and ISC-CNR, Sapienza University of Rome, P.le A. Moro 2, 00185 Rome, ITALY
[3]Tata Institute of Fundamental Research, Homi Bhabha Rd, Colaba, Mumbai 400005, INDIA
[4]National High Magnetic Field Laboratory, Florida State University, Tallahassee, FL 32310, USA
[5]Western Kentucky University, USA
E-mail: ilaria.maccari@psi.ch

The melting transition in two dimensions can occur in two steps via an intermediate phase called "hexatic" phase. The 2D vortex lattice forming in type-II superconducting films is a paradigmatic system to study this two-step melting transition [1].

In a recent work [2], we succeeded in extracting signatures of the hexatic phase directly from transport measurements. By using Monte Carlo simulations on a 2D XY model, we show that, in analogy with previous works in soft colloids, a heterogeneous dynamics emerges at the verge of the isotropic to the hexatic transition. Caging phenomena, characterizing this intermediate phase, reflect into a strong suppression of linear resistivity. Experimental data confirmed these theoretical predictions: approching the hexatic liquid phase the linear resistivity deviates from the standard Arrhenius trend following a Vogel-Fulcher-Tamman (VFT) law characteristic of fragile glasses. With the increase of the magnetic field, the Arrhenius trend is recovered and system undergoes a fragile-to-strong glass transition. This study points towards 2D vortex lattices being an ideal platform to study the fragile-to-strong glass transition upon variation of a single knob: the magnetic field. We reproduce this phenomenology via Monte Carlo simulations, by increasing the level of disorder in the system while leaving the transverse magnetic field constant [3]. This confirms the theoretical expectation that vortex density is coupled with quenched disorder.

References

[1] I. Roy, S. Dutta, A.N.R. Choudhury, S. Basistha, I. Maccari, S. Mandal, J. Jesudasan, V. Bagwe, C. Castellani, L. Benfatto, P. Raychaudhuri, Phys. Rev. Lett. **122 (4)**, 047001 (2019).
[2] I. Maccari, B.K. Pokharel, J. Terzic, S. Dutta, J. Jesudasan, P. Raychaudhuri, J. Lorenzana, C. De Michele, C. Castellani, L. Benfatto, D. Popović, Phys. Rev. B **107 (1)**, 014509 (2023).
[3] I. Maccari, L. Benfatto, C. De Michele, C. Castellani, In preparation.

Abstract ID: 1017

PLASTIC VORTEX CREEP AND DIMENSIONAL CROSSOVERS IN THE HIGHLY ANISOTROPIC SUPERCONDUCTOR $HgBa_2CuO_{4+x}$

Haley M. Cole[1], Michael B. Venuti[1], Brian Gorman[2], Eric D. Bauer[3], Mun K. Chan[4], Serena Eley[1,5]

[1]*Department of Physics, Colorado School of Mines, Golden, CO USA*
[2]*Department of Materials Engineering, Colorado School of Mines, Golden, CO USA*
[3]*Los Alamos National Laboratory, Los Alamos, NM USA*
[4]*Pulsed Field Facility, National High Magnetic Field Laboratory, Los Alamos National Laboratory, Los Alamos, NM USA*
[5]*Department of Electrical & Computer Engineering, University of Washington, Seattle, WA USA* **E-mail: serename@uw.edu**

In type-II superconductors exposed to magnetic fields between upper and lower critical values, H_{c1} and H_{c2}, penetrating magnetic flux forms a lattice of vortices whose motion can induce dissipation. Consequently, the magnetization M of superconductors is typically progressively weakened with increasing magnetic field $B \propto n_V$ (for vortex density n_V). However, some materials exhibit a non- monotonic $M(B)$, presenting a maximum in M at what is known as the second magnetization peak. This phenomenon appears in most classes of superconductors, including low T_c materials, iron-based, and cuprates, complicating pinpointing its origin and garnering intense interest. Here, we report on vortex dynamics in optimally doped and overdoped $HgBa_2CuO_{4+x}$ crystals, with a focus on a regime in which plastic deformations of the vortex lattice govern magnetic properties. Specifically, we find that both crystals exhibit conspicuous second magnetization peaks and, from measurements of the field- and temperature-dependent vortex creep rates, identify and characterize phase boundaries between elastic and plastic vortex dynamics, as well as multiple previously unreported transitions within the plastic flow regime. We find that the second magnetization peak coincides with the elastic-to-plastic crossover for a very small range of high fields, and a sharp crossover within the plastic flow regime for a wider range of lower fields. Moreover, we find evidence that this transition in the plastic flow regime is due to a dimensional crossover, specifically a transition from 3D to 2D plastic dynamics.

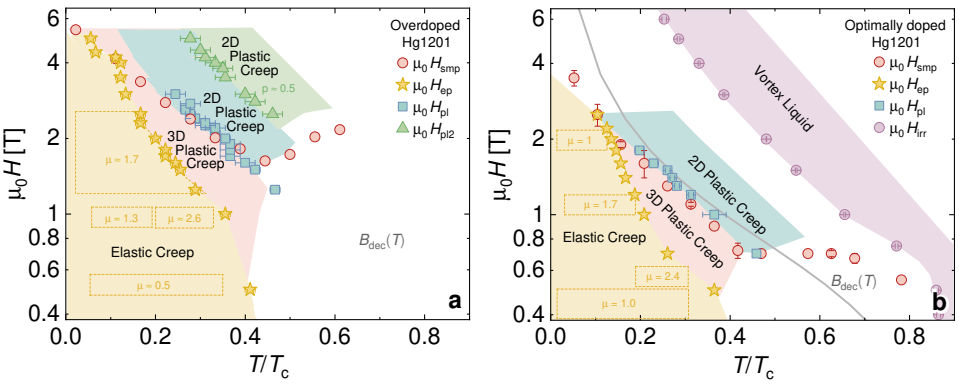

Fig. 1: *Vortex phase diagram determined from creep measurements overlaid with position of second magnetization peak at H_{smp} for (a) overdoped and (b) optimally doped Hg1201 crystals. The gray curve is the prediction for the temperature dependence of the 3D-to-2D decoupling field $B_{dec}(T)$. Overlap with B_{dec} suggests that the second magnetization peak originates from a 3D-to-2D dimensional crossover from 3D-to-2D plastic dynamics.*

Vortex Matter, Dynamics and Pinning IV

02.05.2024 THURSDAY

Abstract ID: 1621

VORTEX PENETRATION INTO THE PUTATIVE CHIRAL SUPERCONDUCTOR 4Hb-TaS_2 BY LOCAL MAGNETIZATION MEASUREMENTS

J. Juraszek[1], Y.M. Thiebes[2], Ł. Luszyński[1], M. Konczykowski[3], R. Niewa[2], T. Cichorek[1]

[1] *Institute of Low Temperature and Structure Research, Polish Academy of Sciences, 50-422 Wroclaw, POLAND*
[2] *Institute of Inorganic Chemistry, University of Stuttgart, 70569 Stuttgart, GERMANY*
[3] *LSI, École Polytechnique, CNRS, Institut Polytechnique de Paris, 91120 Palaiseau, FRANCE*
E-mail: t.cichorek@intibs.pl

Heterostructures formed by alternating magnetic and superconducting layers are predicted systems for the realization of exotic topological quantum phases and resultant Majorana bound states. A promising route to realize topological superconductivity is related to a van der Waals material 4Hb-TaS_2 (a critical temperature $T_c \simeq 3.0$ K). This naturally occurring heterostructure is composed of strongly correlated phases with drastically different ground states [1]. In bulk form, 2H-TaS_2 is a conventional superconductor ($T_c = 0.7$ K), while 1T-TaS_2 is a Mott insulator and can host a quantum spin liquid. Chiral superconductivity in 4Hb-TaS_2 is suggested from, e.g., muon spin relaxation experiments that revealed a spontaneous appearance of magnetic moments at $T \leq T_c$ [1]. Furthermore, an intriguing vortex memory effect [2], which has been observed slightly above T_c, is a topic of present debate whether topological order is involved in vortex nucleation in the thermal cycling process.

Here, we investigate vortex penetration into platelet-shaped 4Hb-$Ta_{1.000(8)}S_{1.97(4)}Se_{0.017(2)}$ samples for a magnetic field H parallel to the layers stacking direction. Using micro-Hall-probe magnetometry, we focus on the field of first flux penetration and the resultant temperature dependence of the lower critical field $H_{c1}(T)$ as a function of sample thickness d. For thick samples ($d \simeq 180$ μm), we observe an anomalous enhancement of H_{c1} at $0.5T_c$ that consists of a non-saturating T-dependence down to 0.007 K being preceded by a concave curvature below 0.5 K. Above 1.5 K, the $H_{c1}(T)$ data show a single-band isotropic s-wave behavior predicted by the Bardeen-Cooper-Schrieffer (BCS) theory. A rather sharp anomaly in $H_{c1}(T)$ far below T_c and no sign of saturation in the limit $T = 0$ suggest that the superconducting state of 4Hb-TaS_2 is both multiband and multisymmetric. This scenario is similar to that realized in the other putative chiral superconductor $PrOs_4Sb_{12}$ ($T_c \simeq 1.85$ K) where multiband order parameters are composed of a sign-changing smaller gap and a large isotropic s-wave gap [4]. However, when the thickness is reduced, the anomaly in $H_{c1}(T)$ of 4Hb-TaS_2 is shifted toward lower temperatures and its magnitude substantially diminishes. For a thin sample ($d \simeq 4$ μm), the lack of saturation is absent and the entire $H_{c1}(T)$ dependence is well described by the conventional BCS relation. We emphasize that T_c does not depend on d. Our findings are at odds with the effect produced by the Bean-Livingston and geometric barriers, and thus point at the presence of an unknown yet factor determining a chiral superconductivity in 4Hb-TaS_2.

This work was supported by the Polish National Science Centre NCN (Project OPUS23 No. 2022/45/B/ST3/04117).

References

[1] A. Ribak *et al.*, Sci. Adv. **6**, eaax9480 (2020).
[2] B. Persky, *et al.,* Nature **607**, 692 (2022).
[3] J. Juraszek *et al.*, Phys. Rev. Lett. **124**, 027001 (2020).

Abstract ID: 1269

INTERTYPE SUPERCONDUCTIVITY EVOKED BY THE INTERPLAY OF DISORDER AND MULTIPLE BANDS

P.M. Marychev, A.A. Shanenko, A.V. Vagov

Centre for Quantum Metamaterials, HSE University, Moscow, 101000, RUSSIA
E-mail: pmarychev@hse.ru

It is well known that nonmagnetic impurity scattering increases the Ginzburg–Landau parameter $\varkappa$ in superconductors. In scenarios where the system begins in type I superconductivity, this impurity scattering can induce a change in its magnetic response, causing it to traverse the intertype domain with $\varkappa \sim 1$, and ultimately making the system to become a type II superconductor.

Our research reveals that the influence of disorder becomes more pronounced when coupled with the multiband structure of the charge carrier states [1]. Specifically, when there is a notable discrepancy in the band diffusivities, the intertype domain undergoes significant expansion, reaching values of $\varkappa \gg 1$ indicative of a deep type-II superconductivity regime (see Fig.1). Our calculations incorporate both intra- and inter-band impurity scattering, demonstrating that the enhancement of the intertype superconductivity domain is primarily governed by intra-band scattering, while inter-band scattering contributes only moderately to its reduction.

Our analysis unveils the intricate role of disorder in shaping the magnetic properties of superconductors, shedding light on the highly nontrivial dynamics of the intertype domain. Importantly, these findings complement earlier results on the enlargement of the intertype domain observed in clean multiband materials [2,3].

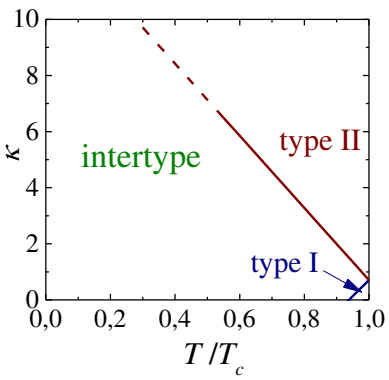

Fig. 1: *The intertype domain in the $\varkappa$-T phase diagram for Θ=200, where Θ is the ratio of the band diffusivities.*

References

[1] P.M. Marychev, A.A. Shanenko, A.V. Vagov, Front. Phys., in press
[2] A. Vagov, A.A. Shanenko, M.V. Milǒsevíc, V.M. Axt, V.M. Vinokur, J.A. Aguiar, F. M. Peeters, Phys. Rev. B **93**, 174503 (2016).
[3] A. Vagov, S. Wolf, M.D. Croitoru, A.A. Shanenko, Commun. Phys. **3**, 58 (2020).

Abstract ID: 1256

MICROSCOPIC ANALYSIS OF THE CROSSOVER BETWEEN TYPE I AND II SUPERCONDUCTIVITY

V.D. Neverov[1,2], A.V. Krasavin[1,2], A.E. Lukyanov[1,2], M.D. Croitoru[1], A. Vagov[1,3]

[1]HSE University, 101000 Moscow, RUSSIA
[2]National Research Nuclear University MEPhI, Moscow, RUSSIA
[3]Moscow Institute of Physics and Technology, Dolgoprudny, RUSSIAN FEDERATION
E-mail: slavesta10@gmail.com

Superconductors exhibit distinctive behaviors in response to externally applied magnetic fields, leading to their classification into two primary types. Type I superconductors expel the magnetic field entirely, while type II materials permit penetration, resulting in a mixed state. However, a class of superconductors, characterized by a proximity of the Ginzburg-Landau parameter to unity, defy this dualism. Observations reveal the existence of an intermediate mixed state (IMS) in these materials, characterized by a diversity of spatial profiles of the magnetic flux and superconducting condensate, which include arbitrary arrangements of Meissner phase, vortex clusters, chains, and liquid droplets [1].

We investigate the crossover between type I to type II superconductivity by solving the microscopic the Bogoliubov – de Gennes equations. The solution methodology employs a recently proposed algorithm that ensures self-consistency with respect to gap, particle density, and the magnetic field [2]. The study unveils various phenomena associated with the IMS, such as vortex clustering and the multi-vortex character of vortex interactions. The latter gives rise to unconventional vortex patterns, vividly illustrated in Fig. 1. The study confirms the universal character of the crossover which is practically independent on the model details.

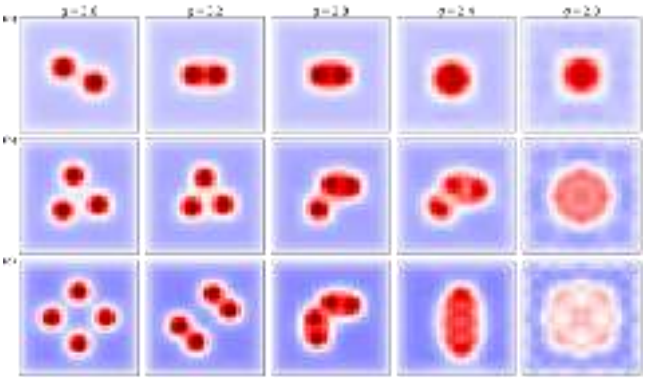

Fig. 1: *Color density plot of the spatial profile of the magnetic flux inside a superconducting sample at various values of the coupling constant g (columns) and the magnetic field (rows a, b, c).*

The work was supported by HSE University Basic Research Program and MEPhI Program Priority 2030, by Ministry of Science and Higher Education of Russian Federation (No. FSWU-2023-0031, FSMG-2023-0014), and by RSF grant 23-72-30004.

References

[1] A. Vagov *et al.*, Comm. Phys. **3**, 58 (2020).
[2] V. Neverov *et al.*, MDPI Condensed Matter, to be published (2024).

Abstract ID: 1652

HELICITY-CONTROLLED SWITCHING OF SUPERCONDUCTING STATES BY RADIATION PULSE: THEORETICAL ANALYSIS AND STABILITY ASSESSMENT

M.D. Croitoru[1], B. Lounis[3,4], A.I. Buzdin[2,5]

[1] HSE University, Moscow 101000, RUSSIA
[2] LOMA, UMR-CNRS 5798, University of Bordeaux, Talence F-33405, FRANCE
[3] LP2N, Université de Bordeaux, Talence F-33405, FRANCE
[4] LP2N, Institut d'Optique and CNRS, Talence F-33405, FRANCE
[5] World-Class Research Center "Digital biodesign and personalized healthcare" Sechenov First Moscow State Medical University Moscow 119991, RUSSIA
E-mail: Mikhail.croitoru@uni-bayreuth.de

Pitaevskii's theoretical framework predicts that circularly polarized light can act as a primary source of the dc magnetization through the inverse Faraday effect (IFE) [1]. Generally, IFE stands out as an efficient tool for non-thermal manipulation of magnetic moments in ferromagnetic materials using light [2]. Notably, recent observations have confirmed the occurrence of IFE in plasmonic gold nanoparticles [3]. However, experimental evidence supporting IFE in superconductors is currently lacking, despite qualitative indications suggesting that the phenomenon may arise from light-induced gap modulation attributable to the concentration-dependent behavior of the superconducting gap function [4-6].

In this study, we present a comprehensive theoretical analysis exploring the feasibility of utilizing a circularly polarized radiation pulse to induce transitions between two distinct quantum states in a superconducting nanoring exposed to half quantum flux. Employing numerical modeling within the framework of the time-dependent Ginzburg–Landau equation, our investigation delineates the conditions necessary for achieving on-demand switching between current-carrying states characterized by different helicities, with a 100% probability of success [7]. Remarkably, our calculations demonstrate the robust stability of the obtained results even in the presence of impurities and reasonable deviations in the external magnetic flux from half quantum values.

The proposed experimental demonstration of this effect would unequivocally establish the existence of the inverse Faraday effect in superconductors. Moreover, such a demonstration would open avenues for the development of light-operated superconducting devices.

References

[1] L.P. Pitaevskii, *Electric forces in a transparent dispersive medium*, ZhETF **39**, 1450 (1961) [Sov. Phys JETP **12**, 1008 (1961)].

[2] A. Kirilyuk, A.V. Kimel, T. Rasing, *Ultrafast optical manipulation of magnetic order*, Rev. Mod. Phys. **82**, 2731–2784 (2010).

[3] O.H. Cheng, D.H. Son, M. Sheldon, *Light-induced magnetism in plasmonic gold nanoparticles*, Nat. Photonics **14**, 365–368 (2020).

[4] S. Mironov, A.S. Mel'nikov, I.D. Tokman, V. Vadimov, B. Lounis, A.I. Buzdin, *Inverse Faraday Effect for superconducting condensates*, Phys. Rev. Lett. **126**, 137002 (2021).

[5] M.D. Croitoru, S.V. Mironov, B. Lounis, A.I. Buzdin, *Toward the light-operated superconducting devices:circularly polarized radiation manipulates thecurrent-carrying states in superconducting rings*, Adv. Quantum Technol. **5**, 2200054 (2022).

[6] M.D. Croitoru, B. Lounis, A.I. Buzdin, *Influence of a nonuniform thermal quench and circular polarized radiation on spontaneous current generation in superconducting rings*, Phys. Rev. B **105**, L020504 (2021).

[7] M.D. Croitoru, B. Lounis, A.I. Buzdin, Hel*icity-controlled switching of superconducting states by radiation pulse*, Appl. Phys. Lett. **123**, 122601 (2023).

High Temperature Superconductors for fusion applications I

02.05.2024 THURSDAY

Abstract ID: 1153

RECENT STATUS OF R&D AND PRODUCTION OF 2G HTS WIRES FOR FUSION APPLICATION AT FARADAY FACTORY JAPAN

S. Lee, V. Petrykin, I. Matvian, M. Nakamura, K. Vereschagin, M. Gaifullin, R.Valikov, H. Nanjyo, A. Borisov, V. Vyatkin, I. Veschunov, M. Okube, J. Renel, L. Pak, A. Li, S. Hasuo, V. Cheremin, M. Oka, S. Samoilenkov, A. Molodyk

Faraday Factory Japan, 192-0032, Tokyo, JAPAN
E-mail: sergey@faradaygroup.com

Since its establishment in 2011 our company has been developing the second generation of high-temperature superconducting wires (2G HTS) using ion beam assisted deposition (IBAD)-pulsed laser deposition (PLD) approach [1]. We offer 2G HTS wires for operation in a wide range of temperatures and magnetic fields and customized for various applications [2]. In a past few years the main driver for scaling up the production was related to our involvement in the compact fusion projects. To satisfy the technical specification of wires for fusion we improved more than 2 times the performance of our "standard" product at 20K and 20 Tesla by modification of YBCO basic composition with Y_2O_3 nanoparticles [3]. Since 2020 such a wire became our main product and rapid acceleration of production is shown on Fig.1. In a past year the annual production capacity exceeded 2000 km and average engineering critical current density (Je) approaching 1000A/mm², which makes Faraday Factory Japan (FFJ) a recognized world leader in manufacturing of 2G HTS. Following the growing demand from our existing customers and taking into account the opening of several new fusion startup companies all over the world, FFJ continuously working for further scaling up and opened a new factory in 2024 with the projected capacity in a range of 0.5-1.0 GAm/year. Our further outlook is based on the assumption that there are no actual alternatives to the 2G HTS wires for fusion and in a next decades the demand will continue to grow [4].

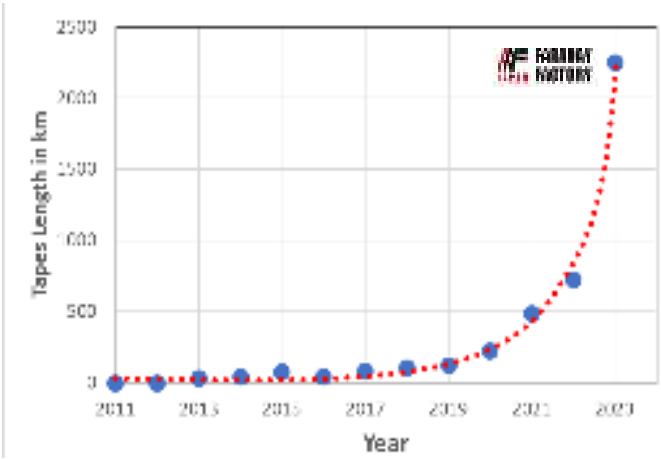

Fig. 1: *Annual production of 4 mm wide 2G HTS wires at Faraday Factory Japan in FY 2011-2023.*

References

[1] S. Lee *et al.*, Superconductor Science and Technology **27**, 044022 (2014).
[2] S. Samoilenkov *et al.*, Superconductor Science and Technology **29**, 024001 (2016).
[3] A. Molodyk *et al.*, Scientific Reports **11**, 2084 (2021).
[4] A. Molodyk, D.C. Larbalestier, Science **380**, 1220 (2023).

Abstract ID: 1159

STUDY OF NEUTRON RADIATION EFFECTS IN YBCO FOR FUSION REACTORS

D. Torsello[1,2], D. Gambino[3], D. Fischer[4], F. Ledda[1,2], S. Sparacio[1,2], Z. Hartwig[4], A. Trotta[5], F. Laviano[1,2]

[1]*Department of Applied Science and Technology, Politecnico di Torino, Torino 10129, ITALY*
[2]*Istituto Nazionale di Fisica Nucleare, Sezione di Torino, Torino 10125, ITALY*
[3]*Linköping University, Department of Physics, Chemistry and Biology, Linköping SE-58183, SWEDEN*
[4]*MIT Plasma Science and Fusion Center, 167 Albany St, Cambridge, MA 02139, USA*
[5]*Eni Venezia, Marghera, 30175 ITALY*
E-mail: daniele.torsello@polito.it

Among the key enabling technologies of compact fusion reactors there are high-temperature superconducting (HTS) magnets. Despite the great improvements recently achieved, one of the main challenges that still need to be faced is the evaluation of radiation effects in HTS tapes [1-3].

In this talk, we present a simulation workflow for the analysis of the impact of neutrons and secondary particles on HTS tapes in compact fusion reactors [4].

First, the radiation environment is evaluated by Monte Carlo simulations performed with the PHITS code [5] on 3D CAD-imported models of the full reactor [6] and of HTS cables [7]. This yields the expected neutron and secondary particles spectra and flux impinging on the HTS material, the map of the deposited power and the damage in terms of displacement per atom (dpa).

The output of such simulations is then used as input for detailed thermal and electromagnetic analysis of the cable and tape behavior at the operation conditions via FEM models [8], and for the study of the distribution and morphology of defects using Molecular Dynamics [4].

We compare the obtained simulations results with existing experimental data, and employ them to design useful experiments for the investigation of radiation effects on HTS.

Finally, we argue that expanding this approach, a comprehensive evaluation of radiation effects in superconducting materials can be achieved, starting directly from the reactor design.

Acknowledgments

This work is partially supported by the European Cooperation in Science and Technology (COST) action CA19108: "High-Temperature Superconductivity for Accelerating the Energy Transition", by the Italian Ministry of Foreign Affairs and International Cooperation, grant number PGR01173, and by Eni S.p.A.. D.T. also acknowledges that this study was carried out within the Ministerial Decree no. 1062/2021 and received funding from the FSE REACT-EU - PON Ricerca e Innovazione 2014-2020. This manuscript reflects only the authors' views and opinions, neither the European Union nor the European Commission can be considered responsible for them.

References

[1] W. Iliffe, *et al.*, Superconductor Science and Technology **34**, 09LT01 (2021).
[2] A. Kuang, *et al.*, Fusion Engineering and Design **137**, 221 (2018).
[3] D.X. Fischer, *et al.*, Superconductor Science and Technology **31**, 044006 (2018).
[4] D. Torsello, *et al.*, Superconductor Science and Technology **36**, 014003 (2023).
[5] T. Sato, *et al.*, Journal of Nuclear Science and Technology **50**, 913 (2013).
[6] F. Ledda, *et al.*, Fusion Engineering and Design (submitted)
[7] F. Ledda, *et al.*, IEEE Transactions on Applied Superconductivity (submitted)
[8] S. Sparacio, *et al.*, IEEE Transactions on Applied Superconductivity (submitted)

Abstract ID: 1178

THE PATH TOWARDS AN HTS STELLARATOR FUSION POWER PLANT IN EUROPE

N. Riva
on behalf of the Proxima Fusion Team

Proxima Fusion, Munich, GERMANY
E-mail: nicorp@proximafusion.com

Stellarators are magnetically confined fusion devices that are capable of operating in inherently-stable and steady-state scenarios, resulting in evident advantages in the scaling to commercially-viable fusion power plants. However, despite their relatively simple operation, stellarators have historically been hard to design and build. Now, thanks to emerging capabilities to numerically optimize stellarators, their large number of degrees of freedom is turning from a *liability* into an *advantage*. Moreover, advances in High-Temperature Superconductors (HTS) offer opportunities to significantly increase magnetic field intensity on the plasma, resulting in radically improved fusion performance.

Proxima Fusion is a spin-out company from the Max Planck Institute for Plasma Physics (IPP), which built and operates W7-X, the most advanced stellarator on the planet. Proxima is implementing an "engineering-first" philosophy to the design of steady-state stellarators. The company is committed to the concept of "quasi-isodynamic" (QI) stellarators, where no net toroidal current is present within the plasma. In the absence of toroidal currents, current-driven instabilities are eliminated and engineering constraints can be significantly relaxed, enabling a path to commercial viability for fusion energy. Moreover, the key performance metrics in fusion devices (both tokamaks and stellarators) scale rapidly with the magnetic field, making HTS magnets crucial to realize a compact fusion device.

In this talk, we will introduce the Proxima Fusion approach to combine high-field magnet technology with a "simulation-first" approach for QI stellarators. Building on the legacy of W7-X, and in partnership with leading scientific and technology fusion institutions, Proxima Fusion aims to deliver a demonstration of effective net-energy production in steady-state.

High Temperature Superconductors for fusion applications II

02.05.2024 THURSDAY

Abstract ID: 1309

INVESTIGATION OF THE QUENCH BEHAVIOR AT FUSION RELEVANT CONDITIONS OF THE ALUMINUM SLOTTED-CORE HTS REBCO CABLE

G. Celentano[1], A. Augieri[1], V. Corato[1], S. Chiarelli[1], G. De Marzi[1], R. Freda[1], M. Marchetti[1], A. Masi[1], L. Muzzi[1], V. Pinto[1], G. Romanelli[1], A. Rufoloni[1], A. Vannozzi[1], A. della Corte[2], A. Formichetti[2], A. Bragagni[3], M. Seri[3], R. Bonifetto[4], A. Zappatore[4], G. Colombo[5], H. Bajas[6], K. Sedlak[6]

[1]ENEA Superconductivity Section, Frascati Research Centre, 00044, Frascati, ITALY
[2]ICAS, 00044, Frascati, ITALY
[3]Tratos Cavi S.p.A., 52036, Pieve S. Stefano, ITALY
[4]NEMO Group, Politecnico di Torino, 10124, Torino, ITALY
[5]Bologna University, Department of Electrical, Electronic and Information Engineering, 40136, Bologna, ITALY
[6]EPFL, Swiss Plasma Center, CH-5232, Villigen, SWISS
E-mail: giuseppe.celentano@enea.it

The emergence of High Temperature Superconducting (HTS) technology based on Rare-Earth-Barium-Copper Oxide (REBCO) tapes, called coated-conductors or 2G tapes, is expected to have a great impact in the energy sector promoting innovative applications and enabling new technologies. In particular, HTS tapes will play a technological key role in the road map towards the development of commercially affordable nuclear fusion power plant. With this perspective, in the last decade a lot of efforts was spent on the technological development of HTS based conductors for fusion magnets. Among others, the aluminum slotted-core concept was proposed, being characterized by stacks of HTS tapes incorporated into the slots created in an extruded Al stabilizer [1]. The peculiarity of this cable is mainly related to the nature of HTS stacks formed by tapes which are not soldered together but simply piled up and mildly compacted during the jacketing process with an external aluminum tube. So far, the cable layout and manufacturing process have been successfully assessed by investigating the electric performances and mechanical behaviour either experimentally or implementing dedicated codes.

In this contribution, we reported the experimental results carried out at the SULTAN facility (Paul Scherrer Institute, PSI – Villigen, Swiss) on the investigation of quench behavior of HTS slotted-core samples under fusion relevant conditions. Conductors were designed for operation at 4.2 K forced-flow cooled by supercritical He under a background magnetic field of 11 T with a critical current in excess of 15 kA. In agreement with the SULTAN facility requirements, the sample consists of two 3.6 m long conductors electrically connected by a joint at the bottom and connected to the terminals of the facility current leads at the top. Every conductor was equipped with 76 HTS tapes, arranged in 4 stacks of 19 tapes each.

Conductor quench events were triggered by increasing the He gas temperature at given bias current and magnetic field and monitoring the temperature and voltage signal traces with sensors arranged along the conductor length and within the conductor cross-section. Sample were subjected to quenches with different maximum hot-spot temperatures (up to 200 K) and cooling gas flow conditions, in order to explore a wide range of possible fusion magnet operation scenario. The measured conductor critical current, I_c, and current sharing temperatures, T_{cs}, were used as reference for the performance degradation assessment after several quench events. The thermal behavior and quench propagation features of the conductors were analyzed and discussed with the support of electromagnetic and thermal-hydraulic simulation codes [2,3].

References

[1] G. Celentano, *et al.*, IEEE Trans. Appl. Supercond. **24**, 4601805 (2014).
[2] G. De Marzi, *et al.*, Supercond. Sci. Technol. **34**, 035016 (2021).
[3] A. Zappatore, *et al.*, IEEE Trans. Appl. Supercond. **31**, 4800805 (2021).

CANCELLED

Abstract ID: 1316

PERFORMANCE DEGRADATION IN REBCO TAPES AFTER IRRADIATIONS BETWEEN 20 K AND 300 K

D.X. Fischer, A.R. Devitre, K.B. Woller, Z.L. Fischer, Z.S. Hartwig

Massachusetts Institute of Technology, MA 02139, Cambridge, UNITED STATES
E-mail: dafisch@mit.edu

Fusion power plants based on magnetic confinement will rely on high-field superconducting electromagnets to maintain the required plasma temperatures of over 100 million K. The deuterium-tritium reactions produce high energy neutrons that damage the microstructure of many essential components of the fusion device like the superconducting magnets. The magnets in compact high-field fusion power plants will use Rare Earth Barium Copper Oxides (REBCO) tapes and will operate at around 20 K.

While irradiation studies are a valuable tool to learn about the effect of radiation damage on material properties, it is important to conduct these experiments under fusion relevant conditions for trustworthy results. To address this issue, we have developed a facility for cryogenic ion irradiation of REBCO tapes which features in-situ transport current measurements. This enables us to assess radiation induced changes of critical current (I_c) and transition temperature (T_c) without warming samples up. Therefore we avoid unrepresentative annealing effects.

We have irradiated REBCO tapes with 1.2 MeV protons at various temperatures from 20 K up to 300 K and observed a distinctly different behavior after cold and warm irradiation. For irradiations at 300 K, a 50% higher fluence is required to reach the same I_c degradation as for 20 K irradiations. However, irradiations at 77 K and 20 K do yield the same results. This finding might significantly decrease the complexity and cost of future irradiation experiments since it allows cooling with liquid nitrogen without compromising the fusion relevance of the results.

Abstract ID: 1312

CORRELATING THE DETERIORATION OF THE SUPERCONDUCTING PROPERTIES OF CCs BY NEUTRON IRRADIATION WITH SMALL DEFECTS

Raphael Unterrainer*[1], Davide Gambino[2], Florian Semper[1], Alexander Bodenseher[1], Daniele Torsello[3,4], Francesco Laviano[3,4], Michael Eisterer[1]

[1]*Atominstitut, Technische Universität Wien, Vienna, AUSTRIA*
[2]*IFM, Linköping University, Linköping, SWEDEN*
[3]*Department of Applied Science and Technology, Politecnico di Torino, Torino, ITALY*
[4]*Istituto Nazionale di Fisica Nucleare, Sezione di Torino, Torino, ITALY*
E-mail: raphael.unterrainer@tuwien.ac.at

Recently published simulations have shown that reactor designers of compact fusion devices will face major issues concerning the expected lifetime of their magnet systems. While a commercially feasible reactor should ideally be affordable, robust and on top of that compact, currently available data suggests that compact reactor designs, relying on coated conductors will face major costs and downtimes to exchange their centrepiece on a regular basis. This is obviously in contradiction to two of the three above proposed advantages of these systems. Considering future improvements in shielding technology and that these designs are still in their infancy and may change in size, a lifespan of 10 years may be feasible but could be an upper limit for the magnets. This raises the question how and if the radiation resistance of coated conductors can be improved. To answer this question, however, it is necessary to understand which types of defects degrade the superconducting properties to subsequently develop mitigation strategies or inherently more resistant conductors.

We irradiated commercial coated conductors based on Gadolinium-Barium-Copper-Oxide (GdBCO) in our TRIGA MARK II fission reactor to work out which types of defects are responsible for the degradation of the critical current J_c and temperature T_c of coated conductors. The fission reactor spectrum is believed to resemble the expected fusion spectrum if the samples are shielded from the thermal peak ($E_{kin} < 0.55$ eV) with a neutron absorber material such as Cadmium. By irradiating samples with or without shielding, it is possible to introduce distinct defect landscapes to the superconductor. This is enabled by the utilization of a defect formation process where Gd isotopes possessing a large absorption cross section for thermalized neutrons, lead to the formation of small mainly oxygen defects upon the absorption of a slow neutron. By comparing the results of these two irradiation techniques, we are able to distinguish between the contribution of small defects versus large cascades on J_c and T_c. The data shows similarities in the degradation behaviour of the superconducting properties despite the different introduced defect landscapes. Consecutive annealing experiments in pure O_2 atmosphere revealed identical recovery rates at increasing temperatures. These results strongly suggest that the defects responsible for the degradation of the superconducting properties are of the same type.

Since the defect formation process in the thermal neutron experiments is well understood and the energy of the primary knock-on-atom (PKA) is known to be approximately 30 eV, it is possible to simulate the expected defect structures by molecular dynamics simulations. Further studying the defect classes with DFT allows us to make an estimation on their influence on the local DOS of the CuO_2 planes and thus on their degrading effects on the superconducting properties.

High Temperature Superconductors for fusion applications III

02.05.2024 THURSDAY

Abstract ID: 1627

CURRENT STATUS OF R&D OF SCSC CABLES

N. Amemiya[1], Y. Sogabe[1], Y. Tejima[2], H. Hara[2], H. Sakamoto[3]

[1]*Kyoto University, 6158510, Kyoto, JAPAN*
[2] *Furukawa Electric Co., Ltd., 3211493, Nikko, JAPAN*
[3] *SuperPower Inc., 12302, Grenville, U.S.A.*
E-mail: amemiya.naoyuki.6a@kyoto-u.ac.jp

A bottle neck toward various applications of REBCO coated superconductors is their tape shape. It is difficult to assemble REBCO tapes for increasing current carrying capacity. Note that their simple stack is not preferred in many applications, because its bending orientation is limited. Furthermore, their wide tape shape, typically 4 mm-wide causes the generation of large ac loss as well as magnetization. Note that simple filamentaization of superconductor layer of a tape does not work, because filaments are coupled electromagnetically when the tape is subjected to the normal ac magnetic field.

We have been developing the Spiral Copper-plated Striated Coated-conductor cables, abbreviated to the SCSC cables or the double "SC" cables, in which the combination of filamentizing (striating) superconductor layer of a coated conductor and winding such coated conductors spirally plays similar role to that of filamentizing and twisting of a low T_c superconductor wire, and, hence, ac losses as well as magnetization can be reduced effectively. Assembling coated conductors in multiple layers increases the current carrying capacity.

We will present the current status of research and development of SCSC cables, whose applications to accelerator magnets, plasma confinement systems for fusion, and various electrical machines are promising.

This work was supported in part by JSPS KAKENHI Grant Number JP22H00142 and in part by JST-ALCA-Next Program (JST-Mirai Program Grant Number JPMJMI19E1).

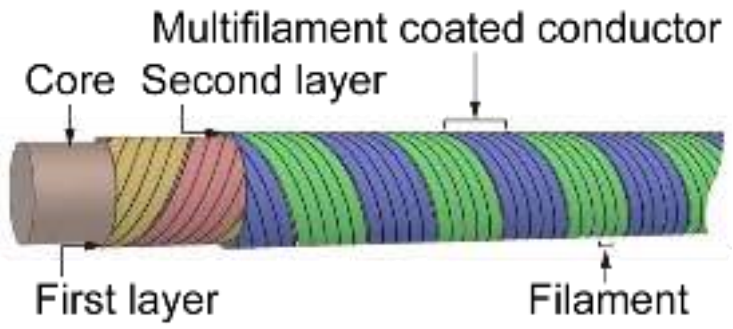

Fig. 1: *Schematic view of SCSC cable [1].*

References

[1] N. Amemiya *et al.*, Supercond. Sci. Technol. **36**, 025003 (2022).
[2] N. Amemiya *et al.*, IEEE Trans. Appl. Supercond. **33**, 4701507 (2023).

Abstract ID: 1323

CHANGE IN STRUCTURAL AND SUPERCONDUCTING PARAMETERS OF 2G HTS TAPES UNDER THE INFLUENCE OF IRRADIATION

P. Pęczkowski

Cardinal Stefan Wyszyński University, Institute of Physical Science, Faculty of Mathematics and Natural Sciences, School of Exact Sciences, K. Wóycickiego 1/3, 01-938 Warsaw, POLAND
E-mail: p.peczkowski@wp.pl

Controlled change of superconductivity parameters, the so-called "superconductivity suppression" occurs under the influence of various dopants to the pure superconductor, e.g. Fe [1], $YMnO_3$ multiferoics [2] or various rare earth elements (*RE*) [3]. In my talk, I will discuss the impact of noble gas ion additions on the critical parameters of 2G HTS (second-generation high-temperature superconducting) tapes based on *RE*BCO ($REBa_2Cu_3O_{7-\delta}$ where δ – oxygen coefficient, *RE* – gadolinium Gd). Such tapes have a very wide range of applications in various industries, including the space industry, and can be used to protect spacecraft and astronauts against radiation in space, where temperatures are low [4]. In space, tapes are exposed to various types of radiation, including: cosmic radiation, solar wind and various ions, including noble gas ions such as Ne [5], and Ar, Kr, Xe [6]. Under the influence of radiation, various types of defects appear in the tape structure, including: Frenkel and Schottky defects, which act as centers of fixation of Abrikosov vortices. The resulting defects affect the superconducting and structural parameters of the irradiated tapes. In order to determine the influence of radiation on the superconducting parameters of 2G HTS SF (stabilizer free) 12050 tapes from SuperPower Inc. [7] the Ag protective layer was removed by a catalytic process. Then, during the implantation process, noble gas ions Ne^+ with an energy of 250 keV and four different fluences were implanted into the superconducting layer of the tape: 10^{12}, $5\cdot10^{12}$, 10^{13}, and 10^{14} Ne^+/cm^2 [5]. The 2G HTS SF 12050 tapes were prepared to obtain a uniform implantation surface on the sample surface. Microstructural studies were carried out using SEM (scanning electron microscopy) with EDS (energy dispersive spectroscopy) and structural XRD (X-ray diffraction from 2 to 300 K). Structural studies have shown that the *c* lattice parameter decreases with longer exposure time, which may be related to the decrease in the oxygen factor in the superconducting layer. In the magnetic investigation, we noted a decrease in the critical current density (J_c) for irradiated samples compared to non-irradiated samples and a slight decrease in the critical temperature (T_c) of 1.5 – 2.0 K for the irradiated tapes (T_c for the non-irradiated 93.5 K tape).

References

[1] P. Pęczkowski, P. Zachariasz, M. Kowalik, W. Tokarz, S.P. Kumar Naik, J. Żukrowski, C. Jastrzębski, J.L. Dadiel, W. Tabiś, Ł. Gondek, J. Eur. Cer. Soc. **41(14)**, 7085–7097 (2021).
[2] P. Pęczkowski, P. Zachariasz, M. Kowalik, R. Zalecki, C. Jastrzębski, Cer. Int. **45(15)**, 18189–18204 (2019).
[3] P. Pęczkowski, M. Łuszczek, E. Szostak, N. Kumar Chogondahalli Muniraju, A. Krztoń-Maziopa, Ł. Gondek, Acta Materilia **222**, 117437 (2022).
[4] P. Spillantini, Acta Astronautica **68(9-10)**, 1430–1439 (2011).
[5] P. Pęczkowski, R. Zalecki, P. Zachariasz, E. Szostak, J. Piętosa, M. Turek, K. Pyszniak, M. Zając, J. Czub. Ł. Gondek, App. Surf. Sci. **636(5)**, 157780 (2023).
[6] L. Antonova, A. Troitskii, G. Maikhailova, T. Demikhov, S. Kuzmichev, V. Skuratov, V. Semina, Phys. Stat. Soli. B **256(5)**, 1800255 (2019).
[7] SuperPower Inc., *SuperPower 2G-HTS wire specifications*, https://www.superpower-inc.com/specification.aspx, 2023 (accessed January 11, 2024).

Abstract ID: 1321

THE INFLUENCE OF ION IRRADIATION ON THE SUPERCONDUCTING PROPERTIES OF 2G HTS WIRE

P. Degtyarenko[1,2], V. Skuratov[3], A. Vasiliev[4], V. Amelichev[1], S. Gavrilkin[5], A. Ovcharov[4], V. Semina[3], M. Novikov[3], A. Petrzhik[1], A. Tsvetkov[5], A. Malyavina[6]

[1]S-innovations LLC, 117246, Moscow, RUSSIA
[2]JIHT RAS, 125412, Moscow, RUSSIA
[3]FLNR JINR, 141980, Dubna, Moscow region, RUSSIA
[4]NRC "Kurchatov institute", 123182, Moscow, RUSSIA
[5]LPI RAS, 119991, Moscow, RUSSIA
[6]NRNU "MEPhI", 115409, Moscow, RUSSIA
E-mail: degtyarenkopn@gmail.com

We systematically studied the superconducting properties of 2G HTS wire samples in magnetic field before and after irradiation. The samples were irradiated with 167 MeV Xe and 670 MeV Bi ions at the IC-100 and U-400 FLNR JINR cyclotron facilities. The samples were fabricated by PLD, using commercial production equipment and conditions at S-Innovations LLC. Superconducting properties were measured using PPMS in the field range from 0 to 9 Tesla. The samples were uniformly irradiated at room temperature by scanning the ion beam over their whole surface at an average ion flux of 2×10^8 cm^{-2} s^{-1}. For the Xe ion exposed targets we determined the optimum fluence values (the number of particles passing through 1 cm^2 of the sample surface) for obtaining the maximum critical current at different temperatures and external magnetic field strength. Increasing the external magnetic field leads to a shift of the critical current peak towards higher fluences in the whole temperature range. Microstructural examination using transmission electron microscopy (TEM) showed that swift heavy ion irradiation results in formation of ion tracks with diameters about of 5-8 nm, which act as effective pinning centers. X-ray diffraction analysis also indicates a decrease in texture sharpness. For the samples irradiated by Bi-ions an increasing of the critical current by 1.4 times at a fluence 1 10^{11} cm^{-2} was observed with a simultaneous decrease of the critical temperature by 3 K in comparison with the non-irradiated sample. The results of TEM studies of the morphology and microstructure are compared with the data of electrophysical studies for all samples. The obtained results will be used in the design of superconducting magnetic systems for new generation accelerators.

Role of Superconductivity Roadmap For Net Zero Carbon Emission Targets by 2050: Superconductivity Global Alliance (ScGA) III

02.05.2024 THURSDAY

Abstract ID: 1567

SUPERCONDUCTIVITY GLOBAL ALLIANCE –ANALYSIS AND ROADMAPS OF TRANSITIONING SUPERCONDUCTING TECHNOLOGIES TO THE MARKETPLACE IN INDUSTRY, ENERGY, POWER, AND TRANSPORT SECTORS

Sastry Pamidi, Michael Parizh, Peter Cheetham, Mohammad Yazdani-Asrami, Loic Queval, Arno Godeke, Marco Breschi, Ziad Melhem

E-mail: pamidi@caps.fsu.edu

The Superconductivity Global Alliance (ScGA) is organizing a large international group of research institutions, professional societies, and industry to establish public-private partnerships to achieve a green, healthy, prosperous, and sustainable future using superconducting technologies. Experts forming multiple working groups have evaluated the status of various superconducting technologies for industry, energy, power, and transport.

The paper discusses the findings of the holistic assessment of superconducting technologies for a green energy future and the investments necessary to realize the dream of superconducting technologies for a sustainable and equitable energy future. The discussion covers the market potential, the challenges in lowering the costs of superconducting technologies to be competitive, solutions for effective supply chains, and the need to develop a skilled workforce to transition from R&D to the marketplace. The group's mission is to advocate for superconducting technologies and educate the decision-makers on the enormous potential of superconducting technologies in tackling climate change by benefiting from the synergy of renewable energy generation, transmission and distribution, and efficient energy. Superconducting technologies effectively integrate the generation of green energy and green fuels to address the intermittent nature of renewable energy sources. Liquid hydrogen provides the energy density and the cryogenic environment needed to support the superconducting technologies for significantly lowering capital and operating costs. Additionally, there is an urgent need for regional industrial commons to support rapid technology development and effectively nurture industry and small businesses with demonstrations and standards development. The plans of the global alliance to establish public-private partnerships to attract investments for rapidly transitioning superconducting technologies to the marketplace are discussed in the paper.

Abstract ID: 1575

NOVEL METHODOLOGY FOR SMART MANUFACTURING AND INSPECTION OF INDUSTRIAL SCALE REBCO COATED CONDUCTOR WIRES

Takanobu Kiss[1,2], Z. Wu[2], K. Higashikawa[1,2], T. Terazaki[2], S. Sera[2], Y. Tanaka[2], R. Valikov[3], M. Nakamura[3], A. Li[3], V. Petrykin[3], S. Lee[3]

[1] *Res. Inst. of Superconductor Science and Systems, Kyushu Univ., Fukuoka 819-0395, JAPAN*
[2] *Dept. of Electrical Engineering, Kyushu Univ., Fukuoka 819-0395, JAPAN*
[3] *Faraday Factory Japan LLC, Kanagawa 252-0132, JAPAN*
E-mail: kiss@sc.kyushu-u.ac.jp

With the progress of research and development of such applications as compact fusion power generation and superconducting motor, which are expected as a key technology for the realization of long-term carbon zero emission, the production of rare-earth based (REBCO) high temperature superconducting coated conductor (CC) wire is shifting to the mass production. Here, a technology for stably low-cost manufacturing of high performance CC is required, but in the present state, empirical approach by try and error is used in most cases based on the wire performance centering the critical current (I_c) of the liquid-nitrogen temperature due to the limitation of the throughput of the wire property characterization. It is an urgent issue to establish an advanced wire manufacturing process by feeding back the wire performance at an actual operation condition, together with upgrading on in-process inspection and shipping inspection. In this talk, recent progress is described on the upgrading of REBCO wire manufacturing technology by the fusion of measurement technology, fabrication process, and informatics which the authors are working on. Combining the high-speed reel-type magnetic microscopy, which was developed by the authors, optical microscopic inspection and image analysis by machine-learning, we have succeeded in automatic detection of local flaw in the tape plane and inhomogeneity of I_c which is difficult to detect by the conventional method, and statistical analysis became feasible. Furthermore, using combinatorial CC wires produced by systematically changing production conditions of an industrial-scale PLD equipment, we have collected more than 20,000 data on the relationship between wire I_c and the production conditions, and by using a deep learning model trained based on these enourmous data, we have succeeded in developing a model which allows us to predict wire I_c with high-precision from the combination of control parameters in manufacturing even though the I_c shows complicated behavior. The importance of these new methodologies based on data-driven approach for manufacturing and evaluating industrial scale REBCO CC wires and its future prospects will be also discussed.

Acknowledgements

This work was supported by JSPS KAKENHI Grant Number JP19H05617.

Abstract ID: 1547

SUPERCONDUCTING WIND ENERGY – AIR-CORED HTS C-GEN MACHINE

Hongye Zhang

The University of Edinburgh, Edinburgh, UK
E-mail: zhang_hongye@qq.com

Wind turbine generators play a crucial role in the global transition towards sustainable and renewable energy sources, and superconducting wind turbine generator provides a promising solution for the challenging global wind targets. C-GEN is an innovative multi-stage air-cored generator technology with permanent magnets (PMs) developed by the University of Edinburgh, which has been demonstrated at a laboratory scale. Based on the PM C-GEN machine prototype, an air-cored high temperature superconducting (HTS) C-GEN machine topology has been proposed. This talk will outline the hurdles faced by traditional wind energy systems and introduce the innovative concept of the air-cored HTS C-GEN machine, highlighting its potential to revolutionize wind power generation.

Quantum Transport and Novel Broken Symmetry Ground States I

02.05.2024 THURSDAY

Abstract ID: 1026

HIGHER-SPIN PAIRING AND EXOTIC SUPERCONDUCTIVITY IN LUTTINGER SEMIMETALS

Igor Herbut

Simon Fraser University, Department of Physics, V5A 1S6, Burnaby, CANADA
E-mail: iherbut@sfu.ca

Luttinger semimetals represent a family of spin-orbit-coupled materials that feature electrons with an effective spin 3/2 and quadratic band touching. In spite of their low carrier density they often exhibit robust superconducting states at low temperatures, the nature of which has been a subject of many experimental and theoretical investigations. I will review our recent work on weakly-coupled exotic superconducting states that result from Cooper pairing of such higher-spin electrons. In particular, I will discuss the five-component d-wave superconducting states at zero and finite chemical potential, the interplay of s- and d-wave components, and the generalized phase diagram of p-wave superconducting states. Particular attention will be paid to possible breaking of time reversal symmetry and the resulting quasiparticle excitation spectrum. Comparison with the experiments on YPtBi will be attempted.

References

[1] M. Kheirkhah, I.F. Herbut, e-print arXiv:2310.18157.
[2] J. Link, I.F. Herbut, Phys. Rev. B **105**, 134522 (2022).
[3] J. Link, I.F Herbut, Phys. Rev. Lett. **125**, 237004 (2020).
[4] I.F. Herbut, I. Boettcher, S. Mandal, Phys. Rev. B **100**, 104503 (2019).
[5] I. Boettcher, I.F. Herbut, Phys. Rev. Lett. **120**, 057022 (2018).

Abstract ID: 1241

DYNAMICAL CONDUCTIVITY OF A TWO-DIMENSIONAL WEAKLY DOPED HOLSTEIN SYSTEM

Z. Rukelj[1], D. Radić[1], J. Krsnik[2], O.S. Barišić[2], A.S. Mishchenko[2], I. Kupčić[1]

[1] *Department of Physics, Faculty of Science, University of Zagreb, Bijenička 32, 10000 Zagreb, CROATIA*
[2] *Institute of Physics, Bijenička 46, 10000 Zagreb, CROATIA*
E-mail: zrukelj@phy.hr

The generalized Drude formula is used to study conductivity properties of the two-dimensional weakly doped Holstein model with a free-electron-like dispersion [1]. The relaxation processes associated with the scattering of conduction electrons by optical phonons are described in terms of a frequency- and temperature-dependent memory function [2]. The imaginary and real parts of the memory function are analyzed in detail in the regime when characteristic energy scales of the problem, i.e., electron Fermi energy and optical phonon energy, are comparable in size. Results obtained at zero temperature and at finite temperatures are used to determine temperature effects in the real part of the dynamical conductivity as well as the frequency dependence of the optical electron mass and the electron relaxation rate. Finally, the characteristic fingerprints of a Holstein system with multiple phonon branches are identified in the dynamical electron conductivity.

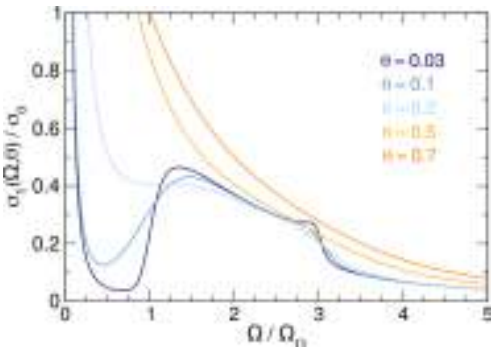

Fig. 1: *The real part of the dynamical conductivity as a function of photon energy Ω scaled to the optical phonon energy Ω_O, calculated for Fermi energy $\varepsilon_F = 2\Omega_O$, and for several values of temperature $\theta = k_B T / \Omega_O$.*

References

[1] Z. Rukelj, D. Radić, J. Krsnik, O.S. Barišić, A.S. Mishchenko, I. Kupčić, Phys. Rev. B **108**, 155151 (2023).
[2] Z. Rukelj, Phys. Rev. B **102**, 205108 (2020).

Abstract ID: 1242

CHARGE STRIPES AND MAGNETOTRANSPORT IN THE GRAPHENE-BASED MATERIALS

D. Radić[1], P. Grozić[1], B. Keran[1], A.M. Kadigrobov[1,2]

[1]University of Zagreb Faculty of Science, Department of Physics, 10000 Zagreb, CROATIA
[2]Theoretische Physik III, Ruhr-Universitaet Bochum, D-44801 Bochum, GERMANY
E-mail: dradic@phy.hr

We present a novel mechanism of charge ordering appearing in graphene sheets within the intercalated graphite CaC_6 compound [1]. This instability mechanism yields the experimentally observed [2] uniaxial charge stripes of periodically modulated electron density, i.e. charge density wave – CDW (Fig. a), accompanied with appearance of a pseudo-gap in electron spectrum (Fig. b). It is coupled to the softest phonon mode of the superlattice, consisting of the Ca atoms intercalated between graphene planes, resulting in the specific type of the Ca lattice deformation (Fig. c). The Fermi surface of the chemically doped graphene undergoes the novel type of instability driven by the mechanism that gains the condensation energy of the stripe state by the topological reconstruction of the Fermi surface, with finite electron-phonon coupling to the above-mentioned phonon mode larger than critical. This mechanism appears to be entirely different from the one based on the Fermi surface nesting, which has been considered a paradigm in the present literature concerning the onset of charge density waves. The magnetoconductivity along the open sheets of the reconstructed Fermi surface, under conditions of magnetic breakdown, shows strong quantum oscillations, being not the mere correction to the classical part, but altering it as its inherent part, rendering it essentially nonclassical.

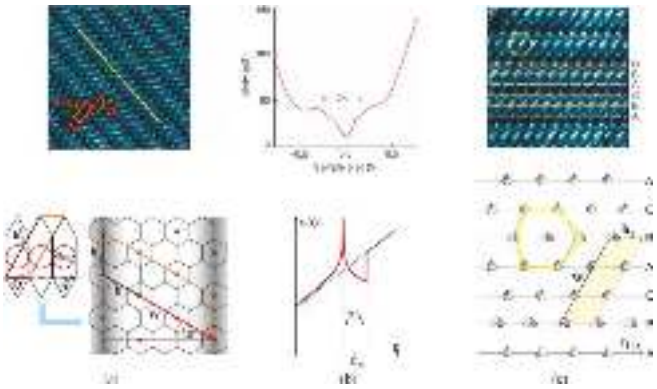

Fig. 1: *Comparison of experimental observation (upper panel) [2] and theoretical prediction (lower panel) [1]: (a) CaC_6 structure, unit cell, charge stripes (shaded); (b) pseudo-gap in electron spectrum; (c) deformation of the Ca superlattice.*

References

[1] P. Grozić *et al.*, Scientific Reports **8**, 18931 (2023).
[2] K. Rahnejat *et al.*, Nature Communications **2**, 558 (2011).

Quantum Transport and Novel Broken Symmetry Ground States II

02.05.2024 THURSDAY

Abstract ID: 1355

TOMASCH OSCILLATIONS AS ABOVE-GAP SIGNATURE OF TOPOLOGICAL SUPERCONDUCTIVITY

Antonio Štrkalj[1], Xi-Rong Chen[2,3], Wei Chen[2], D.Y. Xing[2], Oded Zilberberg[4]

[1]*University of Zagreb, Faculty of Science, Department of Physics, 10000 Zagreb, CROATIA*
[2]*National Laboratory of Solid State Microstructures, School of Physics, and Collaborative Innovation Center of Advanced Microstructures, Nanjing University, Nanjing 210093, CHINA*
[3]*School of Microelectronics and Physics, Hunan University of Technology and Business, Changsha, Hunan Province, 410205, CHINA*
[4]*Department of Physics, University of Konstanz, 78464 Konstanz, GERMANY*
E-mail: astrkalj@phy.hr

The identification of topological superconductors usually involves searching for in-gap modes that are protected by topology. However, in current experimental settings, the smoking-gun evidence of these in-gap modes is still lacking – partially due to difficulties in distinguishing them from disorder effects. In this work, we propose to support the distinction between two-dimensional conventional *s*-wave and topological *p*-wave superconductors by above-gap transport signatures [1]. Our method utilizes the emergence of Tomasch oscillations [2] of quasiparticles in a junction consisting of a superconductor sandwiched between two metallic leads, see Figs. 1(a) and (b). We demonstrate that the behaviour of the oscillations in conductance as a function of the interface barriers provides a distinctive signature for s-wave and *p*-wave superconductors, see Fig.1(c). Specifically, the oscillations become weaker as the barrier strength increases in *s*-wave superconductors, while they become more pronounced in *p*-wave superconductors, which we prove to be a direct manifestation of the pairing symmetries. Our method can serve as a crucial complementary probe for identifying some classes of topological superconductors through the above-gap transport.

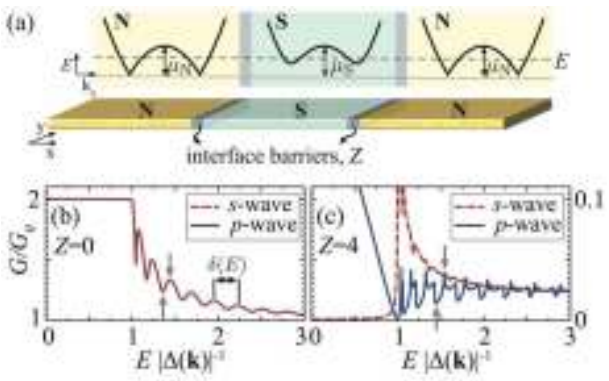

Fig. 1: *(a) Sketch of the NSN junction consisting of a superconductor (S) coupled to two normal metal leads (N) with the interface barrier Z. (top panels) The quasiparticle dispersion for $k_y = 0$ in all three regions. We consider an incident particle from the left lead with energy E (dashed line). (b) Differential conductance as a function of energy for both the s- and p-wave superconductors in the absence of barriers (Z = 0) [3,4] and with the magnitude of the pair potential set to be equal, i.e., $|\Delta(k)| = \Delta_S = \Delta_p k_F$. The period of the conductance oscillations, δ(E), increases with energy. (c) Same as (b) in the presence of finite barriers with equal strengths Z = 4. Grey arrows denote the extremal points of a single oscillation.*

References

[1] A. Štrkalj *et al.*, e-print arXiv:2305.09530 (2022).
[2] W.J. Tomasch, Phys. Rev. Lett. **15**, 672 (1965).
[3] M. Karalic, A. Štrkalj *et al.*, Phys. Rev. X **10**, 031007 (2020).
[4] A. Štrkalj, Ph.D. thesis (2021).

Abstract ID: 1415

UNCONVENTIONAL ELECTRODYNAMICS ACROSS THE CHARGE-DENSITY-WAVE TRANSITION IN $TiSe_2$

Dino Novko

Centre for Advanced Laser Techniques, Institute of Physics, 10000, Zagreb, CROATIA
E-mail: dnovko@ifs.hr

Charge-order states of broken symmetry, such as charge density wave (CDW), are able to induce exceptional electrodynamical properties, however, our understanding of the underlying physics is still incomplete. For instance, the origin of unconventional CDW in 1*T*-$TiSe_2$ and its corresponding optical and plasmonic response is still highly debated, where proposed mechanisms are discussed in terms of purely electronic as well as purely lattice driven processes [1].

Here, we first explore fundamentals of collective electronic excitations in single-layer $TiSe_2$ by using the ab-initio electromagnetic linear response and unveil intricate scattering pathways of two-dimensional (2D) plasmon mode near the CDW phase [2]. We found the dominant role of plasmon-phonon scattering, which in combination with the CDW gap excitations leads to the anomalous temperature dependence of the plasmon linewidth across the CDW transition. Below the transition temperature T_{CDW} a strong hybridization between 2D plasmon and CDW excitations is obtained. These optical features are highly tunable due to temperature-dependent CDW-related modifications of electronic structure and electron-phonon coupling and make CDW-bearing systems potentially interesting for applications in optoelectronics and low-loss plasmonics.

Furthermore, we use fluctuational electrodynamics and density functional theory to reveal a unconventional thermophotonic effect in $TiSe_2$, which we call thermophotonic-CDW (*tp*-CDW) [3]. The interplay of 2D plasmon polariton and CDW electron excitations give rise to an anomalous temperature dependency in thermal photon transport, which could be used as a fingerprint of a electron order transformation. Additionally, the demonstrated nontrivial features of *tp*-CDW-transition also holds promise for a controllable manipulation of heat flow, which could be extensively utilized in various fields such as thermal science and electron dynamics, as well as in next-generation energy devices.

References

[1] D. Novko, Z. Torbatian, I. Lončarić, Phys. Rev. B 106, 245108 (2022).
[2] Z. Torbatian, D. Novko, *Plasmon excitations across the charge-density-wave transition in single layer $TiSe_2$*, (under review), e-print arXiv:2307.11370 (2023).
[3] C.-L. Zhou, Z. Torbatian, S.-H. Yang, Y. Zhang, H.-L. Yi, M. Antezza, D. Novko, C.-W. Qiu, *Unconventional thermophotonic charge density wave*, (under review) (2024).

Abstract ID: 1371

EMERGENT ELECTRONIC PROPERTIES IN A PLASTICALLY DEFORMED QUANTUM MATERIAL

D. Pelc[1,2]

[1]*Faculty of Science, University of Zagreb, Bijenička 32, HR-10000 Zagreb, CROATIA*
[2]*School of Physics and Astronomy, University of Minnesota, Minneapolis MN-55455, USA*
E-mail: dpelc@phy.hr

Strain is one of the most prominent means to manipulate the properties of quantum materials, and is increasingly being applied to study a diverse range of material systems. Most of these investigations, however, remain within the regime of reversible, elastic sample deformation, where the attainable strain levels are relatively low. In contrast, irreversible plastic deformation can lead to very large local strain levels due to the creation and motion of dislocations. While well known in the materials engineering community, this approach has been virtually unexplored in the context of quantum materials. In his talk, I will discuss the consequences of extensive plastic deformation of a model quantum material, strontium titanate ($SrTiO_3$, STO). We use a set of complementary experimental techniques, including neutron and x-ray diffuse scattering, transport, magnetic resonance, Raman spectroscopy and scanning magnetometry, to characterize the structural and electronic properties of deformed STO in detail [1-3]. We show that the large strains and translation symmetry breaking associated with dislocations lead to a number of interesting phenomena: significant enhancement of superconducting transition temperatures [1], the appearance of quantum-critical ferroelectric fluctuations [1], and strain-induced magnetism and multiferroicity [2]. These results also showcase the potential of plastic deformation to tune the electronic properties of quantum materials more broadly, opening up a host of new opportunities in the field.

References

[1] S. Hameed *et al.*, Nat. Mater. **21**, 54 (2022).
[2] X. Wang *et al.*, e-print arXiv:2308.14801 (2023).
[3] I. Khayr *et al.*, in preparation (2024).

Quantum Transport and Novel Broken Symmetry Ground States III

02.05.2024 THURSDAY

Abstract ID: 1417

THE EGZOTIC ELECTROMAGNETIC MODES IN LAYERED VAN DER WAALS HETEROSTRUKTURES

Vito Despoja[1,2]

[1]*Institute of Physics, Bijenička 46, 10000 Zagreb, CROATIA*
[2] *Donostia International Physics Center (DIPC), P. Manuel de Lardizabal, 4, 20018 San Sebastián, SPAIN*
E-mail: vdespoja@ifs.hr

The 2D heterostructures of transition metal dichalcogenides (TMDs), hexagonal boron nitride (hBN) and graphene (Gr) can support some exotic electromagnetic modes. Here we present the results of our recently proposed theoretical approach [1] applied to study the electromagnetic eigen-modes in layered conducting and semiconducting van der Waals (vdW) heterostructures. We will present the efficiency of excitation of 2D plasmon-polaritons (PPs) in hBN/graphene heterostructures by using the monocromatic radiation and silver nano-spheres and compare with recent Scanning Near-Field Microscopy (SNOM) measurements. **Fig. 1(a)** shows the electric field $E_x(\rho)$ carried by the combination of Dirac and Linear PPs (DP+LP) in gr/hBN/gr/hBN/gr composite excited by **x** polarised radiation of frequency ω=300meV. The conditions necessary for emergence of exotic, transversal plasmon (called *trapped photon*) in semiconducting vdW heterostructures will be demonstrated [2,3]. We show that the *trapped photon* (T-ph), built from inter-band electron-hole excitations (not necessarily from excitons) and the transversal photons, is the transversal counterpart to PP in conductive 2D materials, built from intra-band electron-hole excitations and the longitudinal photons. We present the results for T-ph intensities in WS_2/hBN multilayers. **Fig. 1(b)** shows the propagation of the **x** polarised current $j_x^{ind}(\rho)$ in WS_2/hBN/WS_2/hBN/ WS_2 composite, driven by **x** polarised point dipole ocillating at frequencies ω_T=1.96eV, representing strong T-ph.

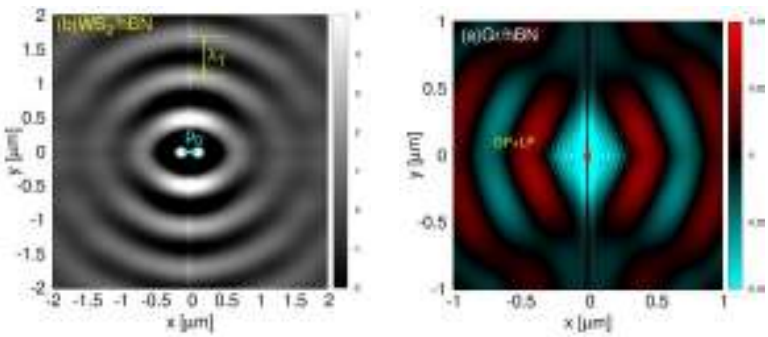

Fig.1: *(a) DP+LP plasmon polariton in gr/hBN/gr/hBN/gr composite excited by **x** polarised infrared radiation of frequency ω=300meV; (b) Propagation of trapped photon in WS_2/hBN/WS_2/hBN/WS_2 composite excited by **x** polarised point dipole ocillating at frequencies ω_T=1.96eV.*

References

[1] D. Novko, K. Lyon, D.J. Mowbray, V. Despoja, Phys. Rev. B **104**, 115421 (2021).
[2] S.A. Mikhailov, K. Ziegler Phys. Rev. Lett. **99**, 016803 (2007).
[3] N. Golenić, V. Despoja, Phys. Rev. B **108**, L121402 (2023).

Abstract ID: 1505

DESIGNING SUPERCONDUCTIVITY IN NANODEVICES

Nina Markovic

Goucher College, Dept. of Physics, 21204, Baltimore, USA
E-mail: ninazagreb@gmail.com

As the dimension of a superconducting wire approaches the coherence length, its superconducting state becomes increasingly sensitive to factors such as the disorder, texture, non-equilibrium effects and details of the interfaces with other materials. While this may present a difficulty for some applications, it also provides an opportunity for controlled manipulation of quantum states that is essential for creating tunable quantum devices. Full understanding and control of the physics at the interfaces is essential to understanding and control of the quantum state of a nanowire that may by dominated by such interfaces. I will describe the fabrication of nanopatterned superconducting samples with controlled physical texture and will show how tunable interfaces with graphene and topological materials lead to unusual transport properties.

Abstract ID: 251

EXPERIMENTAL INVESTIGATION OF THE ELECTROMAGNETICALLY INDUCED TRANSPARENCY FOR DIFFERENT D2-LINE TRANSITIONS OF ^{87}RUBIDIUM

Zahra Heydarinasab, Mohammad Karami, Farrokh Sarreshtedari

Quantum Resonance Research Laboratory, Department of Physics, College of Science, University of Tehran, 143-9955961, Tehran, IRAN

E-mail: m19heydarinassab@gmail.com

Electromagnetically induced transparency (EIT) is a quantum interference effect in which the atomic medium becomes transparent to the weak probe field in the presence of a strong control field [1]. This phenomenon has different applications in various fields, such as slow light, light storage, quantum memory, nonlinear optics, atomic clock, magnetometry, etc.[2-6]. The characteristics of the EIT window, like its bandwidth and slope play important roles in such applications. In this work, we have experimentally investigated the characteristics of EIT window for all different D2 transition lines of ^{87}Rb and compared them with each other. Figure 1 shows the schematics of our Zeeman EIT experimental setup. The wavelength of the laser (a homemade ECDL) is locked on the $5S_{1/2}$-$5P_{3/2}$ transition (D2 line) of the Rubidium [7]. When the output beam of the laser passes from the half-wave plate (HWP) and polarizing beam splitter (PBS), it is divided into two parts, each of which enters a double-pass acousto-optic modulators (AOM) setup to produce the pump and probe beams. After the pump and probe lights are adjusted to the required frequencies, they are coupled in an optical fiber to be directed into the cell. The linear polarization of the light changes to circularly polarization using a quarter-wave plate (QWP) before entering the atomic cell. After the cell, using another QWP and a PBS, the probe beam is separated from pump for EIT observation.

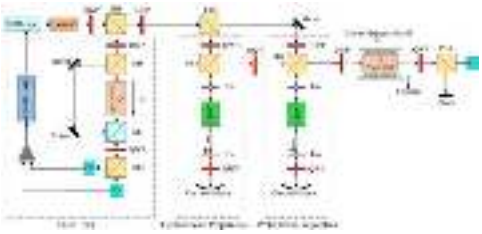

Fig.1: *The schematics of experimental setup for EIT.*

References

[1] S.E. Harris, *Electromagnetically induced transparency*, Physics Today **50, no. 7**, 36-42 (1997).

[2] L.V. Hau, S.E. Harris, Z. Dutton, C.H. Behroozi, *Light speed reduction to 17 metres per second in an ultracold atomic gas*, Nature **397, no. 6720**, 594-598 (1999).

[3] D.F. Phillips, A. Fleischhauer, A. Mair, R.L. Walsworth, M.D. Lukin, *Storage of light in atomic vapor*, Phys. Rev. Letters **86(5)**,783 (2001).

[4] H. Wu, M. Xiao, J. Gea-Banacloche, *Evidence of lasing without inversion in a hot rubidium vapor under electromagnetically-induced-transparency conditions*, Phys. Rev. A **78, no. 4**, 041802 (2008).

[5] R.G. Beausoleil, W.J. Munro, D.A. Rodrigues, T.P. Spiller, *Applications of electromagnetically induced transparency to quantum information processing*, J. Modern Optics **51, no. 16-18**, 2441-2448 (2004).

[6] V.I. Yudin, A.V. Taichenachev, Y.O. Dudin, V.L. Velichansky, A.S. Zibrov, S.A. Zibrov, *Vector magnetometry based on electromagnetically induced transparency in linearly polarized light*, Phys. Rev. A **82(3)**, 033807 (2010).

[7] M. Karami, Z. Heydarinasab, F. Sarreshtedari, *Sub-Doppler dichroism as a useful tool in alkali atom hyperfine spectroscopy*, Laser Physics, **vol. 33, no. 12**, pp. 125701 (2023).

Quantum Transport and Novel Broken Symmetry Ground States IV

02.05.2024 THURSDAY

Abstract ID: 246

QUANTUM TRANSPORT EQUATIONS IN 2D AND 3D DIRAC SYSTEMS: SELF-CONSISTENT RPA APPROACH

I. Kupčić

Department of Physics, Faculty of Science, University of Zagreb, Bijenička 32, 10000 Zagreb, CROATIA
E-mail: kupcic@phy.hr

The generalized Drude approach represents a model-independent method of analyzing measured reflectivity spectra. [1] In this approach, the dynamical conductivity formula is given in terms of a phenomenological frequency-dependent memory function. The same expression for the dynamical conductivity can be obtained theoretically by using different types of quantum transport equations. Here, we present the results for the memory-function dynamical conductivity in weakly doped graphene and in anisotropic 3D Dirac semimetals obtained by using a common self-consistent RPA approach. [2,3] We will show that a seemingly inconsistent dependence of the dc conductivity of ultraclean and dirty lightly doped samples on doping can be easily understood if in the calculations the momentum distribution functions are used instead of the Fermi-Dirac distribution functions. [4] We will also show that the redistribution of the intraband conductivity spectral weight over a wide frequency spectral range, clearly seen in experiments, can be explained by replacing the intraband relaxation rate by the corresponding intraband memory function. For the scattering of conduction electrons by phonons, the real and imaginary parts of the intraband memory function depend on frequency and temperature in the way shown in Fig. 1(a). [3] Fig. 1(b) illustrates the total dynamical conductivity in doped graphene in the same model.

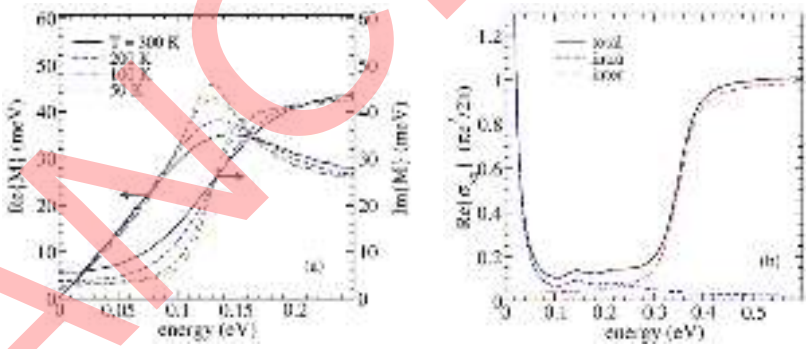

Fig. 1: (a) *The real and imaginary parts of the phonon contribution to the memory function in graphene, for typical values of model parameters.* **(b)** *The corresponding total dynamical conductivity.*

References

[1] S.I. Mirzaei *et al.*, Proc. Natl. Acad. Sci. USA **110**, 5774 (2013).
[2] I. Kupčić, Phys. Rev. B **90**, 205426 (2014).
[3] I. Kupčić, Phys. Rev. B **95**, 035403 (2017).
[4] I. Kupčić, G. Nikšić, Z. Rukelj, D. Pelc, Phys. Rev. B **94**, 075434 (2016).

CANCELLED

Abstract ID: 1665

MANON-DRIVEN QUANTUM DOT BASED SPIN SEEBECK HEAT ENGINE AND REFRIGERATOR

P. Trocha

Faculty of Physics, ISQI, Adam Mickiewicz University, 61-614 Poznan, POLAND
E-mail: piotrtroch@gmail.com

We present results on generation of spin and charge current by means of temperature gradient in a quantum dot based hybrid systems. In particular, we study thermoelectric properties of a quantum dot hybrid device consisting of a quantum dot coupled to a magnetic insulator and magnetic metallic electrode. Each electrode is kept at a different temperature. In the considered system spin current is generated by means of temperature gradient set between the electrodes. Furthermore, spin current of the magnonic (electric) type is converted to electric (magnonic) spin current. An influence of magnonic energy-dependent density of states on thermally induced spin current is investigated [1]. Moreover, we take into account many-body magnon interactions and analyze its influence on spin current. Furthermore, a spin Seebeck engine based on quantum dot is investigated. We also present the conditions under which the considered device works as thermal spin-diode. Apart from that, linear response regime is also considered [2]. We show that in this regime the system can convert heat into electrical power with Carnot efficiency.

Moreover, we present a nanoscale refrigerator composed of two ferromagnetic metals and a magnetic insulator coupled to a quantum dot. By applying temperature gradient to the metals an imbalance in the occupations of the electronic states is created. This leads to the flow of electrons from hot to cold terminal. However with the energy input from outside it is possible to force the net current of electrons from above of Fermi level (hot electrons) to flow in the opposite direction with electrons from below Fermi level (cold electrons) still flowing in the direction of the temperature gradient. This leads to the cooling of the electrons in the cold lead - phenomenon called cooling by heating [3]. In the system under study one of the metals is cooled by the help of the outside source of the energy delivered by magnons coming from the magnetic insulator. The inclusion of quantum dot allows the transport to take place through discrete level which has a beneficial influence on the efficiency of the cooling. We investigate the flow of heat in the system and calculate coefficient of performance of such a device for various system's parameters.

References

[1] P. Trocha *et al.*, J. Magn. Magn. Mater. **589**, 171495 (2024).
[2] P. Trocha *et al.*, Sci. Rep. **12**, 5348 (2022).
[3] B. Cleuren *et.al.*, Phys. Rev. Lett. **108**, 120603 (2012).

Acknowledgements

We acknowledge support of the National Science Center in Poland through the research Project No. 2018/31/D/ST3/03965.

Abstract ID: 1402

ENTANGLEMENT OF MANY-BODY MIXED STATES

F.-H. Wang[1], X.Y. Xu[1,2]

[1]*Key Laboratory of Artificial Structures and Quantum Control (Ministry of Education), School of Physics and Astronomy, Shanghai Jiao Tong University, Shanghai 200240, CHINA*
[2]*Hefei National Laboratory, Hefei 230088, CHINA*
E-mail: xiaoyanxu@sjtu.edu.cn

Many-body entanglement unveils additional aspects of quantum matter and offers insights into strongly correlated physics. While ground-state entanglement has received much attention in the past decade, the study of mixed-state quantum entanglement using negativity in interacting fermionic systems remains unexplored. We demonstrate that the partially transposed density matrix of interacting fermions, similar to the reduced density matrix, can be expressed as a weighted sum of Gaussian states describing free fermions, enabling the calculation of rank-n Rényi negativity within the determinantal quantum Monte Carlo framework. We conduct the first calculation of rank-two Rényi negativity for the half-filled Hubbard model and the spinless t-V model and find that the area law coefficient of the Rényi negativity has a singularity at the finite-temperature transition point. Our work contributes to the calculation of entanglement and sets the stage for future studies on quantum entanglement in various fermionic many-body mixed states.

References

[1] F.-H. Wang, X. Y. Xu, arXiv:2312.14155.

Abstract ID: 1434

DIAGNOSING QUANTUM PHASES USING LONG-RANGE QUANTUM RESOURCE BEHAVIORS

L.-L. Su[1,2], J. Ren[1,3], W.-L. Ma[2,4], Z.D. Wang[3], Y.-K. Bai[1,3]

[1]College of Physics and Hebei Key Laboratory of Photophysics Research and Application, Hebei Normal University, Shijiazhuang, Hebei 050024, CHINA
[2]State Key Laboratory of Superlattices and Microstructures, Institute of Semiconductors, Chinese Academy of Sciences, Beijing 100083, CHINA
[3]Department of Physics, HK Institute of Quantum Science & Technology, and Guangdong-Hong Kong Joint Laboratory of Quantum Matter, The University of Hong Kong, Pokfulam Road, Hong Kong, CHINA
[4]Center of Materials Science and Opto-Electronic Technology, University of Chinese Academy of Sciences, Beijing 100049, CHINA
E-mail: renjun0726@outlook.com

We propose and demonstrate that the behaviors of long-range, two-site quantum resources can effectively diagnose quantum phases. In an XX spin chain with symmetry-breaking quantum phase transitions, we reveal that the asymptotic and oscillating decay modes of quantum coherence or quantum discord, along with two-site distance, can identify two spin-liquid phases. Furthermore, based on our analytical results of spin correlation functions, we confirm the existence of long-range entanglement in the system and establish a connection between two-site entanglement and quantum phases. Additionally, for the extended Ising model with topological phase transitions, we find that coherence and quantum discord behaviors can also signify topological quantum phases. In particular, we discover the quantum resource freezing phenomenon, where topologically protected long-range quantum resources may have potential applications in quantum information processing. In addition, we study the properties of multipartite quantum correlation (MQC) in a one-dimensional spin-1/2 XY chain, where the three-spin reduced states are focused on and the four introduced MQC measures are based on entanglement negativity and entanglement of formation. It is found that, even in the Ising case, the three-spin subsystems have long-range MQCs and the tripartite quantum correlations beyond the nearest-neighbor three spins can detect the quantum phase transition and obey the finite-size scaling around the critical point.

The work was supported by the NSFC/RGC JRS grant (RGC Grant No. N_HKU774/21), the CRF (Grant No. C6009-20G) and GRF (Grant Nos. 17310622 &17303023) of Hong Kong. J.R. acknowledges support from NSF-China (Grants Nos.11575051 and 11904078) and project of China Postdoctoral Science Foundation (Grant No. 2020M670683).

References

[1] L.-L. Su, J. Ren, Z.D. Wang, Y.-K. Bai, Phys. Rev. A **106**, 042427 (2022).
[2] L.-L. Su, J. Ren, W.-L. Ma, Z.D. Wang, Y.-K. Bai, e-print arXiv:0704.3011 (2023).

Superconductivity in Bi-layer Nickelates I

02.05.2024 THURSDAY

Abstract ID: 1405

THEORY FOR HIGH TEMPERATURE SUPERCONDUCTIVITY IN $La_3Ni_2O_7$

Fu-Chun Zhang

Kavli Institute for Theoretical Physics, University of Chinese Academy of Sciences, Beijing, 100190, CHINA
E-mail: fuchun@ucas.ac.cn

Recent discovery of high temperature superconductivity $La_3Ni_2O_7$ under high pressure has attracted a lot of attention. In this talk, I shall present our theory [1-3] for electronic structure of the compound and address the similarity and difference of this newly discovered bilayer nickelate superconductor in comparison with high temperature superconducting cuprates [4,5] and with infinite layer nickelate superconductors [6,7].

References

[1] Yi-Feng Yang, Guang-Ming Zhang, Fu-Chun Zhang, Phys. Rev. B **108**, L201108 (2023).
[2] Kun Jiang, Zi-Qiang Wang, Fu-Chun Zhang, Chine Phys. Letts **41**, 017402 (2024).
[3] Yuxin Wang, Kun Jiang, Ziqiang Wang, Fu-Chun Zhang, Jiangping Hu, e-print arXiv submitted (2024).
[4] P.W. Anderson, P.A. Lee, M. Randeria, T.M. Rice, N. Triveli, F.C. Zhang, J. Phys.: Condens. Matter **16**, R755 (2004).
[5] F.C. Zhang, T.M. Rice, Phys. Rev. B **37**, 3759 (1988)
[6] Danfeng Li, Kyuho Lee, Bai Yang Wang, Motoki Osada, Samuel Crossley, Hye Ryoung Lee, Yi Cui, Yasuyuki Hikita, Harold Hwang, Nature **572**, 624 (2019).
[7] Guang-Ming Zhang, Yi-Feng Yang, Fu-Chun Zhang, Phys. Rev. B **101**, 020501 (2020).

Abstract ID: 1139

ORBITAL-DEPENDENT ELECTRON CORRELATION IN DOUBLE-LAYER NICKELATE $La_3Ni_2O_7$

Xingjiang Zhou

Ntaional Lab for Superconductivity, Institute of Physics, Chinese Academy of Sciences, Beijing 100190, CHINA
E-mail: xjzhou@aphy.iphy.ac.cn

The latest discovery of high temperature superconductivity near 80K in $La_3Ni_2O_7$ under high pressure has attracted much attention[1]. Many proposals are put forth to understand the origin of superconductivity. The determination of electronic structures is a prerequisite to establish theories to understand superconductivity in nickelates but is still lacking. Here we report our direct measurement of the electronic structures of $La_3Ni_2O_7$ by high-resolution angle-resolved photoemission spectroscopy[2]. The Fermi surface and band structures of $La_3Ni_2O_7$ are observed and compared with the band structure calculations. A flat band is formed from the Ni-3dz^2 orbitals around the zone corner which is ~50meV below the Fermi level. Strong electron correlations are revealed which are orbital- and momentum-dependent. Our observations will provide key information to understand the origin of high temperature superconductivity in $La_3Ni_2O_7$.

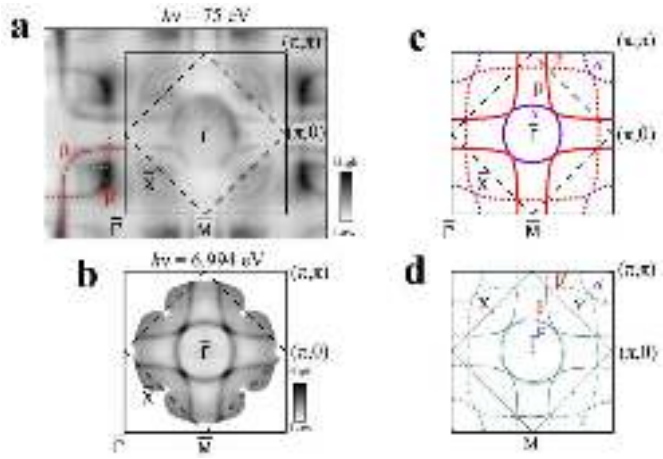

Fig. 1: *Measured Fermi surface of $La_3Ni_2O_7$ and its comparison with the band structure calculations.*

References

[1] H.L. Sun *et al.*, Nature **621**, 493 (2023).
[2] J. Yang, L. Zhao, X.J. Zhou *et al.*, e-print arXiv:2309.01148 (2023).

Abstract ID: 1379

RESONANT X-RAY SCATTERING ON SUPERCONDUCTING NICKELATES

J. Pelliciari

NSLS-II, Brookhaven National Laboratory, Upton, 11772, USA
E-mail: pelliciari@bnl.gov

The discovery of superconductivity in infinite layer nickelates thin films has spurred a lot of attention in the scientific community [1]. These materials appear to be analog to the cuprates with parent compounds having a single hole in the *d* orbitals and upon hole doping they become superconducting. The detection of spin excitations and charge density waves [2-5] further corroborated such similarities even if major differences such as the role of rare earth and the balance between Hubbard (U) and charge transfer energies raise questions on their actual similarity. Additionally, superconducting nickelates have few peculiarities such as their existence only in thin films and the possible effects of the $SrTiO_3$ capping layer which require scrutiny to identify intrinsic from extrinsic effects.

In my talk, I will present our latest high resolution Resonant Inelastic X-Ray Scattering (RIXS) investigations on infinite layer nickelates. Thanks to our data, we can unveil the role of the capping layer for the spin and orbital excitations in $NdNiO_2$ and optimal-doped $Nd_{1-x}Sr_xNiO_2$ disentangling intrinsic and extrinsic effects associated to the scattering signal. Indeed, we observe the presence of damped spin excitations in parent and superconducting samples regardless of the presence of capping. In our data, we can rule out the presence of charge density waves contrary to previous reports. In superconducting $Nd_{1-x}Sr_xNiO_2$, independently of the presence of capping, we observe an overall softening of the spin excitations compared to the parent compound in agreement with a magnetic dilution effect. Overall, the spin excitations spectrum is suppressed in uncapped samples indicating an influence of the capping layer on the magnetism in these compounds, possibly due to extrinsic effect due to a lower quality of the samples or a minimal hybridization with the substrate. Remarkably, the spectral weight of the Ni-Nd charge transfer is also highly suppressed in uncapped samples. To prove the generality of these arguments I will also report on RIXS measurements performed on high quality $Nd_{1-x}Eu_xNiO_2$ where we could generalize the universality of spin excitations in infinite layer nickelates and their softening upon doping.

These pieces of evidence uncover the intrinsic properties of superconducting infinite layer nickelates as a function of capping and doping type which have strong implications in the understanding of nickelate superconductivity.

References

[1] D. Li, *et al.*, *Superconductivity in an infinite-layer nickelate*, Nature **572**, 624–627 (2019).
[2] H. Lu, *et al.*, *Magnetic excitations in infinite-layer nickelates*, Science **373**, 213–216 (2021).
[3] C.C. Tam, *et al.*, *Charge density waves in infinite-layer $NdNiO_2$ nickelates*, Nat. Mater. (2022); doi:10.1038/s41563-022-01330 -1.
[4] G. Krieger, *et al.*, *Charge and spin order dichotomy in $NdNiO_2$ driven by the capping layer*, Phys. Rev. Lett. **129**, 027002 (2022).
[5] M. Rossi, *et al.*, *A broken translational symmetry state in an infinite-layer nickelate*, Nat. Phys. 1–5 (2022); doi:10.1038/s41567-022-01660-6.

Superconductivity in Bi-layer Nickelates II

02.05.2024 THURSDAY

Abstract ID: 1063

MAGNETIC FLUCTUATIONS, SUPERCONDUCTING INSTABILITY AND SPIN RESONANCE IN $La_3Ni_2O_7$ UNDER HIGH PRESSURE

F. Lechermann, S. Bötzel, J. Gandolf, Ilya M. Eremin

Institut für Theoretische Physik III, Ruhr-Universität Bochum, 44801 Bochum, GERMANY
E-mail: ilyaeremin@yahoo.de

Motivated by the report of superconductivity in bilayer $La_3Ni_2O_7$ at high pressure, we examine the interacting electrons and the resulting spin fluctuations in this system. First-principles many-body theory is utilized to study the normal-state electronic properties. Below 100K, a multi-orbital non-Fermi liquid state resulting from loss of Ni-ligand coherence within a flat-band dominated low-energy landscape is uncovered. The incoherent low-temperature Fermi surface displays strong mixing between Ni-d_{z2} and Ni-d_{x2-y2} orbital character. In a model-Hamiltonian picture, spin fluctuations originating mostly from the Ni-d_{z2} orbital give rise to strong tendencies towards a superconducting instability with either d_{x2-y2}-wave or interlayer s+-wave order parameter in pressurized $La_3Ni_2O_7$. We show that the bilayer structure of the spin response allows to elucidate the role of the interlayer interaction and the Cooper-pairing in a very efficient way. In particular, we demonstrate the key difference between the potential s+- and d-wave gaps, discussed recently, by comparing the corresponding response in the even and odd channels of the spin susceptibility. We show that mostly interlayer driven s+- Cooper-pairing produces a single large spin resonance peak in the odd channel whereas several resonances are predicted for the d-wave scenario.

References

[1] F. Lechermann, J. Gondolf, S. Bötzel, I. M. Eremin, Phys. Rev. B, **L201121** (2023).

Abstract ID: 1411

THEORETICAL ANALYSIS ON THE POSSIBILITY OF UNCONVENTIONAL SUPERCONDUCTIVITY IN $La_3Ni_2O_7$ AND $La_4Ni_3O_{10}$ UNDER HIGH PRESSURE

Kazuhiko Kuroki

Dept. of Physics, Osaka University, Machikaneyama, Toyonaka, Osaka, JAPAN
E-mail: kuroki@presto.phys.sci.osaka-u.ac.jp

Recent discovery of high T_c superconductivity in a bilayer nickelate $La_3Ni_2O_7$ has sparked a vast wave of new interest [1]. In fact, this very material was previously proposed as a good starting point for seeking high T_c superconductivity by the present author and his colleagues [2]. Discussed there was the possibility of realizing a nearly half-filled bilayer Hubbard model with large interlayer hopping utilizing the $d_{3z^2-r^2}$ orbitals.

In the present study, we construct a four-orbital ($d_{3z^2-r^2}+d_{x^2-y^2}$, x 2) model of $La_3Ni_2O_7$ under high pressure through DFT calculations and Wannierization, and apply FLEX to study superconductivity [3]. We find that the T_c can be comparable to those of the high T_c cuprates, and the effects of the $d_{x^2-y^2}$ orbitals are limited, so that the experimental T_c ~ 80 K can be understood as a consequence of realizing the bilayer Hubbard model comprising the $d_{3z^2-r^2}$ orbitals.

We next study the possibility of superconductivity in a trilayer nickelate $La_4Ni_3O_{10}$ [4]. We perform structural optimization calculations at high pressures, which results in tetragonal symmetry of the lattice. Using the obtained structure, the possibility of superconductivity is studied using FLEX, which shows that superconductivity with T_c comparable to that of relatively low T_c cuprates is possible. These results are compared with experiments.

References

[1] H. Sun *et al.*, Nature **621**, 493 (2023).
[2] M. Nakata *et al.*, Phys. Rev. B **95**, 214509 (2017).
[3] H. Sakakibara *et al.*, arXiv: 2306.06039.
[4] H. Sakakibara *et al.*, arXiv: 2309.09462.

Abstract ID: 1448

SUPERCONDUCTING TRANSITION BEHAVIOR OF $La_3Ni_2O_\delta$ ($\delta \sim 7$) POLYCRYSTALLINE SAMPLES WITH DIFFERENT OXYGEN CONTENT UNDER HIGH PRESSURE

Ke Wang, Qiang Hou, Sheng Li, ZhiXiang Shi

School of Physics, Southeast University, Nanjing 211189, CHINA
E-mail: wangke_1701@163.com

Recently, signatures of superconductivity near 80 K have been discovered in the single crystal of $La_3Ni_2O_{??}$ under pressure[1,2], marking it as a new candidate for high-temperature superconductors dominated by 3*d* transition elements following the cuprate and iron-based superconductors. This discovery has garnered significant attention. Subsequently, we successfully prepared $La_3Ni_2O_\delta$ ($\delta \sim 7$) samples using solid-state reaction, sol-gel and other methods, and effectively controlled the oxygen content through high oxygen pressure annealing, CaH_2 annealing, and other techniques. Resistance measurements of all samples under pressure were conducted using a diamond anvil cell (DAC). We observed that the resistance of samples prepared via different processes decreased within the range of 40-90 K. Although zero resistance was not achieved in these samples under pressure, combined with magnetic transport measurements and findings from other research teams, we provisionally confirmed that this transition represents superconducting transition. The failure to measure zero resistance may be closely related to the oxygen content. Interestingly, all our measurements exhibited resistance upwarping at low temperatures, possibly due to the localization of non-superconducting components.

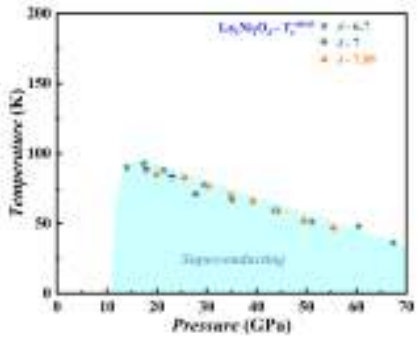

Fig. 1: *Temperature-pressure phase diagram of $La_3Ni_2O_\delta$ with different oxygen contents. Different shapes represent the superconducting transition temperature T_c^{onset} measured under different pressure.*

References

[1] Hualei Sun, *et al.*, *Signatures of superconductivity near 80 K in a nickelate under high pressure*, Nature **621. 7979**, 493-498 (2023).

[2] Jun Hou, *et al.*, *Emergence of high-temperature superconducting phase in pressurized $La_3Ni_2O_7$ crystals*, Chinese Physics Letters **40. 11**, 117302 (2023).

Superconductivity in Bi-layer Nickelates III

02.05.2024 THURSDAY

Abstract ID: 1458

EFFECTS OF OXYGEN REDUCTION ON THE SUPERCONDUCTIVITY AND Ni-3D ORBITALS OF THE INFINITE LAYER NICKELATE

Ariando

Department of Physics, National University of Singapore, SINGAPORE
E-mail: ariando@nus.edu.sg

Topotactic reduction utilizing metal hydrides as reagents emerges as a highly effective approach to achieve exceptionally low oxidization states of metal ions and unconventional coordination networks, leading to the discovery of novel physical properties in transition-metal oxides. A notable example is the discovery of superconductivity in nickelates, in which the perovskite precursor is transformed to infinite-layer structure. However, the reduction effect on the atomic reconstruction and electronic structures, which is crucial to the emergence of superconductivity in nickelates, remains largely unresolved. Here we design two sets of $Nd_{0.8}Sr_{0.2}NiO_2$ thin films, with pure infinite-layer phase and mixed phases respectively, to address the origin of reduction effect on the superconductivity. Secondary ion mass spectroscopy shows negligible hydrogen intercalation in pure infinite-layer phase, in contrast to previous observation. X-ray absorption spectroscopy shows a significant linear dichroism with dominant Ni $3d_{x2-y2}$ orbitals on superconducting samples, indicating a Ni single-band nature of infinite-layer nickelates. Superconductivity is found to manifest dome-like reduction duration dependence, consistent with the Ni 3*d* orbitals asymmetry. Our results unveil the critical role of reduction in modulating the Ni-3*d* orbital polarization and its impact on the superconducting properties.

Acknowledgement

Funding: MOE Tier 2
Collaboration: Shengwei Zeng, Chi Sin Tang, Zhaoyang Luo, Lin Er Chow, Zhi Shiuh Lim, Saurav Prakash, Ping Yang, Caozheng Diao, Xiaojiang Yu, Zhenxiang Xing, Rong Ji , Xinmao Yin, Changjian Li, X. Renshaw Wang, Qian He, Mark B. H. Breese, Huajun Liu

Abstract ID: 1473

SUPERCONDUCTING PHASE TRANSITIONS IN GRANULAR ALUMINIUM THIN FILM

R. Pervin[1,2], U.C. Thuwal[1]

[1]*Indian Institute of Techlogy Kanpur, Dept. of Physics, 208016, Kanpur, INDIA*
[2]*Beijing Institute of University, Dept. of Physics, 102401, Beijing, CHINA*
E-mail: rukshanapervin92@gmail.com

The in-plane resistivity has been measured in granular aluminium superconducting thin film. This film was grown on Si/SiO_2 substrate, and about 40 nm thickness. The in-plane conductivity induced by superconducting fluctuations above the superconducting transition (the so called in-plane conductivity $\Delta\sigma_{ab}$) was extracted from these data in the reduced temperature range $10^{-2} \leq \varepsilon \leq 1$. This $\Delta\sigma_{ab}$ (ε) was then analyzed in terms of the mean-field-like Gaussian-Ginzburg-landau (GGL) approach extended to the high-ε region by means of the introduction of a total-energy cutoff, which takes into account both the kinetic energy and the quantum localization energy of each fluctuation mode. We show that superconducting fluctuations give rise to an appreciable decrease in the resistance even at temperatures well exceeding the superconducting transition temperature, with this decease being dominated by the Aslamazov-Larkin and Maki-Thompson mechanisms. According to our comprehensive analysis of quantum contributions to conductivity, thin superconducting films exhibit non-monotonic temperature resistance because of the competition between weak localization, electron-electron interaction, and superconducting fluctuations.

References

[1] T.I. Baturina, S.V. Postolova, A.Y. Mironov, A. Glatz, M.R. Baklanov, V.M. Vinokur, EPL **97**, 17012 (2012).
[2] S. Yadav, V. Kaushik, M.P. Saravanan, S. Sahoo, Phys. Rev. B **107**, 014511 (2023).

CANCELLED

Abstract ID: 1206

EFFICIENT COOPER PAIR SPLITTING WITHOUT COULOMB BLOCKADE

E.S. Tikhonov, V.S. Khrapai

Osipyan Institute of Solid State Physics RAS, 142432 Chernogolovka, RUSSIAN FEDERATION
E-mail: etikhonov89@gmail.com

Cooper pair splitter (CPS) is a solid-state device producing spin-entangled electron pairs. The first theoretical proposal [1] suggested the use of a superconductor coupled to two normal reservoirs via Coulomb blockaded quantum dots so that Cooper pairs constituting current through the superconductor are forced to split into the different leads of the setup. Another thoroughly studied CPS candidate may be represented by hybrid NSN devices.

Operation of a CPS is described by (i) the splitting probability, p_{11}, determining the magnitude of the current of split pairs and (ii) the splitting efficiency, K, showing which part of the total superconductor current results in the separated entangled electrons. In our talk we will discuss the NSN-based realization of a CPS and how its operating characteristics are related to the scattering matrix of the device.

Fig. 1: *Left side: the system under consideration. Right side: interfering processes contributing to the splitting event.*

We study a spin-degenerate NSN device with single-mode normal terminals depicted schematically on the left side of Fig. 1. The superconducting terminal is connected to the scattering region via either single or two-mode lead. On the one hand, the average current and current fluctuations in this system may be described using the scattering matrix approach [2], on the other hand – by considering the current flow as a stochastic process with the probability p_{11} corresponding to the splitting of a Cooper pair [3]. The comparison of expressions for auto- and cross-correlators from two approaches allows us to obtain explicitly

$$p_{11}=2|s_{11}^{ee}s_{12}^{he}-s_{11}^{he}s_{12}^{ee}|^2,$$

where s_{ij}^{ab} is the amplitude of a particle of type b to be scattered from j-th to i-th terminal as a particle of type a. This expression suggests the splitting events include the two-particle interference between two processes with indistinguishable results shown on the right side of Fig. 1. The most important consequences are that (i) splitting doesn't necessarily rely on crossed Andreev reflection thus allowing for the unit efficiency at zero energy and (ii) for a given system the most negative possible cross-correlator may coexist with the largest p_{11} and K.

The work was supported by the Russian Science Foundation project 22-12-00342.

References

[1] P. Recher, E.V. Sukhorukov, D. Loss, Phys. Rev. B **63**, 165314 (2001).
[2] M. P. Anantram, S. Datta, Phys. Rev. B **53**, 16390 (1996).
[3] E.S. Tikhonov, V.S. Khrapai, e-print arXiv:2311.11954 (2023).

CANCELLED

Superconductivity in Lower Dimensions I

02.05.2024 THURSDAY

Abstract ID: 1104

IMPACT OF DISORDER IN THE CHARGE-DENSITY-WAVE STATE OF Pd-INTERCALATED $ErTe_3$ REVEALED BY THE ELECTRODYNAMIC RESPONSE

L. Degiorgi

Laboratorium für Festkörperphysik, ETH - Zürich, 8093 Zürich, SWITZERLAND
E-mail: degiorgi@phys.ethz.ch

The interplay between broken-symmetry ground states, either via competition or coexistence, belongs to the mostly explored topics of modern solid-state physics. The discovery of a charge-density-wave (CDW) phase in the middle of the pseudogap region of the high-temperature superconducting cuprates (HTC) brought into focus the intrinsic nature of those very different cooperative electronic phenomena, suggesting novel concepts such as intertwined order. However, in HTC and other materials, like the iron-based superconductors, any kind of broken-symmetry ground state also arises in the presence of significant disorder, because of the large doping required in order to destroy the phase of the parent compound. We study here the disorder-induced suppression of the in-plane CDW orders in the two-dimensional Pd-intercalated $ErTe_3$ compositions, by exploring the real part of the optical conductivity with light polarised along the in-plane *a* and *c* axes. Our findings [1] reveal an anisotropic charge dynamics (Fig. 1) with respect to both incommensurate unidirectional CDW phases of $ErTe_3$, occurring within the *ac*-plane. The anisotropic optical response gets substantially washed out with Pd-intercalation, hand-in-hand with the suppression of both CDW orders. We will show that the CDW phases evolve from a (partially) depleted Fermi surface already above their critical onset temperatures. We therefore argue that the long-range CDW orders of $ErTe_3$ tend to be progressively dwarfed by Pd-intercalation, which favours the presence of short-range CDW segments for both crystallographic directions persisting in a broad temperature (*T*) interval up to the normal state, and being suggestive of precursor effects of the CDW orders as well as possibly coexisting with superconductivity at low *T*.

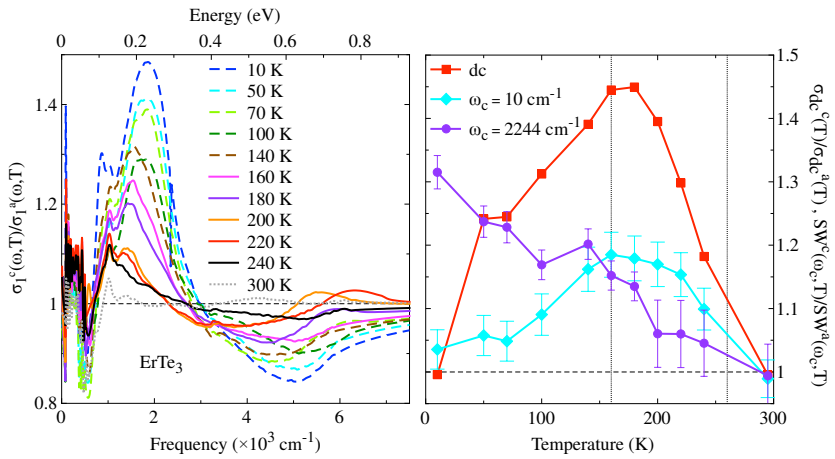

Fig. 1: *Anisotropy of the optical conductivity and of its spectral weight compared to the anisotropic dc transport properties of $ErTe_3$.*

Reference

[1] M. Corasaniti *et al.*, Phys. Rev. Research **5**, 033140 (2023).

Abstract ID: 1414

VOLTAGE FLUCTUATIONS IN A SYSTEM OF CAPACITIVELY COUPLED SUPERCONDUCTING NANOWIRES

A. Latyshev[1,2], A.G. Semenov[2,3], A.D. Zaikin[2,3]

[1]*Departement de Physique Theorique, Universite de Geneve, CH-1211 Geneve, SWITZERLAND*
[2]*National Research University Higher School of Economics, 101000 Moscow, RUSSIA*
[3]*I.E. Tamm Department of Theoretical Physics, P.N. Lebedev Physical Institute, 119991 Moscow, RUSSIA*
E-mail: Aleksandr.Latyshev@unige.ch

In the present work, we explored the interplay between quantum phase slips (QPS) phenomena and the transport properties within a system comprising two capacitively coupled ultrathin superconducting wires. Our findings revealed that QPS events in one of the coupled wires can induce voltage fluctuations in both wires, manifesting as dynamic voltage pulses propagating through the first and second wires. Our investigation established the presence of two plasma modes in such structures, each propagating at different velocities along the wires. We precisely determined these velocities and demonstrated that these plasma modes are identical for both wires, creating a unified dissipative quantum environment that interacts with electrons within the structure [1].

The implications of our results extend to the low-temperature transport properties of coupled superconducting nanowires. Notably, our findings highlight specific characteristics of voltage fluctuations induced in the second wire by a QPS event in the first wire: these fluctuations exhibit zero average voltage and non-zero voltage noise [2]. In particular, non-equilibrium voltage noise in the second wire at non-zero frequencies remains non-zero and non-trivially depends on the external bias current flowing in the first wire.

References

[1] A. Latyshev, A.G. Semenov, A.D. Zaikin, Beilstein Journal of Nanotechnology, **№. 1**, 292-297 (2022).

[2] A. Latyshev, A.G. Semenov, A.D. Zaikin, Journal of Superconductivity and Novel Magnetism, **№. 8**, 2329-2334 (2020).

Abstract ID: 1425

SUPERCONDUCTIVITY INDUCED BY EXTREMELY SMALL AMOUNT OF Li IN $SnSe_2$

Daniel Duong[1], Jie Xing[1], Eklavya Thareja[2], Silu Huang[1], Scott Crittenden[1], Williams A. Shelton[2], Rongying Jin[1]

[1]*Center for Experimental Nanoscale Physics, Department of Physics and Astronomy, University of South Carolina, Columbia, SC 29208, USA*
[2]*Department of Physics and Astronomy, Louisiana State University, Baton Rouge, LA 70803, USA*
E-mail: rjin@mailbox.sc.edu

Unconventional superconductivity often occurs in materials with low dimensionality. We report unusual superconductivity observed in layered Li_xSnSe_2 with T_c ~ 6 K, which is realized by Li^+ intercalation in semiconducting $SnSe_2$. Single crystal x-ray diffraction, Hall effect, and first-principle calculations indicate that the Li concentration x is less than 2×10^{-4}, which is at least two orders lower than the required superconductivity onset condition. More surprisingly, superconductivity is observed in both in-plane and out-of-plane directions with the superconducting anisotropy ~ 2.2 estimated from the coherence lengths. The implication of these results will be discussed.

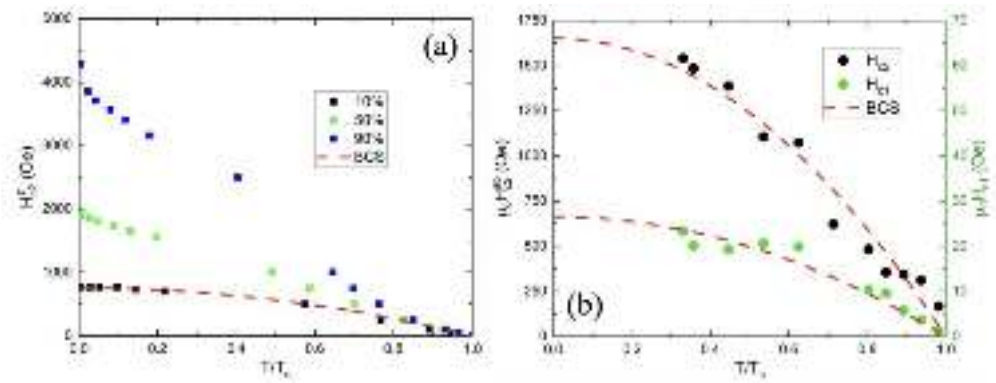

Fig. 1: ***Phase diagrams of superconducting Li_xSnSe_2:*** *(a) magnetic field along the c direction and (b) magnetic field along the ab plane.*

Abstract ID: 254

TRANSPORT OF NON-EQUILIBRIUM QUASIPARTICLES IN A SUPERCONDUCTOR

Konstantin Yu. Arutyunov[1,2], Anatoly S. Gurskiy[1], Dmitry L. Shapovalov[2]

[1]HSE University, 101000, Moscow, RUSSIA
[2]P. L. Kapitza Institute for Physical Problems RAS, 119334, Moscow, RUSSIA
E-mail: asgurskiy@edu.hse.ru

Advances in technology are leading to increased miniaturization of electronic components. However, this progress entails the emergence of new problems associated with heat dissipation per unit volume and the necessity to take into account various quantum effects. One of the potential solutions of the described problems is the utilization of hybrid structures based on superconductors, which are already actively used in a wide variety of applications: from medical field to quantum computing. Although utilization of superconductors has many advantages, such as non-dissipative electric current leading to zero heat generation, new aspects arise related to mandatory cryogenics and new physics. One of the factors hindering the development of some superconducting nanoelectronics devices, for instance, superconducting qubits, single-electron transistors, microrefrigerators, is the presence of non-equilibrium quasiparticles even at temperatures much lower than the superconducting transition temperatures [1,2]. That is why it is relevant to study non-equilibrium quasiparticle relaxation in hybrid superconducting systems of mesoscopic dimensions, where the entire sample can be considered as an 'interface'. Initial studies considered sandwich-type systems at temperatures near the critical temperature of the superconductor [3]. Later works made it possible to obtain spatial resolution of non-equilibrium relaxation processes in hybrid structures based on superconductors [4-7]. Here we report the results of our recent experiments indicating the presence of coherent non-equilibrium transport in normal metal-insulator – superconductor nanostructures representing the solid-state analogue of a 'double-slit' optical interferometer. The work was supported by Russian Science Foundation project No. 23-72-00018.

References

[1] K.M. Lang, S. Nam, J. Aumentado, C. Urbina, J.M. Martinis, IEEE Transactions on Applied Superconductivity **13**, 989–993 (2003).
[2] K. Serniak *et al.*, Phys. Rev. Lett. **121**, 157701 (2018).
[3] M. Tinkham, J. Clarke, Phys. Rev. Lett. **28**, 1366–1369 (1972).
[4] R. Yagi, Phys. Rev. B **73**, 134507 (2006).
[5] T.E. Golikova *et al.*, Phys. Rev. B **89**, 104507 (2014).
[6] K. Yu. Arutyunov, H.-P. Auraneva, A.S. Vasenko, Phys. Rev. B **83**, 104509 (2011).
[7] K. Yu Arutyunov *et al.,* J. Phys. Condens. Matter **30**, 343001 (2018).

Superconductivity in Lower Dimensions II

03.05.2024 FRIDAY

Abstract ID: 1068

JOSEPHSON DYNAMICS AT HIGH TRANSMISSIONS: PERTURBATION THEORY

A.V. Galaktionov[1], A.D. Zaikin[2,3]

[1]I.E. Tamm Department of Theoretical Physics, P.N. Lebedev Physical Institute, 119991 Moscow, RUSSIA
[2]Karlsruhe Institute of Technology, 76021, Karlsruhe, GERMANY
[3]Higher School of Economics, National Research University, 101000 Moscow, RUSSIA
E-mail: andrei.zaikin@kit.edu

We theoretically analyze Josephson dynamics of superconducting weak links with transmissions T not much smaller than unity at subgap bias voltages V . Employing the effective action approach combined with the Keldysh technique, we develop a regular perturbation theory in $R = 1 - T$ and derive the first-order correction to the current across the weak link, which consists of two different contributions. One of them is negative, effectively corresponding to a decrease of the excess current at small V due to breaking of the multiple Andreev reflection cycle by normal reflection for some subgap quasiparticles. These quasiparticles, in turn, generate the second (Josephson-like) contribution to the current, which increases with decreasing V down to very small voltages, where the perturbation theory in R ceases to be valid. Some of the above features are not reproduced within the physical picture involving Landau-Zener tunneling between subgap Andreev states [1].

Reference

[1] A.V. Galaktionov, A.D. Zaikin, Phys. Rev. B **107**, 214507 (2023).

Abstract ID: 1080

MECHANISM OF QUANTUM PHASE TRANSITIONS IN ONE- AND TWO-DIMENSIONAL SUPERCONDUCTORS: MICROSCOPIC SCALE AND NATURE OF CRITICAL FLUCTUATIONS

A. Rogachev, S. Feldman, K. Davenport

University of Utah, Dept. of Physics and Astronomy, 84112, Salt Lake City, Utah, USA
E-mail: rogachev@physics.utah.edu

We show that the pair-breaking mechanism gives a unifying and consistent description of magnetic-field driven quantum phase transitions (QPTs) in amorphous MoGe, Pb and TaN films as well as in high-temperature superconductor $La_{1.92}Sr_{0.08}CuO_4$ and 1d MoGe nanowires [1]. The pair-breaking QPT occurs only in the superconducting part of the system and, at the critical point, is masked by the dominant non-critical contribution of normal electrons. In all systems, the correlation scale exponent is the same, $\nu \approx 1$. The discovery was facilitated by the development of a novel theoretical approach, which allows (from the slope of the scaled data shown in the figure) the extraction of a microscopic seeding length scale, L_0, and dephasing length, L_φ, controlling the transitions. We found that L_0 matches the superconducting coherence length and L_φ the thermal length, thus identifying the critical fluctuations to be of Aslamazov-Larkin type involving both amplitude and phase of order parameter. Using the same generic model, we found that in the "phase-only" QPT in 1d array of Josephson junction SQUIDs (panel c in the figure), L_φ is given by the distance travelled by superconducting plasmons over the Planckian time and L_0 by Cooper pair screening length. This approach has also been successfully applied to many other QPTs in complex, non-superconducting systems [2,3].

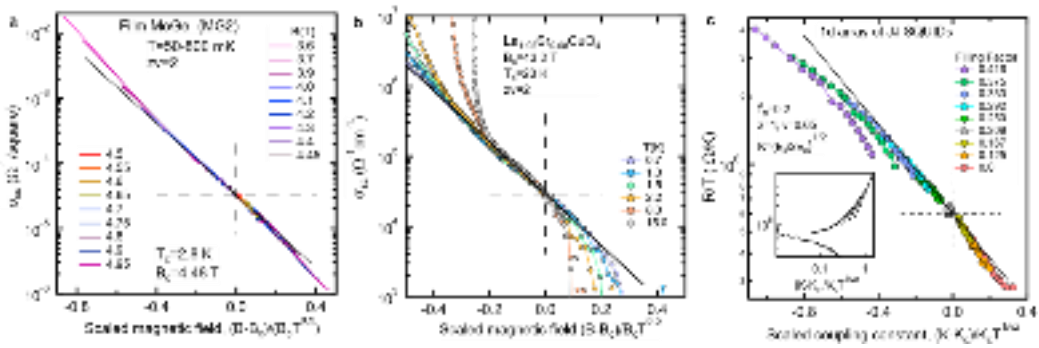

Fig. 1: *(a) Conductivity of the superconducting subsystem versus scaled magnetic field for amorphous MoGe film. (b) The same plot for $La_{1.92}Sr_{0.08}CuO_4$. (c) Scaled resistance versus scaled normalized coupling constant for 1d array of 100 JJ SQUIDs. The data in all panel display roughly exponential variation. Solid lines indicate the fit from which* L_0 was determined.

References

[1] A. Rogachev, S. Feldman, K. Davenport, *Microscopic scale of pair-breaking quantum phase transitions in superconducting films, nanowires and $La_{1.92}Sr_{0.08}CuO_4$*, e-print arXiv:2309.00747 (2023).

[2] A. Rogachev, *Microscopic scale of quantum phase transition: from doped semiconductors to spin chains, cold gases and moiré superlattices*, e-print arXiv:2309.00749 (2023).

[3] A. Rogachev, *Quantum phase transitions in quantum Hall and other topological systems: role of the Planckian time*, e-print arXiv:2309.00747 (2023).

Abstract ID: 1329

QUASIPARTICLE RESPONSE IN SEMICONDUCTOR-SUPERCONDUCTOR NSN STRUCTURES

Vadim Khrapai

Osipyan Institute of Solid State Physics RAS, 142432, Chernogolovka, RUSSIAN FEDERATION
E-mail: dick@issp.ac.ru

Influence of induced superconductivity on the subgap quasiparticle response attracts significant fundamental interest recently, mainly in relation to the physics of Majorana zero modes [1], generation of entanglement in Cooper-pair splitters [2], charge conversion into heat [3] and nonequilibrium superconductivity [4,5]. Hybrid semiconductor-superconductor structures with a pair of normal and one superconducting contact (NSN) are perhaps best suited for studying these questions. For example, in non-local transport mode [6], one of the normal terminals can be used as a source, and the second one as a detector of quasiparticles. Or in Cooper splitting mode, when both N-terminals act as absorbers of entangled electrons from a decayed pair. The presence of Andreev reflection from the superconductor makes characterization of the quasiparticle response a nontrivial problem. The fact is that such a response consists of a superposition of electron and hole excitations and in the general case cannot be completely characterized using just one transport measurement (conductance or resistance).

In this talk I will discuss how measuring spontaneous fluctuations of electric current complements transport measurements, thereby allowing to understand the electrical and thermal response of quasiparticles at sub-gap energies [3]. How quasiparticle nonequilibrium affects the superconducting order parameter and what is the role of electron-phonon relaxation here [4, 6]. Finally, I might have time to briefly talk about the recently proposed model NSN configuration - the Bogoliubov interferometer – allowing to control such effects by means of the Aharonov-Bohm phase in quantum Hall regime [7].

References

[1] A.R. Akhmerov, J.P. Dahlhaus, F. Hassler, *et al.*, Phys. Rev. Lett. **106**, 057001 (2011).
[2] G. Wang, T. Dvir, G.P. Mazur, *et al.*, Nature 612, 448 (2022); A. Bordoloi, V. Zannier, L. Sorba, *et al.*, Nature **612**, 454 (2022); Z.B. Tan, A. Laitinen, N.S. Kirsanov, *et al.*, Nat Commun **12**, 138 (2021).
[3] A.O. Denisov, A.V. Bubis, S.U. Piatrusha, *et al.*, Super. Sci. Technol. **36**, 09LT04 (2021); Nanomaterials **12**, 1461 (2022).
[4] A.V. Bubis, E.V. Shpagina, A.G. Nasibulin, V.S. Khrapai, Phys. Rev. B **104**, 125409 (2021).
[5] A. Ibabe, M. Gómez, G.O. Steffensen, *et al.*, Nat Commun **14**, 2873 (2023).
[6] D. Puglia, E.A. Martinez, G.C. Ménard, *et al.*, Phys. Rev. B **103**, 235201 (2021).
[7] E.V. Shpagina, E.S. Tikhonov, D. Ruhstorfer, *et al.*, arXiv 2311.10676 (2023).
[8] V. Khrapai, Phys. Rev. B **107**, L241401 (2023).

CANCELLED

Superconductivity in Lower Dimensions III

03.05.2024 FRIDAY

Abstract ID: 1317

OBSERVATION OF THE CURRENT STEPS IN JOSEPHSON JUNCTIONS UNDER MICROWAVE RADIATION

V.N. Antonov[1,2], R.S. Shaikhaidarov[1,2], O.V. Astafiev[3,4]

[1]*Physics, Royal Holloway University of London, Egham, Surrey, TW20 0PN, UK*
[2]*National Physical Laboratory, Teddington, TW11 0LW, UK*
[3]*Skolkovo Institute of Science and Technology, 121205, Moscow, RUSSIA*
[4]*Moscow Institute of Physics and Technology, Dolgoprudny, 141701, RUSSIA*
E-mail: O.Astafiev@skoltech.ru

Thirty years ago, it has been predicted that current steps should be induced in transport characteristics of small Josephson junctions illuminated by microwave radiation [1]. The steps are results of synchronization of the Bloch-oscillations with the microwaves and are equal to the Cooper charge multiplied by the microwave frequency and integer. Similar steps have been earlier observed in superconducting nanowires [2]. One of the key elements for the observation was high but compact inductance in series with the nanowires. Now, we succeed in the step demonstration in Josephson junctions instead of the wire. The Josephson junction is embedded in the high impedance environment with the inductances similar to the experiments with nanowires. Without microwave irradiation, current blockade coexists with an apparent supercurrent (Fig. 1(a)). When microwave is turned-on, current steps are induced, as it is shown in Fig. 1(b). In addition, we characterize a large number of different junctions and find the conditions for the effect observation. One limitation is related to the Landau-Zener tunneling to higher states. The work is a big progress because previously only a signature of the steps has been observed in the differential I-V characteristics [3]. The finding can be used for building current standards, which is very important for metrology. The Josephson junctions make the device fabrication easier and reproducible, comparing to the devices with nanowires.

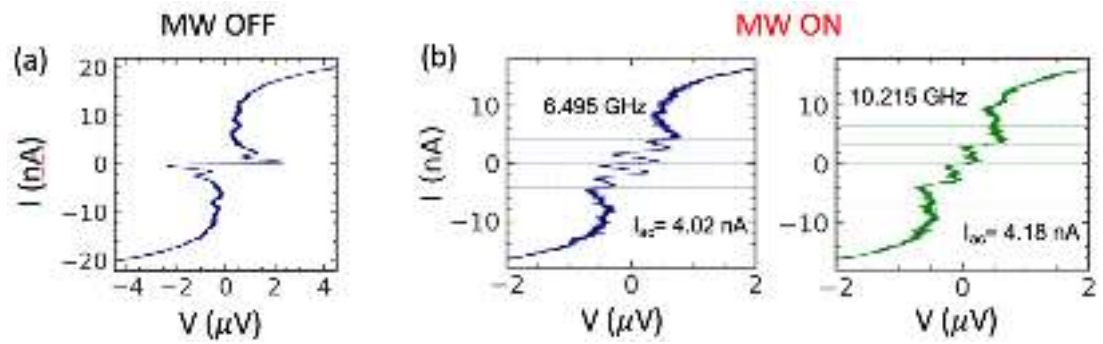

Fig. 1: *I-V characteristics: (a) without microwave; (b) with microwave at two different frequencies.*

References

[1] D.V. Averin, A.B. Zorin, K.K. Likharev. Sov. Phys. JETP **61**, 407 (1985).
[2] R.S. Shaikhaidarov, K.H. Kim, J.W. Dunstan, I.V. Antonov, S. Linzen, M. Ziegler, D.S. Golubev, V.N. Antonov, E.V. Il'ichev, O.V. Astafiev. Nature **608**, 45 (2022).
[3] L.S. Kuzmin, D.B. Haviland. Phys. Rev. Lett. **67**, 2890 (1991).

Abstract ID: 1318

DRAG EFFECT IN CAPACITIVELY COUPLED JOSEPHSON JUNCTIONS AND THIN SUPERCONDUCTING NANOWIRES

Alex Latyshev[1], Andrew G. Semenov[2,3], Andrei D. Zaikin[2,4]

[1]*Universite de Geneve, CH-1211, Geneve, SWITZERLAND*
[2]*P.N. Lebedev Physical Institute, 119991, Moscow, RUSSIA*
[3]*Skolkovo Institute of Science and Technology, 121205, Moscow, RUSSIA*
[4]*Higher School of Economics, 101000, Moscow, RUSSIA*
E-mail: an.semenov@skoltech.ru

It is well known that if two thin metallic films are placed at a short distance from each other, then the Coulomb drag effect will occur in the system. It manifests in the appearance of a current in one of the films when a voltage is applied to another one. And conversely, voltage drop generated in the second film if the first one is current biased. This happens due to the Coulomb interaction between electrons in different films.

In the talk we will present our recent results [3] in the investigation of the similar drag effect in electrostatically coupled quasi-one-dimensional superconductors (Q1DS) [1] and Josephson junctions (JJ). In this case, the phenomenon is in the appearance of a voltage drop in first system (Q1DS or JJ) when current is passed through the another one. It turns out that quantum phase slips play a key role in this effect. Moreover in our talk we will argue that the drag effect is deeply connected with the fluxon cotunneling in both Q1DSs and JJs [2,3].

References

[1] A.G. Semenov, A.D. Zaikin, Phys. Usp. **65**, 883 (2022).
[2] A. Latyshev, A.G. Semenov, A.D. Zaikin, Condensed Matter **8**, 5 (2023).
[3] A. Latyshev, A.G. Semenov, A.D. Zaikin, preprint (2024).

Abstract ID: 233

NONLINEAR MICROWAVE RESPONSE OF CLEAN SUPERCONDUCTING FILMS

A.A. Radkevich[1], A.G. Semenov[1,2]

[1]*I. E.Tamm Department of Theoretical Physics, P. N. Lebedev Physical Institute, 119991 Moscow, RUSSIA*
[2]*Skolkovo Institute of Science and Technology, Moscow 121205, RUSSIA*
E-mail: radkevich@lpi.ru

Over the last decade, the response of a superconductor to an applied electromagnetic field has gained a lot of attention as a result of the experimental progress in the field of Terahertz (THz) spectroscopy. We develop an explicitly gauge-invariant semiclassical approach suitable for the calculation of the high-order response which automatically respects charge conservation. We apply this approach to investigate the nonlinear response of a thin clean superconducting film to monochromatic THz radiation and show that clean superconductors with quadratic electron spectrum do not exhibit nonlinear response to uniform fields. We specifically address the photoinduced electric current and find that it exhibits a strong dependence on the incidence angle and the polarization of the electromagnetic wave. A major simplification of perturbative expansion of the spatially-uniform photoinduced current valid for a wide class of translationally-invariant systems is found.

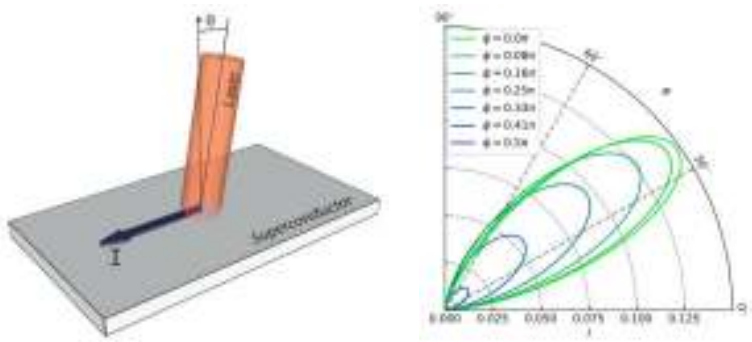

Fig. 1: *Left panel: Schematic depiction of the system under consideration. A large quasi-two-dimensional superconducting film subject to monochromatic electromagnetic plane wave falling at an incidence angle θ. Right panel: Dependence of the second-order photoinduced current I on the incidence angle θ for different angles φ in the limit c → ∞. At φ = 0 the incident wave is transverse magnetically (TM) polarized, while at φ = π / 2 the polarization is transverse electric (TE).*

References

[1] A.A. Radkevich, A.G. Semenov, *Nonlinear microwave response of clean superconducting films*, Phys. Rev. B **106**, 094505 (2022).

Nonuniform Magnetic Textures VI

03.05.2024 FRIDAY

Abstract ID: 1389

ZERO-FIELD SPIN WAVE TURNS

Jan Klíma[1], Ondřej Wojewoda[2], Václav Roučka[1], Tomáš Molnár[2], Jakub Holobrádek[2], Michal Urbánek[1,2]

[1]*Faculty of Mechanical Engineering, Institute of Physical Engineering, Brno University of Technology, Technická 2, Brno, 616 69, CZECH REPUBLIC*
[2]*CEITEC BUT, Brno University of Technology, Purkyňova 123, Brno, 612 00, CZECH REPUBLIC*
E-mail: ondrej.wojewoda@vutbr.cz

The magnon-based computing is one of the promising candidates to complement and surpass CMOS-based technologies [1]. Lot of spin-wave-based logic devices, such as a magnon transistor [2], various types of gates [3] or adders [4] have already been demonstrated experimentally. However, the integration of these devices to complex magnonic circuits is cumbersome, because the spin waves have anisotropic dispersion relation. E.g. the steering of the spin wave to 90 degrees corner is still a major challenge [5].

We tackled this challenge by locally controlled effective field, which stabilizes the magnetization of different parts of the magnonic circuit in the desired direction. By carful design, we can match both, spin-wave group velocity and frequency. This will prevent reflection and energy dissipation. In the presented experiments we employ corrugation of the waveguides to locally control the effective field. This is achieved by sinusoidal modulation of the substrate on which the magnetic wave is deposited. The surface curvature in the films locally modifies the contributions of dipolar and exchange energies and can be described as an effective uniaxial anisotropy term that is perpendicular to the corrugation direction [6]. Using this approach, one can design non-trivial magnonic circuits functioning without the need for an external magnetic field and pave the way towards complex magnonic circuits and all-magnon data processing.

References

[1] A.V. Chumak *et al.*, IEEE Trans. Magn. **58**, 6 (2022).
[2] A.V. Chumak *et al.*, Nat. Commun. **5**, 4700 (2014).
[3] T. Schneider *et al.*, Appl. Phys. Lett. **92**, 022505 (2008).
[4] U. Garlando *et al.*, IEEE Trans. Emerg. Top. Comput. (2023).
[5] K. Vogt *et al.*, Appl. Phys. Lett. **101**, 042410 (2012).
[6] I. Turčan *et al.*, Appl. Phys. Lett. **118**, 092405 (2021).

Abstract ID: 1143

REALIZATION OF MAGNETIC CIRCUITS EXPLOITING EXCHANGE AND CHIRAL LATERAL COUPLINGS

Aleš Hrabec[1,2]

[1] *Laboratory for Mesoscopic Systems, Department of Materials, ETH Zurich, 8093 Zurich, SWITZERLAND*
[2] *Laboratory for Multiscale Materials Experiments, Paul Scherrer Institute, 5232 Villigen PSI, SWITZERLAND*
E-mail: ales.hrabec@psi.ch

In order to go beyond traditional CMOS logic technology, novel spin-based logic architectures are being developed to provide high-performance nonvolatile data retention and processing. Such a new technology is based on strong magnetic couplings in vertical stacks. Due to the nature of these couplings, their implementation in lateral devices is very limited. We have recently developed two new lateral couplings based on (i) the Dzyaloshinskii–Moriya interaction (DMI) in systems with non-uniform anisotropy [1] and (ii) on the exchange interaction in ferrimagnetic films [2], which significantly boost the possibility to design novel planar magnetic circuits.

The first concept exploits the chiral coupling mechanism between adjacent magnets where the non-collinear magnetic anisotropy competes with the interfacial DMI in Pt/Co/AlOx trilayers [3-5]. When an in-plane (IP) magnetized region is fabricated next to an out-of-plane (OOP) magnetized region, as illustrated in Fig. 1(a), the adjacent magnetic moments are coupled in a chiral manner. The chiral IP-OOP structure can be implemented in a domain wall inverter, the essential building block for all implementations of Boolean logic. Based on this principle, we realized reconfigurable NAND and NOR logic gates, making our concept for current-driven DW logic functionally complete [6-8].

The second coupling makes use of the strong lateral coupling mechanism in a single GdCo ferrimagnetic layer relying on the exchange interaction [2], shown in Fig. 1(b). This interaction is achieved by spatially patterning the compensation temperature of the ferrimagnet. We have shown that the strength of the interaction can be manipulated by tuning the geometrical parameters. We also implemented this interaction in devices to demonstrate electrical switching of compensated ferrimagnetic domains utilizing spin-orbit torques.

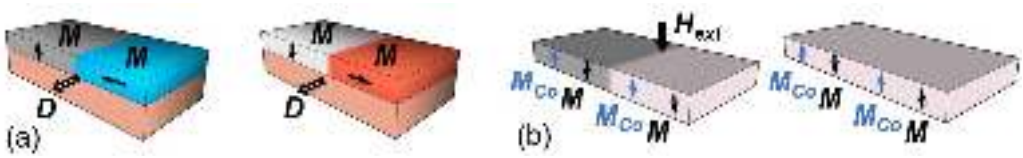

Fig. 1: *Lateral magnetic couplings effective in films with patterned magnetic properties. (a) Chiral coupling between out-of-plane and in-plane magnetized regions mediated via DMI. (b) Exchange coupling between two regions of a ferrimagnet, in light and dark gray, with compensation temperatures above and below room temperature, respectively. On application of a field (left), the magnetization (in black) prefers parallel orientation. When the field is removed, the preferred parallel orientation of the Co sub-lattice (in blue) then results in an effective antiparallel coupling of the net magnetization vectors.*

References

[1] Z. Luo, *et al.* Science **363**, 1435 (2019).
[2] Z. Liu, *et al.* Phys. Rev. B **107**, L100412 (2023).
[3] A. Hrabec, *et al.* Appl. Phys. Lett. **115**, 130503 (2020).
[4] P.D. Dao, *et al.* Nano Lett. **19**, 5930 (2019).
[5] Z. Liu, *et al.* Phys. Rev. Appl. **16**, 054049 (2021).
[6] Z. Luo, *et al.* Nature **579**, 214-218 (2020).
[7] Z. Luo *et al.* Phys. Rev. Appl. **15**, 034077 (2021).
[8] Z. Zeng *et al.*, Appl. Phys. Lett. **118**, 222405 (2021).

Abstract ID: 1375

TOPOTRONICS WITH MAGNETIC TOPOLOGICAL MATERIALS

O.A. Tretiakov

School of Physics, University of New South Wales, 2052, Sydney, AUSTRALIA
E-mail: o.tretiakov@unsw.edu.au

I will discuss topological magnetic textures, such as skyrmions, half-skyrmions (merons), bimerons and their anti-particles, which constitute tiny whirls in the magnetic order. They are promising candidates as information carriers for next generation electronics (thus called topotronics), as they can be efficiently propelled at very high velocities employing current-induced spin torques [1]. First, I will talk about skyrmions [2,3] and bimerons [4,5] in ferromagnetic systems coupled to heavy metals and topological materials. Then I will show that antiferromagnets can also host a variety of these textures, which have gained significant attention because of their potential for terahertz dynamics, deflection free motion [6], and improved size scaling due to the absence of stray field. Finally, I will demonstrate that topological spin textures, merons and antimerons, can be generated at room temperature and reversibly moved using electrical pulses in thin film CuMnAs, a semimetallic antiferromagnet that is a test-bed system for spintronic applications [7].

References

[1] B. Göbel, I. Mertig, O.A. Tretiakov, Phys. Rep. **895**, 1 (2021).
[2] D. Kurebayashi, O.A. Tretiakov, Phys. Rev. Research **4**, 043105 (2022).
[3] M.-G. Han, F. Camino, P.A. Vorobyev, J. Garlow, R. Rov, T. Söhnel, J. Seidel, M. Mostovoy, O.A. Tretiakov, Y. Zhu, Nano Lett. **23**, 7143 (2023).
[4] B. Göbel, A. Mook, I. Mertig, O.A. Tretiakov, Phys. Rev. B **99**, 060407(R) (2019).
[5] K. Ohara, ..., O.A. Tretiakov, *et al.*, Nano Lett. **22**, 8559 (2022).
[6] J. Barker, O.A. Tretiakov, Phys. Rev. Lett. **116**, 147203 (2016).
[7] O.J. Amin, ..., O.A. Tretiakov, K.W. Edmonds, P. Wadley, Nature Nano. **18**, 849 (2023).

CANCELLED

Nonuniform Magnetic Textures VII

03.05.2024 FRIDAY

Abstract ID: 1137

DIPOLAR-STABILIZED SKYRMIONS AND ANTISKYRMIONS IN MAGNETIC MULTILAYERS

M. Albrecht

University of Augsburg, Institute of Physics, 86135, Augsburg, GERMANY
E-mail: manfred.albrecht@physik.uni-augsburg.de

Topologically protected nontrivial spin-textures such as skyrmions are very promising for the next generation of spintronic devices [1]. Magnetic skyrmions can be hosted in different magnetic systems relying on distinct stabilization mechanisms. Skyrmions are most commonly stabilized in systems, where the inversion symmetry is broken due to the presence of Dzyaloshinskii-Moriya interaction. Another mechanism that leads to the formation of skyrmions is the competition between the long-range ordered dipolar interaction, perpendicular magnetic anisotropy and the short-ranged exchange interaction. Recently, we have shown the possibility to stabilize skyrmions and antiskyrmions in Gd/Fe based multilayers [2], as presented in the Lorentz transmission electron microscope (LTEM) image of Fig. 1. With micromagnetic simulations, we confirmed our observations and concluded that the reduction of saturation magnetization and uniaxial magnetic anisotropy leads to the existence of this zoo of different spin objects and that they are primarily stabilized by dipolar interactions.

In a further study, we have recently observed higher-order skyrmions and antiskyrmions of arbitrary topological charge at room temperature in a Co/Ni multilayer system. This system exhibits a high number of vertical Bloch lines, which are essential to the formation of these novel higher-order skyrmions and antiskyrmions if exposed to an out-of-plane magnetic field. The observed coexistence of different topological protected spin objects provides great potential for further studies on quasi-particle interactions, spin dynamics as well as for possible future applications.

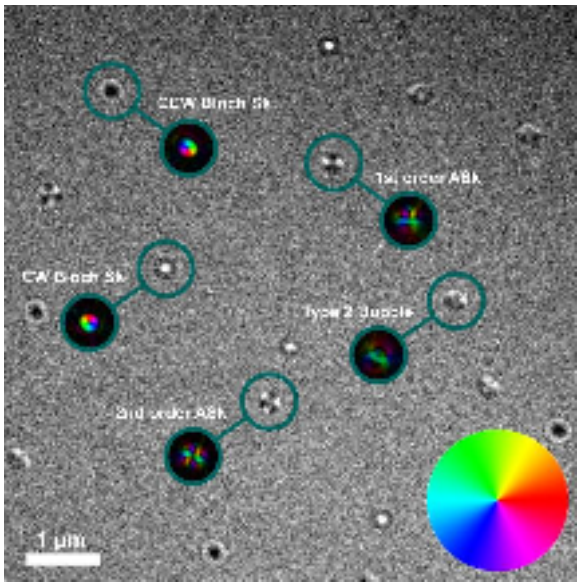

Fig. 1: *LTEM image revealing various spin objects at room temperature in an out-of-plane magnetic field of 100 mT. Extracted induction maps showing the spin texture and its orientation (color wheel) are artificially positioned next to the corresponding spin objects.*

References

[1] C. Back *et al.*, J. Phys. D: Appl. Phys. **53**, 363001 (2020).
[2] M. Heigl *et al.*, Nat. Commun. **12** (2021).

Abstract ID: 217

REVERSIBLE TOPOLOGICAL TRANSFORMATION OF SKYMIONS AND TRIVIAL BUBBLES

T. Schmidt[1], S. Koraltan[2], M. Albrecht[1]

[1]*University of Augsburg, 86159, Augsburg, GERMANY*
[2]*University of Vienna, 1010, Vienna, AUSTRIA*
E-mail: timo.schmidt@physik.uni-augsburg.de

Magnetic skyrmions and type-2-bubbles represent topologically distinct spin textures that have garnered significant attention in the field of condensed matter physics due to their unique properties and potential applications in information storage and processing. While these objects can be stabilized in a wide variety of materials by different mechanisms, this work focusses on dipolar stabilized spin textures in amorphous Fe/Gd-multilayer thin films. These systems are sputter-deposited on SiN-membranes.

Using Lorentz transmission electron microscopy (LTEM) round spin textures can be imaged as they nucleate from the stripe domain state by applying a magnetic field in out-of-plane direction. We observe distinct locations on the membrane where certain types of spin objects are stabilized predominantly and attribute this to the wrinkling of the membrane. Due to this wrinkling, which originates in the sample manufacturing process, there are intrinsically tilted regions on the membrane, resulting in an effective in-plane field component. Tilting of the whole sample in the range of up to 18° shows, that by changing the contribution of the ip-field, topologically trivial type-2-bubbles can be transformed into topologically protected skyrmions and vice versa.

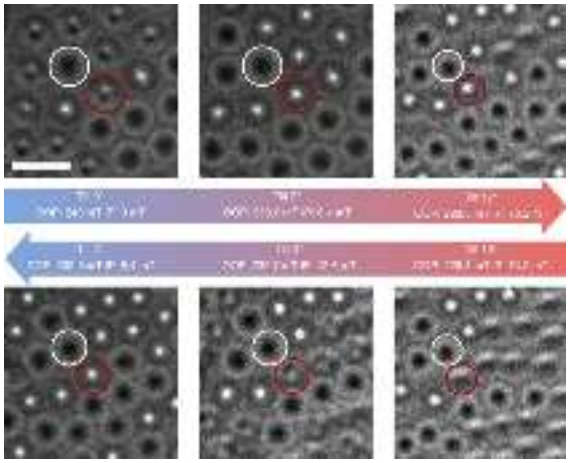

Fig. 1: *LTEM tilting series at -2 mm defocus and an applied OOP-field of 240 mT. The spin object circled in red undergoes transformations based on the tilt angle and the resulting OOP- and IP-field distribution.*

References

[1] S.A. Montoya, Phys. Rev. B **95**, 024415 (2017).
[2] M. Heigl, S. Koraltan, Nat. Commun. **12**, 2611 (2021).
[3] L. Kong, Phys. Rev. B **107**, 174425 (2023).

Abstract ID: 1320

TUNABLE MAGNETIC EQUILIBRIUM CONFIGURATIONS IN DIPOLAR HELICES

Ot Garcés, Òscar Iglesias

Dpt. de Física de la Matèria Condensada and IN2UB, Univ. de Barcelona, Martí i Franquès 1, 08028 Barcelona, SPAIN
E-mail: oscariglesias@ub.edu

The role that geometry and topology play in emergent order parameters has become an important topic in theoretical and experimental studies in different areas of physics [1]. A general theoretical framework to describe statics and dynamics of curved magnetic wires and surfaces has been developed recently, providing a starting point to study magnetization configurations in curvilinear structures [2]. New terms such as induced effective anisotropies and emergent DM interactions appear as a consequence of curvature, which are responsible for magnetochiral effects, not present in the conventional cases. In this work, we have particularized the study to anti- and ferromagnetic (FM) helices, that are the simplest curves with constant κ and τ. By performing atomistic Monte Carlo simulations, we have validated the micromagnetic theoretical framework that predicts stable magnetization transitions between quasi-tangential (QT) to onion-like configurations [2]. Varying the curvature κ (or radius R) and torsion τ (or pitch p), we have obtained phase diagrams for the FM and AF cases for different kinds of anisotropies, extending them beyond the limits of application of the micromagnetic model. In a second part of the work, we will study the effects of curvature in systems where exchange determines the global magnetization direction, but the global magnetic order is dominated by dipolar interactions. This is the case of nanoparticle assemblies, colloidal magnets, magnetic beads or molecular clusters, that can be treated as magnetic macro-dipoles [3]. We will show that in dipolar helices a rich variety of equilibrium configurations can be reached by tuning the angle between consecutive dipoles. They include QT states, entwined head-to-tail magnetic helices that have a periodicity different from the generative helix and FM or AF ordered chains along the helix axis. Varying the radius or the pitch, abrupt transitions between states having zero and sizable net magnetization can be induced, which could be achieved experimentally by applying stress to the helix ends and be used as magneto-mechanic sensors.

Work supported by Spanish MINECO (PID2021-127397NB-I00), Catalan DURSI (2021SGR0032) and EU FEDER funds (Una manera de hacer Europa) also CSUC for supercomputer facilities.

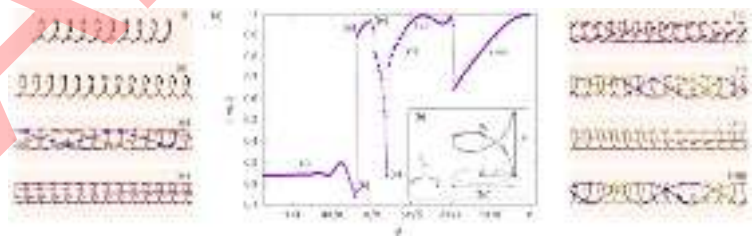

Fig. 1: *Ground states of a dipolar helix (R=1, p=π/2) and their staggered magnetization along the helix axis.*

References

[1] C. Donnelly *et al.*, Nature Nanotechnol. **17**, 136 (2022).
[2] D.D. Sheka *et al.*, Small **18**, 2105219 (2022); Phys. Rev. B **92**, 054417 (2015).
[3] I. Stankovic, *et al.*, Nanoscale **11**, 2521 (2019); A. Edström, *et al.*, Phys. Rev Lett. **128**, 177202 (2022).

CANCELLED

Abstract ID: 1361

SYNTHESIS, STRUCTURAL AND MAGNETIC PROPERTIES OF $Cu_xMn_{1-x}Fe_2O4$ NANOPARTICLES

P.P. Majozi, J.Z Msomi, S.J.C Masuku

Walter Sisulu University, Dept. of Chemical and Physical Sciences, P/Bag X01, 5117, Mthatha Eastern Cape, SOUTH AFRICA
E-mail: jmsomi@wsu.ac.za

The structural and the magnetic properties of the nanosized $Cu_xMn_{1-x}Fe_2O_4$ ($0 \leq x \leq 1$) compounds with particles size between 8 nm and 22 nm produced by glycol-thermal reaction are reported. X-ray diffraction (XRD) data reveal cubic spinel phase. The lattice parameter reduces with increasing Cu content according to the Vegard's law. An increase in the X-ray density as a function of composition observed is attributed to the strengthening effect of Cu atoms. SQUID measurements show superparamagnetic nature of the fine particles with blocking temperature of about 125 K. FC and ZFC data are indicative spin-glass behaviour and bifurcation temperature of about 257 K. The enhancement of coercive fields and saturation magnetization with reducing temperature observed can be explained by spin freezing.

CANCELLED

Spintronics Materials-Devices and Applications

03.05.2024 FRIDAY

Abstract ID: 1218

ENABLING OFFSET-FREE SENSING USING SPIN-ORBIT TORQUES

Sabri Koraltan

Physics of Functional Materials, University of Vienna, Vienna, AUSTRIA
E-mail: sabri.koraltan@univie.ac.at

The discovery of tunnel magnetoresistance (TMR) has sparked considerable interest in developing novel spintronic devices. A key challenge lies in the elimination of the offset observed at vanishing magnetic fields, limiting the resolution to measure absolute fields [1].

Recently, we proposed a differential measurement sensing concept that uses spin-orbit torques (SOT) to eliminate the sensing offset [2]. In contrast to the recent advances in SOT enabled sensors, we show a single device sensing principle of high and scalable linear range. We eliminate the sensing offset by a differential measurement scheme, and employ micromagnetic simulations using magnum.np to predict the sensor properties. The sensitivity and linear range are tunable by varying the injected in-plane SOT current. Experimental validation is performed on Ta/CoFeB/MgO trilayer [2] and [W/CoFeB/MgO]xN multilayers [3]. The multilayers device exhibits a high density of skyrmions, as can be verified by anomalous Hall response to the out-of-plane field skyrmionic characteristics (Fig. 1a). Micromagnetic simulations allow to identify distinct skyrmion phases.

Experimentally measured transfer curves for opposing currents yield a sensor signal with cancelled offset; see Fig. 1b. The skyrmionic stack, with hysteresis-free stripes breathing at high currents for out-of-plane (OOP) fields and in-plane (IP) fields, enables 3D sensing. Micromagnetic simulations reveal how skyrmions/stripes respond to injected currents and magnetic fields. In conclusion, our study presents a differential measurement sensing concept using SOT to cancel the sensing offset. Experimental validations on traditional and skyrmionic devices confirm its effectiveness and versatility in magnetic field sensing.

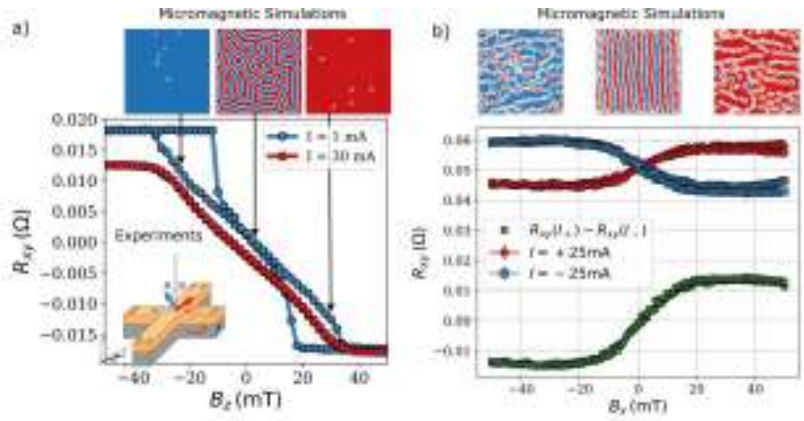

Fig. 1: *Measured transverse voltages for an OOP field (a) and the according magnetization states as obtained per micromagnetic simulations, and for an IP field (b) with the corresponding snapshots of magnetizations.*

References

[1] P. Ripka *et al.*, IEEE Sensors journal **10.6**, 1108-1116 (2010).
[2] S. Koraltan *et al.*, Phys. Rev. Applied **20**, 044079 (2023).
[3] S. Koraltan *et al.*, in Preparation (2024).

Abstract ID: 1231

SPIN PUMPING FROM INSULATING ANTIFERROMAGNETS WITH STRONG DZYALOSHINSKII-MORIYA INTERACTION

A. Safin

Kotel'nikov Institute of Radioengineering and Electronics, RAS, 125009 Moscow, RUSSIA
E-mail: arsafin@gmail.com

Antiferromagnets (AFMs) are of significant interest in spintronics and magnonics due to their unique characteristics [1]. These features include high resonant frequencies, reaching hundreds and thousands of gigahertz, and spin-wave velocities of a few kilometres per second. It's worth noting that-AFMs do not have dipole stray fields and exhibit high magnetostriction. Recent advancements in the measurement of terahertz (THz) radiation have facilitated experiments on spin pumping from diverse antiferromagnetic dielectrics into layers of normal (NM) heavy metals such as Pt, Ta, and W [2-4]. Demonstrations have shown that AFM-NM heterostructures can be used as selective detectors for sub-THz oscillations. These structures have achieved sensitivities ranging from several to tens of μV/W at room temperature [5].

A crucial objective in constructing detectors based on AFMs involves electronic frequency tuning. To achieve this goal, researchers have explored materials with high magnetostriction, such as easy-plane hematite α-Fe2O3 and iron borate FeBO3. These materials are noteworthy for their weak ferromagnetism arising from the Dzyaloshinsky-Moriya interaction. Experiments have been conducted on spin pumping from these materials into layers of normal metals [6-9]. However, a comprehensive theoretical framework that enables the calculation of spin currents and the voltage observed in experiments has not yet been presented.

This study provides a thorough study of spin pumping from different antiferromagnetic dielectrics. The study covers a frequency range that starts from a few to tens of gigahertz (for weak ferromagnets [6-9]) and goes up to hundreds and thousands of gigahertz (for NiO, MnF2, Cr2O3 [2-4]). Phenomenological considerations based on coupled Landau-Lifshitz-Gilbert equations and approximate equations of the "σ-model" are discussed through mathematical models. In this work, the total magnetization vector is considered a subordinate variable to the antiferromagnetic vector, forming the basis for subsequent analyses. The approximate theory proves capable of providing a quantitatively accurate description of the majority of existing experiments on spin pumping from AFM to NM.

References

[1] V. Baltz *et al.*, Rev. of Mod. Phys. **90**, 015005 (2018).
[2] P. Vaidya *et al.*, Science **368**,160-165 (2020).
[3] P. Ross *et al.*, Journ. of Appl. Phys. **118**, 233907 (2015).
[4] P. Stremoukhov *et al.*, arXiv:2211.00353 (2022).
[5] A. Safin *et al.*, Magnetochemistry **8**, 26 (2022).
[6] I. Boventer *et al.*, Phys. Rev. Lett. **126**, 187201 (2021).
[7] H. Wang *et al.*, Phys. Rev. Lett. **127**, 117202 (2021).
[8] R. Lebrun *et al.*, Nat. Comm. **11**, 6332 (2020).
[9] D. Gabrielyan *et al.*, arXiv:2310.20422 (2023).

Abstract ID: 1612

BISMUTH FERRITE NANOSTRUCTURES; MAGNETIC-DEPENDENT CYCLOIDAL ORDERING AND PHOTOCATALYTIC ACTIVITY

N. Thabet Mliki[1], I. Mallek Zouari[1,2], W. Ben Taazayet[1], J-M. Grenèche[3], L. Bessais[4], B. Dkhil[5]

[1] *Université de Tunis El Manar, Faculté des Sciences de Tunis, Laboratoire Matériaux, Organisation et Propriétés (LMOP), Tunis, TUNISIA*
[2] *Institut Supérieur des Etudes Technologiques en Communications de Tunis, TUNISIA*
[3] *IMMMUMR CNRS 6283, Université du Maine, 72085, Le Mans Cedex 9, FRANCE*
[4] *Université Paris Est Créteil, CNRS, ICMPE, UMR 7182, , 94320, Thiais, FRANCE*
[5] *SPMS, CentraleSupélec, UMR CNRS 8580, 91190 Gif-sur-Yvette, FRANCE*
E-mail: najeh.mliki@fst.utm.tn

Investigating the concert of nanoscale multiferroic materials is a noteworthy challenge since the physical properties of these materials vary noticeably on this scale and depend closely on the synthesis method.

In the present work, pure $BiFeO_3$ (BFO) and pure $Bi_2Fe_4O_9$ single phases were successfully synthesized by tailoring a hydrothermal synthesis route. rather monodisperse $BiFeO_3$ nanoparticles were synthesized with an average size of 8±1 nm determined using x-ray diffraction analysis and confirmed using transmission electron microscopy. We combined macroscopic magnetic measurements and in situ Mössbauer spectroscopy as a local probe of the magnetization for investigating the magnetic response and stability of those as-synthesized BFO nanoparticles. Interestingly, while the average size (8 nm) and narrow particle size distribution (5-11 nm), the Mössbauer spectroscopy reveals an asymmetry in the Fe^{3+}-sextet spectrum, which unambiguously indicates that the spin cycloid persists in nanoparticles with sizes five-seven times smaller than the bulk period. Nevertheless, due to magnetic anisotropy due to magnetoelastic and surface-confinement effects, the cycloid is unstable as only a magnetic field of 0.2 T is enough to destroy it and lead to a homogenous antiferromagnetic state. More interestingly, increasing the external magnetic field up to 8 T leads to multiple Mössbauer sextets that we interpret as the consequence of a flexomagnetic effect arising from strain gradients due to a continuous variation of the coupling between magnetization and the structural distortion from the surface to the particle core. However, Mössbauer spectrometry (MS) measurement reveals that substituting Fe atoms with Mn/Zn destabilizes the cycloidal modulation to lead to a homogenous antiferromagnetic state. The main substitution causes an important modification in the crystal field and the band structure. It, mainly, reduces the band gap value. Thus, the photocatalytic activity of doped samples for the degradation of Methylene blue (MB) under solar irradiation is remarkably better than that of pure BFO.

CANCELLED

Theory of Magnetism II

03.05.2024 FRIDAY

Abstract ID: 1083

GROWING CRYSTALLINE ARTIFICIAL MAGNET ICE IN A KAGOME LATTICE

Jun-Yi Ge[1,2,*], Jia-Jie Zhang[1], Li-Ming Tu[1], Vladimir N. Gladilin[3]

[1]Materials Genome Institute, Shanghai University, 200444 Shanghai, CHINA
[2]Zhejiang Laboratory, 311100 Hangzhou, CHINA
[3]Theory of Quantum and Complex Systems, Universiteit Antwerpen, B-2610 Antwerpen, BELGIUM
E-mail: junyi_ge@t.shu.edu.cn

Geometric frustration has been the focus of studying complex many-body interactions where exotic phenomena are widely observed. Among all systems possessing geometric frustration, artificial ice based on nanomagnets and interactive particles allows imaging individual interaction units and designing exotic frustrated lattices, which are difficult to access in traditional ice systems such as water ice and pyrochlore spin ice. However, the relatively weak interaction between nanomagnets and commonly existing quenched disorder hamper the observation of truly long-range ordered (LRO) crystalline state as well as the experimental investigation of the underlying physics. Here we report a totally new design of artificial ice based on macromagnets arranged in a geometrically frustrated kagome lattice. The unique advantage of our design is that the frustrated crystalline lattice is grown by adding the magnets into the system one by one, thus facilitating the minimization of both local and global interaction energy. As a result, an LRO ferromagnetic phase (FM-I) with charge order, as has been predicted for artificial colloidal ice, can be easily realized even in a sample with weak interactions. We also develop a magnetic comb to locally write and erase the FM-I phase at will. Moreover, a totally new ordered ferromagnetic phase (FM-II) emerges following the breakdown of FM-I phase under strong enough interactions. Our results provide unique testbed to probe the up to now elusive states in artificial ice systems.

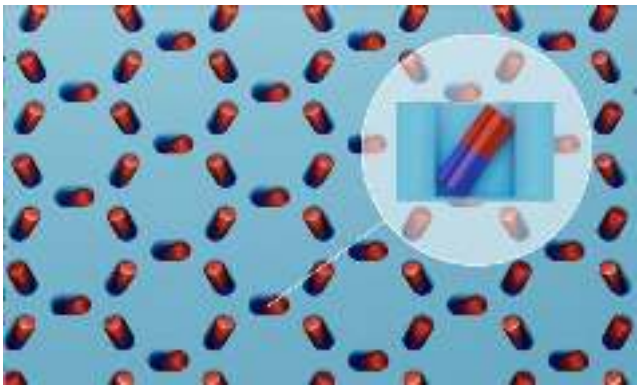

Fig. 1: *Schematic image showing the as growing crystalline kagome magnet ice.*

References

[1] Jun-Yi Ge, Jia-Jie Zhang, Li-Ming Tu, Vladimir Gladilin, (preprint is available at https://doi.org/10.21203/rs.3.rs-3466056/v1)

Abstract ID: 1498

THEORETICAL DESCRIPTION OF SPIN-DRIVEN FERROELECTRICITY IN SYSTEMS WITH SYMMETRIC AND ANTISYMMETRIC EXCHANGE INTERACTIONS

Mariya Iv. Trukhanova[1,2], Pavel Andreev[1]

[1]*Faculty of Physics, Department of General Physics, Lomonosov Moscow State University, Leninskie Gory 1, 119991 Moscow, RUSSIA*
[2]*Theoretical Physics Laboratory, Nuclear Safety Institute, Russian Academy of Sciences, B. Tulskaya 52, 115191 Moscow, RUSSIA*
E-mail: trukhanova@physics.msu.ru

In rare earth manganites, a strong coupling between magnetism and ferroelectricity was found, where the electric polarization could be induced by special magnetic ordering. We have made a bold attempt to build a macroscopic model of spin-driven ferroelectricity from the microscopic behavior of spins. A novel description of the ferroelectricity of spin origin for type-II multiferroics is proposed [1, 2].

The electric dipole moment appears in the cell of magnetic ions with non-collinear spins and negatively charged non-magnetic ligand ion as a result of spin-orbit coupling (fig. 1), and is proportional to the vector product of the spins of the ions. The polarization evolution equation (electric dipole moment density) for such a system is obtained using the many-particle quantum hydrodynamics method. The primary mechanisms of evolution in this regime include the exchange Coulomb interaction, which is modeled by the Heisenberg Hamiltonian, and the interaction of magnetic moments with the external magnetic field, which is modeled by the Zeeman energy. The resulting polarization evolution equation contains the spin density and the nematic tensor density, arising as an anti-commutator of spins for particles with spin $s>1$. For the closed theoretical apparatus, equations for the spin density and the nematic tensor evolution are also obtained. The dependence of the macroscopic polarization on the spin density associated with the dipole moment operator is derived. And with accuracy up to the proportionality coefficient, the obtained definition for the polarization coincides with the results represented in the model of M. Mostovoy [3].

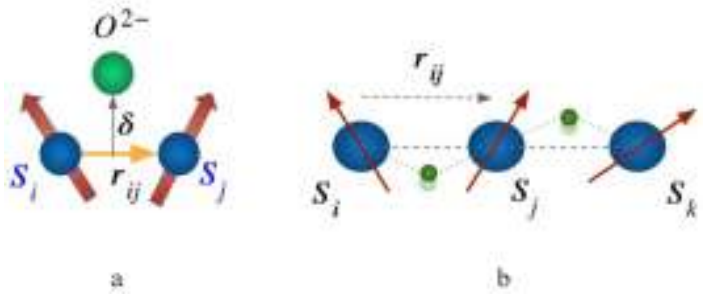

Fig. 1: *(a) - A noncollinear spin pattern (cell/cluster), which consists of positively charged metal ions (blue spheres) and a negatively charged ligand ion (green spheres). (b) - Clockwise cycloidal spiral spin structure with oxygen displacement.*

References

[1] P.A. Andreev, M.Iv. Trukhanova, *Polarization evolution equation for the exchange-strictionally formed II-type multiferroic materials*, e-print arXiv:2312.16321 (2023).

[2] M.Iv. Trukhanova, P.A. Andreev, Y.N. Obukhov, *A new quantum hydrodynamic description of ferroelectricity in spiral magnets*, e-print arXiv:2311.03610v3 (2023).

[3] M. Mostovoy, *Ferroelectricity in spiral magnets*, Phys. Rev. Lett. **96**, 067601 (2006).

HTS Cuprates: Advances in Fundamentals and Experimental Studies VII

03.05.2024 FRIDAY

Abstract ID: 1467

RECENT DEVELOPMENT OF Bi-2223 HIGH TEMPERATURE SUPERCONDUCTING TAPES IN NIN

S. Zhang, L. Jin, X. Liu[1], X. Ma, B. Shao, G. Liu, J. Feng, C. Li, J. Li, P. Zhang

Northwest Institute for Nonferrous Metal Research, Superconducting Materials Research Center, 710076, Xi'an, CHINA

E-mail: 963645802@qq.com

As one of the practical high temperature superconductors (HTS) with well-developed fabrication techniques, Bi-2223 HTS tapes have been successfully applied in many practical applications, such as high voltage current transport, superconducting motors, and current lead, etc. So far, the major supplier of Bi-2223 tapes is Sumitomo Electronic Industrial, who can supply Bi-2223 tapes with the length of over 1000 m and critical current of >200 A. Since 1990s, Northwest Institute for Nonferrous Metal Research started to develop the fabrication technique of Bi-2223 HTS tapes. After, nearly 30 years of study, we can provide the Bi-2223 tapes with the critical current of ~80 A under the ambient atmosphere heat treatment. Recently, new techniques have been developed in order to further enhance the current capacity of Bi-2223 tapes, including the introduction of spray pyrolysis technique for precursor powders fabrication and groove rolling process as well as the cryogenic drawing process for cold deformation. Meanwhile, key parameters, such as the chemical composition of precursor powders, filament structure configuration, and the rolling parameters have been systematically optimized. Therefore, based on these optimization, critical current has been obviously enhanced for 50% to over 120 A. And further optimization is on the way.

CANCELLED

Abstract ID: 1469

FABRICATION OF BSCCO HTS WIRES BY CRYOGENIC DRAWING AND ROLLING UNDER LIQUID NITROGEN TEMPERATURE

X. Liu[1,2], S. Zhang[1], J. Li[1], J. Liu[1], J. Feng[1], C. Li[1], P. Zhang[1]

[1]*Northwest Institute for Nonferrous Metal Research, Superconducting Materials Research Center, 710016, Xi'an, CHINA*
[2]*Northwestern Polytechnical University, State Key Laboratory of Solidification Processing, 710072, Xi'an, CHINA*
E-mail: xueqianliu66@163.com

BSCCO (Bi-2212 and Bi-2223) high temperature superconductors (HTS) are expected to have great potential in terms of applications, for their high critical current capacities and stable multi-filamentary wire structures. However, during the forming process of wire, namely powder-in-tube (PIT) method, the workability of BSCCO wire is restricted by mechanical mismatch between brittle ceramic precursor powders and ductile metal sheath/matrix. Such problems would get worsen in less Ag-Superconductor ratio design for lower material cost. Moreover, to reach higher powder densification state as preferred, higher radial stress would be applied during deformation, causing the deterioration of deformation homogeneity. The problems above could be alleviated to improve the quality of final product by improving the mechanical strength of matrix/sheath. Nano-twinning induced synergistic improvement of strength and ductility under cryogenic temperature had been reported in many metals with certain stacking fault energy, including silver, the commonly used BSCCO matrix and sheath material. In this study, a novel fabrication method for the BSCCO wires was developed by introducing cryogenic temperature during the deformation process. Simultaneous improvements in both strength and plasticity of Ag and AgMg alloys were found under cryogenic temperature close to 77 K. The filament densification effect, filament deformation uniformity, and superconducting properties of BSCCO wires with different wire structures and silver-superconductor ratios were systematically evaluated and analyzed. It has been found that better densification effect with high uniformity could be achieved in single core wires by in-situ strengthening of silver sheath, which can provide and transfer extra hydrostatic pressure for powder densification during the cryogenic deformation process. Wires with cryogenic deformation showed well preserved structures without internal breakage with less intermediate annealing, indicating better plasticity of sheath metal. Higher critical current capacity with higher uniformity was also observed in cryogenic deformed specimens with nearly 20% improvement comparing with the wires fabricated under room temperature. The above results provided the feasibility of cryogenic deformation for bismuth-based wires and tapes, and the extra deformation tolerance might enable new structure designs with smaller filament size and lower Ag/SC ratios.

CANCELLED

Abstract ID: 1274

MASS OF CHARGE CARRIER IN THE $La_{2-x}Sr_xCuO_4$ FROM BIPOLARONIC MODEL

B.Ya. Yavidov[1], S.M. Otajonov[1], D.E. Uskenbaev[2], T. Saparbaev[2], A.N. Kurmantayev[3]

[1] *Nukus State Pedagogical Institute named after Ajiniyaz, 230105 Nukus, UZBEKISTAN*
[2] *S.Seifullin Kazakh Agrotechnical University, 010011 Astana, KAZAKHSTAN*
[3] *Kh.A. Yasawi International Kazakh-Turkish University, 161200 Turkestan, KAZAKHSTAN*
E-mail: bakhrom.yavidov@gmail.com

We have studied the dependence of the mass of charge carrier (CC) on the doping level (x) in $La_{2-x}Sr_xCuO_4$ (LSCO) cuprate superconductor (SC). While doing that we deal with the extended Holstein model and bipolaronic mechanism (BpM) of high-T_c superconductivity (HTSC) [1]. BpM-HTSC has shown itself as a model capable of explaining various properties of HTSC [2] and there is much evidences showing that CC in the cuprates are (bi)polarons, too [3]. Assuming that bipolarons form an ideal Bose-gas, we put their Bose-Einstein condensation (BEC) temperature (T_{BEC}) to be equal to the SC critical temperature (T_C) of LSCO. Then, we calculated three dimensional polaron's mass (m_p) according to the formula $T_{BEC} = 3.31\hbar^2 n^{2/3}/2k_B m_p$. Concentration of bipolarons is expressed through doping level (x) and unit cell volume (V_a) of LSCO: $n = x/2V_a$. The values of T_C and V_a at different x were taken from well-known experimental data. Then, we used the formulas $m_p = m_{p,ab}^{2/3} m_{p,c}^{1/3}$ and $\gamma_m = m_{p,c}/m_{p,ab}$ in order to extract CuO_2 or *ab*-plane polaron's mass $m_{p,ab}$ from m_p taking into account mass anisotropy factor γ_m which itself is doping dependent [4]. Calculated values of m_p and $m_{p,ab}$ are presented in Fig.1 as a function of x. Both dependencies are consistent with the available experimental data, in particular, with the results of work [5] on doping dependence of CC cyclotron mass m_c. The last work reports an increase of m_c with doping level x. So does *ab*-plane polaron's mass $m_{p,ab}$ in our study.

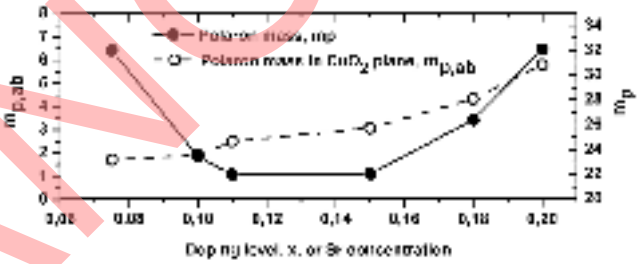

Fig. 1: *Doping dependence of m_p (solid circles) and $m_{p,ab}$ (open circles) in the LSCO (in units of m_e).*

Our results convincingly demonstrate the significant role of electron-phonon interaction in determining the properties of LSCO and support the BpM of HTSC [6].

References

[1] A.S. Alexandrov, *Theory of Superconductivity* (IOP Publishing Ltd., Bristol, 2003).
[2] A. Bussmann-Holder, H. Keller, Condens. Matter **7**, 10 (2022).
[3] K.A. Müller, J. Supercond. Novel Magn. **30**, 3007 (2017).
[4] T. Kimura *et al.*, *In Advances in Superconductivity VII*, Editors K.Yamafuji, T.Morishita (Springer, Tokyo, 1995), p.539.
[5] A. Legros *et al.*, Phys. Rev. B **106**, 195110 (2022).
[6] S. Dzhumanov *et al.*, Mod. Phys. Lett. B (2024) DOI: 10.1142/S0217984924501471

CANCELLED

Superconducting Spintronics: Novel Quantum Circuits VII

03.05.2024 FRIDAY

Abstract ID: 1583

MUTUAL SYNCHRONIZATION OF Bi-2212 THz EMITTERS

O. Kizilaslan[1,2], R. Wieland[2], E. Dorsch[2], N.V. Kinev[3], A.B. Ermakov[3], D.Koelle[2], H.B. Wang[4], P.H. Wu[4], V.P. Koshelets[3], R. Kleiner[2]

[1] *Department of Biomedical Engineering, Faculty of Engineering, Inonu University, Malatya, TURKEY*
[2] *Physics Institute, Center for Quantum Science and LISA+, University of Tübingen, Tübingen, GERMANY*
[3] *Kotel'nikov Institute of Radio Engineering and Electronics RAS, Moscow, RUSSIA*
[4] *Research Institute of Superconductor Electronics, Nanjing, CHINA*
E-mail: olcaykizilaslan@gmail.com

The layered superconductor $Bi_2Sr_2CaCu_2O_8$ (Bi-2212) is known to coherently emit electromagnetic waves in the THz regime [2]. The radiation power of the best stacks exceeds several tens of μW, however a limitation is given by Joule heating. This limitation can at least partially be overcome by using arrays of side-coupled stacks connected by a common Bi-2212 base crystal [2-5]. The highest reported power output is almost 1 mW, achieved with 3 synchronized stacks [3]. However, also for these arrays overheating is severe and presumably prevents the synchronization of a larger number of stacks. A potential way out is to use stand-alone stacks sharing a common gold electrode. In this talk we report on the mutual synchronization of two of such stacks, each biased separately. The observed coupling indicates a potential for enhancing emission properties while keeping Joule heating reasonably low.

We gratefully acknowledge financial support by The Scientific and Technological Research Council of Türkiye, TUBİTAK 2219-2020/2-1059B192000817 and the Research Fund of Inonu University, Türkiye under Grant Contract No. FOA-2023-3260.

References

[1] L. Ozyuzer *et al.*, Science **318**, 1291 (2007).
[2] N. Orita *et al.*, Physica C **470**, S786 (2010).
[3] T. M. Benseman *et al.*, Appl. Phys. Lett. **103**, 022602 (2013).
[4] M. Tsujimoto *et al.*, Phys. Rev. Appl. **13**, 051001 (2020).
[5] R. Kobayashi *et al.*, Phys. Rev. Appl. **17**, 054043 (2022).

Abstract ID: 1605

INTERPLAY BETWEEN MAGNETISM AND SUPERCONDUCTIVITY IN A HYBRID MAGNON-PHOTON BILAYER SYSTEM IN THE ULTRASTRONG COUPLING REGIME

A. Ghirri[1], C. Bonizzoni[1,2], M. Maksutoglu[3], A. Mercurio[4], O. Di Stefano[4], S. Savasta[4], M. Affronte[1,2]

[1] *Istituto Nanoscienze—CNR, Centro S3, via G. Campi 213/A, Modena 41125, ITALY*
[2] *Dipartimento di Scienze Fisiche, Informatiche e Matematiche, Università di Modena e Reggio Emilia, via G. Campi 213/A, Modena 41125, ITALY*
[3] *Institute of Nanotechnology, Gebze Technical University, Gebze, Kocaeli 41400, TURKEY*
[4] *Dipartimento di Scienze Matematiche e Informatiche, Scienze Fisiche e Scienze della Terra, Università di Messina, Messina 98166, ITALY*
E-mail: marco.affronte@unimore.it

Spin wave excitations coherently interact with cavity photons and there is a subtle interplay when a low loss magnetic material is combined with superconducting resonator.

Here, we present the prototypical case of bilayer stack made of a 5-μm-thick insulating Yttrium Iron Garnet (YIG) film and a high-T_c YBCO superconducting coplanar resonator. By putting in direct contact the magnetic and superconducting layers, we obtain very large values of the collective magnon-photon coupling strength (2 GHz) and cooperativity (50000) [1]. The coupling between magnon and photon modes exceeds 0.2 times the cavity frequency, thus demonstrating the achievement of the ultrastrong coupling regime. Our analysis, based on a modified Hopfield model, shows a vanishing contribution of the diamagnetic coupling term, which is a peculiarity of pure spin systems, and which represents a critical prerequisite for the observation of the superradiant phase transition.

We further investigated the interplay between the magnetic and superconducting layers by systematic study of the temperature dependence of the transmission spectra acquired across the critical temperature of YBCO (T_c=88 K). We observe a progressive increase of the magnon-photon coupling strength and of the shift of the hybrid mode frequency with respect to the quasi-uniform thickness mode of the film as the temperature decreases. We correlate this evolution to the temperature dependence of the penetration depth of YBCO, which is extracted within the framework of the two-fluid model. We show that the penetration depth essentially governs the frequency of the resonator through the kinetic inductance, thus the magnon-photon coupling. The shift of the hybrid mode frequency also depends from the penetration depth as an effect of the diamagnetism of the superconductor [2].

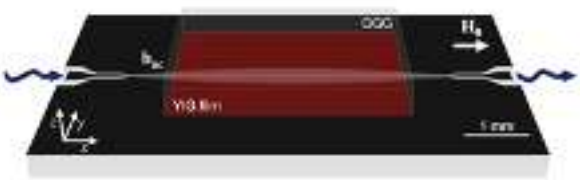

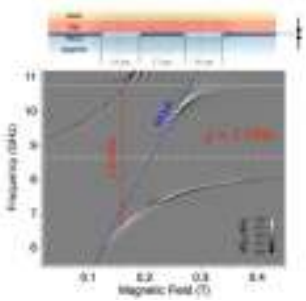

References

[1] A. Ghirri *et al.*, Phys. Rev. Appl. **20**, 024039 (2023).
[2] A. Ghirri *et al.*, submitted (2023). Preprint on arXiv:2312.02785 (2023).

Abstract ID: 1482

UNCONVENTIONAL SUPERCONDUCTOR'S IMPACT ON SPIN DEPENDENT TRANSPORT PROPERTIES OF MULTI-TERMINAL QUANTUM DOT HYBRID

Vrishali Sonar, Piotr Trocha

Institute of Spintronics and Quantum Information, Faculty of Physics, Adam Mickiewicz University, 61-614 Poznan, POLAND

E-mail: vrison@amu.edu.pl

The well-known BCS theory of superconductivity presents the Cooper pair of electrons having a net zero spin (S=0). On the other hand, the unconventional superconductors [1] can exhibit electron pair with non-zero angular momentum, triplet spin pairing and anisotropy in the superconducting gap parameter. As the electron-phonon interaction is responsible for conventional BCS (s-wave) superconductors, the phenomenological reason for triplet superconductors is not uniquely defined. The production, tunability and inter-action with magnetic order of such finite spin supercurrent is crucial to the spintronics devices [2].

In this work, we evaluate the spin dependent charge/heat transport in a hybrid structure of quantum dot coupled to triplet superconductor of chosen phase(s) and ferromagetic electrodes. Our approach is theoretical and computational in nature. The analytical method of non-equilibrium Green's function is employed to calculate the observables. Since this is a three terminal device, both local and non-local transport coefficients [3] such as electrical conductance, thermopower, thermal conductance are presented. In the system driven out-of-equilibrium and in nonlinear response regime, we investigate the prospects of this device to function as a particle exchange heat engine and present the obtainable power and efficiency. It is possible that the triplet superconductor breaks time reversal and point group symmetry and thus we evaluate how this affects the transport properties in the system.

References

[1] M. Sigrist, *Introduction to unconventional superconductivity*, AIP Conference Proceedings **789**, 165-243 (2005).

[2] J. Linder, J. Robinson, *Superconducting spintronics*, Nature Phys., **11**, 307–315 (2015).

[3] F. Mazza, R. Bosisio, G. Benenti, V. Giovannetti, R. Fazio, F. Taddei, *Thermo-electric efficiency of three-terminal quantum thermal machines*, New Journal of Physics **16**, 085001 (2014).

Magnetic Materials Processing and Physical Properties II

03.05.2024 FRIDAY

Abstract ID: 1585

UNLOCKING MULTIFUNCTIONAL POTENTIAL: Mn-Ru CO-DOPING BOOSTS CATALYTIC AND MAGNETIC PROPERTIES IN $La_{0.62}Bi_{0.05}Ba_{0.33}Mn_{1-x}Ru_xO_3$ (x = 0.0 AND 0.1) COMPOUNDS

A. Osman Ayaş[1], S. Kılıç Çetin[2], G. Akça[2], D. Kaya[2], A. Ekicibil[2]

[1] *Adıyaman University, Department of Physics, 02030 Adıyaman, TÜRKIYE*
[2] *Çukurova University, Department of Physics, 01330 Adana, TÜRKIYE*
E-mail: a.ekicibil@gmail.com

Energy demand is constantly increasing and is expected to continue rising. This is pushing mankind to search for new energy-efficient and environmentally friendly technologies. Among these attempts, fuel cells are one of the most promising Technologies due to the several advantages like sustainability, environmentally friendly behavior and energy efficiency [1]. Current research on fuel cells is generally focus on to reduce high costs, increase activity and stability by alloying noble metals with earth-abundant metals in nature [2-4]. Researchers are also developing multifunctional materials that exhibit multiple properties, such as catalytic performance, magnetic properties, and optical functions. Perovskite materials are particularly attractive for this purpose because they have the potential to exhibit these properties simultaneously, including oxygen evaluation reaction (OER), oxygen reduction reaction (ORR), and magnetic properties [5]. For this purpose, in this work, we have synthesized $La_{0.62}Bi_{0.05}Ba_{0.33}MnO_3$ (LBBM), $La_{0.62}Bi_{0.05}Ba_{0.33}Mn_{0.90}Ru_{0.1}O_3$ (LBBMR) samples by using solid state reaction method and characterized their structural, morphological, magnetic, and ORR/OER activity properties. The crystal structure analysis obtained by analyzing the XRD data showed that the samples had a rhombohedral crystal structure, and this structure did not change with a small amount (0.1) of Mn-Ru substitution. The analysis of morphological characteristics showed that the average particle size was less than 3 mm. Temperature dependent magnetization measurements showed that the ferromagnetic-paramagnetic phase transition temperature (Curie temperature) was 334 K and 327 K for LBBM and LBBMR samples, respectively. A decrease in the magnetic entropy change value, which is an important parameter in terms of showing the magnetic cooling capacity, was also observed with 0.1 Mn/Ru substitution. This substitution also reduces the onset potential to 51 mV for OER and 74 mV for ORR. ORR durability test for 6 h shows that ORR efficiency of the LBBM catalyst enhanced by 60% with Ru substitution. All results show that LBBMR sample gains multifunctional properties including magnetocaloric and catalytic performance by Mn substitution with Ru.

References

[1] S. Kılıç Çetin, G. Akça, D. Kaya, A.O. Ayaş, A. Ekicibil, International Journal of Hydrogen Energy **47**, 40999-41009 (2022).
[2] Y. Zhang, F. Gao, H. You, Z. Li, B. Zou, Y. Du, Coordination Chemistry Reviews **450**, 214244 (2022).
[3] C. Zhao, *et al.*, Energy & Environmental Science, **13**, 53-85 (2020).
[4] Y. Zheng, *et al.*, Chemical Society Reviews **46**, 1427-1463 (2017).
[5] A.S. de Dios, M.E. Díaz-García, Analytica Chimica Acta, **666**, 1-22 (2010).

Abstract ID: 1564

EXCELLENT ELECTROMAGNETIC WAVE ABSORPTION OF Fe_3O_4:MoS_2 HYBRID COMPOSITES

M. Akyol[1], C. Aka[1], O. Akgöl[2], M. Karaaslan[2]

[1] *Adana Alparslan Türkeş Science and Technology University, Dept. of Materials Science and Engineering, 01250, Adana, TÜRKIYE*
[2] *İskenderun Technical University, Dept. of Electrical-Electronic Engineering, 31200, Hatay, TÜRKIYE*
E-mail: makyol@atu.edu.tr

Radars, which can be defined as a device that transmits an electromagnetic (EM) wave and detects objects by means of energy emitted after communication with an object, can detect the altitude, orientation, and speed of objects. While the radar can operate at any microwave frequency, military and satellite communication systems mostly operate in the X and Ku bands. In these bands, it is important to develop a thin and light EM absorption material having high absorption capacity and a wide absorption band gap. It is known that materials with high microwave absorption performance must meet two important requirements; i) impedance matching, ii) converting the energy of the absorbed wave into heat or other types of energies as much as possible. In this study, the research on PANI/Fe_3O_4:MoS_2 hybrid nanocomposites will be conducted on the formation of the nanocomposite structure, researching some of its physical properties, and the electromagnetic wave absorption performance. 2-dimensional MoS_2 nanosheets were synthesized by hydrothermal method. After that, the nanosheets were modified by the Fe_3O_4 magnetic nanoparticles at various concentrations. Some physical properties (structural, morphological, and magnetic) were studied by various characterization techniques. For the electromagnetic wave absorption properties, the samples were fabricated by dispersing the hybrid nanocomposites (40%) into the epoxy matrix (60%). It is found that the content of magnetic Fe_3O_4 nanoparticles enhances the electromagnetic wave absorption performance of up to 15% of magnetic particles in the whole matrix. Moreover, MoS_2 nanosheets modified by Fe_3O_4 nanoparticles behave with excellent absorption properties in X and Ku bands. The highest absorption performance was observed in a hybrid nanocomposite at -66 dB at 10.1 GHz frequency with a 7.1 GHz bandwidth. This indicates that the fabricated hybrid nanocomposites can absorb 90% and above the X band and some parts of the Ku band.

Acknowledgement

This work was supported by The Scientific and Technological Research Council of Türkiye (TUBİTAK) under project number 121F367.

Abstract ID: 1579

SINTERING TEMPERATURE EFFECT ON STRUCTURAL, MAGNETIC AND MAGNETOCALORIC PROPERTIES OF SOME PEROVSKITE MANGANITE MATERIALS

A. Osman Ayaş[1], A. Kandemir[2], M. Akyol[3], A. Ekicibil[2]

[1] *Adıyaman University, Department of Physics, 02030 Adıyaman, TÜRKIYE*
[2] *Çukurova University, Department of Physics, 01330 Adana, TÜRKIYE*
[3] *Adana Alparslan Türkeş Science and Technology University, Department of Materials Science and Engineering, 01330, Adana, TÜRKIYE*
E-mail: aayas@adiyaman.edu.tr

Perovskites, both single-layer perovskite materials with the chemical formula of ABO3 and double perovskite materials with the chemical formula of ABB'O6, are material families that have the potential to exhibit rich physical properties depending on the potential for doping many elements into the structure. One of the interesting features of these perovskites is their magnetocaloric effect (MKE) [1-4]. MKE is the response of a material in the form of temperature change when exposed to a magnetic field or when the magnetic field is removed. This effect can be used as an alternative to conventional gas compression refrigeration methods in cooling systems such as refrigerators and air conditioners. Perovskite materials are one of the ideal candidate for coolant material in magnetic cooling applications due to their high MKE values [4]. There are many factors affecting the MKE properties of these materials. These factors include chemical composition, crystal structure, grain size, magnetic field exchange rate and heat treatment processes applied in the material preparation process. In this study, the effect of sintering temperature on the structural, magnetic and magnetocaloric properties of some perovskite materials.

References

[1] K.A. Gschneidner, V.K. Pecharsky, International Journal of Refrigeration, **31**, 945-961 (2008).
[2] K.A. Gschneidner, V.K. Pecharsky, Annual Review of Materials Science, **30**, 387-429 (2000).
[3] M.-H. Phan, S.-C. Yu, Journal of Magnetism and Magnetic Materials, **308**, 325-340 (2007).
[4] A.O. Ayaş, S.K. Çetin, G. Akça, M. Akyol, A. Ekicibil, Materials Today Communications, **35**, 105988 (2023).

Abstract ID: 1094

CHARACTERIZATION OF Gd^{3+} DOPED MAGNESIUM FERRITE SYNTHESIZED BY SOL- GEL METHOD

Haroon Mazhar, M. Anis-ur-Rehman

Applied Thermal Physics Laboratory, Department of physics, COMSATS University Islamabad, 45550, PAKISTAN
Email: haroonmazhar1234@gmail.com & marehman@comsats.edu.pk

Ferrite materials have been investigated in view of versatile and technological applications.Rare earth (RE) ions substitution in spinel ferrite resulting in Fe–Re interactions which leads to strong 3d–4f orbital coupling. This strong 3d–4f orbital coupling creates structural distortion and hence changing the physical properties of ferrite materials [1].Pure and gadolinium (Gd) doped magnesium ferrite were synthesized by WOWs Sol-gel Method. The structural, electrical, dielectric and I-V properties of these ferrites were studied. X-ray diffraction (XRD) of pure and Gd doped magnesium ferrite confirmed the spinel cubic structure. Fourier transform infrared spectroscopy (FTIR) showed the formation of spinel structure. The dielectric tangent loss, dielectric constant, dielectric loss, ac conductivity and impedance was investigated in the frequency range of 20Hz-3MHz. Tangent loss, dielectric loss, dielectric constant and ac conductivity decreases with doping of Gd concentration as compared to pure magnesium ferrite. From the study of conductivity and impedance, the role of grain and grain boundaries in the spinel ferrite nanoparticles was investigated. I-V curve of pure and Gd doped magnesium ferrite in the current study exhibit a hysteresis loop type behavior. Fig.1 has been showed that hysteresis trend confirmed the resistive switching effect exists in gadolinium doped magnesium ferrite nanoparticles. Our study suggest that Gadolinium doped magnesium ferrites have high potential for resistance switching memory devices like Resistive Random-Access Memory (ReRAM).

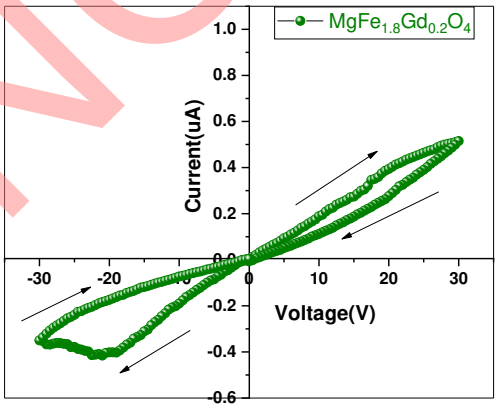

Fig.1: *Current-Voltage (I-V) loop for $MgFe_{1.8}Gd_{0.2}O_4$.*

References

[1] M.D. Hossain, M.A. Hossain, S.S. Sikder, *Hysteresis loop properties of rare earth doped spinel ferrites*: A review. Journal of Magnetism and Magnetic Materials. **564**, 170095, (2022).

CANCELLED

Magnetic Materials Processing and Physical Properties III

03.05.2024 FRIDAY

Abstract ID: 1640

DEVELOPMENT OF PERSISTENT JOINTS FOR SUPERCONDUCTING Bi-2212 COILS

Tayebeh Mousavi[1], Petr Zagura[2], Ingon Kim[2], Frederick Follows[2], Ziad Melhem[3], Steven Ball[3], Andrew Twin[3], Susannah Speller[2], Chris Grovenor[2]

[1] Department of Engineering, King's College London, WC2R 2LS, London, UK
[2] Department of Materials, University of Oxford, 16 Parks Rd, OX1 3PH, Oxford, UK
[3] Oxford Instruments, Tubney Woods, Abingdon, OX13 5QX, UK
E-mail: tayebeh.mousavi@kcl.ac.uk

Bi-2212/Ag multifilamentary wire is the only high-temperature superconductor manufactured in the form of a round wire, and so offers a number of advantages for the designers of high-field magnets (>25 T). The development of a reliable joining process with ultra low-resistance ($R < 10^{-12}$ Ω) is the key step to manufacturing Bi-2212 high-fields magnets and taking the advantage of excellent properties of Bi-2212 wire. This study focuses on the development of persistent mode joints for Bi-2212/Ag multifilamentary round wires that are sufficiently small to be considered for an in-winding joint strategy. A number of different approaches and joint geometries have been explored to introduce Bi-2212 powder between the ends of two wires wound into small coils, and then to melt-process to form a closed loop. The decay characteristics of current induced into the coils have been measured using the inductive method, and the microstructure of joints with different geometries was studied in detail using analytical Scanning Electron Microscopy to understand how to optimize the formation of continuous superconducting paths between the wires during the melt processing stage.

Our optimized technique offers small coils with melt-processed joints that occupy very small volumes but can still carry high currents. We will report on the persistence measurements of the currents induced in the coils as a function of the background magnetic field, and correlate these results with the microstructure in the different joint designs.

Abstract ID: 1645

NUMERICAL MODELLING OF HIGH-VELOCITY EDS HYPERLOOP SYSTEMS WITH DIFFERENT PMG-ALUMINIUM RAIL CONFIGURATIONS

Murat Abdioglu[1,2], Hakki Mollahasanoglu[1,3], Ufuk Kemal Ozturk[1,4], Elvan Coskun[4], Ali Gencer[4,5]

[1] *Electromagnetic Guidance and Acceleration Research Group (EMGA), Department of Physics, Faculty of Science, Karadeniz Technical University, 61080, Trabzon, TÜRKIYE*
[2] *Department of Mathematics and Science Education, Faculty of Education, Bayburt University, 69000, Bayburt, TÜRKIYE*
[3] *Department of Electrical-Electronics Engineering, Faculty of Engineering and Architecture, Recep Tayyip Erdogan University, 53100, Rize, TÜRKIYE*
[4] *Ankara University, Center of Excellence for Superconductivity Research, 50th Year Campus, 06830, Golbasi, Ankara, TÜRKIYE*
[5] *Ankara University, Science Faculty, Phys. Dept., 06100-Tandogan- Ankara, TÜRKIYE*
E-mail: hakki.mollahasanoglu@erdogan.edu.tr

Permanent magnet (PM) electrodynamic suspension (EDS) Maglev systems have been becoming more important in recent years depending on the increasing needs of the people for safe and fast transportation. As a basis, a PM-EDS Maglev system consists of a special arrangement of PMs above a conducting rail [1]. In this study, we have conducted comprehensive numerical simulations to obtain optimum geometric parameters of aluminium rail and PM arrangements for higher levitation and lower drag force values and lower rail fabrication cost. The numerical simulations were performed in "Magnetic Field Formulation (mf)" physics in COMSOL Multiphysics 5.6. In this formulation, the magnetization directions and values of the PMs are defined by Faraday's law while the velocity up to 1100 km/h is defined by Lorentz Term. We have observed that the levitation and drag forces can be optimized and the fabrication cost of EDS hyperloop systems can be decreased by the appropriate arrangement of PMG and rail units.

Acknowledgement

This work and the attendance at the conference were supported by the Scientific and Technological Research Council of Türkiye (TUBITAK), with project number 122F432 and the Scientific Research Projects Coordination Unit of Karadeniz Technical University with project No. FBA-2021-9814.

References

[1] L. Beauloye, B. Dehez, *Permanent magnet electrodynamic suspensions applied to maglev transportation systems: a review*, IEEE Transactions on Transportation Electrification, **9(1)**, 748-758 (2022).

Abstract ID: 1629

HRTEM STUDIES AND SUPERCONDUCTING PROPERTIES OF THE $KCa_2Fe_4As_4F_2$ SINGLE CRYSTALS

Alena Yu. Degtyarenko[1], Andrey V. Sadakov[1], Alexey S. Usoltsev[1], Juniy Ge[2]

[1] *V.L. Ginzburg Centre for High-Temperature Superconductivity and Quantum Materials P.N. Lebedev Physical Institute of the RAS, 53, Leninsky ave., 119991 Moscow, RUSSIA*
[2] *Materials Genome Institute, Shanghai University, 200444 Shanghai, CHINA*
E-mail: degtyarenkoayu@lebedev.ru

The single crystals of the new iron - based superconducting layered 12442 family have been studied in this work [1]. Achieving homogeneous phase of this family of superconductors is a difficult task. The 12442 ($KCa_2Fe_4As_4F_2$) compound is self-doped, it has a narrow crystallization range and is formed from two phases 1111 (CaFeAsF) and 122 (KFe_2As_2) [2]. The single crystals of the $KCa_2Fe_4As_4F_2$ were grown by "self-flux" method (KAs) [2]. The XRD measurements are confirmed the high quality of single crystal with sharp (00l) reflections and minimum trace of the second phase. The measurements of temperature dependence of magnetic susceptibility show superconducting transition about 34 K. Using HRTEM studies (HAADF and EDX) planar defect were observed. It's clearly seen that these defects are monolayers of CaFeAsF and KFe_2As_2. It was found that the volume fraction of these defects is about 4%. However we were able to detect contribution of such defects into a tunneling current. During Andreev reflection spectroscopy experiment we have found the value of the large gap of CaFeAsF and its temperature behavior up to its local T_c(28K) which is lies below $KCa_2Fe_4As_4F_2$ T_c (34K). Analogously to many related compounds of iron-based superconductors [3,4], these compounds can act as additional pinning centers. Therefore, the critical current density J_c and the nature of the pinning mechanism in these samples were also examined. The magnetic hysteresis loops are highly symmetrical, which suggests bulk pinning in the sample for both orientations. The calculated critical current density is ~10^6A/cm^2. We have found second magnetization peak (SMP) at high temperatures (near Tc), which is not in line with usual SMP position of parent compounds. Additionally, we have measured lower critical field in both orientations, and observed a striking difference in temperature dependencies H_{c1}(T).

This research was supported by Russian Science Foundation (№ 23-12-00307).

References

[1] Z.C. Wang, *et al.*, J. Am. Chem. Soc. **138(25)**, 7856-7859 (2016).
[2] T. Wang, *et al.*, J. Phys. Chem. C. **123(22)**, 13925-13929 (2019).
[3] S. Ishida, *et al.*, NPJ Quantum Mater. **4**, 272019 (2019).
[4] A.Y. Degtyarenko, *et al.*, Nanomaterials. **12(21)**, 3801(2022).

Ferrites and Rare Earth Magnetic Materials

03.05.2024 FRIDAY

Abstract ID: 1109

EMERGING RRAM MATERIALS: AN OVERVIEW OF RECENT ADVANCES IN FERRITES

M. Anis-ur-Rehman

Applied Thermal Physics Laboratory, Department of Physics, COMSATS University Islamabad, Islamabad 45550, PAKISTAN

Email: marehman@comsats.edu.pk

Resistive Random Access Memory (RRAM) (Fig 1) is an emerging non-volatile memory technology that utilizes resistive switching mechanisms to achieve high-density data storage and low-power operation, making it a promising candidate for next-generation memory applications. Ferrites' tunable resistive switching makes them promising for RRAM, enabling low power consumption and high-speed operation [1]. This study delves into the exploration of ferrite nanoparticles across three distinct series, investigating their potential for RRAM applications. Three series have been developed, with the first series involving $Co_{1-x}Mg_xFe_2O_4$, the second series comprising $Zn_{0.6}Mn_{0.4-x}Co_xFe_2O_4$, and the third series featuring barium hexa-ferrite with $BaFe_{12-x}Co_xO_{19}$ using WOWs sol-gel method. Structural parameters for the samples were characterized using X-ray diffraction (XRD), providing detailed insights into their crystalline composition and lattice properties. The electrical properties of the samples were carefully examined, AC properties in the frequency range of 20 Hz to 3 MHz, encompassing, DC properties over a temperature range of 30 to 400°C and IV characteristics providing a comprehensive understanding of their behavior under diverse operational conditions. All samples exhibit the expected frequency-dependent behavior of ferrites, displaying enhanced conductivity at higher frequencies. The DC resistivity of the samples decreases as the temperature increases. The sample of $BaFe_{12}O_{19}$ exhibits the highest resistive switching effect (Fig 2), indicating its potential suitability for applications in Resistive Random Access Memory (RRAM). Notably, IV curves for all prepared samples exhibited the hysteresis loop, showing resistive switching effect.

Fig. 1: *Schematic of MIM structure for RRAM [2].*

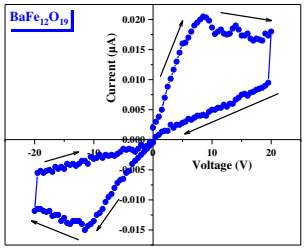

Fig. 2: *I-V curve for $BaFe_{12}O_{19}$.*

References

[1] M. Kamran, M. Anis-ur-Rehman, *Study of dielectric and electrical properties in Co-(Fe–Ce-Nd) nanosized spinel ferrites*, Materials Science in Semiconductor Processing, **153**, 107111 (2023).

[2] F. Zahoor, F.A. Hussin, U.B. Isyaku, S. Gupta, F.A. Khanday, A. Chattopadhyay, H. Abbas, *Resistive random access memory: Introduction to device mechanism, materials and application to neuromorphic computing*, Discover Nano, **18**, 36 (2023).

Abstract ID: 208

CLIMATE CHANGE, CLEAN ENERGY TECHNOLOGIES AND RESOURCE RECOVERY-A PATHWAY FOR SUSTAINABLE DEVELOPMENT

Rizwan Raza

Department of Physics, COMSATS University Islamabad, 54000, Lahore, PAKISTAN
E-mail: rizwanraza@cuilahore.edu.pk

Climate change and negative emissions are among the top global challenges. In the last 200 years, the atmospheric CO_2 has increased and in the last decades caused severe consequences, particularly increased global temperatures and climate change. CO_2 emissions are the major contributor towards climate issues and are continually increasing. Thus, in order to achieve the "Paris agreement" goal for a negative emission society, there is a need to control such greenhouse gas emissions. There are several technologies that have been introduced to tackle these issues; among these, carbon capture and storage has the potential for significant reductions in emissions and thus great impact. Since the industrial revolution the climate issues especial global warming has been increased because of greenhouse emission which leads to the many concerns all over the world.

The clean energy devices got higher attraction towards scientific research and investigation due environment friendly nature. Among conventional resources energy technologies, these clean energy technologies can considerably decrease the impact of emission to the environment. The development of clean energy is the only way to mitigate the effects of climate change and its unprecedented impacts on society. The development of advanced energy technologies has a big challenge. There are many energy technologies, but research activities on fuel cell technology in Pakistan have been reviewed and it is also discussed how this technology can resolve the current energy crises in Pakistan and can be the source of sustainable energy. It has been also reviewed that the country would greatly benefit from Clean energy devices e.g. Fuel Cells and Fuel cell hybrid system (environmentally friendly technology), which could be the best solution for electricity production as well for automobile industry.

CANCELLED

Abstract ID: 1562

LARGE MAGNETORESISTANCE OF AMORPHOUS CARBON FILM

Awais Siddique Saleemi[1], Ali Abdullah[2], M. Anis Ur Rehman[3]

[1] *International College of Guangzhou College of Technology and Business @ Northeastern State University USA (GCTB-NSU), Foshan, CHINA*
[2] *Department of Physics, University of Management and Technology, Sialkot Campus, Lahore, PAKISTAN*
[3] *Department of Physics. COMSATS University, Islamabad, PAKISAN*
E-mail: assaleemi@yahoo.com

Magnetoresistance (MR) of pure amorphous carbon thin films deposited by pulsed laser deposition at various deposition temperatures was studied. Maximum MR of 46% was observed at 2 K under the magnetic field of 7 T for the sample deposited at temperature of 500 ^{o}C. No tendency of MR saturation was observed up to 7 T. The MR decreases rapidly with the increase in measurement temperature and vanishes after 40 K. The transport mechanism of all the samples follow Efros-Shklovskii variable range hopping model. The characteristics temperature decreasing from 2540 K to 1290 K and localization length increasing from 5.3 nm to 10.7 nm with increasing fraction of C(sp^2) from 72% to 84%. The lower disorder degree may results in higher MR.

CANCELLED

Abstract ID: 1183

CONTINUOUS TUNING OF COMPENSATED FERRIMAGNETISM IN $Gd_{3-x}Ho_xFe_5O_{12}$ THIN FILMS

Hao Bai[1,2,*], Wenlong Si[3,*], Heng-An Zhou[1,2,*], Ledong Wang[1,2], Teng Xu[1,2], Yiqing Dong[1,2], Jing Zhu[3,†], Wanjun Jiang[1,2]

[1]*State Key Laboratory of Low-Dimensional Quantum Physics and Department of Physics, Tsinghua University, Beijing 100084, CHINA*
[2]*Frontier Science Center for Quantum Information, Tsinghua University, Beijing 100084, CHINA*
[3]*Key Laboratory of Advanced Materials (MOE), School of Materials Science and Engineering, Tsinghua University, Beijing 100084, CHINA*
E-mail: bh19@mails.tsinghua.edu.cn

Rare-earth iron garnets (ReIGs) are attracting considerable attention because they could enable many intriguing spintronic phenomena. Material choices of these garnets are, however, limited to rather simple compositions, such as $Y_3Fe_5O_{12}$, $Tm_3Fe_5O_{12}$, and $Gd_3Fe_5O_{12}$, amongst many others. The magnetic properties of these garnets, including saturation magnetization, and damping parameter are accordingly limited within a narrow parameter space. In this study, we will first grow a series of substituted ReIGs of composition $\mathrm{Gd}_{3-x}\mathrm{Ho}_x\mathrm{Fe}_5\mathrm{O}_{12}$ ($x_{\mathrm{Ho}} = 0 - 3$). Subsequently, a continuous tuning of magnetic parameters, including the net saturation magnetization (M_S), the magnetization compensation temperature (T_M) and the damping parameter (α) are also demonstrated through linearly changing the Ho concentration. By invoking the molecular-field theory, we can quantitatively characterize both the temperature-dependent and the Ho concentration-dependent compensated ferrimagnetism. Meanwhile, the linear increase of the damping parameter is attributed to the increased spin-orbit coupling with the increased Ho concentration (x_{Ho}) [1]. The present method could be useful for designing garnets with desired material parameters, which could be incorporated for enabling novel spintronic devices based on compensated ReIGs.

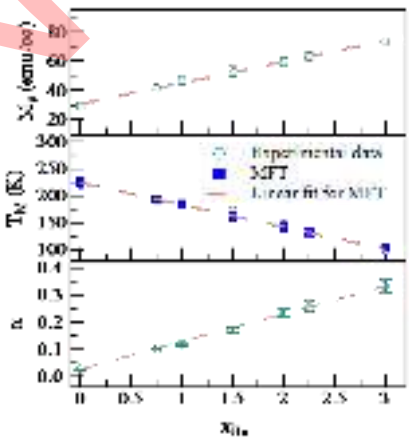

Fig. 1: *The evolution of* $M_S, T_M, and\ \alpha$ *as a function of Ho concentrations.*

References

[1] H. Bai, W. Si, H.-A. Zhou, L. Wang, T. Xu, Y. Dong, J. Zhu, W. Jiang, Physical Review Materials **7**, 094401 (2023).

CANCELLED

Quantum Transport and Novel Broken Symmetry Ground States V

03.05.2024 FRIDAY

Abstract ID: 1513

ELECTRICAL BREAKDOWN OF EXCITONIC INSULATORS

Yuelin Shao[1,2], Xi Dai[2]

[1]Beijing National Laboratory for Condensed Matter Physics and Institute of Physics, Chinese Academy of Sciences, Beijing 100190, CHINA
[2]Department of Physics, The Hongkong University of Science and Technology, Clear Water Bay, Kowloon 999077, Hong Kong, CHINA
E-mail: daix@ust.hk

In this paper, we propose a new electrical breakdown mechanism for exciton insulators in the BCS limit, which differs fundamentally from the Zener breakdown mechanism observed in traditional band insulators. Our new mechanism results from the instability of the many-body ground state for exciton condensation, caused by the strong competition between the polarization and condensation energies in the presence of an electric field. We refer to this mechanism as "many-body breakdown". To investigate this new mechanism, we propose a BCS-type trial wave function under finite electric fields and use it to study the many-body breakdown numerically. Our results reveal two different types of electric breakdown behavior. If the system size is larger than a critical value, the Zener tunnelling process is first turned on when an electrical field is applied, but the excitonic gap remains until the field strength reaches the critical value of the many-body breakdown, after which the excitonic gap disappears and the system becomes a highly conductive metallic state. However, if the system size is much smaller than the critical value, the intermediate tunnelling phase disappears since the many-body breakdown happens before the onset of Zener tunnelling. The sudden disappearance of the local gap leads to an "off-on" feature in the current-voltage (I−V) curve, providing a straightforward way to distinguish excitonic insulators from normal insulators.

Abstract ID: 1439

DIRAC PLASMON EMISSION IN PHOTO-EXCITED HEAVILY DOPED GRAPHENE KC_8

Josip Jakovac

Institute of Physics, Bijenička 46, 10000 Zagreb, CROATIA
E-mail: jjakovac@ifs.hr

Decay mechanisms and plasmon satellites formed in the spectrum of a photo-excited hole in doped graphene is a phenomenon that has been investigated for a long time using angle resolved photoemission spectroscopy (ARPES) measurements [1-3]. I will present the *ab initio* simulation of the photo-hole spectra in doped graphene KC_8 in the framework of our recently developed *many body* RPA-G_0W_0 method [4]. The obtained results show that the hole decay width along the C(π) and K(σ) bands behaves according to the exponential law

$\Gamma \sim |E_{\sigma,\pi\mathbf{K}}-E_F|^{\alpha}$, where $\alpha=3/2$ (**Fig1a**), which perfectly agrees with the previous experimental predictions [1] and deviates from the standard Fermi liquid behavior $\alpha=2$. At deeper energies (below the Fermi energy), the width of the π band shows a peak that comes from the decay due to Dirac plasmon emission, also predicted experimentally [1]. I will also present the plasmonic satellites appearing in the hole spectrum (**Fig1b**), whose intensities are much lower than experimentally predicted [2,3]. However, the plasmaron binding energy of $\Delta=|E_{DP1}-E_D|\sim0.5$eV is in excellent agreement with recent experiments [2,3]. Our simulations predict that even two plasmon satellites DP_1 and DP_2 appear in the KC_8 photo-hole spectrum (**Fig1b**).

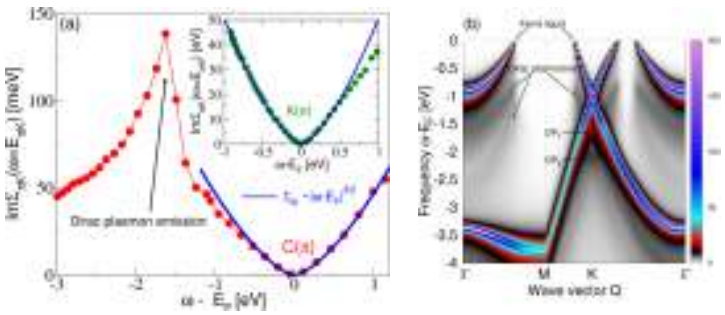

Fig. 1: (a) *The imaginary part of self-energy along π band [ImΣ(ω=$E_{\pi K}$)] in doped graphene KC_8. The insert shows the same for K(σ) band (b) The simulation of the spectral intensity of the holes created in K(σ) and C(π) bands along high symmetry path (Γ-K-M-Γ) in heavily doped KC_8 graphene.*

References

[1] A. Bostwick, T. Ohta, T. Seyller, K. Horn, E. Rotenberg, Nature Phys. **3**, 36 (2007).
[2] H. Zhang, S. Wang, E. Wang, *et al.,* npj Quantum Mater. **6**, 83 (2021).
[3] A. Bostwick, F. Speck, T. Seyller, *et al.*, Science **328**, 999 (2010).
[4] L.A. Barišić, V. Despoja, Phys. Rev. B **109**, 035301 (2024).

Abstract ID: 240

STUDY OF ELECTRIC AND ATOMIC PROPERTIES AT THE GRAIN BOUNDARY IN PEROVSKITE MATERIALS

M.R. Samatov, D. Liu, A.S. Vasenko

HSE University, 101000 Moscow, RUSSIA
E-mail: samatovmichael@gmail.com

Grain boundaries play an important role in determining optoelectronic properties of perovskites, requiring an atomistic understanding of the underlying mechanisms. Strain engineering is recently employed in perovskite solar cells, providing a novel perspective on the role of perovskite GBs. Despite the fact that the metal halide perovskites are not strongly susceptible to defect formation, we still observe carrier recombination at grain boundaries [1]. In addition, we assume that these boundaries contribute to ion migration, which leads to stability problems. In this paper, we examined the migration of Br ions in $CsPbBr_3$ at the grain boundary. Fig. 1a and c show graphs of the Mean squared displacement (MSD) dependence on time for Br atoms. Based on these results, it can be concluded that these atoms change their positions over time. However, our assumption suggests that only atoms at the boundaries should escape from their stationary states. This is well illustrated in Fig. 1b, where the MSD dependence for Br atoms is constructed at a certain point in time depending on the position of the atoms along the z axis. It is clearly seen here that the atoms are more mobile at the boundaries (z = 0, 53 and 106 A). Also, considering the average MSD value for mobile atoms, one can notice an increase in their mobility over time (Fig. 1d).

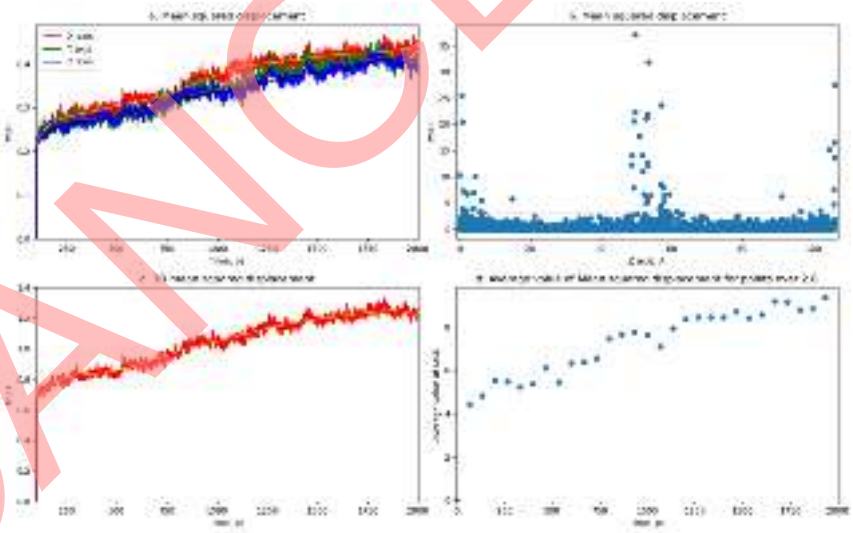

Fig. 1: *Mean squared displacement for Br atoms in $CsPbBr_3$.*

References

[1] J.Y. Woo, Y. Kim, J. Bae, T.G. Kim, J.W. Kim, D.C. Lee, S. Jeong, Chem. Mater. **29**, 7088-7092 (2017).

CANCELLED

Abstract ID: 1597

UNCONVENTIONAL ELECTRONIC INSTABILITIES IN KAGOME METALS: INSIGHTS FROM ARPES

Yong Hu

Center of Quantum Materials and Devices and Department of Applied Physics, Chongqing University CHINA
E-mail: yong.hu@psi.ch

Exploring exotic electronic orders and their underlying driving forces remains a central pursuit in the field of quantum materials. Within this context, the kagome lattice, a corner-sharing triangle network, has emerged as a versatile platform for exploring unconventional correlated and topological quantum states. Due to the unique correlation effects and frustrated lattice geometry inherent to kagome lattices, several families of kagome metals have been found to display a variety of competing electronic instabilities and nontrivial topologies, including quantum spin liquid, unconventional superconductivity, charge density wave orders, and Dirac/Weyl semimetals. Against this backdrop, kagome systems offer an exceptional quantum playground for delving into the intricate interplay among electron correlation effects, geometric frustration, and band topology. In this talk, I will present our recent work, focusing specifically on the unconventional electronic instabilities observed in kagome metals AV_3Sb_5 (A = K, Rb, Cs) [1-4], ATi_3Bi_5 [5], and RV_6Sn_6 (*R* = Gd, Sc) [6,7]. Drawing particularly from the insights derived from angle-resolved photoemission spectroscopy (ARPES), I will highlight the unique characteristics of these systems, shedding light on their intriguing electronic behaviors and elucidating their underlying mechanisms.

References

[1] Y. Hu *et al.*, Nat. Commun. **13**, 2220 (2022).
[2] Y. Hu *et al.*, Sci. Bull. **67(5)**, 495-500 (2022).
[3] Y. Hu *et al.*, Phys. Rev. B **106**, L241106 (2022).
[4] Y. Hu *et al.*, npj Quantum Mater. **8**, 67 (2023).
[5] Y. Hu *et al.*, Nat. Phys. **19**, 1827-1833 (2023).
[6] Y. Hu *et al.*, Sci. Adv. **8**, eadd2024 (2022).
[7] Y. Hu *et al.*, Nat. Commun **15**, 1658 (2024).

CANCELLED

Bulk Superconductors II

03.05.2024 FRIDAY

Abstract ID: 1065

IN SITU SELF-ASSEMBLED DOUBLE-SEEDS WITH EXACT-(110)/(110) ALIGNMENT FOR GROWING HIGH-PERFORMANCE YBCO BULKS

Xin Yao

School of Physics and Astronomy, Shanghai Jiao Tong University, Shanghai 200240, CHINA
E-mail: xyao@sjtu.edu.cn

The application of $YBa_2Cu_3O_{7-\delta}$ (YBCO) superconductor bulks as high-field permanent magnetics requires development towards large size with desired performance. Normally, sizable bulks are fabricated by multi-seeded melt-growth for time saving. However, the performance of such bulks has long suffered from certain methodological barriers related to artificially-induced unreliable precision in seed alignment. Here, inspired by the self-assembly strategy, we report a facile but effective in situ self-assembly (ISSA) approach for seeding structural design, in which exactly (110)/(110) aligned twin-seeds naturally arose through the self-replication of crystallographic orientation from one small seed during thermal procedure, distinctively generating a [110]-oriented rapid-growth zone. This characteristic evolution leaded to a connection between two induced grains and then a fully-grown single grain. Benefiting from the enlarged c-GS and the clean grain-boundary structure, the ISSA seeded YBCO single grains of 25mm diameter demonstrate superior trapped fields up to 0.89 T with a mono-peak profile, which make them ideal candidates for various applications as permanent magnets. The developed seeding architecture in this work, with its nature in achieving exact seed alignment, represent a crucial step beyond conventional approaches of artificially-aligned multi-seeding and will advance the fabrication of high-performance and sizable REBCO superconductors based on architecture optimization.

Abstract ID: 1527

PRODUCTION OF LARGE-SIZE Bi-2212 PLATES USING LASER-FURNACE TECHNOLOGIES

C. Özçelik[1], H. Amaveda[1], M. Mora[1], E. Martínez[1], G.F. de la Fuente[1], L.A. Angurel[1], B. Özçelik[2]

[1] *Instituto de Nanociencia y Materiales de Aragón, INMA (CSIC-Universidad de Zaragoza), María de Luna, 3, 50018 Zaragoza, SPAIN,*
[2] *Cukurova University, Faculty of Science&Letters, Physics Department Adana, TURKEY*
E-mail: ozcelik@cu.edu.tr

Due to the anisotropy problem in high temperature (HT_c) superconductors, the technological applications of these materials are always a major challenge. For this reason, materials having improved mechanical, microstructural and superconducting properties are needed. Recently, laser induced solidification techniques have been used to modify the microstructure of technological materials as *HTc* superconductors. Among these techniques, the Laser Floating Zone (LFZ) and the Electrically Assisted Laser Floating Zone (EALFZ) techniques have been used to fabricate fibers/rods with attractive physical properties due to the well-orientated grain alignment induced after solidification [1,2]. Later, the laser technique has been modified to fabricate materials in planar geometries [3]. Controlling the energy distribution along the laser scanned line, the Laser Zone Melting (LZM) can be applied to texture large area samples [3]. Controlling the scanning laser parameters, it is possible to generate a thin molten volume parallel to the scanning direction. On the other hand, during laser treatment on ceramic materials, high thermal stresses can induce some unwanted cracks that can deteriorate their physical and transport properties. This problem can be handled by performing the laser treatment inside a furnace at high temperatures [4]. The laser furnace system permits to focus a laser beam on a sample moving inside a rolling furnace, at temperatures that minimize crack generation. In this study, we have fabricated Bi-2212 superconducting samples with dimensions up to 10 cm x10 cm by using a laser line scanning protocol. The flatness reached in the solidification front allows obtaining misorientation angles lower than 5º in the full width of the sample. Transport properties of these superconducting materials have been correlated with the level of texture and the distribution of grain size reached during the laser induced solidification process. Additional micromachining protocols using fs lasers have been applied to fabricate samples with different geometries without deteriorating the superconducting properties.

Acknowledgements

B. O. acknowledges to the Scientific and Technological Research Council of Turkey (TUBITAK) for a grant via 2219-Science Fellowships and Grant Programmes Department, with the project number:1059B192000390. Work funded by the Spanish MCIN/AEI/10.13039/501100011033 (project PID2020-113034RB-I00) and by Gobierno de Aragón (research group T54_23R). Authors also would like to acknowledge the use of Servicio General de Apoyo a la Investigación-SAI, Universidad de Zaragoza.

References

[1] R.S. Fiegelson *et al.*, Science, **vol. 240, no. 4859**, pp. 1642–1645 (1988).
[2] M.F. Carrasco *et al.*, Appl. Surf. Sci., **vol. 257, no. 12**, pp. 5283–5286 (2011).
[3] V. Lennikov *et al.*, J. Supercond. Nov. Magn., **vol. 26, no. 4**, pp. 947–952 (2013).
[4] M. Mora *et al.*, Supercond. Sci. Technol., **vol. 17, no. 11**, pp. 1329– 1334 (2004).

CANCELLED

Abstract ID: 1307

INFLUENCE OF LOW OXYGEN PRESSURE ON Tl-BASED HTS PHASE FORMATION

I.R. Metskhvarishvili[1,2], D.L. Surmanidze[1,3], T.E. Lobzhanidze[3], G.N. Dgebuadze[1], V.M. Gabunia[1,4], B.G. Bendeliani[1], M.R. Metskhvarishvili[5]

[1]*Ilia Vekua Sukhumi Institute of Physics and Technology, Laboratory of Cryogenic Technique and Technologies, Mindeli St. 7, 0186 Tbilisi, GEORGIA*
[2]*Georgian Technical University, Faculty of Informatics and Control Systems, Department of Microprocessor and Measurement Systems, Kostava St. 77, 0175 Tbilisi, GEORGIA*
[3]*Ivane Javakhishvili Tbilisi State University, Faculty of Exact and Natural Sciences, Department of Chemistry, Chavchavadze Ave. 3, 0179 Tbilisi, GEORGIA*
[4]*Petre Melikishvili Institute of Physical and Organic Chemistry of the Iv. Javakhishvili Tbilisi State University, Jikia st. 5, 0186, Tbilisi, GEORGIA*
[5]*"Talga" Institute of Georgian Technical University, Zurab Anjaparidze 5, 0186 Tbilisi, GEORGIA*
E-mail: i.metskhvarishvili@sipt.org.ge

The structurally related Tl–Ba–Ca–Cu–O Tl-based superconducting compounds are represented by the chemical formula $Tl_mBa_2Ca_{n-1}Cu_nO_y$, where m=1 or 2 and $1 \leq n \leq 5$. In the synthesis process, it can form multiple phases with different numbers of copper oxide layers: Tl-2201→Tl-2212→Tl-2223→Tl-1223 with critical temperatures of 90, 110, 127, 125, and 115K, respectively.

In this study, we report the influence of low oxygen pressure from 1 to 8 atm on the formation of Tl-based high-temperature superconductors. For this study, we used the in-situ polymerization method for synthesizing high-purity and reaction-ability precursors.

Our experimental results showed the 1 atm pressure formed a non-pure Tl-1223 phase containing precursor $BaCuO_2$ phase, with the onset transition temperature T_c at 115 K and transport critical current density at 25 A/cm². Unlike this, at 2 atm, formed Tl-1223 near the single phase consists small amount of impurity phases with critical temperature and current density 118 K and 129 A/cm², respectively. Enhancement of oxygen gas partial pressure at 3 atm leads to the formation of Tl-2223 phases, with $T_c \approx 125$K and $J_{cJ} \approx 82$ A/cm², and finally, cases 4 - 8 atm formed only the Tl-2212 phases. In resume, we can say the Tl-1223, Tl-2223, and Tl-2212 single phases are formed at 2, 3, and 4 atm oxygen pressure, respectively [1].

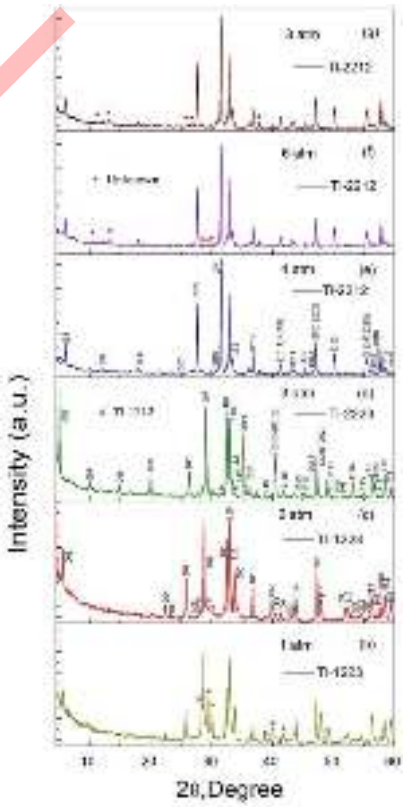

Fig. 1: *XRD patterns of the Tl-based superconductors prepared under 1 up to 8 atm.*

References

[1] D.L. Surmanidze, T.E. Lobzhanidze, I.R. Metskhvarishvili, G.N. Dgebuadze, B.G. Bendeliani, M.R. Metskhvarishvili, V.M. Gabunia, Low Temperature Physics/Fizika Nizkikh Temperatur, **50**, 37 (2024): doi: 10.1063/10.0023889

Abstract ID: 1328

W-Nb-Mo-V-Ta-Cr-Al REFRACTORY HIGH-ENTROPY ALLOYS FOR POTENTIAL SUPERCONDUCTING MATERIALS

Burçak Boztemur, M. Lütfi Öveçoğlu, Duygu Ağaoğulları

Istanbul Technical University, Faculty of Chemical and Metallurgical Engineering, Department of Metallurgical and Materials Engineering, Particulate Materials Laboratories (PML), Graphene & 2D Materials Laboratory, 34469 Maslak, Istanbul, TÜRKIYE

E-mail addresses: boztemur15@itu.edu.tr & bozkurtdu@itu.edu.tr

We present a study of superconductivity in W-Nb-Mo-V-Ta-Al-Cr refractory high-entropy alloys (RHEAs) by investigating nine samples of different atomic concentrations (equimolar and off-equimolar) and number of components (5-7), subjected to different thermal treatments. The mechanical alloying (MA) for 6 hours was applied to obtain RHEA powders. According to the X-ray diffraction (XRD) method, the body-centered cubic (BCC) phase and NbTa phase with a small amount of WC impurity that comes from vials and balls were determined after 6 h MA. Also, RHEA powders were consolidated with the spark plasma sintering (SPS) method (1500 ºC, 30 MPa, and 10 min). After the SPS method, (Nb,Ta)C and $W_2C_{0.85}$ phases were obtained with the decomposition of WC and stearic acid that is added during MA based on XRD results. Superconductivity was found to be a robust phenomenon, being quite insensitive to the actual structure of the material. All investigated samples were superconducting in the entirety of their volumes. The superconducting transition temperatures T_C of the samples are scattered in the range between 10 and 250 K and this scatter could be related to the degree of structural and chemical inhomogeneity of the samples. In the samples with partially ordered nanostructure, short-range atomic clusters possess a slightly different T_C than the Ta- and Nb-rich matrix. Our results also demonstrate the important fact that the formation, stability and structure of a regular (non-ideal) RHEA mixture are determined by both, the minimization of the mixing enthalpy that favors local atomic ordering and the maximization of the mixing entropy that favors a random solid solution. Also, the BCC phase was obtained for the all samples. While the Al_2O_3 phase with a small intensity was seen for the Al addition RHEA samples, the Ta_2VO_6 phase was determined for the other samples. These phases were observed as three different regions according to scanning electron microscopy (SEM). All elements were distributed homogeneously on the white region by measuring of electron probe micro-analyzer (EPMA) coupled with a wavelength dispersive spectroscope (WDS). Also, the grey region of the WNbMoVTa and Cr addition-RHEA samples were rich for Ta, V, and O elements. However, the amount of Al and O elements was higher for the grey region of the Al addition-RHEA sample. The high amount of Nb, Ta, and C elements was determined for both samples. Archimedes' densities that were measured with alcohol media were closer to the theoretical densities of RHEAs.

Bulk Superconductors III

03.05.2024 FRIDAY

Abstract ID: 1508

BULK TRAPPED-FIELD SUPERCONDUCTING MAGNETS ARRANGED IN A LINEAR HALBACH ARRAY: IMPORTANT POINTS TO ACHIEVE THE FULL POTENTIAL OF THE MAGNETIZED SUPERCONDUCTORS

M. Houbart[1], N. Rotheudt[1], J.F. Fagnard[1], J. Dular[2], A.R. Dennis[3], D.K Namburi[4], J.H. Durrell[3], C. Geuzaine[1], B Vanderheyden[1], P. Vanderbemden[1]

[1]*Department of Electrical Engineering and Computer Science, Montefiore Research Unit, University of Liege, Liege, BELGIUM*
[2]*CERN, TE-MPE-PE, Geneva, SWITZERLAND*
[3]*University of Cambridge, Bulk Superconductivity Group, Cambridge, U.K.*
[4]*University of Glasgow, Quantum Sensors Group, U.K.*
E-mail: Philippe.Vanderbemden@ulg.ac.be

Bulk superconductors can act as very powerful permanent magnets, referred to as trapped-field superconducting magnets. These superconducting magnets can generate magnetic field gradients much larger than those typically achievable with conventional ferromagnetic materials [1]. This property is exploited for generating remotely a magnetic force in a number of engineering applications including magnetic separation or magnetic drug delivery [2]. Arranging trapped-field superconducting magnets with mutually perpendicular magnetization directions allows one to make a linear Halbach array. Building such arrays opens the prospect of generating magnetic field gradients exceeding significantly those generated by a single superconductor. One of the main challenges in achieving this goal is to ensure that the superconductors remain fully magnetized during the assembly process of the array [3]. In this communication, different solutions are described and compared to overcome the demagnetization of the trapped-field superconducting magnets. We consider either taking advantage of an additional superconductor removed at 90° from the axis of the array [4], using bulk superconductors with triangular cross-section or creating a vertical offset between the central and peripheral samples. Experimental results are presented on a linear array made of three magnetized bulk large grain melt-textured $YBa_2Cu_3O_{7-\delta}$ superconductors at 77 K. The experimental spatial distribution of the magnetic flux density above the assembly is compared to analytical calculations and finite-element simulations. In addition, arrangements involving non-cubic superconductors are characterized using a bespoke cryogenic 3-axis Hall probe [5]. We show how the various solutions modify the distribution of the magnetic flux density at reasonable distance from the assembly while ensuring a minimal demagnetization effect. By examining the 'useful' spatial zone where the magnetic field gradient exceeds a given threshold (e.g. 1 T/m), it is possible to obtain array configurations for which the extension of the useful zone is significantly larger than that of a single magnetized superconductor.

References

[1] J.H. Durrell *et al.*, Supercond. Sci. Technol. **31**, 103501 (2018).
[2] A. Arsenault *et al.*, IEEE Trans. Appl. Supercond. **33**, 4401409 (2023).
[3] M. Houbart *et al.*, Supercond. Sci. Technol. **35**, 064005 (2022).
[4] M. Houbart *et al.*, Supercond. Sci. Technol. **36**, 115012 (2023).
[5] N. Rotheudt *et al.*, Cryogenics **133**, 103693 (2023).

Abstract ID: 1623

BULK MgB_2 FOR APPLICATIONS AT LIQUID HYDROGEN TEMPERATURES

Tetiana Prikhna[1, 4, 5], Michael Eisterer[2], Canan Aksoy[3], Viktor Moshchil[1], Bernd Büchner[4], Tersa Puig[5], Dirk Lindackers[4], Paul Sass[6], Anton Shaternik[1], Volodymyr Sverdun[1], Semyon Ponomarov[7], Ali Gencer[8]

[1] *V. Bakul Institute for Superhard Materials of the National Academy of Sciences of Ukraine, 2, Avtozavodskaya Str., Kiev 07074, UKRAINE*
[2] *Institute of Atomic and Subatomic Physics, TU Wien, Stadionallee 2, 1020 Vienna, AUSTRIA*
[3] *Karadeniz Technical University, Faculty of Technology, Department of Electronics and Communication Engineering, 61850, Trabzon, TURKIYE*
[4] *Leibniz-Institut für Festkörper- und Werkstoffforschung Dresden e. V., Helmholtzstraße 20, 01069 Dresden, GERMANY*
[5] *Institut de Ciencia de Materials de Barcelona, CSIC, Universitat Autònoma de Barcelona, Campus de la, Carrer dels Til·lers, s/n, 08193 Bellaterra, Barcelona, SPAIN*
[6] *ScIDre – Scientific Instruments Dresden GmbH, Gutzkowstraße 30, 01069 Dresden, GERMANY*
[7] *Institute of Semiconductor Physics of the National Academy of Sciences of Ukraine, 41, Nauky Ave., Kyiv 03028, UKRAINE*
[8] *Ankara University, Center of Excellence for Superconductivity Research, 06500, Golbasi, Ankara, TURKEY*
E-mail: aksoycanan0@gmail.com

Intensive development of hydrogen technologies makes very promising application of one of the cheapest and easily produced bulk MgB_2-based superconductors capable of operating effectively at liquid hydrogen temperatures (around 20 K) and being used as elements of various devices such as magnets, magnetic bearings, fault current limiters, electrical motors, and generators. High-performance submersible liquid hydrogen pumps, for example, requires superconducting bearings which can trap magnetic fields of about 500-600 mT at 20 K. The superconducting properties and microstructure of differently prepared MgB_2 with additions of Ti, Ti-O and TiC (under high pressure of 2 GPa and by hot pressing under 30 MPa) were compared. The ability of different composite materials to trap magnetic fields was studied using hollow cylinders of the same geometry which were manufactured from hot pressed blocks. The field at 20 K in the center of cylinder prepared from hot pressed MgB_2 sample with Ti-O addition remains close to zero (nearly perfect shielding) until the first flux jump appears at about 1.7 T. Screening of the field change remains then again nearly perfect before the next flux jumps appears. The behavior changes at about 3.7 T when the field change in the center of the cylinder is not caused by another flux jump but by a continuous flow of vortices through the superconductor. The field in the center changes faster than the applied field because critical current density, J_c, decreases with field and shielding is monotonously reduced. The field change is first continuous on the decreasing field branch, but shielding becomes more efficient due to the increasing J_c; thus the field in the cylinder changes less than the applied field, until a field jump releases the trapped flux. Finally, the field remains frozen resulting in a remanent trapped field of about 2.8 T. Very similar at 20 K behaved hot pressed material with Ti addition, while that with TiC addition demonstrated much lower characteristics. The study of the materials stability for 7 days in hydrogen at room temperature under 4.2-1.4 bar pressure did not revealed essential variation of their ability to trap magnetic field, while traditional NdFeB and SmCo magnets were turned into powders.

Abstract ID: 1589

SUPERCONDUCTING PROPERTIES OF A SEED INFILTRATION GROWTH (BSIG) PROCESSED REBCO SINGLE CRYSTALS

E. Coskun[1], F. Al-mokdad[1,2], C. Aksoy[1,3], E. Aksu[4], Y.Oznal[1], B. Cakır[5], K. Sonmez[1], S. Celik[6], A. Gencer[1,2]

[1] Ankara University, Superconductor Technologies Application and Research Center, Gölbaşı, Ankara, TURKIYE
[2] Ankara University, Faculty of Sciences, Physics Department, 06100-Beşevler-Ankara, TURKIYE
[3] Electronics and Communication Engineering, Faculty of Technology, Karadeniz Technical University, 61830 Trabzon, TURKIYE
[4] Tenmak, Nüken, Saray Mahallesi Atom Caddesi No:27 06980 Kahramankazan, Ankara, TURKIYE
[5] Vocational School of Health Services, Artvin Çoruh University, 08000 Artvin, TURKIYE
[6] Department of Energy Systems Engineering, Faculty of Engineering and Architecture, Sinop University, Sinop, TURKIYE

E-mail: aligencer06@gmail.com

Several methods have been used in the production of REBCO single crystals using seed infiltration growth, for producing good quality superconductors for large-scale applications. In this study, a single grain YBCO bulk superconductor has been fabricated by using the bottom-seeded infiltration growth (BSIG) method in which a MgO thin film seed crystal was placed under the YBCO sample instead of using conventionally used SmBCO or NdBCO seeds. We have measured a high trapped field about half of the applied 0.2T magnetic field of the permanent magnet. The superconducting properties of the sample are the superconducting transition temperature, T_c, which was found to be 90.5 K, and critical current density J_c was 8.7 x 10^3 A/cm^2 at 77 K at 4 T. Detailed characterization measurements have been performed on the samples prepared by various seeds, with comparative studies in terms of T_c, J_c, trapped field, and levitation forces together with harmonic susceptibility measurements as a function of Temperature, ac field amplitude, ac filed frequency, in the magnetic field range from 0 to 12 T.

POSTER PRESENTATIONS

28.04.2024 SUNDAY - 30.04.2024 TUESDAY

Abstract ID: 1407

MICROSTRUCTURE EVOLUTION AND MAGNETIC PROPERTIES OF NANOCRYSTALLINE $Ni_{75}Fe_{25}$ THIN FILMS DEPOSITED ONTO GLASS, Al_2O_3 KAPTON SUBSTRATES

A. Kaibi[1,2], A. Guittoum[3], R.M. Öksüzoğlu[4], C.Yavru[4], S. Özgün[4], M. Boudissa[5]

[1]*Physics of Materials laboratory (PML), Faculty of physics, Algiers, USTHB, BP 32 El Alia, ALGERIA*
[2]*University Larbi Tbessi, rout de constantine Tebessa, ALGERIA*
[3]*Nuclear Research Centre of Algiers, Algiers, 02 Bd Frantz Fanon, BP 399, ALGERIA*
[4]*University of Anadolu, Faculty of Engineering, Department of Materials Sciences and Engineering, Eskişehir İki Eylül Campus, 26555, TURKEY*
[5]*ENMC Laboratory, Physics Department, University of Sétif, 19000, ALGERIA*
E-mail: kaibi_amel@yahoo.fr

Permalloy (Py) thin films were evaporated from nanocrystalline soft $Ni_{75}Fe_{25}$ powder onto glass and Al_2O_3 kapton substrates [1]. The thicknesses of these films range from 16 nm to 250 nm. The as deposited films were characterized by Grazing incidence X-ray diffraction (GIXRD), Scanning Electron Microscopy (SEM), Atomic Force Microscopy (AFM) and vibrating sample magnetometry (VSM). From GIXRD spectra, we have shown that the films are amorphous for the thinner films. However, for the thicker films, a polycrystalline fcc structure is present. For the intermediate thicknesses, the nature of substrate determines the texture of the films. The SEM micrographs indicate that the nature of substrate influences on the morphology and grains size of Py films. From AFM observations, the nanocrystalline nature of the grains is evidenced. Hysteresis loops reveals the ferromagnetic character of Py films. We have shown that the values of coercive field, H_c, generally, decrease with increasing thickness. Moreover, the H_c values are higher for films deposited onto kapton substrate than those on glass one. The nature of substrate and thickness seems to influence the magnetic properties of Py films. A correlation between these physical properties will be established and discussed.

References

[1] A. Kaibi, A. Guittoum, R.M. Öksüzoglu, A.M. Yagci, M. Boudissad, M. Kechouane, Appl. Sur. Sc. **350**, 50–56 (2015).

Abstract ID: 1322

INVESTIGATION OF THE PHYSICO-CHEMICAL AND SUPERCONDUCTING PROPERTIES OF SUPERCONDUCTING FOAMS PRODUCED BY THE TOP-SEED INFILTRATION-GROWTH (TSIG) METHOD

Paweł Pęczkowski[1], Piotr Zachariasz[2], Ryszard Zalecki[3], Jarosław Piętosa[4], Jan Marek Michalik[3], Cezariusz Jastrzębski[5], Michał Ziętala[6], Marcin Zając[7], Łukasz Gondek[3]

[1]*Cardinal Stefan Wyszyński University, Institute of Physical Sciences, Faculty of Mathematics and Natural Sciences, School of Exact Sciences, K. Wóycickiego 1/3, 01-938 Warsaw, POLAND*
[2]*Łukasiewicz Research Network – Institute of Microelectronics and Photonics, Center for Functional Materials, Zabłocie 39, 30-701 Kraków, POLAND*
[3]*AGH University of Science and Technology, Faculty of Physics and Applied Computer Science, Department of Solid State Physics, A. Mickiewicza 30, 30-059 Kraków, Poland*
[4]*Institute of Physics Polish Academy of Sciences, Division of Physics of Magnetism, Group of Phase Transition, Lotników 32/46, 02-668 Warsaw, POLAND*
[5]*Warsaw University of Technology, Faculty of Physics, Koszykowa 75 Street, 00-662 Warsaw, POLAND*
[6]*Cardinal Stefan Wyszyński University, Multidisciplinary Research Center, M. Konopnickiej 1, 05-092 Dziekanów Leśny, POLAND*
[7]*Jagiellonian University, National Synchrotron Radiation Centre SOLARIS, Czerwone Maki 98, 30-392 Kraków, POLAND*
E-mail: p.peczkowski@wp.pl

The open-cell polyurethanes with various densities, flexibilities, and skeleton types (T-18/30, CL-25/33, T-25/38, HR-30/38, T-30/42, T-35/38, T-40/50) and Melamine were employed to fabricate the $YBa_2Cu_3O_{7-\delta}$ (YBCO or Y-123) superconducting foams in a top-seeded infiltration-growth (TSIG) method. During the TSIG process, precursor foams were infiltrated with a green phase (Y-211) and thermally converted to Y-123 superconductors using $NdBa_2Cu_3O_{7-\delta}$ (NdBCO) single-crystal seeds oriented in the [100] direction. Interestingly, the Y-123 structure growth tendency preserves the crystallographic direction of the NdBCO nucleation agent regardless of the initial orientation of the polyurethane skeleton fiber. The highest porosity of foam structures emerges for congruous densities and elasticities (T-25/38, HR-30/38). In contrast, the outermost mechanical parameters (T-18/30 or T-40/50) prevent high porosity of foam architectures due to pore heterogeneity and their size miscellaneousity. Raman and XAS spectra confirmed the superconducting phase (orthorhombic Y-123) through the characteristic vibrational mode around 500 cm^{-1} and the dominance of ZRS (Zhang-Rice singlets) contribution over UHB (upper Hubbard band), respectively. High-density and stiffness foams favor Y-123 phase evolution, while more flexible foam structures weakly transform Y-211 into Y-123. Moreover, research shows that foam structures preserved the critical temperature (T_c) of YBCO. Essentially, T_c is not significantly influenced by the preparation methodology (specimens T-25/38(1-4)), foam mechanical parameters, or their architecture (porosity). However, the listed-above features affect the nature of superconductivity through the Y-211 assimilation by foam structures and Y-211 to Y-123 conversion efficiency at the TSIG process.

Acknowledgments

Paweł Pęczkowski would like to thank the National Science Centre for support under the MINIATURA 5 project No. DEC-2021/05/X/ST5/00865.

The authors would like to thank "JAG" PTC PLC (Lisków, Poland) for sending polyurethane foams, which were the skeleton for the production of superconducting foams using the Top Seeded Infiltration Growth (TSIG) method.

This work (in the part concerning synchrotron measurements) was developed under the provision of the Polish Ministry and Higher Education project "Support for research and development with the use of research infra-structure of the National Synchrotron Radiation Centre SOLARIS" under contract No. 1/SOL/2021/2. We acknowledge SOLARIS Centre for the access to the PIRX beamline, where the measurements were performed.

Abstract ID: 1331

LASER-INDUCED ULTRAFAST INSULATOR-METAL TRANSITION IN $BaBiO_3$

A.E. Lukyanov[1,2], V.D. Neverov[1,2], Ya.V. Zhumagulov[3], A.P. Menushenkov[1], A.V. Krasavin[1,2], Alexei Vagov[2,4]

[1]*National Research Nuclear University MEPhI, Moscow, RUSSIAN FEDERATION*
[2]*HSE University, Moscow, RUSSIAN FEDERATION*
[3]*Institute for Theoretical Physics, University of Regensburg, Regensburg, GERMANY*
[4]*Moscow Institute of Physics and Technology, Dolgoprudny, RUSSIAN FEDERATION*
E-mail: lukyanov9567@gmail.com

This study explores the ultrafast dynamics of BaBiO3 when subjected to an intense laser pulse [Fig. 1]. The investigation employs the Holstein model for the material, solved within the time-dependent dynamic mean field theory approach and complemented by the self-consistent Migdal approximation for the self-energy. This comprehensive approach takes into account quantum coherences, enabling the calculation of the ultrafast time evolution of the system.

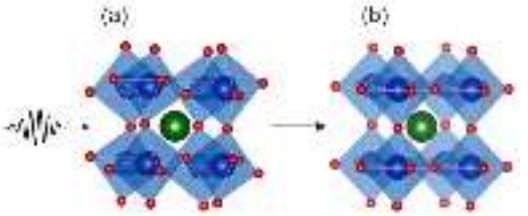

Fig. 1: *(a) Schematic crystal structure of $BaBiO_3$ distorted by CDW; (b) The laser excitation removes the lattice distortion.*

The results illuminate a brief transition between insulating and metallic states within the system, accompanied by the disappearance of the charge density state and the corresponding energy spectrum gap [Fig. 2]. Notably, this transition occurs on a timescale of tens of femtoseconds, comparable to the period of lattice vibrations. The intricate dynamics arise from the complex interplay of particle-hole excitations across the gap and tunneling through it. This interplay generates a highly nontrivial time evolution characterized by the presence of high harmonics and periodic reappearance of the gap [1].

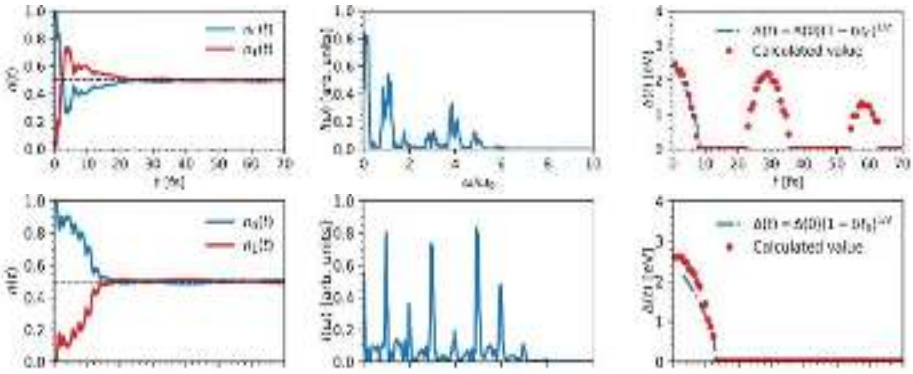

Fig. 2: *Time evolution of the driven system: electronic occupation in different octahedra (left), spectra of electron dynamics (middle), time evolution of dielectric gap (right).*

The work was supported by HSE University Basic Research Program and MEPhI Program Priority 2030, by Ministry of Science and Higher Education of Russian Federation (No. FSWU-2023-0031, FSMG-2023-0014), and by RSF grant 23-72-30004.

References

[1] A.E. Lukyanov *et al.*, Phys. Rev. Research **2**, 043207 (2020).

Abstract ID: 1360

INVESTIGATION OF THE MECHANICAL BEHAVIOUR OF PARTIALLY SUBSTITUTED Tb/Y AND Zn/Cu Y-358 SUPERCONDUCTORS

Ö. Öztürk[1], G. Güdücü[1], S. Kurnaz[2], T. Seydioğlu[1], S. Safran[3]

[1]Kastamonu University, Dept. of Electrical&Electronics Engineering, 37150, Kastamonu, TURKEY
[2]Kastamonu University, Central Research Laboratory, 37150, Kastamonu, TURKEY
[3]Department of Physics, Ankara University, 06100 Ankara, TURKEY
E-mail: oozturk@kastamonu.edu.tr

The quest for superconductors with superior mechanical properties drives the exploration of homovalent substitutions. In this work, we have systematically incorporated Tb/Y and Zn/Cu dopants into $Y_{3-x}(Tb)_xBa_5Cu_8O_{7-\delta}$ and $YBa_2Cu_{1-x}(Zn)_xO_{7-\delta}$ based superconductors using the sol-gel technique. By varying the dopant concentration (0-15%), we aim to elucidate the underlying mechanisms governing the interplay between substitution, processing, and mechanical performance. This knowledge can contribute to the design of robust and high performance superconducting materials for various technological applications. They are extensively investigated by X-ray diffraction, Vickers microhardness analysis and related calculations. Microhardness measurements are analysed using the Meyer's law, the proportional sample resistance (PSR) model, the elastic/plastic deformation (EPD) model, the Hays-Kendall (HK) approach, and the indentation-induced cracking (IIC) model. In this investigation, the fundamental mechanisms behind the altered properties of Y-358 superconductors upon Tb/Y and Zn/Cu substitutions are investigated in depth.

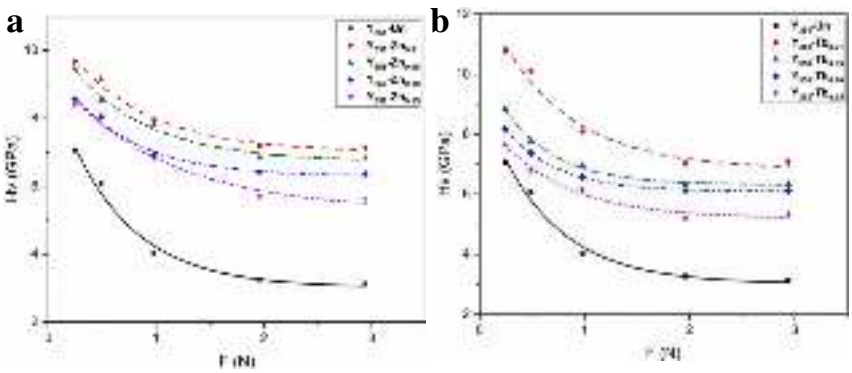

Fig. 1: *Microhardness of (a) Zn and (b) Tb doped Y-358 samples.*

Abstract ID: 1431

SOLAR TECHNOLOGY FOR THE PRODUCTION OF Bi/Pb SUPERCONDUCTING CERAMICS AND ITS PROPERTIES

D.D. Gulamova[1], E.B. Eshonkulov[1], T.I. Gulamov[2], V.R. Li[2], G.I. Mamniashvili[3], G.J. Donadze[3], V.A. Peikrishvili[3]

[1]*Institute of Materials Science, NPO Physics-Sun, Academy of Sciences of the Republic of Uzbekistan, Tashkent, UZBEKISTAN*
[2]*Almalyk branch of National University of Science and Technology, "MISIS", Almalyk, UZBEKISTAN*
[3]*E. Andronikashvili Institute of Physics, I.Javakhishvili State University, Tbilisi, GEORGIA*
E-mail: donadze_g@yahoo.com

The prospect of solar synthesis of Bi/Pb bulk superconducting ceramics is presented based on the experience of solar synthesis of isostoichiometric and isostructural oxides of various compositions [1]. The technology for producing of BSCCO precursors with an oriented structure of crystallites-nuclei in the Large Solar Furnace (Parkent) and the connection of the innate properties with the lamellar morphology of massive ceramics are described. The homophase composition of Bi/Pb ceramics was determined. Graphs of resistance and voltage in the temperature range of the 80-320K are presented. The Meissner effect has been demonstrated in Bi/Pb ceramics at room temperature and normal atmospheric pressure, in daylight and under the influence of light. The properties of Bi/Pb ceramics are explained by effects at grain boundaries caused by a homophase layered structure

References

[1] G.I. Mamniashvili, G.J. Donadze, V.M. Tavkhelidze, D.D. Gulamova, *On the origin of superconducting precursors in Bi/Pb HTSC phases synthesized using solar and explosion energies*, International Journal of Applied Engineering and Technology, **Vol. 5, No. 3**, 98-105, (2023).

Abstract ID: 1501

AN INVESTIGATION COMPARING THE DIFFERENT PHASES OF YBCO SUPERCONDUCTORS DOPED WITH Tb PRODUCED BY THE SOL-GEL ROUTE

Serap Safran[1], Gülnur Güdücü[2], Özgür Öztürk[2], Sedat Kurnaz[3], Elif Aşikuzun Tokeşer[4], Gürcan Yildirim[5]

[1]Department of Physics, Ankara University, 06100 Ankara, TURKEY
[2]Department of Electrical and Electronics Engineering, Kastamonu University, 37210, Kastamonu, TURKEY
[3]Central Research Laboratory, Kastamonu University, 37210, Kastamonu, TURKEY
[4]Department of Metallurgy and Materials Engineering, Kastamonu University, 37210, Kastamonu, TURKEY
[5]Department of Mechanical Engineering, Bolu Abant Izzet Baysal University, 14280 Bolu, TURKEY
E-mail: safranserap@gmail.com

This study examines the superconducting properties of $Y_{1-x}(Tb)_xBa_2Cu_3O_{7-\delta}$ (Y-123) and $Y_{3-x}(Tb)_xBa_5Cu_8O_{7-\delta}$ (Y-358) materials, which are synthesized using sol-gel synthesis and involve the replacement of terbium with yttrium. The samples are sintered at a temperature of 930 degrees Celsius in order to transform them into a superconducting bulk form utilizing chemicals based on acetate. X-ray diffraction (XRD), scanning electron microscopy (SEM), and energy distribution spectroscopy (EDS) are employed to analyze the structural characteristics of the samples. Doping with Tb lowers the critical temperature (T_c) values for superconductivity transition in both YBCO phases. The analysis of the fluctuation induced conductivity of the Y-123 and Y-358 samples is carried out by means of ρ-T measurements. The values of the c-axis coherence length (ξc(0))at zero temperature of the fluctuation analyses based on the resistivity measurements are also in the same trend. The magnetic properties are determined from hysteresis curves obtained by vibrating sample magnetometry (VSM). The critical current density (J_c) and pinning force (F_p) values obtained from hysteresis curves of magnetic measurements generally decrease with Tb doping levels, except for the 0.01 wt. doped Y-123 sample.

Abstract ID: 1504

UNCONVENTIONAL SUPERCONDUCTIVITY IN $PbMo_6Se_8$

Souvik Banerjee, A. Sundaresan

Chemistry and Physics of Materials Unit, Jawaharlal Nehru Centre for Advanced Scientific Research, 560064, Bengaluru, INDIA

E-mail: souvikbanerjee@jncasr.ac.in

We present a comprehensive investigation of superconducting properties in the Chevrel phase compound $PbMo_6Se_8$ by X-ray diffraction, DC magnetization, resistivity, heat capacity, and magnetic relaxation experiments. We determine a bulk superconducting transition temperature T_c of 3.8 K. Key superconducting parameters such as, lower ($\mu_0H_{c1}(0)$) and upper ($\mu_0H_{c2}(0)$) critical fields, coherence length (ξ), penetration depth (λ_{GL}), Ginzburg-Landau parameter (κ) and Pauli paramagnetic field ($\mu_0H_P^{str}$), Maki parameter (α) are obtained. The electronic specific heat in the superconducting state suggests an average energy gap $\Delta \sim 1.56\ k_BT_c$, being close to the weak coupling limit of a BCS limit ($\Delta = 1.76\ k_BT_c$). The electronic specific heat jump ($\Delta C_e/\gamma_eT_c \sim 1.11$) is notably below the conventional BCS limit (1.43), indicating the presence of strong electron-electron correlations in the system and aligning with the potential for a multi-gap phenomenon, as observed in other Chevrel phase compounds [1]. An unconventional vortex state is evident from the investigation of the unusual fishtail effect and unconventional magnetic field dependency [2] of the pinning energy obtained from the magnetic relaxation experiments, indicating a deviation from the ideal type II BCS behavior that suggests unconventional superconductivity in $PbMo_6Se_8$. The μ_0H-T phase diagram illustrates a multiphase vortex crossover.

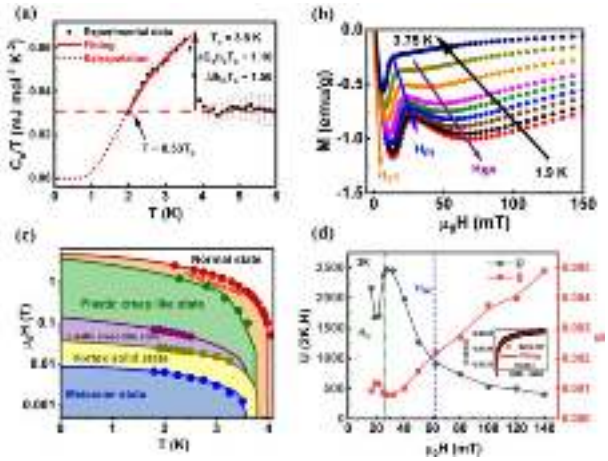

Fig. 1: *(a) Electronic specific heat with exponential fitting. (b) Observation of 'fishtail' in isothermal magnetization. (c) Multi-vortex phase crossover. (d) Unconventional vortex pinning.*

References

[1] P. Petrovic, Phys. Rev. Lett. **106**, 017001 (2011).
[2] A. Pramanik, Phys. Rev. B. **83**, 094502 (2011).

Abstract ID: 1577

SYNTHESIS, CRYSTAL AND ELECTRONIC STRUCTURE OF THE ATM_2Bi_2 SERIES (*TM* = d-METAL, *A* = ALKALI OR ALKALI-EARTH METAL)

E.O. Rakhmanov[1], A.I. Shilov[1,2], A.V. Sadakov[2], A.S. Usoltsev[2], A. Yu. Degtyarenko[2], K.A. Lyssenko[1,3], A.N. Kuznetsov[1,4], I.V. Morozov[1], A.V. Shevelkov[1]

[1] *Lomonosov Moscow State University, Dept. of Chemistry, 119991, Moscow, RUSSIA*
[2] *V.L. Ginzburg Centre for High-Temperature Superconductivity and Quantum Materials P.N. Lebedev Physical Institute of the Russian Academy of Sciences (LPI RAS), 53, Leninsky Ave., 119991 Moscow, RUSSIA*
[3] *National University Higher School of Economics, Faculty of Chemistry, 109028, Moscow, RUSSIA*
[4] *Kurnakov Institute of General and Inorganic Chemistry of RAS, 119991, Moscow, RUSSIA*
E-mail: ra-jenya@yandex.ru

Using a "self-flux" technique, we have grown $BaAg_{1,8}Bi_2$ and $BaAu_{1,8}Bi_2$ single crystals. The latter compound was prepared for the first time [1], whereas the first one was already known [2]. Accoding to XRD single crystal analysis both compounds crystallize in distorted monoclinic variant of $CaBe_2Ge_2$ structure type. The crystal structure of $BaTM_{1.8}Bi_2$ (*TM* = Au, Ag) consists of two types of layers: fluorite-like [Bi*TM*] and antifluorite-like [*TM*Bi] layers along the c-axis. Ba^{2+} cations are located between the layers. *TM* atoms in the [*TM*Bi] layer are locally disordered into four (Au) or two (Ag) equally occupied positions. Also, the fluorite-like layer contains a partial occupancy of the positions of *TM* atoms.

For all the experiments, the samples mounting was made in a dry argon atmosphere. Their chemical composition probed by EDX spectroscopy was found to be $Ba_{1.06(3)}Ag_{1.81(2)}Bi_{2.13(4)}$ and $Ba_{0.97(5)}Au_{1.80(6)}Bi_{2.23(5)}$, which corresponds well to the crystal structure data.

Below $T_c \approx 5{,}5$ K, the sample of $BaAg_{1.8}Bi_2$ turns to the SC state. The width of the resistive SC transition is $\Delta T_c \approx 0.5$ K, which demonstrates a high quality of the crystals.

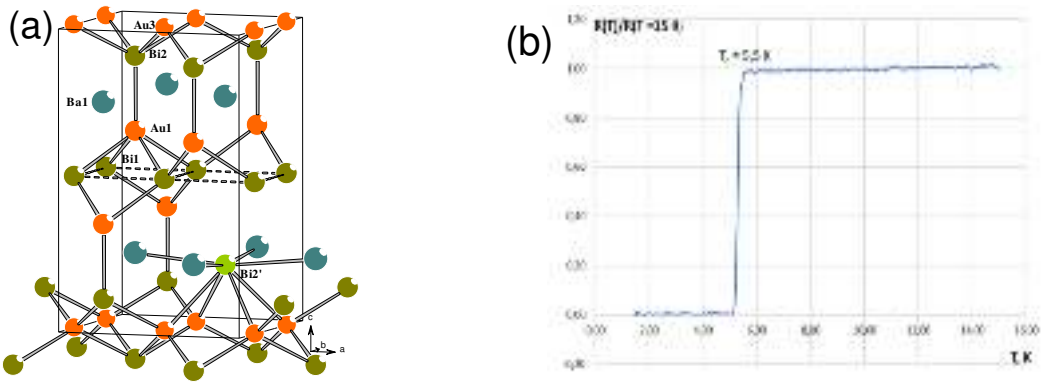

Fig. 1: (a) *Crystal structure of $BaAu_{1.8}Bi_2$. Au3 occupies the ideal 4g position instead of locally split positions Au2 and Au2';* (b) *Temperature dependence of normalized resistance of a bulk $BaAg_{1.8}Bi_2$ single crystal.*

This work was supported by RSCF grant 22-43-02020.

References

[1] A.I. Shilov, E.O. Rakhmanov, K.A. Lyssenko, A.N. Kuznetsov, I.V. Morozov, A.V. Shevelkov, Crystals, **14(2)**, 155 (2024).
[2] Z.-M. Sun, J.-Y. Xie, D.-C. Pan, J.-G. Mao, J. Alloys Compd., **430**, 71–76 (2007).

Abstract ID: 1656

IRRADIATION INFLUENCE ON STRUCTURAL AND MAGNETIC PROPERTIES OF YBCO-123 SUPERCONDUCTOR: AN INVESTIGATION

F. Al-Mokdad[1], E. Aksu[2], S.B. Guner[3], E. Coskun[1], Y. Oznal[1]. K. Sonmez[1], A. Gencer[1]

[1] *Ankara University, Center of Excellence for Superconductiviy Research, 06500, Golbasi, Ankara, TURKIYE*
[2] *Technology Department, Sarayköy Nuclear Research and Training Centre, Turkish Atomic Energy Authority, 06983 Ankara, TURKIYE*
[3] *Department of Physics, faculty of Arts and Sciences, Recep Tayyip Erdogan University, 53100, Rize, TURKIYE*
E-mail: fatima.al.mokdad@outlook.com

Single crystal $YBa_2Cu_3O_7$ (YBCO-123) superconductor samples were prepared using the conventional top seeded melting growth (TSMG) method. This study investigates the influence of irradiation with Co-60 gamma radiation between 50 kGy-500 kGy on the creation of artificial defects within the samples' crystal structure. Various analytical techniques, including X-ray diffraction (XRD) and scanning electron microscopy (SEM), were employed to study the structural effects induced by the irradiation. The magnetic properties of the samples, such as magnetization vs. magnetic field (MH) and temperature (MT) analyses, were conducted in the temperature range of 2K-77K and magnetic field range of 0.5T-3T, respectively, both pre- and post-radiation exposure to understand potential alterations in superconducting properties. Preliminary results suggest radiation-induced modifications, particularly in the formation of artificial pinning centers within the YBCO crystal lattice. These findings emphasize the significant relationship between radiation effects and the superconducting behavior of YBCO materials, with implications for enhancing superconducting device performance and advancing our understanding of superconductor-radiation interactions.

Abstract ID: 1037

THE COMPRESSION SYSTEM OF THE NICA CRYOGENIC COMPLEX

N.N. Agapov, A.E. Emelyanov, A.V. Konstantinov, Iu.A. Mitrofanova, D.S. Shvidkiy

Joint Institute for Nuclear Research, 141980, Dubna, RUSSIA
E-mail: shvidkiy@jinr.ru

The NICA accelerator complex includes three superconducting rings: the Nuclotron, the Booster and the Collider. The Nuclotron and the Booster are operating accelerators; the Collider is currently being under construction.

The operating temperature of the NICA accelerator rings is equal to 4.5 K. Liquid helium for cooling and cryostatting of the superconducting magnetic cryostat systems of the accelerators is provided by the cryogenic facilities: refrigerators and liquefiers. The compressed helium at the input to each of the refrigerators is provided by the compressors of various types and capacities. Two screw aggregates "Kaskad-80/25" are the main compressors at the existing machine hall. These compressors provide with the compressed helium of the cryogenic facilities of the Booster and the Nuclotron. The first stage of the "Kaskad-80/25" contains two compressors operating in parallel, driven by a single electrical motor of power 0.8 MW with a voltage of 6 kV.

To provide with the compressed gas the cryogenic facilities of the collider two new screw compressor aggregates "Kaskad-110/30" will be put into operation. These two-stage compressors were mounted in the new machine hall. The first stage of the "Kaskad–110/30" includes two compressors, but, in comparison with the "Kaskad-80/25", each of them is placed on a separate frame and driven by its own electrical motor with the power of 0.4 MW. This solution together with using of the slide valves allows one to adjust of the compressor capacity from 100 to 20% of the nominal value. Each compressor "Kaskad-110/30" have a capacity of 6600 Nm^3/h and an operating pressure of 30 bar.

In addition to helium cryogenic system the new closed-cycle nitrogen cryogenic system is being under construction for the NICA accelerator complex. This system includes three nitrogen turbo compressors: "Aerokom-179/18" and "Samsung SM5000". Also, two piston compressors with the smaller capacity will be used in the cryogenic system for pumping out of the evaporating nitrogen. All nitrogen compressors are mounted in the new machine hall. Information about the compression system of the NICA cryogenic complex will be given.

References

[1] N. Agapov, *et al.*, *Cryogenic technologies of the superconducting NICA accelerator complex*,Proceedings of 15th IIR Conference Cryogenics 2019, Prague (2019).

[2] N. Agapov, *et al.*, *Status of the NICA cryogenics at JINR*, Proceedings of 1st International IIR Conference ICCRT 2016, Bucharest (2016), p. 183.

[3] N. Agapov, *et al.*, *Nitrogen cryogenic system for the NICA accelerator complex at JINR*, IEEE Transactions on Applied Superconductivity, **Volume: 28**, Issue: 4, (2018).

Abstract ID: 235

DERIVATION OF EFFECTIVE TIGHT-BINDING MODEL FOR COUPLED JOSEPHSON JUNCTION AND SEMICONDUCTOR QUANTUM DOT SYSTEMS

K. Pomorski[1,2], P. Pęczkowski[3], M. Kowalik[4]

[1]Łódź University of Technologies, Institute of Physics, Wólczańska 271/221, 90-451 Łódź, POLAND
[2]Quantum Hardware Systems, Babickiego 10/195, 94-056 Łódź, POLAND
[3]Cardinal Wyszyński University, Faculty of Mathematics and Natural Sciences, School of Exact Sciences, Institute of Physical Sciences, K.Wóycickiego 1/3, 01-938 Warsaw, POLAND
[4]Rzeszów University of Technology, Faculty of Mathematics and Applied Physics, Powstańców Warszawy 8, 35-959 Rzeszów, POLAND
E-mail: kdvpomorski@gmail.com

New Josephson junction [1] systems are proposed [2-4] and go into direction of integration between semiconductor and superconducting electronics. Replacement of microwave waveguides inducing the state of Josephson junctions with chain of coupled semiconductor quantum dots gives chance for more compact scalable superconducting qubits. At the same time topologically protected states are emerging what gives the perspective of scalable and repetitive quantum circuits. All considerations are done in framwork of Wannier qubits [5] interacting perturbatively with Josephson junction basing on Schroedinger model of quantum dots and Bogoliubov-de Gennes model of superconducting nanostructures.

Reference

[1] B.D. Josephson, Phys. Lett. **1(7)**, 252 (1962).
[2] K. Pomorski, P. Pęczkowski, R. Staszewski, Cryogenics **109**, 103117 (2020).
[3] K. Pomorski, P. Giounanlis, E. Blokhina, D. Leipold, P. Pęczkowski, R. Bogdan Staszewski, Proc. SPIE **11054**, 11054M (2019).
[4] K. Pomorski, R. Staszewski, Acta Phys. Pol. A **5(138)** 728-739 (2020).
[5] K. Pomorski, Math. Comp. Simul. **209**, 362-407 (2023).

Abstract ID: 237

INDUCTIVELY COUPLED SUPERCONDUCTING RINGS AND SEMICONDUCTOR RINGS TREATED BY BOGOMOLNY FORMALISM AND SCHROEDINGER-GINZBURG-LANDAU RELAXATION METHOD

Ł. Stępień[1], K. Pomorski[2,3], M. Kowalik[4], P. Pęczkowski[5]

[1]The Pedagogical University in Cracow, Podchorążych 2, 30-084 Cracow, POLAND
[2]Lodz University of Technologies, Institute of Physics, Wólczańska 271/221, 90-451 Łódź, POLAND
[3]Quantum Hardware Systems, Babickiego 10/195, 94-056 Łódź, POLAND
[4]Rzeszów University of Technology, Faculty of Mathematics and Applied Physics, Powstańców Warszawy 8, 35-959 Rzeszów, POLAND
[5]Cardinal Wyszyński University, Faculty of Mathematics and Natural Sciences, School of Exact Sciences, Institute of Physical Sciences, K.Wóycickiego 1/3, 01-938 Warsaw, POLAND
E-mail: kdvpomorski@gmail.com

The case of coupled semiconductor and superconducting rings [1-2] gives new way of controling hybrd quantum electronics. Bogomolny equations [3] allows to obtain various solutions and quite straightforward way. They are confirmed with solutions obtained by Ginzburg-Landau relaxation method [4] that is generalized for coupled Schroedinger and Ginzburg-Landau equation and case of 2 inductively coupled superconducting structures.

References

[1] K. Pomorski, P. Pęczkowski, R. Staszewski, Cryogenics **109**, 103117 (2020).
[2] K. Pomorski, *Intelligent Computing. Lecture Notes in Networks and Systems*, **vol 283**, Springer, 2022.
[3] Ł. Stępień, Acta Physica Polonica B **50(1)**, (2019).
[4] K. Pomorski, H. Akaike, A. Fujimaki, K. Rusek, COMPEL - Internat. J. Comp. Math. Electr. Electr. Eng. **38(1)**, 395-414 (2017).

Abstract ID: 1039

ON THE PATH TO SUPERCONDUCTOR BROADBAND RECEIVERS

V.K. Kornev, N.V. Kolotinskiy

Lomonosov Moscow State University, 119991, Moscow, RUSSIA
E-mail: nkolotinsky@gmail.com

Further progress in communication and information technologies that we need now with increase in the number and variety of the involved information data [1,2] cannot be provided by the only semiconductor-based technologies.

In this work, we review progress in developing the software-defined radio communication systems [3] through using both the rf and digital superconductive technologies.

Both the outstanding sensitivity and the high spurious-free dynamic range (SFDR) of the state-of-the-arts superconductor analog-to-digital converters (ADC) enable broadband receiving systems with direct signal digitizing and following digital extraction of sub-bands. To raise the overall system performance, one can use an active superconductor electrically-small antenna (ESA) instead of a standard passive antenna and a following low-noise amplifier both providing lower performance as compared to the ADC. Both the attainable characteristics and design issues of the superconductor active ESAs are reviewed and discussed in detail.

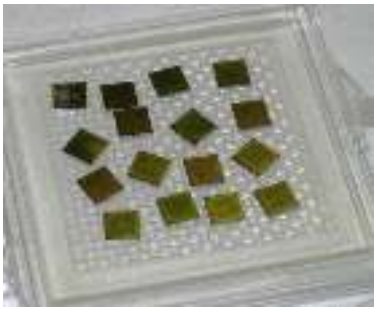

Fig. 1: *Examples of the fabricated electrically-small antenna prototypes. Chip area is 5x5 mm².*

This research was funded by Russian Science Foundation (RSCF), grant number 19-72-10016-P.

References

[1] T. Simonite, *Intel puts the brakes on moore's law*, MIT Tech. Review (23 March 2016). https://www.technologyreview.com/s/601102/intel-puts-the-brakes-onmoores-law/

[2] I.I. Soloviev, N.V. Klenov, S.V. Bakurskiy, *et al.*, *Beyond Moore's technologies: Operation principles of a superconductor alternative*, Beilstein Journal of Nanotechnology, **vol. 8**, pp. 2689–2710 (2017).

[3] T. Ulversoy, *Software defined radio: Challenges and opportunities*, IEEE Communications Surveys & Tutorials **12 (4)**, 531–550 (2010); doi:10.1109/surv.2010.032910.00019.

Abstract ID: 1042

SUPERCONDUCTING PERCEPTRON NETWORK USING HYBRID QFP-RSFQ NEURONS

M. Ameen Jardine[1], Coenrad J. Fourie[2]

[1]*Stellenbosch University, Dept. of Electrical and Electronic Engineering, 7600, Stellenbosch, SOUTH AFRICA*
[2]*Stellenbosch University, Dept. of Electrical and Electronic Engineering, 7600, Stellenbosch, SOUTH AFRICA*
E-mail: ameenjardine98@gmail.com

Neuromorphic computing presents an interesting solution to the limitations imposed by Moore's law on modern-day neural networks. With an ever growing use-case for these networks, the need for improved speed and effciency can no longer be satisfied by solely software and algorithmic optimisations. Neuromorphic computing aims to achieve these improvements through bio-mimicry of the human brain. We present a superconducting perceptron network that makes use of our novel hybrid QFP-RSFQ based neuron [1]. The proposed network can be arranged in both single-layer and multi-layer configurations. These networks exploit the adjustable 3-bit SFQ-based weighting resolution of the neurons, and are thus capable of being trained from scratch, for a number of different applications. Using a simple single-layer perceptron-based learning approach, the net- work is able to tackle simple classification tasks. Extending this to a multi-layer configuration, non-linearly separable learning examples such as XOR and XNOR gate functionality are achievable. We aim to demonstrate these training capabilities on a number of different applications, in both single and multi-layer perceptron configurations. Furthermore, the design of the complex interconnect circuitry between neuron layers are discussed. Through JoSIM simulations, we are able to observe not only the neuron states, but the also the propagation of the data through the network. The limitations of both the neuron model and the chosen architectures are also discussed. Our conclusion shows that our neuromorphic networks are capable of tackling a range of different learning and classification tasks, setting a firm foundation for real-world applications of the proposed superconductive neuromorphic system.

References

[1] M.A. Jardine, C.J. Fourie, *Hybrid RSFQ-QFP superconducting neuron*, IEEE Transactions on Applied Superconductivity, **vol. 33, no. 4**, pp. 1–9 (2023).

Abstract ID: 1667

DESIGN OF A SUPERCONDUCTING RF SWITCH FOR CRYOGENIC 4-12 GHz BAND APPLICATIONS

A.O. Sakın, A.C. Sonğur, B. Akçay, M. Demircioğlu, H.A. Güneş, D. Doğan[1,2], A. Bozbey[1,2], M. Ünlü[1,2]

[1] *TOBB University of Economics and Technology, 06560, Ankara, TÜRKİYE*
[2] *Phi0 Quantum Technologies, 06800, Ankara, TÜRKİYE*
E-mail: bozbey@etu.edu.tr

This paper presents the design of a superconducting (SC) RF switch for cryogenic measurement systems operating at the 4-12 GHz band. The RF switch is based on a coplanar waveguide (CPW) structure, and the switching is achieved by controlling the superconductivity of a serial connected SC region that is connected between the input and output CPW terminals. The control is attained by locally heating the serial connected SC region by means of a closely spaced heating line, which is used for increasing the temperature of SC region and moving it out of the SC mode. This results in a high resistance between the input and output CPW terminals, and hence, increasing the isolation and moving the switch from ON state to OFF state.

The Nb is selected as the SC material for the implementation platform, and the switch operation temperature is selected as 4K. The RF performance of the switch is calculated using both circuit and finite element method (FEM) simulations. The ON-state performance is first simulated by the equivalent circuit model, and then, it is verified by full-wave FEM simulations. The OFF-state performance is calculated only the equivalent circuit model, where the kinetic and geometric impedance is calculated using closed form formulas based on experimental results [1]. The simulations show that the switch has an ON-state insertion loss better than -2 dB and OFF state isolation better than -14 dB in 4-12 GHz band.

The thermal analysis of the proposed switch is also performed using FEM simulations. The simulation results show that the switching area can be locally heated up to 10K approximately in 4 μs and can be cooled down to 4K approximately in 3 μs, both of which determine the switching speed of the RF switch.

The fabrication of the RF switch is performed the AIST process [2], and the measurement results will be presented at the conference.

References

[1] A.J. Annunziata, D.F. Santavicca, L. Frunzio, G. Catelani, M.J. Rooks, A. Frydman, D.E. Prober, Nanotechnology, **1 (44)**, 445202 (2010).
[2] https://www.aist.go.jp/

Abstract ID: 1299

INFLUENCE OF DEFECT STRUCTURE ON SUPERCONDUCTING PROPERTIES IN ALKALI METAL-BASED IRON PNICTIDES AND SELENIDES

A. Yu. Degtyarenko[1], I.V. Morozov[2], E. O. Rakhmanov[2,3], A.V. Sadakov[1], A.I. Shilov[1], S. Yu. Gavrilkin[1], A. Yu. Tsvetkov[1], S. A. Kuzmichev[3,1], T.E. Kuzmicheva[1]

[1]*V.L. Ginzburg Centre for High-Temperature Superconductivity and Quantum Materials P.N. Lebedev Physical Institute of the Russian Academy of Sciences (LPI RAS), 53 Leninsky Ave., 119991 Moscow, RUSSIA*
[2]*Department of Chemistry, Moscow State University, 119991, Moscow, RUSSIA*
[3]*Faculty of Physics, Moscow State University, 119991, Moscow RUSSIA*
E-mail: degtyarenkoayu@lebedev.ru

The layered superconducting compounds tend to the formation of planar, point, columnar, etc. defects [1-3]. Such inclusions in the material volume can act as pinning centers of Abrikosov vortices [4]. In this work single crystals of the iron pnictide of $NaFe_{1-x}Co_xAs$ and selenide $K_xFe_{2-y}Se_{2-z}S_z$ grown by "self-flux" method were studied [5]. The high quality a single crystallinity for both samples was confirmed by X-ray diffraction, magnetic susceptibility χ (T) and resistivity R(T) data. The defect structure at the atomic level has been studied in detail by high-resolution electron microscopy (HRTEM). The vortex pinning mechanism in the single crystals $NaFe_{1-x}Co_xAs$ and $K_xFe_{2-y}Se_{2-z}S_z$ is established.

The work was performed using equipment of the Lebedev Physical Institute Facility Center. This research was funded by the RSF project number 22-72-10082.

References

[1] S. Ishida, *et al.*, NPJ Quantum Mater. **4**, 272019 (2019).
[2] A.V. Ovcharov, *et al.*, Sci Rep. **9**, 15235 (2019).
[3] A.Y. Degtyarenko *et al.*, Nanomaterials, **12**, 3801 (2022).
[4] A. A. Abrikosov, Sov. Phys. JETP **5**, 1174 (1957).
[5] S.A. Kuzmichev *et al.*, JETP Letters **117**, 8, 614 (2023).

Abstract ID: 218

THE LARGE THERMAL-VOLTAGE OF YTTRIUM IRON OXIDE ($Y_3Fe_5O_{12}$)/TUNGSTEN (W) HYBRID STRUCTURE ON SPIN SEEBECK EFFECT MEASUREMENT

P. Wongjom, C. Wongsakulkhamkhot

[1]*Division of Physics, Faculty of Science and Technology, Thammasat University, Pathum Tani 12120, THAILAND*
E-mail: pwongjom@tu.ac.th

The generation of pure spin current by thermal is known as spin Seebeck effect (SSE) (1). The junction of ferrimagnetic insulator as spin injector and paramagnetic metal as spin detector is proposed for longitudinal spin Seebeck effect. This study, we propose the preparation of $Y_3Fe_5O_{12}$ (YIG)/W thin film for SSE detection. The RF-power supply of 100 Watt was applied to YIG target in Ar atmosphere of 5 mTorr pressure operation for 200 nm thickness while the W was coated on top of YIG for 15 nm thickness. The samples were annealed at 800 °C for 2 hr stabilization in air atmosphere. The magnetic, crystal structure and surface properties were analyzed by vibration sample magnetometer (VSM), x-ray diffraction (XRD) and scanning electron microscopy (SEM), respectively. The results show that the polycrystalline of YIG is illustration for ferrimagnetic behavior. The sample is clearly smooth after annealed. For the SSE, the thermal voltage is shown the reverse signal between non-annealed and annealed sample. The large thermal voltage conversion is detected about -140 μV at 12 K temperature difference in which non-annealed sample while the signal is reversed to +80 μV at 12 K difference when the sample was annealed. We conclude that the preparation of YIG/W thin film by sputtering technique can be used to obverse SSE. The large spin conversion is shown reverse between non-annealed and annealed sample.

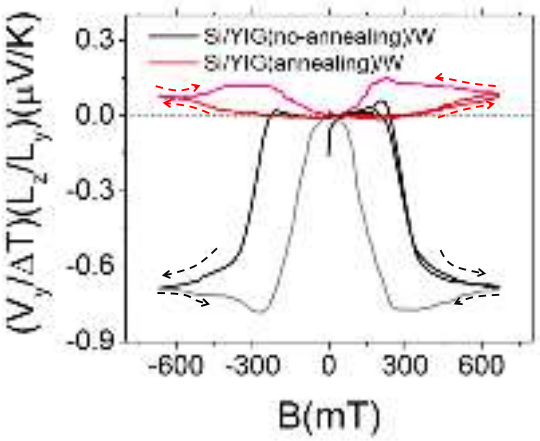

Fig. 1: *The normalized voltage from ISHE, the black line represents non-annealed of Si/YIG/W while the red line shows the voltage of annealed sample.*

References

[1] K. Uchida, S. Takahashi, K. Harii, J. Ieda, W. Koshibae, K. Ando, *et al.*, *Observation of the spin Seebeck effect*, Nature **455 (7214)**,778–81 (2008).

Abstract ID: 222

ENHANCED THE IONIC CONDUCTIVITY AT HIGH TEMPERATURE IN RE DOPED MAGNESIUM FERRITE FOR APPLICATIONS OF FUEL CELL

Haroon Mazhar, Haris Farooq Kiani, M. Anis-ur-Rehman

Applied Thermal Physics Laboratory, Department of Physics COMSATS University Islamabad, Islamabad 45550, PAKISTAN

Email: haroonmazhar1234@gmail.com & harisfarooqkiani@gmail.com & marehman@comsats.edu.pk

Solid oxide fuel cells (SOFCs) are an all-solid energy conversion device from the chemical energy of fuels to electric energy at intermediate and high temperatures. Up to now, massive efforts have been made in developing different components of solid oxide fuel cells, including electrolyte, anode, cathode and interconnect materials. Rare earth elements play an indispensable role in different components of SOFCs which have been extensively studied in the recent decades [1]. $MgFe_{2-x}La_xO_4$ (x = 0.0, 0.02) was prepared by a sol-gel method in which lanthanum was added as a dopant. The material was sintered at 950°C for 3h. To analyze the structural properties of the sample, x-ray diffraction (XRD) technique was used, which confirmed the spinel cubic structure. XRD data was used to analysis the crystallite size (26nm), lattice parameters (8.40), experimental and theoretical density and volume of samples. A precision component analyzer was used for dielectric study of the samples in the frequency range of 20 Hz to 3 MHz at different temperatures (100°C to 500°C). AC conductivity increased at higher frequency. Impedance has progressively decreased at higher frequency. DC conductivity was measured using a two-probe method that showed a increasing trend with increasing temperature. The doped samples demonstrated highly improved structural and electrical properties as compared to those of the undoped sample. The increased conductivity and improved stability of the samples make them a potential candidate for SOFCs.

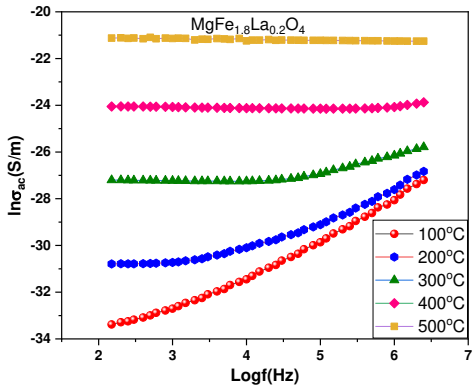

Fig.1: *AC conductivity of different temperature for $MgFe_{1.8}La_{0.2}O_4$.*

References

[1] Rohi Zahra, Sammar Tayyab, M. Anis-ur-Rehman, *Enhancement of conductivity in phase pure and doped ceria for fuel cell applications*, Journal of Electronic Materials: p.2545–2551 (2022).

Abstract ID: 1089

EXPLORING STRUCTURE-ELECTRICAL CORRELATIONS IN (Mn-Zn) NANOMATERIALS FOR MEMORY APPLICATION

Rehana Rasool, M. Anis-ur-Rehman

Applied Thermal Physics Laboratory (ATPL), Department of Physics COMSATS University Islamabad, Islamabad 45550, PAKISTAN

Email: marehman@comsats.edu.pk

A ferrite is a ceramic substance consisting mainly of iron oxide (Fe_2O_4) along with tiny quantities of shiny metallic elements like Mn. The synthesis and characterization of Mn-Zn ferrites are of great significance to researchers because of their many possibilities in various fields. A type of soft magnetic material with good electrical, magnetic, and optical characteristics is called Mn-Zn ferrites [1]. In the present research, Mn-Zn ferrites with cobalt doping and general $Zn_{0.6}Mn_{0.4-x}Co_xFe_2O_4$ were synthesized using WOW'S sol-gel method, with x having values ranging from (x= 0.0-0.1). X-ray diffraction (XRD) investigation confirmed that the synthesized samples formed a single-phase cubic spinel structure, and crystallite size (26nm-41nm), lattice constant (8.5±0.1Å-8.42±0.08Å), unit cell volume (607.39Å^3-596.25Å3), porosity (52.01%-48.7%) have been determined using XRD data [2]. The frequency range of (20Hz–3MHz), the frequency-dependent AC electrical conductivity (σ_{ac}(S/m)) has been examined. As Cobalt content was added, AC conductivity and dielectric loss tangent were all reduced. DC electrical Analysis (ϱ_{dc} (Ωm)), Co-doped Mn-Zn ferrite as their resistivity reduces as the temperature rises (figure 1). The resistive switching effect on the produced samples at room temperature has been investigated using the IV measurement. The samples confirmed the RS effect as doping increased also showed the switching effect. So, for the potential applications of these materials in electrical computer-based products for multi-electronics, and switching resistive applications (figure 2).

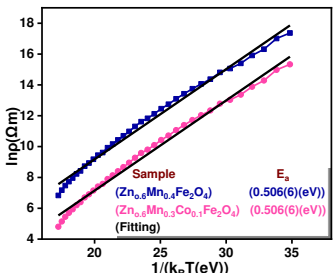

Fig. 1: *DC resistivity (lnρ) Vs Activation Energy (E_a) for sample $Zn_{0.6}Mn_{0.4-x}Co_xFe_2O_4$ (x=0.0, 0.1).*

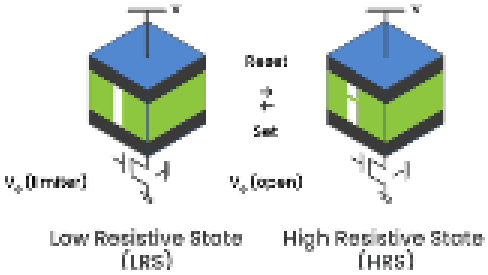

Fig. 2: *Schematic diagram of R-RAM.*

Reference

[1] H. Mahajan, S.K. Godara, A.K. Srivastava, *Synthesis and investigation of structural, morphological, and magnetic properties of the manganese doped cobalt-zinc spinel ferrite*, J. Alloys Compd., **896**, 162966 (2022).

[2] M. Kamran, M. Anis-ur-Rehman, *Study of dielectric and electrical properties in Co-(Fe–Ce-Nd) nanosized spinel ferrites*. Materials Science in Semiconductor Processing, **153**, 107111 (2023).

Abstract ID: 1090

BARIUM HEXAFERRITE DOPED WITH COBALT: A STUDY ON ELECTRICAL BEHAVIOR FOR MEMORY APPLICATIONS

Rabia Tariq, M. Anis-ur-Rehman

Applied Thermal Physics Laboratory, Department of Physics, COMSATS University Islamabad 45550, PAKISTAN

E-mail: rt622052@gmail.com & marehman@comsats.edu.pk

Resistive random-access memory (RRAM) is recognized as significant developing technology with impressive features: low cost, dense storage, fast access, versatile applications, and exceptional adaptability (Fig 1). One of the possible option for RRAM applications is ferrites. The peculiar properties of ferrites include high magnetic permeability, substantial electrical resistance, minimal eddy current and dielectric losses, and potent magnetic characteristics [2]. A series of $BaFe_{12-x}Co_xO_{19}$ materials with varying cobalt content (x=0.0-0.8) were successfully synthesized using the sol-gel method.. The structural properties like lattice constant (a=5.886(2)Å-5.888(2)Å and c=23.205(3)Å-23.161(3)Å), volume (696.2(5)Å-695.4(4)Å), crystallite size (48nm-41nm) have been examined by using Cu-Kα radiation (λ=1.5405Å) within the range 2θ (20°-80°). All samples exhibited the expected frequency (20Hz-3MHz) dependence of ferrites, displaying decreasing dielectric tangent loss and constant due to relaxation phenomena, concurrent with a rise in ac conductivity ($3.31x10^{-4}$S/m–$5.9x10^{-4}$S/m) arising from enhanced charge hopping mechanisms. DC resistivity was characterized w.r.t temperature (30℃-450℃). Higher temperatures induced a decline in DC resistivity ($1.1x10^{7}$Ωm–$3.5x10^{6}$Ωm). Activation energy (E_a) showed that resistivity linearly decreased with increasing temperature (0.90eV-0.85eV). The I-V curves displayed hysteresis loops and non-linear behavior, confirming resistive switching in the samples (Fig 2).

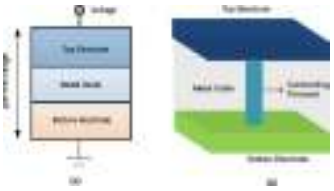

Fig 1: *(a) Schematic diagram of MIM structure for R-RAM. (b) Cross-sectional view of R-RAM.*

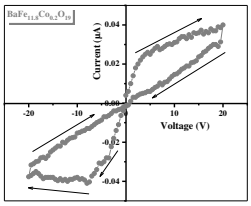

Fig 2: *Current Vs Voltage (I-V) loop of $BaFe_{11.8}Co_{0.2}O_{19}$.*

References

[1] J. Vijaykumar, S. Shubhangi, T. Umakant, M. Rajaram, "Chapter 3 - Properties of ferrites", *In Micro and Nano Technologies, Spinel Ferrite Nanostructures for Energy Storage Devices*, Micro and Nano Technologies, (2020), pp. 35-50.

[2] F. Zahoor, Z. Azni, Z. Tun, A. Khanday, *Resistive Random-Access Memory (RRAM): An Overview of Materials, Switching Mechanism, Performance, Multilevel Cell (mlc) Storage, Modeling, and Applications*, Nanoscale Res. Lett., **15(1)**, pp. 1-26 (2020).

Abstract ID: 1093

TEMPERATURE DEPENDENT ELECTRICAL AND DIELECTRIC PROPERTIES OF $MgFe_{1.8}Ce_{0.2}O_4$ FERRITE

Haroon Mazhar, M. Anis-ur-Rehman

Applied Thermal Physics Laboratory, Department of Physics COMSATS University Islamabad, Islamabad 45550, PAKISTAN

E-mail: haroonmazhar1234@gmail.com & marehman@comsats.edu.pk

Spinel ferrites gain great attraction in view of their extraordinary properties such as low electrical conductivity, high magnetic permeability, low coercive force, high Curie temperature and low eddy current loss [1]. In present work, $MgFe_{1.8}Ce_{0.2}O_4$ ferrite's electrical and dielectric properties at different temperature have been synthesized by WOWS sol-gel method. X-ray diffraction (XRD) confirmed the spinel structure of the prepared compositions. XRD data was used to analysis the crystallite size (32nm), lattice parameters (8.421), experimental density, theoretical density, and volume of samples. The electrical properties including the tangent loss, dielectric constant, dielectric loss, ac conductivity and real and imaginary part of impedance have been studied in the frequency range of 20Hz-3MHz using precision analyzer at a temperature range from RT to 500°C. Tangent loss as shown in fig.1, dielectric loss, dielectric constant decreased by increasing frequency. AC conductivity increased at higher frequency. Impedance has progressively decreased at higher frequency. DC resistance was measured using a two-probe method that showed a decreasing trend with increasing temperature revealing semiconductor nature of prepared sample. High value of dc resistivity makes this ferrite suitable for the high frequency applications which can reduce losses caused by eddy current.

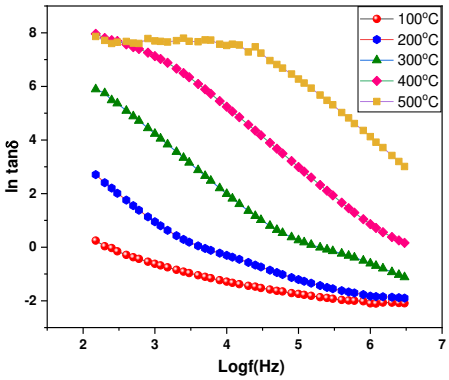

Fig.1: *Tangent loss of different temperature for $MgFe_{1.8}Ce_{0.2}O_4$*

References

[1] M. Zahid, H.M. Khan, M.Z. Manzoor, H.E. Ahmed, T. Akhter, T. Alshahrani, M. Imran, M.A. Assiri, *Optimization of structural, dielectric, and magnetic properties of nanocrystalline copper doped spinel ferrites*, Materials Science and Engineering: B, **297**, 116739 (2023).

Abstract ID: 1120

DOPING IN PYROCHLORE LANTHANUM ZIRCONATES TO TUNE TRANSPORT PROPERTIES FOR RAMS APPLICATIONS

Arouba Abbas, M. Anis-ur-Rehman

Applied Thermal Physics Laboratory, Department of Physics, COMSATS University Islamabad, Islamabad 45550, PAKISTAN

Email: marehman@comsats.edu.pk

The unique structure in lanthanum zirconates influences special electrical and thermal properties, but with proper doping, emerges as a promising option for thermal barrier coatings (fig 1) [1]. In this study, we synthesized lanthanum zirconates with Gd doping utilizing the without water and surfactants (WOWs) sol-gel method. X-ray diffraction analysis has confirmed the pyrochlore structure of lanthanum zirconates. Interestingly, the introduction of gadolinium triggers a notable phase transition from pyrochlore to defective fluorite structure. Thermal transport properties were investigated by using a well-known technique known as advantageous transient plane source (ATPS) method. Lanthanum zirconates with pyrochlore structure exhibit intrinsically low thermal conductivity approximately 0.74 W/(m.K.) and addition of Gd facilitates a further reduction in thermal conductivity, reaching about 0.37 W/(m.K.). A precision analyzer was used to explore electrical behavior, including AC conductivity and impedance, within the frequency range of 20Hz-3MHz at room temperature. AC conductivity shows an upward trend, in contrast impedance in figure 2 exhibits a decrease with increase in frequency. IV measurements reveal switching behavior in $La_{2-x}Gd_xZr_2O_7$ (x=0.0,0.3), as depicted by the hysterisis loop.

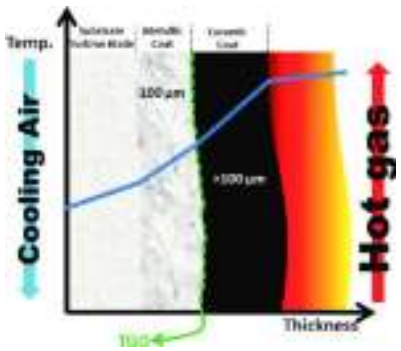

Fig. 1: *Thermal Barrier Coatings (TBCs) [2].*

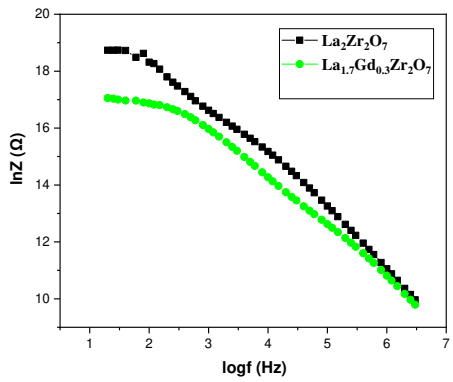

Fig. 2: *Impedance vs freq of $La_{2-x}Gd_xZr_2O_7$ (x=0.0,0.3).*

References

[1] Y Fan, Q Wao, J Wang, *Temperature effect on mechanical and thermal properties of multicomponent rare-earth zirconate pyrochlores*, Journals of the American Society, 118-190, (2023).

[2] Y Chen, R Zhang, J Song, *Toughening mechanism of thermal barrier coatings, International journal of thermophysics*, 565-576, (2021).

Abstract ID: 1168

TUNING ELECTRICAL CHARACTERISTICS OF COBALT FERRITE THROUGH MAGNESIUM DOPING FOR IMPROVED R-RAM PERFORMANCE

Irsa Kanwal Abbasi, M. Anis-ur-Rehman

Applied Thermal Physics Laboratory, Department of Physics, COMSATS University Islamabad, Islamabad 45550, PAKISTAN

Email: marehman@comsats.edu.pk

As memory technologies continue to advance, Resistive Random Access Memory (R-RAM) (shown in Fig 1) becomes a more attractive option for next-generation computer architectures. Cobalt ferrite stands out in R-RAM applications due to its exceptional combination of magnetic properties and electrical performance [1]. The magnesium-doped cobalt ferrite nanoparticles are studied in this study as potential resistive filament materials for RRAM applications. $Co_{1-x}Mg_xFe_2O_4$ nanoparticles with different magnesium (Mg) doping concentrations (x = 0.0-0.5) were created using sol-gel synthesis. The crystal structure, lattice constant, crystallite size, and unit cell volume were characterized using X-ray diffraction (XRD). An X-ray diffraction (XRD) (shown in Fig 2) analysis verified the prepared samples cubic structure. The lattice constant is observed to vary within a range of 8.40 Å to 8.45 Å, while the crystallite size varies from 42nm to 44 nm. Furthermore, DC electrical properties, such as resistivity, were measured at various temperatures. The resistive switching (RS) behavior of the samples was studied by current-voltage (IV) measurements at room temperature. Notably, all prepared samples exhibited the RS effect, and the switching behavior intensified with Mg doping concentration.

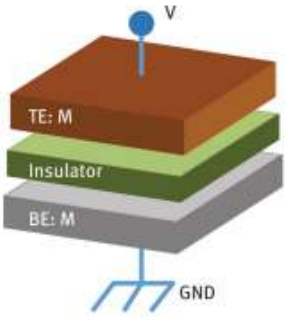

Fig 1: *Schematic diagram of R-RAM [2].*

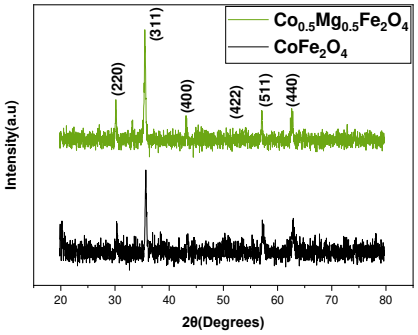

Fig 2: *XRD pattern for Mg-doped $CoFe_2O_4$.*

References

[1] M. Kamran, M. Anis-ur-Rehman, *Enhanced transport properties in Ce doped cobalt ferrites nanoparticles for resistive RAM applications*, Journal of Alloys and Compounds, **822**, 153583 (2020).

[2] A. Prakash, H. Hwang, *Multilevel cell storage and resistance variability in resistive random access memory*, Physical Sciences Reviews, **1(6)**, 20160010 (2019).

Abstract ID: 1217

ENHANCED ENERGY STORAGE PROPERTIES OF Nd-DOPED CALCIUM BISMUTH COBALTITE'S NANOPARTICLES VIA WET CHEMICAL METHOD

Haris Farooq Kiani, Haroon Mazhar, M. Anis ur Rehman

Applied Thermal Physics Laboratory (ATPL), Department of Physics, COMSATS University Islamabad, Islamabad 45550, PAKISTAN

Email: harisfarooqkiani@gmail.com & haroonmazhar1234@gmail.com & marehman@comsats.edu.pk

Renewable energy resources are becoming more popular around the world as a nonpolluting energy generation choice with a substantial impact on the green economy. Calcium Bismuth Cobaltite's $Ca_{2.7}Bi_{0.3}Co_4O_{9+\square}$ were synthesized using WOWS (Without water & surfactants) Sol-gel technique with concentration of (x=0.0,0.20) doped with Neodymium (Nd). For further characterizations, pellets of various compositions were formed and sintered. The Average crystallite size of the sample was determined to be between 17nm and 25nm. Nanoparticle imaging characterization was done by Scanning Electron Microscope (SEM). The properties of calcined samples were further investigated using Fourier transform infrared spectroscopy (FTIR). The Transport properties AC conductivity (σ_{ac}) and Dielectric properties include dielectric constant (ε') dielectric loss (ε''), tangent loss (tan□), Impedance real (Z') & imaginary parts (Z'') were measured at various frequencies and in the variable range (100Hz– 3MHz). The composition $Ca_{2.7}Bi_{0.10}Nd_{0.20}Co_4O_{9+\square}$ achieved higher dielectric constant and lower dielectric loss than other compositions. $Ca_{2.7}Bi_{0.10}Nd_{0.20}Co_4O_{9+\square}$ showed the highest value of AC conductivity. $Ca_{2.7}Bi_{0.10}Nd_{0.20}Co_4O_{9+\square}$ showed that the most auspicious material for energy storage applications.

Abstract ID: 1227

THE MAGNETIC AND ELECTROPHYSICAL PROPERTIES OF $(FeIn_2S_4)_{0,97}(CuIn_2S_4)_{0,03}$

S.S. Ragımov [1,2], Sh. S. Abdullaeva[3]

[1]Baku State University, Institute for Physical Problems, AZ1148, Baku, AZERBAIJAN
[2]Institute of Physics of Azerbaijan Ministry of Science and Education, AZ-1143, Baku, AZERBAIJAN
[3]M.Nagiyev Institute of Catalysis and Inorganic Chemistry of Azerbaijan Ministry of Science and Education, AZ-1143, Baku, AZERBAIJAN
E-mail: sadiyar@mail.ru

$FeIn_2S_4$ is a promising material for magnetic semiconductors of the $MB^{III}{}_2C^{VI}{}_4$ (M – Mn, Fe) type. Compounds of this type have both charge and spin properties. These compounds can be used to create various functional devices controlled by a magnetic field. A doping semiconductor compound with magnetic impurities, as well as the synthesis of solid solutions based on them, makes it possible to obtain compositions with new characteristics. The preparation of solid solutions based on these materials and the study of their transport and magnetic properties are of particular interest. The electrical and magnetic properties of solid solutions based on $FeIn_2S_4$ have not been sufficiently studied.

This work presents the results of a study of the electrical and magnetic properties of the $(FeIn_2S_4)_{0,97}(CuIn_2S_4)_{0,03}$ solid solution.

The temperature dependence of electrical conductivity and the Hall effect of the $(FeIn_2S_4)_{0,97}(CuIn_2S_4)_{0,03}$ solid solution was studied in 100-400K temperature intervals.

The concentration of charge carriers and the electron activation energy (E_a=0.026 eV) was estimated. Based on X-ray diffraction analysis the lattice parameters and type of space group were determined.

The specific magnetic moment of the $(FeIn_2S_4)_{0,97}(CuIn_2S_4)_{0,03}$ was investigated in the temperature range 10–300 K in magnetic fields of 0-5 kOe. It was observed that the specific magnetic moment monotonically increases with decreasing temperature. According to the results of the magnetic measurements, $(FeIn_2S_4)_{0,97}(CuIn_2S_4)_{0,03}$ are paramagnets up to ~30 K.

Abstract ID: 1228

ADDITIVE MANUFACTURING OF R-Fe-B TYPE PERMANENT MAGNETS

V. Maltseva, A. Urzhumtsev, S. Andreev, A. Volegov

Ural Federal University, Institute of Natural Science and Mathematics, Kuibysheva st., 48, Yekaterinburg, 620026, RUSSIA
E-mail: viktoriamaltseva5@gmail.com

Hard magnetic materials belong to the class of functional materials, which are the base of modern technological processes, devices for everyday use, electrical transport, etc. The rate of improvement of the magnetic hysteresis properties of permanent magnets is constantly decreasing, since the potential of the $Nd_2Fe_{14}B$ compound in industrial production is already almost completely realized [1]. To further improve the functional properties of products with permanent magnets, it is necessary to apply new approaches to the design of such products. One of the options for creating magnets of complex shape as well as local variation of material properties is the use of additive manufacturing technologies [2].

This work is devoted to the study of additive manufacturing methods used for 3D-printing of permanent magnets, establishing the relationship between the magnetic hysteresis properties of samples of single-layer permanent magnets of the NdFeB and conditions of their synthesis by selective laser sintering experimentally. Since additive manufacturing involves building an object layer by layer, understanding the potential of magnetic properties in a single layer will allow predicting the upper limit of magnetic hysteresis properties of a bulk permanent magnet sample.

The obtained samples are in the form of squares, with linear dimensions equal to 10 x 10 mm^2 and a thickness of less than 1 mm. For 3D-printing, a mechanical mixture of two powders was used: MQP-B (Magnequench Int. production) and the low melting eutectic alloy $Pr_{75.0}Cu_{6.2}Co_{18.8}$ in an 80% to 20% weight ratio. The alloys were milled using a ball mill in alcohol to prevent oxidation of the powders. 3D-printing was carried out by means of the additive system of selective laser melting Orlas Creator RA: a specially chiseled platform made of brass was inserted into the build chamber, on which the powder was evenly distributed in a recess with a depth of 1 mm. The printing process was carried out in an argon atmosphere with an oxygen content in the build chamber of no more than 0.5 %.

To obtain optimal mechanical and magnetic properties, the following parameters were varied: laser beam power (P, W), number of laser beam passes over the sintered sample (N, times), distance between the subsequent and the previous laser beam passages (h, μm), laser beam speed (v, mm/s), direction of laser beam passage (α, deg.), laser beam diameter (d, μm). All magnetic hysteresis properties were measured at room temperature by means of a KVANS-1 vibrating sample magnetometer and at T = 300 K by a PPMS DynaCool T9 magnetometer with the VSM option (Quantum Design, USA). The possibility of obtaining the coercivity of 19.5 kOe on single-layer magnets without the use of heavy rare-earth metals was shown.

The report will present the results in more detail and suggest ways to carry out further research.

Support by grant RSF № 21-72-10104 is acknowledged.

References

[1] D.Yu. Vasilenko *et al.*, Phys. Metals Metallogr. **122, 12,** 1173–1182 (2021).
[2] A.S. Volegov *et. al.*, Acta Materialia, **188**, 733-739 (2020).

Abstract ID: 1230

MAGNETOMETRIC APPROACH TO ESTABLISHING THE BASIC MECHANISM OF MAGNETIZATION REVERSAL PROCESSES IN Nd-Fe-B TYPE PERMANENT MAGNETS

A. Urzhumtsev, V. Maltseva, A. Volegov

[1]*Ural Federal University, Institute of Natural Science and Mathematics, Kuibysheva st., 48, Yekaterinburg, 620026, RUSSIA*

E-mail: andrej707@bk.ru

The permanent magnets Nd-Fe-B type is the main part of engine of electric cars and scooters. The way to further improve these hard magnetic materials lies in understanding the peculiarities of their magnetization processes and the mechanism of formation of high coercivity. Today the ideas about the nature of hysteresis properties of $Nd_2Fe_{14}B$ magnets are rather ambiguous. In the report presents the results of studies of magnetization and remagnetization processes in Nd-Fe-B type permanent magnets of N35, N48 and N48SH grades. The peculiarities of their microstructure are established. It is shown that the presence of oxide phases in the magnet grains complicates the magnetization process of their thermo-magnetized state. An approach to the establishment of the prevailing mechanism of coercivity is presented, based on the evaluation of the curves of the reversible contribution of magnetization change from the acting field. It is demonstrated how grains with a nucleation mechanism lead to anomalous magnetization behavior on partial hysteresis loops as shown on Fig 1. For a material with a large number of defects on the grain boundaries the pinning mechanism is the main one, in the case of approaching an ideal structure nucleation begins to prevail.

It is shown that the mechanism of remagnetization in permanent magnets based on the $Nd_2Fe_{14}B$ phase is more complicated than the purely nucleation or pinning models predict [1]. In general, it is not correct to consider the processes of remagnetization within the framework of one mechanism or one method, since this process is very multifaceted and may be unique for each sample of permanent magnet. The development of magnetometric techniques has a high potential for obtaining insights into changes in the magnetic state of complex heterogeneous objects, which include permanent magnets.

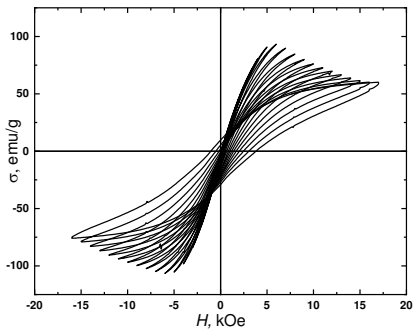

Fig. 1:. *The partial hysteresis loops for the magnet N48SH from initial state.*

This work was financially supported by RSF grant № 21-72-10104.

References

[1] A.N. Urzhumtsev, Physics of Metals and Metallography **123(11)**, 1054–1060 (2022).

Abstract ID: 1364

MAGNETIC AND MAGNETOCALORIC PROPERTIES OF RARE EARTH SUBSTITUTED Zn-Ni NANOSIZED FERRITES

S.J.C. Masuku[1], J.Z. Msomi[1], A.M. Strydom[2], A. Xhakaza[2]

[1]*Walter Sisulu University, Dept. of Chemical and Physical Sciences, P/Bag X01, 5117, Mthatha Eastern Cape, SOUTH AFRICA*
[2]*University of Johannesburg, Dept. of Physics, P. O. Box 524, 2006, Auckland Park, SOUTH AFRICA*
E-mail: smasuku@wsu.ac.za

Magnetic and magnetocaloric properties of $Zn_{0.7}Ni_{0.3}Fe_2O_4$ and $Zn_{0.7}Ni_{0.3}$ $(Re)_{0.1}Fe_{1.9}O_4$ (Re = Gd, Sm, Dy) fine powders with particle size in the range 8 to 13 nm, confirmed by TEM analysis, were investigated by SQUID magnetometry. XRD and FTIR data confirmed cubic spinel phase with no impurity phases. Magnetization results revealed superparamagnetic behaviour of the compounds investigated. Both composition and particle size have significant effects on the magnetic and magnetocaloric properties. The blocking temperature (T_B) for pure Zn-Ni was found to be 180 K and increased with increasing particle size due higher anisotropic energy. The variation of magnetization with reducing temperature showed transformation paramagnetic to ferromagnetic spin state at Curie points. Magnetocaloric properties were analysed by measuring a family of *M-H* curves at temperature intervals of interests and calculating the magnetic entropy change (ΔS_m) by Maxwell equation. ΔS_m increased with increasing applied magnetic field and reached a maximum around T_C. The large ΔS_m and relative cooling power near room temperature found for $Zn_{0.7}Ni_{0.3}Fe_2O_4$ and $Zn_{0.7}Ni_{0.3}$ $(Re)_{0.1}Fe_{1.9}O_4$ (Re = Gd, Sm, Dy) indicate potential applications in magnetic refrigeration technologies.

Abstract ID: 1365

OBSERVATIONS OF THE NOVEL LOW FIELD MICROWAVE ABSORPTION IN $Zn_xCo_{1-x}Fe_{2-x}Al_xO_4$ FERRITES

S.J.C. Masuku[1], P.P. Majozi[1], J.Z. Msomi[1], S. Mahule[2]

[1]*Walter Sisulu University, Dept. of Chemical and Physical Sciences, P/Bag X01, 5117, Mthatha Eastern Cape, SOUTH AFRICA*
[2]*University of South Africa, Dept. of Physics, 1710, Johannesburg, SOUTH AFRICA*
E-mail: smasuku@wsu.ac.za

Nanocrystalline $Zn_xCo_{1-x}Fe_{2-x}Al_xO_4$ with particles size between 6 nm and 13 nm were synthesized were synthesized by glycol-thermal reaction under low reaction temperature of 200 °C. The as-prepared compounds were investigated by XRD, TEM, SEM, FTIR, Raman spectroscopy and ESR measurements. Structural, vibrational and electron spin dynamics are sensitive to particle size and Zn and Al concentrations. Broad ESR signals are attributed to dipolar-dipolar interactions and random orientations of magnetic anisotropy axes. Results show evidence of the novel low field microwave absorption, making $Zn_xCo_{1-x}Fe_{2-x}Al_xO_4$ compounds interesting for potential applications in low magnetic field sensors, magnetic field-controlled absorbers, spin valves etc.

Abstract ID: 1472

MODULATED MAGNETIC STRUCTURE IN WEAK FERROMAGNET $FeBO_3$:Mg AND IRON-GARNETS $Tb_{0,26}Y_{2,74}Fe_5O_{12}$, $Ho_{0,6}Y_{2,4}Fe_5O_{12}$

D.R.Djurayev[1], L.N.Niyazov[1], Sh.Sh.Fayziyev[1]

[1]Bukhara State University, M.Iqbol, 11, 200000 Bukhara, UZBEKISTAN
[2]Bukhara State Medical Institute, Str., A. Navoi, 1, Bukhara 200118, UZBEKISTAN
E-mail: djurayev2002@mail.ru

In this work, we will represent new experimental results on the effect of temperature and optical illumination on the conditions of formation and parameters of the modulated magnetic structure of the single crystals of $FeBO_3$ and doped $FeBO_3$:Mg with weak ferromagnetism, as well as determining the type of the observed phase transition and the structure of the modulated magnetic state. As well as there we will represent new experimental results on spontaneous and induced by external influences phase transitions in magnetically ordered crystals, as well as the development based on these provisions of the existing thermodynamic theory of magnetic orientation phase transitions are single crystals of iron garnets $Tb_{0,26}Y_{2,74}Fe_5O_{12}$, $Ho_{0,6}Y_{2,4}Fe_5O_{12}$.

For the first time carried out direct visual observation of the evolution of the domain structure of iron garnet $Tb_{0,26}Y_{2,74}Fe_5O_{12}$ during spontaneous reorientation direction of the easy axis, and it is shown that near the phase transition temperature of the studied magneto-optical susceptibility of the crystal has a narrow sharp peak, and the coercive force - is reduced.

The model of restructuring of the domain structure of iron garnet $Tb_{0,26}Y_{2,74}Fe_5O_{12}$ in the temperature region of spontaneous reorientation of the easy axis, allowing consistently describe (qualitatively) the totality of the experimental results.

For the first time carried out experimental studies of the magnetic orientation phase transitions induced biaxial mechanical stresses in a cubic ferromagnetic.

For the first time, the type of the orientational phase transition emerging in the easy-plane weak ferromagnet $FeBO_3$:Mg during its magnetization is established and the structure of the modulated magnetic state of this crystal is determined;

For the first time, the magnetic phase diagram of $FeBO_3$:Mg was established experimentally, which establishes the existence boundaries for a homogeneous and modulated magnetic state in this crystal;

It is shown that the transition of a crystal to a modulated magnetic state leads to a significant change in its basic magnetic characteristics (coercive force, initial magnetic susceptibility, magnetic hysteresis loop shape);

It was established that the degree of light influence on the parameters and conditions for the existence of MMS $FeBO_3$:Mg depends essentially both on the duration of exposure and on the orientation of the antiferromagnetism vector at the time of exposure;

On the basis of the theory of "magnetic ripples", a theoretical description of the revealed regularities of the transition of $FeBO_3$:Mg to a modulated magnetic state is carried out, and the main physical causes responsible for the spatial modulation of the magnetic order of this crystal are determined.

Abstract ID: 1491

CORRELATION OF STRUCTURAL AND ELECTRICAL CHARACTERIZATION OF La(Mn-Zn) FERRITES FOR GREEN ENERGY APPLICATIONS

Sumaira Komal, M. Anis-ur-Rehman

Applied Thermal Physics Laboratory (ATPL), Department of Physics COMSATS University Islamabad, Islamabad 45550, PAKISTAN

Email: marehman@comsats.edu.pk

Due to the depletion of non-renewable energy sources, there has been an increased focus on renewable energy sources in recent years. Ferrites are one of the potential candidates to utilize renewable energy resources [1]. Lanthanum is introduced at varying concentrations in manganese zinc ferrite nanoparticles. The synthesis of the nanoparticles ($Zn_{0.8}Mn_{0.2}La_xFe_{2-x}O_4$) is achieved through the sol-gel method. Subsequently, the material undergoes calcination at 870°C and sintering at 900°C for 6 hours in furnaces. The cubic structure and crystalline nature of the material are validated through X-ray diffraction technique [Figure1]. The electrical characteristics of the prepared samples, encompassing AC and DC properties such as conductivity, dielectric constant, loss factor, and impedance, were assessed at fixed frequencies and under room temperature conditions. Doped samples exhibited enhanced properties compared to the pure sample. These samples demonstrate promising potential as candidates for renewable energy sources due to their improved stability and higher conductivity [Figure2].

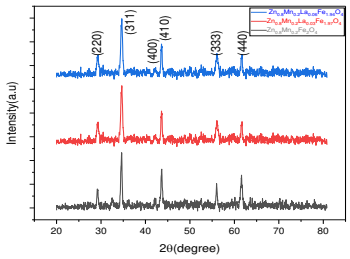

Fig. 1: *XRD pattern of ($Zn_{0.8}Mn_{0.2}La_xFe_{2-x}O_4$) with (x=0.00, 0.03,0.06).*

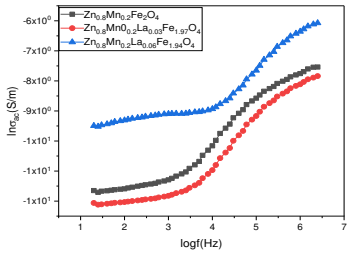

Fig. 1: *AC Conductivity (ln(σ(S/m)) of $Zn_{0.8}Mn_{0.2}La_xFe_{2-x}O_4$ (x=0.00, 0.03,0.06) as a function of frequency at room temperature.*

Reference

[1] P.A. Vinosha, A. Manikandan, A.S.J. Ceicilia, A. Dinesh, G.F. Nirmala, A.C. Preetha, Y. Slimani, M.A. Almessiere, A. Baykal, B. Xavier, *Review of recent advances of zinc substituted cobalt ferrite nanoparticles: Synthesis characterization and diverse applications*, Ceramics International, **47(8)**, pp. 10512-10535 (2021).

Abstract ID: 1552

PHYSICAL PROPERTIES OF $Zn_{0.5}Co_{0.5}Fe_2O_4$ FERRITES DOPED WITH BISMUTH AND TIN

Sajida Rmeid[1], Khulud Habanjar[1], Amani Aridi[2], R. Awad[3]

[1] Beirut Arab University, Dept. of Physics, Beirut, LEBANON
[2] Beirut Arab University, Dept. of Chemistry, Beirut, LEBANON
[3] Alexandria University, Dept. of Physics, Alexandria, EGYPT
E-mail: sajida_rmeid@hotmail.com

Nanoparticles based on zinc-cobalt ferrite ($Zn_{0.5}Co_{0.5}Fe_2O_4$) are suitable for magnetic, optical, and electrical applications. In this study, bismuth and tin are used as dopants in $Zn_{0.5}Co_{0.5}Fe_2O_4$ to create ($Co_{0.5-x}Bi_xZn_{0.5-y}Sn_y$) Fe_2O_4 nanoparticles (x = y = 0, 0.02, 0.04, 0.06 and 0.1), prepared via co-precipitation procedure. X-ray diffraction (XRD) was used to analyze the crystal structure, average crystalline size, volume of the cell, and lattice parameters of the samples. The results confirmed the cubic spinel structure of $Zn_{0.5}Co_{0.5}Fe_2O_4$ ferrite with a decreasing crystalline size from 14.04 nm to 7.28 nm. The morphology of the investigated samples, examined via transmission electron (TEM) and scanning electron microscopes (SEM), showed a cubic agglomerated shape. The elemental compositions of the samples were also verified by energy dispersive X-ray (EDX). From X-ray photoelectron spectroscopy (XPS), the cation distribution and oxidation state of the consisting elements are determined. Based on hysteresis loops, examined via a vibrating sample magnetometer (VSM), magnetic studies of the samples at room temperature reveal the soft ferromagnetism behavior of ferrites. The saturation magnetization (M_s), remanence magnetization (M_r), and coercivity (H_{ci}) showed an alteration with an increase of x and y.

Abstract ID: 1185

NONLINEAR SHIFT OF EXCEPTIONAL POINTS IN COUPLED SPIN TORQUE NANOOSCILLATORS

O. Temnaya

Kotel'nikov Institute of Radioengineering and Electronics, RAS, 125009 Moscow, RUSSIA
E-mail: ostemnaya@gmail.com

This work explores the nonlinear dynamics of interconnected spin-torque nano oscillators (STNOs) and examines the relationship between nonisochronism and the appearance of exceptional points (EPs). EPs are spectral singularities of classical and open quantum dynamics where eigenvalues and their corresponding eigenvectors coalesce [1]. Recent investigations on EPs report a heightened sensitivity of eigenvalues to external perturbations [2], and this is perhaps the most fascinating effect concerning EPs. This effect naturally leads to an excellent opportunity to create ultrasensitive sensors.

However, systems with exceptional points have inherent limitations, primarily stemming from a stringent requirement for their construction. Specifically, these systems must consist of at least two precisely identical parts with perfectly balanced intrinsic loss and gain. Only under these conditions can an EP be observed, and a fixed set of parameters defines it since it is constrained by the structural dimensions. The pivotal question is whether it is feasible to manipulate these EP parameters, effectively shifting the degeneracy within the parametric space by introducing additional degrees of freedom.

We demonstrate that in systems of coupled STNOs, it is possible to observe and fine-tune the position of EPs by manipulating the amplitudes of the driving force and the angles of the external bias magnetic field and spin-polarized current. Namely, the EP shifts most significantly when the azimuth angle of the equilibrium state is approximately 90°, and the system's nonisochronism reaches its peak. The results of this investigation provide valuable insights for enhancing the performance of spintronic devices in applications such as microwave signal generation, spin-based computing, and sensing.

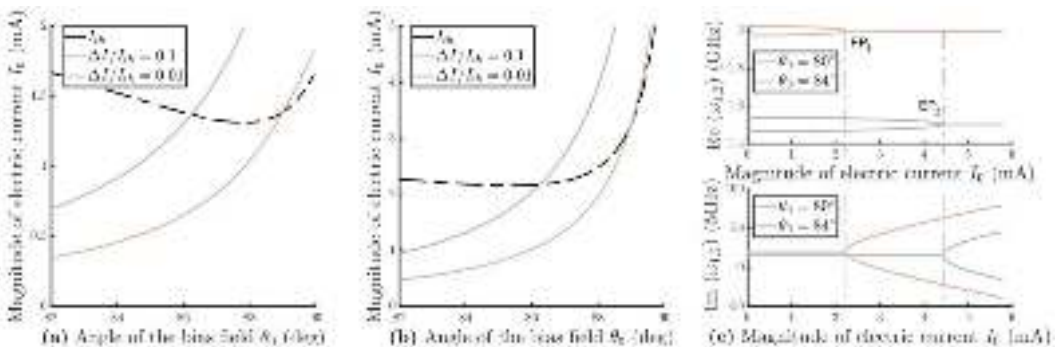

Fig. 1: *Dependencies of critical currents where the system of two coupled STNOs becomes unstable on azimuth angle of the bias magnetic field θ_0 for (a) perpendicular ($\theta_p = 90°$) and (b) parallel ($\theta_p = 5°$) polarization of spin current. (c) represents reliance of real and imaginary parts of normal modes $\omega_{1,2}$ on the electric current magnitude for two different angles of the bias magnetic field $\theta_0 = 80°$ and $\theta_0 = 84°$.*

References

[1] Tosio Kato, *A Short Introduction to Perturbation Theory for Linear Operators* (Springer New York, NY, first edition, 2011).

[2] Jan Wiersig, Phys. Rev. A **93**, 033809 (2016).

Abstract ID: 1121

ENHANCING IONIC CONDUCTIVITY: A COMPREHENSIVE STUDY OF PHASE PURE AND DOPED LANTHANUM ZIRCONATES FOR SOLID OXIDE FUEL CELLS

Arouba Abbas, M. Anis-ur-Rehman

Applied Thermal Physics Laboratory, Department of Physics, COMSATS University Islamabad, Islamabad 45550, PAKISTAN

Email: marehman@comsats.edu.pk

Lanthanum zirconates play a vitol role in solid oxide fuel cells (SOFCs), offering strong ionic conductivity and stability, crucial for enhancing cleaner and sustainable energy conversion technologies [1]. $La_{2-x}Gd_xZr_2O_7$ (x=0.0,0.9) have been synthesized by using a novel approach WOWs sol-gel method. X-ray diffraction pattern verifies the presence of pyrochlore structure of lanthanum zirconates and addition of gadolinium induces observable phase transition in the material. The crystallite size decreases from 49 nm to 35 nm. We conducted electrical analysis by measuring both AC and DC conductivity. The AC conductivity was determined by using a precision analyzer, revealing an increase in value with the rising frequency. DC conductivity was measured by using two probe method in temperature range 30 to 440 °C. Results showed a clear trend, as temperature increased, so did the conductivity. This behavior suggests its suitability for efficient energy conversion in high temperature environments like SOFCs. In figure 2, undoped sample exhibits a consistent activation energy determined through a single linear fit, upon Gd doping reveals a distinct slope break, providing clear evidence of phase transition.

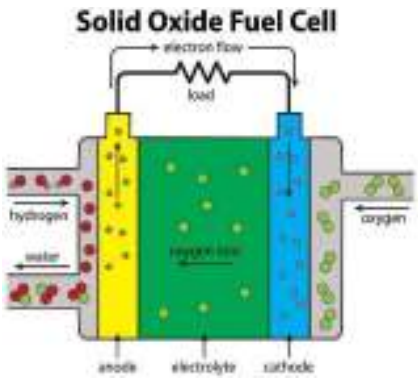

Fig. 1: *Solid Oxide Fuel Cell [2].*

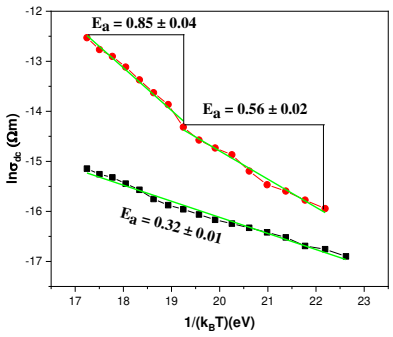

Fig 2: *Activation energy vs DC conductivity ($\ln\sigma_{dc}$) $La_{2-x}Gd_xZr_2O_7$ (x=0.0,0.9).*

References

[1] M. Zapata, A. Larrea, *Lanthanide nickelates for their application on SOFCs*, Electrochimia Acta, **Volume 16**, (2023).

[2] S. Opakhai, *Metal supported SOFCs*, Review, Open Acess Journal, **Volume 16**, (2023).

Abstract ID: 1123

STRUCTURAL AND ELECTRICAL PROPERTIES OF (Mn–Zn) COBALT DOPED SPINEL FERRITES FOR HIGH ENERGY APPLICATIONS

Rehana Rasool, M. Anis-ur-Rehman

Applied Thermal Physics Laboratory (ATPL), Department of Physics COMSATS University Islamabad, Islamabad 45550, PAKISTAN

Email: marehman@comsats.edu.pk

Due to their various applications, Mn-Zn ferrites manufacture and characterization have become significant for physicists. These materials are important as soft magnetic materials because they have useful electrical, magnetic, and optical characteristics. They are mostly composed of iron oxide (Fe_2O_4) with traces of metallic elements as Mn [1]. The current study used the WOWS sol-gel method with general formula $Zn_{0.6}Mn_{0.4-x}Co_xFe_2O_4$ and Mn-Zn ferrites with cobalt doping, where x ranges from (x=0.0-0.4). The formation of single-phase cubic spinel structures in the synthesized samples was confirmed by X-ray diffraction (XRD) analysis. Parameters like crystallite size (26nm-46nm), lattice constant (8.5±0.1Å-8.415±0.006Å), unit cell volume (607.39Å-595.93Å) were determined from the XRD data. The investigation of the frequency-dependent AC electrical conductivity (σ_{ac}) between 20Hz and 3MHz showed that the AC conductivity [fig1] and dielectric loss tangent decreased as the cobalt concentration increased [2]. Moreover, the DC electrical investigation showed a decrease in resistivity of the Co-doped Mn-Zn ferrite with increasing temperature. These outcomes provide opportunities for electrical component application in modern electronics and renewable energy [fig2].

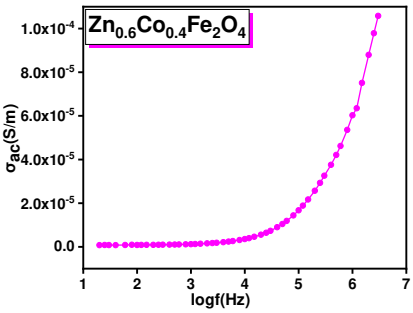

Fig. 1: *Ac Conductivity (σ_{ac}) as function of frequency logf(Hz) for sample $Zn_{0.6}Mn_{0.4-x}Co_xFe_2O_4$ (x=0.0 - 0.4) at room Temperature T (K).*

Fig. 2: *Schematic diagram of renewable energy.*

Reference

[1] H. Mahajan, S.K. Godara, A.K. Srivastava, *Synthesis and investigation of structural, morphological, and magnetic properties of the manganese doped cobalt-zinc spinel ferrite*, Journal of Alloys and Compounds, **896**, 162966 (2022).

[2] M. Kamran, M. Anis-ur-Rehman, *Influence of La^{3+} substitutions on structural, dielectric and electrical properties of spinel cobalt ferrite*, Ceramics International, **49**, pp. 7017-7029 (2022).

Abstract ID: 1156

EVALUATING THE ELECTRICAL CONDUCTIVITY OF COBALT-INCORPORATED BARIUM HEXAFERRITE FOR FUEL CELL APPLICATIONS

Rabia Tariq, M. Anis-ur-Rehman

Applied Thermal Physics Laboratory, Department of Physics, COMSATS University s Islamabad 45550, PAKISTAN
E-mail: rt622052@gmail.com & marehman@comsats.edu.pk

Fuel cells represent innovative devices that revolutionize conventional energy generation through electrochemical processes, providing a sustainable and environmentally friendly solution compared to combustion-based methods (Fig1) [1]. The ferrimagnetic character of hexaferrites arises from their ordered arrangement of oxide ions within the hexagonal magnetoplumbite structure. The remarkable combination of chemical stability, mechanical hardness, and low eddy current loss at high frequencies in hexaferrites renders them durable and high-performing materials for diverse applications [2]. A range of $BaFe_{12-x}Co_xO_{19}$ compositions (x=0.0-0.8) were systematically prepared via sol-gel method, enabling control over cobalt incorporation. Cu-Kα X-ray diffraction (XRD) with λ=1.5405Å was employed over a 2θ (20°-80°) to analyzed lattice constants a=5.893(2)Å-5.890(2)Å and c=23.207(3)Å-23.230(2)Å, leading to V_{cell}= 697.8(5)Å-698.5(5)Å, and crystallite size was estimated to be 43-45nm. Investigating the frequency dependence of AC conductivity and impedence solidified the expected trends in all samples. The increase in AC conductivity (4.1×10^{-5}-7.1×10^{-4}S/m) (Fig 2(a)) and decrease in impedence (2.14×10^{4}-1.2×10^{4} Ω) (Fig 2(b)) across the 20Hz-3MHz frequency range towards the dominance of charge hopping mechanisms influencing these electrical properties. DC resistivity (ϱ_{DC}) sharply decreased (8.43×10^{6}-1.79×10^{6}Ωm) with increasing temperature (50-400°C) due to enhanced charge carrier mobility and E_a decreased linearly (0.94-0.77eV), suggesting thermal activation of charge carriers driving the drop in ϱ_{DC}.

Fig 1. *Application range of fuel cell over power.*

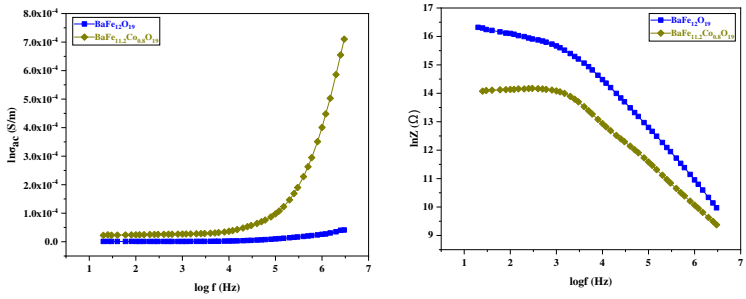

Fig 2. *(a) AC conductivities (b) Impedences for $BaFe_{12-x}Co_xO_{19}$ (0.0-0.8).*

References

[1] A.G. Muhammad, A.R. Hami[illegible] *barium strontium cobalt ferrite cathode for solid oxide fuel cell application: A Short Review*, Malaysian Journal of Microscopy, **V. 19, No. 2**, pp. 220-233 (2023).

[2] D.D. Omid, S. Hooman, M. Shirazi, *A review of synthesis, characterization, and magnetic properties of soft spinel ferrites*, Inorganic Chemistry Communications, **V. 153** (2023).

Abstract ID: 1163

ELECTRICAL ANALYSIS OF $NiCo_2O_4$ AND ITS COMPOSITE WITH CNTS AS ELECTRODE MATERIAL FOR ENERGY STORAGE DEVICES

Hira Sultan, M. Anis-ur-Rehman

Applied Thermal Physics Laboratory (ATPL), Department of Physics COMSATS University Islamabad, Islamabad 45550, PAKISTAN
Email: marehman@comsats.edu.pk

Energy storage devices are crucial tools for storing and releasing energy as needed. They are available in a various form, including batteries, supercapacitors, and fuel cells. Supercapacitors (SCs) have garnered a lot of attention because of its high energy and power density, extended stability [1], [Figure1]. WOWs sol-gel method is used to synthesize the $NiCo_2O_4$ and $NiCo_2O_4$/CNTs composite. X-ray diffraction (XRD) confirmed the spinel structure of the prepared sample and its data is used to measure crystallite size, lattice parameters, Porosity and phase purity. Precision analyzer was used to measure the frequency-dependent (20Hz-3MHz) electrical properties such as ac conductivity and impedance at room temperature. Adding CNT's to $NiCo_2O_4$ increases the electrical conductivity of the sample [Figure2] from 8.738×10^{-4} S/m to 1.23×10^{-3} S/m. From impedance study, the role of grain and grains boundaries of prepared samples were investigated. DC Conductivity was measured by using a two-probe method at temperature range 50 to 435°C presenting a decreasing trend in conductivity with increasing temperature which is further explained by the hopping mechanism. Measured value of DC conductivity are 8.5×10^{-2} S/m and 6.9×10^{-2} S/m respectively. Activation energies were calculated by employing the Arrhenius plot [2]. Cyclic voltammetry is used for electrochemical analysis and to find out the specific capacitance.

Fig. 1: *Merging of Battery and supercapacitor technology.*

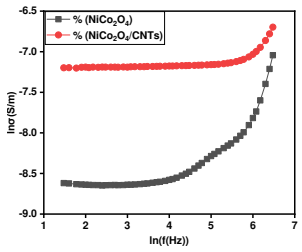

Fig. 2: *AC Conductivity(ln(σ(S/m)) of $NiCo_2O_4$, $NiCo_2O_4$/CNTs as a function of frequency at room temp.*

Reference

[1] M.Z. Iqbal, U. Aziz, *Supercapattery: Merging of battery-supercapacitor electrodes for hybrid energy storage devices*, Journal of Energy Storage, **46**, 103823 (2022).

[2] M. Kamran, M. Anis-ur-Rehman, *Enhanced transport properties in Ce doped cobalt ferrites nanoparticles for resistive RAM applications*, Journal of Alloys and Compounds, **822**, 153583 (2020).

Abstract ID: 1220

Nd DOPING IMPACT ON THE DIELECTRIC PROPERTIES OF (Ca-Bi) COBALTITE'S NANOPARTICLE SYNTHESIZED BY WOWs SOL-GEL PROCESS FOR SOLID OXIDE FUEL CELL APPLICATION

Haris Farooq Kiani[1], Haroon Mazhar[1], Rabia Shahid[2], M. Anis ur Rehman[1]

[1]*Applied Thermal Physics Laboratory (ATPL), Department of Physics, COMSATS University Islamabad, Islamabad 45550, PAKISTAN*
[2]*Fatima Jinnah Women University, Rawalpindi, PAKISTAN*
Email: harisfarooqkiani@gmail.com & haroonmazhar1234@gmail.com & rabiashahid1025@gmail.com & marehman@comsats.edu.pk

As a sustainable way to fulfill the rising global energy demand while minimizing environmental effects, renewable energy sources have drawn a lot of attention. The connections between fuel cells and renewable energy, highlighting the latter's capacity to provide a more robust and environmentally friendly energy system. Calcium Bismuth Cobaltite's $Ca_{2.7}Bi_{0.3}Co_4O_{9+\square}$ were synthesized using WOWS (Without water & surfactants) Sol-gel technique with concentration of (x=0.05,0.10, 0.15) doped with Neodymium (Nd). For further characterizations, pellets of various compositions were formed and sintered. The Average crystallite size of the sample was determined to be between 17nm and 25nm. Morphological Analysis of nanoparticles was done by Scanning Electron Microscope (SEM) The properties of calcined samples were further investigated using Fourier transform infrared spectroscopy (FTIR). The Transport properties AC conductivity (σ_{ac}) and Dielectric properties include dielectric constant (ε') dielectric loss (ε''), Tangent loss (tan□), Impedance real (Z') & imaginary parts (Z'') were measured at various frequencies and in the variable range (100Hz– 3MHz). The composition $Ca_{2.7}Bi_{0.15}Nd_{0.15}Co_4O_{9+\square}$ achieved higher dielectric constant and lower dielectric loss than other compositions. $Ca_{2.7}Bi_{0.15}Nd_{0.15}Co_4O_{9+\square}$ showed the highest value of AC conductivity. $Ca_{2.7}Bi_{0.15}Nd_{0.15}Co_4O_{9+\square}$ showed that the most auspicious material for energy storage applications.

Abstract ID: 1327

MAGNON-POLARITONS AT THE JUNCTION OF TWO ANTIFERROMAGNETIC SUPERLATTICES WITH GRAPHENE AT THE CONTACT INTERFACES

R.T. Askerbeyli, Hiba Elharkati

Karabuk University, Dept. Of Business Administration and Dept. of Physics, Karabuk, TURKEY
E-mail: raskerbeyli@karabuk.edu.tr

We present a theoretical study for the surface and guided magnon-polaritons in superstructure which consist of two antiferromagnetic superlattices (antiferromagnetic materials and nonmagnetic spacers) divided by the contact slab with graphene at the interfaces. The aim our study investigation of influency of the Fermi energies in the graphene which can be varied by employing different electronic doping levels, and as resulting in a strong influence exerted by the presence of graphene on the surface-guided magnon-polariton modes spectrum. The dispersion relation for localized magnon-polaritons modes are derived using Maxwell's electromanetic theory (see Ref 1, 2). The effects include localization of the modes and control of the group velocities of the modes as the Fermi energies of the graphene sheets are varied, along with an important role for the phenomenological damping in the graphene sheets. The dispersion curves for different value of Fermi energy are numerically calculated and the ranges of the existing of these modes are discussed.

References

[1] M.G. Cottam, D.R. Tilley, *Introduction to Surface and Superlattice Excitations*, 2nd Ed. (Boca Raton, FL: CRC Press) (2004)

[2] E.L. Albuquerque, M.G. Cottam, Phys. Rep. **233**, 67–135 (1993).

Abstract ID: 1546

ELECTRONIC PROPERTIES OF MONOLAYER Fe_3GeTe_2 UNDER HUBBARD CORRECTION

G.Y. Senguler[1], Y. Mogulkoc[2], A. Mogulkoc[3]

[1]*Ankara University, Graduate School of Natural and Applied Sciences, Dept. of Physics, 06100, Ankara, TURKEY*
[2]*Ankara University, Faculty of Engineering, Dept. of Physics Engineering, 06100, Ankara, TURKEY*
[3]*Ankara University, Faculty of Sciences, Dept. of Physics, 06100, Ankara, TURKEY*
E-mail: senguler@ankara.edu.tr

Density Functional Theory (DFT) is a method in theoretical chemistry and physics used to calculate the electronic structures of atoms and molecules. However, DFT encounters difficulties, especially in systems such as transition metals and locally magnetic materials, where standard applications often yield inaccurate results due to the inability to accurately model electron interactions [1]. The Hubbard correction is employed to enhance DFT results in such systems. Specifically, it is utilized to better characterize electron interactions in systems containing transition metals. This correction involves introducing a parameter called the Hubbard U term, which is employed to model the Coulomb interaction between electrons within the same atom. By incorporating this term into standard DFT results, the electronic structures of systems such as transition metals and local-magnetic materials can be more accurately calculated. Thus, Hubbard correction improves the accuracy of DFT and provides a more comprehensive description of the electronic properties in these systems. In this study, we investigate how the electronic band structures of monolayer Fe_3GeTe_2 structure **(Fig.1)** change under Hubbard correction using first-principles calculations employing the Generalized Gradient Approximation (GGA)-Perdew-Burke-Ernzerhof exchange correlation functional (PBE) [2] and HSE06 hybrid functional methods.

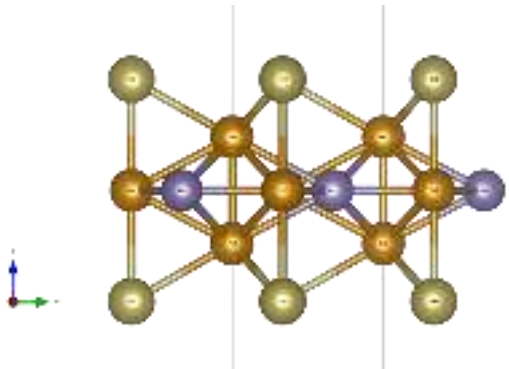

Fig. 1: *Side view of monolayer of Fe_3GeTe_2.*

Acknowledgement

This work was supported by the FLAG-ERA grant MNEMOSYN, by MCIN/AEI/10.13039/501100011033 and European Union "NextGenerationEU/PRTR" under grant PCI2021-122035-2A-2a

References

[1] S.L. Dudarev, G.A. Botton, S.Y. Savrasov, C.J. Humphreys, A.P. Sutton, Phys. Rev. B **57**, 1505 (1998).
[2] J.P. Perdew, K. Burke, M. Ernzerhof, Phys. Rev. Lett. **77**, 3865 (1996).

Abstract ID: 248

SPIN TRANSFER TORQUE AND ANISOTROPIC CONDUCTANCE IN SPIN ORBIT COUPLED GRAPHEME

Razieh Beiranvand

Faculty member, Ayatollah Boroujerdi University, Boroujerd, IRAN
E-mail: razieh.beiranvand@gmail.com

We conducted a theoretical investigation into spin-transfer torque (STT) within a graphene system featuring spin-orbit coupling (SOC). Our study focused on a graphene-based junction with a spin-orbit coupled region positioned between two ferromagnetic (F) segments. We observed that the presence of SOC led to anisotropic modifications in STT, magnetoresistance, and charge conductance relative to the misalignment of magnetization in the F regions. Notably, within the Klein regime, where particles strike the interfaces perpendicularly, spin-polarized Dirac fermions passed perfectly through the boundaries of an F-F junction, resulting in zero reflection and zero STT. However, the introduction of SOC led to a reappearance of nonzero STT due to band structure modification. These findings offer potential for experimental exploration of proximity-induced SOC in graphene systems.

Abstract ID: 1024

INFLUENCE OF MAGNETIC IONS IMPLANTATION ON THE CRITICAL CURRENT OF HTSC COMPOSITES

I. Rudnev[1,2], D. Abin[1], S. Pokrovskii[1,2], R. Batulin[2]

[1]*National Research Nuclear University MEPhI, 115409, Moscow, RUSSIA*
[2]*Kazan Federal University, 420008, Kazan, RUSSIA*
E-mail: iarudnev@mephi.ru

Modern high-temperature superconducting tape composites have a fairly complex composite structure, which consists of a Hastelloy alloy-based substrate, several thin buffer oxide layers and a layer of high-temperature superconductor (HTSC) $Y(Gd)Ba_2Cu_3O_{7-x}$. Such superconducting materials exhibit enormous critical current densities (several MA/cm^2) even at the liquid nitrogen. At the same time, for many practical applications, the problem of increasing the critical current (J_c) of HTSC tapes both in zero field and in magnetic fields and different temperatures remains relevant and requires a solution.

It is well known that an increase in the critical current is achieved through the creation of magnetic flux pinning centers—structural defects—in the HTSC material. For this, various methods are used, from the formation of defects at the synthesis stage to radiation exposure, leading to the appearance of radiation defects of various types. At the same time, pinning can be enhanced by adding magnetic defects to the structural defects, which, due to additional magnetic interaction, will lead to an increase in the pinning force. We have shown earlier that the implantation of magnetic Fe^+ ions can lead to an increase in HTSC composites J_c.

In this report, we provide detailed data on the effect of irradiation with magnetic Co^{2+} ions on the magnetization and critical current of HTSC composites. Irradiation of the samples was carried out with several fluences for four different modes of creating defects in which sequentially there was no implantation of ions, and then the concentration of magnetic ions in the HTSC layer increased until the mode of complete stopping of ions in the superconducting matrix (the Brag peak was in the middle of the HTSC layer). Different implantation modes were implemented by varying the thickness of the silver layer, which led to different projective ion paths, which were previously calculated using the SRIM package. It was shown that under certain irradiation conditions and implantation modes of magnetic Co^{2+} ions, an increase in magnetization and critical current is observed both in zero field and in fields up to 8 T (Fig. 1). In the report we will analyze the results obtained and propose a physical model to explain experimental data.

The study was supported by the RSF grant 23-19-00394, https://rscf.ru/project/23-19-00394/.

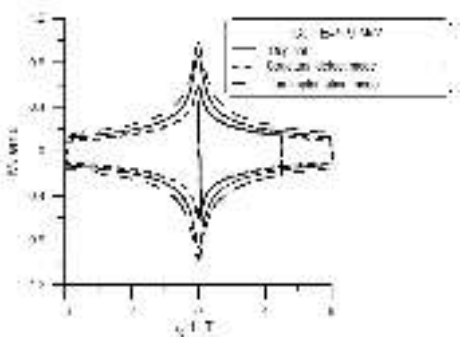

Fig. 1: *Increase in magnetization of HTSC composites upon implantation with Co^{2+} ions.*

Abstract ID: 1460

FLUX JUMPS, CLUSTER DISTRIBUTION MODEL AND VORTEX PHASE DIAGRAM OF OXYGENATED Al-YBCO SINGLE CRYSTAL

Ashna Babu, Deepshikha Jaiswal Nagar

School of Physics, IISER Thiruvananthapuram, Vithura, Kerala, 695551 INDIA
E-mail: ashna19@iisertvm.ac.in

We present the vortex phase diagram for an oxygenated Al-doped YBCO, a type -II superconductor, by analysing the anomalies observed in its magnetization response. One such anomaly is the second magnetization peak (SMP) anomaly expected from the order-disorder transition of the vortex lattice. The thermal evolution of the anomaly differs from that of the as-grown crystal response, which arises due to differences in the pinning characteristics of oxygen-deficient clusters that are proposed to lie in the basal plane of Al-YBCO. The presence of clusters was revealed from the XPS spectra. These clusters also explain the flux jumps observed in the odd quadrants of magnetic hysteresis. The field values of the flux jumps is similar to which a symmetry reorientation transition has previously been reported in the vortex lattice of YBCO via small angle neutron scattering measurements. We propose that the field-induced symmetry reorientation transition in the vortex lattice of Al-YBCO, with clusters having currents in opposite directions triggers the annihilation of the domains and hence a flux jump. Finally, a phase diagram depicting various phases evolved to correspond to the dominant energy on vortices, has been made for the oxygenated crystals, with most of the region independent of the direction of the field, which makes it different from the as-grown crystal vortex phase diagram.

Abstract ID: 1550

EFFECT OF DIFFERENT IMMERSION TIMES IN SEAWATER ON THE MECHANICAL PROPERTIES OF $((Zn_{0.5}Ni_{0.5}Fe_2O_4)_{0.5}(Ba_{0.4}Sr_{0.4}Ca_{0.2}Fe_{12}O_{19})_{0.5})/Bi_{1.6}Pb_{0.4}Sr_2Ca_2Cu_{3.2}O_{10+\delta}$ COMPOSITE

Ahmad Najem[1], M. Anas[2], K. Habanjar[1], R. Awad[1,2]

[1]*Beirut Arab University, Faculty of Science, Dept. of Physics, P.O. Box 11-5020, Riad El Solh, Beirut, LEBANON*
[2]*Alexandria University, Faculty of Science, Dept. of Physics, P.O. Box 21511, Alexandria, EGYPT*
E-mail: ahmadnijim92@gmail.com

Nanocomposite $((Zn_{0.5}Ni_{0.5}Fe_2O_4)_{0.5}(Ba_{0.4}Sr_{0.4}Ca_{0.2}Fe_{12}O_{19})_{0.5})_x/Bi_{1.6}Pb_{0.4}Sr_2Ca_2Cu_{3.2}O_{10+\delta}$ with x=0.00, 0.04, 0.08, 0.16 and 0.40 wt.%, were synthesized using a conventional solid-state reaction method to demonstrate the effect of $(Zn_{0.5}Ni_{0.5}Fe_2O_4)_{0.5}(Ba_{0.4}Sr_{0.4}Ca_{0.2}Fe_{12}O_{19})_{0.5}$ nanocomposites on the mechanical performance of the (Bi, Pb)-2223 superconducting phase. X-ray diffraction (XRD) was used to assess phase purity and structural characteristics. Scanning electron microscopy (SEM) and energy dispersive X-ray spectroscopy (EDX) were used to analyze the morphology and elemental compositions of the investigated samples, respectively. The elemental composition and state of oxidation of every element in the produced samples were identified using X-ray photoelectron spectroscopy (XPS). Vickers microhardness (Hv) measurements were conducted at room temperature for 30 seconds, with varying applied stresses ranging from 0.49 to 9.80 N. Upon the immersion of the prepared samples in seawater at different times (2, 6, 12, and 24 hours), a great improvement in Vickers microhardness (Hv) was obtained. Based on Vickers microhardness (Hv) measurements, the proportional sample resistance (PSR) model offered the most accurate theoretical analysis at the plateau limit region. Furthermore, the introduction of nano-$(Zn_{0.5}Ni_{0.5}Fe_2O_4)_{0.5}(Ba_{0.4}Sr_{0.4}Ca_{0.2}Fe_{12}O_{19})_{0.5}$ into the (Bi, Pb)-2223 superconductor had a significant impact on the mechanical characteristics.

Abstract ID: 1588

THE EFFECT OF Sr SUBSTITUTION ON THE CRYSTAL SYMMETRY AND SUPERCONDUCTIVITY OF THE HIGH TEMPERATURE SUPERCONDUCTOR $La_{2-x}Sr_xCuO_4$

Bassam M. Mustafa

Prof. Dr. Retired from College of Science University of Mosul IRAQ
E-mail: bassam_alemam@yahoo.com

In this research I study the changes in the crystal symmetry during substitution with different amounts of Sr in the High Temperature Superconductor (HTSC) $La_{2-x}Sr_xCuO_4$ and how its distribution and concentration affect the superconductivity in the HTSC compound discussing its changes in the crystal symmetry, from the moment of substitution of Sr in the compound at room temperature, then during cooling till ,triggering of superconductivity, also this linked with the formation and the strange behavior of the charge strips and the appearance of different stages for it. The understanding of these phenomena suggest a new insight for the process of pairing of holes and a model is proposed for that, which explains the changes in the superconducting critical temperature behavior of the HTSC with different concentration of Sr and some other specific characteristics of the high temperature superconductor.

References

[1] T. Yanagisawa, *Mechanism of high-temperature superconductivity in correlated-electron systems*, Condens. Matter, **4(2)**, 57 (2019).

[2] J. Hu, *Identifying the genes of unconventional high temperature superconductivity*, Science Bulletin, **61**, pp. 561-569 (2016).

[3] A. Marouchkine, *Room-Temperature Superconductivity*, Cambridge International Science Publishing, (2004).

Abstract ID: 1533

THE ELECTRICAL PROPERTIES OF THE SEVERAL HTS TAPE JOINTS FOR THE SUPERCONDUCTING FAULT CURRENT LIMITER

D.M. Durão[1], S. Costa[1], C. Aksoy[2], I. Catarino[1,4,5], J.M. Pina[3,4,5], A. Pronto[3,4,5]

[1] *NOVA School of Science and Technology, Department of Physics, Caparica, PORTUGAL*
[2] *Karadeniz Technical University, Electronics&Communication Engineering,61830, Trabzon, TURKIYE*
[3] *NOVA School of Science and Technology, Department of Electrical and Computers Engineering, Caparica, PORTUGAL*
[4] *Centre of Technology and Systems (CTS-UNINOVA), PORTUGAL*
[5] *Intelligent Systems Associate Laboratory (LASI), PORTUGAL*
E-mail: aksoycanan0@gmail.com

Superconducting fault current limiters (SFCLs) represent a transformative advancement in grid protection technology, offering the potential to revolutionize the stability and reliability of modern electrical grids. These devices leverage the remarkable properties of superconducting materials to effectively mitigate fault currents and minimize damage to grid infrastructure during fault events. However, the practical implementation of SFCLs relies heavily on the performance and reliability of the joints connecting superconducting elements within the device. In recent years, significant research efforts have been dedicated to investigating various joint configurations and fabrication techniques to optimize the performance of SFCL. High-temperature superconducting (HTS) tape joints offer unique advantages such as high current-carrying capabilities and low resistance, making them well-suited for applications. In recent years, the integration of high-temperature superconducting (HTS) tape joints into SFCLs has emerged as a promising avenue for enhancing their performance. In this study, the several HTS tape joints were produced by using the soldering method for potential use in SFCL. The I-V characteristic and loses of the joints were investigated in AC and DC. The obtained results of soldered HTS tape joints have provided valuable insights into their suitability for SFCL applications.

Acknowledge

This publication is based upon work from COST Action Hi-SCALE,CA19108, supported by COST (European Cooperation in Science and Technology).

Abstract ID: 1076

INVESTIGATIONS OF SOME PROPERTIES OF HIGH-TEMPERATURE IRON-BASED SUPERCONDUCTOR $Ba_{1-x}Rb_xFe_2As_2$ USING EFFECTIVE TWO-BAND MODEL

Derejaw Gardew, Gebregziabher Kahsay, Tamiru Negussie

Department of Physics, College of Science, Bahir Dar University, Bahir Dar, ETHIOPIA
E-mail: wubetgardew@gmail.com

This paper studies about theoretical investigations of some properties of high temperature iron-based superconductor $Ba_{1-x}Rb_xFe_2As_2$ using effective two-band model. The mathematical expressions of different superconducting parameter are held by the retard double time temperature dependent Green's function formalism. The superconducting order parameter of the material for electron and hole as well as the inter band are plotted with the temperature as well. This parameter is decreased with increasing the temperature and vanishes at the transitional temperature of the superconductor $Ba_{1-x}Rb_xFe_2As_2$. The values of superconducting order parameter coupling strength in electron intra band, hole intra band, intra-inter band and the combined band mathematically determined. The pairing potential of this material is increased as a function of the critical temperature. The phase diagram of temperature-dependent electron and hole-intra-band density of state versus excitation energy for iron-based superconductor $Ba_{1-x}Rb_xFe_2As_2$ are clearly plotted and both are decreased with increasing of the excitation energy. The influences of temperature, pairing potential and critical temperature on condensation energy are expressed graphically in a scientific manner and the condensation energy decreased with increasing of both temperature and pairing potential and vanished at the critical temperature of the superconductor. Furthermore, the densities of state for electron and hole-intra band of different temperatures versus excitation energy are plotted using experimental values. These densities of states are decreased slowly with increasing of the excitation energy and diminished at low temperature values.

Abstract ID: 1199

ELECTRONIC STRUCTURE OF $InCo_2As_2$ AND $KInCo_4As_4$: LDA+DMFT

N.S. Pavlov[1,2], I.R. Shein[3], K.S. Pervakov[2], I.A. Nekrasov[1,2]

[1]*Institute of Electrophysics UB RAS, 620016, Yekaterinburg, RUSSIA*
[2]*Lebedev Physical Institute RAS, 119991, Moscow, RUSSIA*
[3]*Institute of Solid State Chemistry UB RAS, 620990, Ekaterinburg, RUSSIA*
E-mail: pavlovns@gmail.com

A comparative analysis of the electronic structure obtained in the DFT/LDA and LDA+DMFT approaches of the possible isostructural analogues of iron superconductors $InCo_2As_2$ and $KInCo_4As_4$ with the electronic structure of the parent high-temperature superconductor system $BaFe_2As_2$ was carried out [1]. It is established that in spite of the rather large value of the electron-electron correlations (local Coulomb interaction on the Co-3d shell U=4.0 eV, the Hund exchange interaction J=0.85 eV), a relatively small value of the quasiparticle mass renormalization 1.2-1.35 at the Fermi level is observed. The correlation effects lead to an remarkable shift and compression of the spectrum below -0.8 eV. A similar manifestation of correlation effects were earlier observed for $BaCo_2As_2$ [2].

The band structure of $InCo_2As_2$ near the Fermi level is qualitatively similar to the previously studied $BaCo_2As_2$ [3] (but the Fermi level is shifted lower in energy by about 0.3 − 0.5 eV) and differs significantly from the band structure of $BaFe_2As_2$. In the $KInCo_4As_4$ system, the bands near the Fermi level resemble the band structure of $BaFe_2As_2$, and the Fermi surfaces have a similar topology (see Fig. 1). This indirectly points to the possibility of superconductivity formation in $KInCo_4As_4$. Also according to the results of LDA+DMFT calculations it is seen that with a rather small hole or electron doping in the $KInCo_4As_4$ system topological Lifshitz transitions will occur.

We believe that the synthesis of the $InCo_2As_2$ and $KInCo_4As_4$ compounds is important for the study of superconductivity in this class of materials.

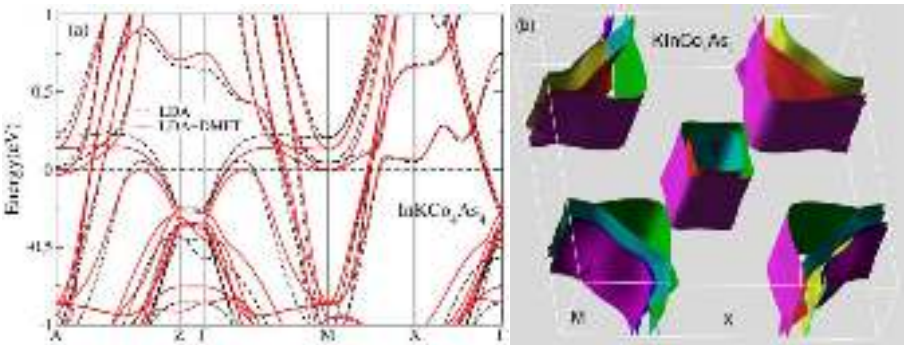

Fig. 1: *LDA (black dashed lines) and LDA+DMFT (red solid lines) calculated band structures for $KInCo_4As_4$ (panel (a)). LDA calculated Fermi surfaces for $KInCo_4As_4$ (panel (b)).*

References

[1] N.S. Pavlov, I.R. Shein, K.S. Pervakov, I.A. Nekrasov, JETP Letters **117**, 61 (2023).
[2] A. van Roekeghem, Th. Ayral, J.M. Tomczak, *et al.*, Phys. Rev. Lett. **113**, 266403 (2014).
[3] N. Xu, P. Richard, A. van Roekeghem, P. Zhang, *et al.*, Phys. Rev. X **3**, 011006 (2013).

Abstract ID: 1209

TUNNELING SPECTROSCOPY OF $Ba(Fe,Ni)_2As_2$ PNICTIDES IN THE NORMAL STATE

I.A. Nikitchenkov[1, 2], A.D. Ilina[2], K.S. Pervakov[2], V.A. Vlasenko[2], S.A. Kuzmichev[1,2], T.E. Kuzmicheva[2]

[1]Faculty of Physics, Lomonosov Moscow State University, Moscow, 119991, RUSSIA
[2]Lebedev Physical Institute, Russian Academy of Sciences, Moscow, 119991, RUSSIA
E-mail: kuzmichevate@lebedev.ru

We report the results of tunneling spectroscopy measurements of current-voltage characteristics (CVC) and dynamic conductance dI(V)/dV spectra of SnS break-junctions [1] in single crystals of superconducting (SC) iron pnictide $BaFe_{2-x}Ni_xAs_2$ within the wide doping range x = 0.06–0.14 and bulk critical temperatures $T_c \approx$ 10–21 K. The single crystals were grown using a "self-flux" method [2]. A strong nonlinearity is reproducibly observed in the obtained curves both in the SC and normal state [3,4], showing humps at $V_{max} \approx$ 10–13 meV and dips at $V_{min} \approx$ 20–25 meV in the out-of-gap region. Below T_c, an Andreev SC gap structure appears on such nonlinear background. We unambiguously show the nonlinearity cannot be caused by the junction overheating, whereas its shape is independent on geometrical properties of the tunneling contact (resistance, area, and transparency). Such effect does not directly relate to the SC state and could be attributed to the normal-state electron density of states features in the vicinity of the Fermi level caused by either band-structure features or electron-boson coupling. The temperature and doping evolution of such nonlinearity are also presented.

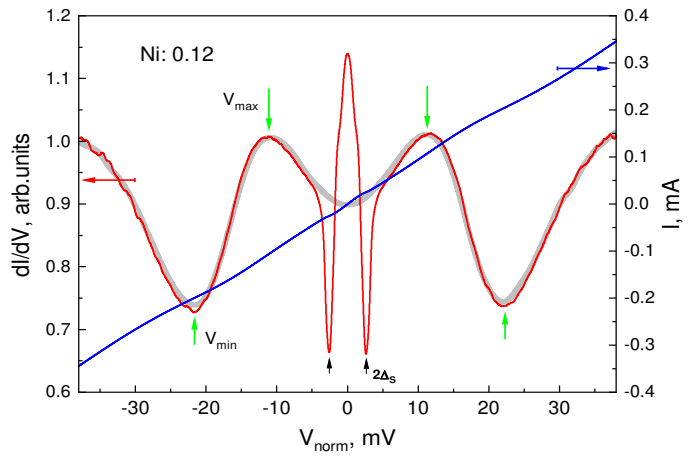

Fig. 1: *CVC (blue line, right axis) and dI(V)/dV spectra measured at T = 4.2 K (red curve, left axis) and in the normal state at $T_c \approx$ 16.2 K (gray curve, left axis) for SnS contact in $BaFe_{1.88}Ni_{0.12}As_2$ single crystal of slightly overdoped composition.*

References

[1] S.A. Kuzmichev, T.E. Kuzmicheva, Low Temp. Phys. **42**, 1008 (2016).
[2] K.S. Pervakov, *et al.*, Supercond. Sci. Technol. **26**, 015008 (2013).
[3] I.A. Nikitchenkov, *et al.*, Moscow Univ. Phys. Bull. **78**, 521 (2023).
[4] T.E. Kuzmicheva, *et al.*, Phys. Rev. B **104**, 174512 (2021).

Abstract ID: 1260

DOPING EVOLUTION OF THE SUPERCONDUCTING GAP STRUCTURE OF THE 122 FAMILY PNICTIDES AND CHALCOGENIDES

T.E. Kuzmicheva[1], S.A. Kuzmichev[1,2], I.V. Morozov[3], A.I. Shilov[1], Ye.O. Rakhmanov[1,3], K.S. Pervakov[1], V.A. Vlasenko[1]

[1]Lebedev Physical Institute, Russian Academy of Sciences, 119991, Moscow, RUSSIA
[2]Lomonosov Moscow State University, Faculty of Physics, 119991, Moscow, RUSSIA
[3]Lomonosov Moscow State University, Department of Chemistry, 119991, Moscow, RUSSIA
E-mail: kuzmichevate@lebedev.ru

Superconducting (SC) pnictides and chalcogenides of the 122 structural family still attract researcher interest due to their unconventional SC properties. In the alkali metal based 122 selenides, a natural phase separation takes place (with bulk volume fraction of the SC phase about 10–15 %), as a result, these unique compound remain still understudied.

Here we compare the structure of the SC order parameter in Fe-based compounds of the 122 structural family: pnictides $Ba(Fe,Ni)_2As_2$ and $(Ba,K)Fe_2As_2$ [1], and chalcogenides $(K,Na)_{0.8}Fe_{2-y}(Se,S)_2$ [2,3] with various doping level and critical temperatures T_c = 11–36 K. Using incoherent multiple Andreev reflection effect (IMARE) spectroscopy of planar "break-junctions" [4], we show a multiple-gap superconductivity in $Ba(Fe,Ni)_2As_2$ and $(Ba,K)Fe_2As_2$, with possibly anisotropic SC condensate with the large SC gap, and a single-gap superconductivity in $(K,Na)_{0.8}Fe_{2-y}Se_{2-z}S_z$. We report the directly determined magnitudes and characteristic ratios of the SC gaps and show their evolution in the unified doping phase diagram. Directly determined temperature dependences of the SC gaps are also presented.

The work is supported by RSF project no. 22-72-10082.

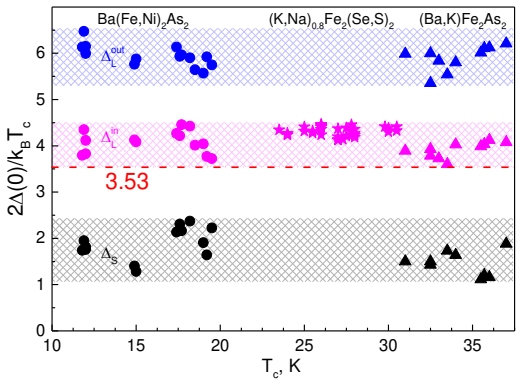

Fig. 1: *Characteristic ratios of the SC order parameters in the 122 family superconductors.*

References

[1] T.E. Kuzmicheva, *et al.*, Phys. Rev. B **104**, 174512 (2021); JETP Lett. **118**, 526 (2023).
[2] A.D. Ilina, *et al.*, Bull. Lebedev Phys. Inst. **50**, 545 (2023).
[3] M.V. Roslova, *et al.*, CrystEngComm **16**, 6919 (2014).
[4] S.A. Kuzmichev, T.E. Kuzmicheva, Low Temp. Phys. **42**, 1008 (2016).

Abstract ID: 1301

ANALYSIS OF THE EFFECT OF ALIOVALENT SUBSTITUTIONS IN Ca/K-1144 IRON BASED SUPERCONDUCTORS

A. Duchenko[1,2], F. Varsano[2], A. Augieri[3], L. Barba[5], G. Campi[4], G. Celentano[2], L. Gigli[6], J.R. Plaisier[6], N. Pompeo[1], A. Rufoloni[3], Z.-H. Sung[7], A. Masi[3]

[1]*Università degli Studi RomaTre, Dipartimento di Ingegneria Industriale, Elettronica e Meccanica, Via Vito Volterra, 62, 00146 Roma, ITALY*
[2]*ENEA, SSPT-PROMAS-MATPRO, Via Anguillarese, 301, 00123 Roma, ITALY*
[3]*ENEA, FSN-COND, Via Enrico Fermi, 45, 00044 Roma, ITALY*
[4]*CNR- Istituto di Cristallografia, Via Salaria Km 29,300, 00015, Monterotondo (Roma), ITALY*
[5]*CNR- Istituto di Cristallografia, Strada Statale 14 km 163,5, 34149 Basovizza (Trieste), ITALY*
[6]*Fermi National Accelerator Laboratory, Batavia, IL, USA*
E-mail: aduchenko@os.uniroma3.it

Among Iron Based superconductors (IBSC), the compounds of the 1144 family are characterized by the chemical composition $A_1AE_1Fe_4As_4$ (A=Alkaline, AE=Alkaline-Earth). In recent years, they have attracted considerable interest due to their high critical currents at high magnetic fields, with further possible improvements by tailoring the pinning landscape by introduction of defects [1]. Despite being usually considered stoichiometric compounds, we recently demonstrated that it is possible to tailor their chemical composition trough targeted substitutions while retaining the crystalline structure. In our previous experiments we obtained 1144 compounds in which Ca is replaced by Na and La and K by Ba or Sr [2,3]. This is reflected on the crystalline structure: the lattice distortion induced by this variation in chemical composition plays a key role on the critical temperature of 1144 compounds. The different chemical composition has furthermore effects on critical currents of polycrystalline samples [4].

In this work, we analyze in detail the effect that the chemical substitution has on the structure, characterizing by means of diffraction and microscopy techniques polycrystalline samples obtained by a solid-state route. We focus on how the nature of the substituting ion affects structural parameters such as the crystalline distortion and its solubility, and eventually how this is reflected on the superconducting properties. Moreover, the role of the different variables commonly identified as crucial for the definition of the critical temperature of IBSCs, such as crystalline geometries, valence of iron ions or disorder is presented and discussed for this 1144 family of IBSCs.

Acknowledgements

This work has been partially carried out within the framework of the EUROfusion Consortium, funded by the European Union via the Euratom Research and Training Programme (Grant Agreement No 101052200 — EUROfusion). Views and opinions expressed are however those of the author(s) only and do not necessarily reflect those of the European Union or the European Commission. Neither the European Union nor the European Commission can be held responsible for them.

References

[1] S. Pyon, *Large and significantly anisotropic critical current density induced by planar defects in $CaKFe_4As_4$ single crystals*, Phys. Rev. B, **99** (10), 10.1103 (2019).
[2] A. Masi, *Tailoring the critical temperature of Ca/K-1144 superconductors: The effect of aliovalent substitution on tetragonality*, Supercond Sci Technol, **35**, 10.1088 (2022).
[3] A. Duchenko, *Influence of Rare-Earth inclusion on structure and properties of Ca/K-1144 IBSC*, has been accepted by IEEE Trans. Appl. Supercond.
[4] A. Augieri, *Pinning properties of 1144 polycrystalline samples with aliovalent doping*, IEEE Trans. Appl. Supercond., **10.1109** (2024).

Abstract ID: 1408

HIGH-PRESSURE SYNTHESIS AND Mn DOPING EFFECT ON $CaKFe_4As_4$ SUPERCONDUCTOR

Manasa Manasa[1], Mohammad Azam[1], Tatiana Zajarniuk[2], Svitlana Stelmakh[1], Tomasz Cetner[1], Andrzej Morawski[1], Andrzej Wisniewski[2], Shiv J. Singh[1]

[1]*Institute of High-Pressure Physics (IHPP), Polish Academy of Sciences, Sokolowska 29/37, Warsaw, POLAND*
[2]*Institute of Physics, Polish Academy of Sciences, aleja Lotników 32/46, 02-668 Warsaw, POLAND*
E-mail: manasa@unipress.waw.pl

$CaKFe_4As_4$ (1144) is one of the stoichiometric high T_c iron-based superconductors (FBS) and depicts the highest transition temperature (T_c) around 35 K with no magnetic or structural transition [1]. The critical current density (J_c) of 1144 is remarkably high and robust of the order 10^8 A/cm^2 compared to other FBS [2]. The high-pressure and high-temperature synthesis (HP-HTS) method is a unique way to improve the superconducting properties [3]. To study the high-pressure growth effect on the superconducting properties of $CaKFe_4As_4$, we synthesize the 1144 bulks by HP-HTS [3-4] and the conventional synthesis process at ambient pressure (CSP) [4-5]. Interestingly, both resistivity and magnetic measurements depict the enhancement of T_c by ~2 K for 1144 samples prepared by HP-HTS compared to that by CSP, and also the improvement of the sample quality and grain connections are observed. Furthermore, J_c is enhanced by one order of magnitude in the whole magnetic field range of 9 T, which suggests the improvement of the pinning centers and the grain connections by high-pressure growth effects. Since $CaKFe_4As_4$ exhibits the superconducting property without any doping, it is worth studying the substitution effect in the superconducting layer (FeAs) of $CaKFe_4As_4$. To understand the electron doping effect on $CaKFe_4As_4$, a series of Mn-doped samples are prepared by CSP as well as HP-HTS. These samples are well characterized by structural, microstructure, transport, and magnetic measurements to understand the superconducting properties of 1144 with these Mn substitution effects. Mn doping reduces the superconducting properties of $CaKFe_4As_4$ prepared by CSP and completely disappears for above 3% Mn doping, whereas the enhancement of the T_c is observed by 4-5 K for some Mn-doped $CaKFe_4As_4$ through the HP-HTS technique. Our study confirms that the substitution of Mn in the superconducting FeAs layer suppresses the superconducting properties of the $CaKFe_4As_4$ samples, but high-pressure growth enhanced the transition temperature and critical current density with improvement of the sample quality [6].

Acknowledgments

The work was funded by SONATA-BIS 11 project (Registration number: 2021/42/E/ST5/00262) funded by National Science Centre (NCN), Poland. SJS acknowledges financial support from National Science Centre (NCN), Poland through Project number 2021/42/E/ST5/00262.

References

[1] W.R. Meier *et al.*,Phys. Rev.B **94**, 064501 (2016).
[2] S.J. Singh *et al.*, Phys. Rev.Materials **2**, 074802 (2018).
[3] M. Azam *et al.*, Materials **16**, 5358 (2023).
[4] M. Manasa *et al.*, IEEE Trans. Appl. Supercond. **34**, 1-5 (2023).
[5] S.J. Singh *et al.*, Supercond. Sci. Technol. **33**, 025003 (2020).
[6] M. Manasa *et al.*, submitted to the journal (under review) (2024).

Abstract ID: 1462

HIGH-PRESSURE SYNTHESIS OPTIMIZATION AND ITS EFFECT ON THE SUPERCONDUCTING PROPERTIES OF Sm-BASED OXYPNICTIDE

Mohammad Azam[1], Manasa Manasa[1], Tatiana Zajarniuk[2], Ryszard Diduszko[3], Tomasz Cetner[1], Andrzej Morawski[1], Andrzej Wiśniewski[2], Shiv J. Singh[1]

[1]*Institute of High Pressure Physics (IHPP), Polish Academy of Sciences, Sokołowska 29/37, 01-142 Warsaw, POLAND*
[2]*Institute of Physics, Polish Academy of Sciences, aleja Lotników 32/46, 02-668 Warsaw, POLAND*
[3]*Łukasiewicz Research Network Institute of Microelectronics and Photonics, Aleja Lotników 32/46, 02-668 Warsaw, POLAND*
E-mail: mohammadazam@unipress.waw.pl

The high-pressure and high-temperature synthesis (HP-HTS) technique can be a promising method to improve the sample quality as well as superconducting properties of iron-based superconductors (FBS) [1,2]. The fluorine-doped Sm-based oxypnictide ($SmFeAsO_{1-x}F_x$: Sm1111) shows the highest critical transition temperature (T_c) of up to 58 K (for $x = 0.25$) for this high T_c superconductors [3,4]. Nevertheless, synthesizing high-quality samples at ambient pressure through the conventional synthesis process (CSP) is a primary challenge which could be due to the evaporation of the lighter elements such as arsenic and fluorine. These issues lead to the formation of impurity phases and a reduction in critical current density (J_c). To overcome these challenges, we optimize the growth conditions for optimally F-doped Sm1111, specifically $SmFeAsO_{0.80}F_{0.20}$ bulks by preparing the 1111 bulks in a broad range of growth temperatures (600-900°C), durations (1-6 hours), and pressures (0-1 GPa) using the HP-HTS method. This technique produces the inert gas pressures up to 1.8 GPa within a cylinder chamber having a large sample space (~15 cm) which is equipped with a three-zone furnace capable of reaching temperatures up to 1700°C [5]. Comprehensive characterization of these samples was performed by structural, microstructural analysis, transport, and magnetic measurements. Our results reveal that the growth conditions: 900°C and 700 MPa for 1 hour are optimal conditions for pure Sm1111 phase formation with improved grain connections. In contrast, the impurity phases and poor grain connections are observed outside these growth conditions. For the optimum Sm1111 bulks, the critical transition temperature is reached up to 54 K, the same as that followed by CSP. However, the critical current density is enhanced by a two-order magnitude (~10^4-10^5 A/cm^2) in comparison with the samples prepared by CSP (10^2-10^3 A/cm^2). More detailed and comparative studies will be presented based on various Sm1111 bulks prepared by CSP and HP-HTS to understand the high-pressure growth effects [6]. These studies will be beneficial for fabricating superconducting wires and tapes of this promising Sm1111 family, where a large amount and high quality of bulks are needed.

Acknowledgments

The work was funded by SONATA-BIS 11 project (Registration number: 2021/42/E/ST5/00262) funded by National Science Centre (NCN), Poland. SJS acknowledges financial support from National Science Centre (NCN), Poland through Project number 2021/42/E/ST5/00262.

References

[1] J. Karpinski *et al.*, Physica C **469**, 370–380 (2009).
[2] M. Azam *et al.*, Materials **16**, 5358 (2023).
[3] S.J. Singh *et al.*, IEEE Trans. Appl. Supercond. **23**, 7300605 (2013).
[4] S.J. Singh *et al.*, Crystals **12**, 20 (2022).
[5] M. Azam *et al.*, Crystals **13**, 1525, (2023).
[6] M. Azam *et al.,* Submitted to journal (under review).

Abstract ID: 1031

COMPARISON OF OPERATING CHARACTERISTICS OF DC CIRCUIT BREAKER ACCORDING TO THE RESPONSE OF SUPERCONDUCTING ELEMENTS IN MMC-HVDC

Dae-Seong Jang, Hyo-Sang Choi

Chosun University, Dept. of Electrical Engineering, Gwang-Ju, SOUTH KOREA
E-mail: jds7142000@naver.com

In order to interrupt fault current generated in the DC system, research on various DC protection technologies is being conducted. Currently, interrupting technologies using semiconductors are in the spotlight, and research on fault current limiting technologies using superconducting elements continues. Resistive-Superconducting Fault Current Limiter (R-SFCL) can reduce fault current by a factor of 3 to 10 within milliseconds due to fast resistance rise when a fault occurs. Additionally, when it is combined with a DC circuit breaker, fast interruption is possible through the fault current limitation. The R-SFCL has a different response speed depending on critical characteristics, which is directly related to the critical current of the R-SFCL and the amplitude of the fault current in a power system. If the critical current is too high, even if a fault occurs, a quench of the R-SFCL may be delayed or not quenched, resulting in a situation in which the fault current is not limited. In this paper, we compared and analyzed the operation characteristics of superconducting DC circuit breakers according to a critical current amplitude of R-SFCL. We modeled a Multi-Terminal High Voltage Direct Current (MTDC) grid and a superconducting DC circuit breaker combined with R-SFCL and DC circuit breaker. We simulated the operating characteristics of a superconducting DC circuit breaker according to the critical current amplitude of the R-SFCL when a short circuit occurred in the middle of a cable within the grid. As a simulation result, interruption times according to the critical current amplitude of the R-SFCL were all the same. However, as a comparison of minimum and maximum values of the critical current, the quenching time of the case of maximum value was about 1 ms later than the case of minimum value. Also, in the case of the maximum value, the amplitude of the fault current flowing through the interrupting module in a superconducting DC circuit breaker increased by about 2.1 times, and the power burden on the interrupting module increased by about 2.3 times than the case of the minimum value.

Abstract ID: 1034

FAULT CURRENT INTERRUPTION IN MTDC SYSTEMS USING SUPERCONDUCTING LC RESONANT DC CIRCUIT BREAKER: RESONANT FREQUENCY

Jihye Kim, Hyosang Choi

Chosun University, Dept. of Electrical Engineering, 61452, Gwangju, REPUBLIC OF KOREA
E-mail: tkdzho06@naver.com

With the increasing demand for renewable energy, there is a growing need for a new system that can integrate it into existing grids. Multi-terminal DC systems have emerged as alternative solutions to address this challenge. However, MTDC systems still face technical challenges [1,2]. In particular, there are concerns about system protection, and a proposed solution to this is the superconducting LC resonant DC circuit breaker. But, there is no standardized design method for this breaker. In the process of selecting the optimal resonant frequency, an arbitrary value is determined until resonance occurs. This paper aims to study the design of the resonant frequency for the superconducting LC resonant DC circuit breaker to be applied in MTDC. The operation characteristics graph of the superconducting LC resonant DC circuit breaker, in cases where resonance fails, is obtained and analyzed in the frequency domain. The design is adjusted to ensure that the analyzed system frequency matches the resonant frequency, thus confirming the occurrence of resonance. The MTDC is modeled in PSCAD/EMTDC, and using the same method, it is verified that the superconducting LC resonant DC circuit breaker reliably interrupts fault currents in just 2.12 ms in the MTDC system.

References

[1] F. LI; L. Zhu; J. Zhou; L. Kou; B. Ren, *Active power control strategy depending on frequency for MMC-HVDC system connected to offshore windfarms*, 22nd International Symposium on High Voltage Engineering, 2022.06

[2] R. Sun; X. Dang; J. Yang, *Application analysis of MMC-HVDC AC tie line transmission in new energy power generation*, Journal of Control Science and Engineering, **vol. 2022**, 2022.09

Abstract ID: 1051

ANALYSIS ON CURRENT LIMITING CHARACTERISTICS OF THREE-PHASE TRANSFORMER TYPE SFCL USING DOUBLE QUENCH DUE TO SINGLE-LINE GROUND FAULT

Shin-Won Lee[1], Tae-Hee Han[2], Seok-Cheol Ko[3], Sung-Hun Lim[4]

[1]*Dept. of Computer Engineering, Jungwon University, KOREA*
[2]*Dept. Semiconductor Engineering, Jungwon University, KOREA*
[3]*Industry University Cooperation Foundation and Regional-Industrial Application Research Institute, Kongju National University, KOREA*
[4]*Dept. of Electrical Engineering, Soongsil University, KOREA*
E-mail: superlsh73@ssu.ac.kr

In this paper, three-phase transformer type superconducting fault current limiter (SFCL) using double quench, which two superconducting moudules were connected in parallel to its three secondary windings, was suggested and its effective fault current limiting operations due to unbalanced three-phase ground faults was analyzed. Similar to three-phase transformer type SFCL with three SCMs, the suggested SFCL with two SCMs could be operated as the peak fault current limiter with the reduced power burden of SCMs. To verify its operation, single-line ground faults at fault angle of 30, 150 and 270 degrees among unbalanced three-phase ground faults were performed. Through analysis on the test results, the power burden of the SCMs and the fault current performance were shown to be effectively accomplished.

Abstract ID: 1052

DC CURRENT LIMITING CHARACTERISTICS OF FLUX-LOCK TYPE SFCL USING TWICE QUENCH

Sung-Hun Lim[1], Seok-Cheol Ko[2], Tae-Hee Han[3]

[1]Department of Electrical Engineering, Soongsil University, Seoul, REPUBLIC OF KOREA
[2]Industry-University Cooperation Foundation, Kongju National University, Chungnam 32586, KOREA
[3]Department of Semiconductor Engineer, Jungwon University, Chungbuk 28024, KOREA
E-mail: superlsh73@ssu.ac.kr & suntrac@kongju.ac.kr & hantaehee@jwu.ac.kr & swlee@jwu.ac.kr

In this paper, the improved DC fault current limiting characteristics of the flux-lock type superconducting fault current limiter (SFCL) using twice quench were investigated. The flux-lock type SFCL using twice quench is composed of two windings connected in series and two superconducting modules (SMs) for twice quench. Each SM is connected in with one coil and in series with another coil.

The flux-lock type SFCLs using twice quench in the DC system are thought to perform the similar fault current limiting operation to AC system. However, since the transient period after the resistance in SM approaches into the constant value, its fault current limiting characteristics in the DC system are expected to be different from one in the AC system as well as its recovery characteristics after the DC fault removes.

To analyze its DC fault current limiting and recovery characteristics, DC short circuit tests were performed and the improved operations of the flux-lock type SFCL using twice quench in DC system were analyzed from the test results.

Abstract ID: 1053

PEAK FAULT CURRENT LIMITING CHARACTERISTICS OF TRIGGER TYPE SFCL USING TWICE QUENCH

Sung-Hun Lim[1], Seok-Cheol Ko[2], Tae-Hee Han[3]

[1]*Department of Electrical Engineering, Soongsil University, Seoul, REPUBLIC OF KOREA*
[2]*Industry-University Cooperation Foundation, Kongju National University, Chungnam 32586, KOREA*
[3]*Department of Semiconductor Engineer, Jungwon University, Chungbuk 28024, KOREA*
E-mail: superlsh73@ssu.ac.kr

The peak fault current limiting characteristics of a trigger-type superconducting fault current limiter (SFCL) using twice quench of two superconducting modules (SCM1, SCM2) were analyzed. The suggested trigger-type SFCL can perform the peak fault current limiting operations by two SCMs and two current limiting resistor (CLR)s through the operational current' setting of the power switch (PS) by the controller. In the case of larger amplitude of the initial fault current, the quench occurrence in SCM2 connected in parallel with one of the separated CLRs after the quench occurrence in SCM1, can make larger fault current more limited. In addition, the power burden of SCM1, which firstly limits larger fault current, can be decreased by the turn-off of PS. Through the analysis on the short-circuit tests, the effective fault current limiting characteristics of the suggested trigger-type SFCL using twice quench of SCMs could be confirmed.

Abstract ID: 1087

50-80 kA CONDUCTORS FOR LARGE HTS FUSION MAGNETS

V. Vysotskiy, E. Zapretilina, V. Zubko, A. Krasilnikov, A. Mednikov, V. Ovsyannikov, I. Rodin, D. Stepanov, V. Sytnikov, S. Fetisov
E-mail: a.mednikov@list.ru

The development of the systems with 14 – 20 T magnetic field seems to be one of the most promising high-temperature superconductor (HTS) application. The high-field magnets are in good demand for science and technology projects, and, in a number of cases, the use of the HTS is the only solution in technical or/and economic terms. The electromagnet systems for advanced fusion projects such as ARC, SPARC, ST160+, FFHRd1 and the Tokamak of Reactor Technology (TRT) being developed in the Russian Federation are among them. The specific feature of such systems is application of a conductor which is able to carry a transport current of several tens of kA. The high-current HTS conductor has a rather complicated design including hundreds of tapes connected in parallel, conductive stabilizer, mechanical structure and channels for coolant circulation.

The paper defines the requirements for the conductors of large electromagnetic systems and considers the final design solutions for the TRT facility. The results of theoretical computation estimates for the performance of the proposed conductors are presented.

The final sections of the paper are devoted to the execution of the experimental program for the study of the TRT conductors including a description of samples and test facility. The results of experimental verification of a current-carrying capability at various magnetic fields and temperatures, as well as the results of AC losses measurements are presented.

Abstract ID: 1215

HIGH-SPEED SUPERCONDUCTING MAGNETIC BEARINGS FOR RING SPINNING: EXPERIMENTAL AND NUMERICAL ANALYSIS

M. Baloochi[1], T. Espenhahn[1], M. Hossain[2], A. Abdkader[2], Chokri Cherif[2], K. Nielsch[1], R. Hühne[1]

[1] *Leibniz Institute for Solid State and Materials Research, Helmholtzstrasse 20, 01069 Dresden, GERMANY*
[2] *Faculty of Mechanical Engineering, Technische Universität Dresden, Institute of Textile Machinery and High Performance Material Technology (ITM), Hohe Strasse 6, 01069 Dresden, GERMANY*
E-mail: armanbaloochi@gmail.com

Superconducting magnetic bearings (SMB) based on a combination of high temperature superconductors and permanent magnets enable the realization of self-stabilized high-speed rotating devices with significant reduced friction. However, external dynamic vibration might couple in the bearing triggering fast oscillations in a resonance case. Such oscillations were observed in an SMB, which was integrated into a ring spinning tester. The ring spinning process is a widely used method in the textile industry for producing yarns from various fiber materials. Conventional ring spinning technologies enable a maximum speed of 25000 rpm due to higher frictional force and heat generation by contact friction of rotating parts, where higher speeds may cause damage or even yarn breakage. Therefore, a SMB consisting of a cooled superconductor in a cryostat and a permanent magnetic (PM) ring were designed to replace the conventional setup, which allows to increase the maximum rotation speed leading to an increase in output and efficiency. For a detailed analysis of the SMB vibration behavior, an array of 5 distance sensors was implemented in the machine to record the PM ring motion in time and space during high speed spinning. This allows not only to study the influence of vibrations on the bearing but also to determine basic SMB properties such as the radial stiffness and the damping ratio for different temperatures and cooling heights. Additionally, a numerical model based on the H-formulation of Maxwell's equations coupled with a motion equation was developed to investigate the effect of cooling height and the temperature of liquid nitrogen on the stability of the bearing. The simulation results will be compared with the experimental data to optimize the SMB itself.

Abstract ID: 1452

PERSISTENT CURRENT SWITCH OF A WHOLE-BODY 1.5 T SUPERCONDUCTING MRI MAGNET

A. Nandawadekar[1,2], M. Singh[1,2], S. Kar[1]

[1]*Inter University Accelerator Centre, 110067, New Delhi, INDIA*
[2]*Delhi Technological University, Department of Electrical Engineering,110042, Shahbad Daultapur, New Delhi, INDIA*
E-mail: ajitnandawadekar@gmail.com

To achieve the stringent requirement of a highly stable magnetic field, the superconducting MRI magnets are operated in the persistent mode through a superconducting switch or persistent current switch (PCS). We have recently developed a PCS for a whole-body 1.5 T superconducting MRI magnet. The PCS is made using a multi-filamentary NbTi conductor embedded in a Cu-30%Ni matrix and having a critical current of >1.1 kA at the 4 T background field. The resistances of the conductor are 2.5 Ω/m and 2.21 Ω/m respectively at 300 K and 15 K. The bifilar technique has been followed for the winding of the PCS to achieve its self-inductance of 5-7 μH which is almost a million times lower than the self-inductance of the main magnet. Several thermo-foil heaters having a resistance of 90 Ω each are placed onto the various layers of the winding pack of the PCS. The wet-winding technique is followed for the PCS using a cryogenic grade epoxy. A 4 K test rig is developed to study the switching behaviour of the PCS along with its test at the operating current of the MRI magnet. A silicon diode temperature sensor is placed inside the PCS to measure the temperature at various operating conditions. The normal resistances of the PCS are measured at various normal temperatures (9-15 K) which are generated by powering its thermo-foil heaters. A smaller amount of current (100-250 mA) is sent through the PCS at its normal condition to estimate the effective resistance by measuring the voltage drop across it. At 15 K, the resistance per unit length is measured to be 1.9 Ω/m which is ~14 % less than the specified resistance at that temperature signifying a non-uniform temperature distribution inside the PCS. The temperature profile of the PCS is studied at various currents (100-500 mA) through its thermo-foil heaters. The PCS exhibited stable operation with 360 mW of power input. The ON-to-OFF and OFF-to-ON switching times are measured to be 20 s and 25 s respectively. The PCS is also tested in a closed-loop operation at the rated current for its suitability in the 1.5 T whole-body MRI magnet application. The PCS showed a 0.17 % energy loss during the normal state. This paper briefly discusses the design and construction of the PCS and its 4 K test rig. This paper also discusses a comparative analysis of the switching behaviour, the thermal behaviour and the corresponding energy losses with the powering of various thermo-foil heaters at various excitation currents to find its suitability and to determine its final operational parameters for the whole-body 1.5 T superconducting MRI magnet.

Abstract ID: 264

COMPRESSION ELIMINATES CHARGE TRAPS BY STABILIZING PEROVSKITE GRAIN BOUNDARY STRUCTURE: AB INITIO ANALYSIS WITH MACHINE LEARNING FORCE FIELD

A.S. Vasenko[1], D. Liu[1], M.R. Samatov[1], O.V. Prezhdo[2,3]

[1] *HSE University, 101000 Moscow, RUSSIA*
[2] *Department of Chemistry, University of Southern California, Los Angeles CA 90089, USA*
[3] *Department of Physics & Astronomy, University of Southern California, Los Angeles CA 90089, USA*
E-mail: avasenko@hse.ru

Grain boundaries (GBs) play an important role in determining optoelectronic properties of perovskites, requiring an atomistic understanding of the underlying mechanisms. [1] Strain engineering is recently employed in perovskite solar cells, providing a novel perspective on exploring the role of perovskite GBs. [2] Here, we theoretically investigate the impact of axial strain on the geometric and electronic properties of a common $CsPbBr_3$ GB. We develop a machine learning force field and perform ab initio calculations to analyze the behavior of GB models with different axial strain on a nanosecond timescale. Our results demonstrate that compressing the GB efficiently suppresses structural fluctuations and eliminates trap states originating from large-scale distortions, see Fig. 1. [3, 4] Moreover, the GB becomes more amorphous under compressive strain, which makes the relationship between electronic structure and axial strain non-monotonic. These results can help clarify conflicts in perovskite GB experiments.

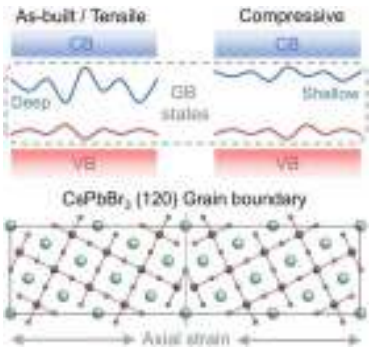

Fig. 1: *Scheme of the impact of axial strain on the electronic structure of $CsPbBr_3$ GB.*

A.S.V. acknowledges support from the Academic Fund Program at HSE University in 2024 (grant №24-00-007 New materials for solar energetics). O.V.P. acknowledges support of the US National Science Foundation, grant CHE-2154367.

References

[1] A.-F. Castro-Méndez, J. Hidalgo, J.-P. Correa-Baena, Adv. Energy Mater. **9**, 1901489 (2019).
[2] J. Wu, Sh.-Ch. Liu, Z. Li, Sh. Wang, D.-J. Xue, Y. Lin, J.-S. Hu, Nat. Sci. Rev. **8**, nwab047 (2021).
[3] D. Liu, Y. Wu, A.S. Vasenko, O.V. Prezhdo, Nanoscale **15**, 285 (2023).
[4] D. Liu, Y. Wu, M.R. Samatov, A.S. Vasenko, E.V. Chulkov, O.V. Prezhdo, submitted to Chem. Mater.

Abstract ID: 1004

HALL EFFECT IN $Sm_xMn_{1-x}S$ SOLID SOLUTIONS

A.M. Kharkov, R.V. Runov, A.V. Gelgorn

Reshetnev Siberian State University of Science and Technology, Krasnoyarsk, RUSSIA
E-mail: khark.anton@mail.ru

Semiconductors form the basis of the electronic component base. Impurity semiconductors are used to manufacture transistors, integrated circuits, lasers and diodes. The article is devoted to the establishment of the type of current carriers at replaced by ions of variable valence [1]. $Sm_xMn_{1-x}S$ compounds were obtained by melt crystallization of obtained powder sulfides. The elementary cell on the basis of X-ray diffraction has a Face-centered cubic lattice type NaCl. Electrical resistance for $Sm_xMn_{1-x}S$ with x = 0.1 was measured by a four-probe method by an Agilent 34410A device at the 80–500 K (Figure 1a). In the magnetically ordered region, a maximum is observed at 102 K. The temperature coefficient of resistance (dR/dT)1/R has several maxima at T = 133 K, 161 K and 253 K. We will find the types of current carriers from Hall measurements in H = 12 kOe with a constant current of 10 μA. Figure 1b shows the Hall constant for $Sm_xMn_{1-x}S$ on temperature. The positive sign R_H indicates that the current carriers are holes in the 80–400 K. The sign of the current carriers has not changed when manganese is substituted by samarium ions.

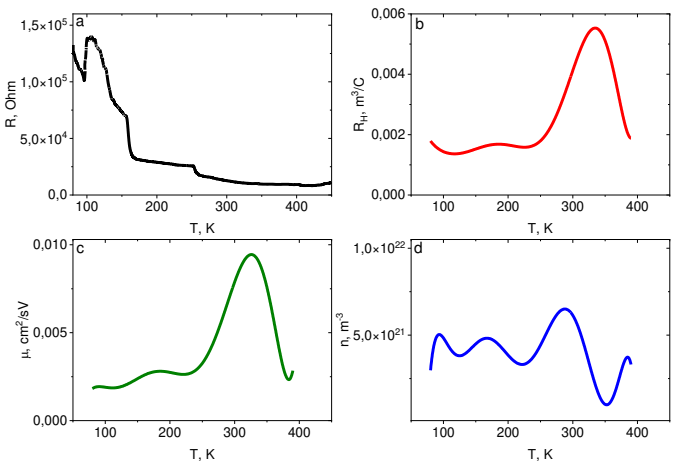

Fig. 1: *(a) – The electrical resistance, (b) – Hall constant, (c) – mobility and (d) – hole concentration in $Sm_{0.1}Mn_{0.9}S$ versus temperature.*

The maximum mobility (Figure 1c) at 180 K and 326 K may be caused by scattering on impurity centers. The hole concentration (Figure 1d) found from $R_H = 1/en$ has small maxima at T = 95 K and 165 K. At these temperatures, spin and lattice polarons are delocalized, that leads to the growth of holes at the Fermi level. Varying the concentration of holes and electrons, different physical properties can be obtained. The type of carriers can be changed by shifting the chemical potential, both in temperature and concentration, under the influence of external factors [2].

References

[1] M.N. Sitnikov, A.M. Kharkov, S.S. Aplesnin, J. Phys.: Conf. Ser. 2573, 012031 (2023).
[2] S.S. Aplesnin, O.B. Romanova, A.M. Kharkov, *et. al.*, Phys. Stat. Sol. B **249**, 812 (2012).

Abstract ID: 1288

GIANT X-RAY CIRCULAR DICHROISM IN A TIME-REVERSAL INVARIANT ANTIFERROMAGNET

Jun Okamoto[1], Ru-Pan Wang[2], Yen-Yi Chu[1], Hung-Wei Shiu[1], Amol Singh[1], Hsiao-Yu Huang[1], Chung-Yu Mou[3], Sucitto The[4], Horng-Tay Jeng[4], Kai Du[5], Xianghan Xu[5], Sang-Wook Cheong[5], Chao-Hung Du[6], Chien-Te Chen[1], Atsushi Fujimori[3,1,7], Di-Jing Huang[1,4]

[1]*National Synchrotron Radiation Research Center, Hsinchu 30076, TAIWAN*
[2]*Department of Physics, University of Hamburg, Luruper Chaussee 149, G610, 22761 Hamburg, GERMANY*
[3]*Center for Quantum Science and Technology and Department of Physics, National Tsing Hua University, Hsinchu 30013, TAIWAN*
[4]*Department of Physics, National Tsing Hua University, Hsinchu 30013, TAIWAN*
[5]*Rutgers Center for Emergent Materials and Department of Physics and Astronomy, Rutgers University,Piscataway, NJ 08854, USA*
[6]*Department of Physics, Tamkang University, Tamsui 251, TAIWAN*
[7]*Department of Physics, University of Tokyo, Bunkyo-Ku, Tokyo 113-0033, JAPAN*
E-mail: djhuang@nsrrc.org.tw

X-ray circular dichroism, arising from the contrast in X-ray absorption between opposite photon helicities, serves as a spectroscopic tool to measure the magnetization of ferromagnetic materials and identify the handedness of chiral crystals. Antiferromagnets with crystallographic chirality typically lack X-ray magnetic circular dichroism because of time-reversal symmetry, yet exhibit weak X-ray natural circular dichroism. Here, we report the observation of giant natural circular dichroism in the Ni L_3-edge X-ray absorption of Ni_3TeO_6, a polar and chiral antiferromagnet with effective time-reversal symmetry. To unravel this intriguing phenomenon, we propose a phenomenological model that classifies the movement of photons in a chiral crystal within the same symmetry class as that of a magnetic field. The coupling of X-ray polarization with the induced magnetization yields giant X-ray natural circular dichroism, reflecting the magnetic susceptibility of Ni_3TeO_6. Our findings provide evidence for the interplay between magnetism and crystal chirality in natural optical activity. Additionally, we establish the first example of a new class of magnetic materials exhibiting circular dichroism with time-reversal symmetry.

Abstract ID: 1658

ENHANCING MAGNETIC SENSING CAPABILITIES BEYOND CONVENTIONAL METHODS

M. Soğan[1,3], M. Dilara Pütkül[2,3], A. Gokce Ozbay[3], A. Ozbay[4] , H. Tatlıpınar[5]

[1] *Yıldız Technical University, Dept. of Physics, 34210, Istanbul, TÜRKIYE*
[2] *Istanbul Technical University, Dept. of Physics Engineering, 34469, Istanbul, TÜRKIYE*
[3] *TUBITAK National Metrology Institute, UME, 41470, Gebze, Kocaeli, TÜRKIYE*
[4] *Istinye University,Dept.of Electrical and Electronic Engineering , 34045, Istanbul, TÜRKIYE*
[5] *Yıldız Technical University, Dept. of Physics, 34210, Istanbul, TÜRKIYE*
E-mail: msogan373@gmail.com

Recent advances in Quantum Technologies sparked enhanced measurement characterization techniques at the nano-scale. Nano-engineered devices play a vital role in quantum sensing. Even though novel examples such as vacancy engineered Nitrogen rich diamond magnetometers emerge, multi-layered magnetic nano-devices displaying the Giant Magneto Resistance (GMR) Effect, Tunneling Magneto Resistance (TMR), and Anisotropic Magneto Resistance (AMR) are well established and remain relevant. They have taken their place in the sensing industry as magnetic recording and reading heads, bio-sensing applications.

In this work, we study magnetic fluctuations in AMR and GMR devices by taking advantage of magnetoresistive coupling of magnetization and resistance fluctuations. We aim to develop a unique characterization tool to understand the magnetic properties of such systems: Magnetic Noise Spectroscopy. The $1/f$ noise, where noise power is inversely scaled with frequency, can be seen in a wide variety of systems. It has been used, for example, to distinguish different types of transport mechanisms in tunnel junction devices [1]. In this study, $1/f$ noise that is magnetic in origin will be studied in AMR and GMR devices [2]. We propose that by studying the dependence of the magnetic $1/f$ noise on temperature and magnetic fields, noise spectroscopy can be used as a tool to image the magnetic energy landscape giving rise to the device characteristics. We utilize the Preisach Model of hysteresis to model magnetic fluctuations showing a $1/f$ power spectrum [3]. Both hysteresis and $1/f$ phenomena originate from two-level systems (TLSs) with characteristic activation energies. Once the energy landscape is obtained, the system response to stimuli can be predicted. Understanding such systems is also crucial in optimizing the signal-to-noise ratios. Consequently, noise imposes a limit on device performances. For instance, ultra-high sensitivities are required in applications like magnetic sensors for the magnetic recording industry or biological applications such as virus detection (where detecting a few nanoparticles is crucial). Therefore, if the origin and nature of magnetic noise can be understood, the impact of noise can be mitigated to enhance device performances.

References

[1] A. Gokce, E.R. Nowak, S.H. Yang, S.S.P. Parkin, J. Appl. Phys., **99**, **8**, 08A906 (2006).
[2] A. Ozbay, A. Gokce, T. Flanagan, R.A. Stearrett, E.R. Nowak, C. Nordman, Appl. Phys. Letters **94**, 202506 (2009).
[3] F. Preisach, Z. Phys. **94**, 277 (1935).

Abstract ID: 1387

ULTRAHIGH CURIE TEMPERATURE IN $Co_2Fe_{1+x}Ge_{1-x}$ HEUSLER ALLOYS VIA POWDER METALLURGY

Yifeng Zhang[1], Chang Xue[1],Zhenjie Feng[1,2], Jincang Zhang[1,2]

[1]*Materials Genome Institute, Shanghai University, Shanghai, 200444, CHINA*
[2]*Zhejiang Laboratory, Hangzhou, 311100, CHINA*
Email: jczhang@shu.edu.cn

This study comprehensively investigates the synthesis and characterization of $Co_2Fe_{1+x}Ge_{1-x}$ Heusler alloys, which were prepared through powder metallurgy techniques. These alloys are remarkable for their highest Curie temperature among known Heusler compounds. The research meticulously explores the synthesis process of $Co_2Fe_{1+x}Ge_{1-x}$ alloy powders through ball milling followed by annealing treatments. The investigation delves into various aspects of these materials, including their crystallographic structure, particle size distribution, flaky particle morphology, and soft magnetic performance characteristics. Notably, the as-milled alloy powder exhibits an exceptional Curie temperature of up to 1212 K and a noteworthy saturation magnetization of 155.07 emu/g. The Heusler alloy structured materials not only exhibit excellent corrosion resistance and stability, but also have great potential for a wide range of industries where robustness and reliability are essential concerns. Thus, this study highlights the significant potential of $Co_2Fe_{1+x}Ge_{1-x}$ Heusler alloys as a versatile and high-performance material option for demanding high-temperature environments.

Abstract ID: 1388

ULTRAHIGH CURIE TEMPERATURE IN $Co_2Fe_{1+x}Ge_{1-x}$ HEUSLER ALLOYS VIA POWDER METALLURGY

Yifeng Zhang[1], Chang Xue[1],Zhenjie Feng[1,2], Jincang Zhang[1,2]

[1]*Materials Genome Institute, Shanghai University, Shanghai, 200444, CHINA*
[2]*Zhejiang Laboratory, Hangzhou, 311100, CHINA*
Email: jczhang@shu.edu.cn

This study comprehensively investigates the synthesis and characterization of $Co_2Fe_{1+x}Ge_{1-x}$ Heusler alloys, which were prepared through powder metallurgy techniques. These alloys are remarkable for their highest Curie temperature among known Heusler compounds. The research meticulously explores the synthesis process of $Co_2Fe_{1+x}Ge_{1-x}$ alloy powders through ball milling followed by annealing treatments. The investigation delves into various aspects of these materials, including their crystallographic structure, particle size distribution, flaky particle morphology, and soft magnetic performance characteristics. Notably, the as-milled alloy powder exhibits an exceptional Curie temperature of up to 1212 K and a noteworthy saturation magnetization of 155.07 emu/g. The Heusler alloy structured materials not only exhibit excellent corrosion resistance and stability, but also have great potential for a wide range of industries where robustness and reliability are essential concerns. Thus, this study highlights the significant potential of $Co_2Fe_{1+x}Ge_{1-x}$ Heusler alloys as a versatile and high-performance material option for demanding high-temperature environments.

Abstract ID: 1581

STABILITY OF THE MAGNETOCALORIC EFFECT IN La-Fe-Si ALLOYS UNDER LONG-TERM EXPOSURE TO THE CYCLIC MAGNETIC FIELDS

N.Z. Abdulkadirova[1], A.G. Gamzatov[1], A.M. Aliev[1], J. Wang[2], Fengxia Hu[2]

[1] *Amirkhanov Institute of Physics of Dagestan Federal Research Centre, Russian Academy of Sciences, Makhachkala, 367003, RUSSIA*
[2] *Institute of physics, Chinese Academy of Sciences, Beijing 100190, P. R. CHINA*
E-mail: nnurizhat@mail.ru & fxhu@iphy.ac.cn

The few available data on the influence of the frequency of the cyclic magnetic field (CMF) on the magnetocaloric effect (MCE) value show the complex nature of the MCE vs. CMF. The observed strong frequency dependence of the MCE for first order phase transition materials can be explained by the presence of hysteresis and the kinetics of the phase transition, while the frequency dependence of the MCE near the second order phase transitions does not lend itself to such an unambiguous interpretation and requires further research.

This paper presents the results of study of the influence of the frequency of the CMF on the value and stability of the MCE in La-Fe-Si alloys, both with a first- and second-order phase transitions. The influence of long-term exposure to CMF of 0.62 and 1.2 T on the stability of the MCE value at various frequencies (up to 30 Hz) was also studied. It is shown that samples with a first-order phase transition ($La_{1-x}Pr_xFe_{13.7}Si_{1.3}$-$H_\delta$) show a strong decrease in the MCE value with increasing frequency of the CMF. As well, these samples are characterized by degradation of the value of the effect upon long-term exposure to CMF. Whereas for second-order phase transition samples ($LaFe_{11.2-x}Co_{0.7}Mn_xSi_{1.1}$) we observe a slight decrease in the MCE with increasing frequency of the CMF and the stability of the effect under a long-term exposure of the 10^5 magnetic field on/off cycles.

This work was supported by RSF № 24-43-00156.

Abstract ID: 1319

CRITICAL ROLE OF THE MAGNETOCRYSTALLINE ANISOTROPY ON THE FREQUENCY-DEPENDENT HYPERTHERMIA PERFORMANCE OF MAGNETITE NANOPARTICLES

D. Failde[1], V. Ocampo[2], D. Serantes[2], Ò. Iglesias[3]

[1]*Centro de Supercomputación de Galicia (CESGA), Santiago de Compostela, SPAIN*
[2]*Applied Physics Dept.and Instituto de Materiais (iMATUS), Univ. de Santiago de Compostela, 15782 Santiago de Compostela, SPAIN*
[3]*Dpt. de Física de la Matèria Condensada and IN2UB, Univ. de Barcelona, Martí i Franquès 1, 08028 Barcelona, SPAIN*
E-Mail: oscariglesias@ub.edu

The role of the magnetocrystalline anisotropy is usually not properly considered when studying the heat release of magnetic nanoparticles (NPs) under AC magnetic fields, building the interpretation of the results upon the assumption that an *effective* uniaxial anisotropy can be a correct description. However, magnetite NPs, which are used in multiple biomedical applications, are characterized by a negative cubic magnetocrystalline anisotropy constant $K_C<0$. Recent works [1,2] have evidenced that the contribution of this kind of anisotropy is non-negligible. With this motivation, we have carried out a theoretical study using simulations based on the LLG equation, computing hysteresis loops to extract the Specific Absorption Rate (SAR) of magnetite NPs. The role of K_C on the SAR of NPs with different aspects ratios (an, therefore, different shape uniaxial anisotropy constants K_U) and sizes has been studied as a function of the frequency f and amplitude of the applied field H_{max}. The results show a complex scenario, with an essentially linear dependence of the SAR on f for the large NPs (cubic with 22 nm side) when H_{max} is large enough to ensure major loop conditions. Significant deviation from the f-independent Stoner-Wohlfarth like behavior (f-independent) are obtained in the entire 0.1-1.0 MHz range, which become more marked the smaller the K_U contribution. Strikingly, when studying the H_{max}/f conditions satisfying either the Brezovich or the Thiesen-Jordan criteria, the magnetocrystalline contribution is shown to play a key role in reaching significant heating, as shown in Fig. 1.

Work supported by Spanish MINECO (PID2019-109514RJ-I00, PID2021-127397NB-I00), Catalan DURSI (2021SGR0032). We thank CESGA for computing support.

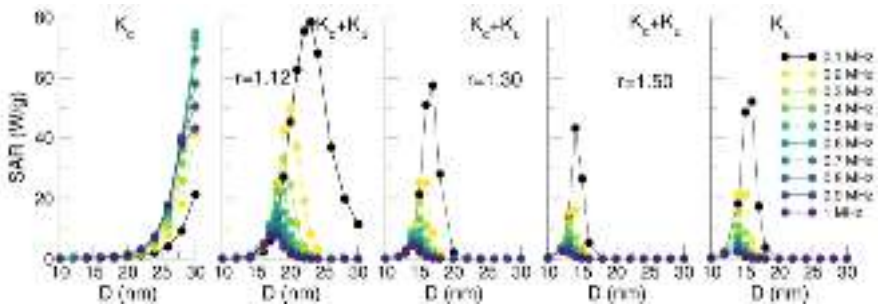

Fig. 1: *SAR vs. f, for H_{max}-f conditions satisfying the Brezovich criteria. Results shown for: only cubic, only uniaxial anisotropy and combined anisotropies for NPs of different aspect ratios r.*

References

[1] H. Gavilán *et al.*, Nanoscale **13**, 15631 (2021).
[2] N.A. Usov *et al.*, Beilstein J. Nanotechnol. **10**, 305 (2019). E.M. Gubanova *et al.*, *ibid.* **12**, 1404 (2021).

Abstract ID: 1602

EFFECT OF MILLING TIME ON THE MOSSBAUER SPECTRA OF $Ni_{50.52}Mn_{9.03}Fe_{11.93}Ga_{28.52}$ AND $Ni_{52.27}Mn_{11.66}Fe_{13.25}Ga_{22.83}$ ALLOYS

H.S. Yilmaz[1], S. Delice[2], H. Güngüneş[2]

[1] *Graduate Student, Graduate Education Institute, Hitit University, 19040 Çorum, TURKEY*
[2] *Department of Physics, Hitit University, 19040 Çorum, TURKEY*
E-mail: hgungunes@gmail.com

In this study, $Ni_{55}Mn_{14}Fe_{12}Ga_{19}$ (S1) and $Ni_{55}Mn_{12}Fe_{14}Ga_{19}$ (S2) alloys, which were used especially as magnetic sensors, were produced by melting the mixture of powders of constituent elements at appropriate proportions in an arc melting furnace. The resulting materials were placed in a vacuumed silica glass tube and subjected to heat treatment for 12 hours at 950 °C in a high temperature furnace to ensure the homogeneity of the alloys. The samples from the produces alloys were prepared and analyzed using scanning electron microscopy (SEM) and energy dispersive X-ray spectroscopy (EDX) measurements. Elemental analyses indicated that the relative ratio of atomic compositions of Ni:Mn:Fe:Ga as 50.52:9.03:11.93:28.52 and 52.27:11.66:13.25:22.83 for S1 and S2, respectively. The bulk samples of the alloys were milled for 20, 50 and 100 ours with the intent of having their nanoparticles using a ball milling. SEM micrographs showed that the size of the resulted particles reduced with increased milling time. The bulk and milled powders were investigated using Mossbauer spectroscopy measurements. Fig. 1 shows the Mossbauer spectra of the bulk and milled samples of the S1.

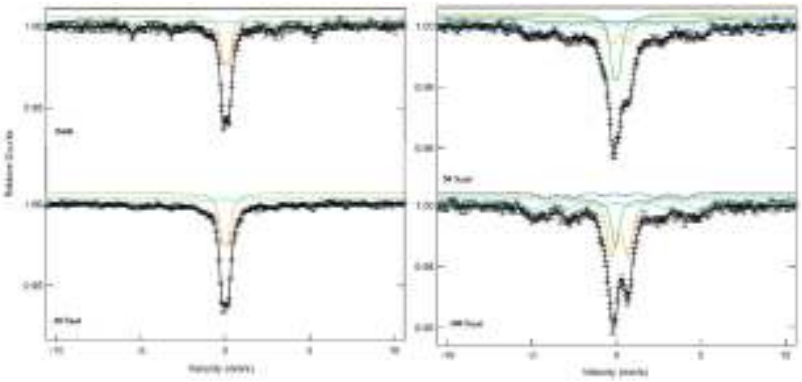

Fig. 1: *Mossbauer spectra of bulk and milled samples of $Ni_{52.27}Mn_{11.66}Fe_{13.25}Ga_{22.83}$ alloy.*

Acknowledgement

The authors are grateful to Scientific Research Project Coordinatorship of Hitit University which supports our study under the Grant No: FEF19404.23.005.

Abstract ID: 1351

PREPARATION OF POLYMER-COATED MAGNETIC NANOPARTICLES AS TARGETED DRUG DELIVERY SYSTEMS

O. Gok[1,2], S.N. Ozkan[2] E. Ozkul[1], M.N. Atilmis[1], P.S. Unlu[1]

[1]*Acibadem University, Faculty of Engineering and Natural Sciences, Dept. of Biomedical Engineering, 34752, Istanbul, TURKEY*
[1]*Acibadem University, Graduate School of Natural and Applied Sciences, Biomedical Engineering Program, 34752, Istanbul, TURKEY*
E-mail: ozgul.gok@acibadem.edu.tr

DDS is an expression or device that facilitates the entry of a therapeutic agent into the body and improves efficacy and safety by controlling the rate, time and place of release of drugs in the body [1]. The goal of any drug delivery system is to deliver and maintain therapeutic drug concentrations in the targeted region. Among the nano-sized nanocarriers, iron oxide nanoparticles (Fe-NPs) are used as MR contrast agents due to their superparamagnetic properties. They are known for their low toxicity and biocompatibility, together with large surface-to-volume ratio and need high surface energies [2]. In order for the nanoparticles to penetrate well into the tissue and increase their solubility in water, their surfaces can be coated with PEG. Polyethylene glycol (PEG) is covalently bound to proteins. It is a water-soluble polymer that changes its properties to increase its potential uses [3].

In this study, Fe-NPs were coated with two different natural polymers, namely alginate and chitosan, with a concentration of 0.5% w/v in distilled water and 2% acetic asit solution, respectively. Their PEGylated versions (Mwt of PEG: 2kDa) were also prepared via amidation reaction and used in the coating step, as well. Quercetin, a very well-known anti-inflammatory drug molecule, was successfully encapsulated in this physical process upon Fe-NPs. Especially for the treatment of long-term circulation (desired for PCOS) and permeability/penetration into tissue (desired for breast cancer), the surface of these nanoparticles was decorated by folic acid molecule via EDCI/NHS chemistry, which has a selective and specific affinity to folate receptors on damaged breast and ovarian tissues. The prepared nanoparticles were characterized for their size by DLS, chemical composition by FT-IR Spectroscopy, morphology by SEM and TEM, and the drug release behavior from these nanoparticles concerning time were conducted by dialysis method and the collected samples were analyzed in LC-MS/MS instrument [4]. The size of nanoparticles was switched from 33nm to a range of 90-150 nm. Also, a positive surface charge (+13 mV) indicates the successful coating of chitosan polymer on Fe-NPs. Their drug encapsulation efficiencies were calculated as above 95%. The magnetic field responsiveness of nanoparticles has been under investigation.

References

[1] S.A. Rizvi, A.M. Saleh, *Applications of nanoparticle systems in drug delivery technology*, Saudi pharmaceutical journal, **26(1)**, 64-70 (2018).

[2] B. Issa, I.M. Obaidat, *Magnetic nanoparticles as MRI contrast agents*, Magn. Reson. Imaging, **378**, 40 (2019).

[3] J.M. Harris, N.E. Martin, M. Modi, *Pegylation: A novel process for modifying pharmacokinetics*, Clinical pharmacokinetics, **40(7)**, 539-551 (2001).

[4] R. Arcot, M. Lundahl, O.J. Rojas, J. Laine, *Asymmetric cellulose nanocrystals: thiolation of reducing end groups via NHS–EDC coupling*, Cellulose, **21(6)**, 4209-4218 (2014).

Abstract ID: 249

EVALUATION OF SUPERCONDUCTING PHASE TRANSITIONS IN MgB_2/Fe WIRES PRODUCED THROUGH DIFFERENT METHODS

Naki Kaya

Kafkas University, Kağızman Vocational School, Department of Medical Service Optician Program, Kars, TURKEY
E-mail: nakikaya06@gmail.com

In today's world, where technological advancements progress in parallel with the goal of making life easier, one of the significant obstacles in the forefront of technological developments is the energy losses during the transfer phase. The energy generated for the continuity of the system can decrease due to various factors. Although efforts have been ongoing for a long time to overcome these losses, it is still challenging to claim complete success. At this point, superconductors, where losses are nearly reduced to zero, come into play. The fact that existing superconductors can transition to the superconducting phase under conditions such as temperature and magnetic field that need to be optimal also brings along a series of challenges in terms of practical usage. Therefore, the rapid transition of the structure to the superconducting phase is desired. In this study, a standard MgB_2/Fe wire was produced within an iron sheath using the in-situ method. Additionally, a carbon-doped MgB_2/Fe wire within an iron sheath was produced using the in-situ method with carbon-doped boron through the chemical vapor deposition (*CVD*) method. The wires obtained were characterized through *R-T* (resistance-temperature) and *M-T* (magnetization-temperature) measurements to investigate which structure transitions to the superconducting phase more rapidly. As a result of the measurements, it was found that the carbon-doped MgB_2/Fe wire within an iron sheath, produced using the in-situ method with carbon-doped boron through the *CVD* method, transitions to the superconducting phase more rapidly due to the carbon content in its composition. Additionally, it was observed that the critical temperature (T_c) value is closer to room temperature.

Abstract ID: 1521

EXAMINING THE EFFECT OF CARBON NANOTUBE ON THE DIELECTRIC PROPERTIES OF MgB_2 SUPERCONDUCTOR

P. Oruç[1], A. Seçkin[1,2], N. Kaya[3], S. Cavdar[1], H. Koralay[1]

[1]Gazi University, Faculty of Science, Department of Physics, 06300, Ankara, TURKIYE
[2]Gazi University, GUTMAM, 06300, Ankara, TURKIYE
[3]Kafkas University, Kağızman Vocatinal School, 36700, Kars, TURKIYE
E-mail: hkoralay@gmail.com

In this study, MgB_2 samples were produced using the solid-state reaction method by mixing Mg (Sigma-Aldrich, powder, ≥99%) and B (Sigma-Aldrich, amorphous powder, ≥95%) powders at specific mass ratios. MgB_2 samples in tablet form were prepared with 0%, 1%, 2%, 3%, and 4% multi-walled carbon nanotube (MWCNT) (Sigma-Aldrich, >98% carbon basis, O.D × L 6-13 nm × 2.5-20 µm) additions. The powders subjected to the necessary experimental processes were weighed to 1 g each and compressed into tablet form using a cold pressing method with a pressure of 4 ton/cm^2. The samples were sintered in a closed argon environment at 750°C for 1 hour. The dielectric properties of the obtained samples were examined. Dielectric measurements at room temperature and different bias voltages were performed using the LCR Meter ST 2826 device to measure the frequency-dependent dielectric capacities. The connection equipment called the Kelvin probe of the LCR meter was used, and samples were placed between electrodes in the form of smooth copper tablets with a diameter of 13 mm and a thickness of 1 mm. Oscillation signal with 50 mVrms was applied, and capacitance measurements as a function of frequency were made through the LCR. According to the obtained results, it was observed that the addition of MWCNT reduced the capacitive effect on MgB2 and increased its conductivity properties from a dielectric standpoint.

Abstract ID: 1522

MICROHARDNESS ANALYSIS OF MgB_2 PRODUCED WITH CARBON-ENCAPSULATED BORON

P. Oruç[1], A. Seçkin[1,2], S. Cavdar[1], H. Koralay[1]

[1]Gazi University, Faculty of Science, Department of Physics, 06300, Ankara, TURKIYE
[2]Gazi University, GUTMAM, 06300, Ankara, TURKIYE
E-mail: oruc.pnr@gmail.com

In this study, both chemical vapor deposition and the solid-state reaction method were employed. In the chemical vapor deposition method, ethylene was used as the hydrocarbon source for the carbon encapsulation of amorphous boron powders. The conditions were set as follows: a temperature of 700°C, amorphous boron powders with a purity of 95-97% and particle size <1µm, helium and hydrogen gases as carrier gases, a carrier gas flow rate of 100 ml/min, an ethylene flow rate of 20 ml/min, and a total experiment duration of 90 minutes. For 90 minutes, the carbon-encapsulated amorphous boron powders were mixed with magnesium powders at specific mass ratios and transformed into tablets under a pressure of 5 ton/cm2. The tabletized samples were wrapped in zirconium foils to protect against possible contaminations and sintered in a closed argon atmosphere at 900°C for 1 hour. The microhardness analyses of the obtained samples were conducted using the Vickers method. The saturation point value against the applied load was found to be 2N for all samples, and the hardness number (n_k value) was greater than 2. The WPSR, WHK, and de values were consistently negative for all samples. Plastic deformation was observed in all samples, while no elastic deformation was encountered. Additionally, ISE behavior was observed in the samples.

Abstract ID: 1532

CRYSTAL SIZE ANALYSIS OF MgB_2 SUPERCONDUCTOR PRODUCED UTILIZING CARBON- ACCUMULATED BORON

A. Seckin[1,2], P. Oruç[2], S. Cavdar[2], H. Koralay[2]

[1] *Gazi University Basic and Engineering Sciences Central Laboratory Application and Research Center (GUTMAM), 06300, Ankara, TÜRKIYE*
[2] *Gazi University, Faculty of Science, Department of Physics, 06300, Ankara, TÜRKIYE*
E-mail: aaytenarslan@gmail.com

This investigation delves into synthesizing MgB_2 superconductor by employing carbon-accumulated boron through the Chemical Vapor Deposition (CVD) method at 800°C for 60 minutes, utilizing ethylene hydrocarbon sources. The obtained powders after accumulation were subjected to elemental analysis to verify the percentage of carbon accumulation. The elemental analysis revealed a carbon accumulation rate of 14.57% within the structure. Subsequently, the carbon-accumulated amorphous boron powders were mixed with magnesium powders at a predetermined stoichiometric ratio. Tabletized samples were wrapped in tantalum foils and sintered in a closed argon atmosphere at 700°C for 60 minutes. For the purpose of comparison, the production of MgB_2 without additives was also performed as the base material.

The obtained samples underwent crystallographic analysis using the XRD method, and crystal size calculations were performed using the Scherrer equation. XRD analyses were conducted in the range of $2\theta=20°$ to 80° using a D8 Advanced model XRD device. The measurement results revealed characteristic peaks of MgB_2, including (0 0 1), (1 0 1), (0 0 2), (1 0 2), (2 0 1), and (1 1 2). Shifts were observed in all obtained peaks compared to the base material. Additionally, in the calculations performed with the Scherrer Equation, the crystal size of the base material was found to be 13 nm, while the crystal size of the carbon-accumulated sample was determined to be 18 nm. The analyses indicated that the sample produced using carbon-accumulated boron through the CVD method had a larger crystal size compared to the base material, longer interplanar distances, and angular shifts in all characteristic peaks.

Abstract ID: 1563

SUPEREXCHANGE-COUPLING DRIVEN MAGNETOSTRICTION IN VAN DER WAALS MOLECULAR SOLIDS

Dong-Yang Li, Yuan-Qi Zhai, Yan-Zhen Zheng

Frontier Institute of Science and Technology (FIST), Xi'an Jiaotong University, Xi'an 710054, Shaanxi, CHINA
E-mail: lidongyang@stu.xjtu.edu.cn

Magnetostriction (MS), a process transforming electromagnetic energy into mechanical energy, is commonly linked to domain wall movements in ordered magnets or quadrupole moments in single ions within paramagnets. This phenomenon, which causes magnetic materials to change shape or size during magnetization, finds application in micro-displacement control, precision machinery, and advanced robotics. Initially documented by Joule in 1847, who noted a 21 parts per million (ppm) volume change in iron under a 0.1 Tesla magnetic field, MS involves the translation and/or rotation of magnetic domains in metals, leading to material elongation or contraction. Although superexchange-coupling (EX) interaction in symmetric materials was hypothesized to induce MS, empirical confirmation has been challenging due to demanding conditions. Our study marks the first experimental validation of EX-induced MS in a molecular solid with the highest cubic symmetry (space group *Pn*-3*n*). This material comprises circular $\{Fe_8Gd_8\}$ molecules, connected solely by van der Waals forces. Remarkably, the $\{Fe_8Gd_8\}$ molecular solid displays MS effects starting at 50 K, reaching a peak of 25 ppm at 2 K in a 7-tesla magnetic field. Through extensive analysis using sophisticated magnetometry, high-field/frequency electron paramagnetic resonance, and Ab initio calculations, we ascertained that the EX interaction between iron(III) and gadolinium(III) ions is the primary cause of the observed MS effect, overruling single-ion quadrupole moments. This pivotal discovery not only verifies a new MS mechanism but also opens avenues for designing innovative MS materials based on molecular structures.

References

[1] G. Engdahl, *Handbook of Giant Magnetostrictive Materials* (Academic Press, San Diego, CA, 2000).
[2] B. Bernáth, K. Kutko, S. Wiedmann, O. Young, H. Engelkamp, P.C. Christianen, S. Poperezhai, L.V. Pourovskii, S. Khmelevskyi, D. Kamenskyi, Adv. Electron. Mater. **8**, 2100770 (2022).
[3] M. Doerr, M. Rotter, A. Lindbaum, *Magnetostriction in rare-earth based antiferromagnets*, Advances in Physics, **54**, 1-66 (2005).
[4] A. Behera, *Advanced Materials: An Introduction to Modern Materials Science* (Springer, Cham, Switzerland, 2022).
[5] J.P. Joule, The London, Edinburgh, and Dublin Philosophical Magazine and Journal of Science **30**, 76 (1847).
[6] E.W. Lee, Reports on Progress in Physics **18**, 184 (1955).
[7] L. Qin, J. Singleton, W.P. Chen, H. Nojiri, L. Engelhardt, R.E. Winpenny, Y.Z. Zheng, Angew. Chem. Int. Ed. **129**, 16798 (2017).
[8] H.L. Zhang, Y.Q. Zhai, L. Qin, L. Ungur, H. Nojiri, Y.Z. Zheng, Matter **2**, 1481 (2020).

Abstract ID: 1548

PREPARATION AND CHARACTERIZATION OF DIFFERENT MAGNETIC NANOFERRITES FOR THE TREATMENT OF CONTAMINATED WATER

Mariam Rabaa[1], Amani Aridi[1], Ramadan Awad[2]

[1] *Chemistry Department, Faculty of Science, Beirut Arab University, Beirut, LEBANON*
[2] *Physics Department, Faculty of Science, Alexandria University, Alexandria, EGYPT*
E-mail: Mariam_rabaa@hotmail.com

The increase in environmental pollution, especially water pollution, intensified the requirement for new strategies for the treatment of contaminated water. One promising approach that has been gaining attention in this field is the use of nanoferrites due to their magnetic properties. This work reports the synthesis of $Mg_{0.33}Ni_{0.33}Co_{0.33}Re_xFe_{2-x}O_4$ NPs with Re= Gd^{3+}, La^{3+}, and Sm^{3+} where $0.00 \leq x \leq 0.08$ by the co-precipitation. These samples were characterized by different techniques to explore the effect of the Re^{3+} dopants on the NPs.

The XRD results confirmed the single-phase cubic structure of the NPs with traces of hematite. TEM images revealed spherical-shaped NPs and the average particle size showed a decrease with the increase in Re^{3+} content. The polycrystalline nature of the NPs is verified by the appearance of concentric rings in the SAED images of the samples. The FTIR spectroscopy showed the existence of v_1 and v_2 vibrational bands proving the formation of the spinel ferrite structure. As Re^{3+} content increased, the bandgap energy increased, while the Urbach energy decreased. A sharp PL peak located in the UV region was revealed in NPs, in addition to the presence of oxygen vacancies and other intrinsic imperfections in all samples. The VSM results revealed the existence of a ferromagnetic nature of the NPs, and it is reduced with the dopants. The Re^{3+} dopants have reduced the saturation magnetization of the NPs.

The photocatalytic performance of the prepared NPs is evaluated for the degradation of different dyes under sunlight irradiation. The influence of photocatalyst dosage and pH that exhibit the best photocatalytic performance on the photodegradation reaction was studied. The adsorption performance of the prepared NPs for the removal of Pb (II) and As (III) was tested. Doping $Mg_{0.33}Ni_{0.33}Co_{0.33}Fe_2O_4$ with Re^{3+} ions improved the photocatalytic activity and the adsorption performance of NPs compared with pure.

Abstract ID: 1638

EFFECT OF MILLING TIME ON THE PARTICLE SIZE AND MAGNETIC PROPERTIES OF Fe-25%Ni-5%Si-15%Co AND Fe-28%Ni-5%Si-15%Co ALLOYS

H. Kuyubaşi[1], S. Delice[2], H. Güngüneş[2]

[1] *Graduate Student, Graduate Education Institute, Hitit University, 19040 Çorum, TURKEY*
[2] *Department of Physics, Hitit University, 19040 Çorum, TURKEY*
E-mail: hgungunes@gmail.com

In this study, the effect of milling time on the particle size and magnetic properties of two different Fe-25%Ni-5%Si-15%Co and Fe-28%Ni-5%Si-15%Co alloys in martensite phases by using SEM, VSM and Mössbauer Spectroscopy. The resulting materials were placed in a vacuumed silica glass tube and subjected to heat treatment for 6 hours at 1100 °C in a high temperature furnace to ensure the homogeneity of the alloys. To create a martensite phase in the alloys, the alloys were immersed in liquid nitrogen. The as-cast ingot was crushed to particles less than 0.5 mm in size by using diamond file. Then the alloys were mixer milled at 25 hertz for 25 and 50 h with a ball to power ratio of 10:1 in hexane. The room temperature mössbauer spectra of bulk Fe-28%Ni-5%Si-15%Co alloys in martensite phases composed of five magnetic sextets. SEM micrographs showed that the size of the resulted particles reduced with increased milling time. According to VSM results the saturation magnetization decreased with increase of milling time. Also the paramagnetic phase ratio increased with increase of milling time.

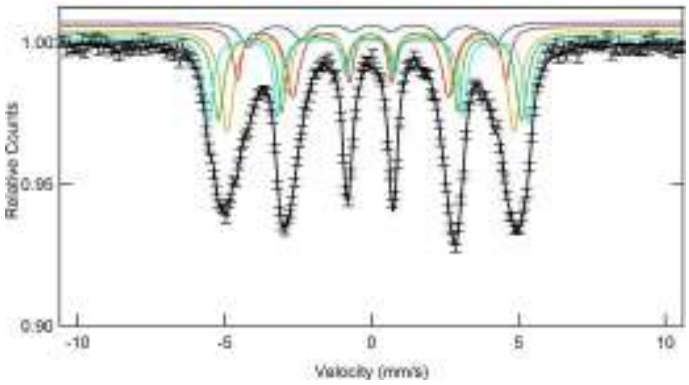

Fig. 1: *Room temperature Mössbauer spectra of Fe-28%Ni-5%Si-15%Co alloys.*

References

[1] H. Hirazawa, S. Kusamoto, H. Aono, T. Naohara, K. Mori, Y. Hattori, T. Maehara, Y. Watanabe, J. Alloys Comp. **46**, 467–473 (2008).
[2] Y. Akin, M. Obaidat, B. Issa, Y. Haik, Cryst. Res. Technol. **44**, 386–390 (2009).
[3] F. Dughiero, S. Corazza, Med. Biol. Eng. Comput. **43**, 40–46 (2005).
[4] Y. Akin, M. Obaidat, B. Issa, Y. Haik, Cryst. Res. Technol. 44, 386–390 (2009).

Abstract ID: 1644

CHARACTERISATION OF A MAGNETIC IRON OXIDE BIOCOMPOSITE FOR WASTEWATER REMEDIATION VIA AN EXTERNAL MAGNETIC FIELD

B. Nasirli[1], İ. Tosun Satir[1,2], Ç. Dönmez Güngüneş[1,3]

[1] *Hitit University, Institute of Graduate Studies, Department of Chemistry, 19030, Çorum, TURKEY*
[2] *Hitit University, Faculty of Arts and Sciences, Department of Chemistry, 19040, Çorum, TURKEY*
[3] *Hitit University, Faculty of Health Sciences, Department of Nutrition and Dietetics, 19200, Çorum, TURKEY*
E-mail: cigdemdz@gmail.com

The purpose of this study was to synthesize a magnetic biocomposite material that can eliminate antibiotics from wastewater by utilizing an external magnetic field. To make this material eco-friendly, magnetic iron oxide nanoparticles were produced using rice husk as a biomaterial. The magnetic biocomposite was examined using FTIR to analyze its composition, and Mössbauer Spectroscopy was used to determine its physical properties. Mössbauer parameters such as hyperfine field (Bhf), quadrupole shift (QS), isomer shift (IS), line width (W), and percent relative area (RA) were determined. According to the Mössbauer study, the Mössbauer spectrum of the magnetic drug carrier consists of 1 doublet and 3 sextets (Figure 1).

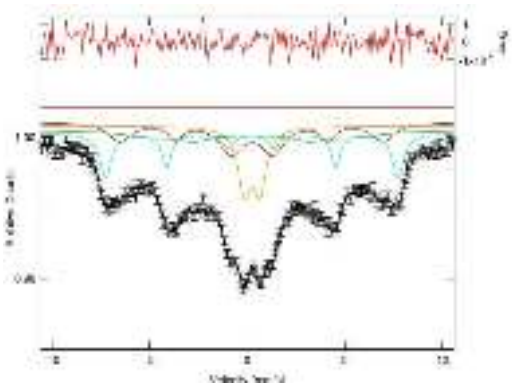

Fig. 1: *Mössbauer spectrum of RH/NFe3O4 magnetic biocomposite.*

References

[1] P. Pillai, N. Kakadiya, Z. Timaniya, S. Dharaskar, M. Sillanpaa, *Removal of arsenic using iron oxide amended with rice husk nanoparticles from aqueous solution*, Materials Today: Proceedings, **28**, 830-835 (2020)..

[2] M. Răcuciu, D.E. Creangă, A. Airinei, *Citric-acid-coated magnetite nanoparticles for biological applications*, The European Physical Journal E, **21**, 117-121 (2006)..

Abstract ID: 1368

SYNTHESIS AND ELECTRON SPIN RESONANCE STUDY OF $Zn_{0.7}Ni_{0.3}(RE)_{0.1}Fe_{1.9}O_4$ (*Re* = Gd, Sm, Dy) NANOSTRUCTURED FERRITES

S.J.C. Masuku[1], J.Z. Msomi[1], S. Mahule[2]

[1]*Walter Sisulu University, Dept. of Chemical and Physical Sciences, P/Bag X01, 5117, Mthatha Eastern Cape, SOUTH AFRICA*
[2]*University of South Africa, Dept. of Physics, 1710, Johannesburg, SOUTH AFRICA*
E-mail: smasuku@wsu.ac.za

$Zn_{0.7}Ni_{0.3}(RE)_{0.1}Fe_{1.9}O_4$ (*Re* = Gd, Sm, Dy) fine powders with particles size between 6 nm and 13 nm were investigated by XRD, TEM, SEM, FTIR, Raman spectroscopy, ESR and magnetization measurements. Structural, vibrational, magnetic and electron spin dynamics are sensitive to particle size and substituted rare earth elements. Broad ESR signals are attributed to dipolar-dipolar interactions and random orientations of magnetic anisotropy axes. FC and ZFC magnetization data reveal the superparamagnetic nature of the as prepared compounds with narrow particle size distribution and T_B = 180 K for pure Zn-Ni, T_B = 171 K and 247 K for Sm- and Dy-substituted Zn-Ni nanosized ferrites, respectively. The evolution of the magnetic parameters as a function of rare earths doping and particle size are also reported.

Abstract ID: 1377

MAGNETIC AND ESR STUDY OF $Cu_xNi_{1-x}Fe_2O_4$ NANOSIZED COMPOUNDS

P.P. Majozi[1], J.Z. Msomi[1], S. Mahule[2]

[1]Walter Sisulu University, Dept. of Chemical and Physical Sciences, P/Bag X01, 5117, Mthatha Eastern Cape, SOUTH AFRICA
[2]University of South Africa, Dept. of Physics, 1710, Johannesburg, SOUTH AFRICA
South Africa
E-mail: jmsomi@wsu.ac.za

$Cu_xNi_{1-x}Fe_2O_4$ nanosized compounds with particle size of about 9 nm were produced by glycol-thermal technique. The as prepared compounds were subjected to annealing from 500 to 1100 ^oC to produce samples with a wide range of particle sizes. TEM and XRD data confirmed particles size of about 45 nm and spherical shapes after annealing at 1100 ^oC. Magnetization and electron spin resonance (ESR) analysis revealed strong dependence of the magnetic properties on particle size. The temperature dependence and zero field magnetization data were indicative of superparamagnetic nature and spin-glass behaviour of the compounds investigated. The evolution of the magnetic properties as a function of particle size and temperature are also reported.

Abstract ID: 1592

TEMPERATURE DEPENDENT STRUCTURAL AND MAGNETIC PROPERTIES OF PERMALLOY ($Ni_{80}Fe_{20}$) NANOTUBES

S. Parajuli[1,2], K. Javed[1,3], M. Irfan[1,4], X. M. Zhang[1], C. Cheng[1], X.F. Han[1,5,6]

[1] *Beijing National Laboratory for Condensed Matter Physics, Institute of Physics, Chinese Academy of Sciences, Beijing 100190, CHINA*
[2] *Nano-Materials Magnetic Materials Research Laboratory, Adana Alparslan Turkes Science and Technology University, Adana, 01250, TURKEY*
[3] *Department of Physics, Forman Christian College (A Chartered University), Lahore 54000, PAKISTAN*
[4] *Institute of Physics, The Islamia University of Bahawalpur, Bahawalpur, 63100, PAKISTAN*
[5] *Centre of Materials Science and Optoelectronics Engineering, University of Chinese Academy of Sciences, Beijing 100049, CHINA*
[6] *SongShan Lake Materials Laboratory, Dongguan, Guangdong 523808, CHINA*
E-mail: sparajuli@atu.edu.tr

One dimensional Permalloy ($Ni_{80}Fe_{20}$) nanotubes (NTs) were successfully fabricated using Anodic Aluminum Oxide (AAO) templates with 100 nm diameter by employing a low-cost electrodeposition route at room temperature. As prepared $Ni_{80}Fe_{20}$ NTs morphology, elemental analysis and structural details have been investigated by using field-emission scanning electron microscopy (FE-SEM), energy dispersive X-ray spectroscopy (EDS) and X-Ray diffraction (XRD) respectively. The structure of prepared Permalloy nanostructures has face centered cubic (FCC) phase with polycrystalline in nature. The $Ni_{80}Fe_{20}$ NTs were annealed at 200°C, 400°C and 600°C. The vibrating sample magnetometer (VSM) showed that all the samples have ferromagnetic nature. Furthermore, VSM has been employed to study the saturation magnetization (M_S), Squareness (SQ) and Coercivity (H_C) as the function of annealing temperature. A comparative study of magnetization reversal mechanism has also been done. The easy axis lies in the direction perpendicular to the NTS axis due to the dominance in shape anisotropy. Annealing temperature improved the magnetic properties of Permalloy (PA) NTs. This work will provide significant applications in the field of spintronics and high-density data storage devices.

Abstract ID: 243

EXCEPTIONALLY SLOW, LONG RANGE, AND NON-GAUSSIAN FLUCTUATIONS ANTICIPATE THE CRITICAL SINGULARITY FAR AWAY FROM THE CHARGE DENSITY WAVE TRANSITION

Sk Kalimuddin,[1] Sudipta Chatterjee,[2] Arnab Bera,[1] Hasan Afzal,[1] Satyabrata Bera,[1] Deep Singha Roy,[1] Soham Das,[1] Tuhin Debnath,[1] Bhavtosh Bansal,[3] Mintu Mondal[1]

[1]*School of Physical Sciences, Indian Association for the Cultivation of Science, Jadavpur, Kolkata 700032, INDIA*
[2]*Department of Condensed Matter and Materials Physics, S. N. Bose National Centre for Basic Sciences, Kolkata 700106, INDIA*
[3]*Indian Institute of Science Education and Research Kolkata, Mohanpur, Nadia, West Bengal 741246, INDIA*
E-mail: intsk@iacs.res.in

$(TaSe_4)_2I$ is a quasi-one-dimensional compound long-known to have a charge-density wave (CDW) transition at around 263 K. We experimentally establish that this transition, unlike what is seen in other CDW compounds such as TaS_2, is a second-order critical transition. Critical fluctuations in the CDW condensate, which couple to the dissipative normal carriers, are slow enough to survive the thermodynamic limit and dominate the low-frequency resistance noise. Around the transition region, we find a rapid increase in their relaxation time, as well as a shift of the spectral weight of fluctuations to lower frequencies. These are direct signatures of the critical slowing down on account of the softening at the hydrodynamic amplitude modes. Critical opalescence on the account of diverging isothermal susceptibility is also seen in the very sharp growth of the variance. The distribution of fluctuations in the transition region is skewed and strongly non-Gaussian. This is on account of the breakdown of the validity of the central limit theorem as the diverging coherence volume becomes comparable to the macroscopic sample size. The temperature window, where the fluctuations manifest as slow and extended hydrodynamic modes is found to be very wide ($\delta\epsilon \approx \pm 0.1$, where ϵ is the reduced critical temperature) but consistent with the Ginzburg criterion.

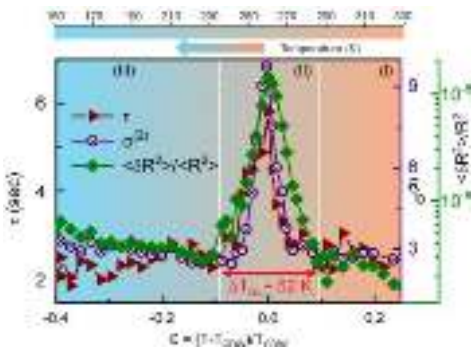

Fig1: ***Fluctuations around the CDW singularity;*** *Variation of the relaxation time τ (wine triangle), the relative variance $\langle\delta R^2\rangle/R^2$ (green rectangular), and the second variance $s^{(2)}$ (violet circle) of the resistance noise with reduced temperature $\epsilon = (T - T_{CDW})/T_{CDW}$, where $T_{CDW} = 263$ K. This combined plot clearly reveals three distinct fluctuation regions, marked (I), (II), and (III) respectively.*

References

[1] Sk. Kalimuddin, S. Chatterjee, A. Bera, H. Afzal, S. Bera, D.S. Roy, S. Das, T. Debnath, B. Bansal, M. Mondal, e-print arXiv:2308.09756v1 (2023).

Abstract ID: 205

MOLECULAR MAGNETISM BASED ON RARE-EARTH DIMER ENCAPSULATED IN FULLERENE CAGES

Matheus Barbosa[1,2], Wei Yang[1,2], Fupin Liu[1], Alexey Popov[1]

[1]*Leibniz Institute for Solid State and Materials Research, 01069, Dresden, GERMANY*
[2]*Technische Universität Dresden, 01069, Dresden, GERMANY*
E-mail: m.f.de.souza.barbosa@ifw-dresden.de

Paramagnetic molecules with energy barriers avoiding rapid spin-reversal are ascribed as Single Molecule Magnets (SMM). When the temperature is sufficiently low, the reduced number of available phonons attenuates the spin relaxation process and then the magnetic moment is considered blocked, exhibiting quantum memory effects. In the last years, molecules formed by rare-earth metals encapsulated in fullerene cages (Endohedral Metallofullerenes) are recognized as good Single Molecule Magnets as they exhibit significantly slow relaxation processes at low temperatures. In special, encapsulated Terbium (Tb) and Dysprosium (Dy) dimers (Dimetallofullerenes) have been demonstrating high potential applicability owing to the strong ferromagnetic coupling of 4f-electrons and trapped valence electron of the bond between them. In the specific case do Dy-Dy dimer inside the fullerene cage C_{80} [called $Dy_2@C_{80}$], due to the energy mismatch between the metal dimer HOMO and the carbon cage LUMO, only $5e^-$ are transferred to fullerene and then each dysprosium assumes the valence $Dy^{2.5+}$. Previous investigation in Lanthanide-based dimetallofullerenes suggest that the delocalization of unpaired electron spin between two Ln atoms glues their magnetic moments together (Ln^{3+} - e^- - Ln^{3+})[1,2] and, therefore, strong ferromagnetic couplings emerge from these interactions. Moreover, the combination of exchange coupling, single-ion anisotropy and collinearity of magnetic moments makes the Dy-based dimetallofullerene a good SMM. Nevertheless, the fullerene cage is a vital component of such class of di-Lanthanide Endohedral Metallofullerene as it protects the metal dimers bonds from the environment. The question however remains how the "container" affects static and dynamics magnetic properties of encapsulated Dy dimers. In this work, we address answering this question by synthesizing a series of Dy-based metallofullerene derivatives with varied structures and studying their SMM behavior. Among the variations we considered the nature of the exohedral group (necessary to stabilize the molecule) and the isomeric structure of the fullerene cage and found that the magnetic behavior is strongly affect by these structural modifications.

References

[1] F. Liu, D. Krylov, L. Spree, *et al.*, Nat. Commun., **8**, 16098, 1-9, (2017).
[2] F. Liu, G. Velkos, D. Krylov, *et al.*, Nat. Commun., **10**, 571, 1-11, (2019).

Abstract ID: 207

TUNING STRATEGY FOR CURIE-TEMPERATURE ENHANCEMENT IN THE VAN DER WAALS MAGNET $Mn_{1+x}Sb_{2-x}Te_4$

M. Sahoo[a,b], M.C. Rahn[b], E. Kochetkova[a,d], A. Tcakaev[e], V.B. Zabolotnyy[e], E. Weschke[h], V. Hinkov[e,c], A. Alfonsov[a], V. Kataev[a], B. Büchner[a,c,b], A.U.B. Wolter[a,c], J.I. Facio[f], L.T. Corredor[a], A. Isaeva[a,d]

[a] *Leibniz IFW Dresden, Helmholtzstraße 20, D-01069, Dresden, GERMANY*
[b] *Institut für Festkörper und Materialphysik, Technische Universität Dresden, 01062, Dresden, GERMANY*
[c] *Van der Waals-Zeeman Institute, Department of Physics and Astronomy, University of Amsterdam, Science Park 094, 1098 XH, Amsterdam, THE NETHERLANDS*
[d] *Universität Würzburg, Physikalisches Institut, Experimentelle Physik IV, Am Hubland, 97074, Würzburg, GERMANY*
[e] *Centro Atomico Bariloche, Instituto de Nanociencia y Nanotecnología (CNEA-CONICET) and Instituto Balseiro, Av. Bustillo 9500, Bariloche, 8400, ARGENTINA*
E-mail: m.sahoo@ifw-dresden.de

The van-der-Waals antiferromagnetic topological insulator $MnBi_2Te_4$ is one of the limited materials exhibiting the desired quantum anomalous Hall (QAH) state and quantized surface charge transport. Following the exploration of $MnBi_2Te_4$, its isostructural counterpart $MnSb_2Te_4$ gained popularity due to its high transition temperature and potential ferromagnetic interlayer interaction among septuple layers. Recent findings suggest that non-stoichiometry in $Mn_{1\pm x}Sb_{2\mp x}Te_4$ serves as an effective means to achieve a net spin-polarized state, surpassing the magnetic ordering temperature of $MnBi_2Te_4$.

Our study presents a comprehensive investigation, combining theory and experiments (bulk and surface magnetism) on two new $Mn_{1+x}Sb_{2-x}Te_4$ samples. Structural probes on both powders and single crystals are employed for a thorough assessment of site mixing. Subsequently, bulk, local (electron spin resonance), and spectroscopic (x-ray magnetic circular dichroism) probes are used to establish connections between structural insights and the magnetism of the materials. Our findings indicate that Mn over-stoichiometry up to x = 1.0, along with a specific Mn/Sb intermixing pattern and an increasingly three-dimensional magnetic order, leads to an increase in T_C. The trend towards more robust ferromagnetism, facilitated by stronger interlayer exchange in $Mn_{1+x}Sb_{2-x}Te_4$ as x increases, is supported by bulk magnetometry and a series of density-functional-theory calculations involving model structures with varying intermixing.

References

[1] M Sahoo *et.al.*, Materials Today Physics **38**, 101265 (2023).

Abstract ID: 1061

MAGNETIC PROPERTIES OF THE DOUBLE PEROVSKITE Ba_2CoNbO_6

D.V. Popov[1], R.G. Batulin[2], M.A. Cherosov[2], I.V. Yatsyk[1], T.I. Chupakhina[3], Yu.A. Deeva[3], R.M. Eremina[1]

[1]*Zavoisky Physical-Technical Institute, Federal Research Center, "Kazan Scientific Center of RAS", 420029 Kazan, RUSSIA*
[2]*Kazan (Volga Region) Federal University, 420008 Kazan, RUSSIA*
[3]*Institute of Solid State Chemistry of the Russian Academy of Sciences (UB), Yekaterinburg, 620990, RUSSIA*
E-mail: reremina@yandex.ru

Double perovskite Ba_2CoNbO_6 was obtained using a new method of pyrolysis of nitrate-organic mixtures of the corresponding components and was studied by XRF, magnetization, and EPR methods. The oxygen content was obtained from X-ray fluorescence analysis and magnetization data. The magnetic moment of the magnetization saturation corresponds to $3.87\mu_B$ per cell. The phase transition to an ordered state in the temperature 30K was detected. The antiferromagnetic nature of the exchange interactions between the spins of cobalt ions follows from the negative Curie Weiss temperature θ_{CW}=-60K obtained from the approximation of the inverse magnetic susceptibility. An exchange narrowed line from cobalt ions is observed in the EPR spectrum in the temperature range 5-80 K. A sharp increase in the linewidth near 80K is associated with the dynamic Jan-Teller effect.

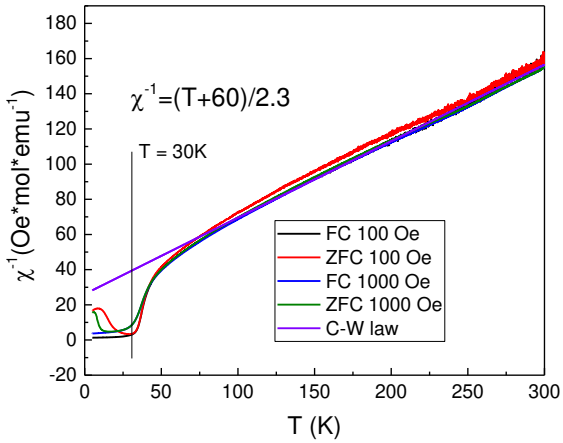

Fig. 1: *Temperature dependence of the inverse magnetic susceptibility of Ba_2CoNbO_6. The blue line represents the Curie-Weiss law approximation.*

This research was supported by the Russian Science Foundation (Project No. 22-42-02014).

Abstract ID: 1219

MAGNETIC PHASE DIAGRAM OF KITAEV QUANTUM SPIN LIQUID CANDIDATE $Na_3Co_2SbO_6$

K.K. Bestha[1,2], M. Sahoo[1,2], R.C. Morrow[1], A. Malyuk[1], B. Buechner[1,2], L.T.C. Bohorquez[1], A.U.B. Wolter[1]

[1]*Institute for Solid State Research, Leibniz IFW Dresden, 01069, Dresden, GERMANY*
[2]*Institute of Solid State and material Physics, TU Dresden, 01062, Dresden, GERMANY*
E-mail: k.k.bestha@ifw-dresden.de

Kitaev Quantum Spin liquid (KQSL) is an exotic state with many-body quantum entanglement which can host Majorana fermions and gauge fluxes. KQSL is an exactly solvable ground state of spin-1/2 model with the bond-dependent Ising interactions on a 2D honeycomb lattice[1]. The quest for Kitaev Quantum Spin Liquid candidates, has posed significant challenges in the last two decades. The presence of non-Kitaev interactions has been a primary obstacle, as they destabilize the QSL ground state[2]. To overcome this hurdle, a search for candidates with more localized d-orbitals, such as 3d cobaltates, was proposed, aiming to eliminate non-Kitaev interactions despite their weak spin-orbit interaction[3]. In this study, we employed thermodynamic methods to characterize such a cobaltate KQSL candidate, $Na_3Co_2SbO_6$. Our investigations, including magnetic and specific heat studies on high quality single crystals, confirm AFM order in $Na_3Co_2SbO_6$ at T_N = 7 K. Our *M(T)* data reveal that $Na_3Co_2SbO_6$ is an easy-plane magnet with large anisotropy in ab-plane and the metamagnetic transitions, manifestation of field-induced phases in the ordered phase. From the *M(H)*, *M(T)* and $C_p(T)$ data we mapped out the detailed anisotropic magnetic phase diagram of $Na_3Co_2SbO_6$ in the light of theoretical predictions.

References

[1] A. Kitaev, Annals of Physics **321**, 2 (2006).
[2] H. Takagi, T. Takayama, G. Jackeli, G. Khaliullin, S.E. Nagler, Nat. Rev. Phys. **1**, 265-280 (2019).
[3] H. Liu, J. Chaloupka, G. Khaliullin, Phys. Rev. Lett. **125**, 047201 (2020).

Abstract ID: 1429

MAGNETIC ORDERING IN $(Ni,Mn,Cu)_3BO_5$

R.M. Eremina[1], R.G. Batulin[2], V.A. Shustov[1], E.M. Moshkina[3], I.I. Fazlizhanov[1]

[1]Zavoisky Physical-Technical Institute, FRC KSC of RAS, 420029 Kazan, Russia
[2]Kazan (Volga Region) Federal University, Kremlevskaya st., 18, 420008 Kazan, RUSSIA
[3]Kirensky Institute of Physics, FRC KSC SB RAS, 660036 Krasnoyarsk, RUSSIA
E-mail: ilshat2004@yandex.ru

Nickel ludwigites $(Ni,Mn,Cu)_3BO_5$ exhibit interesting magnetic behavior - sequences of magnetic phase transitions, as a result of a cation ordered lattice and a multi-lattice magnetic structure, a high dependence of magnetic properties on even a small change in composition, magnetization reversal and temperature hysteresis below the temperature of the first transition in many compositions.

The aim of the work was to determine the model of magnetic ordering and temperature features of the structure of Ludwigites $(Ni,Mn,Cu)_3BO_5$, based on the study of structural properties by neutron diffraction and magnetometry. The neutron measurements were carried out on a DISK installation (λ = 1.544 Å) of the Kurchatov Institute Research Center. For research, samples containing only ^{11}B isotopes were grown by the solution-melt method. The recent experiments with the addition of copper oxide to the melt solution have significantly increased the size of the crystals, practically without changing the composition - the difference in solubility of copper and nickel is such that copper practically does not enter the crystal, and nickel fills the entire 2-valence subsystem.

The neutron diffraction spectra of ceramics $(Ni,Mn, Cu)_3BO_5$ were measured at temperatures of 7, 30, 70 and 296 K (see Fig.1). The unit cell parameters, atomic positions and the Pbam spatial group are set using the Fullprof program. The coordinates of the atoms in the crystal cell and the position filling parameter for ceramics, the unit cell parameters at several temperatures for ceramics $(Ni,Mn,Cu)_3BO_5$ are obtained.

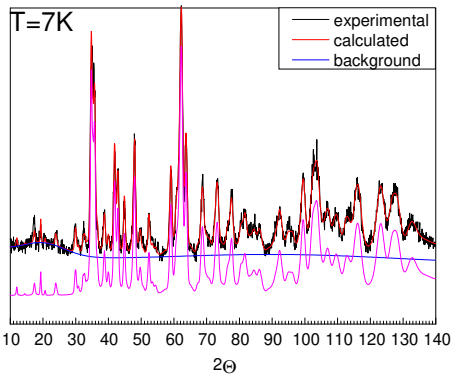

Fig. 1: *The neutron diffraction spectra of ceramics $(Ni,Mn, Cu)_3BO_5$.*

The work was performed with the financial support from the RSF 23-72-00047.

References

[1] D.V. Popov *et al.*, J. Alloys and Compd., **976**, 173143 (2024).

Abstract ID: 1642

TUNABLE CARRIER-MEDIATED FERROMAGNETISM IN A VAN DER WAALS SEMICONDUCTOR UP TO ROOM TEMPERATURE

Xiao Chang, Tingyu Qu, Barbaros Oezyilmaz

Department of Physics, National University of Singapore, SINGAPORE
E-mail: chang_xiao@u.nus.edu

Ferromagnetic semiconductors, marrying electrical tunability with nonvolatility, herald promise for the innovation of spin-based logic devices. However, the realization of room-temperature ferromagnetic order has been elusive despite relentless pursuits spanning decades. In this study, we exploit the ability to intercalation-dope layered Van der Waals semiconductors, ensuring minimal disruption to lattice coherency, resulting in the achievement of ferromagnetism in Co-doped black phosphorus (Co-BP) up to room temperature while preserving its semiconductor characteristics. This heralds a transformative advance, as evidenced by the gate-tunable, carrier-mediated room-temperature ferromagnetism, further authenticated through its resilient performance as a ferromagnetic contact in semiconducting tunnelling spin-valves and a notable anisotropic magnetoresistance. This work unveils the capability of electric field in dictating the dominant majority/minority spins, facilitating unprecedented gate-controllable inversion and a deliberate suppression of tunnelling magnetoresistance as needed. The Anomalous Hall Effect is presented to substantiate the consistent lateral transport performance of Co-BP, reinforcing the manifestation of ferromagnetism within the system. This breakthrough not only unveils a novel class of ferromagnetic semiconductors but also inaugurates a versatile pathway to imbue atomically-thin layered materials with engineered ferromagnetism, broadening the horizon of feasible applications of magnetic semiconductors previously conceived.

Abstract ID: 1354

MATHEMATICAL MODEL AND NEURAL NETWORKS FOR THE DYNAMIC HYSTERESIS LOSSES CALCULATION

A. Nouicer

University of Oumelbouaghi, Dept. of Electrical engineering, Oumelbouaghi, ALGERIA
E-mail: anouicer@gmail.com

Magnetic hysteresis is a complex phenomenon, which is important both from theoretical and practical points of view. It affects the dynamic behaviour of ferromagnetic materials, thus it should be taken into account in engineering calculations.

A realistic hysteresis model must be able to take into account the diversity of the operating conditions of the systems such the variation of the excitation field frequency and the temperature.

Several models are existing in the literature and can describe all facets of the magnetic hysteresis. The two most common ones are the Jiles- Atherton and Preisach models. The first one is of considerable interest due to its relative simplicity and the physical meaning of its parameters. Recently, some improvements have been introduced to this model [1] in order to describe the magnetization processes in ferromagnetic materials in dependence of the temperature and the frequency. However, its numerical implementation is quite complex, especially the modified models, and requires the identification of four parameters. Among the phenomenological hysteresis models, the Preisach model is the most common approach as well as its numerous extensions which are often summarized as Preisach-like hysteresis models. The Preisach model rests upon the weighted elementary hysteresis operators whose superposition determines the whole hysteresis behaviour. Numerous reformulations of the scalar Preisach model have been further elaborated in order to obtain the Preisach operator in a general vectorial form [2]. The numeric implementation of this model is also quite complex and requires more CPU times.

In this paper, an artificial neural network has been used to learn directly the relation between coercivity and frequency. The obtained neuronal model is introduced in mathematical hysteresis model to achieve accurate and computationally efficient hysteresis loss prediction.

The frequency dependent hysteresis and its influence on the core loss in Fe81B13Si14C2 amorphous alloy sample at frequencies in the range of 50–1000Hz has also been presented and discussed. The simulation results are compared with the experimental data published in [3].

References

[1] A. Nouicer, E.Nouicer, M. Felaichi, JMMM **V373** (2015).
[2] S. Rosenbaum *et al.*, IEEE transactions on magnetics, **V.46** (2010).
[3] B. Koprivica *et al.*, JMMM **V422** (2017).

Abstract ID: 1440

MOTION OF A CHARGED PARTICLE IN A MUTUALLY PERPENDICULAR UNIFORM MAGNETIC AND ELECTRIC FIELDS

M.R. Rajabov, B.G. Pashayev

Baku State University AZ1148, Baku, AZERBAIJAN
E-mail: m_rajabov@mail.ru

In quantum theory, the theoretical investigation of the motion of a particle with spin in uniform magnetic and electric fields is of great importance. The study of such tasks allows to clearly demonstrate the basic principles of quantum theory and the nature of quantum formalism.

The Hamiltonian operator of the motion of a charged particle with spin in mutually perpendicular uniform magnetic and electric fields has been written and the Schrödinger equation has been solved. It is known that in experiment, to determine the energy of a particle, the electric and magnetic field intensity vectors $\vec{\varepsilon}, \vec{H}$ are chosen so that the particle moves along a straight line. This is possible when the electric and magnetic forces acting on the particle are equal in modulus and opposite in direction. Then the electric and magnetic field intensities must be perpendicular to each other. If we orient the magnetic field along the z axis and the uniform electric field along the y axis, then the particle moves along the x axis. Thus, in the classical case, the energy of a non-relativistic particle is equal to

$$E = \frac{mv^2}{2} = \frac{mc^2\varepsilon^2}{2H^2} \tag{1}$$

In the same conditions, when we consider the motion of a quantum non-relativistic particle, its energy is determined by

$$E = \hbar\omega(n+1/2) + \frac{\varepsilon c P_x}{H} - \frac{mc^2\varepsilon^2}{2H^2} + \frac{\hbar\omega}{2}\sigma_z \tag{2}$$

From the comparison of the expressions (1) and (2) we see that they differ sharply from each other.

Abstract ID: 1196

FULLY SUPERCONDUCTING ELECTRICAL MACHINES IN VARIOUS APPLICATIONS

N. Ivanov, V. Kaderov, N. Malevich

Moscow Aviation Institute, 125993, Moscow, RUSSIA
E-mail:

This project is aimed at the research and development of HTS electric machines, which are part of hybrid power plants, for use in the transport sector. Electrification of the transport sector is one of the key directions of transport development in the world. It has a number of advantages related to reducing emissions of harmful substances, increasing fuel efficiency and reducing dependence on hydrocarbon fuels. The electrification process in the transportation sector consists of replacing internal combustion engines with electric motors or hybrid systems that use electric machines as energy sources and propulsion systems. However, the transition to electric transport requires solving technological and scientific problems, which slows down this process.

At the moment, the creation of large fully electric machines is difficult due to the low specific characteristics of traditional electric machines. High power characteristics can be achieved by switching from traditional electric machines to superconducting ones using advanced technologies.

The main objective of the project is to develop methods for calculating and designing HTS machines with high specific power for hybrid power plants.

In this paper, an overview of transport systems in various fields of application is carried out. As a result, up-to-date source data for electric machines in their composition have been formed. This takes into account the limitations that exist in each area.

In order to demonstrate the improvement in specific characteristics during the transition to fully superconducting electric machines, calculations of analogues of promising global projects have been performed. As a result, electric machines with higher specific capacities than in the initial designs were designed. This proves the prospects of switching to fully HTS electric machines.

Since the calculated machines are completely superconducting, it is important to consider the AC losses in the HTS winding. To study losses, a 1200W submersible generator with liquid nitrogen cooling was manufactured and tested. During the tests, data were obtained for calculating HTS losses.

Abstract ID: 1421

STUDY OF A NEW SUPERCONDUCTING INDUCTOR FOR AN AXIAL FIELD SYNCHRONOUS MACHINE

Hakim Douar[1], Larbi Hadjout[1], Ailam El Hadj[2]

[1]LSEI-Houari Boumediene University of Science and Technology, BP NO 32, 16111 Algiers, ALGERIA
[2]LESI-University of Djilali Bounaama, Faculty of Sciences and Technologies Khemis Miliana, 44001, ALGERIA
E-mail: douarhakim@yahoo.fr

In this work, a new topology of an inductor of axial flux synchronous machine is presented and tested. It is executed by combining superconducting (SC) bulks and six solenoids. It consists of six superconducting solenoids connected in series stuck in a non-magnetic disc and supplied by direct current. The presence of two SC bulks which by their magnetic field screening property, modulate and redirect the flux density lines produced by the six solenoids. Thus, we can generate a periodic spatial variation of the axial flux density component.

A 3D Electromagnetic modeling based on finite elements solution is developed to demonstrate the suitability of using the magnetic shielding properties of the SC bulks. In order to check the screening properties of the SC bulk, a prototype of the proposed inductor has been constructed at the laboratory. it consists of six copper solenoids and two circular shape superconducting YBCO bulks.

Abstract ID: 1443

SIGNATURES OF SPIN-TRIPLET-PAIRING STATE IN TWO-DIMENSIONAL NIOBIUM DISELENIDE

T. Qu, X. Chang, B. Oezyilmaz

Department of Physics, National University of Singapore, 117542 SINGAPORE
E-mail: ty.qu@nus.edu.sg

Triplet superconductivity is a rare natural occurrence, with conclusive observations limited to heavy fermions [1], $ZrZn_2$ [2], and stacked graphene [3]. However, recent attention has turned to niobium diselenide ($NbSe_2$) as a potential platform for exploring the spin-triplet pairing state because of the Ising spin-orbit coupling [4] and sizeable singlet-triplet mixing in its 2D form [5]. In our study, we interface few-layer BN-encapsulated $NbSe_2$ with ferromagnetic nanoribbons (as the spin injectors and detectors). Using non-local spin-valve measurements, we directly resolved the transport of spin-polarized supercurrents. Our findings reveal long-range spin diffusion through the superconducting $NbSe_2$ channel deep inside the superconducting gap, suggesting $NbSe_2$ hosts intrinsic spin-triplet Cooper pairs with extended spin relaxation. The resolved spin carriers have several potential interpretations, including non-centrosymmetric superconductors, coherent and incoherent components stemming from spin-orbit coupling, and activated quasiparticles with spin-charge separation. Furthermore, we delve into the role of interfacial magnetism in facilitating the injection of supercurrents. This not only minimizes the conductance mismatches but also enables the occurrence of triplet Andreev reflection. Our results highlight $NbSe_2$ as a promising candidate for future research in superconducting spintronics.

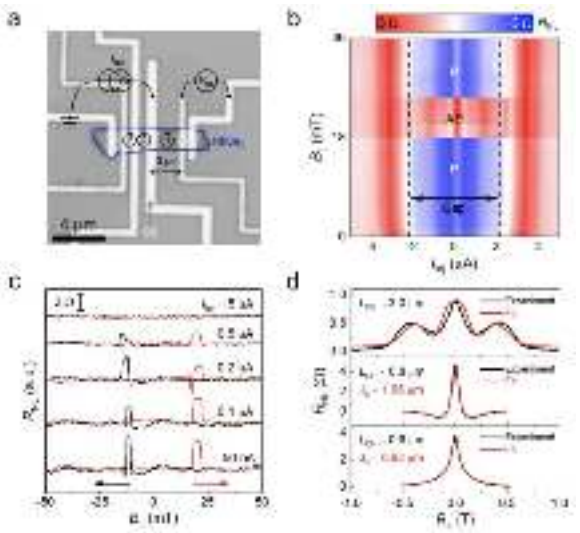

Fig. 1: *Non-local spin supercurrent and Hanle precession. a, Micrograph of the device for non-local measurement. The three different channels are labelled by #1 (~0.6 μm), #2 (~0.8 μm) and #3 (~3.0 μm), respectively. b, 2D mapping of R_{NL} as a function of $B_{||}$ and I_{Inj} at T = 53 mK. A sign change of R_{NL} occurs at finite $B_{||}$ near the coercive field of the Co detector and at finite I_{Inj} for the potential inside the gap. A DC bias is swept from −5 μA to +5 μA with 0.05 μA in each step as the injection source and an AC bias equal to 0.05 μA is applied to resolve the non-local signal with a Lock-in amplifier. c, Examples of non-local switches with different I_{Inj} at T = 53 mK. The injection current tunes the magnitude of the switching but does not obviously affect the switching fields. d, R_{NL} by sweeping $B_{\perp}$ at T = 46 mK, with L_{CH} = 0.6, 0.8 and 3.0 μm, respectively.*

References

[1] S. Ran, *et al.*, Science **365**, 684-687 (2019).
[2] C. Pfleiderer, *et al.*, Nature **412**, 58-61 (2001).
[3] Y. Cao, *et al.*, Nature **595**, 526-531 (2021).
[4] X. Xi, *et al.*, Nat. Phys. **12**, 139-143 (2016).

Abstract ID: 1427

DYNAMICS AND INFLUENCE OF HELIUM AND VACUUM ON GAP RELAXATION TIME IN SUPERCONDUCTING BRIDGES

A. Mekki[1,2], K. Harrabi[1,3], M. Milosevic[4]

[1]Physics Department, King Fahd University of Petroleum and Minerals, 31261 Dhahran, SAUDI ARABIA
[2]Center for Advanced Material, King Fahd University of Petroleum and Minerals, Dhahran 31261, SAUDI ARABIA
[3]Interdisciplinary Research Center (RC) for Intelligent Secure Systems, KFUPM, Dhahran 31261, SAUDI ARABIA
[4]Department of Physics & NANOlab Center of Excellence, University of Antwerp, BELGIUM
E-mail: akmekki@kfupm.edu.sa

Our investigation focused on characterizing non-equilibrium states in NbTi films deposited on fused silica, exploring the effects of varying environmental conditions through the electrical current pulse technique. The emergence of a voltage across the filament, following a current pulse surpassing the depairing current (I_c), *was* observed after a specific delay time (t_d). Despite the significant size of our samples compared to the coherence length (ξ), the resulting micro-metric regions exhibited hotspot behavior. To analyze the delay times, we employed the Time-Dependent Ginzburg-Landau (TDGL) theory proposed by M. Tinkham. This approach allowed us to determine the filament cooling times for samples subjected to either liquid helium or vacuum conditions. Remarkably, our investigation revealed a delay time (τd) of approximately 6.0 ns in vacuum and 5.3 ns in liquid helium. Notably, the impact of liquid helium on filament cooling time was found to be minimal, leading to the inference that the majority of generated heat is effectively evacuated towards the substrate, facilitated by phonons. These findings contribute valuable insights into the thermal dynamics of NbTi films in different environments, shedding light on the mechanisms governing heat dissipation in these systems.

Abstract ID: 1465

ADVANCES IN THE THERMOELECTRIC MEASUREMENTS OF 2D SUPERCONDUCTOR UTILIZING CONTACT PRINTED CIRCUIT BOARDS

S. Shokri[1,2], C.N. Saggau[1], T. Confalone[1], M. Martini[1,2], Y. Lee[1,2], F. Caglieris[3], H. Reith[1], D. Berger[1], G.D. Gu[4], V.M. Vinokur[5], K. Nielsch[1,2], N. Poccia[1]

[1] *Institute for Metallic Materials, IFW Dresden, Dresden,Germany, IFW Dresden, Helmholtzstraße 20, Dresden, 01069, Saxony, GERMANY*
[2] *Institute for Materials Science, Dresden University of Technology, Helmholtzstr. 7, Dresden, 01069, Saxony, GERMANY*
[3] *Department of Physics, Universit`a degli studi di Genova, 16126, ITALY*
[4] *Department of Condensed Matter Physics and Materials Science, Brookhaven National Laboratory, Street, Upton, 11973, New York, USA*
[5] *Terra Quantum AG, St. Gallerstrasse 16a, Rorschach, 610101, St. Gallen, SWITZERLAND*
E-mail: s.shokri@ifw-dresden.de

This study introduces an innovative approach to overcome challenges in contact pad fabrication for air-sensitive materials by incorporating a freestanding SiNx nanomembrane with variable thickness (ranging from 200 nm to 800 nm). The nanomembrane serves a crucial role in constructing a circuit tailored for thermoelectric transport measurements, housing thermoelements, a heater, and vertical contacts within its structure. This setup is designed for the investigation of a 2D Cuprate superconductor.

Functioning as a versatile interconnection medium, the nanomembrane seamlessly links bottom contacts with the underlying 2D materials and larger-scale pads through via contacts created by dry etching via reactive ion etching. Following the PDMS cryogenic transfer technique onto our material, this integration facilitates wire bonding on top of the nanomembrane. This, in turn, enables the electrical connection of our sample to the chip carrier on the PPMS puck, which is then loaded into the Cryostat. Notably, this approach eliminates the need for chemical solvents, photolithography, and traditional metal deposition on top of the nanomaterial, resulting in an exceptionally pristine surface morphology.

The utilization of thermoelectric measurements becomes particularly relevant due to the presence of van Hove singularities in the density of states, which can lead to an amplified Seebeck coefficient in 2D materials. This serves as an additional experimental tool to explore quantum transport phenomena in 2D materials. Furthermore, thinning down the Van der Waals heterostructure superconductor, such as $Bi_2Sr_2Cu_2O_{(8+\delta)}$ (Bi-2212), in hall measurements indicates an increase in the additional part arising from superconductivity vortices. Therefore, Nernst measurements, which also indicate the formation and movement of superconductivity vortices, can be a valuable tool to study superconductivity by thinning down the heterostructure superconductor.

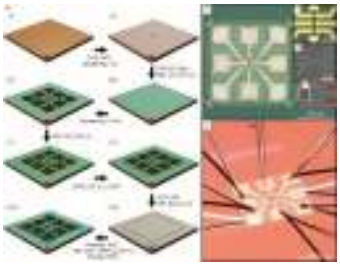

References

[1] C.N. Saggau, S. Shokri, *et al.*, *2D high-temperature superconductor integration in contact printed circuit boards*, ACS Applied Materials & Interfaces **15.44**, 51558-51564 (2023).

Abstract ID: 1476

QUASI-TWO-DIMENSIONAL ANISOTROPIC SUPERCONDUCTIVITY IN Li INTERCALATED 2H-TaS_2

T. Agarwal, C. Patra, A. Kataria, Rajeswari R. Chowdhury, R. P. Singh

Department of Physics, Indian Institute of Science Education and Research Bhopal, Bhopal 462066, INDIA
E-mail: tarushi19@iiserb.ac.in

Superconductivity in two-dimensional (2D) materials have sparked great interest due to emergence of various novel quantum phenomena [1]. Recent experimental studies of 2D superconductivity in anisotropic layered materials propose both conventional and unconventional electron pairing. In this series, layered transition metal dichalcogenides (TMDs) are intriguing class of materials which are the potential candidates to realise Ising superconductivity, spin-valley coupling, quantum spin Hall effect, and non-trivial topologically protected band structure [2]. Chemical doping or intercalation in such materials provides a suitable way to tune the interlayer coupling and thereby to tune dimensionality.

Here, I will present my work on the enhanced superconductivity in 2H-TaS_2 by Li intercalation and demonstrate modified superconducting properties of parent compound 2H-TaS_2 after intercalation [3]. The magnetisation, resistivity, and specific heat measurement of single crystals confirmed weakly coupled bulk anisotropic superconductivity having transition temperature at $T_c \sim 3.3(1)$ K. Moreover, the cusp-like feature in angle-dependent magnetotransport measurement and the appearance of Berezinskii-Kosterlitz-Thouless (BKT) phase transition in bulk crystal Li_xTaS_2 suggested quasi-2D nature of superconductivity. These findings suggest the weakening of interlayer coupling by Li intercalation. There are very few studies in intercalated materials where BKT transition is observed which makes Li_xTaS_2 a valuable candidate for understanding the superconductivity with BKT mechanism and provide a new insight towards the intercalated materials.

References

[1] Y. Saito, T. Nojima, Y. Iwasa, Nat. Rev. Mater**. 2(1)**, 1 (2016).
[2] R.A. Klemm, Physica C: Superconductivity and its Applications, **514**, 86 (2015).
[3] T. Agarwal *et. al.*, Phys. Rev. B **107**, 174509 (2023).

Abstract ID: 1201

ANATOMY OF BAND STRUCTURE OF NEWEST APPARENT NEAR-AMBIENT SUPERCONDUCTOR $LuH_{3-x}N_x$

N.S. Pavlov[1,2], I.R. Shein[3], K.S. Pervakov[2], V.M. Pudalov[2], I.A. Nekrasov[1,2]

[1]*Institute of Electrophysics UB RAS, 620016, Yekaterinburg, RUSSIA*
[2]*Lebedev Physical Institute RAS, 119991, Moscow, RUSSIA*
[3]*Institute of Solid State Chemistry UB RAS, 620990, Ekaterinburg, RUSSIA*
E-mail: pavlovns@gmail.com

It was claimed that nitrogen-doped lutetium hydride exhibited a near-ambient superconducting transition with a temperature of 294 K at a pressure of only 10 kbar [1]. This pressure being several orders of magnitude lower than previously demonstrated for hydrides under pressure. After half a year, this article [1] was retracted. And no other scientific group has been able to reproduce the first experiment. Nevertheless, the theoretical study of the band structure of $LuH_{3-x}N_x$ compound is an area of interest. We investigate within DFT+U the electronic structure of both parent lutetium hydride LuH_3 and nitrogen doped lutetium hydride $LuH_{2.75}N_{0.25}$ [2]. Bands, density of states and Fermi surfaces with and without spin-orbit coupling (SOC) was calculated. It is shown that in the stoichiometric system the Lu-5d states cross the Fermi level while the H-1s states make almost no contribution at the Fermi level. However, with nitrogen doping, the N-2p states enter the Fermi level in large quantities and bring together a significant contribution from the H-1s states.

A minimal band model for reproducing the DFT band structure near the Fermi level has been determined. It includes H-1s states of hydrogen ions in octahedral environment and N-2p states of nitrogen (see Fig. 1). The presence of N-2p and H-1s states at the Fermi level in a doped compound can facilitate the emergence of superconductivity. Surprisingly, SOC splits quite significantly (0.1-0.25 eV) nitrogen bands in $LuH_{2.75}N_{0.25}$ just below the Fermi level. For instance, nitrogen doping almost doubles the value of DOS at the Fermi level. Simple BCS analysis shows that the nitrogen doping of LuH_3 can provide T_c more than 100 K and even increase it with further hole doping.

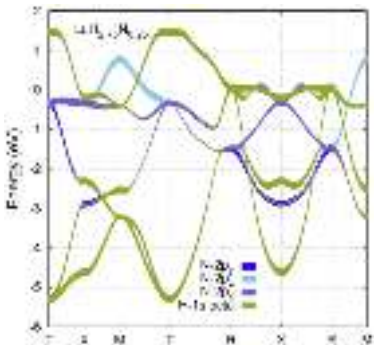

Fig. 1: *Band structure of $LuH_{2.75}N_{0.25}$ on wannier functions, which correspond to minimum basis set. Zero energy is the Fermi level.*

References

[1] N. Dasenbrock-Gammon, E. Snider, R. McBride, *et al.*, Nature **615**, 244 (2023).
[2] N.S. Pavlov, I.R. Shein, K.S. Pervakov, *et al.*, JETP Letters **118**, 693 (2023).

Abstract ID: 210

EXCEPTIONALLY SLOW, LONG RANGE, AND NON-GAUSSIAN FLUCTUATIONS ANTICIPATE THE CRITICAL SINGULARITY FAR AWAY FROM THE CHARGE DENSITY WAVE TRANSITION

Sk Kalimuddin[1], Sudipta Chatterjee[2], Arnab Bera[1], Hasan Afzal[1], Satyabrata Bera[1], Deep Singha Roy[1], Soham Das[1], Tuhin Debnath[1], Bhavtosh Bansal[3], Mintu Mondal[1]

[1]*School of Physical Sciences, Indian Association for the Cultivation of Science, Jadavpur, Kolkata 700032, INDIA*
[2]*Department of Condensed Matter and Materials Physics, S. N. Bose National Centre for Basic Sciences, Kolkata 700106, INDIA*
[3]*Indian Institute of Science Education and Research Kolkata, Mohanpur, Nadia, West Bengal 741246, INDIA*
E-mail: intdydt@gmail.com

$(TaSe_4)_2I$ is a quasi-one-dimensional compound long-known to have a charge-density wave (CDW) transition at around 263 K. We experimentally establish that this transition, unlike what is seen in other CDW compounds such as TaS_2, is a second-order critical transition. Critical fluctuations in the CDW condensate, which couple to the dissipative normal carriers, are slow enough to survive the thermodynamic limit and dominate the low-frequency resistance noise. Around the transition region, we find a rapid increase in their relaxation time, as well as a shift of the spectral weight of fluctuations to lower frequencies. These are direct signatures of the critical slowing down on account of the softening at the hydrodynamic amplitude modes. Critical opalescence on the account of diverging isothermal susceptibility is also seen in the very sharp growth of the variance. The distribution of fluctuations in the transition region is skewed and strongly non-Gaussian. This is on account of the breakdown of the validity of the central limit theorem as the diverging coherence volume becomes comparable to the macroscopic sample size. The temperature window, where the fluctuations manifest as slow and extended hydrodynamic modes is found to be very wide ($\delta\epsilon \approx \pm 0.1$, where ϵ is the reduced critical temperature) but consistent with the Ginzburg criterion.

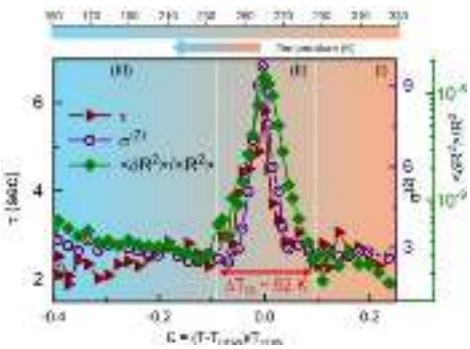

Fig. 1: ***Fluctuations around the CDW singularity;*** *Variation of the relaxation time τ (wine triangle), the relative variance $\langle\delta R^2\rangle/R^2$ (green rectangular), and the second variance $s^{(2)}$ (violet circle) of the resistance noise with reduced temperature $\epsilon = (T - T_{CDW})/T_{CDW}$, where $T_{CDW} = 263$ K. This combined plot clearly reveals three distinct fluctuation regions, marked (I), (II), and (III) respectively.*

References

[1] Sk Kalimuddin, Sudipta Chatterjee, Arnab Bera, Hasan Afzal, Satyabrata Bera, Deep Singha Roy, Soham Das, Tuhin Debnath, Bhavtosh Bansal, Mintu Mondal, e-print arXiv:2308.09756v1 (2023).

Abstract ID: 1277

OPTICAL CONDUCTIVITY OF DYNES SUPERCONDUCTORS: EXPERIMENT AND THEORY

M. Šindler[1], C. Kadlec[1], and F. Herman[2]

[1]*Institute of Physics, Czech Academy of Sciences, 18200 Prague 8, CZECH REPUBLIC*
[2]*Department of Experimental Physics, Comenius University, Mlynská Dolina F2, 842 48 Bratislava, SLOVAKIA*
E-mail: sindler@fzu.cz

One of the major achievements of the BCS theory was the correct description of the optical conductivity [1,2]. The optical conductivity provide valuable information about condensate, quasiparticles and vortex behavior in both equilibrium and non-equilibrium states of superconductors. Later, electrodynamics of superconductors was generalized for the case including either pair-breaking [3] or pair-conserving scattering [4]. Recently, the model by Herman and Hlubina [5] (HH model) allows to account for both cases at the same times for so-called Dynes superconductors (their density of the states is described by phenomenological Dynes formula [6]). The scattering rate in the normal state is $G_n = G_s + G$ where G_s (G) is the pair-conserving (pair-breaking) scattering rate in the superconducting state. Each term modifies the superconducting spectrum differently.

Here, we demonstrate the power of the HH model by interpreting various THz spectra. The model was used to describe zero magnetic field THz spectra of thin films near the superconductor-insulator transition. We also used the model to describe the properties of the superconducting fraction in the effective medium model for inhomogeneous state in a magnetic field parallel [7] and perpendicular to the surface. We propose an alternative interpretation for the parallel field THz measurements by Lee [8].

References

[1] J. Bardeen, L.N. Cooper, J.R. Schrieffer, Phys. Rev. **108**, 1175 (1957).
[2] D.C. Mattis, J. Bardeen, Phys. Rev. **111**, 412 (1958).
[3] S.B. Nam, Phys. Rev. **156**, 470 (1967).
[4] W. Zimmermann *et al.*, Physica C **183**, 99-104 (1991).
[5] F. Herman, R. Hlubina, Phys. Rev. B **97**, 014517 (2018).
[6] R.C. Dynes, V. Narayanamurti, J.P. Garno, Phys. Rev. Lett. **41**, 1509 (1978).
[7] M. Šindler, F. Kadlec, C. Kadlec, Phys. Rev. B **105**, 014506 (2022).
[8] Ji Eun Lee *et al.*, Nat. Commun. **14**, 2737 (2023).

Abstract ID: 1450

PROBLEMS ON REPRESENTING MECHANISM OF THE PHENOMENON OF HIGH TEMPERATURE SUPERCONDUCTIVITY

Djuraev Davron Rahmonovich[1], Ahadov Abdullo Amrullojon ogli[1,2]

[1]Bukhara State University, Bukhara, UZBEKISTAN
[2]Bukhara State Medical Institute, Bukhara, UZBEKISTAN
E-mail: ahadovabdullo42@gmail.com

It is known that the interest in theoretical and practical research in the field of high-temperature superconductivity (HTS) is related to the possibility of achieving important and effective solutions in technical, economic, environmental and various other directions. This determines the relevance of this research topic. Therefore, this direction is one of the modern and relevant directions of physics. To date, there is no single theoretical mechanism that accounts for the various physical properties observed in HTS experiments. Solving this problem requires further strengthening of research in the field of superconductivity, especially in the field of HTS. This article presents some mechanisms describing HTS phenomena and related research results, and also highlights some theoretical models and underlying mechanisms proposed in research to explain the observed features of HTS and show their shortcomings.

Abstract ID: 1471

CORRELATION CARRIER CONCENTRATION WITH CRITICAL TEMPERATURE OF SUPERCONDUCTORS

D.R. Djuraev, J.S. Abdulloyev, A.A. Turayev

Bukhara State University, M.Iqbol, 11, 200000 Bukhara, UZBEKISTAN
E-mail: djurayev2002@mail.ru

The current work is dedicated to study the connection of the superconducting and electronic characteristics of the compounds with A15, B1 and perovskite-type structures. The critical temperature, T_c, of the superconducting transition, the superconducting energy gap Δ and concentration N of carriers (conduction electrons), the London depth, λ_L, of magnetic field penetration are considered. The study results have demonstrated that there is correlation between T_c, Δ and N. It has been found that the correlation dependence obeys the power law ($T_c \sim N^{-2/3}$; $\Delta \sim N^{-2/3}$).

Abstract ID: 1255

BOOSTING THE SOLUTION OF BOGOLIUBOV – de GENNES EQUATIONS BY THE NEURAL NETWORK

A.V. Krasavin[1,2], V.D. Neverov[1,2], A.E. Lukyanov[1,2], M.D. Croitoru[1], A. Vagov[1,3]

[1]HSE University, Moscow, RUSSIAN FEDERATION
[2]National Research Nuclear University MEPhI, Moscow, RUSSIAN FEDERATION
[3]Moscow Institute of Physics and Technology, Dolgoprudny, RUSSIAN FEDERATION
E-mail: avkrasavin@gmail.com

The Bogoliubov – de Gennes (BdG) equations serve as a crucial tool for examining the local electronic structure in inhomogeneous superconductors, particularly in the presence of strong disorder and external magnetic fields. Achieving their numerical solution involves multiple self-consistency cycles for essential system variables, such as the local order parameter, carrier density, and magnetic field [1,2]. The convergence rate of the solution critically hinges on the initial guess for the spatial configuration of the system.

In this study, we propose an innovative approach to obtain an accurate initial guess by utilizing a carefully constructed and trained neural network (NN) model [Fig. 1]. This initial guess significantly reduces the time required to solve the BdG equations for inhomogeneous materials. The NN architecture comprises three hidden layers, each housing 500 neurons with Rectified Linear Unit (ReLU) activation functions. Leveraging the distribution of the disorder potential in the vicinity and microscopic parameters of the system, the NN effectively determines the initial guess for the local order parameter value. This novel strategy enhances the efficiency and accuracy of solving BdG equations for strongly disordered superconductors.

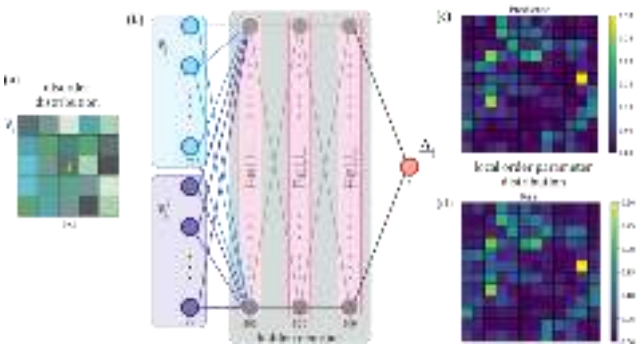

Fig. 1: *(a) For each site i of the lattice, the inputs for NN are the values of the disorder potential at the sites surrounding site i, the squares of these values, and other parameters of the BdG Hamiltonian; (b) The architecture of NN; (c) The predicted and (d) real local order parameter distribution.*

The work was supported by HSE University Basic Research Program and MEPhI Program Priority 2030, by Ministry of Science and Higher Education of Russian Federation (No. FSWU-2023-0031, FSMG-2023-0014), and by RSF grant 23-72-30004.

References

[1] V. Neverov *et al.*, Comm. Physics **5**, 177 (2022).
[2] V. Neverov *et al.*, MDPI Condensed Matter, to be published (2024).

Abstract ID: 265

QUANTUM HALL AND LIGHT RESPONSES IN A 2D TOPOLOGICAL SEMIMETAL

Sariah Al Saati, Karyn Le Hur

CPHT, CNRS, Institut Polytechnique de Paris, Route de Saclay, 91120 Palaiseau, FRANCE
E-mail: sariah_alsaati@hotmail.fr

We investigate the topological characteristics of a recently discovered class of semimetals in two dimensions on the honeycomb lattice. These semimetals reside at the transition between two distinct topological insulators, each existing in a nontrivial topological phase. As a result, these semimetals exhibit specific topological properties, including the presence of edge modes. In a preceding work [1], we demonstrated the topological robustness of this semimetal phase against disorder and interactions. In this work [2], we delve deeper into the semimetal's electronic properties, providing a precise calculation of its Hall conductivity and response to circularly polarized light, elaborating further on its bulk-edge correspondance leading to a half topological semimetal.

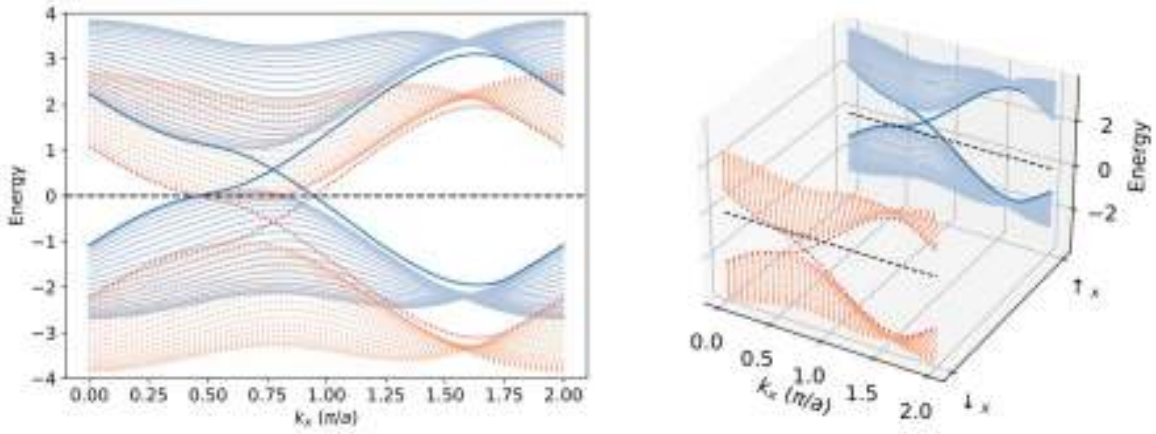

Fig. 1: *(left) One-dimensional energy bands of the topological semimetal showing the two underlying band structures of opposite spin polarization, with the spin polarization shown in the third direction. (Right) Resulting energy bands in the momentum-Energy axis.*

References

[1] Karyn Le Hur, Sariah Al Saati, *Topological nodal ring semimetal in graphene*, Physical Review B, **107(16)** (2023).

[2] Sariah Al Saati, Karyn Le Hur, *Quantum hall and light responses in a 2d topological semimetal*, arXiv:2311.13922 (2023).

Abstract ID: 1074

VORTEX DYNAMICS AND DISSIPATION EFFECTS IN NON-SIMPLY CONNECTED THIN FILMS

V. Pashkovskaia[1], A. Vagov[1], A. Shanenko[1], A. Vasenko[1,2], T.T. Saraiva[1]

[1]HSE University, Moscow 101000, RUSSIA
E-mail: vdpashkovskaya@edu.hse.ru

The Bogomolny point of the Ginzburg-Landau (GL) theory marks a point of infinite degeneracy of the stationary states. The solutions to the Bogomolny equations in superconductors have very particular properties [1] and go beyond Meissner and vortex solutions, e.g. vortex lines, giant vortices, etc [2] . As we decrease the temperature and keep the GL parameter next to $\varkappa \approx 1/\sqrt{2}$, the degeneracy is broken, the condensate and magnetic characteristic lengths become well defined and several elements of the system may influence in the electromagnetic response of the superconductor. In this work, we investigated non-simply connected 2D systems submitted to a perpendicular magnetic field using a generalization of the Time-Dependent Ginzburg-Landau theory, admitting local variations of temperature due to heat dissipation [3]. We simulated a continuous increase of the external magnetic field for different thermal parameters of the system, i.e. thermal diffusivity, conductivity, etc and different sizes of the sample. We found that in the vicinity of the critical penetration field, H_{c1}, where the first magnetic fluxes moved through the sample, the local increase in temperature produced a trail of dissipation causing more elongation of vortices, resembling "vortex lines" found in the analytic solutions to the Bogomolny equations.

References

[1] G.N. Gol'tsman *et al.*, *Picosecond superconducting single-photon optical detector*, Appl. Phys. Lett. **Vol. 79, № 6**, pp. 705–707 (2001).

[2] A. Vagov *et al.*, *Superconductivity between standard types: Multiband versus single-band materials*, Phys. Rev. B. **Vol. 93, № 17**, Pp. 174503 (2016).

[3] E.C.S. Duarte *et al.*, *Comparing energy dissipation mechanisms within the vortex dynamics of gap and gapless nano-sized superconductors*

Abstract ID: 1114

THE EFFECT OF PINNING ARRAYS WITH MOIRÉ STRUCTURE ON THE CRITICAL CURRENT DENSITY IN SUPERCONDUCTING MEDIA

Z. Owjifard[1], M. Hosseini[2], A. Tavana[1]

[1]*Department of Physics, University of Mohaghegh Ardabili, 56199-13131, Ardabil, IRAN*
[2]*Department of physics, Shiraz University of Technology, Shiraz, 313-71555, IRAN*
E-mail: pqmehdi@gmail.com

Researchers have been attracted to exploring artificial vortex pinning with various geometries owing to the possible increase of critical current [1-6]. Moiré patterns arise from the interference effects that emerge when two identical lattices are overlaid, and subsequently one of the lattices is shifted or rotated [1-3]. In this study, we investigate the influence of the twisted angle θ between two sheets of graphene lattice pinning pattern on the critical current density of a superconducting thin film. The critical current density versus number of vortices (magnetic field) is derived by solving the equation of motion for vortices in a viscous medium through molecular dynamics simulations [6]. The results indicated that at certain angles, we have a noticeable increase in critical current density.

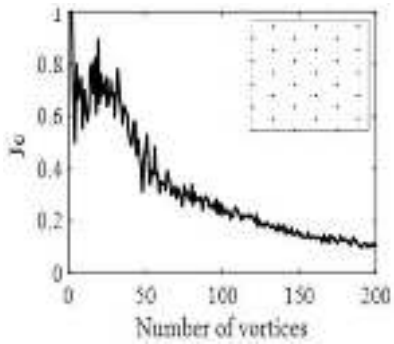

Fig. 1: *Critical current density versus vortices number for hexagonal lattice.*

References

[1] H. Miao, A. Panna, A.A. Gomella, E.E. Bennett, S. Znati, L. Chen, H. Wen. Nature Phys. **12**, 830–834 (2016).
[2] S. Kezilebieke, V. Vano, M.N. Huda, M. Aapro, S.C. Ganguli, P. Liljeroth, J.L. Lado, Nano Lett. **22(1)**, 328-333 (2022).
[3] K. Kobayashi. Phys. Rev. B **53**, 11091–11099 (1996).
[4] G.R. Berdiyorov, M.V. Milosevic, F.M. Peeters,Phys. Rev. Lett. **96**, 207001 (2006).
[5] M. V´elez, J.I. Mart´ın, J.E. Villegas, A. Hoffmann, E.M. Gonz´alez, J.L. Vicent, I.K. Schuller, J. Mag. Mag. Mater. **320**, 2547 (2008).
[6] D. Ray, C. Reichhardt, C.J. Olson Reichhardt Phys. Rev. B **90**, 094502 (2014).

Abstract ID: 1233

CURRENT-INDUCED VORTEX DYNAMICS IN SUPERCONDUCTING DIABOLO AND SCREW GEOMETRIES

A.J.M. Deenen[1], D. Grundler[1,2]

[1]*Laboratory of Nanoscale Magnetic Materials and Magnonics (LMGN), Institute of Materials (IMX), School of Engineering, Ecole Polytechnique Fédérale de Lausanne (EPFL), Lausanne, 1015, SWITZERLAND*
[2]*Institute of Electrical and Micro Engineering, EPFL*
E-mail: axel.deenen@epfl.ch

Superconducting 3D curvilinear nanoarchitectures have generated interest due to their potential use in next-generation computing architectures and sensors [1]. To harvest such functionalities a microscopic understanding of the behavior of 3D superconducting structures under transport currents is necessary. At moderate currents, the magnetotransport characteristics are dominated by the interplay of (screening) currents and topological defects such as Abrikosov vortices [2]. Here, we present 3D finite-element simulations of the magnetotransport behavior of tubular type-II superconductors based on the Time-Dependent Ginzburg-Landau formalism.

In our simulations, we consider a Nb diabolo (Fig. 1a) placed in an external magnetic field perpendicular to the central axis. A transport current is applied along the long axis of the structure, which due to its bended shape gives rise to an inhomogeneous current density. The ensuing vortex motion influences the magnetotransport properties. We additionally present results on vortex motion in screw-like structures as displayed in Fig. 1b.

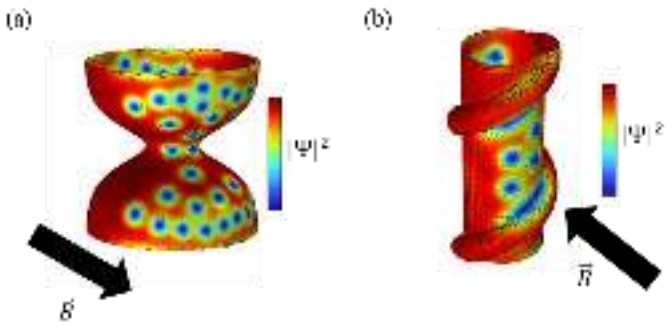

Fig. 1: *(a) The color-coded magnitude of the order parameter of a Nb diabolo in an external magnetic field of 58 mT.. The structure has a major and minor radius of 890 nm and 232 nm respectively. The thickness of the shell amounts to 0.47 times the coherence lenth. (b) Right handed Nb shell with a screw-like surface topography in an external field of 45 mT. The length of the tube is 1.6* μm.

To summarize, using a finite-element approach we studied the magnetotransport properties of tubular constrictions and 3D spiral nanoarchitectures which are important building blocks in non-trivial 3D superconductor networks. This work is an important step towards understanding and exploring advanced functionalities of 3D superconductors.

References

[1] D. Makarov *et al.*, Advanced Materials **34**, 2101758 (2022).
[2] V.M. Fomin *et al.*, Appl. Phys. Lett.**120**, 090501 (2022).

Abstract ID: 1376

DYNAMIC CHANGES IN THE CRITICAL STATE AND THE STRUCTURE OF MAGNETIC FLUX FRONTS IN AN NbTi SUPERCONDUCTOR

V.V. Chabanenko[1], I. Abaloszewa[2], V.F. Rusakov[3], O.I. Kuchuk[2], O.M. Chumak[2], A. Abaloszew[2], A. Nabialek[2], R. Puźniak[2]

[1]*Donetsk Institute for Physics and Engineering, Academy of Sciences, 03028 Kyiv, UKRAINE*
[2]*Institute of Physics, Polish Academy of Sciences, 02-668 Warsaw, POLAND*
[3]*Igor Sikorsky Kyiv Polytechnic Institute, 03056 Kyiv, UKRAINE*
E-mail: vikchabanenko@gmail.com

The superconducting materials with trapped magnetic flux are used as permanent magnets in technical devices such as motors and generators. During operation, such magnets are subject to constant magnetic impacts (for example, the interaction of stator and rotor magnets in an electro-motor). Therefore, it is crucial to study the stability of the critical state of a superconductor (SC) under the influence of a stepwise change in an external magnetic field. Magneto-optical (MO) studies [1] were carried out on a SC disk made from NbTi material after hydroextrusion and subsequent heat treatment [2]. The structure of magnetic flux fronts under mechanical-thermal influence is visualized at various temperatures (5÷7 K) in an external magnetic field (B_{ext}) of 600 G. The following findings were made: **1.** Pulses of decreasing or increasing magnetic fields in experiments result in a corresponding increase or decrease in the magnitude of the trapped flux. The magnitude of these changes depends on the parameters of the superconductor. For instance, in the case of NbTi at a temperature T=5 K, the maximum value of induction in the trapped flux increases by 40-50%. Such flux dynamics lead to additional energy release and heating of technical products. **2.** A sudden reversal of the external magnetic field, opposite to the orientation of the trapped flux, initiates thermomagnetic anti-flux avalanches (Fig. (a): B_{ext}=0 after field cooling (FC) at 600 G; Fig. (b): B_{ext}=-600 G after (a); T=6 K). In the images, white color represents one direction of flux, and black indicates the opposite direction of flux. This behavior of superconducting magnet properties is detrimental to technical applications. Avalanches of thermomagnetic flux during a jump in the external field (0 G → 600 G) are not observed in the shielding mode at such a temperature. **3.** Analysis of rough flux fronts allowed the determination of the range of their roughness exponent α (0.44÷0.48) and Hausdorff dimension (1.52÷1.56) for magnetic induction levels of 150÷600 G. The roughness exponent α is derived from the slope of the power spectrum log$S(k)$ versus log(k) [3]. A comprehensive study of induction profiles at the boundary of the Meissner state and behind the flux front at different levels was conducted. The analysis suggests that if we assume the fractal nature of the flux front, then the SC system in the case under consideration follows the model of dynamic stochastic disorder [4]. Other aspects of field penetration into SC were discussed.

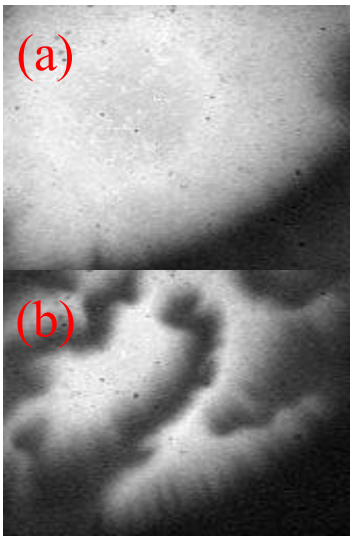

References

[1] Ch. Jooss, J. Albrecht, H. Kuhn, S. Leonhardt, H. Kronmuller, Rep. Prog. Phys. **65,** 651 (2002).
[2] L.D. Cooley, L.R. Motowidlo, Supercond. Sci. Technol. **12**, R135 (1999).
[3] V. Vlasko-Vlasov, U. Welp, V. Metlushko, G. Crabtree, Phys. Rev. B **69**, 140504(R) (2004).
[4] M. Kardar, G. Parisi, Y.-C. Zhang, Phys. Rev. Let. **56**, 889 (1986).

Abstract ID: 1529

TRANSPORT PROPERTIES OF MgB_2/Fe SMALL MONO-CORE WIRES FABRICATED BY MAGNETIC INDUCTION

M. Akdoğan, A. Rajab Ahmed, B. Albayrak

Abant Izzet Baysal University, Dept. of Physics, 14280, Bolu, TURKEY
E-mail: akdogan_m@ibu.edu.tr

Iron sheathed MgB_2 mono-core wires with an outer diameter of 1.80 mm were fabricated using an in-situ PIT method. We applied a magnetic induction heat treatment process with different time intervals, starting from 2 min to 20 min, and different temperatures, starting from 800 °C to 950 °C, to obtain suitable superconducting phase. We used ~2.5 cm long MgB_2/Fe wire and tested it in a helium gas-contact Cryo-Industries cryostat system. T_c^{onset} value of the mono-core MgB_2/Fe wire was 36.4 K with a ΔK=1.1 K transition temperature range for 800 °C-2 min sample (sample A). The critical current values were measured at 25 K under applied magnetic field strengths of up to 7 T. We observed 26.34 A/cm^2 critical current value at 25 K under $\mu_o H$ = 3 T for sample A.

Abstract ID: 262

OPTOELECTRONIC PROPERTIES OF ORGANIC THIN FILM Al/N-Si/ZnCo2O4/TPA-DA-IPA/Al HETEROJUNCTION

Şükrü Çavdar[1], Pınar Oruc[1], Haluk Koralay[1], Serkan Eymur[2], Nihat Tuğluoğlu[2]

[1] *Ankara, Turkey Advanced Technologies, Gazi University, 06500 Ankara, TÜRKIYE*
[2] *Department of Energy Systems Engineering, Faculty of Engineering, Giresun University, 28200 Giresun, TÜRKIYE*
E-mail: sukru.cavdar@gmail.com

Organic semiconductors offer numerous advantages in diode manufacturing due to their variable electrical properties, flexibility, and cost-effective production processes. In this research, the organic compound TPA-DA-IPA (tetramethyl 4,4'-(((1E,1'E) -((phenylazanediyl)bis(4,1-phenylene))bis(methaneylylidene))bis(azaneylylidene)) disophthalate; C40H33N3O8) was utilized for the Al/N-Si/ZnCo2O4/ TPA-DA-IFA/Al Schottky structure. The impact of TPA-DA-IFA on the electrical properties provide many advantages in diode fabrication due to their variable electrical properties of the produced diode was investigated through current-voltage measurements conducted in both dark and under various illumination intensities. Key electrical parameters such as barrier height (ϕ_B), ideality factor (n), series resistance (Rs), and interface state density (Nss) were derived from the I-V characteristics. Additionally, the fabricated device displayed photodiode behavior, as evidenced by photodiode behavior, as evidenced by photocurrent measurements that varied with illumination intensity. İt was observed that the Al/N-Si/ZnCo2O4/ TPA-DA-IFA /Al diode generated a higher photocurrent under illuminated conditions compared to dark conditions. These findings collectively suggest that the Al/N-Si/ZnCo2O4/ TPA-DA-IFA /Al diode holds potential for optoelectronic device applications.

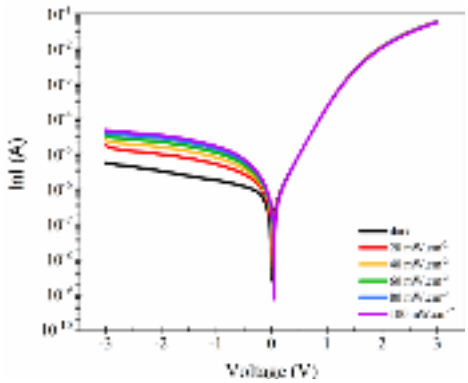

Fig. 1: *Current-voltage measurements of Al/N-Si/ZnCo2O4/ TPA-DA-IFA/Al heterojunction diode*

Abstract ID: 1540

STRUCTURAL AND MAGNETIC PROPERTIES OF (Co/Eu) DOPED ZnO NANOPARTICLES

Y. Kandil[1], A. Guler[1], C. Boyraz[2], L. Arda[3]

[1] *Marmara University, Department of Electrical and Electronics Engineering, Faculty of Technology, Marmara University, 34854, Maltepe, Istanbul, TURKEY*
[2] *Marmara University, Department of Mechanical Engineering, Faculty of Technology, 34854, Maltepe, Istanbul, TURKEY*
[3] *Bahcesehir University, Department of Mechatronic Engineering, 34349 Istanbul, TURKEY*
E-mail: lutfi.arda@eng.bau.edu.tr

We investigated the annealing effect of Cu and Eu-doped ZnO nanoparticles synthesized by the sol-gel technique [1]. A step-like heat treatment was applied to the obtained samples at 450 ^{0}C for 10 minutes and at 630 ^{0}C for 30 minutes. Through the X-ray diffraction technique, the structural phase properties were revealed, and Rietveld analysis was performed to figure out both nano and microstructural parameters. Microstructural parameters were also obtained using theoretical equations. The morphology of the samples was also studied by Scanning Electron Microscopy technique. Detailed magnetic measurements were performed for variation of magnetization under constant temperature (M-H). The temperature dependence of magnetizations (M-T) was also provided from low to room temperature to reveal the magnetic response of the studied samples.

References

[1] A. Guler, L. Arda, N. Dogan, C. Boyraz, E. Ozugurlu, Ceram. Int., **45(2)**, pp. 1737-1745 (2019).
[2] C. Boyraz, N. Doğan, L. Arda, Ceram. Int., **43**, pp.15986-15991 (2017).

Abstract ID: 1541

THE IMPACT OF DEFECTS ON STRUCTURAL AND MAGNETIC PROPERTIES IN Y/B CO-DOPED ZnO NANOPARTICLES

S. Veziroğlu[1,2] K. Özdoğan[1], L. Arda[3]

[1] *Yildiz Technical Üniversity, Department of Physics, 34220 Esenler, İstanbul, TURKEY*
[2] *Marmara University, Faculty of Science, Department of Physics, 34722 Istanbul, TURKEY*
[3] *Bahcesehir University, Faculty of Engineering and Natural Sciences, Department of Mechatronic Engineering, 34353, Besiktas, Istanbul, TURKEY*
E-mail: lutfi.arda@eng.bau.edu.tr

The sol-gel method was used to synthesize $Zn_{0.95-x}Y_xB_{0.05}O$ (x=0.00 to 0.05 with a 0.01 increment) nanoparticles. The effect of defects formed during synthesis in Y/B doped ZnO nanoparticles on their structural, and magnetic properties was investigated [1-2]. The X-ray diffraction method was used to provide the structural analysis. It was observed that all Y/B co-doped ZnO nanoparticles are single phases. The Scanning Electron Microscope (SEM) and electron dispersive spectroscopy (EDS) was used to investigate the surface morphology, shapes, size, and elemental compositions of the Y/B co-doped ZnO nanoparticles. Magnetic properties of $Zn_{0.95-x}Y_xB_{0.05}O$ nanoparticles were investigated by a Quantum Design Physical Property Measurement System. Positron annihilation lifetime spectroscopy were used to study the defect type and density of Y/B co-doped ZnO nanoparticles The study presents the influence of defects formed in Y/B co-doped ZnO nanoparticles with varying doping ratios, synthesized via the sol-gel method, on their structural and magnetic properties.

References

[1] L. Arda, J. Magn. Magn. Matter., **475**, pp. 493-501 (2019).
[2] S.D. Senol, E. Ozugurlu, L. Arda, J. Alloys Compd. **822**, 153514 (2020).

Abstract ID: 1542

THE INFLUENCE OF DEFECTS ON THE STRUCTURAL, MAGNETIC, AND PHOTOCATALYTIC PROPERTIES OF Mg/Fe CO-DOPED ZnO NANOPARTICLES

K. Senturk[1], L. Arda[2]

[1] *Istanbul Gelisim University, Department of Mechatronics Engineering, 34310, Istanbul, TURKEY*
[2] *Bahcesehir University, Faculty of Engineering and Natural Sciences, Department of Mechatronic Engineering, 34353, Besiktas, Istanbul, TURKEY*
E-mail: lutfi.arda@eng.bau.edu.tr

Mg/Fe co-doped ZnO nanoparticles were successfully synthesized via the sol-gel technique to investigate the impact of defects on their structural, magnetic, biological, and photocatalytic characteristics [1-2]. Through X-ray diffraction analysis, the formation of single phases exhibiting ZnO wurtzite hexagonal structures was confirmed. Surface properties, particle size, and shapes of the nanoparticles were examined using scanning electron microscopy. Elemental compositions were determined with insights provided by electron dispersive spectroscopy. Photoluminescence spectrophotometry was employed to explore defect types and assess crystal quality. SEM images revealed dense, quasi-spherical, and agglomerating magnifications of the Mg/Fe-co-doped ZnO nanoparticles. To evaluate photocatalytic activities and blood compatibilities, photocatalytic degradation tests of crystal violet (CV) and hemolysis tests were conducted, respectively. Furthermore, comprehensive magnetic measurements were performed to analyze the variation of magnetization under constant temperature (M-H) and to investigate the temperature dependence of magnetizations (M-T), spanning from low to room temperature, to uncover the magnetic response of the samples under study. The study elucidates the effects of defects in Mg/Fe co-doped ZnO nanoparticles, synthesized using the sol-gel method with different doping ratios, on their structural, magnetic, biological, and photocatalytic properties.

References

[1] L. Arda, J. Magn. Magn. Matter., **475**, pp. 493-501 (2019).
[2] S.D. Senol, E. Ozugurlu, L. Arda, J. Alloys Compd. **822**, 153514 (2020).

INDEX LIST

A

Aarts
Jan 454
Abaloszew
A. 748
Abaloszewa
I. 748
Abbas
Arouba.....662, 674
Yasir.....429
Abbasi
Irsa Kanwal 663
Abdallah
A. M. 425
A.M. 423, 424
Abdioglu
Murat.....288, 620
Abdkader
A. 700
Abdulkadirova
N.Z. 708
Abdullaeva
Sh. S. 665
Abdullah
Ali 625
Abdullo
Ahadov 741
Abdulloyev
J.S.....742
Abel
Mathieu 104
Abert
Claas 115, 502
Abin
D. 682
Acet
M. 489
Adams
Jeremy 278
Addamane
Sadhvikas J.....61
Adler
S. 457
Adolff
Christian F.....381
Affronte
M. 202, 611
Afzal
Hasan.....723, 739
Agapov
N.N. 651
Agarwal
T. 737
Agterberg
D.F. 211
Aguilà
David 194
Ağaoğulları
Duygu 636
Ahangaran
Zahra Gholami.... 367
Ahmed
A. Rajab 749
Aichner
B. 118
Aka
C. 615
Akashi
R. 348
Akay
L. Nur..... 368, 373
Akça
G. 614, 616
Akdoğan
M. 749

Å

Åkerman
J. 33, 385, 389

A

Akgöl
O. 615
Akramov
M. 372
Aksenov
S. 352
Aksoy
C. 686
Canan 639
Akyol
M. 615, 616
Aladyshkin
A. Yu. 362
Albayrak
B. 749
Albrecht
M. 592, 593
Manfred 509
Alcalà
J. 119, 337
Aldica
G. 395
Alekseev
Pavel A.....464
Aleman
A. 389
Alexandru-Dinu
Andrei Alexandru 438
Alfonsova
A. 725
Ali
Q. 265
Aliev
A.M..... 493, 708
Alimenti
A. 518
Allen
Elle 278
Portia..... 61
Al-Mokdad
F. Al 445
Alp
T. 182
Althammer
M. 132
Alvarez-Alonso
Pablo Alvarez..... 303
Álvarez-Alonso
P. Álvarez 492
Amaveda
H. 634
Amelichev
V. 540
Amemiya
N. 73, 538
Anane
A. 497
Anar
Kerem..... 260
Anas
M. 684
Andreev
Pavel..... 604
S. 666
Angelis
M. De..... 335
Angurel
L.A. 149, 445, 634
Luis A..... 150
Anikin
A. 294
Anis-ur-Rehman
M. Anis 429, 617, 623, 658, 659, 660, 661, 662, 663, 671, 674, 675, 676, 677
M. Anis-ur . 429, 617, 623, 658, 659, 660, 661, 662, 663, 671, 674, 675, 676, 677
Anlage
Steven M. 94, 121, 215
Anthofer
D. 56
Antonov
V.N. 584
Arda
L. 428, 751, 752, 753
Ardavan
A. 87
Ariando
Ariando 571
Aridi
A. 423
Amani.....672, 717
Aristov
D.N. 269
Armenio
A. Angrisani..... 335
Aromí
Guillem..... 194
Arregi
J.A. 110
Arroyo-Fructuoso
A. Arroyo..... 108
Arutyunov
Konstantin Yu..... 578
Arzeo
M. 457
Asano
S. 474
Y. 460
Askerbeyli
R.T. 679
Askerzade
I.N.Askerzade..... 420
Astafiev
O.V. 584
Atilmis
M.N. 711
Atkinson
W.A. 37
Atlı
Eren..... 404
Augieri
A. 335, 518, 534, 691
Autieri
Carmine 144
Avcı
Doğan..... 400
Avci
Can Onur..... 136
Avdoshenko
S.M.....195, 207
Avola
Carl..... 278
Awad
A.A. 33, 385, 389
R. 423, 424, 425, 426, 672, 684
Ramadan..... 717

Awaji
S. 283
Awoga
O.A. 248
Oladunjoye A. 244
Ayala
C. 90
Ayaş
A. Osman 614, 616
Aydogan
B. 373
Aygit
E. 182
Azam
Mohammad 692, 693

B

Babij
Michal 400
Babu
Ashna 683
Back
C. 392, 592
Tyson 405
Backmeister
L. 108, 118
Badcock
Rodney 278
Badel
A. 283
Badger
J.R. 351
Badía-Majós
A. Badía 149, 150, 288
Antonio Badía 150
Badica
P. 395, 401, 518
Petre 401, 438
Bael
M.J. Van 186, 256
Bai
Hao 626
Y. K. 561
Baigutlin
D. 292
Bajas
H. 534
Hugues 278
Bal
M. 184, 476, 700
Balakrishnan
Geetha 502, 510
Balcells
L.L. 119
Ll. 110, 140
Balédent
V. 156
Ball
Steven 619
Baloochi
M. 700
Bandur
D. 325
Banerjee
Souvik 648
Bansal
Bhavtosh 723, 739
Baptiste
B. 477
Barba
L. 321, 335, 691
Barbosa
Matheus 724
Barišić
Neven 25
O.S. 547
Barra
A. L. 87
Barrera
A. 110, 119, 140, 337
Barrios
Leoní A. 194
Bartha
Cristina 438
Bartkowiak
M. 163, 376
Basov
S. 186
Batov
I.E. 448
Battistelli
R. 329, 499
Riccardo 509
Batulin
R. 399, 682
R.G. 145, 726, 728
Bazarnik
M. 243
Beach
G.S.D. 383
Beckmann
B. 494
Beiranvand
Razieh 681
Belenli
İbrahim 400
Belkhou
Rachid 502
Belyaev
V.K. 294
Belzig
Wolfgang 93
Bendeliani
B.G. 635
Bending
S. 110, 140
S.J. 513
Beneke
G. 128
Béneut
K. 477
Benfatto
L. 522
Benhabib
S. 37
Benzing
Jake 278
Bera
Arnab 723, 739
Satyabrata 723, 739
Berger
C. 465
D. 736
H. 347
Bergmann
K. von 205, 243
Bessais
L. 600
Bestha
K.K. 727
Betouras
J. 221
Bian
M. 167
Billington
D. 511
Birch
M.T. 391, 510
Max 502, 510
Birge
N.O. 383, 458
Noman O. 458
Black-Schaffer
A.M. Black 248
Blanco
J.A. 147
J.M. 299, 480
Jesús A. 303
María Valeria 473
Blatter
Gianni 461
Bobkov
A.M. 449, 450, 452
G.A. 419, 449, 452, 453
Bobkova
I.V. 419, 449, 450, 452, 453, 462
Bocklage
Lars 381
Bodenseher
A. 287
Alexander 151, 536
Bohorquez
L.T.C. 727
Bokai
K.A. 419
Bondarenko
Vladimir I. 65
Bonifetto
R. 534
Bonizzoni
C. 202, 611
Borisov
A. 530
Borth
R. 210
Bort-Soldevila
N. Bort 110, 140
Bostrem
I.G. 319
Bouchard
B. 279
Boudissa
M. 642
Boulle
O. 507
Bouthillette
A. 279
Boyraz
C. 428, 751
Bozat
O. 373
Bozbey
A. 414, 420, 421
Bożek
Rafał 144
Bozin
Emil 222
Božović
Ivan 10
Boztemur
Burçak 636
Böhm
D. 265
Bötzel
S. 567
Bragagni
A. 534
Braggio
A. 28, 189
Brahim
K. 256
Braithwaite
D. 209, 214
Brando
M. 210
Braunecker
Bernd 114
Brems
M. A. 128
Breschi
Marco 433, 542
Breslavskaya
N.N. 206
Brownell
Elizabeth 278
Brunner
Daniel 278
Bruyant
N. 37
Buchelnikov
V. 292, 301, 439
V.D. 314, 488, 495
Bud'ko
Sergey L. 375
Budniak
A.K. 259
Buechner
B. 727

Buke
Goknur Cambaz . 404, 405
Bunkov
Yu. M. 371
Burghard
M. 391
Marko 510
Burmistrov
S.N. 310
Bussmann-Holder
Annette Bussmann 42
Butch
Nicholas P. 215
Buzdin
A.I. 458, 528
Büchner
Bernd 32, 639
Büchnera
B. 725
Büttner
F. 261, 329, 383, 499
Felix 509

C

Caeyers
J. 186
Caglayan
R. 313
Caglieris
F. 736
Cahay
Marc 405
Cai
Jingnan 94
Calderón
María José 107
Campi
G. 202, 321, 335, 611, 691
Campo
Javier 473
Cano
A. 184
Cao
H.B. 351
Carlton-Jones
Arthur Carlton 215
Carpentieri
M. 123, 124, 313, 387
Carrillo-Cabrera
Wilder Carrillo 115
Castellani
C. 522
Castro
C. Di 322
Catarino
I. 686
Cavdar
S. 713, 714, 715
Caylan
Omer Refet 404
Celentano
G. 335, 518, 534, 691
Celik
S. 445
Cesari
E. 482
Cetner
Tomasz 692, 693
Chabanenko
V.V. 748
Chajewski
G. 211
Chakrabortty
S. 444
Chamberlain
Sarah 278
Chan
M. K. 36
Chang
X. 734
Xiao 729
Chatterjee
Sudipta 723, 739
Chaurasiya
A.K. 389
Chavarria
David 278
Chaves
D.A.D. 256
Che
P. 31, 111, 286, 497, 716
Cheetham
Peter 542
Cheghabouri
A. Mousavi 263
Arash Mousavi 261
Chen
Chien Te 704
G.F. 252
J. 27, 477
Wei 550
Xi Rong 550
Cheng
C. 722
H. P. 27
J.L. 226
JL 278
Cheong
Sang Wook 704
Cherednichenko
S. 257
Cheremin
V. 530
Cherif
Chokri 700
Chernyshev
A.L. 160
Cherosov
M.A. 726
Chiarelli
S. 534
Chikurov
D.S. 332
Chirolli
L. 28, 189
Cho
Soohyun 101
Choi
Deung Jang 205
Hyo Sang 694
Hyosang 695
Chow
Calvin C. T. 79
Chowdhury
Rajeswari R. 737
Chu
Yen Yi 704
Chumak
O.M. 748
Chumlyakov
Y. 482
Chupakhina
T.I. 145, 726
Churikova
A. 383
Cichorek
T. 211, 525
Cindro
N. 207
Cole
Haley M. 523
Collienne
Simon 331
Colombo
G. 534
Colque
Julio 278
Colson
D. 37
Comanescu
Cezar 438
Confalone
T. 736
Conte
R. Lo 243
Cools
I. 186
Corato
V. 534
Córdoba
R. 108, 115
Coronado
E. 27, 83, 207, 317
Corredora
L.T. 725
Corte
A. della 534
Coskun
Elvan 620
Costa
S. 686
Cova
Federico H. 473
Craighill
Christopher 278
Crisa
F. 184
Crisan
A. 356, 514, 515, 518
Crittenden
Scott 577
Crivillers
N. 203
Croitoru
M.D. ...526, 527, 528, 743
Cros
V. 263, 497, 507
Vincent 128
Croteau
A. 279
Cubukcu
M. 259
Culbertson
C. 465
Cunill-Subiranas
J. Cunill 110, 140
Cunningham
J.E. 264
Czaja
P. 485

Ç

Çamsarı
Kerem Y. 123
Çavdar
Şükrü 750
Çelik
M. Eren 95, 177
Çetin
S. Kılıç 614

D

Dabrowski
M. 259
Dadhich
A. 77
Dai
Xi 628
Daibo
M. 230
Damatopoulou
Tatiana 295
Danilov
G.E. 440
Danilyuk
A.L. 224
Darwin
E. 505
Das
D. 241, 376
Soham 723, 739
Dausy
H. 186
Davenport

K. 173, 581
Davies
Mike.....278
Debnath
Tuhin.....723, 739
Deenen
A. J.M.....111
A.J.M.....747
Deeva
Yu.A. 145, 726
Degiorgi
L. 575
Degtyarenko
A. Yu. 649, 656
A.Yu. 68, 70
Alena Yu.....65, 621
P. 540
Deinhart
V. 499
Delaporte
M. Jasiurkowska 316, 318
Delforge
C. 55
Delice
S. 710, 718
Del-Valle
N. Del.....110
Demsar
J. 38, 152
Denawi
Adam Hassan.....104
Dennis
A.R. 638
Desplat
Louise 498
Despoja
V. 412, 554, 629
Vito.....554
Devitre
A.R. 535
Dgebuadze
G.N.....635
Diamantini
M.C. 11
Diaz-Pacheco
Rui Diaz.....278
Diduszko
Ryszard 693
Diko
P. 443
Dimino
A. 279
Djuraev
D.R. 742
Djurayev
D.R. 240
D.R.Djurayev.....670
Dkhil
B. 600
Dolgos
M. 465
Domagala
Jaroslaw..... 144
Domański
T. 248
Donadze
G.J..... 646
Donez
Kai..... 278
Dong
Q. X..... 252
Yiqing..... 626
Donnelly
Claire 115, 502
Donner
W. 494
Dorsch
E. 610
Douar
Hakim 733
Drung
Dietmar 194
Du
Chao Hung..... 704
Kai..... 704
Duan
Y. 27, 83
Dubinin
Mikhail..... 284
Dubovskii
L.B..... 310
Duchenko
A. 691
Duke
Owen..... 278
Dular
J. 638
Duong
Daniel 577
Dupé
Bertrand 498
Durão
D.M..... 686
Durrell
J.H..... 638
Dutta
S.Dutta..... 522
T. 505
Dziarmaga
Jacek..... 120

E

Eaton
A.G..... 213
Eda
G. 259
Efimov
N.N. 206
Efremov
D.V..... 221
Egger
R. 411
Eggert
B. 494
Eginligil
M. 272
Egorov
S.V. 448
Eisebitt
S. 329, 499
Eisterer
M. 287
Michael151, 536, 639
Ekicibil
A. 614, 616
Elatresh
Sabri 50
Eley
Serena 61
Elharkati
Hiba..... 679
Elson
F. 466
Emelyanov
A.E. 651
Engel
D. 499
Engert
S. 180
Eo
Yun Suk..... 215
Eremin
Ilya M. 176, 567
Eremina
R.M..... 726, 728
Ermakov
A.B..... 610
Ertekin
Ercan 79
Eshonkulov
E.B. 646
Espenhahn
T. 700
Evans
W. 27, 83
Evcimen
Sera 278
Eymur
Serkan 750

F

Faciof
J.I. 725
Fagnard
J.F. 638
Fähler
S. 488
Failde
D. 709
Fang
Junyang 441
Fatema
Mehroosh..... 298
Fayziyev
Sh.Sh.Fayziyev 670
Fazlizhanov
I.I. 728
Fazlizhanova
D.I..... 145
Febvre
P. 414
Feldman
S. 581
Feng
J. 606, 607
Zhenjie 706, 707
Fermin
Remko..... 454
Fernandez-Pacheco
Amalio Fernandez 115
Fernández-Pacheco
A. Fernández 502, 503
Fernández-Rodríguez
A. Fernández 119, 331
Ferreira
Marina Raboni ... 502
Fert
A. 128, 263, 507, 509
Fetisov
S. 699
Filippov
Timur V. 95, 177
Finizio
Simone 502
Finocchio
G. 123, 124, 313, 387
Fischbacher
J. 265
Fischer
D. 531
D.X. 531, 535
Z.L. 535
Fistul
Mikhail V. 176
Fitta
M. 316, 318
Flatté
M.E..... 13
Follows
Frederick 619
Fomin
V.M. 12, 747
Vladimir M. 115
Forget
A. 37
Formichetti
A. 534
Forslund
O.K. 466
Forton
E. 276
Fourie
C. 414
C.J.....191, 414, 418, 655
Coenrad J. 655

Fourneau
E. 55, 110, 119, 140, 149
Emile..... 150, 331
Foury
P. 156
Förster
J. 380
Fracasso
M. 517
Francis
Ashleigh 226, 278
Frechilla
J. 149
Javier 150
Freda
R. 534
Freeman
C.W.F. 259
Friedemann
S. 513
Fry
Vinny 278
Fu
Ying Shuang 198
Fuente
G.F. de la.... 149, 445, 634
Germán F. de la .. 150
Fujimori
Atsushi 704
Fujita
Kazuhiro..... 40
M. 22, 474
S. 230
Fukami
Shunsuke 133
Fukushima
K. 255

G

Gabunia
V.M. 635
Gaggioli
Filippo 461
Gaifullin
M. 530
Gaita-Ariño
A. Gaita .. 27, 83, 207, 317
Gajda
Daniel 400
Galaktionov
A.V. 580
Gallardo
R.A. 391
Galluzzi
A. 356, 514, 515, 519
Gambardella
Pietro 17
Gambarella
S. 87
Gambino
D. 531
Davide 536
Gamzatov
A.G..... 495, 708
Adler 493
Gan
Zizhao 394
Gandolf
J. 567
Ganiev
O.K..... 239
Gao
Weiguang 34
Garcés
Ot 594
García
P. Vidal 518
García-Pons
D. García..... 57, 112
Gardew
Derejaw 687
Garescì
F. 124
Garst
M. 31, 309, 497
Gas
Katarzyna..... 144
Gati
Elena..... 341
Gauzzi
A. 340, 477
Gavriliuk
A. 352
Gavrilkin
S. 540
S. Yu..... 656
S.Yu..... 66
Gawryluk
Dariusz..... 344
Gazquez
J. 337
Ge
Jun Yi 603
Juniy 621
Geibel
C. 210
Gelgorn
A.V. 703
Gella
Diego 194
Gencer
A. 3, 445
Ali 620, 639
Gerbaldo
R. 517
Geresdi
A. 186
Gerhards
P. 128
Gerlinger
K.Gerlinger 499
Geshkenbein
Vadim B. 461
Geuzaine
C. 638
Ghiami
Amir 47
Ghigo
G. 517, 518
Ghirri
A. 202, 611
Ghorbani
Fatemeh 47
Giazotto
F. 28, 189
Gigli
L. 691
Gilioli
E. 477
Gilmutdinov
I. 37
Giordano
A. 124
Gironcoli
S. de 412
Gladilin
Vladimir N. 603
Godeke
A. 275
Arno 433, 542
Godinho
J. 392
Gok
O. 711
Goldobin
E. 118, 181
Golenić
N. 412, 554
Golfinopoulos
Theodore..... 278
Golikova
T.E. 448, 578
Gollwitzer
Jakob 381
Golubov
A.A..... 415, 416, 449, 450, 453, 460, 462
Gomez
L. 187
Gomonay
O. 383
Gondek
Łukasz..... 643
Gonzalez
V. 385
González
C.A. 57
Gorria
P. 147, 303
Pedro..... 303
Goryacheva
O.A. 304
Goswami
Partha..... 141
Gouéré
D. 497
Goukassov
A. 470
Goyal
Amit 14
Gozzelino
L. 517
Graham
J.N. 376
Grassellino
A. 184
Grebenshchikov
Yu.B. 440
Greenberg
Aliya 278
Greer
J.A. 383
Grenèche
J M. 600
Grigoriev
S.V. 269
Grigoroscuta
M. 395
Mihai 438
Grimaldi
A. 123, 124, 387
G. 514, 515, 519
Grinenko
Vadim.....345, 363
Grovenor
Chris 619
Grozić
P. 548
Grundler
D. 31, 111, 497, 747
Gruner
M.E.....488, 494
Grzybowski
Michał J. 144
Gu
G.D. 736
Gubina
A. 165
Gudoshnikov
S.A. 440
Guennic
Boris Le 194
Guguchia
Z. 97, 102, 340, 376
Zurab.....97, 344
Guittoum
A. 147, 642
Gulamov
T.I. 646
Gulamova
D.D. 646
Guler
A. 751
Gumarov
A. 399
Guner
S.B. 395, 445
Gunes

H. Alper.....421
Guo
Chen 394
H. 111
Gupta
Deepnarayan 95, 177
Ramesh.....278
Guravova
A.V. 416
Gurevich
A. 294
Gurpinar
Erhan 405
Gurskiy
Anatoly S.....578
Gusenbauer
M. 265
Gutfleisch
O. 494
Güdücü
G. 645
Gülnur.....647
Güler
Zişan 404
Güner
Sait Barış.....401
Güngüneş
Ç. Dönmez 719
H. 710, 718
Günkel
T. 119, 337
Günther
C.M. 329, 499

H

Haase
J. 325
Habanjar
K. 423, 424, 425, 684
Khulud 426, 672
Habib
Mustapha 95
Hadj
Ailam El.....733
Hadjout
Larbi.....733
Haghighirad
Amir Abbas 47
Hahn
Horst.....174
Haidar
M. 602
Han
Jiahao 133
Tae Hee.....696, 697, 698
X.F. 722
Hanisch
D. 181
Hänisch
J. 154
Hanstorp
D. 389
Hara
H. 538
Harb
O.J.Y.....256
Harmant
A. 275
Harrabi
K. 91, 735
Harrison
N. 36
Hartwig
Z. 531
Z.S. 535
Harvey
J.S. 351
Hase
I. 312
Hasegawa
Y. 30, 90, 199
Hasekioglu
Atilla 23
Orkun 23
Hashimoto
Katsushi 193
Hassinger
E. 210
Hasuo
S. 530
Hata
S. 30
Hatefi
Maryam 367
Hattar
Khalid 61
Hauck
D. 309
Hayami
S. 86
Hayashi
Kazuhiko 436
Hayes
Ian 215
Hayn
Roland 104
Hegg
Anthony.....334
Heller
Sam.....278
Hellwig
O. 392
Hemmous
M. 147
Herbut
Igor 546
Herman
F. 740
Heydarinasab
Zahra 367, 556
Hicken
R.J. 259
Hicks
Matt 278
Hidayati
Rahmatul..... 253
Higashikawa
K. 236, 280, 436, 543
Kohei 436
Hill
S. 27, 83, 207, 317
Stephen 27
Hillebrands
B. 20
Hinkove
V. 725
Hirano
Naoki 436
Hirata
W. 230
Hiroi
K. 469
Hitti
B. 466
Hlawacek
G. 108
Hoffman
S. 27
Hofmann
David 151
Holenstein
Manuel 278
Holmvall
P. 248
Holobrádek
Jakub 588
Holzapfel
B. 154
Hong
Fang..... 219, 349
HONG
Fang..... 349
Hosoda
Hideki 290
Hosono
H. 30, 376, 398
Hossain
M. 700
Hosseini
M. 746
Hou
Jinning 334
Qiang..... 71, 569
Houbart
M. 638
Houtput
M. 238
Hovorka
Ondrej 510
Höflich
K. 499
Hrabec
Aleš 589
Hristoforou
Evangelos 295
Hruby
J. 83
Hrubý
J. 27
Hu
Bin..... 85
Fengxia..... 708
W. 18, 272, 329
Y. 255, 330, 631
Yong 631
Hua
Weicheng 473
Huai
C. 167
Huang
Di Jing.....330, 704
Hsiao Yu 704
Silu 577
Hubbard
Amanda..... 278
Hug
H.J. 505
Hans Josef 509
Hughes
Annie..... 278
Hunt
R.G. 264
Hunze
Arvid..... 278
Hur
Karyn Le 744
Husain
Shahid 298
Hussain
A. 77
Hutt
R. 118
Hübers
H. W. 257
Hühne
R. 700

I

Iacob
Nicu..... 438
Ianovskaia
A.S. 419
Ibragimov
I. 410
Ibusuki
K. 280
Igarashi
D. 469
Iglesias
Ò. 709
Òscar..... 594
Iida
K. 30
Iijima
Y. 230
Ilina
A.D. 689, 690
Illige
T. Newhouse 383

Ilyukhin
A.B. 206
Imamura
K. 280
Ioannidis
Ioannis 244
Ionescu
A. 515
A. M. 356, 514
A.M. 356, 395
Ipatov
M. 299, 480
Irfan
M. 722
Isaevaa
A. 725
Isber
S. 425
Ishida
Shigeyuki 360
Ishii
A. 30
Islam
S.S. 376
Itahashi
Y. 178
Ito
Tatsuya 486
Ivan
I. 356, 514, 515
Ivanov
N. 732
Iwasa
Y. 178, 737

J

Jackman
K. 191
Jaffrès
H. 128
Jakovac
Josip 629
Jang
Dae Seong 694
Jangid
S. 446
Jardine
M. Ameen 655
Jastrzębski
Cezariusz 643
Javed
K. 722
Jeng
Horng Tay 704
Jenni
Markus 278
Jiang
Ruoshi 334
Wanjun 135, 626
Wei 62
Zhicheng 101
Jin
L. 418, 606
Rongying 577
Joshi
Piyush 278
Shresht 278
Jungxiang
Yao 454
Juraszek
J. 211, 525
Jurczyk
J. 503

K

Kaczorowski
D. 211
Kaderov
V. 732
Kadigrobov
A.M. 548
Kadirbardeev
A.T. 493
Kadlec
C. 41, 740
Kahsay
Gebregziabher 687
Kaibi
A. 147, 642
Kainuma
Ryosuke 486
Kakimoto
K. 230
Kakudate
Toshiyuki 193
Kaleta
Anna 144
Kalimuddin
Sk 723, 739
Kamiyama
T. 476
Kammerbauer
F. 56
Kandemir
A. 616
Kandil
Y. 751
Kanj
A. El 497
Kapon
Y. 56
Kar
S. 701
Karaaslan
M. 615
Karabassov
T. 416, 450, 462
Karaboğa
Fırat 400
Karadeniz
B. 207
Karaman
Tamer 509
Karami
Mohammad 367, 556
Karrer
M. 118
Kashcheev
Andrey 284
Kataev
V. 168, 195, 725
Kataeva
V. 725
Kataria
A. 737
Katmış
Ferhat 260
Kato
Yusuke 60
Katoh
Keiichi 193
Kavkhani
Roya 260
Kawaguchi
Ryo 193
Kawamura
Y. 469
Kawashima
K. 64, 305, 312, 340
Kaya
D. 614
N. 713
Naki 712
Kazakova
O. 259
Keatley
P.S. 259
Kechouane
M. 147, 642
Kent
Andrew D. 29
Keran
B. 548
Kern
L. M. 499
M. 203
Khan
M.R. 519
Khanna
D.L. R. 492
Kharkov
A.M. 703
Khasanov
R. 97, 340, 376
Rustem 344
Khim
S. 210, 211
Khrapai
V.S. 573, 582
Vadim 582
Khymyn
R. 385, 389
Kiani
Haris Farooq 658, 664, 678
Kim
Ingon 619
Jaeyong 343
Jihye 695
Jin Hee 253
Junyeon 34
Kimura
Akio 484
Kinev
N.V. 610
Kinoshita
Yuto 486
Kirichenko
Dmitri E. 95, 177
Kiselev
Nikolai S. 501
Kishine
J. 59, 271, 272, 319
Jun ichiro 59
Kiss
Takanobu ...236, 280, 436, 543
Kitaguchi
Hitoshi 436
Kizilaslan
O. 610
Kläui
M. 128
Klauss
Hans Henning 339
Klavins
P. 351
Kleiner
R. 118, 181, 610
Klíma
Jan 588
Klimin
S. N. 238
Klimovskikh
I.I. 347
Klose
C. 329, 499
Christopher 509
Knobloch
K. 128
Ko
Seok Cheol .696, 697, 698
Kobayashi
H. 75
Kobiałka
A. 98, 248
Koch
D. 494
Kochetkovaa
E. 725
Koda
A. 469
Koelle
D. 118, 181, 418
D.Koelle 610
Koláček
J. 41
Kolb-Bond
Dylan Kolb 278

Kolotinskiy
N.V. 185, 654
Komaba
S. 469
Komal
Sumaira 671
Komeda
Tadahiro 193
Komiya
W. 90
Konczykowski
M. 211, 525
Kondo
Takahiro 398
Konstantinov
A.V. 651
Koo
H. J. 164
Kopera
L. 77
Koralay
H. 713, 714, 715
Haluk 750
Koraltan
S. 593, 597
Sabri 597
Korner
P.A. 118
Kornev
V.K. 185, 654
Koroteev
P.S. 206
Korshunov
M.M. 323
Koshelets
V.P. 610
Kostifakis
Nick 278
Kotani
Y. 511
Kováč
J. 77
Kovacs
A. 265
Kowalik
M. 187, 539, 652, 653
Kowalska
M. 485
König
Markus 115
Köse
Selçuk 456
Köstler
S. 362
Krajnc
A. 207
Krasavin
A.V. 527, 644, 743
Krasilnikov
A. 699
Krasnikova
Y. 184
Krasucki
Cezary 144
Kremer
R.K. 164
Kret
Sławomir 144
Krishnia
S. 128
Kronast
F. 383
Krsnik
J. 547
Kruk
Robert 174
Ku
Wei 334
Kubetzka
A. 243
Kucharova
V. 443
Kuchuk
O.I. 748
Kucukyilmaz
Emre 421
Kuncser
A. 395
Andrei 438
Victor 438
Kundu
A.K. 347
K. 27, 83
Kunwar
Shankar 361
Kupčić
I. 547, 558
Kurauchi
K. 271
Kurbakov
A.I. 139
Kurebayashi
H. 259
Kurmantayev
A.N. 608
Kurnaz
S. 645
Sedat 647
Kuroki
Kazuhiko 568
Kushwaha
R.K. 446
Kusunose
Hiroaki 59
Kuyubaşi
H. 718
Kuzmichev
S. A. 656
S.A. 66, 70, 656, 689, 690
Kuzmicheva
T.E.. 66, 70, 656, 689, 690
Kuzmin
V.I.Kuzmin 323
Kuznetsov
A.N. 68, 649
Sergey 278
Küß
Matthias 386
Kveder
M. 207

L

L'vov
Victor 290
Laamanen
Eric 278
Lahabi
Kaveh 454
Lakunov
I.S.448
Lamura
G. 340
Lanceros-Mendez
Senentxu Lanceros 290
Landaeta
J. 210
Lang
Eric J 61
W. 118
LaRoca
P. 492
Lasthofer
F. 265
Latyshev
A. 576, 585
Alex 585
Laviano
F. 517, 531
Francesco 536
Lebedev
S.G. 406
Lebrun
R. 497, 598
Leca
Aurel 438
Lechermann
F. 567
Ledda
F. 531
Lee
A. 325, 559, 563
Hunju 232
J. 127, 184
S. 40, 227, 530, 543
Shin Won 696
Y. 736
Leijnse
Martin 244
Lejeune
N. 55, 110, 149, 150, 186, 256
Lenz
K. 380
Leo
A. 514, 515, 519
N. 503
Leon
P Corte 299
Leonard
O. 110
Leupold
Olaf 381
Levchenko
S.V. 145
Levermore
G.J. 6
Li
A. 33, 385, 530, 543, 716
C. 103, 290, 361, 394, 606, 607
Dong Yang 716
J. 87, 243, 380, 494, 546, 606, 607, 612
Sheng 569
Tiefu 366
V.R. 646
Y. 159, 203, 255, 321, 702
Liao
Z.Y. 300
Lill
J. 494
Lim
Sung Hun 696, 697, 698
Lin
Ben Chuan 103
Jiunn Yuan 41
Shizeng 267
Lindackers
Dirk 639
Lindner
J. 380
Lipavský
P. 41
Litvinenko
A. 33, 385
Litzius
K. 329, 383, 391, 499, 510
Kai 509, 510
Liu
D. 630, 702
Fan 441
Fupin 724
G. 606
J. 87, 607
Timothy 278
X. 394, 606, 607
Zheng 308
Ljubicic
Paul 278
Llamazares
José L. Sánchez... 303
Llobet
Jordi 509
Lobzhanidze

T.E. 635
Locovei
C. 395
Claudiu..... 438
Long
J.R. 27
Lopez-Diaz
L. Lopez..... 264
López-García
J. López 492
Lorente
Nicolás 52, 82
Lorenzana
J. 522
Lortz
Rolf 307
Lostao
Anabel 194
Lotsch
B.V. 391
Lounis
B. 528
Lu
Li 169
Tzu Ming 61
Ludbrook
Bart 278
Ludwick
Jon 405
Ludwigs
S. 203
Luetkens
H. 97, 376
Luis
F. 27, 57, 112, 207, 317
Fernando 194, 317
Lukyanov
A.E. 527, 644, 743
Lupi
S. 477
Lupo
F. 457
Luszyński
Ł. 525
Lyakhov
A.D. 319
Lyssenko
K.A. 68, 164, 649
Lyubutin
I. 352
Lyubutina
M. 352

M

Ma
W. L. 561
X. 606
Yanwei 394
Maccari
I. 522
Maeno
Y. 255
Magen
C. 181
Magén
C. 118
Mahule
S. 669, 720, 721
Majozi
P.P. 595, 669, 721
Maksimov
Pavel A. 159
Maksutoglu
M. 611
Malevich
N. 732
Malhotra
Kara 278
Mali
G. 207
Mallah
T. 87
Maltseva
V. 666, 667
Malyavina
A. 540
Malyuk
A. 727
Mamniashvili
G.I. 646
Manasa
Manasa 692, 693
Manchon
A. 127, 136, 313, 599
Aurélien 127
Mandal
Hasan 5
Mandru
A. O. 505
Andrada Oana 509
Månsson
M. 466, 469
Mao
Ho kwang 21
Maraytta
Nour 47
Marbey
J. 27
Marchetti
M. 534
P.A. 336
Marinkovi
S. 149, 155, 186, 331, 337
Marinkovic
S. 149, 155, 337
Marinković
S. 331, 337
Stefan 331
Markovic
Nina 555
Martínez
E. 149, 634
E.Martínez 150
Marisel Di Pietro 502
Martínez-Blanco
D. Martínez 147
Martínez-Pérez
María José Martínez 57, 112, 194
Martini
M. 123, 578, 736
Martovetsky
Nicolai 278
Martucciello
N. 519
Marychev
P.M. 526
Maryyam
Arooba 260
Marzi
G. De 534
Mascot
E. 116, 243
Masdeu
F. 482
Masell
J. 506
Masi
A. 335, 518, 534, 691
Masuku
S.J.C 595
S.J.C. 668, 669, 720
Matrasulov
D. 146, 372, 411, 420
J. 410
Matsuki
Jun 54
Matsumura
T. 271
Matvian
I. 530
Matyakubov
H. 146
Matyunina
M. 301
M.V. 314
Mawass
M. 383
Mayoh
Daniel 510
Mayr
S. Mayr 380
Mazaj
M. 207
Mazhar
Haroon 617, 658, 661, 664, 678
McCormack
Colin 278
McGahn
D. 234
Mednikov
A. 699
Meena
P.K. 446
Meichsner
M. 181
Meier
Guido 381
Mekki
A. 91, 735
Melhem
Ziad 7, 431, 433, 542, 619
Menana
Hocine 74
Mentink
Johan 128
Menushenkov
A.P. 321, 644
Mercurio
A. 611
Merz
Michael 47
Mestres
N. 110, 119, 140, 337
Narcís 331
Metcalfe
Kristen 278
Metskhvarishvili
I.R. 635
M.R. 635
Metternich
Daniel 509
Miao
P. 156, 476
Ping 472
Michael
Phillip 278
Michalik
Jan Marek 643
Michele
C. De 522
Michelsen
Andreas Bock 114
Michioka
C. 466
Miclea
C.F. 356
Mielke
C. Mielke 97, 102, 376
Mila
Frédéric 163
Milosevic
M. 735
Miloševic
M.V. 91
Milošević
M.V. 513
Minasian
S. 27
S. G. 83
Minin
V.V. 206
Miniotaite
U. 466
Mironov
A. Yu. 49

Mironovich
A. 352
Miroshkina
O. N. 494
O.N. 488
Vlada V. 305
Miryala
M. 445
Mishchenko
A. 51
A.S. 238, 547
Mishra
Archana 244
Mitrofanova
Iu.A. 651
Miyake
Atsushi 486
Mliki
N. Thabet 600
Mochizuki
Masahito 54
Moeller
C. 180
Mogulkoc
A. 313, 680
Y. 313, 680
Mohapatra
N. 444
Moharana
A. 56
Mollahasanoglu
Hakki 620
Molnár
Tomáš 588
Molodyk
A. 227, 530
Mondal
Mintu 723, 739
Moore
T.A. 264
Mora
M. 634
Morawski
Andrzej 692, 693
Moriyam
K. 466
Morozov
I.V. . 66, 68, 649, 656, 690
Morr
D.K. 116, 243
Dirk K. 247
Morris
G.D. 466
O. 110
Morrow
R.C. 727
Moshchil
Viktor 639
Moshkina
E.M. 728
Motoky
T. 443
Motta
M. 155
Mou
Chung Yu 704
Mousavi
Tayebeh 619
Moustafa
H. 265
Mpaliou
Angeliki 295
Msomi
J.Z 595
J.Z. 668, 669, 720, 721
Mucchietto
A. 497
Mueller
Christoph 278
Markus 78
Mukhanov
Oleg 457
Mukhin
S.I.321
Muller
David 61
Muralidhar
S. 33, 389
Muratov
A.V. 66
Murthy
A.A. 184
Mustafa
Bassam M. 685
Yerzhan 456
Muto
S. 230
Muyeen
S.M. 436
Muzzi
L. 534

N

Nabiałek
A. 748
Nachtigal
J. 325
Nagar
Deepshikha Jaiswal 683
Nagasako
Makoto 486
Nagayama
R. 280
Nagel
Peter 47
Najem
Ahmad 684
Nakamura
J. 398, 469
M. 280, 530, 543
N. 230
S. 271
T. 73, 511
Namburi
D.K. 638
Nan
Tianxiang 129
Nandawadekar
A. 701
Nanjyo
H. 530
Narkowicz
R. 380
Nasimov
D.A. 49
Nasirli
B. 719
Navau
C. 110, 140
Nazarenka
A.A. 224
Nazhestkin
I.A. 448
Nealey
Justin 278
Neethirajan
Jeffrey 502
Nefedova
E.I. 305
Negussie
Tamiru 687
Nehruji
Vanessa 510
Neill
A. 465
Nekrasov
I.A. 64, 688, 738
Nemirovich
M.A. 305
Neverov
V.D. 527, 644, 743
Nevirkovets
Ivan 457
Ney
A. 380
Ngo
D. 27
Nicklas
M. 210
Nielsch
K. 488, 700, 736
Niewa
R. 525
Nigro
A. 519
Nikitchenkov
I.A. 689
Nikolaev
S.V.Nikolaev 323
Nikolaeva
A.N. 185
Ninomiya
H. 271, 340
Niyazov
L.N.Niyazov 670
Nouicer
A. 730
Novikov
M. 540
Novko
Dino 551
Novoselov
Kostya S. 461
Nowicka
B. 316, 318
Nsouli
B. 424
Nulens
L. 186, 256

O

Obata
K. 255
Ocampo
V. 709
Oda
Y. 280
Odintsov
V.I. 440
Oezelt
H. 265
Oezyilmaz
B. 734
Barbaros 729
Ogino
H. 340, 360
Hiraku 360
ogli
Amrullojon 741
Ogurtani
Omer Tarik 404
Ohara
S. 271
Ohishi
K. 466, 469
Ohsaki
H. 435
Ohsugi
M. 230
Ohya
M. 75
Oka
M. 161, 530
Okada
T. 283
Okai
K. 75
Okamoto
Jun 704
Okay
Elif 404
Okube
M. 530
Okvátovity
Z. 252
Oliviero
V. 37

Ollefs
K. 494
Onbasli
Mehmet C. ... 261, 263
Onbaşlı
Mehmet Cengiz .. 260
Ono
T. 8
Orlov
V.G. ... 223
Ortlepp
T. 180, 414, 418
Oruc
Pınar ... 750
Oruç
P. 713, 714, 715
Otajonov
S.M. ... 327, 608
Otani
YoshiChika ... 34
Otto
A. 279
Otxoa
R.M. ... 392
Ovcharov
A. 540
Alexey V. ... 65
R. 385
Ovchinnikov
A.S. ... 59, 271, 319
S.G.Ovchinnikov .. 323
Ovsyannikov
V. 699
Owjifard
Z. 746
Ozatay
O. 182
Ozhan ... 131
Ozbay
A. 705
A. Gokce ... 368, 373, 705
Ozkan
S.N. ... 711
Ozkul
E. 711
Ozturk
U. Kemal ... 288
U.K. ... 395
Ufuk Kemal ... 620
Y. 182
Ozvat
T. 201

Ö

Öksüzoğlu
R.M. ... 642
Önel
Aykut Can ... 260
Öveçoğlu
M. Lütfi ... 636
Özçelik
B. 634
C. 634
Özdoğan
K. 752
Özgün
S. 642
Öztürk
Adil ... 23
Kemal ... 401
Ö. 645
Özgür ... 647

P

Pacanowska
A. 316, 318
Pacuski
Wojciech ... 144
Padukone
Ronak ... 278
Paglione
Johnpierre ... 215
Pak
L. 530
Pakhira
Santanu ... 47
Palau
A. 110, 119, 140, 337
Anna ... 331
Pallarés
María Carmen ... 194
Palm
R. 466
Palmer
Lex ... 278
Palotás
K. 243, 245
Paltiel
Y. 56
Pamidi
Sastry ... 542
Sastry V. ... 286
Pan
Yongqiang ... 69
Panina
L.V. ... 294, 305
Parajuli
S. 722
Pardo
E. 77
Parisiades
P. 477
Parizh
Michael ... 542
Park
Hee Chul ... 365
Pashayev
B.G. ... 731
Pashkovskaia
V. 745
Patra
C. 737
Manas ... 509
Pavlov
N.S. ... 64, 688, 738
Nikita ... 65
Pavlukhina
O. 439
Pęczkowski
P. 187, 539, 652, 653
Paweł ... 643
Pei
Xiaoze ... 432
Peikrishvili
V.A. ... 646
Pelc
D. 552, 558
Pelliciari
J. 565
Peng
Wei ... 190
Peremedathil-Pradeep
R. Peremedathil . 505
Perez
M.M. Seker ... 428
Pérez-Bailón
J. Pérez ... 57, 112
Pérez-Landazabal
J.I. Pérez ... 492
Perucchi
A. 477
Pervakov
K.S. .64, 70, 688, 689, 690, 738
Kirill S. ... 65
Pervin
R. 157, 572
Petrovic
Cedomir ... 357
Petrykin
V. 227, 530, 543
Petrzhik
A. 540
Pfau
B. 329, 499
Bastian ... 509
Pfeiffer
M. 210
Piętosa
Jarosław ... 643
Pile
S. 380
Pilon
Laurent ... 235
Pina
J.M. ... 686
Pinto
V. 335, 518, 534
Pirottin
Th. ... 110
Plaisier
J.R. ... 691
Plokhikh
I. 97, 102
Poccia
N. 321, 736
Pokharel
B. 522
Pokrovskii
S. 682
Polat
M. 409
Polichetti
M. 356, 514, 515, 519
Pomorski
K. 187, 652, 653
Pompeo
N. 517, 518, 691
Ponomarov
Semyon ... 639
Pons
J. 482
Popov
A.A. ... 195, 207
Alexey ... 724
D.V. ... 726, 728
R. 154
Popova
A.V. ... 440
Popovic
D. 522
Porro
Jose M. ... 481
Porta-Velilla
L. Porta ... 149
Luis Porta ... 150
Posske
Thore ... 244
Powalla
L. 89, 391, 510
Lukas ... 510
Pradeep
Reshma Peremadathil. 509
Prezhdo
O.V. ... 702
Prikhna
Tetiana ... 639
Prischepa
S.L. ... 224
Prokscha
T. 184
Pronto
A. 686
Proust
C. 37
Pröpper
M. 181
Ptok
A. 98
Pudalov
V.M. ... 377, 738
Vladimir M. ... 65, 377
Puig
Tersa ... 639
Puz´niak
R. 748
Pütkül
M. Dilara ... 705

Q

Qaiumzadeh
Alireza 171
Qiu
X.G. 300
Zhishu 79
Qu
T. 734
Tingyu 729
Queval
Loic 542
Quéval
Loïc 433

R

Raab
K. 128
Rabaa
Mariam 717
Radić
D. 547, 548
Radkevich
A.A. 586
Radovinsky
Alexey 278
Raes
B. 186, 256
Ragımov
S.S. 665
Rahimpour
A. 182
Rahman
Muneeb ur 142
Rahmonovich
Djuraev Davron ... 741
Rahnb
M.C. 725
Raimondo
E. 124
Rajabov
M.R. 731
Rakhmanov
E. O. 656
E.O. 68, 649
S. 411
Ye.O. 66, 690
Rakhmonov
Z. 239
Ramazani
Ali 46
Ramires
Aline 216
Rams
Marek M. 120
Rappé
A. 201
Rasool
Rehana 659, 675
Raychaudhuri
P. 522
Raza
Rizwan 624
Recarte
V. 492
Recher
Patrik 114
Rehman
M. Anis 625
Reichhardt
Charles 521
Reinhardt
A. 180
Reith
H. 736
Ren
J. 257, 530, 561
Jie 190
T. 513
Renel
J. 530
Rentz
Ross 278
Repollés
Ana 194
Rex
S. 309
Reyren
N. 128, 507
Rhyee
Jong Soo 253
Riva
N. 532
Rizzo
F. 335, 518
Rmeid
Sajida 672
Rodin
I. 699
Rodionova
V.V. 294
Roditchev
D.Y. 362
Rodrigues
A. De Giovanni 477
D.R. 387
Rodriguez
A. Fernández 337
Rodríguez
Alejandro Fernández 331
Rodríguez-Velamazán
J.A. Rodríguez 478, 492
Rogachev
A. 173, 581
Rogal
Ł. 485
Rogalev
A. 296, 468
Romanelli
G. 534
Romanenko
A. 184
Ross
Caroline A. 19
Rossi
S. 274
Rotheudt
N. 638
Roubeau
Olivier 194
Roučka
Václav 588
Rout
P.K. 392
Roy
Deep Singha 723, 739
Rózsa
L. 243, 245
Röhlsberger
Ralf 381
Rudnev
I. 399, 682
Rudominskiy
A.E. 332
Rufoloni
A. 335, 534, 691
Rui
W.B. 44
Rukelj
Z. 547, 558
Runov
R.V. 703
Rusakov
V.F. 748
Ryazanov
V.V. 448, 458

S

Saati
Sariah Al 744
Sabirianov
R. 167
Sadakov
A.V. 68, 377, 649, 656
Andrey V. 65, 377, 621
Safin
A. 598
Safran
S. 645
Serap 647
Saggau
C.N. 736
Saha
Shanta 215
Sahoo
M. 725, 727
Sahooa
M. 725
Sahu
Anubhav 95, 177
Saitoh
Eiji22
Sakai
Naomichi 360
Sakamoto
H. 538
Salaheldeen
M. 480
Salazar
Daniel 490
Erica 278
Saleemi
Awais Siddique ... 625
Salikhov
R. 392
Salinas
Daniel Pérez 509
Salman
Z. 184
Samatov
M.R. 630, 702
Samoilenkov
S. 227, 530
Samwer
Konrad 509
Sanabria
Charlie 278
Sanchez
A. 110
S. 201
Sánchez
Pedro Alonso 473
Sánchez-Alarcos
V. Sánchez 492
Sandoval
M.A. Cascales 503
Sanz
A. Manjon 465
Saparbaev
T. 327, 608
Saraco
L. 279
Saraiva
T.T. 362, 745
Sarkar
Abhishek 174
Sarreshtedari
Farrokh 367, 556
Sasaki
T. 474
Sass
Paul 639
Sassa
Y. 466
Satheesh
S. 391
Satir
İ. Tosun 719
Sato
K. 474
Satoh
Takuya 59
Savaskan
B. 395
Savasta
S. 611

Savaşkan
Burcu 401
Savchenkov
Pavel S. 464
Sawicki
Maciej.....144
Sazgari
V. 376
Schaffner
N. 201
Schäfter
D. 203
Scheerder
J.E. 256
Scheibel
F. 494
Schilling
M. 181
Schillo
M. 275
Schlage
Kai.....381
Schmid
C. 118, 181
Schmidt
T. 593
Thomas L. 114
Timo.....509
Schneider
M. 329, 499
Michael.....509
Scholz
T. 391
Schrefl
T. 265
Schulz
F. 391
Frank.....510
Schuppler
Stefan 47
Schurig
Thomas.....194
Schütz
G. 296, 383, 391, 497
Gisela.....510
Scipioni
L. 383
Sebe
N. 128
Seckin
A. 715
Seçkin
A. 713, 714
Sedlak
K. 534
Selvamanickam
Venkat 231
Semenok
Dmitrii V. 377
Semenov
A.D. 257
A.G. 576, 585, 586
Andrew G.....585
Semina
V. 539, 540
Semper
Florian 536
Senguler
G.Y. 680
Senturk
K. 753
Sera
S. 280, 543
Serantes
D. 709
Sergeev
G.S. 223
Ilya..... 381
Seri
M. 534
Sesé
Javier 194
Sevinçli
H. 409
Seydioğlu
T. 645
Shabani
Javad 249
Shahid
Rabia 678
Shaikhaidarov
R.S. 584
Shanenko
A. 745
A.A. 362, 526
Shao
B. 606
Yuelin..... 628
Shapovalov
Dmitry L. 578
Sharma
Peter..... 61
Sharrouf
Majed 426
Shaternik
Anton..... 639
Shayeganfar
Farzaneh..... 46
Shchukin
Alexandr 79
Shein
I.R. 688, 738
Shelton
Williams A. 577
Shen
Dawei 101
Shepard
A. 383
Maise..... 278
Shevelkov
A.V. 68, 649
Shi
Kewen 125
Ming 99
Zhixiang 69, 71
Shigiya
K. 474
Shilov
A.I. ..66, 68, 649, 656, 690
Shimada
Y. 30
Shimoyama
J. 358, 443
Shirai
Y. 75
Shiroka
T. 252, 340
Shiu
Hung Wei 704
Shokri
S. 736
Shu
Huchen..... 219
Shuai
J. 264
Shustov
V.A. 728
Shvidkiy
D.S. 651
Sınır
E. 368, 373
Si
Wenlong..... 626
Sidorenko
Anatolie..... 415
Sidorova
M. 257
Silhanek
A. 140
A.V. 55, 110, 119, 149, 186, 256, 337
Alejandro V. 150, 331
Silva
E. 517, 518
Simon
Paul 115
Simsek
Y. 182
Simura
Rayko 360
Šindler
M. 41, 740
Singh
Amol..... 704
M. 701
R. P. 737
R.P. 446
Shiv J. ..358, 692, 693
Sinha
Aritra 120
Sinova
J. 383
Skuratov
V. 539, 540
Slageren
J. van 203
Slavin
A. 385, 390
A.N. 390
Smith
P W..... 83
P.W. 27
Soban
Z. 392
Sogabe
Y. 538
Soğan
M. 705
Sokolovkiy
V.V. 488
Sokolovskiy
V. 292, 301, 439
V.V. 314, 495
Sonar
Vrishali 612
Song
B. 228
Songur
A. Canberk 421
Sorbom
Brandon 226, 278
Sparacio
S. 531
Speller
Susannah..... 619
Stanciu
S. 265
Stano
M. 110
Starkov
Grigory A. 176
Stefano
O. Di 611
Stelmakh
Svitlana 692
Stemmler
F. 203
Stepanov
D. 699
Stępień
Ł. 187, 653
Stoffels
Daniel..... 331
Stojewski
B. 187
Stolyarov
V.S. 362, 415, 513
Streltsov
S. 161
Štrkalj
Antonio 550
Strohm
Cornelius..... 381
Struzhkin
V. 21, 352
Strydom
A.M. 668
Su
L. L. 561
Subramanya
M.V.H. 27

Suess
Dieter.....115
Suffczyński
Jan 144
Sugiyama
J. 466, 469
S. 466
Suh
Junho 370
Sultan
Hira 677
Sun
Yue.....71
Sundaresan
A. 648
Suñé
J. 119
Sung
Z. 184
Z. H. 691
Sunko
D.K. 326
Surmanidze
D.L. 635
Suter
A. 184
Suzuki
J. 469
S. I. 460
T.S. 395
Yuta. 60
Süss
Dieter.....502
Sverdun
Volodymyr 639
Sytnikov
V. 699
Victor 284
Szabo
Andras 216
Szczerba
M.J. 485
Szunyogh
L. 243, 245

T

Taazayet
W. Ben 600
Tacon
Matthieu Le 47
Takahashi
K. 283
Kohki.....486
Takata
S. 469
Tamegai
T. 513
Tanaka
Y. 543, 559
Tarasova
Yu.S. 314
Tariq
Rabia 660, 676
Tatara
R. 469
Taufour
V. 351
Tavana
A. 746
Tay
D. 252
Tcakaeve
A. 725
Tejima
Y. 538
Tekci
N. Orhun..... 421
Temnaya
O. 673
Tempere
J. 238
Terao
Y. 75
Terazaki
T. 543
Teresa
J.M. De 118
Terzic
J. 522
Tesař
R. 41
Tesi
L. 203
Thareja
Eklavya 577
The
Sucitto 704
Thiebes
Y.M. 525
Thuwal
U.C..... 157, 572
Tikhonov
E.S..... 573, 582
Timofeev
V.E. 269
Timokhina
E.N. 206
Tlemsani
I. 87
Togawa
Yoshihiko 59
Tokeşer
Elif Aşikuzun 647
Tokunaga
Masashi 486
Tokuta
S. 30
Tomarchio
L. 477
Tomellini
M. 335
Tonooka
S. 75
Torokhtii
K. 518
Torrens-Serra
J. Torrens..... 482
Torsello
D. 517, 518, 531
Daniele 536
Trafimenko
A.G. 224
Tran
Lan Maria 400
Tretiakov
O.A. 590
Trif
Mircea 244
Trocha
P. 559
Piotr 612
Trotta
A. 531
Troyan
I. 352
Ivan A. 377
Trugenberger
C.A. 11
Trukhanova
Mariya Iv. 604
Trunk
C. 372
Trunov
D. 352
Tsankov
S. 325
Tsuchiya
Y. 283
Tsukagoshi
M. 271
Tsutsumi
K. 474
Tsvetkov
A. 540
A. Yu. 656
Tu
Li Ming 603
Tuğluoğlu
Nihat 750
Turayev
A.A..... 240, 742
O.G. 240
Turnbull
Luke..... 115, 502
Twin
Andrew..... 619
Tyberkevych
V. 385
Tzeng
Wen Yen..... 41

U

Ueda
H. 466
Ugolkova
E.A. 206
Uhlir
V. 140
Uhlíř
V. 110
Ukleev
V. 268
Ullah
R.R..... 351
Ullrich
Aladin..... 509
Umegaki
I. 466, 469
Ummarino
G.A. 106
Ungor
O. 201
Unlu
P.S. 711
Unterrainer
R. 287
Raphael 536
Unuvar
Necdet 4
Uppalapati
Kiran..... 278
Urbánek
Michal 588
Urzhumtsev
A. 666, 667
Uskenbaev
D.E.....327, 608
Usoltsev
A.S. 68, 377, 649
Alexey S..... 621
Ustinov
Alexey 89
Užarević
K. 207

Ü

Ünlü
M. 421

V

Vach
Holger 104
Vagov
A. 362, 526, 527, 743, 745
A.V. 526
Alexei 644
Valenzuela
Sergio 26
Valikov
R. 543
R.Valikov 530
Valla
T. 336, 347
Valvidares
Manuel..... 509
Vanderbemden

P. 638
Vanderheyden
B 638
B. 110
Vannozzi
A. 534
Varga
R. 291
Varsano
F. 691
Vasenko
A. 745
A.S. 416, 450, 462, 578, 630, 702
Vasiliev
A. 540
A.N. 164
Alexander L. 65
Vasudeva
Keshav 278
Vasylkiv
O. 395
Velasco
Verónica 194
Vélez
Saül 382
Venuti
M.B. 61
Vereschagin
K. 530
Verseils
M. 477
Veschunov
I. 530
Veshchunov
I. 513
Veziroğlu
S. 752
Vieira
Rui 278
Vignolles
D. 37
Vilsmeier
F. 392
Vinokur
V.M. . 11, 41, 49, 157, 377, 526, 572, 736
Vlasenko
V.A. 70, 377, 689, 690
Vladimir A. 377
Voccio
J. 279
Volegov
A. 666, 667
Volkov
M.P. 332
Volkova
O. 172
Vondel
J. Van de 186, 256
Vujević
L. 207
Vyatkin
V. 530
Vysotskiy
V. 699
Vysotsky
Vitaly S. 282

W

Wager
Clemens 265
Wan
Xiangang 137
Wang
C. N. 252
Chung Yang 121
Dongliang 394
F. H. 560
H.B. 610
J. 12, 44, 708
Jie 334
Ke 569
Ledong 626
Meng 18
Ru Pan 704
Sansheng 441
Shiyao 441
Yi 169
Z. 255, 267, 510
Z.D. 44, 561
Warner
Alex 278
Watterson
Amy 278
Wederni
A.Wederni 480
Weeks
Dash 278
Wei
Wei 69, 71
Weigand
M. 380, 383, 391
Markus 510
Weinreb
Benjamin 278
Wende
H. 494
Weng
Bicong 190
Weschkeh
E. 725
Whangbo
M. H. 164
White
J. 27
Wieland
R. 610
Wiesendanger
R. 16, 243, 245
Roland 16
Wietek
Alexander 120
Wilcox
J.A. 513
Wilhelm
F. 296
Wille
Hans Christian 381
Winkler
T. B. 128
Wintz
S. 380, 383, 391, 497
Sebastian 502, 510
Wisniewski
Andrzej 692
Wiśniewski
Andrzej 693
Wittmann
A. 56, 383
Wojewoda
Ondřej 588
Wolf
Christoph 197
Woller
K.B. 535
Wolter
A.U.B. ..195, 725, 727
Woltera
A.U.B. 725
Wong
Chi Ho 307
Wongjom
P. 657
Wongsakulkhamkhot
C. 657
Wota
G. 316, 318
Wu
P.H. 610
Y. 176, 351, 702
Z. 236, 280, 543
Zhongyan 343
Wunderlich
J. 392
Wurster
K. 118

X

Xhakaza
A. 668
Xing
Jie 577
Xu
M. 111, 341
Teng 626
Weijie 115
X.Y. 560
Xianghan 704
Xiao 486
Xue
Chang 706, 707
Z. 259

Y

Yagan
R. 261, 263
Rawana 260, 261
Yahia
Anis Ben 278
Yamada
T. K. 199
Y. 228
Yamamoto
A. 30, 398
Rikako 502
Riku 209
Yamanaka
A. 30
Yamane
S. 255
Yamashita
Masahiro 81, 193
Yang
Kun 45
Qian 407
Wei 724
Zhaorong 353
Yanilkin
I. 399
Yao
Xin 633
Y. 255
Yasin
Fehmi 510
Yatsu
Yudai 360
Yatsyk
I.V. 145, 726
Yavidov
B. 239, 327
B.Ya. 327, 608
Yavru
C.Yavru 642
Yazdani-Asrami
Mohammad Yazdani 542
Yetis
Hakan 400
Yıldız
Ali Suat 288
Yılmaz
U. 414
Yildirim
Gürcan 647
Yucel 334
Yilmaz
H.S. 710
Ying
Tianping 376
Yochelis
S. 56
Yonezawa
S. 255
Yoshikawa
N. 90

Yoshimura
K. 466
Yoshinaga
K. 466
You
Shuangrong 78
Yu
Xiuzhen 510
Yudanov
N.A. 305
Yue
Binbin 219, 349
Yuspov
J. 410
Yusupov
J. 146, 372

Z

Zabolotnyye
V.B. 725
Zaccone
A. 106
Zachariasz
Piotr 643
Zadrozny
J. 201
Zagrebin
M. 301, 439
M.A. 314
Zagura
Petr 619
Zahrabi
Ebrahim 260
Zaikin
A.D. 576, 580, 585
Andrei D. 585
Zając
Marcin 643
Zajarniuk
Tatiana 692, 693
Zalecki
Ryszard 643
Zaleski
Andrzej 400
Zampa
A. 283
Zanten
D.M.T. van 184
Zappatore
A. 534
Zapretilina
E. 699
Zatari
Ahmad El 260
Zeng
H. 167
Zervou
A. 221
Zhai
Yuan Qi 716
Zhakina
Elina 115
Zhang
Chi 169
Fu Chun 563
Hongye 544
Jia Jie 603
Jincang 706, 707
Lin169
Min 79
P. 606, 607, 688
S. 606, 607
X. 27, 54, 313, 394
X. M. 722
Xichao 54
Xiyue S. 61
Yifeng 706, 707
Zhao
D. 292, 354
Weisheng 125
Zhibo 174
Zheng
Shu Yu 169
W. 156
Yan Zhen 716
Zhitomirsky
M. E. 165
Zhong
Wei 219, 349
Zhou
Di 377
Heng An 626
Xingjiang 564
Yi 251
Zhu
J M 228
Jing 626
Zhukov
A. 299, 480
Zhukova
V. 299, 480
Zhumagulov
Ya.V. 644
Ziętala
Michał 643
Žilić
D. 207
Ziman
T. 165
Zmorayova
K. 443
Zocco
Diego A. 218
Zouari
I. Mallek 600
Zubko
V. 699
Zueco
D. 57, 112, 317

PLATINUM

SuperMag

TURKISH AIRLINES

SUN Magnetics
INTEGRATED CIRCUIT INDUCTANCE EXTRACTION

GOLD

FYTRONIX Electronic

VACUTECH Based on innovation

Quantum Design EUROPE

CRYOGENIC

SILVER

SHI Cryogenics Group

SuperMag

TURKISH AIRLINES

SUN Magnetics

INTEGRATED CIRCUIT INDUCTANCE EXTRACTION

SUN Magnetics (Pty) Ltd specializes in advanced parameter extraction software and layout verification solutions for the superconductor and quantum electronics industries. Our flagship product, InductEx, is renowned for its comprehensive simulation capabilities. It supports a broad array of features, including flux trapping analysis, external magnetic field analysis, and multi-layer extraction of inductance, capacitance, and impedance. Tailored for superconducting digital circuits, InductEx facilitates layout-vs-schematic verification, parameter sweeps, and direct SPICE compact model extraction from layouts. It also features hybrid tetrahedral/triangular meshing and advanced packaging analysis with customizable wire bonds and interconnects, ensuring accurate and efficient design verification for our clients.

For more details, visit https://sun-magnetics.com/.

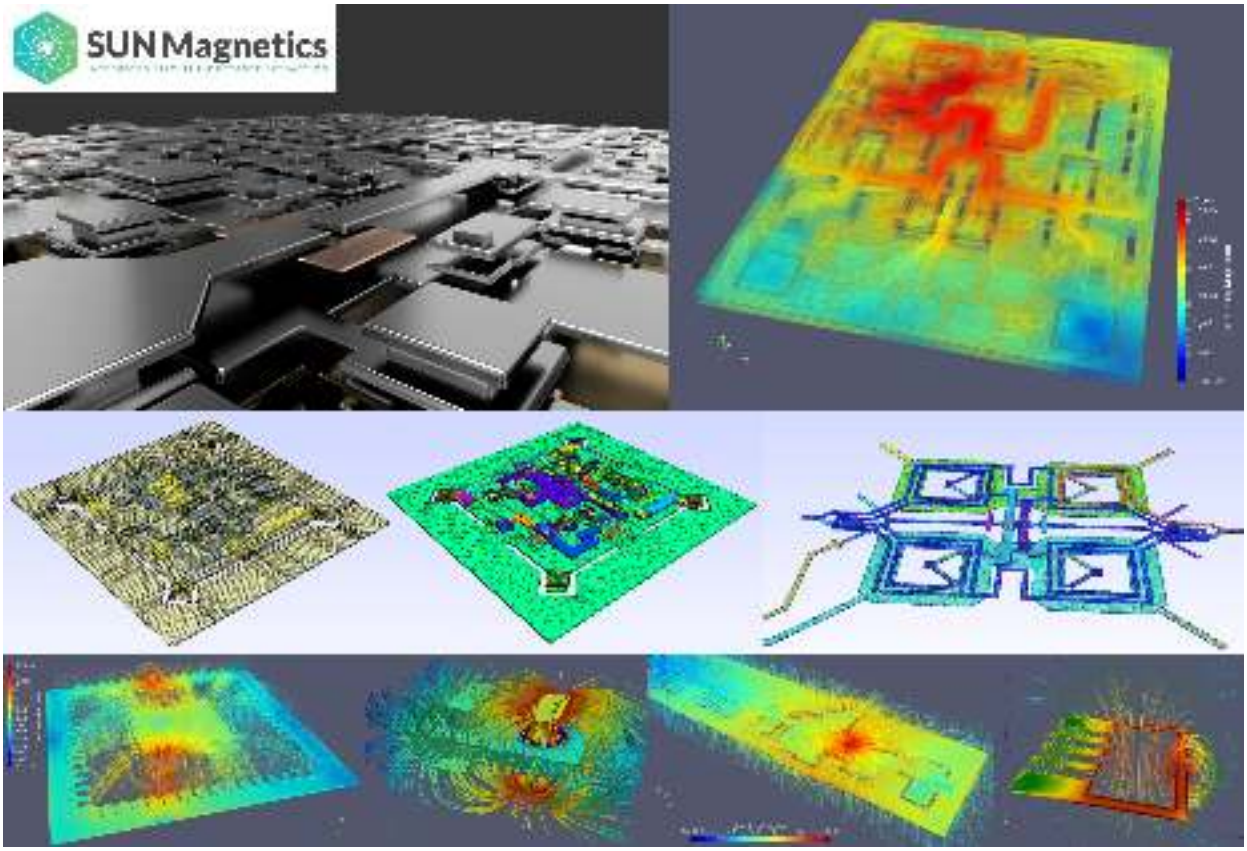

FYTRONIX Electronic

FYTRONIX designs and manufactures advanced technological products to be used in scientific and high technology research.

5 reasons that make us different
Fytronix is competent in Scientific Device Design and Development
FYTRONIX can provide all kinds of support for designing and developing all kinds of devices to be used in scientific research, providing new features to existing products and eliminating deficiencies.

Fytronix Competent in Electronic Device Production and Development
FYTRONIX can provide all kinds of support for the production and characterization of all electronic devices such as solar cells, Schottky diodes, PN joint diodes, Photodiodes, Photodiodes, Photosensors, Field Effect Transistors, Thin Film Transistors, Gas Sensors, Biosensors, Radiation Sensors.

Fytronix is an expert and competent in Solar Energy
FYTRONIX Silicon Solar Cells, Paint Sensitive Solar Cells, Quantum Dots Solar Cells, Organic Solar Cells, Solar Panel Production and Characterization can provide all kinds of support

Fytronix is competent in Material Synthesis and Production
FYTRONIX can provide all kinds of support for the synthesis and production of all kinds of semiconductor, metal,
alloy, composite, biomaterials, nanomaterials and electronic materials to be used in scientific studies.

Fytronix is competent in scientific studies of Master and Ph.D. students
FYTRONIX provides all kinds of support to the scientific studies of master, doctorate and post doctoral students.

VACUTECH
Based on innovation

The Vacuum Technologies Company (Vacutech LTD) is a developer and manufacturer of special vacuum technological thin–film equipment and high-tech productions based on it. The installations produced by our company are widely used in display manufacturing, microelectronics, optics, and the space industry.

Vacutech provides magnetron coating and ion nitriding services for the Customer's products. These services are provided at the company's pilot production facility that meets all the necessary requirements for modern vacuum coating production.
The pilot production includes:

- a coating site, including six vacuum installations of various types and functionality;
- site of chemical preparation of the surface of products
- laboratory for monitoring the properties and characteristics of coatings.

The company specializes exclusively in vacuum and cryogenic equipment and therefore our specialists have extensive technical experience in these areas. They can not only help you choose the right model, but also help in the development of any vacuum system. The company's engineers travel to customers for installation, start-up and maintenance of equipment and staff training.

Our company provides both turnkey project designes:

- Vacuum Chambers
- Turnkey installations for thermal vacuum testing
- We can manufacture vacuum installations to test products and components for leaks-Thinfilm coating equipment
- Cryogenic vacuum systems
- Ultra-precise temperature control systems

Quantum Design EUROPE

Quantum Design GmbH We are a leading European distributor of high-quality scientific instruments and components. We offer components and systems used in materials science, imaging, spectroscopy, photonics, nanotechnology and life science research. We were founded 50 years ago and employ more than 120 dedicated staff across Europe.

CRYOGENIC

Cryogenic Limited has been manufacturing and developing superconducting magnets for nearly 50 years. It has pioneered many technological firsts, including the first company to every deliver a cryogen free superconducting magnet system for material research more than 25 years ago. Cryogenic continues to produce a wide variety of customised superconducting magnet systems, including solenoids to 22 Tesla, split pairs to 14 Tesla, 2D and 3D vector configurations, magnets for UHV soft x-ray, muon, optical and neutron beamline environments, as well asbespoke large bore magnets for gyrotron and mineral separation applications. Our range of measurement systems includes magnets for NMR, EPR, SQUID and vibrating sample magnetometers, electrical and thermal transport measurements, combined with ultra-low temperature capabilities down to 300 mK with 3He or 50 mK with a dilution refrigerator. These configurations are offered as either cryogen free or low boil off liquid helium cooled magnet systems.

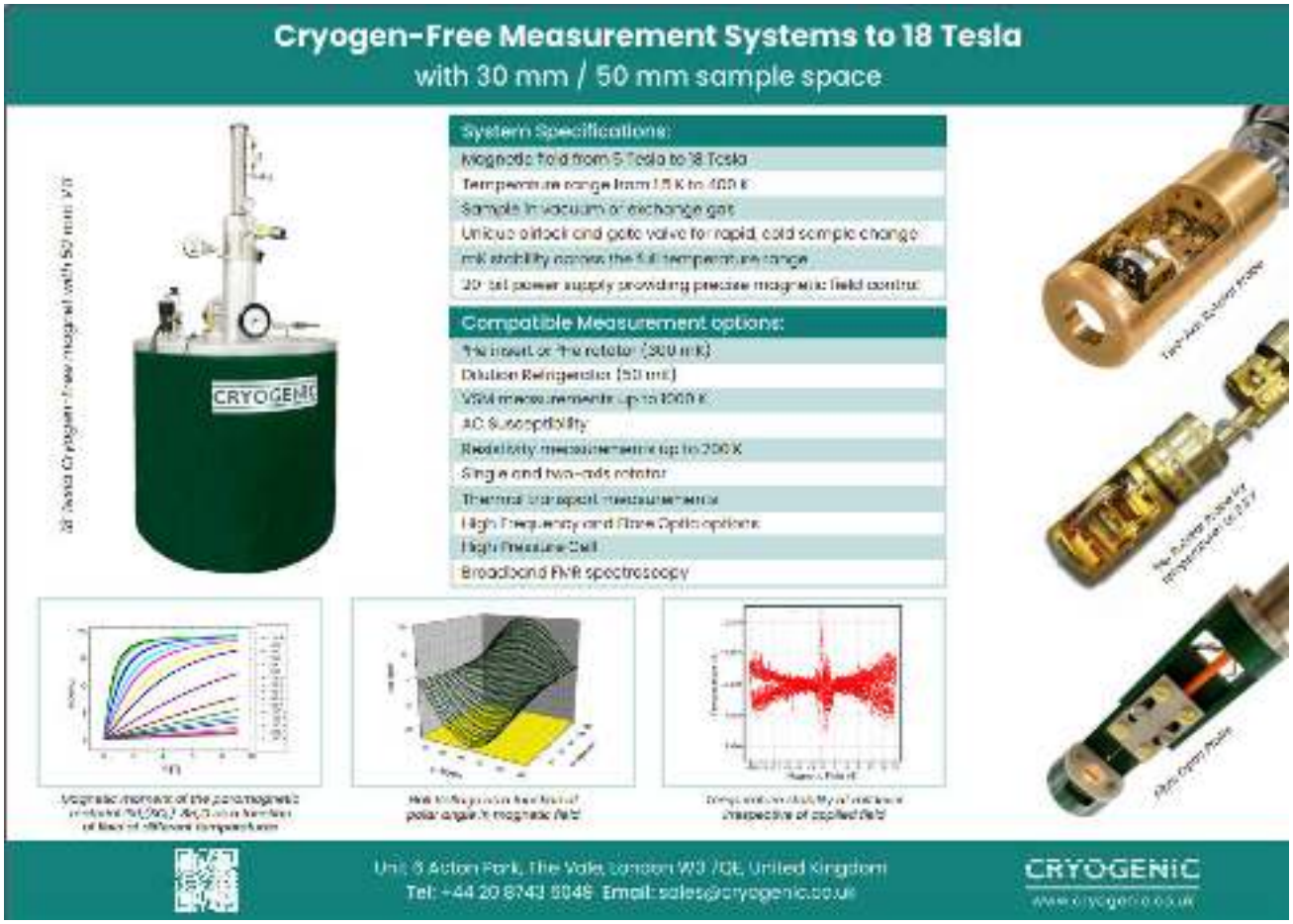

SHI Cryogenics Group

Company profile Sumitomo (SHI) Cryogenics of Europe

As a member of the SHI Cryogenics Group, Sumitomo Cryogenics of Europe GmbH provides high-quality, innovative cryogenic solutions such as cryocoolers, cryopumps and helium compressors for a variety of industries.

PLATINUM

SuperMag

TURKISH AIRLINES

SUN Magnetics
INTEGRATED CIRCUIT INDUCTANCE EXTRACTION

GOLD

FYTRONIX Electronic

VACUTECH Based on innovation

Quantum Design EUROPE

CRYOGENIC

SILVER

SHI Cryogenics Group

Sponsors

PLATINIUM

SuperMag

TURKISH AIRLINES

SUKMagnetics

GOLD

PYROMIX

VADUTECH

CRYOGENIC

SILVER

SHI

Institutional Supporters

HITIT

KTU

Springer